147

SM-47005

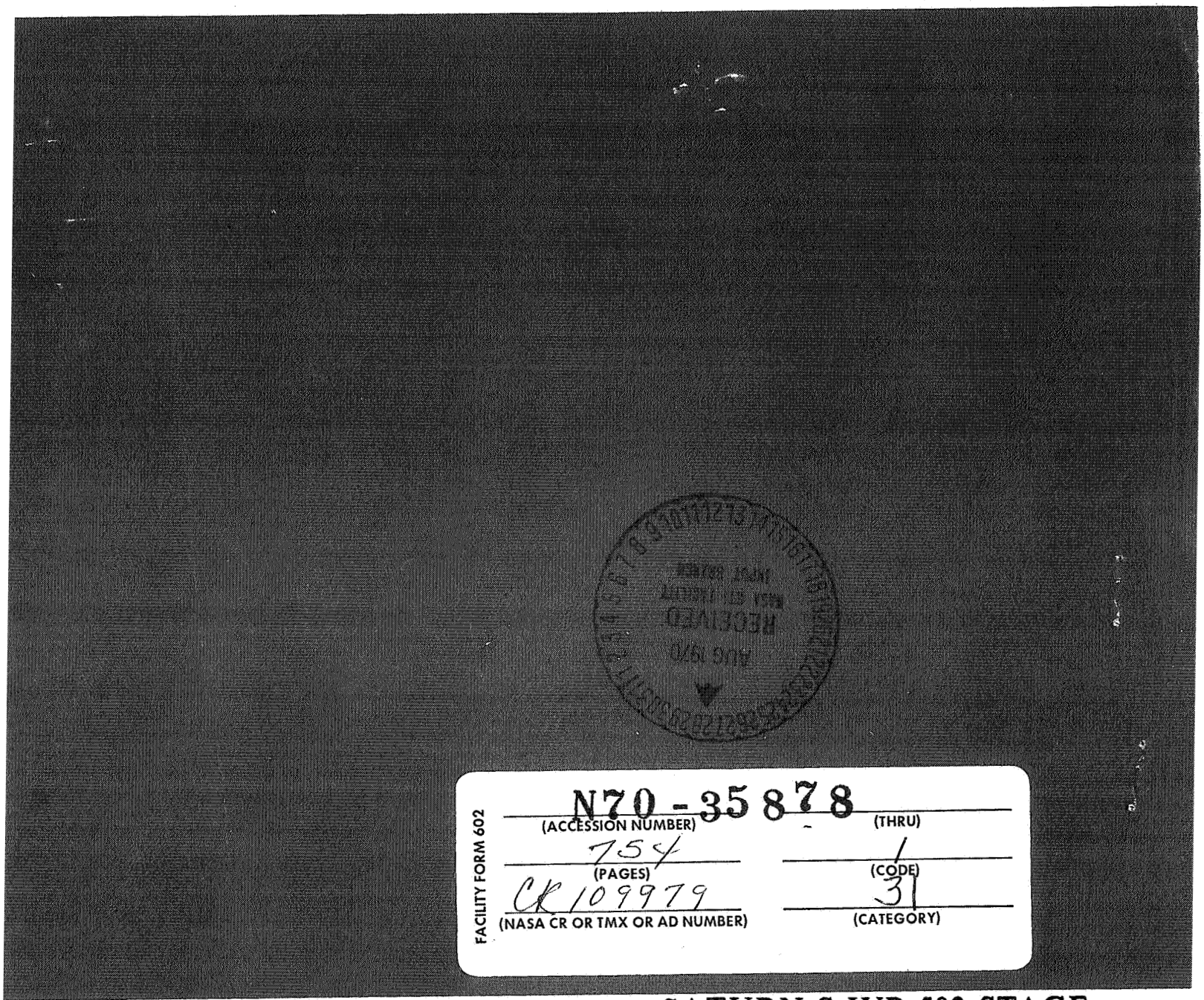

SATURN S-IVB-502 STAGE FLIGHT EVALUATION REPORT

JULY 1968

DOUGLAS MISSILE & SPACE SYSTEMS DIVISION

MCDONNELL DOUGLAS CORPORATION

SATURN S-IVB-502 STAGE
FLIGHT EVALUATION REPORT

DOUGLAS REPORT SM-47005
JULY 1968

PREPARED BY:
SATURN S-IVB TEST PLANNING AND
EVALUATION COMMITTEE AND
COORDINATED BY: J. BUNNELL
PROJECT OFFICE – FLIGHT TEST
SATURN DEVELOPMENT ENGINEERING

PREPARED FOR:
NATIONAL AERONAUTICS AND
SPACE ADMINISTRATION
UNDER NASA CONTRACT NAS7-101

APPROVED BY: A. P. O'NEAL, DIRECTOR
HUNTINGTON BEACH DEVELOPMENT ENGINEERING –
SATURN/APOLLO

MCDONNELL DOUGLAS ASTRONAUTICS COMPANY
WESTERN DIVISION
5301 Bolsa Avenue, Huntington Beach, CA 92647 (714) 897-0311

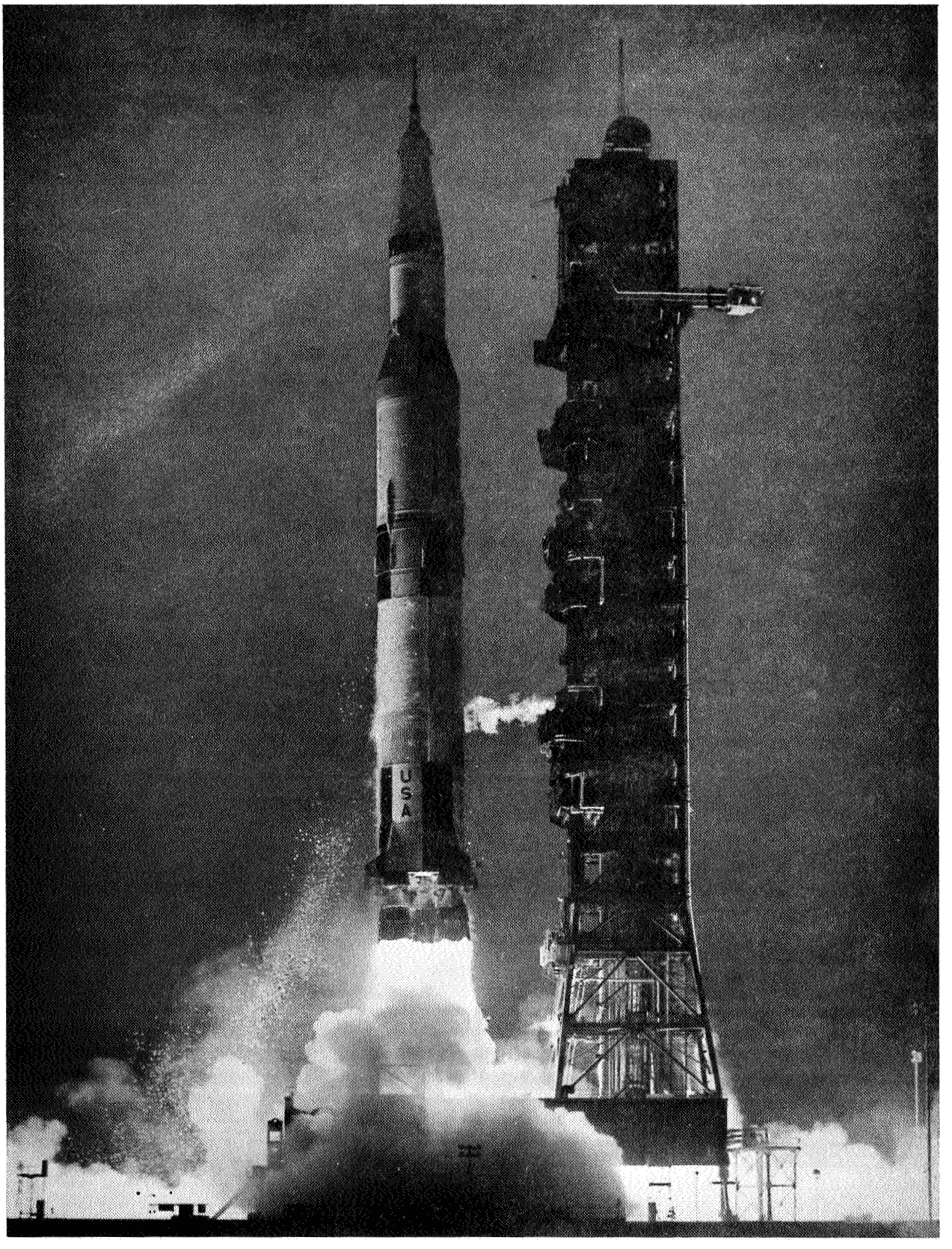

SATURN AS-502 VEHICLE LIFTOFF

ABSTRACT

This report presents the evaluation results of the prelaunch countdown, powered flight, and orbital phase of the S-IVB-502 stage which was launched on 4 April 1968 as the third stage of the Saturn AS-502 vehicle.

The report is a contractual document as outlined in NASA Report MSFC-DRL-021, Contract Data Requirements, Saturn S-IVB Stage and GSE, dated 1 February 1968, Revision A. It was prepared by the Saturn S-IVB Test Planning and Evaluation Committee and coordinated by the Saturn S-IVB Project Office of the McDonnell Douglas Astronautics Company, Western Division.

DESCRIPTORS

data evaluation	S-IVB-502
flight test	Saturn AS-502 vehicle
Saturn V	countdown

PREFACE

The purpose of this report is to present the evaluation results of the prelaunch countdown, powered flight, and orbital phase of the S-IVB-502 stage which was launched on 4 April 1968 as the third stage of the Saturn AS-502 vehicle.

This report was prepared in compliance with the National Aeronautics and Space Administration Contract NAS7-101. It is published in accordance with NASA Report MSFC-DRL-021, Contract Data Requirements, Saturn S-IVB Stage and GSE, dated 1 February 1968, Revision A, which delineates the data required from the McDonnell Douglas Astronautics Company.

This document was prepared by the Saturn S-IVB Test Planning and Evaluation Committee and coordinated by the Saturn S-IVB Project Office of the McDonnell Douglas Astronautics Company, Western Division.

TABLE OF CONTENTS

TABLE OF CONTENTS (Continued)

TABLE OF CONTENTS (Continued)

TABLE OF CONTENTS (Continued)

APPENDICES

LIST OF TABLES

LIST OF TABLES (Continued)

LIST OF TABLES (Continued)

LIST OF ILLUSTRATIONS

LIST OF ILLUSTRATIONS (Continued)

LIST OF ILLUSTRATIONS

LIST OF ILLUSTRATIONS (Continued)

LIST OF ILLUSTRATIONS (Continued)

LIST OF ILLUSTRATIONS (Continued)

LIST OF ILLUSTRATIONS (Continued)

LIST OF ILLUSTRATIONS (Continued)

LIST OF ILLUSTRATIONS (Continued)

LIST OF ILLUSTRATIONS (Continued)

LIST OF ILLUSTRATIONS (Continued)

SECTION 1

INTRODUCTION

1. INTRODUCTION

1.1 General

This report presents the results of analyses that were performed by Douglas personnel on the countdown, launch, and flight of the Saturn S-IVB-502 stage.

This evaluation report also describes tests conducted at Kennedy Space Center (KSC), and pertinent modifications made to the S-IVB and related ground support equipment.

This report is authorized by NASA Contract NAS7-101, and is the final report on the S-IVB-502 by the Douglas S-IVB Test Planning and Evaluation Committee of the Missile and Space Systems Division (MSSD), Huntington Beach, California.

1.2 History

The S-IVB-502 was assembled at the Huntington Beach Space Systems Center. A checkout was performed on 10 May 1966, in the Vehicle Checkout Laboratory prior to shipping the stage to the Sacramento Test Center (STC) on 31 May 1966. The stage was installed in Beta Test Stand I on 6 June 1966, and was acceptance fired on 28 July 1966.

The auxiliary propulsion system (APS) modules were shipped to the manufacturing and assembly (M&A) building at STC for leak and functional checks. The APS modules were then transferred to the Gamma Complex and confidence fired on 19 July and 27 July 1966. After firing, the modules were returned to the M&A building for cleaning and purging prior to shipment to KSC with the S-IVB-502.

All objectives of the acceptance firing tests were successfully completed on 28 July 1966, and are outlined in Douglas Report No. DAC-56357, Saturn S-IVB-502 Stage Acceptance Firing Report, dated 28 September 1966 and in Douglas Report No. SM-37539, S-IVB-502 Stage Acceptance Firing 15 Day Report, dated August 1966.

After completion of acceptance firing tests, the stage was shipped to KSC and installed in the low bay of the Vehicle Assembly Building on 27 February 1967. After installation of the aft interstage and completion of low bay prelaunch checkout, the stage was transferred to the high bay and mated to the AS-502 launch vehicle. The AS-502 launch vehicle was transferred to Launch Complex 39A on 6 February 1968 and was launched at 12:00:01 Greenwich Mean Time (GMT) on 4 April 1968. Figure 1-1 presents significant checkout and test history dates.

The S-IVB ignited successfully and boosted the payload into an elliptical orbit. The S-IVB experienced four significant anomalies during flight.

a. Cold helium leakage

b. Propellant utilization LOX probe malfunction

c. Failure of the hydraulic system to achieve system pressure for restart

d. Failure of the J-2 engine to restart.

These anomalies and related investigations are summarized in section 2 of this report. Detail analyses of system performance and anomalies are evaluated in respective sections of this report.

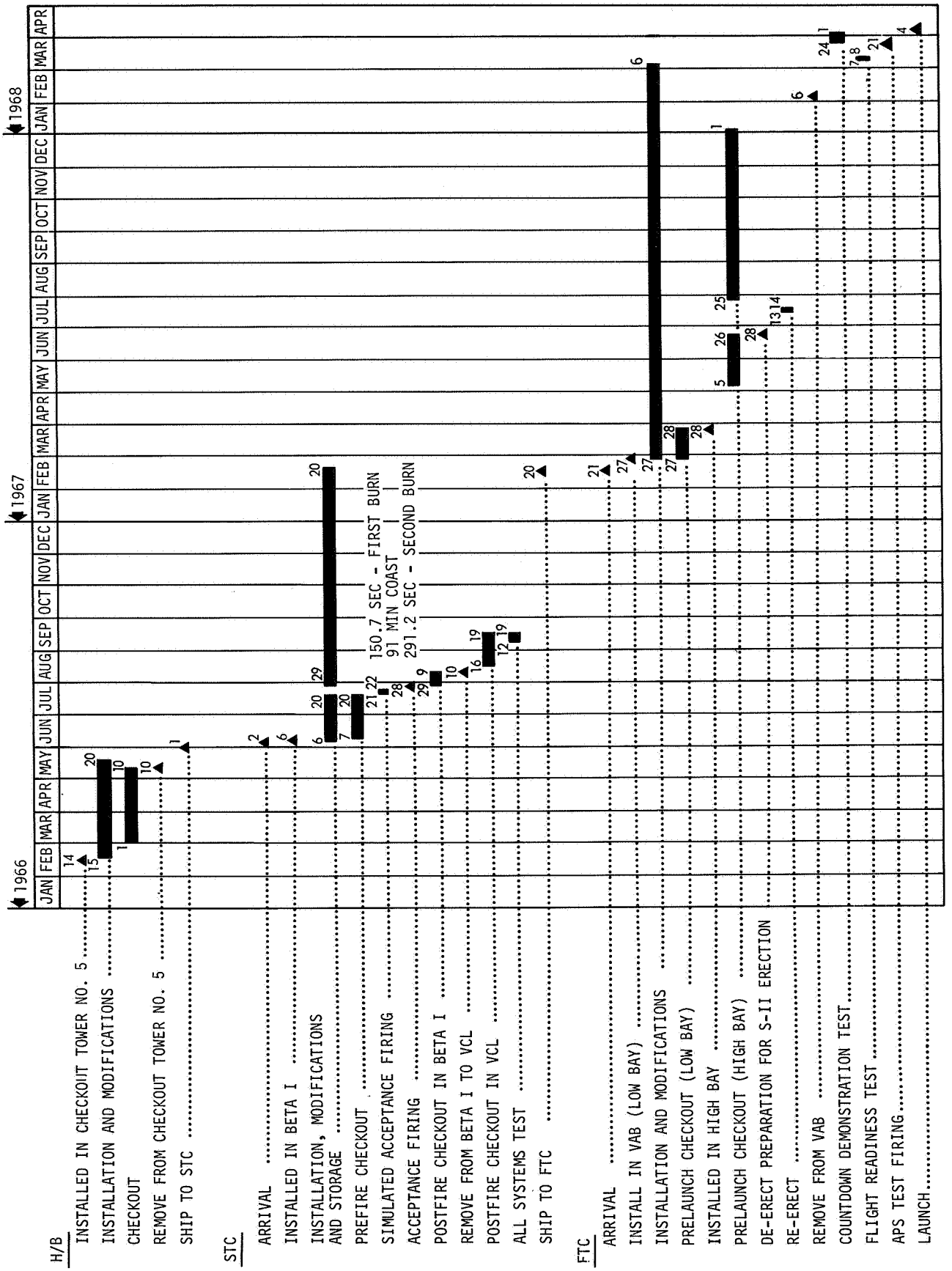

Figure 1-1. S-IVB-502 Stage Checkout and Test History

SECTION 2

FLIGHT DESCRIPTION

2. FLIGHT DESCRIPTION

2.1 Mission

The S-IVB-502 stage was the third stage of the Apollo-Saturn AS-502 Launch Vehicle which served as booster for the Apollo 6 Mission. AS-502 was the second research and development flight of the Saturn V launch vehicle. The payload consisted of a Lunar Test Article (LTA) and an unmanned Command and Service Module (CSM). It was planned that the launch vehicle would place the S-IVB/IU/LTA/CSM combination into approximately a 100 nmi circular parking orbit. During the second orbital pass over Kennedy Space Center (KSC), the S-IVB was to be reignited to inject the combination into a simulated translunar trajectory. After second burn engine cutoff, the CSM was to separate from the S-IVB/IU/LTA, perform a retrograde burn, and the command module was to re-enter and impact in the Pacific.

2.2 Countdown and Launch

After successful completion of the countdown demonstration test (CDDT) and recycle operations, the AS-502 launch countdown was initiated at 05:30:00 GMT on 3 April 1968. At initiation of the final countdown, all stage items with limited lifetimes had more than adequate life cycles remaining for the ancitipated mission. The countdown was successfully completed with no major problems when the vehicle lifted from KSC Launch Complex 39A on 4 April 1968 at 12:00:01.69 GMT.

2.3 S-IC Powered Flight

2.3.1 Sequence of Significant Occurrences

GRR	R0 -16.845 sec
R0 (Nearest even second prior to first motion)	12:00:01 GMT
IU umbilical disconnect (TB1)	R0 +0.69 sec
Mach 1	R0 +60.5 sec
Max q	R0 +75.2 sec
Peak Oscillations	R0 +133 sec
IECO (TB2)	R0 +144.949 sec
OECO (TB3)	R0 +148.405 sec

2.3.2 Vehicle Observations and Effects

The AS-502 vehicle lifted off with a launch azimuth of 90 deg, and following tower clearance, the vehicle executed a tilt and roll maneuver to achieve the desired 72 deg flight azimuth. The vehicle passed through mach 1 and maximum dynamic pressure without any apparent problem. Longitudinal oscillations (POGO) during S-IC boost after maximum q were approximately three times more severe than those experienced on the AS-501 flight. The severity of POGO oscillations resulted from all five engine thrust variations being inphase. At approximately R0 +133 sec, significant perturbations occurred in a number of vehicle measurements. There

is photographic evidence of material separating from the spacecraft lunar module adapter (SLA) panels at this time (figure 2-1). The affected SLA section is located just above the lunar module attach plane. Additional information on this incident is presented in a NASA/MSC report entitled, Anomaly Report No. 6 - Unexpected Structural Indications During Launch Phase, unpublished as of this wiring.

S-IC inboard and outboard engine sequence shutdowns were normal.

2.3.3 S-IVB Observations and Effects

2.3.3.1 POGO

During S-IC boost, the effects of POGO oscillations appeared in the S-IVB LH2 and LOX chilldown systems which exhibited flowrate and pressure oscillations. The effects were also noticed on the S-IVB aft bus No. 2 current, which reflects load changes due to the operation of the chilldown inverters and the auxiliary hydraulic pump. A 5.2 to 5.6 cps oscillation was detected by all of the S-IVB dynamic strain measurements on the forward skirt (S0086 through S0101), by two vibration measurements (E0091, Forward Field Splice, and E0092, Aft Separation Plane), by the forward skirt pitch and yaw body bending accelerometers (E0099 and E0100) and by the aft skirt pitch and yaw accelerometers (E0101 and E0102). The dynamic strain responses were generally inphase indicating that the vibration mode was primarily in the thrust axis. The longitudinal oscillations also appeared to be coupled with the body bending modes.

2.3.3.2 Unusual Indications at Approximately RO +133 Sec

Starting at approximately RO +123 sec, the aft bus No. 2 current (M0022), which supplies the chilldown inverters and auxiliary pump, started to increase from a nominal 76 amps to 80 amps at RO +128 sec. It remained at 80 amps until RO +133 sec and then rose to 84 amps. By RO +135 sec, it decreased to a nominal 76 amps.

S-IVB dynamic strain measurements, static strain measurements, pressure transducers, accelerometer measurements, and microphones responded to a sharp transient encountered at approximately RO +133 sec. Two forward skirt vibration measurements registered a $\pm$17 g response and the forward skirt static and dynamic strains made step changes in magnitude. These occurrences were accompanied by a decrease in indicated S-IVB/IU/SLA static pressure from 0.2 psi to zero psi. Also, the S-IVB pitch actuator pressure measurements registered a differential pressure spike of approximately 400 psid at RO +133 sec.

Available S-IVB data was analyzed to determine, if possible, the probable source of disturbances experienced by the launch vehicle at RO +133 sec. The analysis has eliminated the following possible sources of disturbance and verified that the observed perterbations did not originate on the S-IVB:

a. The strain changes were not thermally induced since:

   (1) The changes were too rapid to be from thermal effects.

   (2) Ten temperature transducers in the forward skirt did not reveal any sudden or drastic changes in skirt temperatures.

b. The strain changes were not inertially induced since vehicle accelerometer recordings were normal at RO +133 sec.

c. The strain changes were not induced by sudden changes in gross mass or by sudden changes in engine thrust as indicated by the continuity and constant slope of the plotted curve from accelerometer readings.

d. The strain changes were not induced by sudden changes in body bending moments since:

(1) The airloads were negligible at RO +133 sec.

(2) There was negligible engine gimbaling recorded at RO +133 sec.

(3) Body bending would be transient from engine gimbaling whereas the strain disturbances were substantially steady-state from RO +133 sec to center engine cutoff.

e. The strain changes were not induced by faulty strain gage system electronics since:

(1) The data were carefully reviewed by electronic specialists with respect to steady voltages, shorts, gage debonding, wiring identifications, data transmission, data reduction, etc., and the data were evaluated as being valid.

(2) The pattern of strain changes at RO +133 sec was not the type expected of faulty electronics which would produce off-scale or zero readings or would result in all similarly wired gages shifting in the same direction by the same amount.

f. The S-IVB forward skirt did not fail and cause the strain changes observed at RO +133 sec since:

(1) The strain gages continued to respond in a normal manner throughout the remainder of powered flight.

(2) The applied flight loads and temperatures did not exceed design loads and design temperatures.

(3) A detailed stress analysis using measured total strains in the forward skirt stringers indicated a minimum margin of safety of 97 percent.

For more detail information concerning S-IVB measurement responses and associated analyses during the S-IC boost phase, refer to sections 18, 19, 23, 25, and 26 of this report.

2.4 S-II Powered Flight

2.4.1 Sequence of Significant Occurrences

S-II Engine Start Command	RO +149.77 sec
S-II No. 2 ENG OUT	RO +412.9 sec
S-II No. 3 ENG OUT	RO +414.2 sec
S-II ECO (TB4)	RO +576.327 sec

2.4.2 Vehicle Observations and Effects

During S-II boost, the No. 2 engine indicated abnormal operation which resulted in a launch vehicle digital computer commanded shutdown at RO +412.9 sec. Shutdown sequence for the No. 2 engine inadvertently shutdown the No. 3 engine as well since the engine circuits had been inadvertently crosswired during stage assembly. Flight control elected not to invoke flight mission rule No. 16 which requires direct staging following the shutdown of more than one S-II engine.

Engines No. 2 and No. 3 are adjacent engines located above the vehicle X-Y plane. The disturbing moment resulting from the shutdown of these engines caused the launch vehicle to assume a nose-up pitch attitude resulting in large deviations from the planned trajectory. Also, since iterative guidance mode (IGM) was programmed to operate with no more than one S-II engine out, a freeze of vehicle attitude commands was initiated, causing a nonoptimum flight path for the remainder of S-II flight. At S-II Engine Cutoff Command (ECC) the vehicle was deviating from the planned trajectory by being higher and slower than predicted.

2.5 S-II/S-IVB Separation

The separation transient in the pitch plane was considerably larger than that experienced on previous flights but was within the capabilities of the control system. This large separation transient was attributed to a large pitch attitude error existing at S-II/S-IVB separation as a result of having two engines out on the S-II. For more detailed separation information, refer to section 17 of this report.

During S-II/S-IVB separation, a 0.25 sec pulse was fired by the pitch engine on module 1. Since the APS was in a coast mode prior to initiation of burn mode, the APS pitch-yaw control was active and was attempting to correct for vehicle attitude error. This pulse had no adverse effect on lateral clearance during S-II/S-IVB separation.

At S-IVB Engine Start Command (ESC), the J-2 engine gimbaled from neutral to 6.3 deg in the pitch plane. During J-2 thrust buildup, this pitch angle increased to 6.7 deg. By the time J-2 engine thrust reached 90 percent, the engine was in the process of returning to a neutral position. This thrust vector control system (TVCS) maneuvering, like the auxiliary propulsion system (APS) response which preceded it, was a normal control system response to attitude errors accumulated during S-II boost. Although the S-IVB engine is gimbaled during all static firings, no engine start had been attempted with the engine in an extreme control position. An examination of engine start data did not reveal any start transient problems with the engine gimbaled to a hardover position.

Retrorocket performance during separation was nominal with good phasing of the thrust-time profiles. Retrorocket heating of the S-IVB structure was similar to that observed on AS-501, indicating only small differences in plume impingement. Calorimeters (C2000 and C2004) indicate that the heat flux to the J-2 engine was somewhat higher on AS-502 than on AS-501, but lower than that experienced on uprated Saturn I flights. The heat fluxes were within the maximum expected envelope. Detail aero/thermo information is provided in section 26.

2.6 S-IVB First Burn

2.6.1 Sequence of Significant Events

S-II/S-IVB separation	RO +577.079 sec
S-IVB ESC	RO +577.28 sec
S-IVB ECO (TB5)	RO +747.298 sec

2.6.2 Trajectory

After separation, guidance commanded the S-IVB to assume a pitch-down attitude to correct for trajectory errors accumulated during S-II boost. The nose-down attitude was maintained until RO +645 sec, when the attitude was commanded nose-up. Trajectory simulations indicate that IGM performed as would be expected throughout first burn considering the greatly perturbed conditions at S-II/S-IVB separation.

2.6.3 Abnormal Measurement Occurrences

Between RO +599 and RO +694 sec, the LH2 turbopump vibration measurement (E0210) increased and reached an apparent value greater than the measurement range. By RO +706 sec, the vibration level returned to normal and continued at this level until S-IVB ECO. The RMS composite time history is shown in figure 25-2. Measurement E0210 has been classified as a failure since it is postulated that it was driven over band edge by a frequency outside of its intended response range. The magnitude of the actual vibration remains unknown, but since LH2 turbopump operation was completely normal, the response of this measurement cannot be considered as valid data (see paragraph 2.11.5 and table 18-4).

The corresponding vibration measurement on the LOX turbopump (E0211) was normal throughout first burn. Between RO +685 and RO +694 sec the vibration measurement on the combustion chamber dome (E0209) became erratic and failed. Continuous data was not available for any of the aforementioned vibration measurements because the information was telemetered on time shared channels.

The earliest significant indications of abnormal temperature were detected at approximately RO +635 sec, when the engine area temperature measurement C0010 began to indicate cooling trends. Ten seconds later, temperature pickup C2005 located on the engine main LOX pneumatic line began to cool abnormally.

After RO +645 sec, a number of other measurements also showed unexpected temperature and vibration response patterns. Attempts to correlate measurement patterns with one or more specific system failures have not been entirely successful. It is possible, however, to distinguish general trends which can be explained for the most part by assuming that there was a failure of the augmented spark ignitor (ASI) fuel feedline, which will be discussed in more detail later. General measurement trends are as follows:

Time Period	Characteristics
a. RO +645 to RO +695 sec	Temperature - Net Cooling Trend Vibration E0210 - Increases E0209 - Fails
b. RO +695 to RO +705 sec	Temperature - Net Heating Trend Vibration E0210 - Decreases
c. RO +705 to RO +715 sec	Temperature - Net Cooling Trend Vibration E0210 - Normal

Table 2-1 summarizes the time sequence and temperature rates for the above measurement trends.

2.6.4 J-2 Engine Performance

The J-2 engine made a normal first burn engine start at RO +577.28 sec. Engine operation was normal and satisfactory until RO +682 sec, when performance began to decline. Engine performance stabilized by RO +702 sec after the following estimated performance degradation:

Thrust	6,200 lbf
Specific impulse	9.5 sec

From RO +702 sec to ECC performance remained essentially unchanged at the reduced level.

2.6.5 Source of Anomalous Conditions

Extensive investigation into the unusual occurrences encountered during S-IVB first burn has indicated that these effects resulted from a failure of the ASI fuel feedline (figure 2-2). This conclusion is supported by special testing covered in paragraph 2.11.2. It is not possible to identify, with complete confidence, the failure mechanism or the chronology of the failure, but the following hypothesis is in good agreement with recorded flight data and test results:

> The failure began as a leak in the 1,200 psia ASI fuel feedline, possibly occurring as early as RO +617 sec. The leakage probably occurred at the upper bellows near the engine injector and resulted from fatigue cracks in the convolutions of the innercore produced by flow induced vibrations. LH2 efflux from the line produced a general cooling trend throughout the thrust structure area which was most pronounced between RO +645 and RO +695 sec. The effect of this leakage was a LOX-rich condition in the ASI chamber, which caused ASI chamber temperatures to increase. These increased temperatures could have resulted in damage to the ASI chamber and J-2 injector

head if the temperature increase was great enough and of sufficient duration. The amount of damage actually incurred, if any, could not be determined from the available data. The ASI fuel feedline leakage continued to increase until the line pressure was sufficiently reduced to cause a flow reversal at the ASI fuel inlet. This reversed flow exposed the ASI fuel feedline to hot combustion gases, resulting in a burn-through of the flex portion of the line. The hot combustion gases released by this burn-through produced the heating trend observed between RO +695 and RO +705 sec. After burn-through, the gases escaping from the ASI chamber were a combination of oxygen from the ASI LOX inlet and combustion products from the main chamber. Hydrogen and oxygen from the J-2 injector head may also have been present, depending on the amount of injector damage incurred prior to burn-through of the ASI fuel feedline. LH2 was also escaping from the lower portion of the burned-through ASI fuel feedline. The combination of all of these escaping gases produced a second general cooling trend in evidence after RO +705 sec. Because of the ruptured ASI fuel feedline, main chamber and gas generator (GG) pressures decreased, resulting in the J-2 engine performance shift previously mentioned. It is probable that RO +690 sec represents the approximate time of ASI fuel feedline burn-through. A detailed description of these occurrences including performance calculations, is provided in section 10 of this report.

Investigative analysis has eliminated the LOX ASI supply line as the possible source of anomalies. A summation of the analysis is presented in section 10 of this report. The investigative effort related to the LOX ASI supply line did reveal one case (S-IVB-508) at the Space Systems Center in which the LOX ASI supply line number identification had been etched beyond specification requirements. Corrective action was taken to eliminate the discrepancy and to guard against repetition on future stages.

2.7 S-IVB First and Second Orbits

Two anomalies were observed during orbit prior to the restart attempt.

2.7.1 Cold Helium Leakage

Between S-IVB first burn engine cutoff and the cold helium dump at RO +22,023 sec, a total of 129 lbm of helium usage could not be accounted for. This would calculate to be an average orbital leakage rate of approximately 0.4 lbm/min. As of this writing, the exact probable source of this leakage had not been determined. During the CDDT, a leak was detected at the cold helium vent port. The cold helium vent valve was cycled, and the leakage stopped. The cold helium vent valve on the dump module was not changed. A small leak (approximately 7 scim) was also detected at a conoseal flange in the cold helium

manifold during post-loading leak checks at KSC. This leak was stopped by retorquing the conoseal flange. Extensive mass decay checks, which were conducted after the CDDT with ambient helium at 950 psia, showed no mass decay. A mass decay check was also performed after fuel loading during the launch countdown; no leakage was noted.

Special tests (paragraphs 2.11.6 and 2.11.7) were conducted to determine if conoseal leakage could be induced by subjecting various flange sizes to temperature and vibration environments. While leakage did result in some instances, the evidence could not be considered conclusive.

The testing did reveal a large amount of torque relaxation on bolts and unions exposed to cold helium. Therefore, it will be proposed that on future stages, the torque be checked after every cold cycle of the system.

Teflon coated aluminum 7075 conoseal gaskets used in conjunction with titanium flanges were proved to be less susceptible to leakage than uncoated 6061 gaskets. An engineering change proposal (ECP) has been written to change all gaskets to teflon coated 7075.

In order to preclude transducer variations induced by severe thermal environments, an ECP has been written to relocate the transducer to a less severe environment for future flights.

2.7.2 PU Probe Problems

The LOX mass bridge operated normally during S-IVB-502 first burn. At approximately RO +10,800 sec (800 sec prior to restart), the LOX mass bridge indicated that the probe was completely filled with propellant. The PU electronics assembly (EA) calibration for S-IVB-502 would allow the coarse mass indication to read approximately 4.5 vdc and the fine mass indication to indicate approximately 2.2 vdc.

At RO +10,610 and RO +10,635 sec into flight, the LOX bridge in the PU EA began to slew at the maximum rate toward the full stop. The bridge recovered each time within 1 sec and operation returned to normal. At RO +10,660 sec, the LOX bridge again slewed at maximum rate to the full stop indicating an over-full indication. The LOX bridge remained in this position until data dropout which occurred at RO +10,880 sec. The next available data beginning at RO +10,960 sec shows the bridge had recovered at some period during data dropout. At RO +10,967 sec into flight, the LOX bridge again slewed at the maximum rate indicating an over-full condition. The bridge recovered within 3 sec and operation returned to normal. At RO +11,066, RO +11,072, RO +11,087, and RO +11,090 sec, the fine mass again indicated an anomaly by starting to slew towards the full stop at the maximum rate. Each of these malfunctions were of less than 1 sec duration. At RO +11,091 sec, the bridge again slewed at the maximum rate and this time reached the full mechanical stop of the output potentiometer. The bridge did not recover from this position for the remainder of the S-IVB flight.

There appear to be two possible causes for the PU system anomaly noted during the S-IVB-502 flight. These causes are:

a. An intermittent open cable shield between the mass probe and the PU electronics assembly.

b. Metallic particle(s) of some type in the LOX tank which caused a short between the inner and outer elements of the PU probe.

PU system operation was normal during first burn and the first appearance of the bridge anomaly occurred during orbiting conditions. Particle(s) in the tank during orbital conditions could be distributed anywhere in the tank and possibly lodge between the probe elements. As the PU system operation was normal during powered flight while the LOX mass probe and its associated cable and PU electronics assembly were under the highest vibration levels experienced during flight, the possibility of an intermittent open cable shield appears to be remote. Therefore, the most probable cause of the PU system anomaly was metallic particle(s) in the LOX tank shorting the inner and outer element of the LOX probe. A complete description of the PU probe malfunction is included in section 16 of this report.

2.8 S-IVB Attempted Restart

2.8.1 Sequence of Significant Events

Initiate restart preparations (TB6)	R0 +11,287.733 sec
S-IVB ESC	R0 +11,614.686 sec
S-IVB ECO (TB7)	R0 +11,630.328 sec
Initiate spacecraft separation	R0 +11,666.1 sec

2.8.2 Restart Attempt

With satisfactory restart conditions a start command signal was given at R0 +11,614 sec. The GG reached 250 psia and the main chamber pressure 40 psia. Spark plug operation was normal, but because of the ASI fuel feedline failure during first burn, the ASI chamber was unable to provide main chamber ignition. Absence of ignition in the main chamber was verified by lack of heat indications in the jacket and increased fuel injector temperature (C0200). Without ignition, there was no back pressure on the flow systems and the GG was unable to stabilize resulting in a GG overtemperature condition. At R0 +11,630 sec the IU was unable to sense mainstage pressures and initiated spacecraft separation.

2.8.3 Hydraulic System

When the auxiliary hydraulic pump was activated at approximately R0 +10,960 sec, it failed to build up system pressure. Aft bus No. 2 current drain for the pump was approximately 12.5 amps indicating that the pump was cavitating. At ESC2, the LOX turbine began to spin up and the engine driven (ED) pump reached approximately 45 percent of operating rpm. There was insufficient fluid pumped to increase system pressure or cause significant actuator movement, indicating that the ED pump was also cavitating. From an analysis of the data, it was determined that a blockage existed in the hydraulic fluid line between the accumulator reservoir assembly on the thrust cone structure and the ED pump inlet. The connecting line runs across the gimbal plane on position III. The blockage apparently resulted from frozen hydraulic fluid in the system. Based on an analysis of flight data and special test results (special testing is summarized in paragraph 2.11.9), it is considered very probable that LH2 which escaped from the ruptured ASI fuel feedline during first burn, caused the hydraulic system to freeze shortly after the auxiliary hydraulic pump was turned off. The system was still frozen when the S-IVB restart was attempted.

Details of the hydraulic system performance are presented in section 22 of this report.

2.8.4 Vibration Occurrence

The vibration measurement on the LH2 turbopump (E0210) indicated a vibration response starting at RO +11,623 sec. At RO +11,624 sec the signal level increased and exceeded band edge. After RO +11,625 sec, the measurement remained offscale high. For a more detailed description of the measurement failure see section 18.

2.9 Launch Vehicle/Spacecraft Separation

The launch vehicle spacecraft (LV/SC) separation was programmed to occur at TB7 +180 sec; however, due to failure of the S-IVB to restart, a ground command was issued to initiate LV/SC separation at TB7 +35.8 sec (RO +11,666.1 sec). The first detectable disturbances resulting from the LV/SC separation occurred at RO +11,667.85 sec, the time at which the separation ordnance was ignited. Telemetry data from both the CSM and S-IVB IU indicated unexpected disturbances were applied to both vehicles during the separation interval. From evaluation of the observed data, it was concluded that SLA panel 1 on position I failed to deploy properly during LV/SC separation possibly due to damage incurred during boost flight (incident occuring at RO +133 sec). Due to the failure of the SLA panel to deploy properly, a momentary interference or hang up with the spacecraft occurred which temporarily affected the motion of the launch vehicle as well as the spacecraft. However, the spacecraft separated successfully and the launch vehicle recovered from the momentary attitude deviation. See paragraph 21.2.5.5 for detailed separation information.

2.10 Post Separation

Following LV/SC separation, the auxiliary hydraulic pump was commanded ON two more times by ground command. Each time the hydraulic system failed to build up pressure and the current drain was 12.5 amps indicating that the pump was still cavitating.

S-IVB attitude control was maintained until approximately RO +22,053 sec when APS module 1 was depleted of propellant. Propellant depletion in module II occurred at approximately RO +22,630 sec. These depletions occurred earlier than normal because of the greater system demands resulting from high angular rates existing at S-IVB first and second engine cutoffs, and large propellant masses remaining after second engine cutoff. Nevertheless, attitude control was maintained beyond the required time period as is discussed in paragraph 7.1.

Details of APS performance and flight control are presented in sections 14 and 21, respectively.

Five days after the launch, photographs were obtained of the S-IVB/IU/SLA in orbit. Although photographic resolution was poor, the adapter panels appeared to be properly deployed, and the assembly appeared to be intact. Tracking data have shown that the S-IVB/IU/SLA remained intact until 9 days after the launch when the vehicle separated into about 15 pieces. At that time, the estimated loads, resulting from S-IVB angular rotation, exceeded the minimum strength of the attach strap fittings and the LTA support struts. Most of the pieces, including the adapter panels, entered the atmosphere within 4 days after the 13 April breakup. The S-IVB entered on 26 April 1968. The LTA is expected to remain in orbit until approximately August 1968.

2.11 Special Testing

A number of special tests were conducted to investigate the anomalies encountered in flight. The results of this testing are summarized below:

2.11.1 Low Pressure Transducer Vibration Test - Douglas/Santa Monica

Pressure transducer D0051, located in the S-IVB forward skirt (internal), registered a static pressure decrease from approximately 0.2 to 0 psi at approximately RO +133 sec. Because of the small pressure values involved, it was suspected that the transducer might have responded to vibration rather than pressure. To investigate this possibility, a similar transducer was subjected to various vibration and pressure environments. Test results were as follows:

a. The maximum response time required to release the transducer mechanical static friction pressure buildup was 70 ms. The maximum response time for a sudden pressure drop from 0.2 to 0 psia was 180 ms. The flight data were recorded every 250 ms. Therefore, it was possible for either a pressure drop or a static friction drop to occur during the flight since both drops occurred in less than 250 ms during the tests.

b. Preflight and pretest calibrations on the flight and test transducers compared to test calibrations of the test transducers showed that age can increase the static friction buildup percentage. Based on test data and the latter fact, it was possible for the flight transducer to build up an indicated static friction pressure of 0.2 psi or greater.

It must be concluded that the tests were inconclusive since a response to either a static friction release or an actual pressure drop of 0.2 psi could have occurred in less than 250 ms.

2.11.2 Testing to Investigate J-2 Engine ASI Fuel Feedline Failures - Rocketdyne/ Santa Susanna

A number of tests were conducted by Rocketdyne to investigate possible failure methods for the ASI fuel feedline. In one test, a leak in the ASI line was simulated by permitting fuel to flow from a tee junction, near the bellows back to the facility. After 10 sec of simulated leakage, fuel flow to the ASI line was terminated, which resulted in a burn-through of the ASI line and an engine performance shift. The amount of performance shift was less than occurred during the S-IVB-502 flight. In another test, fuel flow to the ASI chamber was restricted for approximately 20 sec after which the ASI LH2 flow was terminated completely and a burn-through of the ASI fuel feed line was simulated by opening a tee junction near the ASI chamber. Fire was observed to sepw from the vicinity of the ASI chamber from the time the flow was reversed until termination of the engine test. Post-test inspection revealed considerable erosion of the ASI chamber, J-2 injector head, and gimbal block. Both the LOX and LH2 portions of the J-2 injector were eroded. The associated degradation in J-2 engine performance was somewhat comparable to that observed during the S-IVB-502 flight; however, ASI LH2 was not permitted to dump overboard as must have occurred during actual flight.

It was not possible in any of this testing to exactly simulate flight conditions; however, the testing did demonstrate that flow reversed at the ASI fuel inlet, and subsequent burn-through of the ASI fuel feedline could be produced by leakage in the ASI fuel feedline.

It was also demonstrated that leakage in the ASI fuel feedline could result in damage to the ASI chamber and J-2 injector head.

2.11.3 Testing to Investigate Possible ASI LOX Feedline Failure - Rocketdyne/Santa Susanna

A special test was also conducted to simulate failure of the LOX ASI feedline. The ASI oxidizer supply valve was closed and a line failure was simulated by opening a tee between the orifice and the ASI. Simultaneously, a tee valve was opened between the main oxidizer valve and the ASI to simulate leakage. When line failure was simulated, hydrogen backflowed through the ASI and an explosion occurred. Cause of the explosion has not been determined, and the test results are considered inconclusive.

2.11.4 Investigation of Flexible Metal Hose and Bellows Critical Resonant Conditions - Douglas/Santa Monica

Various worse case J-2 component metal flex hose and bellows are to be subjected to various flowrates to determine critical resonant conditions and to establish additional confidence in present system application. Testing was begun on 14 May 1968 and is in progress as of this writing.

2.11.5 Vibration Test of LH2 Turbopump Accelerometer, and Cable Assembly - Douglas/Santa Monica and Huntington Beach

The instrumentation cable for the LH2 turbopump lateral accelerometer measurement (E0210) passed through a clip on the ASI fuel feedline and then entered a bundle of wires also containing the instrumentation cable for the J-2 dome accelerometer measurements (E0209) on the S-IVB. This arrangement can be seen in figure 2-2. The nature of this physical arrangement and the anomalous behavior reported in paragraph 2.6.3 led to speculation that E0210 and E0209 may have responded to vibrations of the ASI fuel feedline or to sudden changes in the temperature environment rather than to actual vibrations in the LH2 turbopump and J-2 engine. To investigate this possibility, an accelerometer and cable system identical to that used for E0210 was vibrated at levels simulating the S-IVB-502 flight environment while being subjected to the following environmental conditions:

a. Ambient temperature.

b. Non-turbulent LN2 spray on accelerometer and cable.

c. Turbulent LN2 on accelerometer and cable.

d. Pouring LN2 on accelerometer and cable.

e. Heated cable to 2,400 deg F.

f. Heated cable to 600 deg F.

The output of the flight type transducer system was monitored during this testing. The testing was unable to simulate or reproduce the anomalous conditions experienced in flight on E0210. The failure of E0209 was simulated by shorting out the cable.

Additional testing of the transducer system was conducted including the 245 multiplexer, single sideband (SSB) and ground support demultiplexer equipment. The system response was recorded on magnetic tape which was used to generate power spectral density (PSD) plots. These plots were compared to those constructed from flight data. Overdriving by high frequency random signal (4,000 Hz to 12,000 Hz) did not duplicate characteristics observed on the flight data. Severe overdriving of the amplifier using low frequency random signal (20 to 2,000 Hz) resulted in distortion of the SSB wave shape. PSD plots of this response exhibited very similar characteristics to those obtained from the flight data. Summarizing, severe overdriving of the amplifier by high levels of low frequency random signal simulated the flight data recovered from S-IVB-502.

2.11.6 S-IVB-505N Special Cold Helium Leak Test - Douglas/Sacramento

Special cold helium leak tests were conducted at Sacramento Test Center (STC), Beta Test Stand I, utilizing S-IVB-505N. The test objectives were to obtain confidence in the cold helium system in support of S-IVB-503N launch activities, and to investigate possible leak sources with respect to cold helium leakage experienced during the S-IVB-502 flight. Examination of overall test results revealed that cold helium leakage was quite small and no information was obtained that would explain the abnormal loss of cold helium during the S-IVB-502 flight. The testing did reveal that bolts and unions exposed to cold helium are subject to a significant amount of torque relaxation.

2.11.7 Conoseal Flange and Gasket Vibration and Low Temperature Testing - Douglas/Santa Monica

Conoseal flanges and gaskets were subjected to vibration and low temperature environments to gain data related to S-IVB-502 cold helium leakage. Similar to the testing at STC, a significant amount of torque relaxation was experienced with cold helium components.

Teflon coated aluminum 7075 gaskets used in conjunction with titanium flanges were found to be less susceptible to leakage than uncoated 6061 gaskets.

2.11.8 PU Connector Assembly Temperature and Pull Test - Douglas/Santa Monica

There were three different types of electrical connectors used on the S-IVB-502 between the PU probe and the PU computer. To investigate the PU system anomaly, the three types of connectors were subjected to constant pull forces of 1, 2, 4 and 8 lbf under the following environmental conditions:

Deutsch Connectors

a. High temperature soak at 160 deg F for 2 hr.

b. Low temperature soak at -310 deg F for 3 hr.

Bendix Connectors

a. High temperature soak at 160 deg F for 2 hr.

b. Low temperature soak at 30 deg F for 1 hr.

The tests were conducted on 32 samples at a time, and continuity was monitored continuously on two 16 channel oscillographs. Upon completion of the low temperature soak, the connectors were subjected to a pull test to destruction. Half of the connectors were pulled at low temperature and half were pulled at room temperature. Results of the test showed that several samples indicated intermittencies and discontinuities during various phases of the test. The cause of the intermittencies and discontinuities is unknown. However, it was observed that all the properly assembled connectors exhibited no discontinuities at any time.

Additional tests were also conducted on 36 samples of Deutsch connectors similar to the aforementioned tests, but with the addition of a flame test. For the flame test, the connectors were heated with an acetylene torch to an estimated 2,500 deg F temperature. No anomalies were revealed during this additional testing at any time, and the samples did not indicate any loss of continuity during the flame test.

2.11.9 Special Hydraulic Testing - Douglas/Santa Monica

A special test was conducted at Santa Monica to determine susceptibility of the hydraulic system to freezing when exposed to cryogenics. Test results indicated that the system will not freeze under conditions of fluid flow, but will become frozen approximately 85 sec after termination of flow when subjected to liquid nitrogen. With the return line frozen, the auxiliary pump current measured 12.5 amps similar to the current level experienced in flight.

2.12 Conclusions

Perturbations experienced by the launch vehicle during S-IC boost at about RO +133 sec did not originate on the S-IVB. Although POGO oscillations during S-IC boost were more severe than expected, there is no known connection between these occurrences and S-IVB anomalies experienced later in flight.

S-II/S-IVB separation was successfully completed without collision. Control system response was normal for conditions which existed at the time of separation.

Four S-IVB anomalies were experienced in flight:

a. J-2 engine performance degradation during first burn and failure of the engine to restart.

b. Cold helium leakage.

c. PU LOX probe malfunction.

d. Failure of the hydraulic system to develop pressure during the attempted restart.

Failure of the S-IVB to restart during the second revolution as well as the J-2 engine performance shift and the unusual measurement occurrences during first burn are attributed to a failure of the ASI fuel feedline. It should be emphasized that if a failure of the

ASI fuel feedline should reoccur on some future mission, there is no assurance that the first burn would be successfully completed. Premature shutdown of the S-II No. 2 engine was attributed by North American Rockwell Corporation to a failure of the No. 2 engine ASI fuel feedline, but there is no known connection between the S-II and S-IVB engine failures. Every effort must be made to preclude a repetition of ASI fuel feedline failures. There was no evidence during the S-IVB flight of malfunction in the LOX ASI feedline, but in view of the nature of the ASI fuel feedline problems, additional investigation and testing of both ASI feedlines is necessary to insure a high degree of confidence in this system for future missions. This effort is in progress at Rocketdyne.

Source of the reported cold helium leakage remains unknown, but the investigation did reveal the necessity of torque checks after every cold cycle of the system. Relocation of the pressure transducers to a less severe environment should eliminate any instrumentation problems which might have resulted from severe temperature environment. Additionally, all conoseal gaskets in the system will be changed to teflon coated 7075 aluminum.

The most probable cause of the PU system anomaly was metallic particles in the LOX tank shorting the inner and outer element of the LOX probe. A method is being investigated to guard against this type of electrical short and to minimize the possibility of metallic particles in the system for future stages.

The S-IVB hydraulic anomaly resulted from cryogenic leakage associated with the ASI fuel feedline failure during first burn. The following hardware changes were considered with the realization that cryogenic leaks can occur during future flights:

a. Insulate lines to protect them from hot or cold fluid impingement.

b. Multiple thermal switches to initiate flow and protect from cold condition.

c. Redundant path fluid lines.

The contractor's position is that redesign of the hydraulic system, in an attempt to preclude freezing from leaking cryogenic fluids is impractical because there is no definition of the extent of the leak or how long it would persist.

The solution is to redesign the ASI fuel feedline (which has been done) to guard against the possibility of any future leaks.

2.13 Mission Objectives

Douglas considers the SA-502 Launch Vehicle Mission Directive prepared by the Saturn V Test Office, Marshall Space Flight Center, Huntsville, Alabama, dated April 26, 1966, as the official document for providing identification and control of launch vehicle mission requirements. Eleven of the 16 primary objectives and both of the secondary objectives, as defined in the mission directive, directly involve the S-IVB. The AS-502 mission objectives are summarized and discussed in table 2-2.

TABLE 2-1 (Sheet 1 of 2)
MEASUREMENT RESPONSE TRENDS

MEASUREMENT GROUP		MEASUREMENT	TREND AS-502	RATE DEG F/SEC	
				AS-502	AS-501
A					
645 to 695 sec net cooling	C0010	Eng area temp	Cooling	-0.80	0
	C0050	ED hyd pump oil inlet	Heating	+0.05	+0.13
	C0087	Thrust struct - position I	Cooling	-0.35	+0.05
	C0088	Thrust struct - position I-IV	Cooling	-0.20	-0.10
	C0152	LOX main supply line flange wall	Cooling	-0.65	-0.07
	C0153	LOX main support line	-	0	+0.05
	C0154	LOX prevalve bypass wall	-	0	+0.03
	C0203	Pitch act oil temp	Cooling	-0.05	0
	C0204	Yaw act oil temp	Cooling	-0.05	0
	C0275	Gas, interstage area	Cooling	-2.36	-0.08
	C2005	Eng main pneumatic line	Cooling	-6.40	+0.20
	C2013	LH2 turbine manifold ext wall	Less heating	+1.75	+2.50
	C2014	LH2 turbine collector ext wall	Heating	+5.50	0
	C2037	GG LOX boot strap	Cooling	-0.46	0
	E0209	J-2 dome vibration	Fails		
	E0210	LH2 turbopump vibration	Increase and becomes clipped		
B					
695 to 705 sec net heating	C0010	Eng area temp	Heating	+30.7	0
	C0050	ED hyd pump oil inlet	-	0	+0.30
	C0087	Thrust struct - position I	Heating	+2.50	+0.05
	C0088	Thrust struct - position I-IV	Heating	+0.50	0
	C0152	LOX main supply line flange wall	Off-scale high	Failed	-0.005
	C0153	LOX main support line	Heating	+0.78	+0.05
	C0154	LOX prevalve bypass wall	Heating	+0.22	+0.03
	C0203	Pitch act oil temp	Cooling	-0.05	0
	C0204	Yaw act oil temp	Cooling	-0.10	0
	C0275	Gas, interstage area	Heating	+25.6	-0.08
	C2005	Eng main pneumatic line	Cooling	-7.10	0
	C2013	LH2 turbine manifold ext wall	Less heating	+1.00	+3.50
	C2014	LH2 turbine collector ext wall	Heating	+4.00	0
	C2037	GG LOX boot strap	Heating	+16.70	0
	E0210	LH2 turbopump vibration	Decreases to normal		

TABLE 2-1 (Sheet 2 of 2)
MEASUREMENT RESPONSE TRENDS

MEASUREMENT GROUP		MEASUREMENT	TREND AS-502	RATE DEG F/SEC	
				AS-502	AS-501
C					
705 to 715 sec net cooling	C0010	Eng area temp	Off-scale low	Failed	0
	C0050	ED hyd pump oil inlet	Heating	+2.90	+0.30
	C0087	Thrust struct - position I	Cooling	-1.80	+0.05
	C0088	Thrust struct - position I-IV	Cooling	-0.25	0
	C0152	LOX main supply line flange wall	Off-scale high	Failed	-0.005
	C0153	LOX main support line	Heating	+0.41	+0.05
	C0154	LOX prevalve bypass wall	Cooling	-0.10	+0.03
	C0203	Pitch act oil temp	Cooling	-0.10	0
	C0204	Yaw act oil temp	Cooling	-0.40	0
	C0275	Gas, interstage area	Cooling	-5.00	-0.08
	C2005	Eng main pneumatic line	Cooling	-5.00	0
	C2013	LH2 turbine manifold ext wall	Less heating	+1.00	+2.00
	C2014	LH2 turbine collector ext wall	Heating	+3.00	0
	C2037	GG LOX boot strap	Cooling	-0.21	0
	E0210	LH2 turbopump vibration	Normal		

TABLE 2-2
MISSION OBJECTIVES SUMMARY

PRIMARY OBJECTIVES	S-IVB MISSION ACCOMPLISHMENT
1. Demonstrate the S-IVB restart capability.	Objective not achieved. The J-2 engine failed to restart (sections 2 and 10).
2. Demonstrate the adequacy of the S-IVB CVS while in earth orbit.	Objective achieved.
3. Demonstrate the capability of the S-IVB auxiliary propulsion system during S-IVB powered flight and orbital coast periods to maintain attitude control and perform required maneuvers.	Objective achieved.
4. Demonstrate the S-IVB propulsion system including the propellant management systems, and determine inflight system performance parameters.	Objective partially achieved. The propulsion system suffered performance degradation during first burn and failed to restart. The LOX PU probe malfunctioned in the second orbit prior to restart (sections 2, 10, & 16). Inflight system performance parameters were evaluated.
5. Demonstrate S-II/S-IVB separation.	Objective achieved.
6. Demonstrate structural and thermal integrity of launch vehicle throughout powered and coasting flight, and determine inflight structural loads and dynamic characteristics.	Objective achieved.
7. Determine inflight launch vehicle internal environment.	Objective achieved.
8. Demonstrate the launch vehicle guidance and control system during S-IVB powered flight, achieve guidance cutoff and evaluate system accuracy.	Objective partially achieved. The main and auxiliary hydraulic pumps cavitated during the attempted restart. If restart had occurred, the thrust vector control system may have been inoperative.
9. Demonstrate launch vehicle sequencing	Objective achieved.
10. Evaluate performance of the emergency detection system in a closed-loop configuration.	Objective achieved.
11. Demonstrate compatibility of the launch vehicle and spacecraft.	Objective achieved.
SECONDARY OBJECTIVES	**MISSION ACCOMPLISHMENT**
1. Determine launch vehicle powered flight external environment.	Objective achieved.
2. Determine attenuation effects of exhaust flames on RF radiating and receiving systems during main engine, retrorocket and ullage rocket firings.	Objective achieved.

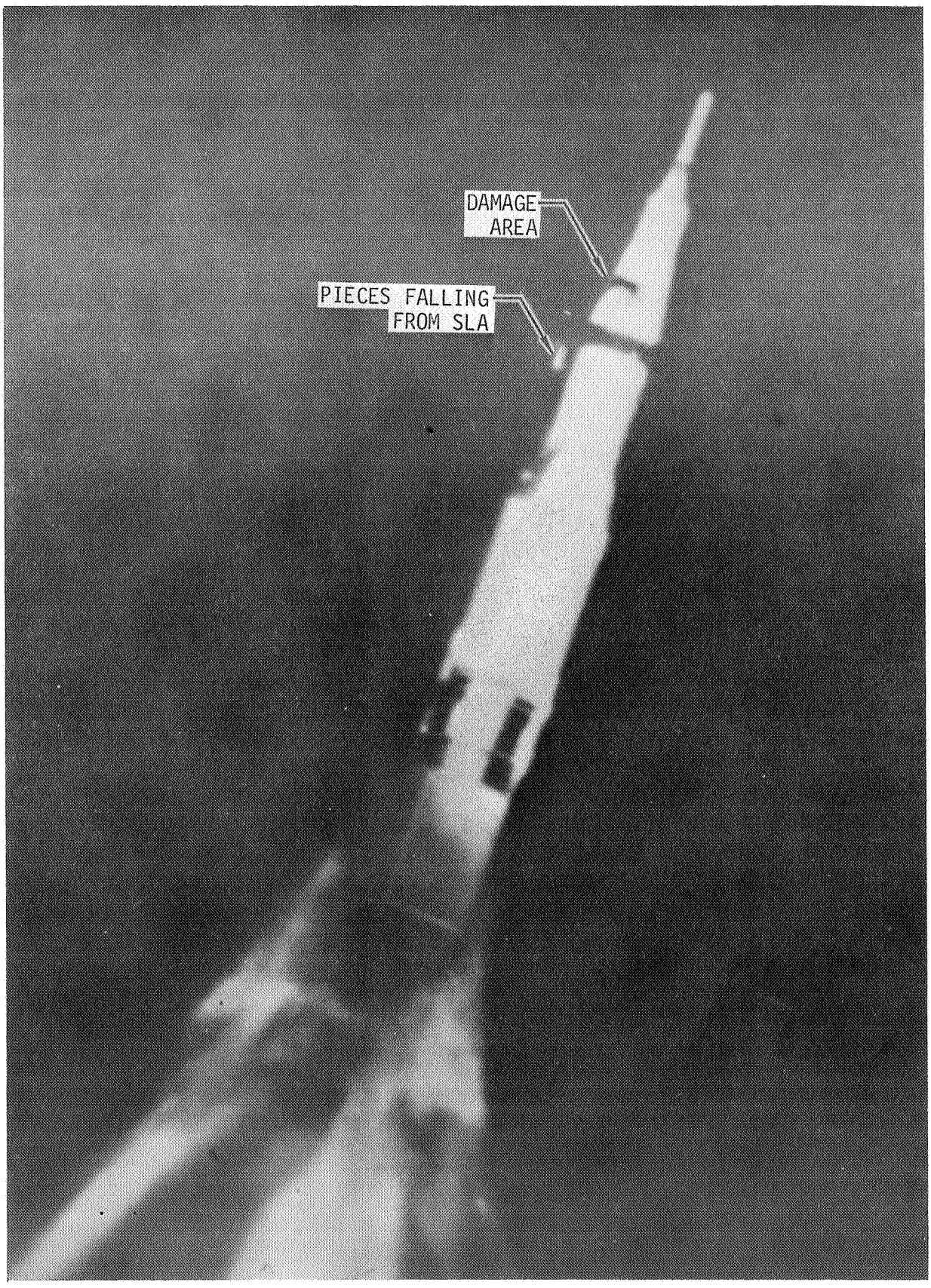

Figure 2-1. AS-502 Launch Vehicle at RO +133.54 Sec

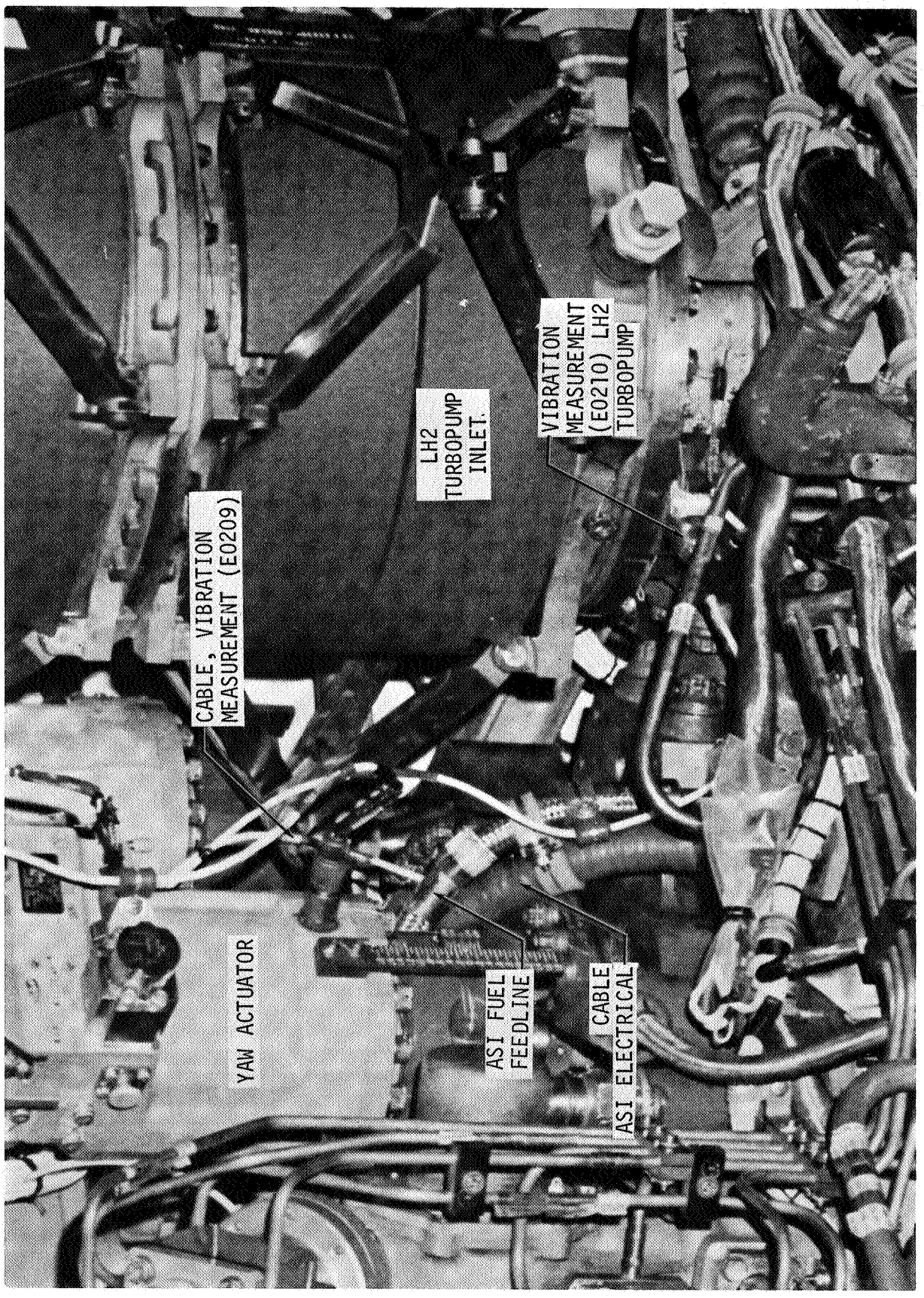

Figure 2-2. S-IVB-502 ASI Fuel Feedline

SECTION 3

SUMMARY

3. SUMMARY

The AS-502 was launched from Kennedy Space Center (KSC), Complex 39A, at 12:00:01.69 GMT on 4 April 1968. Performance of the Douglas built S-IVB stage was satisfactory during countdown and boost, although a slight degradation in J-2 engine performance occurred during first burn. Subsequent analysis disclosed that the performance degradation was caused by a failure of the J-2 engine augmented spark ignitor (ASI) fuel feedline. The S-IVB first burn time was extended because of two premature engine shutdowns on the Saturn V second stage booster. The orbit achieved deviated from that predicted by approximately +94 nmi at apogee and -6 nmi at perigee because of trajectory deviations accumulated during second stage boost. During orbital coast there was evidence of cold helium leakage, and the LOX propellant utilization (PU) probe malfunctioned, indicating off-scale high. Although conditions for restart were completely satisfactory, the earlier ASI fuel feedline failure precluded main chamber ignition. During the attempted restart, the hydraulic system failed to build system pressure or to accomplish significant actuator movement because of frozen hydraulic fluid blocking the system. Freezing of the hydraulic fluid has been attributed to the ASI fuel feedline failure during first burn.

3.1 Countdown Operations

No significant S-IVB or equipment problems occurred during the launch countdown activity, and Douglas ground support equipment (GSE) sustained no significant damage during liftoff.

3.2 Cost Plus Incentive Fee

The incentive evaluation of the AS-502 flight performance includes flight mission accomplishment and telemetry performance. Performance of the S-IC and S-II stages provided preconditions of flight (PCF) at S-II/S-IVB Separation Command that were outside of allowable tolerances. Due to failure to achieve restart of the S-IVB stage, end conditions of flight (ECF) at translunar orbit injection were not attained. Pitch attitude error and rate exceeded allowable tolerance early in S-IVB first burn. It was concluded for incentive purposes: PCF were outside of allowable tolerances; S-IVB flight was prematurely terminated because of J-2 engine failure (not the fault of Douglas); acceptable ECF would have been achieved if proper PCF had existed and the J-2 engine had functioned properly. The telemetry system operated at 98.3 percent efficiency during the telemetry performance evaluation period (TPEP) phase I and 97.6 percent efficiency during TPEP phase II.

3.3 Trajectory

The AS-502 trajectory deviated greatly from predicted, due to anomalies experienced during the boost to parking orbit. As a result of a rupture of the fuel ASI line at approximately RO +690 sec, the S-IVB engine failed to reignite, and second burn was not achieved.

Until approximately RO +413 sec the trajectory of the AS-502 was close to predicted. At this time the shutdown of two S-II engines began. Since the iterative guidance mode (IGM) was programmed to operate with no more than one S-II engine out, a non-optimum trajectory

resulted for the remainder of S-II flight, causing trajectory conditions at S-II/S-IVB separation to deviate greatly from predicted. These off-nominal conditions at separation were responsible for an overspeed at S-IVB engine cutoff, where the velocity was 160.2 ft/sec greater than the target velocity. S-IVB burntime was 30.8 sec longer than predicted because of the non-optimum S-II burn.

The AS-502 parking orbit was elliptical, with an apogee altitude of 194.4 nmi and a perigee altitude of 93.5 nmi. The longer period of the elliptical orbit caused restart preparations to occur 214 sec later than predicted. Second burn was not achieved.

3.4 Mass Characteristics

The S-IVB-502 stage flight mass characteristics that appear in section 9 and appendix 1 of this document are best estimate mass characteristics for the first burn and computed from available data for restart attempt. The total vehicle mass at first burn Engine Start Command was 354,232 $\pm$476 lbm and 265,234 $\pm$400 lbm at first burn Engine Cutoff Command.

3.5 Engine System

The J-2 engine did not meet all objectives during the AS-502 mission. The augmented spark ignitor fuel feedline failed during first burn and resulted in engine performance degradation and subjected the thrust structure to environmental changes. Because of the failure, fuel was prevented from reaching the ignitor for restart and the environmental changes prevented the hydraulic system from functioning properly.

3.6 Solid Rockets

The solid rocket motors on the S-II and S-IVB stages performed satisfactorily and accomplished their intended purpose. The S-II was separated from the S-IVB by the retrorockets, and the S-IVB propellants were settled prior to engine ignition by the ullage rockets.

3.7 Oxidizer System

The oxidizer system performed adequately, supplying LOX to the engine pump inlet within the specified operating limits throughout J-2 engine operation. The available NPSP at the LOX pump inlet exceeded the engine manufacturer's minimum requirement at all times. Ambient helium repressurization of the LOX tank was satisfactorily accomplished. Because of leakage, the cold helium sphere pressure decreased 518 psi between first burn engine cutoff and second burn Engine Start Command, but the supply would have been adequate for normal second burn operations.

3.8 Fuel System

The fuel system supplied LH2 to the engine as designed, and the NPSP exceeded the engine manufacturer's minimum requirement at all times. The LH2 tank was satisfactorily repressurized by a normal ambient helium repressurization cycle. Because of ullage pressure collapse, a second cycle was required shortly before second burn Engine Start Command.

3.9 Auxiliary Propulsion System

The auxiliary propulsion system (APS) fulfilled the attitude control, maneuvering, and ullaging requirements of the mission until APS propellant depletion. The APS propellant usage was greater than predicted as a result of booster problems encountered during the mission. All flight objectives were accomplished, and both modules performed satisfactorily except that the pitch engine chamber pressure of both modules was low at various times during the mission.

3.10 Pneumatic Control and Purge System

The pneumatic control and purge system performed satisfactorily throughout the flight. The helium supply was adequate to meet all mission requirements and to accomplish all purges; the orbital leakage rate was near zero. The only deviation was late initiation of the engine pump purge, but this was not a fault of the pneumatic system components and did not detrimentally affect the mission.

3.11 Propellant Utilization

The propellant utilization system successfully accomplished the requirements associated with propellant loading and first burn propellant management. Prior to the restart attempt a malfunction was experienced by the LOX mass measurement system and would probably have resulted in improper PU system operation had second burn operation been achieved.

The loading system performed loading of the S-IVB to 100.07 and 99.88 percent of desired load for LOX and LH2 respectively. The required stage loading inacurracy is $\pm$1.39 percent.

First burn PU system operation was entirely nominal with the PU valve at the LOX rich (full closed) stop. Proper operation of the PU electronics slosh filter was exhibited by a non-response of the PU system valve to first burn propellant slosh.

3.12 S-II/S-IVB Separation Dynamics

The S-II/S-IVB separation was accomplished satisfactorily within the desired time period. Separation was initiated at RO +577.079 sec; it was completed 0.99 sec later.

The S-II and S-IVB angular velocities and lateral accelerations utilized 6.7 in. of the available 83 in. of lateral clearance. The engine gimbal position at the time of separation utilized an additional 12 in. The S-II rates were all approximately 0 deg/sec at firt motion. A combination of engines two and three being out on the S-II stage and a possible retrorocket misalignment caused the pitch and yaw rates to increase to 2 deg/sec and 0.95 deg/sec by separation complete. The S-II roll rate remained approximately zero throughout separation. The S-IVB rates were all small with pitch and yaw rates remaining below 0.2 deg/sec and the roll rate remaining below 0.5 deg/sec.

3.13 Data Acquisition System

Data acquisition system performance during the mission was excellent, and is summarized as follows:

Measurements assigned	616
Measurements monitored by S-II	4
Measurements inoperative due to stage configuration	1
Checkout measurements	11
Measurements deleted prior to flight	9
Measurements prevented from being transmitted	
Phase I	0
Phase II	3
Measurements active for flight	
Phase I	591
Phase II	588
Phase I measurement failures	10
Phase I measurement efficiency	98.3%
Phase II measurement failures	14
Phase II measurement efficiency	97.6%

The RF system blackout period during S-IC/S-II separation was not evaluated because the airborne tape recorder playback data were not recovered. Data loss was observed at RO +149.23 for 0.83 sec. Flame attenuation was not observed during S-II/S-IVB separation.

Tape recorder performance was satisfactory. It recorded all analog data on fast record, PCM data on slow record, and played it back on command.

3.14 Electrical System

The electrical control system, with the exception of the PU system and the electrical power system, performed satisfactorily. All responses to switch selector commands were satisfactory with 17 nonprogrammed commands initiated to command the S-IVB from the Carnarvon, Hawaii, and Guaymas ground stations. All event measurements verified that the engine control system had responded properly to the Engine Start Command and Engine Cutoff Commands given for first burn and for the restart attempt. All telemetry event measurements of engine performance occurred in the proper sequential order. The APS electrical control system performed within prescribed limitations. All batteries performed within expected limits. The chill-down inverters performed satisfactorily for first burn and for the restart attempt. Both 5 v excitation modules performed satisfactorily. The static inverter/converter operated within design limits with the exception of the 5 vdc output. The out-of-tolerance performance did not affect operation of the PU control system.

3.15 Range Safety System

The range safety system was not required for propellant dispersion during the flight. All indications were that the system was operating properly and would have properly executed its function had it been called upon to do so.

3.16 Flight Control

The thrust vector control system (TVCS) responded satisfactorily to instrument unit command signals providing pitch and yaw control during S-IVB first burn. The separation transient in the pitch plane was considerably larger than that experienced on previous flights but was within the capabilities of the control system. This large separation transient was attributed to a larger pitch attitude error existing at S-II/S-IVB separation. The TVCS responded normally during this interval and provided adequate control following S-II/S-IVB separation.

The auxiliary attitude control system (AACS) provided satisfactory roll stabilization during powered flight and satisfactory pitch, yaw, and roll control during orbit. During S-II/S-IVB separation, a 0.3 sec pitch AACS firing (engine I_p) occurred commencing with the S-II/S-IVB Separation Command and terminating with the S-IVB Burn Mode ON Command. The design characteristics of the flight control computer resulted in a temporary transfer to the S-IVB coast mode between the S-II/S-IVB Separation Command and the S-IVB Burn Mode ON Command. The noted temporary S-IVB coast mode and subsequent pitch AACS firing although undesirable was not detrimental. This occurrence is normal for a Saturn V vehicle and may happen on any or all missions.

All orbital maneuvers were accomplished as planned, and vehicle attitude control was verified until approximately RO +22,040 sec (Hawaii - fourth revolution) at which time the yaw angular rate began diverging to approximately -7.5 deg/sec followed by an oscillatory vehicle motion. AACS propellant depletion and a LOX vent occurring near this time accounted for the diverging angular rate. Depletion of AACS propellants and subsequent loss of attitude control at this time is much earlier than expected for a nominal mission, however, this is reasonable when considering the relatively large and unexpected demands on the attitude control system, particularly following first burn engine cutoff and following the attempted restart and launch vehicle/spacecraft (LV/SC) separation.

3.17 Hydraulic System

The S-IVB hydraulic system performance was satisfactory from liftoff to the end of first burn, although some system temperature data were abnormal during first burn. The temperature abnormalities resulted from a failure of the augmented spark igniter (ASI) fuel feedline as discussed in sections 2, 10, and 26. The pitch actuator experienced a large excursion during S-II/S-IVB separation, which was a normal system response to guidance commands.

When the auxiliary hydraulic pump was activated in preparation for second burn, it failed to build system pressure and current drain was approximately 12.5 amps indicating that the pump was cavitating. The engine driven pump also cavitated and failed to build system pressure or cause significant actuator movement. Data analysis has indicated that the system failure resulted from frozen hydraulic fluid in the system. Apparently the ASI fuel feedline rupture during first burn released cryogenics which caused the hydraulic system to become frozen shortly after the auxiliary pump was turned off. The system was

still frozen when the restart was attempted. Following launch vehicle/spacecraft separation, the auxiliary pump was commanded on two more times and each time the system failed to build pressure and current drain was 12.5 amps indicating that the pump was still cavitating.

3.18 Stage Structure and Environment

Strain, acceleration, pressure, and temperature data indicated that adequate structural strength existed in the stage for the conditions encountered. During S-IC stage boost at RO +133 sec, the S-IVB experienced an unusual load redistribution in the forward skirt as indicated by strain gage measurements at skirt stringers. This load redistribution was evident throughout the remainder of the high axial loads of first stage boost to CECO (Center Engine Cutoff) at RO +144 sec. The combined loads from the load redistribution and from unusually severe 5 1/2 cps longitudinal (POGO) vibrations were within the structural capability of the forward skirt. The load distribution to the aft skirt was normal but included the 5 1/2 cps longitudinal (POGO) vibrations. The anomaly experienced by the forward skirt at RO +133 sec is attributed to sudden changes in structure located above the forward skirt, and the character and causes of these structural changes are being reported in a special report by NASA, referenced in paragraph 23.1.

S-IVB body bending moments and skin differential pressures were less than the maximum predicted values due to moderate winds. Vehicle axial accelerations were close to predicted values except for the structurally noncritical anomaly of two S-II engines cutting out prematurely at about RO +414 sec. Axial loads were in agreement with computed loads from liftoff to approximately RO +60 sec. Beyond this time, the axial load values computed from stringer strain gage data appear to be low apparently because of aerodynamic heating and because of a partial integration resulting from the limited number of instrumented stringers. Flight temperatures did not exceed maximum predicted temperatures. Propellant tank pressures did not exceed design pressures, and differential pressures on the common bulkhead were as expected. Common bulkhead internal pressure remained substantially constant at less than 1 psia as predicted.

3.19 Environmental Stage Systems

The stage environmental control systems functioned satisfactorily throughout the preflight and flight periods.

3.20 Acoustic and Vibration Environment

The acoustic and vibration amplitudes were generally similar to those measured on the AS-501 flight. The dynamic strain levels were higher than those measured on the AS-204 flight; however, there were no indications of panel flutter.

The POGO amplitudes were higher than those measured on the AS-501 flight. There were no adverse effects on the S-IVB due to POGO.

3.21 Aero/Thermodynamic Environment

The aero/thermodynamic evaluation of the S-IVB-502 stage indicated that the aerodynamic heating environment was as expected, propellant heating was nominal, and the APS and the

forward and aft skirt mounted electrical components were within their thermal limits. The boost phase pressure environment was nominal except for an apparent pressure drop in the forward compartment which occurred 133 sec after liftoff. A test was performed on pressure transducers identical to that flown to determine if the noted pressure drop was real or a mechanical friction release in the instrument. The test was inconclusive due to flight data limitations. In support of the J-2 engine restart problem, the thermal environment was defined in the thrust structure engine area covering the time period from the J-2 first burn engine start through the restart attempt.

SECTION 4

TEST CONFIGURATION

4. TEST CONFIGURATION

The general configuration and those stage and ground support equipment (GSE) modifications and deviations that were necessitated by parts shortages or other exigencies are briefly described in this section. The details of specific system modifications are discussed in the appropriate sections of this report.

Figure 4-1 is a schematic of the S-IVB-502 propulsion system and shows the locations of the telemetry instrumentation from which the test data were obtained. Figure 4-1 also lists the functional components except those in the APS system, which are shown on the APS schematic. Figure 4-2 shows the locations of the major propulsion components. Tables 4-1 and 4-2 present the propulsion system orifice characteristics and pressure switch settings. The propulsion GSE is shown in figure 4-3.

4.1 General Configuration

The general configuration of the S-IVB-502 is described in Douglas Report No. SM-46999, S-IVB-502 Stage Flight Test Plan, dated 23 October 1967. This stage was equipped with a Rocketdyne 200,000 lb-thrust engine, serial number (S/N) J-2042; additional stage information is presented in the following documents:

a. Douglas Report SM-47378B, Saturn S-IVB-502 Stage Acceptance Firing Test Plan, dated April 1966, revised 5 August 1966

b. Douglas drawing 1B63789B, S-IVB-502 Stage End Item Test Plan, dated 22 July 1966

c. Douglas Report DAC-56353, Narrative End Item Report on Saturn S-IVB-502 (DAC S/N 1006), dated September 1966

d. Douglas Report No. SM-47184, Saturn S-IVB/IB Range Safety Report, dated 19 November 1965, revised 28 February 1966.

4.2 Stage and Hardware Modifications

The significant modifications that were accomplished on the S-IVB-502 at the Florida Test Center are briefly described in table 4-3. The GSE modifications are described in table 4-4.

TABLE 4-1 (Sheet 1 of 2)
S-IVB-502 AND GSE FLIGHT ORIFICES

FIND NO.*	DESCRIPTION	ORIFICE SIZE OR NOMINAL FLOWRATE	COEFFICIENT OF DISCHARGE	EFFECTIVE AREA (in.^{2})
	S-IVB-502 Stage			
12	LH2 chilldown valve purge	14 scfm with 3,200 psid	--	Sintered
16	Continuous vent bypass valve bellows purge	300 scim with 3,200 psid	--	Sintered
17	Continuous vent bypass valve switch cavity purge	15 scim with 3,200 psid	--	Sintered
19	Continuous vent No. 1	1.090 in. dia	--	0.92
20	Continuous vent No. 2	1.090 in. dia	--	0.92
21	Continuous vent purge	1 scfm with 3,200 psid	--	Sintered
23	LH2 fill and drain valve purge	15 scim with 3,200 psid	--	Sintered
29	LOX fill and drain valve purge	15 scim with 3,200 psid	--	Sintered
39	LOX tank pressurization module, heat exchanger primary	0.196	0.89	0.0268
40	LOX tank pressurization module, heat exchanger bypass	0.166	0.89	0.0192
44	LH2 tank pressurization module (Overcontrol - second burn)	0.2055 in. dia**	0.85	0.1008***
45	LH2 tank pressurization module (Undercontrol)	0.330 in. dia	0.85	0.0726***
46	LH2 tank pressurization module control (Overcontrol - first burn)	0.2054 in. dia**	0.85	0.1008***
47	LH2 tank repressurization module outlet	0.3124 in. dia	0.86	0.0665
48	LH2 tank nonpropulsive vent purge	1 scfm with 3,200 psid	--	Sintered
49	LH2 tank nonpropulsive vent No. 1	2.180 in. dia	--	--
50	LH2 tank nonpropulsive vent No. 2	2.180 in. dia	--	--
61	LOX chilldown pump purge	37 scim with 490 psid	--	--
61A	LOX chilldown pump purge bypass	10 scim with 475 psid	--	Sintered
73A	LOX sensing line purge	1,728 scim with 3,200 psid	--	Sintered
91	LOX tank vent and relief valve	65 scfm with 3,200 psid	--	Sintered
119	LOX tank ambient repressurization	0.036	--	0.00864
120A	Engine purge control module	0.0180 in. dia	--	--
	Pneumatic Console 432A			
A12119	Stage 1 regulator dome vent	0.018 in. dia	--	--
A12120	Stage 1 regulator 3,100 psig dome loading	0.018 in. dia	--	--
A11852	APS helium supply and purge	0.027 in. dia	--	--
A11841	Console 432A GN2 inerting supply	0.031 in. dia	--	--
A11779	Mainstage OK pressure switch checkout, coarse (used with A12054)	0.025 in. dia	--	--

*Indicates location in figures 4-1 and 4-3.

**Indicates diameter of overcontrol orifice or step orifice only.

***Discharge coefficient and effective area are calculated for overcontrol or step orifices in combination with the undercontrol orifice.

TABLE 4-1 (Sheet 2 of 2)
S-IVB-502 AND GSE FLIGHT ORIFICES

FIND NO.*	DESCRIPTION	ORIFICE SIZE OR NOMINAL FLOWRATE	COEFFICIENT OF DISCHARGE	EFFECTIVE AREA ($in.^2$)
A12054	Mainstage OK pressure switch checkout, fine	0.025 in. dia	--	--
A11824	LH2 system checkout supply, fine	0.016 in. dia	--	--
A11820	LH2 system checkout supply, coarse (used with A11824)	0.016 in. dia	--	--
A11837	LOX system checkout supply, fine	0.016 in. dia	--	--
A11836	LOX system checkout supply, coarse (used with A11837)	0.016 in. dia	--	--
A11748	Console 432A stage 1 bleed	--	--	Variable
A12113	Stage 4 regulator vent	--	--	Variable
A11793	Pressure switch checkout, low pressure, fine	0.025 in. dia	--	--
A11792	Pressure switch checkout, low pressure, coarse (used with A11793)	0.025 in. dia	--	--
A12078	Stage 2 regulator vent	--	--	Variable
	Pneumatic Console 433A			
A11886	2,000 psig cold purge purge valve supply	--	--	Variable
A11897	750 psig cold purge valve supply	--	--	Variable
A11937	Thrust chamber jacket purge and chilldown supply	0.072 in. dia	--	0.00347
A11946	Engine control helium sphere supply	0.125 in. dia	--	--
A11954	LOX tank prepressurization supply (located in model 315 aft umbilical kit)	0.0114 in. dia	--	--
A11954	Cold helium sphere pressurization supply (same orifice as above)	0.0114 in. dia	--	--
A11912	LOX umbilical purge supply	0.305 in. dia	--	--
A11908	Umbilical purge supply vent	--	--	Variable
A12143	Stage 3 regulator inlet	0.018 in. dia	--	--
A12152	Stage 3 regulator outlet bleed	0.0022 lbm/min	--	Sintered
	Heat Exchanger 438A			
A12106	Circuit No. 1 upstream vent (primary)	0.081 in. dia	--	--
A12117	Circuit No. 1 downstream vent (secondary)	0.055 in. dia	--	--
A11971	LH2 tank prepressurization supply	0.113 in. dia	--	0.00853
A12234	GH2 regulator dome bleed	0.0003 lbm/min	--	Sintered

*Indicates location in figures 4-1 and 4-3.

TABLE 4-2
S-IVB-502 PRESSURE SWITCH CHECKOUT DATA

NOMENCLATURE	SPECIFICATION	PICKUP (psia)* CALIPS	DROPOUT (psia)* CALIPS	DEADBAND (psia) CALIPS
LOX tank ullage P/N 1B52624-503 Serial No. 023	Pickup: 41 psia max Dropout: 38 psia min Deadband: 0.5 psi min	40.6	39.3	1.3
LOX chilldown pump purge P/N 1B52624-503 Serial No. 020	Pickup: 41 psia max Dropout: 38 psia min Deadband: 0.5 psi min	40.1	39.2	0.9
LOX tank regulator backup P/N 1B52624-509 Serial No. 021	Pickup: 450-485 psia Dropout: 335-370 psia Deadband: None	460	373	83
Engine pump purge P/N 1B52623-515 Serial No. 012	Pickup: 130 psia max Dropout: 105 psia min Deadband: 5 psia min	122	114	8
Control helium reg backup P/N 1B52624-517 Serial No. 023	Pickup: 585-615 psia Dropout: 465-515 psia Deadband: None	605	499	106
LH2 tank ullage-2nd burn P/N 1B52624-501 Serial No. 008	Pickup: 34 psia max Dropout: 31 psia min Deadband: 0.5 psi min	33.8	32.2	1.8
LH2 tank ullage-1st burn P/N 1B52624-511 Serial No. 010	Pickup: 31 psia max Dropout: 28 psia min Deadband: 0.5 psi min	31.2	29.6	1.6
Mainstage OK No. 1 P/N 308390 Serial No. 25324	Pickup: 50 ±5 psig Dropout = Pickup minus 75 ±25 psig	496	431	65
Mainstage OK No. 2 P/N 308390 Serial No. 25254	Pickup: 500 ±15 psig Dropout = Pickup minus 75 ±25 psig	514	450	64

*These values are the average of three runs.

TABLE 4-3 (Sheet 1 of 2)
S-IVB-502 CONFIGURATION AND HARDWARE MODIFICATIONS

ECP	WRO	DESCRIPTION
J2-470 R1	0223	Redesigned pressure actuated purge control valve and fast shutdown valve, and added filter to inlet ports of both.
J2-542	0538	Replaced main oxidizer valve compensator to ensure operation at low temperature.
J2-567	0223	Replaced start sphere discharge valve.
J2-568	0223	Replaced start sphere and relief valve.
J2-592	0223	Replaced helium high pressure relief valve with one that has more resistance to vibration and additional moisture protection.
J2-594 R3	0223	Redundant instrumentation, critical pressure measurements.
J2-599 R1	0223	Replaced MOV thermal compensator orifice plate.
J2-606 R1	4058	Replaced timer in electrical control assembly (ECA) package.
J2-607	0223	Replaced vent port check valve.
J2-620 R1	0223	Modified oxidizer pump primary seal drain line.
0592 R3	3031	Deleted APS helium fill module.
0622 R3	2901	Replaced 10-amp relay modules with redesigned 1A74218-509 modules.
677 R1	3241	Added a redundant relay for 70-pound ullage engine start.
0951 R3	4100	Elimination of cable clamps on wire harness to the retrorocket pressure transducers.
0953 R1	3132	Added clamps to the ullage rocket jettison system confined detonating fuse (CDF) to take up slack in the CDF.
0958 R1	3918	Added orifice caps to APS module ullage vent ports to prevent excessive decay of APS propellant tank ullage pressure during system venting.
0963 R1	3971	Relocated cable clamp on Rocketdyne augmented spark ignitor (ASI) line support bracket.
0964	3144	Replaced pneumatic control system helium sphere, P/N 1A49990-503, with a P/N 1A49990-505.
0972	4011	Substituded a P/N 1B52623-515 engine pump purge pressure switch for a 1B52623-513 switch.
0973	4018	Corrected mating reference designations of exploding bridge wire (EBW) connectors.
0975	4029	Eliminated cable clamp to provide slack in wire harness to allow proper installation of forward battery 1, unit 2.
0978	4091	Replaced existing fiberglass thermal spacers under panel-mounted actuation control modules in the aft skirt with larger outside diameter spacers.
0979	4093	Installed cover plates over all uncovered connector cutouts located on forward skirt electrical feedthrough in area of main tunnel.
0983	4129	Replaced the LOX chilldown shutoff valve, P/N 1A49965-525, with P/N 1A49965-529-013.
0985	3940	Replaced the first burn flight control pressure switch, P/N 1B52624-1, with P/N 1B52624-511.
0986	3941	Added offset bracket for pressure switch line clamping.
2073 R1	3240	Applied protective coating to the aluminum parts of the hydraulic actuators.
2078 R1	3327	Added a low thermal emissivity shroud between the forward skirt cold plates and the stage structure.
2103	3387	Redesigned LOX tank pressurization lines and installed supports to eliminate unnecessary line connections and thus lighten hardware.
2130 R1	3291	Conducted eddy current test of cold helium bottles that were fabricated with titanium alloys using filler wire to verify filler material was of same composition as vessel parent metal.
2143 R1	3356	Changed printed circuit board connectors in Model 270 multiplexer to correct a connector mismatch.
2170	3368	Modified retrorocket nose fairing bulb seal to prevent water from entering the interstage cavity.
2175	3372	Added a continuous bypass bleed to the LOX chilldown pump container purge line to assure positive pressure in the motor container in event of solenoid failure.

TABLE 4-3 (Sheet 2 of 2)
S-IVB-502 CONFIGURATION AND HARDWARE MODIFICATIONS

ECP	WRO	DESCRIPTION
2180 R2	3519	Replaced LOX relief valve with a redesigned valve with greater poppet shaft strength.
2189 R3	3408	Reworked the LH2 PU probe to supplement the spotwelds holding the outer sleeve and mounting ring together.
2218 R1	3746	Changed the interface bolt holes at S-IVB/V station 2519 to accomodate 3/8-in. bolts.
2224 R3	3711	Added panel flutter instrumentation to the forward skirt.
2235 R1	3510	Replaced, in the 2-amp relay modules used in flight critical applications, the 1B50992 relays that had had thermal cycle tests with high reliability relays P/N 1B66899.
2259	3692	Relocated the engine-driven hydraulic pump discharge temperature measurement and changed number from C0218-401 to C2029-401.
2278 R1	3583	Replaced ambient helium bottles, P/N 1A49990-503, with P/N 1A49990-507 bottles.
2405 R1	3795	Installed temperature transducers externally on the LH2 and LOX chilldown inverter cases.
2425 R1	3756	Installed a teflon overboard line for the J-2 engine LOX pump primary seal cavity drain to accomodate Rocketdyne ECP NA-J2-620 R2.
2454	3776	Replaced the range safety safing plug with one that was rewired to isolate and prevent talkback.
2480 R1	3805	Replaced the APS control relay packages, P/N 1B57731-1, by ones that were redesigned by the vendor to P/N 50M35076-2.
2487	3718	Installed S-II retrorocket motors of a new type to reduce the possibility of burnout.
2572	3873	Added a moisture seal to the tunnel disconnect connector for the LOX PU system.
2583 R2	3893	Modified and added to the existing Korotherm ablative insulation.
2589	3907	Replaced pressure switch, P/N 1B52624-507, with P/N 1B52624-517 after the 507 switch failed with excessive leakage.
2597	3901	Reinforced the main and auxiliary tunnel clips with bonded fiberglass doublers.
2605 R1	3991	Added three temperature sensors to the J-2 engine LOX bootstrap line.
2614 R1	3935	Relocated pressure transducers for D0181-409 and D0182-409 to provide thermal isolation.
2621	3956	Replaced the LOX tank pressurization control module, P/N 1B42290-505, with a module in which the Belleville spring had been installed after August 1967.
2628	3951	Replaced the PU bridge potentiometer with one that had received a shock test.
2630	3954	Removed the orifice from the inlet of the actuation control module.
2633 R1	3962	Replaced orifice, P/N 1B63437-501, in the LH2 tank pressurization system with one of larger size to permit the ambient helium supply pressure to drop below 300 psi in 265 sec.
2634	3961	Replaced the LH2 tank pressurization control module assembly, P/N 1B64443-505, with a calibrated module assembly, P/N 1B66230-505, containing the new sized undercontrol orifice.
2645 R1	3960	Removed the line from the pneumatic power control module regulator backup calip pressure switch calip port and installed a cap on the port.
2646	3969	Replaced the eight fiberglass LH2 tank external temperature sensors with sensors of ceramic construction.
2652	3980	Changed the PU component oven to one that had been fabricated in conformance with MSFC-PROC-158A.
2696	4015	Replaced the LOX tank repressurization system orifice, P/N 1B63437, with a P/N 1B64052-503 orifice.
2706	4008	Replaced the LH2 tank pressurization diffuser tube 1B65512-1 and nylon diffuser 1B65814-1 with a configuration that incorporates the internally baffled, slotted tube design and a 1B65813-1 cylindrical nylon diffuser.
2708	4038	Reduced the forward skirt vent area from 200 sq in. to 150 sq in. by adding doublers to each of the eight vents.

TABLE 4-4
GSE MODIFICATIONS

WRO	ECP	DESCRIPTION
		Model DSV-4B-315, Launch Aft Umbilical Kit
3932	0960 R1	Applied potting compound to plunger switch to prevent moisture from entering the switch housing.
4099	0981	Relocated clamping block to eliminate sideloads on the grounding plug and provide an improved ejection system.
3937	2626	Incorporated an improved balanced umbilical purge system.
3039	0637	Added hazardous gas monitor port bosses to the LH2 and LOX tank fill and drain disconnect assemblies to allow vehicle tank sampling and checkout.
3047	0597	Redesigned the ground half of the propellant fill and drain disconnects to reduce leakage.
3172	2050	Added a check valve in the purge vent port of the anti-debris valve to prevent moisture from entering the valve actuator cavity and thereby causing a failure.
		Model DSV-4B-316, Launcher Forward Umbilical Kit
A41-256	0443	Accomplished modification to accomodate the stage hazardous gas detection system.
3440	2088	Modified the umbilical carrier support legs to prevent inadvertent separation from the vehicle support bracket.
3574	2253	Installed spacers to prevent excessive leakage.
3937	2626	Incorporated an improved balanced umbilical purge system.
		Model DSV-4-303, Common Bulkhead Vacuum Monitor
3919	0966	Modified cabinet by taping and caulking seams to maintain a static pressure of 2 in. of water.
		Model DSV-4B-432A, Pneumatic Console
A41-245	0922	Replaced the 0.68 in. orifice in the ambient helium pressurization line with a union.
3023	0606	Removed the pneumatic plumbing comprising the nitrogen and helium manifold vent system.
3786	2459	Modified cabinet by taping and caulking seams to maintain a static pressure of 2 in. of water.
		Model DSV-4B-433, Pneumatic Console
3967	0970	Added seals to the connection of temperature transducers and the associated pneumatic lines.
		Model DSV-4B-438A, Gas Heat Exchanger
A41-245	0909	Installed a vent line from circuit No. 1 bleed hand valve to the vent line in GH2 control panel assembly.
3107	0933	Modified the LH2 pneumatic shutoff valve to provide for a GN2 purge of the microswitch.
3237	2082	Installed a check valve in the outlet of the LH2 tank pressurization supply vent valve.
3500	2021	Installed a protective cover over the vacuum probe on the heat exchanger inlet shroud.
3786	2459	Modified cabinet by taping and caulking seams as necessary to maintain a static pressure of 2 in. of water.
		Model DSV-4B-472, APS Fuel Installation Kit and Model DSV-4B-473, APS Oxidizer Installation Kit
3920	2611	Replumbed the APS liquid level manometer system to eliminate trapped air, which causes flow restriction in the liquid level indicator.

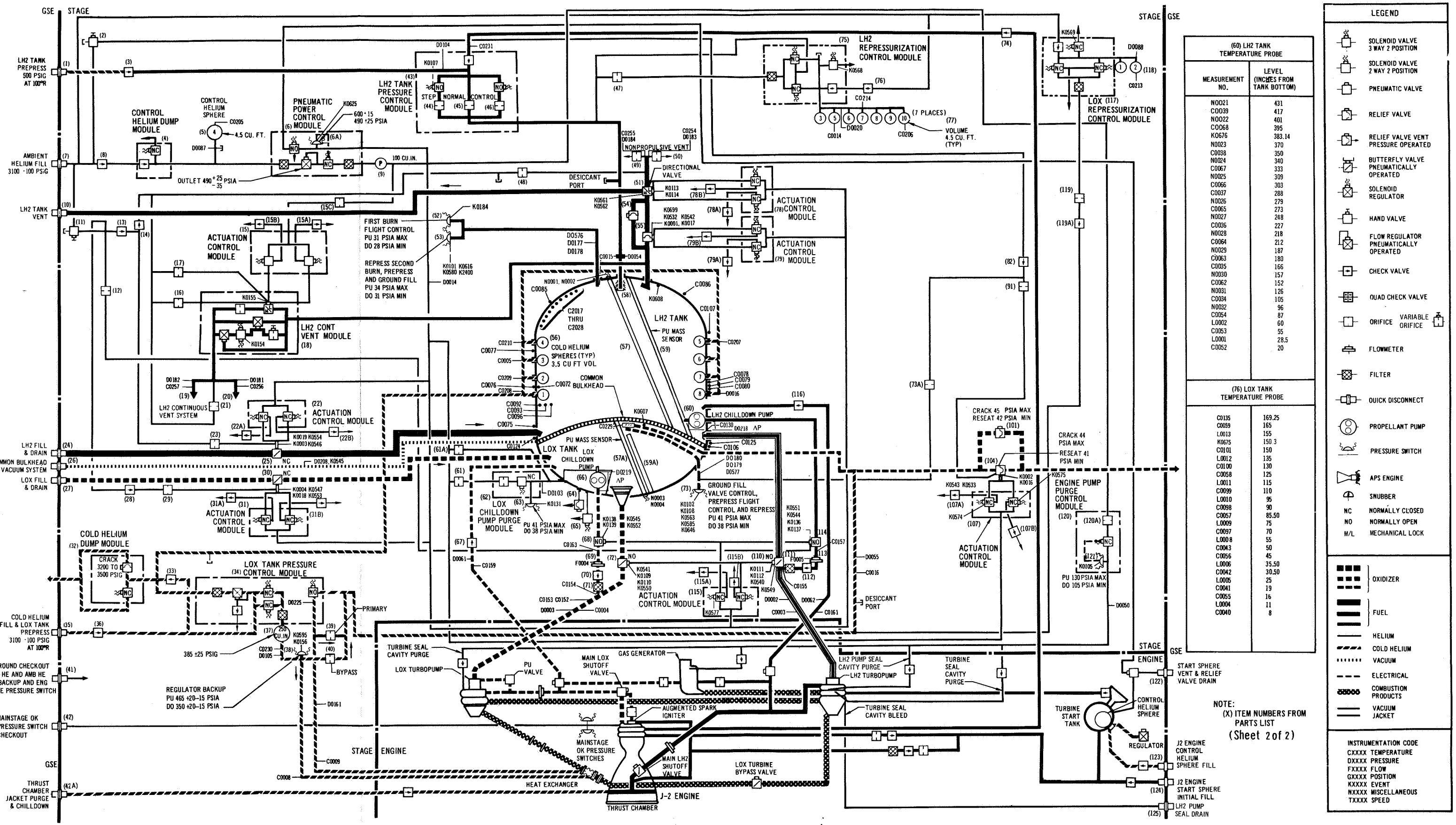

(60) LH2 TANK TEMPERATURE PROBE

MEASUREMENT NO.	LEVEL (INCHES FROM TANK BOTTOM)
N0021	431
C0039	417
N0022	401
C0068	395
K0676	383.14
N0023	370
C0038	350
N0024	340
C0067	333
N0025	309
C0066	303
C0037	288
N0026	279
C0065	273
N0027	248
C0036	227
N0028	218
C0064	212
N0029	187
C0063	180
C0035	166
N0030	157
C0062	152
N0031	126
C0034	105
N0032	96
C0054	87
L0002	60
C0053	55
L0001	28.5
C0052	20

(76) LOX TANK TEMPERATURE PROBE

C0135	169.25
C0059	165
L0013	155
K0676	150.3
C0101	150
L0012	135
C0100	130
C0058	125
L0011	115
C0099	110
L0010	95
C0098	90
C0057	85.50
L0009	75
C0097	70
L0008	55
C0043	50
C0056	45
L0006	35.50
C0042	30.50
L0005	25
C0041	19
C0055	16
L0004	11
C0040	8

LEGEND

- SOLENOID VALVE 3 WAY 2 POSITION
- SOLENOID VALVE 2 WAY 2 POSITION
- PNEUMATIC VALVE
- RELIEF VALVE
- RELIEF VALVE VENT PRESSURE OPERATED
- BUTTERFLY VALVE PNEUMATICALLY OPERATED
- SOLENOID REGULATOR
- HAND VALVE
- FLOW REGULATOR PNEUMATICALLY OPERATED
- CHECK VALVE
- QUAD CHECK VALVE
- ORIFICE / VARIABLE ORIFICE
- FLOWMETER
- FILTER
- QUICK DISCONNECT
- PROPELLANT PUMP
- PRESSURE SWITCH
- APS ENGINE
- SNUBBER
- NC NORMALLY CLOSED
- NO NORMALLY OPEN
- M/L MECHANICAL LOCK

- OXIDIZER
- FUEL
- HELIUM
- COLD HELIUM
- VACUUM
- ELECTRICAL
- COMBUSTION PRODUCTS
- VACUUM JACKET

INSTRUMENTATION CODE
CXXXX TEMPERATURE
DXXXX PRESSURE
FXXXX FLOW
GXXXX POSITION
KXXXX EVENT
NXXXX MISCELLANEOUS
TXXXX SPEED

Figure 4-1. Propulsion System and Instrumentation (Sheet 1 of 2)

FOLDOUT FRAME 1

FOLDOUT FRAME

FOLDOUT FRAME 2

FIND NO.*	PART NO.	NAME
1	7851861-1	Disconnect, LH2 tank prepressurization
2	1B53817-505	Valve hand, LOX vent and relief valve purge
3	1B65673-1	Valve, check, LH2 tank prepressurization line
4	1A57350-507	Module, control helium dump
5	1A49990-503	Sphere, control helium, 4.5 cu ft
6	1A58345-519	Module, pneumatic power control
6A	1B52624-517	Switch, control, helium regulator backup, PU 600 ±15 psia, DO 490 ±25 psia
7	7851823-503	Disconnect, ambient helium fill
8	1B51361-1	Valve, check, control helium fill
9	1A48857-1	Plenum, control helium, 100 cu in.
10	1A48848-505	Disconnect, LH2 ground vent
11	1B53817-505	Valve, hand, LH2 chilldown valve, vent and relief valve, continuous vent, nonpropulsive vent, and fill valves purge
12	1B40622-507	Orifice, LH2 chilldown valve purge
13	1B51361-1	Valve, check, LH2 fill and drain valve, continuous vent system and nonpropulsive vent purge
14	1B51361-1	Valve, check, continuous vent system, and nonpropulsive vent purge
15	1B66692-501	Module, actuation control, continuous vent bypass valve
15A	1B67481-1	Valve, check, continuous vent bypass valve actuation control module vent
15B	1B67481-1	Valve, check, continuous vent bypass valve actuation control module vent
16	1B40622-509	Orifice, continuous vent bypass valve bellows purge
17	1B40622-505	Orifice, continuous vent bypass valve switch cavity purge
18	1B67193-507	Module, continuous vent
19	1B44557-1	Orifice, continuous vent No. 1
20	1B44557-1	Orifice, continuous vent No. 2
21	1B40622-501	Orifice, continuous vent purge
22	1B66692-501	Module, actuation control, LH2 fill and drain valve
22A	1B67481-1	Valve, check, actuation control module vent, LH2 fill and drain valve
22B	1B67481-1	Valve, check, actuation control module vent, LH2 fill and drain valve
23	1B40622-505	Orifice, LH2 fill and drain valve purge
24	1B66932-501	Disconnect, LH2 fill and drain
25	1A48240-505	Valve, LH2 fill and drain
26	1B41065-1	Disconnect, common bulkhead vacuum system
27	1B66932-501	Disconnect, LOX fill and drain
28	1B51361-1	Valve, check, LOX fill and drain valve purge
29	1B40622-505	Orifice, LOX fill and drain valve purge
30	1A48240-505	Valve, LOX fill and drain
31	1B66692-501	Module, actuation control, LOX fill and drain valve
31A	1B67481-1	Valve, check, actuation control module vent, LOX fill and drain valve
31B	1B67481-1	Valve, check, actuation control module vent, LOX fill and drain valve
32	1B57781-503	Module, cold helium dump
32A	1B67481-1	Valve, check, cold helium dump module relief valve vent
33	1B49824-503	Valve, check, cold helium fill
34	1B42290-505	Module, LOX tank pressurization control
34A	1B67481-1	Valve, check LOX tank pressurization regulator vent
35	7851844-501	Disconnect, cold helium fill and LOX tank pressurization
36	1B40824-503	Valve, check, cold helium fill
37	1A49991-1	Plenum, LOX tank pressurization
38	1B52624-509	Switch, pressure, cold helium regulator backup, PU 465 +20, -15 psia, DO 350 +20, -15 psia
39	1B63046-525	Orifice, LOX tank pressurization module, heat exchanger primary
40	1B63047-525	Orifice, LOX tank pressurization module, heat exchanger bypass
41	1A49958-517	Disconnect, ground checkout, cold helium, ambient helium, and engine purge pressure switches
42	1A49958-517	Disconnect, mainstage OK pressure switch checkout
42A	1A49958-519	Disconnect, thrust chamber jacket purge and chilldown
43	1B64443-505	Module, control, LH2 tank pressurization
44	1B64443-505**	Orifice, LH2 tank pressurization control (overcontrol - second burn)
45	1B64443-505**	Orifice, LH2 tank pressurization normal (undercontrol)
46	1B64443-505**	Orifice, LH2 tank pressurization control (overcontrol - first burn)
47	1B63437-507	Orifice, LH2 tank repressurization module outlet
48	1B40622-501	Orifice, LH2 tank nonpropulsive vent purge
49	1A89881-501	Orifice, LH2 nonpropulsive vent No. 1
50	1A89881-501	Orifice, LH2 nonpropulsive vent No. 2
51	1A49988-1	Valve, directional, LH2 tank vent
52	1B52624-1	Switch, pressure, LH2 tank first burn flight control
53	1B52624-513	Switch, pressure, LH2 tank prepressurization, ground fill and repressurization, PU 34 psia max, DO 31 psia min
54	1A49591-523	Valve, relief, LH2 tank, crack 38 psia max, reseat 35 psia min
55	1A48257-511	Valve, LH2 tank vent and relief, crack 37 psia max, reseat 34 psia min
56	1A48858-1	Sphere, cold helium, 3.5 cu ft
57	1A77907-503	Probe, LH2 tank instrumentation
57A	1A48430-507	Probe, LOX mass sensor
58	1B65812-1	Diffuser, LH2 tank pressurization
59	1A48431-501	Probe, LH2 mass sensor
59A	1A69275-503	Probe, LOX instrumentation
60	1A49421-503	Pump, LH2 chilldown
61	1A48854-1	Orifice, LOX chilldown pump purge
61A	1B40622-511	Orifice, LOX chilldown pump purge bypass
62	1A58347-505	Module, LOX chilldown pump purge
63	1B52624-503	Switch, pressure, LOX chilldown pump purge backup, PU 41 psia max, DO 38 psia min
64	1A49423-507***	Valve, relief, LOX chilldown pump purge, crack and reseat 65 to 85 psia (part of dump assembly)
65	1A67913-1	Valve, dump, LOX chilldown pump purge
66	1A49423-507	Pump, LOX chilldown
67	1A49964-501	Valve, check, LOX chilldown return line
68	1A49965-529	Valve, LOX chilldown shutoff
69	1A89104-507	Flowmeter, LOX chilldown
70	1B53920-503	Valve, check, LOX chilldown pump discharge
71	1B52985-501	Filter, LOX chilldown pump discharge
72	1A49968-507	Prevalve, LOX
73	1B52624-503	Switch, pressure, LOX tank prepressurization, ground fill, repressurization and flight control, PU 41 psia max, DO 38 psia min
73A	1B40622-501	Orifice, LOX sensing line purge
74	1B53920-501	Valve, check, GH2 tapoff pressurization line
75	1B56653-513	Module, LH2 repressurization control
76	1B51361-1	Valve, check, LH2 repressurization control module inlet
77	1B49990-503	Sphere, LH2 repressurization, 4.5 cu ft
78	1B66692-501	Module, actuation control, directional valve
78A	1B67481-1	Valve, check, directional valve actuation control module vent
78B	1B67481-1	Valve, check, directional valve actuation control module vent
79	1B66692-501	Module, actuation control, LH2 tank vent and relief valve
79A	1B67481-1	Valve, check, LH2 tank vent and relief valve actuation control module vent
79B	1B67481-1	Valve, check, LH2 tank vent and relief valve actuation control module vent
82	1B51361-1	Valve, check, LOX vent and relief valve and LOX tank sensing line purge
91	1B63206-1	Orifice, LOX tank vent and relief valve purge
101	1A49590-515	Valve, relief, LOX tank, crack at 45 psia max, reseat 41 psia min
104	1A48312-505	Valve, vent and relief, LOX tank, crack 44 psia max, reseat 41 psia min
107	1B66692-501	Module, actuation control, LOX tank vent and relief valve
107A	1B67481-1	Valve, check, LOX tank vent and relief valve actuation control module vent
107B	1B67481-1	Valve, check, LOX tank vent and relief valve actuation control module vent
110	1A49968-509	Prevalve, LH2
111	1B52985-501	Filter, LH2 chilldown pump discharge
112	1B53920-503	Valve, check, LH2 chilldown pump discharge
113	1A89104-509	Flowmeter, LH2 chilldown pump discharge
114	1A49965-523	Valve, shutoff, LH2 chilldown line
115	1B66692-501	Module, actuation control, chilldown valves and prevalves
115A	1B67481-1	Valve, check, chilldown and prevalves actuation control module vent
115B	1B67481-1	Valve, check, chilldown and prevalves actuation control module vent
116	1A49964-501	Valve, check, LH2 chilldown return
117	1B56653-513	Module, control, LOX tank repressurization
118	1A49990-505	Sphere, LOX tank repressurization, 4.5 cu ft
119	1B64052-503	Orifice, LOX tank ambient repressurization module outlet
119A	1B40824-505	Valve, check, LOX repressurization module outlet
120	1A58347-507	Module, engine purge control
120A	1B64598-503	Orifice, engine purge module
121	1B52623-515	Switch, pressure, engine purge module backup, PU 130 psia max, DO 105 psia min
122	1A49958-521	Disconnect, engine start sphere vent and relief valve drain
123	1A49958-515	Disconnect, engine control helium sphere fill
124	1A49958-523	Disconnect, engine start sphere fill
125	1A49958-517	Disconnect, LH2 pump seal drain

*Indicates location in figures 4-1 and 4-2
**Module No.
***Pump Part No.

Figure 4-1. Propulsion System and Instrumentation (Sheet 2 of 2)

FOLDOUT FRAME 1

FOLDOUT FRAME 2

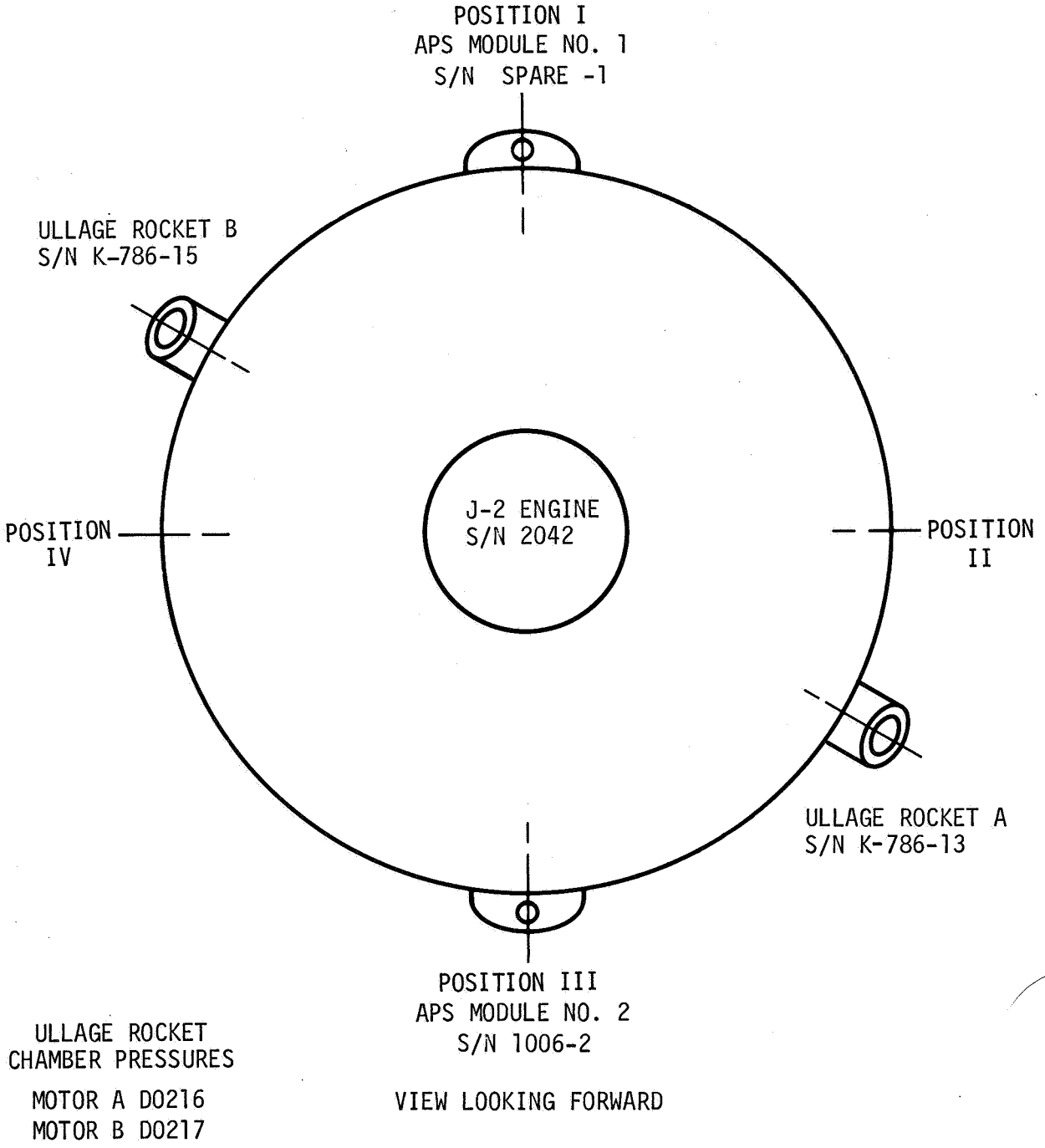

Figure 4-2. Propulsion Major Components Locations

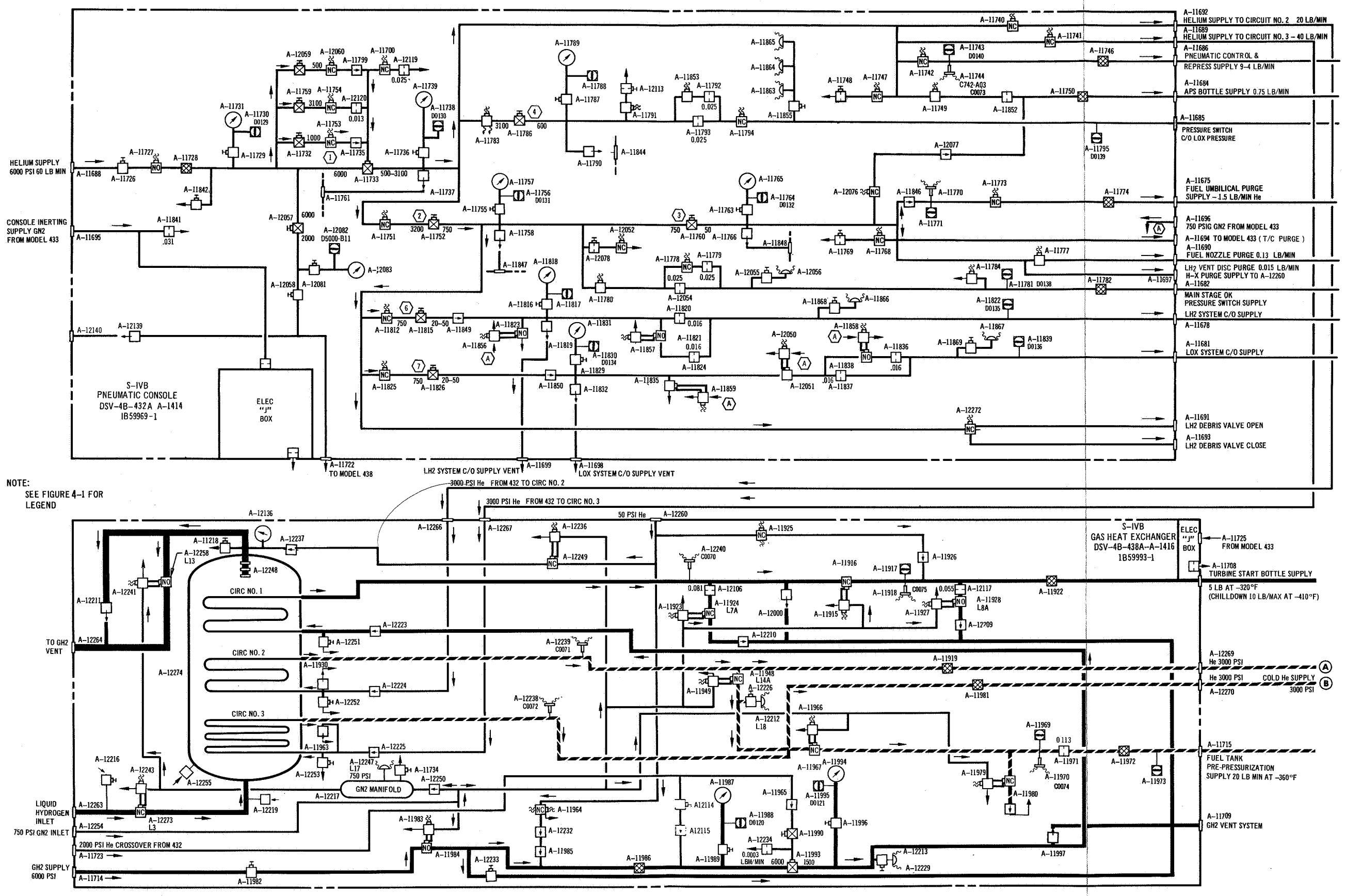
HELIUM SUPPLY
6000 PSI 60 LB MIN
A-11688
CONSOLE INERTING
SUPPLY GN2
FROM MODEL 433
A-11695
A-12140
S-IVB
PNEUMATIC CONSOLE
DSV-4B-432A A-1414
IB59969-1
ELEC
"J"
BOX
A-11722
TO MODEL 438
LH2 SYSTEM C/O SUPPLY VENT
A-11699
A-11698
LOX SYSTEM C/O SUPPLY VENT
NOTE:
SEE FIGURE 4-1 FOR
LEGEND
3000 PSI He FROM 432 TO CIRC NO. 2
3000 PSI He FROM 432 TO CIRC NO. 3
50 PSI He
A-12260
A-11692
HELIUM SUPPLY TO CIRCUIT NO. 2 20 LB/MIN
A-11689
HELIUM SUPPLY TO CIRCUIT NO. 3 – 40 LB/MIN
A-11686
PNEUMATIC CONTROL &
REPRESS SUPPLY 9-4 LB/MIN
A-11684
APS BOTTLE SUPPLY 0.75 LB/MIN
A-11685
PRESSURE SWITCH
C/O LOX PRESSURE
A-11675
FUEL UMBILICAL PURGE
SUPPLY – 1.5 LB/MIN He
A-11696
750 PSIG GN2 FROM MODEL 433
A-11694 TO MODEL 433 (T/C PURGE)
A-11690
FUEL NOZZLE PURGE 0.13 LB/MIN
LH2 VENT DISC PURGE 0.015 LB/MIN
H-X PURGE SUPPLY TO A-12260
A-11682
MAIN STAGE OK
PRESSURE SWITCH SUPPLY
LH2 SYSTEM C/O SUPPLY
A-11678
A-11681
LOX SYSTEM C/O SUPPLY
A-11691
LH2 DEBRIS VALVE OPEN
A-11693
LH2 DEBRIS VALVE CLOSE
S-IVB
GAS HEAT EXCHANGER
DSV-4B-438A-A-1416
1B59993-1
ELEC
"J"
BOX
A-11725
FROM MODEL 433
A-11708
TURBINE START BOTTLE SUPPLY
5 LB AT –320°F
(CHILLDOWN 10 LB/MAX AT –410°F)
A-12269
He 3000 PSI
A
He 3000 PSI
A-12270
COLD He SUPPLY
3000 PSI
B
A-11715
FUEL TANK
PRE-PRESSURIZATION
SUPPLY 20 LB MIN AT –360°F
A-11709
GH2 VENT SYSTEM
CIRC NO. 1
CIRC NO. 2
CIRC NO. 3
TO GH2
VENT
A-12264
LIQUID
HYDROGEN
INLET
A-12263
750 PSI GN2 INLET
A-12254
2000 PSI He CROSSOVER FROM 432
A-11723
GH2 SUPPLY
6000 PSI
A-11714
GN2 MANIFOLD
A-12274
A-12136
A-12266
A-12267
A-12260
A-12240
C0070
A-12106
A-12117
A-12709
A-12210
A-12239
C0071
A-12238
C0072
A-12212
L18
A-12226
A-12213
A-12229
A-12233
A-12232
A-12234
A-12272
A-11740
A-11741
A-11742
A-11743
D0140
A-11744
C742-A03
C0073
A-11746
A-11747
A-11748
A-11749
A-11750
A-11751
A-11752
A-11753
A-11754
A-11755
A-11756
D0131
A-11757
A-11758
A-11759
A-11760
A-11761
A-11762
A-11763
A-11764
D0132
A-11765
A-11766
A-11768
A-11769
A-11770
A-11771
A-11772
A-11773
A-11774
A-11775
A-11776
A-11777
A-11778
A-11779
A-11780
A-11781
D0138
A-11782
A-11783
A-11784
A-11786
A-11787
A-11788
A-11789
A-11790
A-11791
A-11792
A-11793
A-11794
A-11795
D0139
A-11797
A-11798
A-11799
A-11800
A-11801
A-11802
A-11803
A-11804
A-11805
A-11806
A-11807
A-11808
A-11809
A-11810
A-11811
A-11812
A-11813
A-11814
A-11815
A-11816
A-11817
A-11818
A-11819
A-11820
A-11821
A-11822
D0135
A-11823
A-11824
A-11825
A-11826
A-11827
A-11828
A-11829
A-11830
D0134
A-11831
A-11832
A-11833
A-11834
A-11835
A-11836
A-11837
A-11838
A-11839
D0136
A-11840
A-11841
A-11842
A-11843
A-11844
A-11845
A-11846
A-11847
A-11848
A-11849
A-11850
A-11851
A-11852
A-11853
A-11854
A-11855
A-11856
A-11857
A-11858
A-11859
A-11860
A-11861
A-11862
A-11863
A-11864
A-11865
A-11866
A-11867
A-11868
A-11869
A-11870
A-11871
A-11872
A-11873
A-11874
A-11875
A-11876
A-11877
A-11878
A-11879
A-11880
A-11881
A-11882
A-11883
A-11884
A-11885
A-11886
A-11887
A-11888
A-11889
A-11890
A-11891
A-11892
A-11893
A-11894
A-11895
A-11896
A-11897
A-11898
A-11899
A-11900
A-11901
A-11902
A-11903
A-11904
A-11905
A-11906
A-11907
A-11908
A-11909
A-11910
A-11911
A-11912
A-11913
A-11914
A-11915
A-11916
A-11917
A-11918
A-11919
A-11920
A-11921
A-11922
A-11923
A-11924
L7A
A-11925
A-11926
A-11927
A-11928
L8A
A-11929
A-11930
A-11931
A-11932
A-11933
A-11934
A-11935
A-11936
A-11937
A-11938
A-11939
A-11940
A-11941
A-11942
A-11943
A-11944
A-11945
A-11946
A-11947
A-11948
L14A
A-11949
A-11950
A-11951
A-11952
A-11953
A-11954
A-11955
A-11956
A-11957
A-11958
A-11959
A-11960
A-11961
A-11962
A-11963
A-11964
A-11965
A-11966
A-11967
A-11968
A-11969
A-11970
C0074
A-11971
A-11972
A-11973
A-11974
A-11975
A-11976
A-11977
A-11978
A-11979
A-11980
A-11981
A-11982
A-11983
A-11984
A-11985
A-11986
A-11987
A-11988
D0120
A-11989
A-11990
A-11991
A-11992
A-11993
A-11994
A-11995
D0121
A-11996
A-11997
A-11998
A-11999
A-12000
A-12001
A-12002
A-12003
A-12004
A-12005
A-12006
A-12007
A-12008
A-12009
A-12010
A-12011
A-12012
A-12013
A-12014
A-12015
A-12016
A-12017
A-12018
A-12019
A-12020
A-12021
A-12022
A-12023
A-12024
A-12025
A-12026
A-12027
A-12028
A-12029
A-12030
A-12031
A-12032
A-12033
A-12034
A-12035
A-12036
A-12037
A-12038
A-12039
A-12040
A-12041
A-12042
A-12043
A-12044
A-12045
A-12046
A-12047
A-12048
A-12049
A-12050
A-12051
A-12052
A-12053
A-12054
A-12055
A-12056
A-12057
A-12058
A-12059
A-12060
A-12061
A-12062
A-12063
A-12064
A-12065
A-12066
A-12067
A-12068
A-12069
A-12070
A-12071
A-12072
A-12073
A-12074
A-12075
A-12076
A-12077
A-12078
A-12079
A-12080
A-12081
A-12082
D5000-B11
A-12083
A-12084
A-12085
A-12086
A-12087
A-12088
A-12089
A-12090
A-12091
A-12092
A-12093
A-12094
A-12095
A-12096
A-12097
A-12098
A-12099
A-12100
A-12101
A-12102
A-12103
A-12104
A-12105
A-12106
A-12107
A-12108
A-12109
A-12110
A-12111
A-12112
A-12113
A-12114
A-12115
A-12116
A-12117
A-12118
A-12119
A-12120
A-12121
A-12122

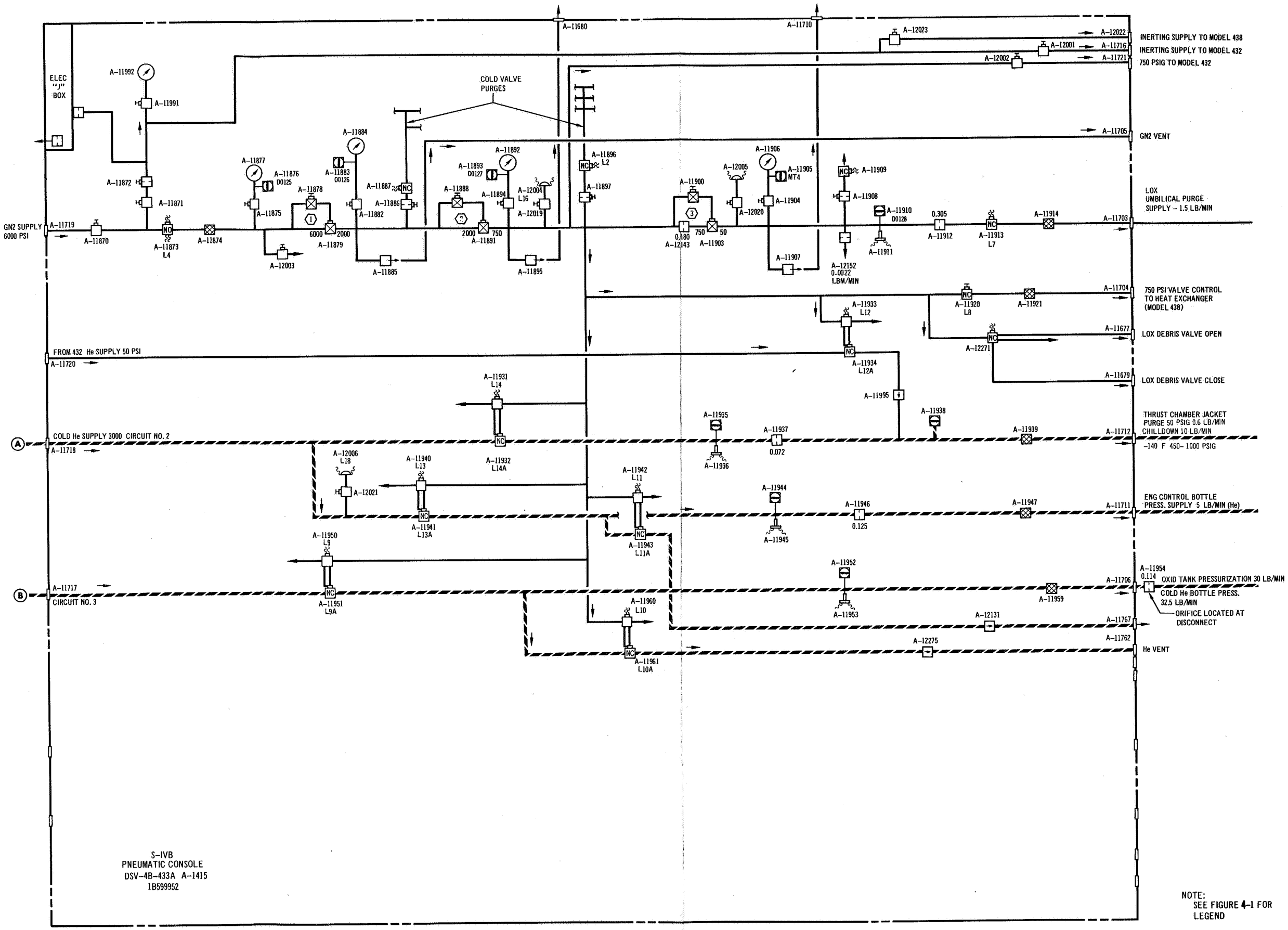

Figure 4-3. Facility Propellant and Pneumatic Loading Systems (Sheet 2 of 2)

FOLDOUT FRAME 1

FOLDOUT FRAME 2

SECTION 5

SEQUENCE OF EVENTS

5. SEQUENCE OF EVENTS

Table 5-1 presents the AS-502 flight sequence of events. Four types of items are included in the sequence.

a. LVDC Commands

These items originate from the Launch Vehicle Digital Computer (LVDC) in the Instrument Unit (IU), and direct vehicle system actions.

b. Events

These items are monitored occurrences resulting from vehicle performance, e.g., the time of maximum dynamic pressure.

c. Responses

These items are responses to commands that are issued from the IU and are monitored in the S-IVB.

d. Ground Commands

These items are manual commands issued from ground stations, which transmit signals to the LVDC in order to direct vehicle system actions.

In the sequence, all commands and events are preceded by an item number. Sequential series of related commands and responses are listed under the same event number with lower case letters distinguishing separate items.

5.1 Predicted and Monitored Times

The predicted times in the sequence were obtained from the Douglas memorandum A3-860-KKBH-68-M-177, published April 26, 1968, entitled S-IVB-502 Stage Predictions. Commands issued from the LVDC to the S-IC, S-II, S-IVB, and IU, were monitored at the LVDC. Times for these items were obtained from Marshall Space Flight Center (MSFC). Commands issued from the LVDC to the S-IVB were also monitored at the S-IVB switch selector. These items were obtained from Douglas data. Ground commands were monitored at the Mission Control Center and at the LVDC if received. Monitored times for events were obtained from Douglas postflight analysis of parameters associated with each event.

The time from range zero is provided for all items. Range zero, which is by definition the even second prior to liftoff, occurred at 12:00:01.0 GMT.

A time-from-base is given for all LVDC commands which were preprogrammed. A time-from-base is not applicable (N/A) for items such as events, command responses, and LVDC commands which were not preprogrammed.

The accuracies listed in table 5-1 are related to the telemetry-channel sampling rates; therefore, the items occurred at the times indicated or earlier by the amount listed in the accuracy column. The accuracy of IU signals is not shown since this information is not available.

5.2 Time Bases

Seven sequential series of preprogrammed commands (time bases) were issued from the LVDC. Each sequential series was initiated by the establishment of its time base in the LVDC. Listed below are the seven time bases with their respective originating events.

a. Time Base One, TB1 - IU Umbilical Disconnect

b. Time Base Two, TB2 - S-IC Inboard Engine Cutoff

c. Time Base Three, TB3 - S-IC Outboard Engines Cutoff

d. Time Base Four, TB4 - S-II J-2 Engines Cutoff

e. Time Base Five, TB5 - First S-IVB Engine Cutoff

f. Time Base Six, TB6 - Begin Restart Preparations (LVDC solves an equation)

g. Time Base Seven, TB7 - Second S-IVB Engine Cutoff

5.3 Ground Commands

Largely due to anomalies occurring during the flight, a number of commands to the LVDC were initiated from the ground by flight controller action. The majority of these commands would not have been transmitted had the flight anomalies not occurred.

The following is a list of the ground commands issued, including comments regarding their purpose and effectiveness. These commands are also included in table 5-1. It should be noted that there are discrepancies of up to 5 sec in table 5-1 between the issuance of certain ground commands and the receipt of the same commands by the S-IVB switch selector. Time delays of this magnitude are possible when considering (a) that in some cases a series of individual commands are stacked together and transmitted by a single ground command, and (b) the amount of time that can be spent in the process of command transmittal, verification, and execution.

Site	Command Time from Range Zero (hr:min:sec)	Command	Results/Comments
CRO	04:09:21	Aux Hydraulic Pump Coast Mode OFF	Verified - Command disables thermal switch. Command was sent to simulate the normal pre-ignition sequence.
CRO	04:09:21	Aux Hydraulic Pump Flight Mode ON	Verified - Command turns on the aux pump. Command was sent in an attempt to turn pump on after failure had occurred during the pre-ignition sequence. A load of 12 amps was observed on Aft Battery No. 2.
CRO	04:10:04	Temeletry Calibrator Inflight Calibrate ON	Verified - Command initiates onboard calibration commands sent to verify proper functioning of onboard switch selector system and ground processing. Also provided an additional calibration for postflight analysis.

Site	Command Time from Range Zero (hr:min:sec)	Command	Results/Comments
CRO	04:10:04	Regular Calibrate Relays ON	Verified - Command initiates onboard calibration commands sent to verify proper functioning of onboard switch selector system and ground processing. Also provided an additional calibration for postflight analysis.
CRO	04:10:37	Aux Hydraulic Pump Coast Mode OFF	Same as above (second attempt)
CRO	04:10:37	Aux Hydraulic Pump Flight Mode ON	Same as above (second attempt)
CRO	04:11:00	Aux Hydraulic Pump Flight Mode OFF	Verified - Command turns off the aux pump. Command sent to remove load from Aft Battery No. 2. A load of 0 amps was observed on Aft Battery No. 2.
CRO	04:11:38	Telemetry Calibrator Inflight Calibrate OFF	SLV Reject - Due to telemetry dropout.
CRO	04:11:38	Regular Calibrate Relays OFF	Same as above.
CRO	04:11:53	Terminate	Ground Reject - Unified S-Band (USB) dropped modulation due to signal dropouts.
CRO	04:12:06	Terminate	Verified - Command sent to reset onboard system because a SLV Reject was received on a previous command.
COR	04:12:15	Telemetry Calibrator Inflight Calibrate OFF	Ground Reject - USB dropped modulation due to signal dropouts.
CRO	04:12:15	Regular Calibrate Relays OFF	Same as above.
CRO	04:12:29	Telemetry Calibrator Inflight Calibrate OFF	Ground Reject - USB dropped modulation due to signal dropouts.
CRO	04:12:29	Regular Calibrate Relays OFF	Same as above.
HAW	04:29:33	Telemetry Calibrator Inflight Calibrate OFF	Verified - Command sent to reset calibration mode for subsequent calibration.
HAW	04:29:33	Regular Calibrate Relays OFF	Same as above.
HAW	04:30:01	Maneuver to Align S-IVB + X Axis with Local Horizontal (Maneuver A - Alternate Sequence 6)	Verified - Command sent to terminate inertial hold and to initiate orbital pitch rate at local horizontal. This would enhance command and telemetry communications. Vehicle was observed to pitch about 160° to achieve local horizontal.

Site	Command Time from Range Zero (hr:min:sec)	Command	Results/Comments
GYM	04:42:07	Slow Record ON	Verified - Command sent to mark end of valid recorded data.
GYM	04:42:07	Slow Record OFF	Verified - Command sent to turn recorder off.
GYM	04:42:07	Tape Playback ON	Verified - Command sent to dump recorded data for postflight analysis.
HAW	06:06:25	Tape Playback OFF	Verified - Command sent to terminate playback to recorded data and provide realtime PCM data.
HAW	06:06:59	LOX Tank Flight Pressure System ON	Verified - Command sent to remove the LOX tank pressure switch from controlling the cold helium shutoff valves.
HAW	06:06:59	Coast Period OFF	Verified - Command sent to power cold helium shutoff valves open. The cold helium sphere pressure was observed to decay from approximately 571 psia to 0 at approximately RO +6 hr 10 min.
HAW	06:06:59	LOX Tank Vent Valve Open	Verified - Command sent to open actuation control module solenoid which allows stage pneumatics to open LOX vent valve.
HAW	06:06:59	LH2 Tank Vent Valve Open	Verified - Command sent to open actuation control module solenoid which allows stage pneumatics to open LH2 vent valve.

NOTE: The above sequence of commands sent at 06:06:59 provided a cold helium dump.

DATA OMISSIONS

A dash (--) was inserted in the flight sequence table for item times which are not available. Some items, such as command responses, had no predicted times. Due to early cutoff, commands 320 through 325 were not issued.

Actual times for items 420a and b, and 421a and b are not included inasmuch as these commands occurred prior to acquisition of signal at Hawaii, revolution 4.

COMMENTS

There are in some instances apparent conflicts in the time of command issuance from the LVDC and command receipt in the S-IVB. This conflict has been recognized by both MSFC and Douglas, but has not been resolved to date.

There are several events for which actual monitored times are not available. For these events the sequence times have been estimated from the last known time. All such derived times are indicated in table 5-1 with an asterisk.

5.4 Ground Sequence of Events

Table 5-2 presents the ground sequence of events from approximately R0 -10 min to liftoff. These events are related to the S-IVB-502 and associated ground support equipment and are derived from the digital events evaluation.

TABLE 5-1 (Sheet 1 of 40)
AS-502 SEQUENCE OF EVENTS

ITEM NO.	EVENT	PREDICTED TIME		SIGNAL MONITORED AT	MONITORED TIME		DATA SOURCE	ACCURACY (ms)
		TIME FROM RANGE ZERO (hr:min:sec) (sec)	TIME FROM BASE (sec)		TIME FROM RANGE ZERO* (hr:min:sec) (sec)	TIME FROM BASE (sec)		
1	Guidance Reference Release	-00:00:16.7 (-16.7)	N/A	IU	-00:00:16.845 (-16.845)	N/A	MSFC	--
2	S-IC Engine Start Sequence Command	-00:00:08.79 (-8.79)	N/A	IU	-00:00:08.77 (-8.77)	N/A	MSFC	--
3	Range Zero	00:00:00.0 (0.0)	N/A	IU	00:00:00.0 (0.0)	N/A	MSFC	--
4	Holddown Arms Release	00:00:00.0 (0.0)		IU	00:00:00.36 (0.36)	N/A	MSFC	--
5	First Motion	00:00:00.0 (0.0)	N/A	GSE	00:00:00.38 (0.38)	N/A	MSFC	--
	TIME BASE 1							
6	AS-502 Liftoff; IU Umbilical Disconnect	00:00:00.3 (0.0)	TB1 +0.0	IU	00:00:00.69 (0.69)	TB1 +0.0	MSFC	--
7	Yaw Maneuver Start	00:00:01.3 (1.3)	N/A	IU	00:00:01.9 (1.9)	N/A	MSFC	--
8	Signal from LVDC for: Auto - Abort Enable Relays Reset	00:00:05.3 (5.3)	TB1 +5.0	IU	00:00:05.643 (5.643)	TB1 +4.953	MSFC	--
9	Sensor Bias ON	00:00:05.5 (5.5)	TB1 +5.2	IU	00:00:05.855 (5.855)	TB1 +5.165		
10	Yaw Maneuver Stop	00:00:09.3 (9.3)	N/A	IU	00:00:09.834 (9.834)	N/A	MSFC	--
11	Pitch Maneuver Start	00:00:11.0 (11.0)	N/A	IU	00:00:11.10 (11.10)	N/A	MSFC	--
12	Roll Maneuver Start	00:00:11.0 (11.0)	N/A	IU	00:00:11.10 (11.10)	N/A	MSFC	--
13	Signal from LVDC for: Multiple Engine Cutoff Enable	00:00:14.3 (14.30)	TB1 +14.0	IU	00:00:14.646 (14.646)	TB1 +13.956	MSFC	--
14	Signal from LVDC for: S-IC Telemetry Calibrate ON	00:00:25.1 (25.1)	TB1 +24.8		00:00:25.442 (25.442)	TB1 +24.752	MSFC	--
15	Signal from LVDC for: Telemetry Calibrator Inflight Calibrate ON	00:00:27.3 (27.3)	TB1 +27.0	IU	00:00:27.657 (27.657)	TB1 +26.967	MSFC	--
16	Roll Maneuver Stop	00:00:29.0 (29.0)	N/A	IU	00:00:31.3 (31.3)	N/A	MSFC	--
17	Signal from LVDC for: S-IC Telemetry Calibrate OFF	00:00:30.1 (30.1)	TB1 +29.8	IU	00:00:30.460 (30.460)	TB1 +29.770	MSFC	--
18	Signal from LVDC for: Launch Vehicle Engines EDS Cutoff Enable	00:00:30.3 (30.3)	TB1 +30.0	IU	00:00:30.663 (30.663)	TB1 +29.973	MSFC	--
19	Signal from LVDC for: Telemetry Calibrator Inflight Calibrate OFF	00:00:32.3 (32.3)	TB1 +32.0	IU	00:00:32.644 (32.644)	TB1 +31.954	MSFC	--

TABLE 5-1 (Sheet 2 of 40)
AS-502 SEQUENCE OF EVENTS

ITEM NO.	EVENT	PREDICTED TIME		SIGNAL MONITORED AT	MONITORED TIME		DATA SOURCE	ACCURACY (ms)
		TIME FROM RANGE ZERO (hr:min:sec) (sec)	TIME FROM BASE (sec)		TIME FROM RANGE ZERO* (hr:min:sec) (sec)	TIME FROM BASE (sec)		
20	Signal from LVDC for: Fuel Pressurizing Valve No. 2 Open and Tape Recorder Record	00:00:49.8 (49.8)	TB1 +49.5	IU	00:00:50.143 (50.143)	TB1 +49.453	MSFC	--
21	Mach 1 Achieved	00:01:01.0 (61.0)	TB1 +60.7		00:01:00.5 (60.5)	N/A	MSFC	--
22	Signal from LVDC for: Start Data Recorders	00:01:14.4 (74.4)	TB1 +74.1	IU	00:01:14.742 (74.742)	TB1 +74.052	MSFC	--
23	Signal from LVDC for: Cooling System Electronic Assembly Power OFF	00:01:15.3 (75.3)	TB1 +75.0	IU	00:01:15.657 (75.657)	TB1 +74.967	MSFC	--
24	Maximum Dynamic Pressure	00:01:19.0 (79.0)	N/A	N/A	00:01:15.2 (75.2)	N/A	MSFC	--
25	Signal from LVDC for: Telemetry Calibrator Inflight Calibrate ON	00:01:30.3 (90.3)	TB1 +90.0	IU	00:01:30.664 (90.664)	TB1 +89.974	MSFC	--
26	Signal from LVDC for: Telemetry Calibrator Inflight Calibrate OFF	00:01:35.3 (95.3)	TB1 +95.0	IU	00:01:35.650 (95.650)	TB1 +94.960	MSFC	--
27	Signal from LVDC for: Fuel Pressurizing Valve No. 3 OPEN	00:01:35.6 (95.6)	TB1 +95.3	IU	00:01:35.949 (95.949)	TB1 +95.259	MSFC	--
28	Signal from LVDC to Flight Control Computer for: Switch Point No. 1	00:01:45.3 (105.3)	TB1 +105.0	IU	00:01:45.658 (105.658)	TB1 +104.968	MSFC	--
29	Signal from LVDC for: S-IC Telemeter Calibrate ON	00:01:55.3 (115.3)	TB1 +115.0	IU	00:01:55.656 (115.656)	TB1 +114.966	MSFC	--
30a	Signal from LVDC for: Regular Calibrate Relays ON	00:01:59.5 (119.5)	TB1 +119.2	IU	00:01:59.845 (119.845)	TB1 +119.155	MSFC	--
30b	Signal Received in S-IVB for: Regular Calibrate Relays ON	--	--	S-IVB	00:01:59.846 (119.846)	TB1 +119.156	DAC (FM)	13
31	Signal from LVDC for: S-IC Telemeter Calibrate OFF	00:02:00.3 (120.3)	TB1 +120.0	IU	00:02:00.658 (120.658)	TB1 +119.968	MSFC	--
32	Signal from LVDC to: Flight Control Computer for: Switch Point No. 2	00:02:00.5 (120.5)	TB1 +120.2	IU	00:02:00.842 (120.842)	TB1 +120.152	MSFC	--
33a	Signal from LVDC for: Regular Calibrate Relays OFF	00:02:04.5 (124.5)	TB1 +124.2	IU	00:02:04.844 (124.844)	TB1 +124.154	MSFC	--

TABLE 5-1 (Sheet 3 of 40)
AS-502 SEQUENCE OF EVENTS

ITEM NO.	EVENT	PREDICTED TIME		SIGNAL MONITORED AT	MONITORED TIME		DATA SOURCE	ACCURACY (ms)
		TIME FROM RANGE ZERO (hr:min:sec) (sec)	TIME FROM BASE (sec)		TIME FROM RANGE ZERO* (hr:min:sec) (sec)	TIME FROM BASE (sec)		
33b	Signal Received in S-IVB for: Regular Calibrate Relays OFF	--	--	S-IVB	00:02:04.846 (124.846)	TB1 +124.156	DAC (FM)	13
34	Signal from LVDC for: Start First PAM-FM/FM Calibration	00:02:10.53 (130.53)	TB1 +129.84	S-II	00:02:10.359 (130.359)	TB1 +129.669	MSFC	--
35	Signal from LVDC for: Fuel Pressurizing Valve No. 4 Open	00:02:13.8 (133.8)	TB1 +133.5	IU	00:02:14.159 (134.159)	TB1 +133.469	MSFC	--
36a	Signal from LVDC for: Fast Record ON	00:02:14.8 (134.8)	TB1 +134.5	IU	00:02:15.158 (135.158)	TB1 +134.468	MSFC	--
36b	Signal Received in S-IVB for: Fast Record ON	--	--	S-IVB	00:02:15.158 (135.158)	TB1 +134.468	DAC (FM)	13
37	Signal from LVDC for: PAM/FM/FM Calibration Stop	00:02:14.9 (134.9)	TB1 +134.7	IU	00:02:15.343 (135.343)	TB1 +134.653	MSFC	--
38	Signal from LVDC for: IU Tape Recorder ON	00:02:15.2 (135.2)	TB1 +134.9	IU	00:02:15.553 (135.553)	TB1 +134.863	MSFC	--
39	Signal from LVDC for: LOX Tank Strobe Lights OFF	00:02:15.4 (135.4)	TB1 +135.1	S-IC	00:02:15.743 (135.743)	TB1 +135.053	MSFC	--
40	Signal from LVDC for: S-IC Two-Engine Out Auto-Abort Inhibit Enable	00:02:15.6 (135.6)	TB1 +135.3	IU	00:02:15.948 (135.948)	TB1 +135.258	MSFC	--
41	Signal from LVDC for: S-IC Two-Engine Out Auto-Abort Inhibit	00:02:15.8 (135.8)	TB1 +135.5	IU	00:02:15.166 (136.166)	TB1 +135.476	MSFC	--
42	Signal from LVDC for: Excessive Rate (P, Y & R) Auto-Abort Inhibit Enable	00:02:16.0 (136.0)	TB1 +135.7	IU	00:02:16.344 (136.344)	TB1 +135.654	MSFC	--
43	Signal from LVDC for: Excessive Rate (P, Y & R) Auto-Abort Inhibit	00:02:16.2 (136.2)	TB1 +135.9	IU	00:02:16.544 (136.544)	TB1 +135.854	MSFC	--
44	Signal from LVDC for: Two Adjacent Outboard Engines Out Enable	00:02:16.4 (136.4)	TB1 +136.1	IU	00:02:16.756 (136.756)	TB1 +136.066	MSFC	--
45	Signal from LVDC for: Inboard Engine Cutoff Enable	00:02:16.6 (136.6)	TB1 +136.3	--	00:02:16.962 (136.962)	TB1 +136.272	MSFC	--

TABLE 5-1 (Sheet 4 of 40)
AS-502 SEQUENCE OF EVENTS

ITEM NO.	EVENT	PREDICTED TIME		SIGNAL MONITORED AT	MONITORED TIME		DATA SOURCE	ACCURACY (ms)
		TIME FROM RANGE ZERO (hr:min:sec) (sec)	TIME FROM BASE (sec)		TIME FROM RANGE ZERO* (hr:min:sec) (sec)	TIME FROM BASE (sec)		
46	Signal from LVDC for: Inboard Engine Cutoff Backup Enable	00:02:16.8 (136.8)	TB1 +136.5	--	00:02:17.143 (137.143)	TB1 +136.453	MSFC	--
47	Stop Pitch Maneuver	00:02:21.7 (141.7)	N/A	IU	00:02:20.9 (140.9)	TB1 +140.21	MSFC	--
48	Inboard Engine Cutoff Interrupt 1520	00:02:23.4 (143.4)	N/A	IU	00:02:24.95 (144.95)	N/A	MSFC	--
	TIME BASE 2							
49	S-IC Inboard Engine Cutoff	00:02:23.4 (143.4)	TB2 +0.0	S-IC	00:02:24.949 (144.949)	TB2 +0.0	MSFC	--
50	Signal from LVDC for: S-II Ordnance Arm	00:02:23.5 (143.5)	TB2 +0.1	IU	00:02:25.028 (145.028)	TB2 +.079	MSFC	--
51	Signal from LVDC for: Separation and Retro EBW Firing Units Arm	00:02:23.7 (143.7)	TB2 +0.3	IU	00:02:25.202 (145.202)	TB2 +0.253	MSFC	--
52	Signal from LVDC for: Separation Camera ON	00:02:23.9 (143.9)	TB2 +0.5	IU	00:02:25.415 (145.415)	TB2 +0.466	MSFC	--
53	Signal from LVDC for: Camera Lights ON	00:02:24.0 (144.0)	TB2 +0.6	IU	00:02:25.513 (145.513)	TB2 +0.564	MSFC	--
54	Signal from LVDC for: S-IC Telemetry Measurement Switch Over	00:02:24.2 (144.2)	TB2 +0.8	IU	00:02:25.702 (145.702)	TB2 +0.753	MSFC	--
55	Signal from LVDC for: Enable Outboard Engines Cutoff	00:02:24.4 (144.4)	TB2 +1.0	IU	00:02:25.912 (145.912)	TB2 +.963	MSFC	--
56	Outboard Engines Cutoff Interrupt 1520	00:02:28.4 (148.4)	N/A	IU	00:02:28.41 (148.41)	N/A	MSFC	--
	TIME BASE 3							
57	S-IC Outboard Engines Cutoff	00:02:28.4 (148.4)	TB3 +0.0	IU	00:02:28.405 (148.405)	TB3 +0.0	MSFC	--
58	Signal from LVDC for: Camera Motor ON	00:02:28.5 (148.5)	TB3 +0.1	IU	00:02:28.486 (148.486)	TB3 +0.81	MSFC	--
59	Signal from LVDC for: S-II LH2 Recirculation Pumps OFF	00:02:28.7 (148.7)	TB3 +0.3	IU	00:02:28.659 (148.659)	TB3 +.254	MSFC	--
60	Signal from LVDC for: S-II Ullage Trigger	00:02:28.9 (148.9)	TB3 +0.5	IU	00:02:28.874 (148.874)	TB3 +.469	MSFC	--
61	Signal from LVDC for: S-IC/S-II Separation	00:02:29.1 (149.1)	TB3 +0.7	IU	00:02:29.078 (149.078)	TB3 +.673	MSFC	--
62	Signal from LVDC for: Camera Event Mark	00:02:29.2 (149.2)	TB3 +0.8	IU	00:02:29.173 (149.173)	TB3 +.768	MSFC	--

TABLE 5-1 (Sheet 5 of 40)
AS-502 SEQUENCE OF EVENTS

ITEM NO.	EVENT	PREDICTED TIME		SIGNAL MONITORED AT	MONITORED TIME		DATA SOURCE	ACCURACY (ms)
		TIME FROM RANGE ZERO (hr:min:sec) (sec)	TIME FROM BASE (sec)		TIME FROM RANGE ZERO* (hr:min:sec) (sec)	TIME FROM BASE (sec)		
63	Signal from LVDC for: Switch Control to S-II Enable S-II Engine Out and S-II Second Separation Indication "A" Enable	00:02:29.3 (149.3)	TB3 +0.9	IU	00:02:29.258 (149.258)*	TB3 + .853	MSFC	--
64	Signal from LVDC for: S-II Engines Cutoff Reset	00:02:29.4 (149.4)	TB3 +1.0	IU	00:02:29.358 (149.358)*	TB3 + .953	MSFC	--
65	Signal from LVDC for: Engines Ready Bypass	00:02:29.5 (149.5)	TB3 +1.1	IU	00:02:29.458 (149.458)*	TB3 +1.053	MSFC	--
66	Signal from LVDC for: Prevalves Lockout Reset	00:02:29.6 (149.6)	TB3 +1.2	IU	00:02:29.558 (149.558)*	TB3 +1.153	MSFC	--
67	Signal from LVDC for: S-II Engine Start	00:02:29.8 (149.8)	TB3 +1.4	IU	00:02:29.758 (149.758)*	TB3 +1.353	MSFC	--
68	Signal from LVDC for: Camera Event Mark	00:02:29.9 (149.9)	TB3 +1.5	IU	00:02:29.858 (149.858)*	TB3 +1.453	MSFC	--
69	Signal from LVDC for: Enable S-II Engine Out and S-II Second Separation Indication "B"	00:02:30.1 (150.1)	TB3 +1.7	IU	00:02:30.058 (150.058)*	TB3 +1.653	MSFC	--
70	Signal from LVDC for: Engine Ready Bypass Reset	00:02:30.3 (150.3)	TB3 +1.9	IU	00:02:30.258 (150.258)*	TB3 +1.853	MSFC	--
71	Signal from LVDC for: Q-Ball Power OFF	00:02:30.8 (150.8)	TB3 +2.4	IU	00:02:30.757 (150.757)	TB3 +2.352	MSFC	--
72	Signal from LVDC for: S-II Hydraulic Accumulators Unlock	00:02:31.4 (151.4)	TB3 +3.0	IU	00:02:31.379 (151.379)	TB3 +2.974	MSFC	--
73	Signal from LVDC for: Chilldown Valves Close	00:02:34.8 (154.8)	TB3 +6.4	IU	00:02:34.759 (154.759)	TB3 +6.354	MSFC	--
74	Signal from LVDC for: S-II start Phase Limiter Cutoff Arm	00:02:35.1 (155.1)	TB3 +6.7	IU	00:02:35.078 (155.078)	TB3 +6.673	MSFC	--
75	Signal from LVDC for: Activate PU System	00:02:35.2 (155.2)	TB3 +6.9	IU	00:02:35.258 (155.258)	TB3 +6.853	MSFC	--
76	Signal from LVDC for: S-II Start Phase Limiter Cutoff Arm Reset	00:02:36.1 (156.0)	TB3 +7.7	IU	00:02:36.074 (156.074)	TB3 +7.669	MSFC	--
77	Signal from LVDC for: Stop Data Recorders	00:02:39.8 (159.8)	TB3 +11.4	IU	00:02:39.780 (159.780)	TB3 +11.375	MSFC	--

TABLE 5-1 (Sheet 6 of 40)
AS-502 SEQUENCE OF EVENTS

ITEM NO.	EVENT	PREDICTED TIME		SIGNAL MONITORED AT	MONITORED TIME		DATA SOURCE	ACCURACY (ms)
		TIME FROM RANGE ZERO (hr:min:sec) (sec)	TIME FROM BASE (sec)		TIME FROM RANGE ZERO* (hr:min:sec) (sec)	TIME FROM BASE (sec)		
78a	Signal from LVDC for: Fast Record OFF	00:02:40.0 (160.0)	TB3 +11.6	IU	00:02:39.960 (159.960)	TB3 +11.555	MSFC	--
78b	Signal Received on S-IVB for: Fast Record OFF	--	--	S-IVB	00:02:39.961 (159.961)	TB3 +11.556	DAC (FM)	13
79	Signal from LVDC for: Tape Recorder Record OFF	00:02:40.2 (160.2)	TB3 +11.8		00:02:40.174 (160.174)	TB3 +11.769	MSFC	--
80	Signal from LVDC for: S-II Second Plane Separation	00:02:59.1 (179.1)	TB3 +30.7	IU	00:02:54.058 (179.058)	TB3 +30.653	MSFC	--
81	Signal from LVDC for: Camera Event Mark	00:02:59.2 (179.2)	TB3 +30.8	IU	00:02:59.158 (179.158)	TB3 +30.753	MSFC	--
82	Signal from LVDC for: Camera Event Mark	00:03:00.2 (180.2)	TB3 +31.8	IU	00:03:00.157 (180.157)	TB3 +31.752	MSFC	--
83	Signal from LVDC for: Water Coolant Valve Open	--	Variable	IU	00:03:02.294 (182.294)	TB3 +33.889	MSFC	--
84	Signal from LVDC for: LET Jettison "A"	00:03:04.8 (184.8)	TB3 +36.4	IU	00:03:04.766 (184.766)	TB3 +36.361	MSFC	--
85	Signal from LVDC for: LET Jettison "B"	00:03:05.0 (185.0)	TB3 +36.6	IU	00:03:04.979 (184.979)	TB3 +36.574	MSFC	--
86	Signal from LVDC for: Camera Eject No. 1	00:03:06.4 (186.4)	TB3 +38.0	IU	00:03:06.374 (186.374)	TB3 +37.969	MSFC	--
87	Signal from LVDC for: Camera Eject No. 2	00:03:07.0 (187.0)	TB3 +38.6	IU	00:03:06:960 (186.960)	TB3 +38.555	MSFC	--
88	Signal from LVDC for: Camera Eject No. 3	00:03:07.5 (187.5)	TB3 +39.1	IU	00:03:07.464 (187.464)	TB3 +39.059	MSFC	--
89	Initiate Iterative Guidance Mode	00:03:10.4 (190.4)	N/A	IU	00:03:10.95 (190.95)	N/A	MSFC	--
90	Signal from LVDC to Flight Control Computer for: Switch Point No. 3	00:03:29.8 (209.8)	TB3 +61.4	IU	00:03:29.764 (209.764)	TB3 +61.359	MSFC	--
91	Initiate Steering Misalignment Correction	00:03:30.01 (210.01)	N/A		00:03:31.99 (211.99)	N/A	MSFC	--
92	Signal from LVDC for: Start Second PAM-FM/FM Calibration	00:05:30.3 (330.3)	TB3 +181.9	IU	00:05:30.258 (330.258)	TB3 +181.853	MSFC	--
93	Signal from LVDC for: Stop Second PAM-FM/FM Calibration	00:05:35.3 (335.3)	TB3 +186.9	IU	00:05:30.269 (335.269)	TB3 +186.864	MSFC	--

TABLE 5-1 (Sheet 7 of 40)
AS-502 SEQUENCE OF EVENTS

ITEM NO.	EVENT	PREDICTED TIME		SIGNAL MONITORED AT	MONITORED TIME		DATA SOURCE	ACCURACY (ms)
		TIME FROM RANGE ZERO (hr:min:sec) (sec)	TIME FROM BASE (sec)		TIME FROM RANGE ZERO* (hr:min:sec) (sec)	TIME FROM BASE (sec)		
94	Signal from LVDC to Flight Control Computer for: Switch Point No. 4	00:05:43.9 (339.8)	TB3 +191.4	IU	00:05:39.759 (339.759)	TB3 +191.354	MSFC	--
95	Signal from LVDC for: Telemetry Calibration Inflight Calibrate ON	00:05:50.3 (350.3)	TB3 +201.9	IU	00:05:50.259 (350.259)	TB3 +201.854	MSFC	--
96	Signal from LVDC for: Telemetry Calibrator Inflight Calibrate OFF	00:05:55.3 (355.3)	TB3 +206.9	IU	00:05:55.271 (355.271)	TB3 +206.866	MSFC	--
97	Signal from LVDC for: Measurement Control Switch No. 2 Activate	00:06:01.1 (361.1)	TB3 +212.7	IU	00:06:01.061 (361.061)	TB3 +212.656	MSFC	--
98	S-II Mixture Ratio Shift (Guidance Sensed)	00:06:52.1 (412.1)	N/A	IU	00:08:10.75 (490.75)	N/A	MSFC	--
99	S-II No. 2 Engine Out	--	--	--	00:06:52.9 (412.9)	N/A	MSFC	--
100	S-II No. 3 Engine Out	--	--	--	00:06:54.2 (414.2)	N/A	MSFC	--
101	Signal from LVDC for: Start Third PAM-FM/FM Calibration	00:07:01.0 (421.0)	TB3 +272.6	IU	00:07:00.981 (420.981)	TB3 +272.576	MSFC	--
102	Signal from LVDC for: Stop Third PAM-FM/FM Calibration	00:07:06.0 (426.0)	TB3 +277.6	IU	00:07:05.965 (425.965)	TB3 +277.560	MSFC	--
103	Signal from LVDC for: S-II LH2 Step Pressurization	00:07:47.4 (467.34)	TB3 +320.0	IU	00:07:48.358 (468.358)	TB3 +319.953	MSFC	--
104a	Signal from LVDC for: Regular Calibrate Relays ON	00:07:57.3 (477.3)	TB3 +328.9	IU	00:07:57.259 (477.259)	TB3 +328.854	MSFC	--
104b	Signal Received in S-IVB for: Regular Calibrate Relays ON	--	--	S-IVB	00:07:57.244 (477.244)	TB3 +328.839	DAC (FM)	13
105	Signal from LVDC for: Telemetry Calibrator Inflight Calibrate ON	00:07:57.5 (477.5)	TB3 +329.1	IU	00:07:57.471 (477.471)	TB3 +329.066	MSFC	--
106a	Signal from LVDC for: Regular Calibrate Relays OFF	00:08:02.3 (482.3)	TB3 +333.9	IU	00:08:02.279 (482.279)	TB3 +333.874	MSFC	--
106b	Signal Received in S-IVB for: Regular Calibrate Relays OFF	--	--	S-IVB	00:08:02.268 (482.268)	TB3 +333.863	DAC (FM)	13
107	Signal from LVDC for: Telemetry Calibrator Inflight Calibrate OFF	00:08:02.5 (482.5)	TB3 +334.1	IU	00:08:02.457 (482.457)	TB3 +334.052	MSFC	--

TABLE 5-1 (Sheet 8 of 40)
AS-502 SEQUENCE OF EVENTS

ITEM NO.	EVENT	PREDICTED TIME		SIGNAL MONITORED AT	MONITORED TIME		DATA SOURCE	ACCURACY (ms)
		TIME FROM RANGE ZERO (hr:min:sec) (sec)	TIME FROM BASE (sec)		TIME FROM RANGE ZERO* (hr:min:sec) (sec)	TIME FROM BASE (sec)		
108a	Signal from LVDC for: Charge Ullage Ignition ON	00:08:02.9 (482.9)	TB3 +334.5	IU	00:08:02.881 (482.881)	TB3 +334.476	MSFC	--
108b	Signal Received on S-IVB for: Charge Ullage Ignition ON	--	--	S-IVB	00:08:02.868 (482.868)	TB3 +334.463	DAC (FM)	13
109	Signal from LVDC for: S-II/S-IVB Ordnance Arm	00:08:03.1 (483.1)	TB3 +334.7	IU	00:08:03.058 (483.058)	TB3 +334.653	MSFC	--
110	Signal from LVDC for: IU Tape Recorder Record ON	00:08:03.3 (483.3)	TB3 +334.9	IU	00:08:03.273 (483.273)	TB3 +334.868	MSFC	--
111a	Signal from LVDC for: Fast Record ON	00:08:03.5 (483.5)	TB3 +335.1	IU	00:08:03.458 (483.458)	TB3 +335.053	MSFC	--
111b	Signal Received in S-IVB for: Fast Record ON	--	--	S-IVB	00:08:03.446 (483.446)	TB3 +335.041	DAC (FM)	13
112	Signal from LVDC for: Start Recorders	00:08:03.7 (483.7)	TB3 +335.3	IU	00:08:03.665 (483.665)	TB3 +335.260	MSFC	--
113	Signal from LVDC for: S-II LOX Depletion Sensor Cutoff Arm	00:08:03.9 (483.9)	TB3 +335.5	IU	00:08:03.879 (483.879)	TB3 +335.474	MSFC	--
114	Signal from LVDC for: S-II LH2 Depletion Sensor Cutoff Arm	00:08:04.1 (484.1)	TB3 +335.7	IU	00:08:04.058 (484.058)	TB3 +335.653	MSFC	--
115	Cutoff S-II J-2 Engines Interrupt 1520	00:08:37.16 (517.16)	N/A	IU	00:09:36.33 (576.33)	N/A	MSFC	--
	TIME BASE 4							
116	S-II J-2 Engines Cutoff	00:08:37.16 (517.16)	TB4 +0.0	IU	00:09:36.327 (576.327)	TB4 +0.0	MSFC	--
117	Signal from LVDC for: Redundant S-II Cut-off SS	00:08:37.16 (517.16)	N/A	IU	00:09:36.410 (576.410)	TB4 +.083	MSFC	--
118	Signal from LVDC for: Start Recorder Timers	00:08:37.26 (517.26)	TB4 +0.1	IU	00:09:36.504 (576.504)	TB4 +.177	MSFC	--
119a	Signal from LVDC for: Prevalves Closed OFF	00:08:37.36 (517.36)	TB4 +0.2	IU	00:09:36.605 (576.605)	TB4 +.278	MSFC	--
119b	Signal Received in S-IVB for: Prevalves Closed OFF	--	--	S-IVB	00:09:36.596 (576.596)	TB4 +.269	DAC (FM)	13
120a	Signal from LVDC for: S-IVB Engine Cutoff OFF	00:08:37.46 (517.46)	TB4 +0.3	IU	00:09:36.697 (576.697)	TB4 +.370	MSFC	--
120b	Signal Received in S-IVB for: S-IVB Engine Cutoff OFF	--	--	S-IVB	00:09:56.687 (576.687)	TB4 +.360	DAC (FM)	13

TABLE 5-1 (Sheet 9 of 40)
AS-502 SEQUENCE OF EVENTS

ITEM NO.	EVENT	PREDICTED TIME		SIGNAL MONITORED AT	MONITORED TIME		DATA SOURCE	ACCURACY (ms)
		TIME FROM RANGE ZERO (hr:min:sec) (sec)	TIME FROM BASE (sec)		TIME FROM RANGE ZERO* (hr:min:sec) (sec)	TIME FROM BASE (sec)		
121a	Signal from LVDC for: Engine Ready Bypass	00:08:37.66 (517.66)	TB4 +.05	IU	00:09:36.789 (576.789)	TB4 +.462	MSFC	--
121b	Signal Received in S-IVB for: Engine Ready Bypass	--	--	S-IVB	00:09:36.779 (576.779)	TB4 +.452	DAC (FM)	13
122a	Signal from LVDC for: LOX Chilldown Pump OFF	00:08:37.76 (517.76)	TB4 +0.6	IU	00:09:36.882 (576.882)	TB4 +.555	MSFC	--
122b	Signal Received in S-IVB for: LOX Chilldown Pump OFF	--	--	S-IVB	00:09:36.872 (576.872)	TB4 +.545	DAC (FM)	13
123a	Signal from LVDC for: Fire Ullage Ignition ON	00:08:37.96 (517.86)	TB4 +0.7	IU	00:09:36.981 (576.981)	TB4 +.654	MSFC	--
123b	Signal Received in S-IVB for: Fire Ullage Ignition ON	--	--	S-IVB	00:09:36.971 (576.971)	TB4 +.644	DAC (FM)	13
124	Signal from LVDC for: S-II/S-IVB Separation	00:08:37.96 (517.96)	TB4 +0.8	IU	00:09:37.079 (577.079)	TB5 +.752	MSFC	--
125	Ullage Thrust Buildup to 75% (Average)	--	--	--	00:09:37.07 (577.07)	N/A	DAC	--
126	S-II Retrorocket Thrust Buildup to 10% (Average)	--	--	--	00:09:37.11 (577.11)	N/A	MSFC	--
127	First Axial Separation Motion	--	--	--	00:09:38.125 (577.125)	N/A	MSFC	--
128	S-II Retrorocket Thrust Buildup to 90% (Average)	--	--	--	00:09:37.13 (577.13)	N/A	MSFC	--
129a	Signal from LVDC for: S-IVB Engine Start Interlock Bypass ON	00:08:38.06 (518.06)	TB4 +0.9	IU	00:09:37.180 (577.180)	TB4 +.853	MSFC	--
129b	Signal Received in S-IVB for: S-IVB Engine Start Interlock Bypass ON	--	--	S-IVB	00:09:37.168 (577.168)	TB4 +.841	DAC (FM)	13
130a	Signal from LVDC for: S-IVB Engine Start ON	00:08:38.16 (518.16)	TB4 +1.0	IU	00:09:37.280 (577.280)	TB4 +.953	MSFC	--
130b	Signal Received in S-IVB for: S-IVB Engine Start ON	--	--	S-IVB	00:09:37.268 (577.268)	TB4 +.938	DAC (FM)	13
130c	J-2 Engine Start Sequence							
	1. Helium Control Solenoid Energized	--	--	S-IVB	00:09:37.268 (577.268)	--	DAC (FM)	25
	2. Main Fuel Valve Closed (Dropout)	--	--	S-IVB	00:09:37.340 (577.340)	--	DAC (FM)	25

TABLE 5-1 (Sheet 10 of 40)
AS-502 SEQUENCE OF EVENTS

ITEM NO.	EVENT	PREDICTED TIME		SIGNAL MONITORED AT	MONITORED TIME		DATA SOURCE	ACCURACY (ms)
		TIME FROM RANGE ZERO (hr:min:sec) (sec)	TIME FROM BASE (sec)		TIME FROM RANGE ZERO* (hr:min:sec) (sec)	TIME FROM BASE (sec)		
3.	Main Fuel Valve Open (Pickup)	--	--	S-IVB	00:09:37.363 (577.363)	--	DAC (PCM)	25
4.	Gas Generator Valve Closed (Dropout)	--	--	S-IVB	00:09:40.839 (580.839)	--	DAC (PCM)	25
5.	Gas Generator Valve Open (Pickup)	--	--	S-IVB	00:09:40.966 (580.966)	--	DAC (PCM)	25
6.	Main Oxidizer Valves Leaves Closed Position (Dropout)	--	--	S-IVB	00:09:40.847 (580.847)	--	DAC (PCM)	25
7.	Start Tank Discharge Valve Open (Dropout)	--	--	S-IVB	00:09:40.880 (580.880)	--	DAC (PCM)	25
8.	Oxidizer Turbine Bypass Valve Open (Dropout)	--	--	S-IVB	00:09:40.988 (580.988)	--	DAC (PCM)	25
9.	Oxidizer Turbine Bypass Valve Closed (Pickup)	--	--	S-IVB	00:09:41.212 (581.212)	--	DAC (PCM)	25
10.	Mainstage OK Pressure Switch No. 1 (Dropout)	--	--	S-IVB	00:09:42.118 (582.118)	--	DAC (PCM)	25
11.	Mainstage OK Pressure Switch No. 2 (Pickup)	--	--	S-IVB	00:09:42.187 (582.187)	--	DAC (PCM)	25
12.	Main Oxidizer Valve Reaches Open Position (Pickup)	--	--	S-IVB	00:09:42.928 (582.928)	--	DAC (PCM)	25
13.	Gas Generator Spark System ON (Dropout)	--	--	S-IVB	00:09:44.013 (584.013)	--	DAC (PCM)	25
14.	Thrust Chamber Spark System ON (Dropout)	--	--	S-IVB	00:09:44.013 (584.013)	--	DAC (PCM)	25
131	Signal from LVDC for: Flight Control Computer S-IVB Burn Mode ON "A"	00:08:38.26 (518.26)	TB4 +1.1		00:09:37.398 (577.398)	TB4 +1.071	MSFC	--
132	Signal from LVDC for: Flight Control Computer S-IVB Burn Mode ON "B"	00:08:38.36 (518.36)	TB4 +1.2	IU	00:09:37.491 (577.491)	TB4 +1.164	MSFC	--
133	Signal from LVDC for: S-IVB Engine Out Indication Enable "A" ON	00:08:38.76 (518.76)	TB4 +1.6	IU	00:09:37.880 (577.880)	TB4 +1.553	MSFC	--

TABLE 5-1 (Sheet 11 of 40)
AS-502 SEQUENCE OF EVENTS

ITEM NO.	EVENT	PREDICTED TIME		SIGNAL MONITORED AT	MONITORED TIME		DATA SOURCE	ACCURACY (ms)
		TIME FROM RANGE ZERO (hr:min:sec) (sec)	TIME FROM BASE (sec)		TIME FROM RANGE ZERO* (hr:min:sec) (sec)	TIME FROM BASE (sec)		
134	Signal from LVDC for: S-IVB Engine Out Indication Enable "B" ON	00:08:38.96 (518.96)	TB4 +1.8	IU	00:09:38.092 (578.092)	TB4 +1.765	MSFC	--
135	Separation Complete (217 in. Axial Clearance)	00:08:34.02 (519.02)	N/A	N/A	00:09:38.106 (578.106)	N/A	DAC	--
136a	Signal from LVDC for: Fuel Chilldown Pump OFF	00:08:39.36 (519.36)	TB4 +2.2	IU	00:09:38.480 (578.480)	TB4 +2.153	MSFC	--
136b	Signal Received in S-IVB for: Fuel Chilldown Pump OFF	--	--	S-IVB	00:09:38.470 (578.470)	TB4 +2.143	DAC (FM)	13
137a	Signal from LVDC for: LOX Tank Flight Pressure System ON	00:08:40.96 (520.96)	TB4 +3.8	IU	00:09:40.081 (580.081)	TB4 +3.754	MSFC	--
137b	Signal Received in S-IVB for: LOX Tank Flight Pressure System ON	--	--	S-IVB	00:09:40.012 (580.072)	TB4 +3.745	DAC (FM)	13
138a	Signal from LVDC for: Fuel Injection Temperature OK Bypass	00:08:41.16 (521.16)	TB4 +4.0	IU	00:09:40.295 (580.295)	TB4 +3.968	MSFC	--
138b	Signal Received in S-IVB for: Fuel Injection Temperature OK Bypass	--	--	S-IVB	00:09:40.281 (580.281)	TB4 +3.954	DAC (FM)	13
139a	Signal from LVDC for: Engine Start OFF	00:08:41.26 (521.26)	TB4 +4.2	IU	00:09:40.480 (580.480)	TB4 +4.153	MSFC	--
139b	Signal Received in S-IVB for: Engine Start OFF	--	--	S-IVB	00:09:40.468 (580.468)	TB4 +4.138	DAC (FM)	13
140a	Signal from LVDC for: First Burn Relay ON	00:08:42.96 (522.96)	TB4 +5.8	IU	00:09:42.081 (582.081)	TB4 +5.754	MSFC	--
140b	Signal Received in S-IVB for: First Burn Relay ON	--	--	S-IVB	00:09:42.070 (582.070)	TB4 +5.743	DAC (FM)	13
141	J-2 Thrust Buildup - 10%	--	--	N/A	00:09:41.308 (581.308)	N/A	DAC	10
142	J-2 Thrust Buildup - 90%	00:08:43.56 (523.56)	N/A	N/A	00:09:42.788 (582.788)	N/A	MSFC	--
143	Guidance Initiation	00:08:43.56 (523.56)	N/A	IU	00:09:44.8 (584.8)	N/A	MSFC	--
144	Start Artificial Tau Mode	00:08:43.56 (523.56)	N/A	IU	00:09:44.8 (584.8)	N/A	MSFC	--
145a	Signal from LVDC for: Emergency Playback Enable ON	00:08:44.96 (524.96)	TB4 +7.8	IU	00:09:44.094 (584.094)	TB4 +7.767	MSFC	--

TABLE 5-1 (Sheet 12 of 40)
AS-502 SEQUENCE OF EVENTS

ITEM NO.	EVENT	PREDICTED TIME		SIGNAL MONITORED AT	MONITORED TIME		DATA SOURCE	ACCURACY (ms)
		TIME FROM RANGE ZERO (hr:min:sec) (sec)	TIME FROM BASE (sec)		TIME FROM RANGE ZERO* (hr:min:sec) (sec)	TIME FROM BASE (sec)		
145b	Signal Received in S-IVB for: Emergency Playback Enable ON	--	--	S-IVB	00:09:44.082 (584.082)	TB4 +7.759	DAC (FM)	13
146a	Signal from LVDC for: Fast Record OFF	00:08:45.6 (525.6)	TB4 +8.0	IU	00:09:44.280 (584.280)	TB4 +7.953	MSFC	--
146b	Signal Received in S-IVB for: Fast Record OFF	--	--	S-IVB	00:09:44.268 (584.269)	TB4 +7.942	DAC (FM)	13
147a	Signal from LVDC for: PU Activate ON	00:08:46.16 (526.16)	TB4 +9.0	IU	00:09:45.300 (585.300)	TB4 +8.973	MSFC	--
147b	Signal Received in S-IVB for: PU Activate ON	--	--	S-IVB	00:09:45.288 (585.288)	TB4 +8.961	DAC (FM)	13
148a	Signal from LVDC for: Charge Ullage Jettison ON	00:08:46.96 (526.96)	TB4 +9.9	IU	00:09:46.094 (586.094)	TB4 +9.767	MSFC	--
148b	Signal Received in S-IVB for: Charge Ullage Jettison ON	--	--	S-IVB	00:09:46.081 (586.081)	TB4 +9.754	DAC (FM)	13
149	S-IVB PU Valve Reaches Hardover Position	00:08:48.16 (528.16)	TB4 +11.0	N/A	00:09:49.0 (589.0)	TB4 +12.673	DAC	100
150	S-IC Impact	00:08:48.762 (528.762)	N/A	N/A	00:08:48.93 (528.93)	N/A	MSFC	--
151a	Signal from LVDC for: Fire Ullage Jettison ON	00:08:49.96 (529.96)	TB4 +12.8	IU	00:09:49.081 (589.081)	TB4 +12.754	MSFC	--
151b	Signal Received in S-IVB for: Fire Ullage Jettison ON	--	--	S-IVB	00:09:49.066 (589.066)	TB4 +12.739	DAC (FM)	13
152a	Signal from LVDC for: Fuel Injection Temperature OK Bypass Reset		TB4 +14.0	IU	00:09:50.280 (590.280)	TB4 +13.953	MSFC	--
152b	Signal Received in S-IVB for: Fuel Injection Temperature OK Bypass Reset			S-IVB	00:09:50.268 (590.268)	TB4 +13.941	DAC (FM)	13
153a	Signal from LVDC for: Ullage Charging Reset	00:08:52.76 (532.76)	TB4 +15.6	IU	00:09:51.880 (591.880)	TB4 +15.55	MSFC	--
153b	Signal Received in S-IVB for: Ullage Charging Reset	--	--	S-IVB	00:09:51.869 (591.869)	TB4 +15.542	DAC (FM)	13
154a	Signal from LVDC for: Ullage Firing Reset	00:08:52.96 (532.96)	TB4 +15.8	IU	00:09:52.088 (592.088)	TB4 +15.761	MSFC	--
154b	Signal Received in S-IVB for: Ullage Firing Reset	--	--	S-IVB	00:09:52.075 (592.075)	TB4 +15.748	DAC (FM)	13

TABLE 5-1 (Sheet 13 of 40)
AS-502 SEQUENCE OF EVENTS

ITEM NO.	EVENT	PREDICTED TIME		SIGNAL MONITORED AT	MONITORED TIME		DATA SOURCE	ACCURACY (ms)
		TIME FROM RANGE ZERO (hr:min:sec) (sec)	TIME FROM BASE (sec)		TIME FROM RANGE ZERO* (hr:min:sec) (sec)	TIME FROM BASE (sec)		
155	Signal from LVDC for: IU Tape Recorder Record OFF	00:08:53.06 (533.06)	TB4 +18.9	IU	00:09:55.181 (595.181)	TB4 +18.854	MSFC	--
156a	Signal from LVDC for: Emergency Playback Enable OFF	00:08:58.46 (538.46)	TB4 +21.3	IU	00:09:57.580 (597.580)	TB4 +21.253	MSFC	--
156b	Signal Received in S-IVB for: Emergency Playback Enable OFF	--	--	S-IVB	00:09:57.567 (597.567)	TB4 +21.240	DAC (FM)	13
157	Signal from LVDC for: Telemetry Calibrator Inflight Calibrate ON	00:08:59.56 (539.56)	TB4 +22.4	IU	00:09:58.680 (598.680)	TB4 +22.353	MSFC	--
158	Signal from LVDC for: Telemetry Calibrator Inflight Calibrate OFF	00:09:04.56 (544.56)	TB4 +27.4	IU	00:10:03.702 (603.702)	TB4 +27.375	MSFC	--
159a	Signal from LVDC for: Regular Calibrate Relays ON	00:09:08.96 (548.96)	TB4 +31.8	IU	00:10:08.095 (608.095)	TB4 +31.768	MSFC	--
159b	Signal Received in S-IVB for: Regular Calibrate Relays ON	--	--	S-IVB	00:10:08.082 (608.082)	TB4 +31.755	DAC (FM)	13
160a	Signal from LVDC for: Regular Calibrate Relays OFF	00:09:13.96 (553.96)	TB4 +36.8	IU	00:10:13.080 (613.080)	TB4 +36.753	MSFC	--
160b	Signal Received in S-IVB for: Regular Calibrate Relays OFF	--	--	S-IVB	00:10:13.070 (613.070)	TB4 +36.743	DAC (FM)	13
161	Introduction of Chi Tilde Guidance Mode	00:10:22.5 (622.5)	N/A	IU	00:11:52.3 (712.3)	N/A	MSFC	--
162a	Signal from LVDC for: Engine Pump Purge Control Valve Enable ON	00:10:43.76 (643.76)	TB5 -7.0	IU	00:12:26.913 (746.913)	TB5 -.395	MSFC	--
162b	Signal Received in S-IVB for: Engine Pump Purge Control Valve Enable ON	--	--	S-IVB	00:12:26.903 (746.903)	TB5 -.394	DAC (FM)	13
163	Freeze Body Attitude (Chi Freeze)	00:10:49.5 (649.5)	N/A	IU	00:12:26.4 (746.4)	N/A	MSFC	--
164a	Signal from LVDC for: S-IVB Engine Cutoff (Guidance Cutoff)	00:10:57.1 (657.1)	N/A	IU	00:12:27.041 (747.041)	N/A	MSFC	13
164b	Signal Received in S-IVB for: S-IVB Engine Cutoff (Guidance Cutoff)	--	--	S-IVB	00:12:27.032 (747.032)	N/A	DAC (FM)	13
165	Cutoff S-IVB Engine Interrupt 1520	00 :10:57.1 (657.1)	N/A	IU	00:12:27.30 (747.30)	N/A	MSFC	--

TABLE 5-1 (Sheet 14 of 40)
AS-502 SEQUENCE OF EVENTS

ITEM NO.	EVENT	PREDICTED TIME		SIGNAL MONITORED AT	MONITORED TIME		DATA SOURCE	ACCURACY (ms)
		TIME FROM RANGE ZERO (hr:min:sec) (sec)	TIME FROM BASE (sec)		TIME FROM RANGE ZERO* (hr:min:sec) (sec)	TIME FROM BASE (sec)		
	TIME BASE 5							
166	LVDC Initiates TB5 Maintain Cutoff Inertial Attitude	00:10:57.1 (657.1)	TB5 +0.0	IU	00:12:27.29 (747.298)	TB5 +0.0	MSFC	--
167a	LVDC Sends Redundant Signal for: S-IVB Engine Cutoff	--	--	IU	00:12:27.380 (747.380)	TB5 +.082	MSFC	--
167b	Signal Received in S-IVB for: S-IVB Engine Cutoff (Redundant Signal)	--	--	S-IVB	00:12:27.37 (747.371)	TB5 +.073	DAC (FM)	13
168a	Signal from LVDC for: Point Level Sensor Disarming	00:10:57.2 (657.2)	TB5 +0.1	IU	00:12:27.473 (747.473)	TB5 +.175	MSFC	--
168b	Signal Received in S-IVB for: Point Level Sensor Disarming	--	--	S-IVB	00:12:27.463 (747.463)	TB5 +.165	DAC (FM)	13
169	S-IVB J-2 Thrust Decay to 5% (Average)	--	--	N/A	00:12:27.496 (747.496)	N/A	DAC	--
170a	Signal from LVDC for: S-IVB Ullage Engine No. 1 ON	00:10:57.4 (657.4)	TB5 +0.3	IU	00:12:27.565 (747.565)	TB5 +.267	MSFC	--
170b	Signal Received in S-IVB for: S-IVB Ullage Engine No. 1 ON	--	--	S-IVB	00:12:27.556 (747.556)	TB5 +.258	DAC (FM)	--
171a	Signal from LVDC for: S-IVB Ullage Engine No. 2 ON	00:10:57.5 (657.5)	TB5 +0.4	IU	00:12:27.659 (747.659)	TB5 +.361	MSFC	--
171b	Signal Received in S-IVB for: S-IVB Ullage Engine No. 2 ON	--	--	S-IVB	00:12:27.652 (747.652)	TB5 +.354	DAC (FM)	13
172	Signal from LVDC for: Ullage Thrust Present ON	00:10:57.7 (657.7)	TB5 +0.6	IU	00:12:27.869 (747.869)	TB5 +.571	MSFC	--
173a	Signal from LVDC for: First Burn Relay OFF	00:10:57.8 (657.8)	TB5 +0.7	IU	00:12:27.966 (747.966)	TB5 +.668	MSFC	--
173b	Signal Received in S-IVB for: First Burn Relay OFF	--	--	S-IVB	00:12:27.958 (747.958)	TB5 +.660	DAC (FM)	13
174a	Signal from LVDC for: PU Activate OFF	00:10:57.0 (658.0)	TB5 +0.9	IU	00:12:28.153 (748.153)	TB5 +.855	MSFC	--
174b	Signal Received in S-IVB for: PU Activate OFF	--	--	S-IVB	00:12:28.143 (748.143)	TB5 +.845	DAC (FM)	13
175a	Signal from LVDC for: LOX Tank Flight Pressure System OFF	00:10:58.2 (658.2)	TB5 +1.1	IU	00:12:28.359 (748.359)	TB5 +1.061	MSFC	--

TABLE 5-1 (Sheet 15 of 40)
AS-502 SEQUENCE OF EVENTS

ITEM NO.	EVENT	PREDICTED TIME		SIGNAL MONITORED AT	MONITORED TIME		DATA SOURCE	ACCURACY (ms)
		TIME FROM RANGE ZERO (hr:min:sec) (sec)	TIME FROM BASE (sec)		TIME FROM RANGE ZERO* (hr:min:sec) (sec)	TIME FROM BASE (sec)		
175b	Signal Received in S-IVB for: LOX Tank Flight Pressure System OFF	--	--	S-IVB	00:12:28.352 (748.352)	TB5 +1.054	DAC (FM)	13
176a	Signal from LVDC for: Coast Period ON	00:10:58.4 (658.4)	TB5 +1.3	IU	00:12:28.551 (748.551)	TB5 +1.253	MSFC	--
176b	Signal Received in S-IVB for: Coast Period ON	--	--	S-IVB	00:12:28.543 (748.543)	TB5 +1.245	DAC (FM)	13
177a	Signal from LVDC for: Engine Pump Purge Control Valve Enable ON	00:10:58.6 (658.6)	TB5 +1.5	IU	00:12:28.752 (748.752)	TB5 +1.454	MSFC	--
177b	Signal Received in S-IVB for: Engine Pump Purge Control Valve Enable ON	--	--	S-IVB	00:12:28.742 (748.742)	TB5 +1.444	DAC (FM)	13
178a	Signal from LVDC for: PU Fuel Boiloff Bias Cutoff ON	00:10:58.8 (658.8)	TB5 +1.7	IU	00:12:28.967 (748.967)	TB5 +1.669	MSFC	--
178b	Signal Received in S-IVB for: PU Fuel Boiloff Bias Cutoff ON	--	--	S-IVB	00:12:28.962 (748.962)	TB5 +1.664	DAC (FM)	13
179	Signal from LVDC for: Flight Control Computer S-IVB Burn Mode OFF "A"	00:11:00.6 (660.6)	TB5 +3.5	IU	00:12:30.755 (750.755)	TB5 +3.457	MSFC	--
180	Signal from LVDC for: Flight Control Computer S-IVB Burn Mode OFF "B"	00:11:00.8 (660.8)	TB5 +3.7	IU	00:12:30.971 (750.971)	TB5 +3.673	MSFC	--
181a	Signal from LVDC for: Aux. Hydraulic Pump Coast Mode ON	00:11:01.0 (661.0)	TB5 +3.9	IU	00:12:31.151 (751.151)	TB5 +3.853	MSFC	--
181b	Signal Received in S-IVB for: Aux. Hydraulic Pump Coast Mode ON	--	--	S-IVB	00:12:31.110 (751.110)	TB +3.812	DAC (FM)	13
182a	Signal from LVDC for: Aux. Hydraulic Pump Flight Mode OFF	00:11:02.2 (662.2)	TB5 +4.1	IU	00:12:31.367 (751.367)	TB5 +4.069	MSFC	--
182b	Signal Received in S-IVB for: Aux. Hydraulic Pump Flight Mode OFF	--	--	S-IVB	00:12:31.330 (751.330)	TB5 +4.032	DAC (FM)	13
183	Signal from LVDC for: S-IVB Engine Out Indication "A" Enable Reset	00:11:07.1 (667.1)	TB5 +10.0	IU	00:12:37.266 (757.266)	TB5 +9.968	MSFC	--

TABLE 5-1 (Sheet 16 of 40)
AS-502 SEQUENCE OF EVENTS

ITEM NO.	EVENT	PREDICTED TIME		SIGNAL MONITORED AT	MONITORED TIME		DATA SOURCE	ACCURACY (ms)
		TIME FROM RANGE ZERO (hr:min:sec) (sec)	TIME FROM BASE (sec)		TIME FROM RANGE ZERO* (hr:min:sec) (sec)	TIME FROM BASE (sec)		
184	Signal from LVDC for: S-IVB Engine Out Indication "B"	00:11:07.3 (667.3)	TB5 +10.2	IU	00:13:37.452 (757.452)	TB5 +10.154	MSFC	--
185	Enable Reset Parking Orbit Insertion	00:11:08.7 (668.7)	N/A		00:12:28.2 (748.2)	N/A	DAC	--
186	Signal from LVDC for: Telemetry Calibrator Inflight Calibrate ON	00:11:09.3 (669.3)	TB5 +12.2		00:12:39.451 (759.451)	TB5 +12.153	MSFC	--
187a	Signal from LVDC for: Regular Calibrate Relays ON	00:11:09.5 (669.5)	TB5 +12.4		00:12:39.660 (759.660)	TB5 +12.362	MSFC	--
187b	Signal Received in S-IVB for: Regular Calibrate Relays ON	--	--	S-IVB	00:12:34.620 (759.620)	TB5 +12.322	DAC (FM)	--
188	Align Axis with Local Horizontal	00:11:12.1	N/A		00:12:44 (764)	N/A	DAC	--
189	Signal from LVDC for: Telemetry Calibrator Inflight Calibrate OFF	00:11:14.3 (674.3)	TB5 +17.2	IU	00:12:44.470 (764.470)	TB5 +17.172	MSFC	--
190a	Signal from LVDC for: Regular Calibrate Relays OFF	00:11:14.5 (674.5)	TB5 +17.4		00:12:44.652 (764.652)	TB5 +17.354	MSFC	--
190b	Signal Received in S-IVB for: Regular Calibrate Relays OFF	--	--	S-IVB	00:12:44.645 (764.645)	TB5 +17.302	DAC	--
191a	Signal from LVDC for: SSB Transmitter OFF	00:11:19.1 (679.1)	TB5 +22.0	IU	00:12:49.255 (769.255)	TB5 +21.957	MSFC	--
191b	Signal Received in S-IVB for: SSB Transmitter Group OFF	--	--	S-IVB	00:12:49.248 (769.248)	TB5 +21.950	DAC (FM)	13
192a	Signal from LVDC for: SSB Group OFF	00:11:19.3 (679.3)	TB5 +22.2	IU	00:12:49.459 (769.459)	TB5 +22.161	MSFC	--
192b	Signal Received in S-IVB for: SSB Group OFF	--	--	S-IVB	00:12:49.452 (769.452)	TB5 +22.154	DAC (FM)	13
193a	Signal from LVDC for: LH2 Tank Continuous Vent Valve Open ON	00:11:56.1 (716.1)	TB5 +59.0	IU	00:13:26.251 (806.251)	TB5 +58.953	MSFC	--
193b	Signal Received in S-IVB for: LH2 Tank Continuous Vent Valve Open ON	--	--	S-IVB	00:13:26.22 (806.22)	TB5 +58.922	DAC (FM)	13
194a	Signal from LVDC for: LH2 Tank Continuous Vent Valve Open OFF	00:11:58.1 (718.1)	TB5 +61.0	IU	00:13:28.257 (808.257)	TB5 +60.959	MSFC	--
194b	Signal Received in S-IVB for: LH2 Tank Continuous Vent Valve Open OFF	--	--	S-IVB	00:13:28.22 (808.22)	TB5 +60.922	DAC (FM)	13

TABLE 5-1 (Sheet 17 of 40)
AS-502 SEQUENCE OF EVENTS

ITEM NO.	EVENT	PREDICTED TIME		SIGNAL MONITORED AT	MONITORED TIME		DATA SOURCE	ACCURACY (ms)
		TIME FROM RANGE ZERO (hr:min:sec) (sec)	TIME FROM BASE (sec)		TIME FROM RANGE ZERO* (hr:min:sec) (sec)	TIME FROM BASE (sec)		
195a	Signal from LVDC for: S-IVB Ullage Engine No. 1 OFF	00:12:25.1 (745.1)	TB5 +88.0	IU	00:13:55.251 (835.251)	TB5 +87.953	MSFC	--
195b	Signal Received in S-IVB for: Ullage Engine No. 1 OFF	--	--	S-IVB	00:13:55.21 (835.21)	TB5 +87.912	DAC (FM)	13
196a	Signal from LVDC for: S-IVB Ullage Engine No. 2 OFF	00:12:25.2 (745.2)	TB5 +88.1	IU	00:13:55.350 (835.350)	TB5 +88.052	MSFC	--
196b	Signal Received in S-IVB for: S-IVB Ullage Engine No. 2 OFF	--	--	S-IVB	00:13:55.31 (835.31)	TB5 +88.012	DAC (FM)	13
197	Signal from LVDC for: S-IVB Ullage Thrust Present OFF	00:12:25.4 (745.4)	TB5 +88.3	IU	00:13:55.560 (835.560)	TB5 +88.262	MSFC	--
198a	Signal from LVDC for: Emergency Playback Enable ON	00:12:25.6 (745.6)	TB5 +88.5	IU	00:13:55.75 (835.75)*	TB5 +88.452	MSFC	--
198b	Signal Received in S-IVB for: Emergency Playback Enable ON	--	--	S-IVB	00:13:55.71 (835.71)	TB5 +88.412	DAC (FM)	13
199	Signal from LVDC for: Tape Recorder Playback Reverse ON	00:12:26.3 (746.3)	TB5 +89.2	IU	00:13:56.452 (836.452)	TB5 +89.154	MSFC	--
200	Roll 180° to Position III Down	00:12:37.1	N/A	N/A	00:13:57 (837)	N/A	DAC	--
201a	Signal from LVDC for: Emergency Playback Enable OFF	00:13:38.6 (818.6)	TB5 +161.5	IU	00:15:08.75 (908.75)*	TB5 +161.452	MSFC	--
201b	Signal Received in S-IVB for: Emergency Playback Enable OFF	--	--	S-IVB	00:15:08.72 (908.72)	TB5 +161.422	DAC (FM)	13
202a	Signal from LVDC for: Slow Record ON	00:13:39.3 (819.3)	TB5 +162.2	IU	00:15:09.45 (909.45)*	TB5 +162.152	MSFC	--
202b	Signal Received in S-IVB for: Slow Record ON	--	--	S-IVB	00:15:09.42 (909.42)	TB5 +162.122	DAC (FM)	13
203a	Signal from LVDC for Slow Record ON	00:13:49.3 (829.3)	TB5 +172.2	IU	00:15:19.45 (919.45)*	TB5 +172.152	MSFC	--
203b	Signal Received in S-IVB for: Slow Record ON	--	--	S-IVB	00:15:19.42 (919.42)	TB5 +172.122	DAC (FM)	13
204	Signal from LVDC for: Tape Recorder Playback Reverse OFF	00:13:50.3 (830.3)	TB5 +173.2	IU	00:15:20.45 (920.45)*	TB5 +173.152	MSFC	--
205	Signal from LVDC for: Water Coolant Valve Closed		Variable	IU	00:18:04.077 (1084.077)	TB5 +336.779	MSFC	--
206	S-II Impact	00:19:41.158 (1,181.158)	N/A	N/A	00:20:51.24 (1,251.24)	N/A	MSFC	--

TABLE 5-1 (Sheet 18 of 40)
AS-502 SEQUENCE OF EVENTS

ITEM NO.	EVENT	PREDICTED TIME		SIGNAL MONITORED AT	MONITORED TIME		DATA SOURCE	ACCURACY (ms)
		TIME FROM RANGE ZERO (hr:min:sec) (sec)	TIME FROM BASE (sec)		TIME FROM RANGE ZERO* (hr:min:sec) (sec)	TIME FROM BASE (sec)		
207a	Signal from LVDC for: Engine Pump Purge Control Valve Enable OFF	00:20:59.7 (1,259.7)	TB5 +602.6	IU	00:22:29.85 (1,349.85)*	TB5 +602.552	MSFC	--
207b	Signal Received in S-IVB for: Engine Pump Purge Control Valve Enable OFF	--	--	S-IVB	00:22:29.852 (1,349.852)	TB5 +602.554	DAC (FM)	13
208a	Signal from LVDC for: Slow Record ON	00:37:50.6 (2,270.6)	TB5 +1,613.5	IU	00:39:20.75 (2,360.75)*	TB5 +1,613.452	MSFC	--
208b	Signal Received in S-IVB for: Slow Record ON	--	--	S-IVB	00:39:20.70 (2,360.70)	TB5 +1,613.402	DAC (FM)	13
209a	Signal from LVDC for: Slow Record OFF	00:38:22.6 (2,302.6)	TB5 +1,645.4	IU	00:39:52.75 (2,392.75)*	TB5 +1,645.452	MSFC	--
209b	Signal Received in S-IVB for: Slow Record OFF	--	--	S-IVB	00:39:52.70 (2,392.70)	TB5 +1,645.402	DAC (FM)	13
210a	Signal from LVDC for: Recorder Playback ON	00:38:22.8 (2,302.8)	TB5 +1,645.7	IU	00:39:52.95 (2,392.95)*	TB5 +1,645.652	MSFC	--
210b	Signal Received in S-IVB for: Recorder Playback ON	--	--	S-IVB	00:39:52.90 (2,392.90)	TB5 +1,645.602	DAC (FM)	13
211a	Signal from LVDC for Recorder Playback OFF	00:41:10.6 (2,470.6)	TB5 +1,813.5	IU	00:42:40.75 (2,560.75)*	TB5 +1,813.452	MSFC	--
211b	Signal Received in S-IVB for: Recorder Playback OFF	--	--	S-IVB	00:42:40.72 (2,560.72)	TB5 +1,813.422	DAC (FM)	13
212a	Signal from LVDC for: Slow Record ON	00:41:10.8 (2,470.8)	TB5 +1,813.7	IU	00:42:40.95 (2,560.95)*	TB5 +1,813.652	MSFC	--
212b	Signal Received in S-IVB for: Slow Record ON	--	--	S-IVB	00:42:40.92 (2,560.92)	TB5 +1,813.622	DAC (FM)	13
213a	Signal from LVDC for: Slow Record ON	00:41:20.8 (2,480.8)	TB5 +1,823.7	IU	00:42:50.95 (2,570.95)*	TB5 +1,823.652	MSFC	--
213b	Signal Received in S-IVB for: Slow Record ON	--	--	S-IVB	00:42:50.92 (2,570.92)	TB5 +1,823.622	DAC (FM)	13
214	Initiate 20° Pitch Down	00:51:57.1 (3,117.1)	N/A	N/A	00:53:27 (3,207)	N/A	DAC	--
215	Signal from LVDC for: Telemetry Calibrator Inflight Calibrate ON	00:54:10.6 (3,250.6)	TB5 +2,593.5	IU	00:55:40.251 (3,340.751)	TB5 +2,593.453	MSFC	--
216a	Signal from LVDC for: Regular Calibrate Relays ON	00:54:10.8 (3,240.8)	TB5 +2,593.7	IU	00:55:40.951 (3,340.951)	TB5 +2,593.653	MSFC	--
216b	Signal Received in S-IVB for: Regular Calibrate Relays ON	--	--	S-IVB	00:55:40.96 (3,340.96)	TB5 +2,593.655	DAC (FM)	13

TABLE 5-1 (Sheet 19 of 40)
AS-502 SEQUENCE OF EVENTS

ITEM NO.	EVENT	PREDICTED TIME		SIGNAL MONITORED AT	MONITORED TIME		DATA SOURCE	ACCURACY (ms)
		TIME FROM RANGE ZERO (hr:min:sec) (sec)	TIME FROM BASE (sec)		TIME FROM RANGE ZERO* (hr:min:sec) (sec)	TIME FROM BASE (sec)		
217	Signal from LVDC for: Telemetry Calibrator Inflight Calibrate OFF	00:54:15.6 (3,245.6)	TB5 +2,598.5	IU	00:55:45.772 (3,345.772)	TB5 +2,598.474	MSFC	--
218a	Signal from LVDC for: Regular Calibrate Relays OFF	00:54:15.8 (3,245.8)	TB5 +2,598.7	IU	00:55:45.963 (3,345.963)	TB5 +2,598.665	MSFC	--
218b	Signal Received in S-IVB for: Regular Calibrate Relays OFF	--	--	S-IVB	00:55:46.02 (3,346.02)	TB5 +2,598.722	DAC (FM)	13
219	Signal from LVDC for: C-Band Transponder No. 1 and No. 2 ON		Variable	IU	00:59:40.803 (3,580.803)	TB5 +2,833.505	MSFC	--
220	Signal from LVDC for: C-Band Transponder No. 1 OFF		Variable	IU	00:59:40.872 (3,580.872)	TB5 +2,833,574	MSFC	--
221	Signal from LVDC for: Telemetry Calibrator Inflight Calibrate ON	01:28:15.6 (5,295.6)	TB5 +4,638.5	IU	01:29:45.75 (5,385.75)*	TB5 +4,638.452	MSFC	--
222a	Signal from LVDC for: Slow Record ON	01:28:15.8 (5,295.8)	TB5 +4,638.7	IU	01:29:45.95 (5,385.95)*	TB5 +4,638.652	MSFC	13
222b	Signal Received in S-IVB for: Slow Record ON	--	--	S-IVB	01:29:45.95 (5,385.93)	TB5 +4,638.632	DAC (FM)	13
223a	Signal from LVDC for: Regular Calibrate Relays ON	01:28:16.0 (5,296.0)	TB5 +4,638.9	IU	01:29:46.15 (5,386.15)*	TB5 +4,638.822	MSFC	--
223b	Signal Received in S-IVB for: Regular Calibrate Relays ON	--	--	S-IVB	01:29:46.12 (5,386.12)	TB5 +4,638.822	DAC (FM)	13
224	Signal from LVDC for: Telemetry Calibrate OFF	01:28:20.6 (5,300.6)	TB5 +4,643.5	IU	01:29:50.749 (5,390.749)	TB5 +4,643.451	MSFC	--
225a	Signal from LVDC for: Regular Calibrate Relays OFF	01:28:21.0 (5,301.0)	TB5 +4,643.9	IU	01:29:51.150 (5,391.150)	TB5 +4,643.852	MSFC	--
225b	Signal Received in S-IVB for: Regular Calibrate Relays OFF	--	--	S-IVB	01:29:51.11 (5,391.11)	TB5 +4,643.812	DAC (FM)	13
226a	Signal from LVDC for: Slow Record OFF	01:28:47.8 (5,327.8)	TB5 +4,670.7	IU	01:30:17.951 (5,417.951)	TB5 +4,670.653	MSFC	--
226b	Signal Received in S-IVB for: Slow Record OFF	--	--	S-IVB	01:30:17.95 (5,417.95)	TB5 +4,670.652	DAC (FM)	13
227a	Signal from LVDC for: Recorder Playback ON	01:28:48.2 (5,328.2)	TB5 +4,671.1	IU	01:30:18.351 (5,418.351)	TB5 +4,671.053	MSFC	--
227b	Signal Received in S-IVB for: Recorder Playback ON	--	--	S-IVB	01:30:18.33 (5,418.33)	TB5 +4,671.032	DAC (FM)	13
228	Initiate 90° Pitch Up Maneuver	01:28:57.1 (5,337.1)	N/A		01:30:27 (5,427)	N/A	DAC	--
229a	Signal from LVDC for: Recorder Playback OFF	01:34:44.6 (5,684.6)	TB5 +5,027.5	IU	01:36:14.751 (5,774.751)	TB5 +5,027.453	MSFC	--

TABLE 5-1 (Sheet 20 of 40)
AS-502 SEQUENCE OF EVENTS

ITEM NO.	EVENT	PREDICTED TIME		SIGNAL MONITORED AT	MONITORED TIME		DATA SOURCE	ACCURACY (ms)
		TIME FROM RANGE ZERO (hr:min:sec) (sec)	TIME FROM BASE (sec)		TIME FROM RANGE ZERO* (hr:min:sec) (sec)	TIME FROM BASE (sec)		
229b	Signal Received in S-IVB for: Recorder Playback OFF	--	--	S-IVB	01:36:14.71 (5,774.71)	TB5 +5,027.412	DAC (FM)	13
230a	Signal from LVDC for: Slow Record ON	01:34:45.0 (5,685.0)	TB5 +5,027.9	IU	01:36:15.151 (5,775.151)	TB5 +5,027.853	MSFC	--
230b	Signal Received in S-IVB for: Slow Record ON	--	--	S-IVB	01:36:15.09 (5,775.09)	TB5 +5,027.792	DAC (FM)	13
231	Roll 180° (Position I Down)	01:34:45.73 (5,685.73)	N/A	--	01:36:27 (5,787)	N/A	DAC	--
232a	Signal from LVDC for: Slow Record ON	01:34:55.0 (5,695.0)	TB5 +5,037.9	IU	01:36:15.152 (5,785.152)	TB5 +5,037.854	MSFC	--
232b	Signal Received in S-IVB for: Slow Record ON	--	--	S-IVB	01:36:25.12 (5,785.12)	TB5 +5,037.822	DAC (FM)	13
233	Roll 180° to Position I Down	01:34:57.1 (5,697.1)	TB5 +5,040.0	N/A	01:36:27 (5,787)	TB5 +5,040	DAC	--
234	Signal from LVDC for: C-Band Transponder No. 1 & No. 2 ON		Variable	IU	01:37:01.509 (5,821.509)	TB5 +5,074.211	MSFC	--
235	Signal from LVDC for: C-Band Transponder No. 1 OFF		Variable	IU	01:37:01.580 (5,821.580)	TB5 +5,074.282	MSFC	--
236	Signal from LVDC for: Water Coolant Valve Open		Variable	IU	01:38:11.178 (5,891.178)	TB5 +5,143.880	MSFC	--
237	Signal from LVDC for: C-Band Transponder No. 1 & No. 2 ON		Variable	IU	01:38:45.512 (5,925.512)	TB5 +5,178.214	MSFC	--
238	Signal from LVDC for: C-Band Transponder No. 2 OFF		Variable	IU	01:38:45.582 (5,925.582)	TB5 +5,178.284	MSFC	--
239	Signal from LVDC for: Water Coolant Valve Closed		Variable	IU	01:43:11.646 (6,191.646)	TB5 +5,444.348	MSFC	--
240	Signal from LVDC for: Telemetry Calibrator Inflight Calibrate ON	01:44:10.6 (6,250.6)	TB5 +5,593.5	IU	01:45.751 (6,340.751)	TB5 +5,593.453	MSFC	--
241a	Signal from LVDC for: Regular Calibrate Relays ON	01:44:10.8 (6,250.8)	TB5 +5,593.7	IU	01:45:40.951 (6,340.951)	TB5 +5,593.653	MSFC	--
241b	Signal Received in S-IVB for: Regular Calibrate Relays ON	--	--	S-IVB	01:45:40.92 (6,340.92)	TB5 +5,593.622	DAC (FM)	13
242	Signal from LVDC for: Telemetry Calibrator Inflight Calibrate OFF	01:44:15.6 (6,255.6)	TB5 +5,598.5	IU	01:45:45.757 (6,345.757)	TB5 +5,598.459	MSFC	--

TABLE 5-1 (Sheet 21 of 40)
AS-502 SEQUENCE OF EVENTS

ITEM NO.	EVENT	PREDICTED TIME		SIGNAL MONITORED AT	MONITORED TIME		DATA SOURCE	ACCURACY (ms)
		TIME FROM RANGE ZERO (hr:min:sec) (sec)	TIME FROM BASE (sec)		TIME FROM RANGE ZERO* (hr:min:sec) (sec)	TIME FROM BASE (sec)		
243a	Signal from LVDC for: Regular Calibrate Relays OFF	01:44:15.8 (6,255.8)	TB5 +5,598.7	IU	01:45:45.957 (6,345.957)	TB5 +5,598.659	MSFC	--
243b	Signal Received in S-IVB for: Regular Calibrate Relays OFF	--	--	S-IVB	01:45:45.92 (6,345.92)	TB5 +5,598.622	DAC (FM)	13
244	Signal from LVDC for: C-Band Transponder No. 1 & No. 2 ON		Variable	IU	01:50:37.210 (6,637.210)	TB5 +5,889.912	MSFC	--
245	Signal from LVDC for: C-Band Transponder No. 1 OFF		Variable	IU	01:50:37.281 (6,637.281)	TB5 +5,889.983	MSFC	--
246a	Signal from LVDC for: Slow Record ON	02:10:17.6 (7,817.6)	TB5 +7,160.5	IU	02:11:47.75 (7,907.75)*	TB5 +7,160.452	MSFC	--
246b	Signal Received in S-IVB for: Slow Record ON	--	--	S-IVB	02:11:47.73 (7,907.73)	TB5 +7,160.432	DAC (FM)	13
247a	Signal from LVDC for: Slow Record OFF	02:10:49.6 (7,849.6)	TB5 +7,192.5	IU	02:12:19.765 (7,939.765)*	TB5 +7,192.476	MSFC	--
247b	Signal received in S-IVB for: Slow Record OFF	--	--	S-IVB	02:12:19.72 (7,939.72)	TB5 +7,192.422	DAC (FM)	13
248a	Signal from LVDC for: Recorder Playback ON	02:10:49.8 (7,849.8)	TB5 +7,192.7	IU	02:12:19.965 (7,939.965)*	TB5 +7,192.667	MSFC	--
248b	Signal Received in S-IVB for: Recorder Playback ON	--	--	S-IVB	02:12:19.92 (7,939.92)	TB5 +7,192.622	DAC (FM)	13
249	Signal from LVDC for: Water Coolant Valve Closed		Variable	IU	02:13:15.446 (7,995.446)	TB5 +7,248.148	MSFC	--
250a	Signal from LVDC for: Recorder Playback OFF	02:15:20.4 (8,120.4)	TB5 +7,463.3	IU	02:16:50.55 (8,210.55)*	TB5 +7,463.252	MSFC	--
250b	Signal Received in S-IVB for: Recorder Playback OFF	--	--	S-IVB	02:16:50.50 (8,210.50)	TB5 +7,463.202	DAC (FM)	13
251a	Signal from LVDC for: Slow Record ON	02:15:20.6 (8,120.6)	TB5 +7,463.5	IU	02:16:50.75 (8,210.75)*	TB5 +7,463.452	MSFC	--
251b	Signal Received in S-IVB for: Slow Record ON	--	--	S-IVB	02:16:50.70 (8,210.70)	TB5 +7,463.402	DAC (FM)	13
252a	Signal from LVDC for: Slow Record ON	02:15:30.6 (8,130.6)	TB5 +7,473.5	IU	02:17:00.752 (8,220.752)*	TB5 +7,473.454	MSFC	--
252b	Signal Received in S-IVB for: Slow Record ON	--	--	S-IVB	02:17:00.70 (8,220.70)	TB5 +7,473.402	DAC (FM)	13
253a	Signal from LVDC for: Regular Calibrate Relays ON	02:28:10.6 (8,890.6)	TB5 +8,233.5	IU	02:29:40.752 (8,980.752)	TB5 +8,233.454	MSFC	--
253b	Signal Received in S-IVB for: Regular Calibrate Relays ON	--	--	S-IVB	02:29:40.74 (8,980.74)	TB5 +8,233.442	DAC (FM)	13

TABLE 5-1 (Sheet 22 of 40)
AS-502 SEQUENCE OF EVENTS

ITEM NO.	EVENT	PREDICTED TIME		SIGNAL MONITORED AT	MONITORED TIME		DATA SOURCE	ACCURACY (ms)
		TIME FROM RANGE ZERO (hr:min:sec) (sec)	TIME FROM BASE (sec)		TIME FROM RANGE ZERO* (hr:min:sec) (sec)	TIME FROM BASE (sec)		
254	Signal from LVDC for: Telemetry Calibrator Inflight Calibrate ON	02:28:10.8 (8,890.8)	TB5 +8,233.7	IU	02:29:40.952 (8,980.952)	TB5 +8,233.654	MSFC	--
255a	Signal from LVDC for: Regular Calibrate Relays OFF	02:28:15.6 (8,895.6)	TB5 +8,238.5	IU	02:29:45.751 (8,985.751)	TB5 +8,238.453	MSFC	--
255b	Signal Received in S-IVB for: Regular Calibrate Relays OFF	--	--	S-IVB	02:29:45.70 (8,985.70)	TB5 +8,238.402	DAC (FM)	13
256	Signal from LVDC for: Telemetry Calibrator Inflight Calibrate OFF	02:28:15.8 (8,895.8)	TB5 +8,238.7	IU	02:29:45.951 (8,985.951)	TB5 +8,238.653	MSFC	--
257a	Signal from LVDC for: Slow Record ON	02:52:00.6 (10,320.6)	TB5 +9,663.5	IU	02:53:30.75 (10,410.75)*	TB5 +9,663.452	MSFC	--
257b	Signal Received in S-IVB for: Slow Record ON	--	--	S-IVB	02:53:30:739 (10,410.739)	TB5 +9,663.441	DAC (FM)	13
258a	Signal from LVDC for: Slow Record OFF	02:52:32.6 (10,352.6)	TB5 +9,695.5	IU	02:54:02.75 (10,442.75)*	TB5 +9,695.452	MSFC	--
258b	Signal Received in S-IVB for: Slow Record OFF	--	--	S-IVB	02:54:02.755 (10,442.755)	TB5 +9,695.457	DAC (FM)	13
259a	Signal from LVDC for: Recorder Playback ON	02:52:32.8 (10,352.8)	TB5 +9,695.7	IU	02:54:02.95 (10,442.95)*	TB5 +9,695.652	MSFC	--
259b	Signal Received in S-IVB for: Recorder Playback ON	--	--	S-IVB	02:54:02.949 (10,442.949)	TB5 +9,695.651	DAC (FM)	13
260a	Signal from LVDC for: Recorder Playback OFF	02:56:57.6 (10,377.6)	TB5 +9,960.5	IU	02:58:27.75 (10,707.75)*	TB5 +9,960.452	MSFC	--
260b	Signal Received in S-IVB for: Recorder Playback OFF	--	--	S-IVB	02:58:27.731 (10,707.731)	TB5 +9,960.433	DAC (FM)	13
261a	Signal from LVDC for: Slow Record ON	02:56:57.8 (10,377.8)	TB5 +9,960.7	IU	02:58:27.95 (10,707.95)*	TB5 +9,960.652	MSFC	--
261b	Signal Received in S-IVB for: Slow Record ON	--	--	S-IVB	02:58:27.931 (10,707.931)	TB5 +9,960.633	DAC (FM)	13
262a	Signal from LVDC for: Slow Record ON	02:57:07.8 (10,627.8)	TB5 +9,970.7	IU	02:58:37.95 (10,717.95)*	TB5 +9,970.652	MSFC	--
262b	Signal Received in S-IVB for: Slow Record ON	--	--	S-IVB	02:58:37.935 (10,717.935)	TB5 +9,970.637	DAC (FM)	13
263a	Signal from LVDC for: Aux. Hydraulic Pump Flight Mode ON	02:58:52.1 (10,732.1)	TB5 +10,075.0	IU	03:00:22.25 (10,822.25)*	TB5 +10,074.952	MSFC	--
263b	Signal Received in S-IVB for: Aux. Hydraulic Pump Flight Mode ON	--	--	S-IVB	03:00:22.231 (10,822.231)	TB5 +10,074.933	DAC (FM)	13

TABLE 5-1 (Sheet 23 of 40)
AS-502 SEQUENCE OF EVENTS

ITEM NO.	EVENT	PREDICTED TIME		SIGNAL MONITORED AT	MONITORED TIME		DATA SOURCE	ACCURACY (ms)
		TIME FROM RANGE ZERO (hr:min:sec) (sec)	TIME FROM BASE (sec)		TIME FROM RANGE ZERO* (hr:min:sec) (sec)	TIME FROM BASE (sec)		
264a	Signal from LVDC for: Aux. Hydraulic Pump Coast Mode OFF	02:58:52.3 (10,732.3)	TB5 +10,075.2	IU	03:00:22.45 (10,822.45)*	TB5 +10,075.152	MSFC	--
264b	Signal Received in S-IVB for: Aux. Hydraulic Pump Coast Mode OFF	--	--	S-IVB	03:00:22.435 (10,822.435)	TB5 +10,075.147	DAC (FM)	13
265a	Signal from LVDC for: LOX Chilldown Pump ON	02:59:42.1 (10,782.1)	TB5 +10,125.0	IU	03:01:12.25 (10,872.25)*	TB5 +10,124.952	MSFC	--
265b	Signal Received in S-IVB for: LOX Chilldown Pump ON	--	--	S-IVB	03:01:12.205 (10,872.205)	TB5 +10,124.907	DAC (PCM)	25
266a	Signal from LVDC for: Fuel Chilldown Pump ON	02:59:47.1 (10,787.1)	TB5 +10,130.0	IU	03:01:17.225 (10,877.25)*	TB5 +129.952	MSFC	--
266b	Signal Received in S-IVB for: Fuel Chilldown Pump ON	--	--	S-IVB	03:01:17.225 (10,877.225)	TB5 +10,129.927	DAC (PCM)	25
267a	Signal from LVDC for: Prevalves Close ON	02:54:57.1 (10,747.1)	TB5 +10,140.0	IU	03:01:27.25 (10,887.25)*	TB5 +10,139.952	MSFC	--
267b	Signal Received in S-IVB for: Prevalves Close ON	--	--	S-IVB	03:01:27.225 (10,887.225)	TB5 +10,139.927	DAC (PCM)	25
268	Signal from LVDC for: C-Band Transponder No. 1 & No. 2 ON		Variable	IU	03:04:29.038 (11,069.038)	N/A	MSFC	--
269	Signal from LVDC for: C-Band Transponder No. 2 OFF		Variable	IU	03:04:29.038 (11,069.109)	N/A	MSFC	--
270	Signal from LVDC for: Telemetry Calibrator Inflight Calibrate ON	03:06:10.6 (11,170.6)	TB5 +10,513.5	IU	03:07:40.751 (11,260.751)	TB5 +10,513.453	MSFC	--
271a	Signal from LVDC for: Regular Calibrate Relays ON	03:06:10.8 (11.170.8)	TB5 +10,513.7	IU	03:07:40.950 (11,260.950)	TB5 +10,513.652	MSFC	--
271b	Signal Received in S-IVB for: Regular Calibrate Relays ON	--	--	S-IVB	03:07:40.93 (11,260.93)	TB5 +10,513.632	DAC (FM)	13
272	Signal from LVDC for: Telemetry Calibrator Inflight Calibrate OFF	03:06:15.6 (11,175.6)	TB5 +10,518.5	IU	03:07:45.757 (11,265.757)	TB5 +10,518.459	MSFC	--
273a	Signal from LVDC for: Regular Calibrate Relays OFF	03:06:15.8 (11,175.8)	TB5 +10,518.7	IU	03:07:45.956 (11,265.956)	TB5 +10,518.658	MSFC	--
273b	Signal Received in LVDC for: Regular Calibrate Relays OFF	--	--	S-IVB	03:07:45.93 (11,265.93)	TB5 +10,518.632	DAC (FM)	13

TABLE 5-1 (Sheet 24 of 40)
AS-502 SEQUENCE OF EVENTS

ITEM NO.	EVENT	PREDICTED TIME		SIGNAL MONITORED AT	MONITORED TIME		DATA SOURCE	ACCURACY (ms)
		TIME FROM RANGE ZERO (hr:min:sec) (sec)	TIME FROM BASE (sec)		TIME FROM RANGE ZERO* (hr:min:sec) (sec)	TIME FROM BASE (sec)		
	TIME BASE 6							
274	Begin Restart Preparations	03:04:34.0 (11,074)	TB6 +0.0	IU	03:08:07.733 (11,287.733)	TB6 +0.0	MSFC	--
275a	Signal from LVDC for: S-IVB Ullage Engine No. 1 ON	03:04:34.2 (11,074.2)	TB6 +0.2	IU	03:08:07.904 (11,287.904)	TB6 +0.171	MSFC	--
275b	Signal Received in S-IVB for: S-IVB Ullage Engine No. 1 ON	--	--	S-IVB	03:08:07.888 (11,287.888)	TB6 +.155	DAC (FM)	13
276a	Signal from LVDC for: S-IVB Ullage Engine No. 2 ON	03:04:34.3 (11,074.3)	TB6 +0.3	IU	03:08:08.005 (11,288.005)	TB6 +.272	MSFC	--
276b	Signal Received in S-IVB for: Ullage Engine No. 2 ON	--	--	S-IVB	03:08:07.989 (11,287.989)	TB6 +.259	DAC (FM)	13
277	Signal from LVDC for: S-IVB Ullage Thrust Present ON	03:04:34.5 (11,074.5)	TB6 +0.5	IU	03:08:08.188 (11,288.188)	TB6 +.455	MSFC	--
278a	Signal from LVDC for: LH2 Tank Vent Valve Boost Close ON	03:04:34.8 (11,074.8)	TB6 +0.8	IU	03:08:08.485 (11,288.485)	TB6 +.752	MSFC	--
278b	Signal Received in S-IVB for: LH2 Tank Vent Valve Boost Close ON	--	--	S-IVB	03:08:08.464 (11,288.464)	TB6 +.731	DAC (FM)	13
279a	Signal from LVDC for: LOX Tank Vent Valve Boost Close ON	03:04:35.0 (11,075.0)	TB6 +1.0	IU	03:08:08.691 (11,288.691)	TB6 +.958	MSFC	--
279b	Signal Received in S-IVB for: LOX Tank Vent Valve Boost Close ON	--	--	S-IVB	03:08:08.672 (11,288.672)	TB6 +.939	DAC (FM)	13
280a	Signal from LVDC for: Continuous Vent Valve Close ON	03:04:35.2 (11,075.2)	TB6 +1.2	IU	03:08:08.886 (11,288.886)	TB6 +1.153	MSFC	--
280b	Signal Received in S-IVB for: Continuous Vent Valve Close ON	--	--	S-IVB	03:08:08.867 (11,288.867)	TB6 +1.134	DAC (FM)	13
281	Signal from LVDC for: C-Band Transponders No. 1 & No. 2 ON	03:04:35.0 (11,075.0)	TB6 +1.4		02:08:09.086 (11,289.086)	TB6 +1.353	MSFC	--
282a	Signal from LVDC for: LH2 Tank Vent Valve Boost Close OFF	03:04:36.8 (11,076.8)	TB6 +2.8	IU	03:08:10.486 (11,290.486)	TB6 +2.753	MSFC	--
282b	Signal Received in S-IVB for: LH2 Tank Vent Valve Boost Close OFF	--	--	S-IVB	03:08:10.47 (11,290.470)	TB6 +2.857	DAC (FM)	13

TABLE 5-1 (Sheet 25 of 40)
AS-502 SEQUENCE OF EVENTS

ITEM NO.	EVENT	PREDICTED TIME		SIGNAL MONITORED AT	MONITORED TIME		DATA SOURCE	ACCURACY (ms)
		TIME FROM RANGE ZERO (hr:min:sec) (sec)	TIME FROM BASE (sec)		TIME FROM RANGE ZERO* (hr:min:sec) (sec)	TIME FROM BASE (sec)		
283a	Signal from LVDC for: LOX Tank Vent Valve Boost Close OFF	03:04:37.0 (11,077)	TB6 +3.0	IU	03:08:10.690 (11,290.690)	TB6 +2.957	MSFC	--
283b	Signal Received in S-IVB for: LOX Tank Vent Valve Boost Close OFF	--	--	S-IVB	03:08:10.674 (11,290.674)	TB6 +2.941	DAC (FM)	13
284a	Signal from LVDC for: Continuous Vent Valve Close OFF	03:04:37.2 (11,077.2)	TB6 +3.2	IU	03:08:10.910 (11,290.910)	TB6 +3.177	MSFC	--
284b	Signal Received in S-IVB for: Continuous Vent Valve Close OFF	--	--	S-IVB	03:08:10.895 (11,290.895)	TB6 +3.162	DAC (FM)	13
285a	Signal from LVDC for: Fuel Chilldown Pump ON	03:04:40.0 (11,080.0)	TB6 +6.0	IU	03:08:13.687 (11,293.687)	TB6 +5.954	MSFC	--
285b	Signal Received in S-IVB for: Fuel Chilldown Pump ON	--	--	S-IVB	03:08:13.667 (11,293.667)	TB6 +5.934	DAC (FM)	13
286a	Signal from LVDC for: LOX Chilldown Pump ON	03:04:45.0 (11,085.0)	TB6 +11.0	IU	03:08:18.686 (11,298.686)	TB6 +10.953	MSFC	--
286b	Signal Received in S-IVB for: LOX Chilldown Pump ON	--	--	S-IVB	03:08:18.671 (11,298.671)	TB6 +10.938	DAC (FM)	13
287a	Signal from LVDC for: Prevalves Close ON	03:04:55.0 (11,095.0)	TB6 +21.0	IU	03:08:28.686 (11,308.686)*	TB6 +20.953	MSFC	--
287b	Signal Received in S-IVB for: Prevalves Close ON	--	--	S-IVB	03:08:28.671 (11,308.671)	TB6 +20.938	DAC (FM)	13
288a	Signal from LVDC for: LOX Repress Valve Open ON	03:06:14.0 (11,174.0)	TB6 +100.0	IU	03:09:37.687 (11,387.687)	TB6 +99.954	MSFC	--
288b	Signal Received in S-IVB for: LOX Repress Valve Open ON	--	--	S-IVB	03:09:37.670 (11,387.670)	TB6 +99.937	DAC (FM)	13
289	Signal from LVDC for: Telemetry Calibration Inflight Calibrate ON	03:07:62.3	TB6 +148.3	IU	03:10:36.004 (11,436.004)	TB6 +148.271	MSFC	--
290a	Signal from LVDC for: Telemetry Calibrate Inflight Calibrate OFF	03:07:07.3 (11,227.3)	TB6 +153.3	IU	03:10:40.985 (11,440.985)	TB6 +153.25	MSFC	--
290b	Initiate Pitch and Yaw Maneuver for Restart Attitude Orientation	03:07:54.0 (11,274.0)	N/A	IU	03:11:27.4 (11,487.4)	N/A	DAC	100
291a	Signal from LVDC for: LH2 Repress Control Valve Open ON	03:07:54.0 (11,274.0)	TB6 +200.0	IU	03:11:27.695 (11,487.695)	TB6 +199.962	MSFC	--

TABLE 5-1 (Sheet 26 of 40)
AS-502 SEQUENCE OF EVENTS

ITEM NO.	EVENT	PREDICTED TIME		SIGNAL MONITORED AT	MONITORED TIME		DATA SOURCE	ACCURACY (ms)
		TIME FROM RANGE ZERO (hr:min:sec) (sec)	TIME FROM BASE (sec)		TIME FROM RANGE ZERO* (hr:min:sec) (sec)	TIME FROM BASE (sec)		
291b	Signal Received in S-IVB for: LH2 Repress Control Valve Open ON	--	--	S-IVB	03:11:27.695 (11,487.695)	TB6 +199.962	DAC (FM)	13
292a	Signal from LVDC for: SSB/FM Group ON	03:08:02.3 (11,282.3)	TB6 +208.3	IU	03:11:35.995 (11,495.995)	TB6 +208.262	MSFC	--
292b	Signal Received in S-IVB for: SSB/FM Group ON	--	--	S-IVB	03:11:35.975 (11,495.975)	TB6 +208.242	DAC (FM)	13
293a	Signal from LVDC for: SSB/FM Transmitter ON	03:08:02.5 (11,282.5)	TB6 +208.5	IU	03:11:36.208 (11,496.208)	TB6 +208.475	MSFC	--
293b	Signal Received in S-IVB for: SSB/FM Transmitter ON	--	--	S-IVB	03:11:36.189 (11,496.189)	TB6 +208.456	DAC (FM)	13
294a	Signal from LVDC for: Regular Calibrate Relays ON	03:09:02.5 (11,342.5)	TB6 +268.5	IU	03:12:36.186 (11,556.186)	TB6 +268.453	MSFC	--
294b	Signal Received in S-IVB for: Regular Calibrate Relays ON	--	--	S-IVB	03:12:36.168 (11,556.168)	TB6 +268.435	DAC (FM)	13
295a	Signal from LVDC for: Regular Calibrate Relays OFF	03:09:07.5 (11,352.5)	TB6 +273.5	IU	03:12:41.197 (11,561.197)	TB6 +273.464	MSFC	--
295b	Signal Received in S-IVB for: Regular Calibrate Relays OFF	--	--	S-IVB	03:12:41.179 (11,561.179)	TB6 +273.446	DAC (FM)	13
296a	Signal from LVDC for: PU Valve Hardover Position ON	03:09:21.0 (11,366.0)	TB6 +287.0	IU	03:12:54.689 (11,574.689)	TB6 +286.956	MSFC	--
296b	Signal Received in S-IVB for: PU Valve Hardover Position ON	--	--	S-IVB	03:12:54.669 (11,574.669)	TB6 +286.936	DAC (FM)	13
297a	Signal from LVDC for: Prevalve Closed OFF	03:09:50.2 (11,390.2)	TB6 +316.2	IU	03:13:23.896 (11,603.896)	TB6 +316.163	MSFC	--
297b	Signal Received in S-IVB for: Prevalve Close OFF	--	--	S-IVB	03:13:23.881 (11,603.881)	TB6 +316.189	DAC (FM)	13
298	Signal from LVDC for: S-IVB Restart Alert	03:09:51.0 (11,391.0)	TB6 +317.0	IU	03:13:24.691 (11,604.691)	TB6 +316.958	MSFC	--
299a	Signal from LVDC for: Engine Cutoff OFF	03:09:59.6 (11,399.6)	TB6 +325.6	IU	03:13:33.290 (11,613.290)	TB6 +325.557	MSFC	--
299b	Signal Received in S-IVB for: Engine Cutoff OFF	--	--	S-IVB	03:13:33.271 (11,613.271)	TB6 +325.579	DAC (FM)	13
300a	Signal from LVDC for: Engine Ready Bypass	03:09:59.8 (11,399.8)	TB6 +325.8	IU	03:13:33.505 (11,613.505)	TB6 +325.772	MSFC	--
300b	Signal Received in S-IVB for: Engine Ready Bypass	--	--	S-IVB	03:13:33.485 (11,613.485)	TB6 +325.793	DAC (FM)	13

TABLE 5-1 (Sheet 27 of 40)
AS-502 SEQUENCE OF EVENTS

ITEM NO.	EVENT	PREDICTED TIME		SIGNAL MONITORED AT	MONITORED TIME		DATA SOURCE	ACCURACY (ms)
		TIME FROM RANGE ZERO (hr:min:sec) (sec)	TIME FROM BASE (sec)		TIME FROM RANGE ZERO* (hr:min:sec) (sec)	TIME FROM BASE (sec)		
301a	Signal from LVDC for: LH2 Repress Control Valve Open OFF	03:10:00.0 (11,400)	TB6 +326.0		03:13:33.686 (11,613.686)	TB6 +325.953	MSFC	--
301b	Signal Received in S-IVB for: LH2 Repress Control Valve Oper OFF	--	--	S-IVB	03:13:33.668 (11,613.668)	TB6 +325.935	DAC	13
302a	Signal from LVDC for: Fuel Chilldown Pump OFF	03:10:00.2 (11,400.2)	TB6 +326.2	IU	03:13:33.899 (11,613.899)	TB6 +326.166	MSFC	--
302b	Signal Received in S-IVB for: Fuel Chilldown Pump OFF	--	--	S-IVB	03:13:33.880 (11,613.880)	TB6 +326.147	DAC (FM)	13
303a	Signal from LVDC for: LOX Chilldown Pump OFF	03:10:00.4 (11,400.4)	TB6 +326.4	IU	03:13:34.087 (11,614.087)	TB6 +326.354	MSFC	--
303b	Signal Received in S-IVB for: LOX Chilldown Pump OFF	--	--	S-IVB	03:13:34.069 (11,614.069)	TB6 +326.336	DAC (FM)	13
304a	Signal from LVDC for: LOX Repress Control Valve Open OFF	03:10:00.8 (11,400.8)	TB6 +326.8	IU	03:13:34.505 (11,614.505)	TB6 +326.772	MSFC	--
304b	Signal Received in S-IVB for: LOX Repress Control Valve Open OFF	--	--	S-IVB	03:13:34.486 (11,614.486)	TB6 +326.767	DAC (FM)	13
305a	Signal from LVDC for: Engine Start ON	03:10:01.0 (11,401.0)	TB6 +327.0	IU	03:13:34.686 (11,614.686)	TB6 +326.953	MSFC	--
305b	Signal Received in S-IVB for: Engine Start ON	--	--	S-IVB	03:13:34.677 (11,614.667)	TB6 +326.936	DAC (FM)	13
305c	J-2 Engine Start Sequence							
	1. Helium Control Solenoid Energized	--	--	S-IVB	03:13:34.667 (11,614.667)	--	DAC (PCM)	25
	2. Main Fuel Valve Close (Dropout)	--	--	S-IVB	03:13:34.729 (11,614.729)	--	DAC (PCM)	25
	3. Main Fuel Valve Open (Pickup)	--	--	S-IVB	03:13:34.752 (11,614.752)	--	DAC (PCM)	25
	4. Gas Generator Valve Closed (Dropout)	--	--	S-IVB	03:13:43.251 (11,623.251)	--	DAC (PCM)	25
	5. Gas Generator Valve Open (Pickup)	--	--	S-IVB	03:13:43.367 (11,623.367)	--	DAC (PCM)	25
	6. Main Oxidizer Valve Leaves Close Position (Dropout)	--	--	S-IVB	03:13:43.239 (11,623.239)	--	DAC (PCM)	25

TABLE 5-1 (Sheet 28 of 40)
AS-502 SEQUENCE OF EVENTS

ITEM NO.	EVENT	PREDICTED TIME		SIGNAL MONITORED AT	MONITORED TIME		DATA SOURCE	ACCURACY (ms)
		TIME FROM RANGE ZERO (hr:min:sec) (sec)	TIME FROM BASE (sec)		TIME FROM RANGE ZERO* (hr:min:sec) (sec)	TIME FROM BASE (sec)		
305d	J-2 Engine Start Sequence (Cont'd)							
	7. Start Tank Discharge Valve Open (Dropout)	--	--	S-IVB	03:13:43.262 (11,623.262)	--	DAC (PCM)	25
	8. Oxidizer Turbine Bypass Valve Open (Dropout)	--	--	S-IVB	03:13:43.342 (11,623.342)	--	DAC (PCM)	25
	9. Oxidizer Turbine Bypass Valve Close (Pickup)	--	--	S-IVB	03:13:43.567 (11,623.567)	--	DAC (PCM)	25
	10. Mainstage OK Pressure Switch 1 (Dropout)	--	--	S-IVB	Not Activated		DAC (PCM)	25
	11. Mainstage OK Pressure Switch 2 (Pickup)	--	--	S-IVB	Not Activated		DAC (PCM)	25
	12. Main Oxidizer Valve Reaches Open Position (Pickup)	--	--	S-IVB	03:13:45.192 (11,625.192)	--	DAC (PCM)	25
	13. Gas Generator Spark System ON (Dropout)	--	--	S-IVB	03:13:46.392 (11,626.392)	--	DAC (PCM)	25
	14. Thrust Chamber Spark System ON (Dropout)	--	--	S-IVB	03:13:46.392 (11,626.392)	--	DAC (PCM)	25
306	Signal from LVDC for: S-IVB Engine Out Indication "A" Enable ON	03:10:01.8 (11,401.8)	TB6 +327.8	IU	03:13:35.486 (11,615.486)	TB6 +327.753	MSFC	--
307	Signal from LVDC for: S-IVB Engine Out Indication "B" Enable ON	03:10:02.0 (11,402.0)	TB6 +328.0	IU	03:13:35.696 (11,615.696)	TB6 +327.963	MSFC	--
308a	Signal from LVDC for: Ullage Engine No. 1 OFF	03:10:04.0 (11,404.0)	TB6 +330.0	IU	03:13:37.686 (11,617.686)	TB6 +329.953	MSFC	--
308b	Signal Received in S-IVB for: Ullage Engine No. 1 OFF	--	--	S-IVB	03:13:37.669 (11,617.669)	TB6 +329.936	DAC (FM)	13
309a	Signal from LVDC for: Ullage Engine No. 2 OFF	03:10:04.1 (11,404.1)	TB6 +330.1	IU	03:13:37.785 (11,617.785)	TB6 +330.052	MSFC	--
309b	Signal Received in S-IVB for: Ullage Engine No. 2 OFF	--	--	S-IVB	03:13:37.767 (11,617.767)	TB6 +330.034	DAC (FM)	13
310	Signal from LVDC for: Ullage Thrust Present OFF	03:10:04.3 (11,404.3)	TB6 +330.3	IU	03:13:37.992 (11,617.992)	TB6 +330.259	MSFC	--
311	Signal from LVDC for: Control Computer S-IVB Burn Mode ON "A"	03:10:08.6 (11,408.6)	TB6 +334.6	IU	03:13:42.286 (11,622.286)	TB6 +334.553	MSFC	--

TABLE 5-1 (Sheet 29 of 40)
AS-502 SEQUENCE OF EVENTS

ITEM NO.	EVENT	PREDICTED TIME		SIGNAL MONITORED AT	MONITORED TIME		DATA SOURCE	ACCURACY (ms)
		TIME FROM RANGE ZERO (hr:min:sec) (sec)	TIME FROM BASE (sec)		TIME FROM RANGE ZERO* (hr:min:sec) (sec)	TIME FROM BASE (sec)		
312	Signal from LVDC for: Computer S-IVB Burn Mode ON "B"	03:10:08.8 (11,408.8)	TB6 +334.8	IU	03:13:42.494 (11,622.494)	TB6 +334.761	MSFC	--
313a	Signal from LVDC for: Injection Temperature OK Bypass	03:10:09.0 (11,409.0)	TB6 +335.0	IU	03:13:42.685 (11,622.685)	TB6 +334.952	MSFC	--
313b	Signal Received in S-IVB for: Injection Temperature OK Bypass	--	--	S-IVB	03:13:42.666 (11,622.666)	TB6 +334.933	DAC (FM)	13
314a	Signal from LVDC for: LOX Tank Flight Press System ON	03:10:09.2 (11,409.2)	TB6 +335.2	IU	03:13:42.899 (11,622.899)	TB6 +335.166	MSFC	--
314b	Signal Received in S-IVB for: Tank Flight Press System ON	--	--	S-IVB	03:13:42.881 (11,622.881)	TB6 +335.148	DAC (FM)	13
315a	Signal from LVDC for: Coast Period OFF	03:10:09.4 (11,409.4)	TB6 +335.4	IU	03:13:43.088 (11,623.088)	TB6 +335.355	MSFC	--
315b	Signal Received in S-IVB for: Coast Period OFF	--	--	S-IVB	03:13:43.069 (11,623.069)	TB6 +335.336	DAC (FM)	13
316a	Signal from LVDC for: Engine Start OFF	03:10:09.6 (11,409.6)	TB6 +335.6	IU	03:13:43.296 (11,623.296)	TB6 +335.563	MSFC	--
316b	Signal Received in S-IVB for: Engine Start OFF	--	--	S-IVB	03:13:43.277 (11,623.277)	TB6 +335.544	DAC (FM)	13
317	J-2 Thrust Buildup (10%)	--	N/A	--	Not Achieved		DAC	10
318	J-2 Thrust Buildup (90%)	03:10:11.4	TB6 +337.4	--	Not Achieved		MSFC	--
319a	Signal from LVDC for: Second Burn Relay ON	03:10:11.6 (11,411.6)	TB6 +337.6	IU	03:12:45.285 (11,625.285)	TB6 +337.552	MSFC	--
319b	Signal Received in S-IVB for: Second Burn Relay ON	--	--	S-IVB	03:12:45.268 (11,625.268)	TB6 +337.535	DAC (FM)	13
320a	Signal from LVDC for: PU Activate ON	03:10:13.8 (11,413.8)	TB6 +339.8	IU	03:12:47.499 (11,627.499)	TB6 +339.766	MSFC	--
320b	Signal Received in S-IVB for: PU Activate ON	--	--	S-IVB	03:12:47.470 (11,627.470)	TB6 +339.737	DAC (FM)	13
321a	Signal from LVDC for: PU Valve Hardover Position OFF	03:10:14.0 (11,414.0)	TB6 +340.0	IU	03:12:47.686 (11,627.686)	TB6 +339.953	MSFC	--
321b	Signal Received in S-IVB for: PU Valve Hardover Position OFF	--	--	S-IVB	03:12:47.669 (11,627.669)	TB6 +339.936	DAC (FM)	13
322	Guidance Initiation	03:10:14.0 (11,414.0)	N/A	IU	03:12:47.73 (11,627.73)	N/A	MSFC	--

TABLE 5-1 (Sheet 30 of 40)
AS-502 SEQUENCE OF EVENTS

ITEM NO.	EVENT	PREDICTED TIME		SIGNAL MONITORED AT	MONITORED TIME		DATA SOURCE	ACCURACY (ms)
		TIME FROM RANGE ZERO (hr:min:sec) (sec)	TIME FROM BASE (sec)		TIME FROM RANGE ZERO* (hr:min:sec) (sec)	TIME FROM BASE (sec)		
323	Start Artificial Tau Mode	03:10:14.0 (11,414.0)	N/A	IU	03:12:47.73 (11,627.73)	N/A	MSFC	--
324	Signal from LVDC for: Fuel Injection Temp OK Bypass Reset	03:10:15.0 (11,415.0)	TB6 +345.0	IU	Not Issued		MSFC	--
325	Signal from LVDC for: Flight Control Computer Switch Point No. 5	03:14:31.0 (11,671.0)	TB6 +597.0	IU	Not Issued		MSFC	--
326	Introduction of Chi Tilde Guidance Mode	03:14:53.0	N/A	IU	Not Achieved		MSFC	--
327	Signal from LVDC for: Freeze Body Attitude (Chi Freeze)	03:15:18.0 (11,718.0)	N/A	IU	Not Achieved		DAC	
328	Signal from LVDC for: Point Level Sensor Arming	03:15:59.2 (11,759.2)	TB6 +663.2	IU	Not Issued		MSFC	--
329a	LVDC Sends Signal for: Cutoff S-IVB Engine (Guidance Cutoff)	03:15:25.6 (11,725.6)	N/A	IU	Not Issued		MSFC	--
329b	S-IVB Receives Signal for: Cutoff S-IVB Engine (Guidance Cutoff)	--	--	S-IVB	Not Issued		DAC (FM)	--
329c	S-IVB Engine Interrupt 1520	--	--		03:13:50.32 (11,630.32)	N/A	MSFC	--
	TIME BASE 7							
330	LVDC Initiates Time Base 7	03:15:25.6 (11,725.6)	TB7 +0.0	IU	03:13:50.328 (11,630.328)	TB7 +0.0	MSFC	--
331a	LVDC Sends Redundant Signal for: Cutoff S-IVB Engine	--	--	IU	03:13:50.410 (11,630.410)	TB7 +0.082	MSFC	--
331b	Signal Received in S-IVB for: Cutoff S-IVB Engine (Redundant Signal)	--	--	S-IVB	03:13:50.394 (11,630.394)	TB7 +0.066	DAC (FM)	13
332	S-IVB J-2 Thrust Decay to 5% (Average)	--	--	N/A	Not Achieved		DAC	--
333a	Signal from LVDC for: LOX Tank Vent Valve Open ON	03:15:25.8 (11,725.8)	TB7 +0.2	IU	03:13:50.506 (11,630.506)	TB7 +.178	MSFC	--
333b	Signal Received in S-IVB for: LOX Tank Vent Valve Open	--	--	S-IVB	03:13:50.490 (11,630.490)	TB7 +0.164	DAC (FM)	13
334a	Signal from LVDC for: Point Level Sensors Disarming	03:15:25.9 (11,725.9)	TB7 +0.3	IU	03:13:50.599 (11,630.599)	TB7 +0.271	MSFC	--

TABLE 5-1 (Sheet 31 of 40)
AS-502 SEQUENCE OF EVENTS

ITEM NO.	EVENT	PREDICTED TIME		SIGNAL MONITORED AT	MONITORED TIME		DATA SOURCE	ACCURACY (ms)
		TIME FROM RANGE ZERO (hr:min:sec) (sec)	TIME FROM BASE (sec)		TIME FROM RANGE ZERO* (hr:min:sec) (sec)	TIME FROM BASE (sec)		
334b	Signal Received in S-IVB for: Point Level Sensors Disarming	--	--	S-IVB	03:13:50.584 (11,630.584)	TB7 +.256	DAC (FM)	13
335a	Signal from LVDC for: LH2 Tank Vent Valve Open ON	03:15:26.0 (11,726.0)	TB7 +0.4	IU	03:13:50.697 (11,630.697)	TB7 +.369	MSFC	--
335b	Signal Received in S-IVB for: LH2 Tank Vent Valve Open ON	--	--	S-IVB	03:13:50.681 (11,630.681)	TB7 +.353	DAC (FM)	13
336a	Signal from LVDC for: Second Burn Relay OFF	03:15:26.4 (11,726.4)	TB7 +0.8	IU	03:13:51.081 (11,631.081)	TB7 +.753	MSFC	--
336b	Signal Received in S-IVB for: Second Burn Relay OFF	--	--	S-IVB	03:13:51.066 (11,631.066)	TB7 +.738	DAC (FM)	13
337a	Signal from LVDC for: LOX Tank Flight Press System OFF	03:15:26.6 (11,726.6)	TB7 +1.0	IU	03:13:51.290 (11,631.290)	TB7 +.962	MSFC	--
337b	Signal Received in S-IVB for: LOX Tank Flight Press System OFF	--	--	S-IVB	03:13:51.274 (11,631.274)	TB7 +.946	DAC (FM)	13
338a	Signal from LVDC for: Coast Period ON	03:15:26.8 (11,726.8)	TB7 +1.2	IU	03:13:51.498 (11,631.498)	TB7 +1.170	MSFC	--
338b	Signal Received in S-IVB for: Coast Period ON	--	--	S-IVB	03:13:51.479 (11,631.479)	TB7 +1.151	DAC (FM)	13
339a	Signal from LVDC for: PU Activate OFF	03:15:27.0 (11,727.0)	TB7 +1.4	IU	03:13:51.705 (11,631.703)	TB7 +1.375	MSFC	--
339b	Signal Received in S-IVB for: PU Activate OFF	--	--	S-IVB	03:13:51.684 (11,631.684)	TB7 +1.356	DAC (FM)	13
340a	Signal from LVDC for: PU Inverter and DC Power OFF	03:15:27.1 (11,727.1)	TB7 +1.5	IU	03:13:51.799 (11,631.799)	TB7 +1.471	MSFC	--
340b	Signal Received in S-IVB for: PU Inverter and DC Power OFF	--	--	S-IVB	03:13:51.781 (11,631.781)	TB7 +1.453	DAC (FM)	13
341a	Signal from LVDC for: LOX Chilldown Pump Purge Control Valve Open OFF	03:15:27.2	TB7 +1.6	IU	03:13:51.892 (11,631.892)	TB7 +1.564	MSFC	--
341b	Signal Received in S-IVB for: LOX Chilldown Pump Purge Control Valve Open OFF	--	--	S-IVB	03:13:51.873 (11,631.873)	TB7 +1.545	DAC (FM)	13
342	Signal from LVDC for: Flight Control Computer S-IVB Burn Mode OFF "A"	03:15:29.1 (11,729.1)	TB7 +3.5	IU	03:13:53.784 (11,633.784)	TB7 +3.456	MSFC	--

TABLE 5-1 (Sheet 32 of 40)
AS-502 SEQUENCE OF EVENTS

ITEM NO.	EVENT	PREDICTED TIME		SIGNAL MONITORED AT	MONITORED TIME		DATA SOURCE	ACCURACY (ms)
		TIME FROM RANGE ZERO (hr:min:sec) (sec)	TIME FROM BASE (sec)		TIME FROM RANGE ZERO* (hr:min:sec) (sec)	TIME FROM BASE (sec)		
343	Signal from LVDC for: Flight Control Computer S-IVB Burn Mode OFF "B"	03:15:29.3 (11,729.3)	TB7 +3.7	IU	03:13:53.999 (11,633.999)	TB7 +3.671	MSFC	--
344a	Signal from LVDC for: Auxiliary Hydraulic Pump Flight Mode OFF	03:15:29.5 (11,729.5)	TB7 +3.9	IU	03:13:54.182 (11,634.182)	TB7 +3.854	MSFC	--
344b	Signal Received in S-IVB for: Auxiliary Hydraulic Pump Flight	--	--	S-IVB	03:13:54.166 (11,634.166)	TB7 +3.838	DAC (FM)	13
345	Signal from LVDC for: Telemetry Calibrator Inflight Calibrate ON	03:15:24.7 (11,724.7)	TB7 +4.1	IU	03:13:54.393 (11,634.393)	TB7 +4.065	MSFC	--
346a	Signal from LVDC for: Regular Calibrate Relays ON	03:15:29.9 (11,729.4)	TB7 +4.3	IU	03:13:54.581 (11,634.581)	TB7 +4.253	MSFC	--
346b	Signal Received in S-IVB for: Regular Calibrate Relays ON	--	--	S-IVB	03:13:54.565 (11,634.565)	TB7 +4.237	DAC (FM)	13
347	Signal from LVDC for: Telemetry Calibrator Inflight Calibrate OFF	03:15:34.7 (11,734.7)	TB7 +9.1	IU	03:13:59.384 (11,639.384)	TB7 +9.056	MSFC	--
348a	Signal from LVDC for: Regular Calibrate Relays OFF	03:15:34.9 (11,734.9)	TB7 +9.3	IU	03:13:59.587 (11,639.587)	TB7 +9.259	MSFC	--
348b	Signal Received in S-IVB for: Regular Calibrate Relays OFF	--	--	S-IVB	03:13:59.572 (11,639.572)	TB7 +9.254	DAC (FM)	13
349a	Signal from LVDC FOR: SSB/FM Transmitter OFF	03:15:35.1 (11,735.1)	TB7 +9.5	IU	03:13:59.804 (11,639.804)	TB7 +9.476	MSFC	--
349b	Signal Received in S-IVB for: SSB/FM Transmitter OFF	--	--	S-IVB	03:13:59.787 (11,639.787)	TB7 +9.459	DAC (FM)	13
350a	Signal from LVDC for: SSB/FM Group OFF	03:15:35.3 (11,735.3)	TB7 +9.7	IU	03:13:59.982 (11,639.982)	TB7 +9.654	MSFC	--
350b	Signal Received in S-IVB for: SSB/FM Group OFF	--	--	S-IVB	03:13:59.964 (11,639.964)	TB7 +9.636	DAC (FM)	13
351a	Signal from LVDC for: LOX Tank Vent Valve Close	03:15:35.6 (11,735.6)	TB7 +10.0	IU	03:14:00.281 (11,640.281)	TB7 +9.953	MSFC	--
351b	Signal Received in S-IVB for: LOX Tank Vent Valve Close	--	--	S-IVB	03:14:00.276 (11,640.276)	TB7 +9.948	DAC (FM)	13
352a	Signal from LVDC for: LOX Tank Vent Valve Boost Close ON	03:15:38.6 (11,738.6)	TB7 +13.0	IU	03:14:03.294 (11,643.294)	TB7 +12.966	MSFC	--
352b	Signal Received in S-IVB for: LOX Tank Vent Boost Close ON	--	--	S-IVB	03:14:03.288 (11,643.288)	TB7 +12.960	DAC (FM)	13

TABLE 5-1 (Sheet 33 of 40)
AS-502 SEQUENCE OF EVENTS

ITEM NO.	EVENT	PREDICTED TIME		SIGNAL MONITORED AT	MONITORED TIME		DATA SOURCE	ACCURACY (MS)
		TIME FROM RANGE ZERO (hr:min:sec) (sec)	TIME FROM BASE (sec)		TIME FROM RANGE ZERO* (hr:min:sec) (sec)	TIME FROM BASE (sec)		
353a	Signal from LVDC for: LOX Tank Vent Valve Boost Close OFF	03:15:40.6 (11,740.6)	TB7 +15.0	IU	03:14:05.283 (11,645.283)	TB7 +14.955	MSFC	--
353b	Signal Received in S-IVB for: LOX Tank Vent Valve Boost Close OFF	--	--	S-IVB	03:14:05.23 (11,645.23)	TB7 +14.83	DAC (FM)	13
354	Initiate Maneuver to Attain Separation Inertial Attitude (End of Chi Freeze)	03:15:45.6 (11,745.6)	N/A	IU	03:14:10.1 (11,650.1)	N/A	DAC	1,000
355	Signal from LVDC for: C-Band Transponder No. 1 and No. 2 ON		Variable	IU	03:14:10.443 (11,650.443)	TB7 +20.115	MSFC	--
356	Signal from LVDC for: C-Band Transponder No. 1 OFF		Variable	IU	03:14:10.540 (11,650.540)	TB7 +20.212	MSFC	--
357	Signal from LVDC for: C-Band Transponder No. 1 and No. 2 ON		Variable	IU	03:14:18.677 (11,658.677)	TB7 +28.349	MSFC	--
358	Signal from LVDC for: C-Band Transponder No. 2 OFF		Variable	IU	03:14:18.749 (11,658.749)	TB7 +28.421	MSFC	--
359	Ground Command Issued for: Initiate Spacecraft Separation 0-1.7 sec: Coast 1.7-10.0 sec: RCS Thruster Burn 10-50 sec: Spacecraft Reorientation 50-100 sec: Spacecraft Coast 100 sec: SPS Ignition	--	--	IU	03:14:26.1 (11,666.1)*	N/A	MSFC	--
360	Signal from LVDC for: C-Band Transponder No. 1 and No. 2 ON		Variable	IU	03:14:59.128 (11,699.128)	TB7 +68.800	MSFC	--
361	Signal from LVDC for: C-Band Transponder No. 1 OFF		Variable	IU	03:14:59.198 (11,699.198)	TB7 +68.870	MSFC	--
362	Signal from LVDC for: C-Band Transponder No. 1 and No. 2 ON		Variable	IU	03:15:08.330 (11,707.330)	TB7 +77.002	MSFC	--
363	Signal from LVDC for: C-Band Transponder No. 2 OFF		Variable	IU	03:15:07.403 (11,707.403)	TB7 +77.075	MSFC	--
364	Signal from LVDC for: C-Band Transponder No. 1 and No. 2 ON		Variable	IU	03:15:22.603 (11,722.603)	TB7 +92.275	MSFC	--

TABLE 5-1 (Sheet 34 of 40)
AS-502 SEQUENCE OF EVENTS

ITEM NO.	EVENT	PREDICTED TIME		SIGNAL MONITORED AT	MONITORED TIME		DATA SOURCE	ACCURACY (ms)
		TIME FROM RANGE ZERO (hr:min:sec) (sec)	TIME FROM BASE (sec)		TIME FROM RANGE ZERO* (hr:min:sec) (sec)	TIME FROM BASE (sec)		
365	Signal from LVDC for: C-Band Transponder No. 1 OFF		Variable	IU	03:15:22.689 (11,722.689)	TB7 +92.361	MSFC	--
366a	Signal from LVDC for: LH2 Tank Vent Valve Close	03:17:25.6 (11,845.6)	TB7 +120.0	IU	03:15:50.281 (11,750.281)	TB7 +119.953	MSFC	--
366b	Signal Received in S-IVB for: LH2 Tank Vent Valve Close	--	--	S-IVB	03:15:50.263 (11,750.263)	TB7 +119.935	DAC (FM)	13
367a	Signal from LVDC for: LH2 Tank Vent Valve Boost Close ON	03:17:28.6 (11,848.6)	TB7 +123.0	IU	03:15:53.291 (11,753.291)	TB7 +122.963	MSFC	--
367b	Signal Received in S-IVB for: LH2 Tank Vent Valve Boost Close ON	--	--	S-IVB	03:15:53.273 (11,753.273)	TB7 +119.945	DAC (FM)	13
368a	Signal from LVDC for: LH2 Tank Vent Valve Boost Close OFF	03:17:30.6 (11,850.6)	TB7 +125.0	IU	03:15:55.281 (11,755.281)	TB7 +124.953	MSFC	--
368b	Signal Received in S-IVB for: LH2 Tank Vent Valve Boost Close OFF	--	--	S-IVB	03:15:55.261 (11,755.261)	TB7 +124.933	DAC (FM)	13
369	Stop Roll Maneuver for CSM Separation Attitude	--	--	--	03:16:14.5 (11,774.5)	N/A	DAC	1,000
370	LV/SC Separation Sequence Start	03:18:25.6 (11,905.6)	TB7 +180.0	IU	03:16:50.280 (11,810.280) (Previously Spacecraft Separated)	TB7 +179.952	MSFC	--
371	Signal from LVDC for: C-Band Transponder No. 1 & No. 2 ON		Variable	IU	03:17:30.657 (11,850.657)	TB7 +220.329	MSFC	--
372	Signal from LVDC for: C-Band Transponder No. 2 OFF		Variable	IU	03:17:30.728 (11,850.728)	TB7 +200.400	MSFC	--
373	Signal from LVDC for: Water Coolant Valve Open		Variable	IU	03:23:23.467 (12,203.467)	TB7 +573.139	MSFC	--
374	Signal from LVDC for: Maneuver to Post-Separation Inertial Attitude	03:25:25.6 (12,325.6)	TB7 +600		03:23:50.1 (12,230.1)	TB7 +599.772	MSFC	--
375	Signal from LVDC for: Switch PCM to Low Gain Antenna (Fail Safe)	03:35:25.6 (12,925.6)	TB7 +1,200.0		03:33:50.28 (12,830.28)*	TB7 +1,199.952	MSFC	--
376	Signal from LVDC for: Switch CCS to Low Gain Antenna	03:35:25.8 (12,925.8)	TB7 +1,200.2		03:33:50.48 (12,830.48)*	TB7 +1,200.152	MSFC	--

TABLE 5-1 (Sheet 35 of 40)
AS-502 SEQUENCE OF EVENTS

ITEM NO.	EVENT	PREDICTED TIME		SIGNAL MONITORED AT	MONITORED TIME		DATA SOURCE	ACCURACY (ms)
		TIME FROM RANGE ZERO (hr:min:sec) (sec)	TIME FROM BASE (sec)		TIME FROM RANGE ZERO* (hr:min:sec) (sec)	TIME FROM BASE (sec)		
377a	Signal from LVDC for: LH2 Tank Continuous Vent Valve Open ON	03:35:26.0 (12,926.0)	TB7 +1,200.4		03:33:50.68 (12,830.68)*	TB7 +1,200.352	MSFC	--
377b	Signal Received in S-IVB for: LH2 Tank Continuous Vent Valve Open ON	--	--		03:33:50.747 (12,830.747)*	TB7 +1,200.419	DAC (PCM)	--
378a	Signal from LVDC for: LH2 Tank Continuous Vent Valve Open OFF	03:35:28.0 (12,928.0)	TB7 +1,202.4		03:33:52.68 (12,832.68)*	TB7 +1,202.352	MSFC	--
378b	Signal Received in S-IVB for: LH2 Tank Continuous Vent Valve Open OFF	--	--		03:33:52.747 (12,832.747)*	TB7 +1,202.419	DAC (PCM)	--
379	Signal from LVDC for: Telemetry Calibrator Inflight Calibrate ON	03:37:15.9 (13,035.9)	TB7 +1,310.3	IU	03:35:40.58 (12,940.58)*	TB7 +1,310.252	MSFC	--
380a	Signal from LVDC for: Regular Calibrate Relays ON	03:37:16.1 (13,036.1)	TB7 +1,310.5		03:35:40.78 (12,940.78)*	TB7 +1,310.452	MSFC	--
380b	Signal Received in S-IVB for: Regular Calibrate Relays ON	--	--		03:35:40.847 (12,940.847)*	TB7 +1,310.519	DAC (PCM)	--
381	Signal from LVDC for: Telemeter Calibrate Inflight Calibrate OFF	03:37:20.9 (13,040.9)	TB7 +1,315.3		03:35:45.58 (12,945.58)*	TB7 +1,315.252	MSFC	--
382a	Signal from LVDC for: Regular Calibrate Relays OFF	03:38:21.1 (13,041.1)	TB7 +1,315.5		03:35:45.78 (12,945.78)*	TB7 +1,315.452	MSFC	--
382b	Signal Received in S-IVB for: Regular Calibrate Relays OFF	--	--		03:35:45.847 (12,945.847)*	TB7 +1,315.519	DAC (PCM)	--
383a	Ground Command Issued for: Aux Hydraulic Pump Coast Mode OFF	--	--	Ground	04:09:21.0 (14,961.0)	N/A	MSFC	--
383b	Signal Received in S-IVB for: Aux. Hyd. Pump Coast Mode OFF	--	--	S-IVB	04:09:21.0 (14,961.0)*	N/A	DAC (FM)	--
384a	Ground Command Issued for: Aux. Hyd. Pump Flight Mode ON	--	--	Ground	04:09:21.0 (14,961.0)	N/A	MSFC	--
384b	Signal Received in S-IVB for: Aux. Hyd. Pump Flight Mode ON	--	--	S-IVB	04:09:21.89 (14,961.89)*	N/A	DAC (FM)	--
385	Ground Command Issued for: Telemetry Calibrator Inflight Calibrate ON	--	--	Ground	04:10:04.0 (15,004.0)	N/A	MSFC	--
386a	Ground Command Issued for: Regular Calibrate Relays ON	--	--	Ground	04:10:04.0 (15,004.0)	N/A	MSFC	--

TABLE 5-1 (Sheet 36 of 40)
AS-502 SEQUENCE OF EVENTS

ITEM NO.	EVENT	PREDICTED TIME		SIGNAL MONITORED AT	MONITORED TIME		DATA SOURCE	ACCURACY (ms)
		TIME FROM RANGE ZERO (hr:min:sec) (sec)	TIME FROM BASE (sec)		TIME FROM RANGE ZERO* (hr:min:sec) (sec)	TIME FROM BASE (sec)		
386b	Signal Received in S-IVB for: Regular Calibrate Relays ON	--	--	S-IVB	04:10:05.29 (15,005.29)*	N/A	DAC (FM)	--
387a	Ground Command Issued for: Aux. Hyd. Pump Coast Mode OFF	--	--	Ground	04:10:37.0 (15,037.0)	N/A	MSFC	--
387b	Signal Received in S-IVB for: Aux. Hyd. Pump Coast Mode OFF	--	--	S-IVB	04:10:37.67 (15,037.67)*	N/A	DAC (FM)	--
388a	Ground Command Issued for: Aux. Hyd. Pump Flight Mode ON	--	--	Ground	04:10:37.0 (15,037.0)	N/A	MSFC	--
388b	Signal Received in S-IVB for: Aux. Hyd. Pump Flight Mode ON	--	--	S-IVB	04:10:38.58 (15,038.58)*	N/A	DAC (FM)	--
389a	Ground Command Issued for: Aux. Hyd. Pump Flight Mode OFF	--	--	Ground	04:11:00.0 (15,060.0)	N/A	MSFC	--
389b	Signal Received in S-IVB for: Aux. Hyd. Pump Flight Mode OFF	--	--	S-IVB	04:10:59.83 (15,059.83)*	N/A	DAC (FM)	--
390	Ground Command Issued for: Telemetry Calibrator Inflight Calibrate OFF	--	--	Ground	04:11:38.0 (15,098.0)	N/A	MSFC	--
391a	Ground Command Issued for: Regular Calibrate Relays OFF	--	--	Ground	04:11:38.0 (15,098.0)	N/A	MSFC	--
391b	Signal Received in S-IVB for: Regular Calibrate Relays OFF	--	--	- - - - - - - - Not Received - - - - - - - -				
392	Ground Command Issued for: Terminate	--	--	Ground	04:11:53.0 (15,113.0)	N/A	MSFC	--
393	Ground Command Issued for: Terminate	--	--	Ground	04:12:06.0 (15,126.0)	N/A	MSFC	--
394	Ground Command Issued for: Telemetry Calibrator Inflight Calibrate OFF	--	--	Ground	04:12:15.0 (15,135.0)	N/A	MSFC	--
395a	Ground Command Issued for: Regular Calibrate Relays OFF	--	--	Ground	04:12:15.0 (15,135.0)	N/A	MSFC	--
395b	Signal Received in S-IVB for: Regular Calibrate Relays OFF	--	--	- - - - - - - - Not Received - - - - - - - -				
396	Ground Command Issued for: Telemetry Calibrator Inflight Calibrate OFF	--	--	Ground	04:12:29.0 (15,149.0)	N/A	MSFC	--

TABLE 5-1 (Sheet 37 of 40)
AS-502 SEQUENCE OF EVENTS

ITEM NO.	EVENT	PREDICTED TIME		SIGNAL MONITORED AT	MONITORED TIME		DATA SOURCE	ACCURACY (ms)
		TIME FROM RANGE ZERO (hr:min:sec) (sec)	TIME FROM BASE (sec)		TIME FROM RANGE ZERO* (hr:min:sec) (sec)	TIME FROM BASE (sec)		
397a	Ground Command Issued for: Regular Calibrate Relays OFF	--	--	Ground	04:12:29.0 (15,149.0)	N/A	MSFC	--
397b	Signal Received in S-IVB for: Regular Calibrate Relays OFF	- - - - - - - - - - - - - - - - - - Not Received - - - - - - - - - - - - - - - - - -						
398	Ground Command Issued for: Telemetry Calibrator Inflight Calibrate OFF	--	--	Ground	04:29:33.0 (16,173.0)	N/A	MSFC	--
399a	Ground Command Issued for: Regular Calibrate Relays OFF	--	--	Ground	04:29:33.0 (16,173.0)	N/A	MSFC	--
399b	Signal Received in S-IVB for: Regular Calibrate Relays OFF	--	--	S-IVB	04:29:32.0 (16,172.0)*	N/A	DAC (PCM)	--
400	Ground Command Issued for: Maneuver to Align S-IVB + X Axis with Local Horizontal	--	--	Ground	04:30:01.0 (16,201.0)	N/A	MSFC	--
401	Signal from LVDC for: C-Band Transponder No. 1 and No. 2 ON		Variable	IU	04:39:46.450 (16,786.450)	TB7 +5,156.122	MSFC	--
402	Signal from LVDC for: C-Band Transponder No. 1 OFF		Variable	IU	04:39:46.521 (16,786.521)	TB7 +5,156.193	MSFC	--
403a	Ground Command Issued for: Slow Record ON	--	--	Ground	04:42:08.816 (16,928.816)	N/A	MSFC	--
403b	Signal Received in S-IVB for: Slow Record ON	--	--	S-IVB	04:42:08.85 (16,928.85)	N/A	DAC (FM)	13
404a	Ground Command Issued for: Slow Record OFF	--	--	Ground	04:42:09.717 (16,929.717)	N/A	MSFC	--
404b	Signal Received in S-IVB for: Slow Record OFF	--	--	S-IVB	04:42:09.74 (16,929.74)	N/A	DAC (FM)	13
405a	Ground Command Issued for: Recorder Playback ON	--	--	Ground	04:42:10.621 (16,930.621)	N/A	MSFC	--
405b	Signal Received in S-IVB for: Recorder Playback ON	--	--	S-IVB	04:42:10.64 (16,930.64)	N/A	DAC (FM)	13
406	Signal from LVDC for: C-Band Transponder No. 1 & No. 2 ON		Variable		04:42:51.006 (16,971.006)	TB7 +5,340.678	MSFC	--
407	Signal from LVDC for: C-Band Transponder No. 2 OFF		Variable		04:42:51.077 (16,971.077)	TB7 +5,340.749	MSFC	--
408	Signal from LVDC for: Switch PCM to High Gain Antenna	04:45:25.6 (17,125.6)	TB7 +5,400.0	IU	04:43:50.281 (17,030.281)	TB7 +5,399.953	MSFC	--

TABLE 5-1 (Sheet 38 of 40)
AS-502 SEQUENCE OF EVENTS

ITEM NO.	EVENT	PREDICTED TIME		SIGNAL MONITORED AT	MONITORED TIME		DATA SOURCE	ACCURACY (ms)
		TIME FROM RANGE ZERO (hr:min:sec) (sec)	TIME FROM BASE (sec)		TIME FROM RANGE ZERO* (hr:min:sec) (sec)	TIME FROM BASE (sec)		
409	Signal from LVDC for: Switch CCS to High Gain Antenna (Fail Safe)	04:45:25.8 (17,125.8)	TB7 +5,400.2	IU	04:43:50.494 (17,030.494)	TB7 +5,400.166	MSFC	--
410	Signal from LVDC Telemetry Calibrator Inflight Calibrate ON	04:47:15.9 (17,235.9)	TB7 +5,510.3	IU	04:45:40.586 (17,140.586)	TB7 +5,510.258	MSFC	--
411a	Signal from LVDC for: Regular Calibrate Relays ON	04:47:16.1 (17,236.1)	TB7 +5,510.5	IU	04:45:40.787 (17,140.787)	TB7 +5,510.459	MSFC	--
411b	Signal Received in S-IVB for: Regular Calibrate Relays ON	--	--	IU	04:45:40.73 (17,140.73)	TB7 +5,510.405	DAC (FM)	13
412	Signal from LVDC for: Telemetry Calibrate Inflight Calibrate OFF	04:47:20.9 (17,240.9)	TB7 +5,515.3	IU	04:45:45.580 (17,145.580)	TB7 +5,515.252	MSFC	13
413a	Signal from LVDC for: Regular Calibrate Relays OFF	04:47:30.1 (17,250.1)	TB7 +5,515.5	IU	04:45:45.781 (17,145.781)	TB7 +5,515.453	MSFC	--
413b	Signal Received in S-IVB for: Regular Calibrate Relays OFF	--	--	S-IVB	04:45:45.71 (17,145.71)	TB7 +5,515.382	DAC (FM)	13
414	Signal from LVDC for: C-Band Transponder No. 1 & No. 2 ON		Variable	IU	04:47:14.535 (17,234.535)	TB7 +5,604.207	MSFC	--
415	Signal from LVDC for: C-Band Transponder No. 1 OFF		Variable	IU	04:47:14.606 (17,234.606)	TB7 +5,604.278	MSFC	--
416	Signal from LVDC for: Water Coolant Valve Close		Variable	IU	04:47:14.288 (17,314.288)	TB7 +5,683.960	MSFC	--
417	Signal from LVDC for: C-Band Transponder No. 1 and No. 2 OFF		Variable	IU	04:52:35.174 (17,555.174)	TB7 +5,924.846	MSFC	--
418	Signal from LVDC for: C-Band Transponder No. 2 OFF		Variable	IU	04:52:35.245 (17,555.245)	TB7 +5,924.917	MSFC	--
419	Signal from LVDC for: Maneuver to Align S-IVB/CSM + X Axis with Local Horizontal	05:15:25.6 (18,925.6)	N/A	- - - - - - - - Not Applicable - - - - - - - -				
420a	Signal from LVDC for: LH2 Tank Continuous Vent Valve Close ON	06:05:25.6 (21,925.6)	TB7 +10,200.0	These Commands occurred prior to acquisition of signal at Hawaii, Revolution 4.				
420b	Signal Received in S-IVB for: LH2 Tank Continuous Vent Valve Close ON	--	--					
421a	Signal from LVDC for: LH2 Tank Continuous Vent Valve Close OFF	06:05:27.6 (21,927.6)	TB7 +10,202.0					
421b	Signal Received in S-IVB for: LH2 Tank Continuous Vent Valve Close OFF	--	--					

TABLE 5-1 (Sheet 39 of 40)
AS-502 SEQUENCE OF EVENTS

ITEM NO.	EVENT	PREDICTED TIME		SIGNAL MONITORED AT	MONITORED TIME		DATA SOURCE	ACCURACY (ms)
		TIME FROM RANGE ZERO (hr:min:sec) (sec)	TIME FROM BASE (sec)		TIME FROM RANGE ZERO* (hr:min:sec) (sec)	TIME FROM BASE (sec)		
422a	Ground Command Issued for: Recorder Playback OFF	--	--	Ground	06:06:27.418 (21,987.418)	N/A	MSFC	--
422b	Signal Received in S-IVB for: Recorder Playback OFF	--	--	S-IVB	06:06:27.39 (21,987.39)	N/A	DAC (FM)	13
423a	Ground Command Issued for: LOX Tank Flight Pressure System ON	--	--	Ground	06:07:01.485 (22,021.485)	N/A	MSFC	--
423b	Signal Received in S-IVB for: LOX Tank Flight Pressure System ON	--	--	S-IVB	06:07:01.45 (22,021.45)	N/A	DAC (FM)	13
424a	Ground Command Issued for: Coast Period OFF	--	--	Ground	06:07:02.389 (22,022.389)	N/A	MSFC	--
424b	Signal Received in S-IVB for: Coast Period OFF	--	--	S-IVB	06:07:02.35 (22,022.35)	N/A	DAC (FM)	13
425a	Ground Command Issued for: LOX Tank Vent Valve Open ON	--	--	Ground	06:07:03.301 (22,023.301)	N/A	MSFC	--
425b	Signal Received in S-IVB for: LOX Tank Vent Valve Open ON	--	--	S-IVB	06:07:03.25 (22,023.25)	N/A	DAC (FM)	13
426a	Ground Command Issued for: LH2 Tank Vent Valve Open ON	--	--	Ground	06:07:04.207 (22,024.207)	N/A	MSFC	--
426b	Signal Received in S-IVB for: LH2 Tank Vent Valve Open ON	--	--	S-IVB	06:07:04.17 (22,024.17)	N/A	DAC (FM)	13
427	Signal from LVDC for: C-Band Transponder No. 1 and No. 2 ON		Variable	IU	06:09:30.389 (22,170.389)	TB7 +10,540.061	MSFC	--
428	Signal from LVDC for: C-Band Transponder No. 1 OFF		Variable	IU	06:09:30.460 (22,170.460)	TB7 +10,540.132	MSFC	--
429	Signal from LVDC for: C-Band Transponder No. 1 and No. 2 ON		Variable	IU	06:16:34.883 (22,594.883)	TB7 +10,964.555	MSFC	--
430	Signal from LVDC for: C-Band Transponder No. 1 OFF		Variable	IU	06:16:34.954 (22,594.954)	TB7 +10,964.626	MSFC	--
431	Signal from LVDC for: C-Band Transponder No. 1 and No. 2 ON		Variable	IU	06:16:51.165 (22,611.165)	TB7 +10,980.837	MSFC	--
432	Signal from LVDC for: C-Band Transponder No. 2 OFF		Variable	IU	06:16:51.253 (22,611.253)	TB7 +10,980.937	MSFC	

TABLE 5-1 (Sheet 40 of 40)
AS-502 SEQUENCE OF EVENTS

ITEM NO.	EVENT	PREDICTED TIME		SIGNAL MONITORED AT	MONITORED TIME		DATA SOURCE	ACCURACY (ms)
		TIME FROM RANGE ZERO (hr:min:sec) (sec)	TIME FROM BASE (sec)		TIME FROM RANGE ZERO* (hr:min:sec) (sec)	TIME FROM BASE (sec)		
433	Signal from LVDC for: C-Band Transponder No. 1 and No. 2 ON		Variable	IU	06:17:54.803 (22,674.803)	TB7 +11,044.476	MSFC	--
434	Signal from LVDC for: C-Band Transponder No. 1 OFF		Variable	IU	06:17:54.873 (22,674.873)	TB7 +11,044.546	MSFC	--
435	Signal from LVDC for: C-Band Transponder No. 1 & No. 2 ON		Variable	IU	06:19:14.560 (22,754.560)	TB7 +11,124.232	MSFC	--
436	Signal from LVDC for: C-Band Transponder No. 1 & No. 2 ON		Variable	IU	06:19:14.631 (22,754.631)	TB7 +11,124.303	MSFC	--
437	Signal from LVDC for: C-Band Transponder No. 1 & No. 2 ON		Variable	IU	06:22:43.268 (22,963.268)	TB7 +11,332.940	MSFC	--
438	Signal from LVDC for: C-Band Transponder No. 1 OFF		Variable	IU	06:22:43.339 (22,963.339)	TB7 +11,333.011	MSFC	--
439	Signal from LVDC for: C-Band Transponder No. 1 and No. 2 ON		Variable	IU	06:23:46.894 (22,026.894)	TB7 +11,396.566	MSFC	--
440	Signal from LVDC for: C-Band Transponder No. 2 OFF		Variable	IU	06:23:46.965 (23,026.965)	TB7 +11,396.637	MSFC	--
441	Signal from LVDC for: C-Band Transponder No. 1 & No. 2 ON		Variable	IU	06:25:22.760 (23,122.760)	TB7 +11,492.432	MSFC	--
442	Signal from LVDC for: C-Band Transponder No. 1 OFF		Variable	IU	06:25:22.831 (23,122.831)	TB7 +11,492.503	MSFC	--

TABLE 5-2 (Sheet 1 of 2)
GROUND SEQUENCE OF EVENTS

TIME		EVENT	TIME		EVENT
MIN	SEC		MIN	SEC	
-9	-25.290	Engine Control Power ON		-53.834	Start Tank Supply Valve Closed
	-22.114	Engine Cutoff Command ON		-53.784	Start Tank Supply Vent Open
	-7.674	Engine Ignition Power ON		-51.708	Start Tank Supply Vent Closed
	-7.666	Engine Ready ON		-49.118	Control Bottle Supply Valve Closed
-8	-54.868	Auxiliary Hydraulic Pump Flt Relay Reset OFF		-49.044	Control Bottle Supply Vent Open
	-54.782	Auxiliary Hydraulic Pump Power ON		-47.514	Start Tank Supply Vent Open
	-54.780	Ready for 4D411 Power OFF		-44.160	LOX Chilldown Pump ON
	-50.784	Auxiliary Hydraulic Pump Coast Reset ON		-44.154	LOX Chilldown Relay Reset OFF
-5	-59.894	LOX Vent Closed		-44.152	LOX Chilldown Pump Inverter Power ON
	-58.166	LOX Vent Open		-35.766	Prevalves Close Command ON
	-55.920	LH2 Vent Closed		-35.618	LH2 Prevalves Closed
	-53.926	LH2 Directional Vent Valve - Flight Position		-35.614	LOX Prevalves Closed
	-52.172	LH2 Directional Vent Valve - Ground Position		-22.840	Switch Selector Inhibit ON
	-49.882	LH2 Vent Open		-18.332	Cold Helium Crossover Valve Closed
	-45.348	S&A Device Armed		-18.250	Terminal Countdown Sequence Ready ON
	-45.324	Ordnance OK Indication ON		-16.276	APS No. 2 Engine Power ON
	-34.314	S-IVB DC Power Supply Commit		-16.266	APS No. 1 Engine Power ON
	-28.968	Heat Exchanger Circuit No. 1 Vent Closed		-16.260	S-IVB Preps Complete ON
	-23.850	All Stages Ready for Power Transfer ON	-3	-06.996	Terminal Countdown Sequence Ready OFF
-4	-59.016	Fuel Chilldown Pump ON	-2	-46.994	Terminal Countdown Sequence Output ON
	-59.008	LH2 Chilldown Pump Inverter Power ON			START OF TERMINAL SEQUENCE
	-59.008	LH2 Chilldown Relay Reset OFF		-46.760	LOX Vent Closed

TABLE 5-2 (Sheet 2 of 2)
GROUND SEQUENCE OF EVENTS

TIME		EVENT	TIME		EVENT
MIN	SEC		MIN	SEC	
	-46.602	LOX Tank Pressurization Command ON		-49.912	S-IVB Stage on Internal Power
	-31.604	LOX 100 Pct Flight Mass ON		-49.562	S-IVB Power Transfer Complete
	-31.046	LOX Fill and Drain Valve Closed		-39.696	Directional Vent In-Flight Position
	-30.324	S-IVB LOX Tank Pressurized		-39.694	S-IVB Ready for Launch
	-30.324	LOX Minimum Liftoff Press OK		-16.986	RSCR's 1 & 2 PD Blocked OFF
	-29.360	GN2 LOX Umbilical Purge Supply Open		-8.894	Ignition Enabled
-1	-36.700	LH2 Tank Vent Valve Closed		-8.892	Ignition Sequence Start ON
	-36.506	LH2 Tank Pressurization Command ON		-8.836	LH2 Tank Prepress Supply Vent
	-36.428	LH2 Tank Ground Prepress Supply Valve Open		-8.814	Engine TC Chilldown Supply Vlave Closed
	-15.072	LH2 Minimum Liftoff Pressure OK		-8.796	Cold Helium Bottle Supply Closed
	-15.072	LH2 Tank Pressurized		-8.704	Cold Helium Bottle Supply Vent Open
	-15.002	LH2 Tank Ground Prepress Supply Valve Closed		-8.574	LH2 Ground Control and Prepress Supply Closed
	-11.720	LOX Vent Open		-8.476	3000 Helium Supply Closed
	-11.394	LOX Vent Closed		-1.414	All Engines Running
	-4.676	LH2 100 Pct Mass ON		-0.008	Time for Commit
	-3.928	LH2 Fill and Drain Valve Closed		-0.008	S-IC Commit
-0	-59.770	LH2 Umbilical Purge Supply Open	R0 = 12:00:01.000 GMT		
	-51.162	GH2 Supply Pressure Switch Mode		+0.068	LH2 Nozzle Purge Supply Closed
	-49.918	S-IVB Aft Bus No. 1 on Internal Power		+0.268	GN LOX Umbilical Purge Supply Closed
	-49.916	S-IVB Aft Bus No. 2 on Internal Power		+0.556	IU Liftoff
	-49.916	S-IVB Fwd Power on Internal		+0.608	S-IC Liftoff
	-49.916	S-IVB On External Power OFF		+0.310	LH2 Debris Valve Closed
				+0.626	LOX Debris Valve Closed

SECTION 6

COUNTDOWN OPERATIONS

6. COUNTDOWN OPERATIONS

No significant S-IVB or equipment problems occurred during the launch countdown activity, and Douglas ground support equipment sustained no significant damage during liftoff. The precountdown and countdown activities are reviewed and evaluated in the following paragraphs which include discussions of the prelaunch checkouts, purges, propellant and pneumatic loading, and the terminal countdown. Significant events occurred at the following times:

Event	Time
LOX loading initiated	05:32:00 GMT
LH2 loading initiated	09:46:00 GMT
Cold helium loading initiated	10:18:42 GMT
Terminal countdown initiated	11:30:01 GMT
Liftoff	12:00:01 GMT

6.1 Propulsion System Checkouts

Preflight checkouts of the S-IVB-502 were conducted in accordance with handling and checkout requirements drawings listed in Douglas report No. DAC-56353, Narrative End Item Report on Saturn S-IVB-502 (Douglas S/N 1006), dated September 1966.

6.2 Launch Vehicle Tests

The S-IVB-502 was subjected to the launch vehicle tests listed in table 6-1 to determine that switch selector, interfaces, etc., were functional for launch. These tests were performed in the vehicle assembly building (VAB) or on Pad 39A.

6.2.1 Countdown Demonstration Test

The AS-502 vehicle countdown demonstration test (CDDT) was initiated at 23:00:00 GMT on 24 March 1968 with the count at T -103 hr. The planned CDDT cutoff at T -8.9 sec occurred at approximately 19:25:46 GMT on 31 March. The test was performed in accordance with NASA procedure V-20044; the Douglas preparations and securing steps were conducted in accordance with procedure V-20043. Three runs were necessary to complete Part III (T -7 hr to T -0) of the CDDT.

Run 1 (29 March 1967) was scrubbed at 23:00:00 GMT while in a hold at T -6 hr because of a leak at the LOX fill quick disconnect/debris valve flange.

Run 2 (30 October 1967) was scrubbed at 14:03:00 GMT with the count at T -4 hr because of S-IC electrical power problems. The LOX aboard the S-IVB was drained without problems.

Run 3 (31 March 1968) was initiated at 11:00:00 GMT with the count at T -7 hr and was completed at 19:25:46 GMT. The first terminal count sequence was terminated at T -32 sec because of a high LOX pump discharge temperature on the S-II.

Several unexpected problems occurred during the CDDT. Leakages were found in the cold helium system, at the LOX debris valve, and in two calips switches at the diaphragm. These were corrected, and mass decay checks that were subsequently performed showed no mass decay. In addition, two redlines were changed for the launch countdown because of the following problems:

a. The LH2 recirculation flowrate was at or near 130 gpm, and the minimum redline limit was changed from 130 to 120 gpm.

b. The LH2 pump inlet temperature was within 0.5 deg of the redline limit, and the maximum redline limit for this parameter was increased by 1 deg.

Inspection of the LH2 recirculation system after the CDDT revealed that a piece of insulation had not been installed. The insulation was installed for the launch countdown, and the LH2 recirculation flowrate and pump inlet temperature were well within limits.

6.2.2 Flight Readiness Test

The AS-502 flight readiness test was conducted on 7 and 8 March 1968 in order to assure the proper functioning of the space vehicle in the launch configuration (except for the overall test [OAT] equipment). This test was conducted at LC 39A in accordance with Kennedy Space Center procedure V-20017, revision 005, dated 8 February 1968. S-IVB preparations, functional testing, and securing operations were conducted in accordance with procedure S-V-31028, dated 23 February 1968.

The APS dry fire was conducted at T -1 hr 30 min without difficulty, and all data stations reported good results. This test verified that the APS firing program and all data stations were ready for the APS hot firing.

6.3 APS Preparations

6.3.1 APS Loading

APS module propellant loading preparations were started on 4 March and satisfactorily completed on 20 March 1968 in accordance with KSC procedure S-V-24-109. The loading data are presented in table 6-2. During module 2 fuel loading, the differential pressure across the bladder in the module 1 fuel tank slowly increased to 38 psid (allowable is 20 psid) because of a temperature differential between the environmental control system air and the propellant. The ullage pressure remained at a constant 29 psia, indicating that the bladder was not damaged, and a waiver was written to accept the excessive differential pressure for AS-502.

6.3.2 APS Gas Removal

Gas removal from APS modules 1 and 2 oxidizer tanks was satisfactorily accomplished before the APS test firing. Propellant loss data are presented in table 6-2.

6.3.3 APS Test Firing

The APS test firing was accomplished on 21 March 1968 in accordance with NASA procedure V-25303, revision 002. The engines were fired in a sequence that consisted of one 250-ms clearing burst and two 65-ms pulses with a 750-ms delay between each pulse, the ullage engines were each fired for one pulse.

The firing sequence was as follows:

a. Minus pitch - engine 2-2

b. Minus roll - engines 1-1 and 2-1

c. Ullage engine (one 400-ms pulse) - engine 1-4

d. Plus pitch - engine 1-2

e. Plus roll - engines 1-3 and 2-3

f. Ullage engine (one 400-ms pulse) - engine 2-4

Evaluation of the data from these firings indicated that the systems were acceptable for flight.

6.4 AS-502 Launch Countdown

The launch countdown activities began at 05:30:00 GMT on 3 April (immediately after the CDDT recycle was completed) and was terminated at 12:00:01.69 GMT on 4 April 1968 with space vehicle launch. The final portion of the countdown progressed without incident or delay to firing command initiation.

6.4.1 Prelaunch Preparations and Purges

The prelaunch preparations and purges were accomplished in accordance with procedures V-20043, S-IVB Support Preparations for Countdown Demonstration and Countdown; and Douglas procedure 1B61615, Pneumatic Console and Heat Exchanger Operating Instructions.

During the preparations the systems were leak checked, purges and valve actuations were verified, and the helium supply was analyzed for purity and moisture content.

The engine purges required by Rocketdyne were accomplished just prior to LOX loading during LOX transfer line chilldown. The LOX and LH2 tank purges included the fill and drain valves, the LOX umbilical vent valve, and the S-IVB umbilical line drain valve.

An APS gas bubble removal test was simulated during CDDT. It was found to be adequate and was not altered for prelaunch preparations.

6.4.2 Loading Operations

LOX and LH2 loading, propellant tank prepressurization, thrust chamber chilldown, and helium and GH2 sphere loading were all satisfactorily accomplished.

6.4.2.1 Propellant Loading

S-IVB LOX and LH2 loadings were conducted in accordance with procedure V-35007-AS-502. Both loadings were uninterrupted and accomplished smoothly. Pressures, temperatures, and flowrates at significant times are presented in table 6-3.

6.4.2.2 Helium and GH2 Loading

Final pressurization of all S-IVB helium spheres, both cold and ambient, was accomplished without difficulty; pressurization of the APS helium tanks from blanket to full pressure was accomplished in one step at T -55 min. Pressurization of the engine control sphere from ambient to full pressure was accomplished in two steps approximately 5 min apart to limit the temperature rise. Sphere pressurization data are presented in table 6-4.

6.4.3 Terminal Count

The launch terminal count was initiated at T -30 min and was completed without any significant problems. During this period, final engine and stage conditioning were accomplished. Table 6-5 presents the sequence of terminal countdown events.

6.4.3.1 Engine Conditioning

The J-2 engine conditioning was initiated with a 50-psig ambient helium purge through the start sphere. After the purge was terminated, the start sphere was chilled with cold GH2 circulated through heat exchanger circuit No. 1; it was maintained at the proper temperature by opening the heat exchanger circuit No. 1 vent valve (primary bleed) at the proper time. Start sphere chilldown was terminated with the initiation of start sphere pressurization by closing the start sphere vent valve. No problems occurred during start sphere conditioning for launch.

The J-2 engine thrust chamber jacket conditioning was initiated with a 50-psig ambient helium purge. The purge was terminated at T -10 min, and thrust chamber chilldown was initiated with cold helium flowing through heat exchanger circuits 2 and 3 for approximately 5 min; chilldown was then continued with cold helium supplied through heat exchanger circuit No. 2 only. Thrust chamber jacket temperature was well within redline limits at both the initiation of automatic sequence and at T -19 sec.

The engine control sphere was pressurized at T -40 min and conditioned during start sphere chilldown. The supply was closed at T -5 min. The differential temperature between the GH2 start sphere and the engine control sphere was +13.7 deg R at T -19 sec, which is within the $\pm$30 deg R required at this time.

6.4.3.2 Stage Conditioning

LOX turbopump chilldown was performed with a LOX flowrate of 40 gpm unpressurized and 43 gpm pressurized. The chilldown was normal in every respect.

LH2 turbopump chilldown was performed at an LH2 flowrate of 92 gpm unpressurized and 133 gpm pressurized. The chilldown was normal and provided satisfactory LH2 pump inlet conditions for launch. The low LH2 chilldown pump flowrate and high LH2 pump inlet temperature encountered during the CDDT did not occur during the launch countdown because the proper insulation had been installed on the recirculation pump and shutoff valve. Chilldown is further discussed in sections 11 and 12.

LOX and LH2 tank prepressurization were completed in the expected times, and the tank ullage pressures were satisfactory at T -19 sec. Two LOX tank ullage pressure makeup cycles were accomplished satisfactorily.

The stage pneumatic system functioned normally during the terminal count. The control regulator discharge pressure during periods of low demand was 540 to 560 psia, as expected.

6.5 Redline Limits

The redline limits for launch vehicle parameters are presented in the Apollo 6 (AS-502) Launch Mission Rules, Rev A, dated 8 March 1968; and in Douglas report SM-46999, Saturn S-IVB-502 Stage Flight Test Plan, dated 23 October 1967; and in the A41 Redline Monitoring Brief. All redlines were satisfied before the launch; however, two were changed after the CDDT because of the poor LH2 chilldown system performance during CDDT. The LH2 pump flowrate redline was decreased from 130 to 120 gpm, and the LH2 pump inlet temperature redline was increased 1 deg R. However, these measurements were well within the original redline limit for launch.

6.6 Countdown Operations

6.6.1 Environmental Control Systems

The aft interstage thermoconditioning and purge system functioned properly during the countdown, maintaining the APS oxidizer temperatures within the launch redline limits of 535 to 560 deg R. At liftoff, the oxidizer temperature in APS module 1 was 556 deg R and in APS module 2 was 545 deg R.

6.6.2 Common Bulkhead Evaluation

The vacuum monitor console setups were started at 15:30:00 GMT on 3 April. A gas sample was taken at 15:51:00 GMT and the vacuum supply valves opened at 16:09:00 GMT with an internal bulkhead pressure of 0.9 psia. Results of the gas sample indicated a satisfactory inert atmosphere inside the bulkhead at liftoff, as shown in the following table.

Results of Gas Sample

Gas	Concentration
H_2	0.16%
He	0.28%
N_2	37.6%
O_2	5.9%
A	53.7%
CO_2	1.9%

The vacuum supply valves were closed on 4 April at 05:08:00 GMT, 24 min prior to LOX loading. A satisfactory internal pressure was maintained throughout the count with a pressure of 0.17 psia at liftoff. During flight and orbital coast, the internal pressure remained steadily at 0.2 psia until loss of signal from KSC, 6-1/2 hr after liftoff.

The bulkhead internal pressure remained well below the relief valve setting of 1.0 psia, and the entire flight pressure history was indicative of a sound bulkhead.

6.6.3 Countdown Problems

The following problems were encountered during the launch countdown:

a. At 21:59:00 GMT on 2 April, after the CDDT and during recycle operations, the pneumatic console Model DSV-4B-432A, 3,200 psia helium dome regulator, A11733, P/N 1A66985-503, S/N 168 was found to be chattering during periods of high flowrate. The regulator was removed and replaced.

b. At 12:19:00 GMT on 3 April 1968, during propulsion preparations for launch, the pneumatic console Model DSV-4B-432A, 500 psi helium dome loader regulator, A12059, P/N 1B37340-519, S/N 10248, was found to be leaking internally. The regulator was removed and replaced.

c. Temperature measurement C0205-403 was recommended for deletion prior to launch. This recommendation was based on a misinterpretation of the data. The transducer appeared to be hung up at 80 percent of full scale, but the temperature was actually being maintained at this level by air from the environmental control system.

6.7 Atmospheric Conditions

The atmospheric conditions for the AS-502 launch on 4 April 1968 were as follows:

Time (GMT)	Ambient Temp. (deg F)	Dew Point Temp. (deg F)	Relative Humidity (percent)	Ambient Press* (in. of HG)	Wind Direction** (deg from N)	Wind Velocity** (knots)
06:00:00	69	62	79	30.16	130	9
07:00:00	69	62	79	30.15	120	6
08:00:00	68	63	84	30.13	140	7
09:00:00	68	64	87	30.12	140	7
10:00:00	69	64	84	30.13	140	9
11:00:00	69	64	84	30.14	140	8
12:00:00 (liftoff)	71	65	81	30.14	140	10

*Ambient pressure at sea level.

**Wind direction and velocity from location 60 ft above ground level and 3 miles West of LC Pad 39A.

TABLE 6-1
LAUNCH VEHICLE TESTS

TEST	NASA PROCEDURE	COMPLETION
AS-502 Launch Vehicle OAT No. 1 (Plugs In)	V-20011	21 Dec 67
AS-502 Launch Vehicle OAT No. 1 (Plugs Out)	V-20035	28 & 29 Dec 67
AS-502 Space Vehicle OAT No. 1 (Plugs In)	V-20010, rev 001	16 Jan 68
AS-502 Launch Vehicle Propellant Simulated Loading Test	V-25166	15 Feb 68
AS-502 Launch Vehicle LH2 Simulated Loading Test	V-25126	12 Feb 68
AS-502 Launch Vehicle LOX Simulated Loading Test	V-25116	13 Feb 68
AS-502 Space Vehicle Cutoff and Malfunction Test	V-20021, rev 004	16 Feb 68
AS-502 Launch Vehicle LOX System Cold Flow Test	V-25333	19 Feb 68
AS-502 LH2 System Cold Flow Test	V-20034, rev 004	24 Feb 68
AS-502 Launch Vehicle MCC-H Interface Command Test (Pad)	V-20027	27 Feb 68
AS-502 Launch Vehicle MCC-H Interface Command Test (VAB)	V-20023	4 & 5 Jan 68
AS-502 Space Vehicle OAT No. 2 (Plugs Out)	V-20012	24 & 25 Jan 68
AS-502 Launch Vehicle OAT No. 2 (Plugs In)	V-20029	29 & 30 Aug 67
AS-502 Launch Vehicle Flight Sequence and EBW Functional	V-20007	10 Aug 67
AS-502 Launch Vehicle OAT No. 1 (Plugs In) S-II Spacer	V-20011S, rev A	13 June 67
AS-502 Launch Vehicle Sequence Malfunction Test with S-II Spacer	V-20019S	5, 6, 7, and 8 June 68
AS-502 Launch Vehicle Sequence and EBW Functional Test with S-II Spacer	V-20007S, rev B	1 June 67

TABLE 6-2
APS LOADING DATA

ITEM	VOLUME ($IN.^3$)	TEMPERATURE (DEG R)
Module 1		
Oxidizer System		
Loaded	4,102	80
Offloaded	372	75
Removed with bubble bleed during burp firing	28	88.5
Removed with bubble bleed during countdown	38	85
Fuel System		
Loaded	4,102	81.5
Offloaded	88	83
Removed during countdown	38	84
Module 2		
Oxidizer System		
Loaded	4,102	82
Offloaded	372	82
Removed with bubble bleed during burp firing	21	91
Removed with bubble bleed during countdown	30	84
Fuel System		
Loaded	4,102	79
Offloaded	88	80.5
Removed with bubble bleed during countdown	28	82

TABLE 6-3
S-IVB-502 STAGE PROPELLANT LOADING DATA

PARAMETER	UNITS	LOX	LH2
Chilldown initiated	GMT	04:57:00	09:46:00
Slow Fill			
Levels	percent	0 to 5	0 to 5
Initiation time	GMT	05:32:00	09:46:00
Flowrate	gpm	720	400
Maximum swing arm pressure	psia	47	20.7
Maximum ullage pressure	psia	23.5	18.5
Fast fill			
Levels	percent	5 to 96	5 to 98
Initiation time	GMT	05:34:00	09:59:00
Flowrate	gpm	950 to 1,050	2,700 to 3,000
Swing arm pressure			
Maximum	psia	44	20.7
Stabilized	psia	42.5 to 44	20.7
Maximum ullage pressure	psia	23.5	17.5
Final slow fill			
Level at initiation	percent	96	98
Initiation time	GMT	05:53:00	10:23:00
Flowrate	gpm	450	500
Swing arm pressure	psia	21	20.7
Maximum ullage pressure	psia	16.5	17.5
Total time required	min	22	40

TABLE 6-4
SPHERE PRESSURIZATION DATA

SPHERE	VOLUME (ft^3)	FINAL PRESSURIZATION		INITIAL PRESSURE (psia)	FINAL PRESSURE (psia)	PRESSURE AT LIFTOFF (psia)	TEMPERATURE AT LIFTOFF (deg R)	MASS AT LIFTOFF (lbm)
		INITIATION TIME	REQUIRED TIME					
Repressurization								
LOX	9.0	80% LH2	8 min	2,625	3,120	3,080	495	18.58
LH2	31.5	80% LH2	8 min	2,580	3,100	3,053	486	66.2
Control helium	4.5	80% LH2	7 min	2,850	3,110	3,100	545	8.54
Cold helium	28.0	80% LH2	16.5 min	1,080	3,100	2,966	38.9	332.0
APS helium								
Module 1	0.540	T -55 min	3 min	3,120	3,120	3,120	558	1.02
Module 2	0.540	T -55 min	3 min	3,100	3,100	3,100	545	1.03
Engine control	0.578	T -32 min	1 min 30 sec*	3,080	2,972	2,968	290	1.87
Engine GH2 start	4.224	T -5 min 30 sec	approx 15 sec	1,100	1,280	1,304	278	3.47

*Pressurized in two steps.

TABLE 6-5
TERMINAL COUNTDOWN SEQUENCE

FUNCTION	TIME FROM LIFTOFF (sec)
Start sphere purge initiated	-1,200
Thrust chamber purge initiated	-870
Start sphere purge terminated	-870
Start sphere chilldown initiated	-870
Thrust chamber purge terminated	-600
Thrust chamber chilldown initiated	-600
Start sphere chilldown terminated	-293.8
Engine control sphere supply closed	-289.1
LOX turbopump chilldown initiated	-284.2
LH2 turbopump chilldown initiated	-299.0
Cold helium crossover valve closed	-258.3
Fuel prevalve closed	-275.6
Oxidizer prevalve closed	-275.6
LOX tank vent valve closed	-166.7
LOX tank prepressurization terminated	-150.3
LH2 tank vent valve closed	-96.7
LH2 tank prepressurization terminated	-75.1
LH2 directional vent to flight position	-39.7
Commit and liftoff (12:00:01.69 GMT)	0

SECTION 7

COST PLUS INCENTIVE FEE

7. COST PLUS INCENTIVE FEE

7.1 S-IVB-502 Flight Mission Accomplishment Results

S-IVB preconditions of flight (PCF) were outside of allowable tolerances as a result of non-nominal lower stage performance caused by the premature shutdown of two S-II stage engines. S-IVB end conditions of flight (ECF) also were not achieved due to premature termination of flight caused by a malfunction of the J-2 engine which is not considered Douglas' fault as defined in paragraphs 3.3.7 and 3.3.9 of Exhibit J to Supplemental Agreement 1100 to Contract NAS7-101. S-IVB performance was satisfactory throughout the S-IVB first burn and parking orbit phases of the mission, and the required ECF would have been achieved if proper PCF had existed and the J-2 engine had not malfunctioned. Substantiation of this position is presented in the following paragraphs.

Table 7-1 presents a comparison of the actual PCF determined from flight data and allowable PCF defined in MSFC Letter I-CO-S-IVB-8-303, dated 27 March 1968. It can be seen that all of the trajectory parameters and the pitch attitude parameter of the PCF differed from nominal by substantially more than the allowable tolerances.

Flight evaluation results have established that the failure of the S-IVB to restart was caused by a failure of the J-2 engine augmented spark igniter (ASI) assembly which occurred during S-IVB first burn. The evaluation results also show that all S-IVB systems were functioning properly until after this failure occurred. The subsequent failure of the S-IVB hydraulic system can be attributed directly to the J-2 engine failure.

S-IVB anomalies that cannot be definitely attributed to the ASI failure are:

a. Excessive S-IVB cold helium leakage in orbit

b. Abnormal operation of the S-IVB propellant utilization system in orbit.

Neither of these problems would have precluded successful attainment of required ECF, if proper PCF had existed and the J-2 engine had not failed. Sufficient cold helium remained for a full duration second S-IVB burn. The propellant utilization system anomaly could have resulted in high engine mixture ratio (5.5:1) operation during the second S-IVB burn phase. If proper PCF had existed, sufficient reserve propellants would have been available to accommodate this mode of operation. As shown in table 7-2, the ECF that would have resulted are within the allowable tolerances stated in MSFC Letter I-CO-S-IVB-8-329, dated 29 March 1968. These ECF were obtained from a trajectory simulation that was based on the following conditions:

a. Nominal PCF

b. Actual S-IVB first burn performance (excluding effects of ASI failure)

c. Propellant utilization valve at the extreme high mixture ratio limit during second S-IVB burn.

S-IVB attitude control ECF were evaluated throughout the portion of the planned mission that was successfully accomplished. This includes first S-IVB burn and parking orbit (until

issuance of the command to restart the S-IVB J-2 engine). Table 7-3 presents the actual and allowable attitude control ECF during this period. The allowable envelopes are those defined in MSFC Letter I-CO-S-IVB-8-303 dated 27 March 1968. Pitch attitude error and pitch rate temporarily exceeded allowable tolerances early in S-IVB first burn. This was caused by the out of tolerance pitch attitude PCF parameter. S-IVB control system performance was normal and all other parameters were within tolerance throughout this period.

7.2 Telemetry Performance

Evaluation of the telemetry performance indicated that the telemetry system operated at 98.3 percent efficiency during the telemetry performance evaluation period (TPEP) phase I (liftoff to first S-IVB engine cutoff +10 sec) and performed at 97.6 percent efficiency during the TPEP phase II (liftoff to planned LV/SC separation as defined in NASA drawing 40M33622, Interface Control Document Definition of Saturn SA-502 Flight Sequence Program).

The results of the telemetry performance analysis are shown in table 7-4.

TABLE 7-1
S-IVB-502 PRECONDITIONS OF FLIGHT

PARAMETER	UNITS	NOMINAL	ACTUAL	ALLOWABLE DEVIATION*	ACTUAL DEVIATION
Range	km	1,505.4	1,815.5	+55.4 -71.1	310.1**
Crossrange	km	40.8	30.7	+3.5 -3.8	-10.1**
Altitude	km	188.8	195.2	+3.4 -3.4	6.4**
Velocity vector magnitude	m/sec	6,834.4	6,728.7	+52.4 -66.1	-105.7**
Velocity vector direction	deg	0.78	1.60	+0.38 -0.34	0.82**
Pitch attitude	deg	-96.3	-82.2	+5.0 -5.0	14.2**
Pitch rate	deg/sec	0.0	-0.1	+1.5 -1.5	-0.1
Yaw attitude	deg	0.3	-1.0	+3.8 -3.7	-1.3
Yaw rate	deg/sec	0.0	-0.2	+1.5 -1.5	-0.2
Roll attitude	deg	0.0	-0.5	+4.0 -4.0	-0.5
Roll rate	deg/sec	0.0	-0.1	+1.5 -1.5	-0.1

NOTE: PCF are evaluated at the instant of Separation Command

*Deviations consist of allowable error plus evaluation uncertainty

**Exceeds allowable tolerance

TABLE 7-2
SIMULATED TRAJECTORY END CONDITIONS OF FLIGHT FOR PU MALFUNCTION
RESULTING IN HIGH EMR OPERATION

PARAMETER	UNITS	NOMINAL	SIMULATED	ALLOWABLE DEVIATION	SIMULATED DEVIATION
Inclination	deg	32.485	32.486	+0.049 -0.052	+0.001
Node	deg	122.490	122.499	+0.220 -0.225	+0.009
Energy (C_3)	m^2/sec^2	-1,491,156	-1,494,147	+125,675 -193,679	-2,991
Eccentricity	--	0.97532	0.97528	+0.00206 -0.00332	-0.00004

NOTE: The Simulated ECF are based on:

a. Nominal PCF

b. Actual S-IVB first burn performance (excluding effect of ASI failure)

c. Propellant utilization valve at the extreme high mixture ratio limit during second S-IVB burn.

TABLE 7-3
ATTITUDE CONTROL END CONDITIONS OF FLIGHT
(TO RESTART ATTEMPT)

PARAMETER	ALLOWABLE ENVELOPE	MAXIMUM FLIGHT VALUE
S-IVB First Burn		
Pitch Attitude Error (deg)	±6	+7.6**
Yaw Attitude Error (deg)	±6	+2.4
Roll Attitude Error (deg)	±13.5	-1.0
Pitch Rate (deg/sec)	±3	-3.5**
Yaw Rate (deg/sec)	±3	+1.0
Roll Rate (deg/sec)	±1.5	-0.6
Parking Orbit		
*Pitch Attitude Error (deg)	±4	+1.3
*Yaw Attitude Error (deg)	±4	-1.1
*Roll Attitude Error (deg)	±13.5	-0.6
Pitch Rate (deg/sec)	±1.2	-0.3
Yaw Rate (deg/sec)	±1.2	-0.5
Roll Rate (deg/sec)	±1.5	-0.6

*Excluding normal transients and maneuvers

**Temporary out of tolerance condition resulting from out of tolerance preconditions of flight.

TABLE 7-4 (Sheet 1 of 3)
FLIGHT TELEMETRY PERFORMANCE SUMMARY

ITEM	DESCRIPTION	TOTAL
1.	Total number of measurements listed in the S-IVB-502 Instrumentation Program and Components List (IP&CL), Douglas Drawing 1B43567, AL Change.	616
2.	Measurements listed in the IP&CL which are not wholly on the S-IVB-502 stage:	7
	Measurements transmitted by the S-II telemetry system:	
	D0153-423 Press - Chamber Retrorocket Posit IV-I	
	D0154-421 Press - Chamber Retrorocket Posit II-III	
	D0155-420 Press - Chamber Retrorocket Posit I-II	
	D0156-422 Press - Chamber Retrorocket Posit III-IV	
	Measurements wholly transmitted landline to the Launch Control Center:	
	D0545-407 Press - Common Bulkhead Internal - H/W	
	D0576-408 Press - Fuel Tank Ullage Umbilical - H/W	
	D0577-406 Press - Oxid Tank Ullage Umbilical - H/W	
3.	Measurements known to be inoperative at start of automatic launch sequence, or became inoperative prior to start of automatic launch sequence:	18

TABLE 7-4 (Sheet 2 of 3)
FLIGHT TELEMETRY PERFORMANCE SUMMARY

ITEM	DESCRIPTION	TOTAL
	The function of the following measurements is to monitor the output voltage of exploding bridgewires (EBW) by means of pulse sensors during checkout. The pulse sensors are removed prior to launch, thus making the measurements inoperative during flight.	
	K0141-411 Event - R/S 1 Pulse Sensor	
	K0142-411 Event - R/S 2 Pulse Sensor	
	K0149-404 Event - Ullage Jettison 1 P/S	
	K0150-404 Event - Ullage Jettison 2 P/S	
	K0169-404 Event - EBW Pulse Sensor Off Indication	
	K0176-404 Event - Ullage Rocket Ignition P/S 1 Ind	
	K0177-404 Event - Ullage Rocket Ignition P/S 2 Ind	
	The following measurement was listed in the IP&CL, and the capability to make the measurements existed on the stage. MSFC did not require the associated rate gyro installation; therefore, the measurement is inoperative.	
	K0152-404 Event - Rate Gyro Wheel Speed OK Ind	
	The following measurement is used for checkout only. The IU flight sequencing tape is not programmed to activate this measurement in flight. Therefore, it is inoperative.	
	K0168-404 Event - Switch Selector Register Test	
	The following measurements malfunctioned and became inoperative prior to the start of automatic sequence	
	C0041-406 Temp - LOX Tank, Posit 2	
	C0056-406 Temp - LOX Tank Ullage Gas, 20 percent	
	C0150-401 Temp - Eng LH2 Pump Surface	
	C0155-404 Temp - LH2 Prevalve Bypass Line	
	C0205-403 Temp - He Prepress Sphere, No. 4 Gas	
	C0301-415 Temp - APS Oxid, Tank 2	
	D0018-401 Press - Eng Reg Outlet	
	D0058-401 Press - PU Valve Inlet	
	S0087-426 Strain - Dyn, Fwd Skirt, Pnl 17	
4.	Measurements from which Douglas could not obtain data due to noise from unknown sources, and measurements which were degraded or prevented from being transmitted.	
	Phase I	0
	Phase II	3
	C0010-403 Temp - Engine Area Ambient	
	C0152-403 Temp - LOX Main Line Flg Wall	
	E0209-401 Vib - Combustion Chamb Dome, Long	
5.	The total number of measurements to be evaluated for incentive performance for both TPEP phase I and phase II is item 1 minus the sum of items 2, 3, and 4.	
	Phase I	591
	Phase II	588

TABLE 7-4 (Sheet 3 of 3)
FLIGHT TELEMETRY PERFORMANCE SUMMARY

ITEM	DESCRIPTION	TOTAL
6.	Measurements which were failures during TPEP phase I (Liftoff to first S-IVB engine cutoff +10 sec). Details regarding these measurement failures may be obtained in section 18 of this report. B0023-404 Acoustic - Aft (2400 - 4800), Int C0008-403 Temp - Heat Exch He Inlet C0049-405 Temp - Electrical Tunnel, Loc 1 C0058-406 Temp - LOX Tank Ullage, 80 percent C0111-426 Temp - Fwd Skirt, Loc 8 C0151-401 Temp - LOX Pump Surface C0286-415 Temp - APS Fairing 2-4 D0105-404 Press - LOX Tank Press Mod, He Gas E0114-411 Vib - Fwd Skirt, EBW R/S Pnl, Radial E0210-401 Vib - LH2 Turbopump - Lateral	10
7.	Measurements which were failures during TPEP phase II (Liftoff to planned LV/SC separation as defined in NASA drawing 40M33622, Interface Control Document Definition of Saturn SA-502 Flight Sequence Program). Details regarding these measurement failures may be obtained in section 18 of this report. All measurements which were failures during TPEP phase I are included as phase II failures because phase II encompasses phase I. These ten measurements are shown in item 6 above. In addition to those measurements which were failures during TPEP phase I, the following four measurements were failures during phase II. C0189-414 Temp - APS Inj Wall, Eng 1-2 C2015-401 Temp - Crossover Duct Ext Wall 1 D0003-403 Press - LOX Pump Inlet D0224-401 Press - LH2 Pump Intrstg Outlet Calculation of phase I performance: Item 5 minus item 6, divided by item 5, multiplied by 100, and rounded off to the nearest one-tenth of one percent. $\frac{591-10}{591} \times 100 = 98.3$ percent Calculation of phase II performance: Item 5 minus item 7, divided by item 5, multiplied by 100, and rounded off to the nearest one-tenth of one percent. $\frac{588-14}{588} \times 100 = 97.6$ percent	14

SECTION 8

TRAJECTORY

8. TRAJECTORY

8.1 Scope

This section presents a discussion of the AS-502 vehicle trajectory. Comparisons are made between the actual observed trajectory and the preflight and postflight predicted trajectories; also results of a simulation of the actual trajectory are presented. Actual observed trajectory deviations from predicted are explained in terms of S-IVB and lower stage system performance deviations.

Also presented is the parking orbit continuous vent system (CVS) thrust determined from trajectory analysis. A comparison of this thrust with predicted is presented.

As areas of interest, discussions are included of the vehicle overspeed problem which occurred at the end of the S-IVB first burn, and the stage motion and breakup after the unsuccessful restart attempt.

8.2 Comparison Between Actual and Preflight Predicted Trajectories

A comparison is made between the actual trajectory (based on tracking and telemetry data) and the preflight predicted trajectory. The predicted trajectory, during S-IC and S-II stage burns, is that presented in the Boeing final operational trajectory. The S-IVB portion of the predicted trajectory is the Douglas final predicted trajectory.

The flight trajectory of the AS-502 was characterized by several anomalies (section 2) resulting in large deviations from the predicted trajectory beginning at approximately R0 +413 sec and continuing throughout the remainder of the boost to parking orbit phase and the parking orbit coast phase. Most significant of the anomalies was a failure of the S-IVB J-2 engine to reignite for boost into translunar orbit. Powered flight comparisons of actual and predicted trajectory conditions as presented in this section will, therefore, be restricted to the boost to parking orbit phase.

Figures are presented comparing the actual and predicted values of altitude, ground range, crossrange position, crossrange velocity, inertial velocity, axial acceleration, inertial flight path elevation angle, and inertial flight path azimuth angle for the powered and orbital coast phases of the flight.

Figures 8-1 through 8-25 compare the actual and predicted histories for each trajectory parameter. Figures 8-26 through 8-31 present a history of the differences between the preflight and postflight predicted and actual trajectory parameters during the S-IVB and orbital phases of flight. Table 8-1 shows conditions at certain significant event times.

The S-IC stage trajectory was close to predicted. As shown in table 8-1, the maximum dynamic pressure was 31.5 lbf/ft^2 higher than predicted and it occurred 4.14 sec earlier than predicted. Approximately 100 sec into the S-IC flight, a longitudinal pogo oscillation of approximately 5 cps was observed. This oscillation lasted through the remaining portion of S-IC flight producing no significant effect on the trajectory. S-IC/S-II separation

occurred 1.35 sec later than predicted. As shown in table 8-1, the altitude at S-IC/S-II separation was 3,379 ft higher than predicted and the inertial velocity was 33.2 ft/sec higher than predicted.

The S-II stage trajectory was close to predicted until RO +412.9 sec. At this time the No. 2 engine prematurely shut down. Reportedly because of prevalve cross wiring, the No. 3 engine was shut down at RO +414.2 sec following the detection of a thrust loss on engine No. 2. As a result of the shutdown of these engines, S-II propellant depletion was not reached until RO +576.3 sec, at which time the three remaining engines cut off normally. The iterative guidance mode (IGM) was not implemented to fly optimally with two engines out. The IGM detected a loss of a single engine and adjusted S-II burn time-to-go by 20 percent. When the second engine shut down, no further adjustment of time-to-go could be made. As a result, the guidance commands were frozen approximately 58 sec prior to S-II cutoff, causing a far-from-optimum trajectory during the latter part of S-II boost. S-II/S-IVB separation occurred at RO +577.08 sec, 59.12 sec later than predicted. At this time the trajectory could be characterized as slow, high, long, and to the right of the predicted path. This is shown in table 8-1. The inertial velocity was 354.9 ft/sec lower than predicted while the altitude was 21,323 ft higher than predicted. The inertial flight path elevation angle was 0.822 deg higher than predicted. Figures 8-1 through 8-14 present the S-IC/S-II trajectory parameter histories.

Because of the nonoptimum trajectory conditions at S-II/S-IVB separation which resulted from the large period of frozen attitude commands, guidance commanded the S-IVB to pitch nose down at the maximum rate of 1 deg/sec for 60 sec. At this time, altitude reached its peak value (figure 8-26) and began to decrease toward the target value. Figure 8-29 shows that at this time inertial flight path angle was decreasing rapidly from the target value of 0 deg which is necessary to obtain the desired orbit. In order to attain target flight path angle, the vehicle was commanded to pitch nose up. This nose up maneuver became rate limited near the end of S-IVB burn. Figure 8-23 presents pitch attitude commands during these maneuvers. When target velocity of 25,561.1 ft/sec was attained at approximately RO +739 sec, the guidance was still attempting to rotate the velocity vector to a 0 deg flight path orientation. At RO +747.04 sec, after guidance had entered the high-speed loop, the velocity magnitude was found to be greater than its target value and engine cutoff was commanded. This overspeed problem is discussed in detail in paragraph 8.5.

Another significant problem occurred during the S-IVB first burn. At approximately RO +690 sec, the LH2 augmented spark igniter (ASI) feedline ruptured. This caused an approximate 5,000 lbf (paragraph 8.4) loss in thrust to occur. The lower acceleration caused by this loss in thrust is shown in figure 8-20. Table 8-1 presents the trajectory conditions at S-IVB first burn Engine Cutoff Command. These conditions can be characterized as low, fast, and long. The altitude was 1,987 ft lower than predicted while the inertial velocity was 160.2 ft/sec higher than predicted. The inertial flight path elevation angle was 0.4 deg lower than predicted. Figures 8-15 through 8-29 present the S-IVB trajectory.

A parking orbit was achieved which had an apogee altitude of 194.4 nmi, a perigee altitude of 93.5 nmi, and a period of 89.8 min, instead of the target 100 nmi circular parking orbit. The elliptical orbit was caused by the vehicle overspeed. Had the vehicle overspeed not occurred and S-IVB cutoff been commanded when target velocity magnitude was reached, the resulting parking orbit would have had a perigee radius of 67 nmi and an apogee radius of 157 nmi since flight path angle would still have been approximately 0.7 deg below the target value. Trajectory conditions and parking orbit elements at insertion are presented in table 8-1. The CVS thrust appeared to be close to nominal throughout the parking orbit (paragraph 8.6). Preparations to restart the S-IVB were begun 11,287.73 sec into the flight. This was 213.7 sec later than predicted because of the higher-than-predicted elliptical parking orbit period. Trajectory conditions at this time are presented in table 8-1. Figure 8-30 and 8-31 present the parking orbit trajectory.

Restart of the S-IVB J-2 engine was attempted at R0 +11,614.7 sec. Table 8-1 presents the trajectory conditions at this time. Following fuel lead, LOX and LH2 were dumped through the engine in the normal manner, and the combination of pumped propellants and gas generator exhaust produced approximately 10,000 lbf of J-2 engine thrust. However, due to the rupture of the LH2 ASI line during first burn, reignition did not occur. The instrument unit automatically initiated TB7 at R0 +11,630.32 sec, when the mainstage pressure switch did not detect sufficient chamber pressure to indicate that ignition was accomplished. Launch vehicle/spacecraft (LV/SC) separation was initiated by ground command at R0 +11,666.1 sec. Trajectory conditions at TB7 and LV/SC separation are presented in table 8-1.

8.3 Postflight Predicted Trajectory Evaluation

To assist in the isolation of S-IVB performance deviations which contributed to trajectory deviations, a postflight S-IVB predicted trajectory was generated. This trajectory was generated using predicted S-IVB performance characteristics and actual S-II/S-IVB separation trajectory conditions. Trajectory deviations between the actual and the postflight predicted are due to S-IVB performance deviations, observed trajectory evaluation errors, and instrument unit navigation or guidance errors.

To support this evaluation, the following set of parameters were selected to define the S-IVB trajectory: Altitude, ground range, crossrange position, crossrange velocity, inertial velocity, axial acceleration, inertial flight path elevation angle, and inertial flight path azimuth angle. Figures 8-26 through 8-31 show that deviations from predicted for each of these parameters are due primarily to lower stage performance deviations. S-IVB performance, with the exception of the ASI fuel feedline rupture at approximately R0 +690 sec, was nearly nominal as indicated by figure 8-32 through 8-35. These figures compare the postflight predicted trajectory with observed data.

Over most of the S-IVB powered flight, the postflight predicted trajectory is long, low, fast, and to the right of actual. Figure 8-34 shows that actual vehicle acceleration was lower than predicted, which accounts for the slower-than-predicted inertial velocity (figure 8-34) and the shorter-than-predicted ground range (figure 8-32). Postflight simulated trajectory analysis (paragraph 8.4) shows that a thrust vector misalignment in both the pitch and yaw planes accounts for the deviations between postflight predicted and actual altitude (figure 8-32), crossrange position and velocity (figure 8-33), and inertial

flight path elevation and azimuth angles (figure 8-35). The impact of the overspeed phenomenon on S-IVB cutoff conditions is evident from figures 8-34 and 8-35. The target cutoff velocity was exceeded by approximately 160 ft/sec, but the overspeed caused both elevation and azimuth flight path angles to more closely approach target values. Guidance responses causing the overspeed are discussed in detail in paragraph 8.5.

The S-IVB burntime was 30.8 sec longer than predicted. The table below shows that the primary contributors to this deviation were deviations in preconditions of flight.

The magnitude of these contributions were obtained from postflight trajectory analysis using the actual preconditions of flight and predicted S-IVB performance. Another large contributor was the overspeed. The magnitude of this contribution was obtained by subtracting from the actual cutoff time the time at which the launch vehicle digital computer (LVDC) output indicated the magnitude of the target velocity was reached. The remainder of the contributions bring the total burntime deviation to 32.6 sec. This is 1.8 sec more than the actual burntime deviation. The additional 1.8 sec of burntime could be accounted for by uncertainties in preconditions of flight and uncertainties in the thrust average obtained from trajectory reconstruction.

CONTRIBUTOR	DEVIATION (ACTUAL MINUS PREDICTED)	CONTRIBUTION TO BURNTIME DEVIATION
Preconditions of flight (simulation)		+23.1 sec
Velocity magnitude	-354.9 deg	
Elevation flight path angle	+0.822 deg	
Altitude	+21,300 ft	
Overspeed (LVDC)	+160.2 ft/sec	+8.1 sec
S-IVB thrust	-1,985 lb	+1.0 sec
S-IVB mass flow	+0.48 lb	+0.4 sec
Total		+32.6 sec

Figures 8-30 and 8-31 compare the postflight predicted and actual parking orbit trajectories. Because of the overspeed at S-IVB cutoff, the AS-502 flight vehicle was inserted into a perturbed parking orbit with an apogee altitude of 194.4 nmi and a perigee altitude of 93.5 nmi. Since the CVS thrust was near predicted (paragraph 8.6), the deviation in postflight predicted and actual parking orbit is due primarily to the guidance overspeed phenomenon.

8.4 Powered Flight Simulated Trajectory Evaluation

Using a five-degrees-of-freedom trajectory simulation program, a trajectory was generated which closely matched the observed trajectory (appendix 3). The simulation program employed a differential correction technique which determined the necessary adjustments to the levels of thrust and weight flow from the engine analysis and adjustments to pitch and yaw engine thrust misalignment angles from the control system analysis to match the observed trajectory.

These adjustments were determined by minimizing, in a least-squares sense, the weighted differences in altitude, earth-fixed velocity, earth fixed velocity azimuth angle, and inertial acceleration between the observed and simulated trajectories.

Differences between the observed and simulated trajectories are presented in figure 8-36. The standard deviation of the differences and the maximum of the differences are:

PARAMETER	UNITS	STANDARD DEVIATION	MAXIMUM DEVIATION
Altitude	ft	97.15	190.1
Earth-fixed velocity	ft/sec	2.618	4.77
Earth-fixed velocity azimuth angle	deg	0.0020	0.0041
Inertial acceleration	ft/sec^2	0.0714	0.179

Figure 8-37 shows the thrust history determined by engine analysis. To obtain a match of the observed trajectory initial results indicated that the thrust level after the performance shift should have been higher than that determined by engine analysis. Consequently, a study was conducted to parameterize the size of the performance shift.

A series of simulations was made in which the thrust level after the performance shift was varied by applying a multiplier from a range time of 700 sec to Engine Cutoff Command before the differential correction procedure was applied. Figure 8-38 shows the resultant behavior of two parameters as a function of this multiplier. The first parameter, L, is the non-dimensional weighted sum of the squares of the differences between the observed and simulated trajectories and is a measure of the trajectory fit. This is the quantity that is minimized by the trajectory hunting procedure. The other parameter, Δw, represents the difference between the weights as determined from the trajectory simulation and that determined by the best estimate of mass technique (section 9). It is interesting to note that where the trajectory weight determination coincides with that determined by the other methods, the trajectory fit parameter, L, is also minimized. These results indicate that the multiplier adjusting the thrust level should be equal to 0.6 percent, which indicates a smaller performance shift than determined by engine analysis.

The following table compares the average performance from 90 percent thrust as calculated by trajectory reconstruction and engine analysis with the predicted performance. The table also compares performance before and after the performance shift as calculated by trajectory reconstruction with that calculated by engine analysis.

PARAMETER	UNITS	PREDICTED	ENGINE ANALYSIS	TRAJECTORY RECONSTRUCTION
Total average thrust	lb	228,310	226,565	227,838
Total average weight flow	lb/sec	538.21	537.91	537.34
Total average specific impulse	sec	424.01	421.19	424.03
Before Performance Shift				
Average thrust	lb	--	229,200	229,897
Average weight flow	lb/sec	--	540.6	539.56
Average specific impulse	sec	--	424	426.09
After Performance Shift				
Average thrust	lb	--	223,000	226,154
Average weight flow	lb/sec	--	536.9	538.77
Average specific impulse	sec	--	414.5	419.77

The S-IVB weights as determined by trajectory reconstruction are:

	PREDICTED	SIMULATED
Engine Start Command (lbm)	353,300	354,175
Engine Cutoff Command (lbm)	280,524	265,300

These weights were derived from the composite best estimate ignition and cutoff weight (section 9). The weights were determined by finding the point on the trajectory reconstruction line (figure 9-5), that has the highest probability of being equal to the best estimate value for ignition and cutoff weight. Using the nonpropellant weights of 117,649 lbm at Engine Start Command and 117,574 lbm at Engine Cutoff Command presented in section 16 and the best estimate of the liquid oxygen to liquid hydrogen ratios presented there, flight simulation results indicate the following propellant consumptions:

	LOX	LH2	TOTAL PROPELLANTS
	ENGINE START COMMAND		
Actual	194,088	42,438	236,526
Predicted	193,273	42,493	235,766
Deviation*	815	-55	760

*Deviation equals actual minus predicted.

	LOX	LH2	TOTAL PROPELLANTS
	ENGINE CUTOFF COMMAND		
Actual	119,219	28,507	147,726
Predicted	132,047	31,185	163,232
Deviation*	-12,828	-2,678	-15,506
	TOTAL CONSUMED		
Actual	74,869	13,931	88,800
Predicted	61,226	11,308	72,534
Deviation*	13,643	2,623	16,266

*Deviation equals actual minus predicted

The pitch and yaw thrust misalignment angles as established by control system and trajectory analysis, compare favorably. The values obtained are given below.

PARAMETER	UNITS	CONTROL ANALYSIS VALUE	SIMULATED VALUE
Pitch thrust misalignment	deg	0.25	0.13
Yaw thrust misalignment	deg	0.42	0.64

A positive pitch misalignment produces a nose-above commanded attitude, and a positive yaw misalignment produces a nose-left of commanded attitude (looking downrange).

The steady-state thrust vector as determined by flight simulation was located relative to the vehicle as shown below:

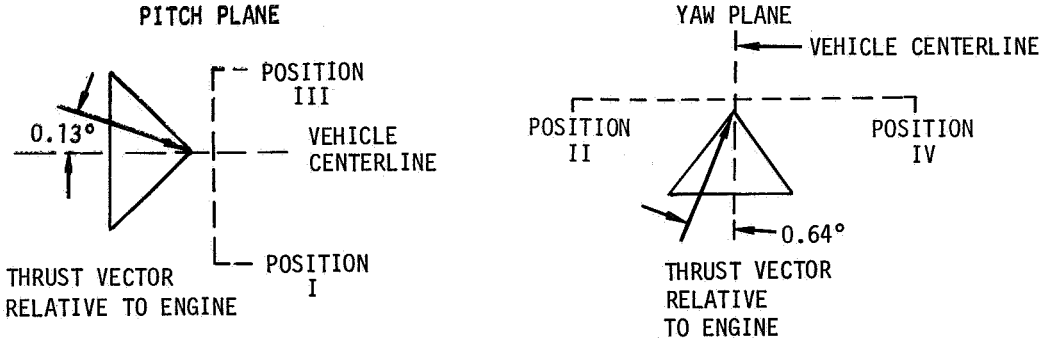

8.5 S-IVB First Burn Guidance Response Analysis

This section presents results of an analysis of the operation of the IGM during AS-502 boost to parking orbit. The IGM response to the S-II double engine-out trajectory, leading to the overspeed phenomenon at S-IVB cutoff, is explained in detail. Results of a trajectory simulation, assuming that direct staging was implemented as per flight mission rule No. 16, are also presented.

On AS-502, the IGM was capable of continuing to provide optimum commanded attitude angles in the event of no more than one S-II engine out. The IGM was not programmed to cope with two S-II engines out, hence guidance was nonoptimum during S-II two engine out operation.

At S-II/S-IVB separation, altitude (h) and inertial velocity flight path angle (γ_{1_I}') were higher and inertial velocity (V_I) lower than predicted. Given those initial conditions and the nonoptimum value of commanded pitch attitude angle (χ_p) at S-IVB IGM initiation, guidance commanded the vehicle to pitch nose down at the maximum rate of 1 deg/sec for 60 sec until optimum X_p was reached. The optimum X_p command rate at that time was nose up, becoming rate limited toward the end of S-IVB burn (figure 8-40).

A key IGM parameter pertinent to the overspeed problem is time-to-go to stage cutoff (T_3). T_3 is determined directly from the root sum square (RSS) of the three velocity-to-go components (difference between present velocity and target velocity). It is important to note that velocity-to-go and hence T_3 are dependent not only on velocity magnitude (V_I) but also velocity direction (γ_{1_I}').

After T_3 becomes less than 35 sec, guidance is based on the assumption that the altitude targeting constraint has been satisfied. Thereafter, guidance strives only to achieve the three components of target velocity. On the AS-502 flight, an unusually large inertial velocity flight path angle change requirement still existed toward the end of S-IVB first burn, causing the RSS of velocity-to-go components to be unusually large, even after target velocity magnitude (V_T) had been exceeded. This is shown in the sequence of diagrams below where the dashed line indicates velocity-to-go.

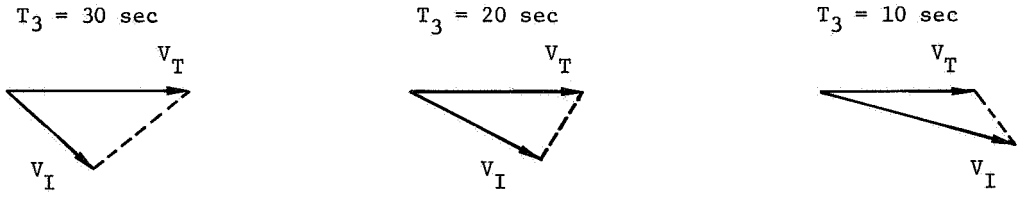

The large velocity-to-go as V_I approached V_T caused T_3 to be large also. The cutoff logic is not entered until after T_3 becomes less than 8 sec. After T_3 becomes less than 8 sec, the commanded attitude angles are frozen and guidance is based on the assumption that the cutoff velocity direction has been achieved and only the cutoff velocity magnitude constraint remains unsatisfied. Thus, all the IGM does once $T_3 < 8$ sec is to order engine cutoff when $V_I \geq V_T$.

Two trajectory simulations were made which resulted in overspeed at S-IVB first burn engine cutoff and allowed the isolation of guidance mechanism which caused the overspeed. In both cases, the actual PCF at S-II/S-IVB separation were perturbed as follows: γ_{1_I}', 10 percent more non-nominal, h, 10 percent less non-nominal. (This was necessary because the post-flight predicted trajectory, starting from observed PCF at S-II/S-IVB separation, did not exhibit overspeed. The postflight predicted trajectory achieved cutoff at the specified velocity 2.5 sec after T_3 < 8 sec.)

Case 1: The trajectory simulation assumed predicted J-2 engine performance and observed trajectory conditions perturbed by the above amounts at S-II/S-IVB separation. IGM and particularly the cutoff logic operation in this case were very similar to actual AS-502 operation. As previously noted, due to the large flight path angle error existing near end of burn, T_3 did not become less than 8 sec until after target velocity magnitude had been exceeded (figure 8-39). On the first guidance compute point after T_3 < 8 sec, IGM entered the velocity cutoff searching logic and cutoff occurred almost immediately.

Case 2 assumed subnominal engine performance as indicated by engine performance data and the perturbed trajectory conditions at separation. This case missed cutoff entirely. As previously noted, cutoff logic is not entered until T_3 becomes less than 8 sec. In this case, T_3 never became less than 8 sec and thus cutoff was not initiated (figure 8-39). It appears from actual 502 data that this situation very nearly occurred.

The results obtained indicate that given the actual initial conditions at S-IVB IGM start and the 1 deg/sec rate limit on X's, it was not possible to achieve the target first burn end conditions.

8.5.1 AS-502 Direct Staging Simulation Summary

A simulation was made of the trajectory that would have resulted if direct staging (TB4A) had been initiated after S-II second engine shutdown as per flight mission rule No. 16. The sequence of events and trajectory conditions achieved at S-IVB first burn engine cutoff are shown below.

To achieve S-IVB second burn ECF, a velocity gain of $\Delta V \sim 10{,}000$ fps is required after the parking orbit conditions are achieved. The direct staging simulation indicates that the desired parking orbit would have been achieved with only W_{LOX} = 57,790 lbm W_{LH2} = 13,275 lbm available for second burn. These propellants are sufficient to provide an available velocity gain of $\Delta V \tilde{=} 6{,}520$ fps. Therefore, translunar injection (TLI) conditions could not have been achieved. This agrees with the alternate mission prediction that TLI will not be achieved for direct staging prior to R0 +505 sec, assuming nominal performance until then.

Direct Staging Sequence of Events

Event	Time from Range Zero (sec)
No. 2 out	412.9
No. 3 out	414.2
S-II Engine Cutoff Command	449.5
Time Base 4A	452.5

Event	Time from Range Zero
S-IVB Engine Start Command	458.2
S-IVB Engine Cutoff Command	764.2

Conditions achieved at S-IVB first burn engine cutoff after direct staging

t	764.2 sec
h	627,275 ft
V_I	25,561 fps
$\gamma 1_I'$	-0.003 deg
$\gamma 2_I'$	90.23 deg

8.6 Orbital Trajectory Simulation Analysis

This paragraph presents a determination of the thrust provided during S-IVB parking orbit by the CVS. The level of CVS thrust is an important factor on normal Saturn V missions from two aspects: first, the accuracy of second burn engine cutoff conditions and, secondly, the S-IVB second burn performance capability.

Three-degrees-of-freedom trajectory simulations were conducted to determine the CVS thrust history required to closely match the observed orbital trajectory. The observed trajectory was generated from guidance accelerometer and tracking data. Figure 8-42 presents a comparison of predicted CVS thrust with the best estimate of actual thrust as determined from trajectory analysis. Figure 8-43 compares the difference between observed altitude during parking orbit and simulated altitude using both predicted and actual CVS thrusts. The actual CVS thrust provides a close fit of the observed altitude. To obtain this close fit, it was necessary to decrease the observed velocity at parking orbit insertion by 0.5 ft/sec, which is well within the 9.84 ft/sec accuracy band quoted for the observed velocity data.

As shown in figure 8-42, the S-IVB parking orbit CVS thrust was close to predicted, with the average thrust only 1.5 percent lower than predicted. This deviation would have had no significant effect on S-IVB performance during second burn, and no significant influence on S-IVB injection accuracy.

8.7 Orbital Motion following LV/SC Separation

Paragraph 21.2.6 discusses the loss of vehicle attitude control following depletion of APS propellant during the fourth parking orbit revolution. This section discusses the motion of the vehicle and orbit characteristic after control loss.

At RO +22,023 sec LOX propulsive venting was initiated by ground command in order to assure APS depletion prior to loss of stage electrical power.

Shortly after this ground action was taken, module 1 depleted at RO +22,053 sec, and yaw control was lost. Following module 2 depletion at RO +22,630 sec, complete stage attitude control was lost and the vehicle assumed conical rotational motion. By the time of

module 2 depletion the LOX venting thrust had decayed from an initial value of 700 lbf to 250 lbf thrust and continued to decrease to 25 lbf at approximately 6,000 sec after the vent was opened and may have sustained this level until loss of electrical power to the LOX vent solenoid valve.

Following loss of electrical power, the valve would close and remain closed until the vent pressure relief setting was reached. The time of electrical power loss to the vent valve and the time of relief venting is not known since these events were preceded by loss of power to the telemetry system.

Figure 8-44 presents the stage angular velocities following loss of attitude control. The motion in pitch and yaw was sinusoidal with one rate being an extremum when the other was zero; these rates induced a nearly flat spin with a half cone angle of 82 deg. To verify that the observed motion during this interval was consistent with known occurrences, such as APS depletion and LOX venting, Euler's equations of rotational motion were solved using estimated mass and LOX vent characteristics. The resultant solution yeilded a sufficiently close match of the actual rate data to indicate that the observed motion was caused by LOX vent thrust. The simulation is included in figure 8-44.

Figure 8-45 presents the orbit semi-major axis and rotational rate to 31 days after launch. Under the influence of LOX tank venting the body rate of the total vehicle continued to increase to approximately 180 deg/sec on the ninth day after launch. The centrifugal acceleration loads resulting from this high rate caused the vehicle to break up into six major parts. Orbital decay and eccentricity of these parts is shown in figure 8-45. One major component to break loose was the LTA. Reportedly, the loads induced by the observed high rotational rate at structural breakup were sufficient to expect LTA attachment failure.

TABLE 8-1 (Sheet 1 of 4)
TRAJECTORY CONDITIONS AT SIGNIFICANT EVENT TIMES

PARAMETER	SYMBOL	UNITS	PREDICTED	ACTUAL	DEVIATION
CONDITIONS AT MAXIMUM DYNAMIC PRESSURE					
Range time	(t)	sec	79.38	75.24	-4.14
Dynamic pressure	(q)	lbf/ft^2	753.0	784.5	31.5
Altitude	(h)	ft	44,760	39,429	-5,331
Mach number	(M)	--	1.79	1.61	-0.18
Ambient pressure	(Pa)	lbf/ft^2	336.4	434.4	98.0
Pitch angle of attack	(α)	deg	0.28	1.56	1.28
Yaw angle of attack	(β)	deg	0.09	0.62	0.53
CONDITIONS AT S-IC/S-II SEPARATION					
Range time	(t)	sec	147.73	149.08	1.35
Downrange distance	(Z_E)	ft	276,470	280,158	3,688
Vertical distance	(X_E)	ft	191,768	195,260	3,492
Crossrange distance	(Y_E)	ft	2,167	-442	-2,609
Downrange velocity	($\dot{Z}_E$)	ft/sec	7,245.9	7,291.3	45.4
Vertical velocity	($\dot{X}_E$)	ft/sec	2,962.1	2,942.6	-19.5
Crossrange velocity	($\dot{Y}_E$)	ft/sec	59.9	-12.5	-72.4
Relative velocity	(V_E)	ft/sec	7,828.2	7,862.7	34.5
Inertial velocity	(V_I)	ft/sec	9,038.8	9,072.0	33.2
Inertial flight path elevation angle	(γ_{1_I}')	deg	19.725	19.530	-0.195
Inertial flight path azimuth angle	(γ_{2_I}')	deg	75.491	74.996	-0.495
Altitude	(h)	ft	193,738	197,117	3,379
Range	(S)	ft	274,162	277,721	3,559
Dynamic pressure	(q)	lbf/ft^2	21.6	19.6	-2.0
Pitch angle of attack	(α)	deg	1.45	-3.72	-5.17
Yaw angle of attack	(β)	deg	0.50	-2.14	-2.64
CONDITIONS AT S-II/S-IVB SEPARATION					
Range time	(t)	sec	517.96	577.08	59.12
Downrange distance	(Z_E)	ft	5,040,251	6,055,052	1,014,801
Vertical distance	(X_E)	ft	21,545	-226,677	-248,222
Crossrange distance	(Y_E)	ft	77,797	100,850	23,053
Downrange velocity	($\dot{Z}_E$)	ft/sec	20,587.8	20,076.7	-511.1
Vertical velocity	($\dot{X}_E$)	ft/sec	-4,630.8	-5,223.2	-592.4
Crossrange velocity	($\dot{Y}_E$)	ft/sec	516.5	567.0	50.5
Relative velocity	(V_E)	ft/sec	21,108.5	20,752.7	-354.8
Inertial velocity	(V_I)	ft/sec	22,430.5	22,075.6	-354.9
Inertial flight path elevation angle	(γ_{1_I}')	deg	0.775	1.597	0.822
Inertial flight path azimuth angle	(γ_{2_I}')	deg	81.641	83.416	1.775
Altitude	(h)	ft	619,247	640,570	21,323
Range	(S)	ft	4,942,133	5,956,445	1,014,312
CONDITIONS AT S-IVB FIRST BURN ENGINE CUTOFF COMMAND					
Range time	(t)	sec	657.12	747.04	89.92
Downrange distance	(Z_E)	ft	8,027,843	9,592,333	1,564,490

Deviation = Actual minus predicted

TABLE 8-1 (Sheet 2 of 4)
TRAJECTORY CONDITIONS AT SIGNIFICANT EVENT TIMES

PARAMETER	SYMBOL	UNITS	PREDICTED	ACTUAL	DEVIATION
Vertical distance	(X_E)	ft	-922,905	-1,626,565	-703,660
Crossrange distance	(Y_E)	ft	170,971	232,687	61,716
Downrange velocity	($\dot{Z}_E$)	ft/sec	22,481.5	21,749.0	-732.5
Vertical velocity	($\dot{X}_E$)	ft/sec	-9,019.1	-11,013.7	-1,994.6
Crossrange velocity	($\dot{Y}_E$)	ft/sec	840.5	973.8	133.3
Relative velocity	(V_E)	ft/sec	24,237.8	24,398.1	160.3
Inertial velocity	(V_I)	ft/sec	25,561.1	25,721.3	160.2
Inertial flight path elevation angle	(γ_{1_I}')	deg	0.000	-0.400	-0.400
Inertial flight path azimuth angle	(γ_{2_I}')	deg	87.133	90.237	3.104
Altitude	(h)	ft	627,681	625,694	-1,987
Range	(S)	ft	7,988,636	9,655,615	1,666,979
CONDITIONS AT PARKING ORBIT INSERTION					
Range time	(t)	sec	667.12	757.04	89.92
Downrange distance	(Z_E)	ft	8,252,204	9,809,284	1,557,080
Vertical distance	(X_E)	ft	-1,014,379	-1,737,882	-723,503
Crossrange distance	(Y_E)	ft	179,463	242,504	63,041
Downrange velocity	($\dot{Z}_E$)	ft/sec	22,384.3	21,633.5	-750.8
Vertical velocity	($\dot{X}_E$)	ft/sec	-9,273.7	-11,253.6	-1,979.9
Crossrange velocity	($\dot{Y}_E$)	ft/sec	857.7	990.3	132.6
Relative velocity	(V_E)	ft/sec	24,244.4	24,405.6	161.2
Inertial velocity	(V_I)	ft/sec	25,567.8	25,728.6	160.8
Inertial flight path elevation angle	(γ_{1_I}')	deg	0.001	-0.377	-0.376
Inertial flight path azimuth angle	(γ_{2_I}')	deg	87.567	90.675	3.108
Altitude	(h)	ft	627,721	623,979	-3,742
Range	(S)	ft	8,223,999	9,892,549	1,668,550
PARKING ORBIT ELEMENTS AT INSERTION					
Range time	(t)	sec	667.12	757.04	89.92
Semi-major axis	(a)	nmi	3,543.9	3,587.9	44.0
Apogee altitude*	(h_A)	nmi	100.0	194.4	94.4
Perigee altitude*	(h_p)	nmi	100.0	93.5	-6.5
Apogee velocity	(V_A)	ft/sec	25,567.7	25,055.7	-512.0
Perigee velocity	(V_p)	ft/sec	25,567.9	25,770.6	202.7
Eccentricity	(e)	--	0.0000	0.0141	0.0141
Inclination	(i)	deg	32.561	32.567	0.006
Period	(P)	min	88.19	89.84	1.65
Inertial velocity	(V_I)	ft/sec	25,567.8	25,728.6	160.8
Inertial flight path elevation angle	(γ_{1_I}')	deg	0.001	-0.377	-0.376
Descending node	(θ_N)	deg	123.176	123.196	0.020
Conic energy	(C_3)	m^2/sec^2	-60,732,254	-59,872,268	859,986
CONDITIONS AT TIME BASE 6					
Range time	(t)	sec	11,074.00	11,287.73	213.73

Deviation = Actual minus predicted
*Measured with respect to a mean earth radius of 3,443.94 nmi.

TABLE 8-1 (Sheet 3 of 4)
TRAJECTORY CONDITIONS AT SIGNIFICANT EVENT TIMES

PARAMETER	SYMBOL	UNITS	PREDICTED	ACTUAL	DEVIATION
Downrange distance	(Z_E)	ft	-8,628,597	-8,922,271	-293,674
Vertical distance	(X_E)	ft	-1,871,562	-1,995,040	-123,478
Crossrange distance	(Y_E)	ft	-5,343,617	-5,530,985	-187,368
Downrange velocity	($\dot{Z}$)	ft/sec	19,692.2	19,626.3	-65.9
Vertical velocity	($\dot{X}$)	ft/sec	11,288.6	11,470.8	182.2
Crossrange velocity	($\dot{Y}$)	ft/sec	8,465.4	8,621.2	155.8
Relative velocity	(V_E)	ft/sec	24,225.6	24,312.4	86.8
Inertial velocity	(V_I)	ft/sec	25,550.0	25,640.2	90.2
Inertial flight path elevation angle	(γ_{1_I}')	deg	-0.013	-0.589	-0.576
Inertial flight path azimuth angle	(γ_{2_I}')	deg	80.296	80.141	-0.155
Altitude	(h)	ft	661,121	718,846	57,725
Range	(S)	ft	10,242,365	10,595,769	353,404
CONDITIONS AT S-IVB SECOND BURN ENGINE START COMMAND					
Range time	(t)	sec	11,401.00	11,614.69	213.69
Downrange distance	(Z_E)	ft	-1,800,704	-2,099,419	-298,715
Vertical distance	(X_E)	ft	473,415	423,629	-39,786
Crossrange distance	(Y_E)	ft	-2,190,662	-2,317,223	-126,561
Downrange velocity	($\dot{Z}_E$)	ft/sec	21,595.4	21,641.2	45.8
Vertical velocity	($\dot{X}_E$)	ft/sec	2,891.5	3,143.8	252.3
Crossrange velocity	($\dot{Y}_E$)	ft/sec	10,603.8	10,821.6	217.8
Relative velocity	(V_E)	ft/sec	24,231.4	24,399.4	168.0
Inertial velocity	(V_I)	ft/sec	25,556.7	25,724.0	167.3
Inertial flight path elevation angle	(γ_{1_I}')	deg	-0.009	-0.334	-0.325
Inertial flight path azimuth angle	(γ_{2_I}')	deg	94.270	94.166	-0.104
Altitude	(h)	ft	660,588	651,462	-9,126
Range	(S)	ft	2,757,853	3,043,955	286,102
CONDITIONS AT S-IVB SECOND BURN ENGINE CUTOFF COMMAND					
Range time	(t)	sec	11,725.56	11,630.32	-95,24
Downrange distance	(Z_E)	ft	6,359,520	-1,760,955	-8,120,475
Vertical distance	(X_E)	ft	-11,688	469,487	481,175
Crossrange distance	(Y_E)	ft	2,023,130	-2,147,518	-4,170,648
Downrange velocity	($\dot{Z}_E$)	ft/sec	29,698.8	21,666.1	-8,032.7
Vertical velocity	($\dot{X}_E$)	ft/sec	-6,429.7	2,723.9	9,153.6
Crossrange velocity	($\dot{Y}_E$)	ft/sec	15,861.7	10,892.6	-4,969.1
Relative velocity	(V_E)	ft/sec	34,244.3	24,402.6	-9,841.7
Inertial velocity	(V_I)	ft/sec	35,581.2	25,727.0	-9,854.2
Inertial flight path elevation angle	(γ_{1_I}')	deg	6.673	-0.320	-6.993
Inertial flight path azimuth angle	(γ_{2_I}')	deg	108.652	94.840	-13.812
Altitude	(h)	ft	1,026,528	649,075	-377,453
Range	(S)	ft	6,463,519	2,702,029	-3,761,490

Deviation = Actual minus predicted

TABLE 8-1 (Sheet 4 of 4)
TRAJECTORY CONDITIONS AT SIGNITICANT EVENT TIMES

PARAMETER	SYMBOL	UNITS	PREDICTED	ACTUAL	DEVIATION
ORBIT ELEMENTS AT LV/SC SEPARATION					
Range time	(t)	sec		11,666.1	
Semi-major axis	(a)	nmi		3,596.1	
Apogee altitude*	(h_A)	nmi		204.8	
Perigee altitude*	(h_A)	nmi		99.5	
Apogee velocity	(V_A)	ft/sec		25,012.7	
Perigee velocity	(V_p)	ft/sec		25,755.9	
Eccentricity	(e)	--		0.0146	
Inclination	(i)	deg		32.568	
Period	(P)	min		90.15	
Inertial velocity	(V_I)	ft/sec		25,733.3	
Inertial flight path elevation angle	(γ_{1_I}')	deg		-0.286	
Descending node	(θ_N)	deg		122.268	
Conic Energy	(C_3	ft^2/sec^2		-59,738,957	

Deviation = Actual minus predicted
*Measured with respect to a mean earth radius of 3,443.94 nmi.

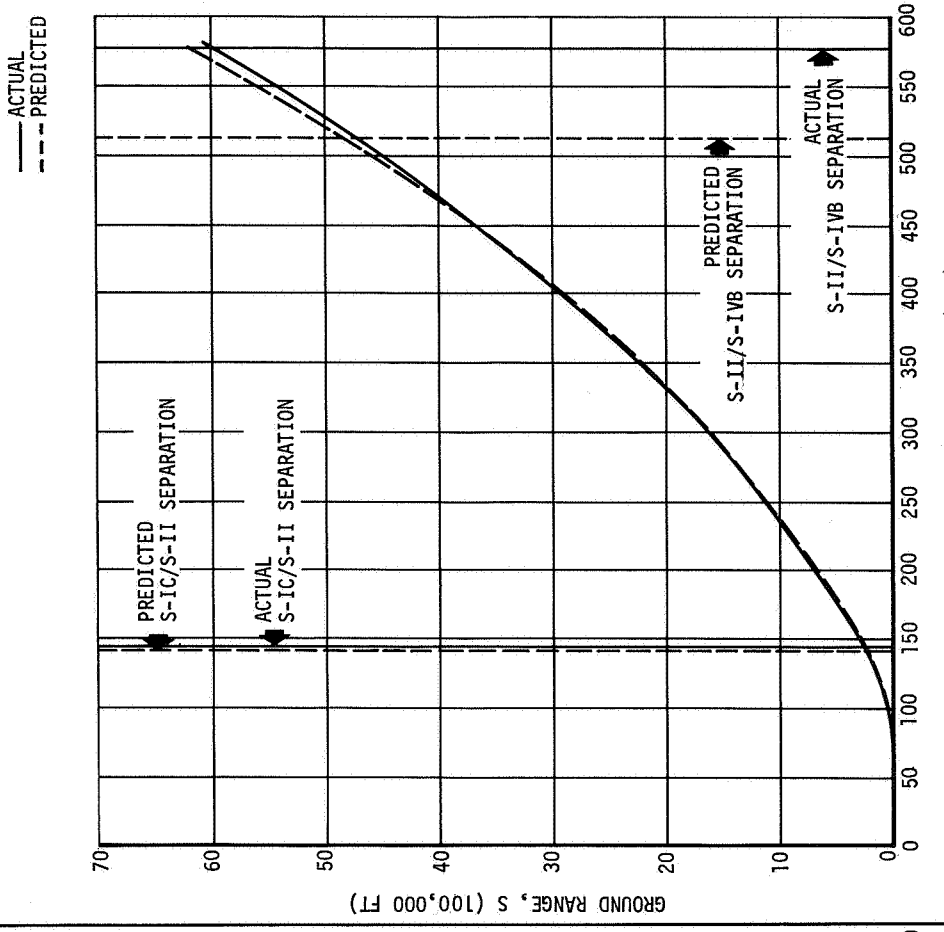

Figure 8-2. S-IC/S-II Ground Range History

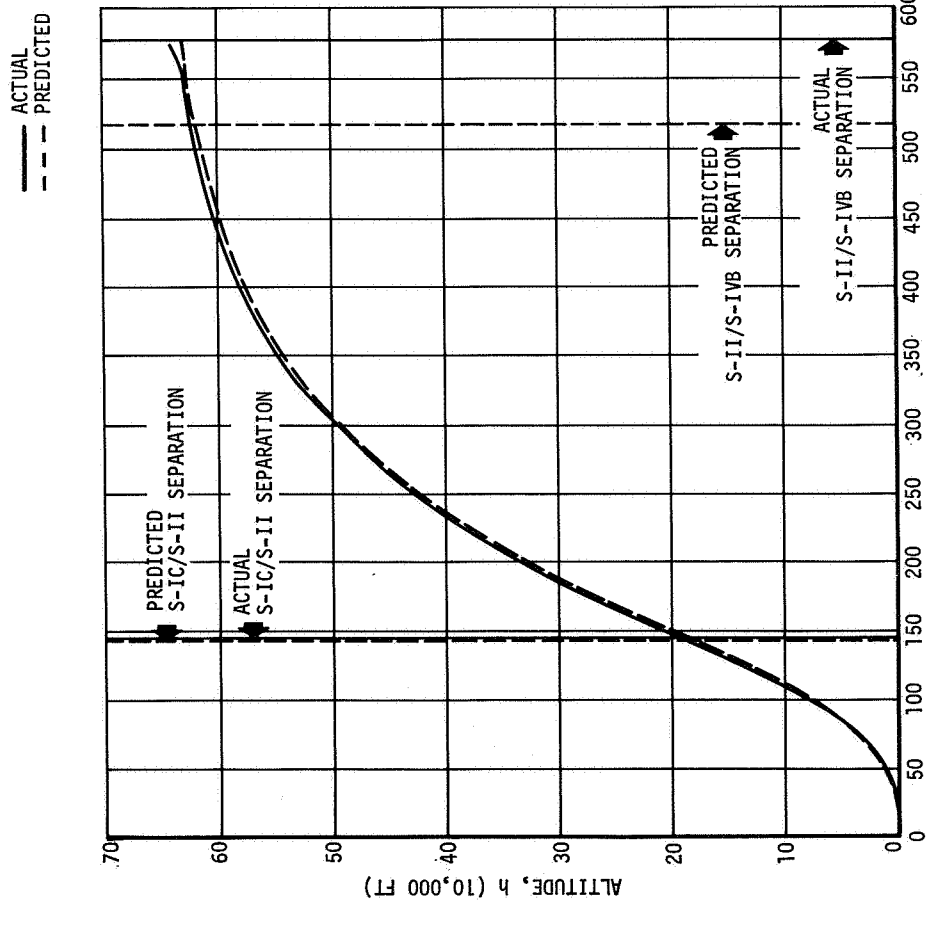

Figure 8-1. S-IC/S-II Altitude History

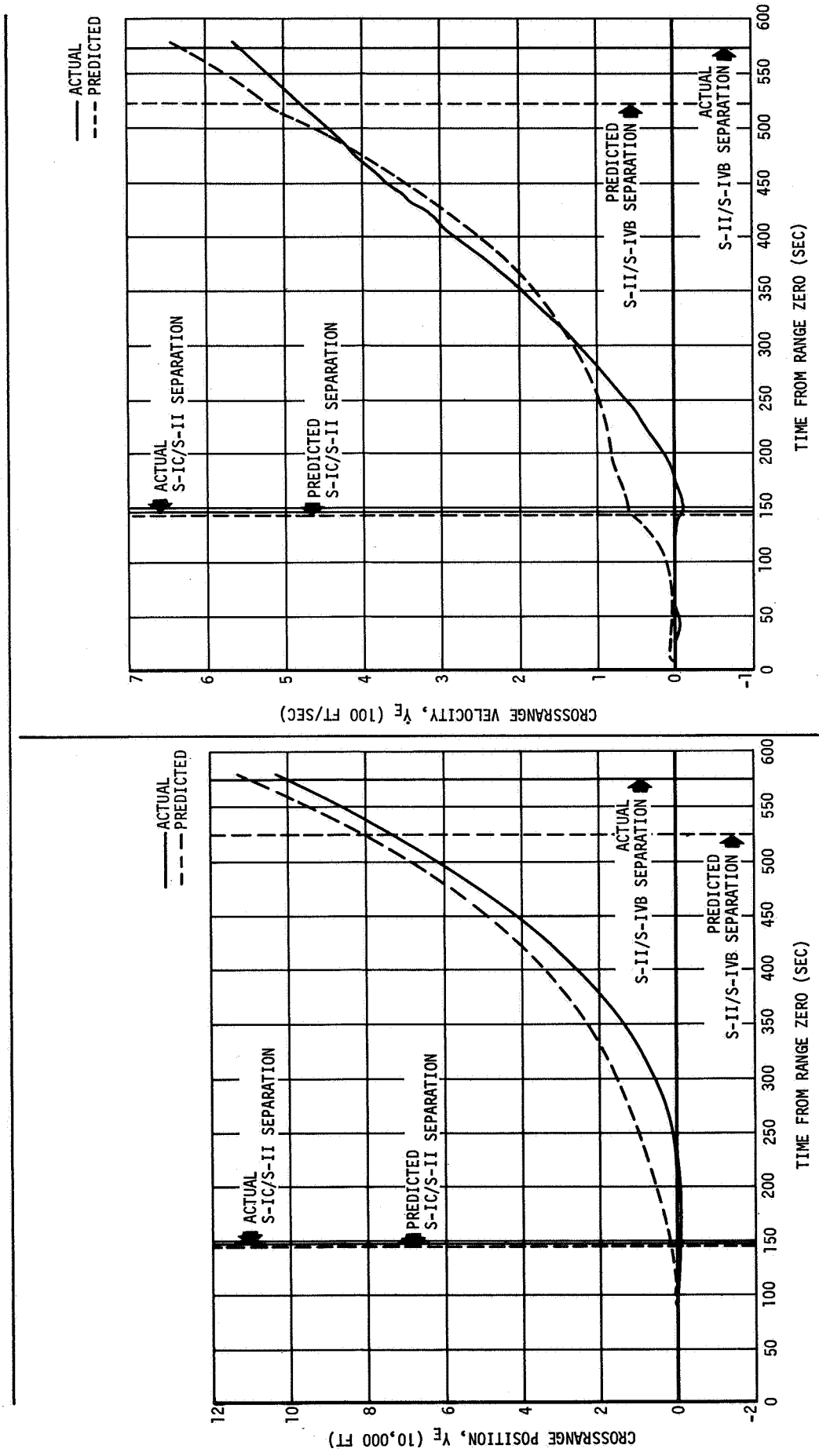

Figure 8-3. S-IC/S-II Crossrange Position History

Figure 8-4. S-IC/S-II Crossrange Velocity History

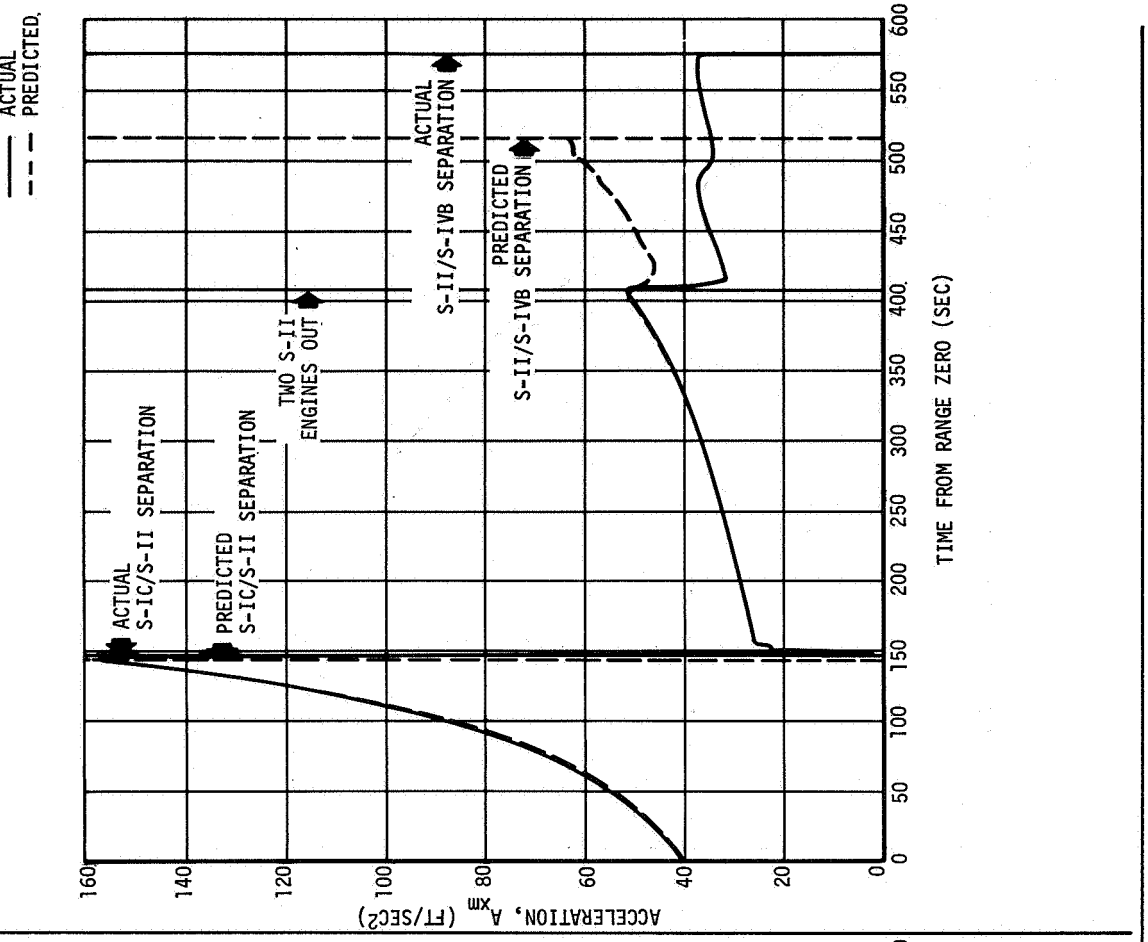

Figure 8-6. S-IC/S-II Axial Acceleration History

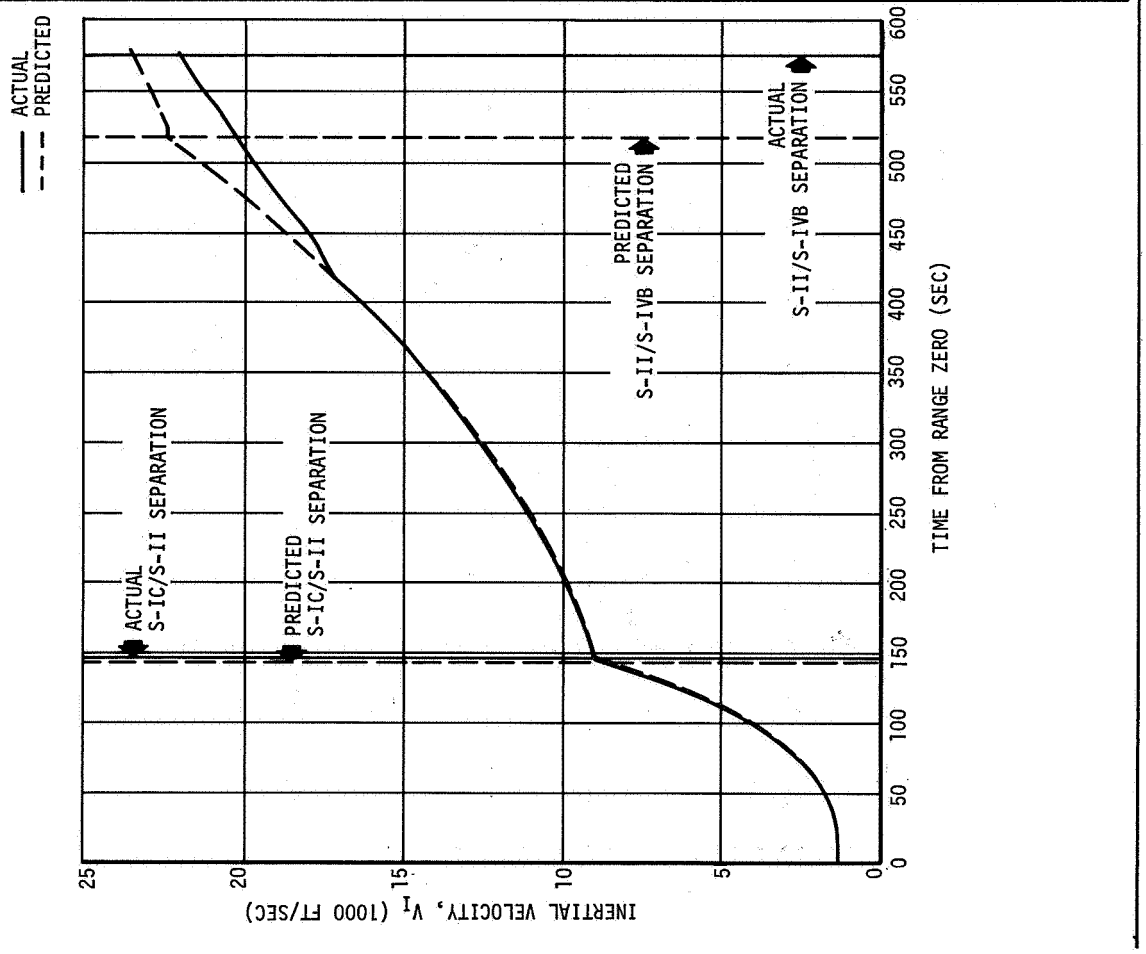

Figure 8-5. S-IC/S-II Inertial Velocity History

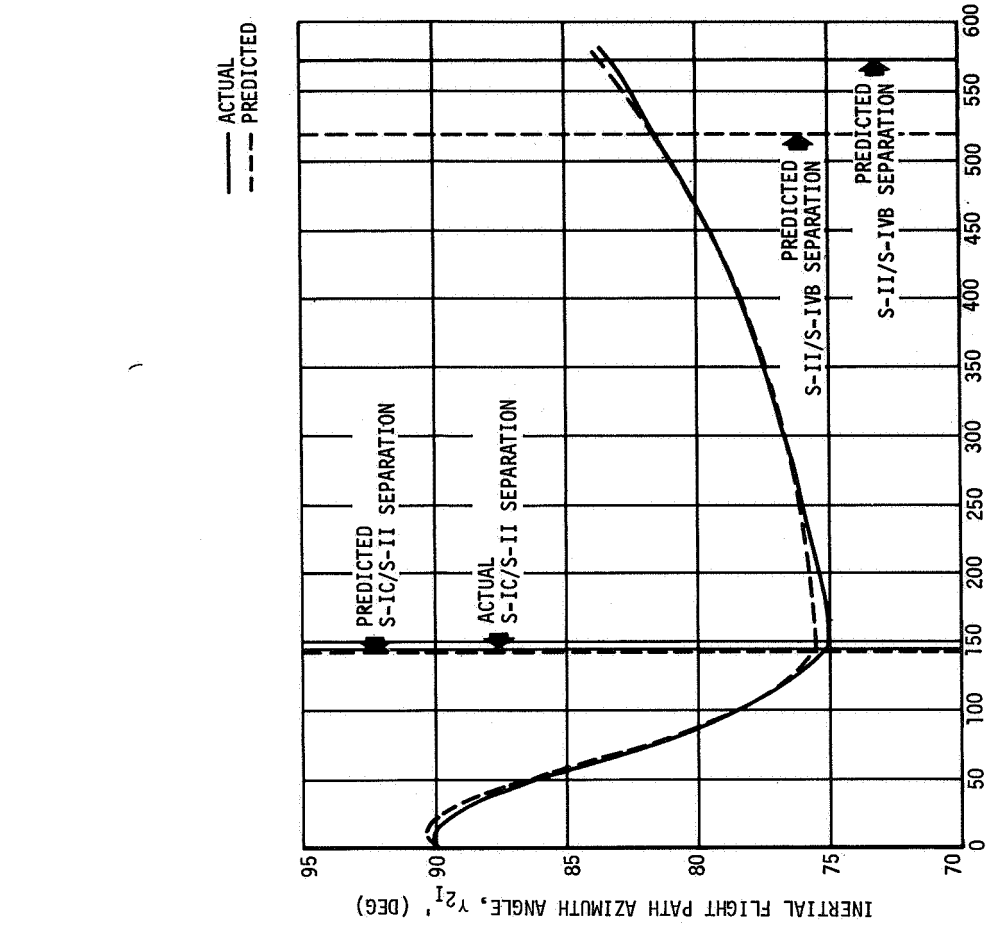

Figure 8-8. S-IC/S-II Inertial Flight Path Azimuth Angle History

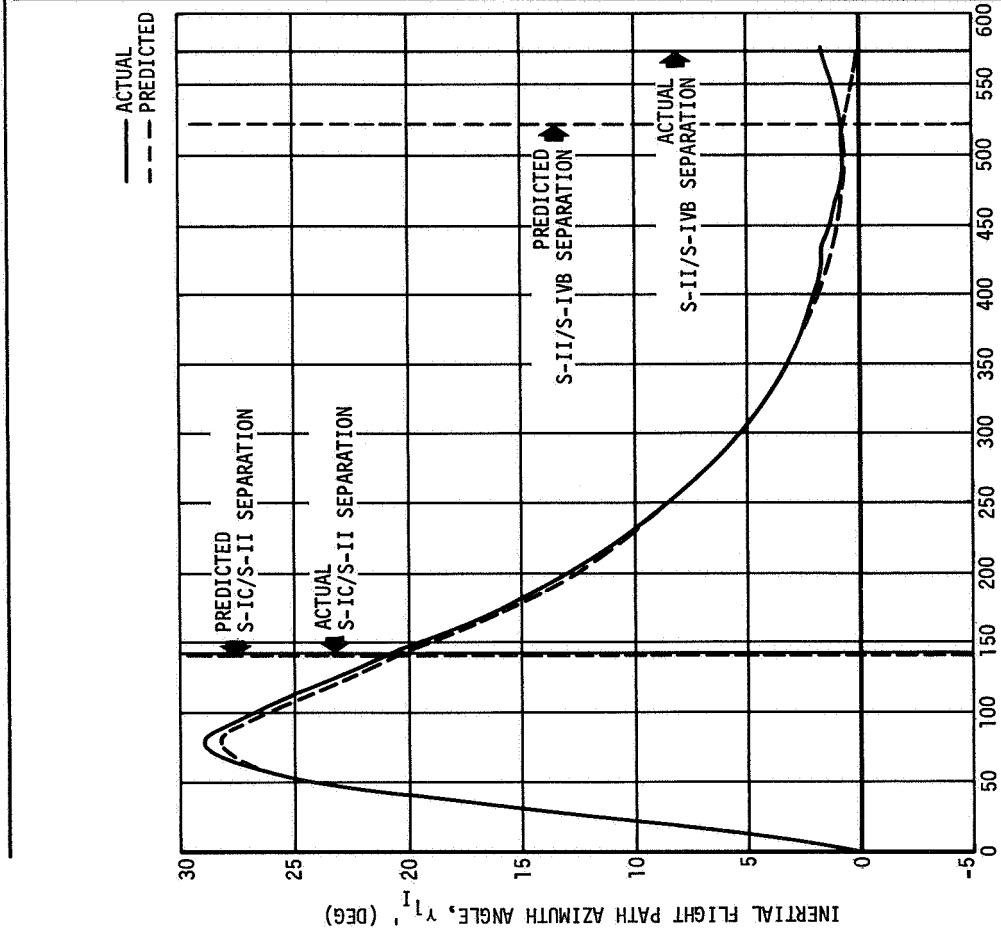

Figure 8-7. S-IC/S-II Inertial Flight Path Elevation Angle History

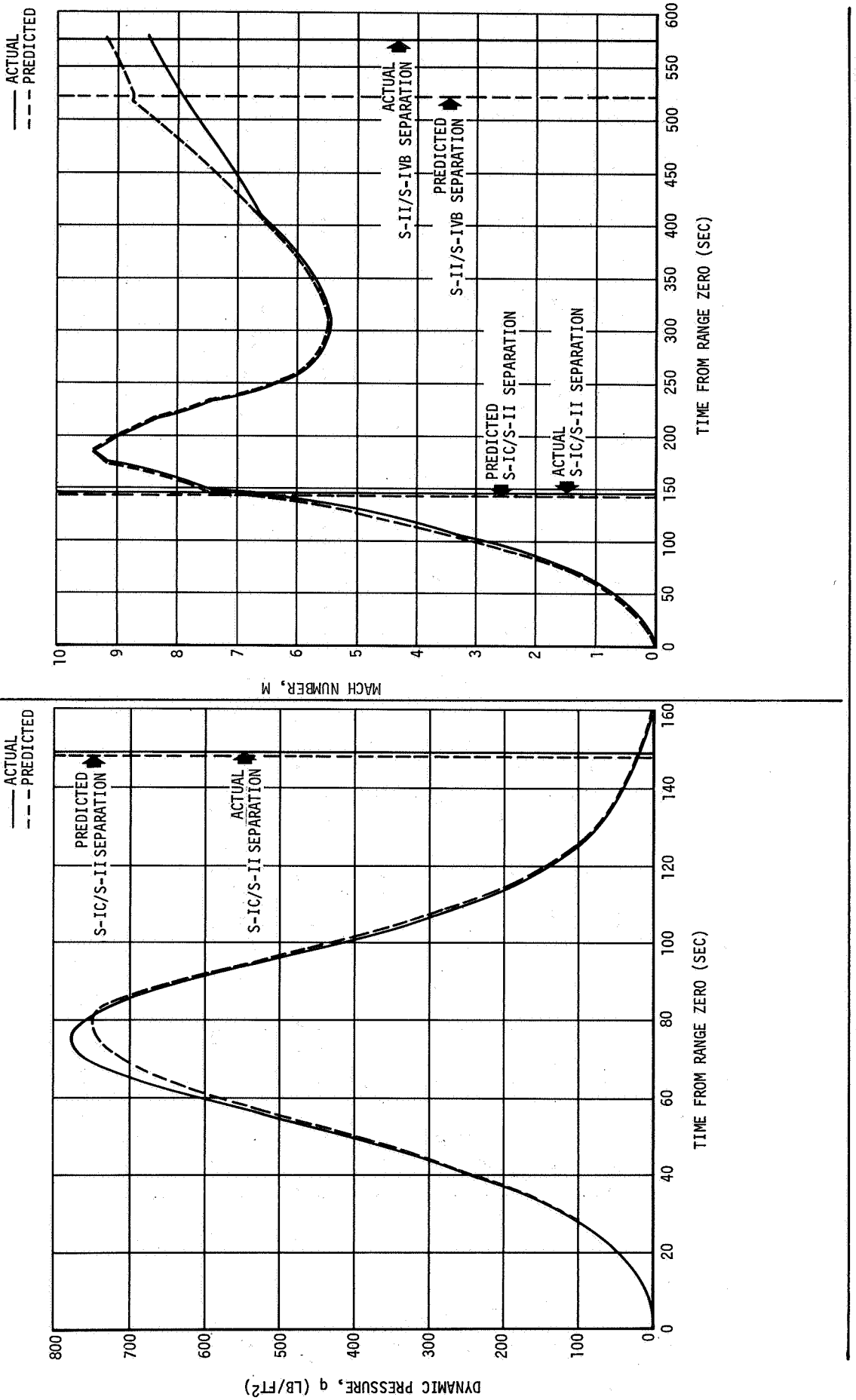

Figure 8-9. S-IC Dynamic Pressure History

Figure 8-10. S-IC/S-II Mach Number History

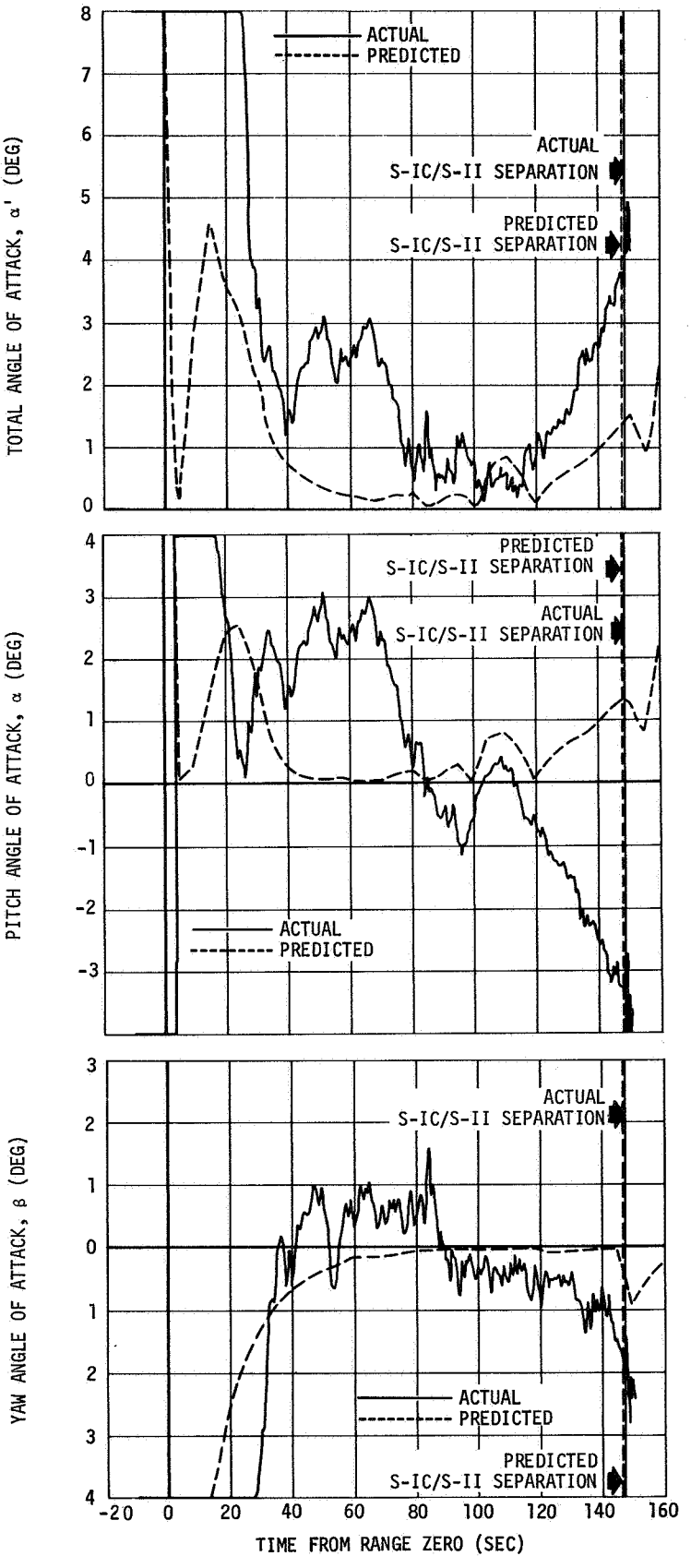

Figure 8-11. S-IC Angle of Attack History

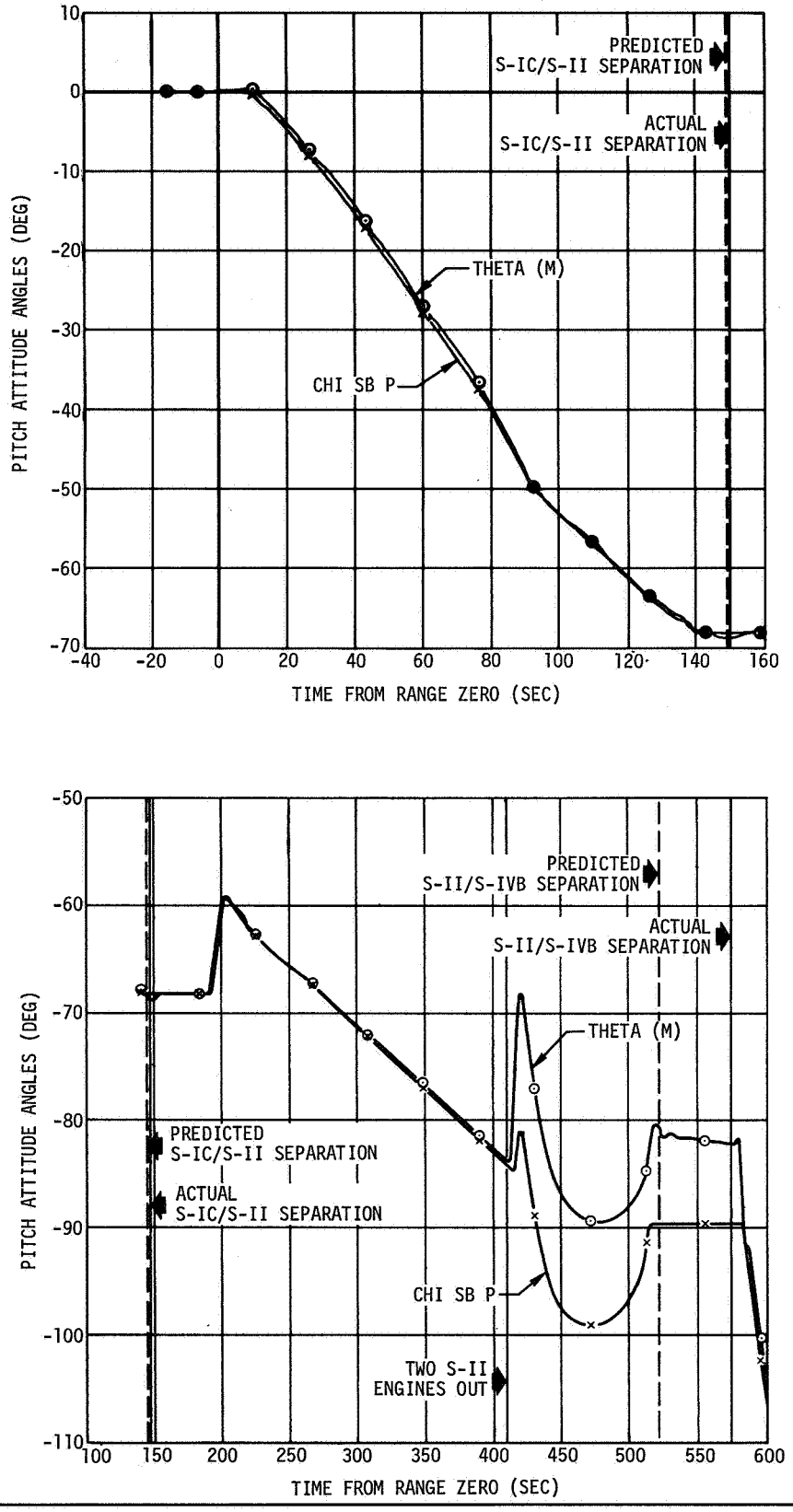

Figure 8-12. S-IC/S-II Pitch Attitude Angle History

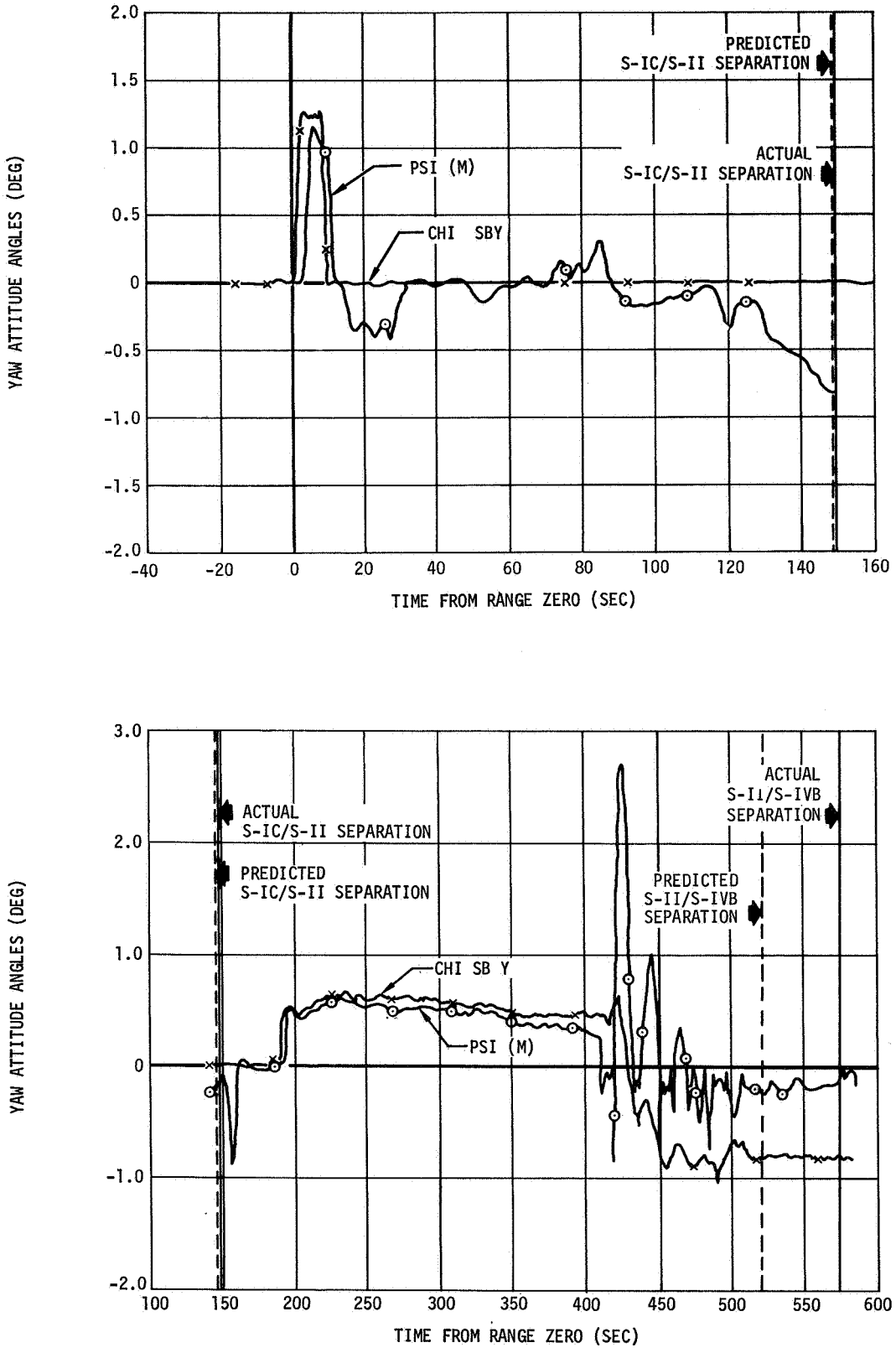

Figure 8-13. S-IC/S-II Yaw Attitude Angle History

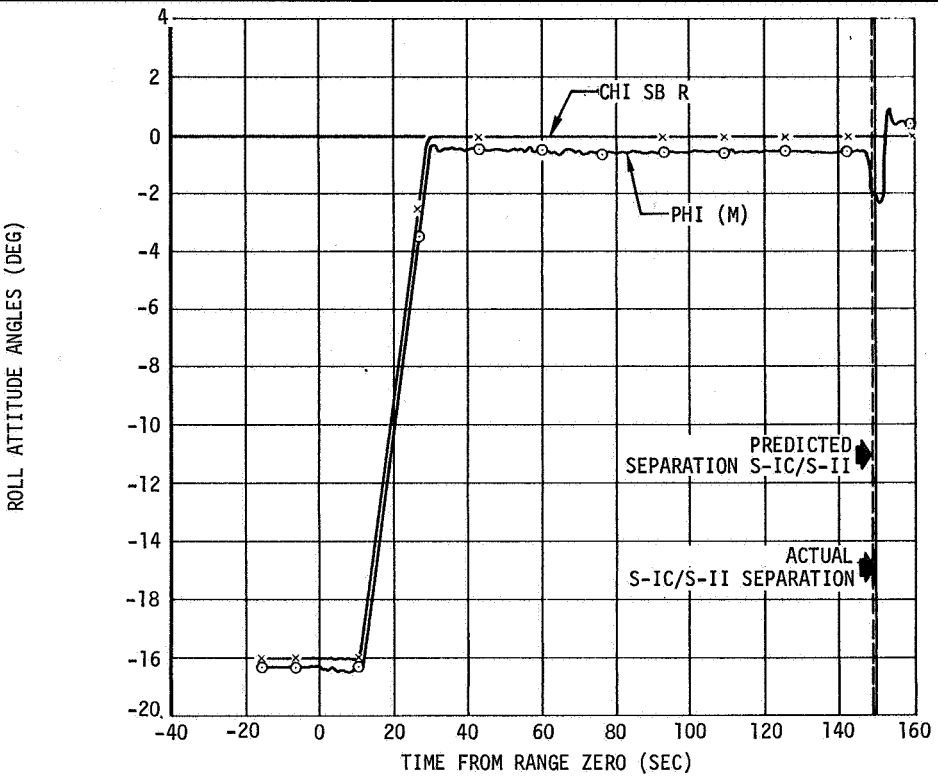

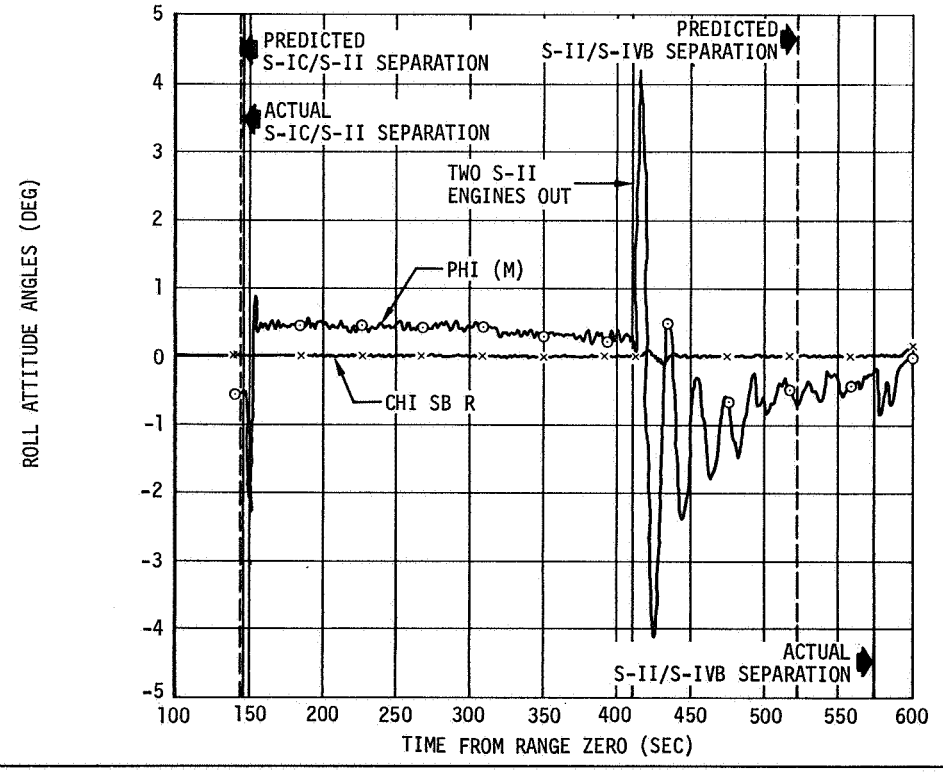

Figure 8-14. S-IC/S-II Roll Attitude Angle History

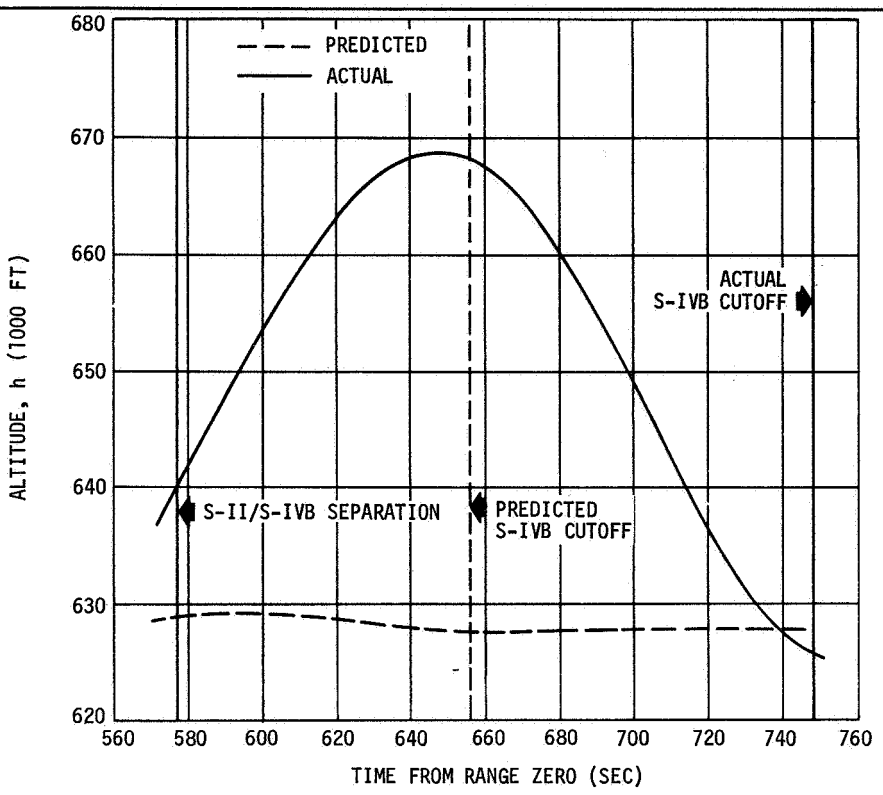

Figure 8-15. Altitude History

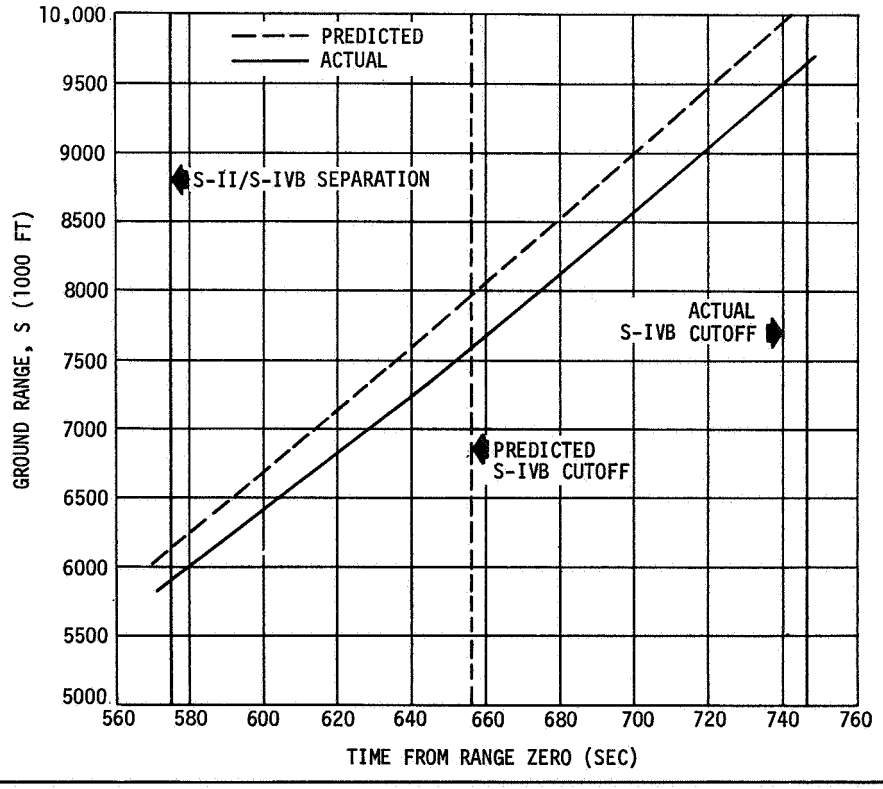

Figure 8-16. Ground Range History

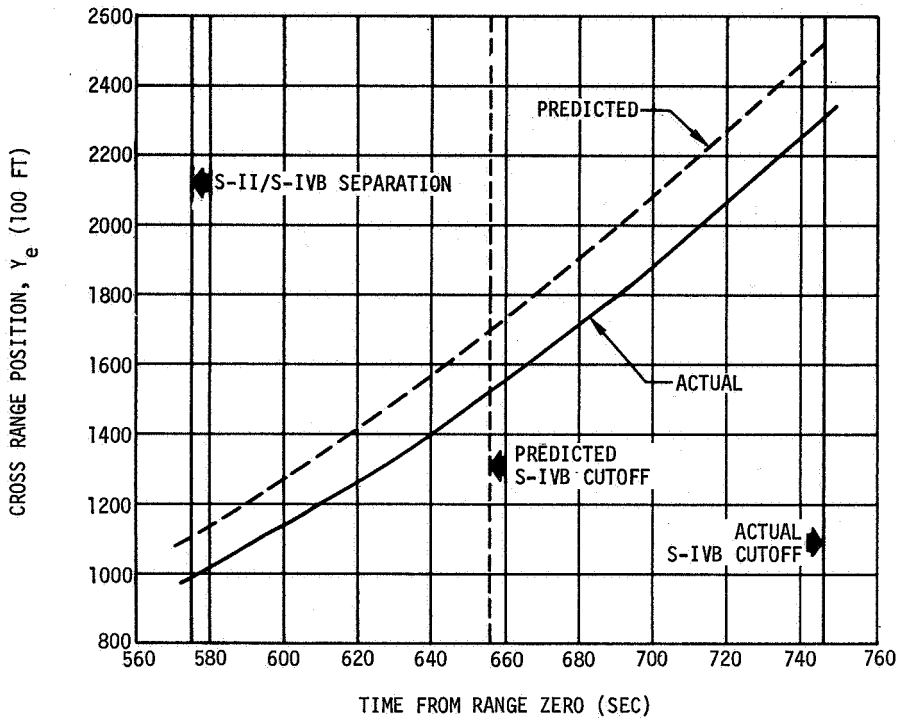

Figure 8-17. Crossrange Position History

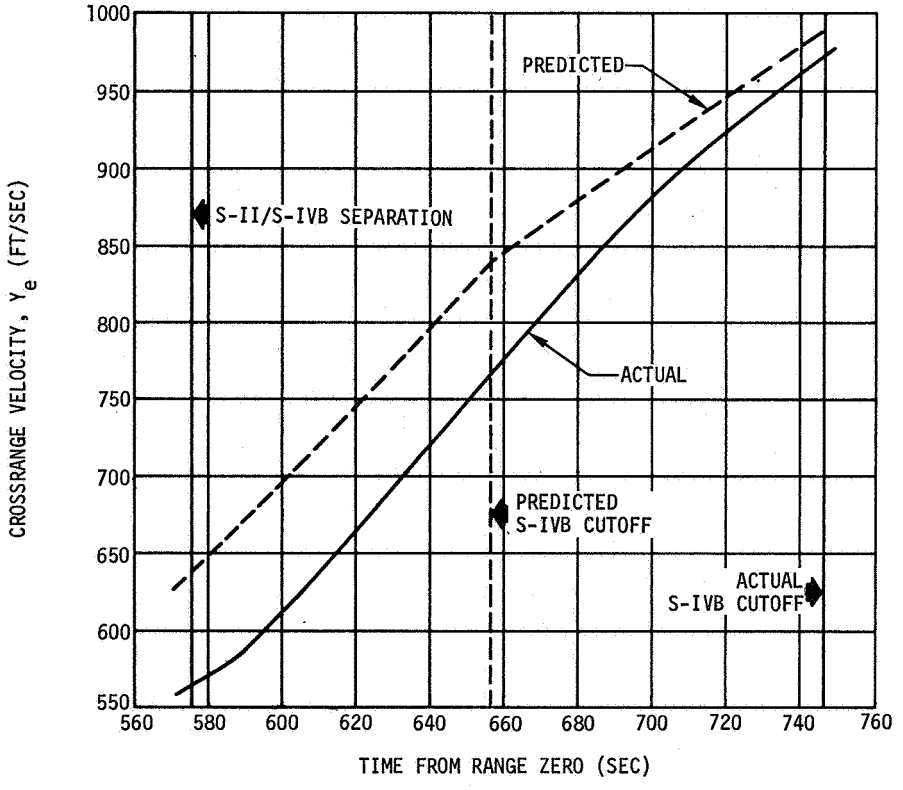

Figure 8-18. Crossrange Velocity History

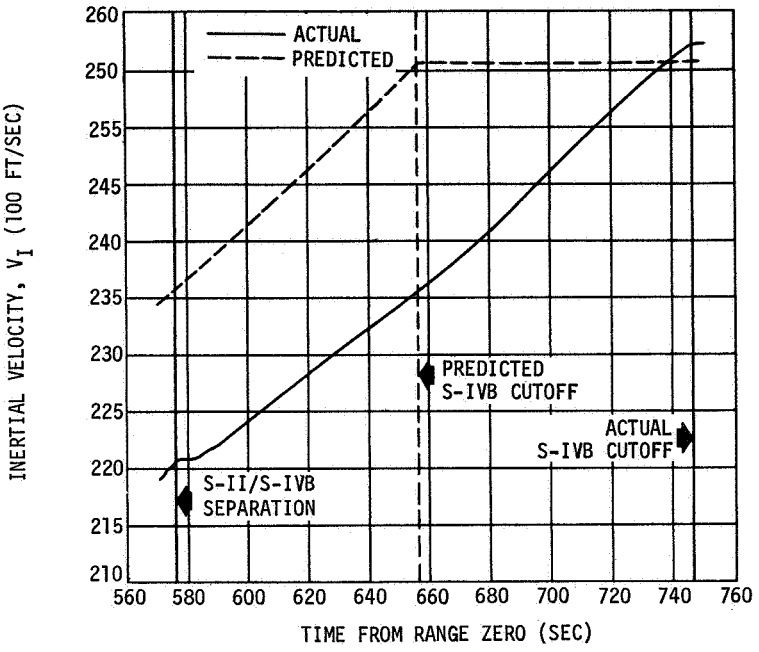

Figure 8-19. Inertial Velocity History

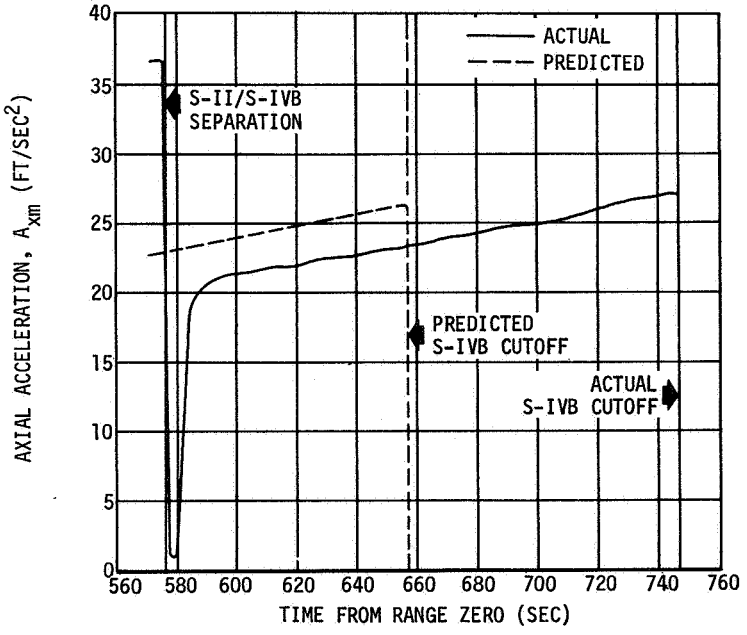

Figure 8-20. Axial Acceleration History

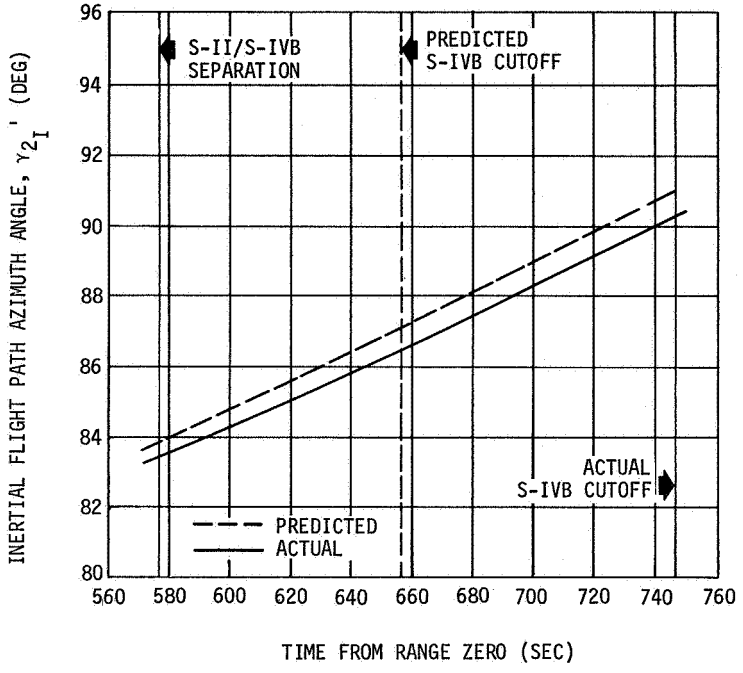

Figure 8-21. Inertial Flight Path Azimuth Angle History

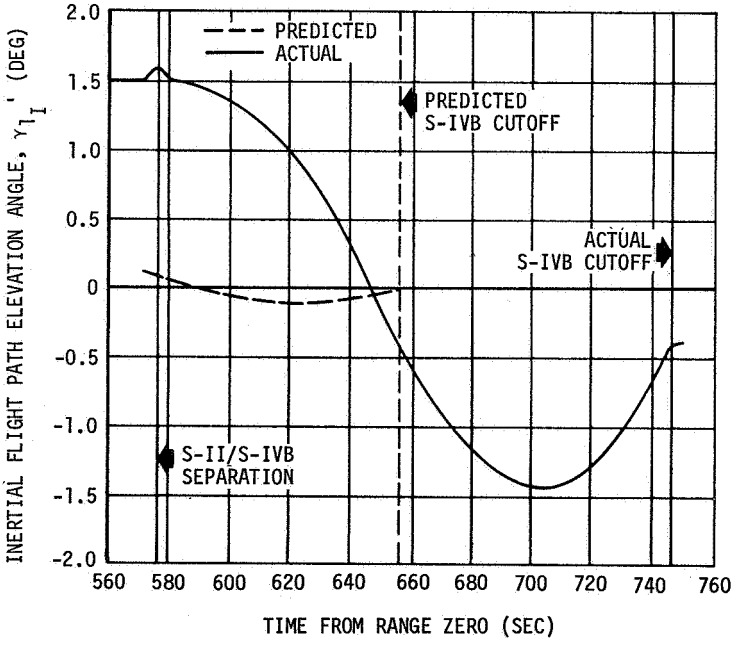

Figure 8-22. Inertial Flight Path Elevation Angle History

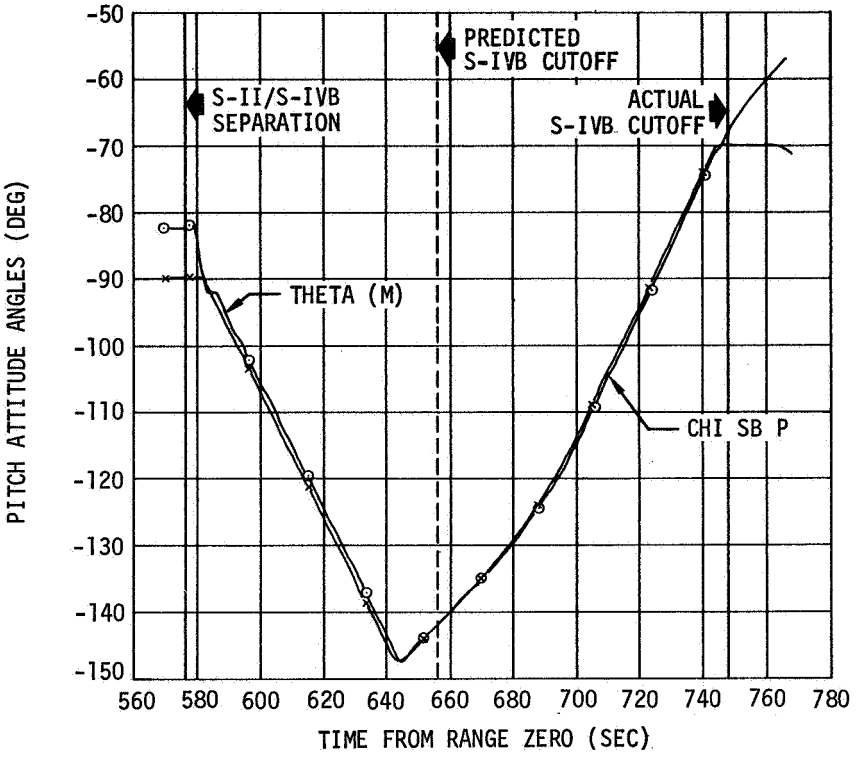

Figure 8-23. Pitch Attitude Angle History

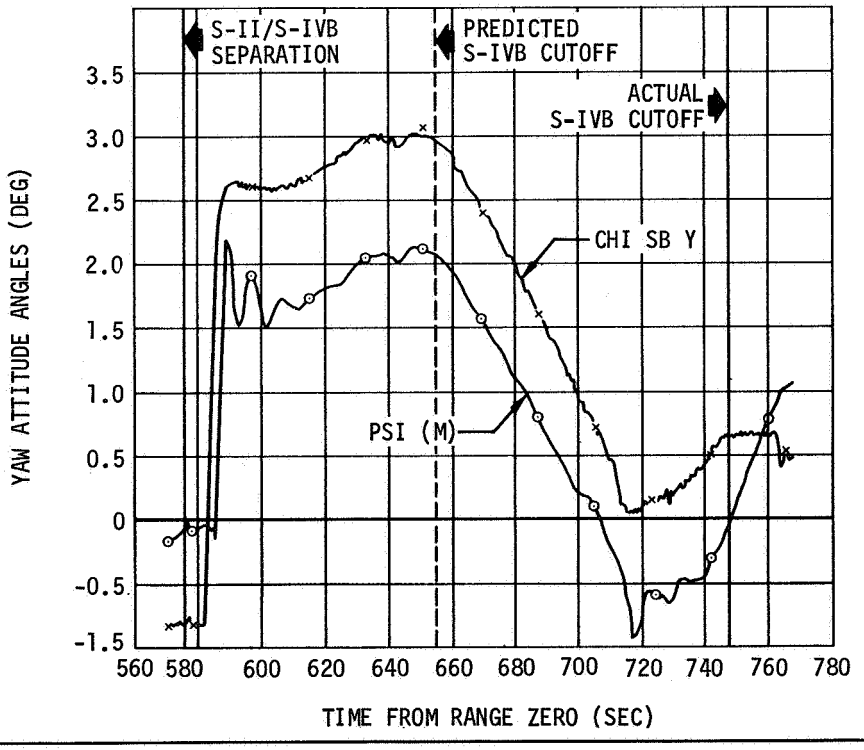

Figure 8-24. Yaw Attitude Angle History

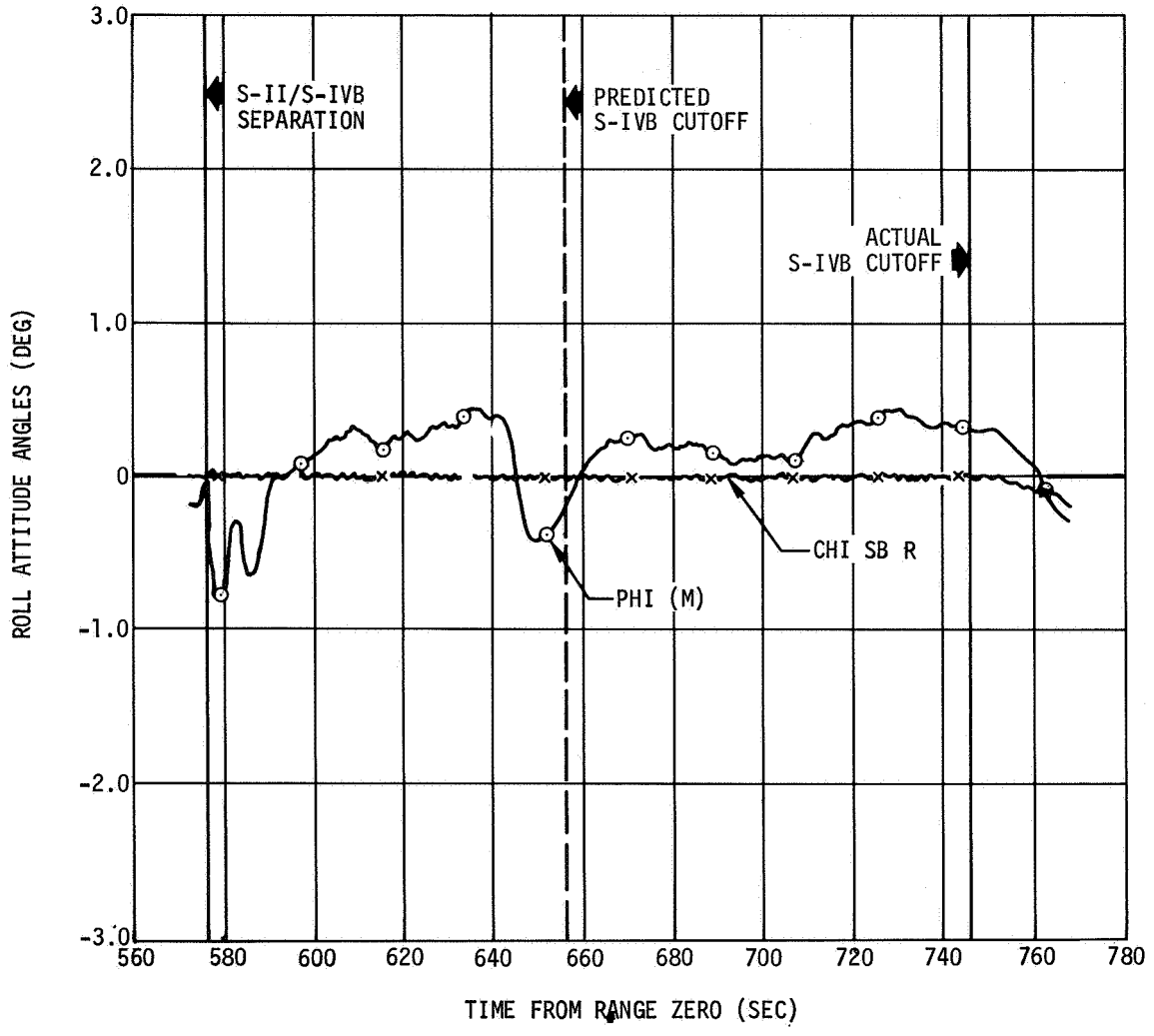

Figure 8-25. Roll Attitude Angle History

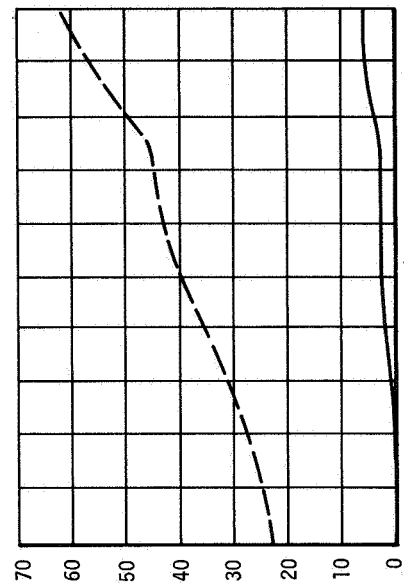

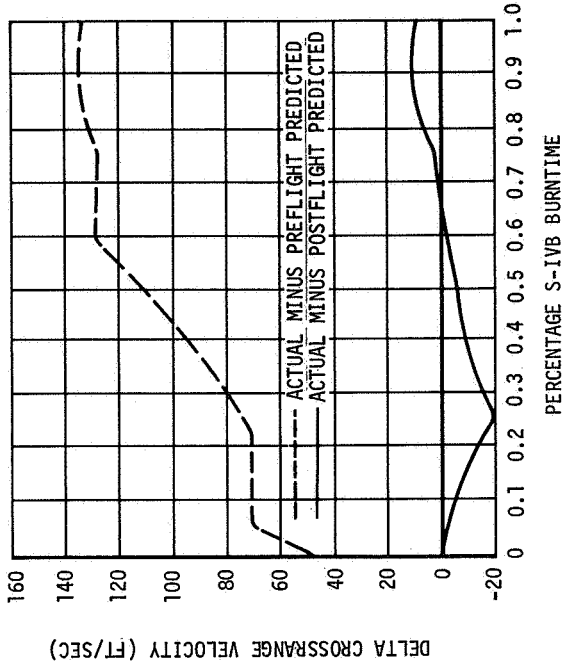

Figure 8-27. Crossrange Position and Crossrange Velocity Difference Histories

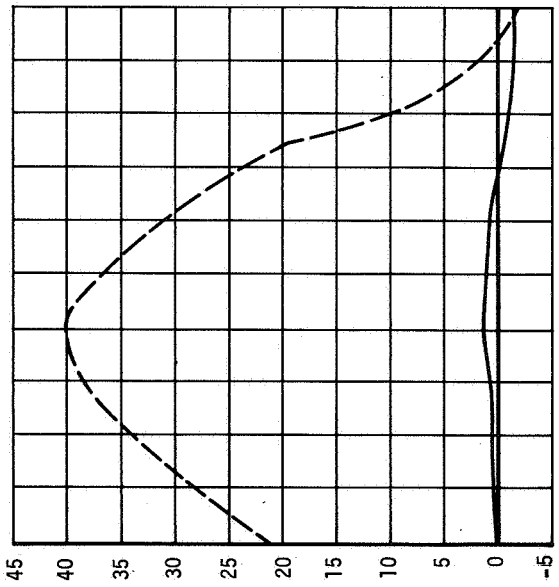

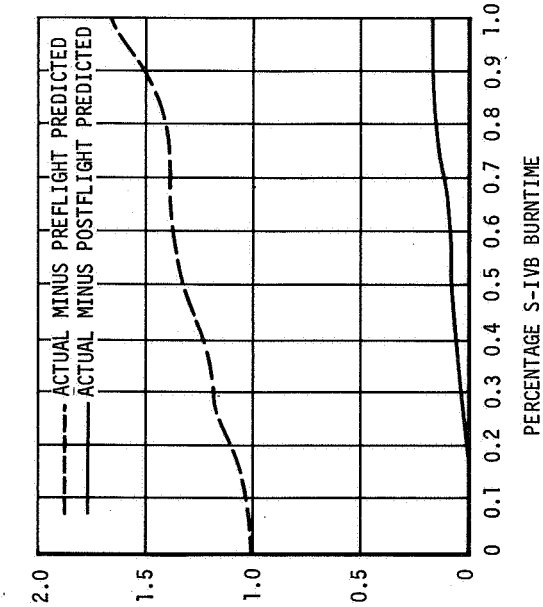

Figure 8-26. Altitude and Range Difference Histories

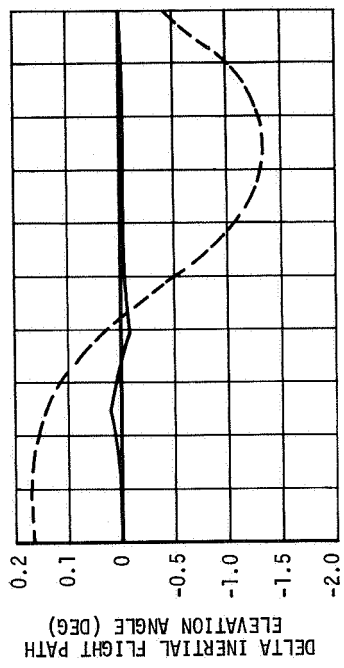

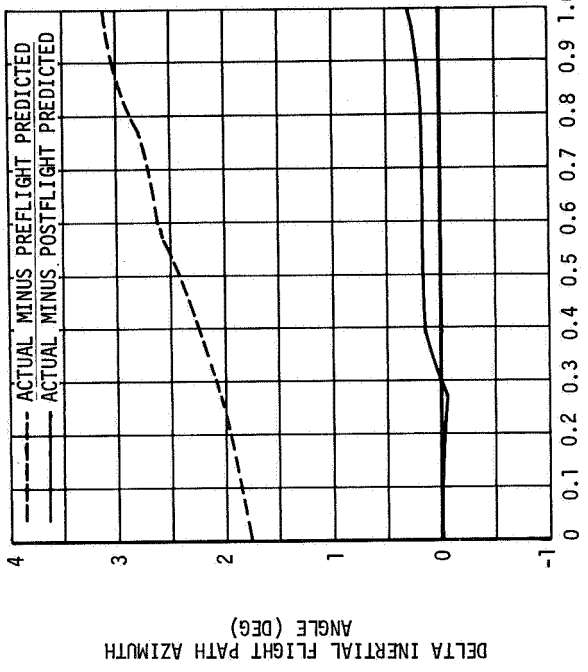

Figure 8-29. Inertial Flight Path Elevation and Azimuth Angle Difference Histories

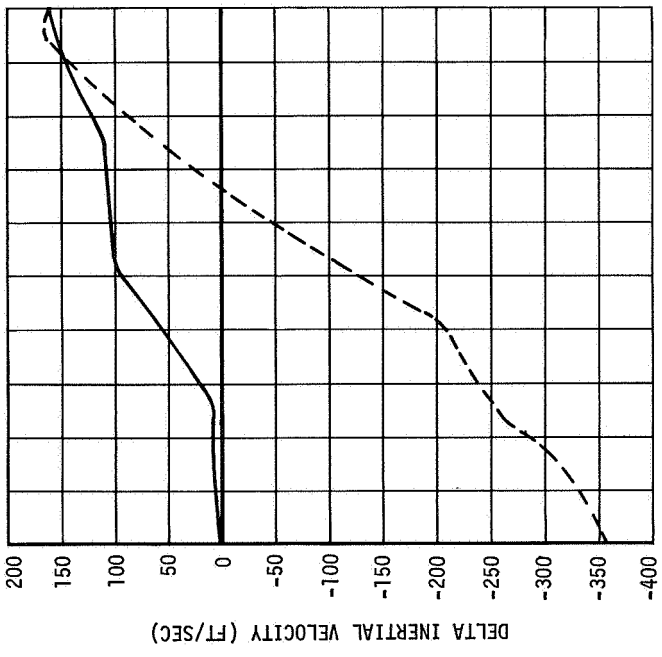

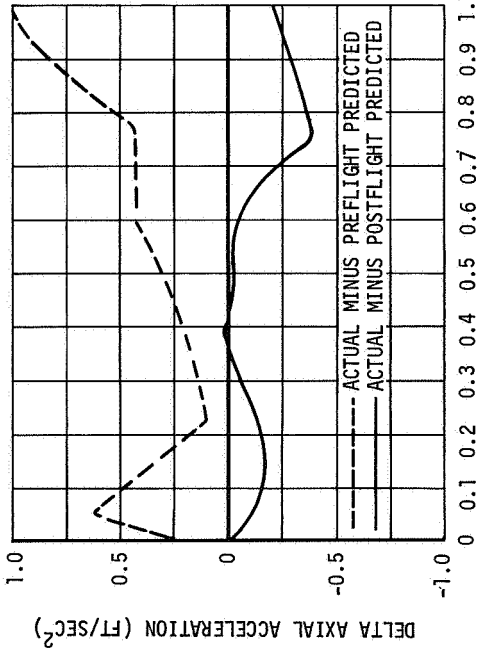

Figure 8-28. Inertial Velocity and Axial Acceleration Difference Histories

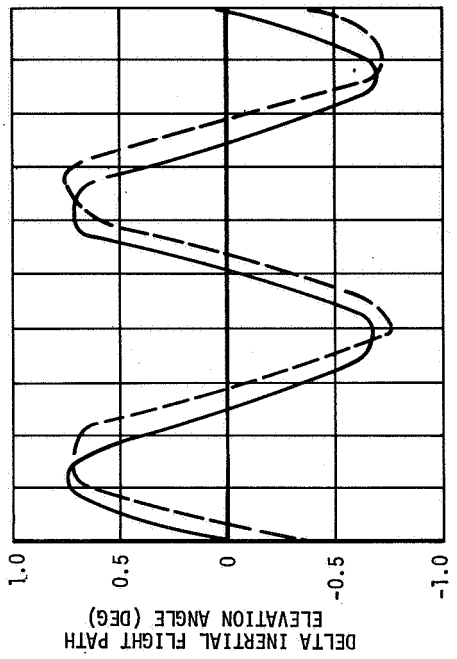

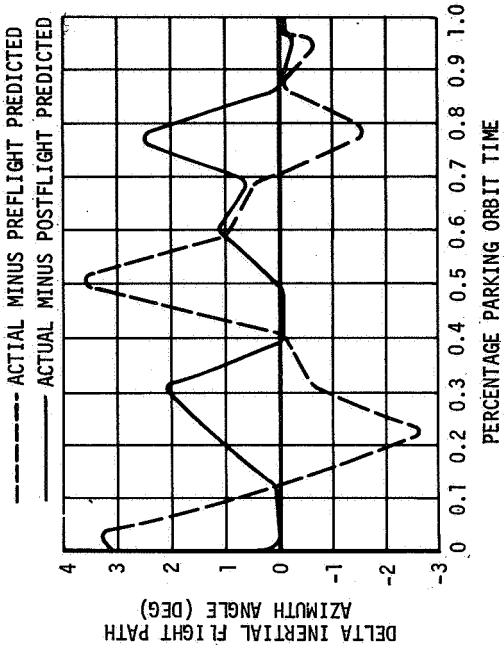

Figure 8-31. Parking Orbit Inertial Flight Path Elevation and Azimuth Angle Difference Histories

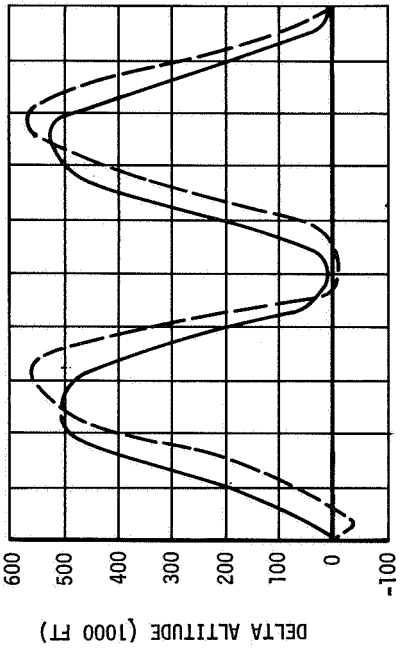

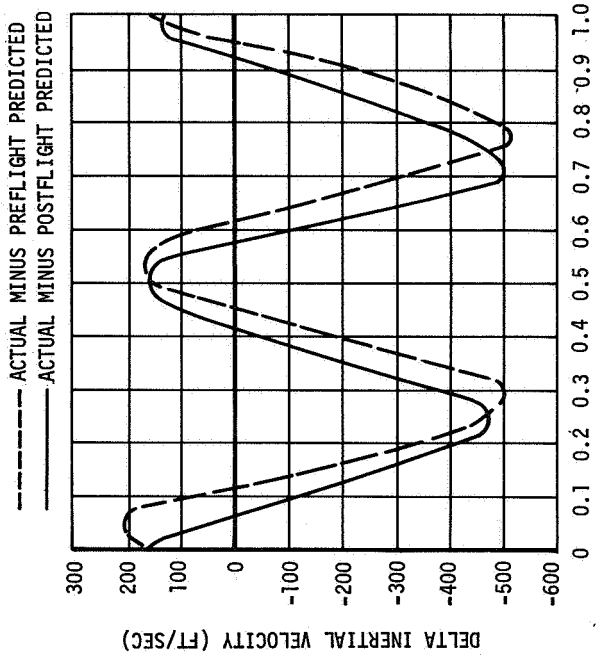

Figure 8-30. Parking Orbit Altitude and Inertial Velocity Difference Histories

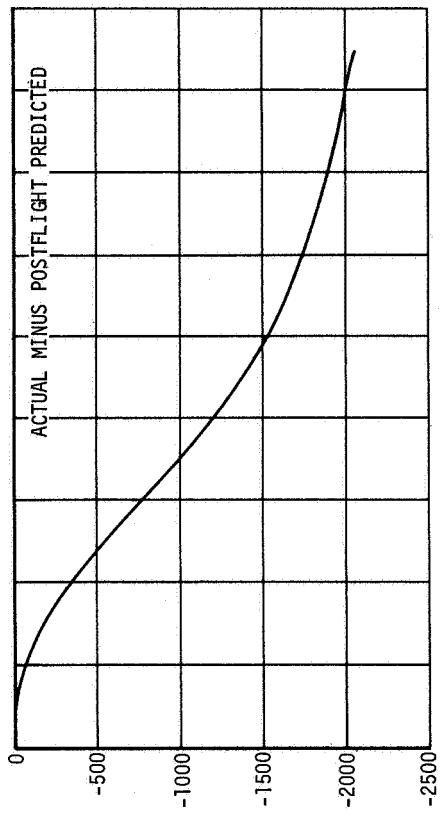

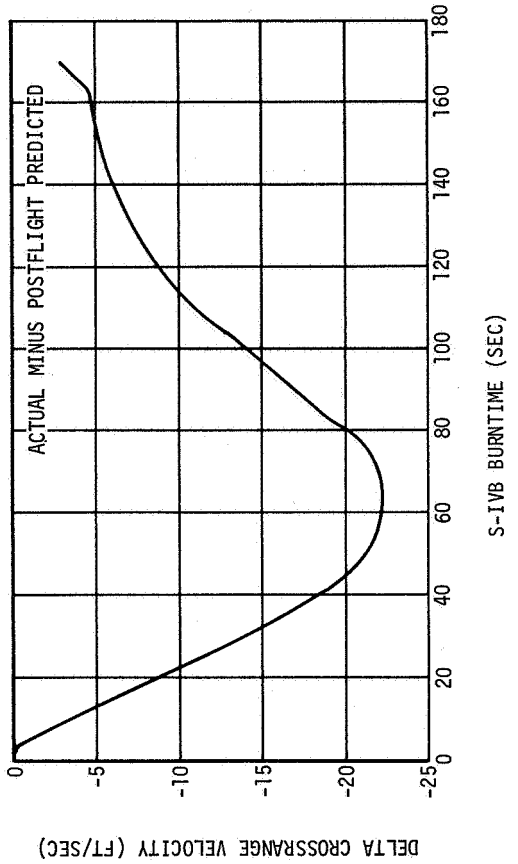

Figure 8-33. Crossrange Position and Velocity Difference Histories Between Postflight Predicted and Actual Trajectories

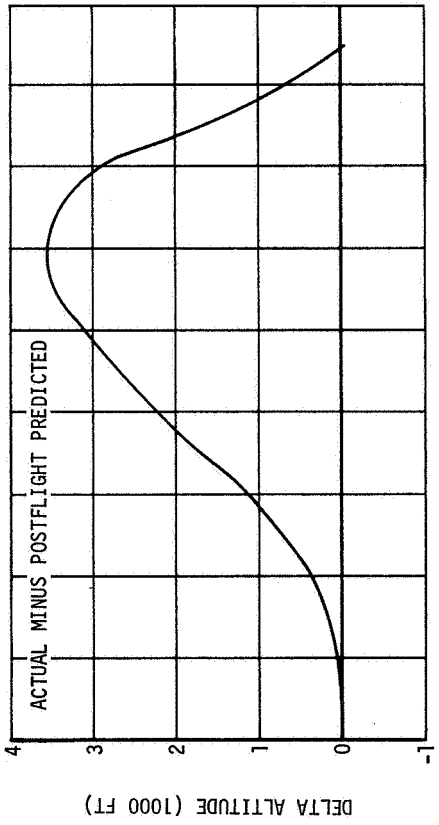

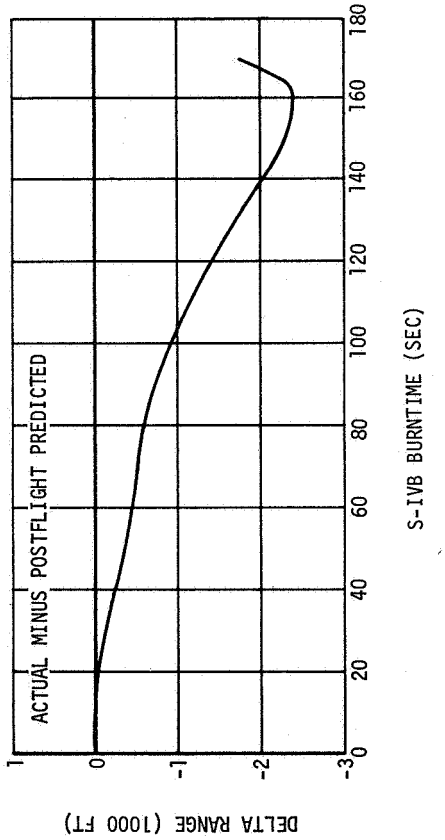

Figure 8-32. Altitude and Range Difference Histories Between Postflight Predicted and Actual Trajectories

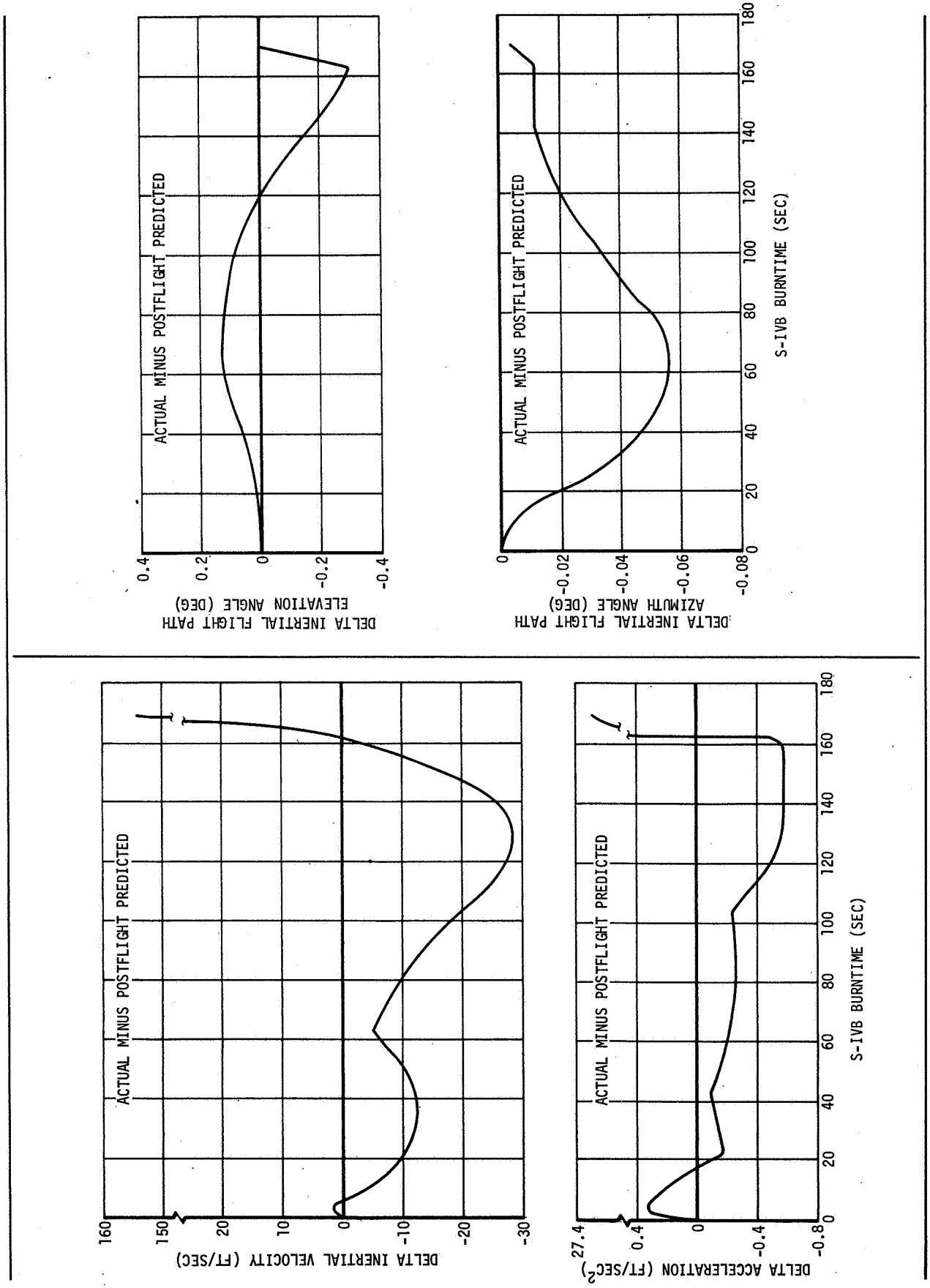

Figure 8-34. Inertial Velocity and Acceleration, Actual Minus Predicted Trajectories

Figure 8-35. Inertial Flight Path Angle, Actual Minus Predicted Trajectories

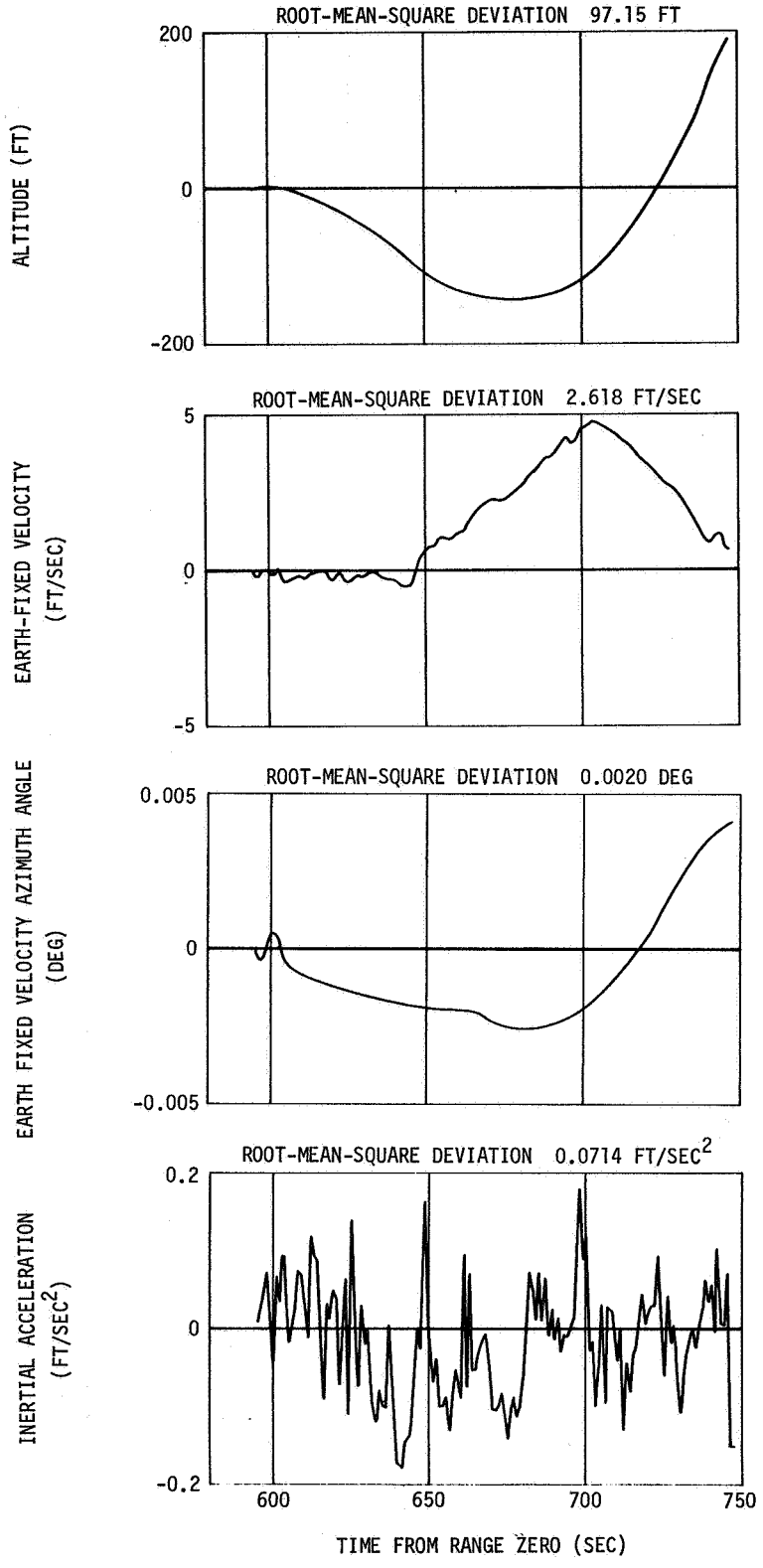

NOTE: DATA IS ACTUAL MINUS SIMULATED

Figure 8-36. Trajectory Reconstruction Simulation Deviations from Observed Mass Point Trajectory

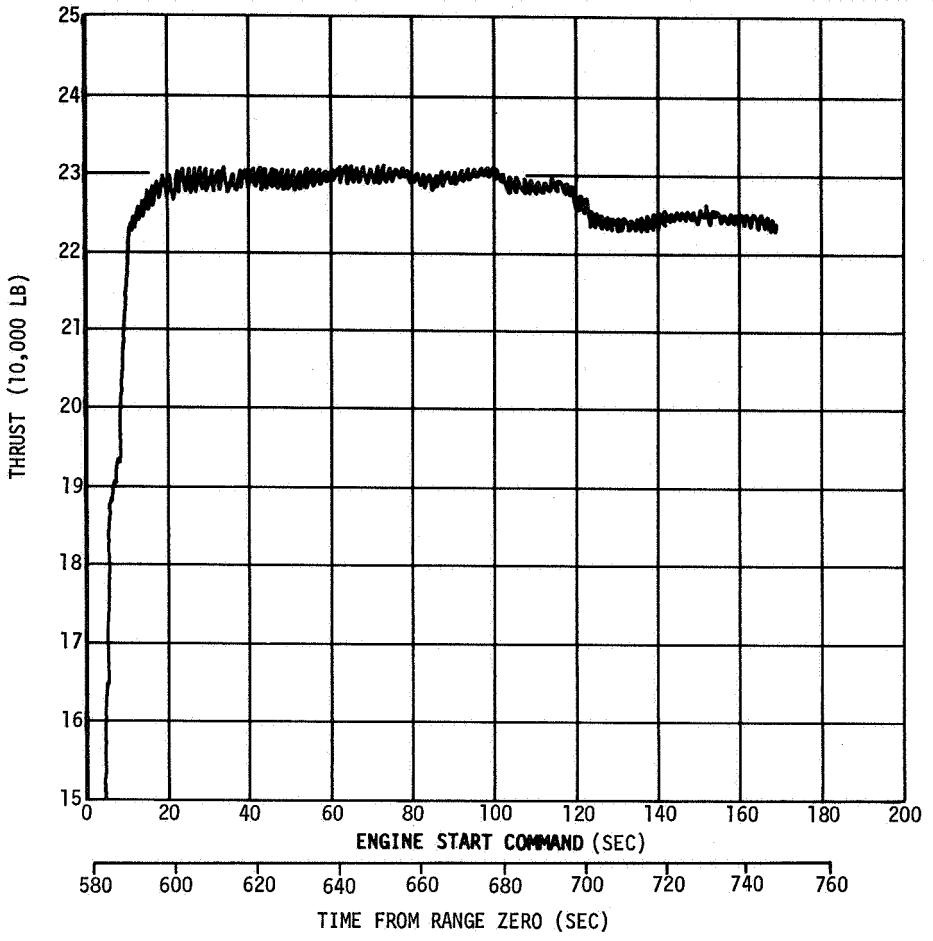

Figure 8-37. Thrust History from Engine Analysis

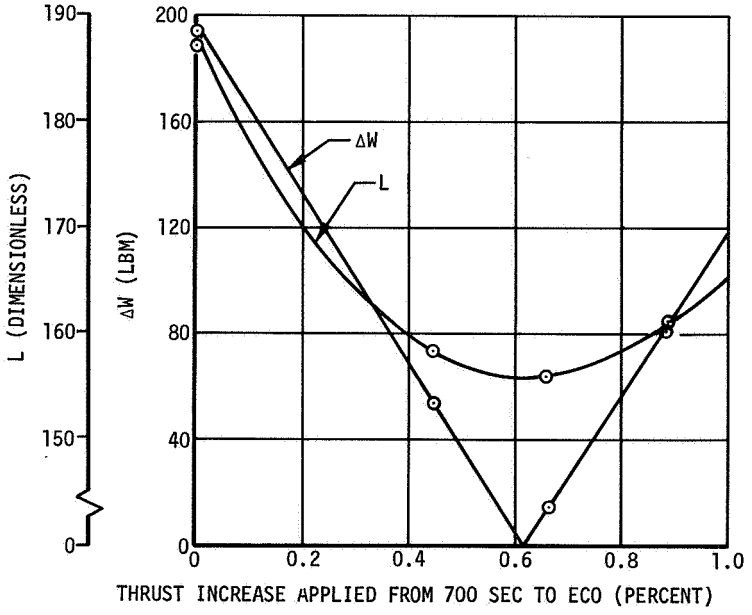

Figure 8-38. Effect of Magnitude of the Performance Shift on the Trajectory and Weight Estimate Fits

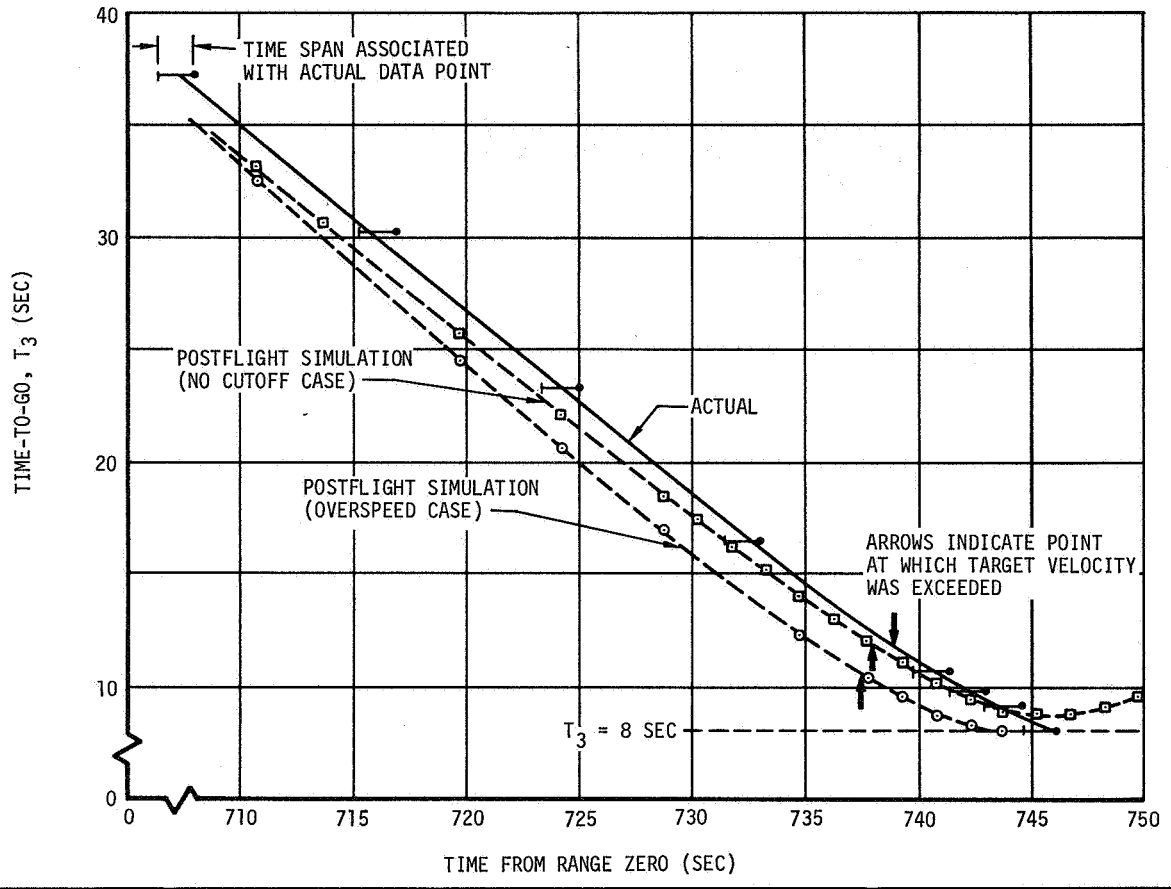

Figure 8-39. Guidance Time-to-Go for Actual, Overspeed, and No Cutoff Trajectories

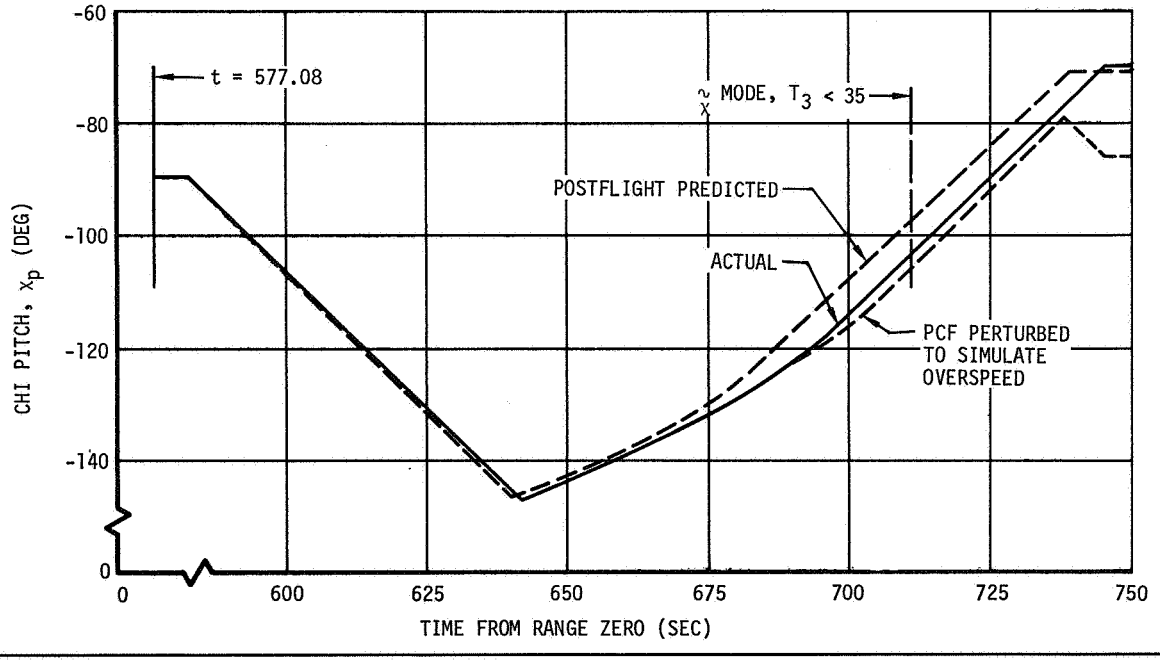

Figure 8-40. Commanded Pitch Attitude Angle for Actual, Postflight Predicted, and Overspeed Trajectories

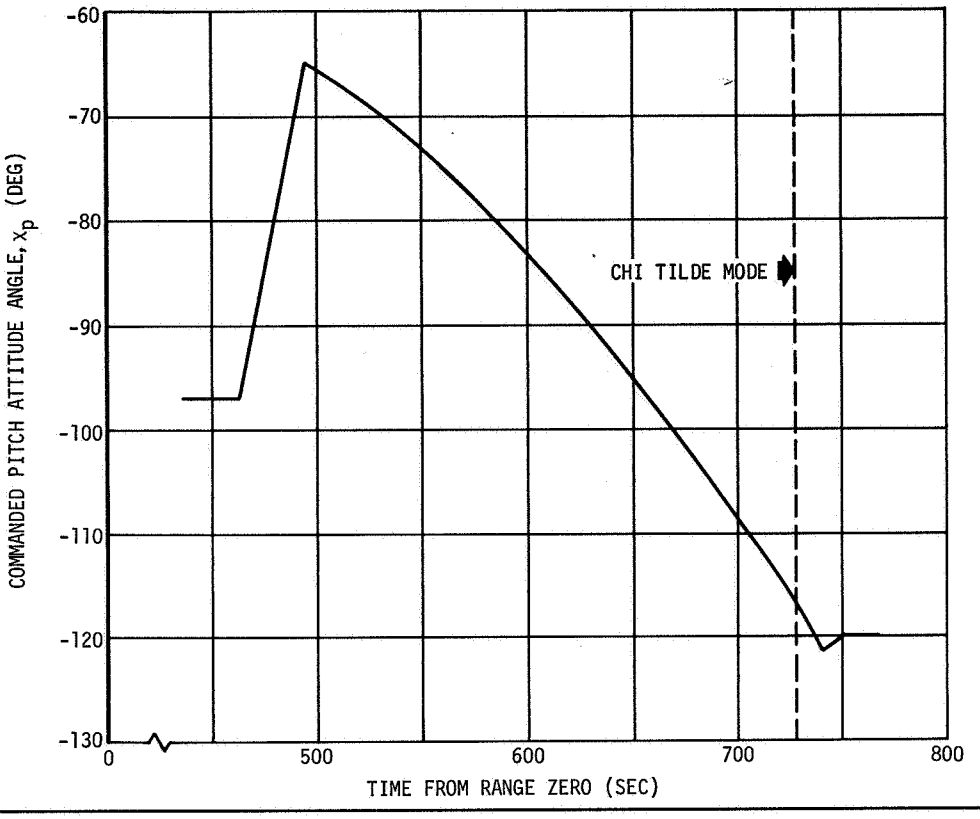

Figure 8-41. Commanded Pitch Attitude History for Direct Staging After Second S-II Engine Shutdown

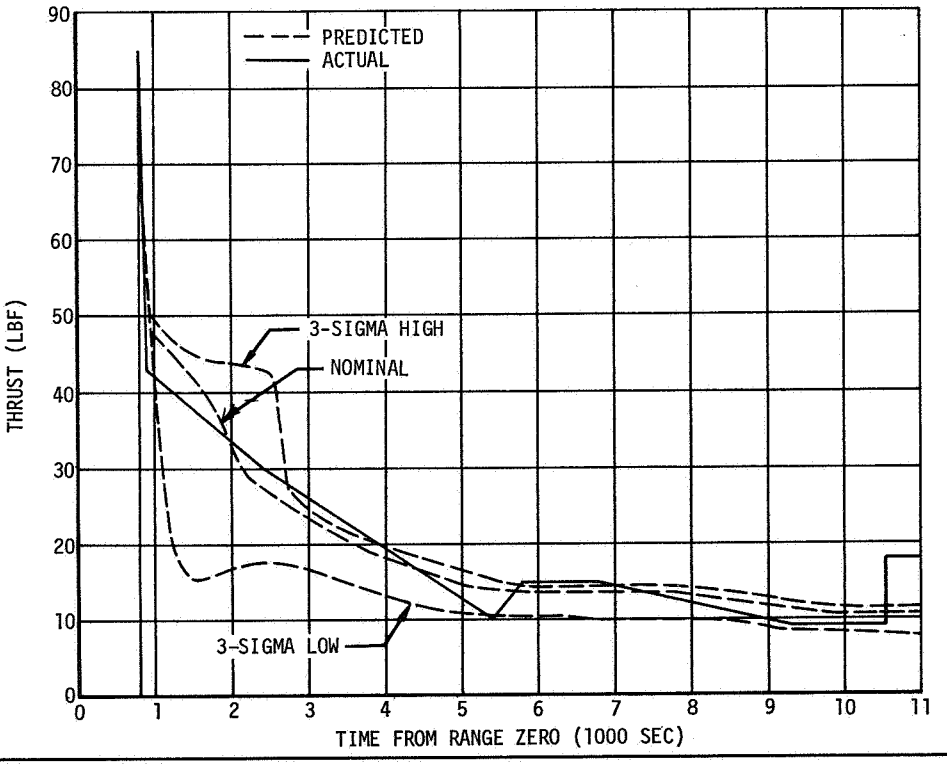

Figure 8-42. Predicted and Best Actual CVS Thrust - Orbital Coast

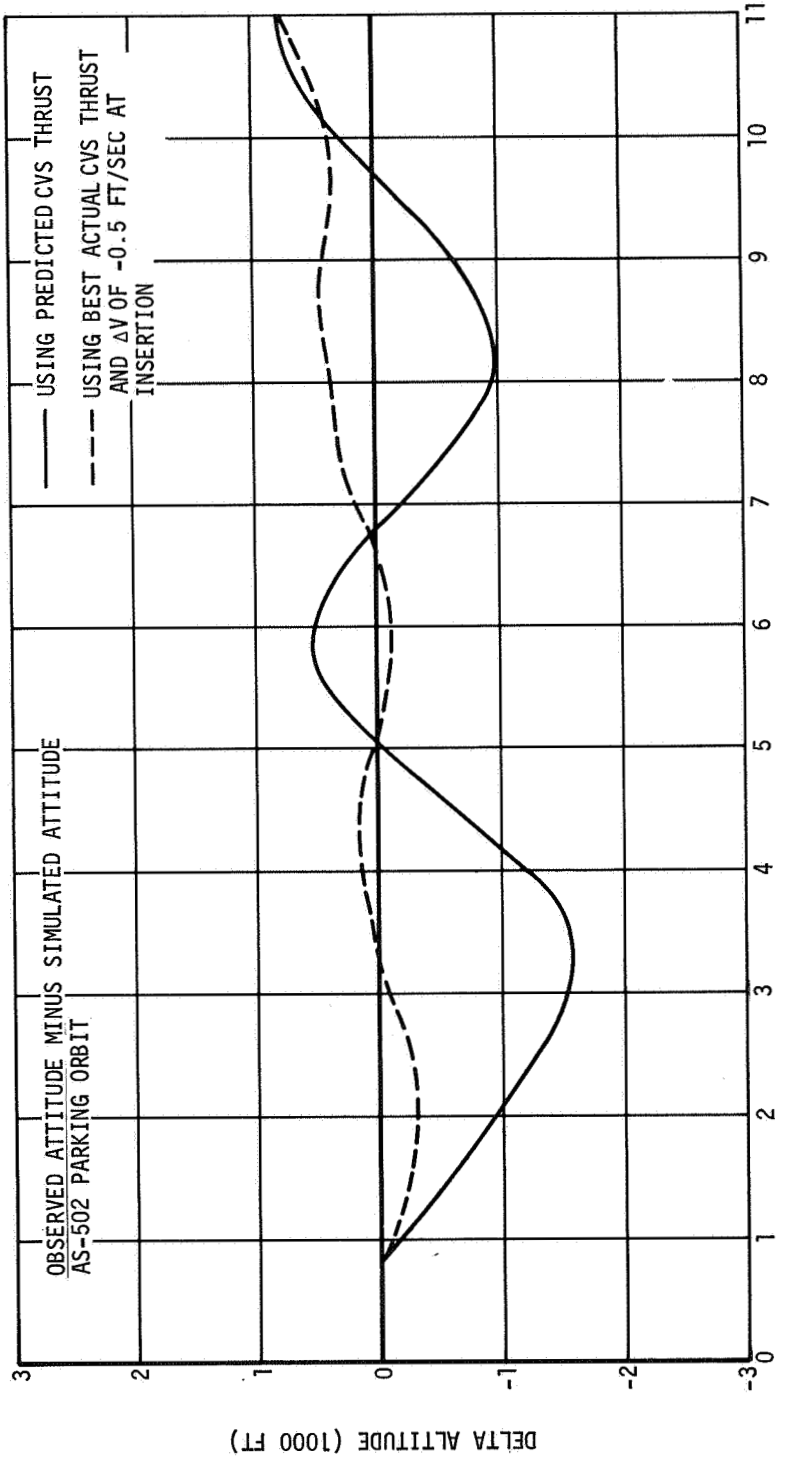

Figure 8-43. Altitude Residual Using Best Estimate of CVS Thrust

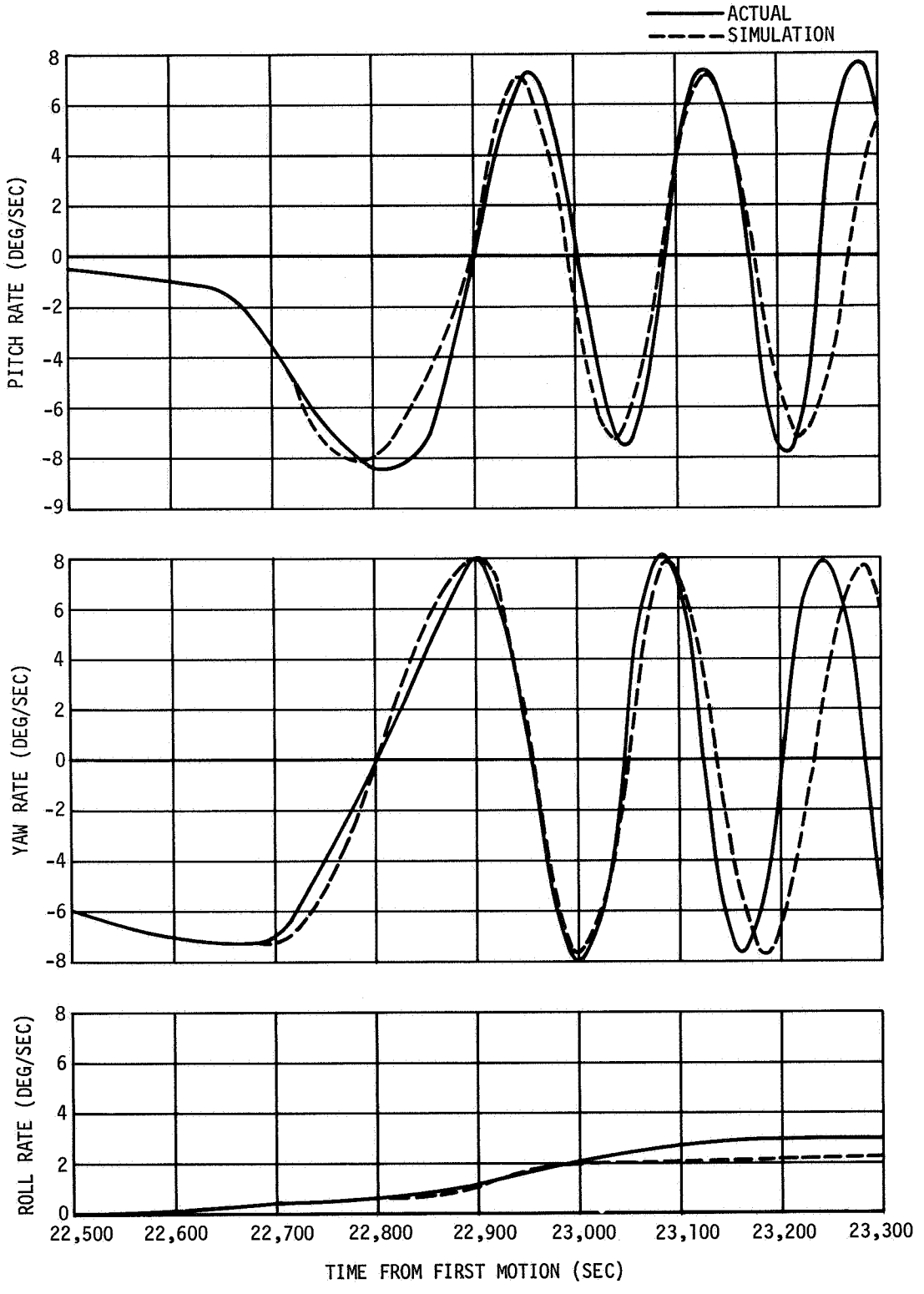

Figure 8-44. Tumbling Rates following APS Depletion

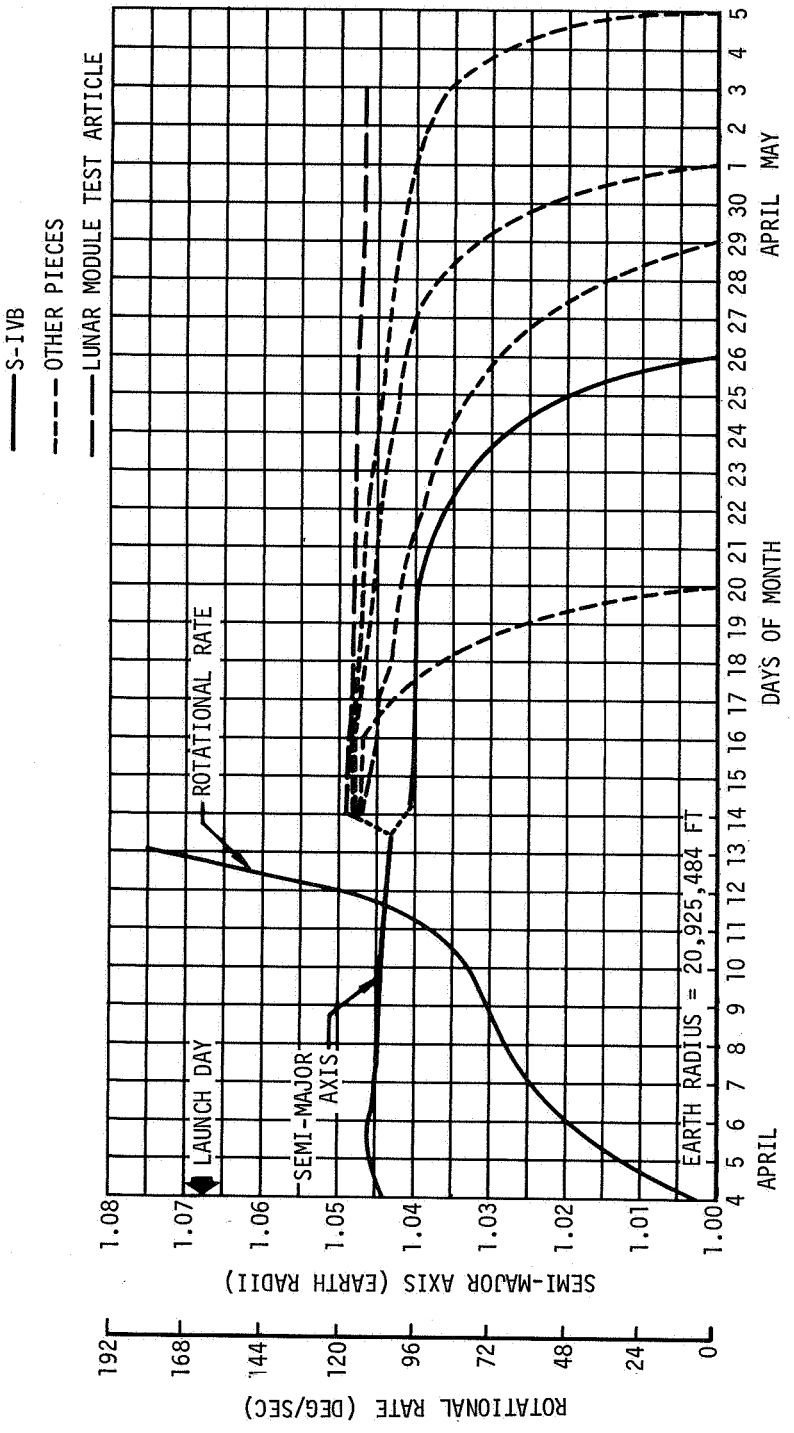

Figure 8-45. Orbit Radii and Rotational Rates

SECTION 9

MASS CHARACTERISTICS

9. MASS CHARACTERISTICS

9.1 Mass Characteristics Summary

The AS-502 third flight stage (S-IVB, IU, and Payload) mass summary presented in table 9-1, and the mass characteristics presented in appendix 1 are best estimate mass characteristics up to, and including first burn engine cutoff. Orbital boiloff and restart attempt mass losses do not represent values derived from statistical analysis.

9.2 Mass Properties Dispersion Analysis

Figures 9-1 through 9-4 present a comparison of the predicted vehicle mass characteristics and three-sigma dispersions, versus postflight actual vehicle mass characteristics during S-IVB first burn. The comparison for second burn is not shown. Figures 9-2 and 9-4 show that the actual longitudinal center of gravity and the pitch and yaw moment of inertia, respectively, were less than the minimum predicted three-sigma dispersions. The cause of this was a change in payload mass distribution which was not included in the predicted values. Had the payload mass distribution change been incorporated in the predicted values the actual values would have been well within the predicted three-sigma dispersions, and would have compared favorably with the predicted nominal values.

The predicted dispersions were determined from a statistical analysis component mass properties uncertainties and are referenced relative to time from Engine Start Command.

9.3 Third Flight Stage Best Estimate Ignition and Cutoff Masses

The best estimate method is a three dimensional statistical analysis of data from five mass measurement systems. This method develops a joint probability density function from which the most probable values and accuracies for ignition and cutoff masses are determined.

Three measurement systems provide unique values for ignition and cutoff masses while two systems provide linear relationships between cutoff and ignition mass. The best estimate method combines the unique values with the linear relationships to compute the most probable value for ignition and cutoff mass.

The five measurement systems used in determining the best estimate masses are: (1) PU indicated corrected (2) flight flow integral (3) PU volumetric (4) level sensors and (5) trajectory reconstruction. A brief description of each measurement system is given in section 16.

Figure 9-5 is a graphical presentation of the best estimate analysis for ignition and cutoff mass. The third flight stage ignition mass was 354,232 $\pm$476 lbm and the cutoff mass was 265,234 $\pm$400 lbm.

9.3.1 Best Estimate Program Input

Table 9-2 presents a summary of the values used in determining the best estimate ignition and cutoff mass. For the unique measurement systems, the LOX, LH2, and non-propellant mass values and their predicted dispersions are presented in addition to the total mass values and dispersions used for computation. The linear relationship slope, intercept, and dispersion values are presented as utilized for the best estimate analysis.

TABLE 9-1
MASS SUMMARY

EVENT	S-IC LIFT-OFF	S-II/ S-IVB SEPAR.	S-IVB FIRST ESC	END FUEL LEAD	FIRST 90 PCT THRUST	S-IVB FIRST ECC	S-IVB FIRST ETD	BEGIN RESTART PREPS.	S-IVB SECOND ESC	END FUEL LEAD	S-IVB SECOND ECC	CSM SEPAR-ATION
LAUNCH ESCAPE	8,886	0	0	0	0	0	0	0	0	0	0	0
FROST	100	0	0	0	0	0	0	0	0	0	0	0
SEPARATION PKG	51	0	0	0	0	0	0	0	0	0	0	0
ULLAGE ROCKETS	253	250	244	153	135	0	0	0	0	0	0	0
COMMAND MODULE	12,543	12,543	12,543	12,543	12,543	12,543	12,543	12,543	12,543	12,543	12,543	0
SERVICE MODULE	9,836	9,836	9,836	9,836	9,836	9,836	9,836	9,836	9,836	9,836	9,836	0
SM PROPELLANT	32,785	32,785	32,785	32,785	32,785	32,785	32,785	32,785	32,785	32,785	32,785	0
ADAPTER RING	91	91	91	91	91	91	91	91	91	91	91	0
ADAPTER (SLA)	3,795	3,795	3,795	3,795	3,795	3,795	3,795	3,795	3,795	3,795	3,795	3,795
LUNAR MODULE	26,001	26,001	26,001	26,001	26,001	26,001	26,001	26,001	26,001	26,001	26,001	26,001
VEH INSTR UNIT	4,874	4,874	4,874	4,874	4,874	4,874	4,874	4,874	4,874	4,874	4,874	4,874
S4B502 DRY STG	26,253	26,253	26,253	26,253	26,253	26,253	26,253	26,253	26,253	26,253	26,253	26,253
LOX IN TANK	193,773	193,768	193,768	193,768	193,470	118,769	118,609	118,378	118,378	118,378	116,685	116,685
LOX ULLAGE GAS	28	33	33	34	35	187	187	418	423	423	423	345
LOX BELOW TANK	367	367	367	367	397	397	367	367	367	367	397	367
LH2 IN TANK	42,400	42,400	42,400	42,392	42,278	28,436	28,407	25,383	25,383	25,098	24,863	24,863
LH2 ULLAGE GAS	78	78	78	79	80	160	160	405	448	448	448	448
LH2 BELOW TANK	48	48	48	53	58	58	48	48	48	56	58	48
COLD HELIUM	332	332	332	331	330	274	274	203	201	200	199	198
APS PROP FP 1	314	314	314	314	314	311	311	189	102	100	98	88
APS PROP FP 3	315	315	315	315	315	312	312	240	139	136	134	122
GH2 IN STRTANK	5	5	5	3	1	7	7	7	7	2	1	1
HELIUM-REPRESS	78	78	78	78	78	78	78	78	30	30	30	30
SERVICE ITEMS	73	73	73	73	73	73	73	73	73	73	73	73
TOTAL MASS	363,279	354,239	354,233	354,138	353,742	265,240	265,010	261,967	261,777	261,489	259,586	204,190
TIME FROM RANGE ZERO (sec)	0.690	577.079	577.280	580.280	582.788	747.032	747.432	11,287.733	11,614.667	11,623.239	11,630.320	11,666.100

TABLE 9-2
BEST ESTIMATE PROGRAM INPUT VALUES

UNIQUE MEASUREMENT SYSTEMS

EVENT	MEASUREMENT SYSTEM	LOX (lbm)		LH2 (lbm)		NON-PROPELLANT (lbm)		TOTAL (lbm)	
		VALUE	ERROR	VALUE	ERROR	VALUE	ERROR	VALUE	ERROR
ESC	PU VOLUMETRIC	194,122	±965	42,214	±271	117,649	±231	353,985	±1,029
	PU INDICATED CORRECTED	193,272	±1,380	42,430	±354	117,649	±231	353,351	±1,443
	POINT LEVEL SENSORS	194,893	±954	42,569	±251	117,649	±231	355,111	±1,013
ECC	PU VOLUMETRIC	119,145	±670	28,265	±214	117,574	±233	264,984	±741
	PU INDICATED CORRECTED	118,235	±844	28,542	±238	117,574	±233	264,351	±907
	POINT LEVEL SENSORS	119,875	±732	28,590	±153	117,574	±233	266,039	±783

LINEAR RELATIONSHIPS

EVENT	MEASUREMENT SYSTEM	SLOPE	INTERCEPT (lbm)	ERROR (lbm)
ESC TO ECC	FLOW INTEGRAL	1.0	88,952	±544
	TRAJECTORY RECONSTRUCTION	1.33501	0	±1,770

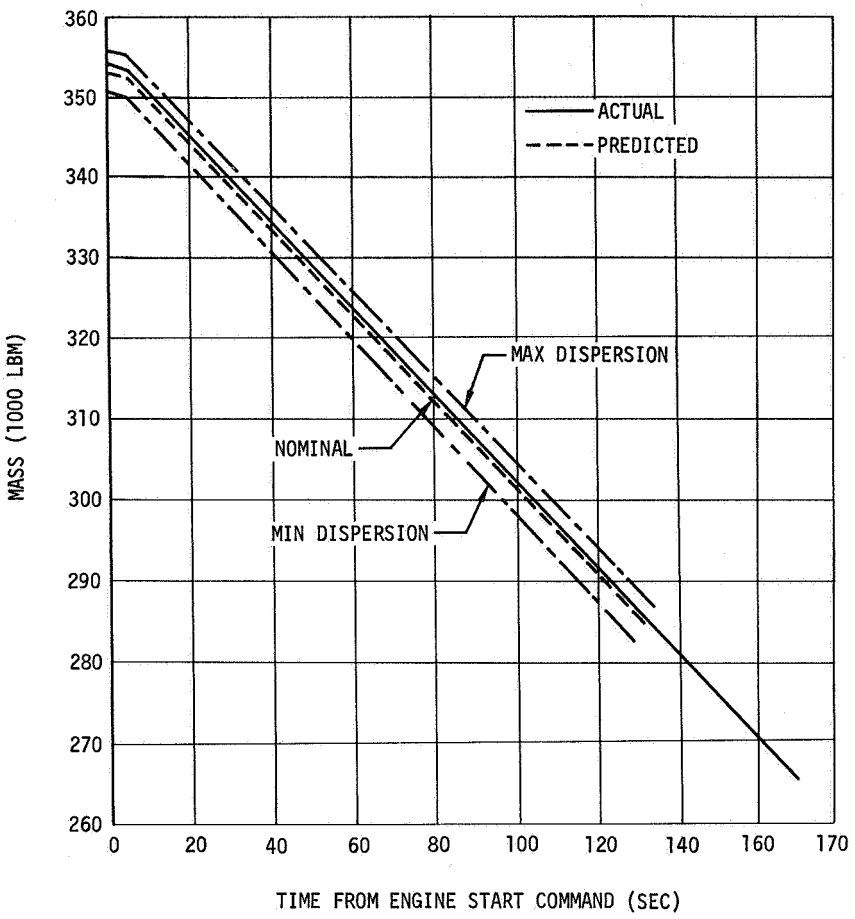

Figure 9-1. Third Flight Stage Vehicle Mass - First Burn

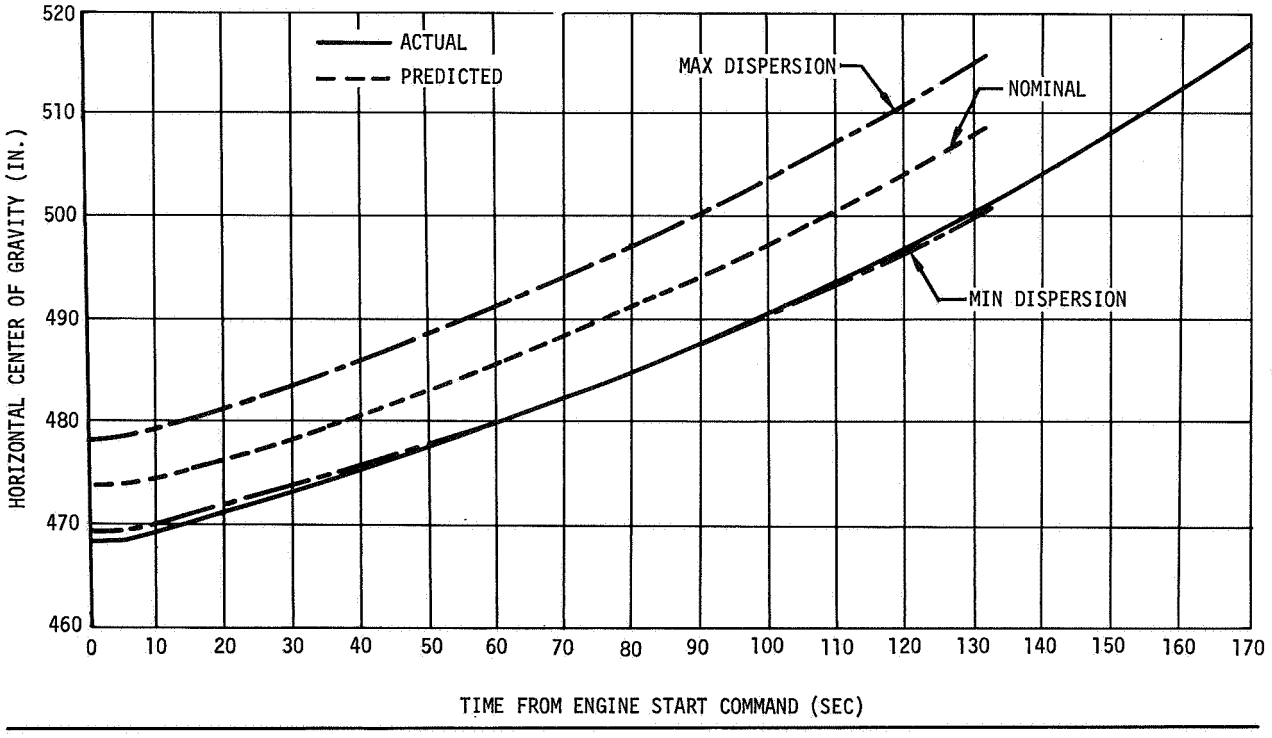

Figure 9-2. Third Flight Stage Vehicle Horizontal Center of Gravity - First Burn

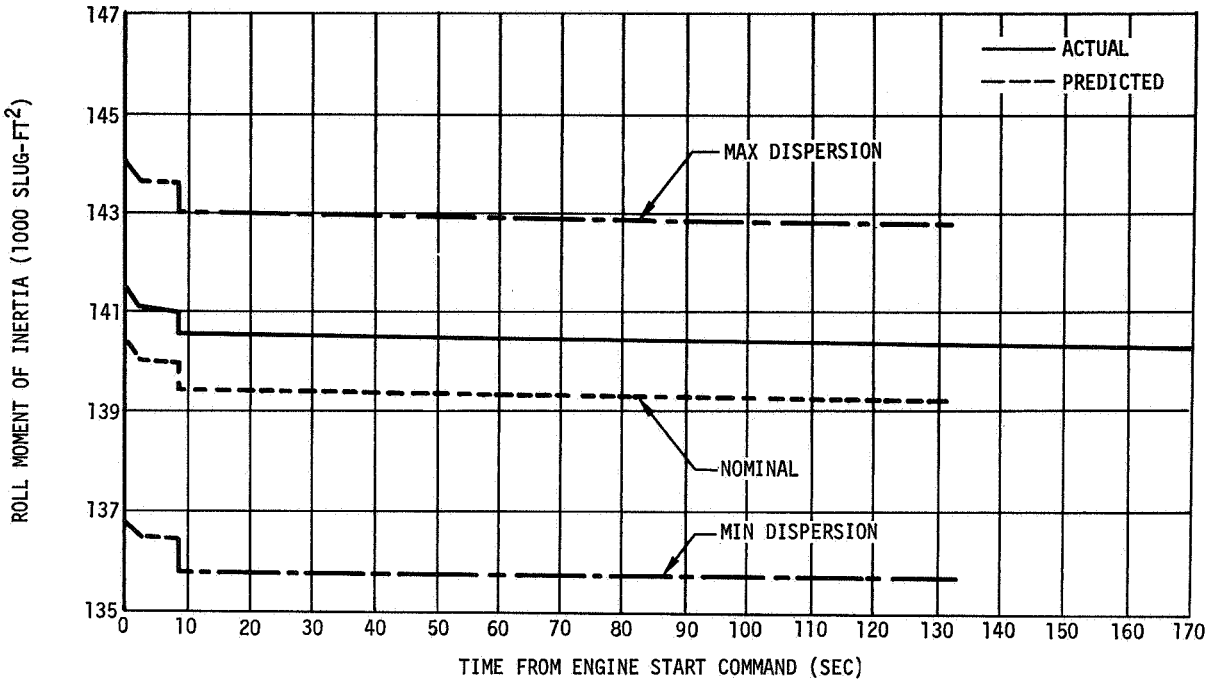

Figure 9-3. Third Flight Stage Vehicle Roll Moment of Inertia - First Burn

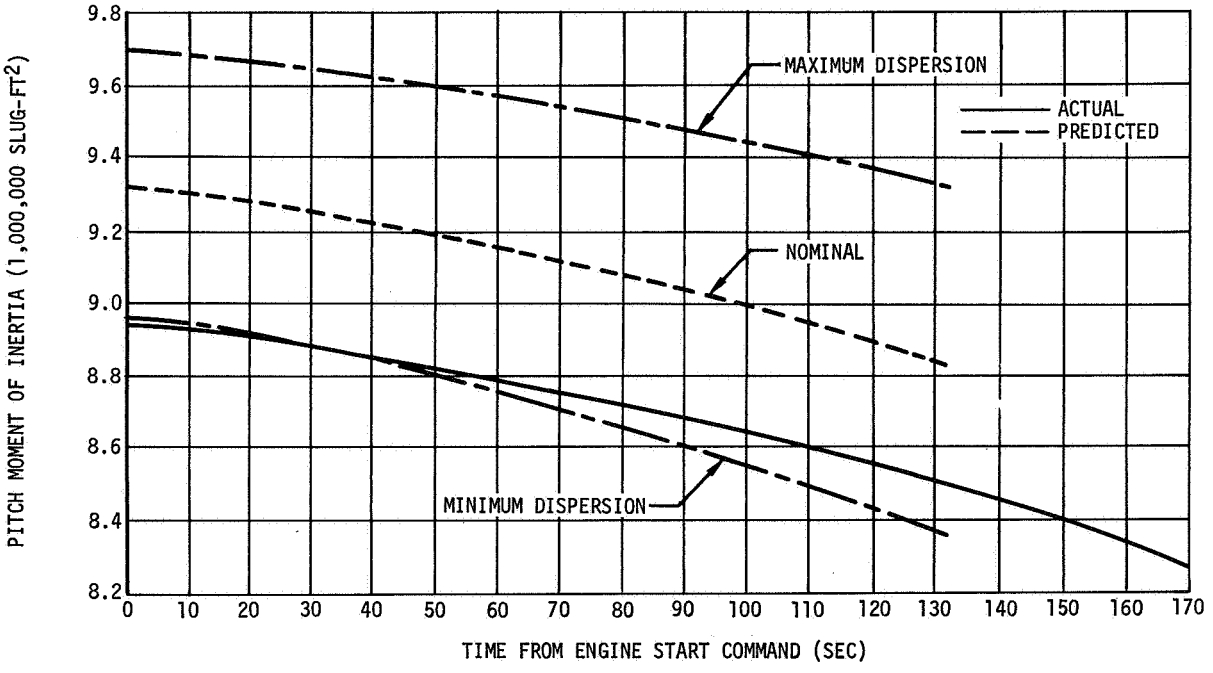

Figure 9-4. Third Flight Stage Vehicle Pitch Moment of Inertia - First Burn

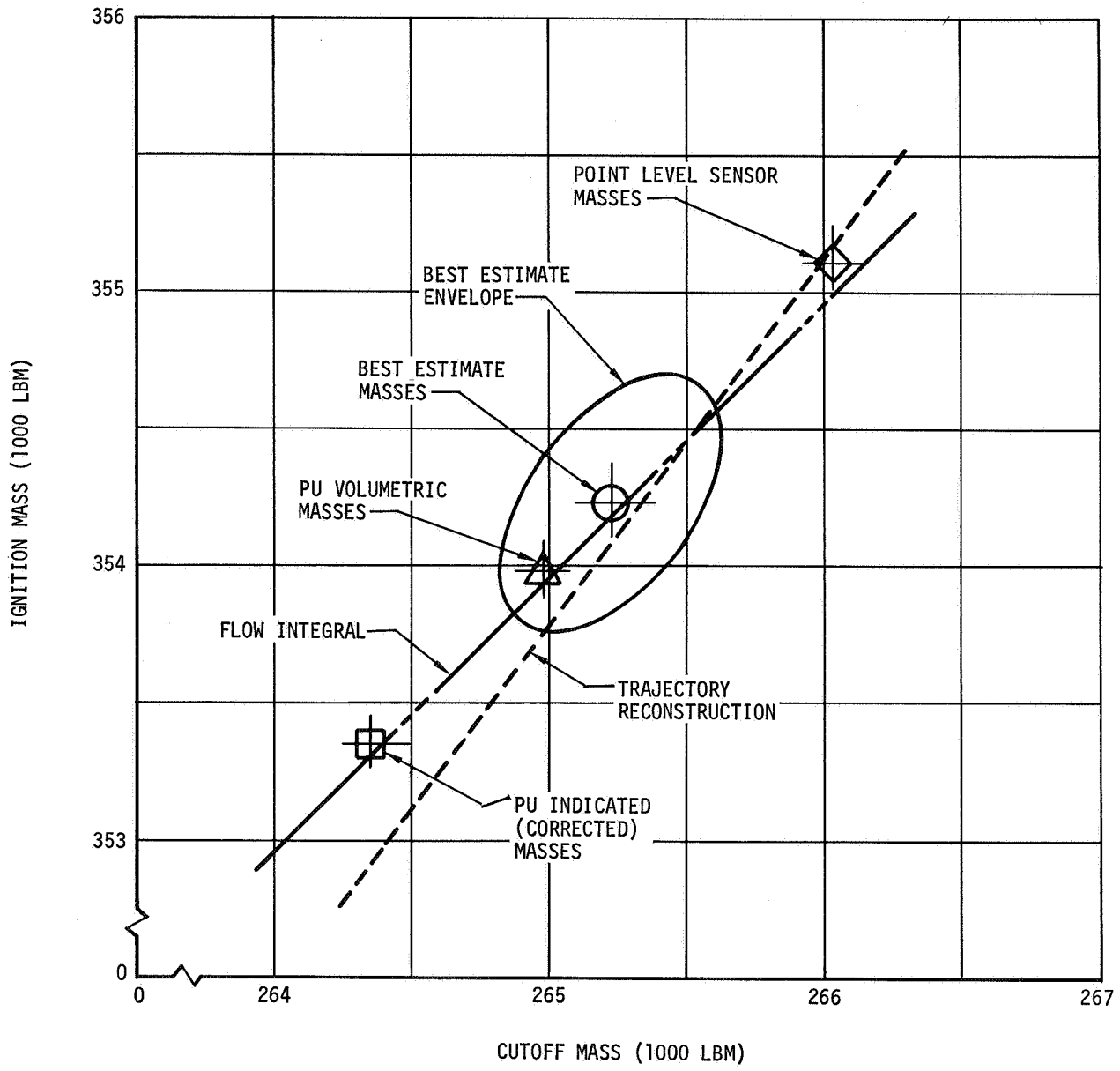

AT IGNITION 354,232 ±476 LBM
AT CUTOFF 265,234 ±400 LBM

Figure 9-5. Third Flight Stage Best Estimate Masses

SECTION 10

ENGINE SYSTEM

10. ENGINE SYSTEM

The main propulsion system of the S-IVB stage of the AS-502 launch vehicle consisted of a Rocketdyne J-2 engine (S/N J-2042) shown schematically in figure 10-1, associated propellant ducting, and conditioning systems. The engine was rated at 225,000 lbf thrust. As a result of the analysis of the engine and stage acceptance tests, the following 60-sec tag values were established with the engine constants presented:

Tag Values	
Thrust	228,980 lbf
Engine mixture ratio (EMR)	5.480
Specific impulse (Isp)	424.77 sec

Engine Constants	
LOX flowmeter	5.5419 cycles/gal
LH2 flowmeter	2.0270 cycles/gal
LOX boot strap orifice	0.268 $in.^2$
LH2 boot strap orifice	0.468 $in.^2$
Oxidizer turbine bypass nozzle	1.202 $in.^2$

The engine was equipped with a 0.640-sec start tank discharge valve (STDV) timer in the engine control circuit; however, actuation of the STDV, which determines the fuel lead duration, was controlled from the stage through the fuel injection temperature bypass circuit. With such control, the fuel leads were nominally 3 and 8 sec for the first and second burns, respectively.

10.1 Modifications

The engine was modified to improve restart capability. These modifications included retiming the main oxidizer valve (MOV) opening rate, reducing the augmented spark igniter (ASI) LOX orifice, and painting the crossover duct black. The stage propellant utilization (PU) system was modified to provide for a second burn engine start with the PU valve full open. A calibrated start tank vent and relief valve was installed to regulate the energy of the start tank, thereby controlling the pump spin up. Other modifications were made involving instrumentation or structures, but are not discussed here as they do not affect performance. Details of these modifications are presented in the Rocketdyne configuration report (R-5788).

10.2 Sequence of Events

Significant engine events during the S-IVB powered flight phase of the S-IVB-502 mission were as follows:

Event	Time (sec) From RO*	From ESC	Predicted From RO*	Deviation
First Engine Start Command (ESC1)	577.270	0.0	518.16	+ 59.51
First Engine Cutoff Command (ECC1)	747.036	169.366	657.12	+ 89.92
Second Engine Start Command (ESC2)	11,614.671	0.0	11,401.00	+213.67
Second Engine Cutoff Command (ECC2)	11,630.397	15.726	11,725.56	- 95.16

*Range Zero

NOTE: There are some differences in the sequence of events (section 5) and engine event times given in this section.

Engine events times are those received at the engine while the times listed in the sequence of events reflect switch selector or IU times. In addition, there is an inherent inaccuracy in both sources of data since neither is continuous.

Comparisons are made to the predicted propulsion system performance as published in memorandum M177-KKBA, dated 26 April 1968. Details of the sequence of events for the first and second starts are given in tables 10-1 and 10-2. Effects of these sequences on the start transients can be seen in figures 10-2 and 10-3.

10.3 Engine Chilldown Conditioning

10.3.1 Turbopump Chilldown

Chilldown of the engine LOX and LH2 turbopumps was adequate to provide the conditions required for proper engine start for both burns. Figure 10-4 shows the condition of the LOX pump. The pump performance is discussed in paragraph 10.5.2. The analysis and results of the chilldown operation at the engine/stage interface is presented in sections 12 and 13.

10.3.2 Thrust Chamber Chilldown

10.3.2.1 Ground Conditioning and Boost

Thrust chamber chilldown was initiated at RO -600 sec and terminated at RO -8.8 sec with a thrust chamber jacket temperature (C0199) of 241 deg R, thus satisfying the maximum allowable redline limit of 300 deg R. At first burn Engine Start Command, the temperature was 287 deg R (figure 10-5) which was within the requirement of 330 $\pm$50 deg R.

For the S-IVB-502 flight, the thrust chamber conditioning time was decreased from the 15 min used for S-IVB-501 flight to 10 min, due to the lower than predicted heating during boost observed on the S-IVB-501 flight. The temperature rise rate at Engine Start Command was calculated to be 16.0 deg/min for S-IVB-502 flight and 22.5 deg/min for S-IVB-501 flight whereas the average temperature rise rate during boost was 48.5 deg R/min for S-IVB-502 flight and 54.3 deg R/min for S-IVB-501 flight.

10.3.2.2 Inflight Conditioning

Inflight conditioning of the thrust chamber is accomplished by the fuel lead which allows hydrogen to flow through the thrust chamber jacket prior to mainstage operation. The time used for this fuel lead period is defined as the time between Engine Start Command and STDV solenoid energize.

Fuel lead times were 3 and 8 sec respectively for the first and second burns. The conditions and characteristics of these fuel lead operations are summarized in table 10-3. Flight measurements are presented in figures 10-6 and 10-7.

Both fuel lead operations (first and second burns) were satisfactory. Engine performance during the fuel lead periods is presented in paragraphs 10.4.2.3 and 10.4.4.3.

10.3.3 Engine Start Sphere Chilldown and Loading

The GH2 start sphere was satisfactory at liftoff with 3.47 lbm of GH2 at 1,303 psia and 279 deg R as shown on figure 10-8. These conditions met the liftoff requirements shown in figure 10-9. Sphere conditions at liftoff are compared to S-IVB-501 flight and S-IVB-502 acceptance firing conditions in table 10-4. The sphere warmup rate from sphere pressurization to blowdown was 1.2 deg/min; the S-IVB-501 warmup rate was 0.9 deg/min. The difference between the GH2 start sphere and engine control helium sphere temperatures on S-IVB-502 and S-IVB-501 after pressurization was 27 deg R and 17 deg R, respectively. At liftoff, the respective differences had decreased to 11 and 9 deg R. The S-IVB-501 and S-IVB-502 warmup rates from pressurization to liftoff were 1.6 and 2.2 deg/min, respectively. From liftoff to sphere blowdown, the respective warmup rates were 0.6 and 0.7 deg/min. These warmup rates reflect the temperature differences before and after liftoff. From these data it can be seen that the greater warmup rate observed on S-IVB-502 was due to the greater temperature difference between the GH2 start sphere and the engine control helium sphere. This warmup rate is within the previous band of experience.

10.3.4 Engine Control Sphere Chilldown and Loading

The engine control helium sphere was satisfactorily loaded at liftoff with 1.87 lbm of helium at 2,963 psia and 290 deg R. These conditions met the liftoff requirements of 3,040 ±240 psia and 279 ±30 deg R, respectively. Control sphere performance data during loading is presented in figure 10-8. Control sphere conditions at liftoff are compared with S-IVB-501 flight and S-IVB-502 acceptance firing conditions in table 10-5.

10.4 Engine Performance

The J-2 engine did not meet all objectives during the AS-502 mission. After inserting the stage and payload into earth orbit, the engine failed to reignite for a second burn, thereby aborting the S-IVB mission. The failure was due to a rupture of the ASI feedline with possible ASI and injector damage during the first burn which prevented fuel from reaching the igniter during the second burn restart transient. The rupture allowed cold hydrogen gas to be sprayed into the thrust structure and engine area causing severe environmental changes for several components resulting in their inability to function properly. These malfunctions are discussed in the appropriate sections. All performance values were within the prediction accuracy of 1 percent prior to the rupture. The malfunction caused a performance degradation at approximately ESC +100 sec, and the 1 percent prediction limits were exceeded. As a result of this performance change and reduced performance in the lower stage, an extended first burn duration was required to achieve orbit.

Plots of selected data showing engine characteristics are presented in figures 10-10 through 10-21 for engine mainstage operation. The engine propellant inlet conditions are discussed in sections 12 and 13. The average stage performance and propellant consumption summary is presented in table 10-6.

10.4.1 Engine Performance Analysis Methods and Instrumentation

The performance of the engine start tank and helium control sphere was analyzed by applying thermodynamic relationships to the measured data. Start and cutoff transient thrust and impulse were determined by computer program PA53. Flowrates and consumption during the transients were determined by a manual count of the flowmeter cycle data. Computer program UT23A was used to investigate internal engine performance. Steady-state performance was calculated by use of computer program G105, which is considered to be the best current estimate of engine performance. The results of the G105 were also used in determining the best estimate of stage propellant consumption. Revised tag values, based on flight data, were generated by computer program G307 (Rocketdyne PAST640). A description of the program operation and a tabulation of the results is presented in table 10-7. Data inputs to the computer programs with the applicable biases are shown in table 10-8.

10.4.2 First Burn

10.4.2.1 Start Tank Performance

The engine start tank conditions at first S-IVB Engine Start Command and Engine Cutoff Command during the AS-502 flight, are shown on table 10-4. The deviations from predictions shown on table 10-9 were due to a higher than anticipated start tank temperature due to heat input from the control sphere which caused a higher flow through the relief valve thereby reducing the mass and pressure at Engine Start Command. The higher initial temperature was reflected throughout the first burn and was due to the heat transfer to the start tank from the control sphere which had not stabilized when the start tank vent was closed.

The STDV was commanded open at ESC1 +3.019 sec and the pressure decay initiated at ESC1 +3.219 sec. The blowdown was terminated by the STDV closure at ESC1 +3.821 sec. It was calculated that 2.839 lbm of GH2 were discharged during the 0.602 sec blowdown with

terminal conditions as shown on figure 10-22 at which time the start sphere began to refill with hydrogen from the fuel injection manifold and pump discharge.

A 0.055 $in.^2$ orifice in the line from the fuel pump discharge controlled the refill rate. The start sphere pressure increased to 793.4 psia at ESC1 +6.7 sec which terminated the gas portion of the refill as shown in figure 10-23. The figure also shows that, at that time, topping was initiated, which involves the flow from the fuel pump discharge only and is characterized by increasing pressure and decreasing temperature. The recharge capability of the start tank, as defined by Rocketdyne, was demonstrated (figure 10-24) at STDV +60 sec. The topping process was terminated at ESC1 +74.0 sec when the start tank pressure and pump discharge pressure were in equilibrium. The pressure and the temperature at this time were 1,185 psia and 187 deg R respectively with no further mass increase in the tank. Heat input from the system caused a temperature increase and a corresponding pressure increase along a constant mass line as shown in figure 10-22. At cutoff the start sphere pressure and temperature were 1,239 psia and 197 deg R, respectively. Cutoff conditions were within the safe engine restart envelope.

10.4.2.2 Engine Control Sphere Performance

The pressure and temperature in the engine control sphere at Engine Start Command were 3,000 psia and 288 deg R, respectively with a mass of 1.9 lbm as shown on table 10-5. Although the fuel lead time for the first burn engine start was 3.019 sec, the ignition phase control timer (0.450 $\pm$0.033 sec) extended the period of high helium usage associated with the fuel lead to 3.480 sec which was normal. However, and additional extension of 0.65 sec was experienced due to the delay in the purge control valve closing. Delays as high as 0.7 sec have been experienced with this valve. As a result of this extension the control sphere pressure drop associated with the fuel lead was 662 psi as compared to the predicted value of 540 psi (figure 10-25). The indicated pressure drop of 1,334 psi from Engine Start Command to ECC1 +1 sec was adjusted to 813 psi when the temperature was corrected to 290 deg R for comparison with specification values. The adjusted pressure was not within the required maximum ΔP (800 psi) due to the slow deactuation of the purge control valve. The performance during the first burn is also shown in figure 10-25. Consumption based on the indicated data was 0.39 lbm. However, when corrected for temperature the consumption was 0.405 lbm leaving 1.495 lbm in the sphere at orbital insertion. Barring any subsequent malfunction there was sufficient helium for the second burn.

10.4.2.3 Fuel Lead and Start Transient

Temperature and pressure data presented in figure 10-6 indicate that the first fuel lead was quite similar to AS-501. The temperature and pressures were also in close agreement with predictions. Flowrates, total flow, thrust, and impulse data in figure 10-26 were calculated using the flowmeter, temperature, and pressure data. All of these first burn fuel lead data appear normal.

The engine performance during the first burn start transient was satisfactory and is summarized in table 10-10. The thrust buildup occurred at a null PU valve position following the fuel lead. During the start transient, the PU valve position and MOV operation were satisfactory. Thrust buildup to the 90 percent performance level (STDV Command +2.5 sec by definition) was within the maximum and minimum thrust limits as shown in figure 10-27.

Thrust buildup was faster during flight than during the acceptance firing. This was largely due to the shorter first stage plateau time during MOV opening during flight. As a result of the shorter plateau time, LOX flowrate to the thrust chamber was higher during the early phases of thrust buildup during flight. The thrust and total impulse at the 90 percent performance level during flight were very similar to the S-IVB-501 flight values and were reasonably close to the log book values. They were considerably higher than the corresponding acceptance firing values due to the faster opening MOV on flight.

Figure 10-27 shows the thrust chamber pressure, the thrust buildup, and total impulse during the start transient. Figures 10-28 and 10-29 show the measured flowrates, consumptions, and pump speeds during the start transient.

10.4.2.4 Engine Steady-State Performance

Plots of selected data showing engine characteristics are presented in figures 10-10 through 10-15.

The PU valve was maintained at the full closed position during the mainstage period as planned. Burntime was 30.4 sec longer than predicted because the combined performance of both the S-II and S-IVB was much lower than expected. Although the overall performance level of the S-IVB was lower than predicted, the engine performance for the first 115 sec was satisfactory. At this time, the effects of a suspected ASI fuel line leak began to change the level of engine operation.

The significant effects of loss of fuel to the injector were to raise the mixture ratio at the injector and cause an increase in fuel injection temperature. However, the mixture ratio at the pumps did not change significantly because the leak occurred downstream of the pumps and flowmeters. Both fuel injection and fuel tank pressurization module temperatures increased 6.4 deg R and 12.5 deg R, respectively, which corresponds to a decrease in fuel flow of from 4.5 to 6 lb/sec.

At approximately ESC1 +127 sec, the engine performance began to stabilize at the lower level of operation. Chamber pressure exhibits the reduction in engine performance. A 17.5 psi drop in chamber pressure occurred due to a drop in total weight flow estimated at approximately 11.0 lb/sec, which was accomplished by a leak or combination of leaks. Gas generator (GG) performance was reduced due to the reduction in pump discharge pressures; however, the mixture ratio remained essentially constant.

Table 10-11 lists the steady-state average performance before and after the malfunction. Table 10-6 presents the average overall performance during the first burn period.

The composite values for standard altitude steady-state performance (engine tag values) with a comparison to the predicted at STDV +60 sec are shown in figures 10-30 and table 10-12.

Flow integral mass analysis indicated the following mainstage propellant consumptions by the engine during mainstage operation first burn: LOX 74,559 lbm, LH2 13,812 lbm.

Table 10-6 presents the total impulse generated during first burn mainstage operation.

Computed engine performance parameters of thrust, Isp, EMR, LOX flow, fuel flow, and total flow are shown in figure 10-31. The variation of Isp with EMR is presented on figure 10-32 which shows the performance shift.

The thrust variations from ESC1 +60 sec to engine cutoff of first burn are shown in figure 10-33. The thrust oscillations that occurred prior to and after the ASI fuel line failure are compared to the contract end item (CEI) specification in table 10-13. Prior to the failure, the thrust oscillations were within specification and would have remained so if the failure had not occurred.

The CEI specification states that if inflight engine performance shifts occur, the thrust variation limits may be exceeded, such was the case. The limits for the oscillations about mean thrust level and rate of change of thrust were exceeded due to the malfunction.

10.4.2.5 Cutoff Transient

The engine performance during the first burn engine cutoff transient was satisfactory. The time lapse between engine cutoff, as received at the engine, and thrust decrease to 11,250 lbf (5 percent of rated thrust) was within the maximum allowable time of 800 ms. Engine performance during the cutoff transient is shown in table 10-14.

The thrust decrease time during flight was greater than the log book value. This was probably due to a colder MOV actuator during flight which resulted in a longer valve closing time. First burn engine cutoff occurred with the PU valve in the closed position (high EMR).

The total cutoff impulse was greater than that of the S-IVB-501 flight and S-IVB-502 acceptance firing. This greater impulse was largely due to a colder MOV actuator temperature during the S-IVB-502 flight (282.5 deg R for -502 flight compared to 305 deg R for -501 flight). This resulted in a slower MOV closing time and increased cutoff impulse. The colder actuator temperature was most likely due to the presence of LH2 from the broken ASI line during the latter stages of first burn.

The flight total impulse can be compared to the log book value by adjusting the flight values to standard conditions (null PU valve position and 460 deg R MOV actuator temperature). The adjusted flight total impulse was in good agreement with the log book value. This indicated that the higher cutoff impulse during flight was due to the higher cutoff thrust and colder MOV actuator temperature during flight as compared to the nominal log book conditions.

The cutoff impulse to zero thrust as computed from MSFC trajectory data was 67,600 lb/sec as compared to a value of 59,376 lb/sec from engine analysis. The trajectory value exceeds the predicted three-sigma maximum cutoff impulse (66,350 lb/sec). This discrepancy remains unexplained as of this writing, but Douglas has a higher degree of confidence in the value derived from engine analysis which has been subjected to review and verification by Douglas.

Figure 10-34 shows the thrust chamber pressure, the thrust decrease, and total impulse during the cutoff transient. Figure 10-35 compares the velocity gain during the cutoff transient as computed by engine analysis and trajectory analysis with the predicted velocity gain.

Approximately 15 sec after first burn Engine Cutoff Command, a 25 psi spike was observed at the fuel pump discharge as shown in figure 10-34. A pressure use was also manifested in the fuel pump interstage outlet pressure, fuel pump inlet pressure, and fuel pump balance piston cavity pressure. The fuel pump discharge temperature showed a corresponding rise. The most probable cause of the pressure spike was the sloshing or flow of liquid to the still spinning fuel pump from the main fuel supply. The magnitude of the pressure rise is a function of the opening time of the fuel bleed valve which allows the trapped gas at the pump discharge to relieve back to the fuel tank. This allows fuel to flow into the pump again, causing the rise in pump discharge pressure.

This phenomenon has been observed during several tests during the Arnold Engineering Development Center (AEDC) test series with both prevalves open and closed following engine cutoff. Present predicted maximum pressure rises at the pump discharge are expected to be 2,400 psi. Tests are currently underway at the AEDC facility to identify the magnitude of the pressure in the bleed return line with special instrumentation. The stage low pressure line is rated at approximately 100 psi; however, the bleed valve and associated hardware resistance may be sufficient to reduce the pressure to a safe level.

An increase in fuel turbine inlet temperature of approximately 90 deg was noted immediately after engine cutoff. This rise in temperature was attributed to a lack of GG purge, which is normally required 7 sec prior to engine cutoff. The purge was not supplied to the engine until 1 sec before cutoff because of instrument unit (IU) difficulty resulting from unexpected stage maneuvers as the required cutoff velocity was approached. The magnitude of the temperature rise was not great enough to cause any hardware damage, and the temperature returned to cutoff level within 20 sec.

10.4.3 First and Second Orbits

10.4.3.1 Start Tank Performance

Figure 10-36 shows a relatively large temperature change at Engine Cutoff Command with very little pressure change which is impossible without a corresponding mass loss. A similar deviation has been noted on AS-203 and AS-501. The resultant analysis concluded that, in the zero g environment, heat transfer becomes very localized because of the lack of free convection. Therefore, the location, installation technique, and type of transducer indicate that the start sphere temperature measurements during orbital coast are not

accurate; however correct interpretation of the data can now be made based on S-IVB-502 and previous flight experience. The pressure measurement can be used to obtain the temperature up to relief setting because the bottle mass is constant. Also, the temperature after the second burn start tank discharge (STD) should be valid due to convective currents set up by the blowdown. The temperature is assumed to be linear between the initiation of venting and second burn STD.

The anticipated temperature rise rate during orbital coast was 0.54 deg/min with a corresponding 2.3 psi/min pressure rise rate. With such rates the relief setting (1,290 psia) of the vent and relief valve would be reached at ECC1 +14 min. The actual relief time was ECC1 +23 min resulting from a mean pressure rise rate of 3.5 psi/min, which corresponds to an isochoric temperature rise rate of 0.561 deg/min compared to the indicated temperature rise rate of 2.5 deg/min. The vent and relief valve did not respond as predicted during orbit maintaining the pressure at 1,320 psia instead of 1,290 psia. This was apparently the effect of the environment change during the first burn and of the orbital maneuvers which varied the heat input into the start tank. The vehicle attitude experiment did not show any appreciable change in start bottle performance.

During the S-IVB-502 orbital coast (181 min) an estimated 0.87 lbm of GH2 was vented through the relief valve to maintain the pressure as indicated on figure 10-36.

10.4.3.2 Control Sphere Performance

The same environmental conditions which affect the start tank temperature effect the control sphere temperature to a lesser degree. The rate of increase agrees well with the predicted as shown on figure 10-37. The pressure and temperature data and temperatures calculated by using perfect gas laws are also shown on figure 10-37. There was no indication of leakage.

10.4.4 Second Burn

10.4.4.1 Start Tank Performance

The engine start sphere conditions, at Engine Start Command and Engine Cutoff Command during the AS-502 flight second burn, are shown on table 10-4. The deviations from normal after the blowdown were due to the malfunction which prevented the start tank from refilling.

The STDV was commanded open at ESC2 +8.007 sec and the pressure decay initiated at ESC2 +8.215 sec. The blowdown was terminated by STDV closure at ESC2 +8.800 sec. Approximately 3.17 lbm of GH2 were discharged during the 0.585 sec blowdown with the terminal conditions as shown on figure 10-38. The start sphere blowdown provided a turbine spin satisfactory for mainstage initiation. The lack of ignition in the thrust chamber prevented a successful mainstage and, although not required, the start tank did not refill as expected.

10.4.4.2 Control Sphere Performance

The pressure and temperature in the engine control sphere at Engine Start Command were 1,918 psia and 247 deg R, respectively, with a mass of 1.48 lbm as shown in table 10-5 and figure 10-39. Although the fuel lead time for the second burn start was 8 sec, the ignition phase timer (0.450 ±0.033 sec) extended the period of high helium consumption associated with the fuel lead to 8.457 sec as anticipated. The fuel lead pressure drop was 740 psi as compared to a predicted value of 800 psi. Because of the failure to restart, comparisons with the prediction during mainstage were not possible; however, the cutoff usage was normal. The pressure profile is shown on figure 10-40.

10.4.4.3 Restart Attempt

The engine did not meet all objectives as second ignition failed to occur. Plots of selected data are presented in figures 10-16 through 10-21.

Second burn fuel lead measurements presented in figure 10-7 appear normal with two exceptions. Injector fuel temperature decreased somewhat faster than was expected and the injector fuel pressure measurement was lower than expected. Fuel injector pressure measurement (D0004) appeared to be erratic during the second burn fuel lead, as compared to D0104 which measures the pressure of the hydrogen bled from the engine for LH2 tank pressurization. These two pressure measurements usually correlate very well and analyses indicate that the tap off pressure was correct. The unusual reading of D0004 following the malfunction may have been caused by injector damage resulting from the ASI line failure discussed in paragraph 10.4.5.

Fuel lead thrust was determined from accelerometer measurement (A0006), and injector fuel pressure was calculated as a check on the validity of this measurement. The resulting pressure schedule is shown in the figure. Since the pressure calculated in this manner correlates reasonably well with the chilldown rates experienced and with the AS-501 chilldown, it is assumed to be valid.

The exceptionally rapid chilldown rate indicated in figure 10-8 is not greatly different than that during AEDC testing. The small differences in chilldown rates are logical considering the differences in bulk temperature and thermal distribution between test and flight. In addition, the possible effects of a general chilling of the area that could occur with an overboard hydrogen leak and a lack of combustion in the ASI are both indicative of an accelerated chilldown.

Second burn flowrates and fuel consumption thrust and total impulse are shown in figure 10-41 for the fuel lead. These are based on flowmeter (F0002) and temperature and pressure measurements. Injector pressure calculated from accelerometer data was used to calculate injector flow and engine thrust. Thrust, specific impulse and engine mixture ratio are shown in figure 10-41 also for the remainder of the restart attempt.

The S-IVB provided adequate conditioning of propellants to the J-2 engine for the restart attempt as discussed in sections 12 and 13. The engine start sphere was recharged properly and maintained sufficient pressure during coast. Although the engine control sphere gas usage was greater than predicted during the first burn, the sphere maintained sufficient system pressure for a proper restart.

All monitored events occurred as required and performance was as predicted until the end of the start bottle blowdown which occurred at approximately ESC2 +8.5 sec. At this time the main engine chamber pressure should have increased with opening of the MOV, and the GG should bootstrap to mainstage operation. However, the main engine chamber pressure did not rise and lack of ignition was indicated by the lack of increase in fuel injector temp C0200 (figure 10-20). The GG was ignited as shown by C0001 (figure 10-21). The temperature rose (see paragraph 10.5.4) just prior to Engine Cutoff Command and the GG chamber pressure increased slightly. This fact plus the absence of any unexplained vehicle moment during second burn suggests that the temperature spike did not burn through the GG combustor wall and that the GG performed satisfactorily.

The start bottle did not recharge due to a lack of system pressure buildup. Engine operation was terminated by instrument unit monitor of the mainstage OK pressure switches.

10.4.5 Malfunction Analysis

10.4.5.1 Failure to Restart

Failure to restart the engine was the major result of the malfunction that occurred during the flight. Proper electrical power was applied to the spark plugs but no ignition occurred. The subsequent failure of the IU to detect the mainstage pressure switch OK signal resulted in engine cutoff.

A failure of this type could only have occurred as a result of two possible malfunctions: (1) The destruction of both spark plugs due to an overtemperature in the ASI chamber which could have resulted from a flow reversal, or from an ASI fuel feedline anomaly which restricted fuel flow to the ASI chamber causing a high mixture ratio and thus extreme temperatures in the chamber shown schematically on figure 10-42; (2) A lack of one or both propellants in the ASI chamber. Since the start system has two independent spark exciters and igniters, a double failure would have been necessary to prevent ignition. A break in the LOX and/or ASI fuel lines was, therefore, considered most likely.

10.4.5.2 First Burn Anomalies

Investigation of pertinent parameters during first burn indicated deviations from normal operation as early as ESC1 +63 sec. Small leaks in the ASI lines, however, may actually have occurred earlier when abnormal engine vibration data was measured at ESC1 +20 sec.

10.4.5.3 Engine Abnormal Vibration

Abnormal engine vibration was indicated by the accelerometer data during first burn. The sensor on the LOX dome (E0209), failed completely at approximately RO +700 sec. The LOX pump exhibited normal vibrations (E0211) but shortly after engine start (ESC +20 sec), the LH2 pump vibration (E0210) indications deviated from normal (section 18). At approximately ESC1 +120 sec, the LH2 pump vibration indication returned to normal for the remainder of first burn. The abrupt changes in vibration indication levels appeared to correspond to engine temperature changes and engine performance levels; however, fuel pump performance was normal as discussed in paragraph 10.5.2. Sections 18 and 25 discuss the vibration effects.

10.4.5.4 Environment Temperatures

The engine area environmental temperature measurements indicated a malfunction as follows:

a. A cooling trend began to appear at approximately RO +610 sec indicating a cryogenic fluid leak.

b. A rapid heating trend was observed from RO +695 to RO +700 sec indicating that hot gas was escaping.

c. After RO +700 sec, a general net cooling trend was again noted in the engine area.

These general trends are shown by a great number of environment temperature measurements. Some of them began showing cooling trends as early as RO +610 sec while some did not show any cooling until approximately RO +680 sec. At approximately RO +695 sec, most of the temperatures rose rapidly until approximately RO +700 sec and then began cooling again.

The GG fuel inlet line wall temperature indicates that the initial cold leak was probably a cryogenic fuel leak because of the temperature drop from 58 to 50 deg R. A temperature reduction at this level could not have been caused by expanding LOX because the temperature was too low. The discussion of the engine performance also points out the malfunction was most probably a failure of the ASI fuel line. Additional discussions of the engine area environment can be found in the thermodynamics section (section 26) of this report.

A few of the temperature measurements during the restart attempt indicated that a leak was present. At the end of fuel lead the thrust structure temperature and the engine main LOX pneumatic line surface temperature show cooling trends which are not normal. Also the gas generator fuel inlet line wall temperature shows a decrease immediately after the second burn Engine Start Command.

No leaks were indicated during the orbital coast period. Also, the roll maneuver during the orbital coast apparently had little effect on any temperatures. The changes in temperatures correlate with entering and leaving the shadow of the earth.

The location of each engine area environment temperature sensor is shown on figure 10-43 and the range is given in table 10-15. This table contains a detailed description of the temperatures and is supported by figures 10-43 through 10-53. The temperature measurements are discussed for the first burn, orbital coast, and second burn periods and are compared to AS-501 data where possible.

10.4.5.5 Engine Parameters

10.4.5.5.1 Fuel Lead

Figures 10-54 and 10-55 present special data particularly relevant to the engine failure that occurred during the first burn. This failure also apparently resulted in the failure of the engine to progress into mainstage operation during the restart attempt.

The figure shows the amount of hydrogen existing between the flowmeter and the injector plotted against injector temperature and against fuel lead time. Examination of this figure shows a degree of correlation between AS-501 and AS-502 first burns.

The second burn does not correlate as well. The AS-502 second burn shows a progressively increasing difference in the quantity of fuel in the thrust chamber compared to that in AS-501. Since AS-501 chilled only to 165 deg R, an extrapolation, shown by the dotted line in figure 10-54, is required to project this characteristic to a fully chilled condition. This curve shows that in the AS-502 chilldown, approximately 13.5 lbm of fuel existed in the thrust chamber at the time the fuel injection temperature reached 40 deg R. A quantity of 10.5 lbm is indicated for AS-501.

If similar conditions are assumed, this difference indicates that 3 lbm of hydrogen leaked from the system between the flowmeter and the injector during this period. This would be an average flowrate of 0.375 lbm/sec during the 8-sec fuel lead. A leakage rate of this magnitude projects, on the basis of percent average total fuel flowrate, to a mainstage leakage rate in the order of 8.6 lbm/sec. This flowrate is compared to the 2 to 11 lbm/sec leakage rate calculated for mainstage operation as discussed in paragraph 10.4.2.4.

Another indication of possible hydrogen leakage based entirely on flowmeter (F0002) data is given in figure 10-55 which shows that AS-502 used considerably more propellant than AS-501. However, it should be pointed out that AS-501 did not chill completely. Therefore some additional amount of propellant, possibly the amount shown by the dotted line in figure 10-54, should be allowed to complete the AS-501 chilldown. The thrust, engine mixture ratio (EMR), and specific impulse (Isp) that occurred between Engine Start Command and the IU commanded cutoff are also shown in the figure. It should be noted that thrust calculated from accelerometer data (A0006) correlates well with thrust calculated from chamber pressure (D0001). The specific impulse during fuel lead (the first 8 sec) was calculated from flowmeter and accelerometer thrust data. The specific impulse values shown are reasonable for a two-phase flow condition during this time. EMR is based entirely on flowmeter (F0001 and F0002) data.

10.4.5.5.2 Mainstage

The major engine parameter indicating the failure was the chamber pressure which began to drop noticeably at ESC1 +107 sec. The exact time was not distinguishable because a pressurization cycle was present at the time. A plot of chamber pressure corrected to exclude the effects of helium pressurization is presented in figure 10-56 which shows an initial decrease of 4 psia between ESC1 +107 and ESC1 +115 sec and a subsequent 12 psia drop during the following 10 sec. The reduction in measured chamber pressure, as indicated on figure 10-10 was validated by correlation with other major engine parameters. At the same time negligible changes were noted in the measured oxidizer and fuel flowrates (figure 10-12) indicating that a propellant loss had occurred at some point downstream of the flowmeters and upstream of the main chamber.

A second major indication of the malfunction can be seen in the fuel tank pressurizstion control module temperature data (figure 10-57). At ESC1 +50 sec the temperature began to deviate from the expected profile, resulting in a deviation of +4.5 deg R at ESC1 +118 sec. The deviation increased sharply to +12.5 deg R and remained at that value until engine cutoff. An increase of 7 to 10 deg R was also exhibited by the fuel injection temperature; however, this transducer had a much larger range and the control module temperature is considered more accurate. The control module temperature may be high, however, due to additional heatup in the line between the fuel injection and the module transducers.

Indications of the performance shift resulting from the malfunction are seen in most engine parameters and are discussed in the steady-state performance paragraph 10.4.2.4.

The initial 4 psi drop in chamber pressure and the subsequent 12 psi decrease, totaling 16 psi, corresponds to a flowrate decrease through the combustion chamber throat of approximately 11 lbm/sec.

The hydrogen pressurization module temperature which was 12.5 deg R higher than expected indicated that there was a 7 lbm/sec decrease in fuel flow through the engine thrust chamber tubes.

As ESC1 +115 sec the fuel flowrate, as shown by the LH2 flowmeter, increased approximately 0.3 lbm/sec. This indicates a decrease in flow resistance, downstream of the flowmeter. At approximately the same time, the LOX flowrate appeared to decrease 1 lbm/sec.

In order to verify the failure reconstruction, the summation of the flow losses must equal the decrease in engine flowrate as a result of the observed drop in chamber pressure. The various losses associated with a broken ASI fuel line are presented below and in table 10-14.

a. As shown in figure 10-58 the loss of fuel from a broken ASI fuel line can vary from 2 to 11 lbm/sec, depending on the break location. The most likely point for the break would be in the vicinity of one of the three flex hose sections, probably at the first flex, resulting in a flow loss of 6 lbm/sec. This agrees within 1.0 lbm/sec of the fuel loss indicated by the increase in the fuel pressurization module temperature.

b. An additional loss would result from the backflow of propellants and/or combustion gases from the combustion chamber. The flow is difficult to predict since injector erosion probably occurred and the temperature in the ASI chamber and degree of mixing cannot be determined. The range of flow, however, is approximately 0.1 to 1.5 lbm/sec.

c. As mentioned previously the fuel pump flowrate increased and the LOX pump flowrate decreased.

d. The final malfunction, which would lead to a loss of gas flow through the engine throat, is a burnthrough in the ASI chamber. The exact magnitude of the loss would, of course, depend on the severity of the erosion.

Considering all the propellant losses that would result from an ASI fuel line failure (table 10-16), it appears that a net loss between 2.8 and 13.2 lbm/sec is possible. The actual loss of 11 lbm/sec, indicated by the decrease in chamber pressure, is well within the range. The expected net loss if 7.7 lbm/sec, 3.2 lbm/sec lower than actual, which indicates that the ASI burned through and the main injector was eroded. The additional loss could result from combustion gases flowing through a hole less than 1 $in.^2$ of effective area.

10.4.5.6 Rocketdyne Failure Simulation

A J-2 engine was calibrated to match the engine used on the S-IVB. The S-IVB-502 failure was then simulated with this engine by slowly reducing the fuel flow to the ASI and then completely bypassing the fuel flow, thus simulating a leak and a subsequent break in the ASI fuel line. The engine was allowed to run for 29 sec following the elimination of fuel flow to the ASI. As a result the main injector was eroded, the ASI chamber was burned through, and the ASI fuel line was burned away along with the spark plug cable. This proved that the ASI could be burned through and severe engine damage caused by a fuel starvation to the ASI. The ASI LOX line was not damaged in the test, and thus helped to substantiate the theory that it had not broken during the flight.

A performance shift similar to that seen during the first burn of S-IVB-502 was noted, thus demonstrating that an ASI fuel line failure was responsible for producing effects seen on S-IVB-502.

Component testing on the upper flex section of the ASI line has been conducted at nominal ASI engine flowrates (0.8 to 1.2 lbm/sec). It has been demonstrated that these bellows sections can fail at near operational flowrates due to resonance under certain conditions. The precise conditions required to establish the resonant conditions are related to the bellows construction, internal flowrate, and external environment as well as installation configuration.

Results to date indicate the following:

a. Bellows supplied from two independent sources resonate at different flowrates. The configuration installed on S-IVB-502 was of the type most susceptible to resonance.

b. Fatigue failures have been demonstrated in short periods at operational flowrates in a vacuum environment.

c. External environment such as air can provide enough damping due to liquefaction within the convolutions to preclude a fatigue failure that might have occurred in a vacuum under the same internal flowrates.

10.4.5.7 Suspected Failures

Suspected engine failures are as follows:

a. The spark plugs were suspected of being damaged by an overtemperature in the ASI chamber due to a leak in the ASI fuel line. This may have been the case; however, an ASI fuel line leak would not account for the high propellant loss encountered.

b. The two-stage increase in the fuel tank pressurization control module temperature strongly indicates that the ASI fuel line leaked for 68 sec and then broke completely at ESC1 +118 sec. A leak from the ASI fuel line would have reduced flow to the ASI resulting in an increase in the mixture ratio in the ASI chamber along with the temperature.

c. An ASI LOX line failure is considered a possibility because this alone or in conjunction with an ASI fuel line failure would have prevented restart. However, a break in the line upstream of the orifice would have resulted in a LOX loss which, in addition to the fuel loss, would have produced a net loss much greater than that experienced. Although a break downstream of the orifice is feasible, the line should not be subject to failure since it is a relatively short line with no flexible sections.

d. High temperatures in the ASI chamber may have induced internal erosion and possible damage to main engine LOX and fuel injectors, other adjacent engine hardware, and the ASI injector and body. A burnthrough could, therefore, have occurred leading to the loss of combustion gases and propellants from the main chamber.

10.4.5.8 Most Probable Failure

Environment temperatures and engine parameters indicate that the failure occurred as follows: During first burn a leak developed in the ASI fuel line. The leak increased with time resulting in a decrease in fuel flowrate to the engine and ASI chamber. This resulted in a decreasing chamber pressure and an increase in ASI mixture ratio until the pressure at the break decreased to a point where backflow could occur. At this time the ASI fuel line was severed and the flowrate to the engine decreased markedly. The ASI and main injector probably suffered erosion and burnthrough, allowing LOX from the ASI feed, propellants from the main injectors, and chamber gases from the injector face, to flow out. After the initial outflow of hot gases from the ASI chamber, a net cooling trend was apparent in environmental temperature. It is therefore concluded that hot gases from the combustion chamber were being cooled by mixing with the ASI LOX and possibly the injector-supplied fuel entering the ASI chamber. They then expanded into a vacuum environment already being cooled by fuel from the broken ASI line, and an effective cooling trend was established. The temperature of the escaping gases is difficult to determine since the degree of injector erosion is impossible to predict. The extent of any burnthroughs in the ASI can, likewise, not be predicted.

10.4.5.9 Corrective Action

Redesign of the ASI fuel line to a rigid 1/2 in. diameter, one piece, butt welded unit has been initiated and will be installed on future flight vehicles. The ASI LOX supply line has likewise been redesigned with the orifice moved to the ASI LOX valve flange. Analytical studies and tests have been made on all critical bellows installations in the engine to determine their susceptibility to failure.

10.5 Component Operation

10.5.1 Main LOX Valve

The main LOX valve performed satisfactorily during the first burn period and the restart attempt as indicated in table 10-17 and figure 10-59. The flight data acquisition accuracy of ±85 ms is considered to be responsible for the apparent deviation of the flight values from the acceptance firing values. This accuracy level is the result of the 10 sample/sec data sampling rate.

The engine MOV actuator skin temperature (C2003) began to decrease at ESC1 +62 sec. This lowered actuator temperature is attributed to the ASI fuel line failure and subsequent LH2 cryogenic spray. The effect of this lower MOV temperature is discussed in paragraph 10.4.2.3.

10.5.2 Pumps and Turbines

The LH2 pump performance was satisfactory during the first burn start transient and the restart attempt with no indication of stall (figure 10-60). These data indicate that both thrust chamber chilldown operations were adequate to prevent excessive fuel pump back pressure. Further information on the chilldown operation and GSE supply system is presented in sections 6, 12, and 13.

The performance of the LH2 and LOX pumps and turbines was satisfactory during the first burn and the restart attempt. Pump speeds, discharge pressures, and temperatures, responded to perturbations and to engine inlet conditions as expected. Pressure and temperature increases across the pumps were satisfactory.

10.5.3 PU Valve

The PU valve control during first burn was as expected. Engine start occurred with the PU valve in the null position (5.0 EMR). At ESC1 +8 sec, PU Activate Command was given, and the valve moved to the full closed position (5.5 EMR) in approximately 1 sec, as predicted. The valve maintained the full closed position for the remainder of the first burn. A history of the valve position is shown in figure 10-11.

Prior to second burn Engine Start Command the PU valve was positioned in the full open position (4.5 EMR) and remained there until PU activate time (ESC2 +13 sec).

After system activation at ESC2 +13 sec, the valve moved to the LOX-rich (high EMR) position as shown on figure 10-17 due to the PU system malfunction as discussed in section 15.

10.5.4 Gas Generator

The GG performance was satisfactory during both the first burn and the restart attempt. The GG performance was noted to shift at the time of the ASI fuel line failure (ESC1 +115 sec). At this time the GG chamber pressure was observed to decrease approximately 20 psi because of the decreased LOX and fuel pump discharge pressures associated with the powering down effect of the ASI fuel line failure (figure 10-61).

During the start of the second burn, the GG temperature spiked (as indicated by the fuel turbine inlet temperature bulb), to 2,300 deg R, the upper limit of the temperature bulb, but an expanded plot of fuel turbine inlet temperature suggests the spike actually reached as high as 2,500 deg R. The spike resulted from a high start mixture ratio in the GG which in turn was caused by the failure of the main chamber pressure to rise above the 40 psia idling pressure it reached during the second burn. With a low main chamber pressure, most of the flow destined for the GG follows the lower pressure drop path to the main chamber, resulting in a low GG total flowrate. However, because the start load of the oxidizer pump is lower than that of the fuel pump, the initial oxidizer flow is less affected than the fuel flow. Thus, as noted in figures 10-21 and 10-61, the GG chamber pressure, a function of both total flowrate and mixture ratio, is low; whereas, the fuel turbine inlet temperature, a function only of GG mixture ratio, is high.

At Engine Cutoff Command, the GG chamber pressure was observed to rise slightly. This fact plus the absence of any unexplained vehicle moment during second burn provides evidence that the temperature spike did not burn through the GG chamber wall.

10.5.5 Engine Drive Hydraulic Pump

The engine-driven hydraulic pump performed satisfactorily during the first burn. The average power required by the pump was 4.67 hp. The auxiliary and main hydraulic pumps failed during and preceding second burn due to cavitation resulting from frozen hydraulic fluid believed to have been a result of the cryogenic leak that occurred during the first burn. A comprehensive analysis of the hydraulic system performance can be found in section 22.

10.6 Powered Flight Simulated Trajectory Evaluation

Using a five-degrees-of-freedom trajectory simulation program, propulsion system parameter histories were adjusted so that an S-IVB trajectory could be generated to closely match the observed trajectory (appendix 5). The simulation program employed uses a differential correction technique which determines the necessary adjustments to thrust and weight flow from the engine analysis and pitch and yaw/engine thrust misalignment angles from the control system analysis to match the observed trajectory. These adjustments were determined by minimizing in a least-squares sense the weighted differences in altitude, earth-fixed velocity, earth fixed velocity azimuth angle, and inertial acceleration between the observed and simulated trajectories.

To obtain a match of the observed trajectory it was necessary to adjust the level of the weight flow and to make separate adjustments to the levels of thrust before and after the performance shift. This is discussed more fully in paragraph 8.4. The weight flow determined by engine analysis was decreased by 0.11 percent. The thrust was increased by 0.30 percent before the performance shift and by 1.41 percent after the performance shift. The corresponding adjustments to the specific impulse were an increase of 0.49 percent before the performance shift and 1.27 percent following the performance shift. The averages of thrust, weight flow, and specific impulse from 90 percent thrust to Engine Cutoff Command were adjusted by +0.56 percent, -0.11 percent, and +0.67 percent, respectively, from the values determined by engine analysis. These averages are compared with predicted and engine analysis values in paragraph 8.4.

TABLE 10-1 (Sheet 1 of 2)
FIRST BURN ENGINE SEQUENCE

CONTROL EVENTS		CONTINGENT EVENTS		NOMINAL TIME FROM SPECIFIED REFERENCE	ACTUAL TIME (ms)	
MEAS NO.	EVENT AND COMMENT	MEAS NO.	EVENT AND COMMENT		FROM ESC	FROM SPECIFIED REFERENCE
K0021 (K0021)	*Engine Start Command P/U			0	0	0
		K0007 (K0531)	Helium Control Solenoid Enrg P/U	Within 10 ms of K0021	0	0
		K0010 (K0454)	Thrust Chamber Spark on P/U	Within 10 ms of K0021	011	011
		K0011 (K0455)	Gas Generator Spark on P/U	Within 10 ms of K0021	011	011
		K0006 (K0535)	Ignition Phase Control Solenoid Enrg P/U	Within 20 ms of K0021	020	020
		K0126 (K0558)	LOX Bleed Valve Closed P/U	Within 130 ms of K0007	068	068
		K0127 (K0557)	LH2 Bleed Valve Closed P/U	Within 130 ms of K0007	151	151
		K0020 (K0627)	ASI LOX Valve Open P/U	Within 20 ms of K0006	112	092
		K0119 (G0506)	Main Fuel Valve Closed D/O	60 ±30 ms from K0006	072	052
		K0118 (G0506)	Main Fuel Valve Open P/U	80 ±50 ms from K0119	095	023
K0021 (K0021)	**Engine Start D/O			Approx 3200 ms from K0021 P/U	3201	3201
K0096 (K0536)	†Start Tank Disc Control Solenoid Enrg			3,000 ±40 ms from K0021 P/U	3019	3019
		K0123 (G0508)	Start Tank Disc Valve Closed D/O	100 ±20 ms from K0096	3162	153
		K0122 (G0508)	Start Tank Disc Valve Open P/U	105 ±20 ms from K0123	3245	083
K0005 (K0538)	Mainstage Control Solenoid Enrg			450 ±30 ms from K0096	3480	461
		K0096 (K0536)	Start Tank Disc Control Solenoid Enrg D/O	450 ±30 ms from K0096	3469	450
		K0121 (G0507)	Main LOX Valve Closed D/O	50 ±20 ms from K0005	3570	090
		K0116 (G0509)	Gas Generator Valve Closed D/O	140 ±10 ms from K0005	3571	091
		K0122 (G0508)	Start Tank Disc Valve Open D/O	95 ±20 ms from K0096	3612	143
		K0117 (G0509)	Gas Generator Valve Open P/U	50 ±30 ms from K0116	3698	127
		K0124 (G0510)	LOX Turbine Bypass Valve Open D/O		3720	
		K0123 (G0508)	Start Tank Disc Valve Closed P/U	250 ±40 ms from K0122	3821	209

(KOXXX) Actual number from acceptance firing event recorder.

*Engine ready and stage separation signals (or simulation) are required before this command will be executed. This command also actuates a 640 ±30 ms timer which controls energizing of the start tank discharge solenoid valve (K0096).

**This signal drops out after a time sufficient to lock in the engine electrical.

†An indication of fuel injection temperature of -150 ±40 deg F (or simulation) is required before this command will be executed. This command also actuates a 450 ±30 ms timer which controls the start of mainstage.

P/U - Pickup D/O - Dropout

TABLE 10-1 (Sheet 2 of 2)
FIRST BURN ENGINE SEQUENCE

CONTROL EVENTS		CONTINGENT EVENTS		NOMINAL TIME FROM SPECIFIED REFERENCE	ACTUAL TIME (ms)	
MEAS NO.	EVENT AND COMMENT	MEAS NO.	EVENT AND COMMENT		FROM ESC	FROM SPECIFIED REFERENCE
		K0125 (G0510)	††LOX Turbine Bypass Valve Closed P/U		3944	
K0158 (K0572)	Mainstage Press Switch #1 Depress D/O				4850	
K0159	Mainstage Press Switch #2 Depress D/O				4919	
		K0120 (G0507)	Main LOX Valve Open P/U	2,435 ±145 ms from K0005	5660	2180
		K0010 (K0454)	Thrust Chamber Spark on D/O	3,300 ±200 ms from K0005 P/U	6745	3265
		K0011 (K0455)	Gas Generator Spark on D/O	3,300 ±200 ms from K0005 P/U	6745	3265
K0013 (K0522)	Engine Cutoff P/U (New time reference)			0	0	0
		K0005 (K0538)	Mainstage Control Solenoid Enrg D/O	Within 10 ms of K0013	002	002
		K0006 (K0535)	Ignition Phase Control Solenoid Enrg D/O	Within 10 ms of K0013	018	018
		K0020 (K0622)	ASI LOX Valve Open D/O		087	
		K0120 (G0507)	Main Oxidizer Valve Open D/O	50 ±15 ms from K0005	109	107
		K0117 (G0509)	Gas Generator Valve Open D/O	75 $^{+25}_{-35}$ ms from K0006	145	127
		K0118 (G0506)	Main Fuel Valve Open D/O	90 ±25 ms from K0006	167	149
		K0121 (G0507)	Main Oxidizer Valve Closed P/U	120 ±15 ms from K0120	235	126
		K0116 (G0509)	Gas Generator Valve Closed P/U	500 ms from K0006	217	199
		K0119 (G0506)	Main Fuel Valve Closed P/U	225 ±25 ms from K0118	419	252
K0158 (K0572)	*Mainstage Press Switch A Depress P/U				233	
K0159 (K0573)	Mainstage Press Switch B Depress P/U			*	233	
K0007 (K0531)	Helium Control Solenoid Enrg D/O			1,000 ±110 ms from K0013	999	999
		K0125 (G0510)	Oxidizer Turbine Bypass Valve Closed D/O		285	
		K0124 (G0510)	Oxidizer Turbine Bypass Valve Open P/U	10,000 ms from K0005	883	881
K0126 (K0558)	LOX Bleed Valve Closed D/O			30,000 ms from K0005	3709	3707
K0127 (K0557)	LH2 Bleed Valve Closed D/O			30,000 ms from K0005	3626	3624

††Within 5,000 ms of K0005 (Normally = 500 ms)

*Signal drops out when pressure reaches 425 ±25 psig.

P/U - Pickup D/O - Dropout

TABLE 10-2 (Sheet 1 of 2)
SECOND BURN ENGINE SEQUENCE

CONTROL EVENTS		CONTINGENT EVENTS		NOMINAL TIME FROM SPECIFIED REFERENCE	ACTUAL TIME (ms)	
MEAS NO.	EVENT AND COMMENT	MEAS NO.	EVENT AND COMMENT		FROM ESC	FROM SPECIFIED REFERENCE
K0021 (K0021)	*Engine Start Command P/U			0	0	0
		K0007 (K0531)	Helium Control Solenoid Enrg P/U	Within 10 ms of K0021	0	0
		K0010 (K0454)	Thrust Chamber Spark on P/U	Within 10 ms of K0021	010	010
		K0011 (K0455)	Gas Generator Spark	Within 10 ms of K0021	010	010
		K0006 (K0535)	Ignition Phase Control Solenoid Enrg P/U	Within 20 ms of K0021	010	010
		K0126 (K0558)	LOX Bleed Valve Closed P/U	Within 130 ms of K0007	152	152
		K0127 (K0557)	LH2 Bleed Valve Closed P/U	Within 130 ms of K0007	152	152
		K0020 (K0627)	ASI LOX Valve Open P/U	Within 20 ms of K0006	112	102
		K0119 (G0506)	Main Fuel Valve Closed D/O	60 ±30 ms from K0006	062	052
		K0118 (G0506)	Main Fuel Valve Open P/U	80 ±50 ms from K0119	085	023
K0021 (K0021)	**Engine Start D/O			Approx 8,200 ms from K0021 P/U	9609	9609
K0096 (K0536)	†Start Tank Disc Control Solenoid Enrg			8,000 ±40 ms from K0021	8007	8007
		K0123 (G0508)	Start Tank Disc Valve Closed D/O	100 ±20 ms from K0096	8154	147
		K0122 (G0508)	Start Tank Disc Valve Open P/U	105 ±20 ms from K0123	8245	091
K0005 (K0538)	Mainstage Control Solenoid Enrg			450 ±30 ms from K0096	8457	450
		K0096 (K0536)	Start Tank Disc Control Solenoid Enrg D/O	450 ±30 ms from K0096	8457	450
		K0121 (G0507)	Main LOX Valve Closed D/O	50 ±20 ms from K0005	8562	105
		K0116 (G0509)	Gas Generator Valve Closed D/O	140 ±10 ms from K0005	8584	127
		K0122 (G0508)	Start Tank Disc Valve Open D/O	95 ±20 ms from K0096	8595	138
		K0117 (G0509)	Gas Generator Valve Open P/U	50 ±30 ms from K0116	8700	116
		K0124 (G0510)	LOX Turbine Bypass Valve Open D/O		8675	
		K0123 (G0508)	Start Tank Disc Valve Closed P/U	250 ±40 ms from K0122	8795	200

(KOXXX) Actual number from acceptance firing event recorder.

*Engine ready and stage separation signals (or simulation) are required before this command will be executed. This command also actuates a 640 ±30 ms timer which controls energizing of the start tank discharge solenoid valve (K0096).

**This signal drops out after a time sufficient to lock in the engine electrical.

†An indication of fuel injection temperature of -150 ±40 deg F (or simulation) is required before this command will be executed. This command also actuates a 450 ±30 ms timer which controls the start of mainstage.

P/U - Pickup D/O - Dropout

TABLE 10-2 (Sheet 2 of 2)
SECOND BURN ENGINE SEQUENCE

CONTROL EVENTS		CONTINGENT EVENTS		NOMINAL TIME FROM SPECIFIED REFERENCE	ACTUAL TIME (ms)	
MEAS NO.	EVENT AND COMMENT	MEAS. NO.	EVENT AND COMMENT		FROM ESC	FROM SPECIFIED REFERENCE
		K0125 (G0510)	††LOX Turbine Bypass Valve Closed P/U		8900	
K0158 (K0572)	Mainstage Press Switch #1 Depress D/O				Did Not Occur	
K0159	Mainstage Press Switch #2 Depress D/O				Did Not Occur	
		K0120 (G0507)	Main LOX Valve Open P/U	2,435 ±145 ms from K0005	10525	2068
		K0010 (K0454)	Thrust Chamber Spark on D/O	3,300 +200 ms from K0005 P/U	11725	3268
		K0011 (K0455)	Gas Generator Spark on D/O	3,300 +200 ms from K0005 P/U	11725	3268
K0013 (K0522)	Engine Cutoff PU (New time reference)			0	0	
		K0005 (K0538)	Mainstage Control Solenoid Enrg D/O	Within 10 ms of K0013	006	006
		K0006 (K0535)	Ignition Phase Control Solenoid Enrg D/O	Within 10 ms of K0013	008	008
		K0020 (K0622)	ASI LOX Valve Open D/O		053	
		K0120 (G0507)	Main Oxidizer Valve Open D/O	50 ±15 ms from K0005	074	068
		K0117 (G0509)	Gas Generator Valve Open D/O	75 +25 -35 ms from K0006	124	116
		K0118 (G0506)	Main Fuel Valve Open D/O	90 ±25 ms from K0006	133	125
		K0121 (G0507)	Main Oxidizer Valve Closed P/U	120 ±15 ms from K0120	211	137
		K0116 (G0509)	Gas Generator Valve Closed P/U	500 ms from K0006	183	175
		K0119 (G0506)	Main Fuel Valve Closed P/U	225 ±25 msffrom K0118	360	227
K0007 (K0531)	Helium Control Solenoid Enrg D/O			1,000 ±110 ms from K0013	1000	1000
SS-22 K0507	PU Activate Switch D/O			N/A		
		K0125 (G0510)	Oxidizer Turbine Bypass Valve Closed D/O		244	
		K0124 (G0510)	Oxidizer Turbine Bypass Valve Open P/U	10,000 ms from K0005	574	568
K0126 (K0558)	LOX Bleed Valve Closed D/O			30,000 ms from K0005	3592	3586
K0127 (K0557)	LH2 Bleed Valve Closed D/O			30,000 ms from K0005	3592	3586

††Within 5,000 ms of K0005 (Normally = 500 ms)

P/U - Pickup D/O - Dropout

TABLE 10-3
FUEL LEAD CONDITIONS

ITEM	UNIT	S-IVB-501 FLIGHT		S-IVB-502 FLIGHT	
		FIRST START	SECOND START	FIRST START	SECOND START
Estimated thrust chamber bulk temperature* at fuel lead start	(deg R)	242	443	265	411
Fuel lead duration	(sec)	3	8	3	8
Fuel temperature at the injector at fuel lead termination	(deg R)	40	165	55	34
Fuel passing through MFV during fuel lead	(lbm)	15	25	14	39
Fuel between injector and MFV at fuel lead termination	(lbm)	4	8	4.5	14.5
Fuel passing through injector during fuel lead	(lbm)	11	17	9.5	24.5
Total effective impulse during fuel lead	(lbf-sec)	1,400	3,200	1,250	3,050

*Average of three temperature measurements: jacket temperature C0199 and exit skin temperatures C0385 and C0386.

TABLE 10-4
ENGINE START SPHERE CONDITIONS

PARAMETER	TEMPERATURE (°R)			PRESSURE (psia)			MASS(lbm)		
	502 FLIGHT	501 FLIGHT	502 ACCPT	502 FLIGHT	501 FLIGHT	502 ACCPT	502 FLIGHT	501 FLIGHT	502 ACCPT
Liftoff	279	262	260	1303	1294	1270	3.47	3.65	3.64
Liftoff requirement	See Liftoff Box			See Liftoff Box			See Liftoff Box		
First Engine Start Command	284	266	272	1267	1270	1335	3.31	3.53	3.64
After first start sphere blowdown	180	171	180	120	100	150	0.50	0.49	0.66
First Engine Cutoff Command	197	187	225	1242	1166	1255	4.75	4.74	4.18
Total GH2 usage during first start	-	-	-	-	-	-	2.84	3.04	2.98
Second Engine Start Command	253	246	263	1327	1286	1320	3.88	3.84	3.70
After second start sphere blowdown	-	170	178	-	140	165	-	0.68	0.73
Second Engine Cutoff Command	162	170	227	182	1185	1286	0.89	5.37	4.21
Total GH2 usage during second start	-	-	-	-	-	-	-	3.16	2.97

TABLE 10-5
CONTROL SPHERE DATA

PARAMETER	TEMPERATURE (deg R)			PRESSURE (psia)			MASS (lbm)**		
	502 FLIGHT	501 FLIGHT	502 ACCEPTANCE	502 FLIGHT	501 FLIGHT	502 ACCEPTANCE	502 FLIGHT	501 FLIGHT	502 ACCEPTANCE
Required at liftoff	279 ±30*	262 ±30*	260 ±30*	2,800 to 3,200 psia			-	-	-
Actual at liftoff	290	271	283	2,963	3,010	3,260	1.87	2.01	2.07
Before first burn engine start	288	271	286	3,000	3,075	3,345	1.90	2.03	2.11
After first burn engine cutoff	210	216	246	1,679	1,989	2,450	1.51	1.56	1.79
Before second burn engine start	247	239	276	1,918	1,878	2,764	1.48	1.48	1.84
After second burn engine cutoff	186	172	236	903	735	1,925	0.97	0.80	1.52
Mass used - first burn	-	-	-	-	-	-	0.39	0.51	0.32
Mass used - second burn	-	-	-	-	-	-	0.37	0.68	0.32

*Actual requirement is start sphere temperature ±30 deg R.

**As calculated from measured temperature and pressure.

TABLE 10-6
ENGINE PERFORMANCE*

PARAMETER	UNIT	CLOSED PU VALVE OPERATION			OVERALL PERFORMANCE 90 PERCENT THRUST TO ECC		
		ACTUAL	PREDICTED	PERCENT DEVIATION	ACTUAL	PREDICTED	PERCENT DEVIATION
Thrust	lbf	227,101	230,524	-1.48	226,293	229,832	1.54
Total flowrate	lbm/sec	539.42	542.52	-0.57	537.21	540.50	0.61
LOX flowrate	lbm/sec	455.93	459.15	-0.70	453.82	457.24	0.75
LH2 flowrate	lbm/sec	83.49	83.37	+0.14	83.39	83.26	+0.16
Engine mixture ratio		5.461	5.507	-0.83	5.441	5.491	-0.91
Specific impulse	sec	421.01	424.91	-0.92	421.29	425.27	-0.94

PARAMETER	UNIT	MAINSTAGE			TO DEPLETION**
		ACTUAL	PREDICTED	PERCENT DEVIATION	
Burntime		163.866	133.5	+22.75	
Consumption					
LOX	lbm	74,559	61,083	+22.06	
LH2	lbm	13,812	11,200	+23.32	
Impulse	lbf/sec	37.08×10^6	30.68×10^6	+20.86	

*All engine performance values are first burn only.

**Depletion figures were considered meaningless as there was no mainstage performance during second burn on which to base calculations.

TABLE 10-7
COMPARISON OF COMPUTER PROGRAM RESULTS

PROGRAM	INPUT	METHOD	RESULTS
G105 Mode 1	LOX and LH2 flowmeters, pump discharge pressures and temperatures, chamber pressures, chamber thrust area	Flowrates are computed from flowmeter data and propellant densities. The C_F is determined from equation $C_F = f(P_c, MR)$ and thrust is calculated from equation $F = C_F A_t P_c$.	$F = 230,343$ $\dot{W}_T = 541.233$ $I_{sp} = 425.59$ $MR = 5.505$
G307	Pump inlet and outlet conditions, PU valve position, chamber pressure, turbine inlet and outlet conditions, flowmeter speed	Math models of rocket engine components are linked together by the program which iterates among the component models until an operating point is reached where the power required by the pumps balances the power available from the turbines.	$F = 230,113$ $\dot{W}_T = 541.62$ $I_{sp} = 424.8$ $MR = 5.52$
F839	Thrust chamber pressure, chamber throat area	The C_F is computed from equation $C_F = f(P_c)$ and thrust is computed from equation $F = C_F A_t P_c$. The impulse is determined from integrated thrust.	Refer to paragraphs 10.4.2.3 and 10.4.2.5

TABLE 10-8
DATA INPUTS TO COMPUTER PROGRAMS

PARAMETER	PROGRAM	SELECTION	BIAS	REASON
Chamber Pressure	G105-1	D0001 (TM/FM)	-15	Rocketdyne estimation of purge effect
	PA53	D0001 (TM/FM)	+4.887	Correct for non-zero indication of transducer at ESC
	(Start)		97.51%	Variable bias -0 at ESC and -15 at ESC +60 sec
	(Cutoff)	D0001 (TM/FM)	+(6.412)	Correct for non-zero indication of transducer at end of thrust decay
			97.27%	Variable bias -0 at end of thrust decay and -15 at ECC
LOX Flowrate	G105-1	F0001	None	
Fuel Flowrate	G105-1	F0002	None	
LOX Pump Discharge Temperature	G105-1	C0133	None	
Fuel Pump Discharge Temperature	G105-1	C0134	None	
LOX Pump Discharge Pressure	G105-1	D0009	None	
Fuel Pump Discharge Pressure	G105-1	D0008	None	
Fuel Turbine Inlet Temperature	G105-1	C0001	None	
Gas Generator Chamber Pressure	G105-1	D0010	None	
	G307			

TABLE 10-9
START TANK PERFORMANCE

TIME	PRESSURE		TEMPERATURE		PREDICTED	ΔM	ACTUAL	ΔM
	PREDICTED	ACTUAL	PREDICTED	ACTUAL				
First Burn Engine Start Command	1,290	1,266.5	275	284.4	3.575		3.31	
STDV 1	1,290	1,265	275	284.4	3.575	0	3.31	0
End of blowdown 1	175	117.6	178	190.3	0.749	-2.826	0.471	-2.839
End of refill 1	825	793.4	226	236.4	2.78	+2.039	2.56	+2.089
End of topping 1	1,115	1,184.9	178	186.8	4.77	+1.99	4.83	+2.27
First Burn Engine Cutoff Command	1,260	1,238.8	195	196.8	4.91	+0.14	4.75	-0.08
Second Burn Engine Start Command	1,285	1,327	230	252.8	4.25	-0.66	3.88	-0.87

TABLE 10-10
FIRST BURN START TRANSIENT

PARAMETER	UNIT	ENGINE LOG BOOK	501 FLIGHT FIRST BURN	502 ACCEPT FIRST BURN	502 FLIGHT FIRST BURN
Time of STDV Command	sec from ESC	1.0	3.008	0.629	3.019
Thrust at 90 percent performance level*	lbf	189,580**	185,599	156,200	188,171
Total Impulse from Engine Start Command to 90 percent performance level*	lb-sec	---	188,864	---	190,543
Total impulse from STDV Command to 90 percent performance level*	lb-sec	197,707**	187,464	135,931	189.158

*Defined as STDV Command +2.5 sec
**Based on stabilized thrust at null PU and standard altitude conditions.

TABLE 10-11
STEADY-STATE ENGINE PERFORMANCE

PARAMETER	UNIT	90 PERCENT THRUST TO 115 SEC	PERCENT DEVIATION FROM PREDICTED	120 SEC TO C/O	PERCENT DEVIATION FROM PREDICTED
Thrust	lbf	227,032	-1.21	224,579	-2.29
Mixture Ratio		5.44	-0.93	5.45	-0.75
LOX Flowrate	lbm/sec	452.61	-1.01	456.6	-0.14
LH2 Flowrate	lbm/sec	83.21	-0.06	83.8	+0.65
Specific Impulse	sec	423.7	-0.37	415.6	-2.27

TABLE 10-12
FLIGHT 60-SEC TAG COMPARISON

PARAMETERS	UNIT	PREDICTED	ACTUAL	DEVIATION
Thrust	lbf	228,980 $\pm$2,901	228,804	-176
EMR		5.4804 $\pm$0.09	5,485	+0.0046
Specific Impulse	sec	424.765 $\pm$2.7	425.0	+0.235
LOX Flowrate	lb/sec	455.889 $\pm$5.34	455.30	-0.589
LH2 Flowrate	lb/sec	83.185 $\pm$1.35	83.01	-0.175

TABLE 10-13
THRUST OSCILLATION SUMMARY

DURING PU VALVE HARDOVER OPERATION	UNIT	CEI SPEC LIMIT	PRIOR TO MALFUNCTION	ACTUAL INCLUDING MALFUNCTION
Variation in mean thrust level	lbf	±5,000	-1,100	-3,500
Oscillations about mean thrust level	lbf	±2,500	±1,000	3,400
Rate of change of thrust	lbf/sec	±500	+134, -133	+134, -632
Thrust acceleration	lbf/sec/sec	±125	+69	+48

TABLE 10-14
FIRST BURN CUTOFF TRANSIENT

PARAMETER	UNIT	J-2 ENGINE LOG BOOK	501 FLIGHT FIRST BURN	502 FLIGHT FIRST BURN	502 FLIGHT RESULTS	
					ENGINE PERFORMANCE CALCULATIONS	FD AND C (AERO) CALC.
Time for Thrust to Decrease to 11,250 lbf*	ms	349	444	451	464	---
Thrust at Engine Cutoff Command	lbf	202,651	223,122	230,525	224,576	---
Total Impulse to 5 percent Thrust	lb-sec	38,031	48,101	48,808	53,177	---
Total Impulse to Zero Thrust	lb-sec	---	54,949	---	59,376	67,600
MOV Actuator Temperature at Engine Cutoff	°R	460	304.9	---	282.5	---
PU Valve Position at Engine Cutoff	deg	0	33.3	---	32.7	---
Total Impulse to 5 percent Thrust Adjusted to Null PU and 460°R Main Oxidizer Valve Actuator Temperature	lb-sec	38,031	---	---	39,005	---

*5 percent rated thrust

TABLE 10-15 (Sheet 1 of 3)
ENGINE AREA ENVIRONMENT TEMPERATURES

TEMPERATURE	MEAS. NO.	RANGE	FIGURE NO.	DISCUSSION
GG Fuel Inlet Line Wall	C0146	35 to 300°R	10-43	At approximately RO +685 sec this measurement began dropping from 58 deg R until it reached 50 deg R at RO +725 sec. It then increased slightly until engine cutoff. This temperature response indicates that fuel must have been spraying on the line because the temperature level is too low for LOX to cause such a reaction. The AS-501 data does not show any temperature change during the first burn. No unusual temperature changes occur during the orbital coast, alghough the level is approximately 50 deg R lower than on AS-501. Prior to second start the temperature increased to the same level as on AS-501. Immediately after the second burn Engine Start Command, the temperature dropped to the same level it reached during the first burn again indicating a fuel leak.
GG LOX Inlet Temp	C2035	100 to 610°R	10-44	At approximately RO +660 sec this temperature stopped increasing at 180 deg R and dropped to 160 deg R at RO +695 sec. It remained constant at this level until engine cutoff. During the second orbit of the coast period, the measurement went off-scale-high at RO +10,400 sec and remained there for the remainder of the mission. This measurement was not on AS-501; therefore, no comparison is possible.
Main LOX Valve Pneumatic Line Surface Temp	C2005	210 to 560°R	10-46	The temperature was normal until RO +650 sec when it dropped rapidly from 395 deg R to offscale at RO +720 sec. The temperature came back on scale after engine cutoff. The AS-501 continued to increase somewhat all during the first burn. The temperature during orbital coast appeared to be normal, although approximately 50 deg R lower than AS-501. At the end of fuel lead for the second start, it again dropped very rapidly approximately 45 deg R from 370 deg R. The AS-501 data increased during the second burn, similar to the first burn profile.
Main LOX Valve Actuator Skin Temp	C2003	110 to 560°R	10-46	During the first burn, the temperature dropped from 333 deg R at RO +640 sec to 280 deg R at engine cutoff with a slight discontinuity between RO +695 and RO +700 sec. On AS-501, this temperature decreased very slightly all during the first burn, but not nearly as much as it did on AS-502. Again, nothing unusual happened during orbital coast. During the period of the second burn the temperature was approximately 30 deg R lower on AS-502 than on AS-501 and showed evidence of a cooling trend following the restart attempt.
GG Bootstrap Line Temp No. 1	C2037	100 to 610°R	10-27	The temperature appeared to be normal until approximately RO +675 sec when it dropped about 5 deg R. At RO +695 sec, it rose very sharply from 165 to 193 deg R and then cooled until cutoff. The temperature appeared to behave as expected during the orbital coast period and the restart attempt. This measurement was not on AS-501 and no comparison is possible.
GG Bootstrap Line Temp No. 2	C2036	100 to 610°R	10-47	This temperature, which was not on AS-501, appeared normal throughout the mission. No abnormal temperature increases or decreases were present.

TABLE 10-15 (Sheet 2 of 3)
ENGINE AREA ENVIRONMENT TEMPERATURES

TEMPERATURE	MEAS. NO.	RANGE	FIGURE NO.	DISCUSSION
Main Hydraulic Pump Discharge Line Temp	C2029	360 to 610°R	10-48	This thermocouple was not on AS-501. The temperature appeared to be normal until approximately RO +685 sec when it stopped increasing and remained near 570 deg R until engine cutoff. Nothing unusual appeared in this temperature for the remainder of the mission from a propulsion view point. It is mentioned, however, due to the hydraulic system anomaly which is discussed in section 22.
Crossover Duct Wall Temp No. 1	C2015	0 to 2000°R	10-49	Compared to the AS-501 data, the temperature appeared to be normal until it went offscale at 718 sec. During the orbital coast, the temperature came back on scale for a short time at approximately the correct level. The thermocouple appears to have short circuited.
Crossover Duct Wall Temp No. 2	C2016	0 to 2000°R	10-49	This temperature was normal until RO +625 sec when the rate of increase was greatly reduced. The AS-501 data shows the temperature increasing throughout the first burn. The low heat uprate present on AS-502 must be due to external cooling because there was no decrease of the gas temperature in the crossover duct. The temperature was normal and very close to AS-501 during the orbital coast. Because of the failure to start the second time, the temperature did not reach its normal level.
Engine Area Ambient	C0010	260 to 960°R	10-50	AS-502 data showed a gradual cooling trend somewhat similar to AS-501. However, at RO +650 sec the cooling rate increased until, at RO +695 sec, a heat spike occurred from about 365 deg R to 422 deg R and then at RO +700 sec dropped completely offscale. This entire cycle of increased cooling rate at RO +650 sec and the heat spike at RO +695 sec are entirely different from AS-501 data. The measurement remained offscale all during orbital coast and the restart attempt. It is concluded that this transducer or its electrical connections failed at RO +700 sec due to the engine malfunction.
Oxidizer Main Supply Line Wall Temp	C0153	160 to 450°R	10-51	The data for AS-501 and AS-502 are similar until approximately RO +690 sec where a rapid heating trend occurs in the AS-502 data. This heating trend peaks out at RO +700 sec and 178 deg R after an increase in temperature of 10 deg. At RO +700 sec it gradually decreases until engine cutoff at which time it begins to heat up again. During orbital coast a linear cooling trend is shown until RO +3,600 sec. At this time the reading dropped offscale and remained there for the duration of the flight. The location of C0153 is on the main LOX line itself while C0010 is on the flange supporting the LOX line. The main difference in the two readings is that while C0010 showed a gradual cooling trend starting at RO +650 sec before the heat spike, C0153 revealed no corresponding cooling trend.

TABLE 10-15 (Sheet 3 of 3)
ENGINE AREA ENVIRONMENT TEMPERATURES

TEMPERATURE	MEAS. NO.	RANGE	FIGURE NO.	DISCUSSION
Oxidizer Main Supply Line Flange Wall Temp	C0152	160 to 370°R	10-51	The main supply line flange wall temperature (C0152) was similar to data from AS-501 until RO +675 sec. At this time the cooling rate increased similar to C0010 but continued for approximately 20 sec. At RO +695 sec the transducer went offscale for the duration of the flight. As shown in figure 10-43 the C0152 sensor is located between C0010 and C0153 sensors on the flange near the main LOX line. However, its data is more like the data from C0010 located farther back on the flange away from the LOX line. This leads to the conclusion that the initial cold leak occurred in an area somewhere to the inside of the main LOX line. Escaping hot gas could easily engulf all three sensors and probably did at approximately RO +695 sec since all these readings were definitely affected radically at this time. In conclusion, these three sensors indicate that the general environment became cooler in the area of the flange supporting the main LOX line. This cooling tendency did not occur in the area of C0153 shown in figure 10-43. Therefore, the hydrogen leak was probably to the inside of the main LOX line and accessible to the flange supporting the line. Two of the sensors (C0010 and C0153) showed a heat spike at RO +695 sec.
Interstage Area 7 Gas Temperature	C0275	160 to 660°R	10-52	The gas interstage area 7 temperature begins a rapid cooling trend at approximately RO +650 sec. This cooling continued until approximately RO +695 sec. A 505 to 575 deg R heat spike occurred at RO +700 sec. The heat spike peaked out and a rapid temperature drop occurred.
Thrust Structure Temp No. 1	C0087	310 to 885°R	10-53	This measurement showed a cooling trend starting at RO +610 sec. This cooling trend continued until RO +700 sec and dropped a total of 10 deg R. At RO +700 sec a heat spike of 30 deg R occurred followed by an immediate temperature drop of 72 deg. During orbital coast the temperature trend for AS-502 is somewhat similar to AS-501 except that AS-502 temperatures are cooler.
Thrust Structure Temp No. 2	C0088	310 to 385°R	10-53	The thrust structure No. 2 temperature exhibited a gradual cooling trend starting at approximately RO +680 sec. At RO +695 sec a rapid temperature increase occurred followed by another cooling trend. The temperature increase was 8 deg and much less exaggerated than the C0087 measurement. The two sensors are in the same general location but they are separated by a flange which could have shielded the C0088 sensor from the temperature extremes experienced by C0087. During orbital coast and restart attempt, the C0088 data is the same general pattern as AS-501 except that it is slightly cooler. In the AS-501 data, there is a gradual increase in temperature at approximately RO +2,000 sec followed by a cooling aid that is not seen in the AS-502 data. All of these sensors (C0275, C0088, and C0087) show a gradual cooling followed by an increase in temperature at approximately RO +700 sec. They are all located on the thrust structure itself. C0088 showed less irregularity in the data than the other two but the flange near it could easily have acted as a shield to protect it from the temperature extremes.

TABLE 10-16
PROPELLANT LOSSES DUE TO FAILURE

		MAXIMUM	MINIMUM	MOST PROBABLE
Total propellant loss indicated by chamber pressure	lbm/sec			-11
Fuel loss from a broken ASI fuel line	lbm/sec	-11.0	-2.0	-6.0
Backflow of gases from ASI chamber	lbm/sec	-1.5	-0.1	-1.0
Fuel flowrate change--flowmeter	lbm/sec			+0.3
LOX flowrate change--flowmeter	lbm/sec			-1.0
LOX loss from a broken ASI LOX line	lbm/sec	-13.0	-1.3	0
Backflow of gases through a burnthrough in the ASI chamber		Depends on size of hole		-3.3*
Net loss		-26.2	-4.1	-11.0
Net loss excluding a broken ASI LOX line		-13.2	-2.8	-11.0

*This is the additional flow required to produce a net loss of 11 lbm/sec.

TABLE 10-17
MAIN LOX VALVE OPENING TIMES

SECTION	NOMINAL TIME (ms)	ACCEPTANCE FIRST START (ms)	FLIGHT FIRST BURN (ms)	ACCEPTANCE SECOND START (ms)	FLIGHT SECOND BURN (ms)
First stage travel	50 ±26	60	150	70	165
First stage plateau	480 ±120	540	315	570	395
Second stage travel	1,825 ±75	1,890	2,030	2,110	1,800
Total	2,355 ±220	2,490	2,495	2,750	2,360

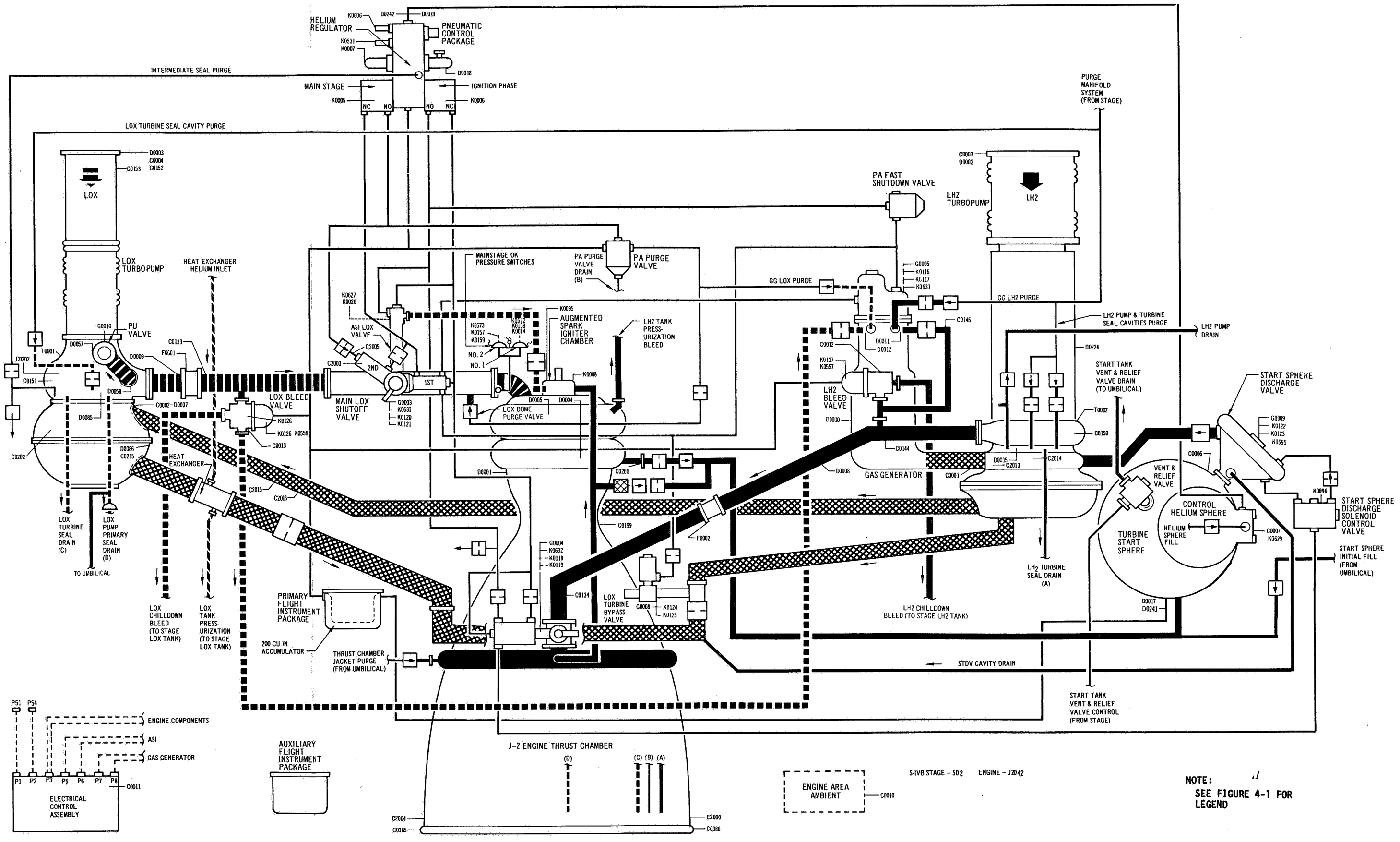

Figure 10-1. J-2 Engine System and Instrumentation

FOLDOUT FRAME 1

FOLDOUT FRAME

FOLDOUT FRAME 2

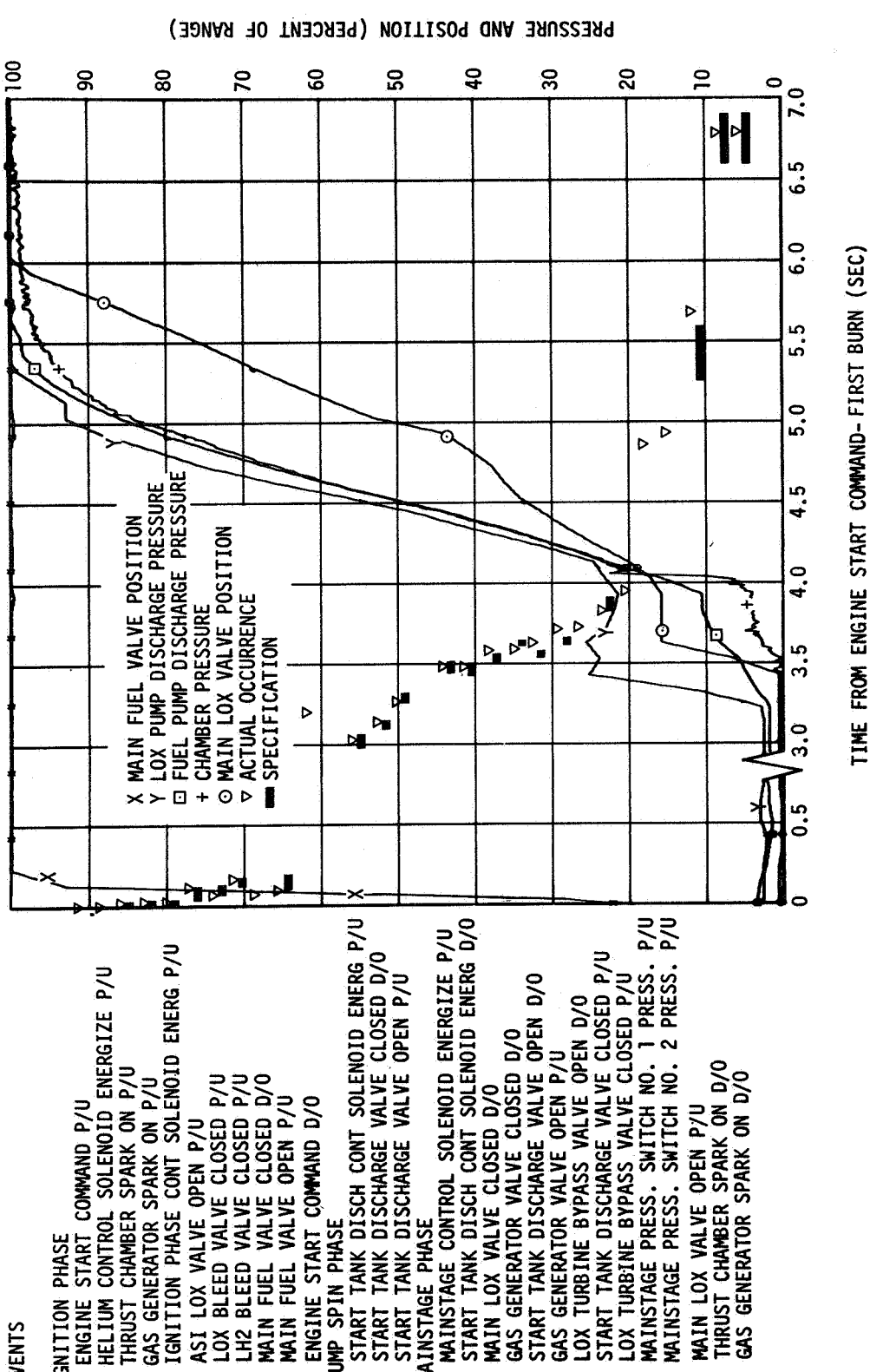

Figure 10-2. Engine Start Sequence - First Burn

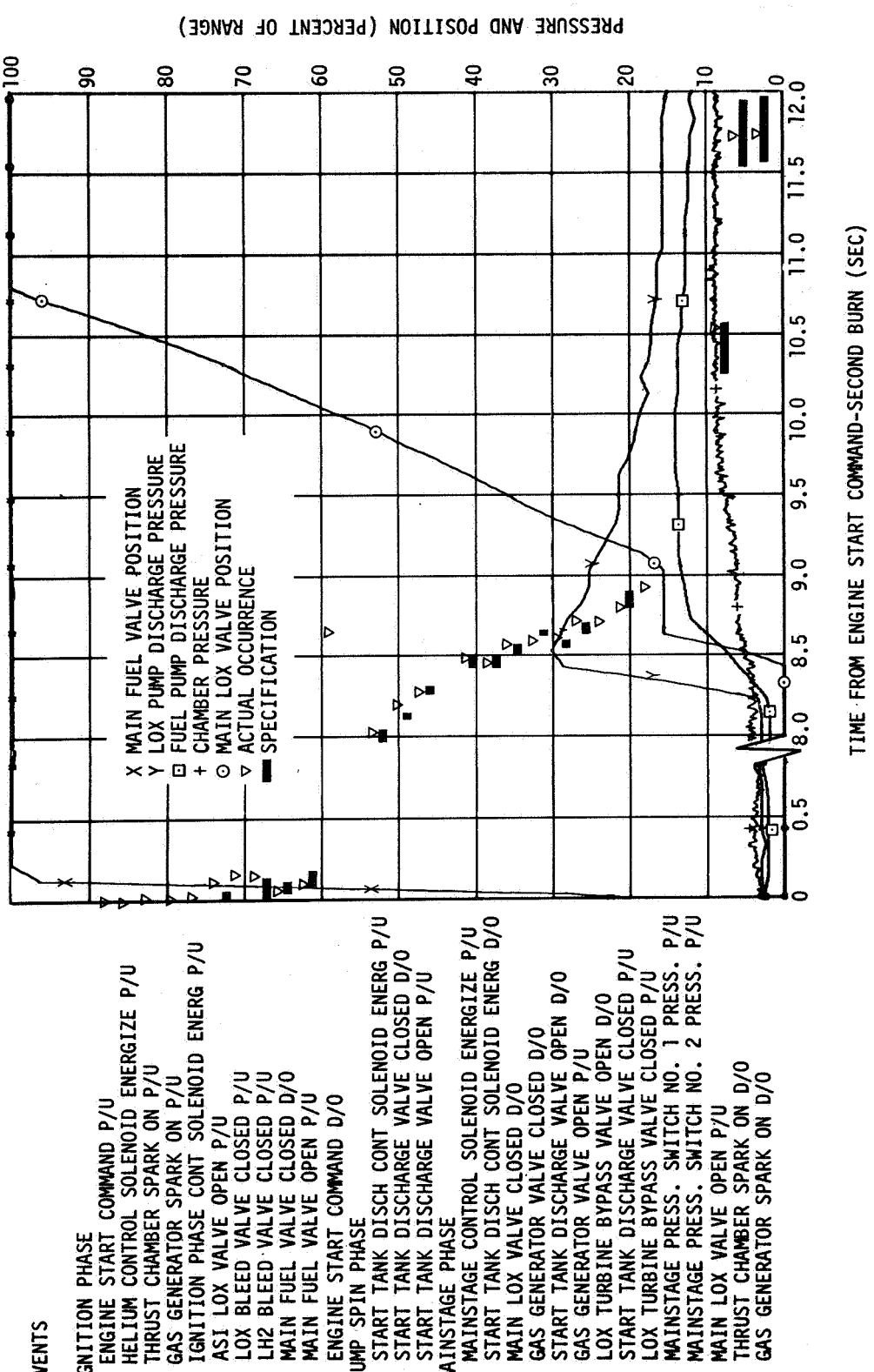

Figure 10-3. Engine Start Sequence - Second Burn

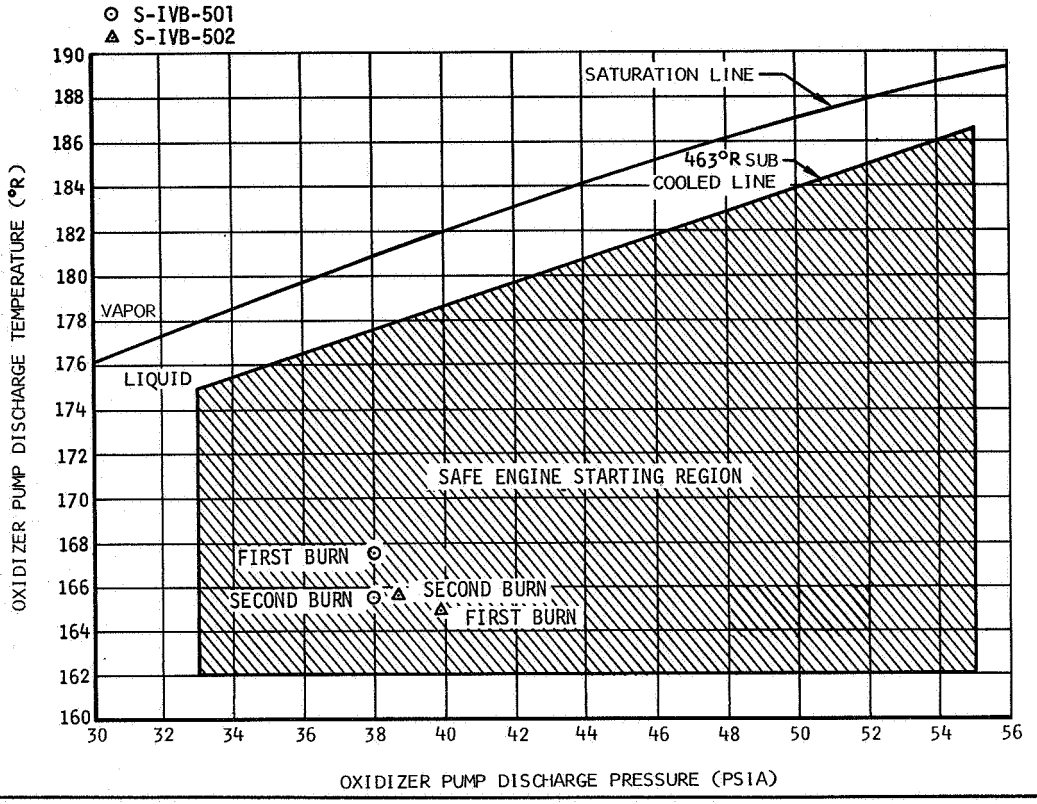

Figure 10-4. Oxidizer Pump Discharge Pressure Versus Temperature

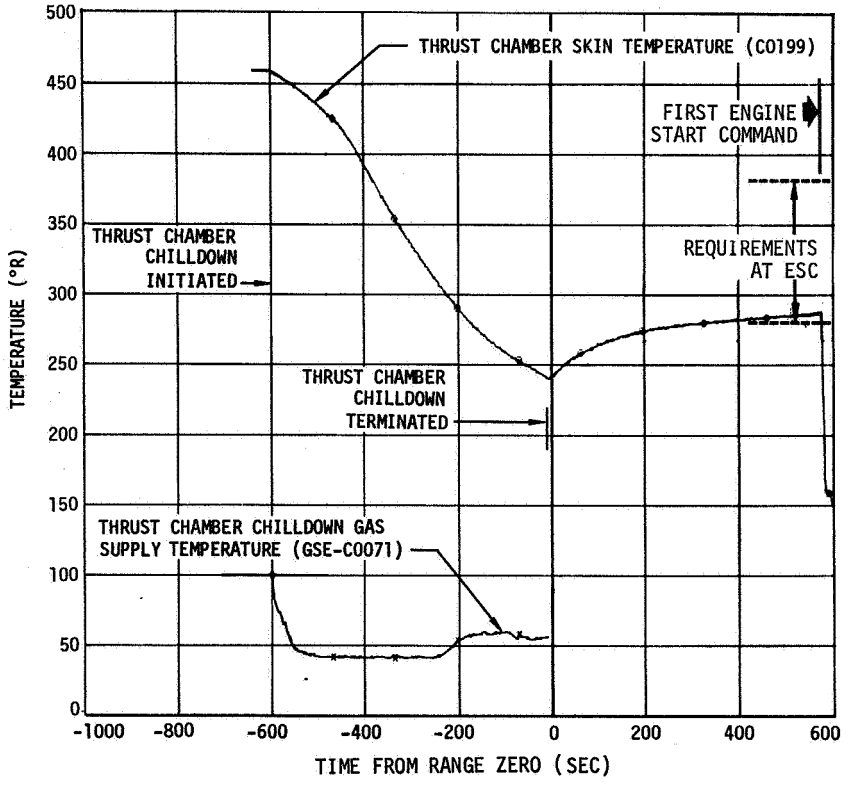

Figure 10-5. Thrust Chamber Chilldown - First Burn

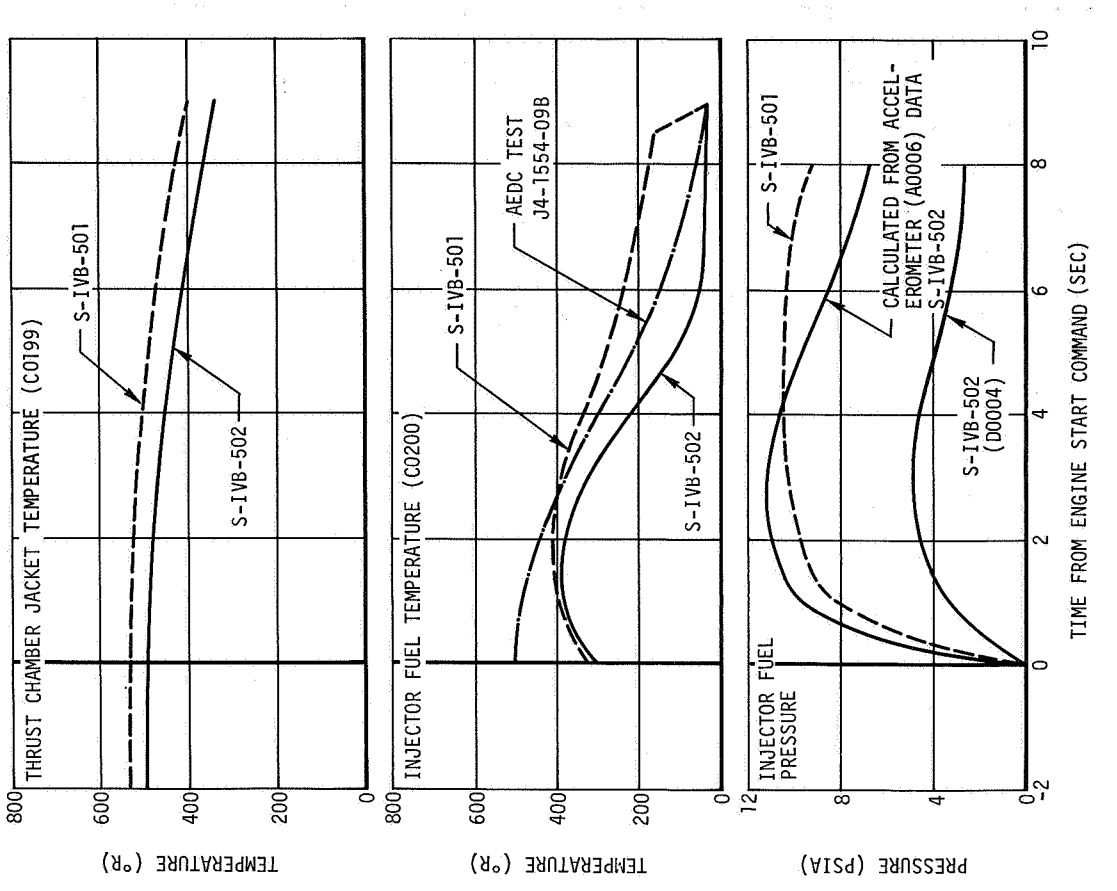

Figure 10-7. Fuel Lead - Second Burn

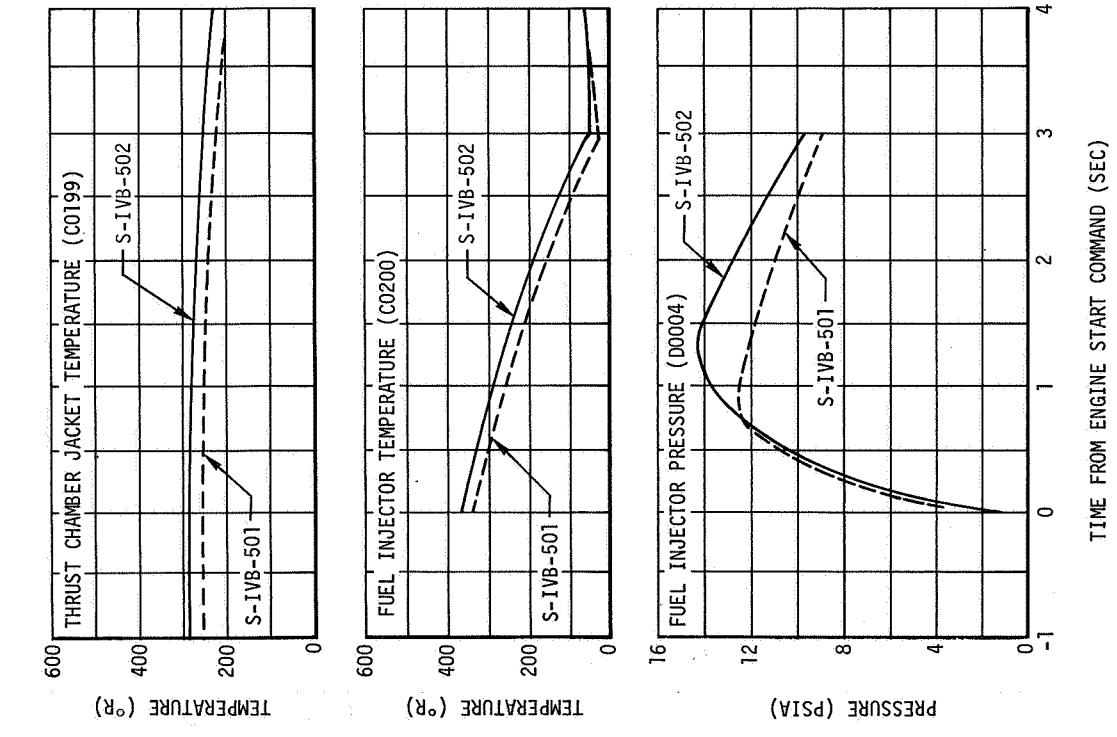

Figure 10-6. Fuel Lead - First Burn

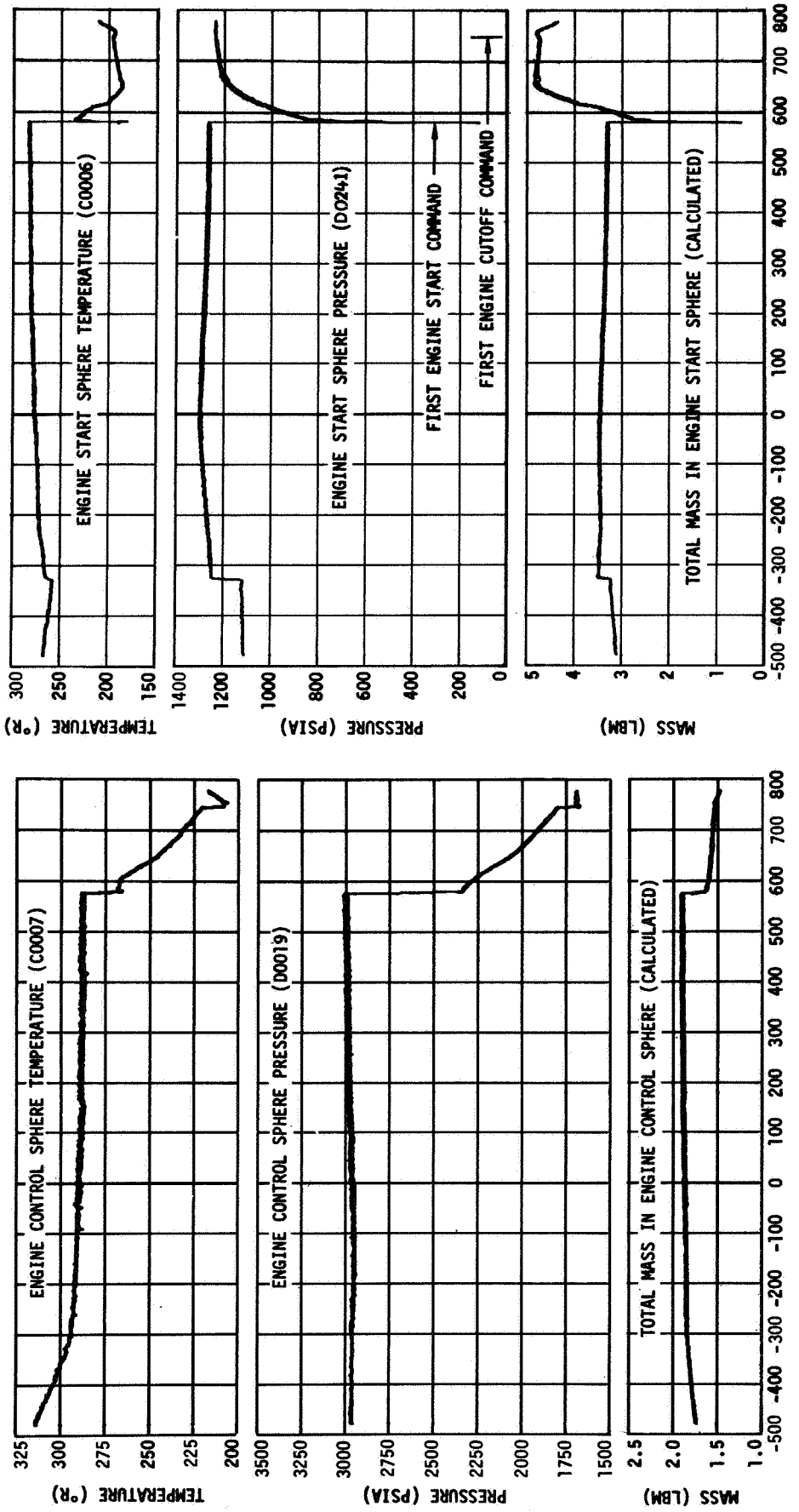

Figure 10-8 Engine Start and Control Sphere Performance - First Burn

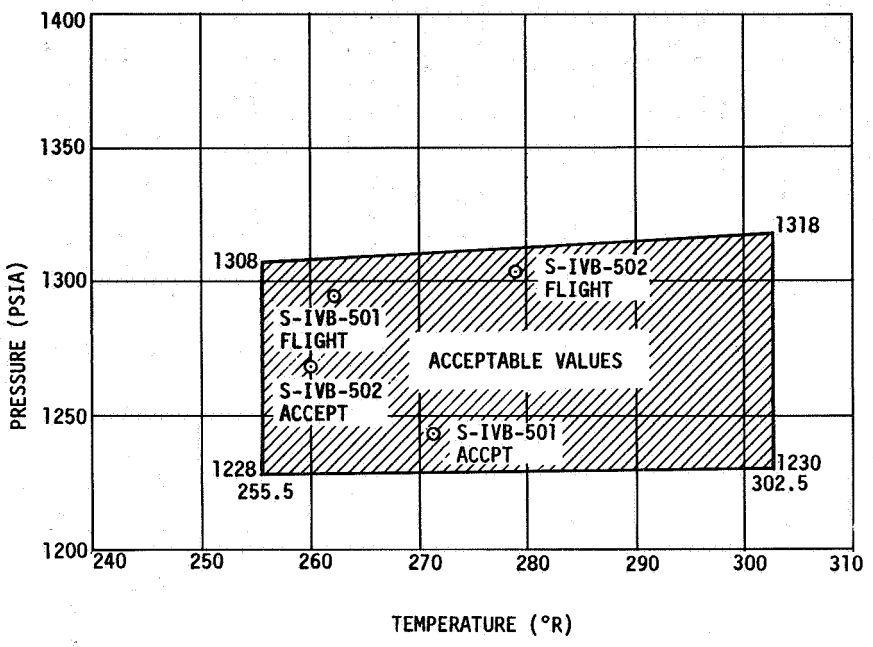

Figure 10-9. GH2 Start Sphere Critical Limits at Liftoff

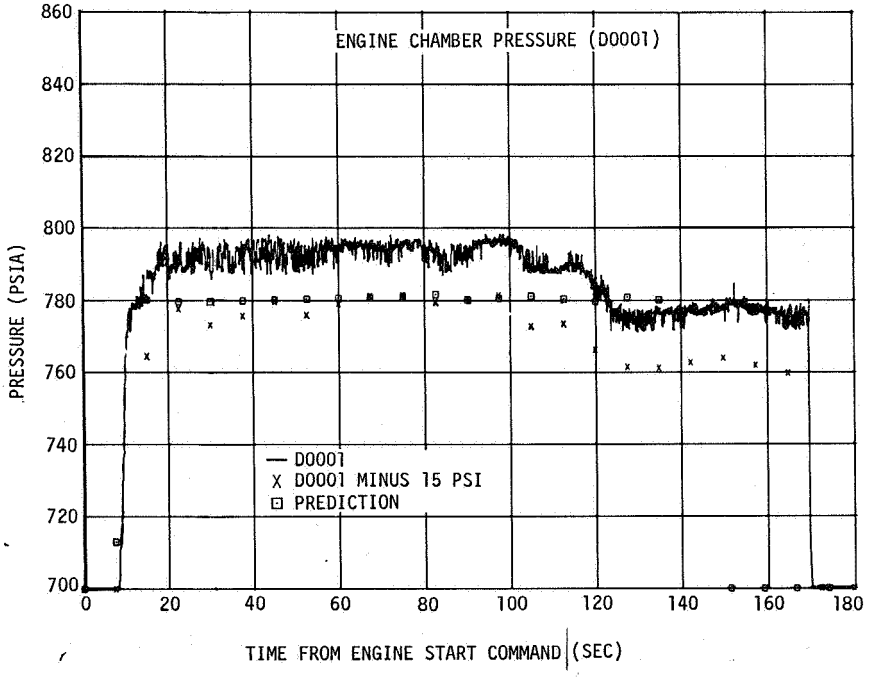

Figure 10-10. J-2 Engine Chamber Pressure - First Burn

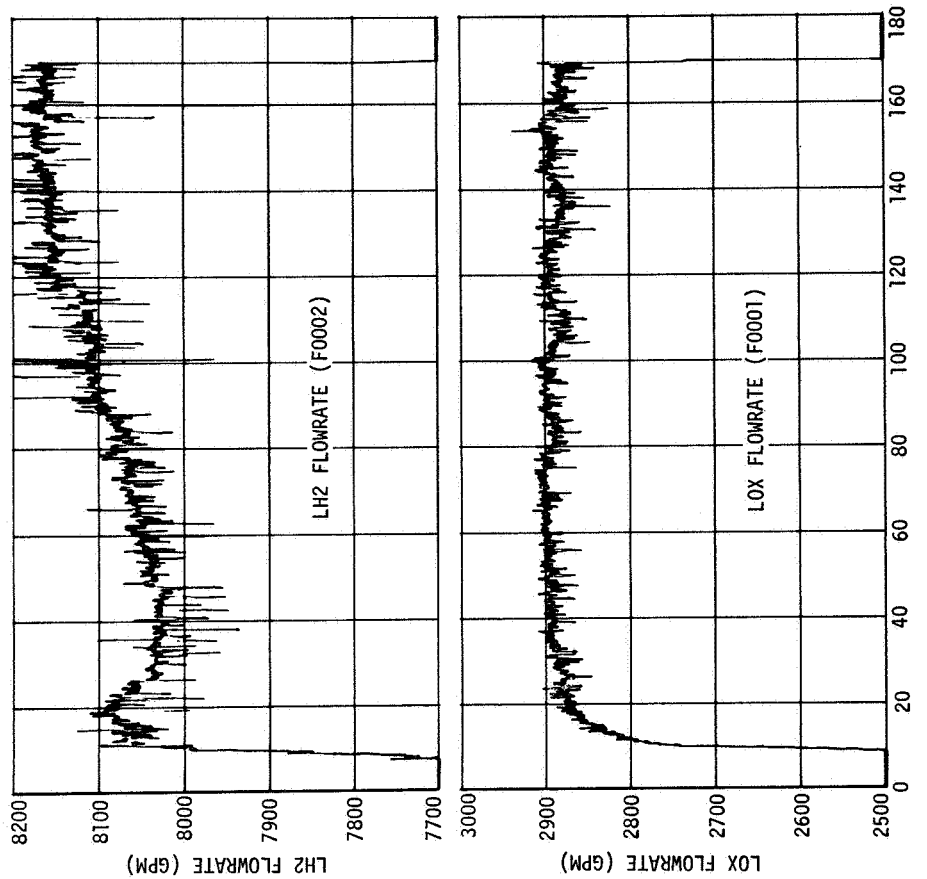

Figure 10-12. J-2 Engine Pump Flowrates - First Burn

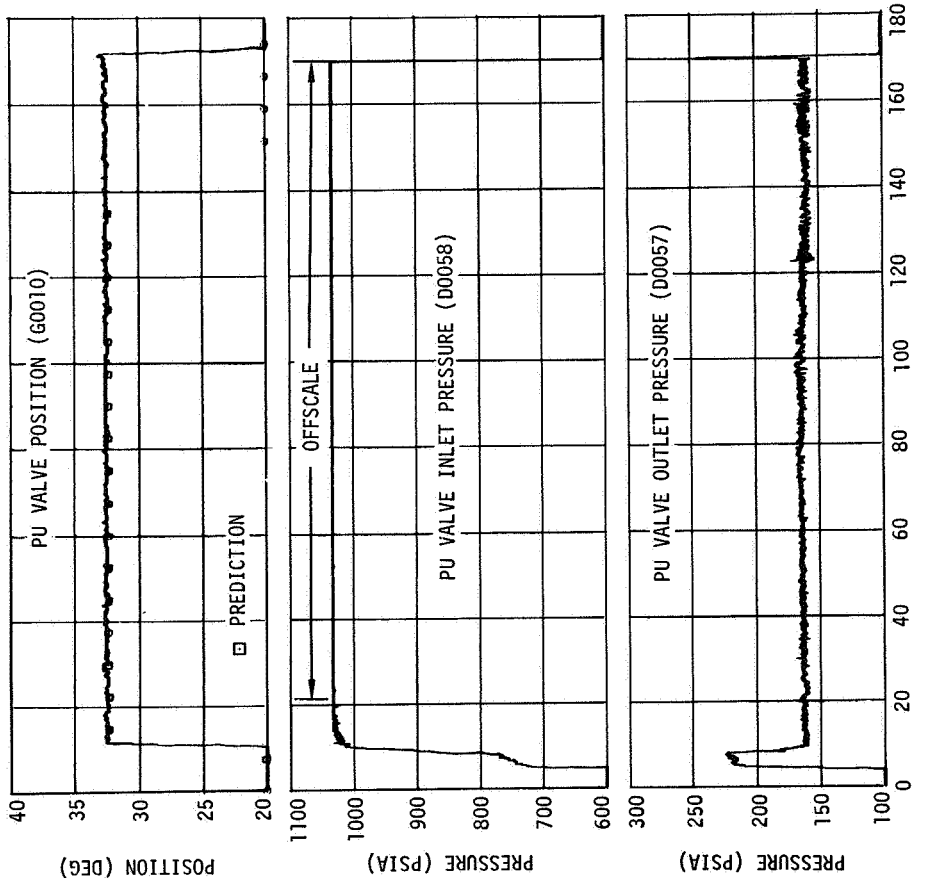

Figure 10-11. PU Valve Operation - First Burn

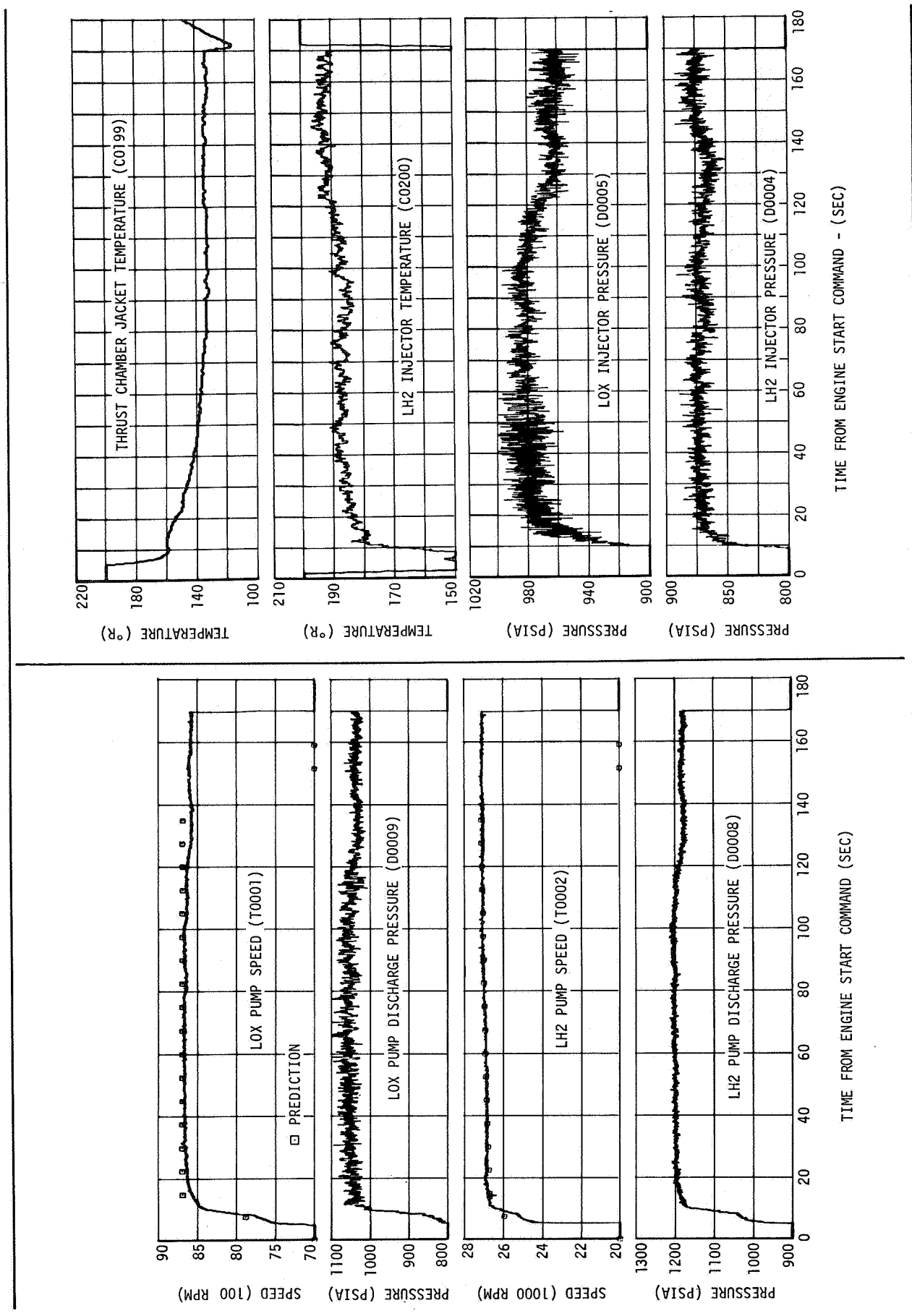

Figure 10-13. J-2 Engine Pump Operating Conditions - First Burn

Figure 10-14. J-2 Engine Injector Supply Conditions - First Burn

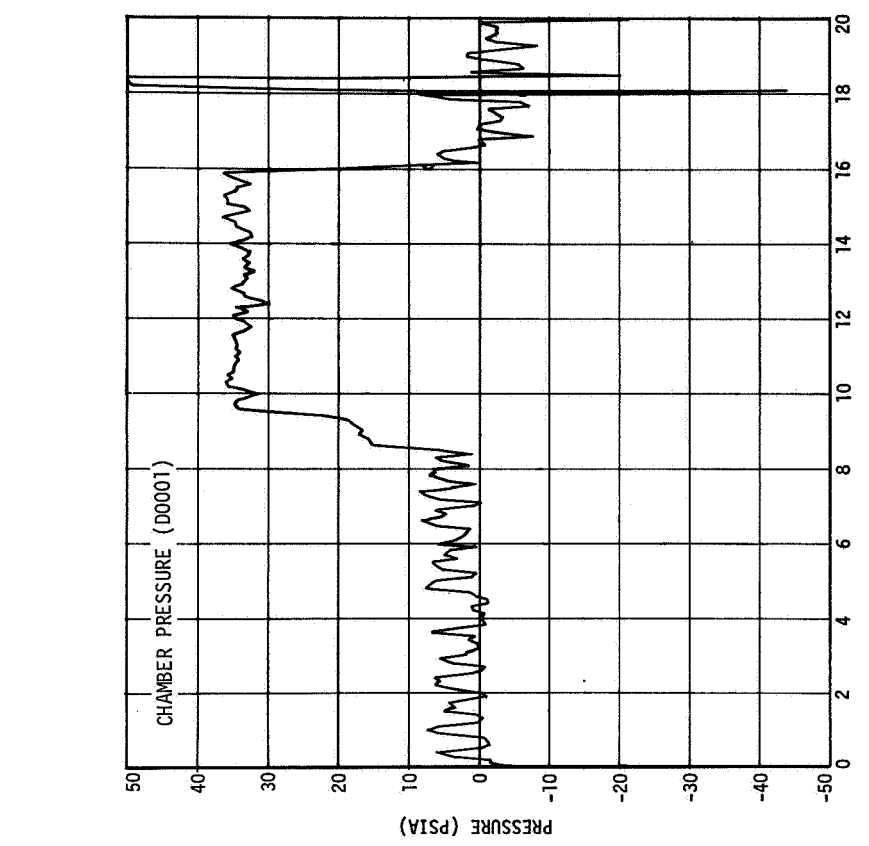

Figure 10-16. Engine Chamber Pressure - Second Burn

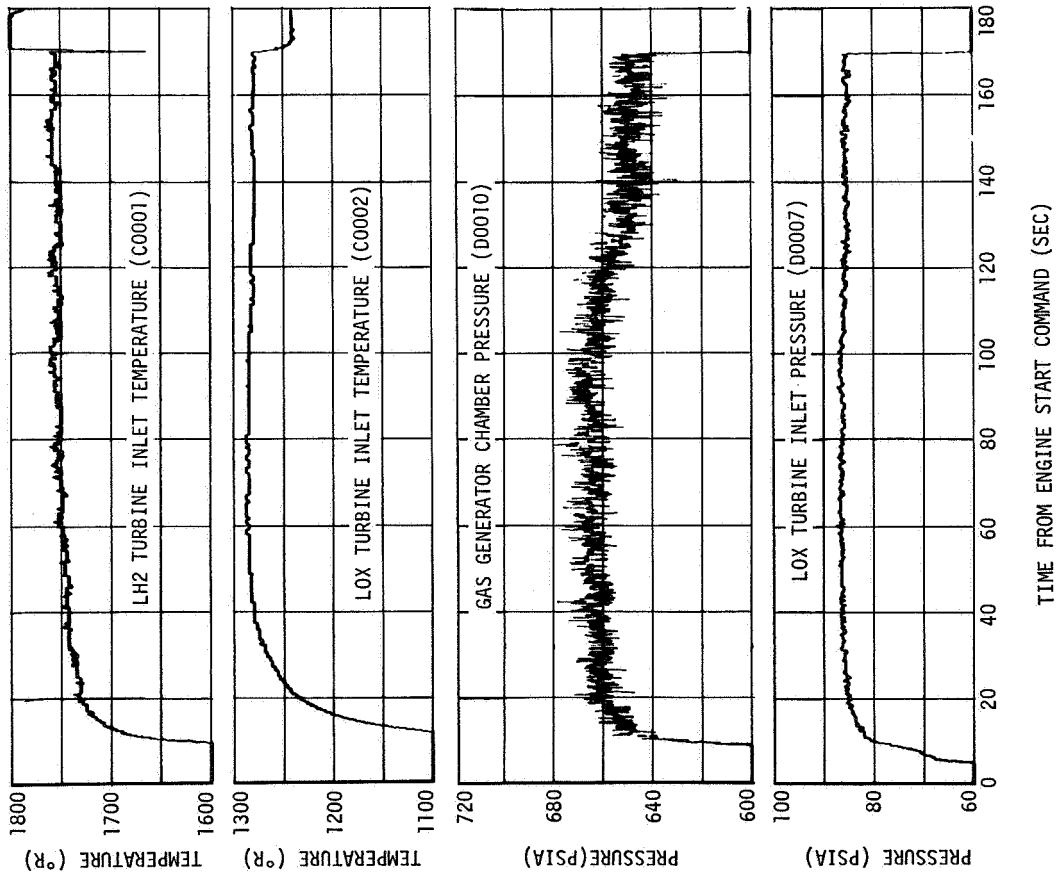

Figure 10-15. Turbine Inlet Operating Conditions - First Burn

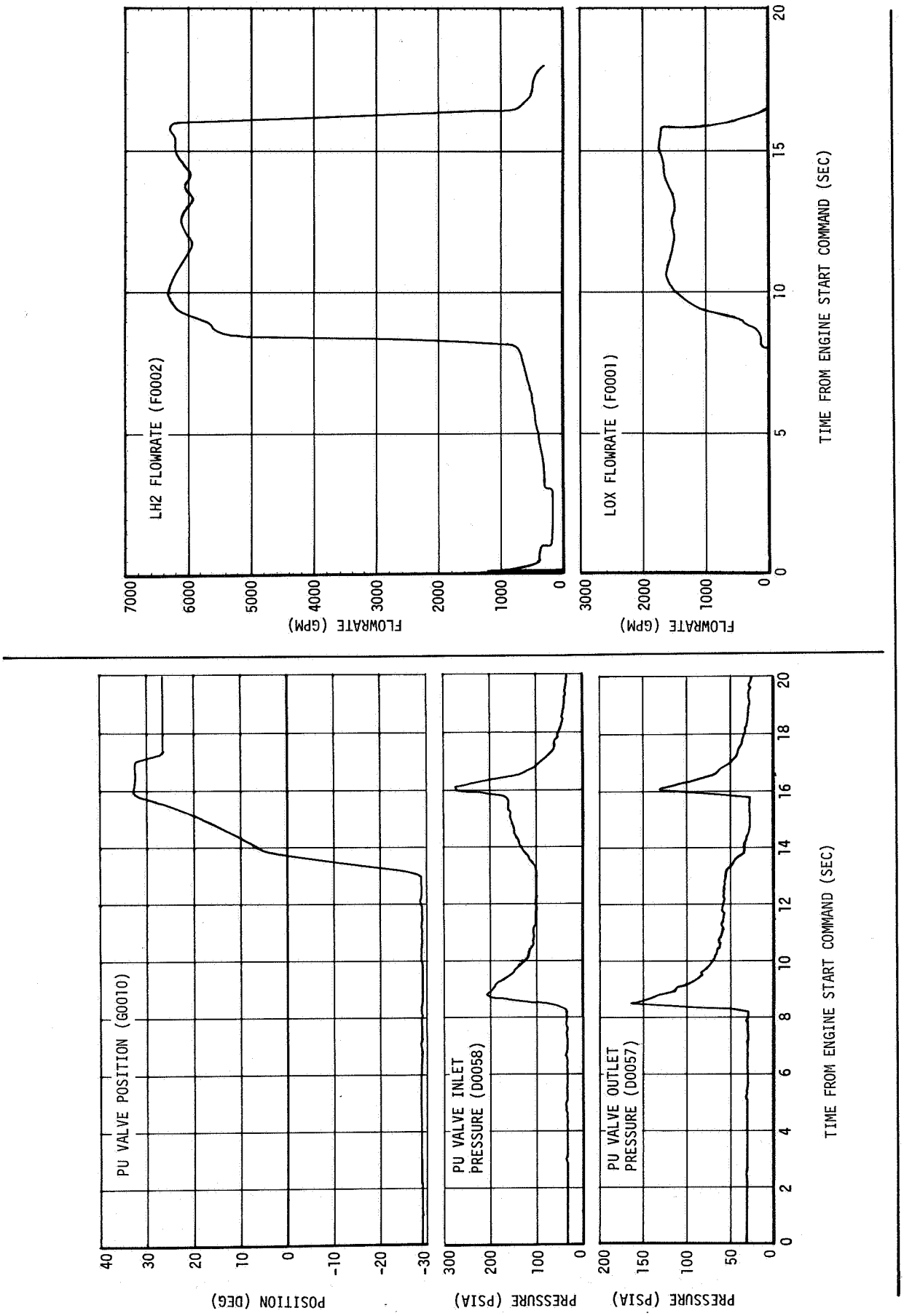

Figure 10-18. J-2 Engine Pump Flowrate - Second Burn

Figure 10-17. PU Valve Operation - Second Burn

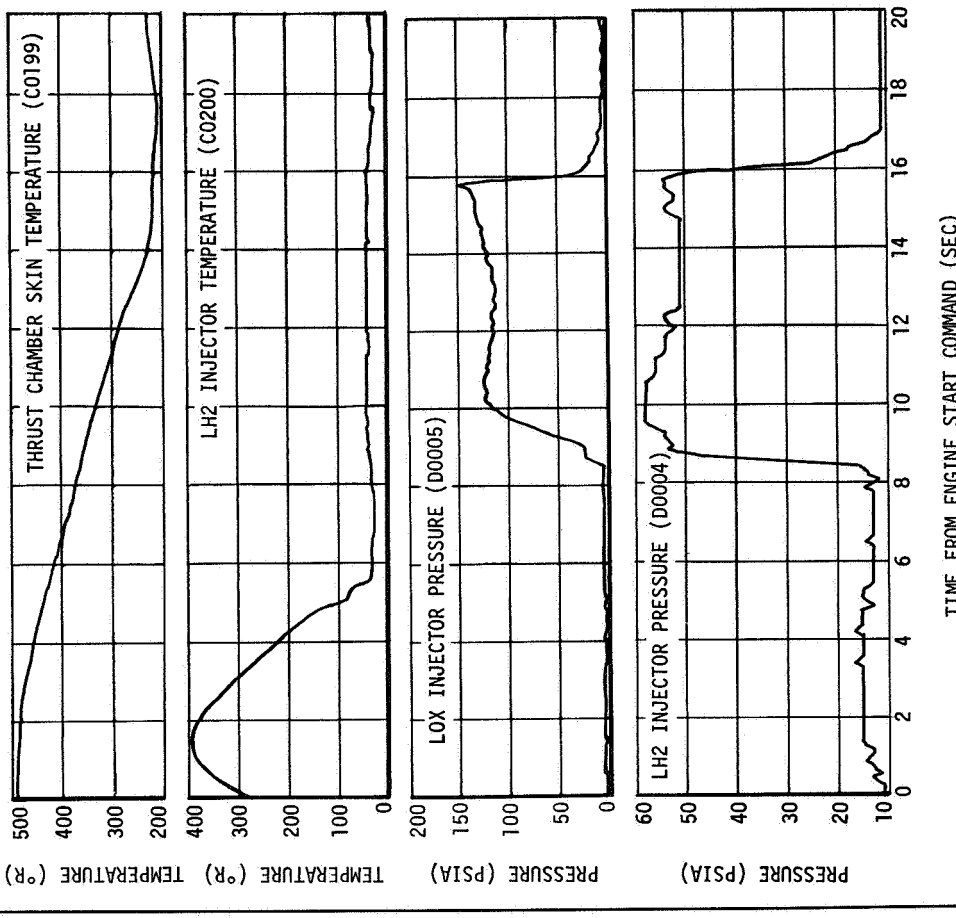

Figure 10-20. J-2 Engine Injector Supply Conditions - Second Burn

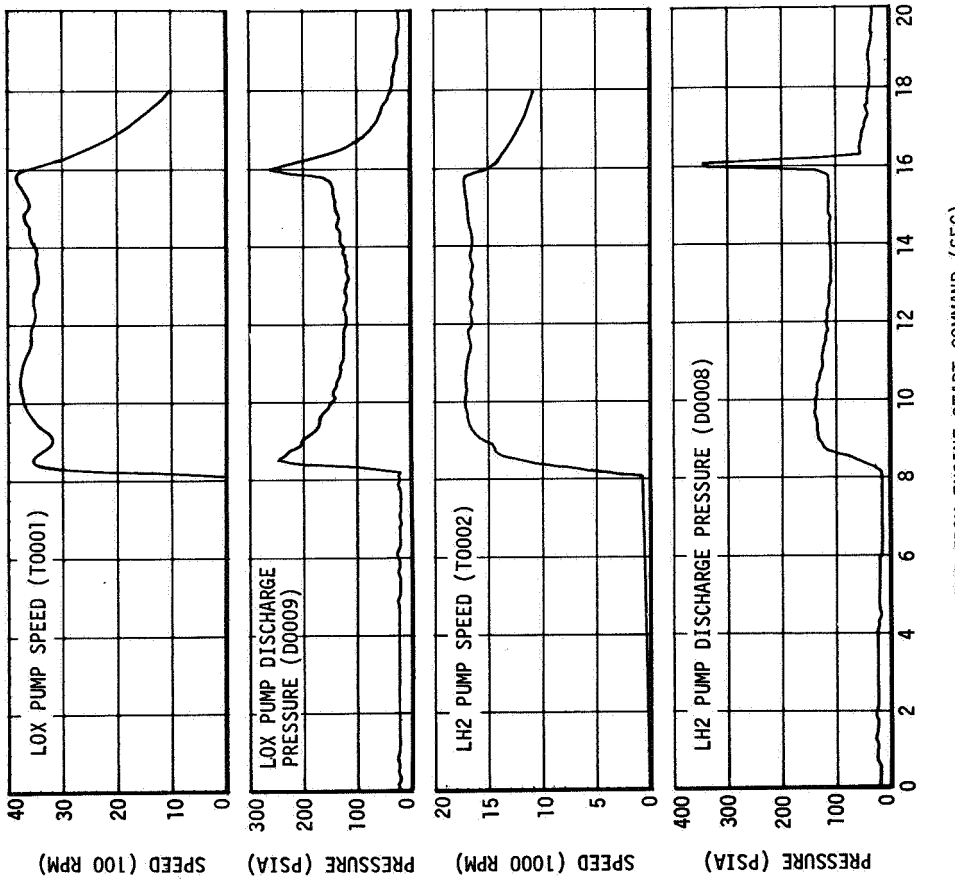

Figure 10-19. J-2 Engine Pump Operating Conditions - Second Burn

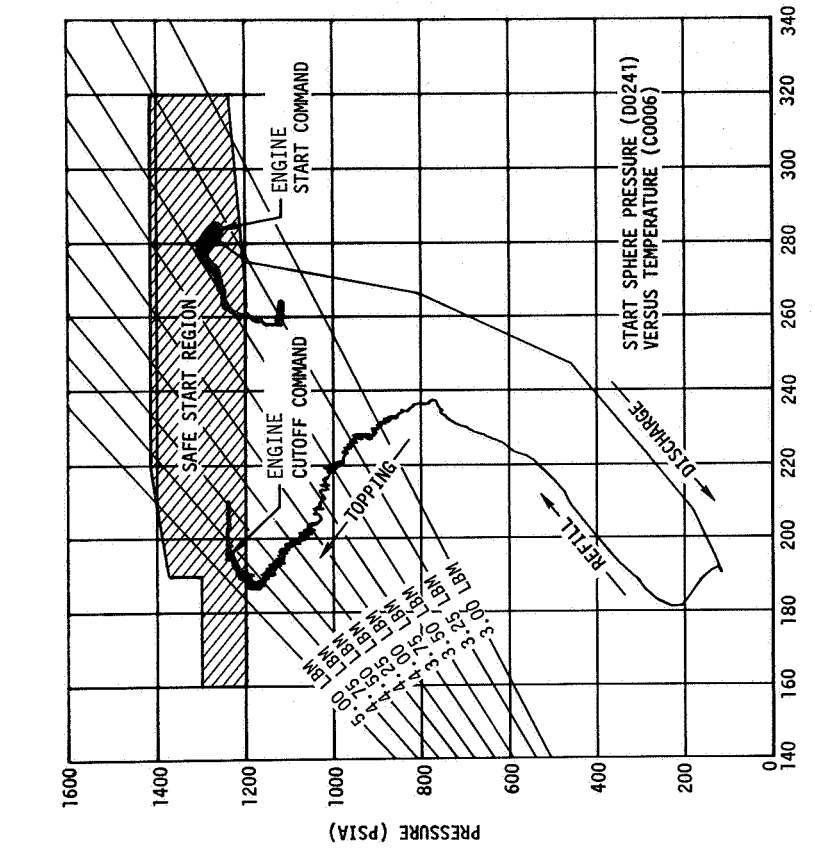

Figure 10-22. Start Sphere Refill Performance - First Burn

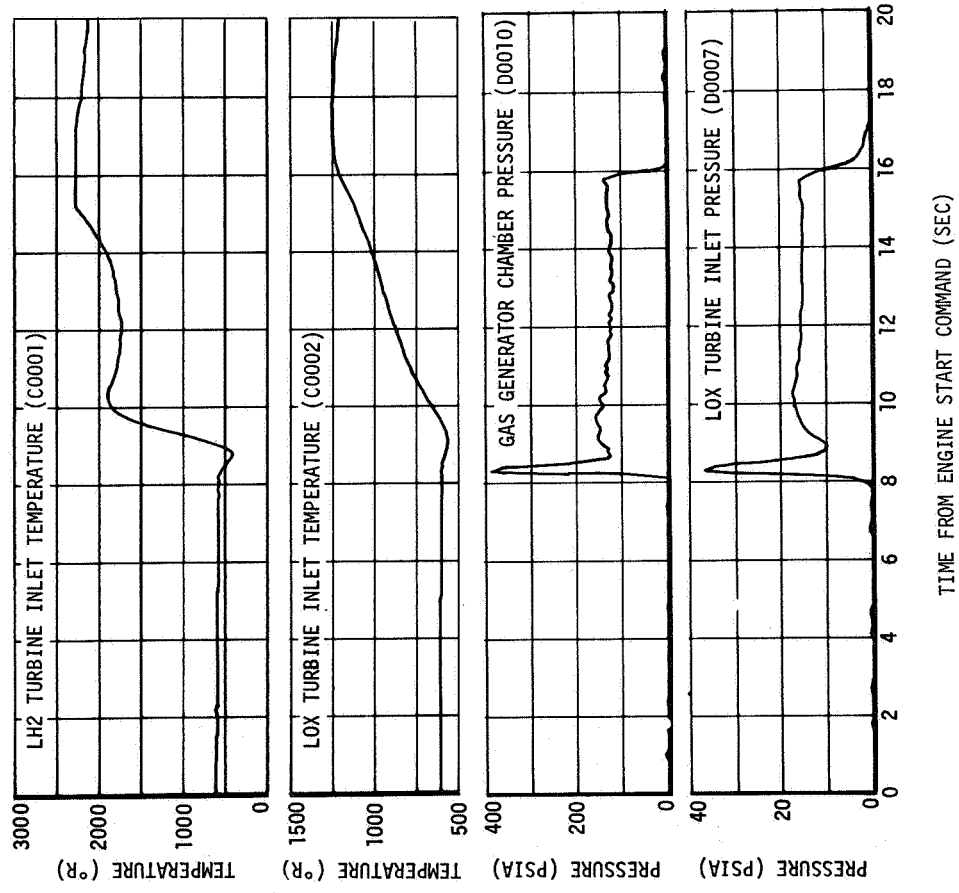

Figure 10-21. Turbine Inlet Operating Conditions - Second Burn

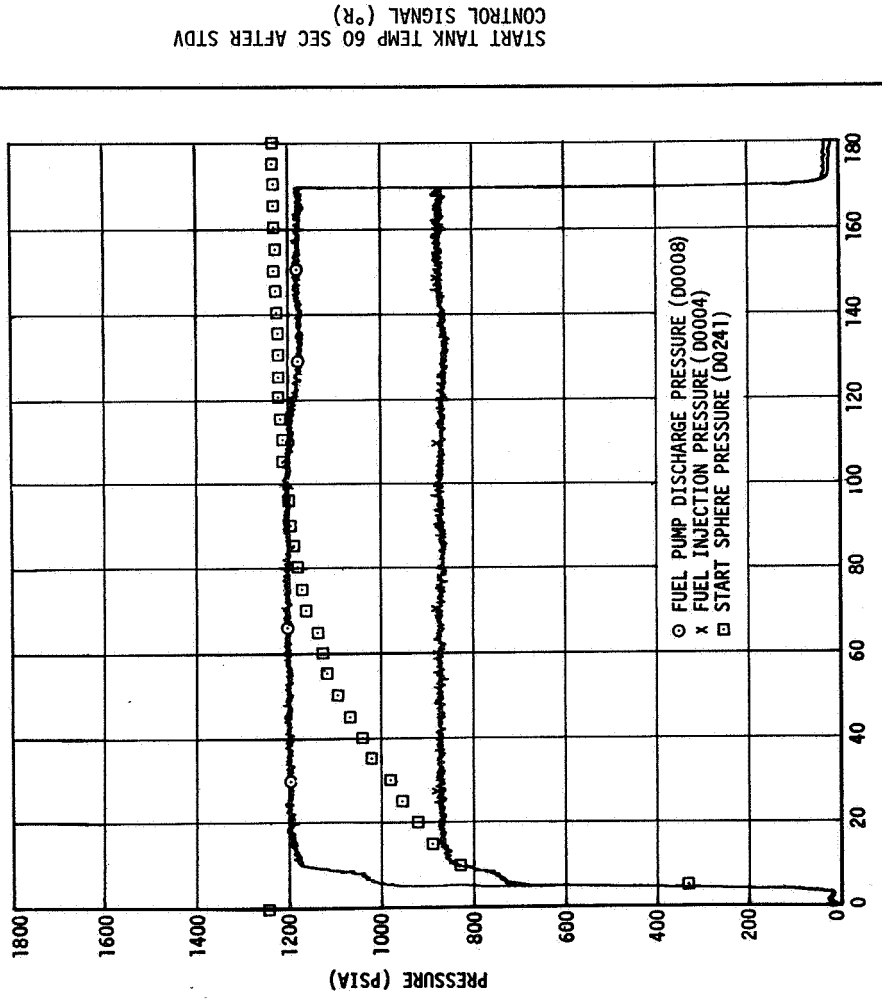

Figure 10-23. Start Sphere Refill

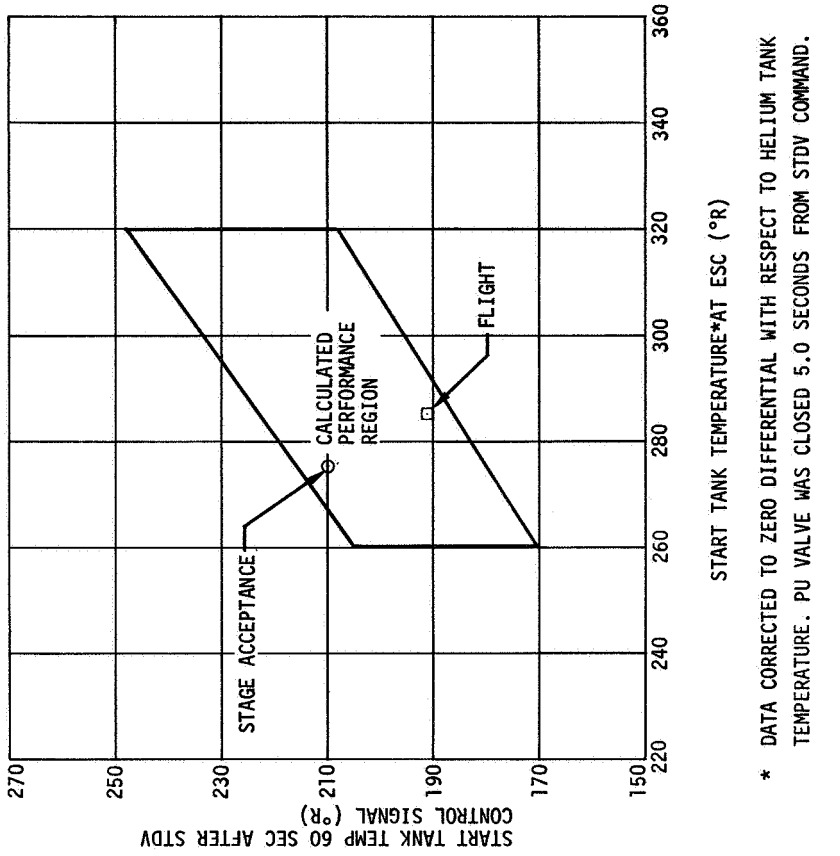

Figure 10-24. Start Tank Recharge Capability

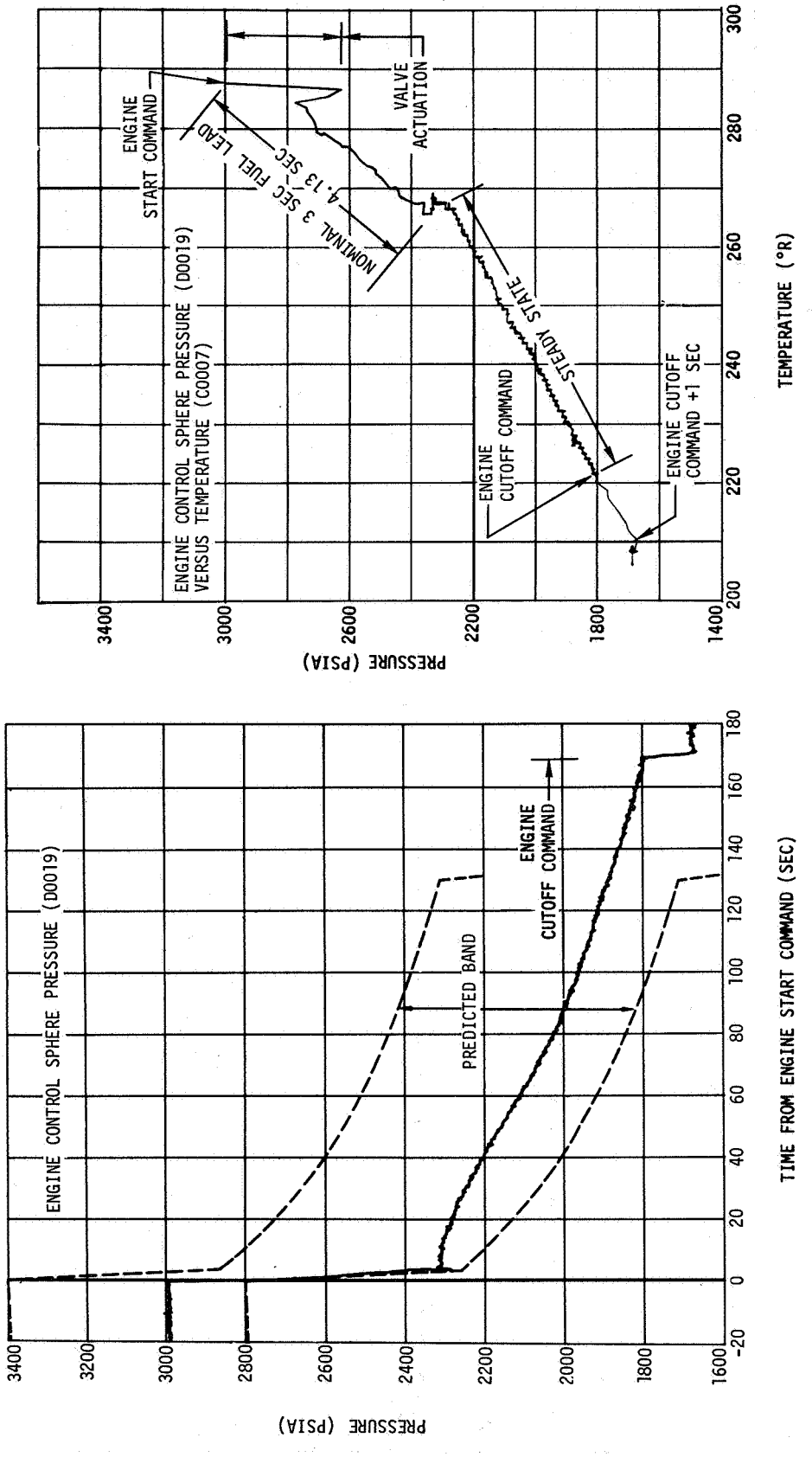

Figure 10-25. Engine Control Sphere Conditions - First Burn

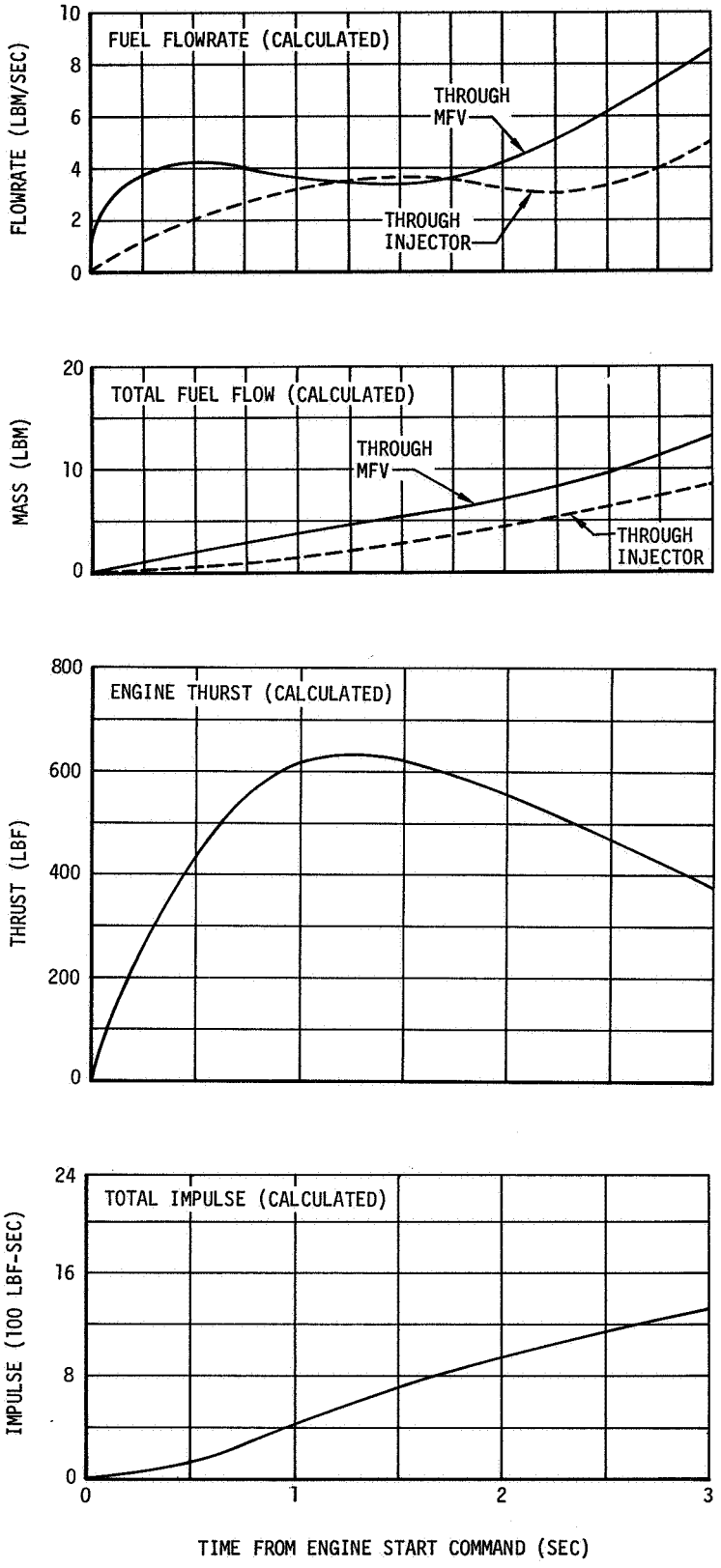

Figure 10-26. Fuel Lead Conditions - First Burn

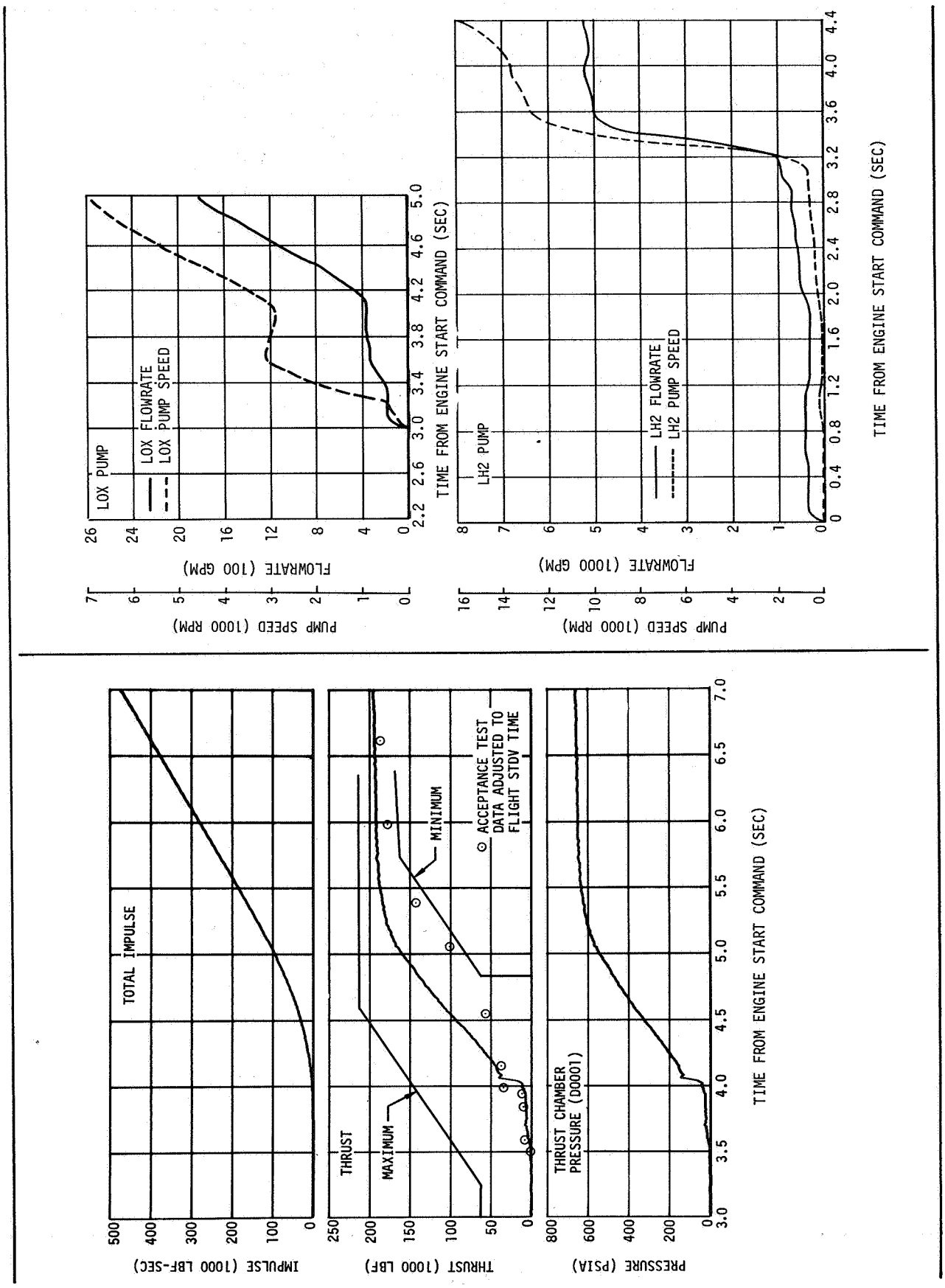

Figure 10-28. LOX and LH2 Pump Performance - First Burn

Figure 10-27. Engine Start Transient Characteristics - First Burn

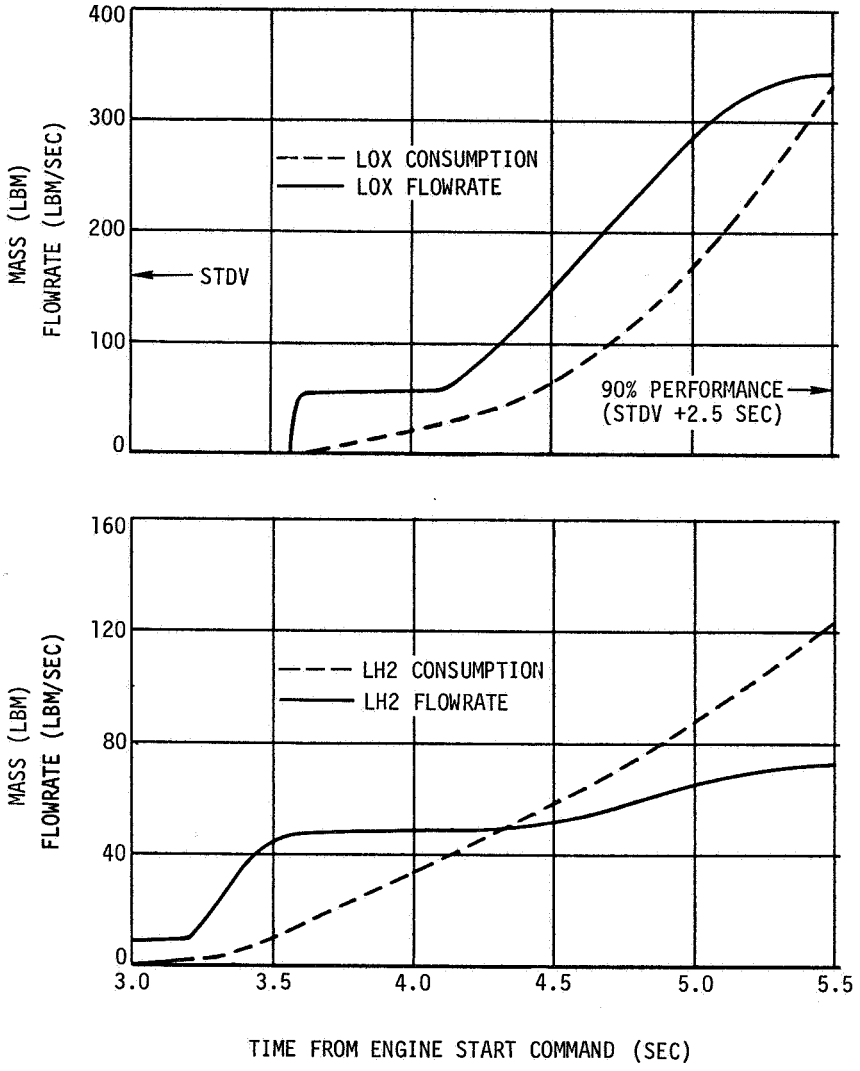

Figure 10-29. LOX and LH2 Consumption - First Burn Start Transient

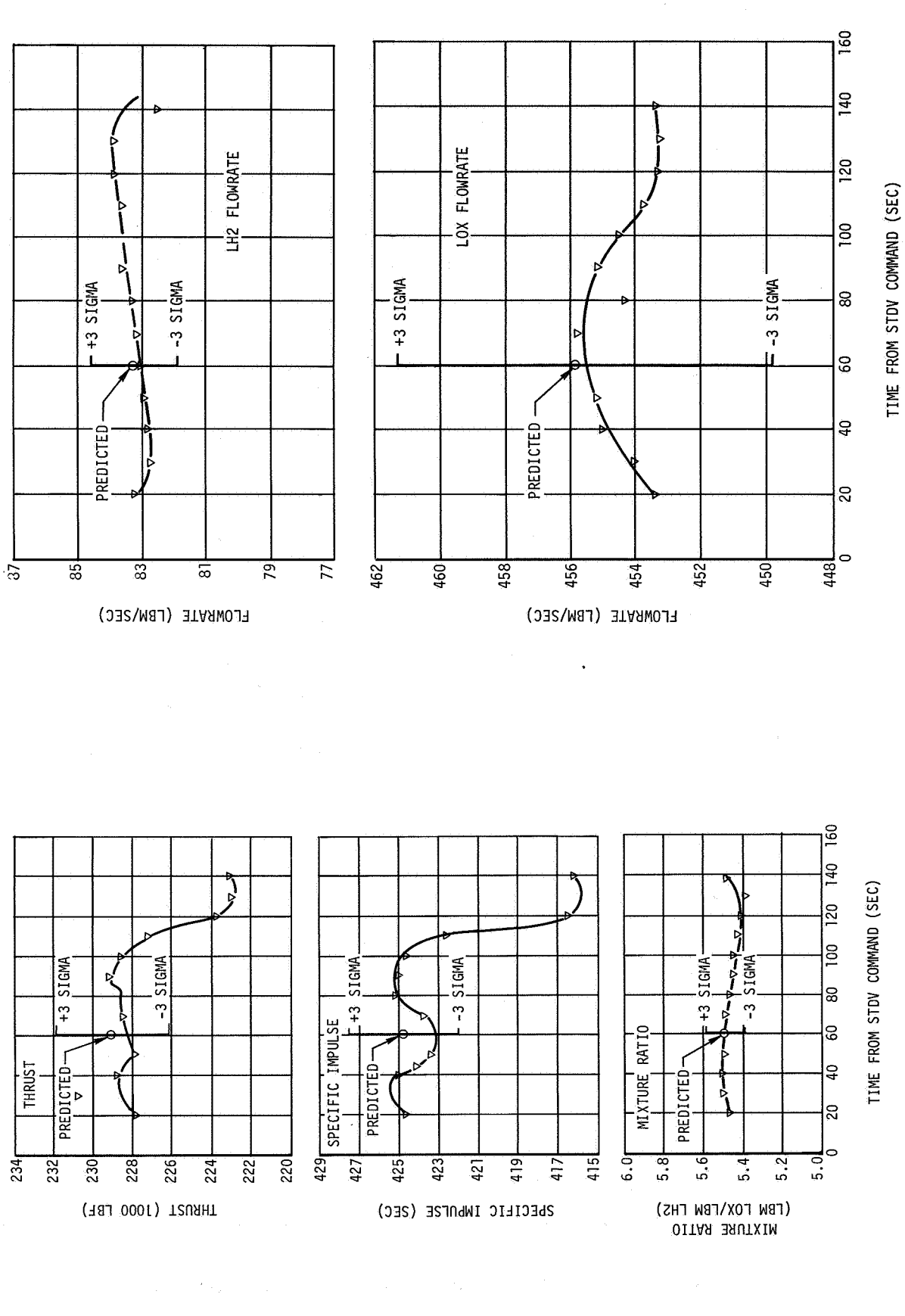

Figure 10-30. First Burn Engine Tag Values at Standard Altitude Conditions

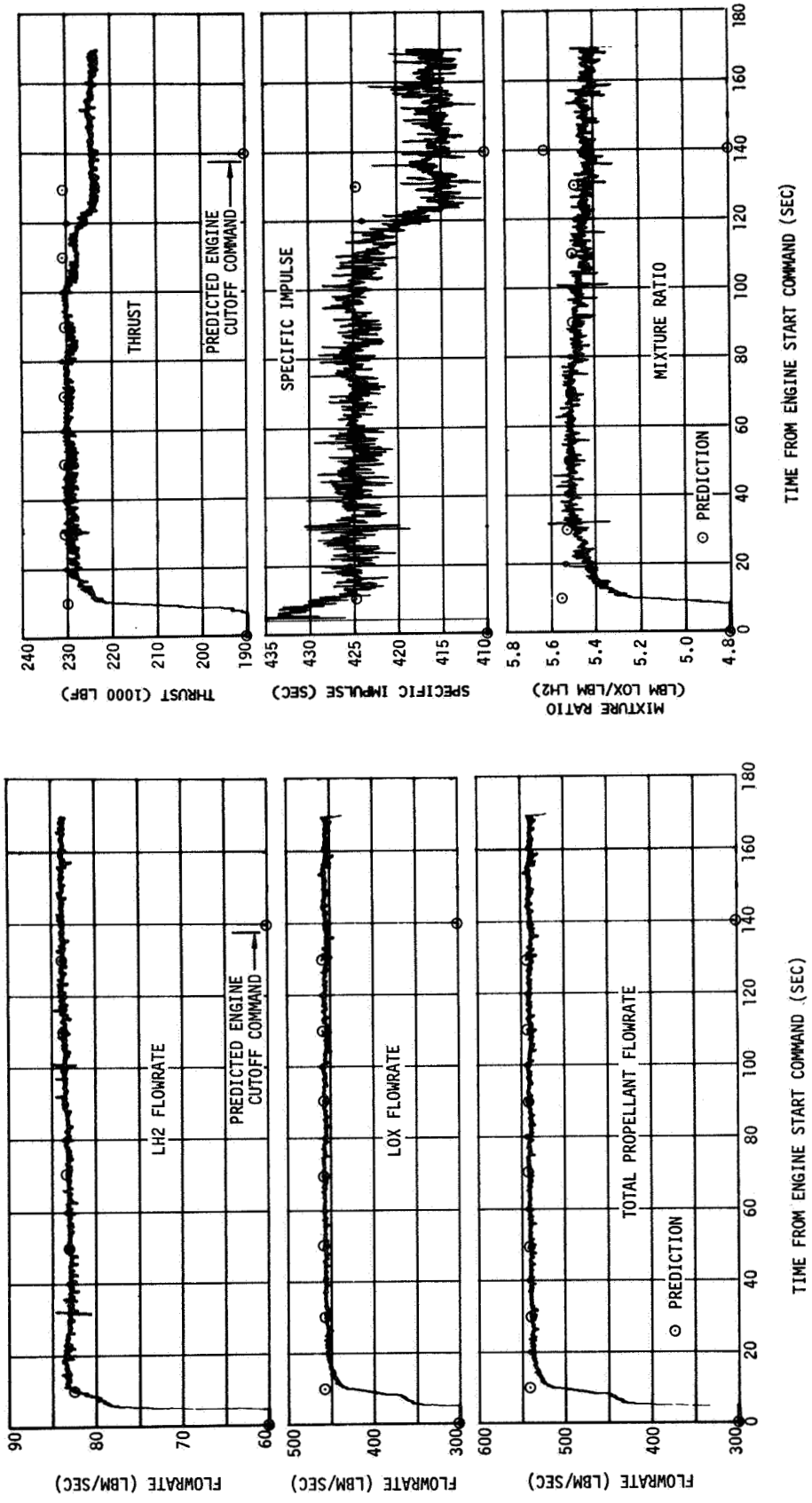

Figure 10-31. Engine Steady-State Performance - First Burn (Sheet 1 of 2)

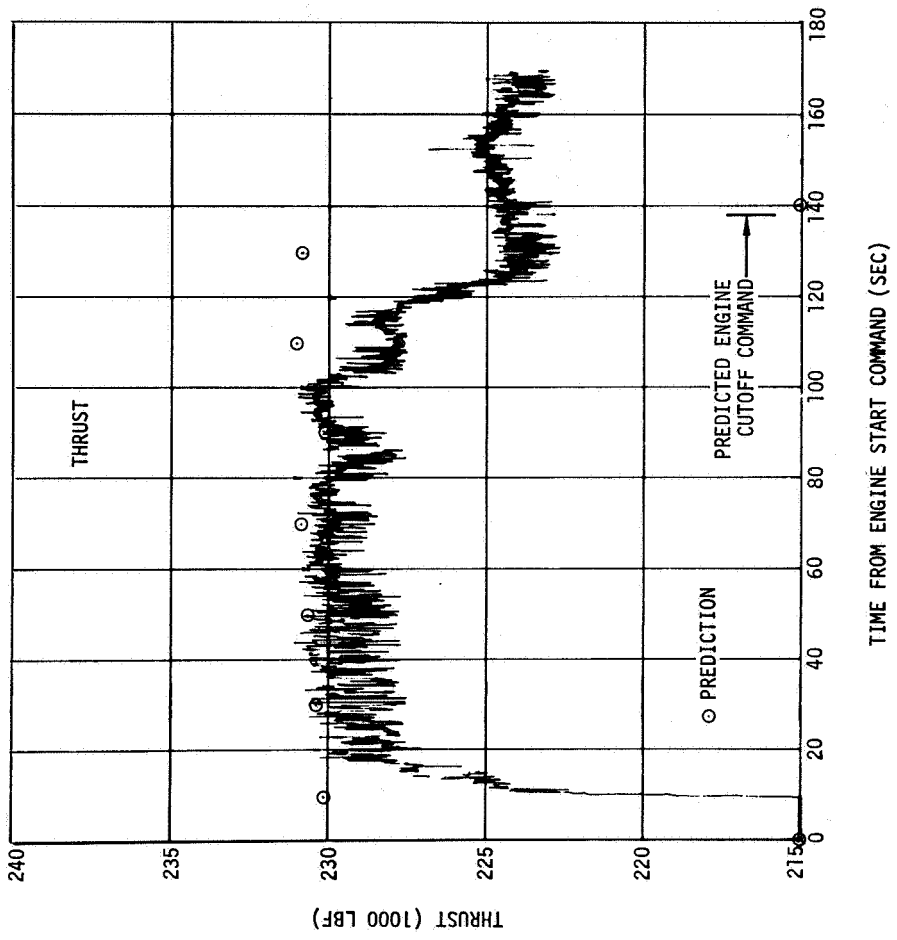

Figure 10-31. Engine Steady-State Performance - First Burn (Sheet 2 of 2)

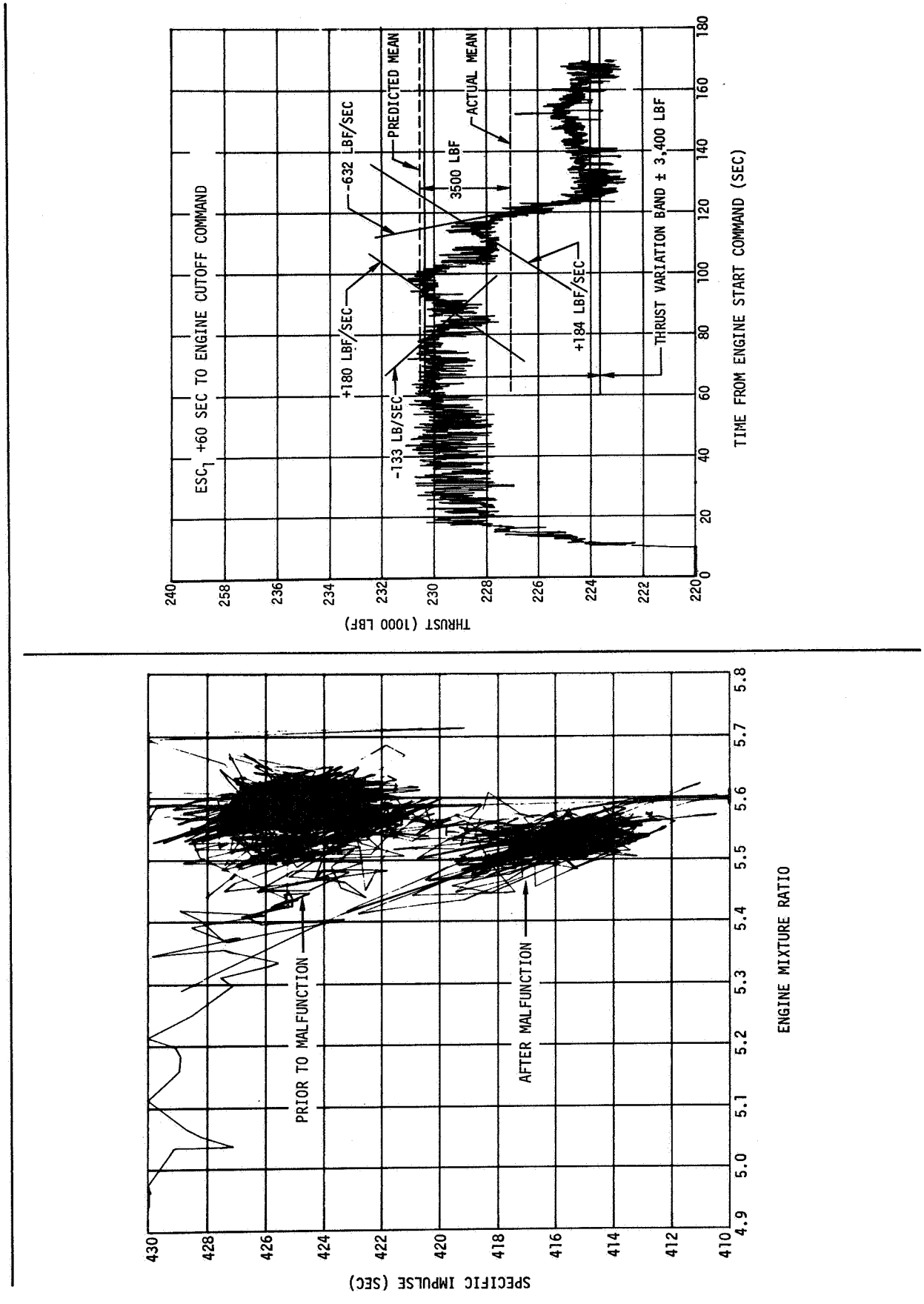

Figure 10-33. Thrust Variation - First Burn

Figure 10-32. Specific Impulse Versus Engine Mixture Ratio - First Burn

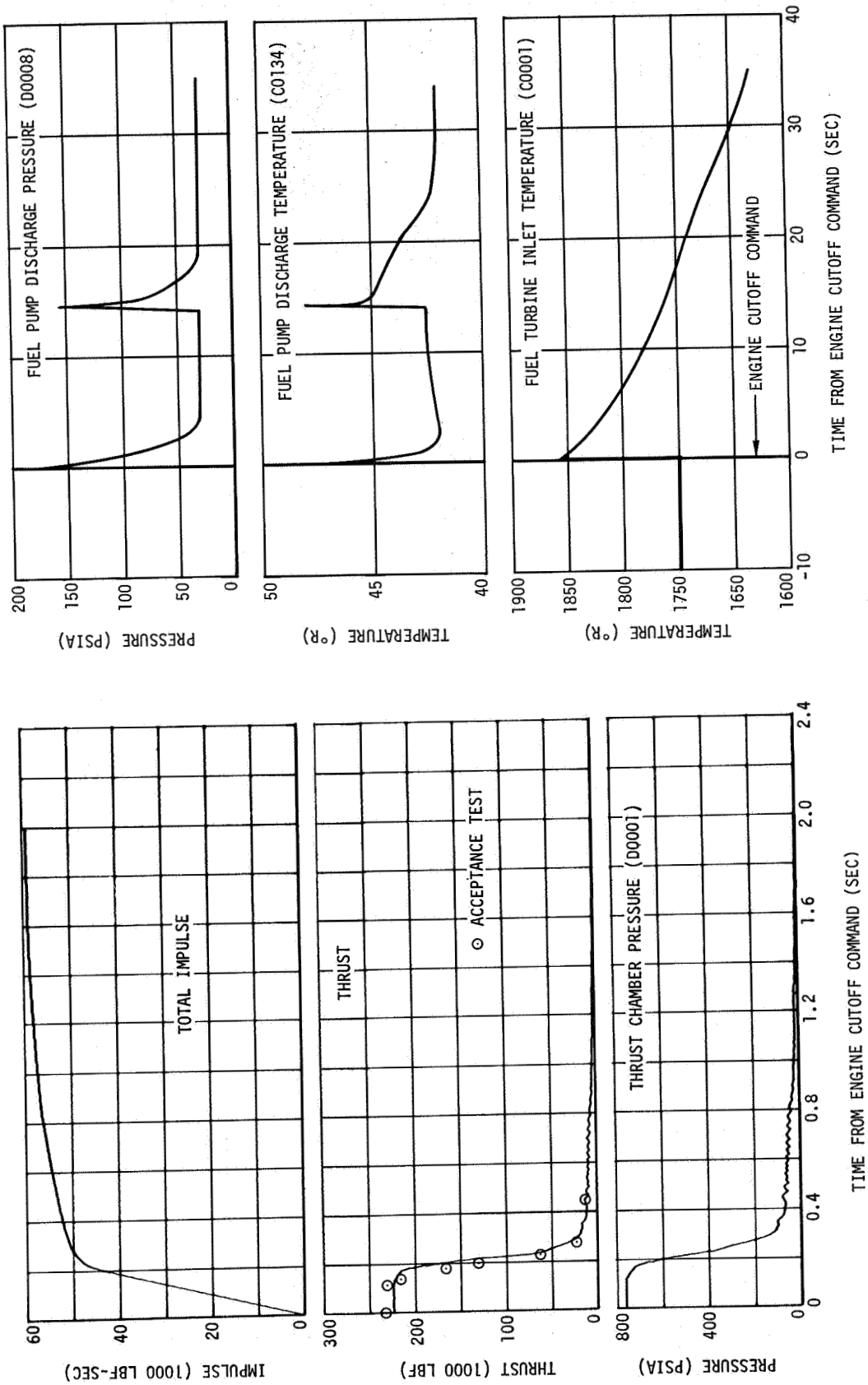

Figure 10-34. Engine Cutoff Transient Characteristics - First Burn

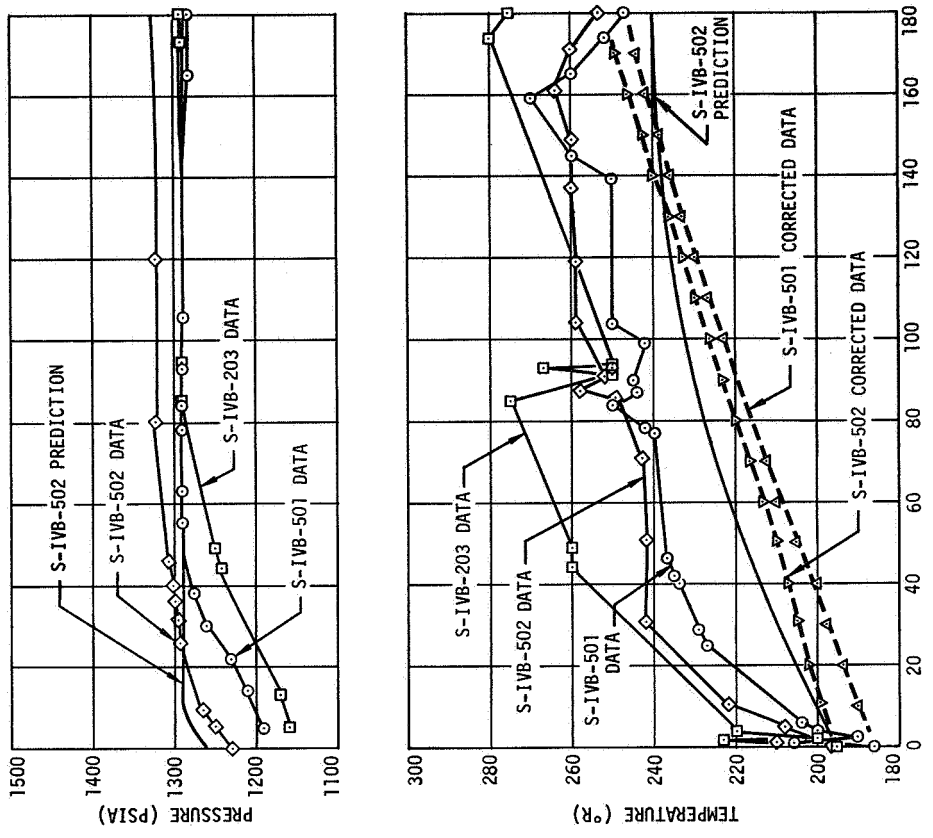

Figure 10-36. Start Sphere Conditions - First and Second Orbits

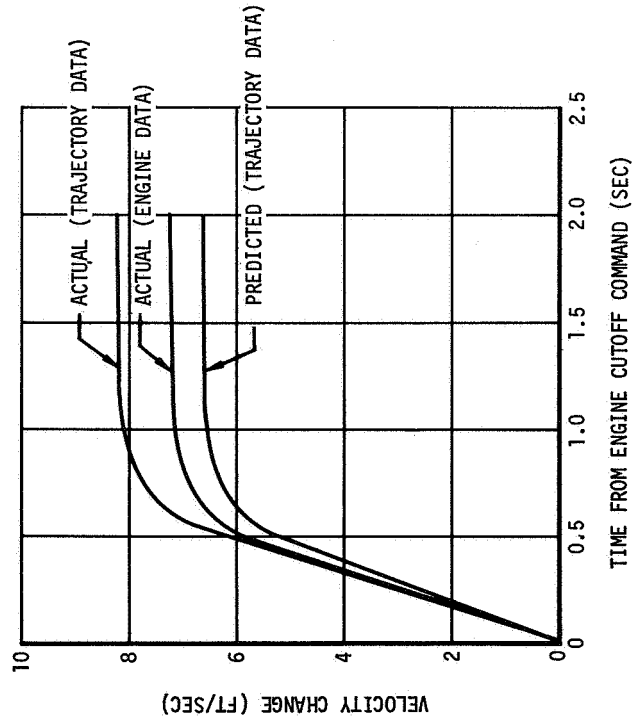

Figure 10-35. Change in Velocity Due to Cutoff Impulse - First Burn

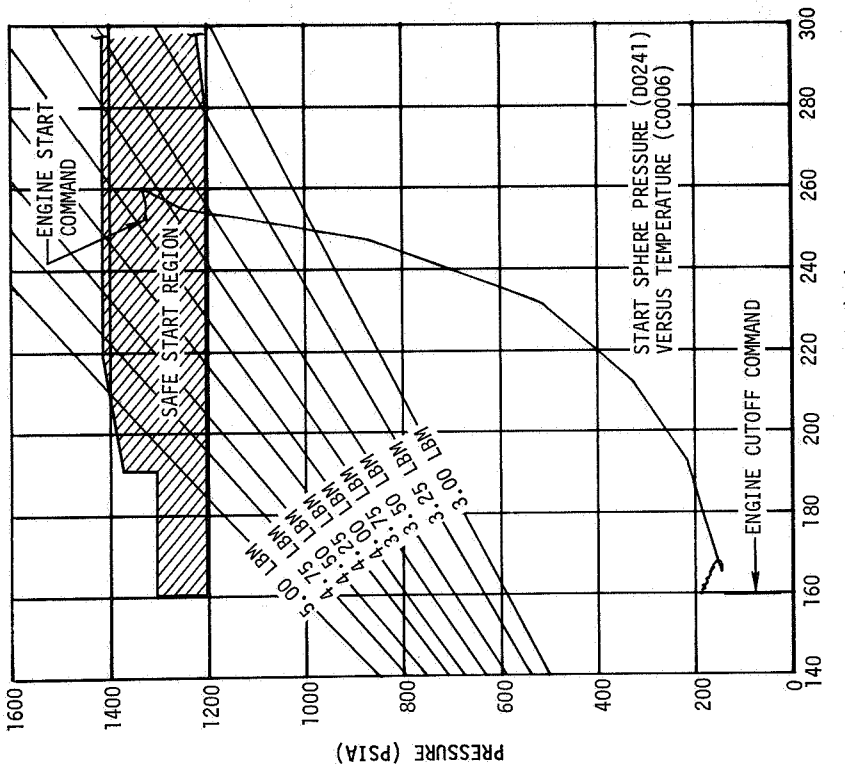

Figure 10-38. Start Sphere Blowdown - Second Burn

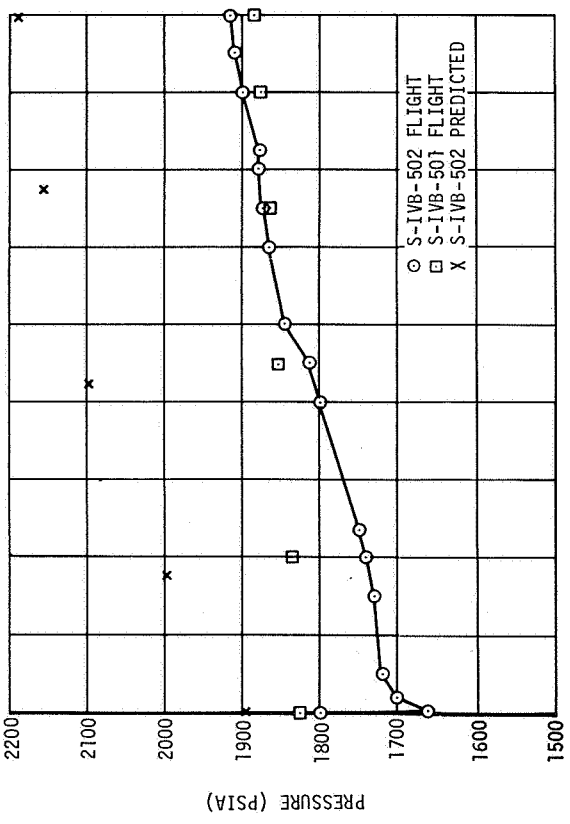

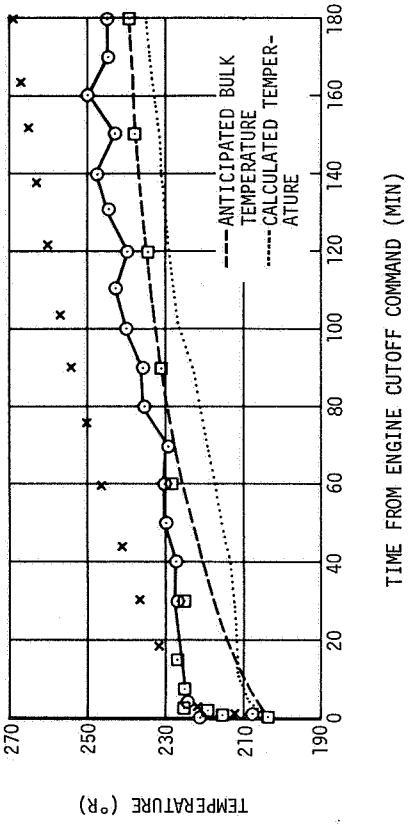

Figure 10-37. Engine Control Sphere Performance - First and Second Orbit

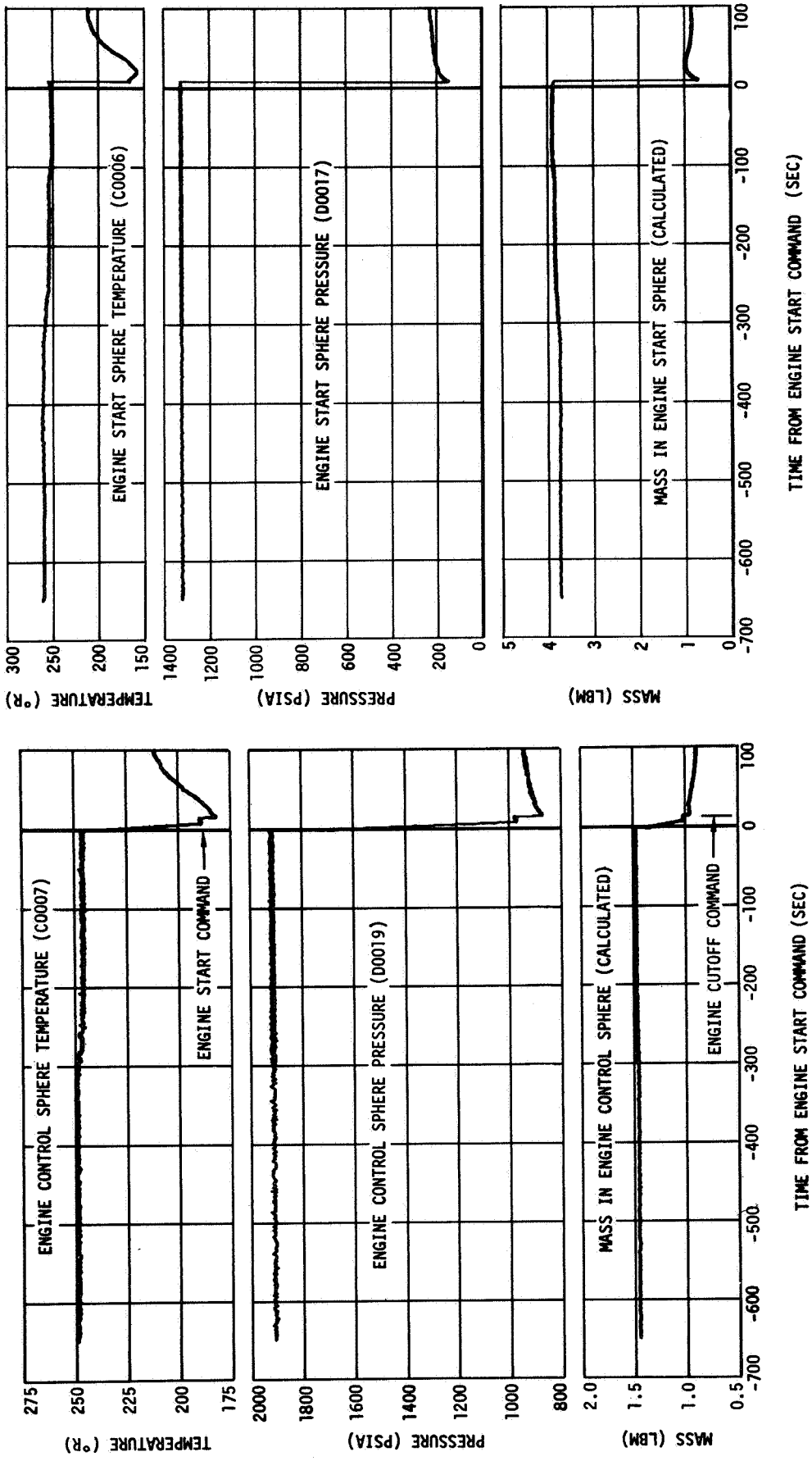

Figure 10-39. Engine Start and Control Sphere Operation - Second Burn

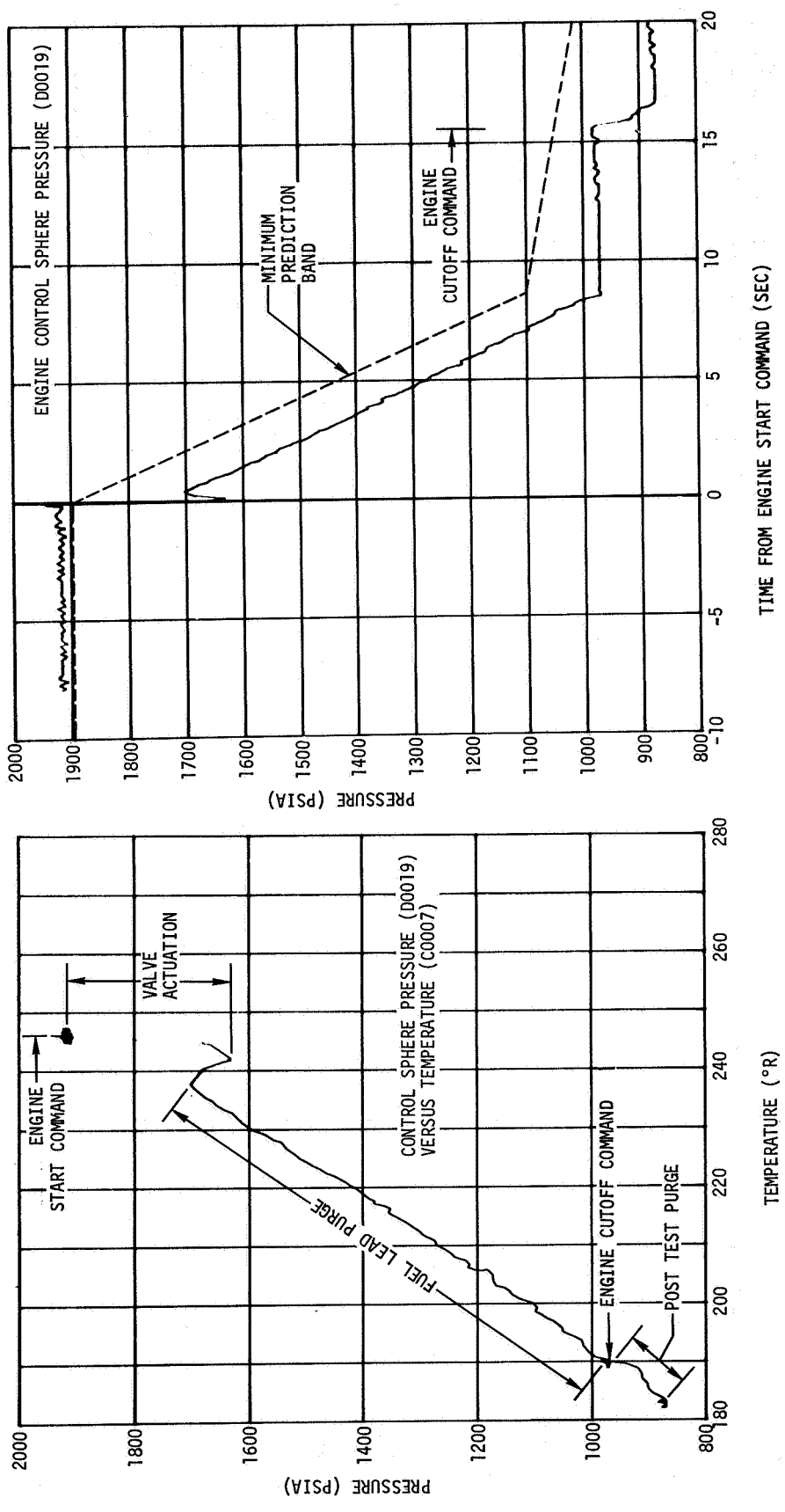

Figure 10-40. Control Sphere Performance - Second Burn

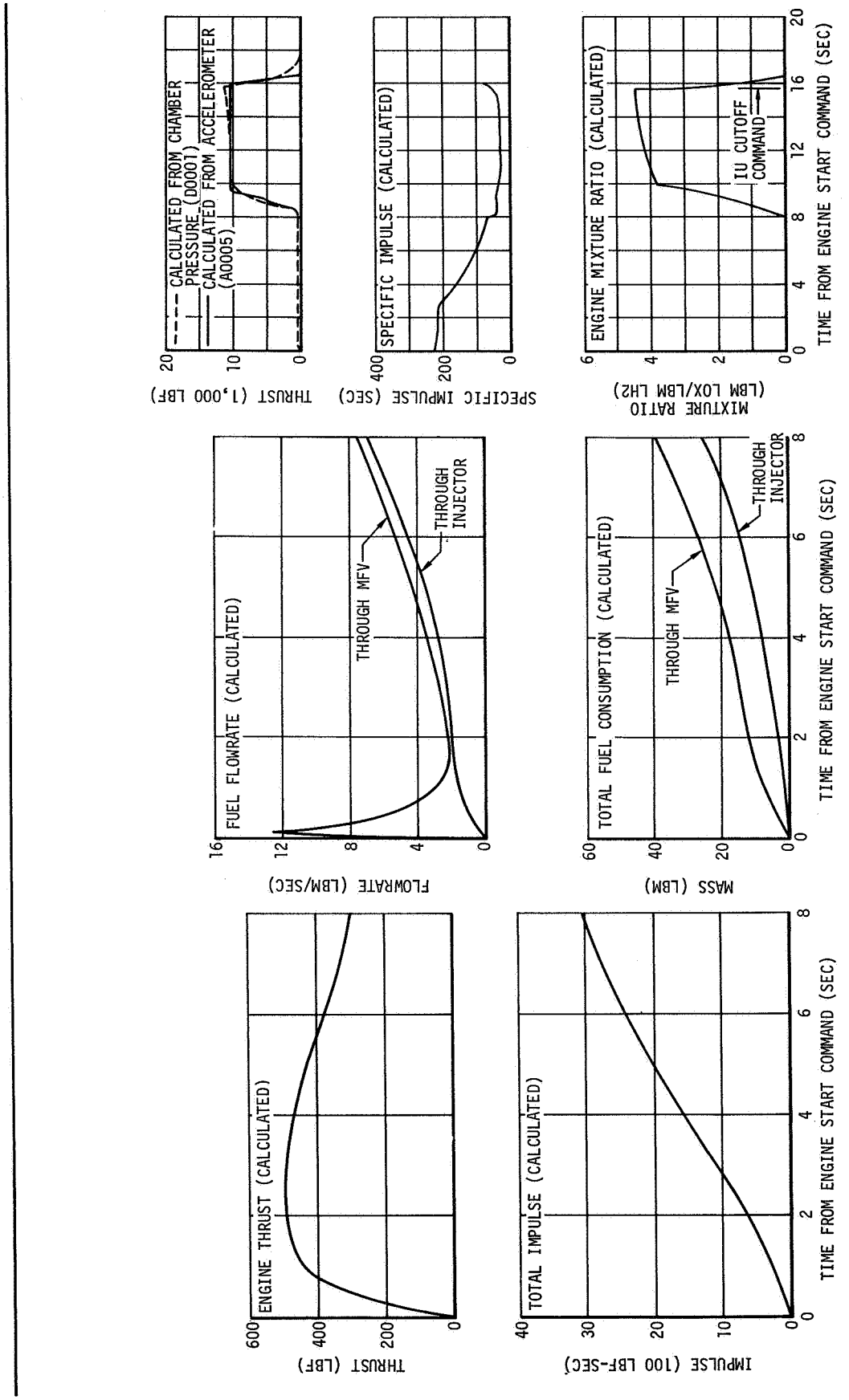

Figure 10-41. Engine Performance During Attempted Second Burn

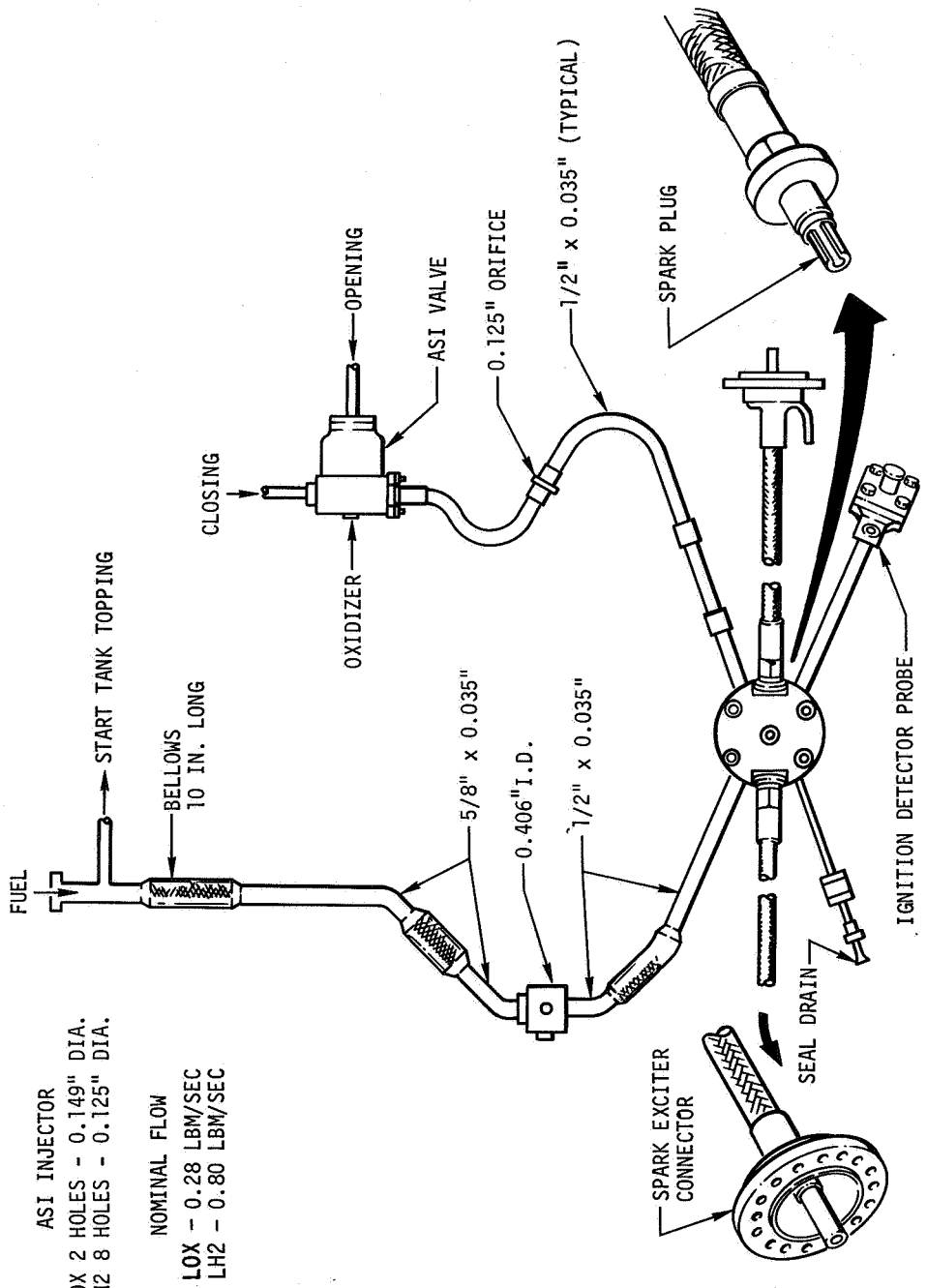

Figure 10-42. ASI Ignition System Schematic

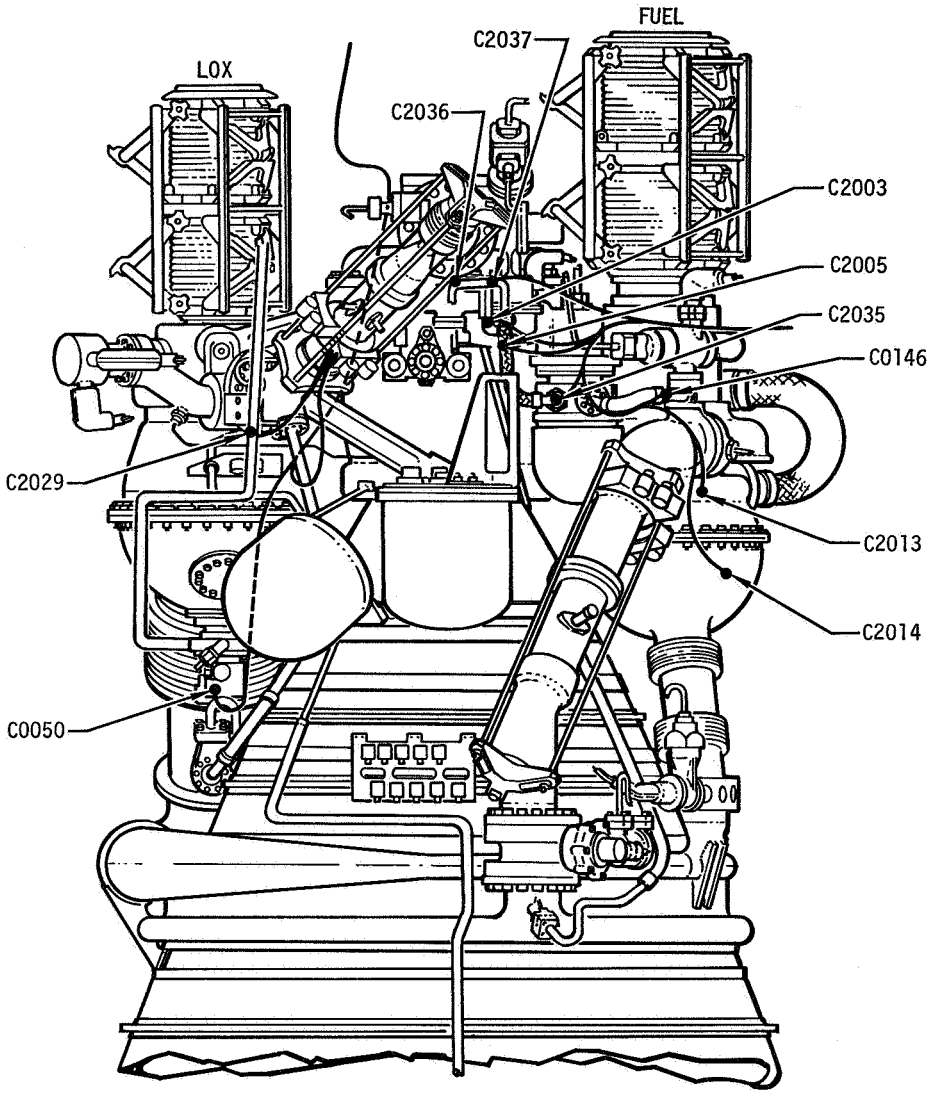

Figure 10-43. Engine Area Transducer Locations (Sheet 1 of 3)

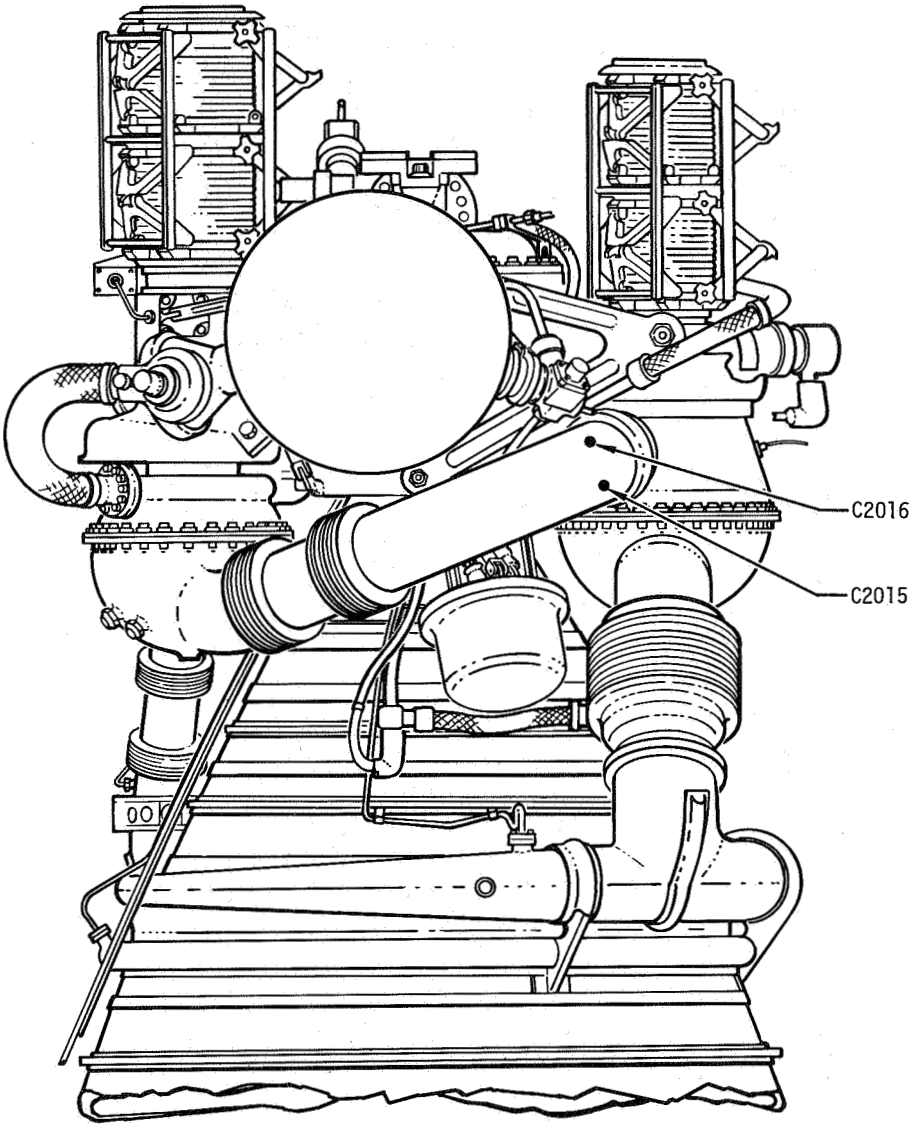

Figure 10-43. Engine Area Transducer Locations (Sheet 2 of 3)

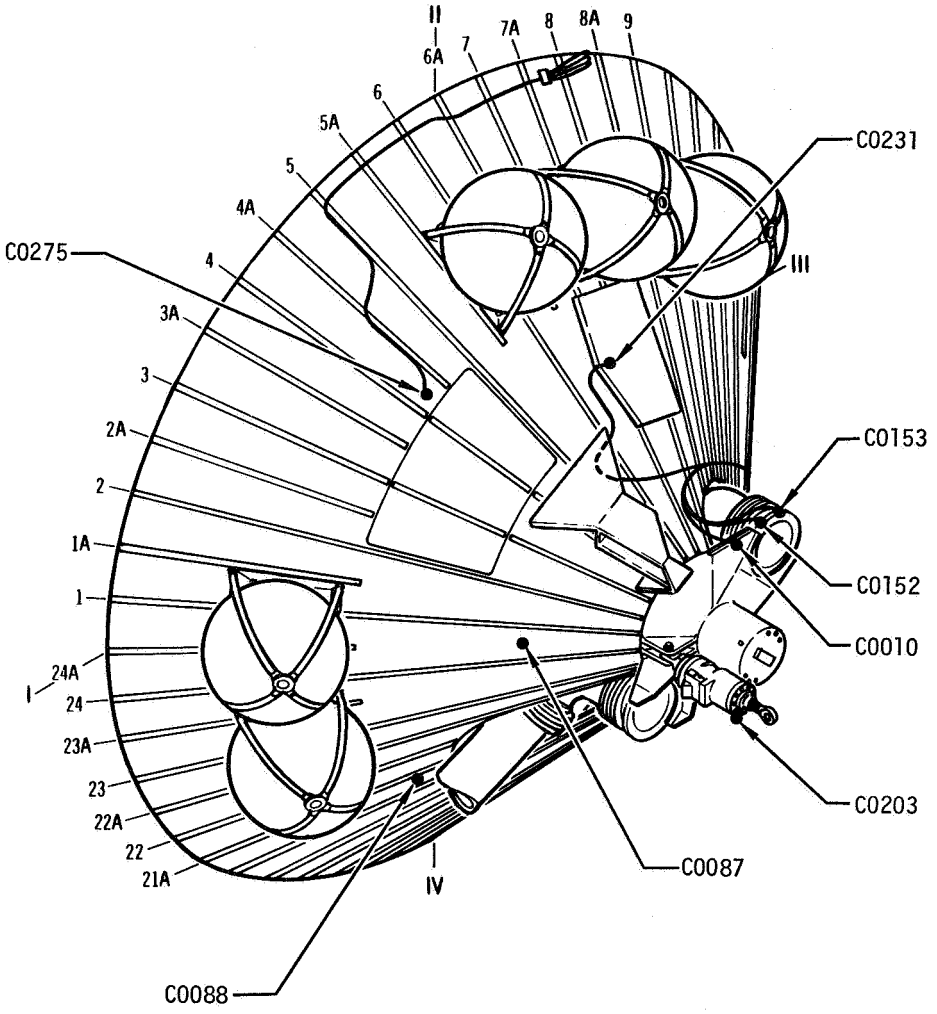

Figure 10-43. Engine Area Transducer Locations (Sheet 3 of 3)

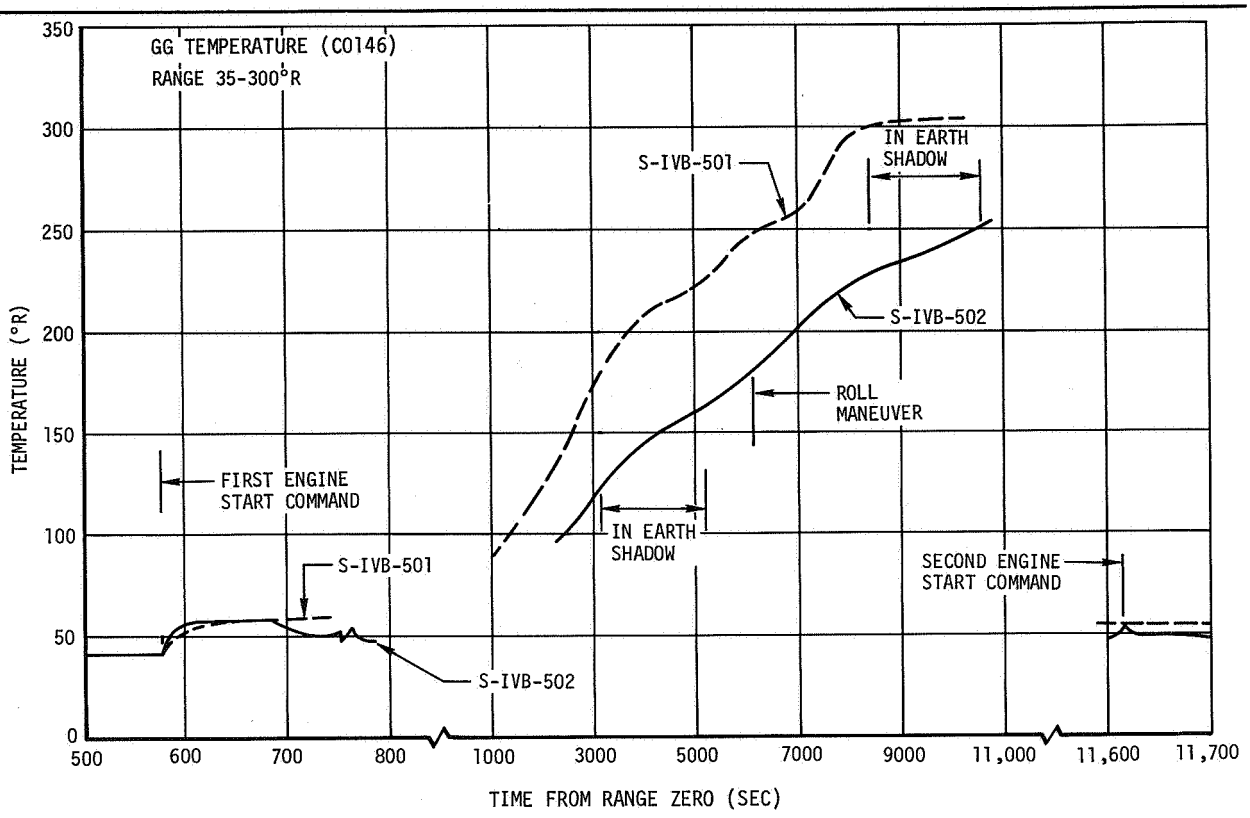

Figure 10-44. Gas Generator LH2 Inlet Line Wall Temperature

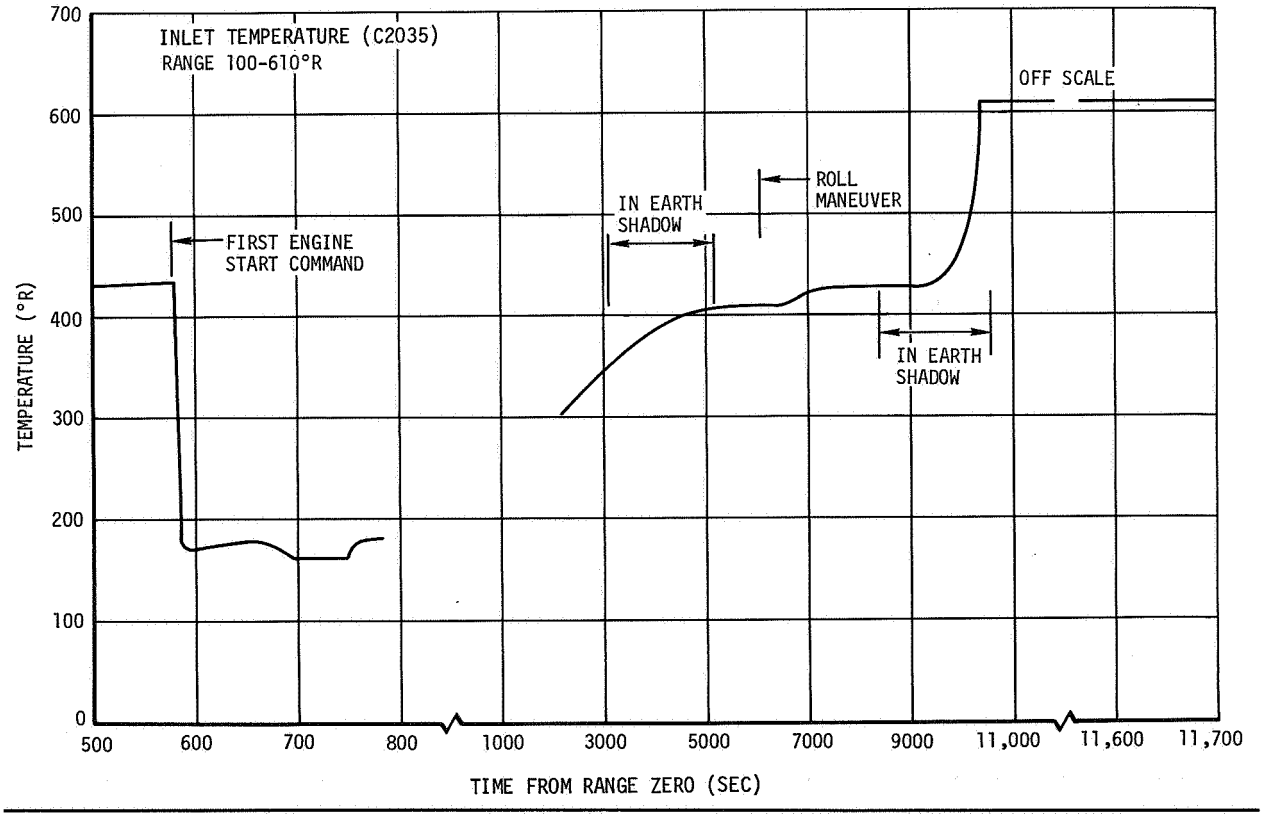

Figure 10-45. Gas Generator LOX Inlet Temperature

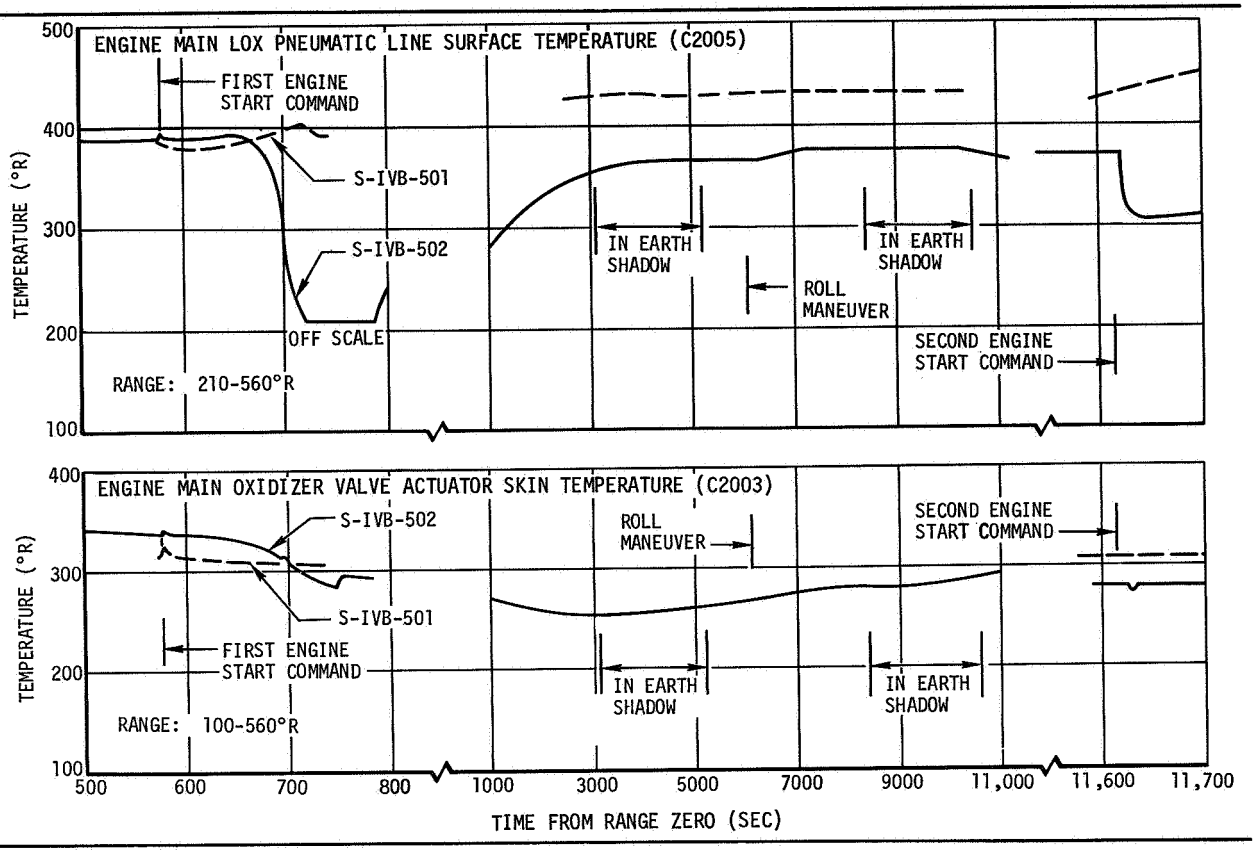

Figure 10-46. Environmental Effects

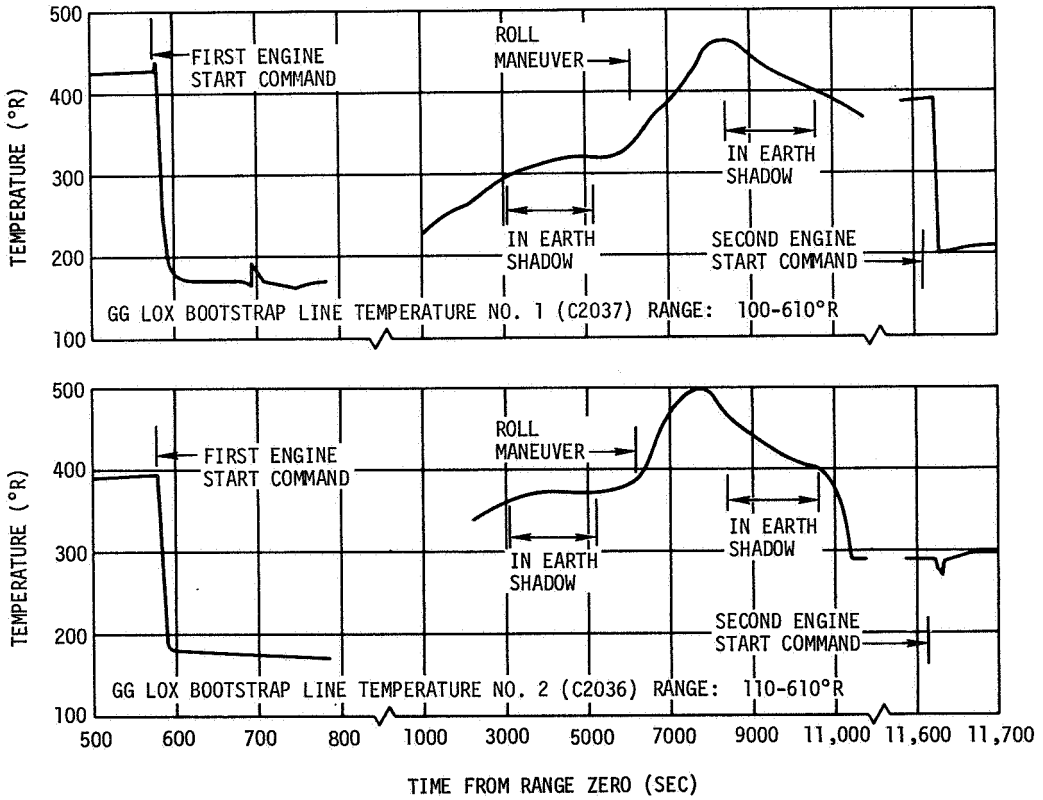

Figure 10-47. Gas Generator LOX Bootstrap Line Temperatures

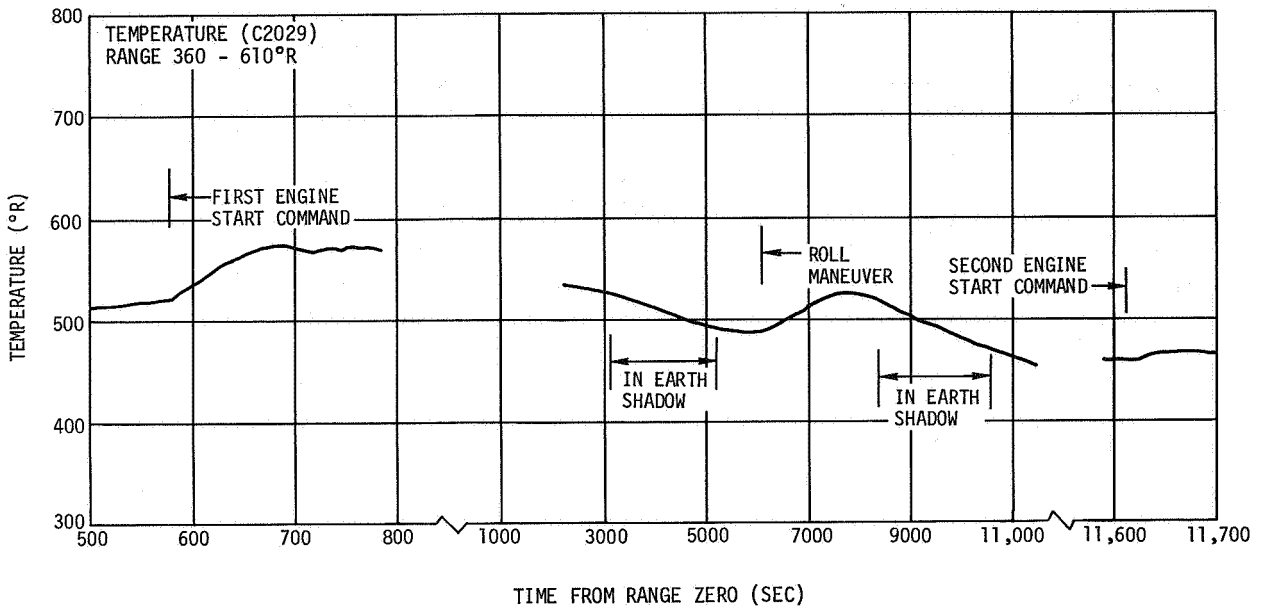

Figure 10-48. Main Hydraulic Pump Discharge Line Temperature

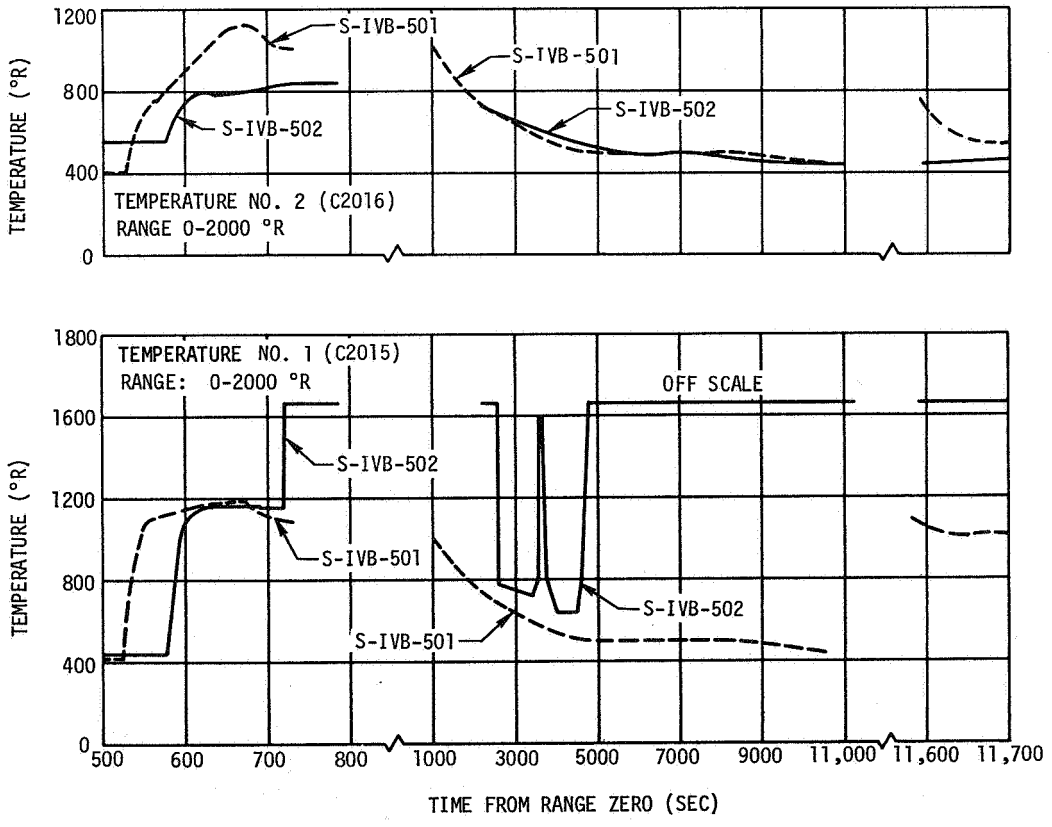

Figure 10-49. Crossover Duct Exterior Wall Temperatures

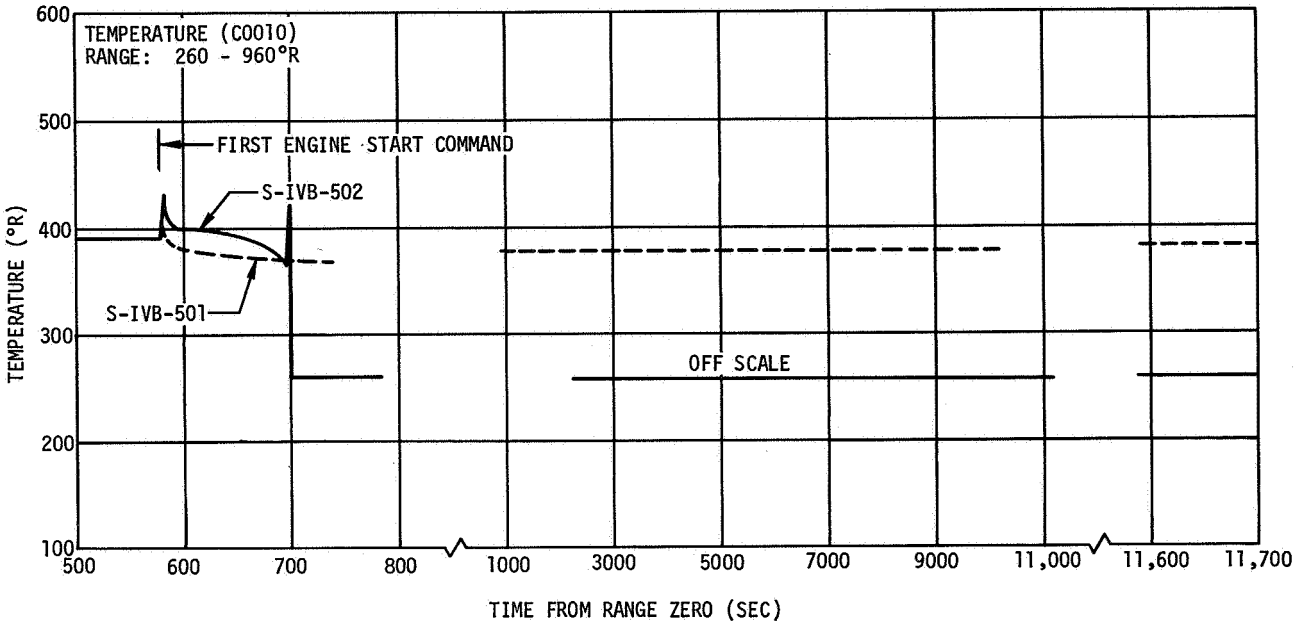

Figure 10-50. Engine Area Ambient Temperature

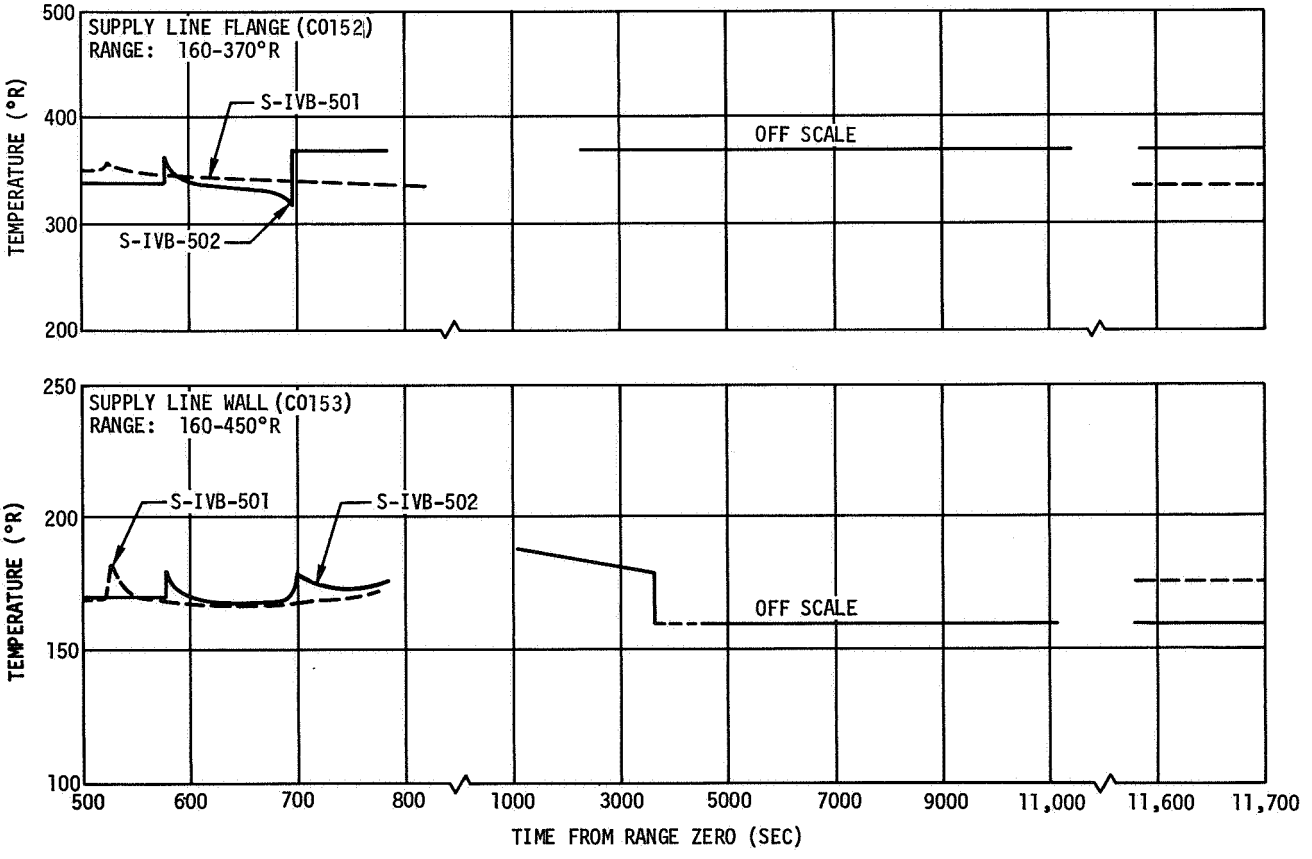

Figure 10-51. Main Oxidizer Supply Line Temperatures

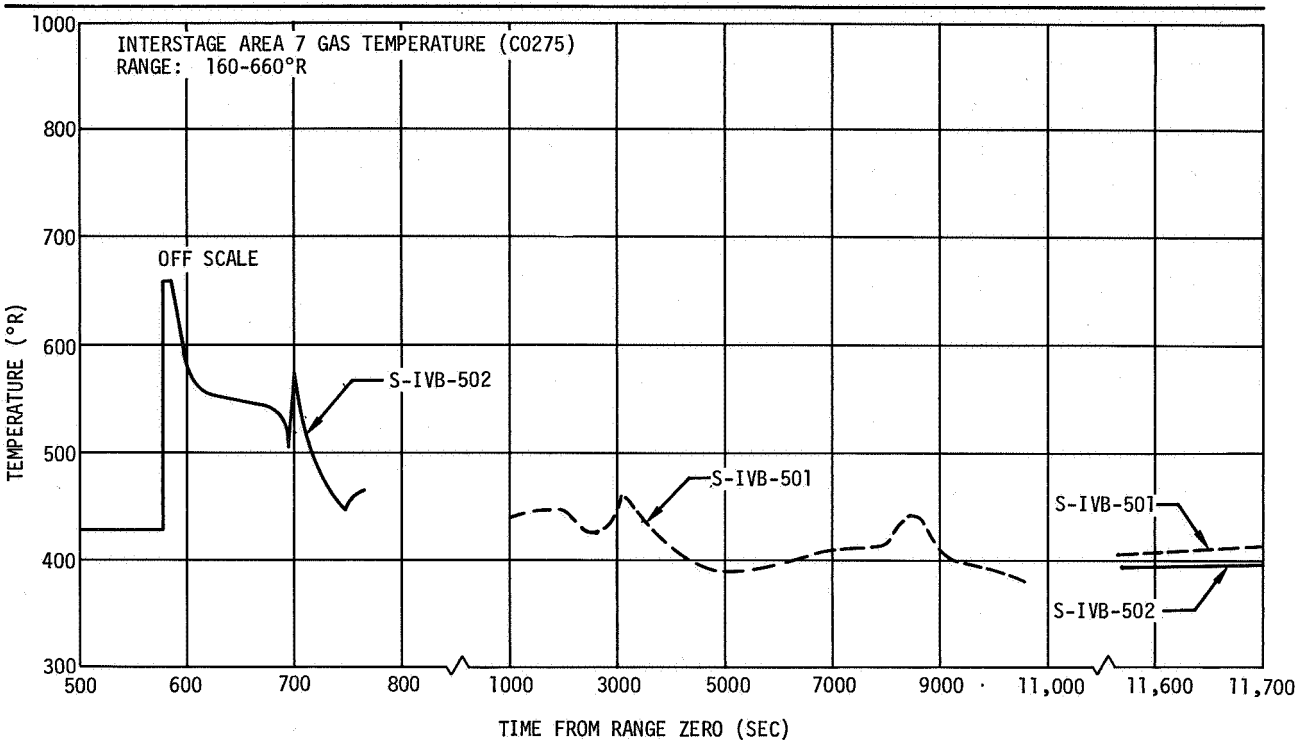

Figure 10-52. Interstage Area 7 Gas Temperature

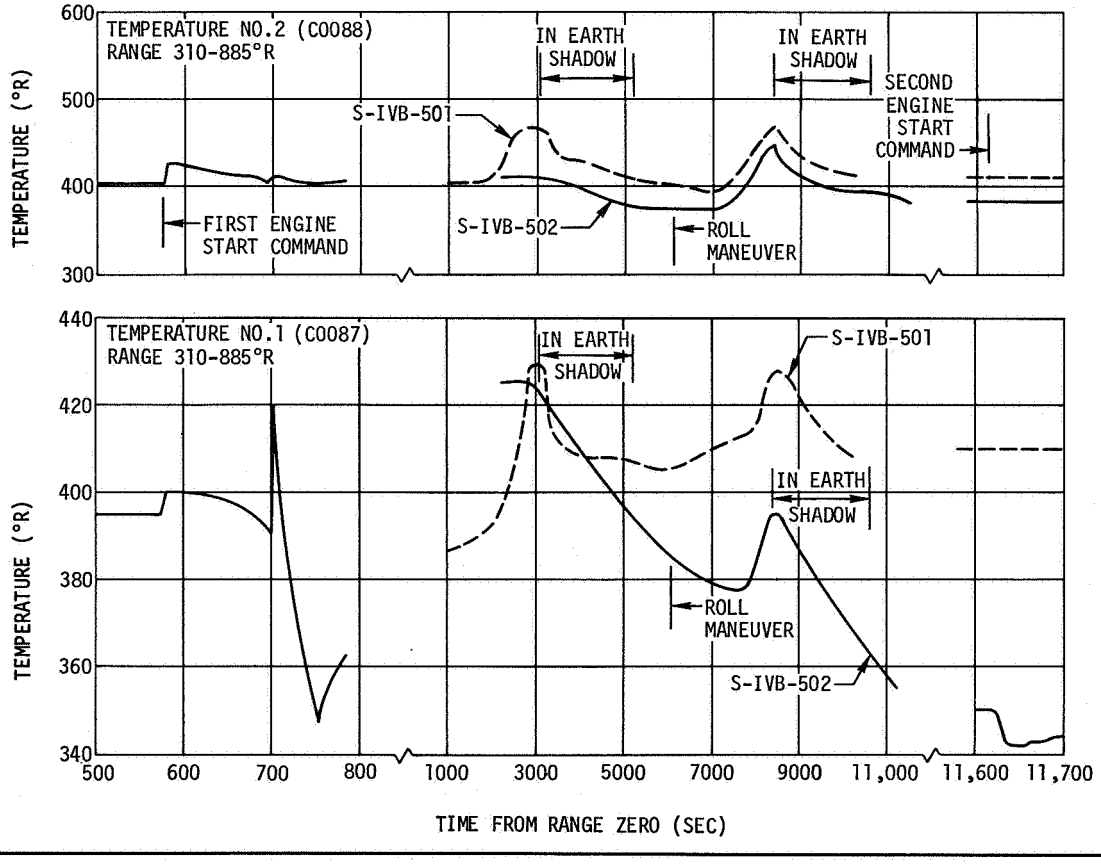

Figure 10-53. Thrust Structure Temperatures

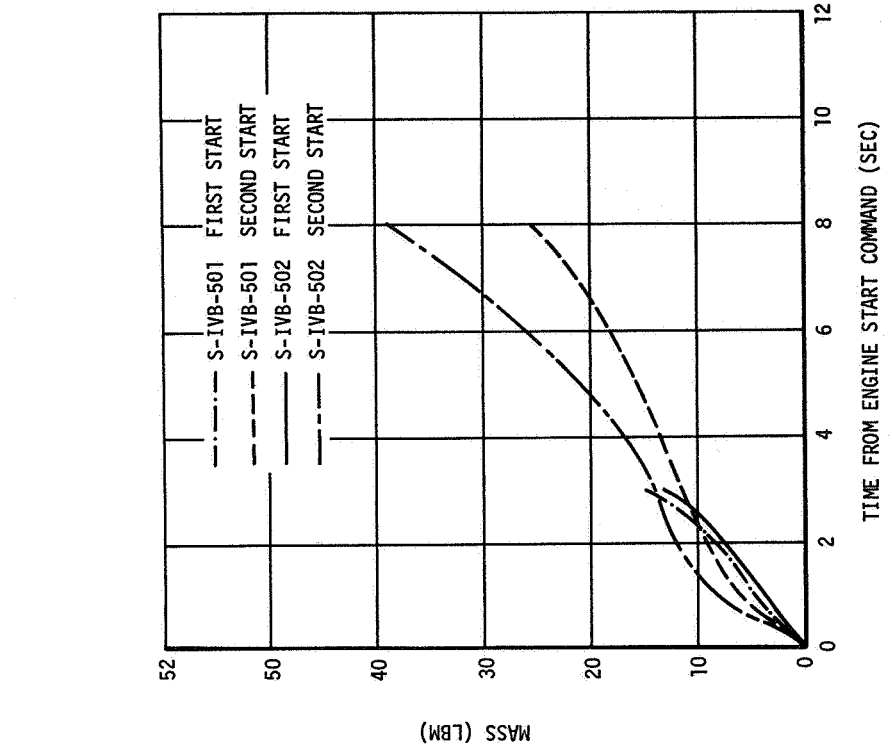

Figure 10-55. Total LH2 Flow Through Main Fuel Valve During Fuel Lead

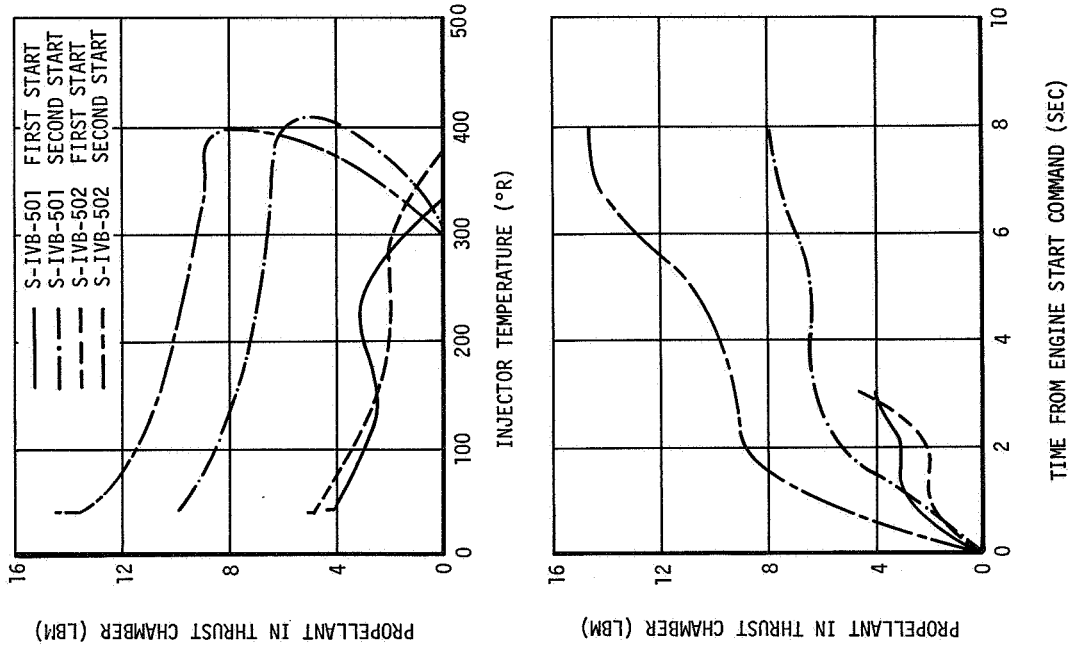

Figure 10-54. Propellant in Thrust Chamber During Fuel Lead

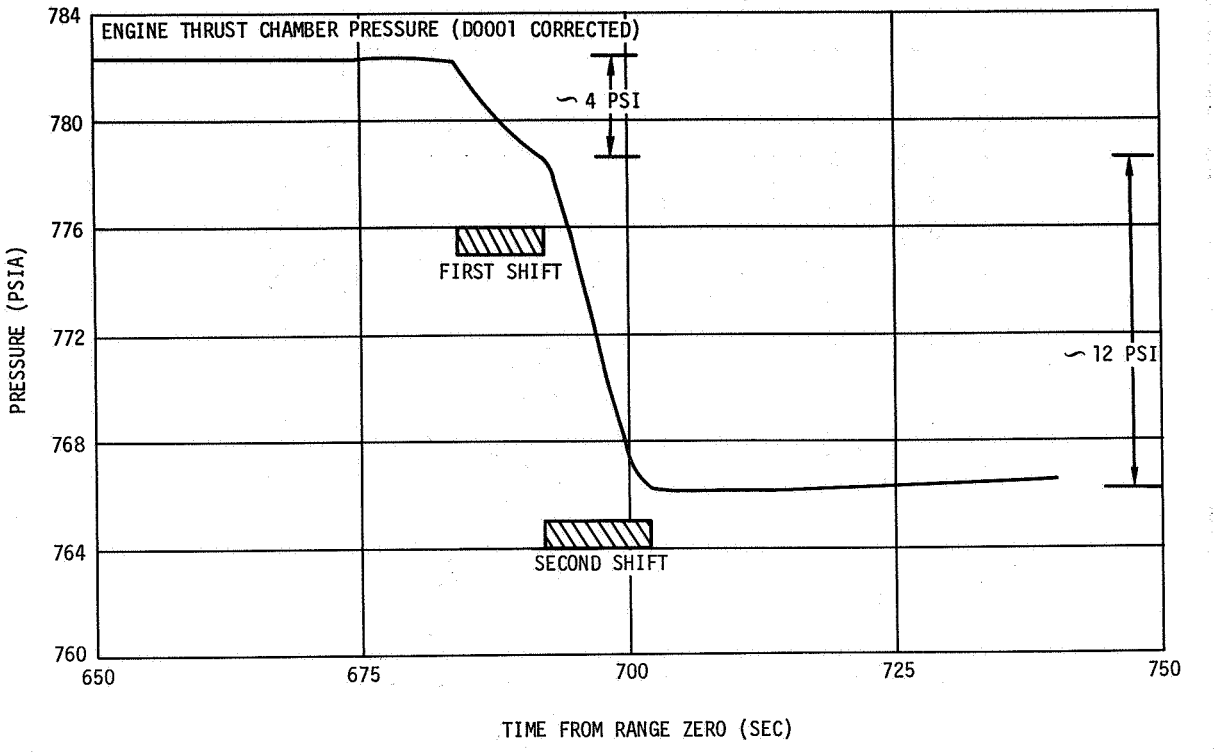

Figure 10-56. Thrust Chamber Pressure Corrected to Constant Heat Exchanger Operation (Reference Rocketdyne)

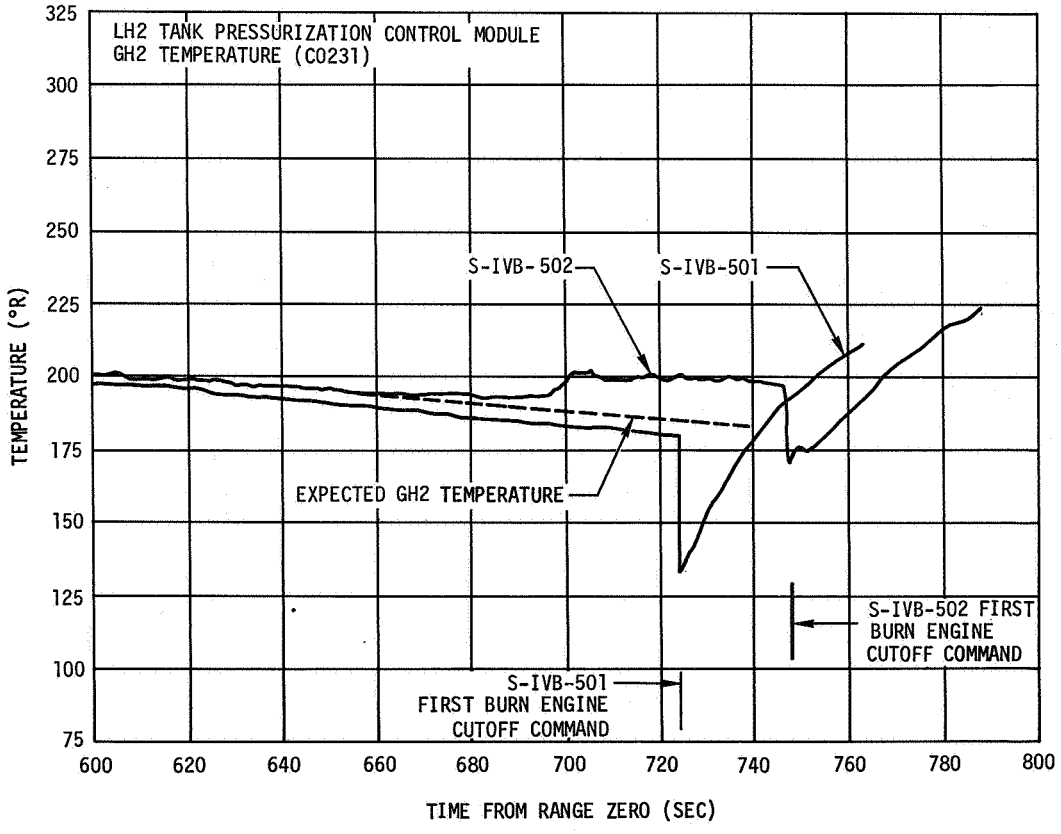

Figure 10-57. Response of LH2 Tank Pressurization GH2 Temperature

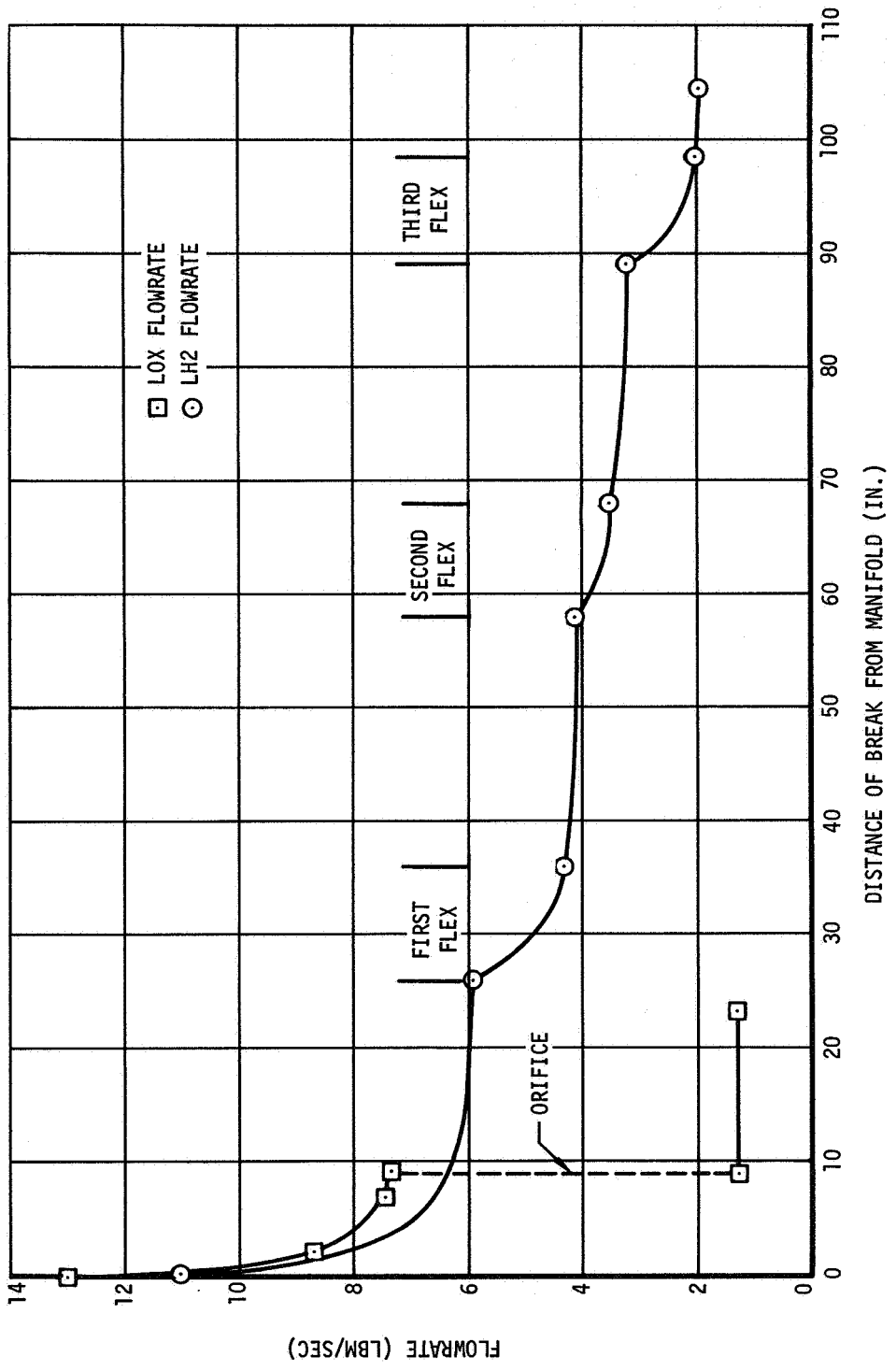

Figure 10-58. Flowrates From Broken ASI Lines

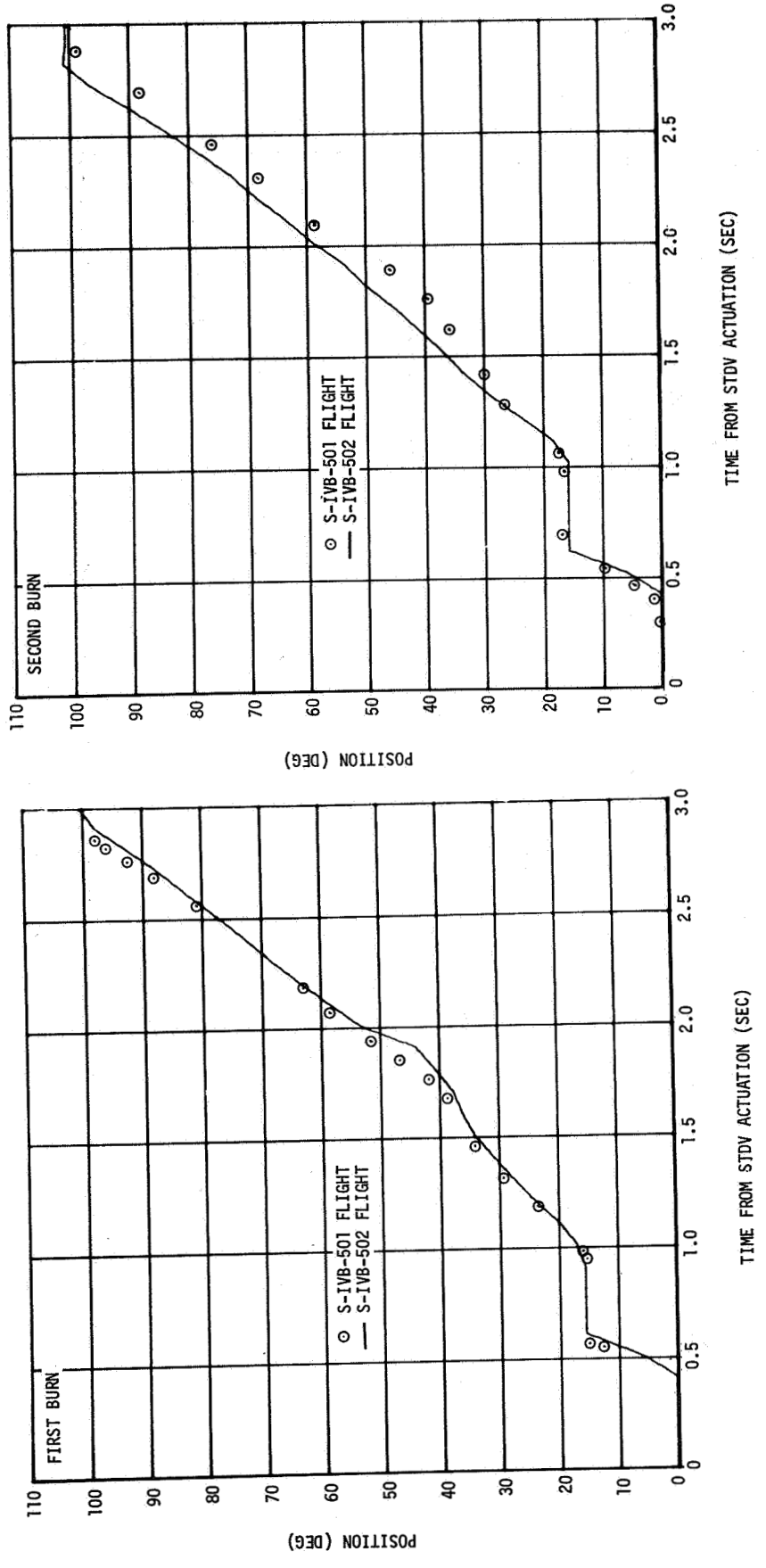

Figure 10-59. Main Oxidizer Valve Position

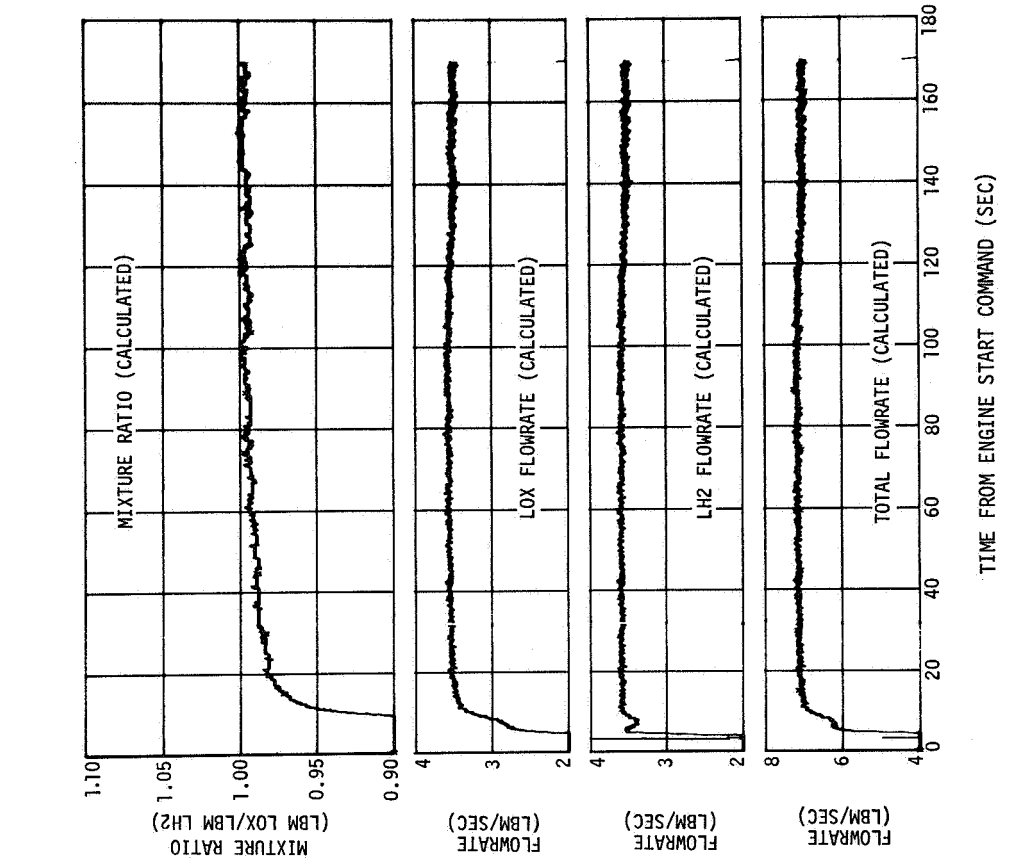

Figure 10-61. Gas Generator Performance - First Burn

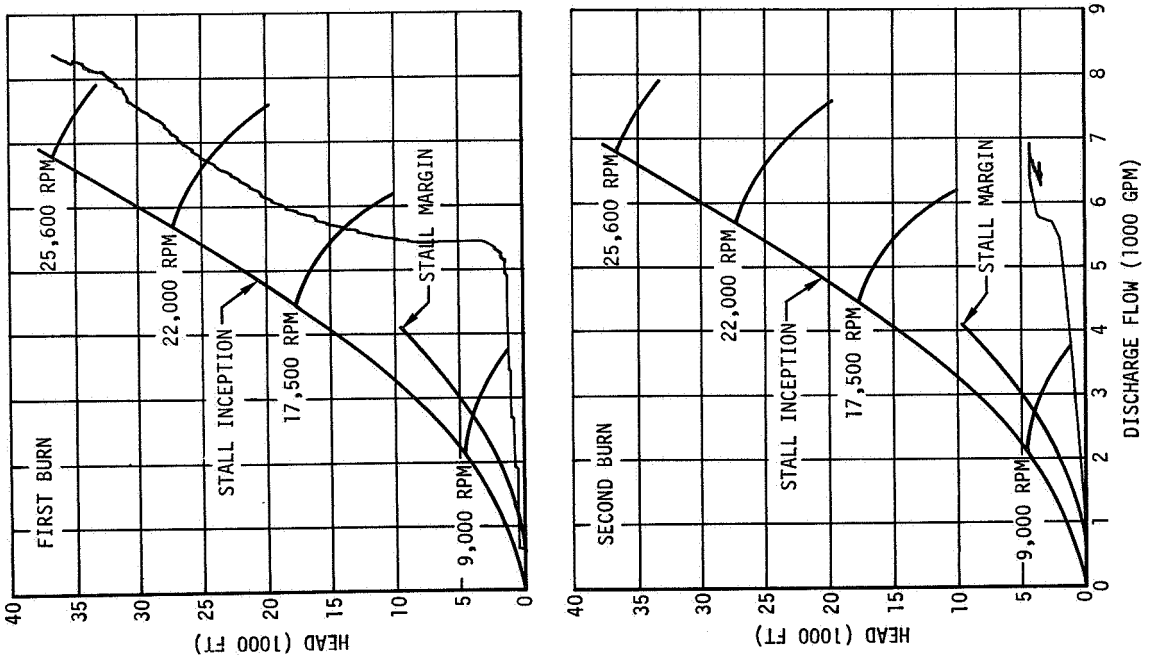

Figure 10-60. LH2 Pump Performance - Engine Start

SECTION 11

SOLID ROCKETS

11. SOLID ROCKETS

The solid rocket motors on the S-II and S-IVB stages performed satisfactorily and accomplished their intended purpose. The S-II was separated from the S-IVB by the retrorockets, and the S-IVB propellants were settled prior to engine ignition by the ullage rockets.

11.1 Retrorockets

The four retrorockets mounted on the S-II performed satisfactorily and separated the S-II from the S-IVB. The ignition command time was not available as it is not transmitted on an S-IVB data link; however, the pressure buildup for all four retrorockets began within 0.02 sec of each other at RO +577.10 sec. The thrust and chamber pressure profiles for the four rockets were very similar and the maximum difference in burntimes was 0.04 sec. Prior to the flight, a correlation between thrust and chamber pressure had been obtained from previous ground tests of similar retrorockets. This correlation was used in a computer program to determine the retrorocket thrust from the chamber pressure data during the AS-502 flight. Table 11-1 presents the performance parameters for the individual rocket motors. All parameters were within the nominal performance limits except for the burntime total impulse for motor A (D0153) which was slightly greater than the nominal maximum value. This had no detrimental effect on motor performance. The chamber pressure data for motor D (D0156) was reading zero before burn and approximately 80 psia after burn, indicating a data shift during burn. A linear skew bias was applied to the data to correct for this shift. The corrected thrust and chamber pressure profiles for the retrorockets are presented in figure 11-1.

11.2 Ullage Rockets

Ullage rocket performance was satisfactory. The Ullage Rocket Ignition Command was given at RO +576.971 sec, with the Jettison Command at RO +589.066 sec. These times, relative to Engine Start Command, were very close to predicted. Table 11-2 presents the individual rocket motor performance parameters as defined in the Thiokol Chemical Company model specification SP-544A, dated November 29, 1965. A comparison of these data with nominal performance limits indicates that both motors performed within design specifications. Figure 11-2 presents the thrust profiles during burn.

TABLE 11-1
RETROROCKET PERFORMANCE

Parameter	Units	Motor A (Pos IV-I D0153)	Motor B (Pos II-III, D0154)	Motor C (Pos I-II, D0155)	Motor D (Pos III-IV, D0156)	Average	Nominal Performance Limits	
							Maximum	Minimum
Burntime*	sec	1.55	1.51	1.51	1.52	1.52	1.67	1.38
Maximum Chamber Pressure	psia	1,930	1,855	1,865	1,920	1,893	2,258	1,822
Average Burn Time Chamber Pressure	psia	1,734	1,720	1,715	1,745	1,729	1,875	1,545
Maximum Thrust	lbf	40,800	39,800	39,300	41,000	40,225	43,420	34,200
Average Burn Time Thrust	lbf	36,371	35,623	35,356	36,241	35,898	39,435	30,190
Burntime Total Impulse	lbf-sec	56,375	53,791	53,387	55,086	54,660	56,300	52,290

*The interval between the time at which the pressure attains 10 percent of the maximum pressure during the buildup portion of the pressure curve, and the time at which the bisector of an angle (formed by the intersection of a line tangent to the pressure curve just prior to decay and a line tangent to the descending portion of the pressure curve) intersects the pressure curve.

TABLE 11-2
AS-502 ULLAGE ROCKET PERFORMANCE

Parameter	Units	Motor A (Pos II-III, D0216)	Motor B (Pos IV-I, D0217)	Nominal Performance Limits	
				Maximum	Minimum
Action Time*	sec	5.80	5.77	6.08	5.01
Burntime**	sec	3.81	3.80	4.10	3.54
Maximum Chamber Pressure	psia	1,016	1,031	1,220	900
Maximum Ignition Chamber Pressure	psia	1,081	1,076	1,470	----
Average Action Time Chamber Pressure	psia	739	758	880	680
Average Burntime Chamber Pressure	psia	975	1,001	1,100	890
Maximum Thrust	lbf	3,526	3,578	4,150	2,600
Maximum Ignition Thrust	lbf	3,751	3,734	5,100	----
Average Action Time Thrust	lbf	2,564	2,630	3,045	2,345
Average Burntime Thrust	lbf	3,383	3,473	3,786	3,090
Action Time Total Impulse	lbf-sec	14,871	15,175	15,595	14,335
Burntime Total Impulse	lbf-sec	12,889	13,197	13,590	12,500

*The time interval between 10 percent of maximum chamber pressure during the start transient and 10 percent of maximum chamber pressure during the cutoff transient.

**The time interval between 10 percent of maximum chamber pressure during the start transient and 75 percent of maximum chamber pressure during the cutoff transient.

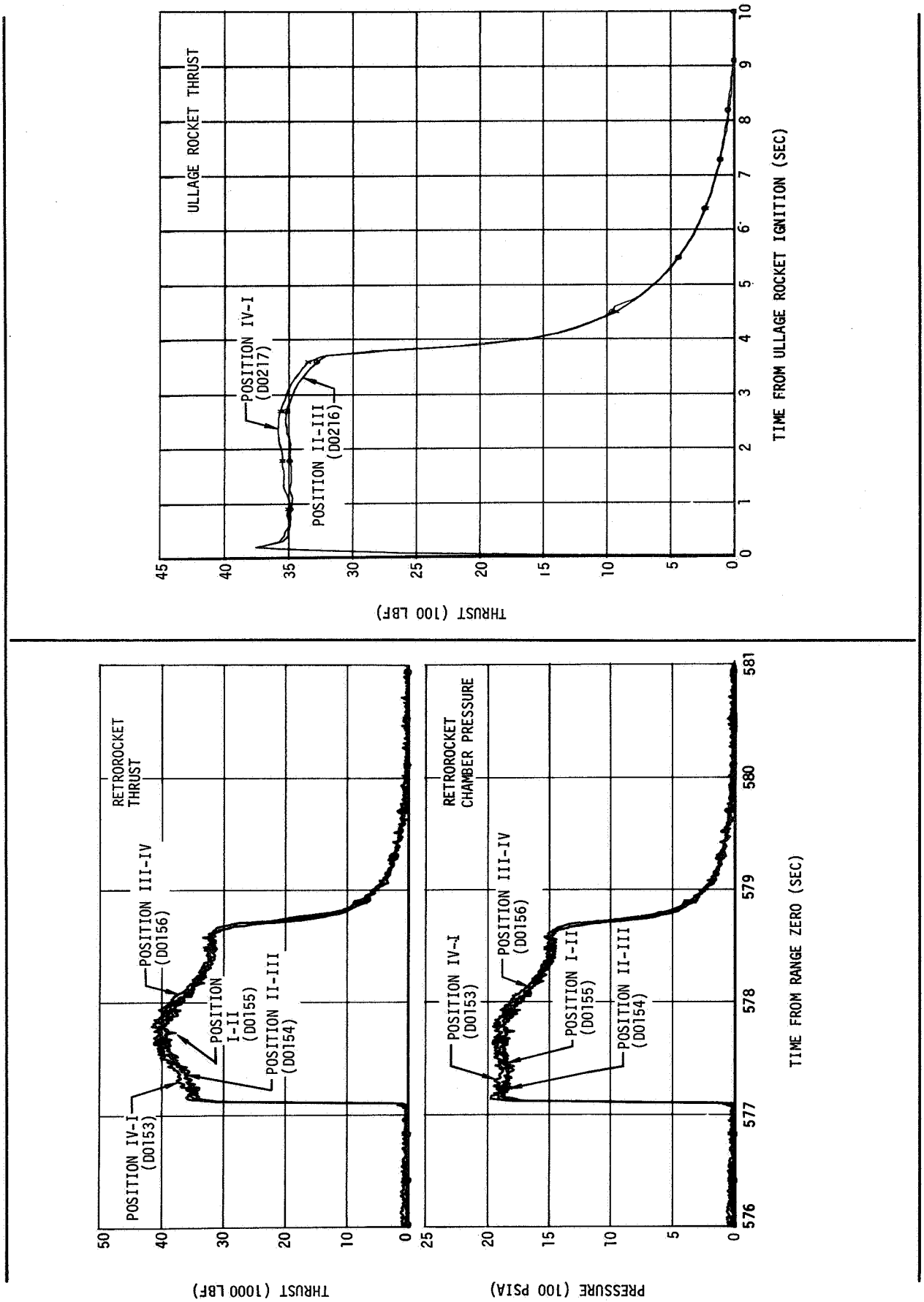

Figure 11-2. Ullage Rocket Performance

Figure 11-1. Retrorocket Performance

SECTION 12

OXIDIZER SYSTEM

12. OXIDIZER SYSTEM

The oxidizer system performed adequately, supplying LOX to the engine pump inlet within the specified operating limits throughout J-2 engine operation. The available NPSP at the LOX pump inlet exceeded the engine manufacturer's minimum requirement at all times.

12.1 LOX Tank Pressurization Control

The LOX tank pressurization systems (figure 12-1) satisfactorily controlled pressure in the LOX tank during all periods of the flight. The cold helium supply was adequate during boost and first burn and would have been sufficient for second burn if the restart had been successful. A significant cold helium leak occurred during orbit but adequate helium was available. The LOX pressurization module regulator performed as expected. The ambient helium repressurization system performed nominally during the restart preparations. Safing of the LOX tank was adequately accomplished subsequent to the aborted second burn.

12.1.1 First Burn

12.1.1.1 Prepressurization and Boost

LOX tank prepressurization started at RO -167 sec and increased the LOX tank ullage pressure from 15.3 to 40.5 psia within 17 sec (figure 12-2). Two makeup cycles were required to maintain the LOX tank ullage pressure above 38.5 psia before the ullage temperature stabilized. At RO -96 sec, the ullage pressure began increasing from 39.6 to 43.1 psia as a result of stage geometric change during LH2 prepressurization, with a minor contribution from the LOX vent valve purge and the LOX pressure sense line purge. At 43.1 psia the vent/relief valve cracked and dropped the ullage pressure to 42.1 psia where it remained until liftoff. Table 12-1 compares prepressurization data from the S-IVB-501 flight and the S-IVB-502 acceptance tests to that of the S-IVB-502 flight.

During the first 10 sec after liftoff (ESC -577 to ESC -567 sec) the ullage pressure decayed 1.4 psi to 40.7 psia. The pressure continued to decay at a lesser rate of 1.75 psi/min throughout S-IC boost, necessitating two makeup cycles from the cold helium spheres to maintain the ullage pressure above the lower pressure switch setting of 38.7 psia. At S-IC engine cutoff two sharp pressure rises occurred corresponding to S-IC inboard and outboard engines off; at S-II engine start the pressure was 42.0 psia. During S-II boost, the ullage pressure decayed at a constant rate of 0.37 psi/min until the S-II engines two and three cut off, at which time the pressure sharply increased 0.3 psi. The pressure then decayed at a constant rate of 0.18 psi/min until S-II engine cutoff when it again rose sharply (from 39.8 to 40.4 psia).

The rate of pressure decay during the various periods is approximately proportional to the rate of increase in axial acceleration during that period $\left(\frac{dp}{dt} \cong 60 \frac{da}{dt}\right)$. Correspondingly, the ullage pressure rise at the various engine cutoffs is proportional to the decrease in acceleration at that time ($\Delta P \cong -0.4\ [\Delta A]$). In addition, the tank ullage temperature data do not indicate the temperature decay which would necessarily accompany the pressure drop if it were caused by an ullage collapse; there is also no temperature response to the pressure

increase at the various engine cutoffs. The conclusion to be drawn from this information is that the ullage pressure decay and subsequent increases are a result of LOX tank ullage volume changes resulting from acceleration forces. Calculations based on ullage conditions indicate a decrease in ullage volume of 4.8 ft^3 as a result of the 4.9 g decrease in acceleration at S-IC engine cutoff. This delta volume is consistent with predictions developed by the Saturn Weights Section in support of PU system performance. This change in LOX tank geometry as a result of stage axial acceleration was not noted on the AS-501 flight. The explanation for this discrepancy is not presently understood and is under investigation.

When the ullage pressure decayed below 38.7 psia during S-IC boost (at ESC -497.6 and ESC -449.1 sec), the tank pressure switch commanded the cold helium shutoff valves open until the pressure had been raised to 40.6 psia (figure 12-2). Each makeup cycle required approximately 1.1 sec and a total of 0.38 lbm of cold helium was added to the LOX tank.

Temperature data at the LOX tank diffuser (C0229) and the LOX pressurization line inlet to the vent line (C0016) suggest a flow out of the LOX tank through the vent line at two different periods during boost. Immediately after liftoff (ESC -577 sec) these two measurements show a rapid temperature drop for 10 sec followed by a gradual warming (figure 12-2). This corresponds to the period of initial rapid ullage pressure decay. (This was also noted on the AS-501 launch.) Later in the boost, at approximately ESC -472 sec, the rates of decrease for both C0016 and C0229 showed an increase; in each measurement the temperature dropped below its previous steady-state level. This rapid temperature decay was interrupted by the second makeup cycle at ESC -449 sec but continued after that cycle until approximately ESC -427 sec (S-IC engine cutoff). At that time C0016 began warming asymptotically to its previous steady-state level, and C0229, which coincidentally was at its previous steady-state level, began following the ullage temperatures (figure 12-2).

It is apparent that these temperature profiles could have been produced by cold gas flowing through the LOX vent line. Since the cold helium shutoff valves are closed during these times and the pressurization system still contains sensible heat, as demonstrated during both makeup cycles, the source of the cold gas could not have been through the pressurization system. The tank ullage temperatures during this period make it evident that the vent line temperature responses could have been caused by ullage gas flowing out through the LOX vent line. This would indicate a loss of ullage gas during the S-IC boost.

Unfortunately, the data are not adequate to precisely determine the mass of ullage gas; however, rough calculations indicate approximately 0.4 lbm of gas lost during the S-IC boost.

Loss of ullage gas in this manner, i.e., by flowing out through the tank vent line, would require flow through the LOX tank vent/relief and/or relief valves. These valves are not at their respective relief settings during these periods and should not have opened. The vent/relief valve talkbacks did not indicate a loss of the closed position (the relief valve has no talkbacks); however, this valve is capable of opening as much as 0.030 in. without affecting the microswitch. The only relevant phenomenon which is common to these two time periods is a longitudinal oscillation of approximately 5 cps.

Since there is no other logical explanation for the preceding data, it is felt that the data are indicative of leakage through the relief and/or vent/relief valve caused in all probability by the 5 cps longitudinal oscillation. The amount of leakage was not excessive from a pressurization aspect. It was, coincidentally, approximately equal to the mass of gas added during the two boost makeup cycles.

12.1.1.2 Pressurization

The LOX tank ullage pressure and temperature and the pressurant flowrate are shown in figure 12-3. The ullage pressure was 40.3 psia at first burn Engine Start Command, satisfying the engine start requirements, and was sufficient throughout S-IVB powered flight to meet the minimum NPSP requirement. During the start transient, the ullage pressure decreased to a minimum of 35.2 psia before the pressurant flowrate became large enough to increase the ullage pressure. During the burn the ullage pressure cycled between the upper and lower pressure settings approximately as predicted, although four overcontrol cycles were required versus the predicted three because the control band was smaller than that used for the prediction, and the burntime was longer.

The ullage pressure increased slightly during the first few seconds after first burn Engine Start Command because the pressurization system was activated at first burn engine start +2.8 sec and allowed the pressurant to flow into the tank for approximately 3 sec before the LOX flow out of the tank attained its steady-state level.

Due to the failure of the cold helium regulator discharge plenum pressure measurement (D0105) and the heat exchanger helium inlet temperature measurement (C0008), these parameters were reconstructed based on available data and relationships developed on past tests. The heat exchanger outlet pressure (D0161) was also biased by +6 psi in order to make it consistent with remaining system data under ambient conditions.

Utilizing this data the LOX tank pressurant flowrate varied from 0.20 to 0.41 lbm/sec during overcontrol system operation, and from 0.25 to 0.31 lbm/sec during undercontrol. This variation is normal because the heat exchanger bypass orifice inlet temperature changes as the system chills down. During S-IVB first burn, 54.7 lbm of helium were used; 332 lbm had been loaded. Table 12-2 compares the pressurization system data from S-IVB-502 flight to that from S-IVB-502 acceptance firing and S-IVB-501 flight tests.

The pressurization system showed no effects from the engine anomaly, as the system is almost independent of the engine. However, both the heat exchanger discharge pressure (D0161) and overcontrol valve inlet pressure (D0225) throughout the burn indicated pressures approximately 30 psi lower than was noted on either the S-IVB-502 acceptance firing or the S-IVB-501 acceptance firing or flight test. There was no system design change to account for this change in operating level; however, the LOX pressurization regulator had been replaced by a later configuration after the acceptance firing. Unfortunately, the failure of D0105 makes it quite difficult to determine whether the lower pressures were the result of regulator performance or of some unusual system condition. These data are undergoing continuing evaluation.

12.1.1.3 Cold Helium Supply

The cold helium supply was adequate to meet boost and first-burn flight requirements. The cold helium supply system data are presented in table 12-3 and figure 12-4. Two makeup cycles, using a total of approximately 0.4 lbm of cold helium, were required during boost. During burn, mass calculations based upon sphere temperatures and pressure agreed closely with the results obtained from flow integration.

12.1.1.4 J-2 Heat Exchanger

The J-2 heat exchanger performance data are presented in figure 12-5 and compared to S-IVB-501 flight and S-IVB-502 acceptance firing data in table 12-4. The failure of the heat exchanger helium inlet temperature (C0008) makes a precise comparison of performance to previous tests impossible; however, the available data indicate that performance was nominal. The effects of the engine anomaly were not reflected in the heat exchanger performance. The heat exchanger outlet temperature had increased to 965 deg R by the end of 50 sec of engine operation and continued to increase to a maximum of 1,005 deg R at ESC1 +115 sec. The flowrate through the heater was relatively constant at the values given in the table.

12.1.2 Second Burn Attempt

12.1.2.1 Repressurization

Ambient helium repressurization of the LOX tank in preparation for second burn engine start was satisfactorily accomplished. Repressurization was initiated at ESC2 -227 sec (figure 12-6) and raised the ullage pressure from 37.4 psia to 40.0 psia in 19.7 sec. Helium supply pressure dropped from 3,095 to 1,925 psia, and 5.2 lbm of helium were utilized. The ullage pressure stabilized at 40.0 psia until ESC2 -100 sec at which time it began to increase. The pressure was 41.6 psia at second burn Engine Start Command, completely satisfying all requirements. The pressure rise from ESC2 -100 sec is discussed in paragraph 12.2.1.

12.1.2.2 Pressurization

The LOX tank pressurization system operated nominally during the second burn attempt. Regulator discharge pressure rose rapidly to approximately 400 psi and remained at that level until the system was deactivated at ESC2 +16.2 sec. Contrary to first burn, when it was off-scale-high, the regulator discharge measurement (D0105) provided good data beginning during the second orbit and continuing through repressurization and second burn. Comparison with other system data verifies its level as correct during these periods.

Because the ullage pressure was above the pressure switch setting, the pressurization system was in the undercontrol mode during the entire 8.4 sec of activation. The ullage pressure was 42.1 psia at engine cutoff; cold helium usage was 2.95 lbm (figure 12-7).

12.1.2.3 Cold Helium Supply

Although orbital leakage (figure 12-8) dropped the cold helium sphere pressure from 1,378 psia at first burn engine cutoff to 860 psia at restart attempt, the cold helium supply would have been adequate for normal second-burn operations. Table 12-3 presents the cold helium supply system data at restart and cutoff; the system was activated for approximately 8 sec. Following the restart attempt the sphere pressure continued to decay, reaching 550 psia by the beginning of the cold helium dump (paragraph 12.2.3).

12.2 Pressurization System Conditions during Orbit

12.2.1 LOX Tank Conditions during Orbit

Evaluation of the LOX tank temperature and pressure data during the first and second orbits is difficult due to the lack of data at some times and the accuracy and response characteristics of the tape recorded data at other times. In general, however, the ullage gas temperatures appear to drop to liquid temperatures at engine cutoff because of liquid diffused through the ullage by the cutoff transients. Throughout the remainder of the orbital period the ullage temperatures appeared to very gradually become progressively colder toward the forward end of the tank (figure 12-9). During the same period the LOX liquid changed from uniform temperatures throughout the tank at engine cutoff to a profile that became progressively warmer toward the bottom of the tank. At no time, however, were liquid saturation temperatures indicated. With the common bulkhead exposed to LH2 and the aft bulkhead, thrust cone, and all of the attached hardware exposed to radiation heating in space, this provile would appear to be reasonable. The gradually decreasing trend of the ullage pressure during this period is consistent with the cooling trend in the ullage temperature.

At three times during orbit (approximately R0 +3,275, R0 +5,450, and R0 +11,520 sec), the trends previously described were interrupted (figure 12-9). All of the temperature probes in the tank, both liquid and gas, converged rapidly on a common temperature of 164 to 165 deg R. Beginning at the same time, the ullage pressure increased 1 to 2 psi over an approximate 125-sec period. In each case, the change in the trend of the ullage data was preceded (100 to 300 sec) by a stage attitude pitch maneuver. Although no temperature data are available, at approximately R0 +16,150 sec another ullage pressure rise occurred that was also preceded by an attitude pitch maneuver.

While the data and supporting analysis are not conclusive, the temperature and pressure responses are presently explained as follows: the ullage achieved a condition in which the proportion of GOX in the ullage gas assumed a gradient along the longitudinal axis as a function of the ullage temperature gradient. The partial pressure of GOX, and consequently the mass, was defined by the saturated vapor pressure at the local temperature.

The execution of the pitch maneuver under very low g conditions abruptly changed the orientation of the LOX in the tank in a manner that resulted in a slosh wave and surface agitation of the liquid. This exposed all of the ullage gas to direct contact with LOX and resulted in warming all of the ullage to LOX temperatures of 164 to 165 deg R. The GOX

in the ullage gas consequently was no longer saturated, and evaporation occurred until the GOX component of the ullage was again at a saturation condition. The rise in temperature and increase in ullage mass caused the noted ullage pressure rise.

Analysis of the data is continuing in an effort to develop a quantitative method of evaluation and prediction of this phenomenon.

12.2.2 LOX Tank Venting during Orbit

The automatic cutoff sequence immediately following the abortive restart attempt incorporated a 10-sec LOX tank vent during which the ullage pressure dropped from 42 to 33 psia. Tank ullage data are presented in figure 12-7. Tank ullage conditions indicate a homogeneous two-gas mixture in the ullage prior to the vent. Calculations based on these tank conditions indicate that 191 lbm of gas were vented including 27 lbm of helium. At the termination of the vent the ullage consisted of 41 lbm of helium and 355 lbm of LOX. The thrust level of the propulsive vent outlet averaged 900 lbf with a total impulse of 8,852 lbf-sec.

At approximately RO +22,022 sec, the LOX tank vent and cold helium shutoff valves were commanded open in order to gain additional information relative to stage safing. The tank temperatures and pressure during the subsequent blowdown are presented in figure 12-10. The ullage pressure dropped rapidly from 34.5 to 24.0 psia within 24 sec and then stabilized for 14 sec before resuming the decay. At RO +22,090 sec with the pressure at approximately 18 psia, the ullage pressure decay rate changed from a rapid blowdown to a gradual decay that followed the vapor pressure for the cooling LOX bulk. The pressure had decayed to 10.5 psia by RO +23,000 sec and to 1.0 psia by 33,000 sec when data were finally lost.

Due to the simultaneous cold helium dump through the same vent valve and line coupled with the lack of instrumentation situated advantageously for this operation, the LOX tank vent flowrate and LOX boiloff have not yet been accurately reconstructed. With the exception of the 14 sec ullage pressure plateau, however, this ullage pressure appeared to follow a normal blowdown profile until the tank pressure reached the vapor pressure of the liquid bulk. At this point (RO +22,090 sec) pronounced boiloff began, as evidenced by the liquid temperatures which began decreasing at this time. Calculations based on LOX mass and the temperature decay rate indicate an initial boiloff rate of approximately 8 to 10 lbm/sec. Since this is the approximate flow capacity of the LOX vent valve and line at the 18 psi ullage pressure, the rate of boiloff, at least initially, was obviously being controlled by the vent system flow capacity. In spite of the limited data available, a review of the excessively long blowdown period (more than 11,000 sec were required to drop the ullage pressure to 1.0 psia), indicates that boiloff is capable of maintaining tank pressure at the vapor pressure level indefinitely. The high rate of boiloff, when compared to the vent flowrate, also tends to confirm that there was no restriction of the vent line or valve.

A thorough analysis of the available LOX tank and pressurization system data has failed to provide a conclusive explanation for the 14-sec plateau in the ullage pressure. Pressurization system parameters show no reflection of this phenomenon, indicating that the cold helium dump flowrate was not affected. A possible cause, and the only one advanced which is

consistent with the data, is blockage of the vent line by liquid oxygen. If this were the case, the ullage volume would be effectively isolated from the vent, and the pressure would show a very small decay over a short period of time.

This liquid blockage of the vent line might well have been caused by a slosh wave in the tank which immersed the LOX vent line inlet as a result of the unbalanced 700-lbf thrust at the LOX vent outlet. As the thrust continued and the stage settled into a stable tumbling pattern, centrifugal force would quickly settle the LOX into the bottom of the tank and vent inlet would be uncovered, allowing the ullage gas to begin venting again.

12.2.3 Cold Helium Supply System during Orbit

Cold helium sphere conditions during orbit are shown in figure 12-8. Following first burn engine cutoff the cold helium sphere pressure (D0016) decreased steadily, dropping from 1,378 psia at cutoff to 860 psia at the restart attempt and to 550 psia by the beginning of the cold helium dump. In addition, the cold helium sphere temperatures were abnormally low during orbit. Both of these trends are indicative of a significant cold helium leak. The fact that D0016 appears somewhat inaccurate (the data approached -200 psia instead of 0 psia in the latter stages of the cold helium dump) does not account for this anomaly. It is therefore concluded that 50 to 75 lbm of cold helium were lost between first burn engine cutoff and second burn restart attempt, with an additional 35 to 58 lbm lost from the restart attempt to the beginning of the cold helium dump. The exact mass loss cannot be determined because of the possible 200 psi error in D0016.

The source of this leakage is not known. However, the curvature of the sphere pressure data indicates the leak was from an unregulated source upstream of the shutoff valves in the LOX pressurization control module. Possible leakage sources include (1) the conoseals at the eight spheres and at the inlet flange of the LOX pressurization control module, (2) the cold helium dump module, (3) the cold helium fill umbilical disconnect, and (4) the pipe joints. Based upon past experience, the conoseals and pipe joints appear to be the most likely sources. All future stages will have improved teflon-coated conoseals at all conoseal joints. Also, in the future all pipe joints and conoseal joints will be torque-checked after each cryogenic loading.

At the beginning of the fifth orbit (R0 +22,023 sec) an experimental cold helium dump was initiated by opening the cold helium shutoff valves and the LOX tank vent valve; these valves were still open when loss of telemetry data occurred two orbits later. Significant parameters for the first 20 min of dump are shown in figure 12-11. As shown, the cold helium sphere pressure data (D0016) dropped toward an indicated level of approximately -200 psia, rather than 0 psia. This discrepancy is under investigation. Approximately 144 sec after dump initiation, the LOX pressurization system data indicated a reduction of cold helium flow, as evidenced by the drop in the system pressure levels and the rise in temperature; the flow recovered 76 sec later, as the pressures rose and the temperature decreased. At dump initiation +680 sec the cold helium flow again diminished. These variations in flow were apparently caused by variations of flow area within the LOX pressurization module. This change in flow area may have been caused by movement of the poppet within the cold helium regulator, partial closure of the cold helium shutoff valves, or an interaction of these. This phenomenon is still being investigated.

12.3 LOX Pump Chilldown

12.3.1 First Burn

The LOX pump chilldown system performed adequately. At Engine Start Command, the pump inlet conditions of 41.7 psia and 164.7 deg R were sufficient to produce an NPSP of 24.9 psi, thus satisfying the requirement of 12.8 psi minimum (table 12-5). At this time, the pump inlet pressure was 1.4 psia higher than the ullage pressure because of the slow prevalve opening.

Recirculation chilldown started at RO -284 sec and continued until RO +576.6 sec when the prevalve started to open with the pump still running. The chilldown system fluid temperature decreased during the first minute of chilldown, then remained relatively constant until prepressurization (figures 12-12 and 12-13) when the LOX became subcooled throughout the recirculation system. The engine pump inlet pressure was constructed for the period from liftoff to RO +145 sec because acceleration caused it to go off-scale high. The pump inlet and return line pressures increased and decreased with acceleration until the prevalve was opened and the chilldown pump developed head was lost. The chilldown pump was cut off at approximately RO +576.8 sec; the prevalve full open signal was received at RO +579.4 sec. The pump inlet pressure then decreased to equal the ullage pressure.

The chilldown flowrate was 39.5 gpm prior to prepressurization and 42.5 gpm afterwards, with a pressurized frictional pressure drop of 11.5 psi through the system. The flow coefficient, a measure of the flow resistance, was calculated from these flowrate and pressure drop values to be 18.3 $sec^2/in.^2\text{-}ft^3$ for pressurized chilldown.

Three of the chilldown system parameters (C0013, C0159, and D0061) showed a change in level at or near the engine performance shift that occurred during first burn. The primary measurement indicating a change is the LOX bleed valve temperature. The temperature started a 0.6 deg R increase at RO +695 sec and reached a maximum at RO +700 sec. At this time the temperature started a decrease to 169.5 deg R which was 0.2 deg R higher than the steady-state temperature prior to the engine performance shift.

The change in the steady-state temperature level seems to be due to a small change in the LOX gas generator (GG) bleed flow. The temperature change at RO +695 sec was apparently due to heating of the GG bleed valve and the LOX chilldown return line. This heating caused some of the liquid near the valve to vaporize and traverse through the return line to the tank. As the slug of vapor and liquid passed the chilldown return line temperature probe, the indicated temperature dropped from 179.4 deg R to approximately 172 deg R. It then increased to 182.4 deg R, indicating the slug had passed the probe. The higher return line temperature after the slug passed the probe was due to and coincidental with the pressure in the return line reaching its relief level which corresponds to the ullage pressure plus head pressure.

12.3.2 Second Burn

The second burn chilldown was initiated at RO +10,872.2 sec, the predicted time. The total chilldown period was approximately 180 sec longer than predicted due to an LVDC time update resulting in a later than expected second burn Engine Start Command.

The LOX pump chilldown system performed satisfactorily (figures 12-14 and 12-15). At second burn Engine Start Command, the pump inlet pressure of 41.6 psia and temperature of 165 deg R were within the start requirements. The NPSP at engine start was 24.7 psi, which was 11.9 psi above the required minimum of 12.8 psi. Significant data are presented in table 12-5.

Due to vehicle position at initiation of the chilldown, many of the parameters required to perform an adequate chilldown analysis were not available. When sufficient data were available (ESC2 -650 sec) the chilldown pump differential pressure, flowrate, and engine LOX pump pressure and temperature had reached steady conditions. At this time the chilldown pump differential pressure was 12 psi, the flowrate was approximately 43 gpm, and the engine pump inlet pressure and temperature were 49.7 psia and 165.9 deg R, respectively. When the prevalve was opened at ESC2 -9.3 sec, the engine LOX pump inlet pressure dropped from 53.4 psia to 44.37 psia. The engine pump inlet temperature went from 165.4 deg R to 165 deg R between the time the prevalve opened and Engine Start Command. The engine pump outlet temperature increased from 165.3 deg R to 165.4 deg R during the same period.

12.4 Engine LOX Supply

The engine LOX supply system (figure 12-16) delivered the necessary quantity of LOX to the engine during first burn. During the restart attempt, the system performed adequately and reasonably in view of system boundary conditions.

12.4.1 First Burn

The NPSP at the engine interface (figure 12-17) was calculated to be 24.9 psi at first burn Engine Start Command. The NPSP then decreased and after 26 sec of powered flight reached a minimum value of 21.1 psi which was 0.8 psi above the 20.3 psi required at the interface at that time. During the remainder of the burn, the NPSP remained between 24.2 and 26.5 psi as it followed the ullage pressure. At the end of first burn the NPSP was 25.3 psi which was 5.1 psi higher than required at that time.

The interface static pressure and temperature are shown in figure 12-17. The interface pressure was 41.7 psia at Engine Start Command and reached a minimum of 34.9 psia after 26 sec of engine operation. The pressure increased to 40.0 psia and then cycled between 38.5 and 41.0 psia as it followed the ullage pressure. The LOX pump interface static pressure became significantly erratic commencing at approximately RO +700 sec. Related system parameters and performance levels indicate the occurrence of this erratic behavior to be external of the LOX feed system. It is believed the behavior is a result of the J-2 failure which produced severe environmental changes which affected the instrumentation. The interface pressure at Engine Cutoff Command was 29.5 psia. The pump interface temperature was 164.7 deg R at Engine Start Command and Engine Cutoff Command.

The LOX pump inlet pressure and temperature were plotted in the LOX pump operating region (figure 12-18) and indicated that the LOX pump interface conditions were met satisfactorily throughout the first period of powered flight. The pump interface temperature was plotted against the mass remaining in the LOX tank during engine operation and is shown in figure 12-19. Table 12-6 compares the LOX supply parameters to those of the AS-501 flight and S-IVB-502 acceptance firing.

12.4.2 Second Burn

The LOX pump NPSP at the engine interface (figure 12-20) was calculated to be 24.7 psi at second burn Engine Start Command. At the end of fuel lead, the LOX NPSP increased rapidly to 25.5 psi. At Engine Cutoff Command, the NPSP was 25.5 psi which was 4.5 psi above the minimum required at that time.

The LOX pump interface static pressure transducer (D0003) was inoperative after first burn, and thus the inlet pressures were calculated from LOX tank conditions. The interface pressure was 41.6 psia at Engine Start Command and at the end of fuel lead; it was 42.0 psia at Engine Cutoff Command.

The interface temperature at Engine Start Command and at the end of fuel lead was 165 deg R; at Engine Cutoff Command it was 165.2 deg R.

The LOX pump interface pressure and temperature were plotted in the engine operating region (figure 12-21) and indicated that the engine LOX pump interface conditions were met satisfactorily during the restart attempt. The S-IVB-502 flight data are compared to the S-IVB-501 flight and the S-IVB-502 acceptance firing data in table 12-6.

TABLE 12-1
LOX TANK PREPRESSURIZATION DATA

PARAMETER	UNITS	S-IVB-502 FLIGHT	S-IVB-501 FLIGHT	S-IVB-502 ACCEPT
Prepressurization duration	sec	17	15	19
Number of makeup cycles		4*	2	1
Prepressurization helium				
Flowrate	lbm/sec	0.28	0.26	0.321
Mass added to LOX tank during prepressurization	lbm	4.8	3.7	6.1
Mass added to LOX tank during makeup cycles	lbm	1.28*	0.39	0.57
Ullage pressure				
At prepressurization initiation	psia	15.2	15.1	14.7
At prepressurization termination	psia	40.5	40.5	40.3
At liftoff**	psia	42.1	42.4	
At Engine Start Command	psia	40.3	40.2	36.8
Events (from liftoff**)	sec			
Prepressurization initiation		-167	-167	-163
Prepressurization termination		-150	-152	-144
Engine Start Command		577.3	520.7	511.0

*0.9 lbm of helium were added to the tank during two GSE-supplied makeup cycles on the ground. Two cold-helium-sphere-supplied makeup cycles during S-IC boost added 0.38 lbm more.
**Liftoff is simulated during acceptance firing.

TABLE 12-2
LOX TANK PRESSURIZATION DATA

PARAMETER	UNITS	S-IVB-502 FLIGHT		S-IVB-501 FLIGHT		S-IVB-502 ACCEPT	
		FIRST BURN	SECOND BURN	FIRST BURN	SECOND BURN	FIRST BURN	SECOND BURN
Number of secondary flow intervals		4	N/A	6	3	3	3
Pressure control band							
Minimum	psia	38.6	N/A	39.0	38.9	38.0	38.0
Maximum	psia	40.3	N/A	40.0	40.0	39.7	39.8
Ullage pressure							
At Engine Start Command	psia	40.3	41.6	40.2	42.6	38.0	35.0
Minimum during start transient	psia	35.2	N/A	35.8	38.8	33.8	34.6
At Engine Cutoff Command	psia	39.0	42.1	40.0	39.0	35.6	39.5
Pressurant total flowrate							
During undercontrol	lbm/sec	0.25 to 0.31	N/A	0.25 to 0.30	0.28 to 0.33	0.26 to 0.28	0.28
During overcontrol	lbm/sec	0.37 to 0.41	N/A	0.38 to 0.42	0.40 to 0.46	0.38 to 0.40	0.40 to 0.41
Maximum LOX tank vent inlet temperature	°R	506	N/A	495	420	550	540

N/A Not applicable

TABLE 12-3
COLD HELIUM SUPPLY DATA

PARAMETER	UNITS	S-IVB-502 FLIGHT		S-IVB-501 FLIGHT		S-IVB-502 ACCEPT	
		FIRST BURN	SECOND BURN	FIRST BURN	SECOND BURN	FIRST BURN	SECOND BURN
Pressure							
At liftoff	psia	2,966	N/A	2,910	N/A	3,280	N/A
At Engine Start Command	psia	2,939	860	2,910	1,430	3,200	2,425
At Engine Cutoff Command	psia	1,378	830	1,570	800	1,670	1,090
Average Temperature							
At liftoff	deg R	38.9	N/A	41.0	N/A	41.0	N/A
At Engine Start Command	deg R	39.1	35.3	40.0	38.5	40.0	56.0
At Engine Cutoff Command	deg R	30.8	34.8	32.5	35.0	31.5	44.0
Helium Mass							
At Engine Start Command	lbm	332	201.0	332	252	345	282
At Engine Cutoff Command	lbm	275	198.5	294	190	295.2	192
Usage calculated from sphere conditions	lbm	57	2.5	38	62	50	90
Usage calculated by integration of flowrate	lbm	55	2.9	47	95	50.2	105.5

N/A Not applicable

TABLE 12-4
J-2 HEAT EXCHANGER PERFORMANCE DATA

PARAMETER	UNITS	S-IVB-502 FLIGHT		S-IVB-501 FLIGHT		S-IVB-502 ACCEPT	
		FIRST BURN	SECOND BURN	FIRST BURN	SECOND BURN	FIRST BURN	SECOND BURN
Flowrate through heat exchanger							
During overcontrol	lbm/sec	0.185	N/A	0.2	0.22	0.20	0.21
During undercontrol	lbm/sec	0.065	N/A	0.073	0.074	0.075	0.075
Heat exchanger inlet temperature							
During overcontrol	deg R	*	N/A	50	50	75	70
During undercontrol	deg R	*	N/A	60	63	100	90
Minimum	deg R	*	N/A	45	39	70	75
Heat exchanger outlet temperature							
At end of 50-sec transient	deg R	965	N/A	925	940	960	940
During overcontrol	deg R	990	N/A	**	930	985	915
During undercontrol	deg R	1,005	N/A	**	985	1,000	940
At Engine Cutoff Command	deg R	1,000	N/A	990	985	995	950
Heat exchanger outlet pressure							
During overcontrol	psia	330	N/A	350	360	360	350
During undercontrol	psia	380	N/A	410	418	420	420
Average LOX vent inlet pressure							
During overcontrol	psia	69	N/A	67	65	64	64
During undercontrol	psia	52	N/A	52	50	47	47
Maximum LOX vent inlet temperature	deg R	506	N/A	495	420	550	540

*Measurement failed.

**Temperature did not stabilize.

N/A Not applicable

TABLE 12-5
LOX CHILLDOWN SYSTEM PERFORMANCE DATA

PARAMETER	UNITS	S-IVB-502 FLIGHT		S-IVB-501 FLIGHT		S-IVB-502 ACCEPT	
		FIRST BURN	SECOND BURN	FIRST BURN	SECOND BURN	FIRST BURN	SECOND BURN
NPSP							
At Engine Start Command*							
With chilldown pump head	psi	24.9	N/A	36.9	N/A	N/A	N/A
Without chilldown pump head	psi	22.8	24.7	23.8	25.0	27.6	22.8
Minimum required at engine start	psi	12.8	12.8	12.8	12.8	12.8	12.8
At opening of prevalve	psi	42.23	27.1	45.5	34.0	36.0	31.5
Pump inlet conditions							
Pressure at Engine Start Command**							
With chilldown pump head	psia	41.7	N/A	50.3	N/A	N/A	N/A
Without chilldown pump head	psia	40.3	41.6	40.2	42.6	44.8	40.2
Temperature at Engine Start Command	deg R	164.7	165.0	164.5	165.75	165.4	165.4
Average flow coefficient	sec^2/in^2ft^3	18.3	18.2	25.0	25.0	14.4	13.27
Heat absorption rate	(Btu/hr						
Section 1 (tank to pump inlet)		500	∿500	500	500	2,900	4,110
Section 2 (pump inlet to bleed valve)		4,000	∿100	3,500	4,000	13,600	24,570
Section 3 (bleed valve to tank inlet)		∿500	0	3,500	2,000	4,400	6,120
Total		5,000	∿600	7,500	6,500	20,900	34,800
Chilldown flowrate							
Unpressurized	gpm	39.5	N/A	33.5	N/A	38.7	38.6
Pressurized	gpm	42.5	42.5	35.0	37.0	40.9	40.9
Chilldown system pressure drop							
Unpressurized	psi	10.0	N/A	9.2	N/A	6.6	6.6
Pressurized	psi	11.5	12.4	11.0	10.5	8.3	7.7
Events***	sec						
Chilldown initiation		-284.152	-742.466	-278.9	-562.7	-203.8	-719.7
Prevalve closed		-274.909	-727.446	-272.5	-552.0	--	--
Prepressurization initiation		-166.602	-227.001	-166.7	-326.0	-159.5	-700.4
Prevalve open command		576.596	-10.79	520.0	-10.8	509.37	-3.14
Prevalve closed signal dropout		577.596	-9.256	520.9	-9.8	510.31	-2.12
Prevalve open signal pickup		579.421	-7.117	522.5	-7.9	511.59	-0.91
Chilldown pump off		576.872	-0.602	520.3	-0.60	511.00	-1.6
Chilldown shutoff valve closed		N/A	N/A	625.298†	Not Sent	511.1	-1.7
Engine Start Command		577.270	0	520.7	0	511.9	0

*During acceptance testing, liftoff is simulated.

**The NPSP and pump inlet pressures are high at this time because the prevalves were slow in opening.

***All first burn data are referenced to liftoff (or simulated liftoff); all second burn data are referenced to second burn Engine Start Command.

†LOX chilldown valve closed switch (K0139) failed before liftoff (open dropout used).

N/A Not applicable

TABLE 12-6
LOX PUMP INLET CONDITION DATA

PARAMETER	UNITS	S-IVB-502 FLIGHT		S-IVB-501 FLIGHT		S-IVB-502 ACCEPT	
		FIRST BURN	SECOND BURN	FIRST BURN	SECOND BURN	FIRST BURN	SECOND BURN
Pump Inlet Conditions							
Static pressure at Engine Start Command*							
With chilldown pump head	psi	41.7	N/A	50.3	N/A	N/A	N/A
Without chilldown pump head	psi	40.3	41.6	40.2	42.6	44.8	40.2
Temperature at Engine Start Command	°R	164.7	165.0	164.5	165.75	165.4	165.4
Temperature at Engine Cutoff Command	°R	164.7	165.2	164.5	165.75	165.0	169.2
NPSP Requirements							
Minimum at Engine Start Command	psi	12.77	12.77	12.8	12.8	12.8	12.8
At high EMR	psi	20.96**	20.96**	20.8	20.8	20.8	20.8
After EMR cutback	psi	14.93**	14.93**	N/A	14.95	14.95	14.95
NPSP Available							
At Engine Start Command*	psi						
With chilldown pump head	psi	24.9	N/A	36.9	N/A	N/A	N/A
Without chilldown pump head	psi	22.8	24.7	23.8	25.0	27.6	22.8
At Start Tank Discharge Valve OPEN Command	psi	23.4	25.5	23.6	25.0	29.0	23.5
Maximum during firing	psi	27.3	25.7	27.5	28.0	29.0	25.0
Time of maximum	sec from ESC	5.7	15.1	15.0	8.5	4.0	118.0
Minimum during firing	psi	21.1	24.6	22.5	24.2	20.2	17.5
Time of minimum	sec from ESC	26.0	3.3	20.0	ECC	ECC	ECC
At Engine Cutoff Command	psi	25.3	25.5	26.0	24.2	20.2	17.5
LOX Feed Duct							
At high EMR							
Pressure drop	psi	2.0	0.8	1.9	1.8	2.6	2.3
Flowrate	lbm/sec	453	250	448	453	462	462
After EMR cutback							
Pressure drop	psi	N/A	N/A	N/A	1.8	N/A	1.6
Flowrate	lbm/sec	N/A	N/A	N/A	381	N/A	400

*The NPSP and pump inlet pressure are high at this time because the prevalves were slow in opening.

**These requirements are variable with acceleration. The values presented are maximum. Figures 12-10 and 12-11 graphically display the requirement.

N/A Not applicable.

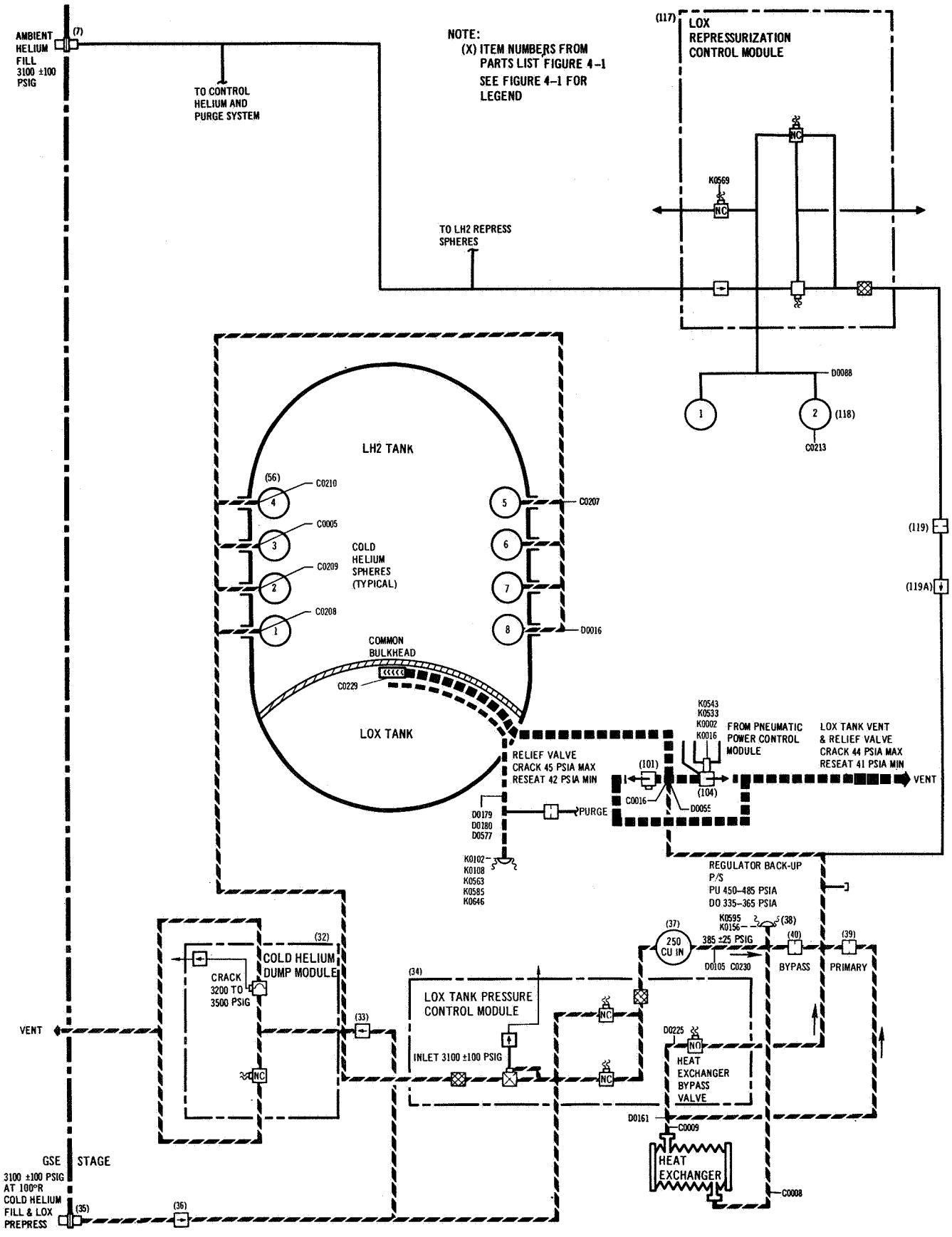

Figure 12-1. LOX Tank Pressurization System

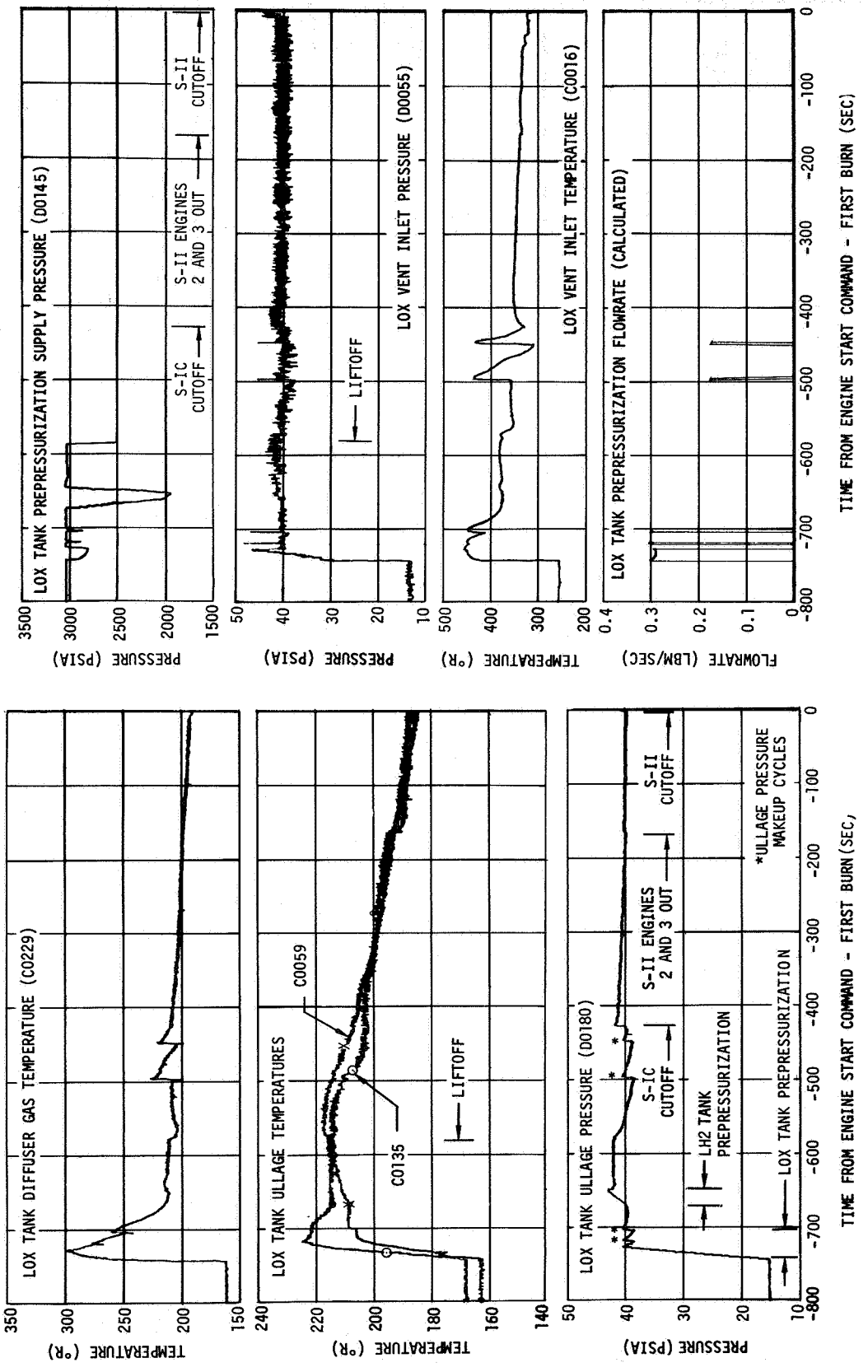

Figure 12-2. LOX Tank Conditions - Prepressurization and Boost

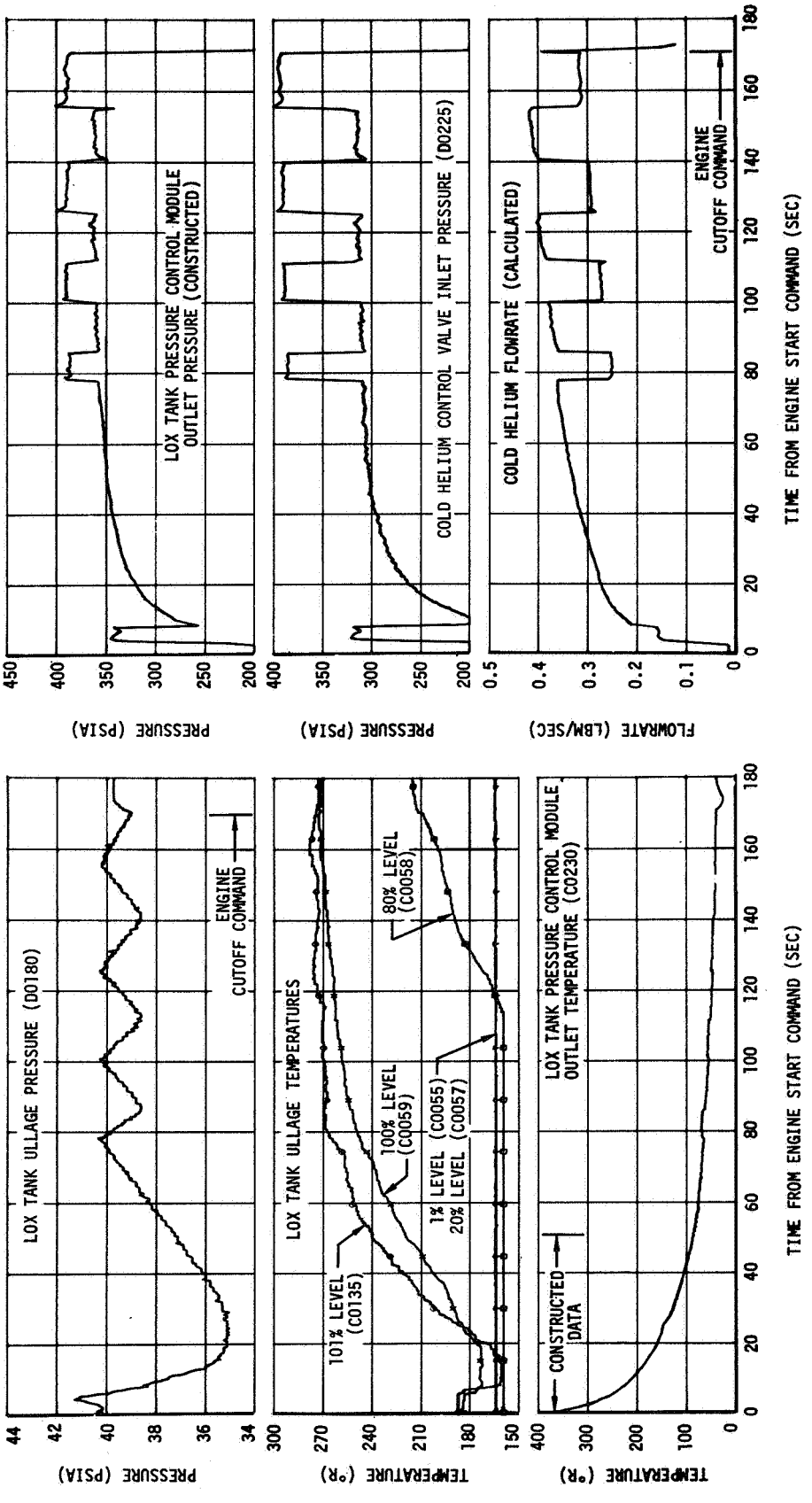

Figure 12-3. LOX Tank Pressurization System Performance - First Burn

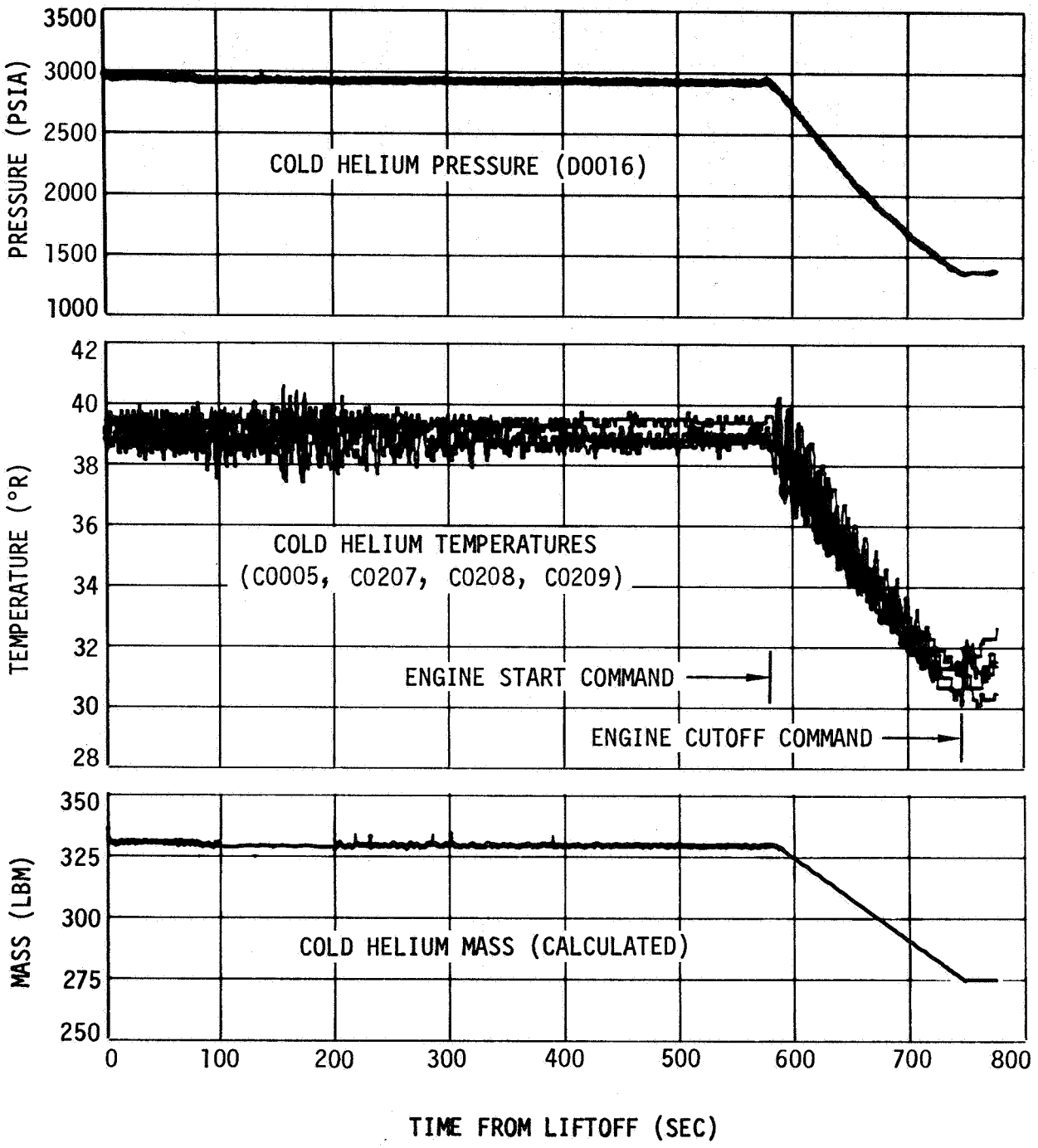

Figure 12-4. Cold Helium Supply - Boost and First Burn

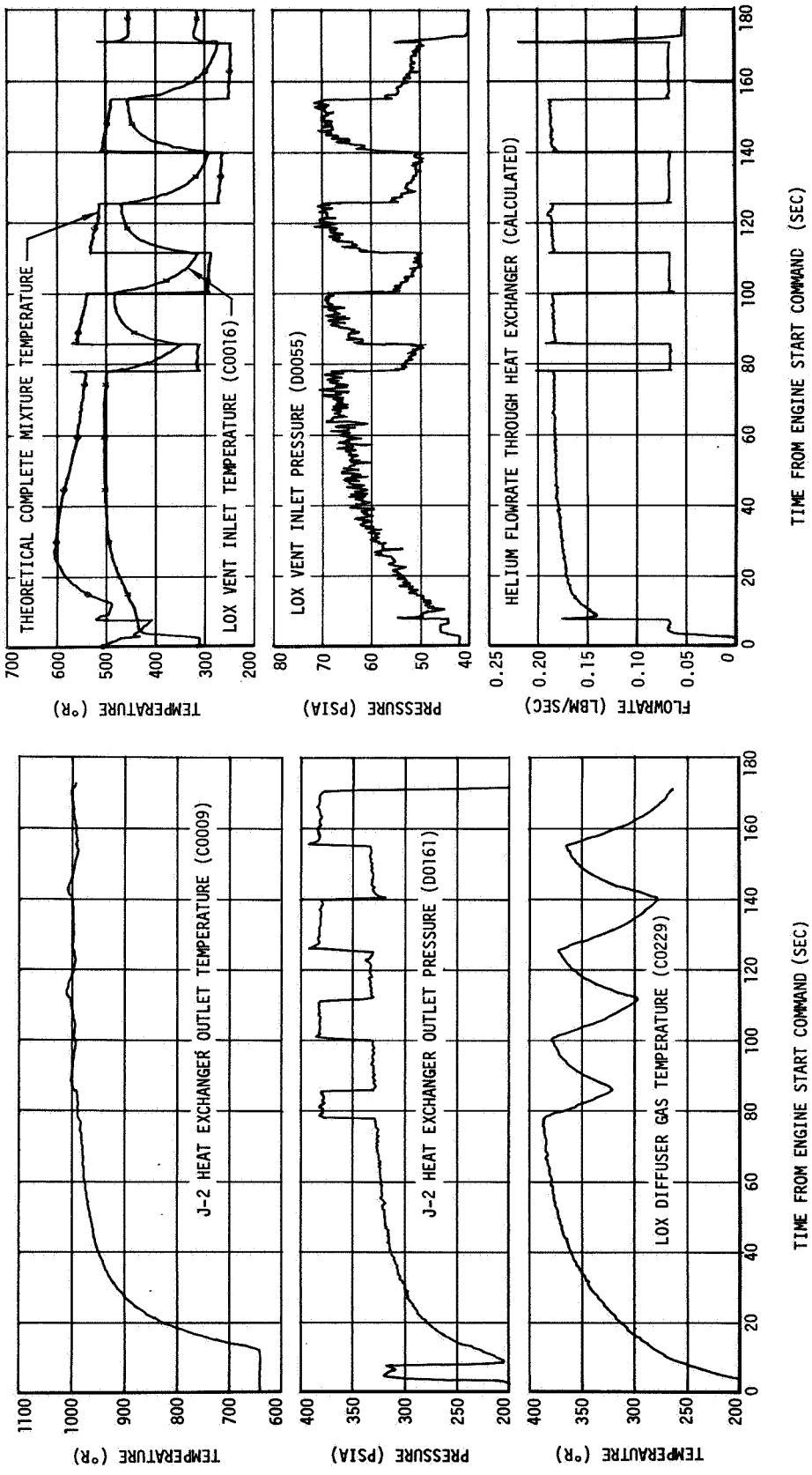

Figure 12-5. J-2 Heat Exchanger Performance - First Burn

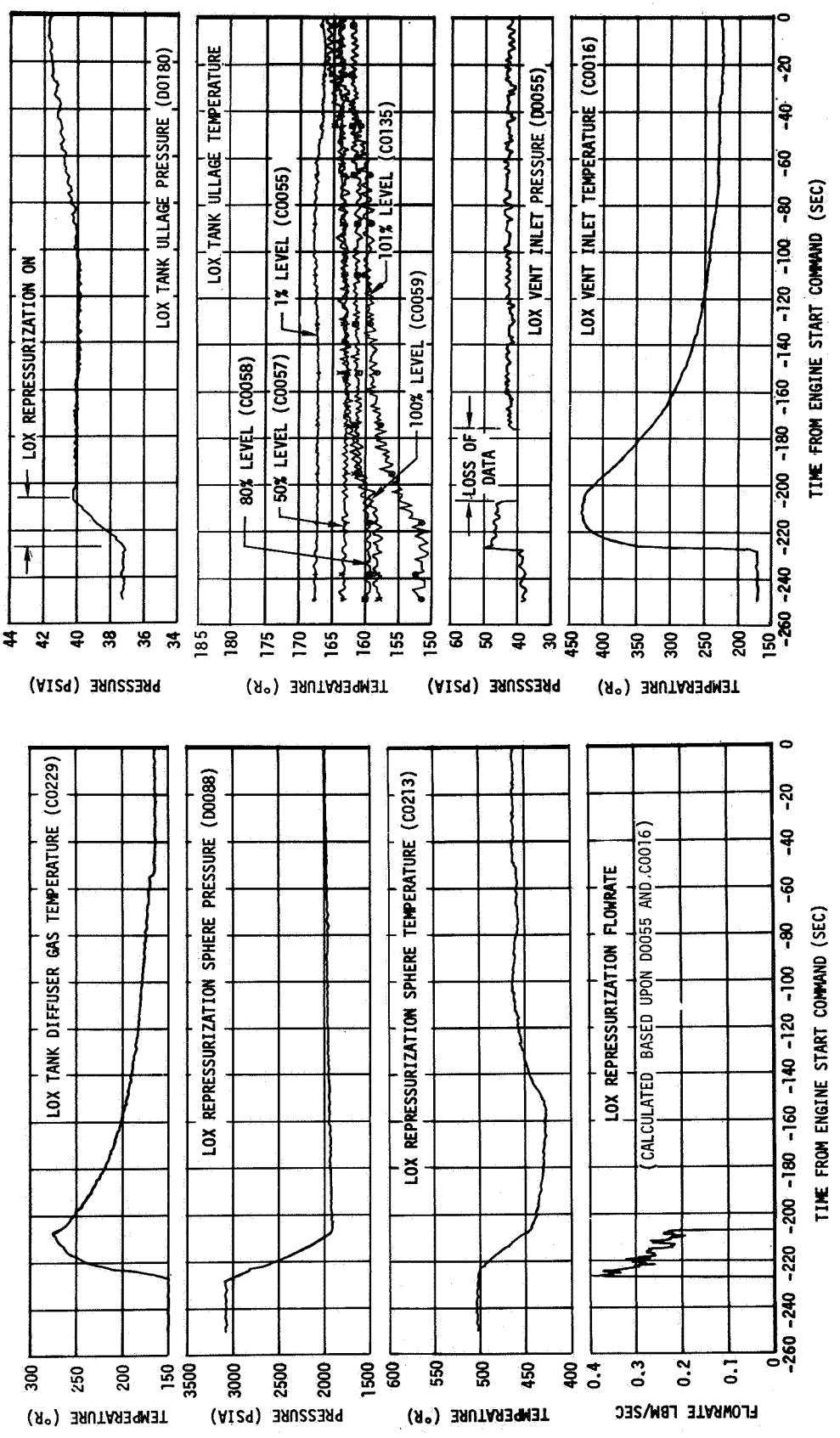

Figure 12-6. LOX Tank Conditions During Repressurization Period - Second Burn

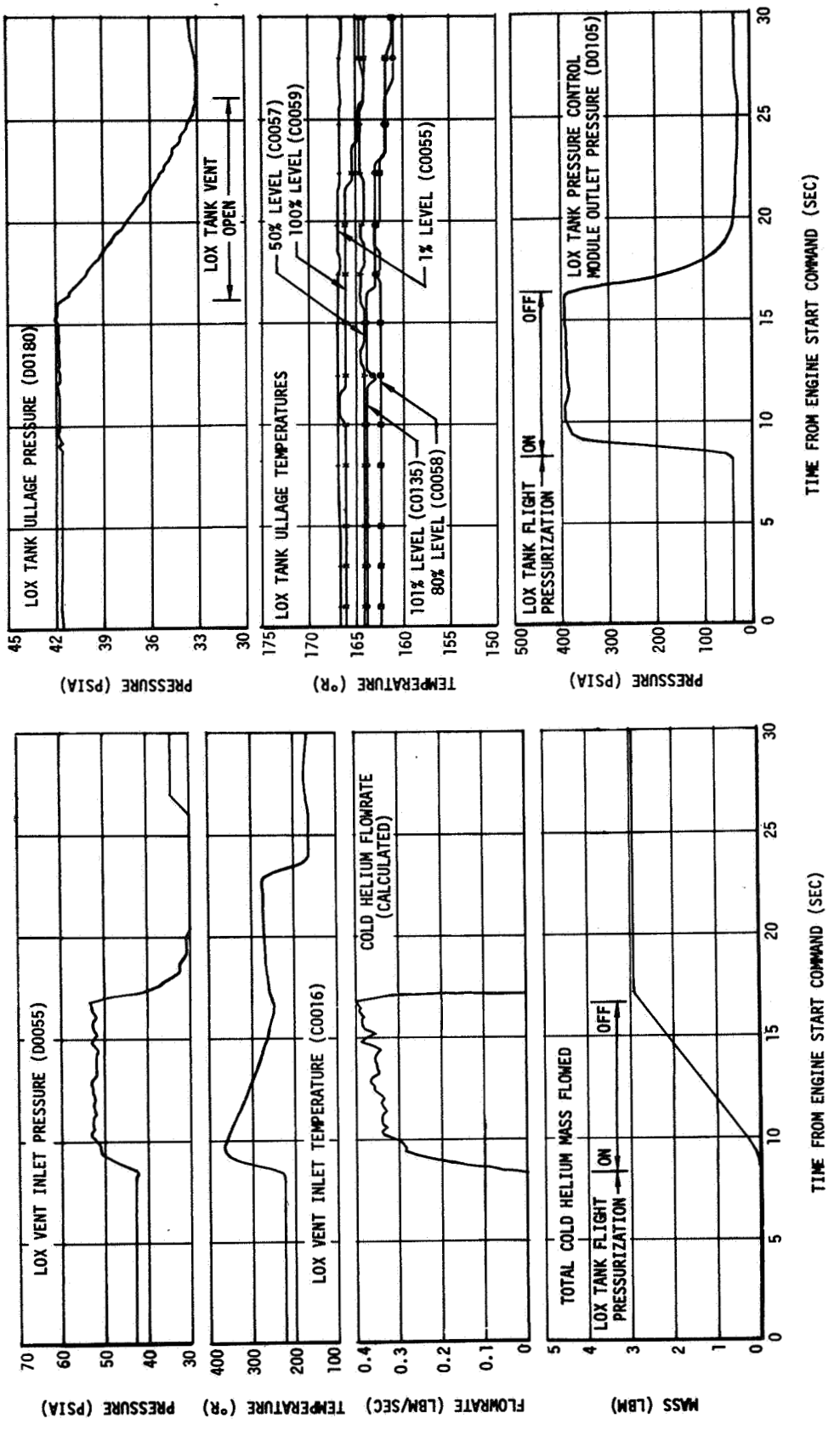

Figure 12-7. LOX Tank Pressurization System Performance - Second Burn

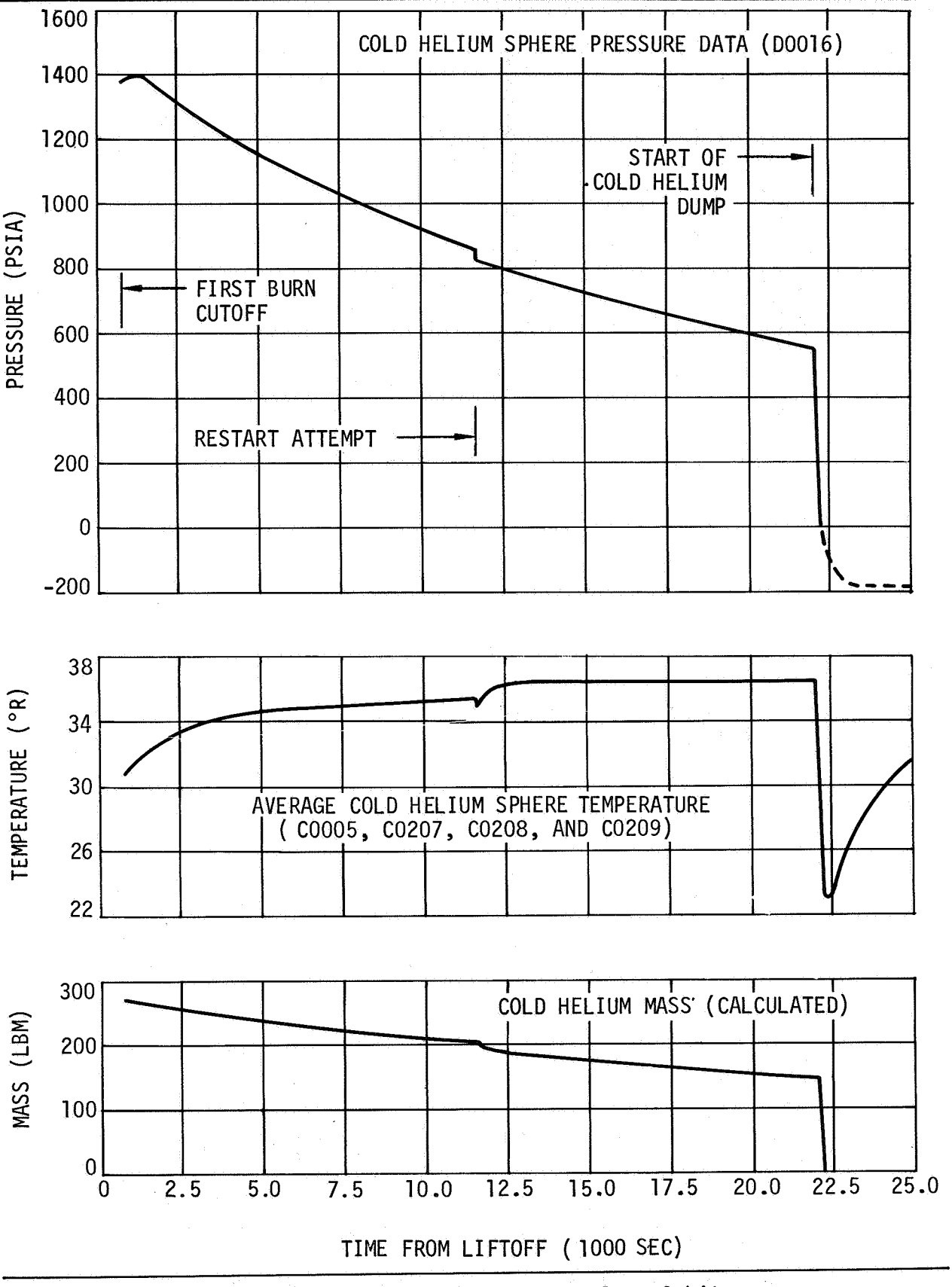

Figure 12-8. Cold Helium Supply - Orbit

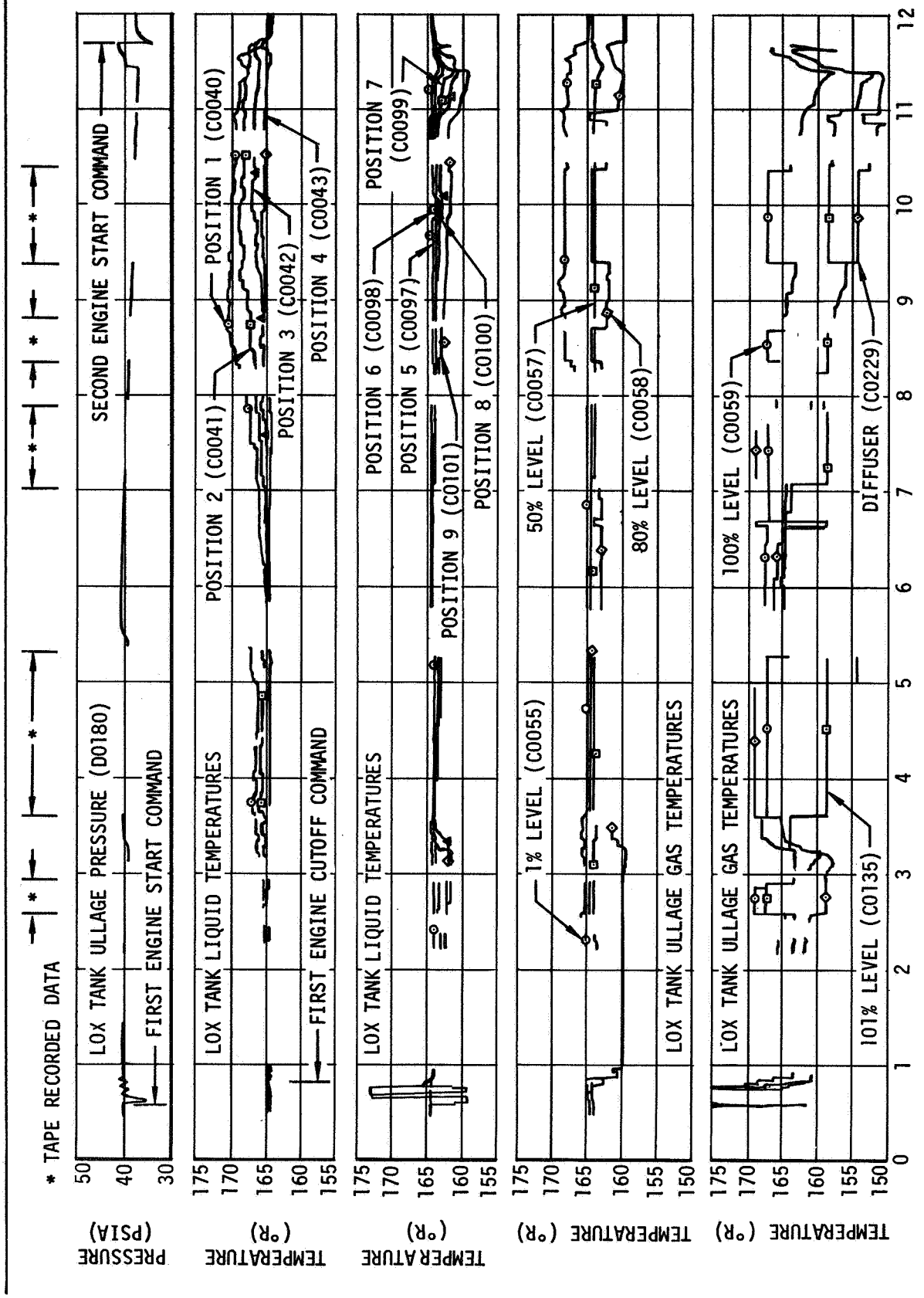

Figure 12-9. LOX Tank Conditions - First and Second Orbits

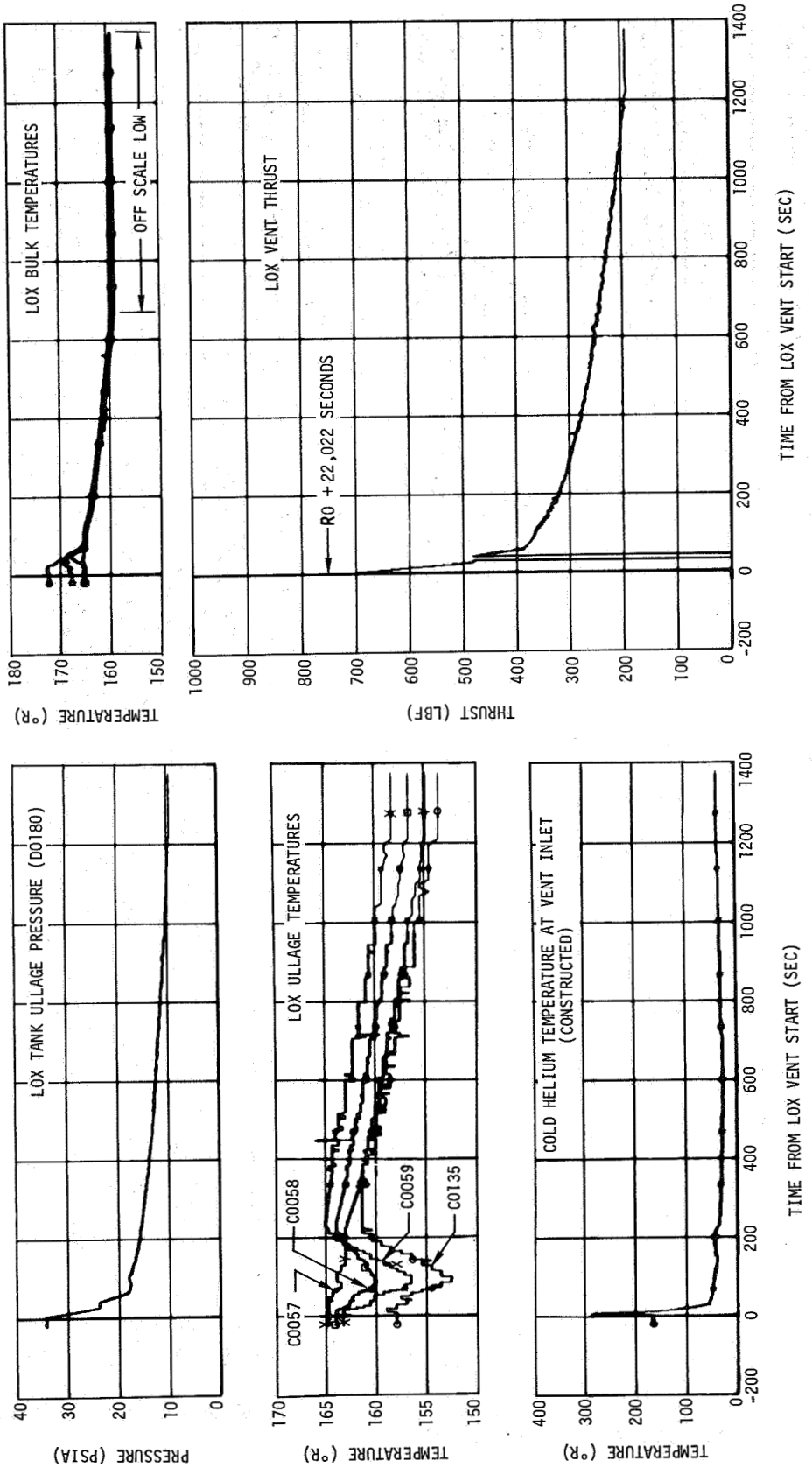

Figure 12-10. LOX Tank Conditions During LOX Tank Cold Helium Vent

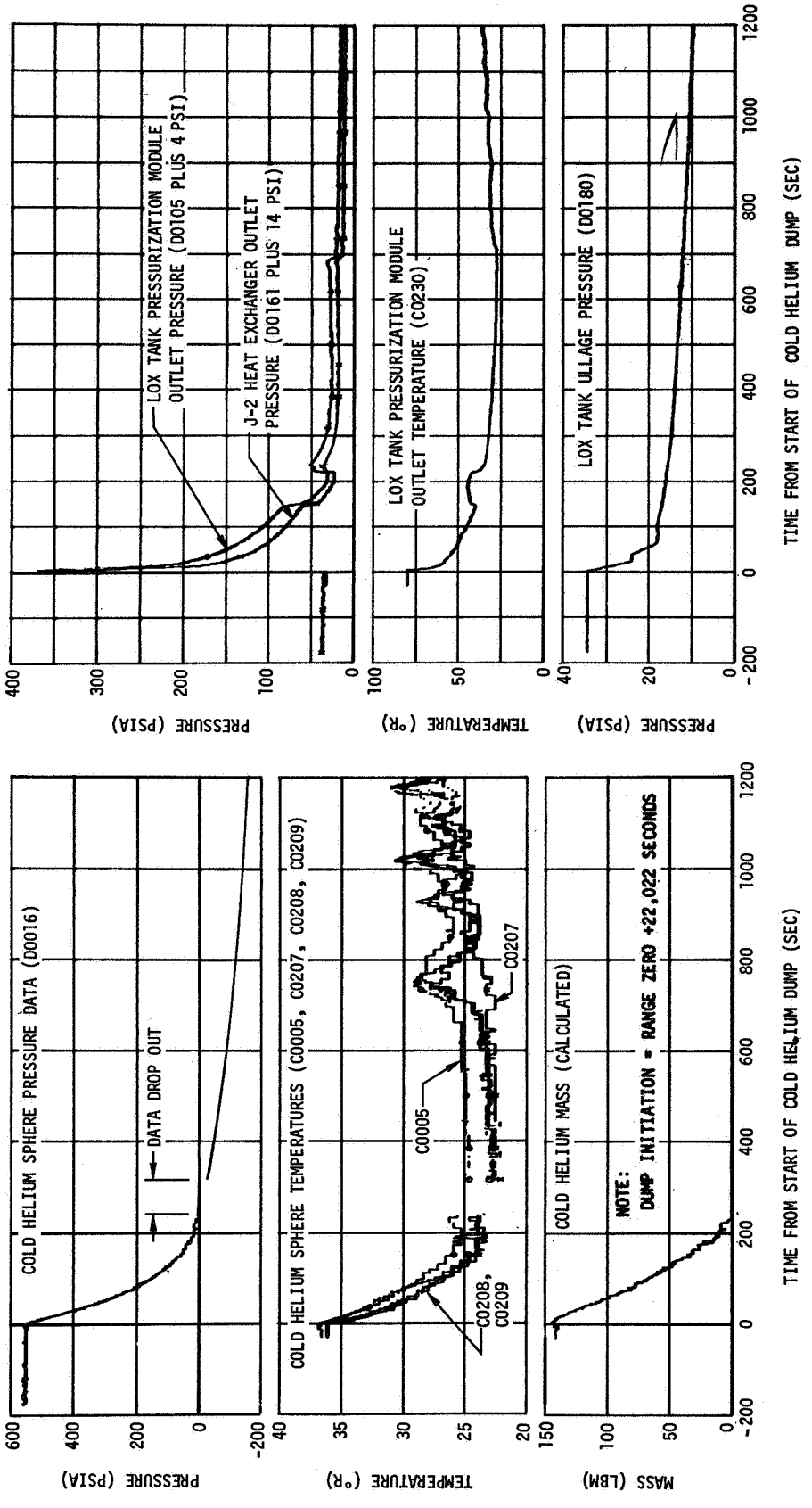

Figure 12-11. LOX Pressurization System Conditions - Cold Helium Dump

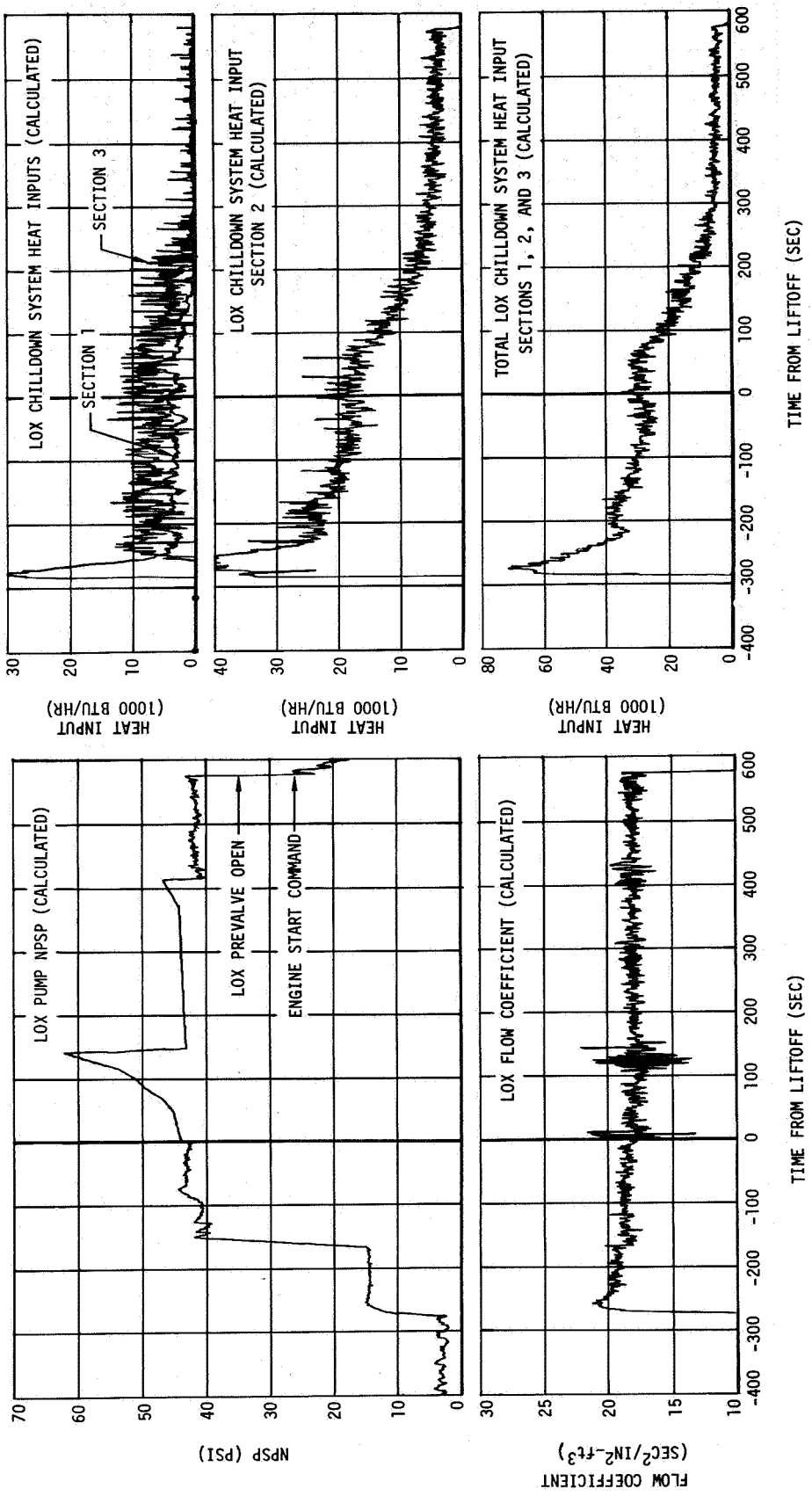

Figure 12-12. LOX Pump Chilldown System Performance - First Burn

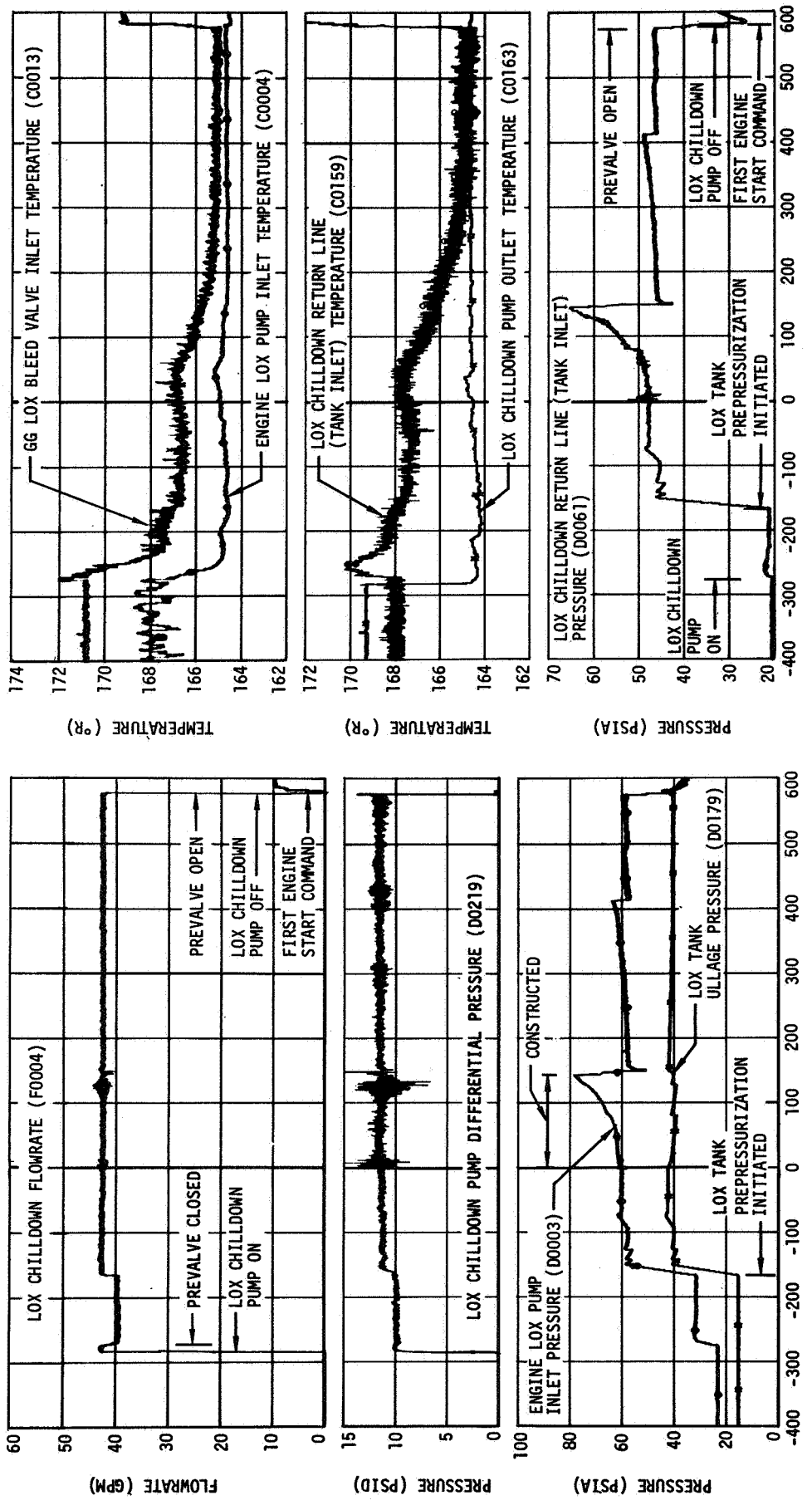

Figure 12-13. LOX Pump Chilldown System Operation - First Burn

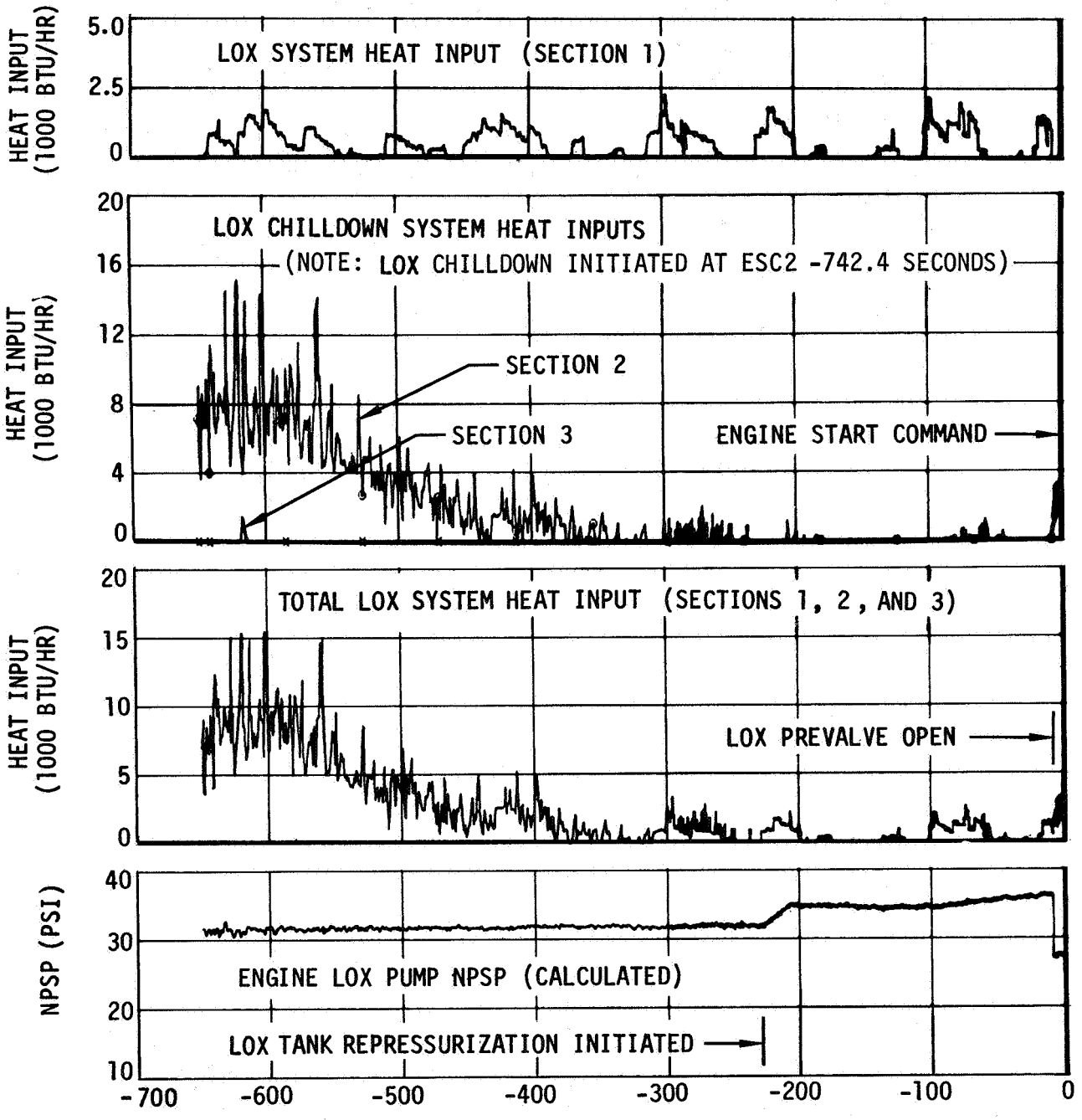

Figure 12-14. LOX Pump Chilldown System Performance - Second Burn

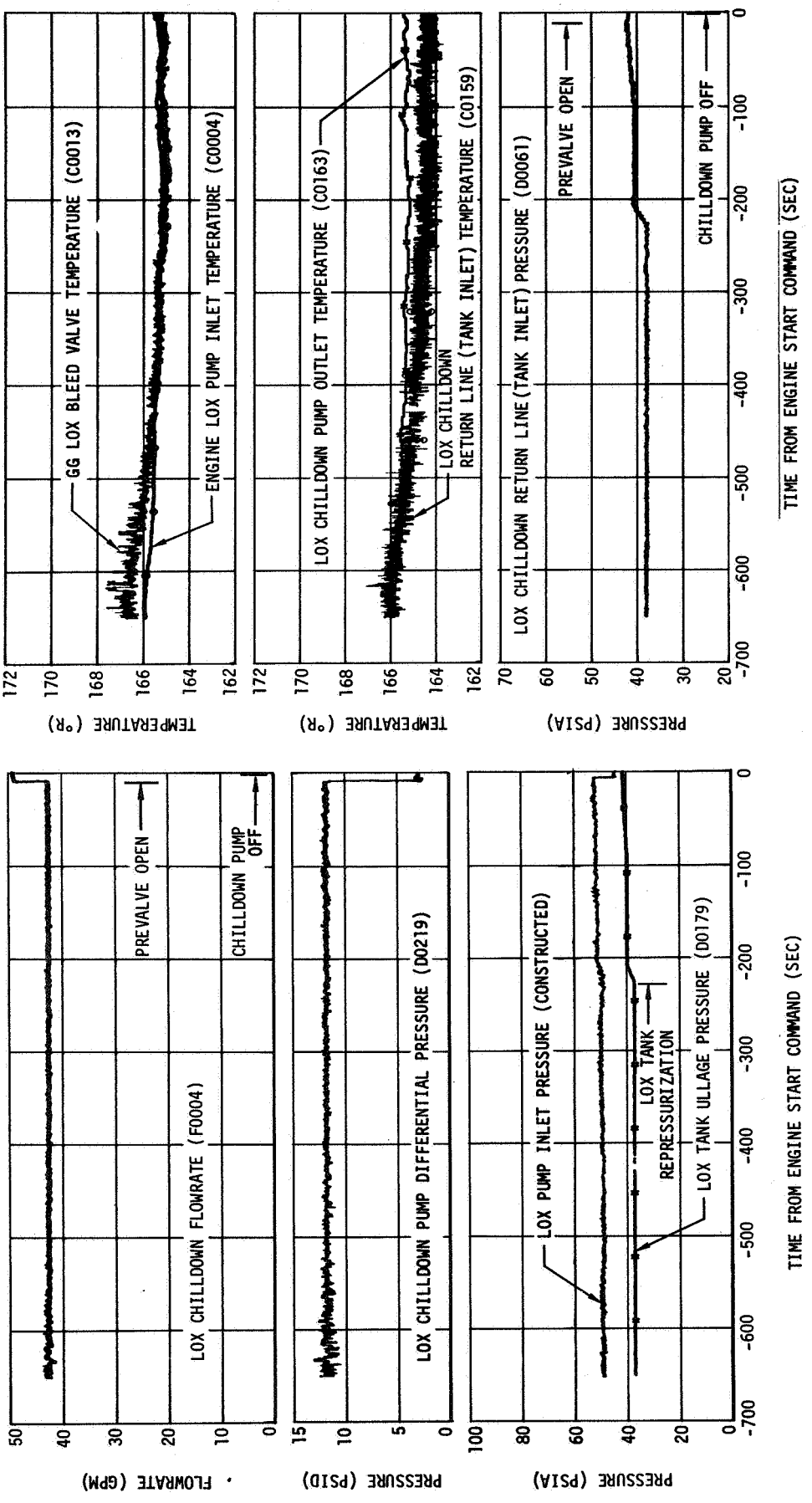

Figure 12-15. LOX Pump Chilldown System Operation - Second Burn

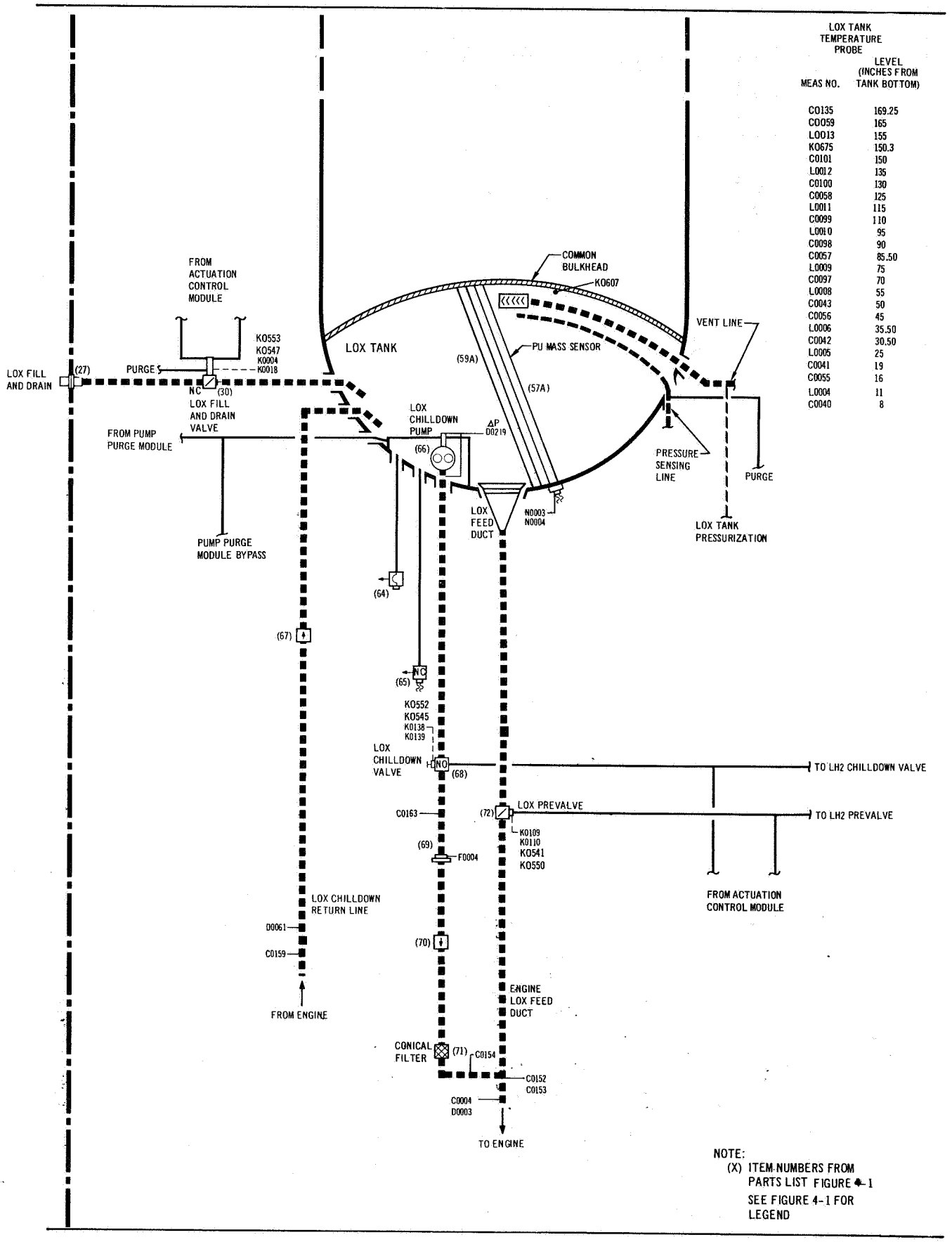

Figure 12-16. LOX Supply System

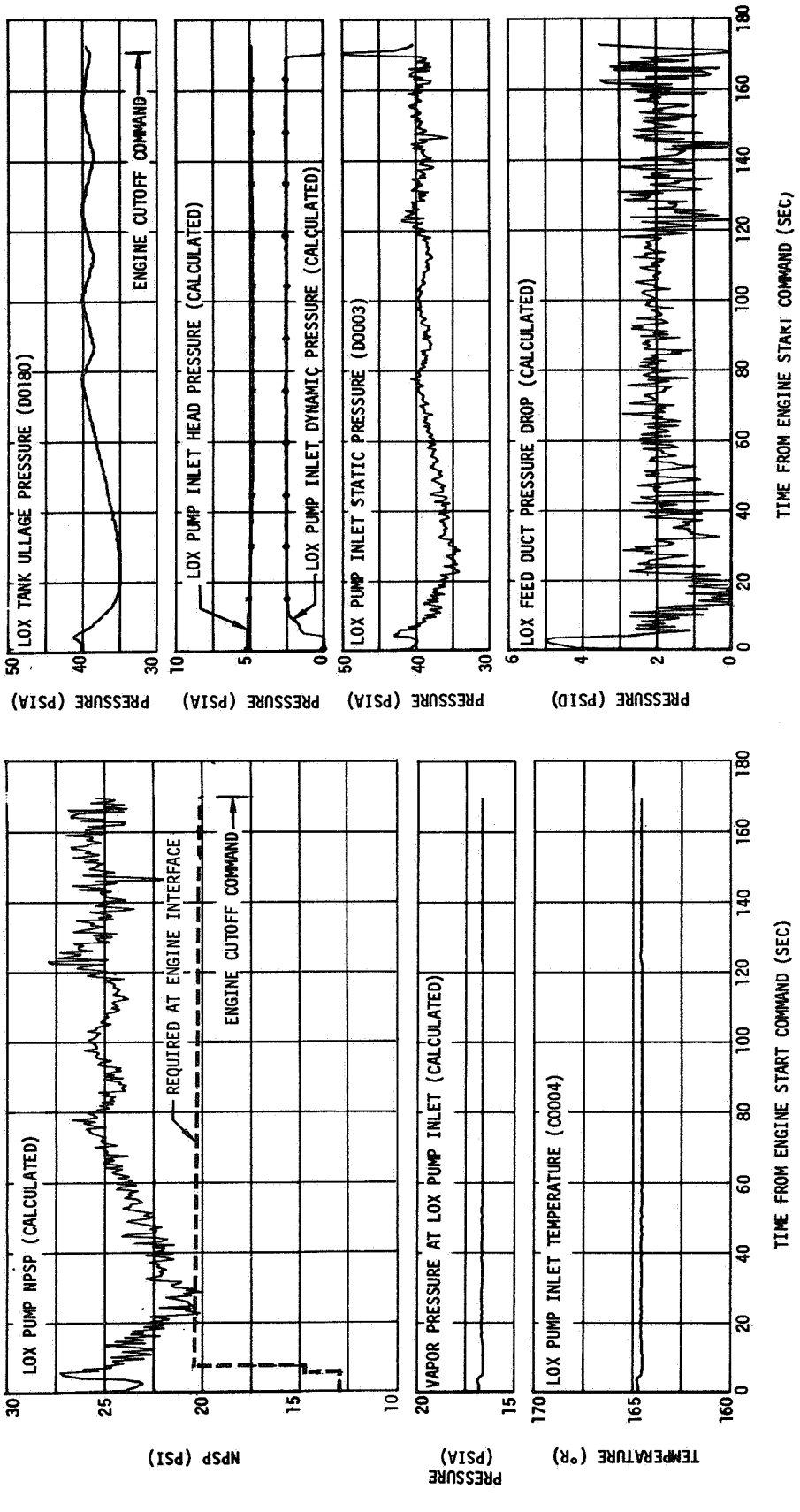

Figure 12-17. LOX Pump Inlet Conditions - First Burn

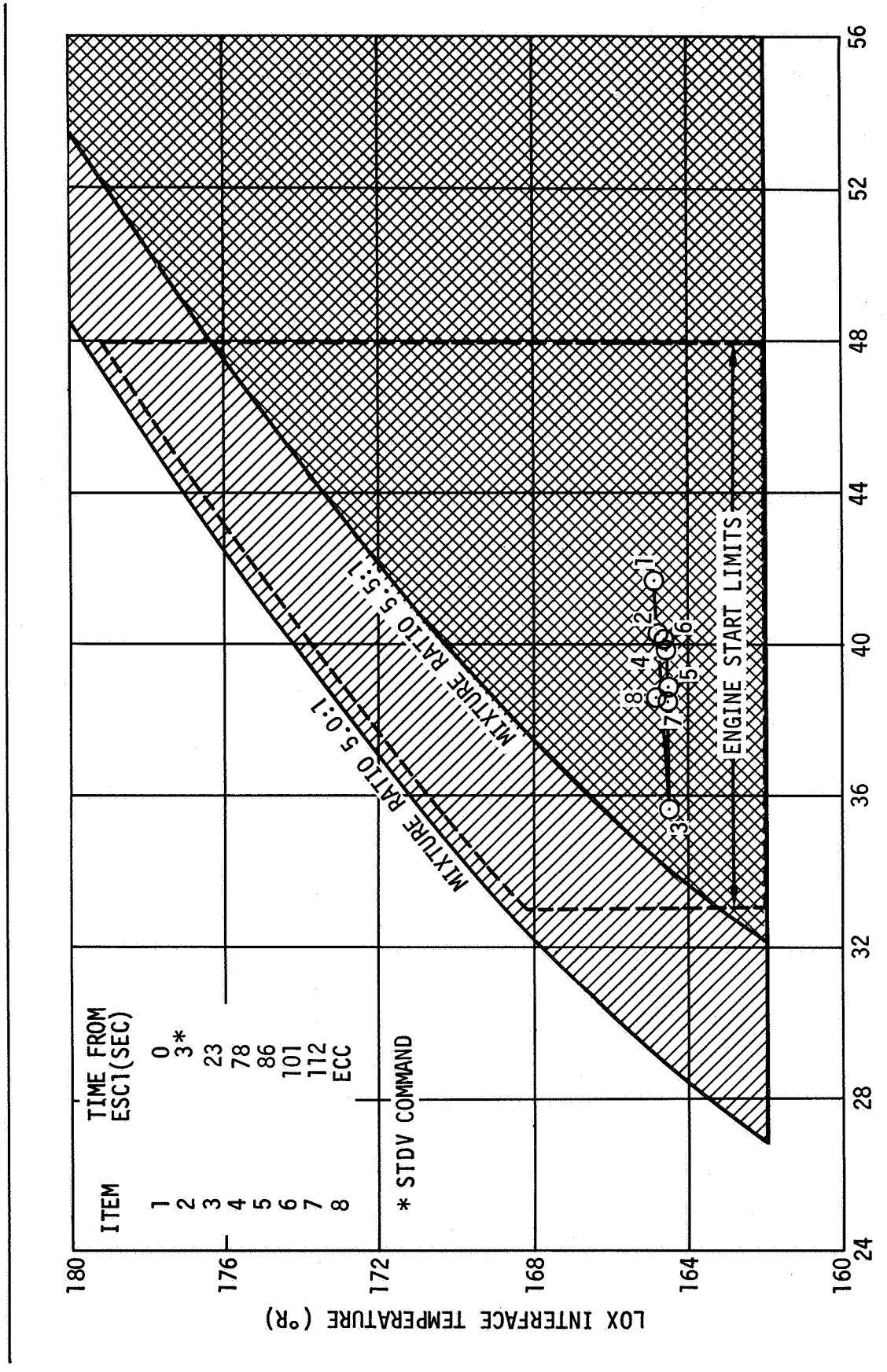

Figure 12-18. LOX Pump Interface Conditions - First Burn

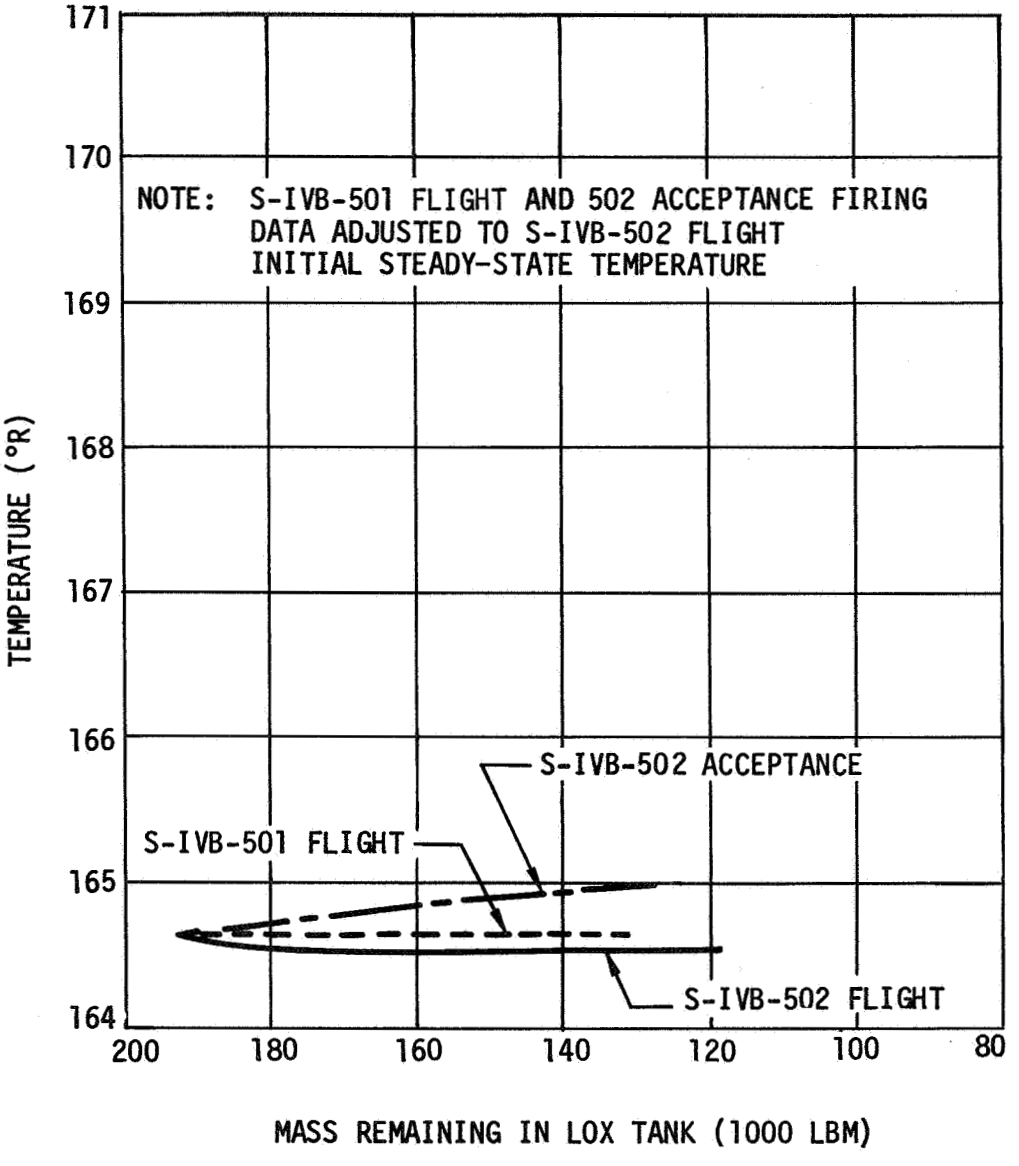

Figure 12-19. Effect of LOX Mass Level on LOX Pump Interface Temperature - First Burn

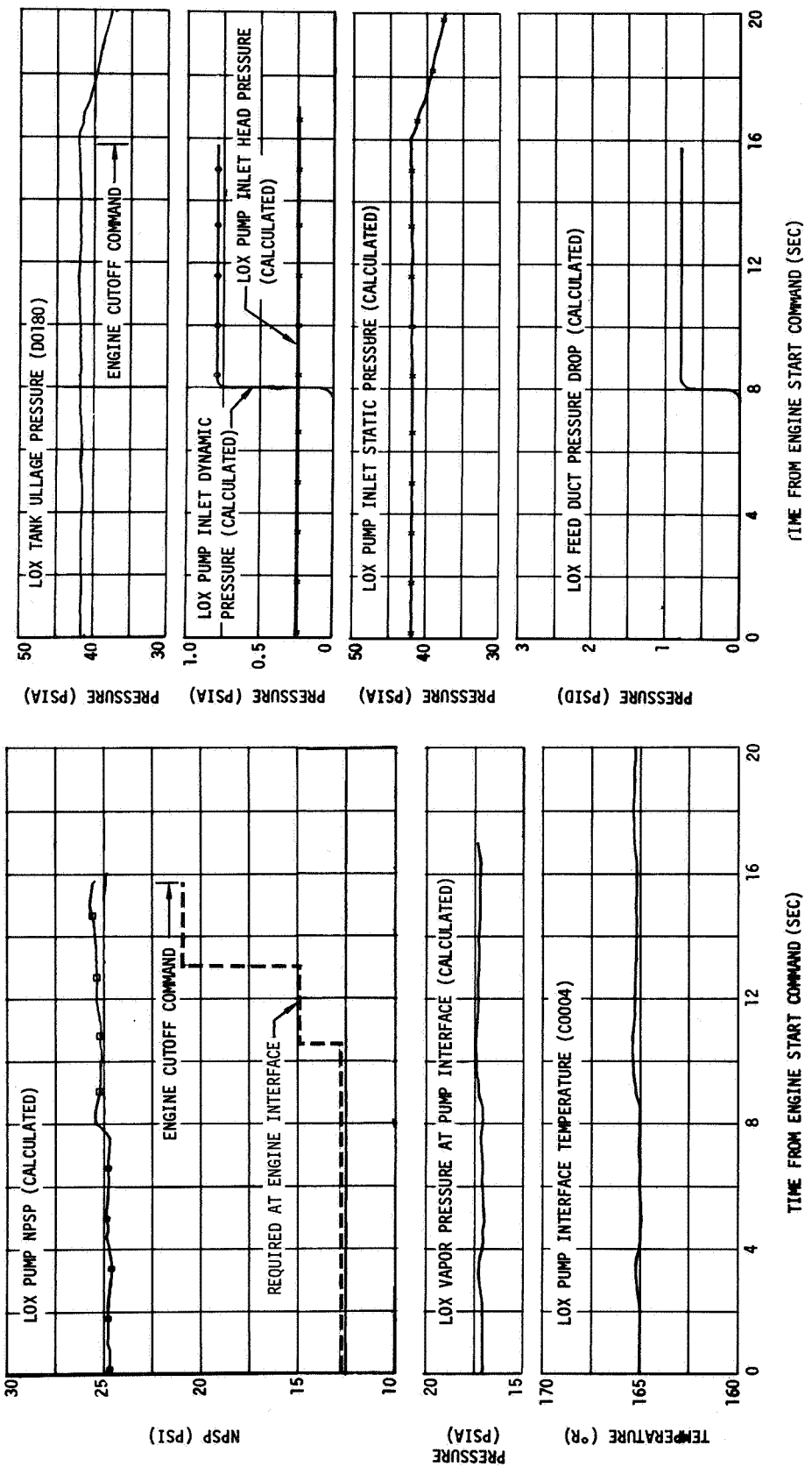

Figure 12-20. LOX Pump Inlet Conditions - Second Burn

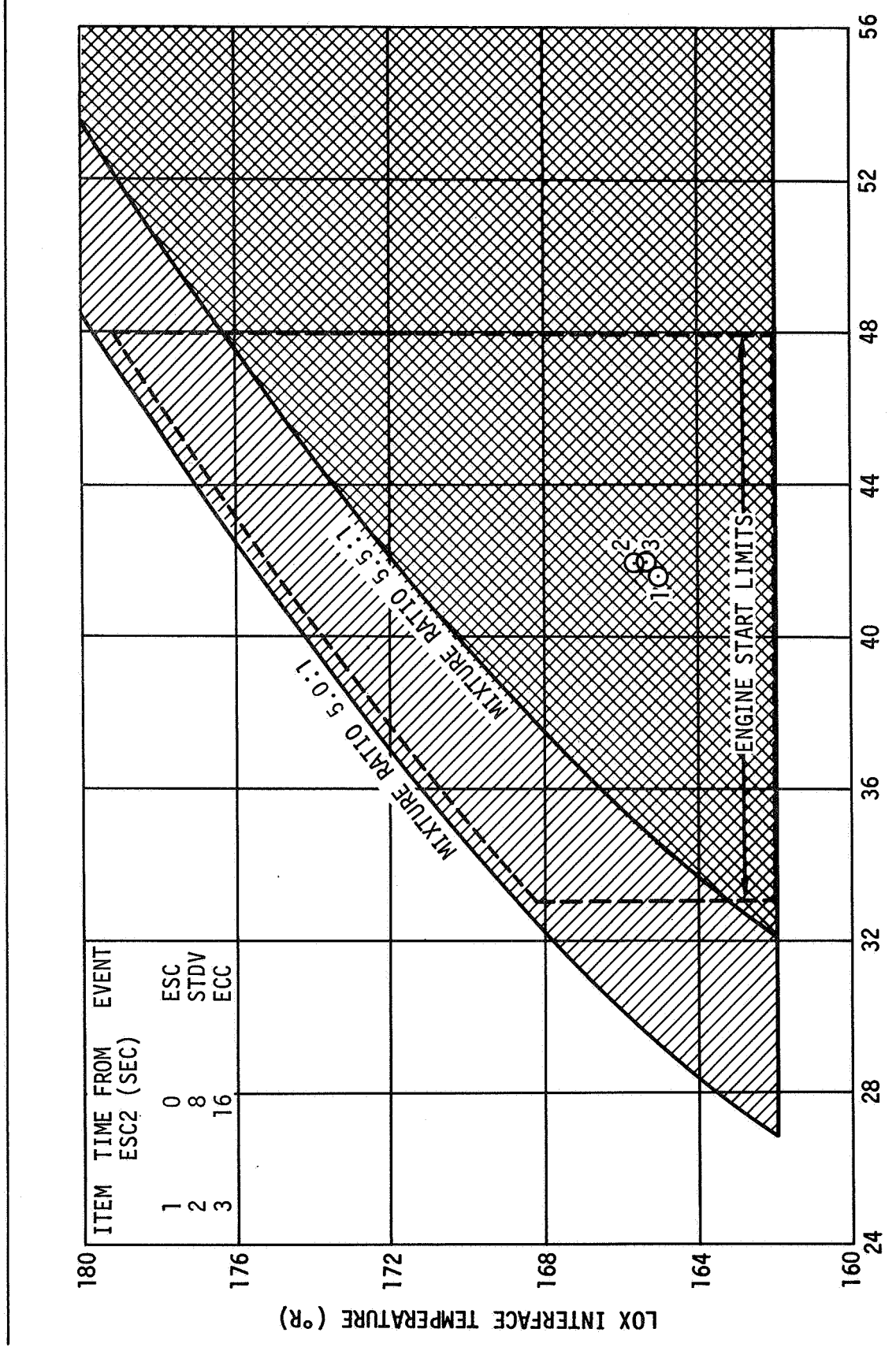

Figure 12-21. LOX Pump Interface Conditions - Second Burn

SECTION 13

FUEL SYSTEM

13. FUEL SYSTEM

The fuel system supplied LH2 to the engine as designed, and the NPSP exceeded minimum requirements at all times.

13.1 Pressurization Control

The LH2 tank pressurization system (figure 13-1) satisfactorily accomplished prepressurization, first burn GH2 pressurization, and second burn ambient helium repressurization. The system did not indicate any GH2 pressurization malfunction during the second burn restart attempt.

13.1.1 First Burn

13.1.1.1 Prepressurization

The LH2 tank conditions prior to prepressurization were 37 deg R and 16 psia. The LH2 prepressurization command was received at RO -96.3 sec, and the LH2 tank pressurized signal was received 21.3 sec later when the LH2 tank ullage pressure reached 33.8 psia. The ullage pressure continued to increase as the ullage warmed, reaching the relief setting of 36.2 psia by liftoff.

Approximately 7.1 lbm of helium were added during prepressurization. Considering the relative ullage volumes, this agrees well with the 8.8 lbm of helium required during the AS-501 flight prepressurization. Conditions from prepressurization to first burn Engine Start Command are summarized in figure 13-2 and compared with S-IVB-501 flight and S-IVB-502 acceptance firing data in table 13-1.

A minor decay and subsequent recovery in LH2 tank ullage pressure occurred immediately following liftoff. This decay, which may have been the result of ullage gas cooling due to sloshing, was probably aggravated by the small initial LH2 ullage volume (719 ft^3). A similar decay followed AS-203 flight liftoff (with an initial ullage volume of 750 ft^3). There was no discernible decay following AS-501 flight liftoff (with an initial ullage volume of 1,019 ft^3). A second ullage pressure decay resulted from a 10-sec LH2 relief vent period beginning at RO +120 sec which was followed by recovery. A short vent occurred at RO +180 sec, when the ullage pressure exceeded the vent relief setting. The relief vent then appears to have feathered with the LH2 ullage pressure at 36.2 psia until first burn Engine Start Command. Approximately 7 lbm of mixed GH2 and helium were vented from the LH2 ullage during the boost period.

13.1.1.2 Pressurization

At first burn Engine Start Command (ESC1) the LH2 tank ullage pressure was 36.2 psia. Between first engine start (which occurred at RO +577.3 sec) and approximately ESC +4.8 sec, the primary, control, and step pressurization orifices were open to provide a high GH2 pressurant flowrate to the LH2 tank during engine start. From ESC1 +4.8 sec until first burn Engine Cutoff Command (ECC1) at ESC1 +169.8 sec, the control and step pressurization orifices were closed, thus limiting the pressurization flow to the primary orifice. The

ullage pressure decreased normally and reached 32.6 psia at engine cutoff command. The ullage pressure profile was somewhat lower than expected, but was higher than the S-IVB-501 flight first burn pressure profile. The higher pressure was the result of the use of a larger undercontrol orifice (effective area of 0.0726 $in.^2$ on S-IVB-502 flight compared to 0.0606 $in.^2$ on S-IVB-501 flight). Minor ullage energy collapse may have occurred during first burn; however, the magnitude of the calculated collapse is of the same order as the error in the method of calculation. If energy collapse actually occurred, it was probably the result of heat loss from the warm ullage gases to the cold tank walls and/or liquid bulk/ullage gas interaction produced by the significant pitch maneuvers occurring throughout first burn. The actual pressure profile, although slightly lower than expected, was satisfactory.

The engine performance shift occurring at approximately ESC1 +120 sec resulted in an increase in LH2 tank inlet and LH2 tank pressurization module temperatures, and in a decrease in LH2 tank pressurization module pressure. These changes reflected similar changes (or shifts) in the LH2 injector temperature and pressure. The changes in pressurization module conditions resulted in a downward shift in LH2 pressurization flowrate. The timing and magnitude of the shift were such that there was no significant effect on the LH2 tank ullage pressure profile.

An LH2 tank vent occurred at ESC1 +7 sec, resulting in the loss of approximately 0.8 lbm of ullage gas. The GH2 pressurization flowrate was approximately 0.62 lbm/sec, providing a first burn total flow of 102 lbm. Conditions during first burn LH2 tank pressurization are summarized in figure 13-3 and compared with S-IVB-501 flight and S-IVB-502 acceptance firing data in table 13-2.

13.1.2 Second Burn

13.1.2.1 Repressurization

The LH2 tank was repressurized with ambient helium from seven repressurization spheres (4.5 ft^3 each). A 199 sec period of self-pressurization due to continuous vent system (CVS) closure preceded repressurization. Repressurization was initiated 127 sec before second burn Engine Start Command (ESC2), with the LH2 tank ullage pressure at 20.8 psia. The first repressurization cycle was terminated at ESC2 -90 sec when the ullage pressure upper switch setting of 33.8 psia was reached. By ESC2 -16 sec the ullage pressure had collapsed to the lower switch setting of 31.4 psia. At this time a makeup cycle was initiated, increasing the LH2 ullage pressure to 32.8 by ESC2 -1 sec when repressurization was automatically terminated. The ambient helium usage was 35.8 lbm during the first repressurization cycle and 8.1 lbm during the makeup cycle.

Reconstruction of the repressurization performance indicates that the initial repressurization cycle was nearly adiabatic and that most of the energy loss during repressurization (approximately 4,500 Btu) occurred during the subsequent pressure decay and makeup cycle. Liquid level measurements indicate that the 200 sec of ullaging prior to LH2 repressurization was successful in removing most of the subsurface GH2 bubbles. This is further substantiated by the lack of significant energy loss during the initial repressurization cycle

(the period during which the greatest loss due to bubble collapse would occur). Therefore the probable cause of the energy loss during the repressurization period was liquid bulk/ullage gas interaction resulting from the stage maneuver which began at the initiation of LH2 repressurization. This conclusion is supported by the temperature sensors which indicated some liquid disturbances prior to Engine Start Command.

Significant pressurization data are presented in figure 13-4 and compared to S-IVB-501 flight and S-IVB-502 acceptance firing data in table 13-3.

13.1.2.2 Pressurization

The LH2 tank ullage pressure at second burn Engine Start Command (RO +11,614.7 sec) was 32.8 psia. As a result of the failure of the engine to ignite, the LH2 tank pressurization GH2 flowrate (which is tapped off of the engine GH2 injector manifold) was negligible, and the LH2 ullage pressure consequently decayed rapidly as LH2 was drained from the tank, dropping to 30 psia by second burn Engine Cutoff Command (ESC2 +15.7 sec). There was no indication of any malfunction by the LH2 pressurization system during the restart attempt.

Second burn cutoff was immediately followed by a 2-min LH2 tank vent which brought the ullage pressure back down to the CVS operational pressure (approximately 20 psia). Significant pressurization data are presented in figure 13-5 and compared to S-IVB-501 flight and S-IVB-502 acceptance firing data in table 13-2.

13.2 Pressurization System Conditions During Orbit

13.2.1 LH2 Tank Nonpropulsive Vent and Relief Valve Operation

The nonpropulsive vent (NPV) and relief valve operated satisfactorily. During boost, the relief valve opened twice (paragraph 13.1.1) and apparently feathered to maintain the ullage pressure at 36.2 psia between the second vent and first burn Engine Start Command. The valve opened again at 36.2 psia at ESC1 +7 sec.

After second burn cutoff, the NPV valve was opened for 120 sec, dropping the ullage pressure from 30.0 to 20.4 psia (figure 13-6). The LH2 tank then self-pressurized to 22.7 psia by RO +12,830 sec, when the continuous vent valve was opened. The ullage pressure remained below the relief setting throughout the orbital portions of the mission.

At RO +22,024 sec, the valve was opened again, dropping the ullage pressure to approximately 0 psia by RO +27,600 sec.

13.2.2 LH2 Tank Continuous Vent System Performance

The CVS performed satisfactorily, maintaining the LH2 tank ullage pressure at an average level of 19.7 psia and providing an average acceleration of 5×10^{-5} g for propellant settling during coast. The LH2 disturbances caused by the 20-deg pitch maneuvers at RO +3,213 and RO +5,428 sec were settled by the CVS acceleration before fuel tank repressurization.

Continuous venting was initiated at RO +806 sec as evidenced by the almost instantaneous increase in nozzle pressures, the decrease in nozzle temperatures, and the rapid decay of ullage pressure (figure 13-7). Two data problems encountered on the AS-501 flight were resolved by the relocation of the nozzle pressure transducers. After continuous venting was terminated, both nozzle pressures, unlike the S-IVB-501 nozzle pressures, dropped to and remained at approximately 0 psia (figure 13-8). Also unlike the S-IVB-501 nozzle pressures, the S-IVB-502 nozzle pressures were generally in good agreement (within 1 psi) during periods of good data.

The nozzle temperatures were lower on S-IVB-502 than on S-IVB-501. This resulted from the lower ullage temperatures, which were caused by the attitude maneuvers. The nozzle temperatures were cycling about a level which caused the tape recorder to alternately pick up and drop a data bit. The nozzle temperature transducer calibration curve was such that the alternate gain and loss of the data bit resulted in an erroneous indicated temperature cycling between approximately 7 and 48 deg R. Since the tape recorded data comprised a significant portion of the data for the first two orbits, only an approximate calculation of 2,870 lbm for the total vented mass was possible. CVS operation and performance are shown in figures 13-7 and 13-9, respectively, for the first and second orbits.

At RO +12,830 sec, following the nonpropulsive venting, continuous venting was initiated again and continued until RO +21,830 sec. During this time, the ullage pressure was maintained at an average pressure of 19.7 psia (figure 13-10).

During the third and fourth orbits, data were available only over ground stations. System operation parameters and system performance calculations are shown for the available third and fourth orbit data in figures 13-10 and 13-11, respectively. Extrapolating between station data yielded a total vented mass of 1,993 lbm during the third and fourth orbits.

13.2.3 LH2 Tank Conditions During Orbit

13.2.3.1 LH2 Tank Conditions During First and Second Orbits

LH2 tank conditions during the first and second orbits are shown in figures 13-7 and 13-8. The ullage temperatures were similar to those observed on S-IVB-501. Except for the 101 percent probe (C0039), the temperature probes indicated an environment which could have been either gaseous or liquid during most of the first two orbits. Prior to the start of ullaging, the forward dome liquid-vapor sensors indicated mainly dry, with erratic wetting, down to S-IVB sta 548. The erratic wetting indicates possible LH2 entrapment under the deflector.

Rapid drying of the S-IVB sta 528 level sensors (C2028 and C2026) occurred during ullaging. A comparison of these levels with those expected from the LH2 mass at first burn cutoff minus the calculated boiloff indicates as much as 1,300 ft^3 of gas were entrapped in the liquid prior to the start of ullaging. Considering meniscus and liquid disturbance effects, an entrapped gas volume of approximately 1,000 ft^3 may be more realistic. Using the first burn cutoff LH2 mass and the CVS vented mass, an approximate boiloff of 3,024 lbm was calculated.

13.2.3.2 LH2 Tank Conditions During Third and Fourth Orbits

Within 50 sec after second burn Engine Start Command, most liquid sensors were wet. This indicates that large liquid disturbances were caused by the restart attempt, venting, and launch vehicle/spacecraft separation. The NPV was opened for 120 sec immediately after the restart attempt and vented a calculated 299 lbm. The nozzle temperatures decreased rapidly, then leveled out at an indicated 39 deg R. Although this is above the saturation temperature, the temperature profile (figure 13-10) indicates that saturated gas was flowing through the vent. The difference between the indicated temperature and saturation temperature is well within transducer accuracy. During the third and fourth orbits only the 101 percent temperature probe occasionally indicated above 60 deg R (figure 13-10). This indicates that conditions in the tank during the third and fourth orbits were similar to the tank conditions during the first and second orbits.

13.2.3.3 LH2 Tank Passivation

LH2 tank passivation was initiated at RO +22,024 sec by opening the nonpropulsive vent. The LH2 tank ullage pressure decayed rapidly until saturated conditions were attained approximately 14 sec later (figure 13-12). Subsequent to this time, the pressure decay rate decreased because of LH2 flashoff. At RO +22,205 sec, the ullage pressure decay rate decreased again while the NPV nozzle pressure decay rate increased sharply. This phenomenon may be explained by a decrease in the quality of the fluid flowing through the NPV lines. Subsequent data indicate that the flow out of the tank was only slightly more than enough to overcome self-pressurization by LH2 boiloff.

Based on nozzle conditions and the assumption of gas flow only, the flowrate through the NPV system would have been 1.9 lbm/sec. Heat input to the tank and the heat available from the liquid bulk as the pressure decreased were sufficient to boil off only 0.35 lbm/sec. These conflicting calculations indicate either that the flow area in the NPV system was restricted or that the fluid flowing through the system was two-phase or liquid. Since the nozzle pressure data do not indicate a restriction in flow area, the two-phase or liquid flow is more probable. This theory is consistent with the indications discussed in the preceding paragraph.

Effective stage attitude control was lost at RO +22,030 sec, and the thrust from the LOX vent caused the stage to tumble. The internal tank temperatures indicated that the centrifugal force developed from this motion could have forced the LH2 to the top of the tank and, thus, over the LH2 vent inlet. This condition would allow only two-phase or liquid flow through the NPV and could provide an explanation for the observed phenomenon. With a flow coefficient calculated for the post restart attempt all-gas blowdown, a liquid flowrate was calculated to be 14.8 lbm/sec. This flowrate would remove most of the liquid from the tank in 1,500 sec; a flow with the quality of 0.01 would deplete the tank sufficiently to uncover the vent in approximately 1,800 sec, and a blowdown of the tank ullage would then be expected. At RO +24,170 sec, when data were recovered after a dropout, a blowdown was occurring. Extrapolating the pressure profile back, the blowdown would have started at approximately RO +23,950 sec, thus indicating approximately 1,700 sec of liquid and/or two-phase flow.

Some liquid would be expected to remain in the tank after the blowdown began. As the tank pressure dropped below the triple point (1.02 psia), solidification and then sublimation would occur. At RO +27,600 sec, after a data dropout, two low-range temperature transducers (C0052 and C0053) were off-scale-low (below 35 deg R), while all other transducers were off-scale-high. The high range transducers indicated from 80 to 115 deg R and were increasing. By RO +33,300 sec, after another data dropout, C0053 was also off-scale-high (about 47 deg R); and C0052 was the only transducer in the LH2 tank indicating cold temperatures. These data suggest that solid hydrogen had formed at the lower end of the instrumentation probe and was slowly sublimating.

13.3 LH2 Pump Chilldown

13.3.1 First Burn

The LH2 pump chilldown system performed adequately. The LH2 chilldown was initiated at RO -299 sec and was continuous until RO +577.4 sec when the LH2 prevalve was opened. The chilldown pump was turned off at RO +578.5 sec. The engine pump inlet pressure and temperature were 42.5 psia and 38.3 deg R at first burn Engine Start Command. Table 13-4 compares significant LH2 chilldown system performance data with S-IVB-501 flight data and S-IVB-502 acceptance firing data. The chilldown system temperatures, pressures, and calculated performance are presented in figures 13-13 and 13-14.

The unpressurized chilldown flowrate stabilized at 92 gpm after the start transients subsided and the prevalve closed. After prepressurization the flowrate was 133 gpm until first engine start. All heat inputs during pressurized chilldown were lower in flight than during acceptance testing. The total rate was constant at 17,000 Btu/hr for 30.0 sec before first engine start as compared to 56,000 Btu/hr during acceptance testing.

During unpressurized chilldown, the LH2 pump inlet was slightly subcooled; immediately following pressurization, the temperature decreased to a minimum of 38 deg R as the flowrate increased. By Engine Start Command, the LH2 pump inlet temperature had increased to 38.3 deg R reflecting the LH2 bulk warming. All chilldown system temperatures reflected this warming.

The bleed valve and return line temperature increased sharply at the initiation of prepressurization because all of the heat input went into heating the pressurized fluid and no vaporization occurred. The LH2 entered the system sufficiently subcooled to absorb all the heat input to the system without reaching saturation temperature. After pressurization the ullage pressure was constant but the pump inlet pressure increased and decreased with acceleration until the prevalve was opened and allowed essentially all flow to return to the LH2 tank through the prevalve with no flow through the chilldown system. The pump inlet pressure then decreased (because of loss of pump head) to 35.9 psia.

The NPSP at the pump inlet followed the ullage pressure during pressurization and reached a maximum of 29 psi when maximum acceleration was reached at S-IC cutoff. The NPSP dropped at S-IC cutoff and increased with S-II acceleration. With the loss of two S-II engines the

NPSP dropped from 25.8 psi to 24.8 psi and maintained that level until S-II cutoff. When the S-IVB LH2 prevalve was opened, the NPSP dropped to 15.9 psi because of the loss of pump head.

The LH2 prevalve was somewhat slow in opening during S-IVB first burn. No opening requirement exists for the prevalve per se, but the prevalve is required to be open to allow a 3-sec fuel lead prior to the start tank discharge valve (STDV) opening. Under the current sequence, the prevalve open command was given 0.672 sec prior to first burn Engine Start Command. The valve started to move 0.187 sec after engine start, as indicated by the drop-out of the closed position microswitch. The full open prevalve position was received 2.418 sec after engine start, and STDV command occured 0.616 sec later. Investigation is continuing to determine the cause of the valve opening slowly and its effects on the fuel lead.

The flow coefficient was calculated from flowrate and chilldown system pressure drop data to be 19.0 $sec^2/in.^2-ft^3$, which was within the range calculated for previous S-IVB stages. The coefficient was used to compute the average fluid quality during the unpressurized phase of the chilldown.

Prior to prepressurization, two-phase flow existed in section 2 (engine pump inlet to the bleed valve) and in section 3 (engine bleed valve to tank inlet); the average fuel quality was 0.046 lbm gas/lbm mixture. The quality decreased to zero during prepressurization when the fluid in the system became subcooled. The LH2 chilldown system pressure drop was relatively steady during the unpressurized and pressurized operations at 9.0 psi and 6.4 psi, respectively.

13.3.2 Second Burn

The LH2 pump chilldown for second burn differed from that for first burn in that it started with no indication of liquid at the engine inlet. The chilldown was initiated at RO +10,877.2 sec, the predicted time. The total chilldown period was approximately 180 sec longer than predicted due to a launch vehicle digital computer time update resulting in a later than expected second burn Engine Start Command.

The recirculation chilldown system performed satisfactorily. At second engine start, the pump inlet pressure and temperature of 32.6 psia and 39.4 deg R were within the engine start requirements. The pump inlet NPSP at Engine Start Command was 9.5 psi, which was 3.2 psi above the required minimum limit of 6.3 psi (figure 13-15 and 13-16).

The LH2 chilldown pump was started at ESC2 -737.4 sec with the LH2 tank pressure being maintained by the continuous vent regulator. At ESC2 -325.8 sec the CVS was terminated allowing the tank to self pressurize until ESC2 -127 sec when the LH2 tank was pressurized. The Prevalve OPEN Command was issued at ESC2 -10.79 sec with the valve starting to open at ESC2 -9.824 sec. The full open position was attained at ESC2 -5.909 sec.

Before termination of the CVS, chilldown was marked by small pressure and flow fluctuations caused by the rapid vaporization of LH2 as it entered the system and came in contact with the warm hardware. This cycling is reflected throughout the system in the pressure and temperature data. The magnitude of the cycling decreased with time during the unpressurized chilldown period as the system hardware was cooled.

After the termination of the CVS, the cyclic action of the system flowrate, pressures, and temperatures stopped due to subcooled liquid caused by the slight self pressurization of the tank. During the tank self pressurization period, the chilldown flowrate increased from 100 to 128 gpm, and the pump inlet temperature and pressure decreased from 39.02 deg R and 27.5 psia to 38.8 deg R and 27.3 psia, respectively. A comparison of the mass of LH2 entering the chilldown system is presented in figure 13-17.

When the LH2 tank was pressurized for second burn at ESC2 -127 sec the chilldown flowrate increased from 128 gpm to 133 gpm. The NPSP dropped from 16.94 psi when the prevalve was commanded open at ESC2 -10.79 sec to 11.24 psi when the prevalve reached the full open position. At second burn Engine Start Command the pump inlet temperature and pressure were 39.4 deg R and 32.6 psia yielding an NPSP of 9.5 psi which is 3.2 psi above the required minimum of 6.3 psi. Figure 13-18 compares the total heat input rate to those obtained from S-IVB-501 and S-IVB-203 flights.

13.4 Engine LH2 Supply

13.4.1 First Burn

The LH2 supply system (figure 13-19) delivered the necessary quantity of LH2 to the engine pump inlet throughout first burn and maintained the pressure and temperature within a range that provided an LH2 pump NPSP that was at least 5.4 psi above the minimum requirement. The data and calculated performance are presented in figure 13-20. Table 13-5 compares the S-IVB-502 flight data with that from previous stages.

The LH2 pump inlet temperature and pressure during engine operation were plotted in the engine operating region in figure 13-21 which shows that conditions were met satisfactorily throughout first burn.

Figure 13-22 is a plot of the pump inlet temperature as a function of the propellant mass remaining within the LH2 tank and includes previous stage data for comparison. As the figure shows, the data from the three tests agree closely.

13.4.2 Second Burn

The NPSP, LH2 pump interface static pressure, and LH2 pump interface temperature during second burn attempt are shown in figure 13-23. The NPSP at second burn Engine Start Command was 3.2 psi above the minimum required.

The fuel pump inlet pressure and temperature were plotted in the second start region (figure 13-24) and indicate that the engine fuel pump inlet conditions were satisfactorily met. Table 13-5 compares the LH2 supply data with that from S-IVB-501 flight and S-IVB-502 acceptance firing.

TABLE 13-1
LH2 TANK PREPRESSURIZATION DATA

PARAMETER	UNIT	S-IVB-502 FLIGHT	S-IVB-501 FLIGHT	S-IVB-502 ACCEPT
Prepressurization duration	sec	21.3	21.5	41.0
Ullage volume	cu ft	719.0	1,019.0	1,174.0
Helium mass added	lbm	7.1	8.8	17.4
Ullage pressure				
At prepressurization initiation	psia	16.0	17.5	15.3
At prepressurization termination	psia	33.8	33.8	33.6
At liftoff*	psia	36.2	35.9	35.0
At Engine Start Command	psia	36.2	35.9	36.0
Rate of increase after prepressurization	psi/min	1.5	1.0	1.3
Events	sec from liftoff*			
Prepressurization initiation		-96.3	-96.5	-114.0
Prepressurization termination		-75.0	-75.0	-73.0
Engine Start Command		577.3	520.7	511.0

*During acceptance testing, liftoff is simulated.

TABLE 13-2
LH2 TANK PRESSURIZATION DATA

PARAMETER	UNITS	S-IVB-502 FLIGHT		S-IVB-501 FLIGHT		S-IVB-502 ACCEPT	
		FIRST BURN	SECOND* BURN	FIRST BURN	SECOND BURN	FIRST BURN	SECOND BURN
Pressure switch setting							
Lower	psia	28.7	32.2	28.0	31.6	29.2	30.1
Upper	psia	30.2	33.8	30.5	33.6	31.5	34.3
Ullage pressure							
At Engine Start Command	psia	36.2	32.8	35.9	27.8	36.2	33.5
At Engine Cutoff Command	psia	32.6	30.0	29.0	31.9	28.7	32.8
GH2 pressurant flowrate							
Undercontrol--high EMR	lbm/sec	0.62	--	0.50	--	0.50	0.50
Undercontrol--low EMR	lbm/sec	--	--	--	--	--	0.47
Overcontrol--high EMR	lbm/sec	--	--	--	0.75	--	--
Overcontrol--low EMR	lbm/sec	--	--	--	0.70	--	0.72
Total GH2 added	lbm	102	--	70.1	206	76	161.8

*GH2 pressurant flowrate during S-IVB-502 restart attempt was negligible.

TABLE 13-3
LH2 TANK REPRESSURIZATION DATA

PARAMETER	UNITS	S-IVB-502 FLIGHT	S-IVB-501 FLIGHT	S-IVB-502* ACCEPT
Repressurization duration	sec	52**	80	279
Helium usage from repressurization spheres during repressurization	lbm	43.9***	47	40.5
Ullage				
Volume	cu ft	4,451	4,260	4,780
Pressure at repressurization initiation	psia	20.8	19.7	15.5
Pressure at repressurization termination	psia	32.8	32.0	32.9
Events	sec from ESC2			
Repressurization initiation		-127	-325	-322
Repressurization termination		-1	-245	-43

*The repressurization system was supplemented by the auxiliary pressurization system. This is not accounted for in mass calculations.

**This includes 37 sec during the first repressurization cycle and 15 sec during the makeup cycle.

***This includes 35.8 lbm used during the first repressurization cycle and 8.1 lbm used during the makeup cycle.

TABLE 13-4 (Sheet 1 of 2)
LH2 CHILLDOWN SYSTEM PERFORMANCE DATA

PARAMETER	UNITS	S-IVB-502 FLIGHT		S-IVB-501 FLIGHT		S-IVB-502 ACCEPT	
		FIRST BURN	SECOND BURN	FIRST BURN	SECOND BURN	FIRST BURN	SECOND BURN
NPSP							
At Engine Start Command*	psi						
With Chill Pump Head		22.8	N/A	21.5	N/A	N/A	N/A
Without Chill Pump Head		15.9	9.5	13.41	0.17	14.3	10.5
Minimum required at engine start	psi	6.3	6.3	6.3	6.3	6.3	6.3
Maximum during chilldown	psi	29.0	18.9	27.3	16.5	25.6	18.6
Average flow coefficient	$sec^2/in.^2ft^3$	19.0	19.0	16.5	16.5	18.8	18.8
Fuel quality in sections** 2 and 3	lb gas/ lb mixture						
Maximum during unpressurized chilldown		0.0495	N/A	0.023	N/A	0.049	0.29
At prepressurization		0.045	N/A	0.020	N/A	0.042	0.065
Fuel pump inlet conditions							
Static pressure at Engine Start command*	psi						
With Chill Pump Head		42.5	N/A	43.9	N/A	N/A	N/A
Without Chill Pump Head		35.6	32.6	35.8	28.0	38.2	35.1
Temperature at Engine Start Command	deg R	38.3	39.4	38.9	40.7	39.6	39.8
Amount of subcooling at engine start (deg below saturation at pump inlet)	deg R	5.7	2.5	3.6	0.08	3.7	2.7
Heat absorption rate during unpressurized chilldown							
Section 1**	Btu/hr	22,000	0.0†	8,200	N/A	19,000	21,000
Sections 2 and 3**	Btu/hr	29,000	28,000†	27,500	N/A	25,000	35,000
Total	Btu/hr	51,000	28,000†	35,700	N/A	44,000	56,000

*The S-IVB-501 flight and S-IVB-502 flight first burn NPSP's and pump inlet pressure's are high at this time as the prevalves were slow in opening.

**Section 1 is tank to pump inlet; section 2 is pump inlet to bleed valve; section 3 is bleed valve to tank.

†Values at repressurization initiation.

N/A = Not Applicable

TABLE 13-4 (Sheet 2 of 2)
LH2 CHILLDOWN SYSTEM PERFORMANCE DATA

PARAMETER	UNITS	S-IVB-502 FLIGHT		S-IVB-501 FLIGHT		S-IVB-502* ACCEPT	
		FIRST BURN	SECOND BURN	FIRST BURN	SECOND BURN	FIRST BURN	SECOND BURN
Heat absorption rate during pressurized chilldown							
Section 1†	Btu/hr	2,500	500	100	3,500	13,500	19,000
Section 2†	Btu/hr	7,000	23,000	12,000	11,500	18,000	21,000
Section 3†	Btu/hr	7,500		1,500		24,500	15,000
Total	Btu/hr	17,000	23,500	13,600	15,000	56,000	55,000
Chilldown flowrate							
Unpressurized	gpm	92	10 to 100	115	32 to 95	91	82
Pressurized — After CVS closure	gpm	N/A	125	N/A	N/A	N/A	N/A
Pressurized — After repressurization	gpm	133	134	143	143	135	133
Chilldown pump pressure differential							
Unpressurized	psi	9.0	2 to 8.5	8.7	2 to 16.5	8.8	9.1
Pressurized	psi	6.4	7.4	7.4	7.8	7.5	7.3
Events	sec††						
Chilldown initiation		-299.008	-737.446	-302.8	-567.7	-200.7	-716.9
Prevalve closed		-275.076	-727.446	-272.8	-551.9	-197.0	-744.5
CVS closed		N/A	-325.696	N/A	-325.8	N/A	N/A
Prepressurization		-96.506	-126.993	-96.5	-326.2	-111.5	-323.3
Prevalve OPEN Command		576.596	-10.79	520.0	-10.8	N/A	N/A
Prevalve closed signal dropout		577.429	-9.839	520.9	-9.8	N/A	N/A
Prevalve open signal pickup		579.671	-5.909	522.8	-7.2	511.3	-0.8
Chilldown pump off		578.470	-0.791	521.9	-0.8	510.9	-0.9
Chilldown pump off		Not Sent	Not Sent	625.5	Not Sent	511.5	-0.5
Engine Start Command		577.270	0	520.7	0	511.9	0

*During acceptance testing, liftoff is simulated.

†Section 1 is tank to pump inlet; section 2 is pump inlet to bleed valve; section 3 is bleed valve to tank.

††All first burn data are referenced to liftoff (or simulated liftoff); all second burn data are referenced to ESC2

N/A = Not Applicable

TABLE 13-5
LH2 PUMP INLET CONDITION DATA

PARAMETER	UNITS	S-IVB-502 FLIGHT		S-IVB-501 FLIGHT		S-IVB-502 FLIGHT	
		FIRST BURN	SECOND BURN	FIRST BURN	SECOND BURN	FIRST BURN	SECOND BURN
Pump Inlet Conditions							
Static pressure at Engine Start Command	psia						
With chilldown head*		42.5	N/A	43.89	N/A	N/A	N/A
Without chilldown head		35.6	32.6	35.8	28.0	38.2	35.1
Static pressure at engine cutoff	psia	30.5	28.2	27.5	31.0	27.0	30.8
Temperature at engine start	deg R	38.3	39.4	38.9	40.7	39.6	39.8
Temperature at engine cutoff	deg R	38.5	38.5	38.8	39.45	38.0	39.0
NPSP Requirements							
Minimum at Engine Start Command	psi	6.3	6.3	6.3	6.3	6.3	6.3
At high EMR	psi	6.37	6.37	6.3	6.3	6.3	--
After EMR cutback	psi	N/A	5.8	N/A	5.8	5.8	5.8
NPSP Available							
At Engine Start Command	psi						
With chilldown head*		22.8	N/A	21.5	N/A	N/A	N/A
Without chilldown head		15.9	9.5	13.41	0.17	14.3	10.5
At Start Tank Discharge Valve Open Command	psi	16.5	11.2	15.1	5.8	17.2	16.0
Maximum during engine burn	psi	16.5	11.5	16.0	11.0	17.8	16.0
Minimum during engine burn	psi	11.8	7.7	7.5	0.17	9.5	10.0
At Engine Cutoff Command	psi	11.8	7.7	7.5	8.75	9.5	10.0
LH2 Feed Duct							
At high EMR							
Pressure drop	psi	1.0	1.25	1.0	0.5	1.0	1.8
Flowrate	lbm/sec	82.5	60	81	80	79.5	78.5
After EMR cutback							
Pressure drop	psi	N/A	N/A	N/A	0.5	N/A	1.7
Flowrate	lbm/sec	N/A	N/A	N/A	77	N/A	76.3

*The NPSP and pump inlet pressure are high at this time because the prevalves were slow in opening.

N/A = Not Applicable

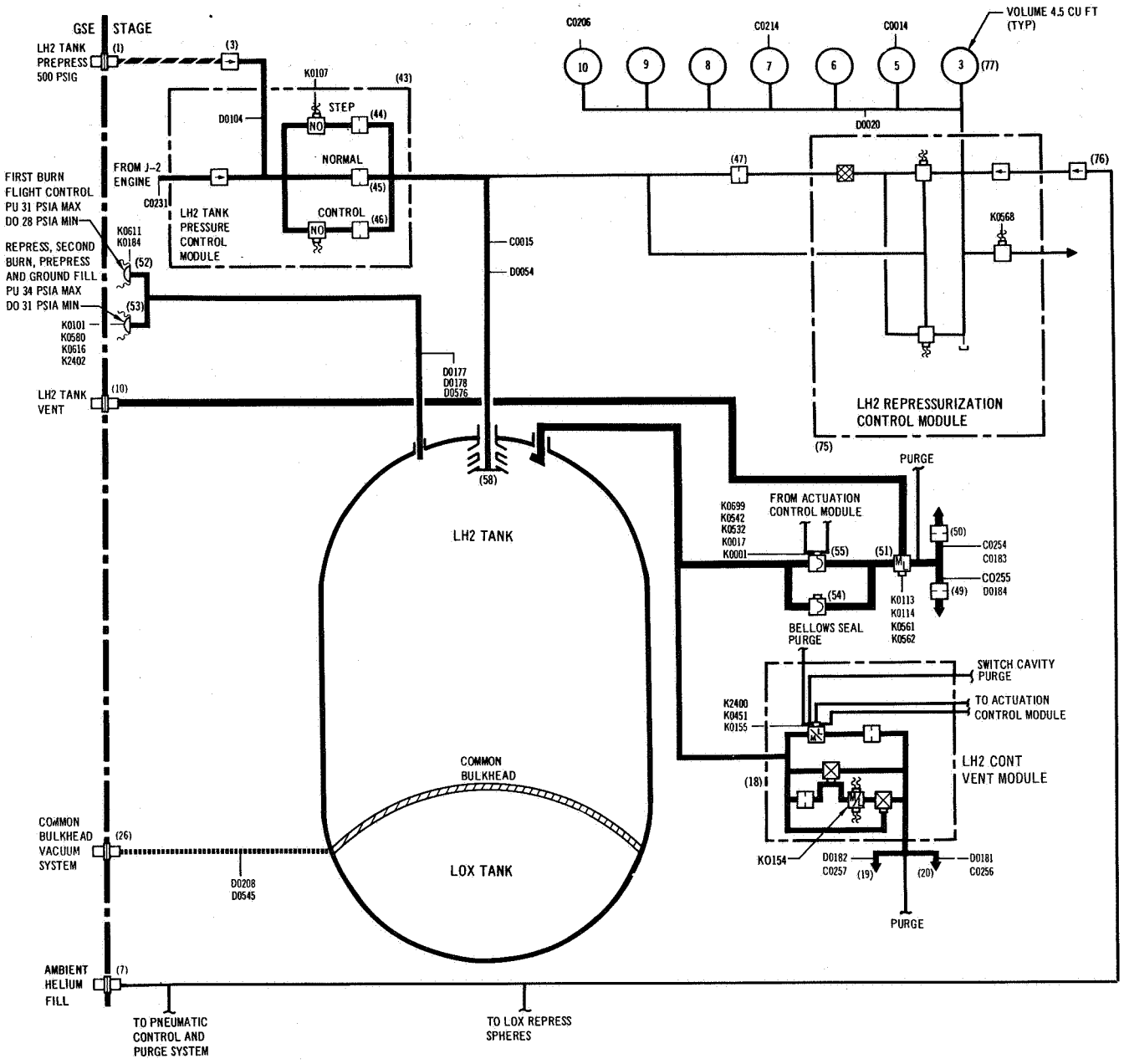

NOTE:
(X) ITEMS
PARTS LIST FIGURE 4-1
SEE FIGURE 4-1 FOR LEGEND

Figure 13-1. LH2 Tank Pressurization System

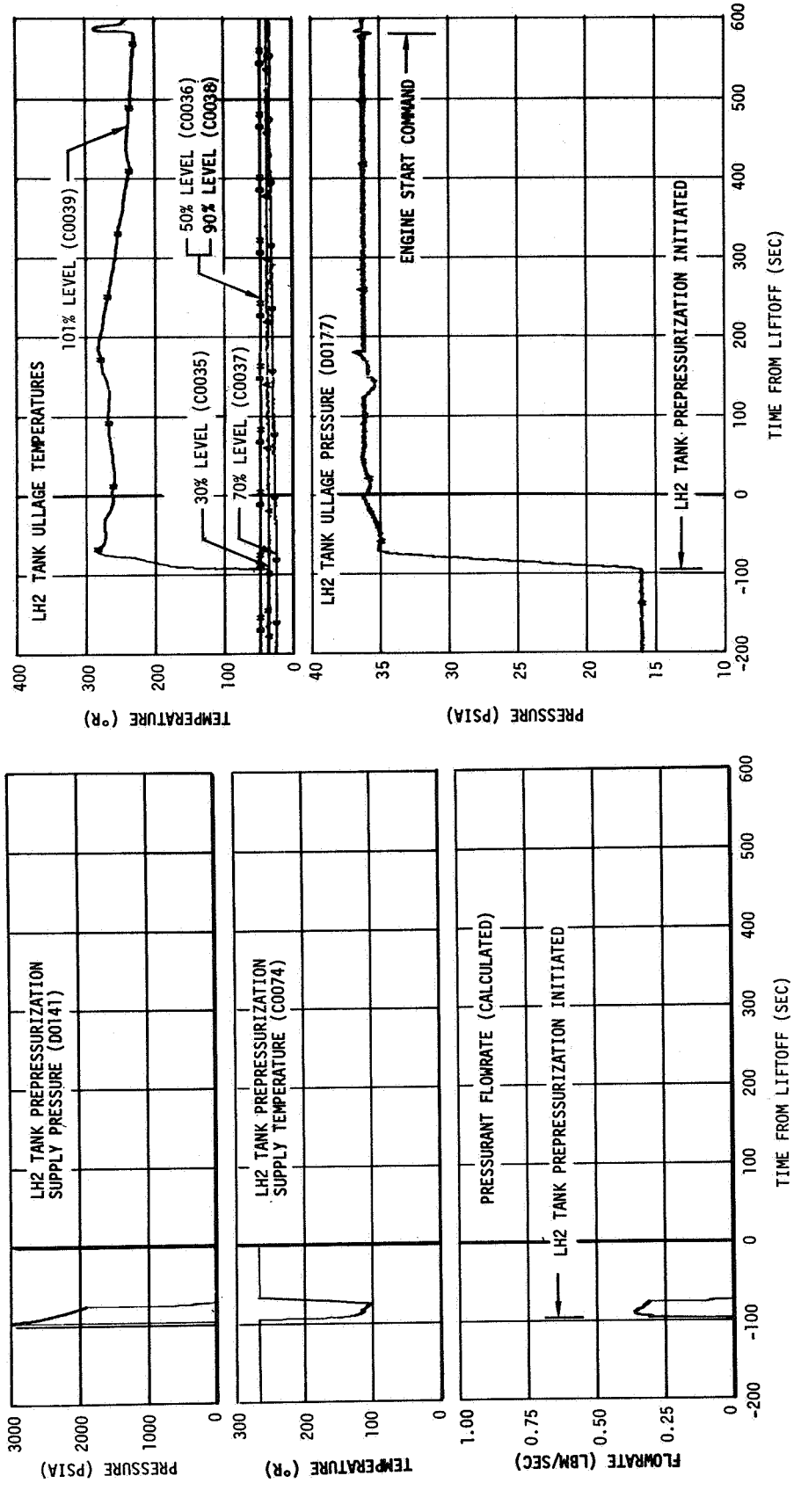

Figure 13-2. LH2 Tank Prepressurization System Performance

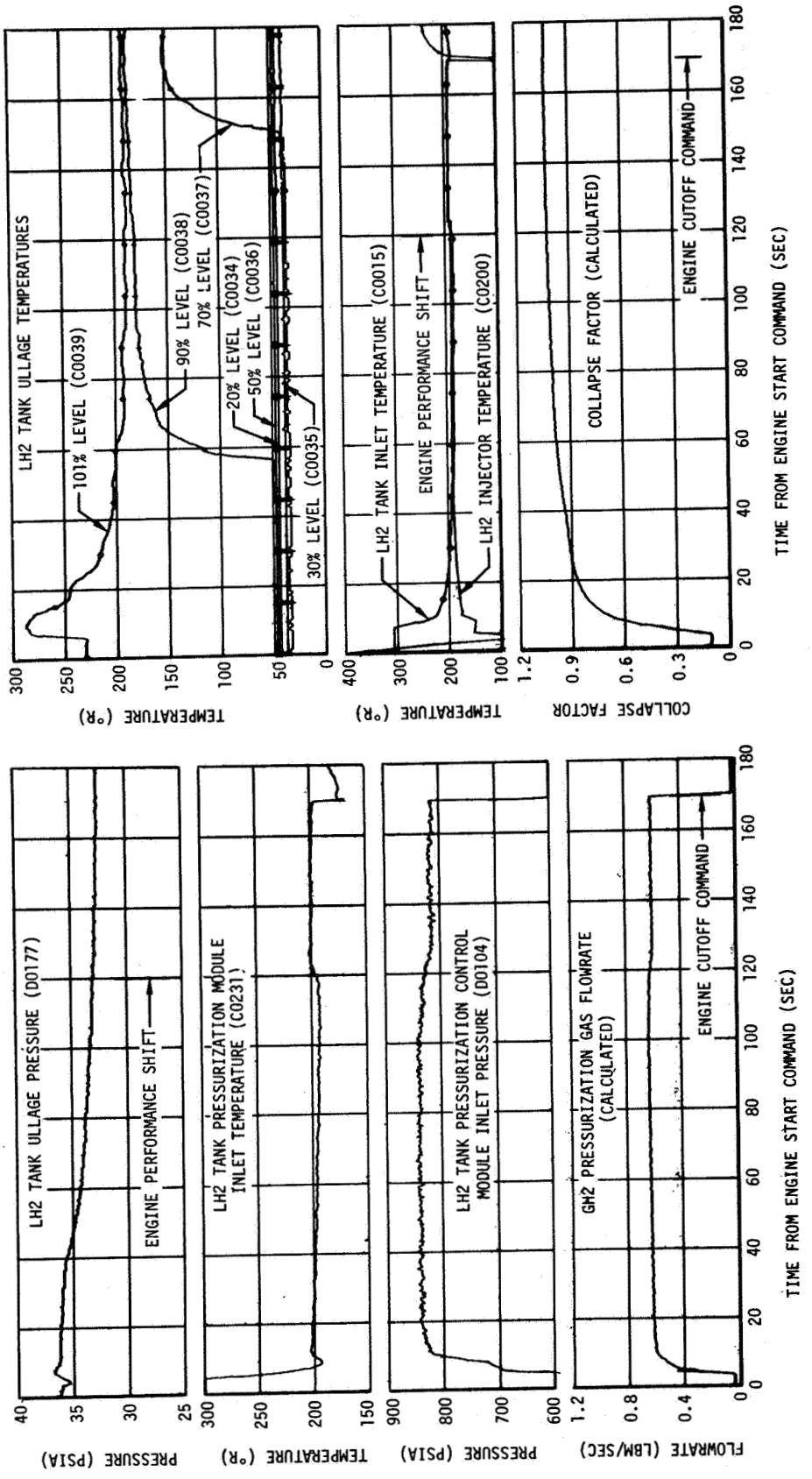

Figure 13-3. LH2 Tank Pressurization System Performance - First Burn

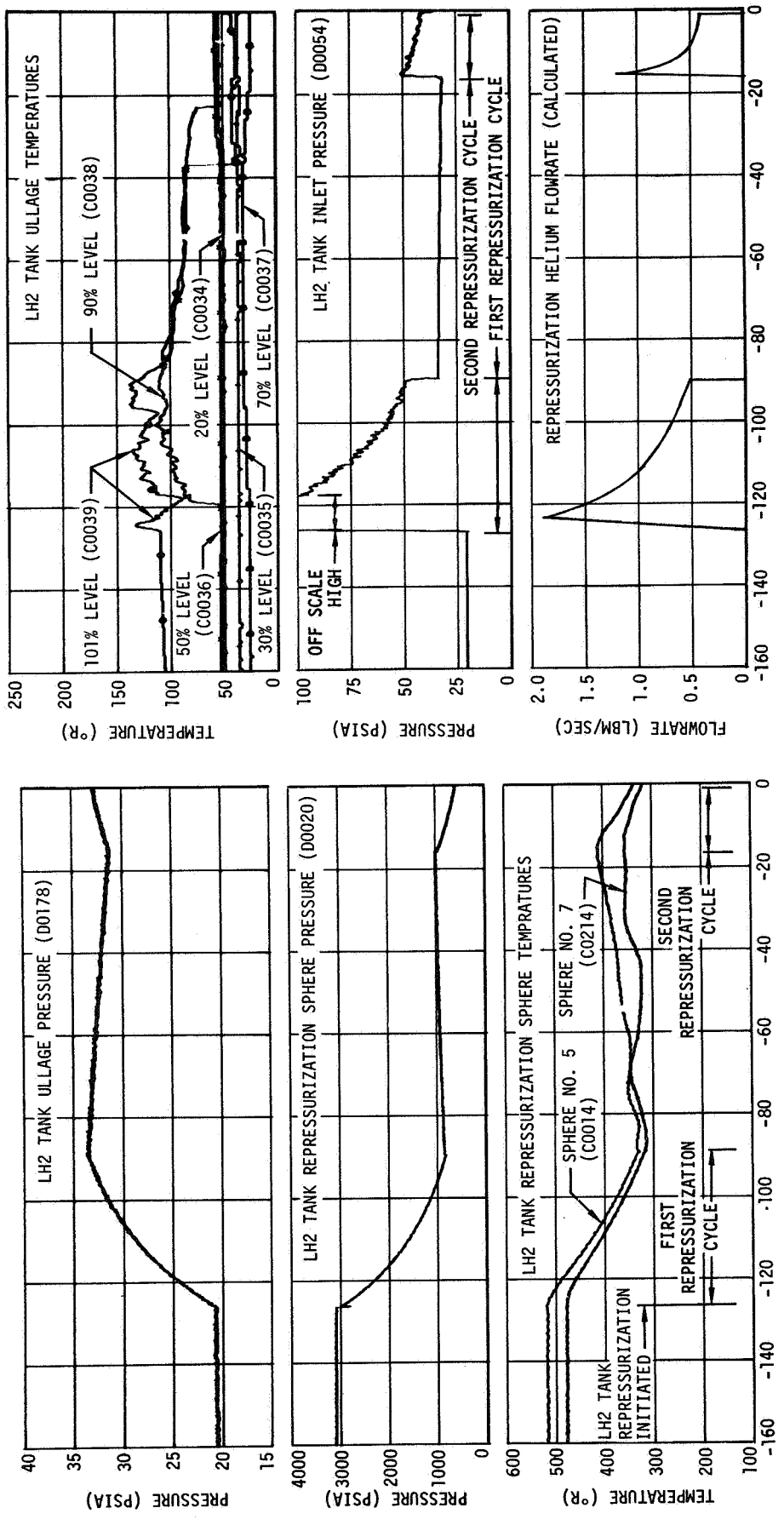

Figure 13-4. LH2 Tank Ambient Repressurization Performance - Second Burn

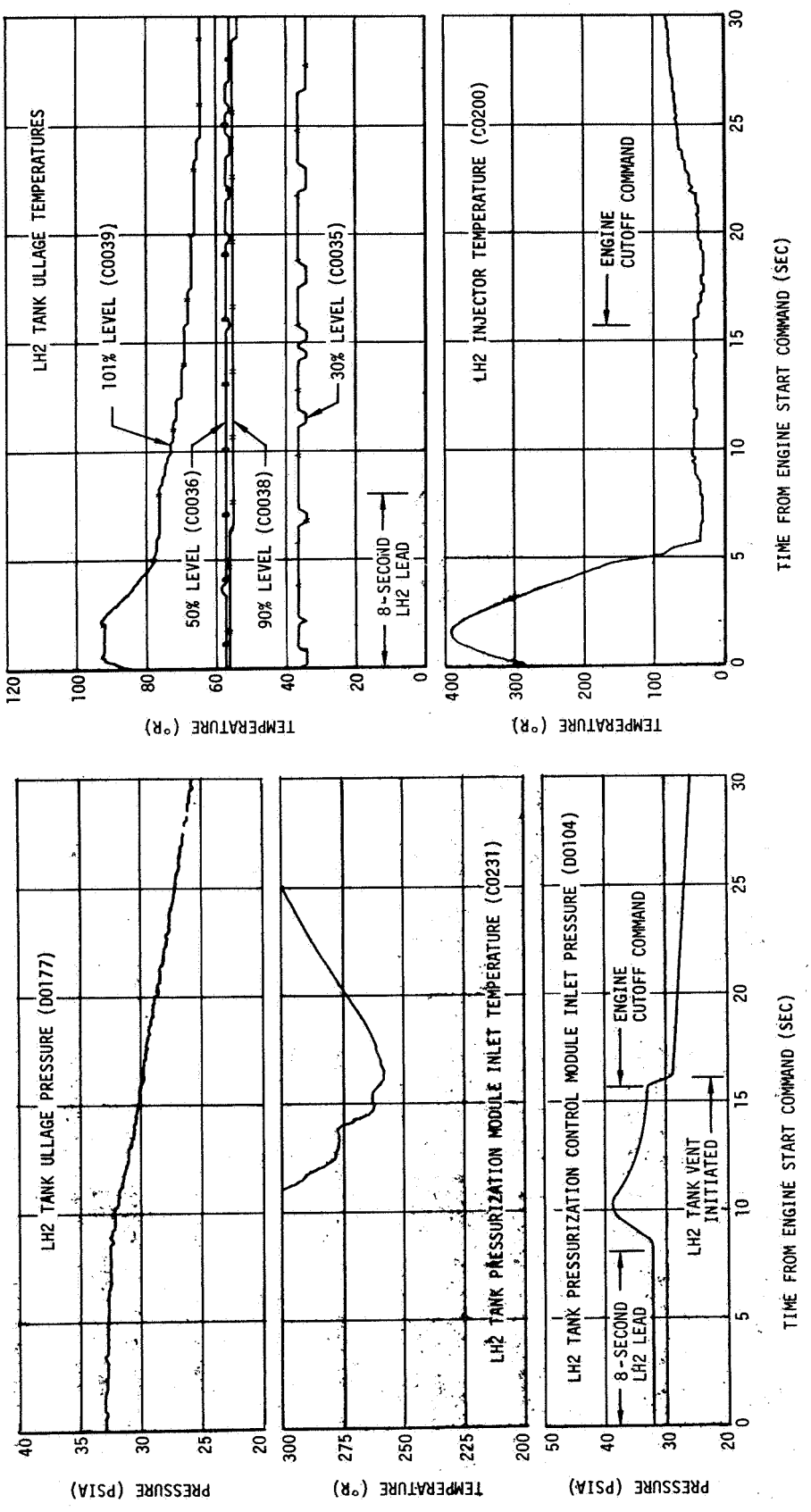

Figure 13-5. LH2 Tank Pressurization System Performance - Second Burn

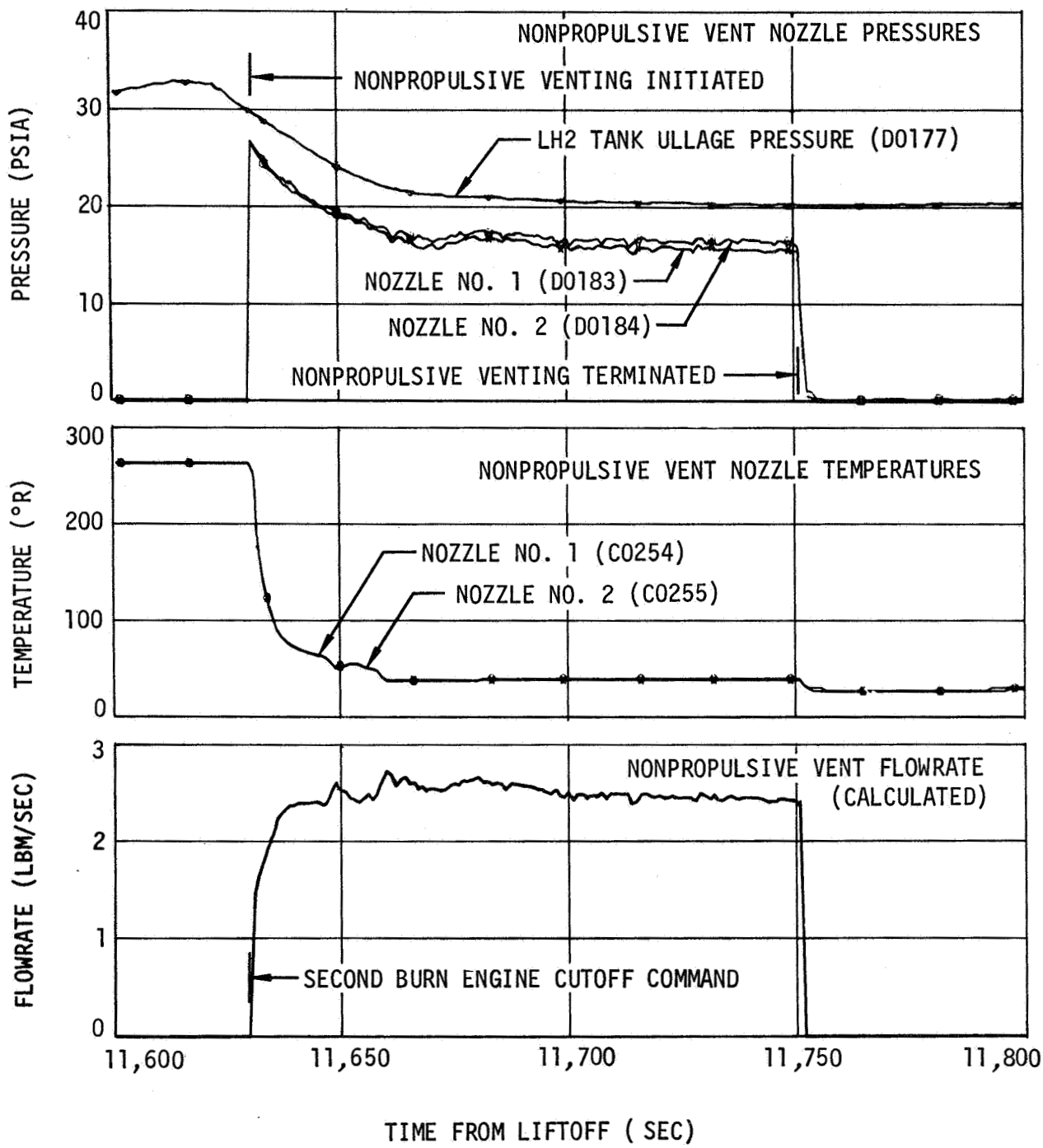

Figure 13-6. Nonpropulsive Vent System Performance

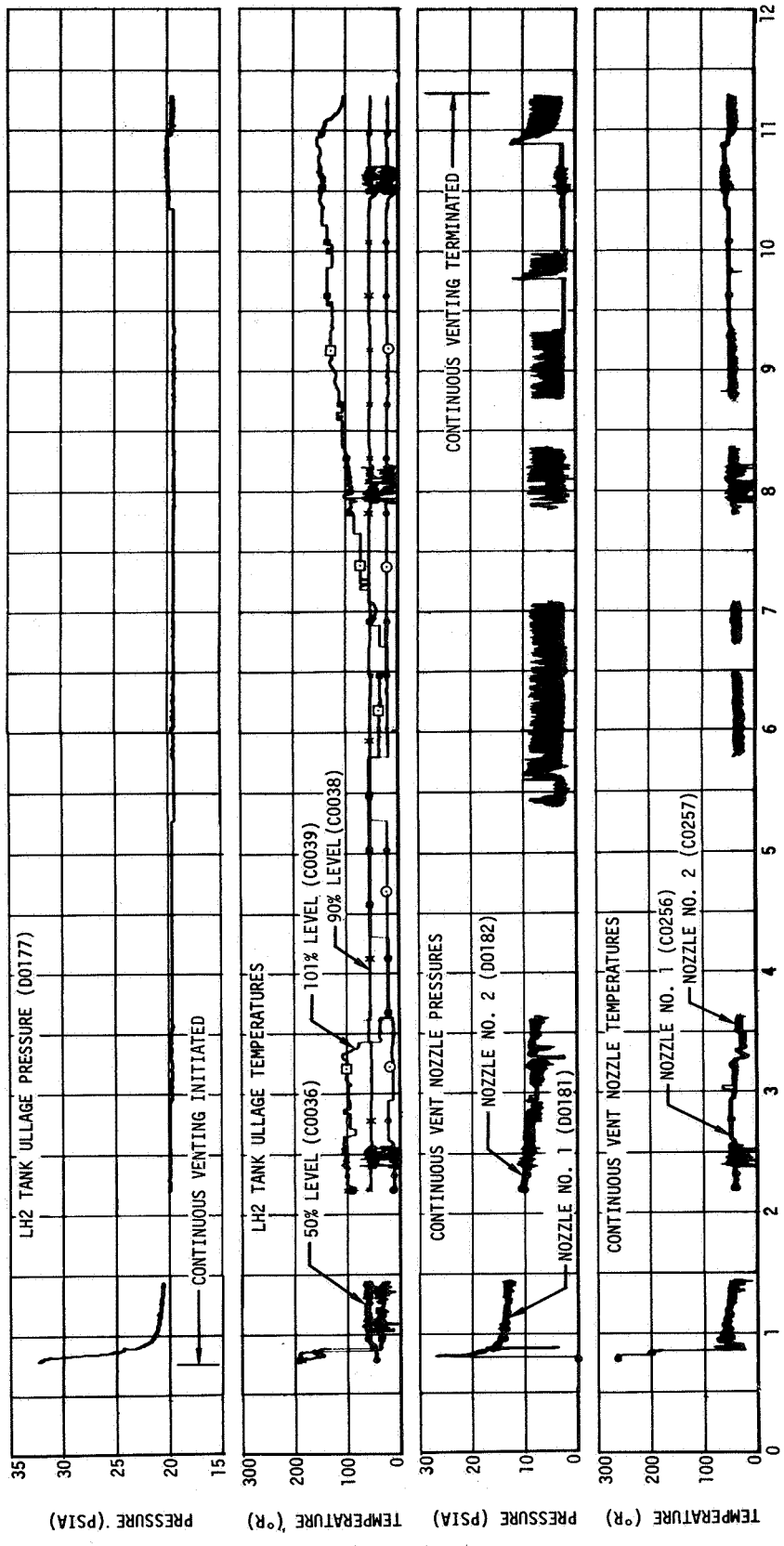

Figure 13-7. LH2 Continuous Vent System Operation - First and Second Orbits

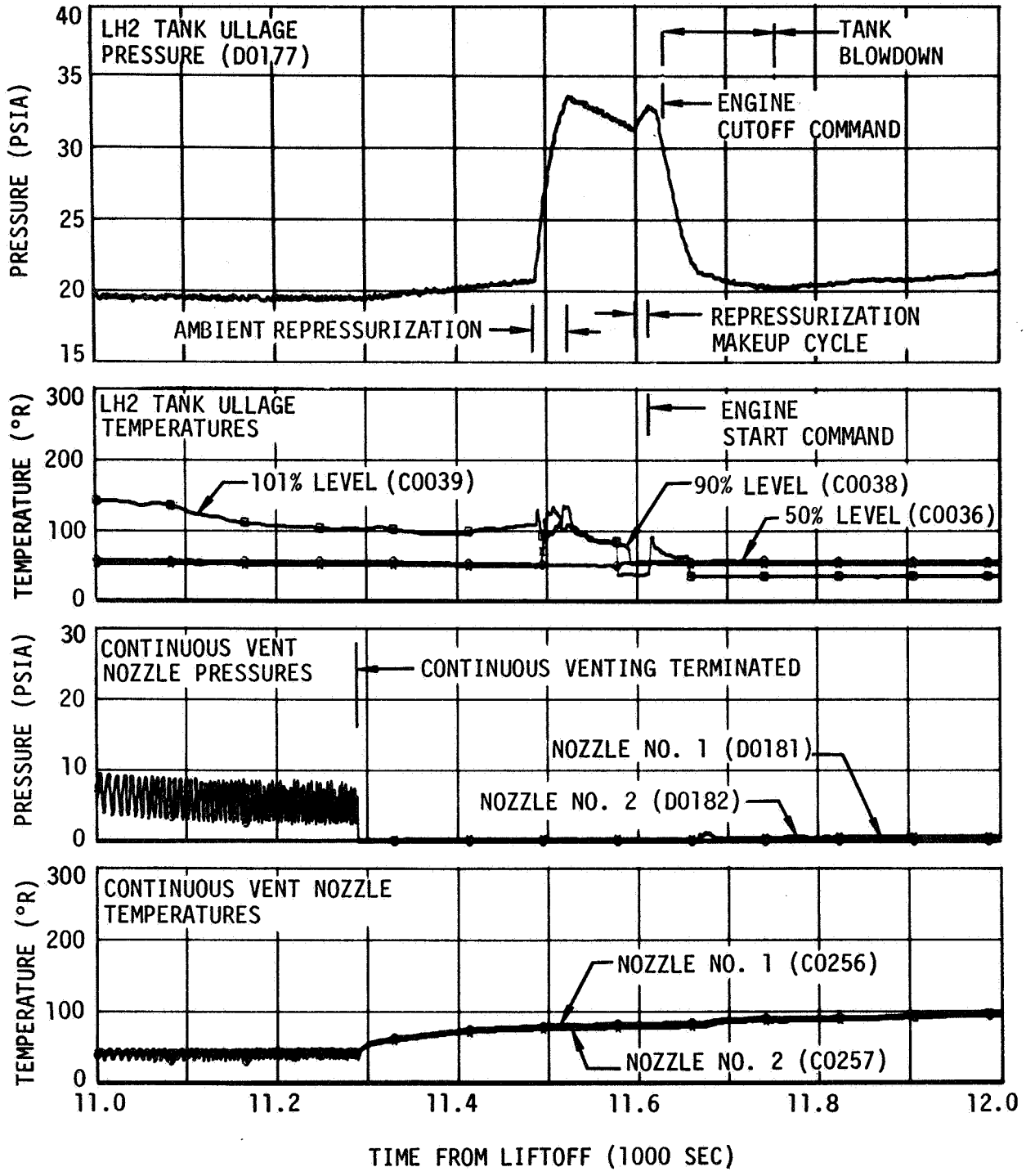

Figure 13-8. LH2 Tank Continuous Vent System Operation - Restart Preparations and Second Burn

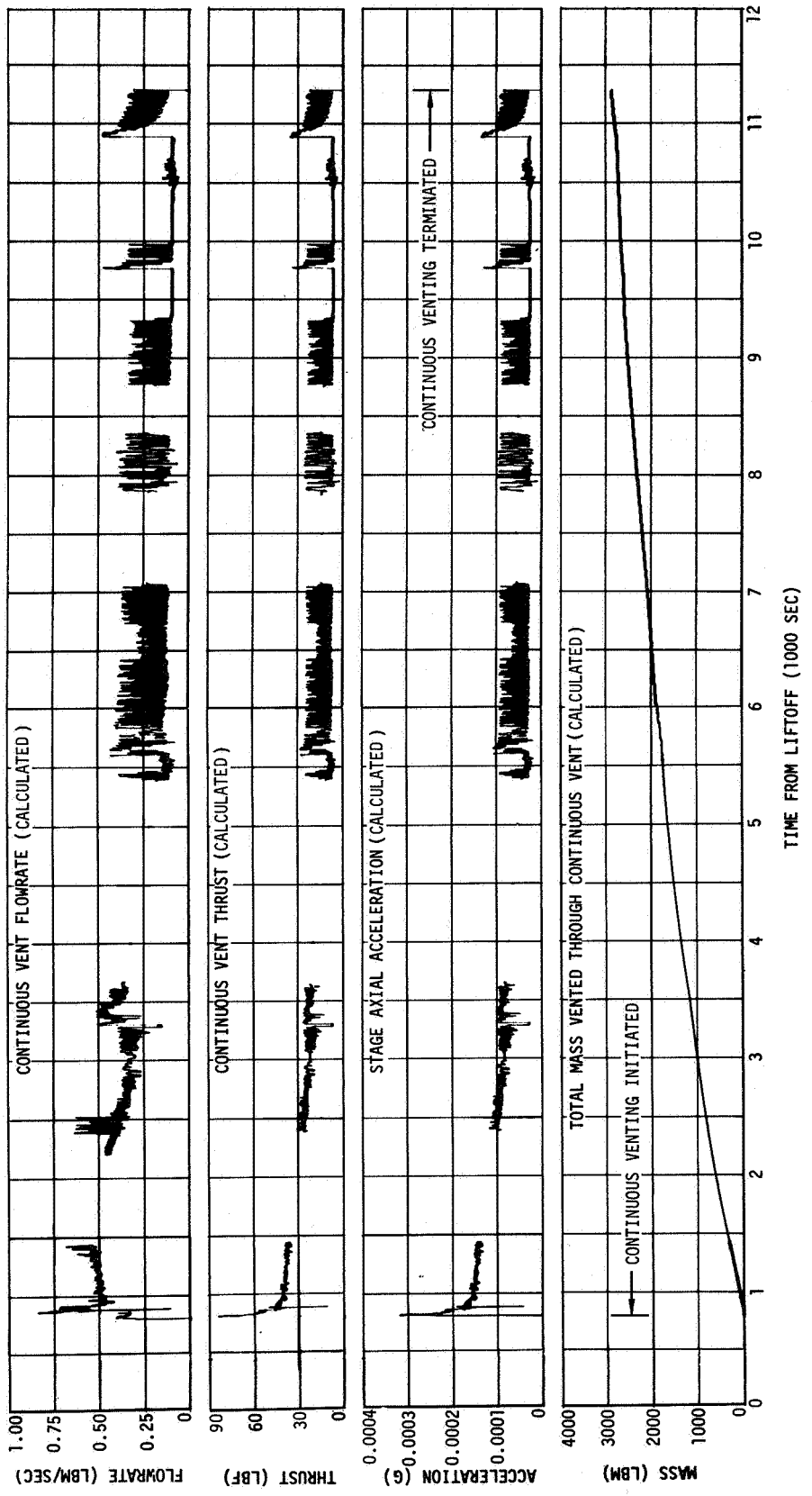

Figure 13-9. LH2 Continuous Vent System Performance - First and Second Orbits

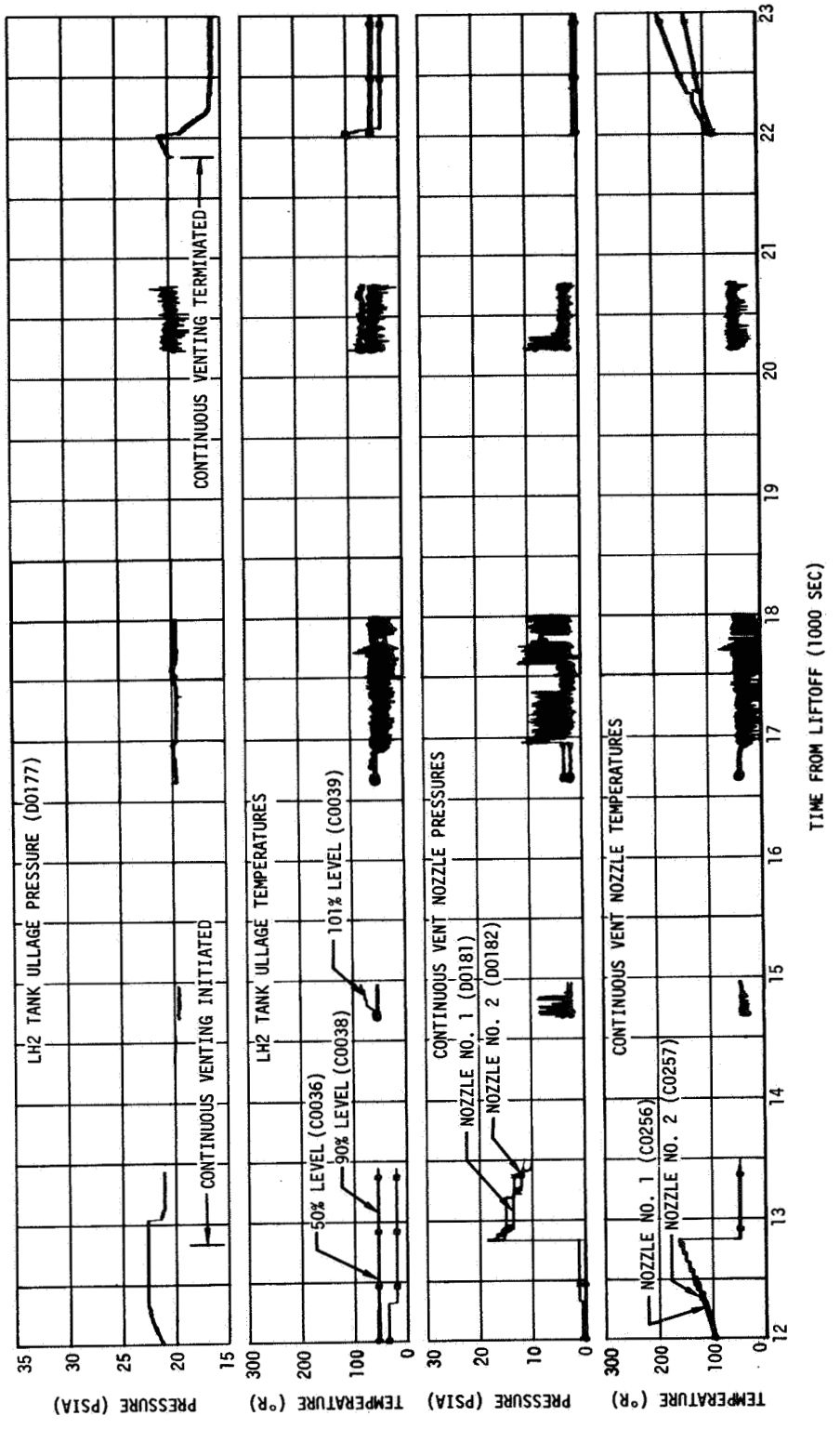

Figure 13-10. LH2 Tank Continuous Vent System Operation - Third and Fourth Orbits

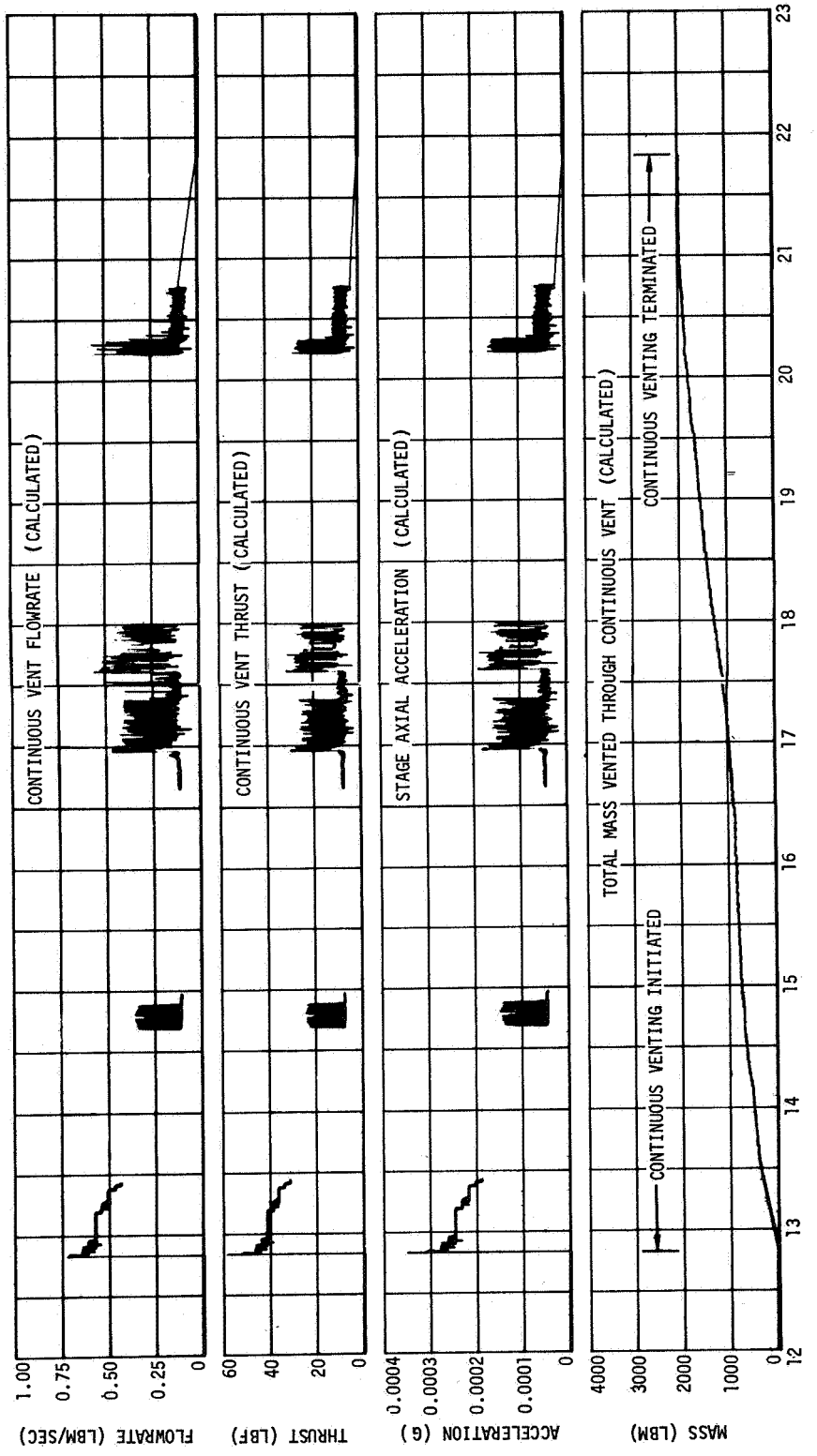

Figure 13-11. LH2 Continuous Vent System Performance - Third and Fourth Orbits

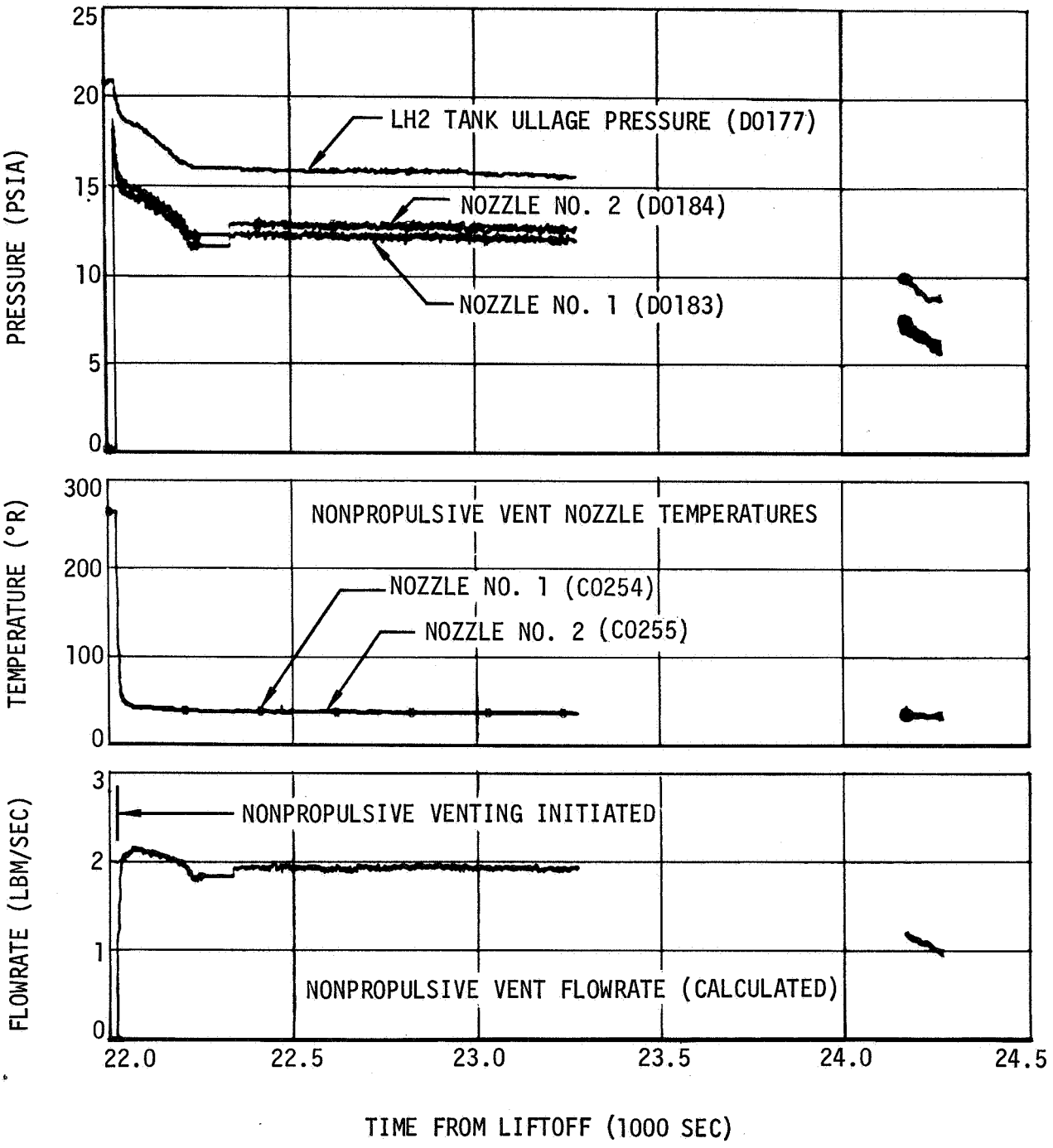

Figure 13-12. Nonpropulsive Vent System Performance – LH2 Tank Passivation

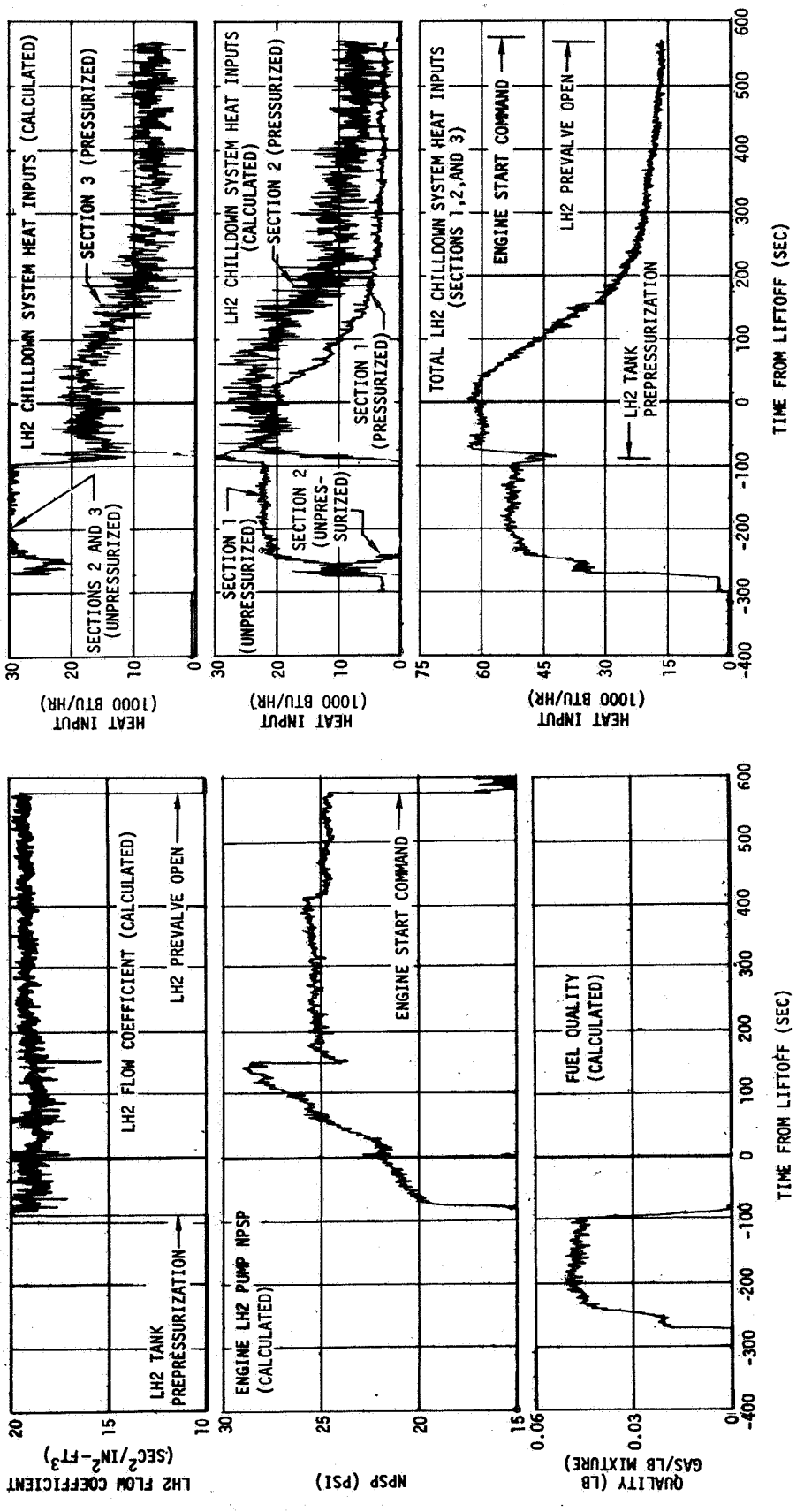

Figure 13-13. LH2 Pump Chilldown Conditions - First Burn

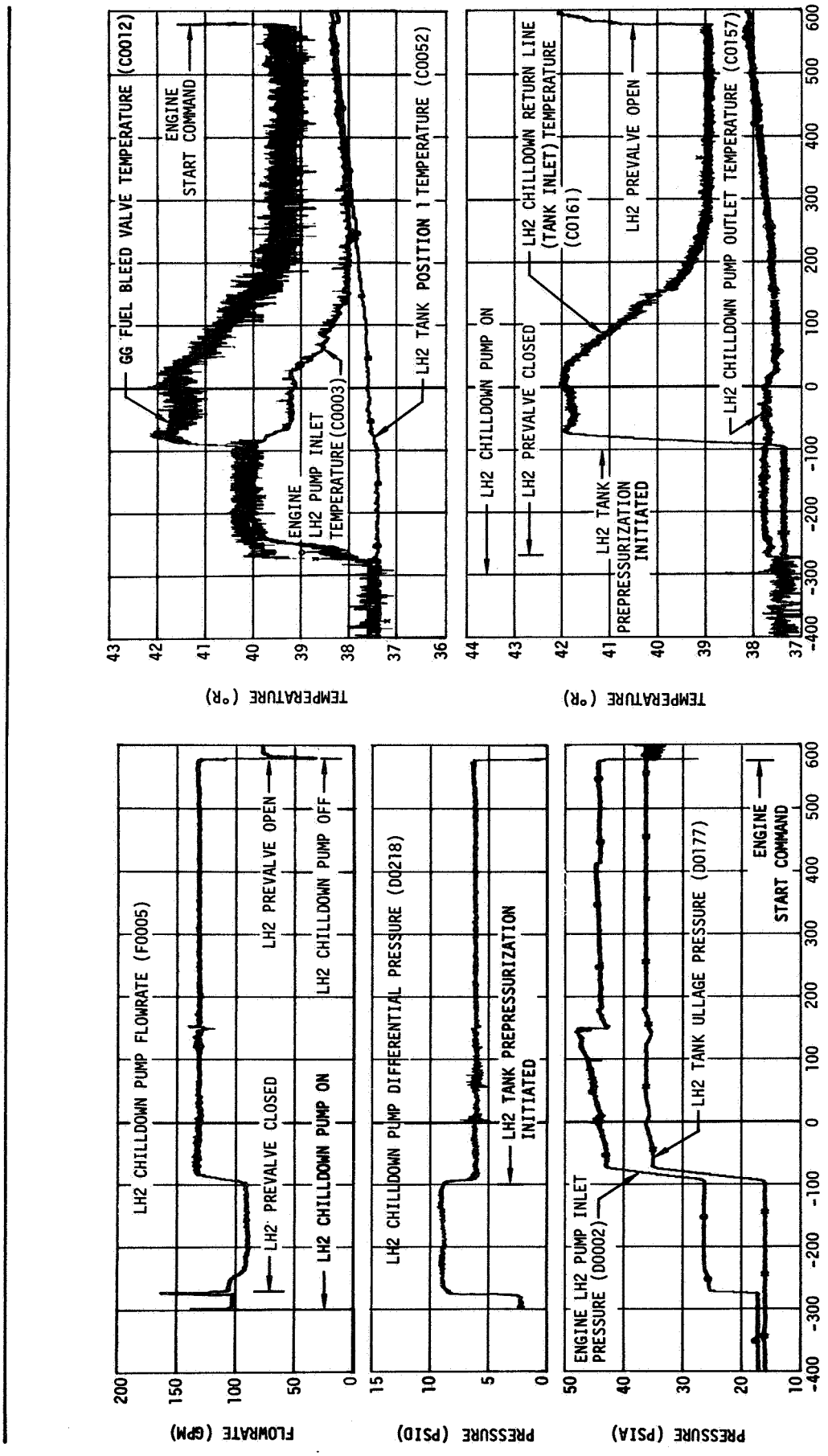

Figure 13-14. LH2 Pump Chilldown - First Burn

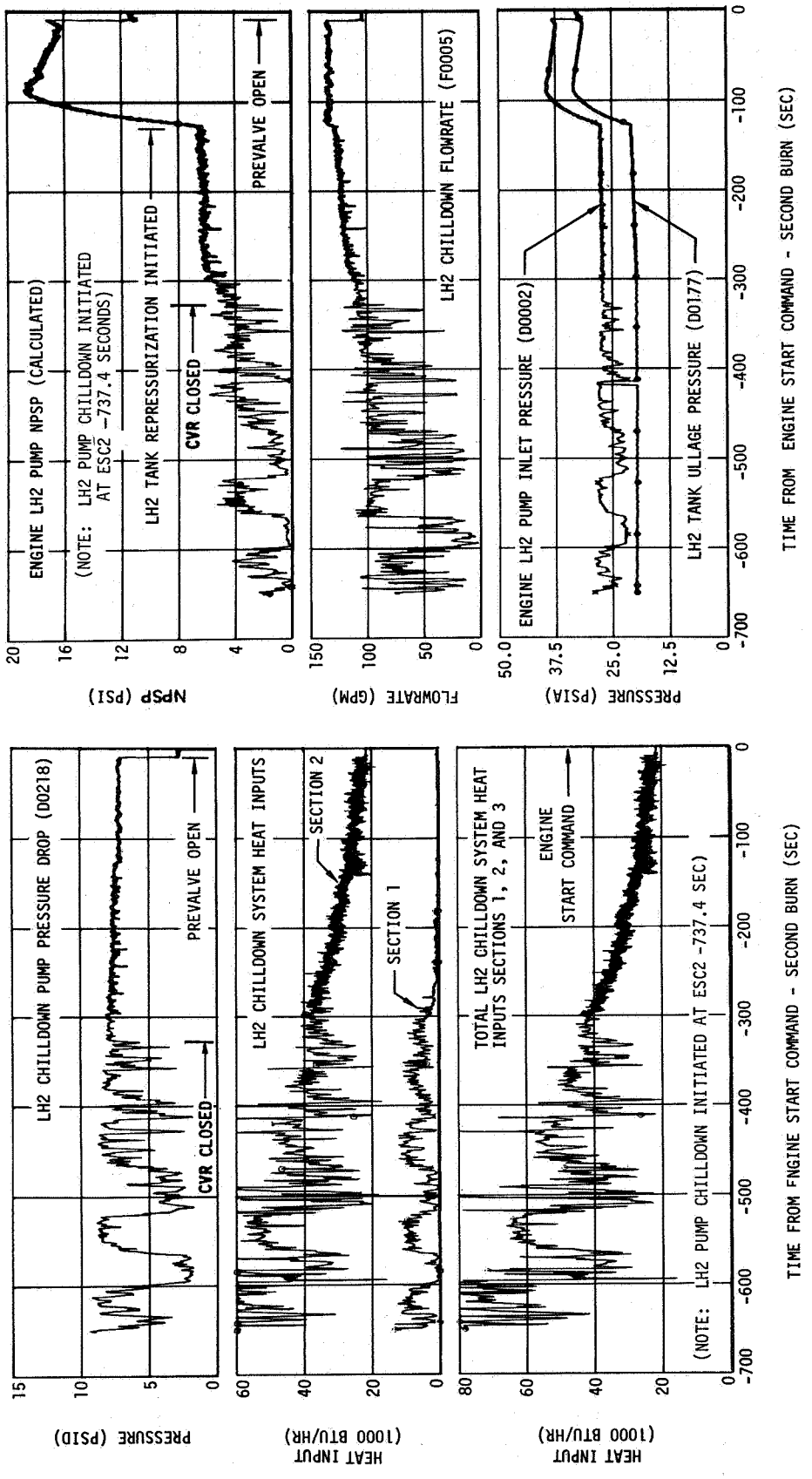

Figure 13-15. LH2 Pump Chilldown Characteristics - Second Burn

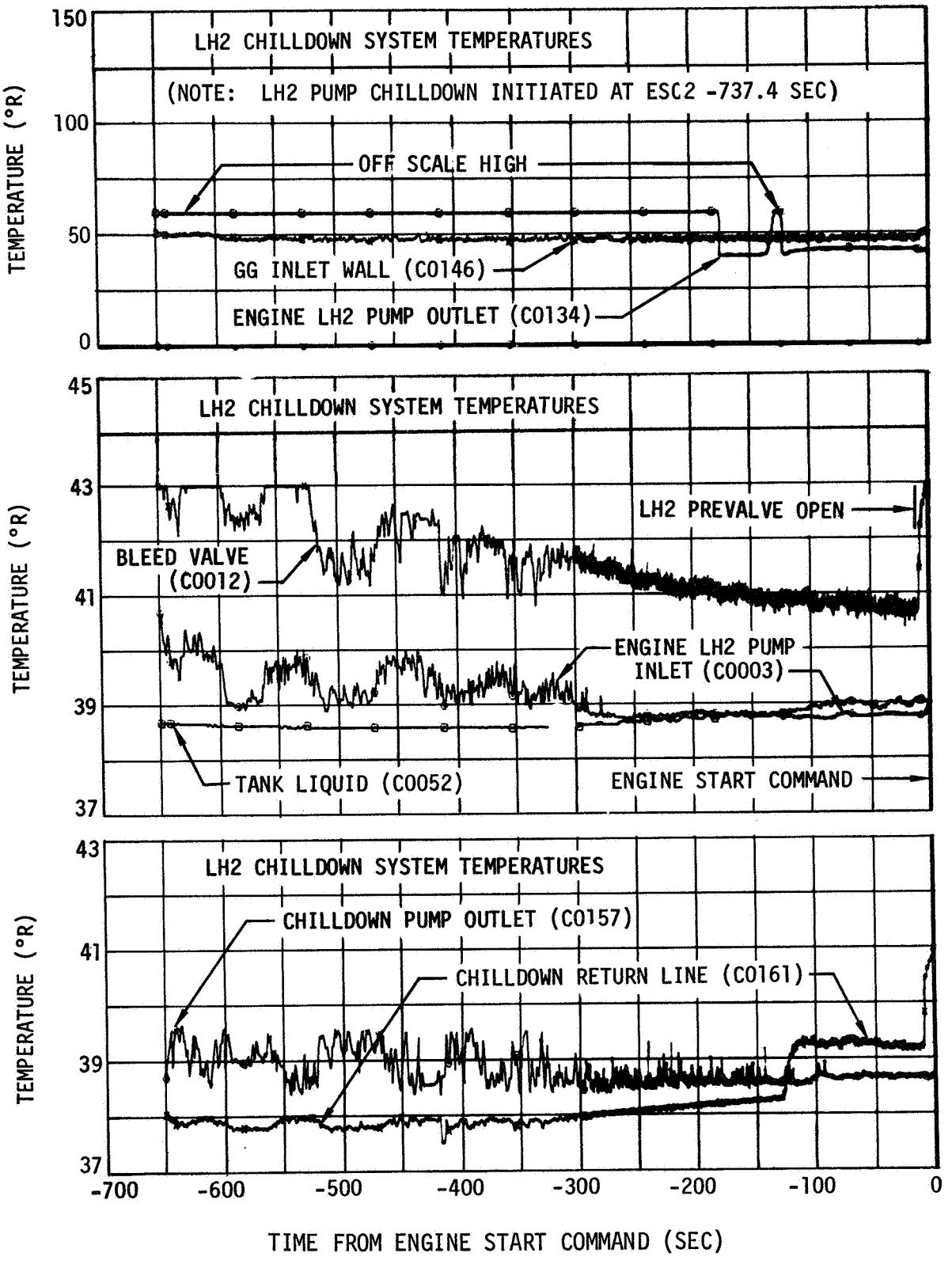

Figure 13-16. LH2 Pump Chilldown - Second Burn

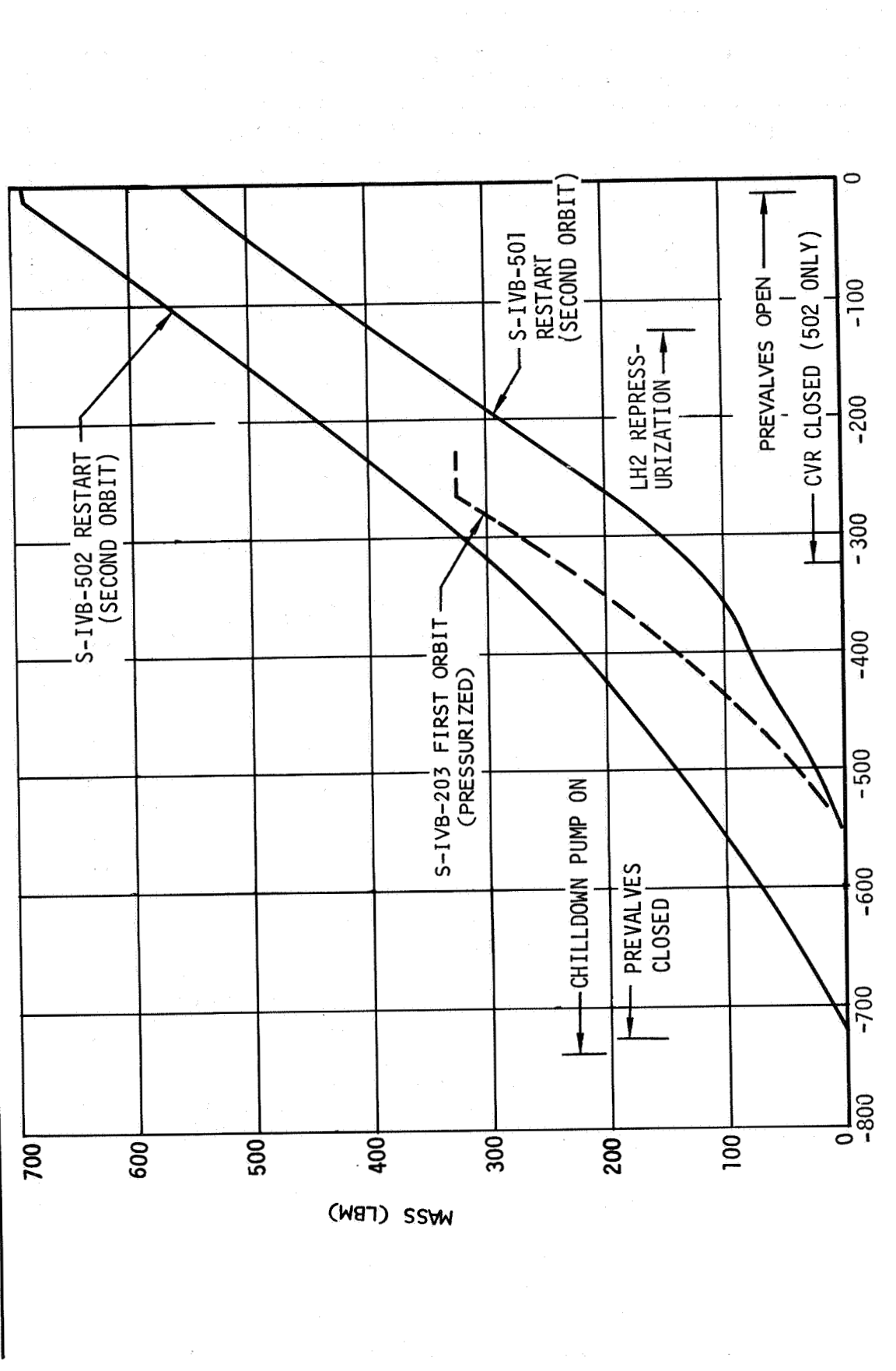

Figure 13-17. Comparison of LH2 Mass Entering Chilldown System

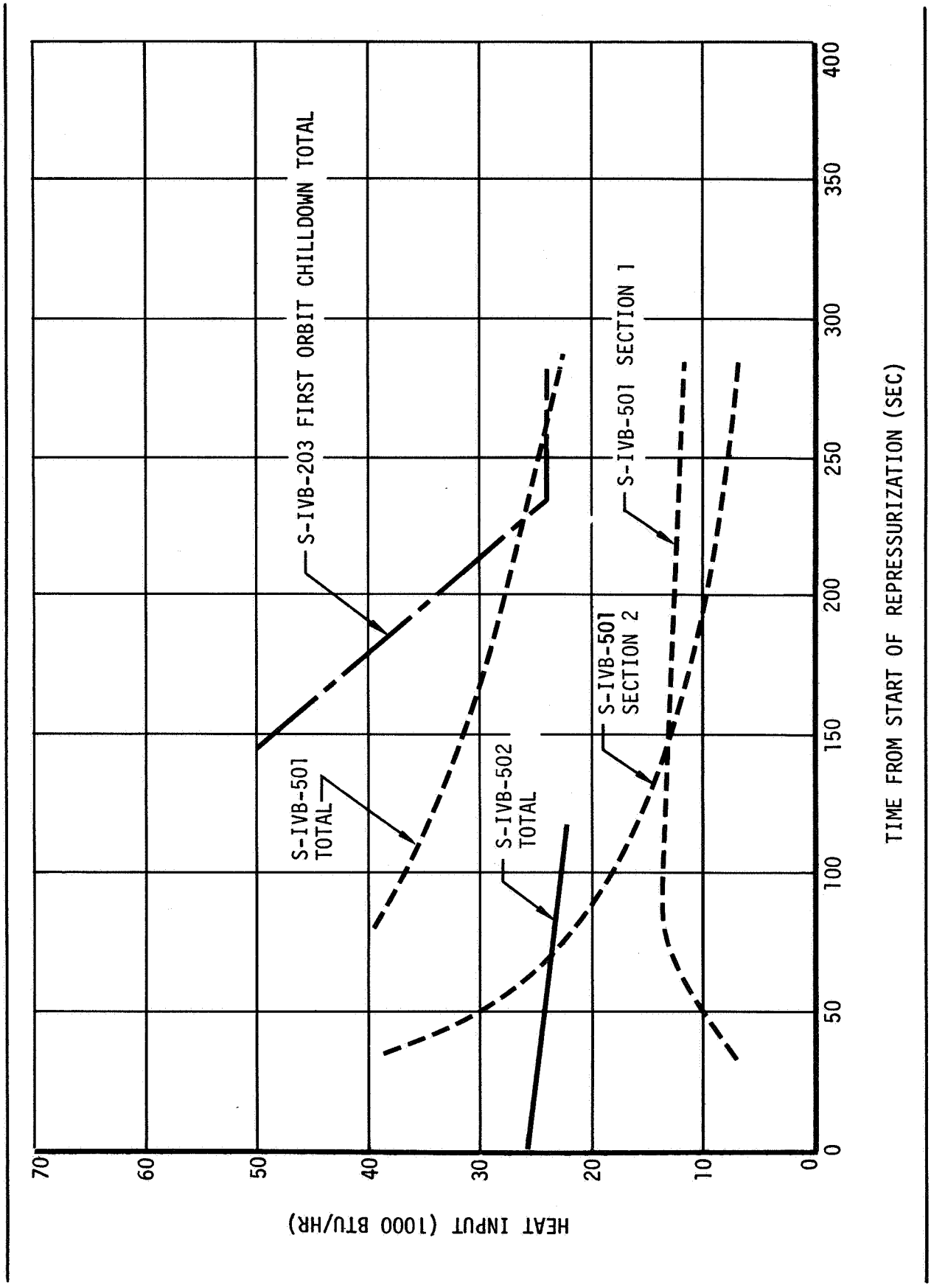

Figure 13-18. Comparison of Heat Input Rates During Flight

NOTE:
(X) ITEM NUMBERS FROM PARTS LIST FIGURE 4-1

SEE FIGURE 4-1 FOR LEGEND

LH2 TANK TEMPERATURE PROBE

MEAS NO.	LEVEL (INCHES FROM TANK BOTTOM)
N0021	431
C0039	417
N0022	401
C0068	395
K0676	383.14
N0023	370
C0038	350
N0024	340
C0067	333
N0025	309
C0066	303
C0037	288
N0026	279
C0065	273
N0027	248
C0036	227
N0028	218
C0064	212
N0029	187
C0063	180
C0035	166
N0030	157
C0062	152
N0031	126
C0034	105
N0032	96
C0054	87
L0002	60
C0053	55
L0001	28.5
C0052	20

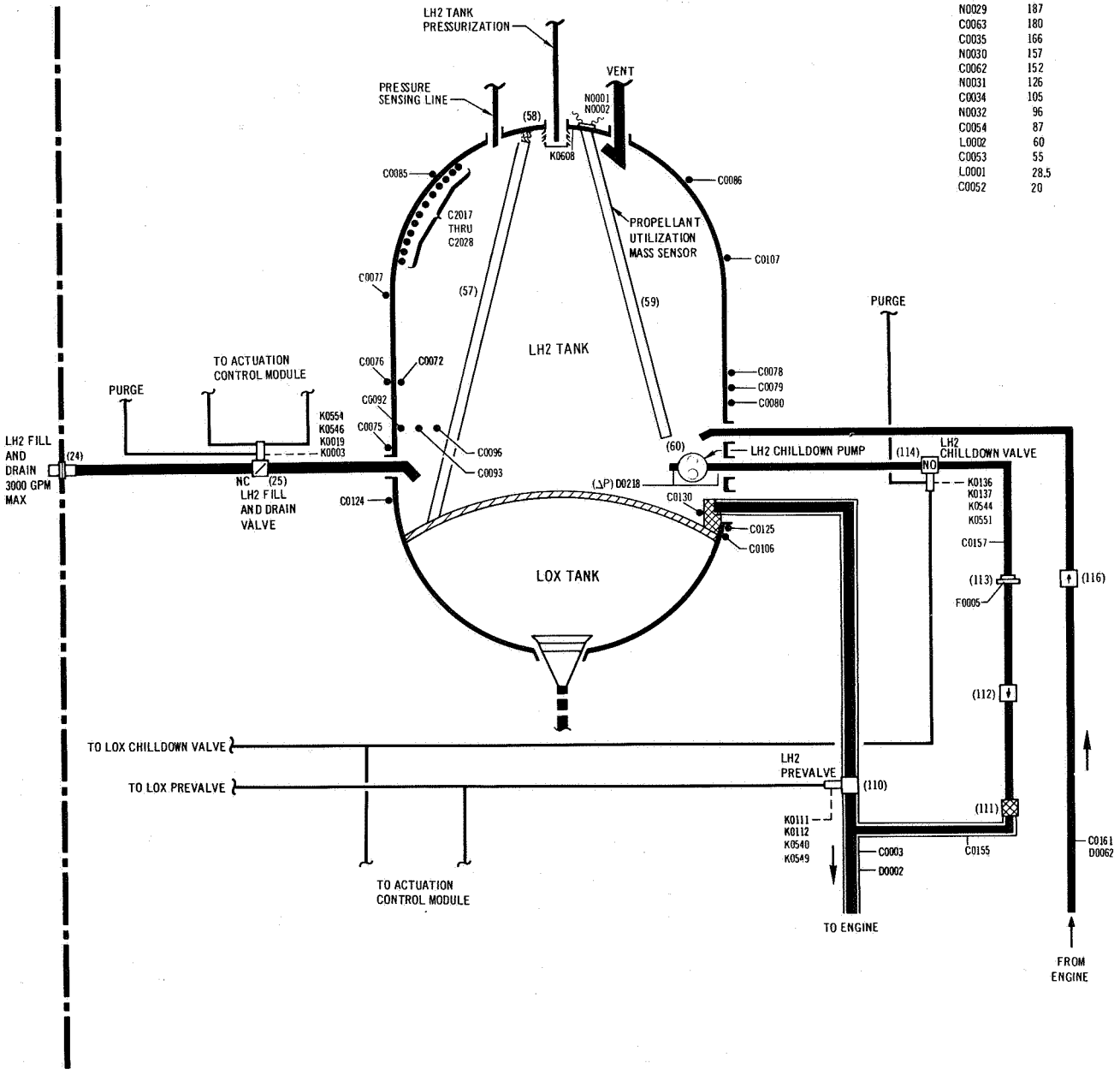

Figure 13-19. LH2 Supply System

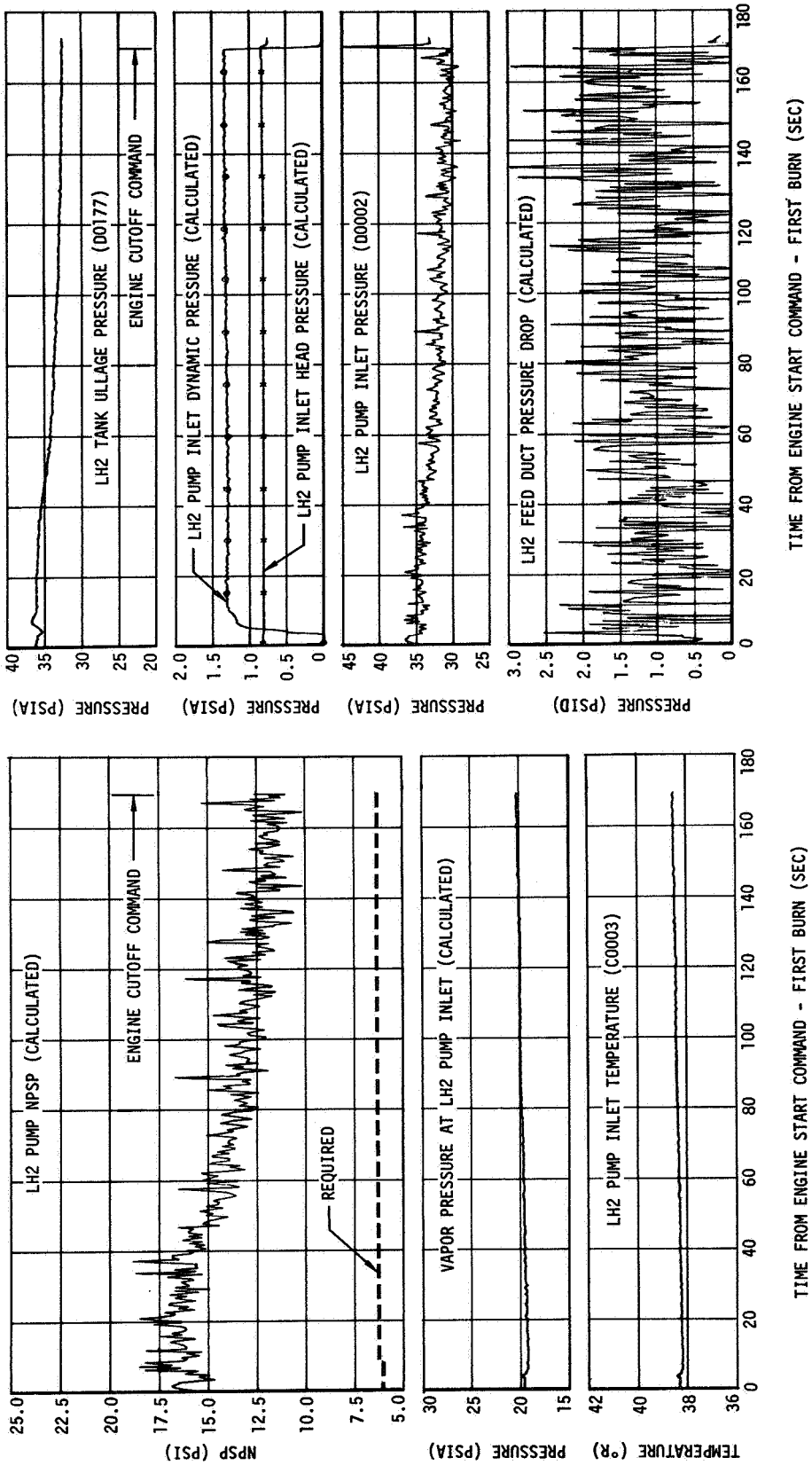

Figure 13-20. LH2 Pump Inlet Conditions - First Burn

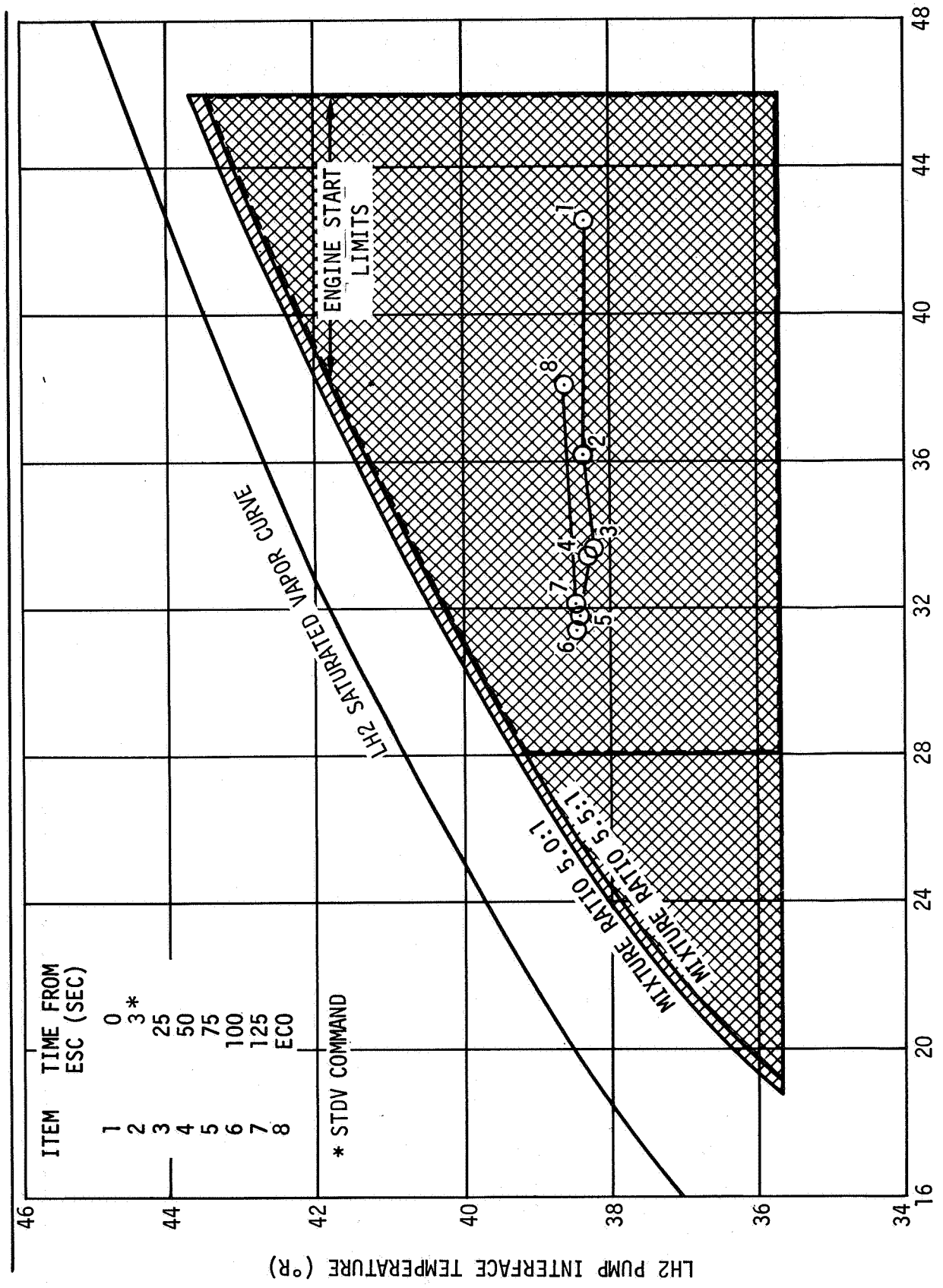

Figure 13-21. LH2 Pump Interface Conditions - First Burn

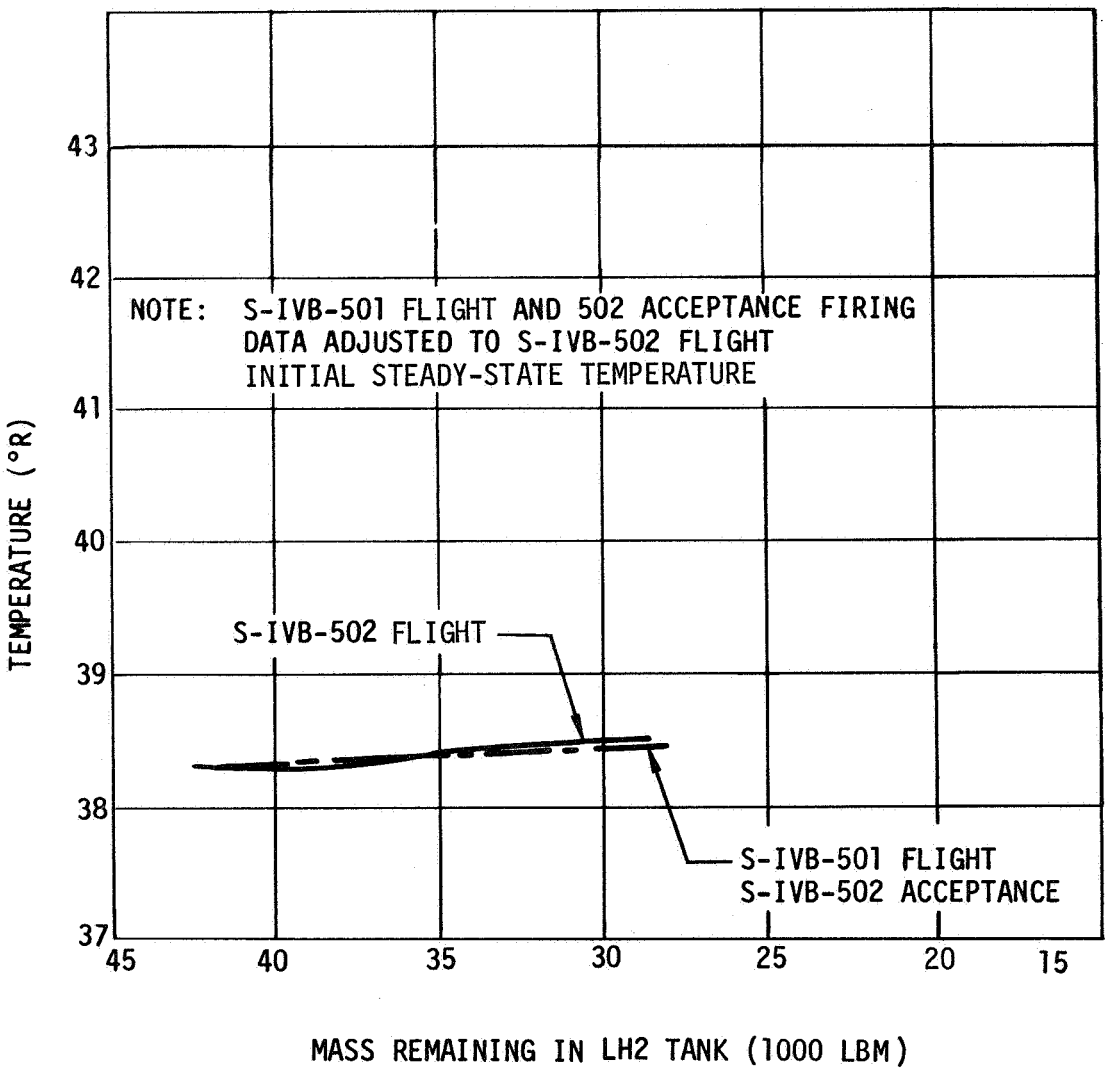

Figure 13-22. Effect of LH2 Mass Level on LH2 Pump Inlet Temperature

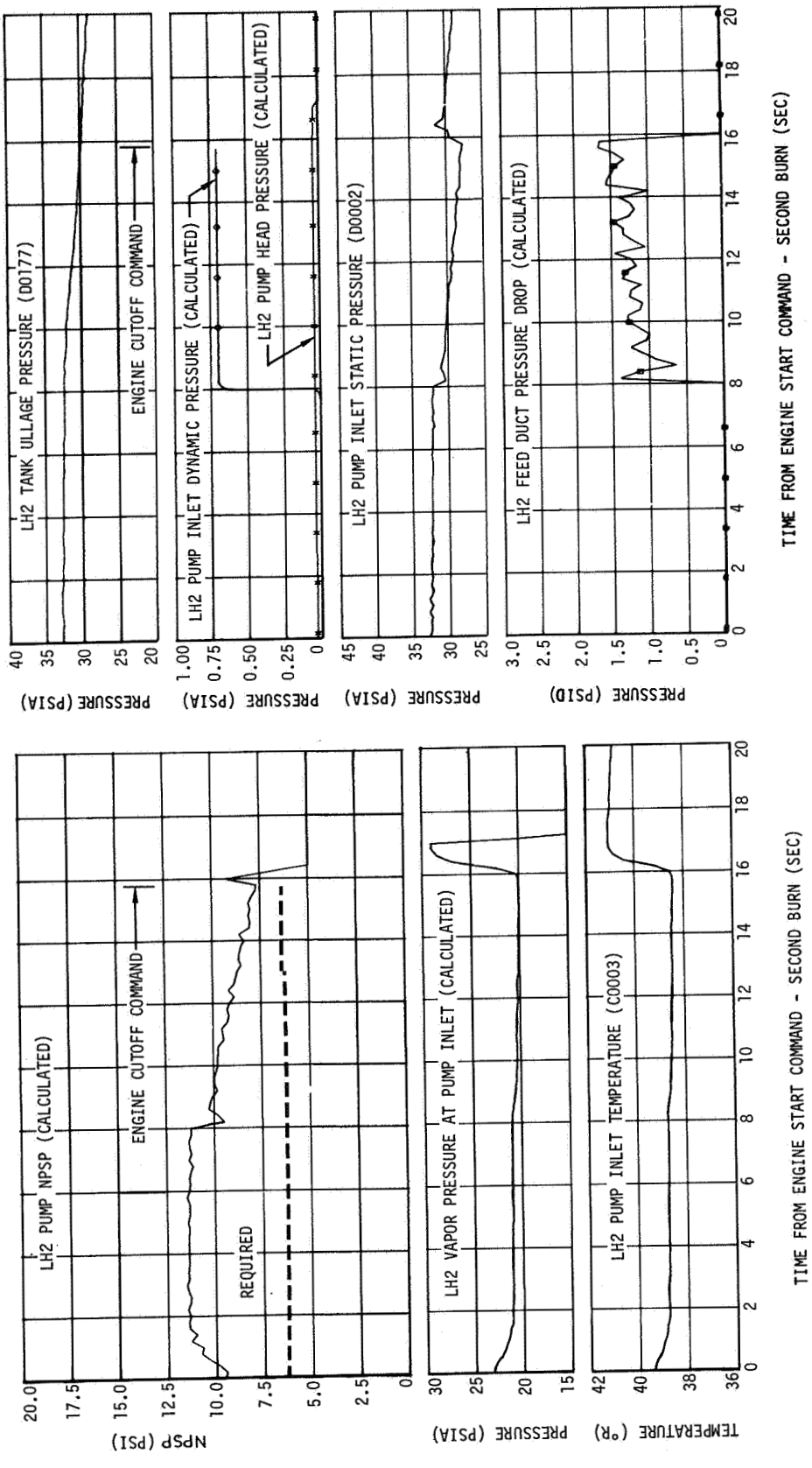

Figure 13-23. LH2 Pump Inlet Conditions - Second Burn

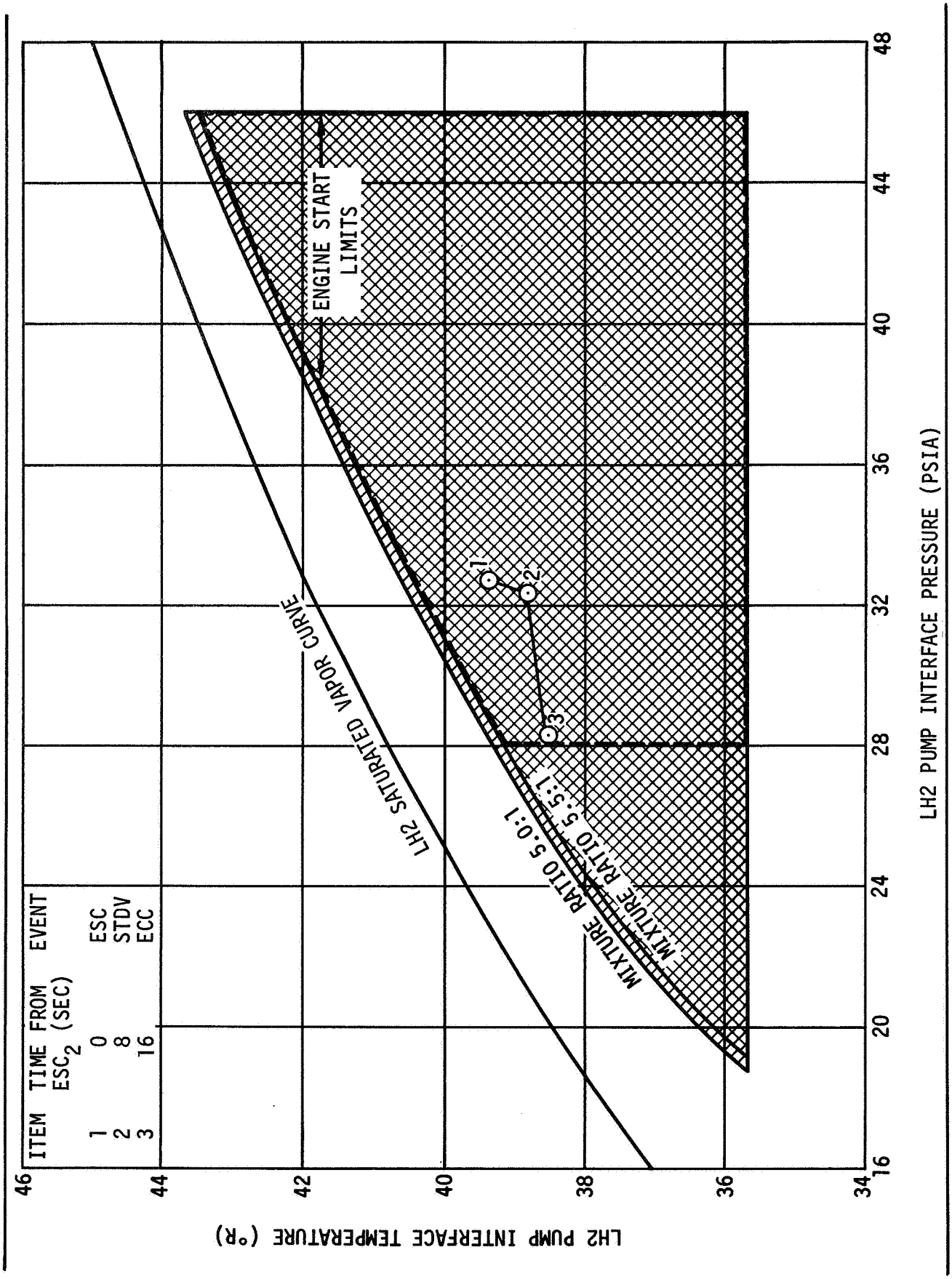

Figure 13-24. LH2 Pump Interface Conditions - Second Burn

SECTION 14

AUXILIARY PROPULSION SYSTEM

14. AUXILIARY PROPULSION SYSTEM

The attitude of the S-IVB is controlled by two auxiliary propulsion system (APS) modules (figure 14-1) mounted 180 deg apart on the aft skirt of the stage. Each module is a self-contained unit composed of four basic systems: (1) Oxidizer system; (2) fuel system; (3) helium pressurization system; and (4) the engines. The instrumentation unit, mounted above the S-IVB, provides signals for operation of the APS modules.

Each module contains two 150-lbf engines which provide roll control during S-IVB powered flight, and yaw and roll control during the coast periods. A third 150-lbf engine in each module provides pitch control during the coast periods. Each module also contains a 72-lbf engine to provide thrust for LOX and LH2 tank ullage control after first burn and during restart preparation.

14.1 APS Flight Operation

The APS operation was adequate to fulfill the attitude control, maneuvering, and ullaging requirements of the mission until APS propellant depletion. The APS propellant usage was greater than predicted as a result of the booster problems encountered during the mission. A discussion of usage is presented in the module 1 oxidizer paragraph 14.2.2.

The pitch engine of each module exhibited reduced chamber pressure at specific times during the mission as shown in figures 14-2, 14-3, and 14-4. The reason for the low chamber pressure is explained in the engine performance paragraph 14-4.

14.1.1 APS Flight Objectives

All objectives of the flight with respect to the APS modules were accomplished. These were as follows:

a. To evaluate APS operation under actual flight conditions
b. To better substantiate APS requirements
c. To evaluate the ability of the APS to fulfill the attitude control, maneuvering, and ullaging requirements.

14.1.2 APS Flight Description

Approximately 1 sec after S-II engine cutoff, the APS was activated to provide roll control during first burn.

Following first burn engine cutoff, APS pitch and yaw control was activated to maintain the vehicle in the desired attitude. The APS ullage engines fired for 88 sec following J-2 first burn to provide slosh control and propellant settling.

Approximately 330 sec prior to restart the APS ullage engines were again ignited to provide ullage control during restart preparations. The ullage engines were shut off 3 sec after second burn Engine Start Command.

During the restart attempt the APS pitch and yaw control was deactivated and the APS provided roll control only. When the J-2 engine failed to restart, APS pitch and yaw control was reactivated. The APS maintained pitch, yaw, and roll control of the stage until module 1 propellant depletion at approximately RO +22,030 sec. At this time the signal from the IU was activating the valves of engine 1-1 continuously, attempting to maintain control.

14.2 APS Module No. 1

The operation of the helium pressurization system of module No. 1 was as expected. The propellant supply system pressure levels and the propellant temperatures measured in the propellant control module were in the expected range.

The performance of the module 1 engines was satisfactory throughout the mission with the exception of the pitch engine which had low chamber pressure at various times during the mission.

14.2.1 Helium Pressurization System - Module 1

The module No. 1 helium pressurization system operation was normal with no problems encountered throughout the flight. Prior to APS activation, the helium bottle pressure was 3,120 psia and the temperature was 558 deg R yielding an initial mass in the bottle of 1.015 lbm.

Figure 14-5 shows the helium temperature, pressure, and mass as a function of mission time. The nominal and three-sigma predictions are included for comparison. The mass of helium remaining in the bottle at module 1 propellant depletion was 0.470 lbm. This corresponds to a helium temperature of 552 deg R and a pressure of 1,330 psia.

Figure 14-5 shows that the module 1 helium usage was greater than nominal but was still less than the three-sigma prediction prior to second ullage burn. However the disturbances resulting from the failure of the J-2 to restart resulted in more propellant usage than predicted.

Following propellant depletion, the helium bottle mass leveled off at approximately 0.45 lbm indicating no leakage in the pressurization system.

The helium regulator outlet pressure was maintained at approximately 192 psia throughout APS operation. The propellant tank ullage pressures were 188 psia, which is on the low end of the expected range of 188 to 203 psia.

14.2.2 APS Oxidizer System - Module 1

The oxidizer manifold supply pressure of module 1 was as expected during the flight. The pressure was approximately 188 psia during APS operation. The oxidizer temperature measured at the propellant control module was also in the expected range. The maximum temperature recorded was 570 deg R. Evaluation of the data indicates that the oxidizer bulk temperature (in the tank) remained near the liftoff value of 557 deg R.

The oxidizer remaining in the APS is shown as a function of mission time in figure 14-6. The nominal and three-sigma predictions are included for comparison. The initial oxidizer load of module 1 was 188.6 lbm. The oxidizer consumption exceeded the predicted immediately following the stage first burn. This was due to a 43-sec steady-state burn by the module 1 pitch engine followed by approximately 43 sec of rapid pulsing. The excessive pitch engine firing was required to correct for an unusually high guidance-induced pitch rate at engine cutoff. Following this attitude correction the oxidizer consumption rate was close to the predicted rate until the restart attempt. When the APS pitch-yaw control was reactivated after the restart attempt, engine 1-3 fired steady-state for 18 sec followed by approximately 30 sec of rapid pulsing. Within the next 300 sec, steady-state pulses of 26 and 34 sec were fired on engine 1-2. These firings were required to correct for error rates induced by the J-2 engine and to perform commanded maneuvers. Because of the large LH2 and LOX residual, the moment of inertia of the vehicle was larger than predicted, and the center of gravity (CG) lower. The low CG resulted in shorter APS pitch and yaw moment arms resulting in the large quantity of propellant usage at this time. Table 14-1 shows the propellant consumption during significant periods of the flight. The oxidizer in module 1 was depleted at RO +22,053 sec after liftoff. The time of depletion was determined by examining the oxidizer manifold pressure. Figure 14-7 shows the oxidizer manifold pressure drop at RO +22,053 sec after liftoff.

14.2.3 APS Fuel System - Module 1

The fuel system of module 1 performed as expected during the flight. The fuel manifold supply pressure remained at approximately 190 psia. The fuel temperature measured at the propellant control module remained below 566 deg R. Again, the data indicate that the fuel bulk temperature remained near the liftoff value of 555 deg R (figure 14-6).

The fuel remaining in module 1 during the mission is shown in figure 14-6. The liftoff value was nominal at 124.4 lbm. Like the oxidizer the fuel consumption exceeded predicted usage immediately following stage first burn for the reason mentioned in the oxidizer section. After the attitude control engine burned to correct for guidance-induced vehicle disturbances, the fuel consumption rate was near nominal. Following the restart attempt, the fuel consumption greatly exceeded that predicted for the reasons mentioned in the oxidizer section. The fuel was depleted at RO +21,953 sec. The time of depletion was determined by examining engine chamber pressure data and fuel manifold pressure. Figure 14-7 shows the decrease in engine 1-2 chamber pressure starting at 21,953 sec. The fuel manifold pressure data were not obtained at this time; however, the drops in pressure can be seen with each pulse after RO +21,993 sec. No problems resulted from the fuel being depleted first.

The fuel consumption during significant portions of the flight is presented in table 14-1.

14.3 APS Module No. 2

The operation of APS module 2 was satisfactory. As in module 1 low pitch engine chamber pressures were recorded at various times in the mission. Also as in module 1 the propellant usage was greater than predicted. Module 2 propellant depletion occurred approximately 600 sec after module 1 depletion.

14.3.1 Helium Pressurization System - Module 2

The module No. 2 helium pressurization system operation was normal with no problems encountered throughout the flight. Prior to APS activation, the helium bottle pressure was 3,100 psia and the temperature was 545 deg R. The mass of helium in the bottle was 1.035 lbm. Figure 14-5 shows the helium temperature, pressure, and mass as a function of mission time. The nominal and three-sigma predictions are included for comparison.

Figure 14-5 shows that the module 2 helium usage was close to nominal until after the restart attempt. At this time the APS burn requirements greatly exceeded predicted for the reason mentioned in paragraph 14.2.2.

Following propellant depletion the helium bottle mass leveled off at approximately 0.45 lbm indicating no leakage in the pressurization system.

The helium regulator outlet pressure was maintained at 193 to 195 psia throughout APS operation. The propellant ullage pressures were 192 psia.

14.3.2 APS Oxidizer System - Module 2

The oxidizer system of module 2 performed as expected during the flight. The manifold supply pressure was approximately 193 psia. The oxidizer temperature (measured at the propellant control module) remained in the expected range throughout the APS operation. The maximum temperature recorded was 561 deg R. As with module 1, the data indicate that the oxidizer bulk temperature (in the tank) remained near the liftoff temperature of 546 deg R.

The oxidizer remaining in the APS as a function of mission time is presented in figure 14-6. The initial oxidizer load was 189.4 lbm. The oxidizer quantity prior to restart attempt was within the three-sigma predicted range. For the reasons mentioned in paragraph 14.2.2 the oxidizer consumption exceeded predicted following the restart attempt. Engine 2-1 was fired steady-state for 31 sec, and engine 2-2 had two long steady-state burns of 69 and 64 sec. Table 14-1 shows the propellant consumption during significant periods of the flight. The oxidizer in module 2 was depleted at RO +22,634 sec. The time of oxidizer depletion was determined from the oxidizer manifold pressure. Figure 14-8 shows the drop in manifold pressure at the time of depletion.

14.3.3 APS Fuel System - Module 2

The fuel system of module 2 performed as expected during the flight. The fuel manifold supply pressure was approximately 193 psia throughout the flight. The fuel temperature measured at the propellant control module remained in the expected range throughout the APS operation. The data indicate that the bulk temperature remained near 545 deg R throughout the flight.

The quantity of fuel remaining in the APS is presented as a function of mission time in figure 14-6. The quantity of fuel in the module 2 APS at liftoff was 124.7 lbm. The fuel usage was slightly less than nominal until the restart attempt. At this time, as in the case of the oxidizer, the fuel consumption exceeded prediction. Table 14-1 shows the fuel consumption during significant portions of the mission. The fuel was depleted at RO +22,602 sec. The time of fuel depletion was determined from the drop in fuel manifold

pressure and the decrease in chamber pressure. As in module 1 the fuel was depleted prior to the oxidizer without any detrimental affects on the module. The fuel was depleted first in both modules because the propellants were loaded for an attitude control engine EMR of 1.65 to 1, while the attitude control engines operate at an EMR of approximately 1.60 to 1 during minimum pulsing of which a large portion of the mission is composed. Another reason for the fuel to deplete first was an apparently reduced oxidizer flow at various times during the mission. This is explained in greater detail in the following paragraphs.

14.4 Engine Performance

The performance of the APS engine was adequate to fulfill the attitude control and ullaging requirements until APS propellant depletion. The two pitch engines, 1-2 and 2-2, had low chamber pressures at various times during the mission. The ullage engine in module 2 had a slightly extended chamber pressure tail-off after the second ullage engine burn.

Low chamber pressure (85 psia) was first observed at RO +5,565 sec on engine 1-2. This was the first pulse of a series on this engine after not having fired for approximately 100 sec. Prior to this, the firing on this engine was quite extensive. The chamber pressure increased with each successive pulse. The second pulse in the series had a chamber pressure of 92 psia, while the third was 94 psia. Figure 14-4 shows the chamber pressure increase in a series of pulses on the module 2 pitch engine later in the mission. The chamber pressure of the initial pulse was 55 psia, but by the seventeenth pulse the chamber pressure was up to 92 psia. This engine had two steady-state firings of 69 and 64 sec as well as extensive pulsing prior to this time. In figures 14-2 and 14-3 the engine chamber pressures, injector temperature, and propellant temperature are presented as functions of mission time. The propellant temperatures measured in the propellant control module remained within the acceptable region throughout the mission. A correlation, however, can be made between the low chamber pressure of the module 2 pitch engine and the injector temperature. Figure 14-3 shows that as the engine injector temperature increases the engine chamber pressure decreases. A similar correlation could not be made directly on the module 1 pitch engine because module 1 injector temperature data were not obtained after RO +2,500 sec. Because of the extensive firing on engine 1-2 prior to the times when low chamber pressures were observed, it is very likely that the injector temperature was high.

The following conclusions have been reached in regard to the low chamber pressures obtained during the flight. Extensive attitude control engine firing as a result of the booster problems caused high engine injector temperatures. Heat soak back from the engines during the off periods increased the injector temperature and propellant temperatures in the lines near the injector. When the engine valves were opened the drop in line pressure caused oxidizer vaporization and helium liberation. The vapor and gas in the lines reduced the oxidizer flow and resulted in the lower chamber pressure during the initial pulses in a series. As the series of pulses continued the cooler propellants, which were not affected by the high engine temperature, entered the injector and decreased the injector temperature. The oxidizer vaporization was reduced and the oxidizer mass flow increased. This resulted in the chamber pressure increase with successive pulses as shown in figure 14-4.

The total APS impulse for the attitude control engines in each module is presented as a function of mission time in figure 14-9. Module 1 had supplied a total impulse of 53,830 lbf-sec for attitude control when the propellants were depleted. The quantity of propellant used for attitude control was approximately 201 lbm. Therefore, the average specific impulse for the module attitude control engines was 268 sec. The module 2 attitude control total impulse at propellant depletion was 55,959 lbf/sec. The quantity of propellant used by module 2 for attitude control was 202 lbm. Therefore, the average specific impulse of the module 2 attitude control engines was 277 sec.

The APS engine total impulse is presented in figure 14-10 as a function of pulse width. The total impulse was obtained by integrating the chamber pressure and multiplying the integral by the thrust coefficient (C_F) and the throat area (A_t). The TRW plus and minus two-sigma impulse variation for single and multiple pulses are included in this figure for comparison purposes. The data points below the TRW two-sigma line are the low performance pulses on the two pitch engines and the pulses which occurred on the engines after the fuel had depleted.

The APS engine average thrust is presented as a function of mission time in figure 14-11. The average thrust of each pulse was determined by dividing the total impulse by the pulse width. TRW nominal plus and minus two-sigma thrust value lines have been included in this figure for comparison. The points which are below the minus two-sigma line are the low thrust values on the pitch engines and the pulses which occurred after fuel depletion.

The slightly extended tail-off (1 sec) of the module No. 2 ullage engine at the end of the second ullage burn is presented in figure 14-12. The module 1 ullage engine chamber pressure is presented for comparison. No tail-off was observed on this engine after the first ullage burn. This slight tail-off is not seen as a problem.

TABLE 14-1
APS PROPELLANT USAGE DURING FLIGHT

Events	Module No. 1				Module No. 2			
	Oxidizer Usage		Fuel Usage		Oxidizer Usage		Fuel Usage	
	lbm	percent	lbm	percent	lbm	percent	lbm	percent
Initial load	188.6		124.4		189.4		124.7	
First burn roll control	1.6	0.8	1.0	0.8	1.6	0.8	1.0	0.8
Engine cutoff to end of first APS ullaging	28.1	14.9	21.6	17.4	14.5	7.7	11.1	8.9
Limit cycle operation	45.3	24.0	28.2	22.7	28.7	15.2	18.0	14.4
Restart preparation (Including second ullage engine burn)	50.5	26.8	37.4	30.1	51.5	27.2	38.1	30.6
Restart attempt to propellant depletion	63.1	33.5	36.2	29.0	93.1	49.1	56.5	45.3
Total usage	188.6	100	124.4	100	189.4	100	124.7	100

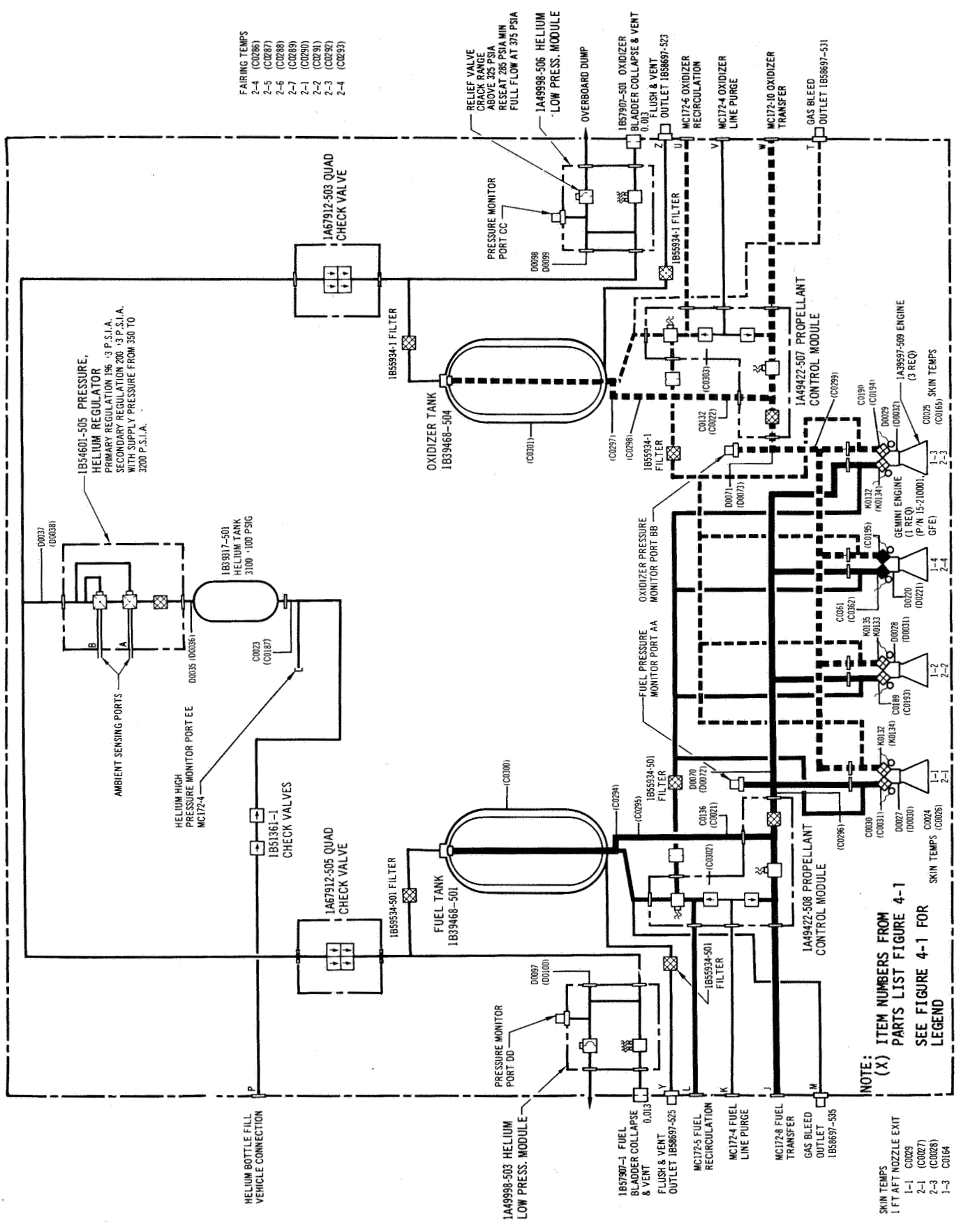

Figure 14-1. Auxiliary Propulsion System and Instrumentation

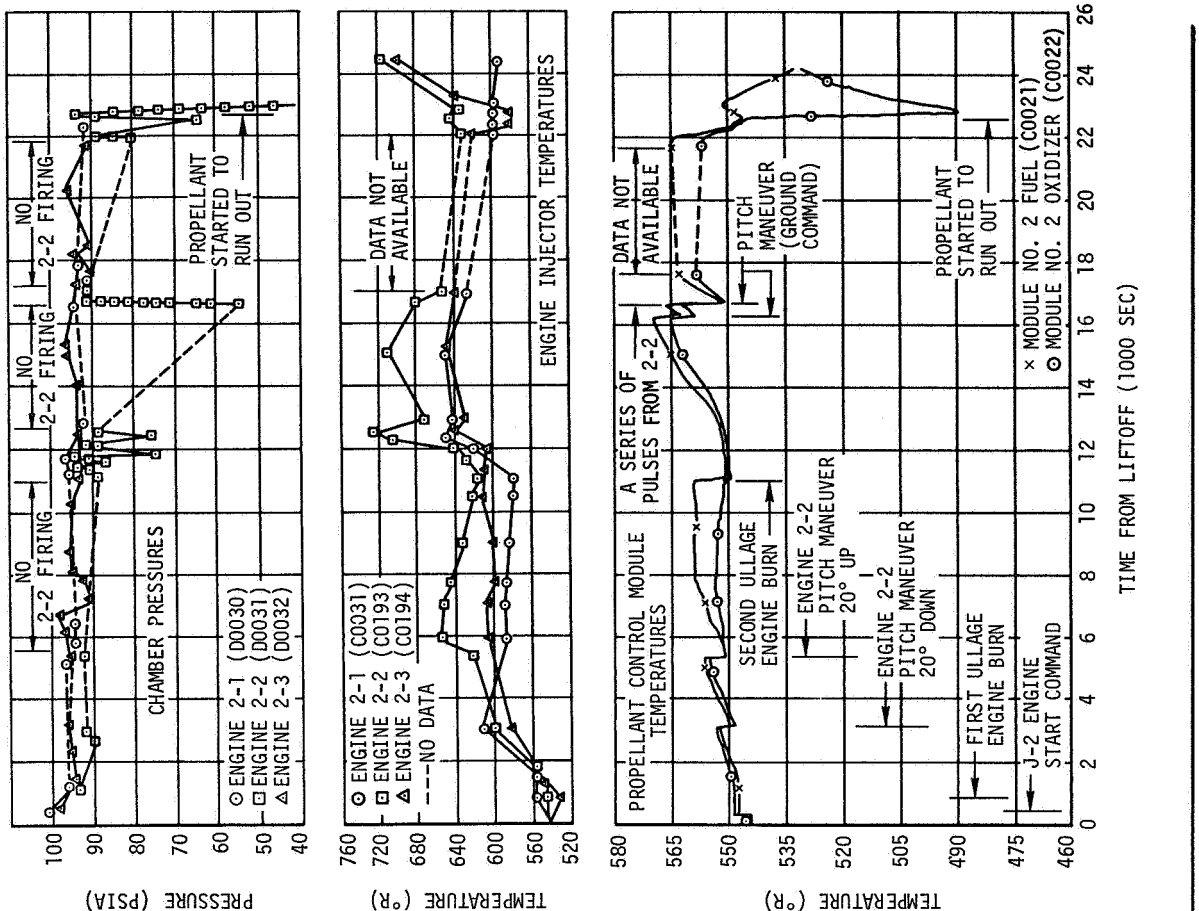

Figure 14-3. Module 2 Performance Correlation

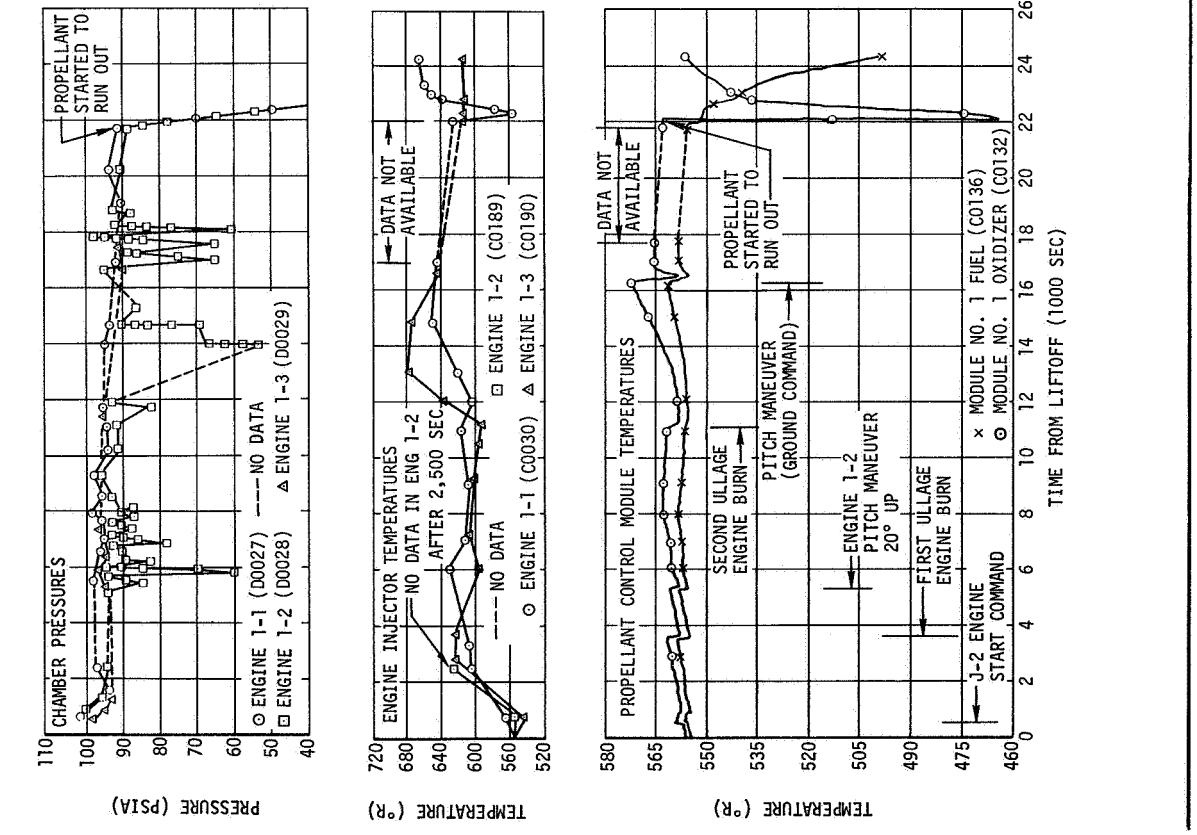

Figure 14-2. Module 1 Performance Correlation

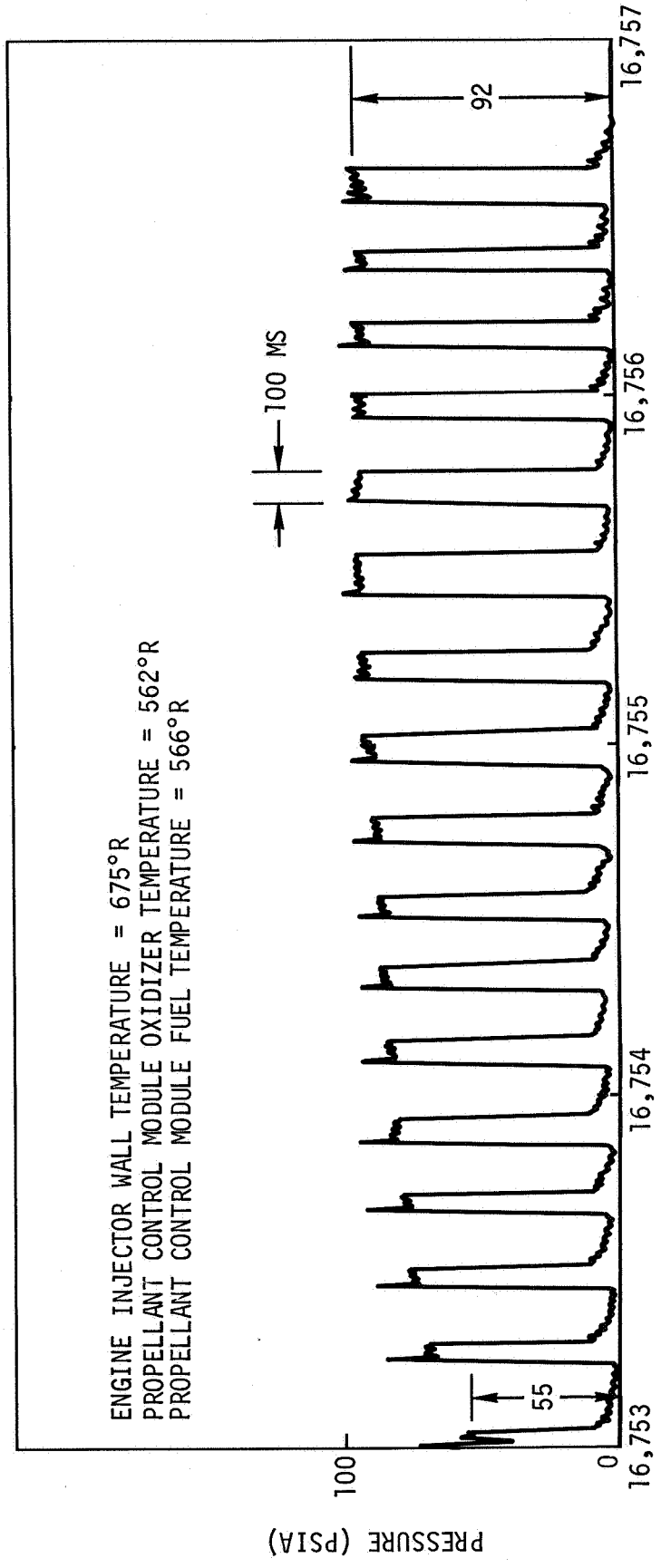

Figure 14-4. Module 2 Pitch Engine 2-2 Chamber Pressure

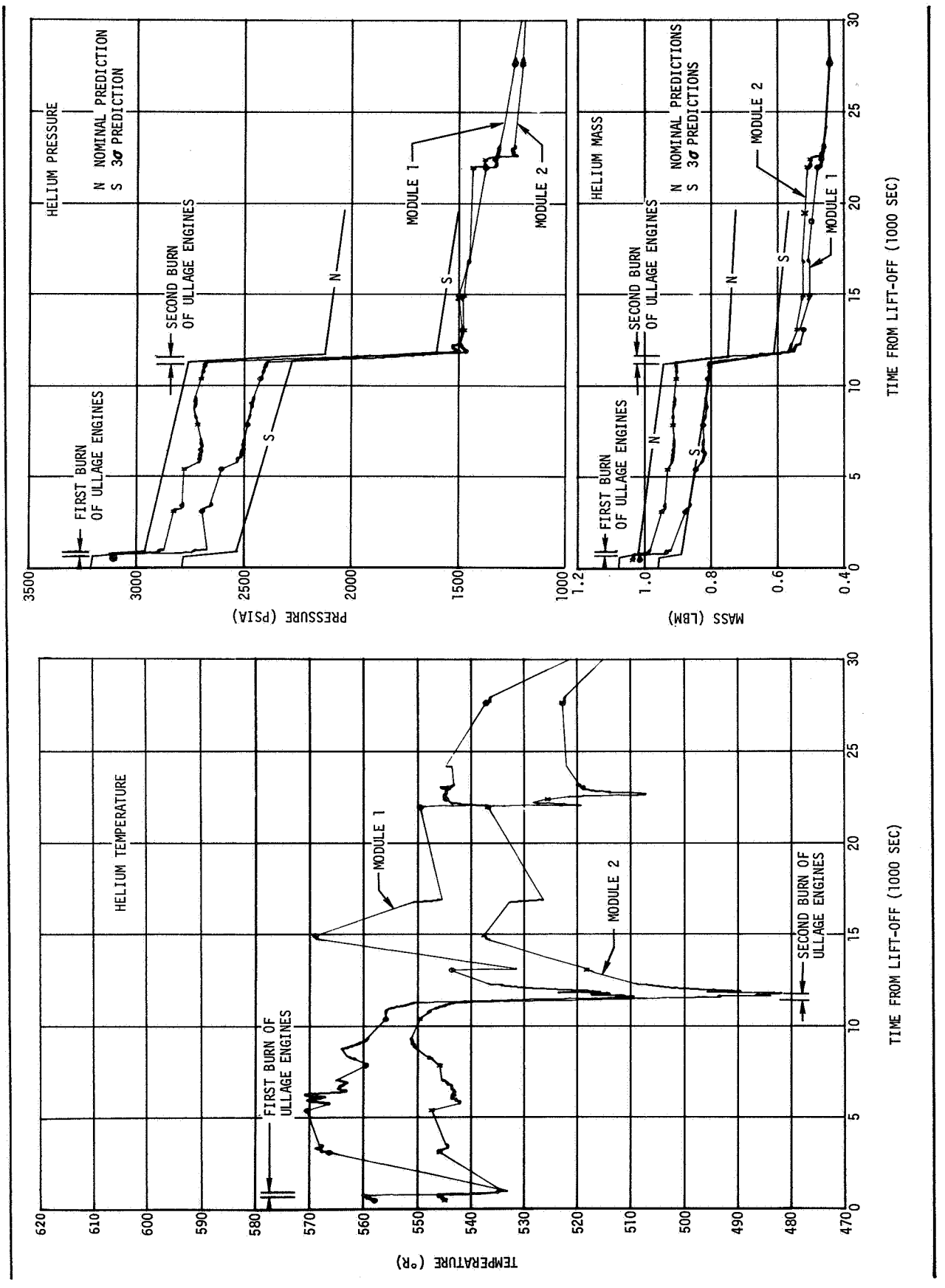

Figure 14-5. Helium Bottle Conditions

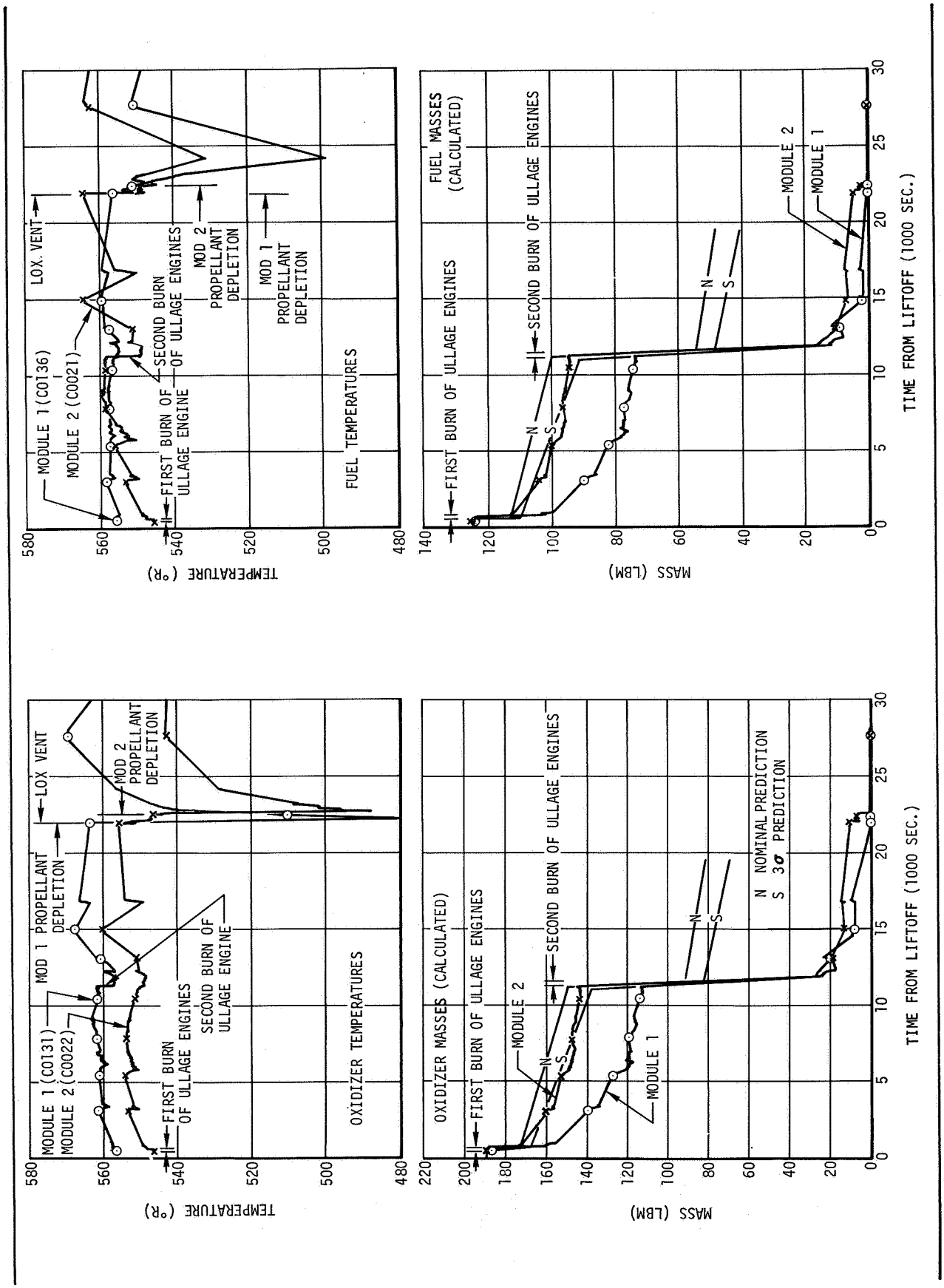

Figure 14-6. APS Propellant Conditions

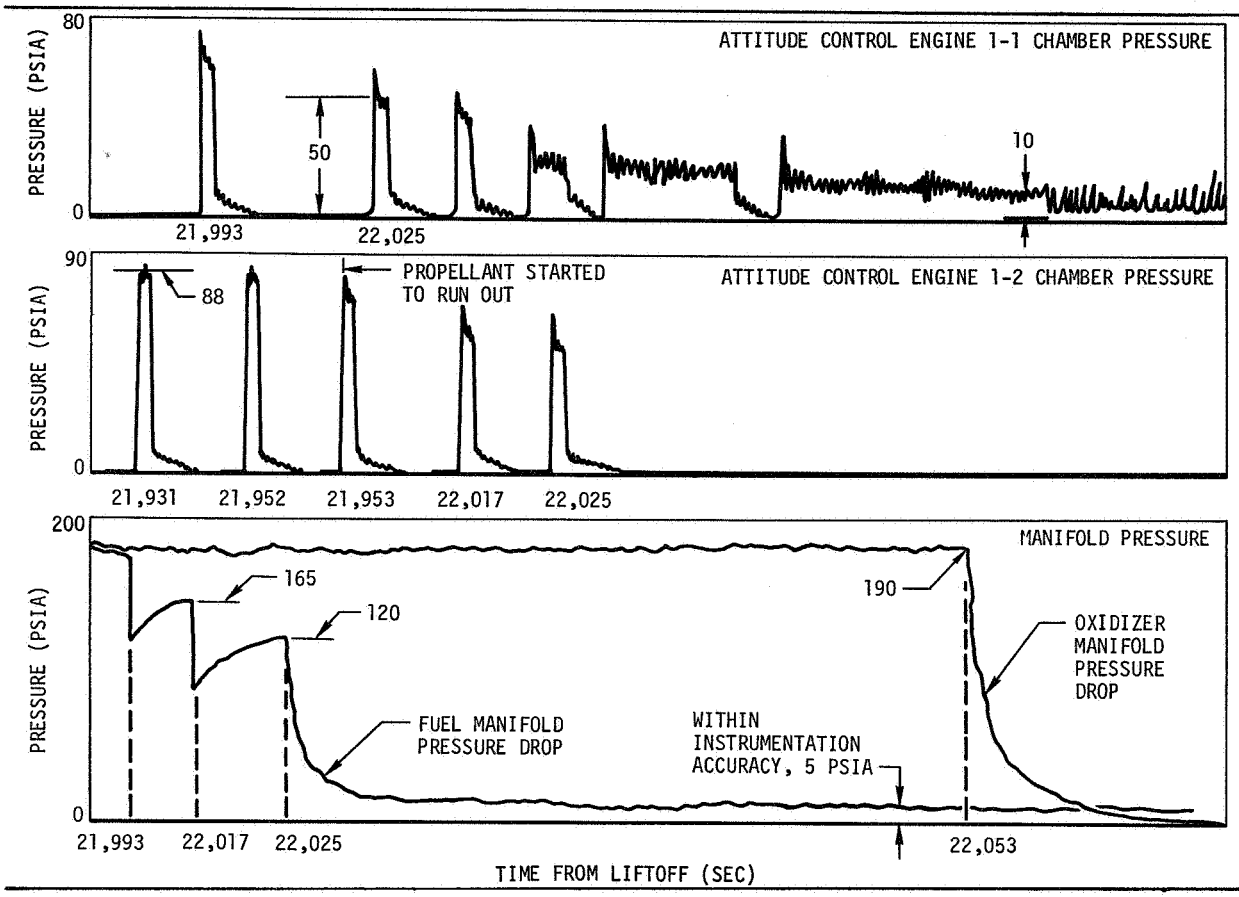

Figure 14-7. APS Module No. 1 Propellant Depletion History

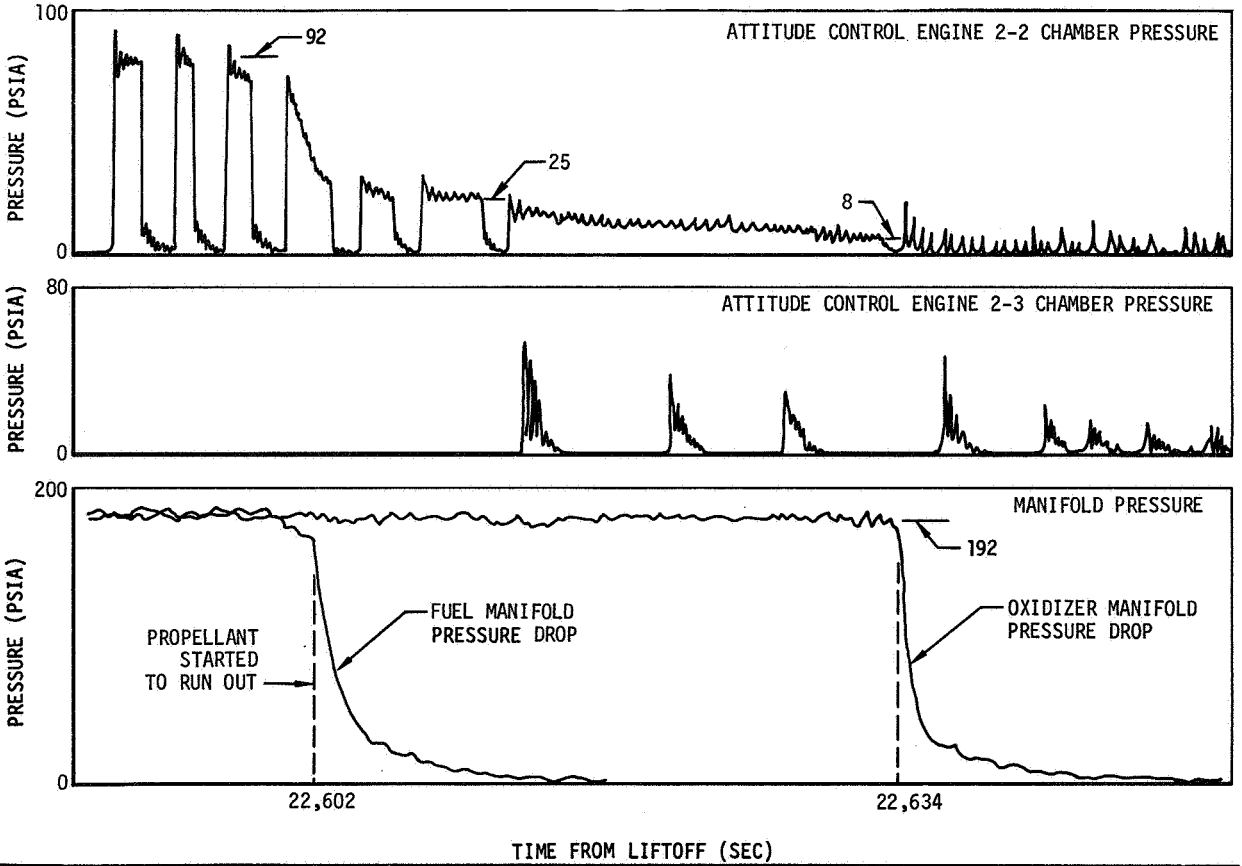

Figure 14-8. APS Module No. 2 Propellant Depletion History

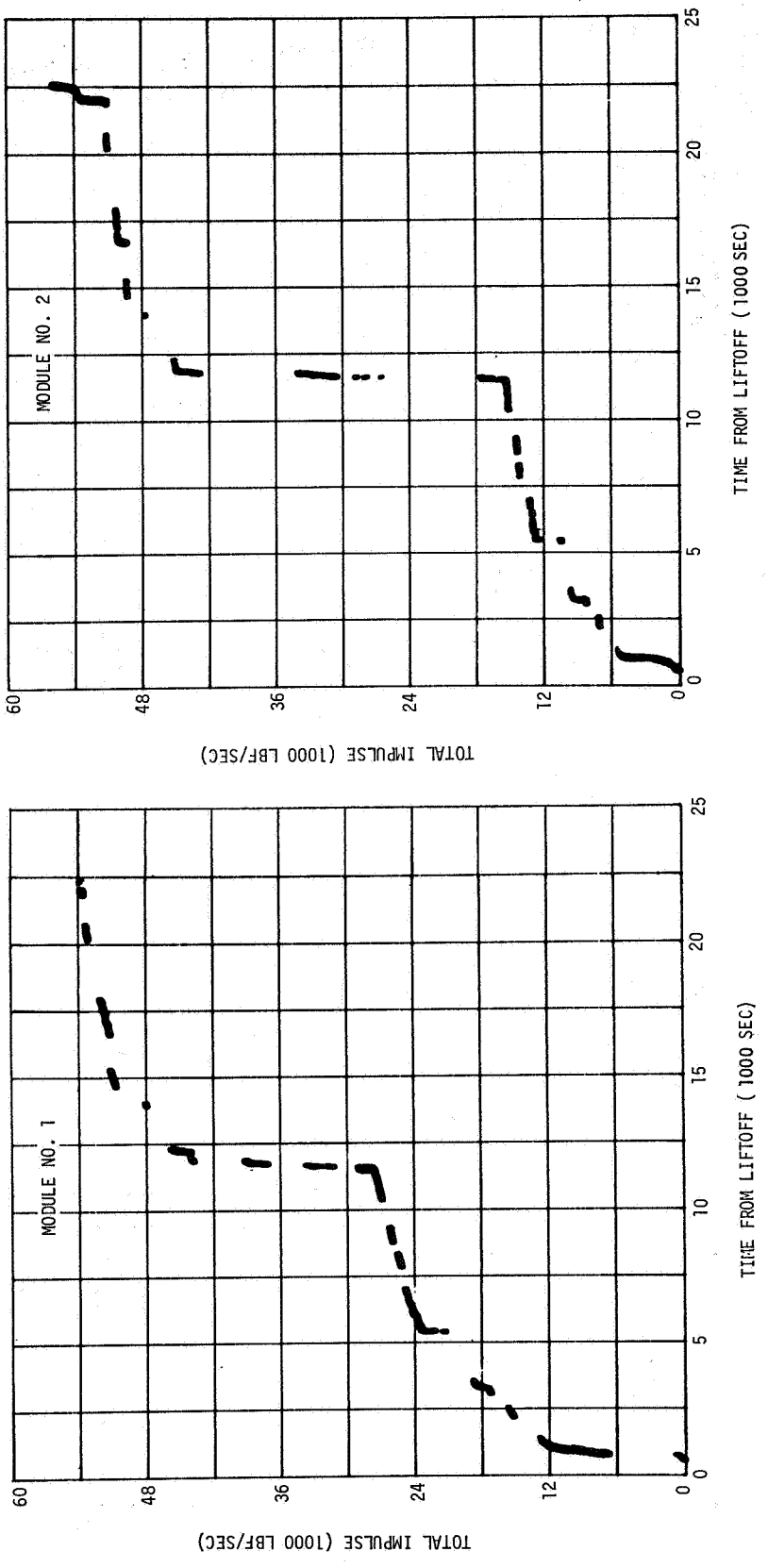

Figure 14-9. APS Total Impulse

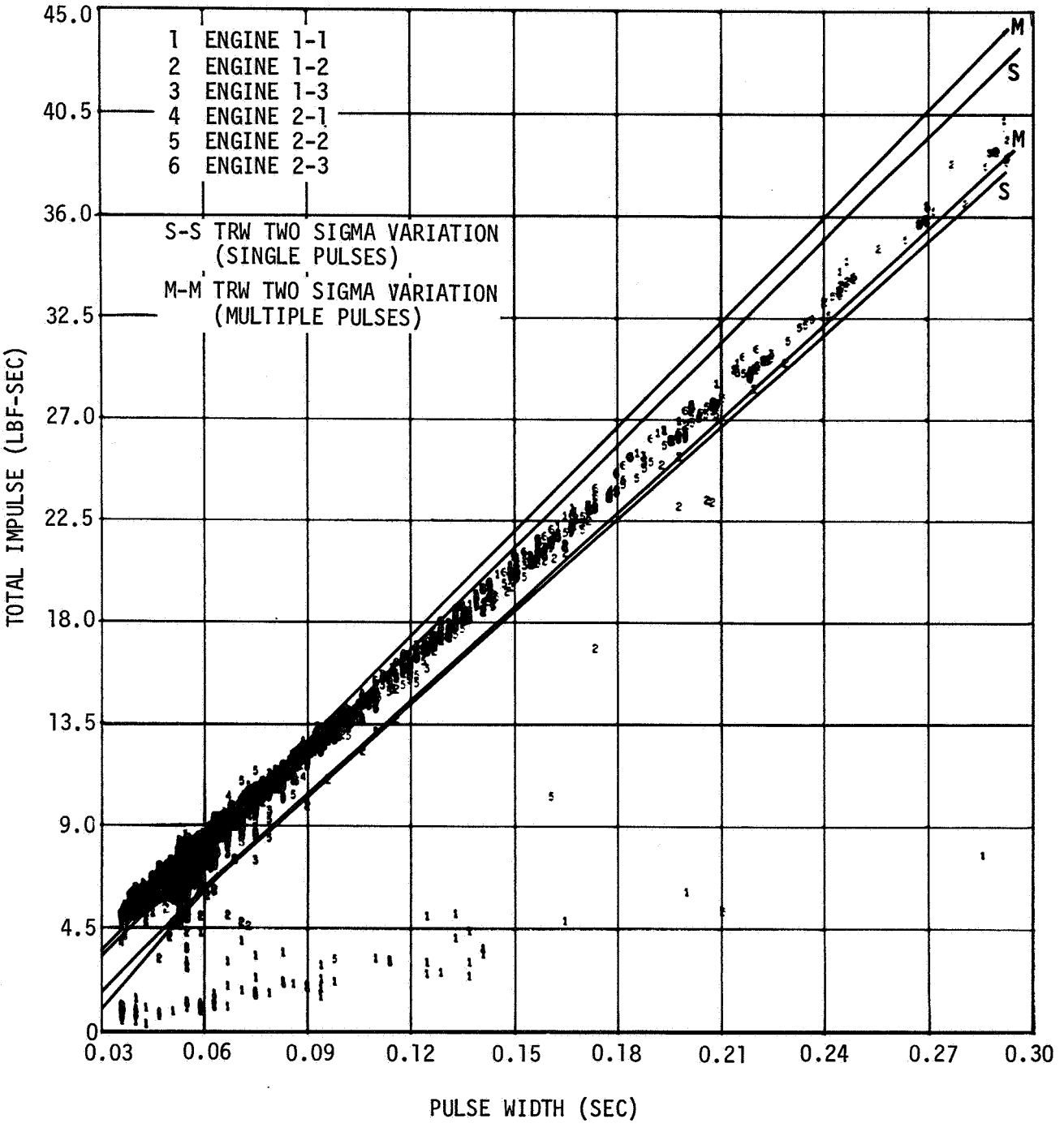

Figure 14-10. APS Total Impulse Per Pulse

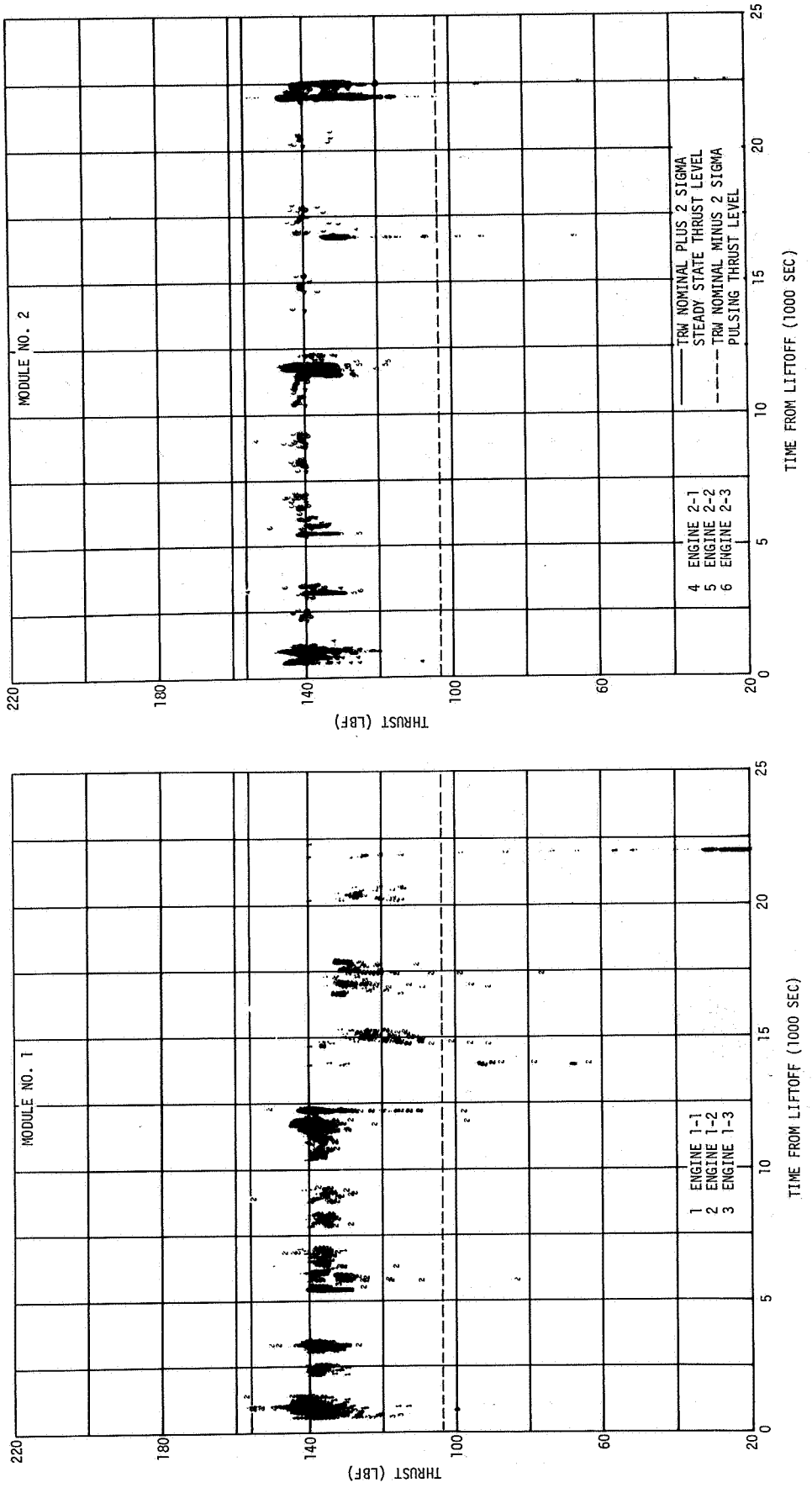

Figure 14-11. APS Thrust

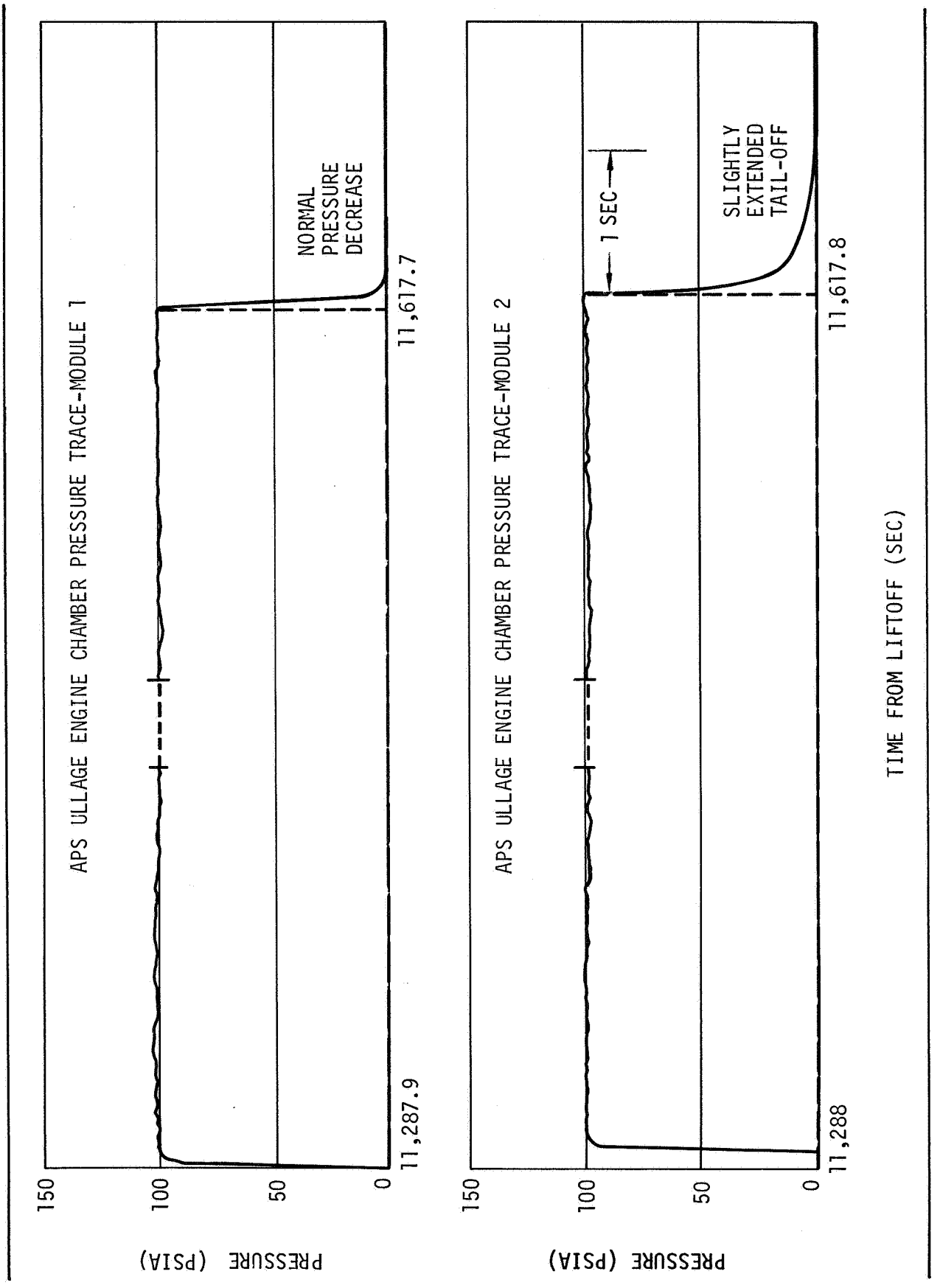

Figure 14-12. APS Ullage Engine Chamber Pressure - Second Burn

SECTION 15

PNEUMATIC CONTROL AND PURGE SYSTEM

15. PNEUMATIC CONTROL AND PURGE SYSTEM

The pneumatic control and purge system (figure 15-1) performed satisfactorily throughout the flight. The helium supply was adequate to meet all mission requirements and to accomplish all purges. The S-IVB-502 was the first to incorporate Sterer actuation control modules, and the modules performed satisfactorily. The orbital leakage rate was near zero.

15.1 Ambient Helium Supply

The pneumatic supply was adequate, and only one deviation in system operation occurred during the flight. The engine pump purge was initiated approximately 0.1 sec before engine cutoff (approximately 7 sec late), and the purge pressure was near operating level within 1.5 sec. This purge initiation is required a minimum of 5 sec before Engine Cutoff Command to ensure that the required conditions are present at the customer connect panel within 0.2 sec of Engine Cutoff Command. The purge is conducted to purge the oxidizer turbine seal, fuel turbine seal, and fuel turbopump primary seal cavities of moisture; to clear the gas generator (GG) combustor of combustion products; and to maintain an inert moisture-free atmosphere at the GG injector face. The only problems likely to be caused by a purge delay are blockage, or partial blocakage, of the GG LH2 injector and freezing, or sticking, of the GG LH2 valve poppet. Since the GG was successfully restarted during the second burn attempt, these problems did not occur; therefore, the purge delay had no detrimental effect. The delay was caused by an error in the launch vehicle digital computer (LVDC) time to go equations and was not a fault of pneumatic system components. It is understood that the LVDC contractor is presently studying means to prevent recurrence of this problem.

During the AS-502 countdown demonstration test, the LOX chilldown pump motor container purge pressure (D0103) reached the vent setting (86 psia) before chilldown was initiated and remained at 86 psia throughout the test. The container pressure during the flight showed a similar profile and is compared with the S-IVB-501 flight in figure 15-2. The lower prelaunch container pressure on S-IVB-501 indicates that the prelaunch static leakage was greater on S-IVB-501. The increases in D0103 during the S-IVB-501 chilldowns occurred because the motor seals were dynamic seals which leak less when the pump is running. During engine burn on S-IVB-501, the chilldown pumps were stopped, resulting in an increased leakage rate. This accounts for the decreases in D0103 during both engine burns.

On S-IVB-502 the D0103 pressure decay, which began at liftoff, indicated an increased leakage rate that could have resulted from poor sealing due to vibration or to a chipped seal. Also, tests have shown that seals can change sealing characteristics during the wearing in process, and that they can seal differently at different speeds. On S-IVB-502 and subsequent stages, the chilldown shutoff valves are normally left open during engine

burn, allowing sufficient flow (approximately 10 gpm) to spin the chilldown pump at low speed. Good sealing at slow speed could account for the low leakage rates observed during the S-IVB-502 flight first engine burn.

Therefore, the difference in seal boundary conditions between S-IVB-501 and -502 during boost (S-IVB-502 experienced significant 5 cps longitudinal vibration) and the variance in system configuration (chilldown shutoff valve closed on S-IVB-501 during burn) support the indicated behavior of the system levels.

15.2 Pneumatic Control

Significant valve actuations through the end of first burn and their respective demands on the system are shown in figure 15-3. The control helium regulator discharge pressure (D0014) responded to the J-2 engine anomaly at RO +700 sec by increasing from 550 to 554 psia, but pneumatic control system performance was not affected by this indicated change in pressure. The control sphere temperature (C0205) during the last half of the engine pump purge was obtained from less accurate tape recorder data, but an extrapolation of the valid data indicated an average mass usage rate of 5.9 scfm, which is near prediction of 6 to 8 scfm. After the engine pump purge was terminated, the mass loss rate was insignificant until RO +10,877 sec when the prevalves were closed for orbital chilldown (figure 15-4). During the period of prevalve closure the average mass usage rate was 1.7 scfm which agrees very well with predictions. The pneumatic system performance parameters during the restart attempt and during the third and fourth orbits are shown in figures 15-5 and 15-6, respectively. During periods of no pneumatic actuations, the mass loss rate continued to be insignificant (approximately zero).

Pneumatic system performance data at significant times are compared with S-IVB-501 flight and S-IVB-502 acceptance firing data in table 15-1.

TABLE 15-1
PNEUMATIC CONTROL AND PURGE SYSTEM DATA

Parameter	Units	S-IVB-502 Flight		S-IVB-501 Flight		S-IVB-502 Accept	
		First Burn	Second Burn	First Burn	Second Burn	First Burn	Second Burn
Sphere Volume	cu ft	4.5	4.5	4.5	4.5	4.5	4.5
Sphere Pressure							
At liftoff	psia	3,063	--	2,921	--	3,205	--
At Engine Start Command	psia	3,003	2,429	2,892	1,474	3,220	2,640
At Engine Cutoff Command	psia	3,010	2,429	2,932	1,515*	3,110	2,640
Sphere Temperature							
At liftoff	deg R	545	--	547	--	555	--
At Engine Start Command	deg R	541	496	543	461	549	545
At Engine Cutoff Command	deg R	541	496	552	473*	549	546
Helium Mass							
At liftoff	lbm	8.54	--	8.19	--	9.75	--
At Engine Start Command	lbm	8.49	7.56	8.17	5.08	8.98	7.39
At Engine Cutoff Command	lbm	8.49	7.56	8.14	5.08*	8.76	7.36
Usage during engine operation	lbm	0.0	0.0	0.03	0*	0.22	0.03
Usage during 10-min postfiring engine pump purge	lbm	0.72	--	0.62	--	0.84	--
Regulator Outlet Pressure							
Maintained pressure band	psia	525 to 560	525 to 560	520 to 555	520 to 540	515 to 545	515 to 545
Minimum system pressure during start and cutoff transient	psia	510	483	420	415	425	425
Average LOX chilldown motor container purge pressure	psia	42	43	65	59	41	41

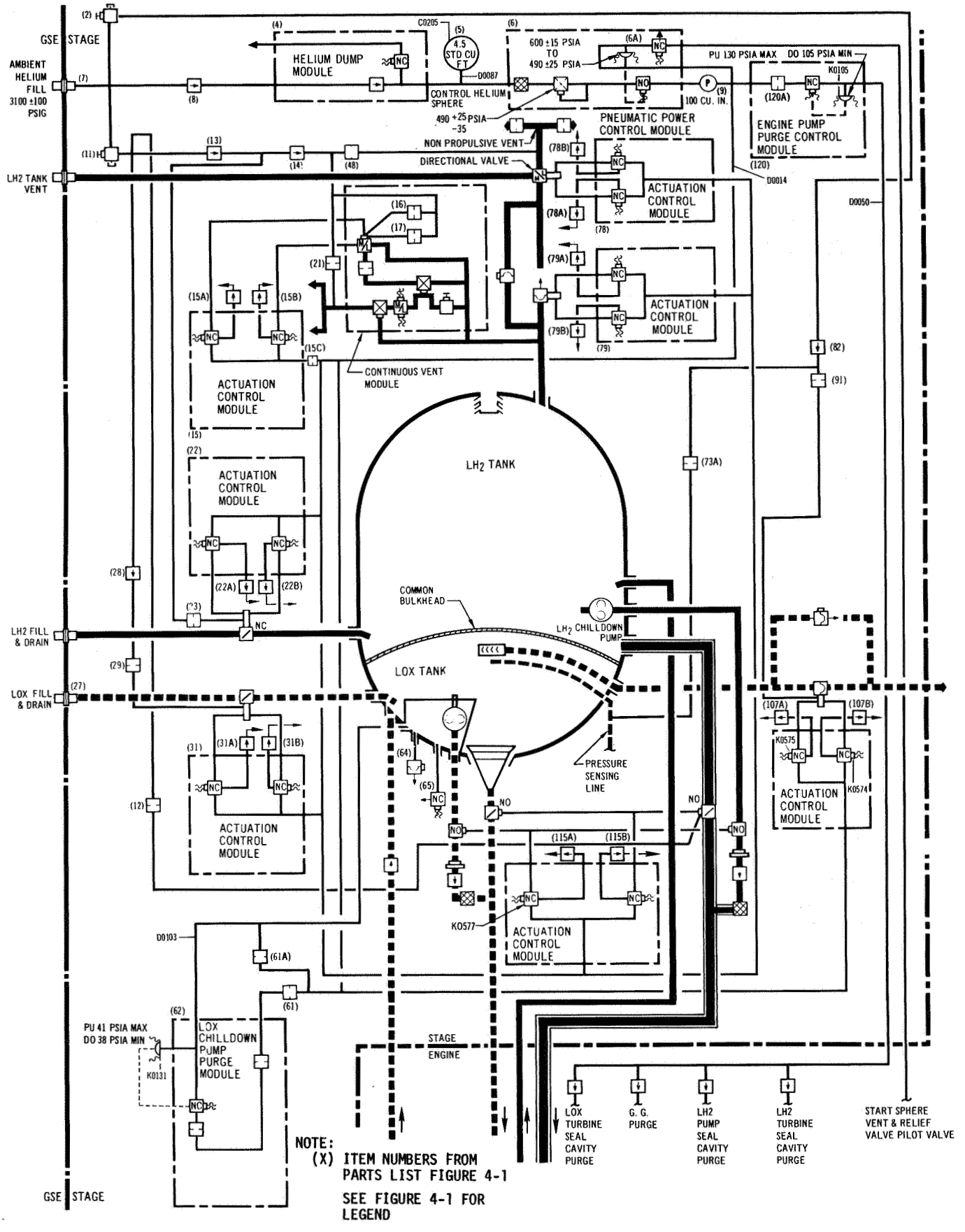

Figure 15-1. Pneumatic Control and Purge System

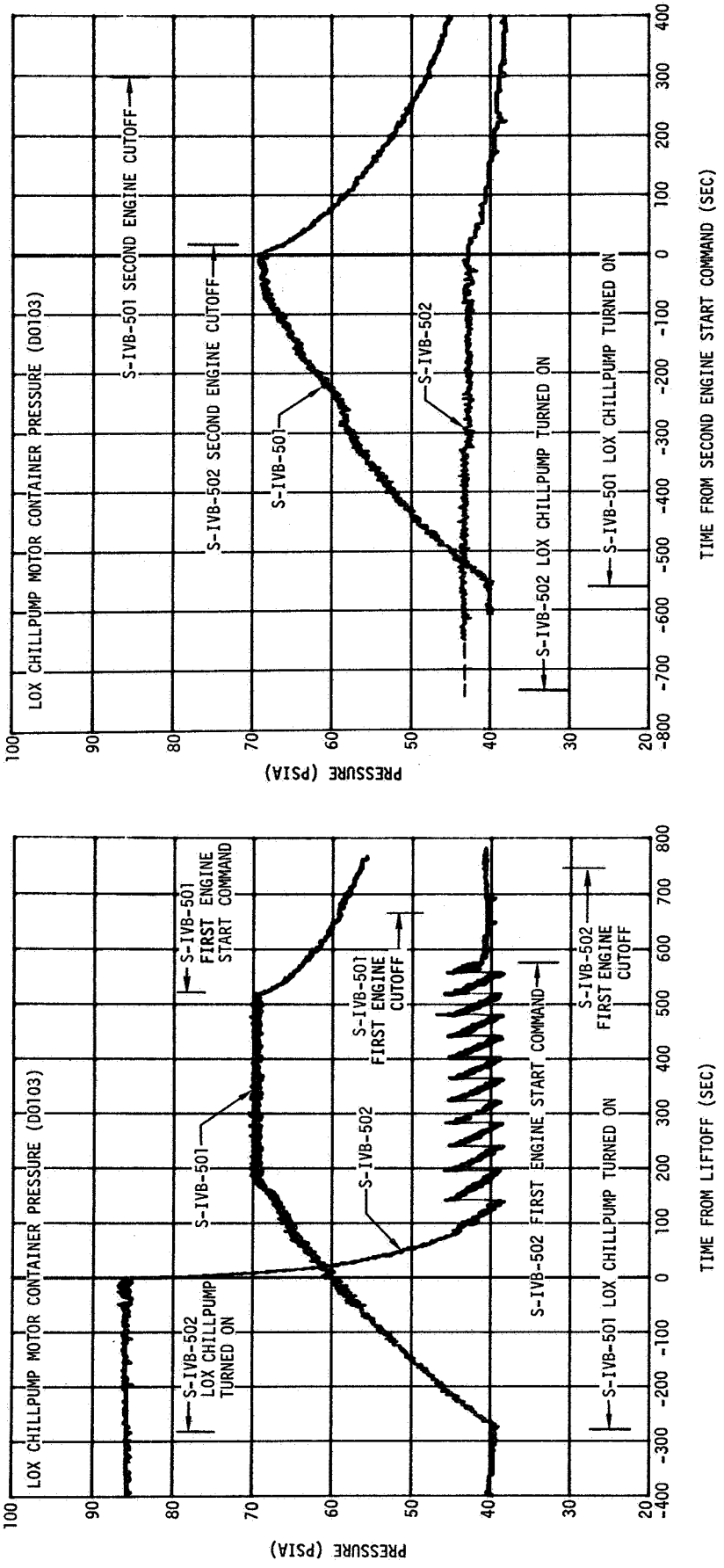

Figure 15-2. LOX Chilldown Motor Container Purge Performance

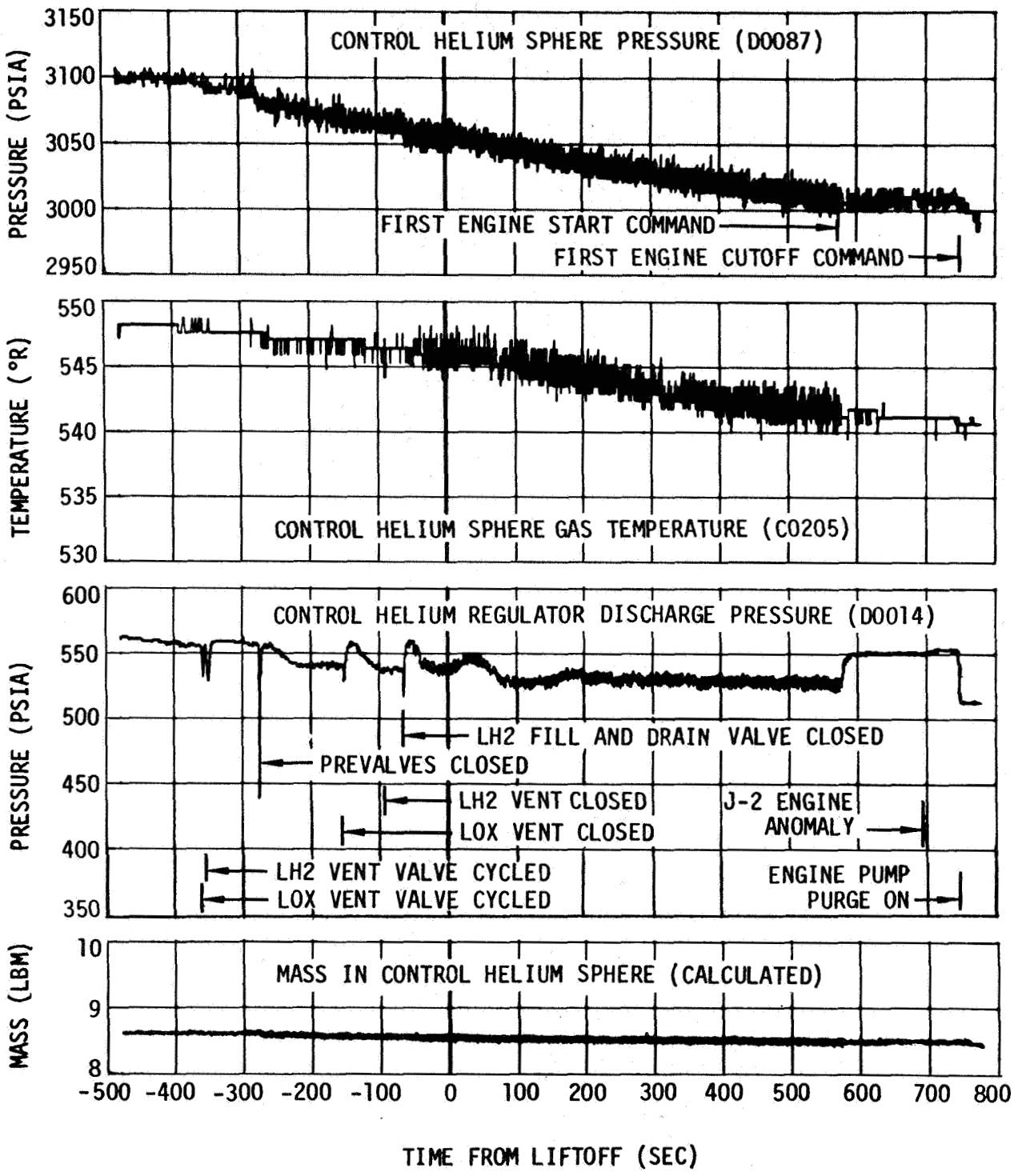

Figure 15-3. Pneumatic Control and Purge System Performance – Boost and First Burn

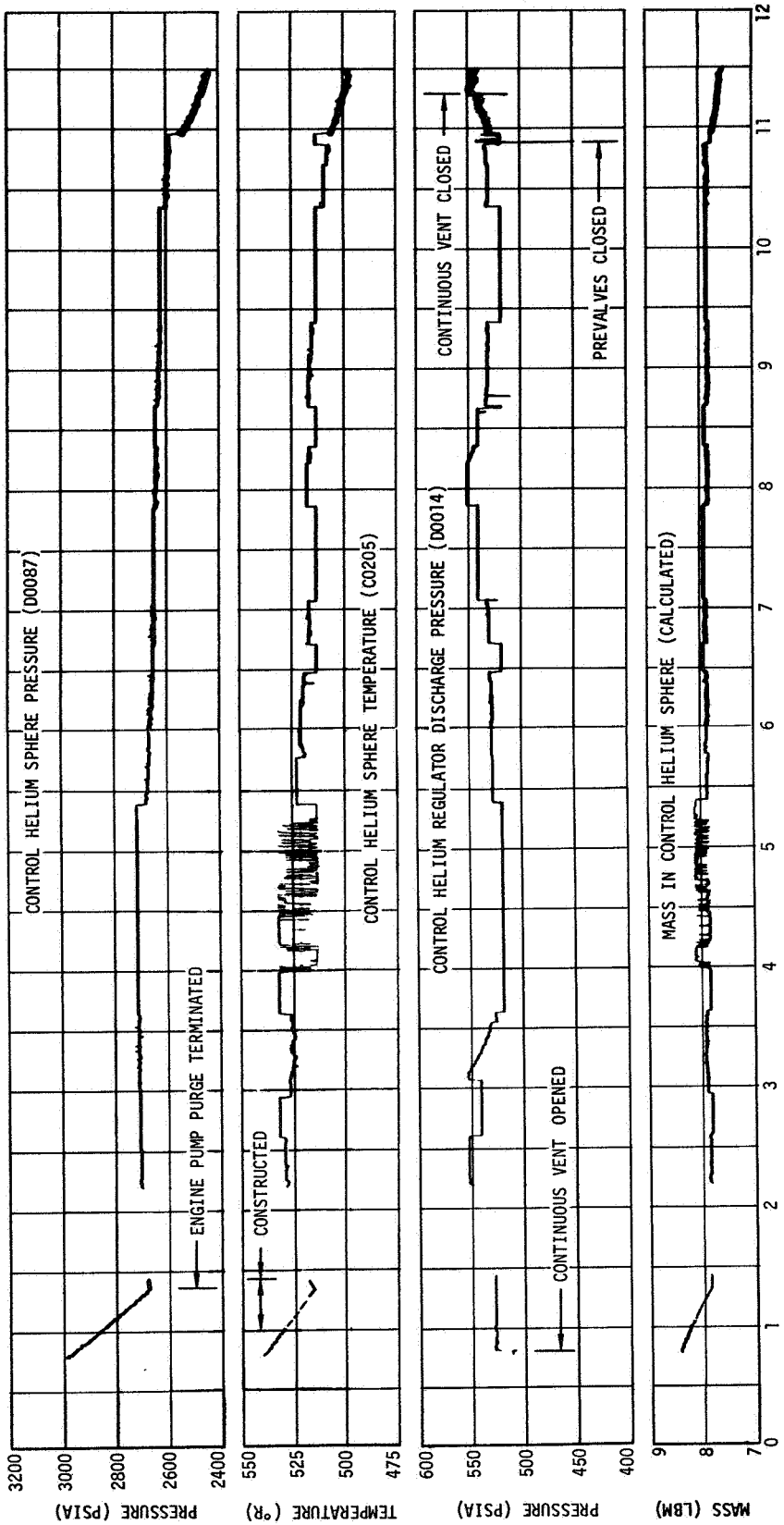

Figure 15-4. Pneumatic Control and Purge System Performance During First and Second Orbits

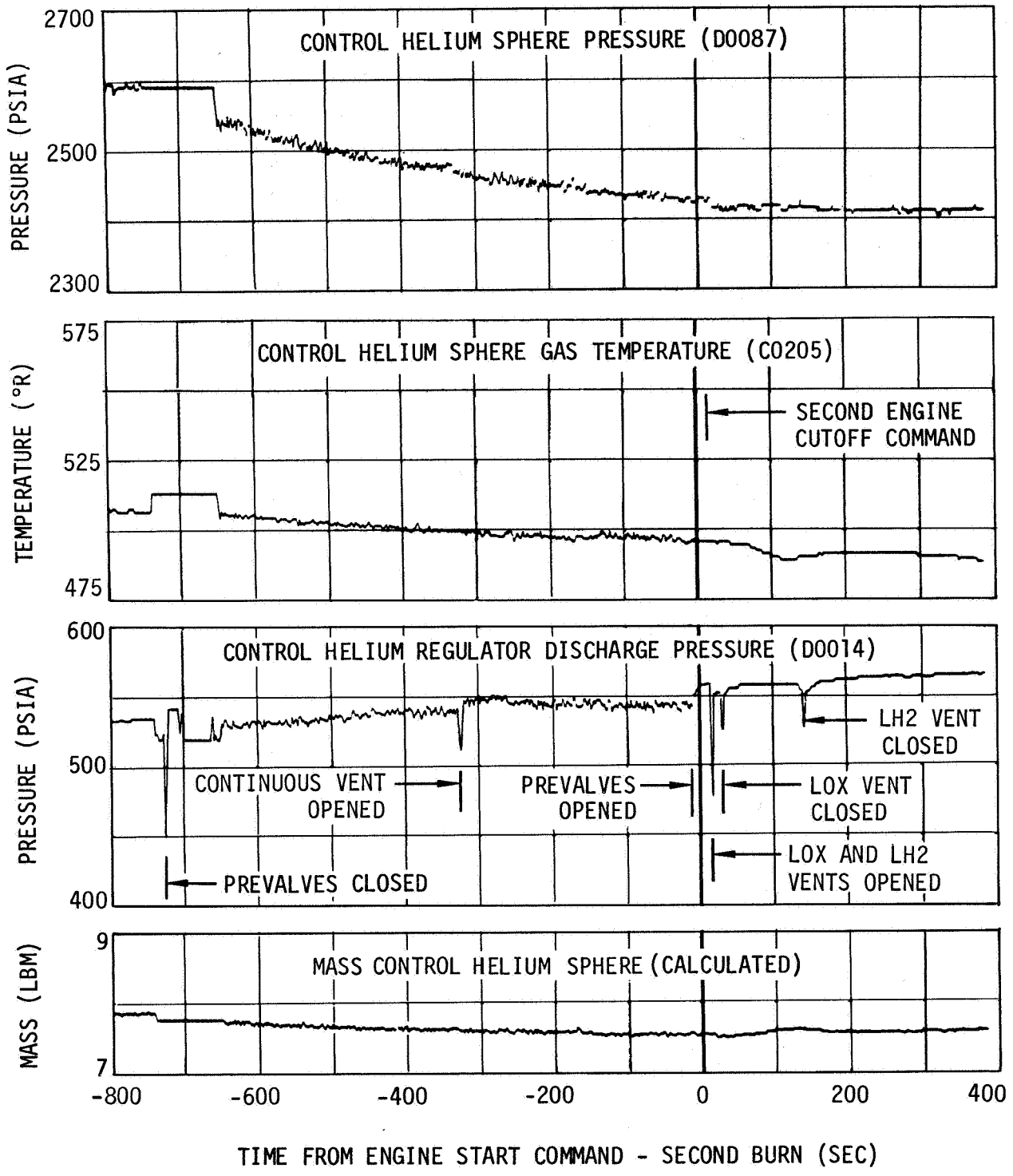

Figure 15-5. Pneumatic Control and Purge System Performance - Second Burn

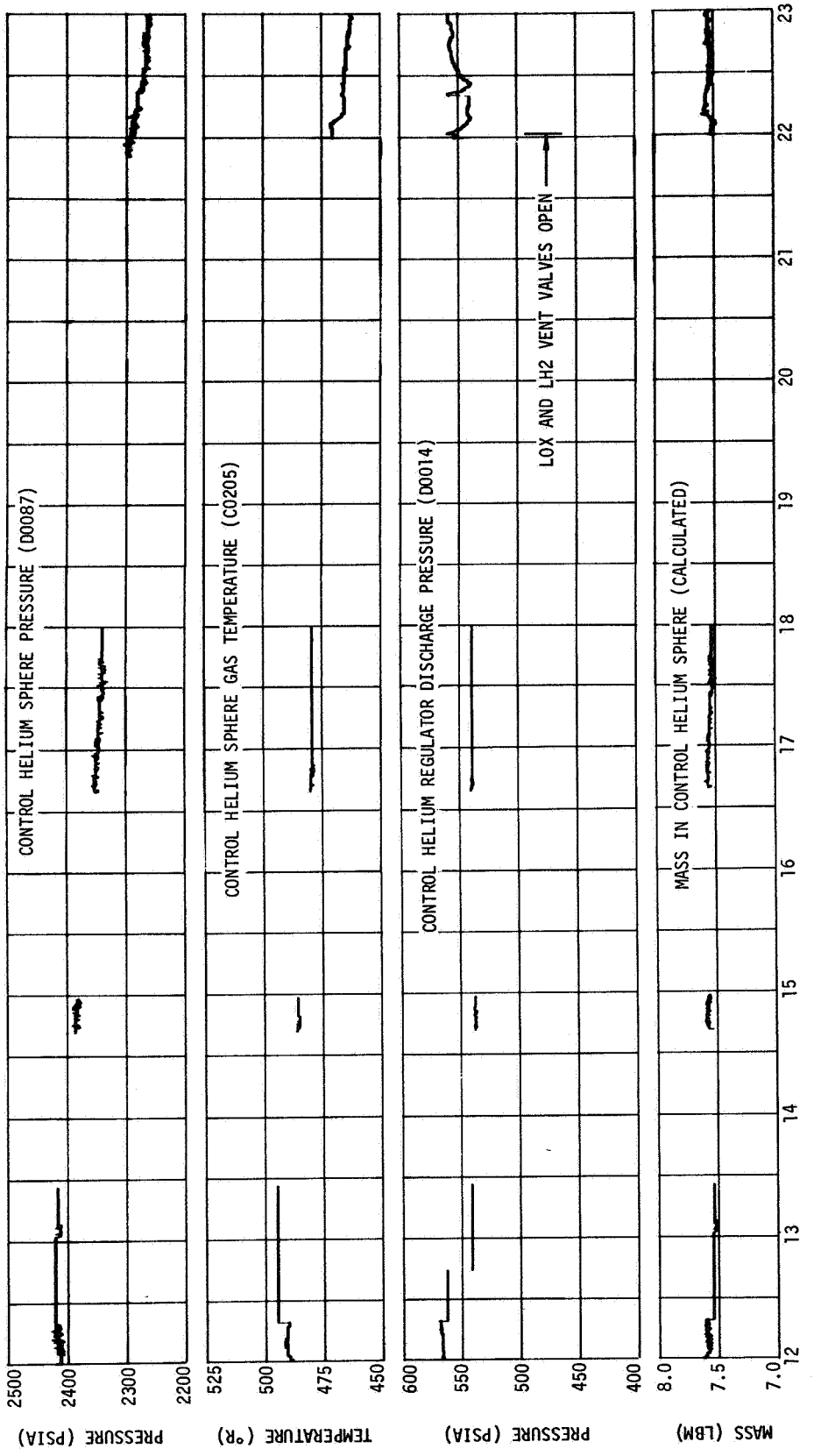

Figure 15-6. Pneumatic Control and Purge System Performance During Third and Fourth Orbits

SECTION 16

PROPELLANT UTILIZATION

16. PROPELLANT UTILIZATION

The propellant utilization (PU) system successfully accomplished the requirements associated with propellant loading and first burn propellant management. A LOX mass measurement system malfunction prior to the attempted restart might have prevented proper operation of the PU system during second burn operation, had restart been achieved.

Loading computer indicated full load propellant values at liftoff were 100.07 and 99.88 percent of the desired indicated values for LOX and LH2, respectively. The actual best estimate propellant mass values at liftoff were 194,140 lbm LOX and 42,448 lbm LH2 as compared to the desired mass values of 193,273 lbm LOX and 42,493 lbm LH2. These values are well within the required $\pm$1.39 percent stage loading accuracy.

The PU valve slewed to the LOX rich (full closed) position after PU activate and remained in that position for the duration of the extended first burn. Second burn PU valve operation, through restart attempt, was consistent with proper sequencing followed by a response to a LOX mass measuring system anomaly.

Similar to the flight of AS-501 the rising of propellants within the sensors due to capillary action was noted during the low acceleration coast period. During the orbital coast period a malfunction of the LOX mass measuring system occurred, resulting in an indication of a LOX tank overfilled condition. Since restart was not achieved the effect of capillary action on the hydrogen mass probe was not completely removed.

Propellant slosh experienced by the stage had no effect on PU operation during first burn because of the high engine mixture ratio (EMR) operation.

Several tests are in progress to further define the PU system failures mode as well as to evaluate proposed fixes and/or product improvement. The results of these studies are not available for inclusion in this report. However, it should be noted that the aft section of the stage was subjected to a high temperature environment which may have degraded the LOX probe wiring during first burn.

16.1 PU Mass Sensor Calibration

The preflight propellant masses at the desired full load calibration point were determined by extrapolating the S-IVB-502 acceptance firing full load data. S-IVB-502 acceptance firing full load data was determined by the flow integral analysis method.

The propellant masses at the lower calibration point were computed from unique tank volumes and predicted propellant density data. The corresponding capacitance values were determined by adding a mean delta capacitance based on measured data to the S-IVB-502 vendor air capacitance values.

The following table presents a summary of the PU mass sensor calibration data:

SENSOR	FULL POINT		EMPTY POINT	
	MASS (lbm)	CAPACITANCE (pf)	MASS (lbm)	CAPACITANCE (pf)
LOX	193,273	412.94	1291	282.33
LH2	42,493	1180.29	202	974.31

16.2 Propellant Mass History

The predicted, measured, and best estimate propellant masses at significant flight events are presented in table 16-1. The best estimate propellant masses are derived by subtracting nonpropellants (dry stage, ullage gases, etc.) from AS-502 third flight stage best estimate masses presented in section 9. The remaining propellant mass is then divided into LOX and LH2 according to the prevailing mixture ratio at the specific flight event time.

The propellant mass measurement systems represented in table 16-1 are (a) PU indicated corrected (b) flight flow integral (c) PU volumetric (d) level sensors, and (e) trajector-reconstruction. A brief description of each measurement system is as follows:

a. The PU indicated corrected method measures propellant mass from raw PU probe output which is reduced according to the preflight flow integral calibration slope and adjusted for acceptance firing flow integral nonlinearity and PU flight dynamics effects.

b. The flight flow integral method consists of determining the LOX and LH2 mass flowrates and integrating as a function of time to obtain total consumed propellant masses during engine burn. The flow integral propellant masses at Engine Start Command (ESC) are determined by adding propellant at Engine Cutoff Command (ECC) to the total propellant consumed by the engine, the fuel pressurant added to the ullage, and the propellant lost to boiloff.

c. The PU volumetric masses are derived from raw PU probe output data which is reduced according to volumetric calibration slopes and adjusted for flight dynamics effects and volumetric tank to sensor mismatch. The calibration slopes (pounds per picofarad) were computed from the capacitance-propellant mass relationships at the upper and lower probe active element extremities. Propellant masses at the extremities were calculated from unique tank volume determined from tank measurements and propellant density.

d. The level sensor system measures propellant mass at sensor activation and these masses are extrapolated to ignition or cutoff masses by the flight flow integral data. Data was obtained from three level sensors in the LOX tank and four level sensors in the LH2 tank.

e. The trajectory reconstruction method determines vehicle mass changes from thrust/acceleration relationships.

The results of the five methods of propellant mass evaluation are presented in table 16-1. The flight flow integral, the PU volumetric, and the trajectory reconstruction total propellant masses agree very closely to the best estimate propellant masses. The PU indicated corrected total propellant masses are 881 and 883 lbm less at Engine Start Command and Engine Cutoff Command, respectively, than the best estimate. The level sensor total propellant masses are 879 and 805 lbm more at Engine Start Command and Engine Cutoff Command, respectively, than the best estimate. Propellant consumption values from the various measurement systems agreed favorably with the best estimate consumption values. The maximum deviation in propellant consumption between all measurement systems was 314 lbm.

16.2.1 Propellant Loading

Table 16-2 presents a tabulation of the LOX, LH2, and total propellant masses at liftoff. The desired, measured, and best estimate masses are presented and the deviations of the desired and measured values from the best estimate are shown. The best estimate liftoff propellants are derived from the AS-502 third flight stage best estimate masses presented in section 9 and from the S-IVB stage propellant mass history presented in paragraph 16.2.

The best estimate total propellant liftoff mass was 822 lbm (0.347 percent) greater than desired; the LOX mass was 867 lbm greater and the LH2 mass was 45 lbm less than desired. Both LOX and LH2 loaded masses were well within the specified loading accuracy.

16.2.2 Orbital Boiloff

LOX loss between first burn Engine Cutoff Command and second burn restart preparations was 343 lbm including first burn engine thrust decay and orbital boiloff.

The LH2 boiloff between first burn Engine Cutoff Command and second burn restart preparations was 3,024 lbm. This value was determined by analysis of the LH2 tank ullage gas and continuous vent system (CVS) flowrate analysis (section 13).

16.2.3 PU Nonlinearity Analysis

A comparison of the LOX and LH2 mass sensor nonlinearities as determined by the PU volumetric and flow integral methods is presented in figure 16-1. The volumetric nonlinearities were obtained by normalizing the volumetric total flight corrections to the observed flight full propellant load and propellant sensor empty point. The predicted flow integral nonlinearity was obtained from smoothed acceptance firing data and predicted inflight dynamics effects. The flow integral actual data are smoothed nonlinearities from the flight flow integral analysis, which inflight dynamics effect.

The total correction to the indicated PU mass for volumetric analysis is the sum of the PU flight dynamics correction, propellant tank to sensor mismatch, and the difference in preflight flow integral and volumetric calibration slopes. A discussion of corrections applied are given in paragraphs 16.2.3.1 and 16.2.3.2.

The deviation of the volumetric derived actual nonlinearity from the predicted (volumetric) is less than 50 lbm for both LOX and LH2.

The magnitude of the flow integral nonlinearities compare favorably with predictions. The maximum deviation of flow integral LOX mass sensor nonlinearity from predicted is 180 lbm. The LH2 flow integral mass history demonstrates good agreement with the prediction except at engine start when the LH2 mass nonlinearity deviates by approximately 210 lbm. This condition demonstrates the effects of the LH2 propellant tilt which had resulted from the launch vehicle response to the S-II engine malfunctions.

16.2.3.1 Inflight Dynamics Effects

The PU mass sensor corrections, due to inflight dynamics, are shown in figure 16-2 for the LH2 and LOX tanks. These corrections are the sum of the tank deflection and CG offset corrections as described in the following paragraphs.

The propellant tank deflection correction to the PU indicated mass is caused by tank skin temperature variations and differential tank pressure difference from those experienced during acceptance firing.

Figure 16-3 and 16-4 present a comparison of the predicted and actual flight tank deflection corrections for the LOX and LH2 mass sensors. The predicted LOX correction shows good agreement with the actual postflight evaluation. The slightly lower actual correction for the LH2 sensor was attributed to a lower skin temperature than predicted prior to the flight. Consequently the actual postflight correction due to this effect was 38 lbm less than predicted at S-IVB Engine Start Command.

The offset correction is caused by tilting of the propellant level due to the engine thrust vector passing through the vehicle cg when the cg is displaced from the longitudinal centerline.

Figure 16-5 and 16-6 present the predicted versus the flight evaluation center of gravity offset correction for the LOX and LH2 mass sensors. The difference between the actual and predicted values is due to a MSFC change in the payload distribution prediction. The payload distribution change was not reflected in the predicted values.

16.2.3.2 Volumetric Propellant Tank to Sensor Mismatch

The volumetric propellant tank to sensor mismatch nonlinearity was computed from the vendor's sensor data and measured unique tank volume-height data. The vendor's raw manufacturing nonlinearity was smoothed for the sensor discontinuity introduced during the test procedure. The smoothed S-IVB volumetric tank to sensor mismatch nonlinearity is presented in figures 16-7 and 16-8 for LOX and LH2 respectively. The nonlinearity was normalized to the sensor active element extremities.

16.2.4 Comparison of Level Sensors and Volumetric PU Mass at Level Sensor Activation

Table 16-3 presents the level sensor mass and volumetric PU mass at each level sensor activation during flight. The level sensor masses were computed from propellant volume at the level sensor height location and propellant density at the level sensor activation time.

Figures 16-9 and 16-10 show the deviations between level sensor and volumetric PU mass at level sensor activation times for acceptance firing, countdown demonstration test (CDDT) and flight. In order to compare the level sensor data to the PU data for the three tests, the PU masses for the acceptance firing were recomputed based upon the pounds per picofarad flight calibration slope. This procedure normalizes the volume data so that the differences between level sensor and PU mass for the three tests (acceptance firing, CDDT, and flight) are a measure of system repeatability.

The general trend and magnitude of the deviations for both the LOX and LH2 tanks are approximately the same as experienced for the S-IVB-501. During first burn, there is good agreement between the CDDT and flight data although the magnitude of the deviations are greater than the acceptance firing data. Further analysis will be conducted in view of the similarity between the S-IVB-501 and S-IVB-502 data and the greater than expected mass deviations.

16.3 PU System Response

The first burn PU valve position is illustrated in figure 16-11. During first burn, the PU valve was positioned at null for start and remained there until PU activate at first burn ESC +8 sec. The PU valve was then commanded to the fully closed (high EMR) position at activation and remained there until ESC +171.9 sec, at which time the PU system was deactivated. The extended burntime resulting from the early shutdown of two of the S-II engine caused 30.7 sec of additional S-IVB operation at the LOX-rich stop.

The actual second burn PU valve position is presented in figure 16-12. At RO +11,574.7 sec (40 sec prior to second burn Engine Start Command) the PU valve low hardover command was issued; 0.8 sec later, the PU valve reached the low stop and remained there until ESC +13 sec, at which time PU activate was commanded by the IU. Following PU activate the valve travelled to the high stop in 3 sec, and remained there until PU deactivate (1 sec later). Following PU deactivate, the valve started back toward null but the removal of the PU system power left the valve at 26.7 deg. Had the power not been shut off, the PU valve would have returned to null.

Had restart been achieved, with a normal LOX mass system operation, it is highly probable the PU system would have described the revised second burn prediction (figure 16-13). This prediction is based on the actual S-IVB first burn and coast data which included the initial LOX overload, extended S-IVB first burn operation, and boiloff data.

During the second revolution, the LOX mass bridge experienced disturbances on nine different occasions which caused the LOX bridge to slew toward the full stop. On each occasion the bridge subsequently recovered except for the last disturbance at RO +11,091 sec of flight when the LOX mass bridge slewed to the full mechanical stop and remained there for the remainder of the S-IVB mission.

Had second burn been sustained with the PU system in the malfunctioned mode, the engine would have operated in the high EMR mode until velocity cutoff. In that mode, guidance cutoff is predicted to occur at second burn ESC +263 sec. In the high EMR hardover malfunction mode, propellant depletion would occur at second burn ESC +265 sec.

16.4 PU System Anomalies

PU system operation was normal during the CDDT and during propellant loading for the S-IVB-502 flight. AS-502 liftoff was at 12:00:01 and first burn engine cutoff occurred approximately 747 sec after liftoff. During this period, PU system operation was normal as shown in figure 16-14. The EMR valve was positioned at 5.5:1 to provide the high thrust required during this initial portion of flight. Some time after engine cutoff, the PU electronics indicated the expected capillary action on both the LOX and LH2 PU probes.

Data is available for the periods: RO +5,400 to RO +6,300 sec, RO +10,300 to RO +10,800 sec, and RO + 10,960 sec up to and including the restart attempt. Figure 16-15 shows that data available for the period RO +10,960 sec through restart. Prior to RO +10,610 sec, the LOX mass bridge indicated that the probe was completely filled with propellant. The PU electronic assembly calibration for the S-IVB would allow the coarse mass indication to read approximately 4.5 vdc and the fine mass indication to indicate approximately 2.2 vdc when the probe is completely filled.

At RO +10,610 and RO +10,635 sec into flight, the LOX bridge began to slew at the maximum rate toward the full stop. The bridge recovered each time within 1 sec and operation returned to normal. At RO +10,660 sec, the LOX bridge again slewed at maximum rate to the full stop indicating an over-full indication. The LOX bridge remained in this position until data dropout, which occurred at RO +10,880 sec. The next available data beginning at RO +10,960 sec shows the bridge had recovered at some period during data dropout.

At RO +10,967 sec into flight, the LOX bridge again slewed at the maximum rate indication an over-full condition. The bridge recovered within 3 sec and operation returned to normal. At RO +11,066, RO +11,072, RO +11,087, and RO +11,090 sec the fine mass again indicated an anomaly by starting to slew towards the full stop at the maximum rate. Each of these malfunctions were of less than 1 sec duration. At RO +11,091 sec the bridge slewed at maximum rate and this time reached the full mechanical stop of the output potentiometer. The bridge did not recover from this position for the remainder of the S-IVB mission.

16.4.1 Failure Analysis

The PU system is an inflight, closed-loop, propellant-mass-ratio control system consisting of two capacitance mass probes, an electronics assembly, and a liquid oxygen flow-control valve with valve-positioning assembly.

The PU system provides continuous 0-5 vdc analog output signals of the propellant masses. These outputs are obtained from the coarse and fine mass telemetry potentiometers and are sent to the stage telemetry system for transmission to the ground station.

In operation, indicated LOX mass is compared to the product of indicated LH2 mass times the predetermined propellant mass-ratio reference. The difference between the actual and predetermined propellant mass is then used to proportionally control the LOX pump bypass flowrate, thereby altering the EMR. A change in the EMR produces a change in the remaining propellant mass ratio.

The LOX mass bridge is a servo balanced capacitance type which converts changes in propellant mass to a proportional output voltage. The bridge consists of a capacitance mass probe in one leg, a stable reference capacitor mounted in a temperature controlled oven in another leg, and transformer voltage sources in the third and forth leg. Figure 16-16 is a schematic diagram of the servo balanced bridge.

The capacitance of the mass probe changes in direct proportion to the variations in propellant mass. This change in capacitance will unbalance the bridge, resulting in an output signal to the bridge amplifier, which in turn drives the servomotor and rebalance potentiometer to seek a null condition. When rebalance occurs, no output is developed by the bridge network, and therefore, the motor and potentiometer will remain in that position.

In order for the capacitance bridge to slew at maximum rate toward the full stop, it is necessary to have a condition which causes the bridge to unbalance so that the rebalance potentiometer will attempt to null at or past the full stop.

In order to create such a condition in the PU electronics assembly, an open circuit is required in the full adjust potentiometer, rebalance potentiometer, or reference capacitor. These open circuits are indicated by X's on the schematic diagram shown in figure 16-16.

The over-full condition could also be caused by the LOX mass probe or its associated cabling. Figure 16-17 indicates the failure modes of the capacitance probe. Summarized below are the four probe and/or cabling failures which could cause the bridge to slew to the full stop.

a. The Inner Element Shorted to Ground

   This will cause the bridge to slew at a slow rate to the full stop.

b. The Inner Element Shield Shorted to the Outer Element

   This will cause the bridge to slew at maximum rate to the full stop if the short is no greater than 2K ohms.

c. Inner Element Shield Open

   This will cause the bridge to slew at maximum rate to the full stop.

d. The Inner Element Shorted to the Outer Element

   This will cause the bridge to slew at maximum rate to the full stop.

The intermittent operation of the LOX bridge prior to restart tends to indicate a condition which eliminates component failures such as resistors, transistors, capacitors, etc. The anomaly appears to be of the type present with either an open wire/cable shield or a short between probe elements.

16.4.2 Anomaly Conclusions

At this time there appears to be two possible causes for the PU system anomaly noted during the S-IVB flight. These causes are:

a. An intermittent cable shield between the mass probe and the PU electronics assembly.

b. Metallic debris of some type in the LOX tank which caused a short between the inner and outer elements of the LOX PU probe.

PU system operation was normal during first burn and the first appearance of the bridge anomaly occurred during orbiting conditions. Debris in the tank during orbital conditions could be distributed anywhere in the tank and possibly lodge between the probe elements. As the PU system operation was normal during powered flight while the LOX mass probe, its associated cable and PU electronics assembly, were under the highest vibration levels experienced during flight, the possibility of an intermittent cable shield appears to be remote. Therefore, the most probable cause of the PU system anomaly was metallic debris in the LOX tank shorting the inner and outer element of the LOX probe, thus causing the LOX bridge to slew at a maximum rate to the over-fill condition.

Figure 16-18 shows the slew rates of the LH2 bridge during the failure that occurred on the S-IVB-503N at Sacramento, the slew rate of the LOX bridge during the S-IVB-502 flight, and the lab test data obtained on a PU system breadboard at Space Systems Center, Huntington Beach, when a LOX mass probe failure was simulated by shorting the elements of a simulated mass probe.

TABLE 16-1
PROPELLANT MASS HISTORY

EVENT		PREDICTED MASS (lbm)	PU INDICATED MASS (lbm)	PU INDICATED CORRECTED MASS (lbm)	FLIGHT FLOW INTEGRAL MASS (lbm)	PU VOLUMETRIC MASS (lbm)	LEVEL SENSOR MASS (lbm)	TRAJECTORY RECONSTRUC-TION MASS (lbm)	BEST ESTIMATE MASS (lbm)
LIFTOFF	LOX	193,273	193,412	193,412	194,097	194,272	194,893	--	194,140
(RO +0)	LH2	42,493	42,442	42,482	42,440	42,266	42,569	--	42,448
	TOTAL	235,766	235,854	235,894	236,537	236,538	237,462	236,526	236,588
ESC 1	LOX	193,273	193,136	193,272	194,097	194,122	194,893	--	194,135
(RO +577.28)	LH2	42,493	42,154	42,430	42,440	42,214	42,569	--	42,448
	TOTAL	235,766	235,290	235,702	236,537	236,336	237,462	236,526	236,583
ECC 1	LOX	132,047	119,991	118,551	119,166*	119,145	119,875	--	119,166*
(RO +747.30)	LH2	31,185	28,580	28,542	28,494*	28,265	28,590	--	28,494*
	TOTAL	163,232	148,571	147,093	147,660	147,410	148,465	147,726	147,660
CONSUMPTION	LOX	61,226	73,145	74,721	74,931	74,977	75,018	74,869	74,969
(ESC 1 TO ECC 1	LH2	11,308	13,574	13,888	13,946	13,949	13,979	13,931	13,954
	TOTAL	72,534	86,719	88,609	88,877	88,926	88,997	88,800	88,923
ORBITAL BOILOFF	LOX	120	--	--	343	--	--	--	--
(ECC 1 TO RE-	LH2	2,964	--	--	3,024	--	--	--	--
START PREPS)	TOTAL	3,084	--	--	3,367	--	--	--	--
ESC 2	LOX	131,402	--	--	118,723	--	--	--	--
(RO +11,614.67)	LH2	28,168	--	--	25,470	--	--	--	--
	TOTAL	159,570	--	--	144,193	--	--	--	--
ECC 2	LOX	N/A	--	--	117,030	--	--	--	--
(RO +11,630.32)	LH2	N/A	--	--	24,950	--	--	--	--
	TOTAL	N/A	--	--	141,980	--	--	--	--

*Best estimate residual propellants

TABLE 16-2
PROPELLANT LOADING SUMMARY

ITEM	LOX (lbm)	LH2 (lbm)	TOTAL (lbm)
PROPELLANT LOAD			
Desired	193,273	42,493	235,766
PU indicated	193,412	42,442	235,854
PU indicated (corrected)	193,412	42,482	235,894
Flight flow integral	194,097	42,440	236,537
PU volumetric	194,272	42,266	236,538
Level sensor	194,893	42,569	237,462
Trajectory reconstruction	--	--	236,526
Best estimate	194,140	42,448	236,588
DEVIATION FROM BEST ESTIMATE			
Desired	-867(-0.447%)	+45(+0.106%)	-822(-0.348%)
PU indicated	-728(-0.375%)	-6(-0.014%)	-734(-0.310%)
PU indicated (corrected)	-728(-0.375%)	+34(+0.080%)	-694(-0.293%)
Flight flow integral	-43(-0.022%)	-8(-0.019%)	-51(-0.022%)
PU volumetric	+132(+0.068%)	-182(-0.429%)	-50(-0.021%)
Level sensor	+753(+0.388%)	+121(+0.285%)	+874(+0.369%)
Trajectory reconstruction	--	--	-62(-0.026%)

TABLE 16-3
LEVEL SENSOR AND VOLUMETRIC PU MASS AT
LEVEL SENSOR ACTIVATION DURING FLIGHT

LEVEL SENSOR	ACTIVATION TIME (sec) FROM RO	LEVEL SENSOR MASS (lbm)	VOLUMETRIC PU MASS (lbm)	DEVIATION LEVEL SENSOR-PU (lbm)
(LOX TANK)				
LO013	586.2	193,508	192,906	+602
LO012	626.1	174,946	174,491	+455
LO011	687.1	147,354	146,761	+593
(LH2 TANK)				
NO023	596.4	141,349	40,994	+355
NO024	637.8	37,800	37,450	+350
NO025	685.6	33,809	33,437	+372
NO026	731.8	29,898	29,580	+318

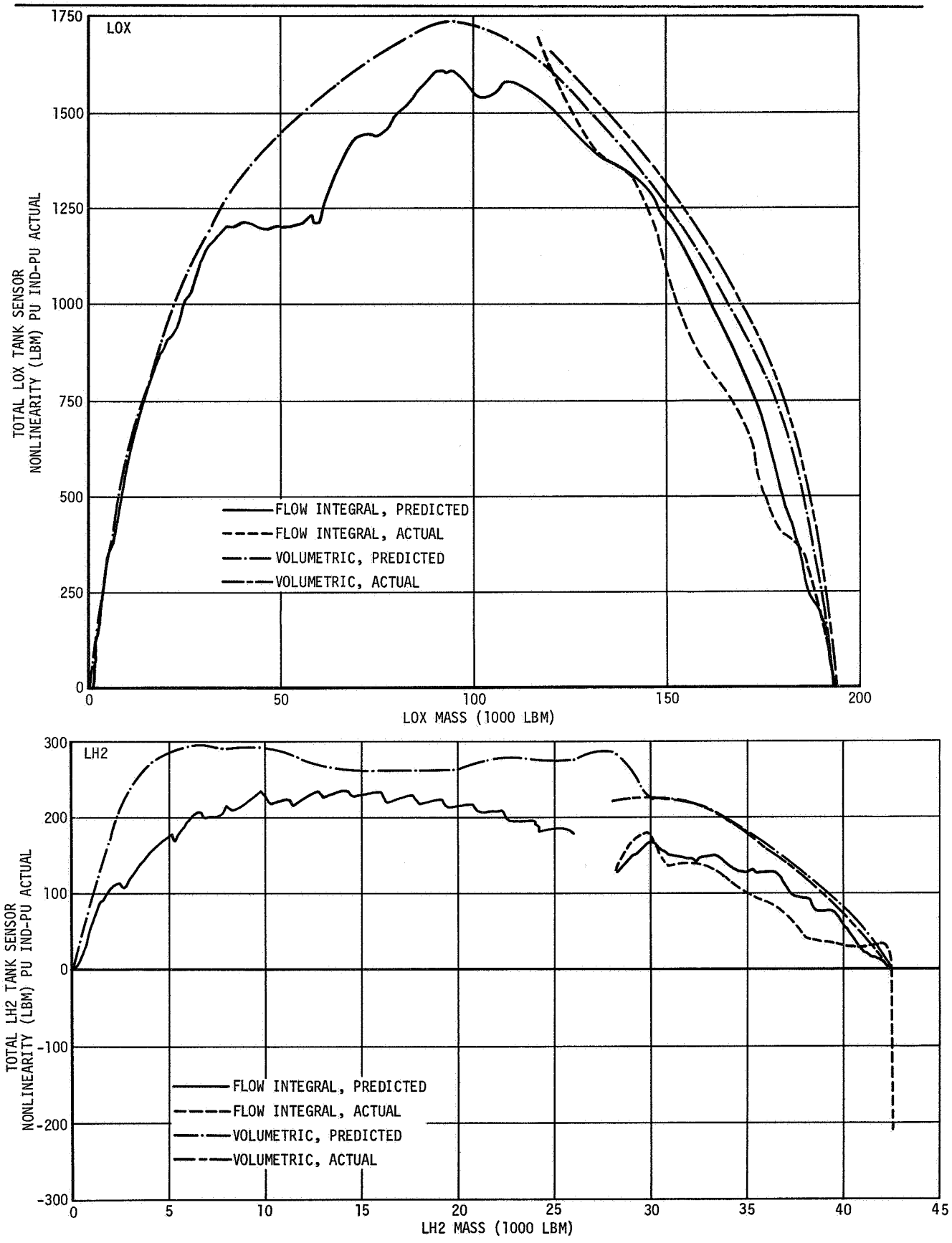

Figure 16-1. Total Mass Sensor Flight Nonlinearity

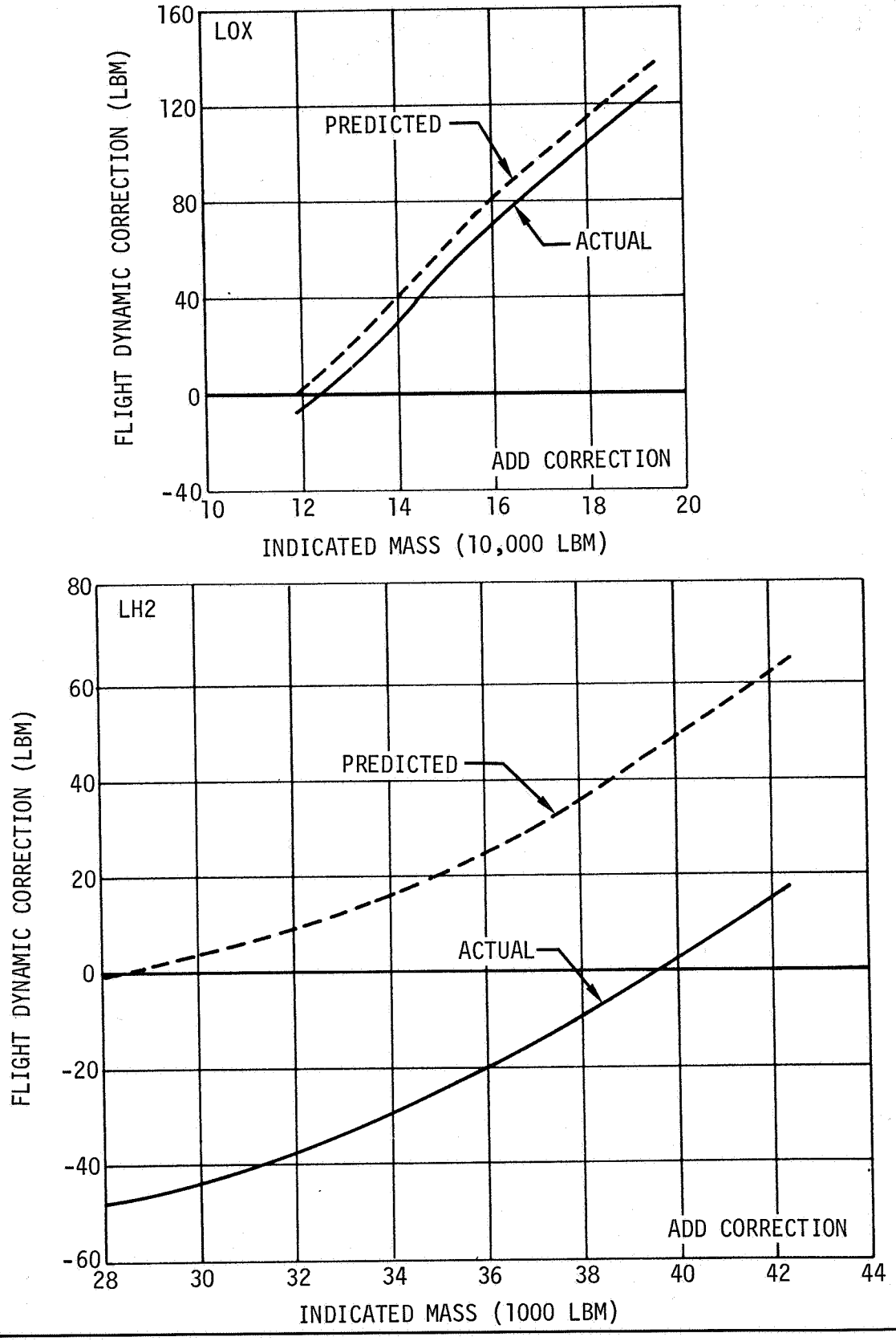

Figure 16-2. PU Mass Sensor Correction Due to Flight Dynamic Effect - CG Offset and Tank Deflection

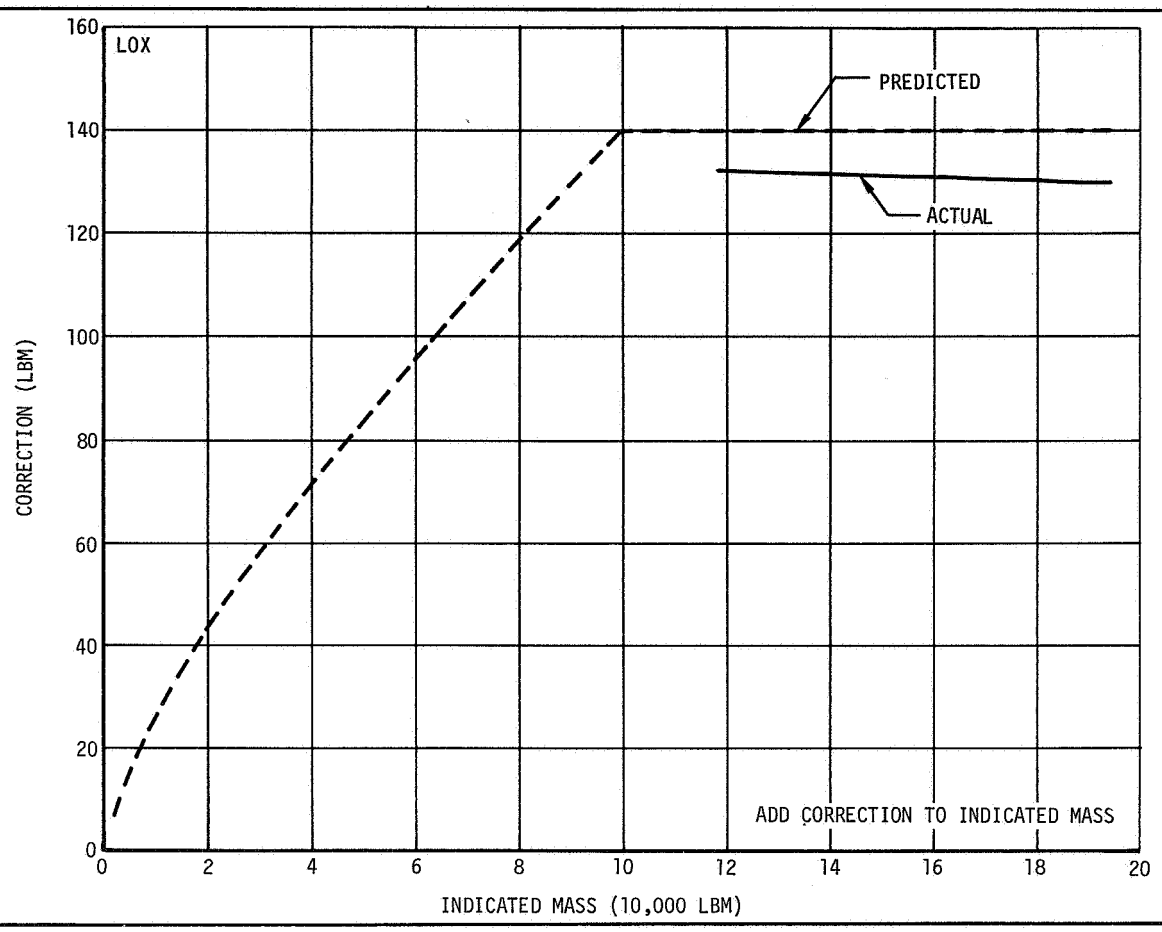

Figure 16-3. Flight PU Correction Due to LOX Tank Deflection

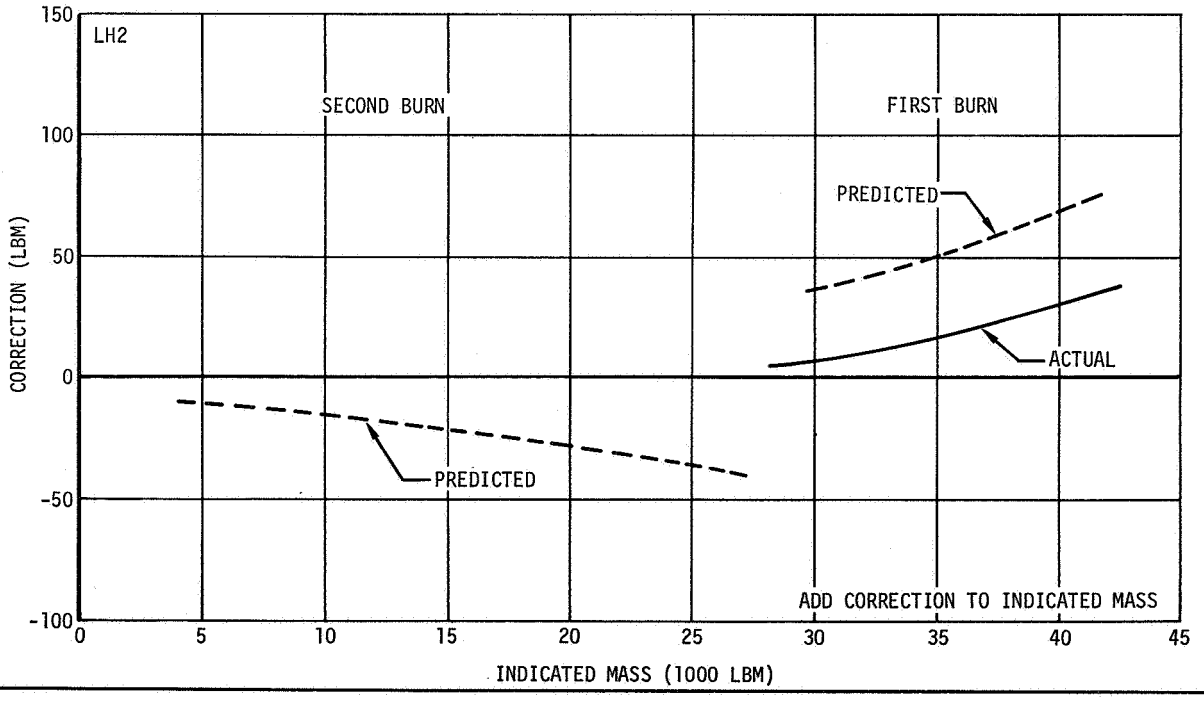

Figure 16-4. Flight PU Correction Due to LH2 Tank Deflection

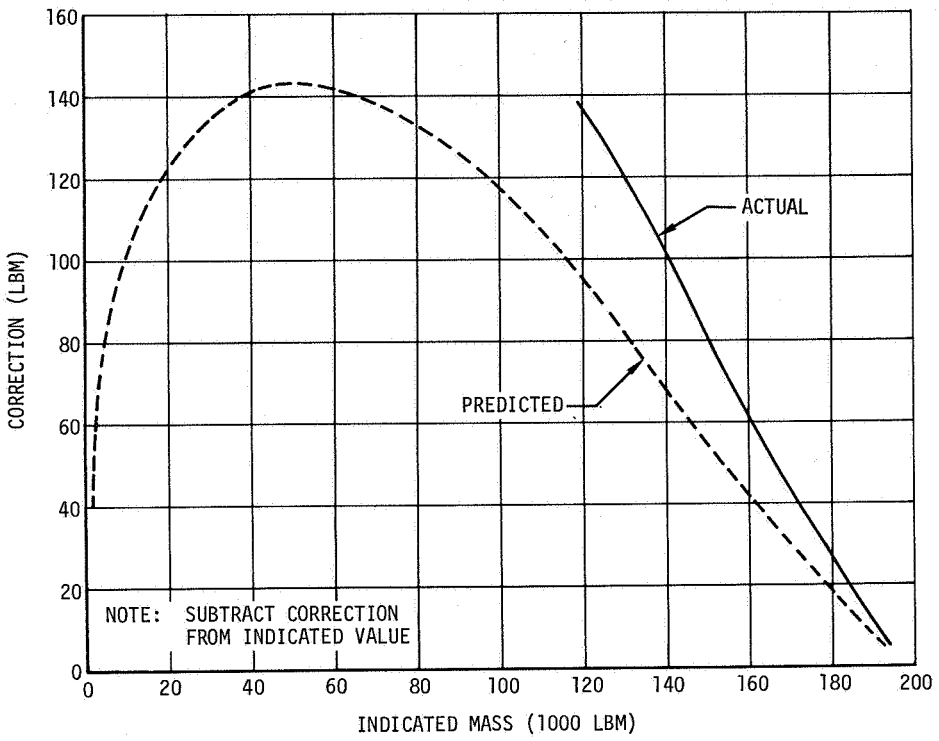

Figure 16-5. LOX PU Mass Sensor Correction Due to CG Offset

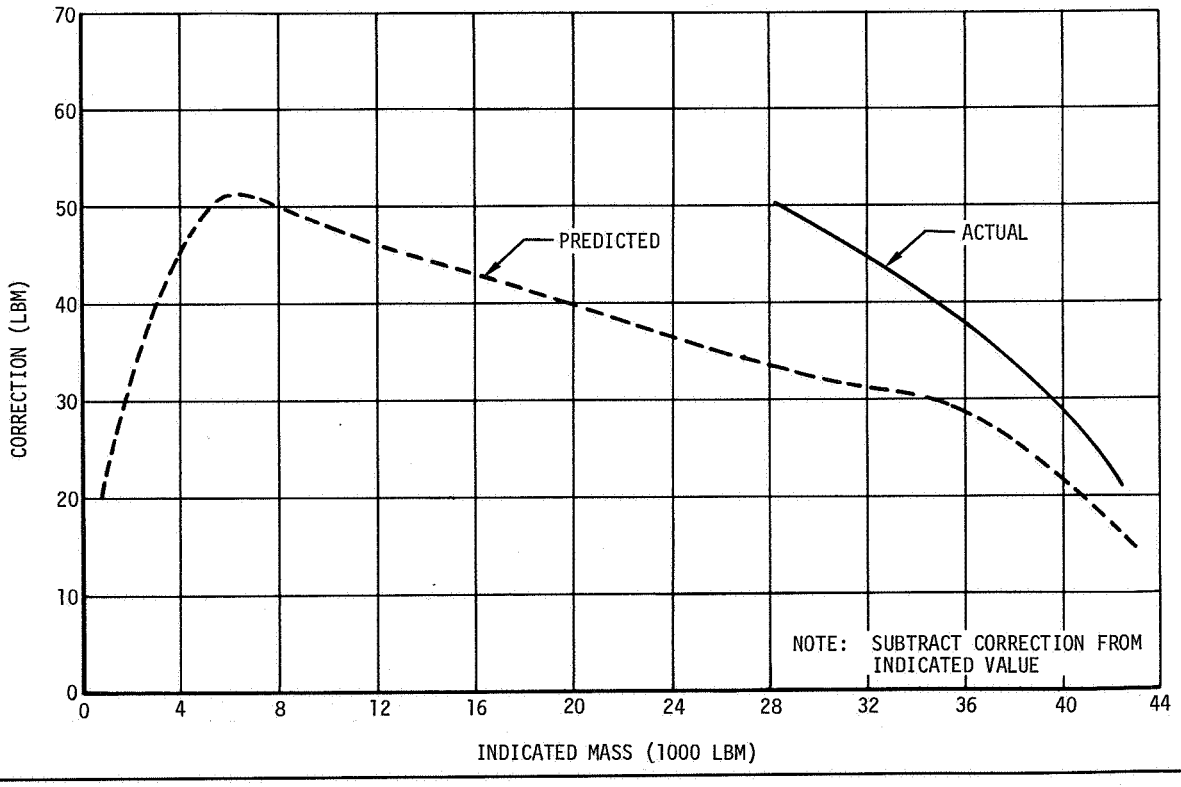

Figure 16-6. LH2 PU Mass Sensor Correction Due to CG Offset

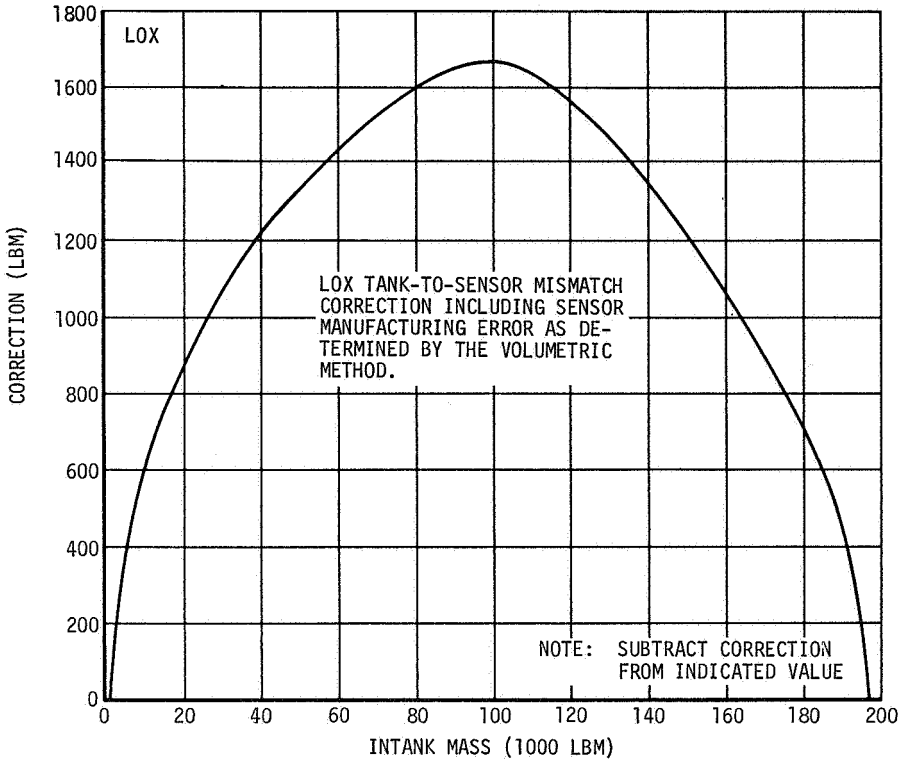

Figure 16-7. Volumetric LOX Tank-to-Sensor Mismatch Correction

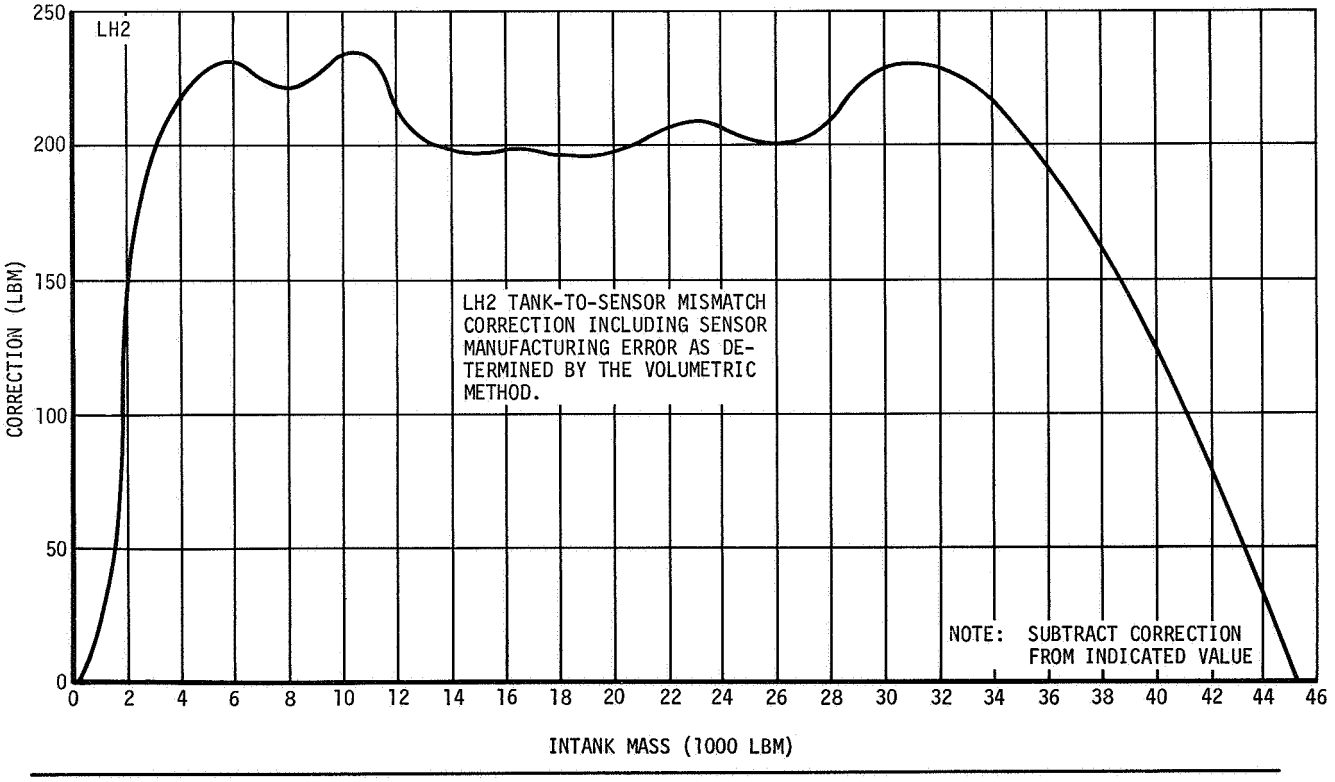

Figure 16-8. Volumetric LH2 Tank-to-Sensor Mismatch Correction

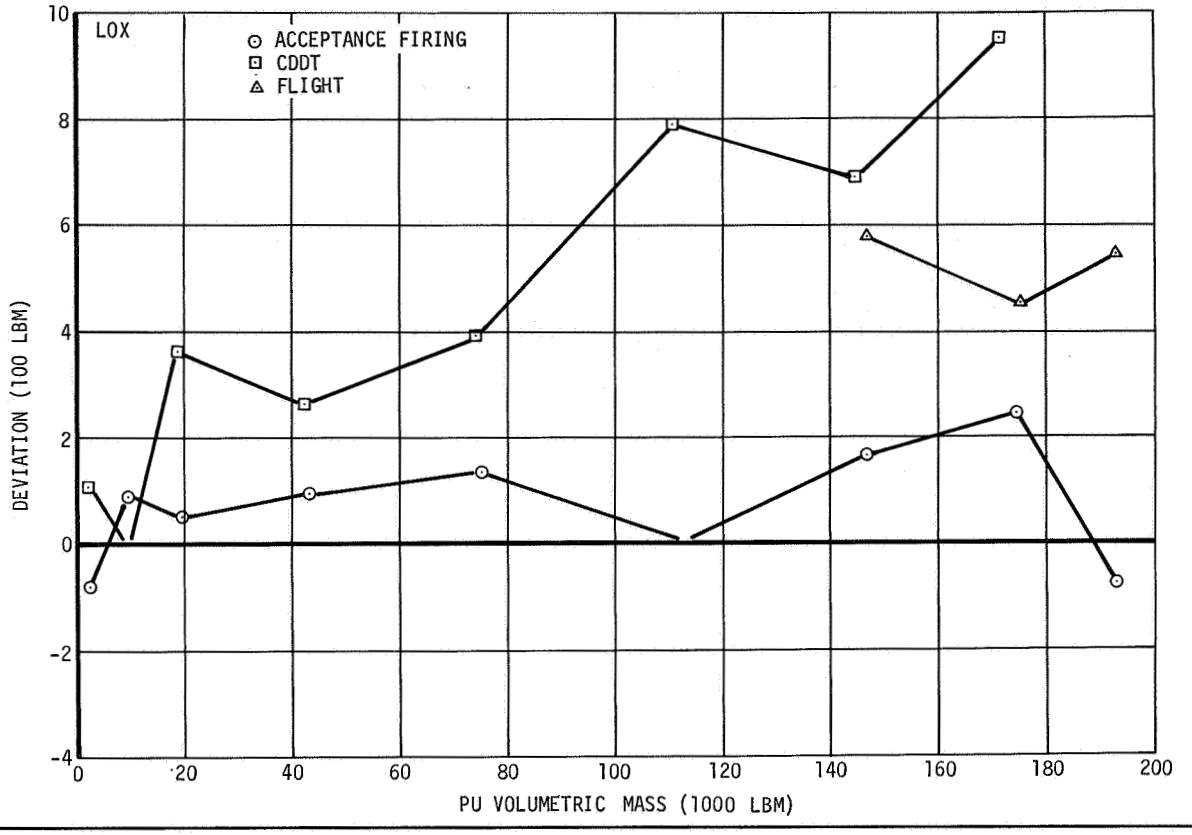

Figure 16-9. Level Sensor and Volumetric PU Mass Comparison - LOX Tank

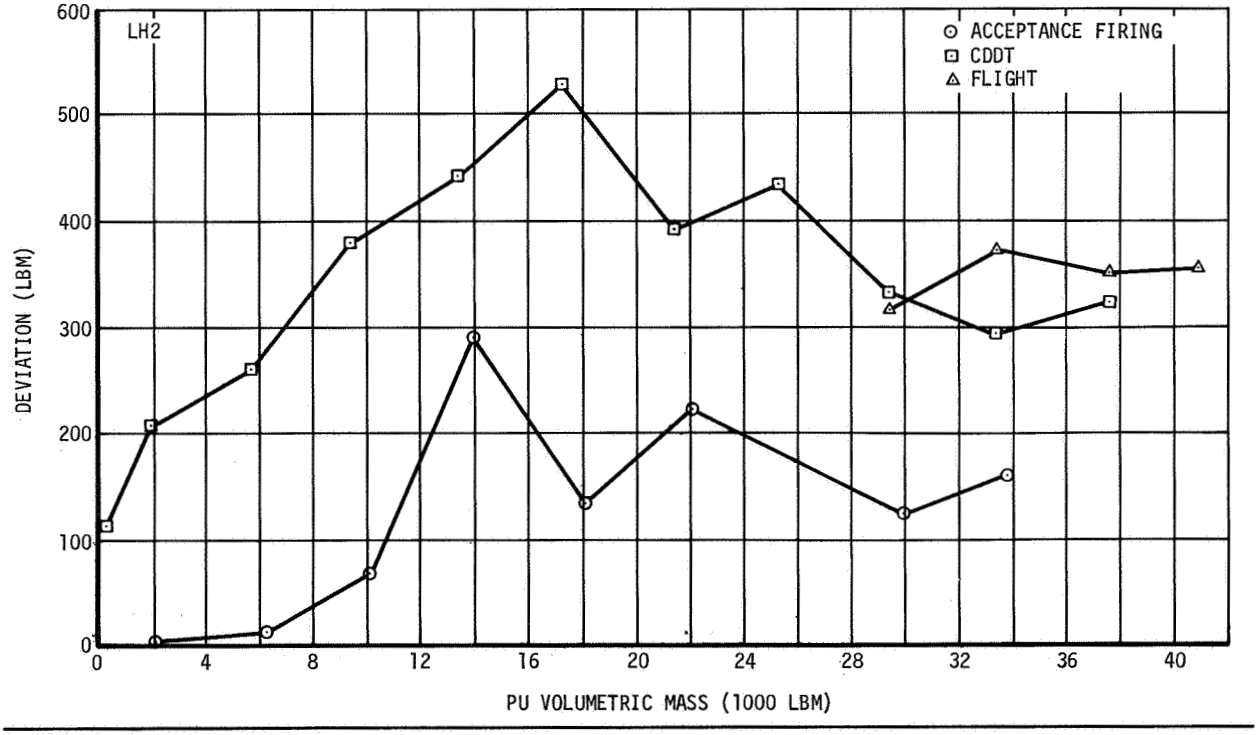

Figure 16-10. Level Sensor and Volumetric PU Mass Comparison - LH2 Tank

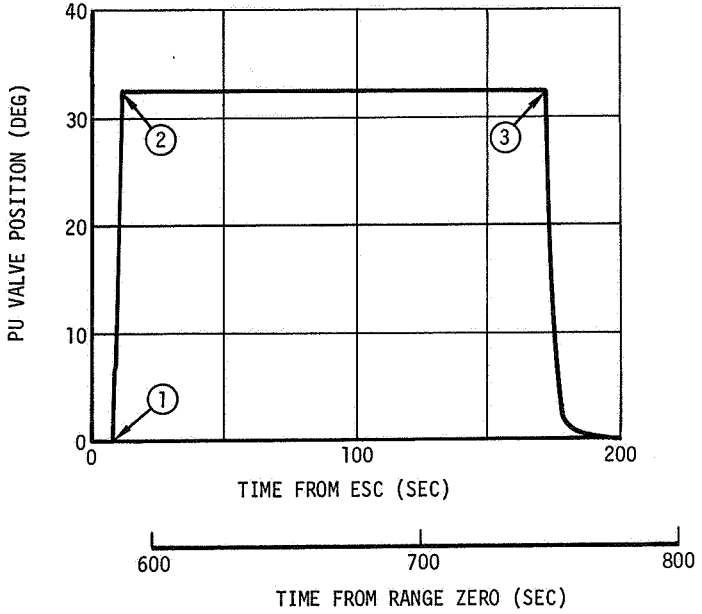

	EVENT	RANGE TIME (SEC)
1	PU ACTIVATE	+585.3
2	VALVE REACHES TOP STOP	+589.0
3	PU DEACTIVATE	+749.2

Figure 16-11. PU Valve Position - First Burn

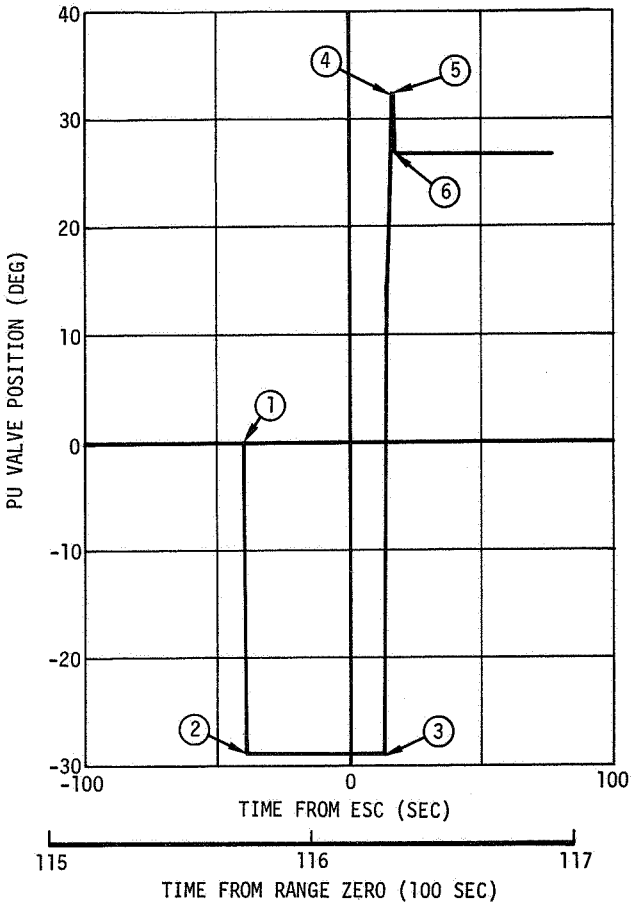

	EVENT	RANGE TIME (SEC)
1	LOW STOP COMMAND	+11,574.7
2	VALVE REACHES LOW STOP	+11,575.5
3	PU ACTIVATE	+11,627.6
4	VALVE REACHES TOP STOP	+11,630.6
5	PU DEACTIVATE	+11,631.6
6	PU POWER OFF	+11,632.0

NOTE: VALVE POSITION REMAINED AT 26.6 DEG AFTER PU POWER WAS SHUT OFF.

Figure 16-12. PU Valve Position - Second Burn

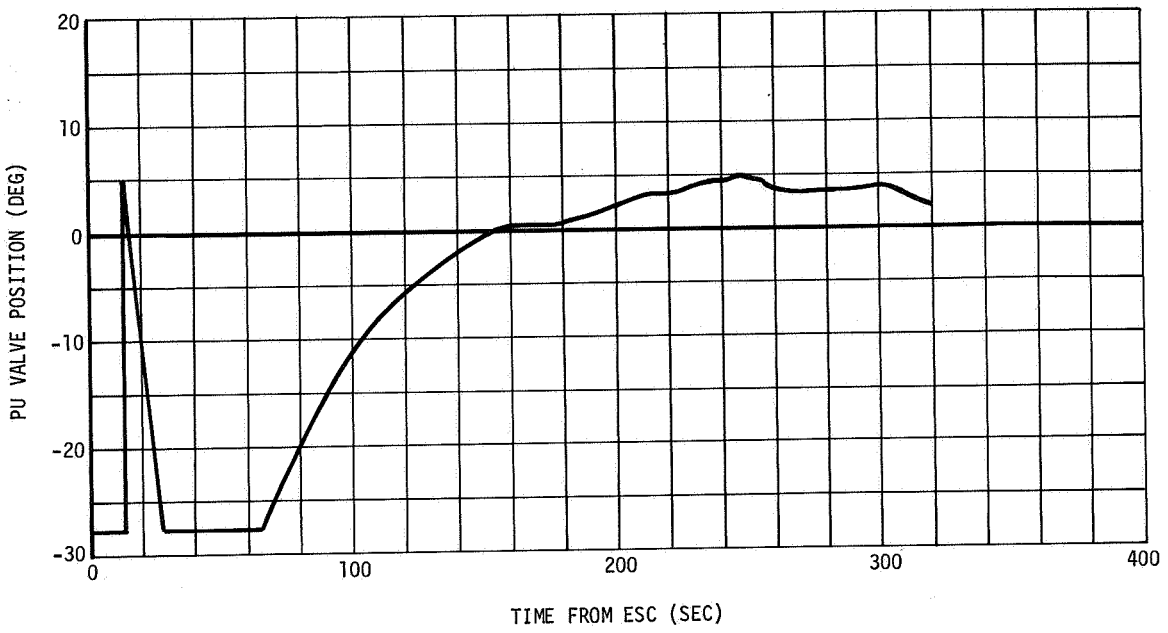

Figure 16-13. Revised Prediction No LOX Measuring System Anomaly - Second Burn

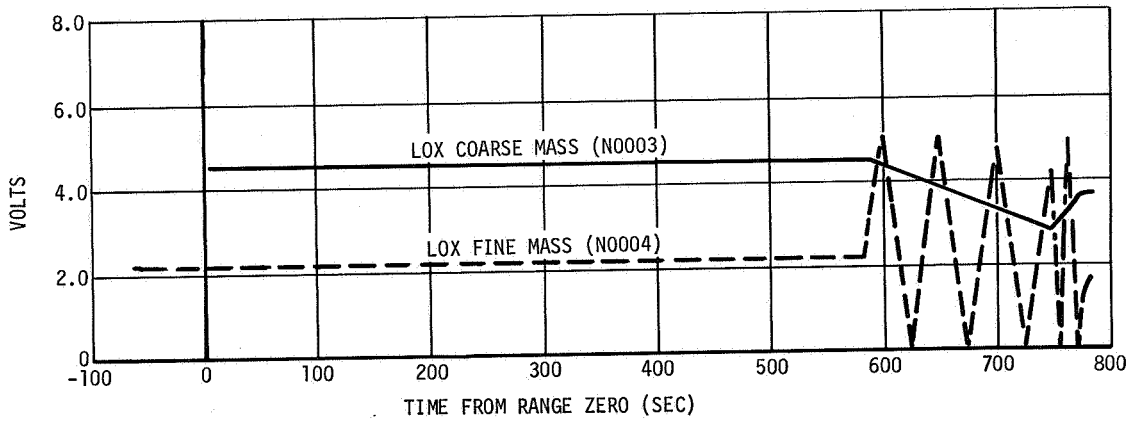

Figure 16-14. LOX Mass History - First Burn

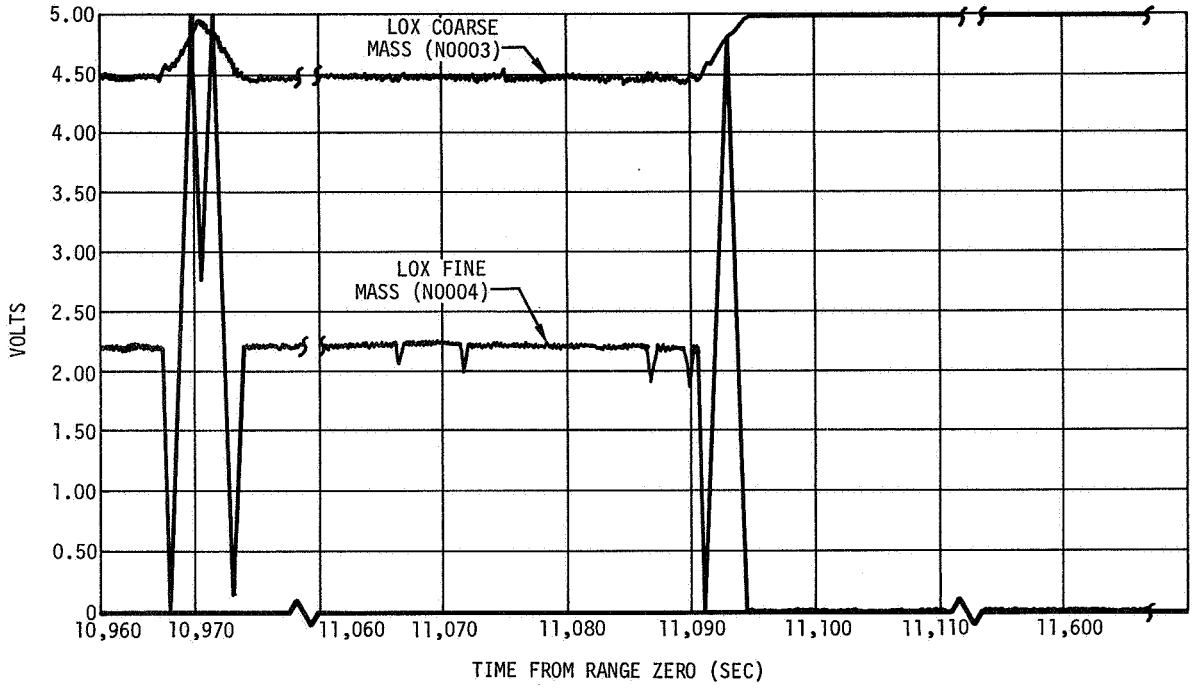

Figure 16-15. LOX Mass History - Restart Preparations

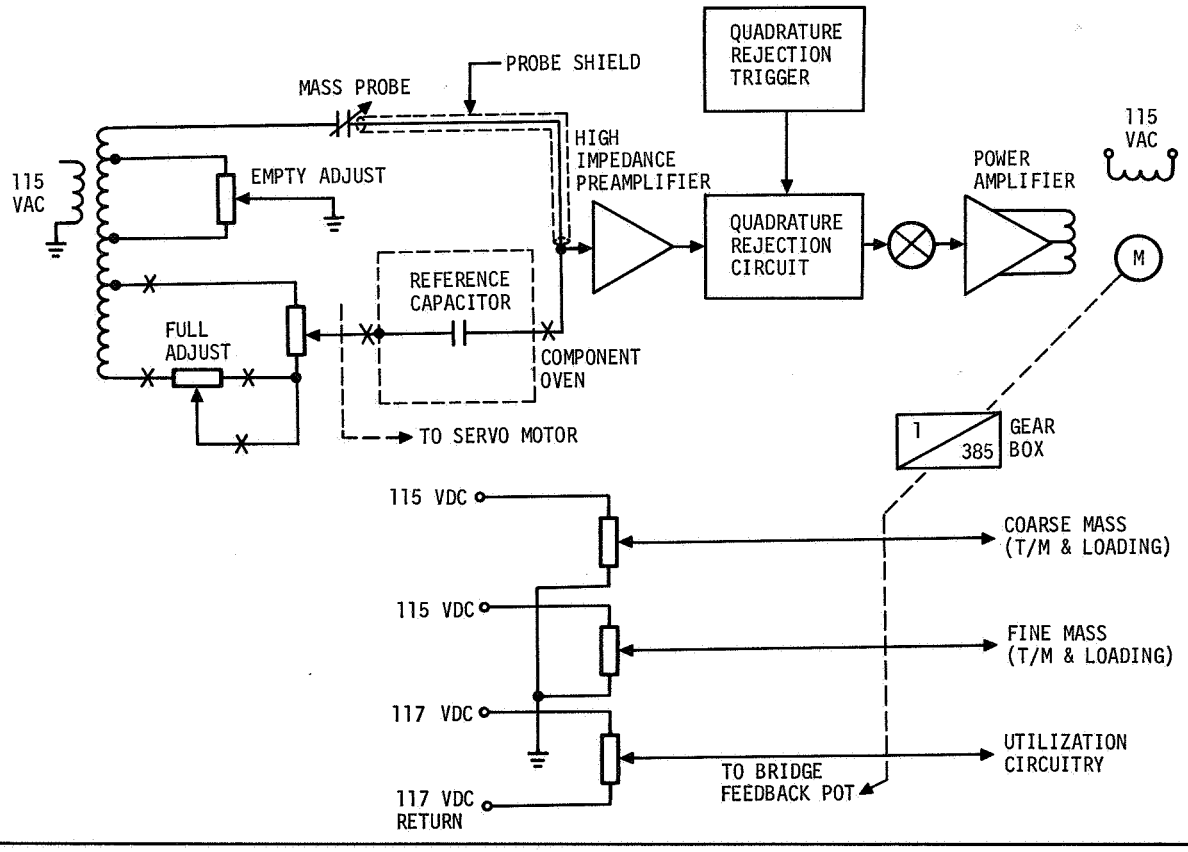

Figure 16-16. Servo Bridge

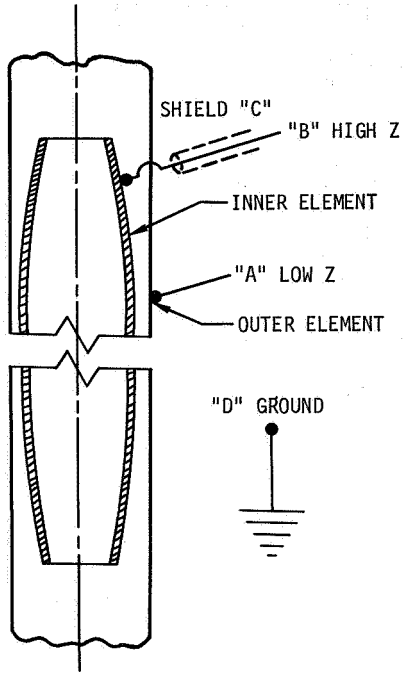

FAILURE MODE	CONDITION BRIDGE WILL GO TO
A SHORTED TO D	EMPTY
B SHORTED TO D	FULL
C SHORTED TO D	SLIGHT SHIFT
B SHORTED TO C	EMPTY
C SHORTED TO A	FULL
B SHORTED TO A	FULL (PROBABLE FAILURE)
A OPEN	EMPTY
B OPEN	EMPTY
C OPEN	FULL

Figure 16-17. Failure Modes of PU Probes

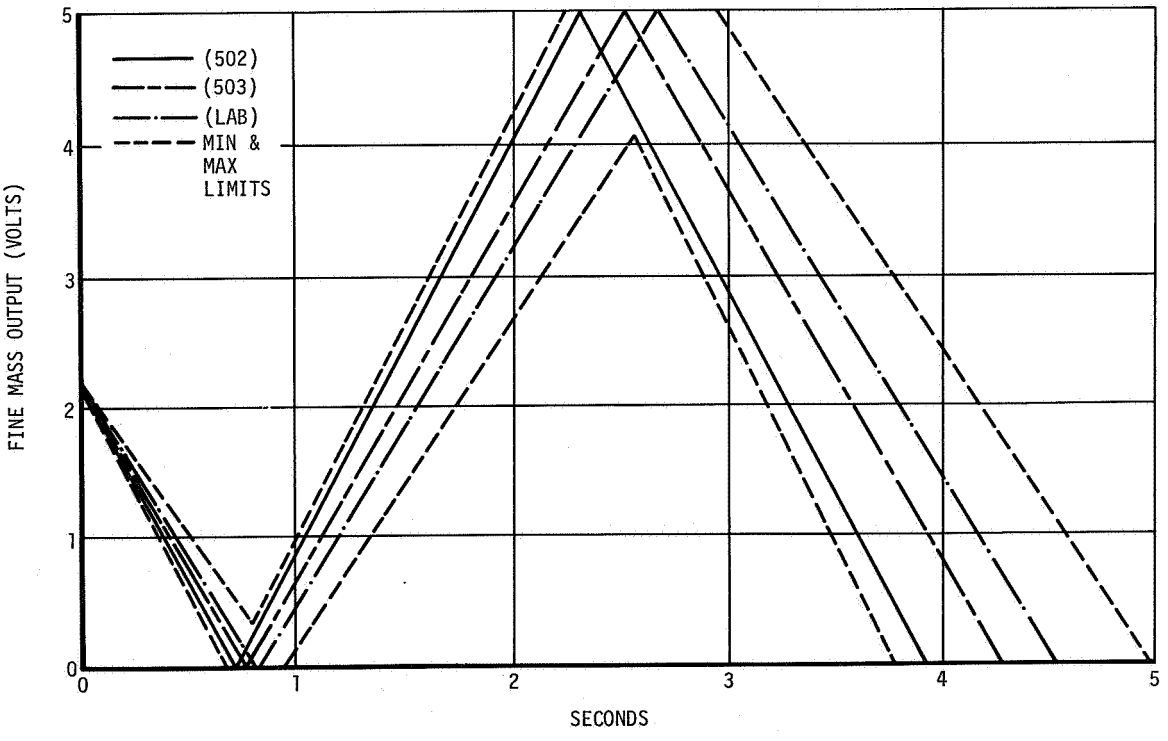

Figure 16-18. PU Bridge Slew Rate

SECTION 17

S-II/S-IVB SEPARATION

17. S-II/S-IVB SEPARATION

Separation of the S-IVB from the S-II was accomplished faster than predicted for a nominal separation by 0.07 sec. This was caused by lower than nominal S-II tail-off thrust level due to two engines out. First axial motion between the stages occurred 0.049 sec after the Separation Command (established from extensometer data). Due to engines two and three being out on the S-II a resultant unbalanced moment is introduced on the S-II causing a positive S-II pitch rate making the critical separation point on position I side of the S-IVB thrust structure. The clearance distance used for separation was approximately 6.7 in. in the direction of position I. In addition, approximately 12 in. were used due to engine gimbal position at the time of separation.

Table 17-1 contains significant times and events for S-II/S-IVB separation.

Figure 17-1 presents the axial separation history of the S-II/S-IVB separation. Also included in this figure are the predicted and actual S-IVB-501 separation histories.

Figure 17-2 shows the longitudinal accelerations for the S-II and S-IVB. The reconstructed acceleration histories were obtained from S-II and S-IVB accelerometer data. A time base was applied to these acceleration histories to compensate for the time lag inherent in the accelerometer data. Retrorocket chamber pressure data was used to determine the time bias.

Figure 17-3 presents the lateral accelerations for the S-II and S-IVB. The S-II pitch acceleration varied between 0.65 ft/sec^2 to -0.4 ft/sec^2 and the yaw acceleration varied between 0.5 ft/sec^2 and -0.4 ft/sec^2. The S-IVB lateral accelerations were for pitch $\pm$0.6 ft/sec^2 and yaw $\pm$0.2 ft/sec^2.

The angular velocity for both the S-II and S-IVB is presented in figure 17-4. The S-II rates were all approximately zero at first motion. The S-II pitch rate increased to approximately 2 deg/sec by the end of separation. The yaw rate increased to 0.95 deg/sec by the end of separation and the roll rate remained approximately zero throughout separation. The increase in both the S-II pitch and yaw rates after first motion were caused by the combination of two engines out on the S-II and retrorocket misalignment of approximately 0.1 deg. The S-IVB rates were all small with pitch and yaw rates remaining below 0.2 deg/sec and the roll rate remaining below 0.5 deg/sec.

The path of the interstage lip during separation is shown in figure 17-5. The closest approach point was a point on the S-IVB engine bell at position I. During separation 6.7 in. of lateral clearance was utilized. The S-IVB engine was in a hardover (6.7 deg) position in the direction of position I but a clearance of approximately 64 in. still remained.

Figure 17-6 presents the relative velocity between the two stages during separation.

TABLE 17-1
SEQUENCE OF EVENTS DURING S-II/S-IVB SEPARATION

EVENT	TIME FROM RANGE ZERO	TIME FROM SEPARATION COMMAND	
		ACTUAL	PREDICTED
S-II ECC	+576.327	-0.766	-0.8
Ullage rocket ignition	+576.956	-0.12	-0.1
75% ullage thrust	+577.07	-0.006	-
Separation Command	+577.079	0.0	0.0
S-II retrorocket ignition	+577.076	0.0	0.0
10% retrorocket thrust	+577.11	0.034	
First axial motion	+577.125	0.049	0.075
90% retrorocket thrust	+577.13	0.054	-
S-IVB ESC	+577.268	0.192	0.2
Separation complete	+578.066	0.99	1.06

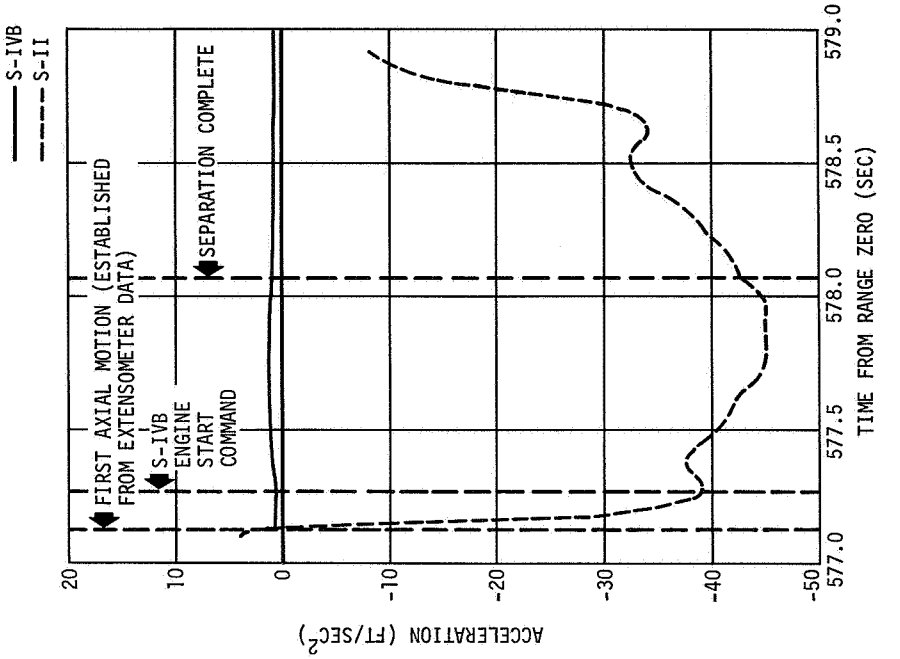

Figure 17-2. Longitudinal Acceleration

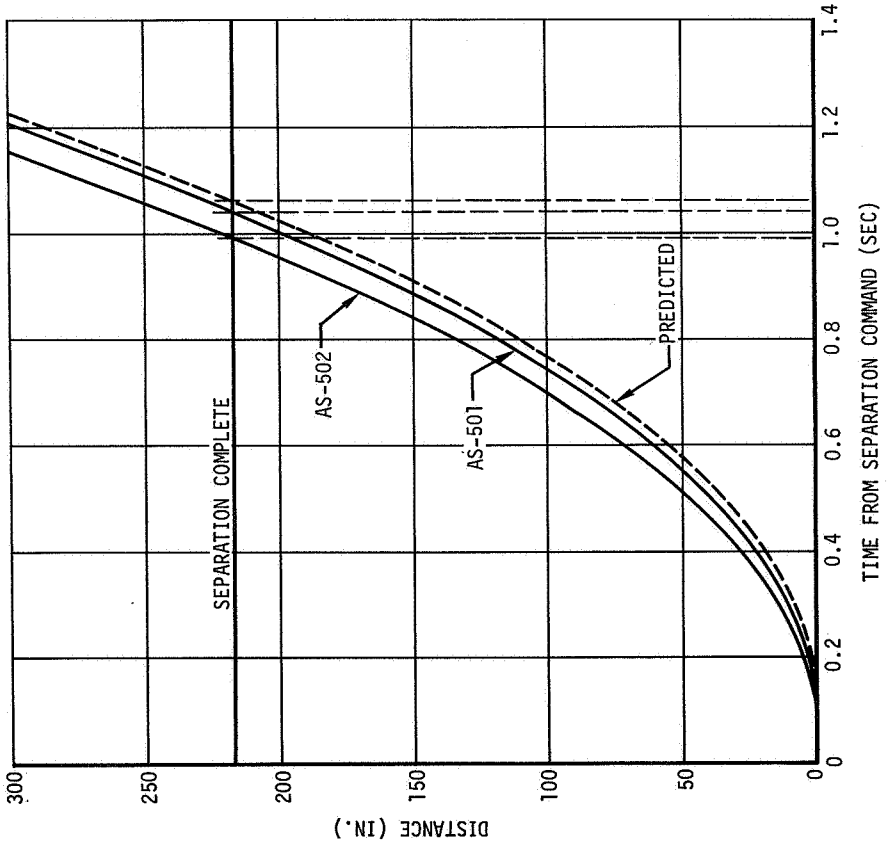

Figure 17-1. Axial Separation History

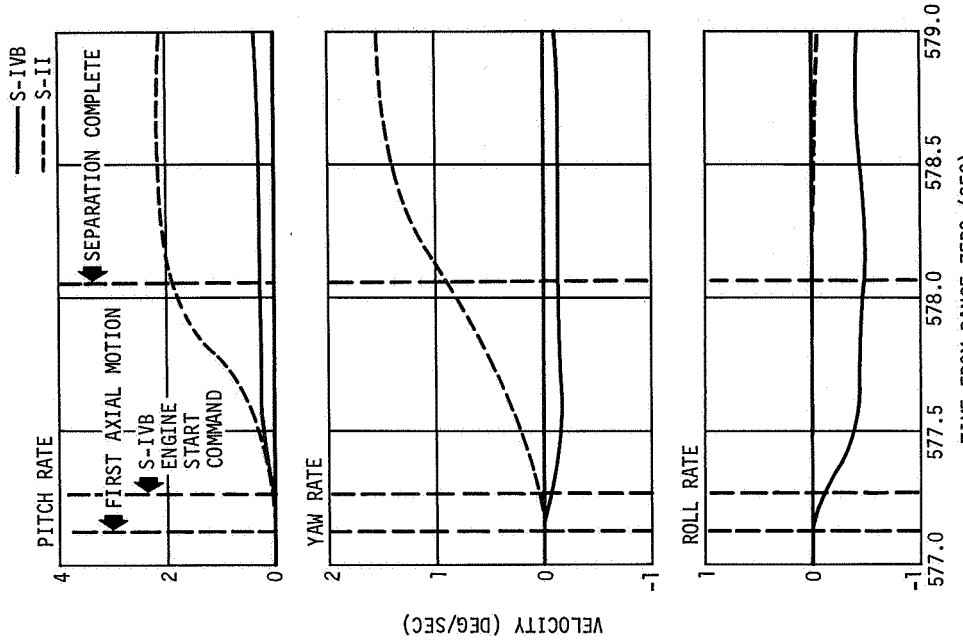

Figure 17-4. Angular Velocity

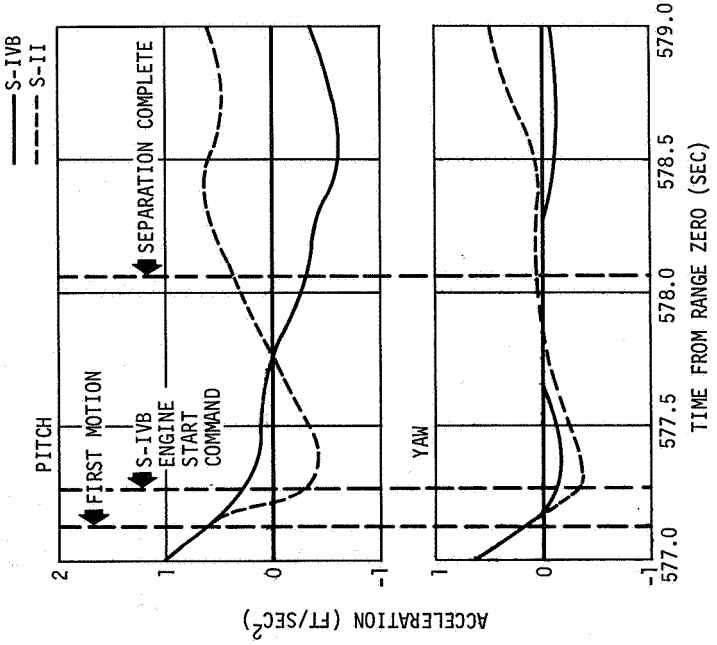

Figure 17-3. Lateral Acceleration

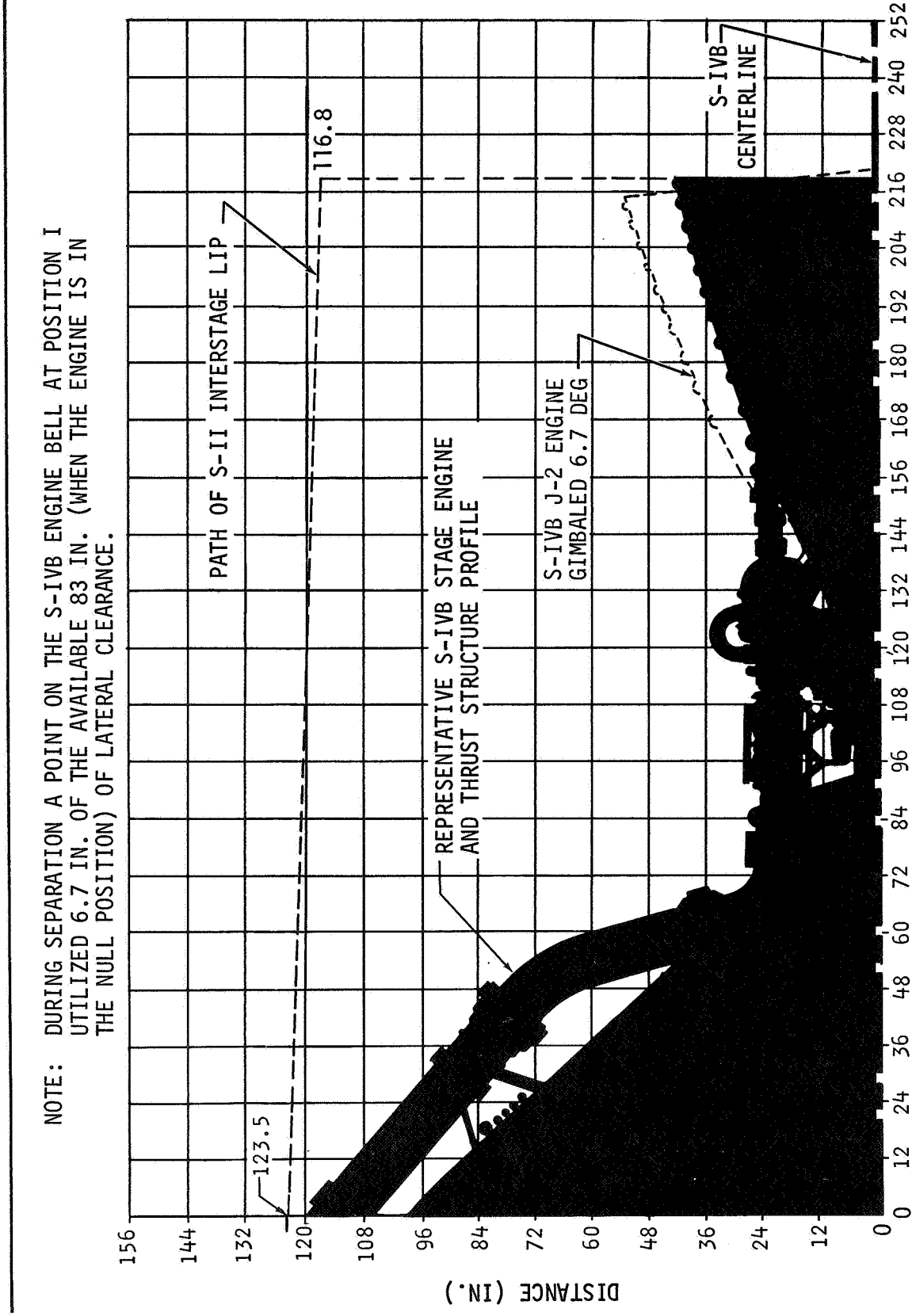

Figure 17-5. S-II Interstage Lip Path - S-II/S-IVB Separation

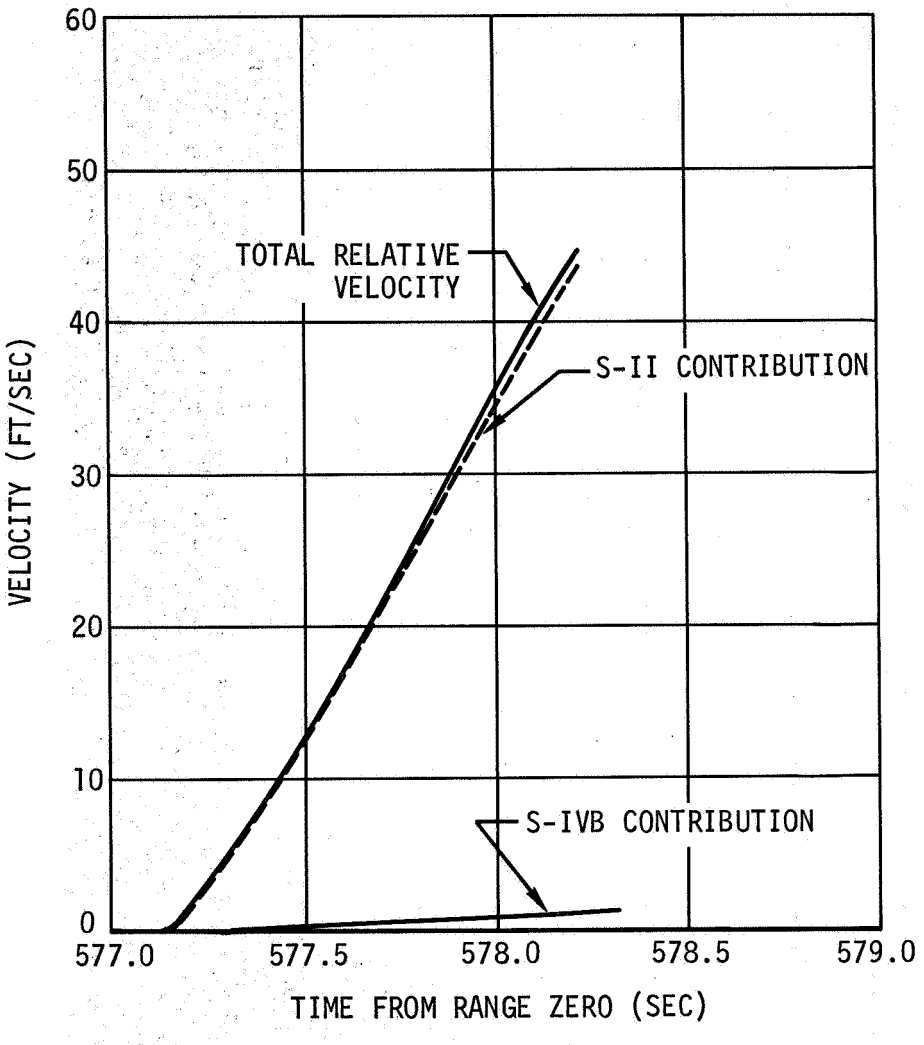

Figure 17-6. S-II/S-IVB Relative Velocity History

SECTION 18

DATA ACQUISITION SYSTEM

18. DATA ACQUISITION SYSTEM

18.1 Data Acquisition System Objective

The objective of the data acquisition system was to gather information describing the performance of stage systems and environments. The measurements collected are specified in the Douglas Drawing 1B43567, "AL" change Instrumentation Program and Components List (IP&CL). The information acquired from the measurements was converted into telemetry format and transmitted to ground stations located throughout the flight path. The final data were processed to conform with the requirements of the measurement requirement drawings.

Data shall be evaluated to requirements specified in the IP&CL, from automatic sequence start through S-IVB Command Service Module separation.

18.2 Summary of Performance

The performance of the data acquisition system was excellent throughout the flight mission. All systems performed as designed, and there were no system malfunctions. The number of measurement failures was low for the two evaluation phases of the AS-502 mission as summarized below:

Measurements assigned	616	
Measurements monitored by S-II	4	
Measurements inoperative due to stage configuration	1	
Checkout measurements	11	
Measurements deleted prior to flight	9	
Measurements prevented from being transmitted		
Phase I	0	
Phase II	3	
Measurements active for flight		
Phase I	591	
Phase II	588	
Phase I measurement failures	10	
Phase I measurement efficiency	98.3	percent
Phase II measurement failures	14	
Phase II measurement efficiency	97.6	percent

A detailed presentation status for the flight mission is presented in table 18-1. The nine deleted measurements prior to the flight are described in table 18-2. The three measurements prevented from being transmitted for phase II are elaborated on in table 18-3.

18.3 Instrumentation System Performance

The performance of the instrumentation system was satisfactory throughout the AS-502 mission. Ten measurements were considered phase I failures (liftoff to first S-IVB engine cutoff +10 sec). An additional four measurements failed after phase I to give a total of 14 phase II measurement failures. Table 18-4 elaborates on each measurement failure. Measurements which were not failures but considered as questionable, are covered in table 18-5.

The remote automatic checkout system (RACS) calibration levels were evaluated at RO -1,161 sec (11:40:40 hr GMT). Three measurements exceeded the 3 percent level tolerance. D0031-415 (Press - APS Chamber 2-2), D0206-404 (Press Int, Aft Skirt, Loc 1), and S0092-426 (Strain - Dyn, Fwd Skirt, Pnl 55). The following list delineates the measurements that exceeded 2 percent.

Measurement No. and Title	RACS Level	PCM Bit Count	Percent from Nominal
D0031-415	High	(FM)	-3
Press - APS Chamb 2-2	Low	(FM)	-3
D0206-404	High	787	-1.7
Press - Int, Aft Skt, Loc 1	Low	188	-3.2
S0092-426	High	(FM)	-3
Strain - Dyn, Fwd Skt, Pnl 55	Low	(FM)	-1
D0192-426	High	827	+2.7
Press - Ext, Aft Intrstg, Loc 14	Low	246	+2.8
D0196-419	High	786	-1.8
Press - Ext, Aft Intrstg, Loc 18	Low	197	-2.6
D0198-419	High	788	-1.6
Press - Ext, Aft Intrstg, Loc 2	Low	194	-2.6
D0199-419	High	795	-0.9
Press - Ext, Aft Intrstg, Loc 21	Low	198	-2.2
D0201-427	High	826	+2.3
Press - Ext, Aft Skt, Loc 5	Low	243	+2.5
D0210-402	High	783	-2.2
Press - Int, Intrstg, Loc 6	Low	199	-2.1

18.4 Telemetry System Performance

The telemetry system performance was within expected nominals. No deviation from the normal was observed.

18.4.1 Pulse Code Modulation Subsystem

All analog multiplexers were properly synchronized with respect to their pulse code modulation (PCM) assemblies. The PCM wave train was properly serialized and sync words properly coded. Analog-to-digital conversion appears uniform throughout the life of the stage.

PCM was utilized as the prime data source for sampled data.

18.4.2 Pulse Amplitude Modulation Subsystem

PAM was the secondary data source for sampled data; therefore, all channels were not reduced for evaluation. However, from the limited reduced data and the PCM/PAM comparison data, the pulse amplitude modulation (PAM) systems appear normal. Higher data noise was observed on PAM as compared to PCM; however, this was expected and is inherent in PAM systems.

18.4.3 Frequency Modulation Subsystem

The frequency characteristic for individual subcarrier oscillators (SCO) are listed in table 18-6. All SCO's were within band tolerances. System calibrations were verified whenever commanded by the switch selector. All calibration levels were present and easily distinguishable.

18.4.4 Single Sideband Subsystem

Data from the single sideband system verified the proper sampling of the 245 multiplexer. The 1,700 Hz calibration signal was actually 1,713 Hz, which was well within the calibrating tolerance. The presence of the calibration signal was verified whenever calibration was commanded.

The system was commanded OFF/ON/OFF at RO +296, RO +11,496, and RO +11,640 sec, respectively. System operation was verified by the presence of the SS/FM transmitter RF output power.

18.4.5 Tape Recorder

The critical data loss period at S-IC/S-II separation was not recovered due to the insufficient preprogrammed playback time that resulted from the over-burn of the S-II flight phase.

The tape recorder was commanded to fast record at RO +135 to RO +160 sec to recover data during S-IC/S-II separation. The second fast record, programmed to recover data during the time of S-II/S-IVB separation, was commanded to fast record at RO +483 sec (TB4 +335 sec) and was not commanded to stop recording until RO +597 sec (TB5 +21 sec). The total time for the second recording was 114 sec. Upon insertion, the tape recorder was commanded to play back at RO +835 sec for the preprogrammed time of 73 sec. This playback time was not sufficient to completely play back the second recording phase.

The short playback from the launch phase fast recording that resulted in an incomplete rewinding of the recorder tape, equivalent to 528 sec of slow recording, was not detrimental to the programmed recovery of out-of-range orbital data.

Except for difficulties in timing correlation due to the abnormal orbit trajectory, all orbital recordings were successfully recovered and reduced.

The evaluation of the fast operation period indicated an average speed of 29.99 in./sec with a wow amplitude of 0.24 in./sec^2 peak to peak (P-P) at the rate of 15.5 Hz and a flutter amplitude of 0.45 in./sec^2 P-P at the rate of 4,690 Hz. The tape recorder required 2.11 sec to attain speed stability in the fast operation mode.

18.4.6 Calibration Subsystem

The remote automatic checkout system (RACS), used for instrumentation system evaluation, was exercised at RO -1,161 sec. High mode was initiated at RO -1,161 sec, low mode at RO -1,144 sec, and returned to run mode at RO -1,130 sec. RACS levels were verified on all channels.

Telemetry system calibration was sent to the voltage controlled oscillator assemblies in the proper sequence and all calibration levels were present.

18.5 Radio Frequency System

The performance of the RF system was within expected nominal as shown in table 18-7. The performance figures were taken at four different places because of data drifts encountered during the launch period. The selected times are: Prelaunch (R0 -1 sec), prior to first burn (R0 +500 sec), post first burn when single sideband was OFF (R0 +780 sec), and prior to second burn (R0 +11,600 sec). Major drifting of the detectors occurred at liftoff and max q; stability was attained by R0 +600 sec.

The transmitter output power of FM/FM 2, FM/FM 3, and SSB/FM was higher than specified by specifications; however, detrimental effects were not observed. The high power output was confirmed during detector calibration.

The RF system blackout period during S-IC/S-II separation was not evaluated because the tape recorder playback data were not recovered. Data loss was observed at R0 +149.23 sec for 0.83 sec. Flame attenuation was not observed during S-II/S-IVB separation.

Good system performance was verified until R0 +33,000 sec when degradation of performance was observed due to the depletion of the electrical power source.

18.6 Signal Strength

Based upon available data reviewed, it is concluded that overall flight coverage was good as indicated by data recovery. The received signal levels were generally as expected when the antenna radiation patterns are considered with respect to the attitude and range of the vehicle.

Figures 18-1 and 18-2 show the signal strength level received at the noted ground stations from the S-IVB-502 PCM telemetry link. The time periods shown were selected to depict the prime interest areas of the first burn (R0 +577 to R0 +747 sec) and second burn (R0 +11,615 to R0 +11,630 sec) portions of the flight. Both left hand circular polarized (LHCP) and right hand circular polarized (RHCP) are shown except for the Tel 4 ground station from R0 +11,500 to R0 +11,980 sec, for which there was no RHCP data available. The derived signal levels shown are theoretical levels expected at the ground stations, computed from the actual flight trajectory.

There were two sets of data received for MILA-CIF RHCP from R0 to R0 +570 sec; one set showed a received signal strength approximately 10 db lower than the other. Figure 18-1 shows the lower level set of signal strength data. However, the signals received at MILA-CIF, both RHCP and LHCP, were approximately 40 db greater than expected throughout the acquisition period. The signal level received at Bermuda for approximately 75 sec starting at R0 +490 sec varied from 10 to 40 db lower than expected. At present, investigation is still in progress to determine the correct level of MILA-CIF RHCP and the reasons for the received signal strength transients.

18.7 Electromagnetic Compatibility

An electromagnetic compatibility (EMC) review of the S-IVB-502 prime flight data disclosed two measurements with marginal noise content. Measurements M0069-404 and M0070-404 displayed between 2 and 2-1/2 percent peak to peak (P-P) noise during chilldown for both burns.

Douglas Report No. SM-47376, Test Plan for the Electromagnetic Compatibility Test of S-IVB/V Systems Saturn S-IVB-501 and Subsequent, limits long term (over 1 sec) variations to 2 percent P-P.

ECP 10012 will reroute wiring in order to eliminate this noise problem on S-IVB-504N and subs.

TABLE 18-1 (Sheet 1 of 2)
MEASUREMENT STATUS

1. Measurements Assigned by IP&CL — 616

2. Measurements Not Flight Active — 12

Landline Measurements Available Prior to Liftoff Only -(3)

D0545-407	Press - Common Bulkhead Int - H/W
D0576-408	Press - Fuel Tank Ullage Umb - H/W
D0577-406	Press - Oxid Tank Ullage Umb - H/W

Inactive Measurement

K0152-404	Event - Rt Gyro Whl Speed OK Ind

Measurements Used for Checkout and Prelaunch Only -(8)

K0141-411	Event - R/S 1 Pulse Sensor
K0142-411	Event - R/S 2 Pulse Sensor
K0149-404	Event - Ullage Rocket Jettison 1 P/S
K0150-404	Event - Ullage Rocket Jettison 2 P/S
K0168-404	Event - Switch Selector Register Test
K0169-404	Event - EBW Pulse Sensor OFF Ind
K0176-404	Event - Ullage Rkt Ign P/S 1 Ind
K0177-404	Event - Ullage Rkt Ign P/S 2 Ind

3. S-IVB-502 Measurements Monitored by S-II Stage — 4

D0153-423	Press - Chamber Retro Rocket Pos IV - I
D0154-421	Press - Chamber Retro Rocket Pos II - III
D0155-420	Press - Chamber Retro Rocket Pos I - II
D0156-422	Press - Chamber Retro Rocket Pos III - IV

4. Measurements Waived from Flight Active List — 9

C0041-406	Temp - LOX Tank, Posit 2
C0056-406	Temp - LOX Tank Ullage Gas, 20%
C0150-401	Temp - Eng LH2 Pump Surface
C0155-404	Temp - LH2 Prevalve Bypass Line
C0205-403	Temp - He Prepress Sphere, No. 4 Gas
C0301-415	Temp - APS Oxid, Tank 2
D0018-401	Press - Eng Reg Outlet
D0058-401	Press - PU Valve Inlet
S0087-426	Strain - Dyn, Fwd Skirt, Pnl 17

5. Measurements Prevented from being Transmitted

Phase I — 0

Phase II — 3

C0010-403	Temp - Engine Area Ambient
C0152-403	Temp - LOX Main Line Flg Wall
E0209-401	Vib - Combustion Chamb Dome, Long

6. Net Measurements Available for Flight Test

Phase I — 591
Phase II — 588

TABLE 18-1 (Sheet 2 of 2)
MEASUREMENT STATUS

7. Measurement Failures

Phase II — 14

C0189-414	Temp - APS Inj Wall, Eng 1-2
C2015-401	Temp - Crossover Duct Ext Wall 1
D0003-403	Press - LOX Pump Inlet
D0224-401	Press - LH2 Pump Intrstg Outlet

Phase I — 10

B0023-404	Acoustic - Aft (2400 - 4800), Int
C0008-403	Temp - Heat Exch He Inlet
C0049-405	Temp - Electrical Tunnel, Loc 1
C0058-406	Temp - LOX Tank Ullage, 80 percent
C0111-426	Temp - Fwd Skirt, Loc 8
C0151-401	Temp - LOX Pump Surface
C0286-415	Temp - APS Fairing 2-4
D0105-403	Press - LOX Tank Press Mod, He Gas
E0114-411	Vib - Fwd Skirt, EBW R/S Pnl, Radial
E0210-401	Vib - LH2 Turbopump - Lateral

8. Partially Successful

C0274-403	Temp - Gas, Intrstg Area, Loc 6
C0305-418	Temp - Aft, Intrstg, Loc 7
D0002-403	Press - LH2 Pump Inlet
D0055-424	Press - LOX Tank Inlet
E0117-411	Vib - Fwd Skirt, Battery 1 and 2, Tan

9. Aberrant Measurements

C0037-408	Temp - LH2 Tank Ullage, 70 percent
C0153-403	Temp - Oxid Main Supply Line Wall
C0205-403	Temp - He Repress Sphere 4
C2035-401	Temp - Gas Generator LOX Inlet
D0016-425	Press - Cold Helium Sphere
D0018-401	Press - Engine Reg Outlet
D0071-414	Press - APS Oxid Sup Manf, Mod 1
D0073-415	Press - APS Oxid Sup Manf, Mod 2
K0008-401	Event - Ignition Detector
M0069-404	Volt - Aft T/M Full Scale Ref
M0070-404	Volt - Aft T/M Zero Volt Ref
N0012-411	Misc - RF Power, T/M Ant 2, Fwd
N0015-411	Misc - RF Power, FM/FM 1 Transmitter
N0016-411	Misc - RF Power, FM/FM 2 Transmitter
N0017-411	Misc - RF Power, FM/FM 3 Transmitter
N0019-411	Misc - RF Power, SS/FM Transmitter
N0033-411	Misc - RF Power, T/M Ant 3, Fwd
N0036-411	Misc - RF Power, T/M Ant 4, Refl
S0054-426	Strain - Axial, Fwd Skirt Loc 10A
S0055-426	Strain - Axial, Fwd Skirt Loc 10B
S0062-426	Strain - Axial, Fwd Skirt Loc 14A
S0063-426	Strain - Axial, Fwd Skirt Loc 14B
S0086-426	Strain - Dyn, Fwd Skirt, Pnl 13
S0087-426	Strain - Dyn, Fwd Skirt, Pnl 17
S0088-426	Strain - Dyn, Fwd Skirt, Pnl 26
S0089-426	Strain - Dyn, Fwd Skirt, Pnl 33
S0090-426	Strain - Dyn, Fwd Skirt, Pnl 40
S0091-426	Strain - Dyn, Fwd Skirt, Pnl 46
S0092-426	Strain - Dyn, Fwd Skirt, Pnl 55
S0093-426	Strain - Dyn, Fwd Skirt, Pnl 61
S0094-426	Strain - Dyn, Fwd Skirt, Pnl 69
S0095-426	Strain - Dyn, Fwd Skirt, Pnl 76
S0096-426	Strain - Dyn, Fwd Skirt, Pnl 80
S0097-426	Strain - Dyn, Fwd Skirt, Pnl 87
S0098-426	Strain - Dyn, Fwd Skirt, Pnl 94
S0099-426	Strain - Dyn, Fwd Skirt, Pnl 101
S0100-426	Strain - Dyn, Fwd Skirt, Pnl 108
S0101-426	Strain - Dyn, Fwd Skirt, Pnl 7

TABLE 18-2 (Sheet 1 of 2)
MEASUREMENT DELETIONS

C0041-406 Temp - LOX Tank, Posit 2

The level prior to liftoff was 6 deg R higher than nominal LOX temperatures. At liftoff, the level abruptly decreased to nominal LOX temperatures and subsequently proper operation was verified. The erroneous temperature data prior to liftoff was probably due to a high resistance contact in the sensor resistance system. The reason for the resistance changes at liftoff (change in acceleration) is presently under investigation.

C0056-406 Temp - LOX Tank Ullage Gas, 20%

The measurement was deleted from the flight list because of its erratic behavior during countdown demonstration test (CDDT) detanking process. During terminal countdown the measurement was off-scale-low. At RO +70 sec, the measurement abruptly came on-scale at the proper LOX temperature. It exhibited good data until RO +575 sec when it suddenly decreased to off-scale-low and remained there throughout the remainder of the mission.

Since the RACS were within specifications, the amplifier/bridge system was operating properly. The characteristic of the data indicates a short circuited sensor; however, the location of the malfunction is still under study.

C0150-401 Temp - Engine LH2 Pump Surface

The data remained in the off-scale-high state throughout the flight test. A debonded temperature sensor is suspected, possibly an open circuit resulted from the debonding. This transducer was bonded using the newer installation method. However, the malfunction was probably the result of improper technique.

C0155-404 Temp - LH2 Pre-Valve Bypass Line

The data level was off-scale-high prior to launch and remainded off-scale through the mission. Since the upper end of the temperature range was 460 deg R, it was expected, even if a debonded condition occurred, the temperature indication would be in-range sometime during flight. It is, therefore, suspected that a similar condition to measurement C0150 occurred, i.e., debonding with an open-circuit sensor.

C0205-403 Temp - He Repress Sphere No. 4 Gas

This measurement was deleted from the flight test list, however, good data was received throughout the mission. The measurement was deleted because of intermittent operation during prelaunch countdown.

C0301-415 Temp - APS, Oxid Tank 2

The measurement indicated off-scale-high prior to liftoff and throughout the mission. The malfunction is characteristic of a debonded temperature transducer that resulted in an open circuit sensor. The transducer was bonded using a method that is susceptible to debonding under environmental conditions.

D0018-401 Press - Engine Regulation Outlet

The measurement presented valid data during the flight test. The measurement was deleted because of an off-scale-low indication during CDDT. During launch countdown the pressure indication was at normal ambient.

TABLE 18-2 (Sheet 2 of 2)
MEASUREMENT DELETIONS

D0058-401 Press PU Valve Inlet

The measurement was deleted because of erratic variations of 40 psi during CDDT. The erratic condition persisted during launch, S-IC, and S-II flight phases. The erratic phenomenon was not exhibited after the initial pressure increase at S-IVB ignition. Data during the attempted restart was good. It was surmised that a restriction in the pressure monitoring line was present which was cleared after the initial pressure surge at S-IVB ignition.

S0087-426 Strain - Dyn, Fwd Skirt, Pnl 17

This measurement could not be calibrated during CDDT and was deleted prior to initiation of the automatic sequence. Evaluation of the preflight RACS indicated the high level was 8.5 percent low and the low level was 2.5 percent low. It appears that the gain setting of the amplifier was 0.87 of the nominal gain. It was not determined if the amplifier gain setting was at its maximum position. The balance adjustment was slightly lower than nominal. However, since the data level was on-scale, no detrimental effects were introduced. The response of the measurement during launch appears normal except for possible amplitude suppression; the measurement could be classified as trend.

TABLE 18-3
DEGRADED MEASUREMENTS PREVENTED FROM BEING TRANSMITTED

The following measurements have been deleted from the Phase II measurement efficiency baseline. The failure of these measurements have been attributed to the rupture of the ASI fuel feedline and the abnormal conditions existing (beyond design limitations) as a result. Since these transducers were subjected to conditions beyond their design limits, it does not reflect on the instrumentation system performance and therefore cannot be considered as instrumentation failures.

C0010-403 Temp - Engine Area Ambient

The measurement failed at RO +699 sec. The transducer was initially subjected to a very high temperature as shown by a 100 deg temperature rise in 3 sec. It then short-circuited indicating an off-scale-low condition. The malfunction was probably caused by excessive heating to the temperature probe and its associated wiring, causing an apparent short circuit to the sensor element.

C0152-403 Temp - LOX Main Line Flange Wall

The measurement failed in the off-scale-high mode at RO +696 sec. The transducer was subjected to a high temperature at RO +695 sec prior to the failure. The failure was probably caused by excessive heat deforming the bonding material that subsequently resulted in an open-circuit sensor.

E0209-401 Vib - Combustion Chamber Dome, Long

The measurement ceased to display valid data at RO +694 sec. The erratic data during the malfunction appears as a coaxial cable problem. It has been surmised that the initial malfunction was caused by a short circuit of the coaxial cable outer conductor to the inner conductor then, due to vibration, an electrical discontinuity occurred. The failure was initiated by the abnormal environment in the engine area.

TABLE 18-4 (Sheet 1 of 3)
MEASUREMENT FAILURES

PHASE I FAILURES

Liftoff to first burn Engine Cutoff Command (ECC) +10 sec.

B0023-404 Acoustic - Aft (2400 - 4800), Int

The measurement did not respond to sound pressures. Some indication of sound pressures was expected at liftoff and max q as extrapolated from measurements B0022 and B0024 in the same area. A redundant transmission of this channel digital in nature indicated some increase of noise quantity during the time of interest; however, the noise was much lower than the expected sound pressure levels. It is suspected that the transducer experienced an input signal adjustment change or an erroneous sound pressure calibration.

C0008-403 Temp - Heat Exchanger, He Inlet

The data exhibited off-scale-high condition throughout the flight test. The temperature was expected to be on-scale during cold helium flow at LOX tank pressurization. Since the RACS levels were within proper limits, the off-scale condition was due to an open circuit sensor.

C0049-405 Temp - Electrical Tunnel, Loc 1

The data indicated a sharp increase to off-scale-high at R0 +70 sec. The off-scale condition was probably caused by an open circuit transducer. This temperature sensor was a patch type bonded by a method that was susceptable to debonding under max q conditions.

C0058-406 Temp - LOX Tank Ullage, 80%

The temperature indicated a decrease at liftoff 5 deg R lower than nominal LOX temperature. The measurement performance characteristics appear normal; the probe uncovering characteristics were similar to those recorded for the S-IVB-501. At the present time, investigation is being conducted to determine the LOX tank influence on electrical components at liftoff.

C0111-426 Temp - Forward Skirt, Loc 8

The measurement did not display valid data during the region of max q. The data appears normal except from liftoff to R0 +148 sec when it was off-scale-high, from R0 +525 to R0 +557 sec when erratic data increases were noted, and after R0 +664 sec when the temperature started increasing until it was off-scale-high at R0 +712 sec. The malfunction was caused by a debonded temperature sensor exhibiting erratic discontinuities and high resistance interface connections. The bonding method was a type susceptable to debonding under environmental conditions.

C0151-401 Temp - LOX Pump Surface

The data indicated off-scale-high condition throughout the flight test. The malfunction was probably caused by a debonded sensor. The debonding could have also caused an open circuit sensor. Since preflight RACS levels were within nominal levels, sensor connections were intact.

C0286-415 Temp - APS Fairing 2-4

The measurement response was very slow with respect to other similar fairing temperatures. The characteristic appears as a partially debonded transducer. The bonding method was a type susceptable to debonding under environmental conditions.

TABLE 18-4 (Sheet 2 of 3)
MEASUREMENT FAILURES

D0105-403 Press - LOX Tank Press Mod He Gas

The measurement displayed invalid data during S-IVB first burn. The data increased to off-scale-high at R0 +92 sec and did not return to nominal level until R0 +7,260 sec and subsequently presented valid data.

E0114-411 Vib - Fwd Skirt, EBW R/S Pnl, Rad

The vibration data was erratic during the presence of stage vibration. The malfunction appears to be a loosened coaxial connection that was susceptible to vibration causing discontinuity of the accelerometer output signal. The vibration spectral power density plots indicate excessive low frequency components, which confirms disturbance from a low response source.

E0210-410 Vib - LH2 Turbopump, Lat

The data indicated very high levels between R0 +667 and R0 +695 sec, and higher than nominal levels at other turbopump operating times. The vibration characteristic appears good with higher than nominal levels at engine start as compared to AS-501. At the R0 +667 sec sample, the level was very high; the peaks were clipped by amplifier limiting. At R0 +699 sec, after three samples, the level decreased to a nominal level. Due to the nature of the data during this period, the measurement did not provide usable information for the purpose of defining the vibration environment and is classified a failure for phase I. However, investigation of the measurement subsequent to the failure indicate that there is sufficient intelligence in the data to provide information useful in correlating engine performance. Total loss of measurement response was observed to occur at R0 +11,625 sec.

Extensive laboratory tests and analyses performed in the investigation of the measurement failure indicate that severe overdriving of the amplifier from high vibration levels at low frequencies can result in the duplication of the flight data observed on AS-502. The vibration transducer is mounted on a block with the block bolted to the turbopump. It is suspected that a problem may exist in the mounting method. Resolution of the problem is under study and the implementation of Change Order 1789 and 1796 is expected to include corrective action.

PHASE II FAILURES - LIFTOFF TO PLANNED LV/SC SEPARATION

C0189-414 Temp - APS Injector Wall, Eng 1-2

The measurement failed in the off-scale-high mode at approximately R0 +2,400 sec. The failure occurred during the first revolution coast period where the APS was enabled. The continual temperature variation associated with APS firings probably caused debonding of the transducer and subsequently open circuited the sensor continuity. The bonding method was a type susceptible to debonding under environmental conditions.

C2015-401 Temp - Crossover Duct, Ext Wall, Loc 1

The data was off-scale-high during the attempted restart. The initial indication of failure occurred at R0 +722 sec when an off-scale-high response was observed. During coast mode the temperature appeared to return to scale. Several erratic temperature rises were noted, then at R0 +4,700 sec it finally remained off-scale-high. Since the upper end of the range was 1,660 deg R, and off-scale-high condition during orbital coast phase seems unlikely.

The malfunction was probably due to a temperature patch debonding causing an intermittent high resistance contact of the sensor wiring. This temperature measurement was installed by Rocketdyne on the J-2 engine.

TABLE 18-4 (Sheet 3 of 3)
MEASUREMENT FAILURES

D0003-403 Press - LOX Pump Inlet

The data indicated off-scale-high subsequent to RO +5,400 sec. The expected pressure was approximately the LOX ullage pressure. This transducer was a potentiometer type transducer. At the present time definite cause of the malfunction has not been determined; however, some possibilities are presented here:

a. Potentiometer deterioration - Deterioration of the potentiometer winding caused by rapid pressure variations as seen between RO +696 and engine cutoff.

b. Diaphragm damage - Overpressurizing at engine cutoff caused over-flexing of the mechanical diaphragm.

c. Internal pressure relief - Loss of internal pressure to reduce the diaphragm backpressure.

d. LOX ingestion - LOX entering the sense tube causing internal damage.

At RO +33,500 sec the data abruptly came on scale to the 47 psia level, still approximately 46 psia above the ullage pressure. This phenomenon is also unexplained.

D0224-401 Press - LH2 Pump Interstage Outlet

The data decreased abruptly from 20 psia to below zero psia. The malfunction occurred at RO +2,730 sec during the coast mode. The data level was approximately 2 percent through the remainder of the mission. The malfunction is still under investigation; the pressure sensing system and the output connector discontinuity are the prime suspects.

TABLE 18-5 (Sheet 1 of 3)
QUESTIONABLE MEASUREMENTS

Partially Successful

C0274-403 Temp - Gas Interstage Area, Loc 6

The measurement abruptly increased to off-scale-high at S-II/S-IVB separation and remained in that state for the duration of the mission. The malfunction occurred after the period of interest. The off-scale-high condition indicates an open circuit of the sensor or to its associated wiring probably caused by temperature shock at S-II/S-IVB separation.

C0305-419 Temp - Aft Interstage, Loc 7

The temperature indication from RO +90 to RO +117 sec increased abnormally rapid with respect to other aft interstage temperatures. The response resembles a partially debonded sensor subjected to localized heating. The sensor eventually reseated itself (due to bond stress or aerodynamic pressures) at RO +117 sec and cooled to ambient skin temperature at RO +119 sec. The bonding method used was a type susceptable to debonding under environmental conditions.

D0002-403 Press - LH2 Pump Inlet

The data level indicated 2.5 psia (4 percent) above ullage pressure during the coast phase. The pressure during this phase was expected to be very close to the ullage pressure because of the very low axial acceleration level. The transducer malfunction occurred at RO +762 sec when a high pressure surge was observed. This pressure surge damaged the pressure sensor and offset its calibration +4 percent. Data were recoverable by a manual calibration shift.

D0055-424 Press - LOX Tank Inlet

Invalid data indication of zero pressure areas from RO +11,410 to RO +11,430 sec and subsequent to RO +11,730 sec was observed. The probable malfunction was the lifting of the potentiometer wiper from the winding in the vicinity of excessive wear. The invalid areas were not detrimental to the evaluation of the LOX pressurization system.

E0117-411 Vib - Fwd Skirt, Battery 1 and 2, Tan

Erratic vibration data were displayed except during liftoff and max q. The malfunction appears to be due to a loose coaxial cable connector. This measurement was not continually monitored (multiplexed); therefore, transition from good to invalid data was not definitely discernable. The malfunction probably occurred just after liftoff, then at max q, good data were obtained for one sample. The spectral power density plots at liftoff and max q appear similar to AS-501.

Aberrant:

C0037-408 Temp - LH2 Tank Ullage, 70 Percent

The temperature level indication was far below LH2 boiling point, and the level changed in irregular steps. The range of this measurement was intended to measure both liquid and gas temperatures. The calibration curve is linear until close to the liquid temperature where it is then exponential. The accuracy of the measurement is markedly degraded by the exponential portion of the curve and cannot be precisely represented by the computer calibration program.

C0153-403 Temp - Oxid Main Supply Line Wall

The measurement reflected a cooling trend during the coast period through RO +3,600 sec. At RO +5,400 sec, which was the next available data period, the measurement indicated off-

TABLE 18-5 (Sheet 2 of 3)
QUESTIONABLE MEASUREMENTS

scale-low and remained there for the duration of flight. Since the measurement was partially successful in phase II with failure occurring between RO +3,600 and RO +5,400 sec, it was considered good for phase II in accordance with the evaluation ground rules.

C0205-403 Temp - He Repress Sphere 4

This measurement was deleted prior to flight test; however, the flight data appear valid.

C2035-401 Temp - Gas Generator LOX Inlet

The measurement went off-scale-high at RO +10,230 sec. A patch-type transducer is utilized and it is suspected that debonding occurred. Since the measurement was partially successful in phase II, it was considered good for phase II in accordance with the evaluation ground rules.

D0016-425 Press - Cold Helium Sphere

The measurement was off-scale-low at RO +22,375 sec, after cold helium dump, on the data plots. Digital data showed the pressure to be below zero at -175 psia. RACS were verified to be within tolerance and the pressure at liftoff was within 50 psia of the ground supply pressure; however, investigation into the measurement history indicates the pressure to be lower than the ambient expected. It is believed that an ambient calibration degradation exists and the problem is being investigated further to correct the lower end point of calibration.

D0018-401 Press - Engine Reg Outlet

This measurement was deleted prior to flight test. It responded properly during flight.

D0071-414 Press - APS Oxid Supply Manf, Mod 1
D0073-415 Press - APS Oxid Supply Manf, Mod 2

Appearance of activity during liftoff, mach 1, and max q was indicated, although no activity was expected. These transducers are potentiometer type pressure transducers which are known to be susceptible to a high vibration environment.

K0008-401 Event - Ignition Detected

No activity was expected from this measurement. A dummy probe was installed for flight test.

M0069-404 Volt - Aft T/M Full Scale Ref
M0070-404 Volt - Aft T/M Zero Volt Ref

These measurements were susceptable to noise created by the chilldown inverters. The noise quantity was discernable; however, it was not detrimental to the telemetry system. Noise in these measurements was observed on previous tests.

N0012-411 Misc - RF Power, T/M Ant 2, Fwd
N0015-411 Misc - RF Power, FM/FM 1 Transmitter
N0017-411 Misc - RF Power, FM/FM 3 Transmitter
N0019-411 Misc - RF Power, SS/FM Transmitter
N0033-411 Misc - RF Power, T/M Ant 3, Fwd
N0036-411 Misc - RF Power, T/M Ant 4, Refl

These measurements indicated drifting characteristics which were quite pronounced during the launch phase. These drifting responses were of a random nature that could not be attributed to the change of RF power. The drifting characteristic manifested itself as an

TABLE 18-5 (Sheet 3 of 3)
QUESTIONABLE MEASUREMENTS

increasing or decreasing step shift at liftoff. After liftoff they slowly increased or decreased to some peak value, then stabilized at a nominal level. The drifts did not exceed system requirements, and they were used for system evaluation. It appears the detectors were sensitive to vibration and temperature changes. Similar characteristics were observed on the S-IVB-501 flight.

N0016-411 Misc - RF Power, FM/FM 2 Transmitter

The measurement indicated a loss of output power at RO +27,950 sec. No telemetry data loss was observed, and the antenna powers did not decrease. Thus, a measurement loss was experienced. Probably a detector loss of sensitivity was incurred.

S0054-426 Strain - Axial, Fwd Skirt Loc 10A
S0055-426 Strain - Axial, Fwd Skirt Loc 10B
S0062-426 Strain - Axial, Fwd Skirt Loc 14A
S0063-426 Strain - Axial, Fwd Skirt Loc 14B

These measurements show polarity reversals. There is no degradation of data and the measurements have been used in analyses of static strain.

S0086-426 Strain - Dyn, Fwd Skirt, Pnl 13
to
S0101-426 Strain - Dyn, Fwd Skirt, Pnl 7

All dynamic strain measurements were inadvertently displayed with their calibration header inverted. Dynamically, the direction of deflection was not critical; however, for static deflection, correction should be applied.

S0100-426 Strain - Dyn, Fwd Skirt, Pnl 108
S0101-426 Strain - Dyn, Fwd Skirt, Pnl 7

These strain measurements indicated behavior questioned by Acoustics and Structural Dynamics. S0101-426 and S0100-426 showed higher than expected data amplitudes between RO +79.5 and RO +82.5 sec, and between RO +84.5 and RO +87.5 sec, respectively. At RO +91.5 sec, S0101-426 showed a dc shift from 52 percent to 70 percent of the measurement range and maintained the dc offset for two data samples. After the return of the data level of S0101-426 to approximately 42 percent of range, S0100-426 exhibited level variations during one sample period of approximately 10 percent from RO +109 sec.

Investigation and analysis of possible electrical malfunctions to the measurements did not produce evidence of electrical failures which would account for the anomalous behavior of the data during the periods specified above. Singular failure modes which can exhibit the type of data observed were investigated and analyzed but no reasonable singular failure mode could be determined. In view of the electrical characteristics, multiple failures of two separate measurements, over a coincident period of time, is possible but is considered unlikely. No laboratory testing was performed since simulation of flight conditions is considered impractical.

TABLE 18-6 (Sheet 1 of 3)
SUBCARRIER OSCILLATOR FREQUENCY

IRIG CHANNEL	NOMINAL		PRELAUNCH (RO -1,266)		POST RESTART (RO +11,634)	
	F_c	f_{BE}	F_c	f_{BE}	F_c	f_{BE}
	FM SYSTEM 1					
5	1300	1398 1202	1301	1400 1202	1300	1400 1202
6	1700	1828 1572	1699	1826 1569	1695	1815 1572
7	2300	2473 2127	2305	2466 2132	2296	2468 2135
8	3000	3225 2775	2993	3217 2768	2988	3190 2784
9	3900	4193 3607	3867	4190 3607	3891	4183 3596
10	5400	5805 4995	5396	5804 4989	5385	5783 4977
11	7350	7901 6799	7346	7899 6797	7332	7878 6778
12	10500	11288 9712	10505	11299 9709	10484	11267 9681
13	14500	15588 13412	14488	15572 13406	14459	15530 13369
14	22000	23650 20350	21980	23632 20341	21944	23576 20290
15	30000	32250 27750	29964	32229 27722	29928	32144 27656
	FM SYSTEM 2					
3	730	785 675	729	784 674	730	783 674
6	1700	1828 1572	1700	1831 1571	1701	1831 1571
7	2300	2473 2127	2301	2477 2126	2303	2479 2129
8	3000	3225 2775	3001	3225 2776	3004	3230 2778

TABLE 18-6 (Sheet 2 of 3)
SUBCARRIER OSCILLATOR FREQUENCY

IRIG CHANNEL	NOMINAL		PRELAUNCH (RO -1,266)		POST RESTART (RO +11,634)	
	F_c	f_{BE}	F_c	f_{BE}	F_c	f_{BE}
9	3900	4193 3607	3906	4197 3611	3905	4201 3611
10	5400	5805 4995	5395	5798 4989	5407	5813 5000
11	7350	7901 6799	7351	7904 6805	7364	7921 6807
12	10500	11288 9712	10500	11289 9710	10514	11307 9722
13	14500	15588 13412	14510	15610 13412	14526	15626 13429
14	22000	23650 20350	21990	23644 20344	22027	23699 20376
15	30000	32250 27750	29969	32211 27715	30032	32302 27780
16	40000	43000 37000	39996	43000 37027	40020	43033 37022
17	52500	56440 48560	52487	56424 48560	52522	56469 48616
18	70000	75250 64750	70089	75350 64848	70122	75453 64837
FM SYSTEM 3						
6	1700	1828 1572	1699	1828 1571	1701	1830 1572
7	2300	2473 2127	2299	2474 2126	2302	2475 2127
8	3000	3225 2775	3000	3224 2774	3003	3228 2777
9	3900	4193 3607	3898	4190 3605	3900	4194 3611
10	5400	5805 4995	5399	5803 4990	5402	5806 4995
11	7350	7901 6799	7346	7895 6794	7353	7907 6802

TABLE 18-6 (Sheet 3 of 3)
SUBCARRIER OSCILLATOR FREQUENCY

IRIG CHANNEL	NOMINAL		PRELAUNCH (R0 −1,266)		POST RESTART (R0 +11,634)	
	F_c	f_{BE}	F_c	f_{BE}	F_c	f_{BE}
12	10500	11288 9712	10505	11298 9708	10514	11304 9714
13	14500	15588 13412	14485	15567 13399	14499	15586 13409
14	22000	23650 20350	21970	23632 20331	22006	23663 20354
15	30000	32250 27750	30004	32238 27766	30032	32271 27801

TABLE 18-7
RF SYSTEM PERFORMANCE SUMMARY

	LAUNCH TIME			
	R0 -1	R0 +500	R0 +780	R0 +11,600
Transmitter output (watts) (min 15w)				
FM/FM 1 (N15)	21.2	20.2	20.0	22.2
FM/FM 2 (N16)	25.2	25.2	25.2	25.2
FM/FM 3 (N17)	27.2	27.6	27.6	29.6
PCM/FM (N18)	22.6	23.0	23.0	24.0
SS/FM (N19)	26.4	25.4	0	23.8
Antenna Power (watts)				
Ant 1 (N1)	10.0	9.8	9.8	10.6
Ant 2 (N12)	9.8	9.4	9.8	11.6
Ant 3 (N33)	20.2	19.4	13.8	20.8
Ant 4 (N35)	17.4	17.2	11.6	17.8
Antenna VSWR (max 1.7:1)				
Ant 1	1.19:1	1.69:1	1.69:1	1.54:1
Ant 2	1.37:1	1.47:1	1.47:1	1.44:1
Ant 3	1.11:1	1.12:1	1.06:1	1.56:1
Ant 4	1.13:1	1.63:1	1.44:1	1.41:1
Insertion Loss (max 7.5 db) (At R0 +500)				
Ant 1		6.88 db		
Ant 2		7.07 db		
Ant 3		5.79 db		
Ant 4		6.31 db		

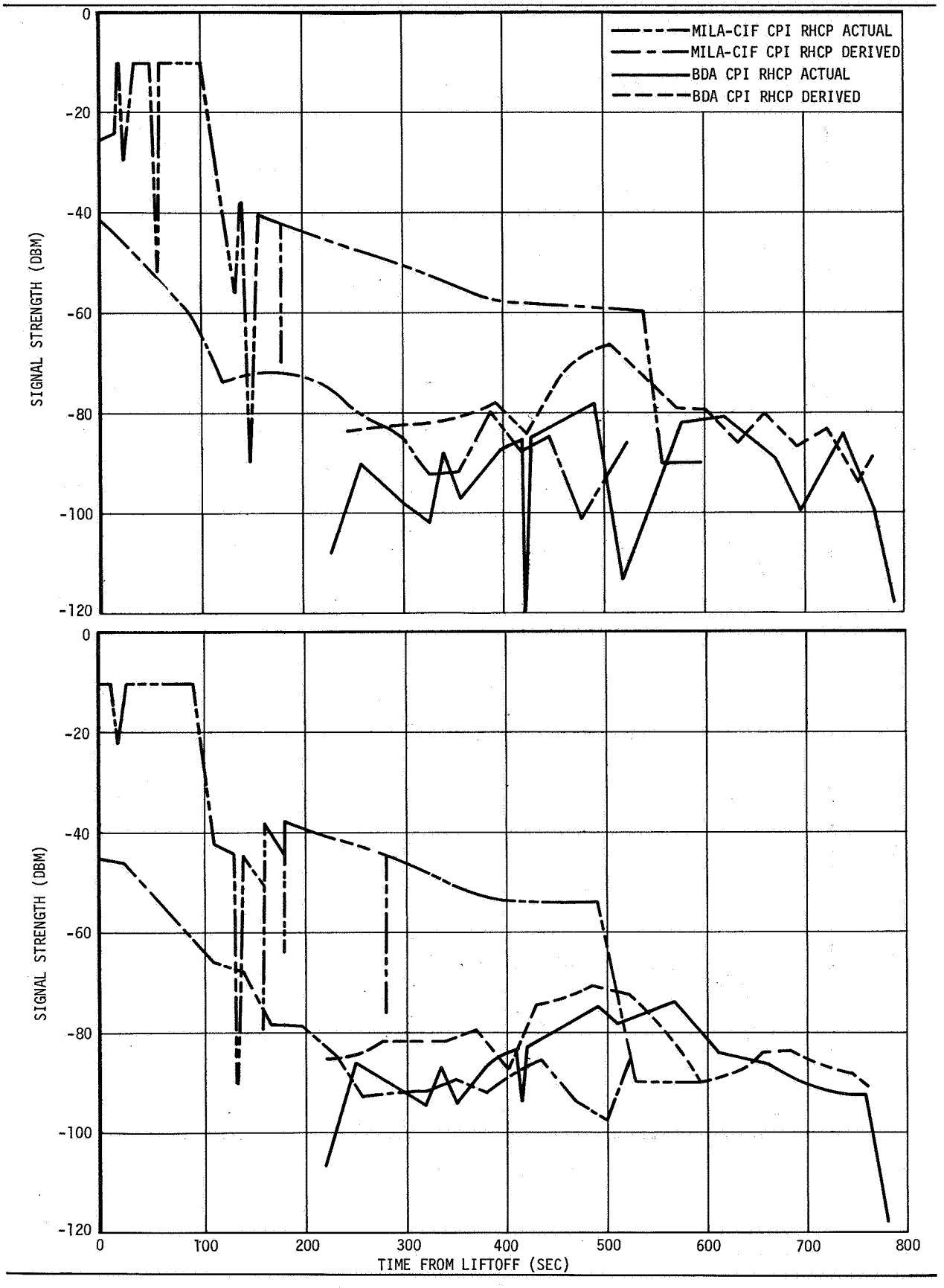

Figure 18-1. Telemetry Signal Strength - MILA and BDA

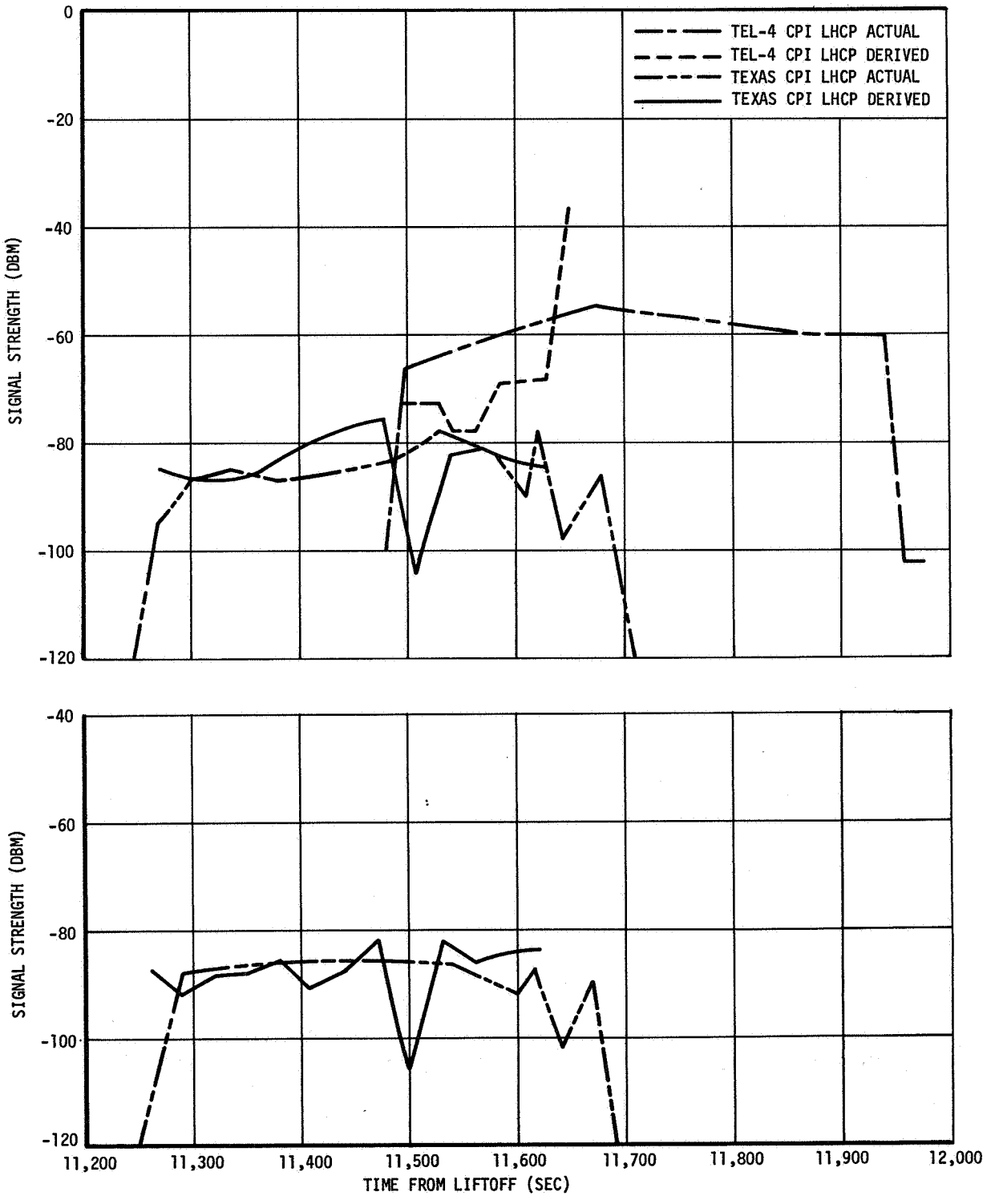

Figure 18-2. Telemetry Signal Strength - Tel 4 and Texas

SECTION 19

ELECTRICAL SYSTEMS

19. ELECTRICAL SYSTEMS

The electrical control system, with the exception of the PU system, and the electrical power system performed satisfactorily throughout phases I and II of the AS-502 flight as defined in Douglas Report No. DAC-56610A, S-IVB-502 Stage Technical Performance Criteria Document, revised March 1968. Although the propellant utilization (PU) system performed satisfactorily throughout phase I, LOX mass measurements went to a LOX tank mass-full condition during restart preparation of phase II, indicating possible PU system malfunction. Subsequent investigation verified the PU system malfunction, and the analysis is delineated in section 16.

Evaluation of the electrical system performance during the critical analysis period of RO +133 sec did not disclose any electrical system malfunction.

19.1 Electrical Control System

The operational integrity of the electrical control system is verified in the sequence of events in section 5 of this evaluation. All responses to switch selector commands were satisfactory. Seventeen nonprogrammed commands were initiated to command the S-IVB from Carnarvon, Hawaii, and Guaymas ground stations. These commands are included in the sequence of events.

19.1.1 J-2 Engine Control System

All event measurements verified that the engine control system had responded properly to the Engine Start Command and Engine Cutoff Command given for first burn and for the engine restart attempt. First burn engine start was initiated at RO +577.268 sec with engine cutoff being initiated at RO +747.032 sec, resulting in a total engine first burn time of 169.764 sec. Second burn engine start was initiated at RO +11,614.667 sec. Due to the failure of the S-IVB engine to restart, the mainstage OK pressure switches did not pick up and engine cutoff was initiated at RO +11,630.394 sec. All telemetry event measurements of engine performance occurred in the proper sequential order.

19.1.2 Control Pressure Switches

A review of the event and pressure measurements associated with the control pressure switches verified that each switch functioned properly. The following paragraphs list these measurements and delineate the performance of each pressure switch.

The engine pump purge control module pressure switch regulates the pressure of the helium gas in the pump purge line to stay between 105 and 130 psia when the Engine Pump Purge Control Valve Enable ON Command is given. Data from the following measurements showed that purge pressure never reached the actuation limit (130 psia) and that the pressure switch, therefore, remained in the de-energized position (105 psia).

K0105-404 Event - Pump Purge Regulator Backup Pressure Switch De-en

D0050-403 Press - Engine Pump Purge Regulator

The LH2 tank first burn flight control pressure switch actuates the first burn bypass control valve so that tank ullage pressure is maintained between 28 and 31 psia during the time that the first burn relay is on. The fuel tank was pressurized to 35 psia prior to first burn and never decreased below 32 psia during mainstage. Therefore, the pressure switch remained in the actuate (31 psia) position during this time. The following measurements verified these conditions.

K0184-404 Event - Fuel Tank Flight Control Pressure Switch

K0107-404 Event - LH2 Tank Step Pressure Valve En

D0177-410 Press - Fuel Tank Ullage EDS 1

D0178-410 Press - Fuel Tank Ullage EDS 2

The LH2 tank prepress, repress, and second burn flight control pressure switch actuates at 34 psia and deactuates at 31 psia. It controls the LH2 repress control valves during the LH2 Repress Control Valve Open ON Command and the LH2 tank step pressurization control valve during the time that the second burn relay is on. During repressurization, the switch allowed ullage pressure to increase from 20 to 34 psia at which time it closed the repress control valves. Prior to the second burn attempt, ullage pressure decreased sufficiently to allow deactuation of the switch. During the second burn attempt the pressure did not reach the actuation limit of the switch before the engine was cut off.

These conditions are verified by the following measurements:

K0101-404 Event - LH2 Repress Control Switch De-en

K0107-404 Event - LH2 Step Pressure Valve En

D0177-410 Press - Fuel Tank Ullage EDS 1

D0178-410 Press - Fuel Tank Ullage EDS 2

The LOX tank prepress and flight control pressure switch regulates the cold helium shutoff valves during the OFF portion of the LOX tank flight pressure system command and the heat exchanger bypass valve during the ON portion of this command. Actuation and deactuation of the switch occurs, respectively, at 41 and 38 psia of LOX ullage pressure. The pressure switch also controls the LOX tank repress control valves after the LOX Tank Repress Control Valve Open ON Command is given. Data from the following measurements verified that the switch responded properly to ullage pressure changes throughout flight.

K0102-404 Event - LOX Prepress Flight Switch En

K0108-404 Event - LOX Prepress Flight Switch De-en

D0179-424 Press - Oxid Tank Ullage EDS 1

D0180-424 Press - Oxid Tank Ullage EDS 2

The LOX chilldown pump purge pressure switch actuates at 41 psia and deactuates at 38 psia of pressure in the pump purge line. It controls the LOX chilldown pump purge control valve

when the LOX Chilldown Pump Purge Control Valve Enable ON Command is given prior to LOX loading. The pressure switch responded to pressure fluctuations in the pump purge line throughout flight as is verified by the following measurements.

K0131-403 Event - LOX Chilldown Purge Switch De-en

D0103-403 Press - Helium Pressure to LOX Motor Control

The control helium regulator backup pressure switch is employed in the pneumatic power control module as a redundant control of the helium line pressure should the module regulator fail for some reason. The switch actuates at 600 $\pm$15 psia and deactuates at 490 $\pm$25 psia. Pressure measurement D0014 showed that the regulator kept the line pressure below the actuation limit of the pressure switch during flight.

D0014-403 Press - Control Helium Regulator Discharge

The operation of the LOX tank regulator backup pressure switch is redundant to that of the cold helium pressure regulator in the LOX tank pressure control module. If the regulator fails, the pressure switch can actuate (450-485 psia) and close the cold helium supply shutoff valves thereby regulating the cold helium supply line pressure. Since the regulator functioned properly, the pressure switch remained in the de-energize (335-370 psia) position during flight. Proper operation was verified by the following measurements.

K0156-404 Event - LOX Tank Regulator Backup Pressure Switch En

D0225-403 Press - Cold Helium Control Valve Inlet

The LOX and LH2 translunar vent termination pressure switches were installed but were not operational for flight.

19.1.3 APS Electrical Control System

A review of the APS feed valve data verified that the APS electrical control system performed within prescribed limitations.

K0132-404 Event - APS Eng 1-1/1-3 Fd Vlv - Op

K0133-404 Event - APS Engine 1-2 Fd Vlv - Open

K0134-404 Event - APS Engine 2-1/2-3 Fd Vlv - Op

K0135-404 Event - APS Engine 2-2 Fd Vlv - Open

19.1.4 Chilldown Shutoff Valves

The LOX and LH2 chilldown shutoff valves responded to the chilldown shutoff pilot valve commands and operated properly.

K0136-409 Event - Fuel SOV Chill System - Cl

K0137-409 Event - Fuel SOV Chill System - Op

K0138-424 Event - Oxid SOV Chill System - Op

K0139-424 Event - Oxid SOV Chill System - Cl

19.1.5 Vent Valves

A review of the following measurements indicated that the LOX and LH2 vent valves responded to their respective commands and operated properly.

K0001-410 Event - Fuel Tank Vent Valve - Cl

K0002-424 Event - Oxid Tank Vent Valve - Cl

K0016-404 Event - Oxid Tank Vent Valve 1 - Op

K0017-410 Event - Fuel Tank Vent Valve 1 - Op

19.1.6 Fill and Drain Valves

The LOX and LH2 fill and drain valves were commanded closed through the umbilical prior to liftoff and remained closed throughout flight.

K0003-427 Event - Fuel Fill Valve - Closed

K0004-404 Event - Oxid Fill Valve - Closed

19.2 Electrical Power System

The electrical power system performed satisfactorily in meeting electrical load requirements throughout phase I and the restart attempt of phase II.

19.2.1 Flight Batteries

All batteries performed within the expected limits as verified from the load profiles and temperature data shown in figures 19-1 through 19-4.

19.2.2 Chilldown Inverters

The chilldown inverters performed satisfactorily during phases I and II of the flight evaluation period. The inverters reacted to the load change demands of the chilldown pumps without difficulties. The operating temperature of the inverters prior to liftoff was 515 deg R. The LOX chilldown inverter temperature increased to 524 deg R and the LH2 chilldown inverter temperature increased to 527 deg R at turnoff. Both the LOX and LH2 chilldown inverter temperatures were at 499 deg R at turnon after the coast period and increased to 511 deg R and 515 deg R respectively at turnoff before the restart attempt.

MEASUREMENT NUMBER	MEASUREMENT NOMENCLATURE	ACCEPTABLE RANGE	ACTUAL VALUE
M0026-404	Volt-Phase A-B Fuel Chilldown Inverter	56 ±4 vac	57.0 vac
M0027-404	Volt-Phase A-B LOX Chilldown Inverter	56 ±4 vac	56.0 vac
M0028-404	Freq-Fuel Chilldown Inverter	400 ±10 Hz	401.0 Hz
M0029-404	Freq-Oxid Chilldown Inverter	400 ±10 Hz	402.0 Hz
M0040-404	Volt-Phase A-C LOX Chilldown Inverter	56 ±4 vac	57.0 vac
M0041-404	Volt-Phase A-C Fuel Chilldown Inverter	56 ±4 vac	57.0 vac
M0044-404	Volt-Phase A1-B1, LOX Chilldown Inverter	56 ±4 vac	58.0 vac
M0045-404	Volt-Phase A1-C1, LOX Chilldown Inverter	56 ±4 vac	58.0 vac
M0046-404	Volt-Phase A1-B1, LH2 Chilldown Inverter	56 ±4 vac	57.0 vac
M0047-404	Volt-Phase A1-C1, LH2 Chilldown Inverter	56 ±4 vac	58.0 vac

19.2.3 5 Volt Excitation Modules

Both 5 v excitation modules performed satisfactorily. The output values are listed below:

MEASUREMENT NUMBER	MEASUREMENT NOMENCLATURE	ACCEPTABLE RANGE	ACTUAL VALUE
M0024-411	Volt-5 Volt Excitation Mod Fwd	5.00 ±0.025 vdc	5.01 vdc
M0025-404	Volt-5 Volt Escitation Mod Aft	5.00 ±0.025 vdc	5.00 vdc
M0042-404	Freq-5 Volt Excitation Mod Aft	2,000 ±200 Hz	2,000 Hz
M0043-411	Freq-5 Volt Excitation Mod Fwd	2,000 ±200 Hz	2,000 Hz

19.2.4 Static Inverter Converter

The static inverter converter operated within design limits with the exception of the 5 vdc output, measured by measurement M0004-411 (Static Inverter Converter, 5 vdc) which was 30 mv higher than the tolerance limit during normal PU operation and 90 mv out of tolerance when the PU Valve Hardover Command was acted upon. The 5 vdc output being out of tolerance does not affect the operation of the PU control system since it is used for telemetry excitation of the mass potentiometers only. No error is introduced into propellant mass calculations since ratios of voltage levels are utilized in evaluating mass potentiometer data.

The inverter frequency went to 406.2 Hz when the PU Valve Hardover Command was given at second burn Engine Start Command. The shift in frequency is expected at the PU Hardover Command, and there is no degradation in the operation of the PU system.

The minimum temperature was 541 deg R at liftoff. At inverter power turnoff, the temperature was 546 deg R.

MEASUREMENT NUMBER	MEASUREMENT NOMENCLATURE	ACCEPTABLE RANGE	ACTUAL VALUE
M0001-411	Volt-Static Inverter Converter	115 $\pm$3.45 vrms	114.5 vrms
M0004-411	Volt-Static Inverter Converter	5.00 $^{+0.10}_{-0.55}$ vdc	5.130 vdc 5.190 vdc*
M0012-411	Freq-Static Inverter Converter	400 $\pm$6 Hz	402 Hz 406.2 Hz*
M0023-411	Volt-Static Inverter Converter, 21 vdc	21.0 $^{+1.5}_{-1.0}$ vdc	21.80 vdc

*Levels during PU hardcver period.

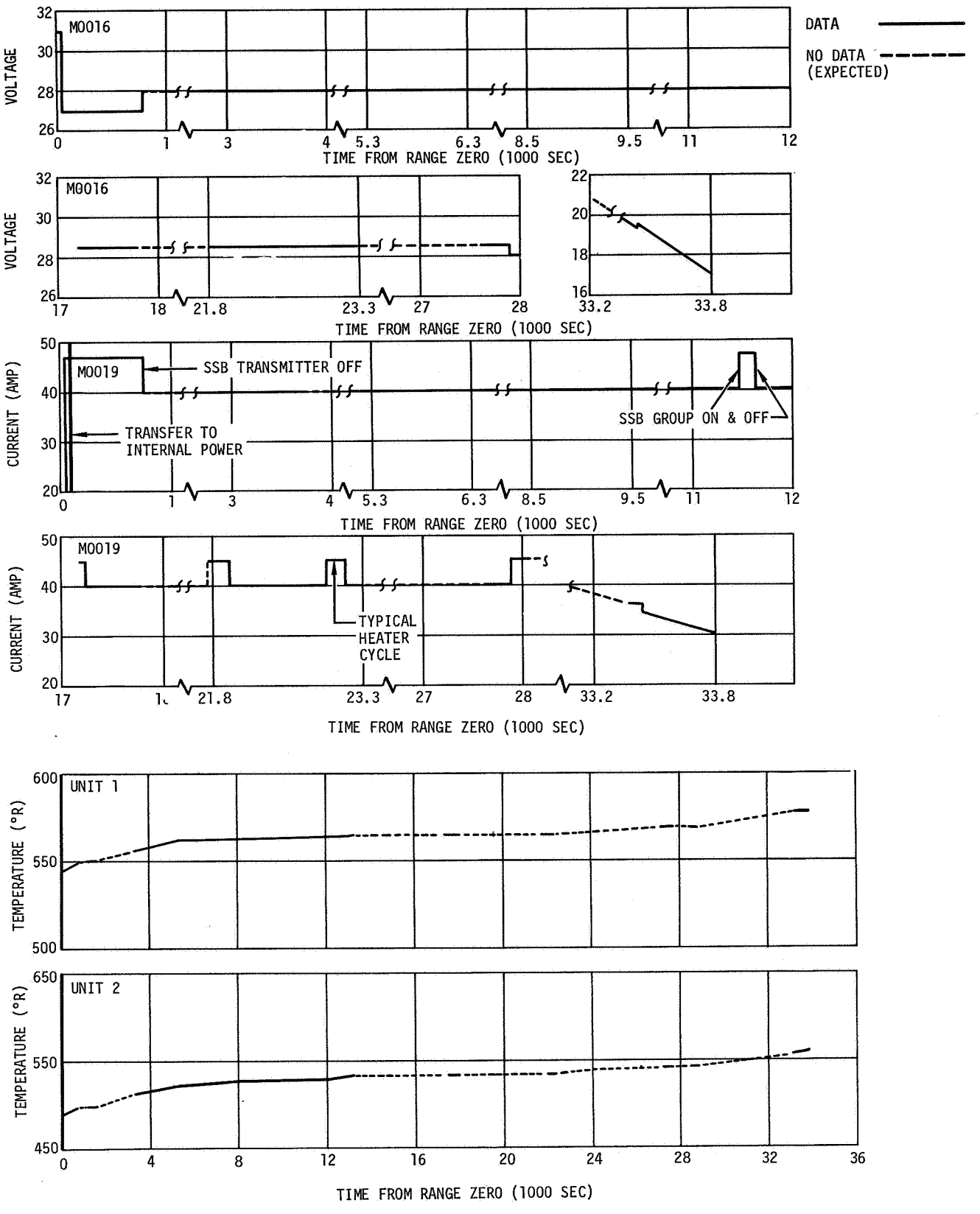

Figure 19-1. Forward Battery No. 1 Performance

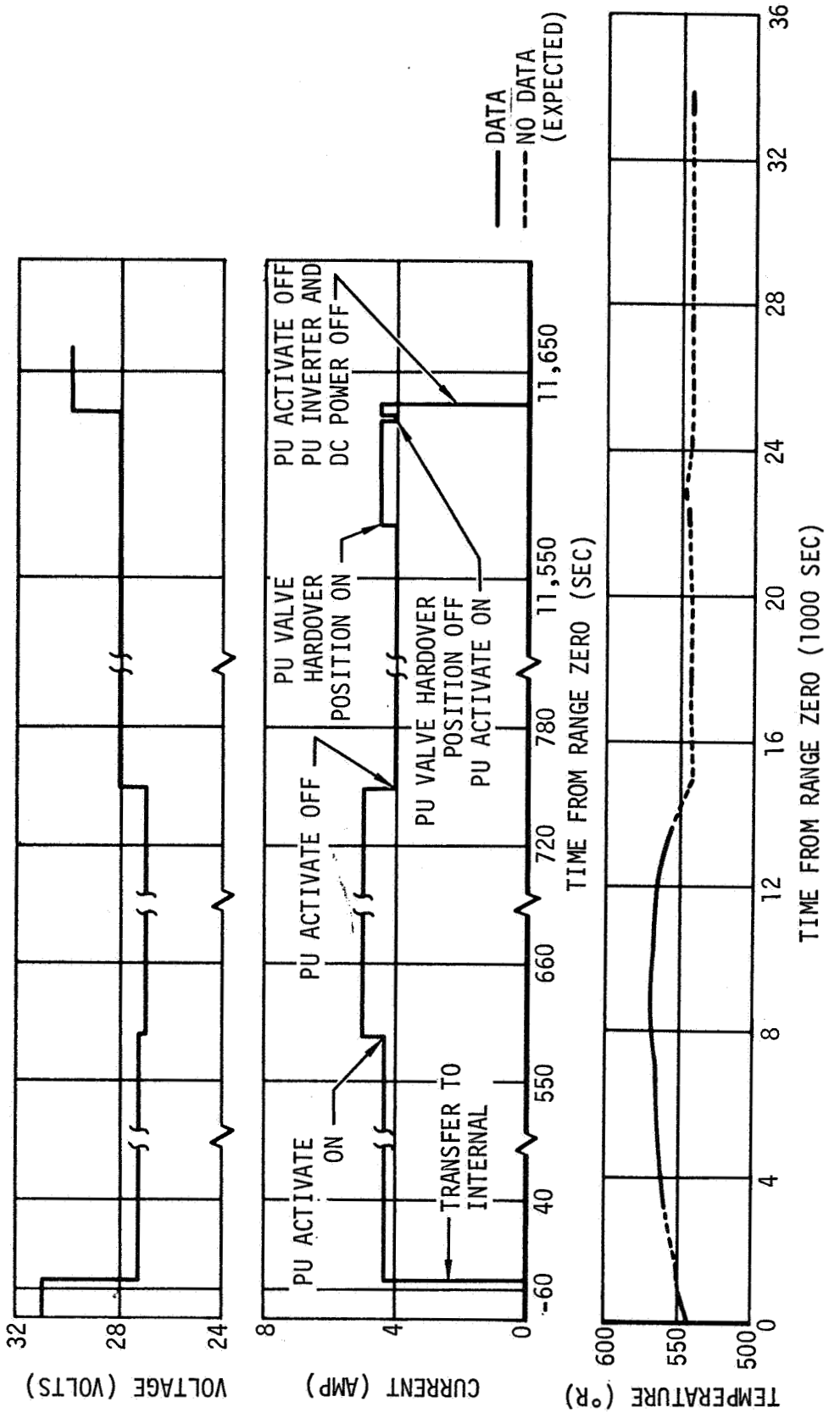

Figure 19-2. Forward Battery No. 2 Performance

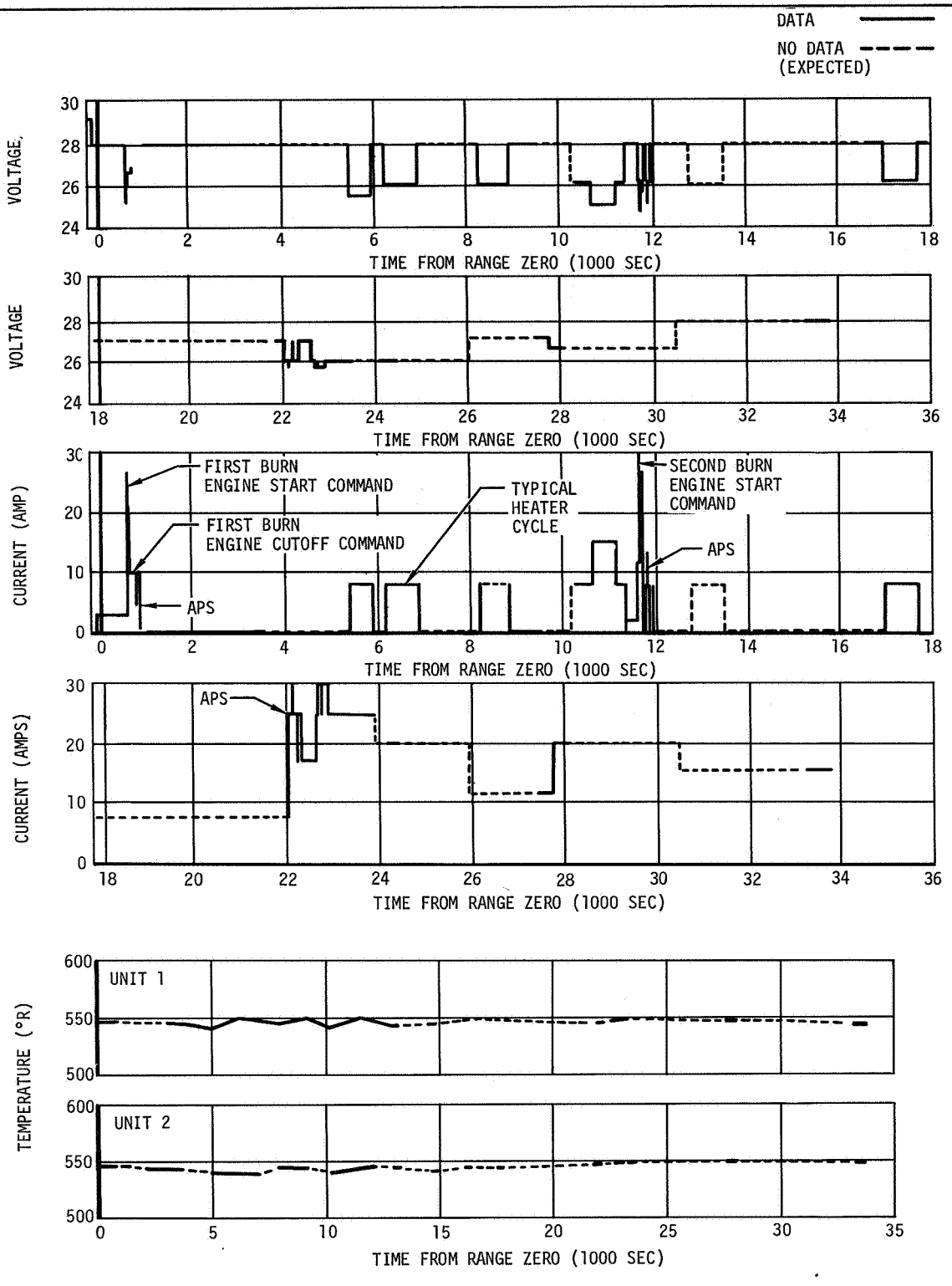

Figure 19-3. Aft Battery No. 1 Performance

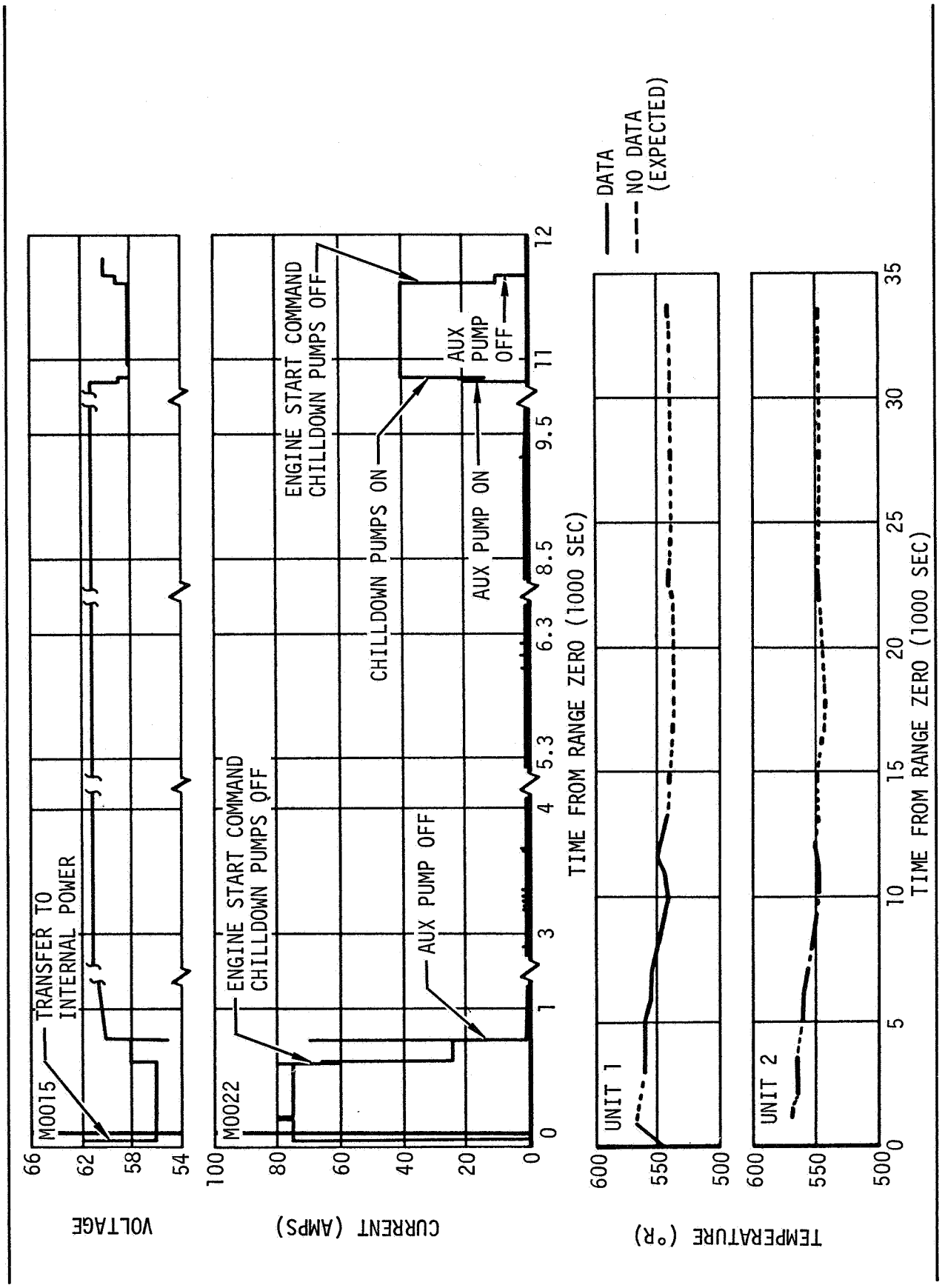

Figure 19-4. Aft Battery No. 2 Performance

SECTION 20

RANGE SAFETY SYSTEM

20. RANGE SAFETY SYSTEM

The range safety system was not required for propellant dispersion during the flight. All indications are that it operated properly and would have satisfactorily terminated an erratic flight.

20.1 Controllers

The controllers are designed to distribute command signals for engine cutoff, exploding bridgewire (EBW) charge and fire, and to distribute power to the range safety components. No abnormal conditions were evident.

20.2 Firing Unit Monitors

The following measurements indicate that the firing units were not charged throughout the flight.

M0030-411 Volt - F/U 1 EBW Range Safety

M0031-411 Volt - F/U 2 EBW Range Safety

20.3 Receivers Signal Strength

The signal strength monitors indicate that the range safety system was on at loss of data at RO +785 sec. Although safe commands were sent from Bermuda during the orbital insertic phase of flight, the range safety system did not respond since the flight vehicle was out of range of the range safety transmitter. This is due to the extended burn times of the S-II and S-IVB stages resulting from the S-II engines-out conditions. The safe command was sent from Bermuda on the first orbital pass and the following measurements verified that the range safety system was safed at RO +5,889 sec.

N0056-411 Misc - Sec R/S Rcvr 2 H/L Sig Str

N0057-411 Misc - Sec R/S Rcvr 1 L/L Sig Str

N0062-411 Misc - Sec R/S Rcvr 2 L/L Sig Str

SECTION 21

FLIGHT CONTROL

21. FLIGHT CONTROL

The thrust vector control system (TVCS) responded satisfactorily to instrument unit (IU) command signals providing pitch and yaw control during S-IVB first burn. The separation transient in the pitch plane was considerably larger than that experienced on previous flights. The maximum pitch engine deflection following S-II/S-IVB separation was approximately 6.7 deg which is near the maximum design engine deflection of 7 deg. This large separation transient was attributed to a large pitch attitude error (7.6 deg) existing at S-II/S-IVB separation. The TVCS responded normally during this interval and provided adequate control following S-II/S-IVB separation. Additional control system transients were experienced during guidance mode changes and first burn engine cutoff. These transients were expected and were well within the capabilities of the control system.

Inadequate hydraulic system supply pressure prior to restart prevented the J-2 engine from being centered at the time of Engine Start Command (ESC). The engine position at Engine Start Command was approximately 1.5 deg in pitch and -2.3 deg in yaw. Disturbances, experienced during the restart interval, resulted in pitch and yaw angular rates of -0.5 deg/sec and 0.45 deg/sec at the time of Engine Cutoff Command. The TVCS did not respond normally to control system commands during this interval because of insufficient hydraulic pressure.

The auxiliary attitude control system (AACS) provided satisfactory roll stabilization during powered flight and satisfactory pitch, yaw, and roll control during orbit. During S-II/S-IVB separation, a 0.3 sec pitch AACS firing (engine I_p) occurred commencing with the S-II/S-IVB Separation Command and terminating with the S-IVB Burn Mode ON Command. The design characteristics of the flight control computer (FCC) resulted in a temporary transfer of attitude control to the S-IVB coast mode following the S-II/S-IVB Separation Command which was terminated by the S-IVB Burn Mode ON Command. The noted temporary S-IVB coast mode and subsequent pitch AACS firing, although undesirable because of unnecessary use of AACS propellants, was not detrimental.

All orbital maneuvers were accomplished as planned, and vehicle attitude control was verified until approximately RO +22,040 sec, at which time the yaw angular rate diverged attaining a maximum angular rate of -7.5 deg/sec followed by an oscillatory vehicle motion. AACS propellant depletion in module 1 (oxidizer - RO +22,053 sec) and a LOX vent (RO +22,020 sec) accounted for the diverging angular rate at this time. Depletion of the AACS propellants and subsequent loss of attitude control at this time is much earlier than expected for a nominal mission; however, this is reasonable when considering the relatively large and unexpected demands on the control system, particularly due to high initial angular rates at first and second burn engine cutoff, large propellant masses remaining following second engine cutoff, and an early LV/SC separation. Although depletion was earlier than expected, attitude control was maintained beyond the time period necessary to meet mission requirements.

LOX and LH2 propellant sloshing during powered flight was comparable to that experienced on previous flights. A large LH2 slosh wave occurred at S-II/S-IVB separation due to the large control system transient experienced at that time, however, the LH2 sloshing was rapidly damped by the LH2 deflector and baffle. LOX and LH2 sloshing did not have an appreciable effect on the control system during first burn.

21.1 Attitude Control - Powered Flight

The TVCS and AACS responded normally to guidance commands during first burn and provided satisfactory control in the pitch and yaw axes and roll axis respectively.

21.1.1 Thrust Vector Control System Performance - First Burn

A large pitch attitude error (7.6 deg) existing at S-II/S-IVB separation resulted in a significant control system transient (6.7 deg engine deflection) following transfer of attitude control from the S-II to the S-IVB (RO +577.4 sec). The large attitude error at S-II/S-IVB separation is attributed primarily to S-II engine trim (engines 1 and 4) required to compensate for the loss of two control engines (engines 2 and 3). These engines are shown in conjunction with the vehicle coordinate system and polarities in figure 21-1. The separation transient was considerably larger than that experienced on any previous flight, however, the control system operation appeared normal during this interval. TVCS capability was demonstrated for the engine in a near hardover position at the time of initial J-2 engine thrust buildup. A sequence of events related to attitude control during powered flight is presented in table 20-1. Maximum values of significant control system parameters are presented in table 20-2.

Following guidance initiation (third phase iterative guidance mode [IGM]) at RO +582.5 sec, the guidance system commanded the S-IVB to pitch nose down at a limited rate of 1 deg/sec to correct for nonoptimum trajectory conditions existing at S-II/S-IVB separation. Discussion of the trajectory conditions existing at S-II/S-IVB separation are presented in sections 8 and 17. Approximately RO +645 sec, the guidance system commanded the S-IVB nose up to achieve the desired target flight path angle at S-IVB engine cutoff. This maneuver became rate limited at 1 deg/sec near the end of S-IVB burn. The S-IVB inertial attitude (θ_y) at first burn engine cutoff was -71 deg, approximately 50 deg above the local horizontal.

Pitch and yaw guidance commands and actual vehicle attitudes (platform gimbal angles) during first burn are shown in figure 21-2. The actual vehicle attitude correlates well with the commanded attitude indicating normal control system operation.

Pitch attitude error, angular rate, and actuator position during first burn are presented in figure 21-3. The corresponding parameters in the yaw plane are shown in figure 21-4. The maximum angular rates experienced during first burn occurred during the interval of S-II/S-IVB separation and initiation of the third phase IGM. The maximum pitch and yaw

angular rates were -3.5 deg/sec and 1 deg/sec, respectively. The separation/guidance initiation transient decayed by approximately 30 sec after activation of the S-IVB attitude control system. The steady-state pitch attitude error during the pitch-down maneuver at 1 deg/sec was 1.5 deg. Following the pitch up maneuver at R0 +645 sec, the pitch attitude error shifted from 1.5 deg to -0.3 deg and gradually increased to -1 deg at approximately R0 +705 sec. At this time the pitch angular rate attained the rate limit of 1 deg/sec and the pitch attitude error remained constant at approximately -1 deg until first burn engine cutoff. The yaw attitude error was approximately -0.9 deg throughout flight. The steady-state attitude errors experienced during powered flight resulted from a combination of constant vehicle angular rates and/or effective thrust vector misalignment. The effective thrust vector misalignment includes the thrust vector misalignment with respect to the J-2 engine centerline, actuator tolerances, engine/stage misalignment, and system electrical biases. The effective pitch and yaw thrust vector misalignments determined for first burn were 0.25 deg and -0.4 deg respectively. These values are comparable to those experienced on previous flights.

LVDC Guidance commands were frozen (chi freeze) approximately 0.9 sec prior to guidance cutoff. Guidance commands are frozen to minimize disturbances at S-IVB cutoff. Immediately following chi freeze, the pitch attitude error became positive and increased as the vehicle attitude deviated from the frozen guidance commands due to angular rates at the time of chi freeze. The pitch actuator retracted responding to attitude control signals to remove the angular rate and resulting attitude error until R0 +750.7 sec at which time the FCC was switched to coast mode enabling the pitch and yaw channels of the AACS. Both pitch and yaw actuators returned to null as expected following activation of coast mode control.

The attitude control system response during first burn was simulated to determine the nature of experienced disturbances and to verify satisfactory control system operation. Initial conditions and constant parameter values required in the simulation are presented in table 21-4. A comparison of actual and simulated pitch and yaw attitude errors, angular rates and actuator positions are shown in figures 21-3 and 21-4, respectively. The results indicate that the TVCS responded normally to attitude control signals.

21.1.2 Auxiliary Attitude Control System

The AACS operation for roll stabilization during S-IVB powered flight appeared normal. During S-II/S-IVB separation a 0.3 sec pitch AACS firing (engine I_p) occurred commencing with the S-II/S-IVB Separation Command and terminating with the S-IVB Burn Mode ON Command. The sequence of events and noted AACS engine firing immediately following S-II/S-IVB separation are shown in figure 21-6. The roll control system is activated by the S-IVB Burn Mode ON Command. This command also enables the TVCS for pitch and yaw control with the J-2 engine during powered flight. Investigation of design characteristics of the FCC

indicate that the attitude control system is temporarily in coast mode operation during the time interval between the S-II/S-IVB Separation Command and the S-IVB Burn Mode ON Command (0.3 sec). As a result, the appropriate initial conditions (attitude errors and angular rates) at S-II/S-IVB separation can induce pitch, yaw, or roll AACS firings during this interval. An initial pitch attitude error of 7.6 deg at S-II/S-IVB separation induced the noted AACS pitch firing. The S-IVB coast mode operation at S-II/S-IVB separation, although undesirable due to unnecessary use of AACS propellants, was not detrimental. Employment of alternate sequence TB4a would place the FCC in coast mode operation for 4.4 sec as opposed to 0.3 sec which was observed during the AS-502 mission. This may result in the unnecessary use of as much as 3 lbm of AACS propellants from one module.

Attitude control system firings during the separation interval have been experienced on one previous flight. During the AS-501 S-II/S-IVB separation, engine I_{IV} pulsed before the FCC was switched to S-IVB burn mode. This pulse is again attributed to attitude control signals commanding engine firings while the FCC was temporarily in coast mode operation.

Roll control during first burn appeared normal. The roll attitude error, angular rate, and attitude control system engine firings required for roll stablization are shown in figure 21-5. Significant roll disturbances were observed during the interval from S-II/S-IVB separation to guidance initiation and following a change in pitch guidance commands at approximately R0 +645 sec. The roll disturbances experienced at S-II/S-IVB separation and guidance initiation were induced by a combination of ullage rocket misalignment (Flight Test Data indicated that the effective ullage rocket misalignment was approximately 0.6 deg), J-2 engine exhaust gas swirl, and coupling resulting from the engine pitch and yaw deflections. The roll disturbance experienced during the change in pitch guidance commands was induced by the pitch transient which occurred at this time.

The frequency of AACS roll engine firings during powered flight was higher than that experienced on previous flights. This is attributed to a higher steady-state roll torque (approximately 40 ft-lbf in a clockwise direction), resulting from J-2 engine exhaust gas swirl. The highest steady-state roll torque experienced previously was 27 ft-lbf (AS-204). AACS engines I_{II} and III_{IV} fired to correct for disturbances resulting from the steady-state roll torque. Propellant requirements and impulse usage for roll control during first burn were approximately 2.8 lbm and 620 lbf-sec for module 1 and 2.6 lbm and 570 lbf-sec for module 2. The propellant usage was determined using impulse data derived from integration of engine thrust data and assuming an Isp of 230 sec. A summary of AACS impulse is presented in table 21-5. The difference in AACS impulse requirements between module 1 and module 2 is attributed primarily to the pitch firing from module 1 (40 lbf-sec) during the separation sequence and also to AACS engine performance variations. The AACS propellant usage for roll control during first burn was higher than expected. The expected propellant usage ranged

between 0.8 and 2.0 lbm. The higher than expected usage is attributed primarily to the roll induced disturbances resulting from the large separation transient and to the relatively high steady-state roll torque.

Investigation of rate gyro data indicated the presence of low amplitude oscillations (17 to 22 cps) similar to that experienced on AS-204. These oscillations were noted primarily on the pitch and roll rate gyros during S-II/S-IVB separation. The amplitude and duration of these oscillations on AS-502 were much less than that experienced on AS-204, and no apparent effect on the attitude control system was noted.

21.2 Attitude Control - Orbit

The AACS responded normally to guidance commands during orbit and provided satisfactory attitude control during orbital disturbances, limit cycle operation, and maneuvering periods. The attitude control system engine firing history during orbit is shown in figure 21-7.

Loss of normal attitude control was evidenced at RO +22,040 sec as the yaw angular rate diverged to approximately -7.5 deg/sec followed by an oscillatory vehicle motion. The large yaw angular rate is attributed to termination of AACS engine firings in module 1 due to AACS propellant depletion (see section 14) and a LOX vent initiated at RO +22,023 sec. AACS propellant depletion of module 2 occurred approximately RO +22,630 sec. Depletion of the AACS propellants occurred earlier than expected for a nominal mission but is reasonable when considering the relatively large and unexpected demands on the control system, particularly during the intervals following first burn engine cutoff and second burn engine cutoff. Attitude control was maintained beyond the required period as covered in section 7 of this report.

21.2.1 First Burn Engine Cutoff

Launch Vehicle Digital Computer (LVDC) guidance commands were frozen approximately 0.9 sec prior to S-IVB engine cutoff. This is normally referred to as chi freeze and is implemented to minimize disturbances at engine cutoff. The guidance commands remained frozen until approximately 15 sec after cutoff at which time guidance commands were issued to align the S-IVB with the local horizontal.

The S-IVB attitude at cutoff was approximately 50 deg above the local horizontal. Initial conditions at first burn engine cutoff are summarized as follows:

Pitch Attitude Error - 0.9 deg	Pitch Angular Rate - 0.7 deg/sec
Yaw Attitude Error - 0.8 deg	Yaw Angular Rate - 0.04 deg/sec
Roll Attitude Error - 0.35 deg	Roll Angular Rate - 0.07 deg/sec

These conditions resulted from guidance operation during S-II and S-IVB burn phases (see section 8). The AACS pitch and yaw channels were activated approximately 3.5 sec after engine cutoff. Following activation of the AACS, pitch engine I_p came full on for

approximately 43 sec to reduce the initial positive rate (0.7 deg/sec) and establish the maneuvering rate of -0.3 deg/sec to align the vehicle with the local horizontal. Prior to achieving the local horizontal, the vehicle was commanded to roll 180 deg (counterclockwise looking forward) to position I up. This command was initiated at R0 +837 sec with a maneuvering rate of -0.5 deg/sec.

The attitude control system operation appeared normal following engine cutoff. AACS propellant usage following engine cutoff was higher than expected and is attributed primarily to the initial pitch rate existing at engine cutoff. Actual and commanded vehicle attitudes following first burn engine cutoff are shown in figure 21-8. The corresponding pitch, yaw and roll control system response following engine cutoff are shown in figures 21-9, 21-10, and 21-11.

21.2.2 20 Deg Pitch Down Maneuver

A 20 deg pitch down maneuver was initiated at R0 +3,207 sec for the purpose of evaluating propellant slosh dynamics. Propellant behavior is presented in paragraph 21.4.4. AACS engine III_p fired to establish the required maneuvering rate of +0.3 deg/sec (nose down) which was maintained until the vehicle attitude approached the commanded attitude; engine I_p then fired to reduce the angular rate to the desired orbital pitch rate. The commanded and actual vehicle attitudes during this maneuver are shown in figure 21-12. The corresponding attitude errors, angular rates and AACS engine firings are shown in figures 21-13, 21-14, and 21-15 for pitch, yaw, and roll, respectively. The AACS response appeared normal during this maneuver.

Low amplitude oscillations at 19.5 to 22 cps (see figure 21-15) were observed on the pitch and roll rate gyro signals beginning at R0 +3,311 sec and terminating approximately 15 sec later. This time correlates with the time period of an AACS engine firing frequency of approximately 5 to 6 firings per sec required to terminate the pitch maneuver. The noted oscillations appeared to terminate as the AACS engine firing frequency was reduced to less than 4 firings per sec. Correlation of the noted oscillations and AACS firings indicates that the oscillations are related to the AACS engine firings. The oscillations appear to be similar to that experienced on previous flights and during other intervals of the AS-502 mission. The observed oscillations were not of sufficient magnitude to effect attitude control system operation.

21.2.3 20 Deg Pitch Up Maneuver

A 20 deg pitch up maneuver to the local horizontal was initiated at R0 +5,427 sec. (An evaluation of propellant sloshing during this maneuver is presented in paragraph 21.4.4) AACS pitch engine I_p fired to remove the existing orbital pitch rate and established a

maneuvering rate of -0.3 deg/sec (nose up). As the actual vehicle attitude approached the commanded attitude, AACS engine III_p fired to remove the maneuver rate and establish an orbital pitch rate (nose down). High frequency oscillations were also observed during this maneuver, particularly on the pitch and roll rate gyros. Again, these oscillations existed during intervals of high frequency AACS engine firings (approximately 5 firings per sec). The attitude control system operation appeared normal during the 20 deg pitch up maneuver.

The commanded and actual vehicle attitudes during this maneuver are shown in figure 21-16. The corresponding attitude errors, angular rates and AACS engine firings are presented in figures 21-17, 21-18, and 21-19 for pitch, yaw, and roll, respectively.

Impulse requirements to initiate and terminate the pitch up maneuver were much larger than for the pitch down maneuver. This is normal since the orbital pitch rate contributes to the maneuvering rate during the pitch down maneuver and opposes the maneuvering rate during the pitch up maneuver. As a result, additional impulse is required to complete the pitch up maneuver. APS impulse requirements to initiate and terminate each of the pitch maneuvers was as follows:

Pitch Down Maneuver

Initiation	1,060 lbf-sec (module 2)
Termination	1,130 lbf-sec (module 1)

Pitch Up Maneuver

Initiation	2,270 lbf-sec (module 1)
Termination	2,220 lbf-sec (module 2)

21.2.4 180 Deg Roll Maneuver (Counterclockwise Looking Forward) Position I Down

A 180 deg counterclockwise roll maneuver was initiated approximately R0 +5,787 sec to rotate position I down. AACS engine III_{IV} fired to establish the required maneuvering rate of -0.5 deg/sec and the attitude error limited at 3.5 deg as expected. The attitude error remained limited until approximately R0 +6,090 sec at which time the actual vehicle attitude approached the commanded attitude and AACS engines I_{IV} and III_{II} fired to reduce the maneuvering rate. The attitude control system response appeared normal during this maneuver. The commanded and actual vehicle attitudes are shown in figure 21-20. The corresponding attitude errors, angular rates, and AACS engine firings are presented in figures 21-21, 21-22, and 21-23 for pitch, yaw, and roll, respectively.

21.2.5 Restart Orientation Maneuver to Spacecraft Separation

21.2.5.1 Restart Orientation Maneuver

Restart preparations were initiated at R0 +11,287.6 sec (TB6). Shortly after this time,

the APS ullage engines were commanded ON to provide acceleration to settle the propellants for restart. During ullaging, a small nose down disturbance was observed with a resulting rate of approximately -0.01 deg/sec which corresponds to an effective ullage thrust unbalance of approximately 0.6 lbf. This effective unbalance was probably a combination of a small ullage engine misalignment and thrust unbalance.

A restart orientation maneuver was initiated at R0 +11,488 sec to position the vehicle in the desired attitude for restart. The commanded pitch attitude was approximately 10 deg below the local horizontal. Upon attainment of this attitude, the pitch guidance commands were frozen resulting in a pitch attitude of approximately 4 deg below the local horizontal at the time of Engine Start Command (R0 +11,614.7 sec). The yaw and roll guidance commands at initiation of the restart orientation maneuver were +0.9 deg (nose right) and 0 deg respectively. The restart orientation maneuver was performed satisfactorily and the attitude control system response appeared normal. The commanded and actual vehicle attitudes during this maneuver are shown in figure 21-24. The corresponding attitude errors, angular rates, and AACS engine firings are presented in figures 21-25, 21-26, and 21-27, for pitch, yaw, and roll, respectively.

21.2.5.2 Restart

The FCC was transferred from the S-IVB coast mode to the S-IVB burn mode at R0 +11,622.3 sec to provide pitch and yaw attitude control with the J-2 engine during second burn. Insufficient hydraulic system pressure (see section 22) prevented the main engine from providing satisfactory pitch and yaw control during this interval. The engine position at Engine Start Command was 1.5 deg in pitch and -2.3 deg in yaw. Disturbances experienced during the restart interval resulted in pitch and yaw angular rates of -0.5 deg/sec and 0.45 deg/sec at Engine Cutoff Command. These rates resulted from the inability of the TVCS to respond normally to control signals due to inadequate supply pressure. The LVDC issued TB7 after failure to restart. The AACS pitch and yaw channels were activated 3.5 sec after initiation of TB7. Roll control during the S-IVB burn mode on phase was minimal and appeared normal. Pitch and yaw attitude errors, angular rates, and actuator positions during the interval are shown in figures 21-28, and 21-29. The roll attitude error, angular rate, and AACS firing history are shown in figure 21-30.

21.2.5.3 Cutoff

Following engine cutoff and initiation of TB7, the pitch, yaw, and roll guidance commands (χ_y, χ_z, and χ_x) were set equal to the stable platform gimbal angles (θ_y, θ_z, and θ_x) and an inertial hold commanded until TB7 +20 sec, at which time the spacecraft separation orientation maneuver was initiated. Noticeable decreases in the pitch, yaw, and roll attitude errors were experienced at the time the guidance commands were set equal to the platform gimbal angles (figures 21-28, 21-29, and 21-30). This change in attitude error is normal.

Prior to engine cutoff, pitch and yaw angular rates increased to approximately -0.5 deg/sec (nose up) and 0.45 deg/sec (nose right). These angular rates at second burn engine cutoff are attributed to inadequate thrust vector control during the restart interval. Following second burn engine cutoff, the attitude error limits and command rate limits are changed to reconfigure for coast mode control (table 21-6). The attitude control system gains are changed (table 21-7) and the pitch and yaw channels of the AACS are activated approximately 3.5 sec after TB7. At this time, AACS engines III_p, I_{II}, and III_{II} came full on to reduce existing initial rates. Pitch and yaw attitude errors, angular rates and actuator positions following second burn engine cutoff are shown in figures 21-28 and 21-29. The roll attitude error, angular rate and AACS engine firing history during this interval is presented in figure 21-30.

21.2.5.4 Launch Vehicle/Spacecraft Separation Maneuver

The pitch and yaw attitude error limits and command rate limits were changed again at TB7 +15 sec (table 21-6) to provide increased maneuvering capability during the spacecraft separation orientation maneuver. Normal step changes in the pitch and yaw attitude error were observed at this time (see figures 21-28 and 21-29).

The launch vehicle/spacecraft (LV/SC) separation maneuver was initiated at TB7 +20 sec. The attitude commands during this maneuver were χ_y (pitch) +158 deg (nose up), χ_z (yaw) -5.5 deg (nose left), and χ_x (roll) 180 deg (clockwise looking forward). The maximum maneuvering rate in all three axes was $\pm$1.2 deg/sec. Commanded and actual vehicle attitudes during the LV/SC separation maneuver are shown in figure 21-31. The corresponding attitude errors angular rates, and AACS engine firings are presented in figures 21-25, 21-26, and 21-27.

21.2.5.5 LV/SC Separation

The LV/SC separation was programmed to occur at TB7 +180 sec; however, due to the restart failure, a ground command was issued to initiate LV/SC separation at R0 +11,666.1 sec (TB7 +35.8 sec). At this time the vehicle attitude was θ_y -128.9 deg (0.2 deg below the local horizontal), θ_z -2.6 deg, and θ_x 15.0 deg. Pitch, yaw, and roll angular velocities were 0.4, -0.9, and 1.3 deg/sec, respectively. The first detectable disturbances resulting from the LV/SC separation occurred at R0 +11,667.85 sec.

Telemetry data from both the CSM, and the S-IVB IU indicated unexpected disturbances were applied to both vehicles during the separation interval. The following information was obtained from available flight data:

a. The spacecraft pitch rate increased by 1.53 deg/sec (from 0.3 to 1.83 deg/sec in the nose up direction) (figure 21-32) over a period of 0.1 sec immediately following physical separation which occurs 1.7 sec after initiation of the LV/SC separation sequence.

b. The S-IVB pitch rate decreased by approximately 0.3 deg/sec (from 0.38 deg/sec to 0.1 deg/sec nose up) (figure 21-32), in a similar interval immediately following physical separation.

c. The S-IVB pitch rate abruptly increased by approximately 0.3 deg/sec (from 0.1 to 0.4 deg/sec nose up) at 1.0 sec following physical CSM separation.

d. Longitudinal acceleration impulses in the aft direction were detected by the IU accelerometer at the time of physical separation and 1.0 sec later.

e. Additional data relating to the noted disturbance were also evaluated and correlated with the above data.

The following phenomena were considered as possible causes of the observed disturbances:

a. A shift in position of a large mass, such as the LM, on the launch vehicle.

b. Unbalanced forces from Spacecraft Lunar Module Adapter (SLA) panel separation ordnance (MDF).

c. CSM RCS (Command service module reaction control system) thrust.

d. CSM RCS plume impingement on the launch vehicle.

e. S-IVB APS thrust.

f. Launch vehicle venting thrust.

g. A momentary interference or hangup between a SLA panel and the CSM.

h. Failure of one or more SLA panels to deploy properly.

Of the phenomena evaluated as possible sources of the moments required to cause the separation disturbances, the following were ruled out as primary causes of the disturbances.

a. A shift of a large mass on the launch vehicle such as the LM was ruled out because it could not contribute to the CSM disturbances, and the sequence of events connected with the launch vehicle behavior is not consistent with a shifting mass.

b. Unbalanced SLA ordnance (MDF) forces during separation could not account for the S-IVB disturbances 1 sec after physical separation.

c. RCS thrust moments were too small to account for CSM rate changes.

d. RCS plume impingement forces on the launch vehicle were too small to account for the observed rate changes, and the pulsing history did not correlate with the observed rate changes.

e. S-IVB APS moments were too small to account for the observed rapid rate changes and the thrusting history did not correlate with the observed rate changes.

f. Launch vehicle venting could not cause the CSM disturbances. Potential venting moments applied to the S-IVB (even with worst case asymmetry) are too small to account for the observed rate changes, and the actual venting history did not correlate with the observed rate changes.

From analysis of the data it was concluded that the primary cause of the disturbances noted previously can be explained by:

a. A momentary interference or hangup between the SLA panel on position I and the CSM during the 0.1 sec following actual separation, which induced the CSM disturbance which resulted in the angular rate change of 1.53 deg/sec.

b. The asymmetrical forces and moments applied to the S-IVB by the acceleration of the SLA panel on position III and the failure to accelerate the SLA panel on position I coupled with the CSM interference during deployment could account for the first observed S-IVB rate change of approximately 0.3 deg/sec.

c. Action of the ordnance at separation can account for the first noted longitidinal acceleration pulse.

d. Deceleration of the SLA panel on position III during panel arrrestment without a corresponding deceleration of the SLA panel on position I accounts for the observed S-IVB rate change of approximately 0.3 deg/sec.

e. The second observed longitudinal acceleration pulse can be accounted for by deceleration of SLA panels on positions II, III, and IV.

From evaluation of the observed data it was concluded that a momentary interference or hangup occurred between the launch vehicle and spacecraft preventing normal deployment of the SLA panel on position I. The momentary interference or hangup temporarily affected the motion of both the launch vehicle and spacecraft, however, the spacecraft separated successfully and the launch vehicle and spacecraft each recovered from the momentary attitude deviation.

21.2.6 Loss of Attitude Control

Orbital attitude control was verified until approximately RO +22,040 sec (Hawaii fourth revolution) at which time the yaw angular rate started to diverge attaining an angular rate of -7.5 deg/sec followed by an oscillatory motion. Two factors were conductive to producing the initial yaw attitude divergence:

a. A LOX vent initiated at RO +22,023 sec

b. AACS propellant depletion (module 1) at RO +22,053 sec (section 14).

Since the LOX vent is oriented approximately 14.5 deg off of position IV toward positon III, venting disturbances were experienced primarily in the yaw plane. AACS engine III_{IV} fired

to correct for the resulting yaw disturbance but introduced a negative roll angular rate and attitude error. Since yaw/roll signal mixing is employed in the FCC during orbital control, engine III_{IV} terminated yaw correction firings (RO +22,227 sec) when the roll angular rate and attitude error increased to a sufficient magnitude to require AACS engine III_{II} to fire for roll attitude correction. Approximately RO +22,112 sec, the yaw platform gimbal angle reached its physical limit (61.3 deg) causing loss of the platform inertial reference. AACS propellants in module 2 were depleted at approximately RO +22,630 sec.

AACS propellant depletion and subsequent loss of attitude control, although earlier than expected for a normal mission, was reasonable when considering control system requirements due to initial angular rates existing at first and second burn engine cutoff, large propellant mass remaining following second burn engine cutoff, and an early spacecraft separation. Commanded and actual vehicle attitudes following loss of attitude control are shown in figure 21-33. The vehicle dynamics and control system response during this interval are shown in figures 21-34 through 21-39.

21.3 Propellant Sloshing During S-IVB Powered Flight

Propellant utilization (PU) system sensor fine mass data was utilized to determine LH2 and LOX slosh frequencies and amplitudes during S-IVB first burn. LH2 and LOX slosh frequencies and amplitudes are shown in figures 21-40 and 21-41, respectively. The LH2 probe sensor data indicated a large slosh wave occurring at S-II/S-IVB separation which has been attributed to the large control system transient experienced at that time. This slosh wave appeared to be rapidly damped by the LH2 deflector. Increased LH2 slosh activity was also indicated at approximately RO +645 sec which coincides with the time of the vehicle pitch maneuver. This sloshing was rapidly damped. LOX slosh amplitudes and frequencies were comparable to those experienced on previous flights. Propellant sloshing did not significantly affect control operation during first burn.

21.4 Propellant Behavior During Orbit

The dynamic behavior of the LH2 and LOX aboard the S-IVB has been evaluated using data from instrumentation inside the tanks, flight AACS impulse usage, attitude error data and angular rate data. The results of this evaluation for the time period between J-2 first burn engine cutoff and restart attempt are presented in this section of the flight evaluation report.

The LH2 behavior was evaluated using data obtained from the internal sensors, but LOX sloshing could not be evaluated during orbit using the tank sensor data. The LOX sensors are mounted internally to the hollow instrumentation probe. For periods of low g coast, capillary action in this probe preclude an accurate evaluation of LOX behavior in the tank.

LOX sloshing behavior has been determined during the orbital maneuver from AACS firings, attitude error data and angular rate data.

21.4.1 Tank Instrumentation

The locations of the sensors in the LH2 tank from which data on propellant behavior has been obtained are shown in figure 21-42. Three types of sensors are used. These are: (1) wall temperature patches, (2) instrumentation probe temperature sensors, and (3) liquid/gas differentiators located on both the tank wall and instrumentation probe. Data from these sensors have been converted into charts (figures 21-43 through 21-46) presenting a continuous display of liquid or vapor condition.

The criteria used to discriminate between liquid and vapor conditions for the various temperature sensors are as follows:

a. Liquid Condition

   Temperature at or below saturation temperature.

b. Vapor Condition

   Temperature above saturation temperature.

c. Transition Condition

   Temperature changing from or to a steady-state condition indicating liquid.

The liquid/gas differentiators give a simple high or low capacitance reading, which indicates vapor or liquid, respectively.

During boost and S-IVB powered flight phase of operation, the various sensors performed satisfactorily. Both the wall temperature patch and instrumentation probe data show a progressive transition from liquid to vapor conditions as the propellant surface level dropped during S-IVB burn. Figure 21-43 shows a comparison between the surface level indicated by the PU probe data and the transition time for the various sensors. This comparison demonstrates that these sensors were operational and performing satisfactorily during high g vehicle operation.

During the orbital coast period data from the wall temperature patches appear to give an accurate indication of the presence of liquid propellant at the sensor. It has been found relatively easy to differentiate between liquid and vapor conditions. When the patches were immersed in the LH2, the data indicated liquid conditions. When the patches were surrounded by vapor, the data indicated a temperature even higher than that of the vapor. This is due to the low heat transfer between the patch and vapor compared with the relatively high thermal conductivity between the patch and the tank wall. Hence, the wall patch temperature data was considered to be giving an accurate differentiation between liquid and vapor conditions.

The instrumentation probe sensors are considered less reliable than the wall temperature patches during orbit coast. After orbital injection and activation of the CVS, the ullage temperature decreases to the liquid hydrogen temperature. Therefore, the probe temperature sensor data cannot be used to differentiate between liquid and vapor conditions. The liquid/gas differentiators have shown a tendancy to be sensitive to condensation and globules on the sensor. Therefore, one of these sensors could be indicating liquid propellant due to small amounts of liquid trapped on the sensor, even though the sensor is well above the liquid level. However, the converse of this does not apply. When these liquid/gas differentiators indicate vapor, the data is considered reliable, since it does not appear to be probable that a submerged sensor would be surrounded by a single large vapor bubble.

21.4.2 LH2 Slosh Behavior at First Burn Engine Cutoff

A baffle and deflector are installed in the LH2 tank of all S-IVB/V vehicles to:

a. Minimize the slosh amplitude at J-2 engine cutoff

b. Increase slosh damping during orbital coast

c. Minimize the amount of liquid which travels into the forward dome area of the LH2 tank.

Slosh amplification during the J-2 engine thrust termination and ullage thrusting could have caused high amplitude sloshing early in the coast period. To minimize the amount of this slosh amplification, the ullage thrusting sequence for the S-IVB was carefully timed. The theoretical maximum possible slosh wave amplification with this thrust sequencing has been determined to be 39. With the slosh wave indicated in the LH2 tank at the time of engine cutoff (less than 1 in.) the theoretical maximum slosh wave due to amplification would have been less than 40 in.

Immediately after engine cutoff, a number of events occurred (rocket ignition and cutoff, CVS activation, pitch down maneuver, and 180 deg roll maneuver) which could have had a significant effect upon propellant behavior. Because of the number and close proximity of these events, it is very difficult to establish a cause/effect relationship for these events and slosh amplification with the attendant propellant behavior.

Within 20 sec after S-IVB first burn engine cutoff, all of the wall sensors in the pitch plane indicated liquid propellant. The same type of response was noted in the yaw plane approximately 20 sec later. The data (figures 21-4 and 21-44) showed that these sensors continued to indicate liquid for quite a time (greater than 7000 sec), unlike data from S-IVB-203 and S-IVB-501 which indicated the liquid motion transients had subsided within 300 sec after engine cutoff. The instrumentation probe data indicate that liquid propellant inundated the probe sensors between 100 and 140 sec after engine cutoff. Unlike S-IVB-501 and S-IVB-203 data, sensors on the instrumentation probe above the level of the deflector (N0023, C0068, N0022, C0039 and N0021) indicated liquid at this time. Hence, the propellant

dynamics at engine cutoff appeared to have been more severe than that indicated on the previous flights. This increased slosh activity could have been the result of a combination of slosh amplification at engine cutoff and attitude control system engine firings. Attitude control system firings were required to remove a high initial pitch rate and maneuver the vehicle to the local horizontal.

21.4.3 LH2 Slosh Behavior During Orbital Coast

The wall sensor data during the orbital coast period (except for that from C2020 and C2021) continuously indicated liquid conditions until approximately R0 +8,200 sec. Starting at this time, a number of sensors in both the pitch and yaw planes indicated a transition from liquid to vapor conditions. The nature of the change in readings for these sensors does not indicate either sloshing or bubble formation (as was postulated in the S-IVB-501 flight evaluation). The topmost sensor in both planes (sta 605) continued to indicate liquid even though sensors lower on the probe indicated vapor.

One possible explanation for the response of these sensors is that after engine cutoff (where large propellant motion was indicated) a substantial amount of propellant became trapped between the tank wall and the bottom of the deflector due to surface tension effects. However, the amount of trapped liquid was greater than could be sustained indefinitely by these surface tension forces and liquid moved down the wall toward the main bulk of LH2 until the volume of this trapped liquid reached a steady-state condition. In the steady-state condition, the sensors above the surface level and below the trapped liquid would become exposed to vapor. This explanation would correlate the wall temperature sensor data to propellant behavior.

If the propellant configuration postulated above is correct, then the propellant would appear to have been settled prior to TB6 and the surface level as determined from wall sensor data would have been between sta 530 and 545.

Data obtained from temperature sensors on the instrumentation probe during orbital coast indicates liquid conditions at all sensors below sta 660. This was not unexpected, since on previous flights data from these sensors did not indicate transition from liquid to vapor conditions during orbital coast periods. This can be attributed to the sensor peculiarities noted in paragraph 21.4.1. Therefore, this data does not necessarily discredit the surface level indicated by the wall patch sensors.

21.4.4 LOX and LH2 Slosh Behavior During Pitch Maneuvers

Two 20 deg pitch maneuvers were performed during the orbital coast in order to assess propellant slosh dynamics resulting from vehicle maneuvers. Propellant slosh behavior resulting from these maneuvers have been determined through comparison of AACS flight data with predictions.

The flight impulse data for both maneuvers were compared to the predicted (dynamic model) impulse requirements and rigid body impulse requirements. The predicted impulse requirements

were obtained from an analog simulation of the S-IVB AACS and included the effects of propellant sloshing. The rigid body impulse requirements were analytically determined and represent the amount of impulse required to start or stop the desired maneuver rate excluding the effects of propellant sloshing. The AACS impulse usage requirements from modules 1 and 2 for the 20 deg pitch down and pitch up maneuvers are given in figures 21-47 and 21-48. The 20 deg pitch down maneuver was initiated by engine firings from module 2 (III_p) and terminated by engine firings from module 1 (I_p). For the 20 deg pitch up maneuver engine firings from module 1 (I_p) initiates the maneuver and firings from module 2 (III_p) terminates the maneuver.

Comparison of actual AACS impulse and calculated rigid body impulse requirements (figures 21-47 and 21-48) during the noted maneuvers indicate the existence of relatively large LOX slosh disturbances following initiation and termination of each maneuver. The actual impulse data, however, did not indicate sustained slosh activity. This was evidenced by the lack of periodic impulse usage following each maneuver. This is also evidenced in the pitch attitude error and angular rate data (figures 21-13 and 21-17) which do not indicate any significant interaction between propellant sloshing and the AACS as would be expected if sustained slosh activity had occurred. As discussed in paragraph 21.4.2, LH2 wall temperature sensor data indicate a wet condition before and during both pitch maneuvers. Therefore, LH2 sloshing during this time cannot be determined.

An investigation of actual impulse usage during these maneuvers is being continued in order to evaluate and improve, if necessary, the existing slosh model used in control system simulations.

21.4.5 LH2 Slosh Behavior During Restart Preparations

Prior to the engine restart attempt, a number of events occurred (ullage rocket ignition, LH2 repressurization, and APS firing to realign the vehicle) which would effect propellant slosh dynamics. The LH2 tank sensor data and the sequence of events related to restart preparation are given in figures 21-45 and 21-46.

After the application of ullage thrust, a number of sensors on the instrumentation probe indicated a transition from liquid to vapor conditions (figure 21-45). The sensors indicating this trend were both temperature sensors (C0068 and C0069) and liquid/gas differentiators (N0022, N0023, and N0024). This transition would correspond either to the expulsion of entrained vapor from the liquid bulk or to the draining of liquid attached to the probe and sensors. Since these sensors are reliable when indicating vapor conditions, data from these sensors give a sound indication that the liquid surface level at Engine Start Command was below sta 550. Within 20 sec after Engine Start Command, sensors N0025 and N0026 also showed a transition from liquid to vapor conditions. Hence, the surface level at that time was below sta 524. This would indicate that the propellant was settled with very little entrained vapor in the bulk at this time.

The wall temperature patch data (figure 21-46) for this same time period (around Engine Start Command) indicated liquid conditions existed as high as sta 605. The discrepancy in the propellant surface level as indicated by instrumentation probe data and wall sensor data must be explained in order to positively establish the propellant configuration at Engine Start Command. The wall temperature patch data in both planes indicated that the sensors became wet during the restart preparation period. The order in which these sensors became wet indicated propellant motion downward along the tank wall. This could be attributed to increased acceleration during ullaging causing the unsettling of propellant which had become trapped between the LH2 deflector and the tank wall during orbit. Hence, wall temperature sensors above the propellant surface level could have been indicating liquid propellant. Therefore, the wall sensor data does not discredit the validity of the surface level postulated from instrumentation probe data prior to engine restart.

Approximately 100 sec after the initiation of repressurization and the attitude realignment maneuver, instrumentation probe sensors high in the tank (N0021 and C0039) indicated the presence of liquid. This phenomenon appears to be quite similar to that experienced on S-IVB-501. Although it is not possible to determine the amount of propellant that reached the forward dome area, the duration of the liquid indication by the sensors would tend to indicate that this response resulted from a small amount of splash.

The repressurization difficulties encountered on S-IVB-501 were not encountered on S-IVB-502. This appears to be the result of the revised restart preparation sequence which employs ullaging prior to repressurization. This sequence appears to have contributed to better propellant control during repressurization and the restart orientation maneuver than on AS-501.

On the S-IVB-501 the realignment maneuver and repressurization occurred immediately after ullage engine ignition. On S-IVB-502 these two events took place about 200 sec after the initiation of ullage thrust. As a result of the duration of this thrust period, a substantial amount of entrained vapor appears to have been purged from the liquid; hence, lowering the surface level as indicated by probe data. At the time of the attitude realignment maneuver this surface was much nearer the level of the slosh baffle, thereby increasing baffle effectiveness for propellant control during restart preparations.

21.4.6 Conclusions

LH2 wall temperature sensor data indicated that LH2 sloshing following first burn engine cutoff was greater than that experienced on S-IVB-501. Propellant sloshing following engine cutoff has been attributed to a combination of slosh amplification and the pitch down maneuver. LH2 slosh amplitudes prior to engine cutoff were greater on S-IVB-502 than S-IVB-501 (0.7 in. compared to 9.1 in.). As a result, the LH2 slosh wave resulting from slosh amplification could be higher on S-IVB-502, depending on the phase angle of the propellant surface. In addition, control system activity following S-IVB-502 engine cutoff was much more severe than that experienced on S-IVB-501, due primarily to a high initial

pitch rate at engine cutoff (approximately 1 deg/sec). The larger LH2 sloshing experienced after engine cutoff on S-IVB-502 is, therefore, attributed to the increased control system activity in conjunction with the initial slosh conditions.

Propellant sloshing activity during the two 20 deg pitch maneuvers remained within acceptable levels. Although there was a relatively large initial LOX slosh wave excited by each maneuver, sustained sloshing was not evident.

During the first portion of the orbital coast, LH2 wall temperature sensor data indicated liquid conditions in both pitch and yaw as high as S-IVB sta 605. Late in the orbital coast, a number of these sensors indicated a transition from liquid to vapor. Because of the manner of this transition, it was postulated that LH2 was trapped in the corner between the wall and the bottom of the deflector and that the propellant surface level was below sta 545 prior to TB6.

The S-IVB-502 data during TB6 indicates conditions in the LH2 tank more conducive to a successful restart than that of S-IVB-501. Instrumentation probe data indicated a surface level in the vicinity of that which would be expected under high acceleration. This would place the LH2 surface level near the baffle, thus increasing the effectiveness of the slosh baffle for propellant control during restart preparations. Since S-IVB-501 restart was successfully completed, the more favorable conditions in the LH2 tank on S-IVB-502 should have enhanced a successful restart.

For additional information concerning propellant behavior refer to paragraph 26.4.

TABLE 21-1
SEQUENCE OF EVENTS RELATED TO ATTITUDE CONTROL
DURING POWERED FLIGHT

EVENT	TIME FROM RANGE ZERO (sec)
Guidance reference release	-16.84
S-II/S-IVB separation	577.12
Engine Start Command	577.27
S-IVB Burn Mode ON	577.40
Guidance initiation	582.50
End of artificial tau guidance	593.90
Chi freeze	746.10
S-IVB first burn engine cutoff (TB5)	747.03
S-IVB Burn Mode OFF	750.76
Time base 6	11,287.73
Ullage engines ON	11,287.89
Engine Start Command	11,614.67
S-IVB Burn Mode ON	11,622.29
Guidance initiation	11,627.73
S-IVB second burn engine cutoff (TB7)	11,630.32
S-IVB Burn Mode OFF	11,633.78
LV/SC separation	11,667.80

TABLE 21-2
MAXIMUM VALUES OF CRITICAL FLIGHT CONTROL PARAMETERS

	UNITS	SEPARATION, GUIDANCE INITIATION AND ARTIFICIAL TAU	CHI TILDE	S-IVB C/O
Pitch attitude error	deg	7.6	-1.0	-0.9
Yaw attitude error	deg	-2.4	-0.9	-0.8
Roll attitude error	deg	-1.0	0.3	0.4
Pitch rate	deg/sec	-3.5	1.1	1.0
Yaw rate	deg/sec	1.0	-0.2	-0.1
Roll rate	deg/sec	-0.6	0.5	0.0
Pitch actuator position	deg	6.7	0.2	0.2
Yaw actuator position	deg	-1.3	-0.5	-0.6

TABLE 21-3
ORBITAL MANEUVERS

COMMANDED MANEUVER	INITIATION TIME (sec)	COMMANDED ATTITUDE PRIOR TO INITIATION OF MANEUVER (deg)			COMMANDED ATTITUDE AT TERMINATION OF MANEUVER (deg)		
		X_y	X_z	X_x	X_y	X_z	X_x
Maneuver to local horizontal following S-IVB cutoff	TB5 +15 (754)	-70.17	.67	0	-131*	+0.05	-47
Roll 180° CCW position I up	TB5 +90 (837)	-99	+0.1	0	-145.94	0.11	180
Pitch 20° nose down	TB5 +2460 (3,207)	74.6	-0.9	+180	51.1*	-0.9	+180
Pitch 20° nose up	TB5 +4680 (5,427)	-91	0.8	0	-74*	1.0	0
Roll 180° CCW position I down	TB5 +5040 (5,787)	-95	0.8	180	-115.6	0.59	0.0
Restart orientation maneuver	TB6 +0.0 (11,288)	-115.6	+0.75	0.0	-128.0	+1.5	0.0
S-IVB second burn engine cutoff	TB7 +0.0 (11,630)	-128.0	-1.51	0	-129.99(x)	4.57(x)	0.47(x)
Spacecraft separation maneuver	TB7 +20 (11,650)	-129.99	4.57	0.47	28.02(x)	-0.85(x)	178.73(x)
Post separation maneuver	TB7 +600 (12,230)	ND	ND	ND	ND	ND	ND
Maneuver to local horizontal (ground command)	TB7 +7200 (16,201)	ND	ND	ND	ND	ND	ND

ND - No data X_y - Pitch X_z - Yaw X_x - Roll (x) - Chi freeze

* - Establish orbital pitch rate

TABLE 21-4

Simulation Initial Conditions and Constant Parameter Values

Initial pitch attitude error - positive nose up	7.21 deg
Initial yaw attitude error - positive nose right	0 deg
Initial roll attitude error - positive clockwise looking forward	-0.2 deg
Initial pitch angular velocity - positive nose up	0.2 deg/sec
Initial yaw angular velocity - positive nose right	-0.1 deg/sec
Initial roll angular velocity - positive clockwise looking forward	0 deg/sec
Initial pitch engine position	0 deg
Initial yaw engine position	0 deg
Initial slosh parameters	0 deg
Initial pitch angle of attack - positive nose up	0 deg
Initial yaw angle of attack - positive nose right	0 deg
Effective pitch thrust vector misalignment	-0.25 deg
Effective yaw thrust vector misalignment	0.418 deg
Steady-state roll torque - positive clockwise looking forward	40 ft-lbf

FIGURE 21-5
APS IMPULSE SUMMARY

	UNITS	MODULE 1	MODULE 2	APS ENGINE					
				I_{IV}	I_p	I_{II}	III_{II}	III_p	III_{IV}
Powered Flight:									
Separation, guidance initiation, and ullage RKT jettison; R0 +577 to R0 +600 sec.	lb-sec	365.5	318.4	216.7	38.3	110.5	207.7	0	110.7
	N-sec	1,625.8	1,416.3	963.9	170.4	491.5	923.9	0	492.4
Limit cycle operation for remainder of first burn; R0 +600 to R0 +747 sec.	lb-sec	253.9	251.6	23.9	0	229.9	22.6	0	229.0
	N-sec	1,129.4	1,119.2	106.3	0	1,022.6	100.5	0	1,018.6
Initial recovery after first burn and alignment to local horizontal including pitch and 180° roll maneuver plus settling usage; CVS ON; *R0 +750 to R0 +1,230 sec.	lb-sec	11,726.0	4,914.4	1,449.0	9,144.5	1,132.7	1,363.4	2,333.8	1,217.3
	N-sec	52,159.8	21,860.3	6,445.5	40,676.7	5,038.5	6,064.7	10,381.2	5,414.8
Pitch down 20° below local horizontal; CVS is ON; R0 +3,210 to R0 +3,475 sec.	lb-sec	1,334.3	1,206.3	111.5	1,222.7	0	30.5	1,062.8	113.0
	N-sec	5,935.2	5,365.9	496.0	5,438.8	0	135.7	4,727.6	502.6
Pitch up maneuver to align with local horizontal; CVS is ON; R0 +5,426 to R0 +5,520 sec.	lb-sec	2,099.6	2,313.4	6.7	2,092.8	0	0	2,283.6	29.8
	N-sec	9,339.5	10,290.5	29.8	9,309.2	0	0	10,158.0	132.6
Roll 180° to fin position I down; CVS is ON; R0 +5,786 to R0 +6,110 sec.	lb-sec	560.7	199.8	146.1	354.3	60.3	52.0	0	147.8
	N-sec	2,494.1	888.8	649.9	1,576.0	268.2	231.3	0	657.4
Pitch and yaw maneuver for restart orientation; R0 +11,485 to R0 +11,600 sec.	lb-sec	1,413.3	2,147.4	97.7	1,266.0	49.6	29.6	2,022.1	95.8
	N-sec	6,286.7	9,552.1	434.6	5,631.4	220.6	131.7	8,994.7	426.1
Recovery following second burn attempt, maneuver to spacecraft separation attitude, spacecraft separation and settling; 10 sec LOX tank venting, 120 sec LH2 tank venting; R0 +11,630 to R0 +11,970 sec.	lb-sec	14,930.1	27,318.6	1,615.9	8,320.5	4,993.7	5,034.0	20,819.8	1,464.8
	N-sec	66,412.4	121,519.1	7,187.9	37,011.4	22,213.1	22,392.3	92,611.0	6,515.8

*Does not include R0 +965 to R0 +1,010 sec because data is not available.

TABLE 21-6
ATTITUDE CONSTANTS

TIME OF CHANGE	LADDER RATE LIMIT (-deg/minor loop)			LADDER MAGNITUDE LIMIT (-deg)			ATTITUDE COMMAND RATE LIMIT (-deg/sec)		
	YAW	ROLL	PITCH	YAW	ROLL	PITCH	YAW	ROLL	PITCH
0 (Initial Values)	0.48	0.48	0.48	15.3	15.3	15.3	1.0	1.0	1.0
TB4 +0	0.48	0.48	0.48	15.3	15.3	15.3	1.0	1.0	1.0
TB5 +0	0.48	0.48	0.48	2.5	15.3	2.5	0.4	0.6	0.4
TB5 +100	0.24	0.24	0.24	2.5	15.3	2.5	0.4	0.6	0.4
TB6 +0*	0.48	0.48	0.48	2.5	15.3	2.5	0.4	0.6	0.4
TB6 +327	0.48	0.48	0.48	15.3	15.3	15.3	1.0	1.0	1.0
TB7 +0	0.48	0.48	0.48	2.5	15.3	2.5	0.4	0.6	0.4
TB7 +15	0.24	0.24	0.24	7.0	7.0	7.0	1.44	1.44	1.44
TB7 +600	0.24	0.24	0.24	2.5	15.3	2.5	0.4	0.6	0.4

*This change should be made when switchover from orbit to boost navigation occurs.

TABLE 21-7
ATTITUDE CONTROL SYSTEM GAINS

TIME (sec)	PITCH AND YAW		ROLL	
	$A_0 \left(\frac{deg}{deg}\right)$	$A_1 \left(\frac{deg}{deg/sec}\right)$	$A_0 \left(\frac{deg}{deg}\right)$	$A_1 \left(\frac{deg}{deg/sec}\right)$
TB4 +1.1	0.809	0.97	1.0	5.0
TB5 +3.7	1.0	5.0	1.0	5.0
TB6 +334.6	0.809	0.97	1.0	5.0
TB6 +597*	0.809	0.698	1.0	5.0
TB7 +3.7	1.0	5.0	1.0	5.0

*Did not occur due to restart failure

NOTES:

1. ALL SIGNAL ARROWS INDICATE POSITIVE VEHICLE MOVEMENTS.
2. VEHICLE PITCHES OVER POSITION 1.
3. ENGINE ACTUATOR LAYOUTS SHOWN AS VIEWED FROM AFT END OF VEHICLE.
4. DIRECTIONS AND POLARITIES SHOWN ARE TYPICAL FOR ALL STAGES.
5. +β INDICATES ENGINE DEFLECTION REQUIRED TO CORRECT FOR POSITIVE VEHICLE MOVEMENT.
   CG = CENTER OF GRAVITY
   F = NOZZLES ON
   EXT = ACTUATOR EXTENDED
   RET = ACTUATOR RETRACTED
   β = THRUST VECTOR ANGULAR DEFLECTION
6. THE ACTION SHOWN IN THE POLARITY TABLES FOR THE ACTUATORS AND NOZZLES WILL TURN THE VEHICLE IN A DIRECTION OPPOSITE TO THE INDICATED ERROR SIGNAL.

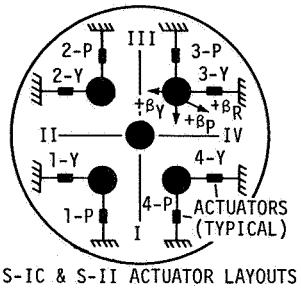

S-IC & S-II ACTUATOR LAYOUTS

S-IVB ACTUATOR AND NOZZLE LAYOUT

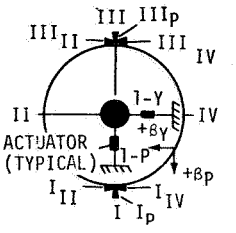

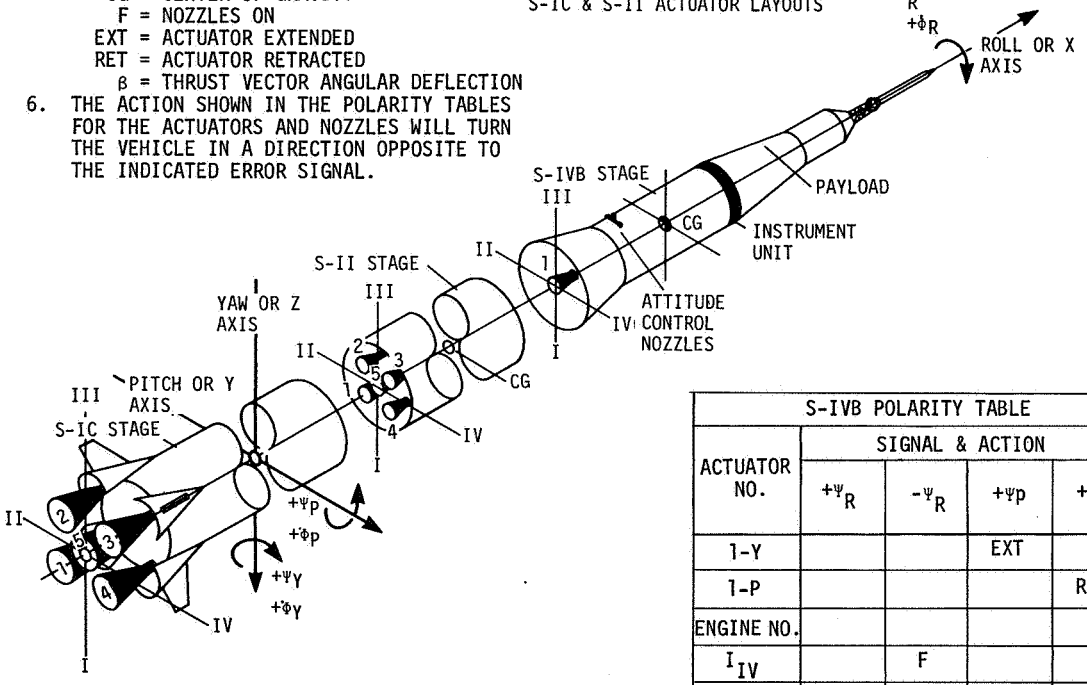

S-IC & S-II POLARITY TABLE			
ACTUATOR NO.	ACTUATOR MOVEMENT		
	$+\dot{\Phi}_R$ / $+\Psi_R$	$+\dot{\Phi}_Y$ / $+\Psi_Y$	$+\dot{\Phi}_P$ / $+\Psi_P$
1-Y	RET	RET	
1-P	EXT		RET
2-Y	EXT	RET	
2-P	RET		EXT
3-Y	RET	EXT	
3-P	EXT		EXT
4-Y	EXT	EXT	
4-P	RET		RET

S-IVB POLARITY TABLE				
ACTUATOR NO.	SIGNAL & ACTION			
	$+\Psi_R$	$-\Psi_R$	$+\Psi_P$	$+\Psi_P$
1-Y			EXT	
1-P				RET
ENGINE NO.				
I_{IV}		F		
Ip				
I_{II}	F			
III_{II}		F		
IIIp				
III_{IV}	F			
CONDITIONS DURING COAST				
	$+\Psi_R$	$-\Psi_R$	$+\Psi_Y$	$-\Psi_Y$	$+\Psi_P$	$-\Psi_P$
I_{IV}		F		F		
Ip					F	
I_{II}	F		F			
III_{II}		F	F			
IIIp						F
III_{IV}	F			F		

Figure 21-1. Saturn V Coordinate System and Polarities

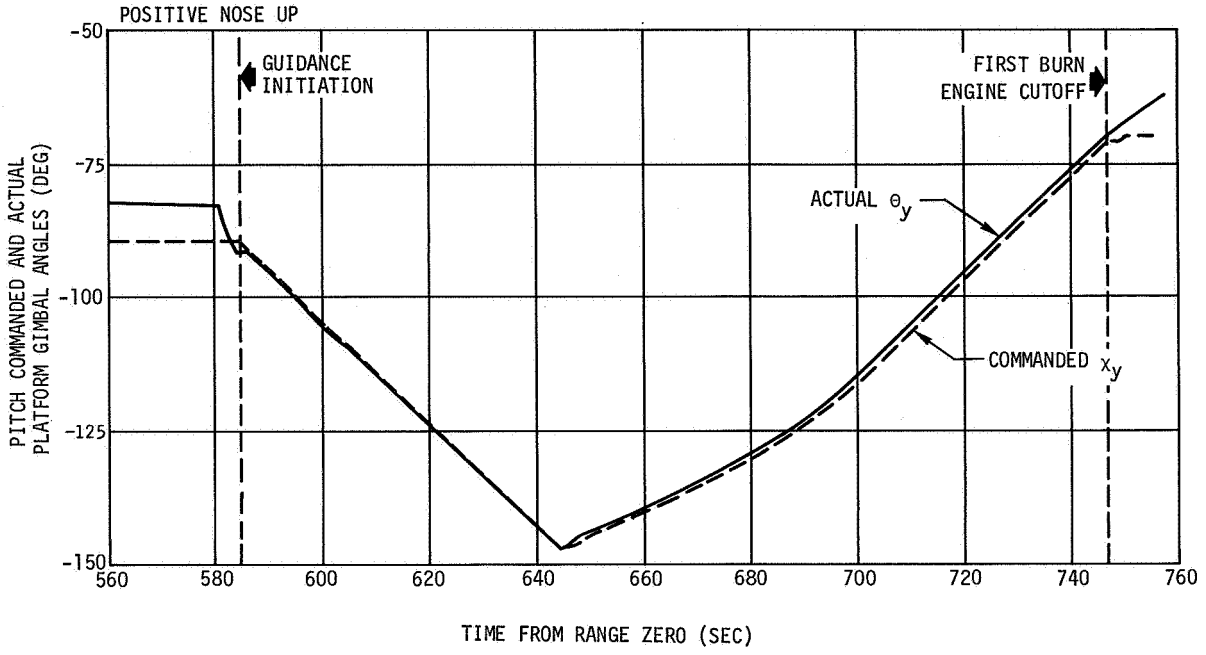

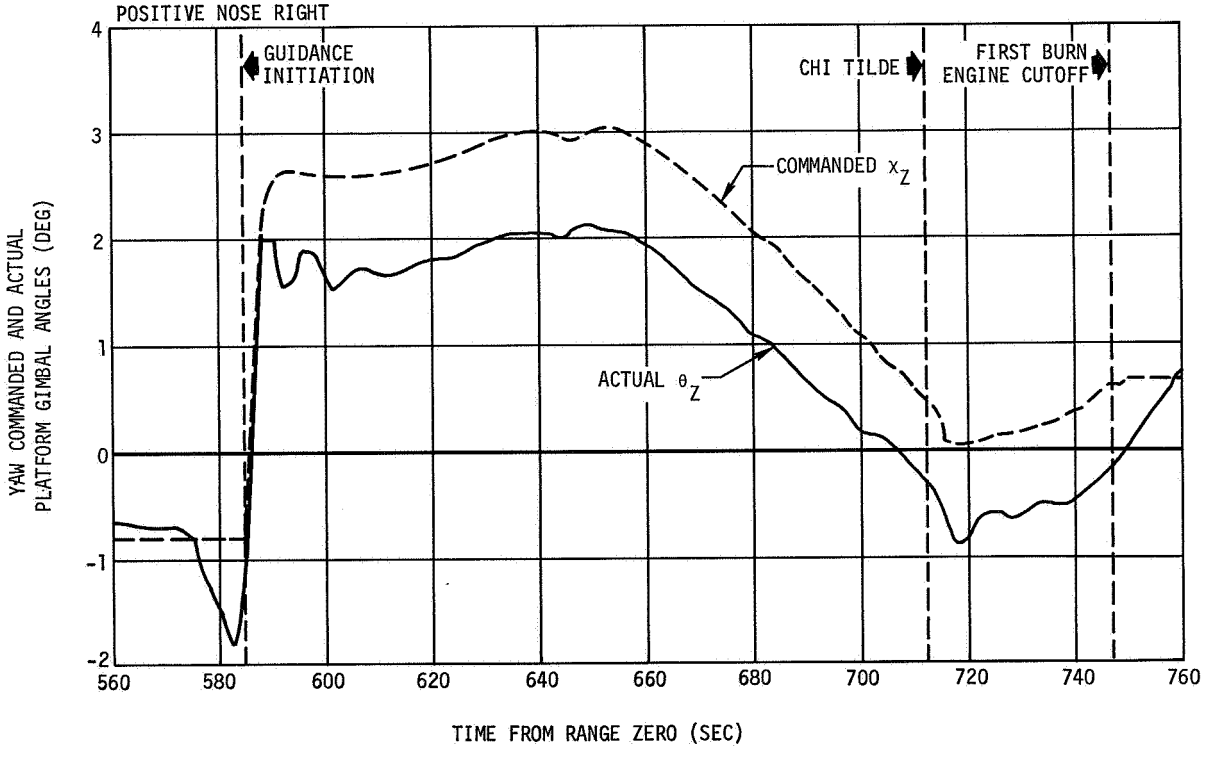

Figure 21-2. Pitch and Yaw Commanded and Actual Vehicle Attitude - S-IVB Powered Flight

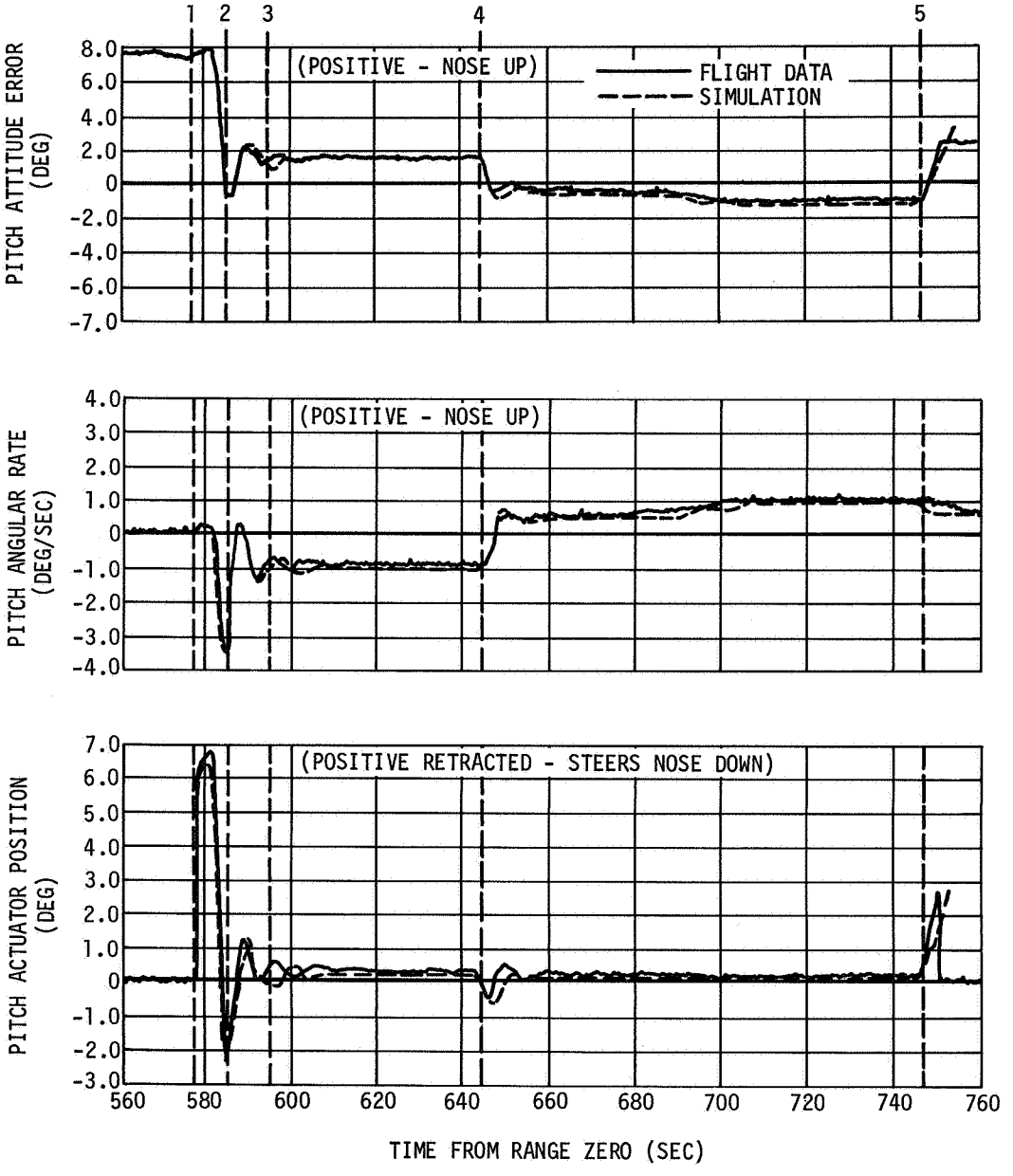

1. ENGINE START COMMAND
2. GUIDANCE INITIATION
3. END ARTIFICIAL TAU GUIDANCE MODE
4. PITCH COMMAND TO NOSE UP ATTITUDE
5. CHI FREEZE AND ENGINE CUTOFF

Figure 21-3. Pitch Attitude Control - First Burn

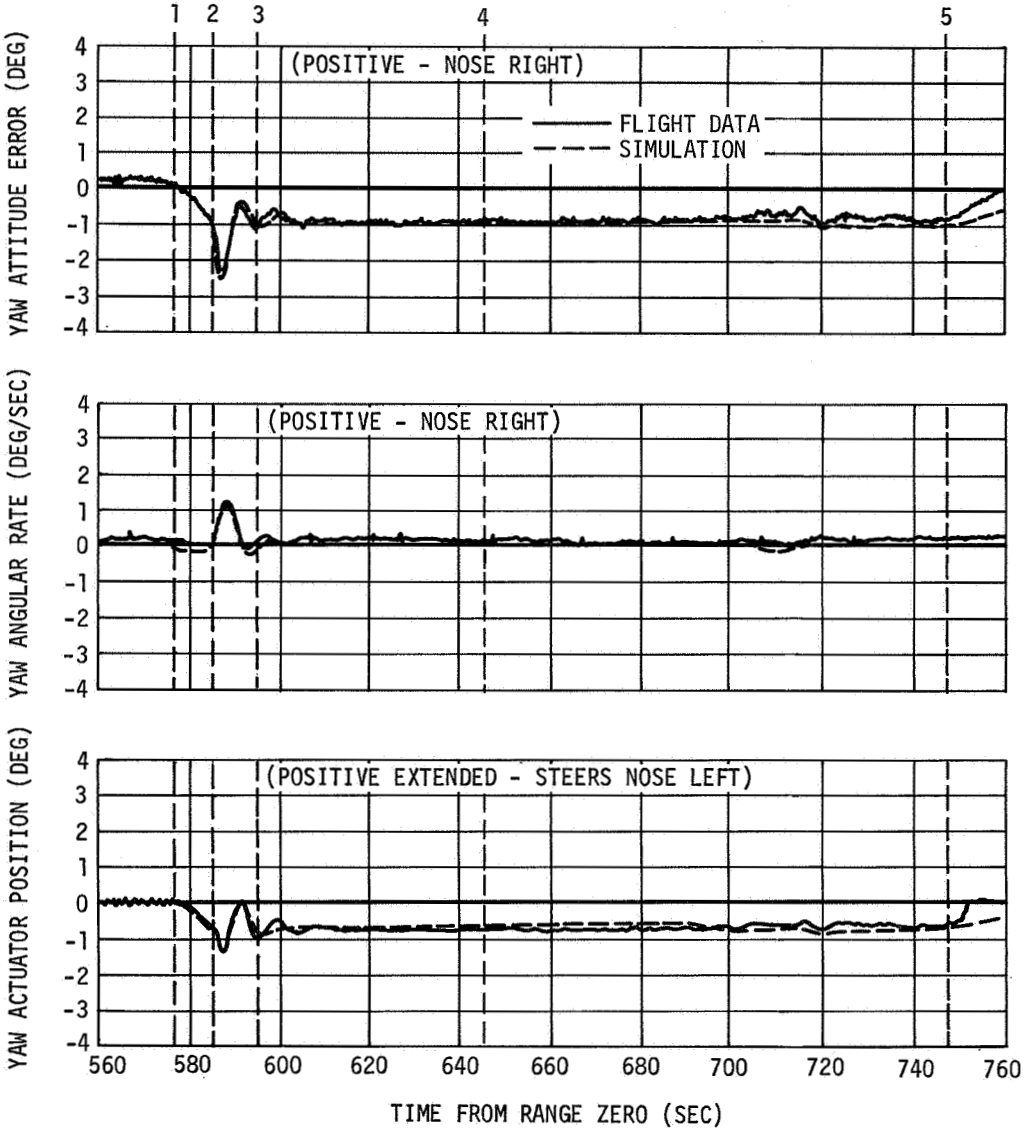

1. ENGINE START COMMAND
2. GUIDANCE INITIATION
3. END ARTIFICIAL TAU GUIDANCE MODE
4. PITCH COMMAND TO NOSE UP ATTITUDE
5. CHI FREEZE AND ENGINE CUTOFF

Figure 21-4. Yaw Attitude Control - First Burn

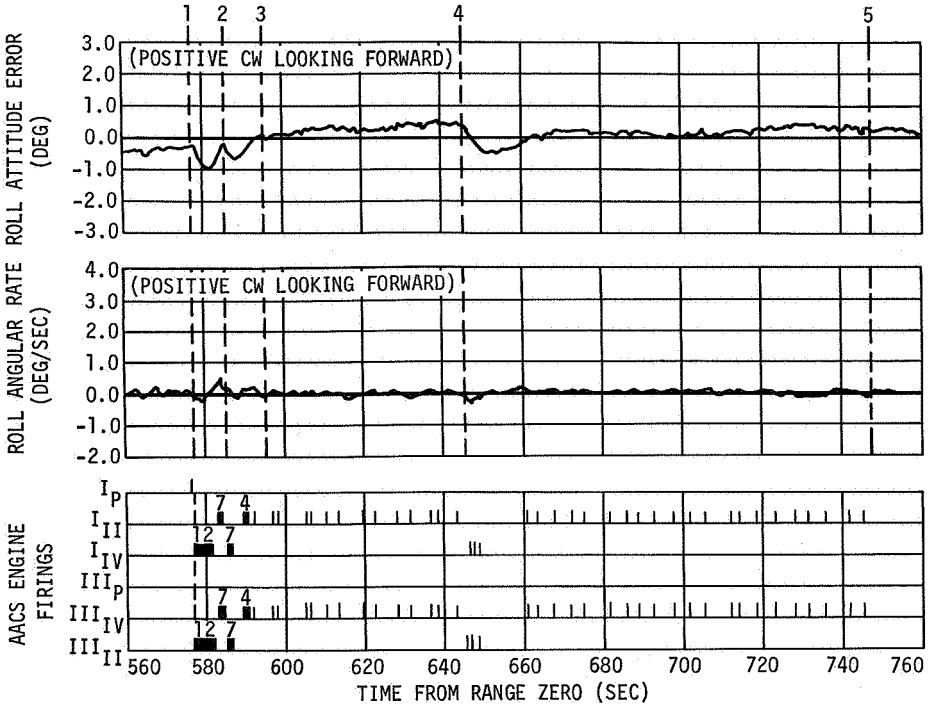

1. ENGINE START COMMAND
2. GUIDANCE INITIATION
3. END ARTIFICIAL TAU GUIDANCE MODE
4. PITCH COMMAND TO NOSE UP ATTITUDE
5. CHI FREEZE AND ENGINE CUTOFF

Figure 21-5. Roll Attitude Control - First Burn

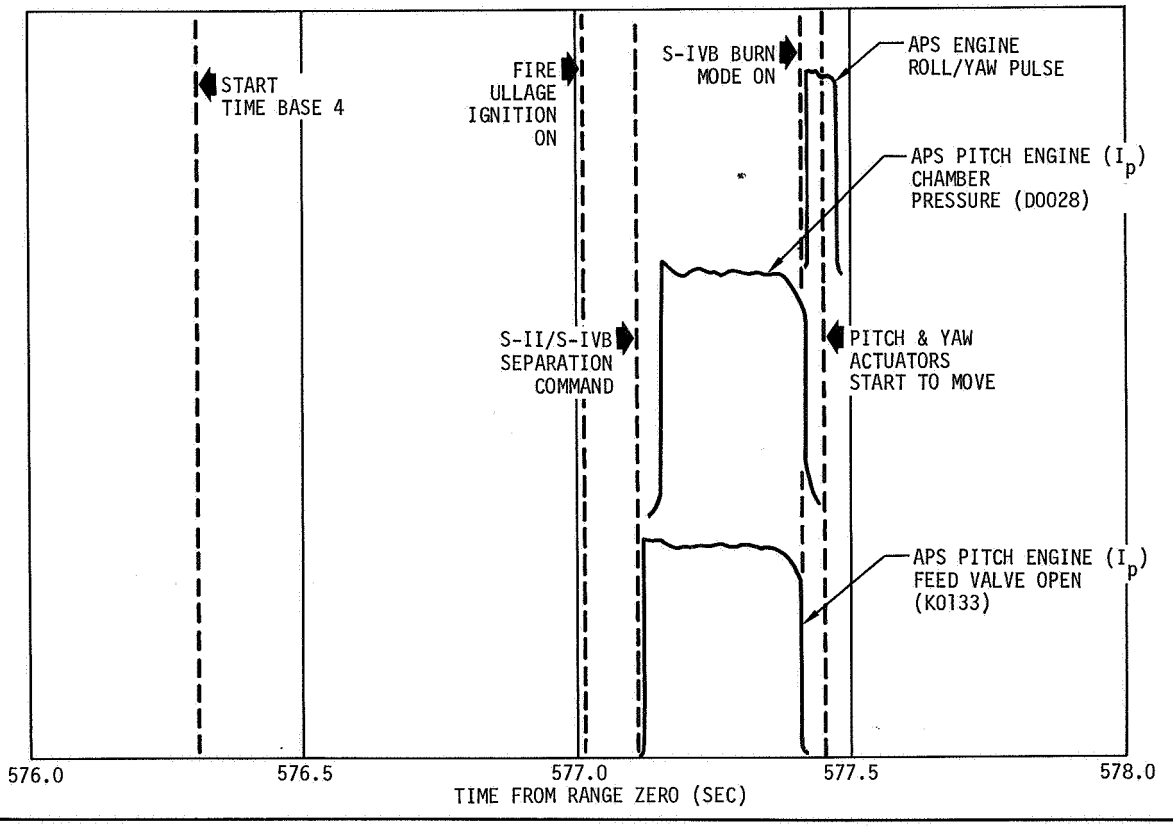

Figure 21-6. Pitch AACS Engine Firing and Related Sequence of Events - S-II/S-IVB Separation

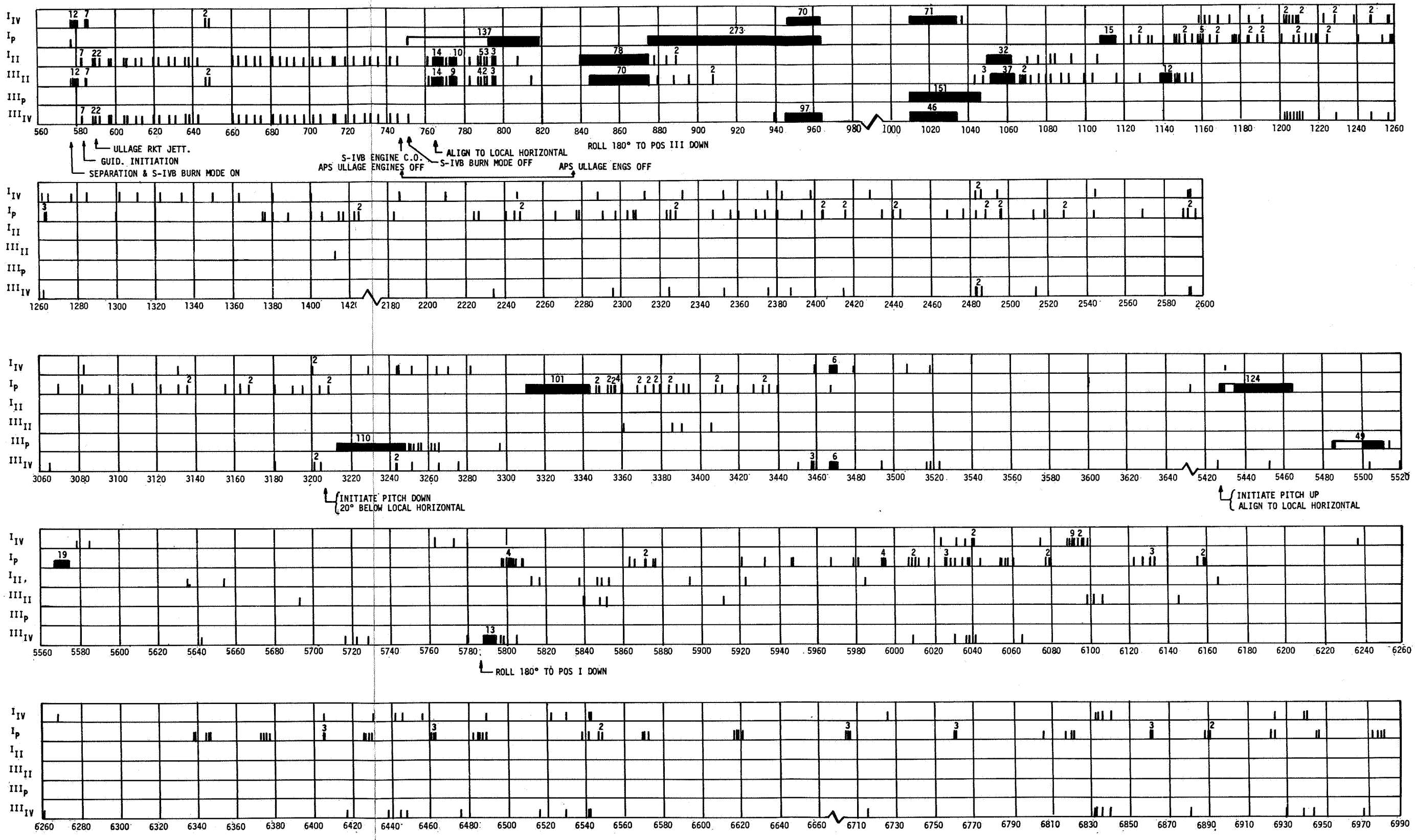

Figure 21-7. Auxiliary Attitude Control System Firing History (Sheet 1 of 3)

FOLDOUT FRAME 1

FOLDOUT FRAME

FOLDOUT FRAME 2

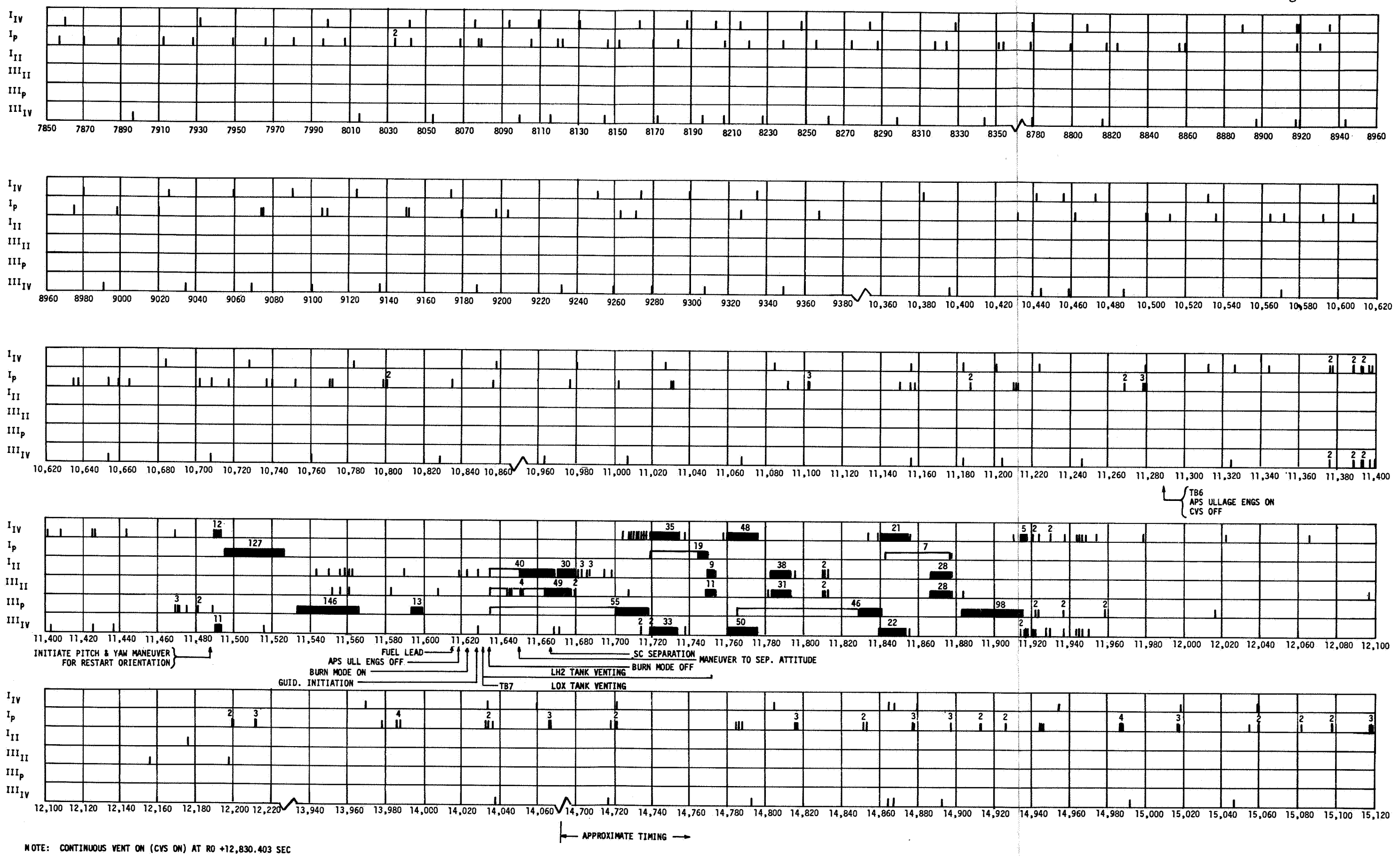

NOTE: CONTINUOUS VENT ON (CVS ON) AT RO +12,830.403 SEC

* INDICATES * INDIVIDUAL PULSES

INDICATES CONTINUOUS FIRING

Figure 21-7. Auxiliary Attitude Control System Firing History (Sheet 2 of 3)

FOLDOUT FRAME 1

FOLDOUT FRAME 2

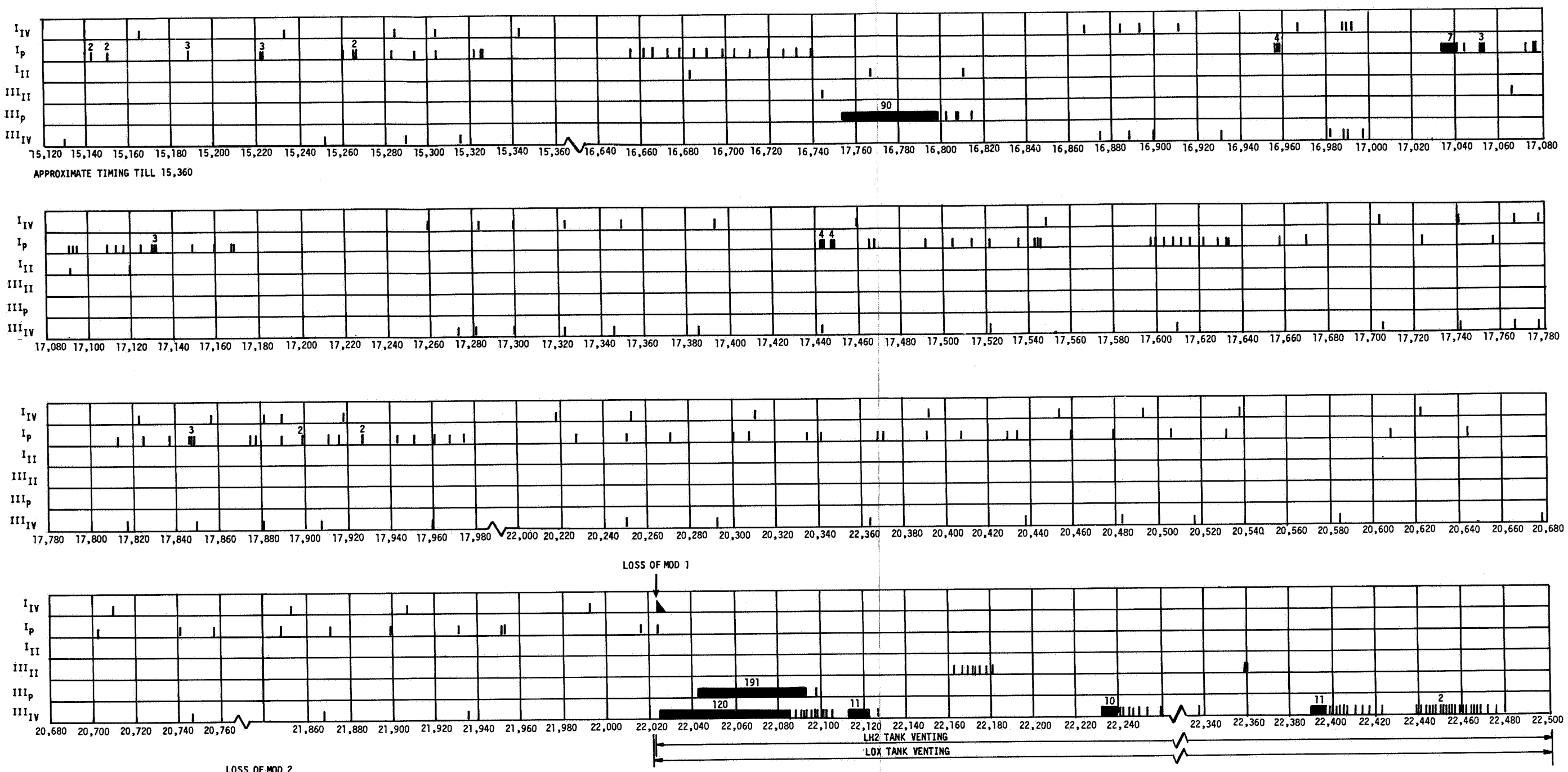

Figure 21-7. Auxiliary Attitude Control System Firing History (Sheet 3 of 3)

FOLDOUT FRAME 1

FOLDOUT FRAME 2

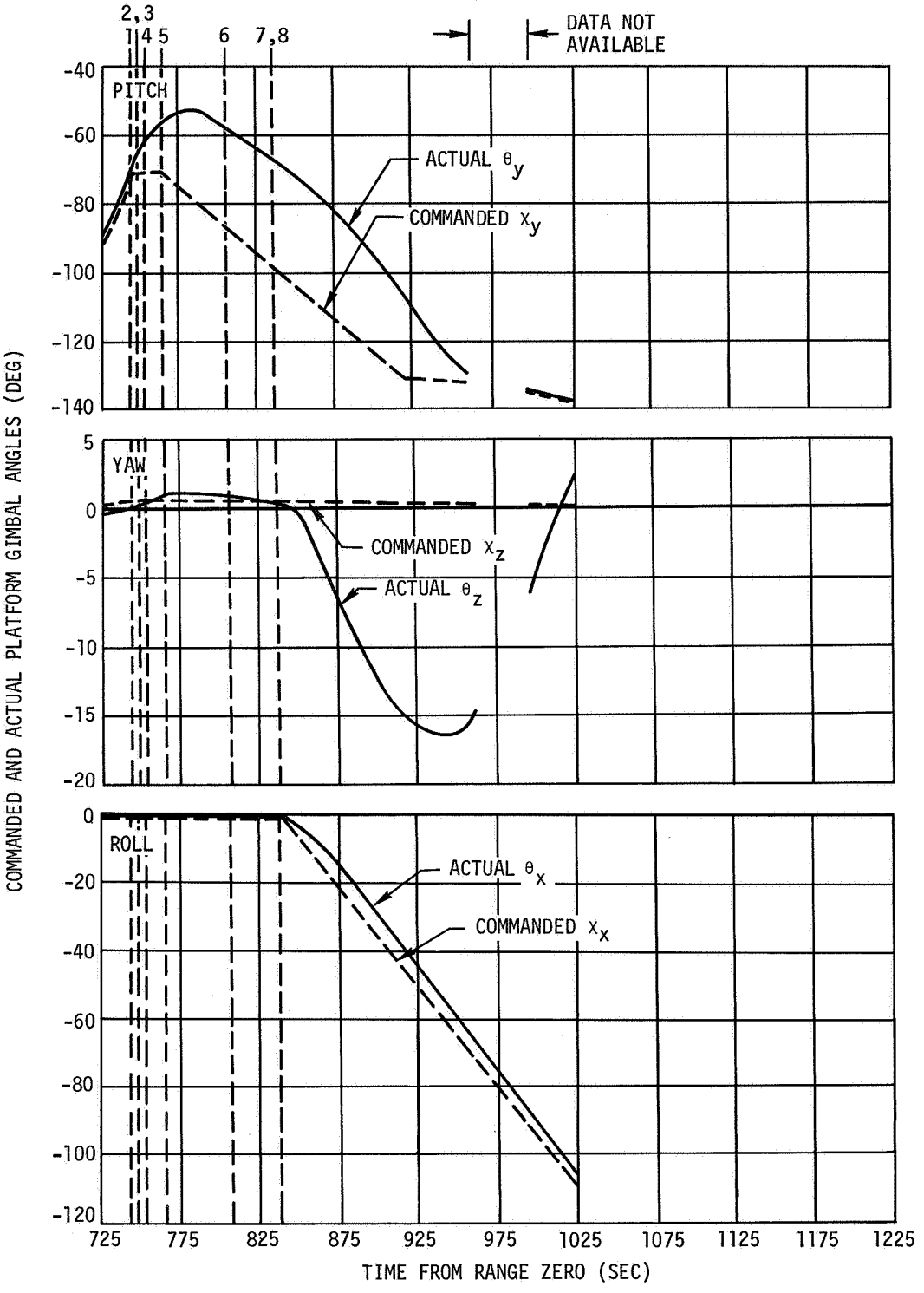

1. COMMAND FREEZE
2. FIRST S-IVB ENGINE CUTOFF
3. ULLAGE ENGINES ON
4. APS ACTIVATE
5. COMMAND LOCAL HORIZONTAL
6. LH2 CVS ON
7. ULLAGE ENGINES OFF
8. COMMAND -180° ROLL POSITION III TOWARD EARTH

Figure 21-8. Commanded and Actual Pitch, Yaw and Roll Attitudes following First Burn

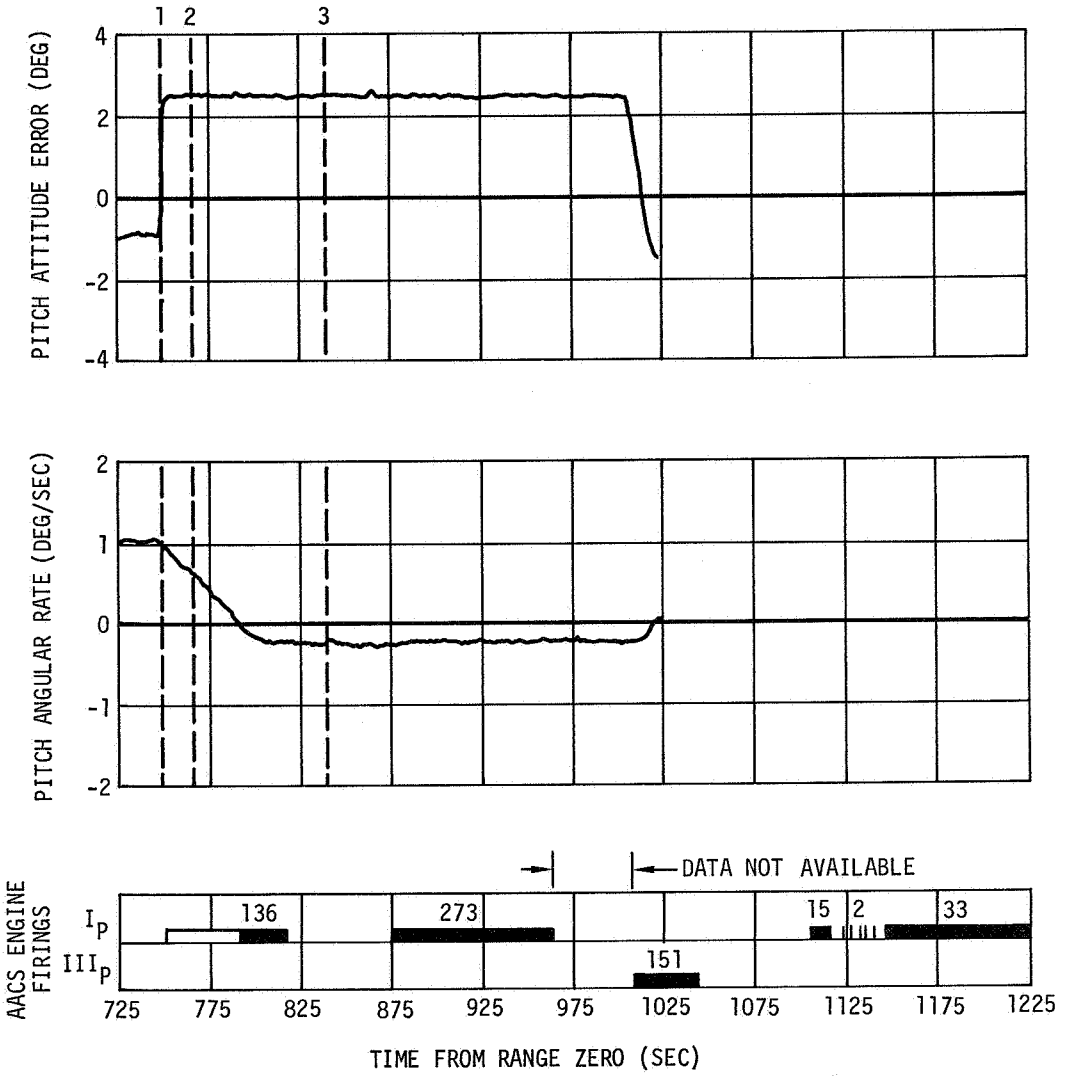

DENOTES FULL ON PULSE

DENOTES MULTIPLE PULSES WITH TOTAL NUMBER OF PULSES ABOVE

1. FIRST BURN ENGINE CUTOFF
2. PITCH DOWN TO LOCAL HORIZONTAL
3. ROLL CCW 180 DEG TO ALIGN POSITION III TOWARD EARTH

Figure 21-9. Pitch Attitude Control following Engine Cutoff

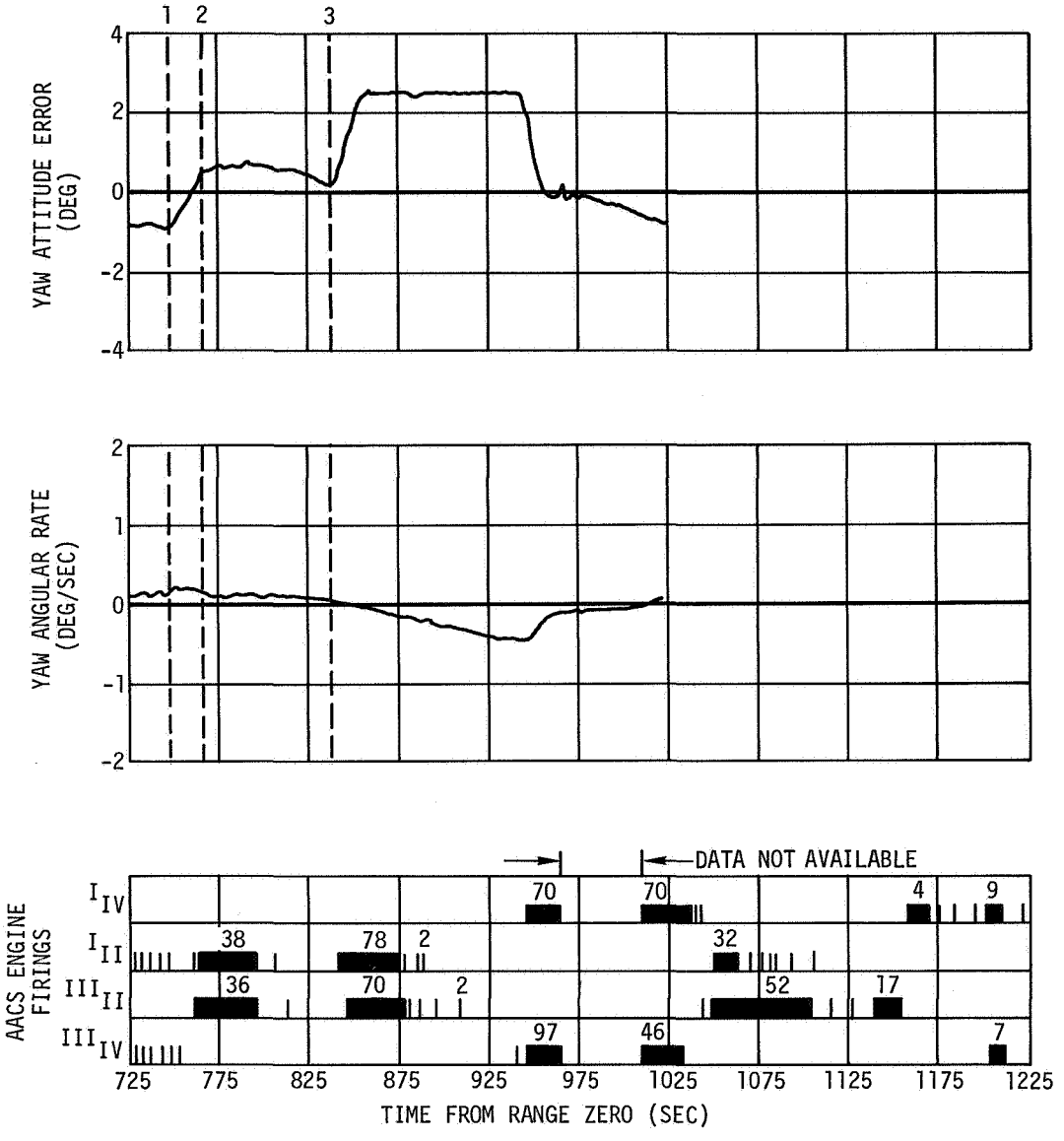

DENOTES FULL ON PULSE

DENOTES MULTIPLE PULSES WITH TOTAL NUMBER OF PULSES ABOVE

1. FIRST BURN ENGINE CUTOFF
2. PITCH DOWN TO LOCAL HORIZONTAL
3. ROLL CCW 180 DEG TO ALIGN POSITION III TOWARD EARTH

Figure 21-10. Yaw Attitude Control following Engine Cutoff

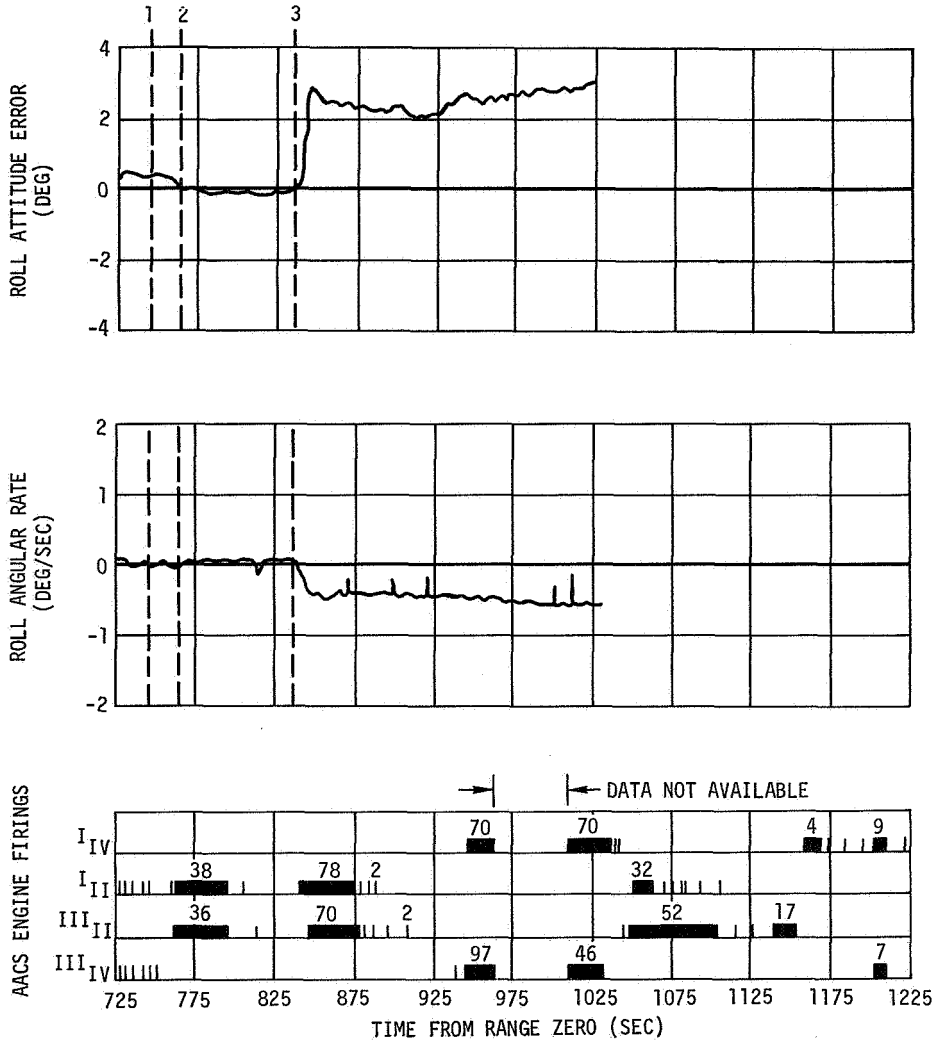

DENOTES FULL ON PULSE

DENOTES MULTIPLE PULSES WITH TOTAL NUMBER OF PULSES ABOVE

1. FIRST BURN ENGINE CUTOFF
2. PITCH DOWN TO LOCAL HORIZONTAL
3. ROLL CCW 180 DEG TO ALIGN POSITION III TOWARD EARTH

Figure 21-11. Roll Attitude Control Following Engine Cutoff

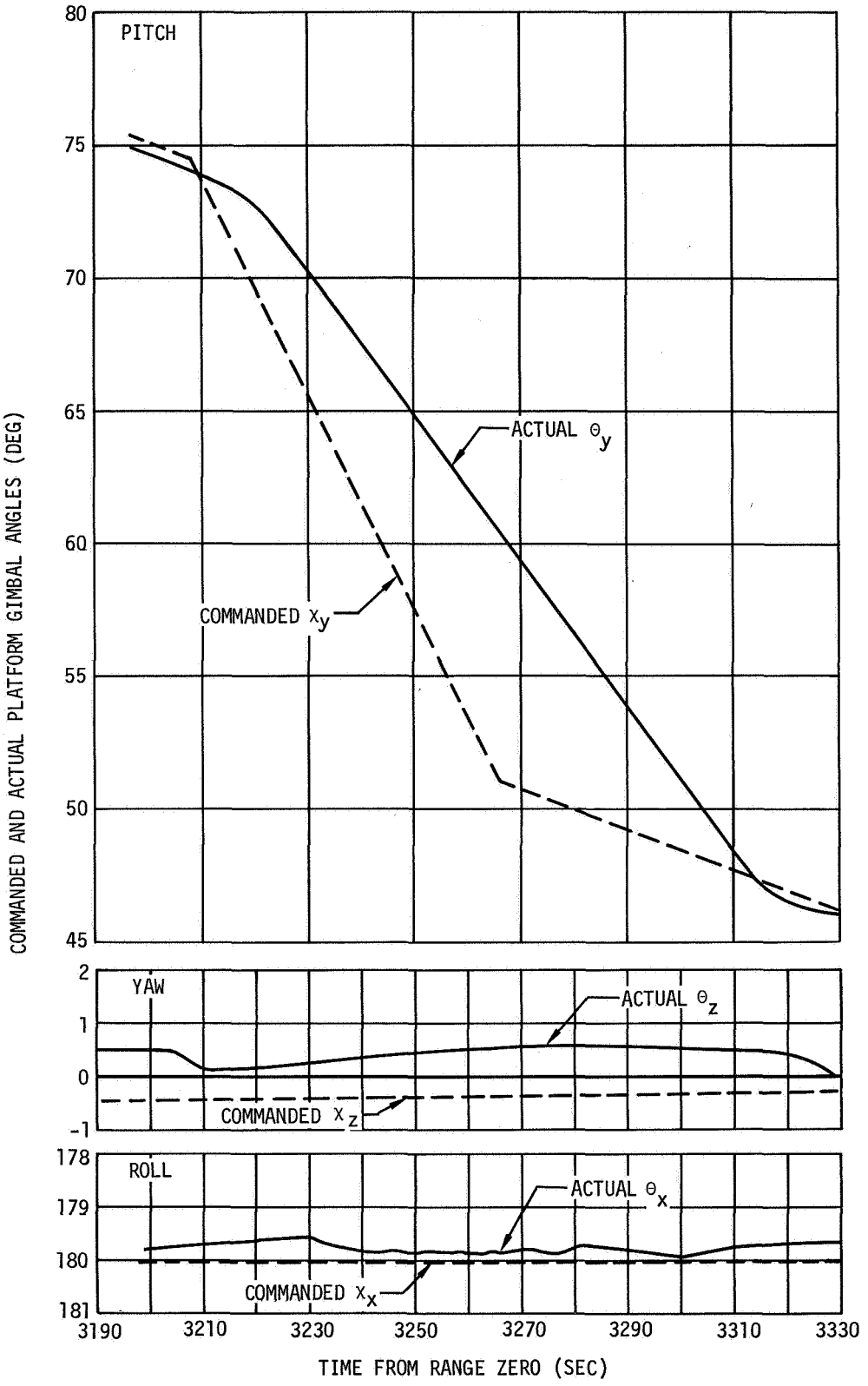

Figure 21-12. Commanded and Actual Vehicle Attitudes - Pitch Down Maneuver

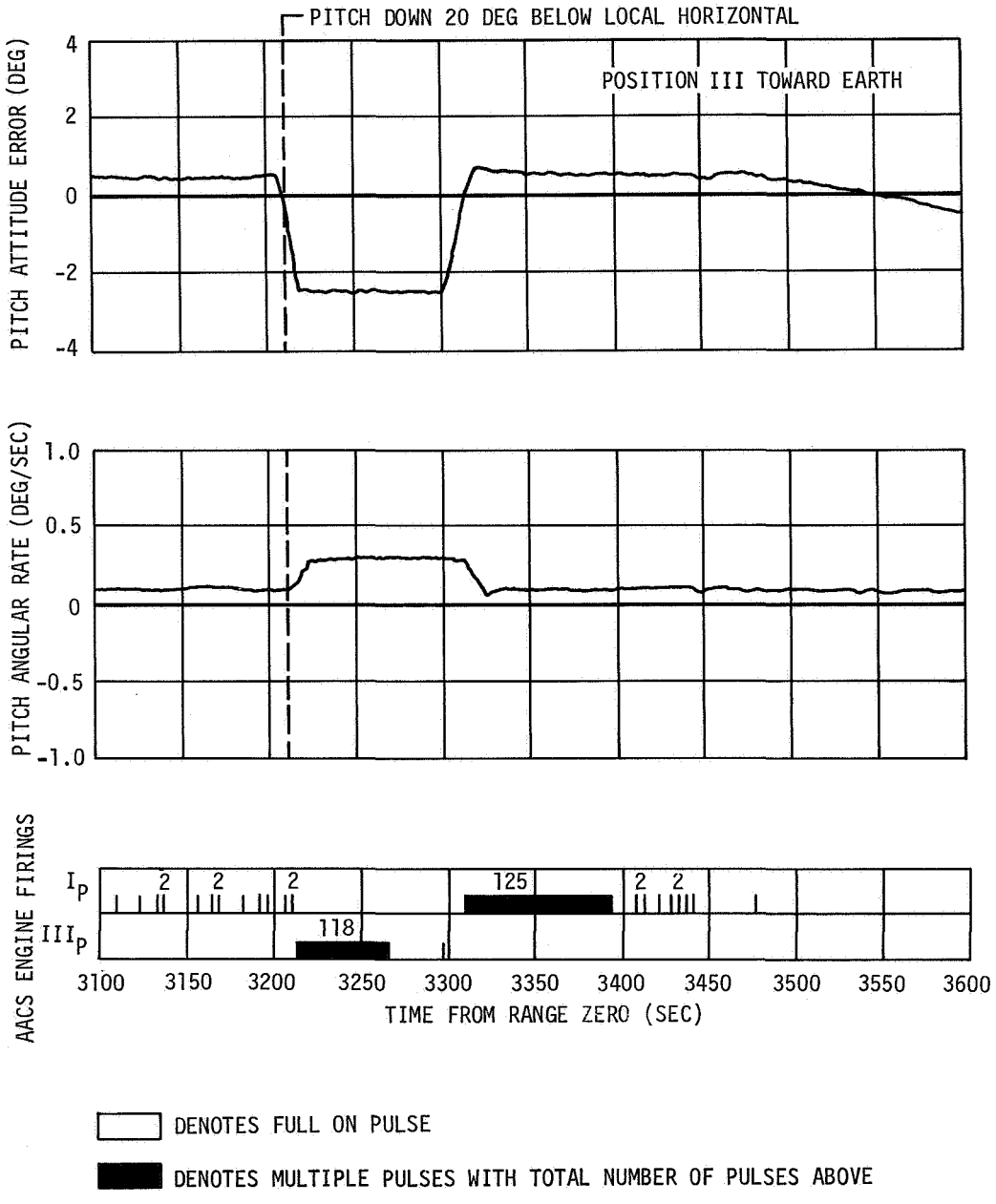

Figure 21-13. Pitch Attitude Control - Pitch Down Maneuver

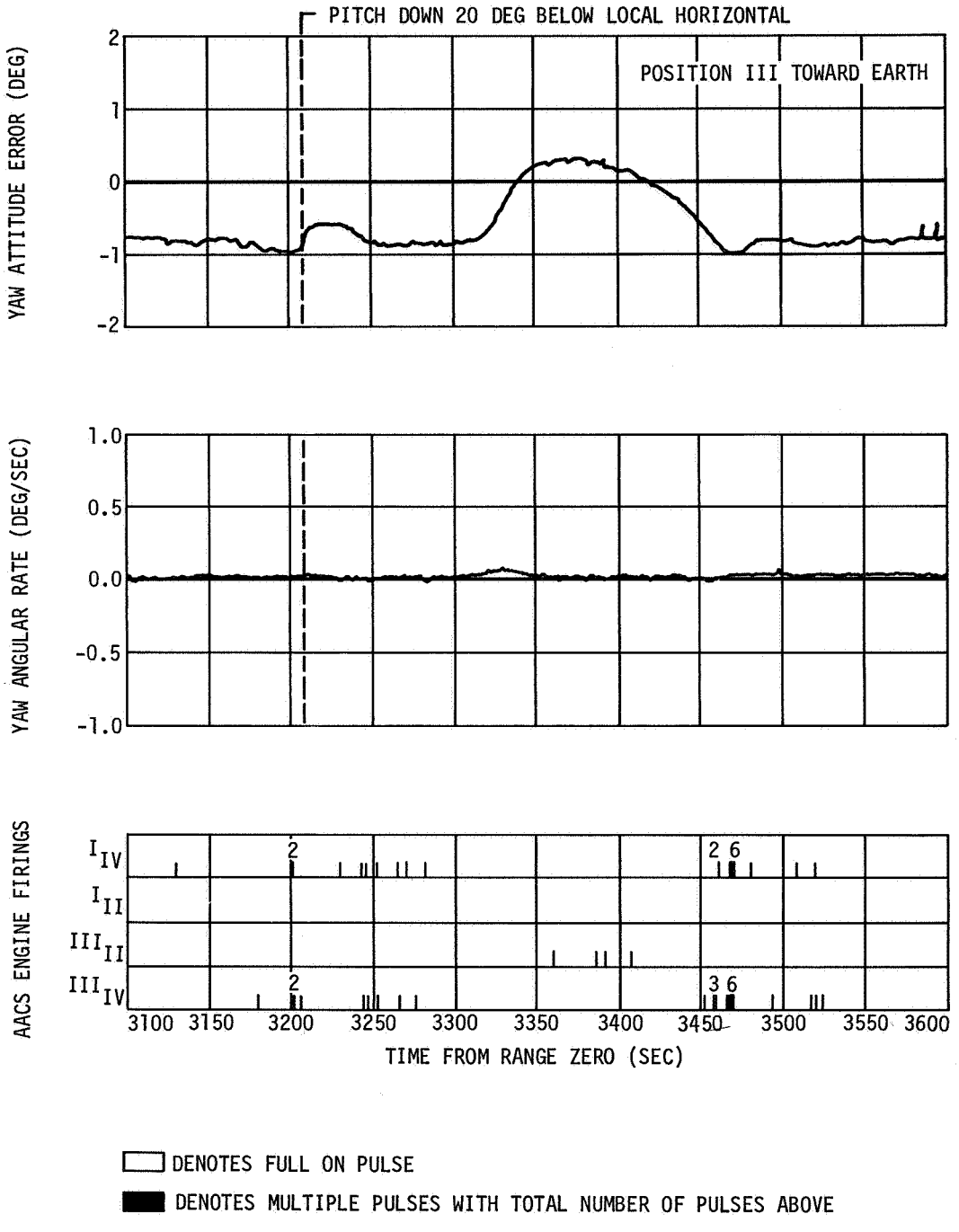

Figure 21-14. Yaw Attitude Control - Pitch Down Maneuver

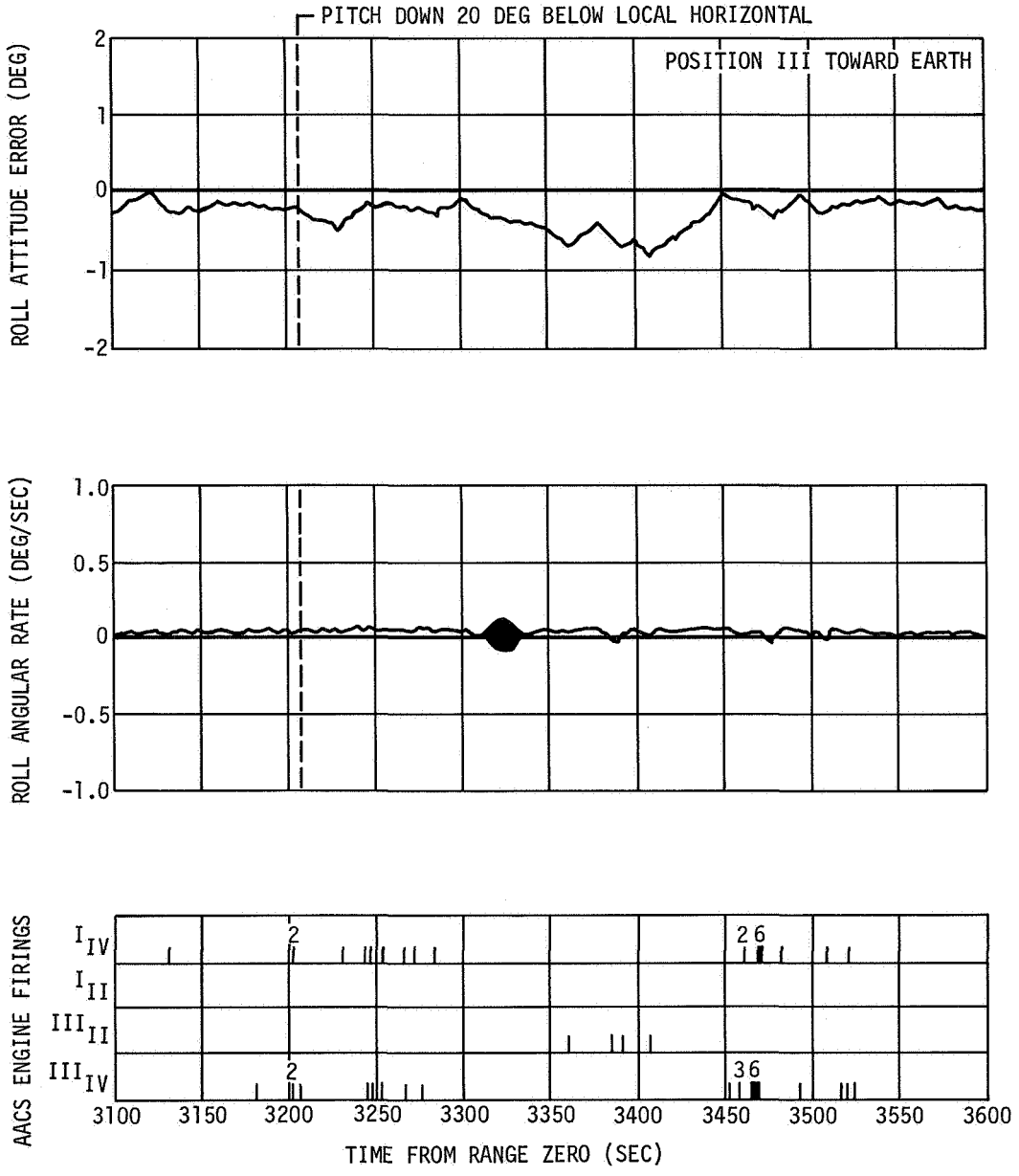

Figure 21-15. Roll Attitude Control - Pitch Down Maneuver

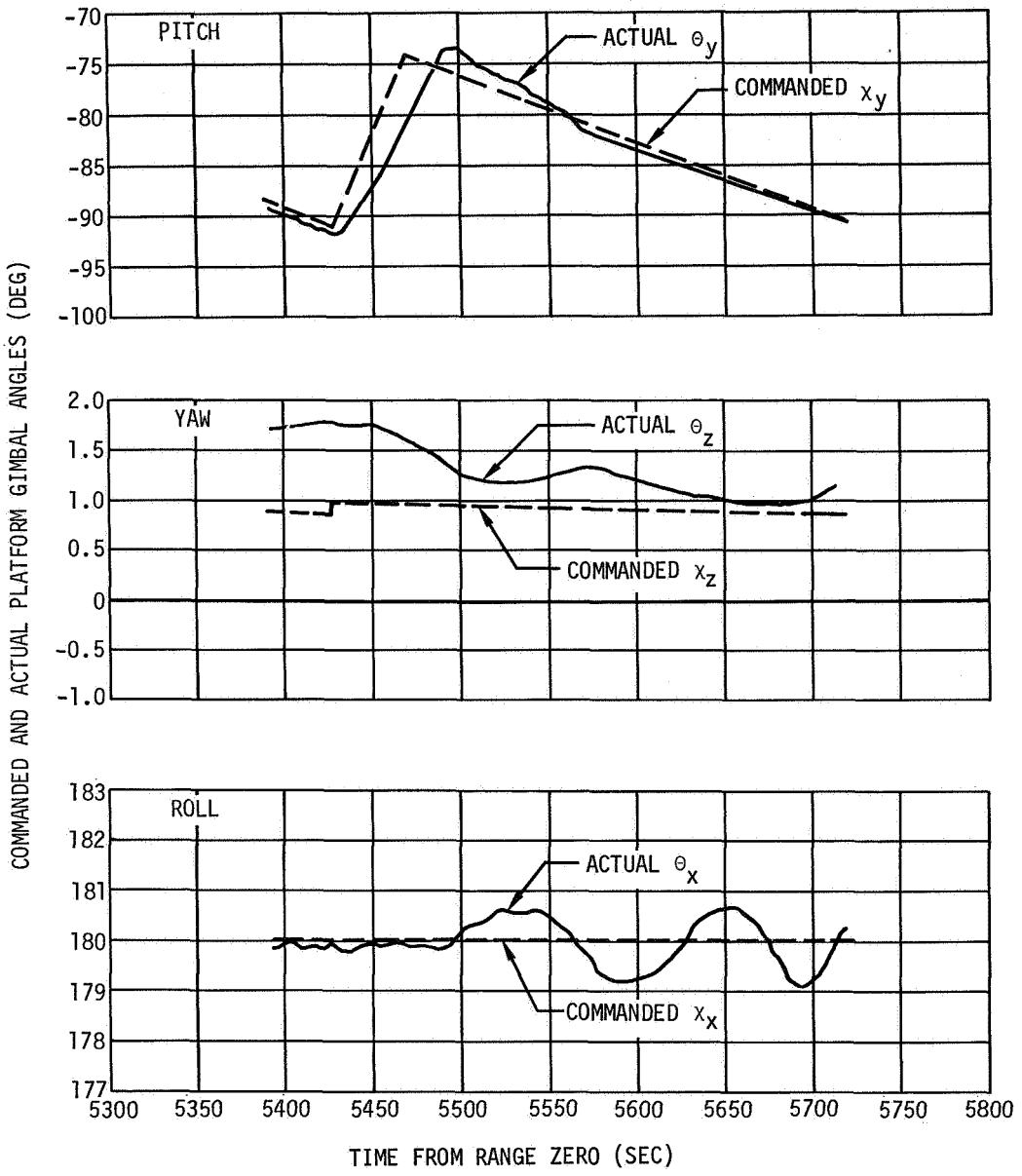

Figure 21-16. Commanded and Actual Vehicle Angles - Pitch Up Maneuver

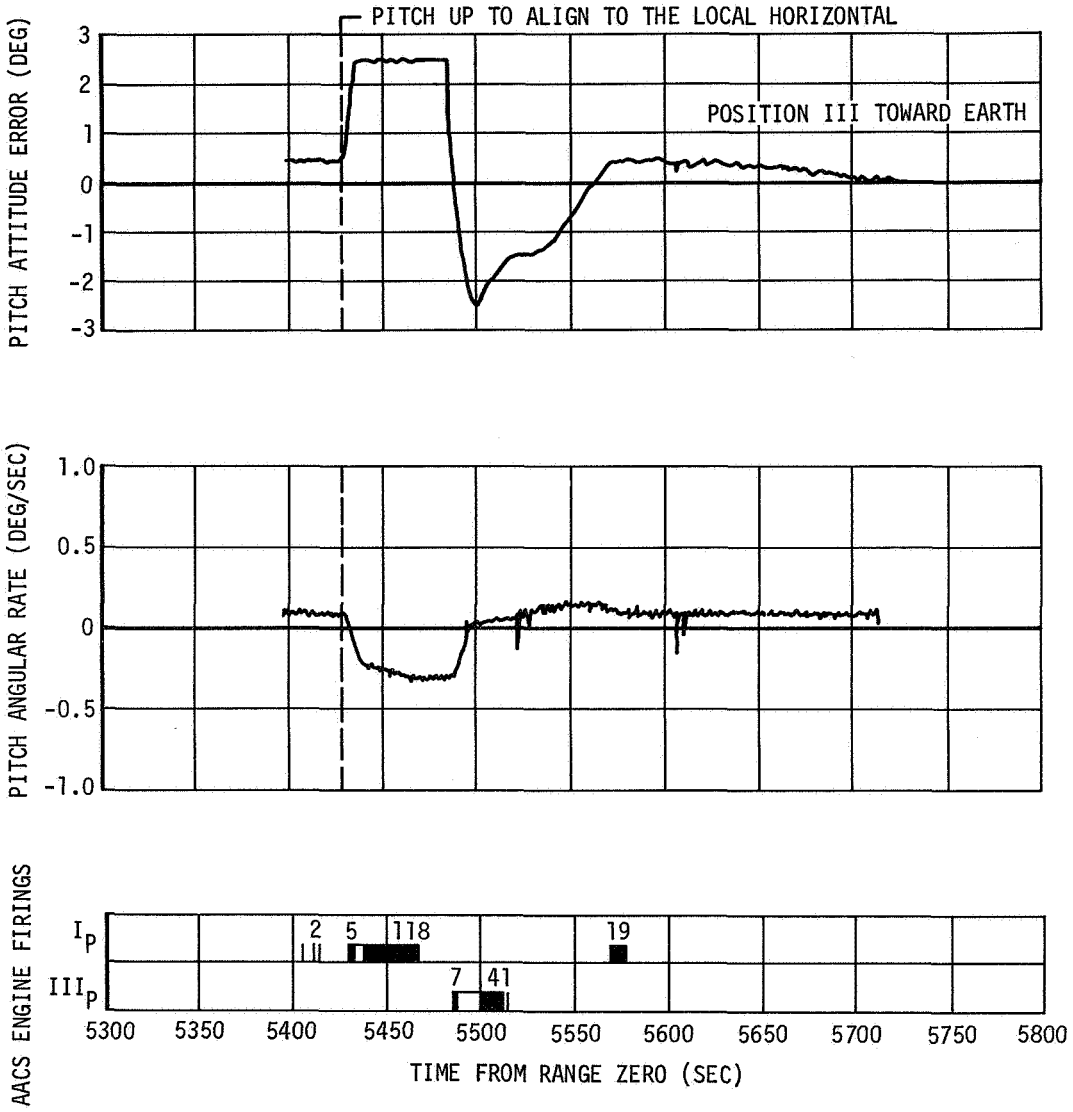

Figure 21-17. Pitch Attitude Control - Pitch Up Maneuver

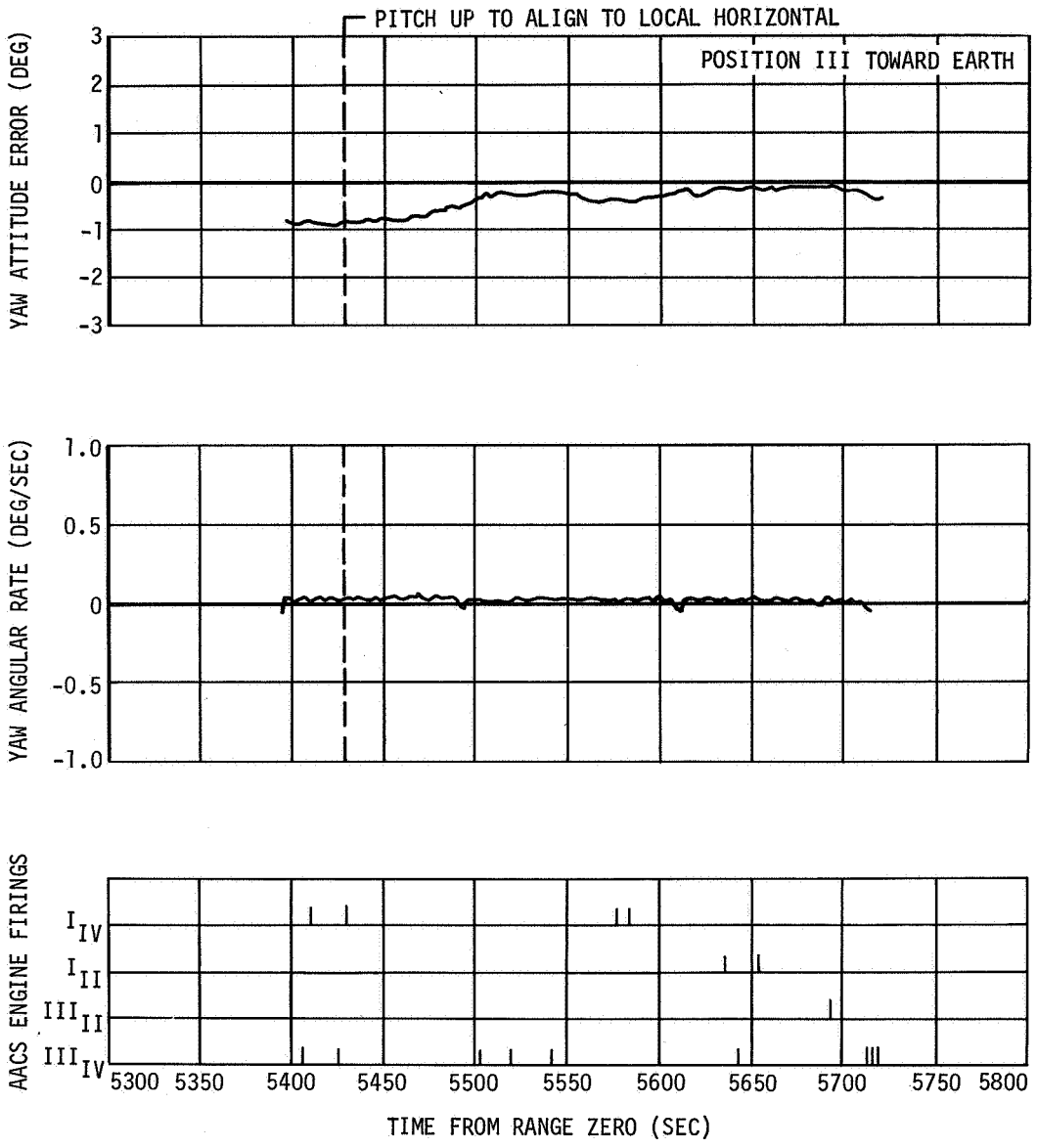

Figure 21-18. Yaw Attitude Control - Pitch Up Maneuver

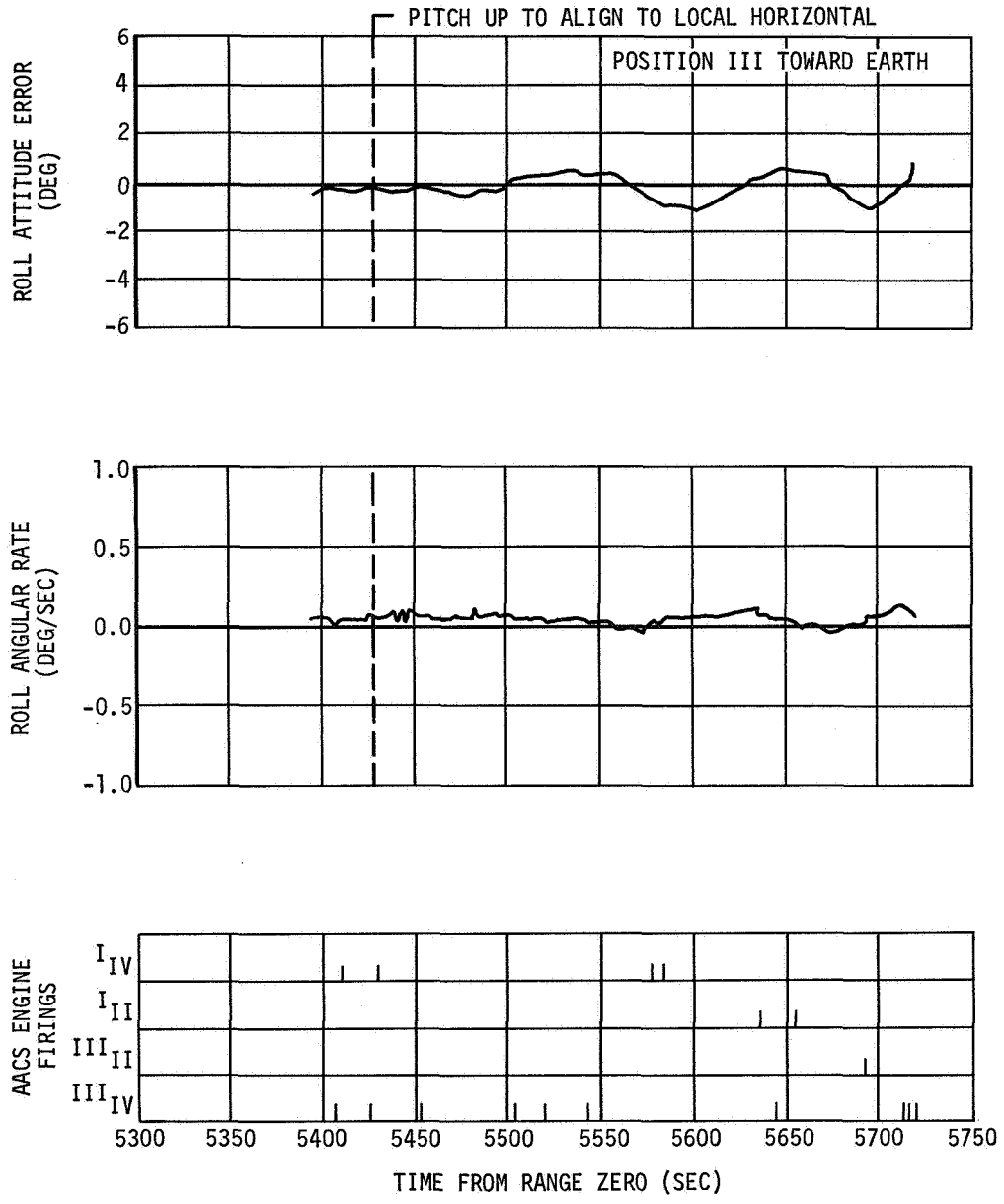

Figure 21-19. Roll Attitude Control - Pitch Up Maneuver

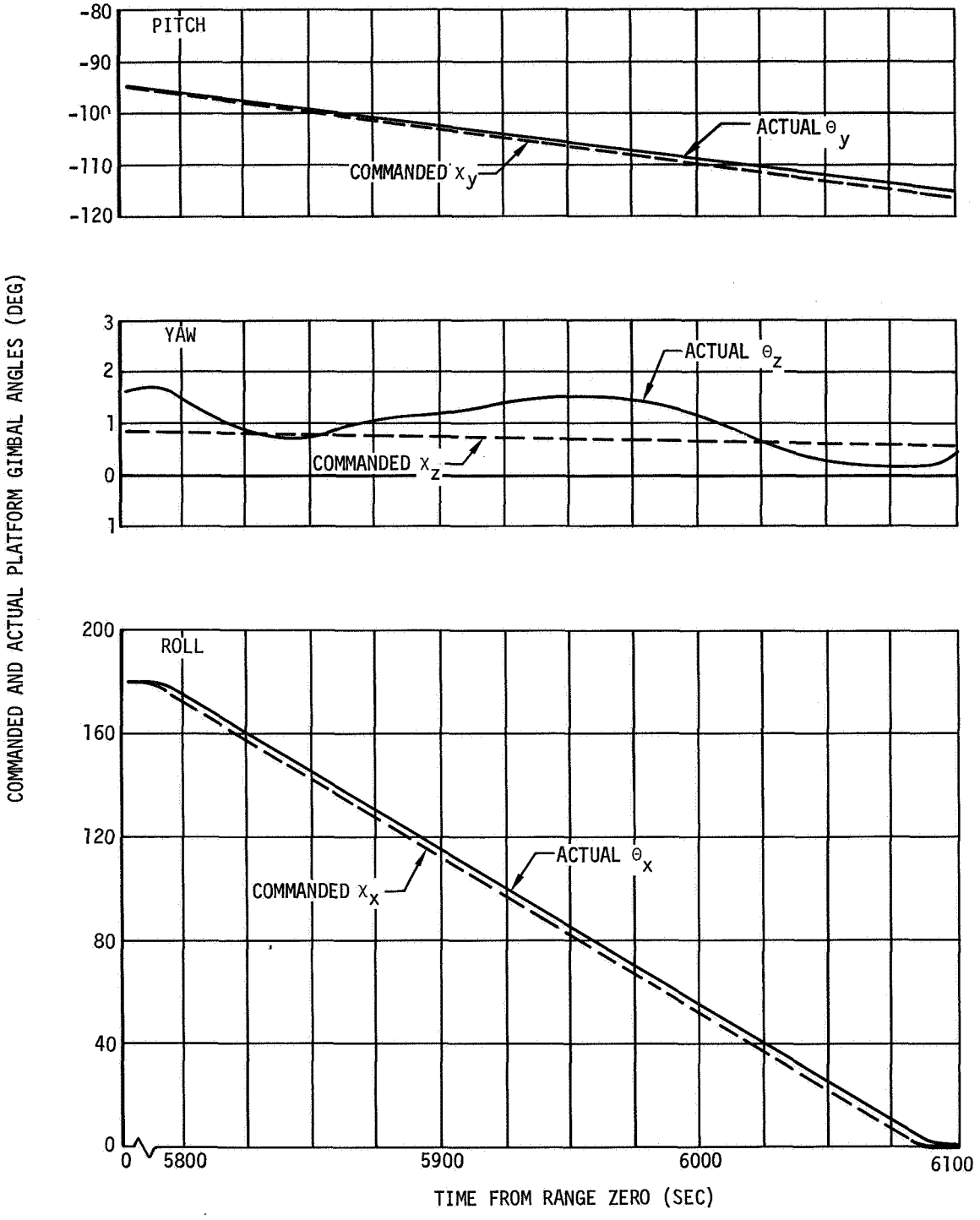

Figure 21-20. Commanded and Actual Vehicle Attitudes - 180 deg Roll Maneuver (CCW Position I Down)

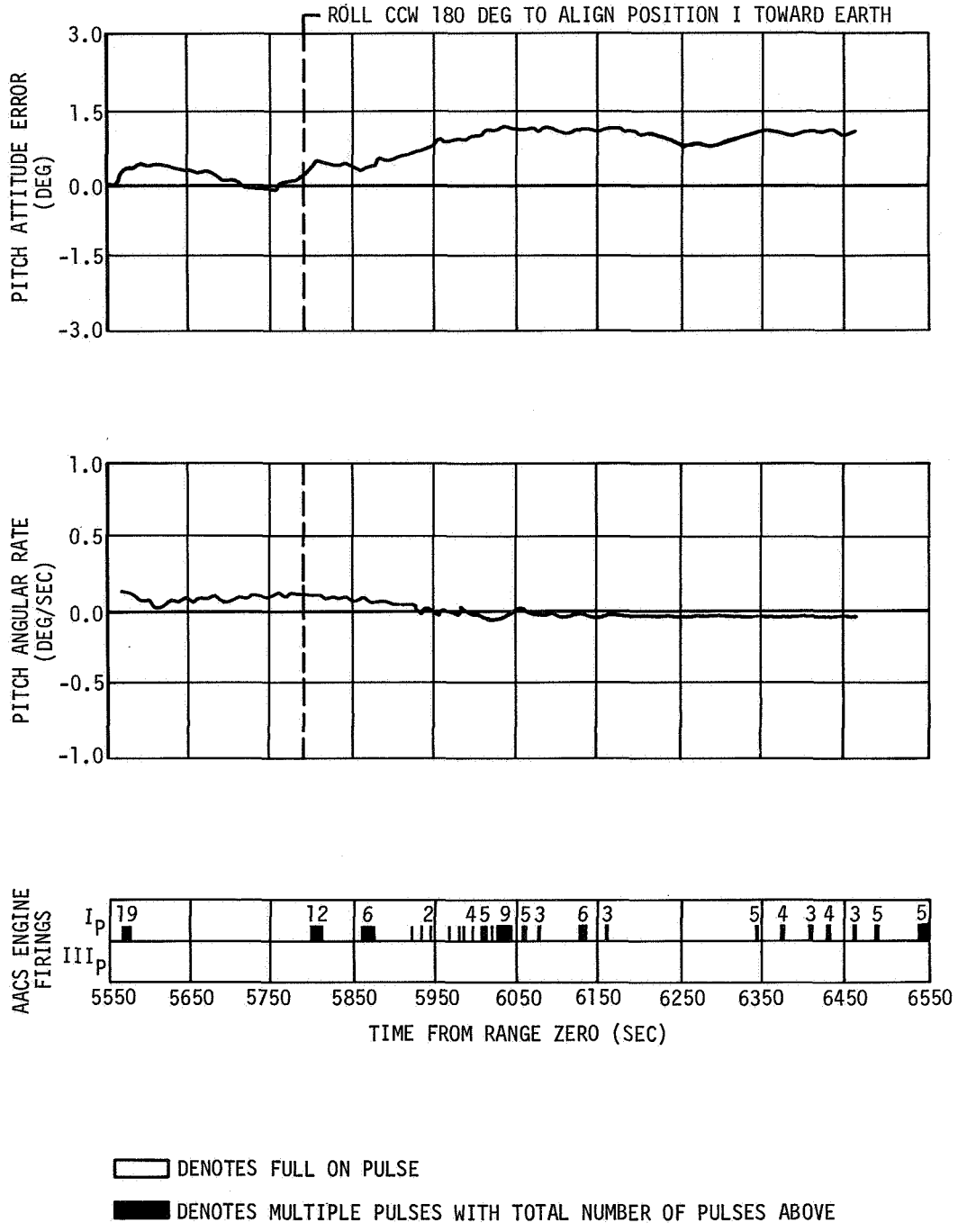

Figure 21-21. Pitch Attitude Control - 180 deg Roll Maneuver (CCW Position I Down)

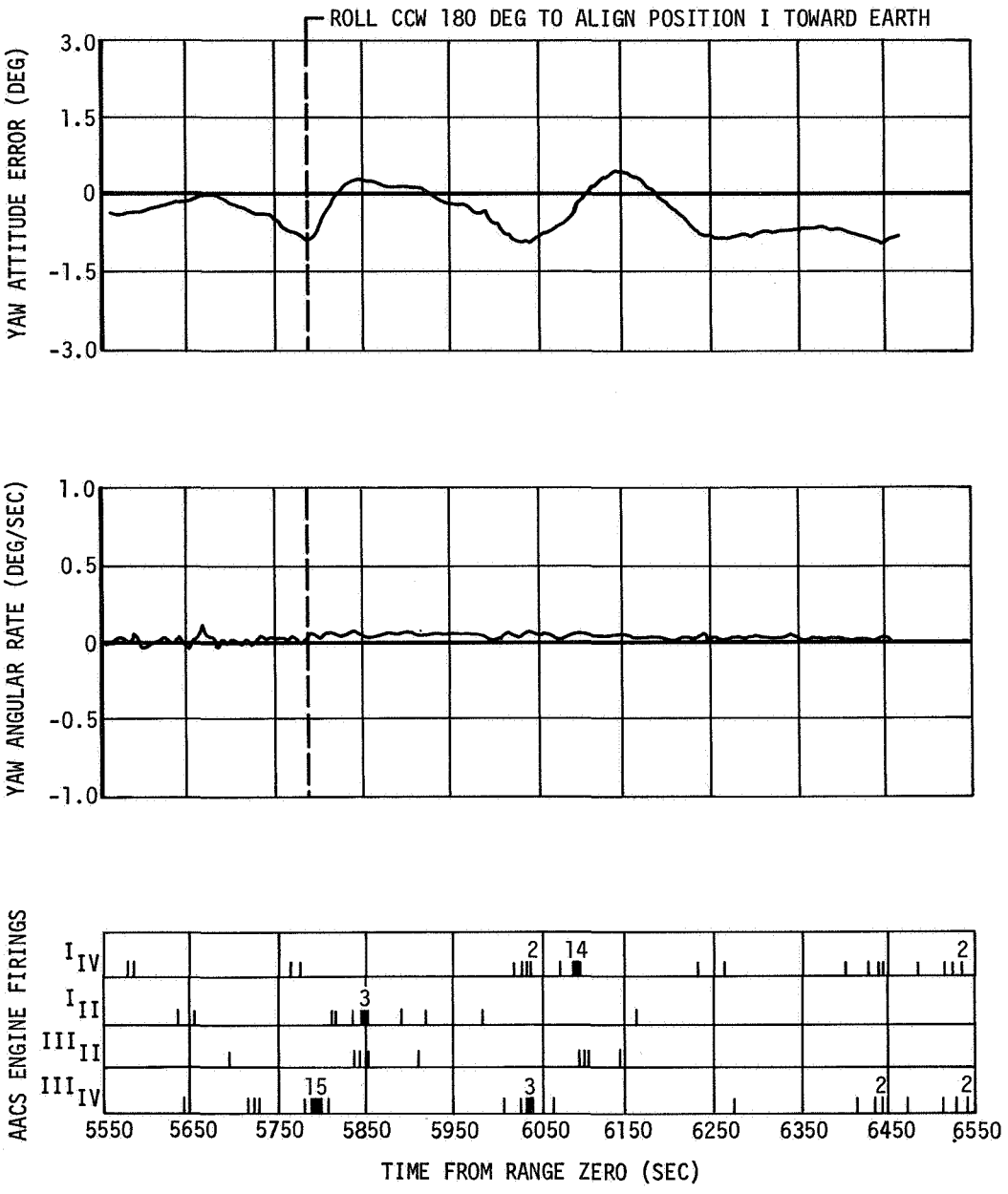

Figure 21-22. Yaw Attitude Control - 180 deg Roll Maneuver (CCW Position I Down)

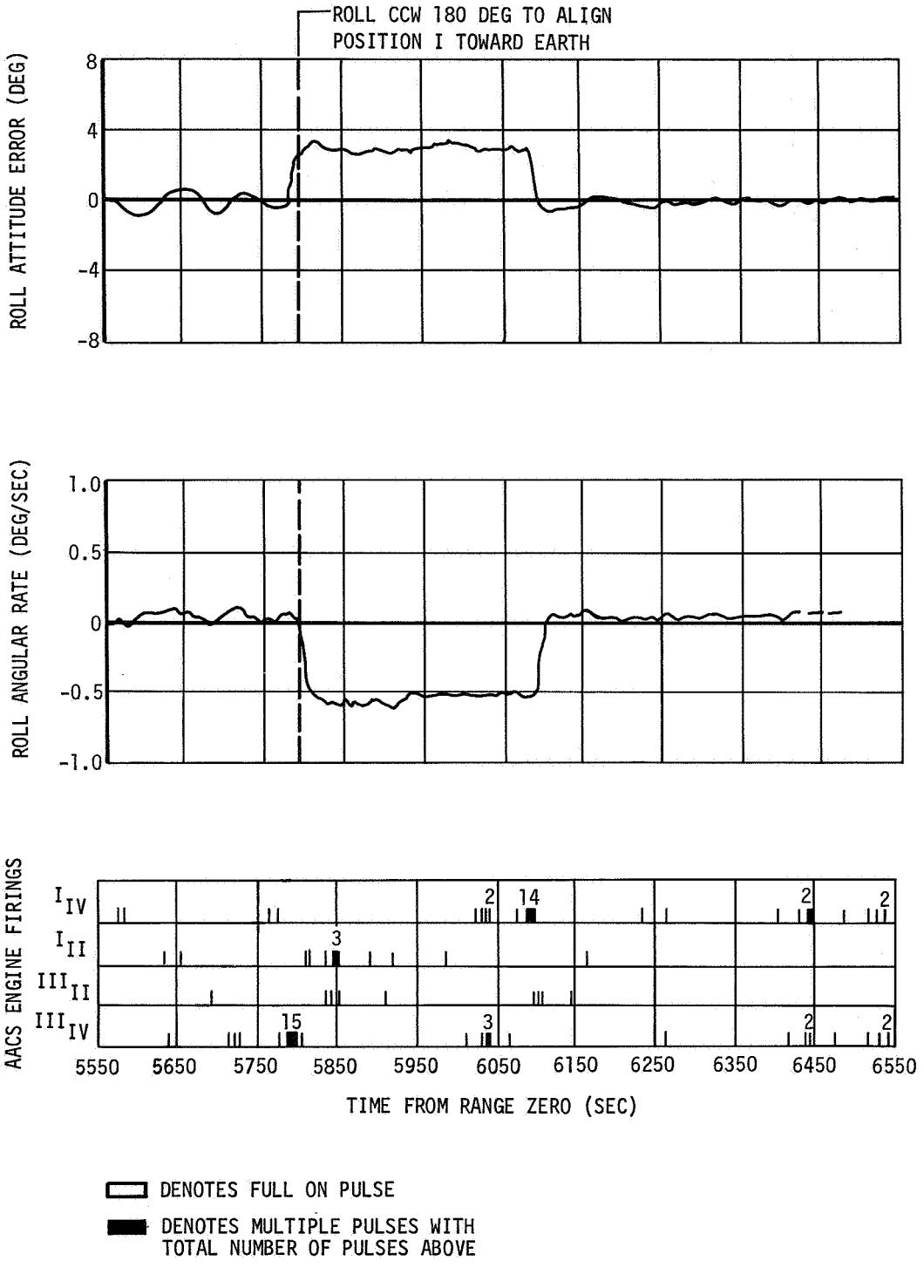

Figure 21-23. Roll Attitude Control - 180 deg Roll Maneuver (CCW Position I Down)

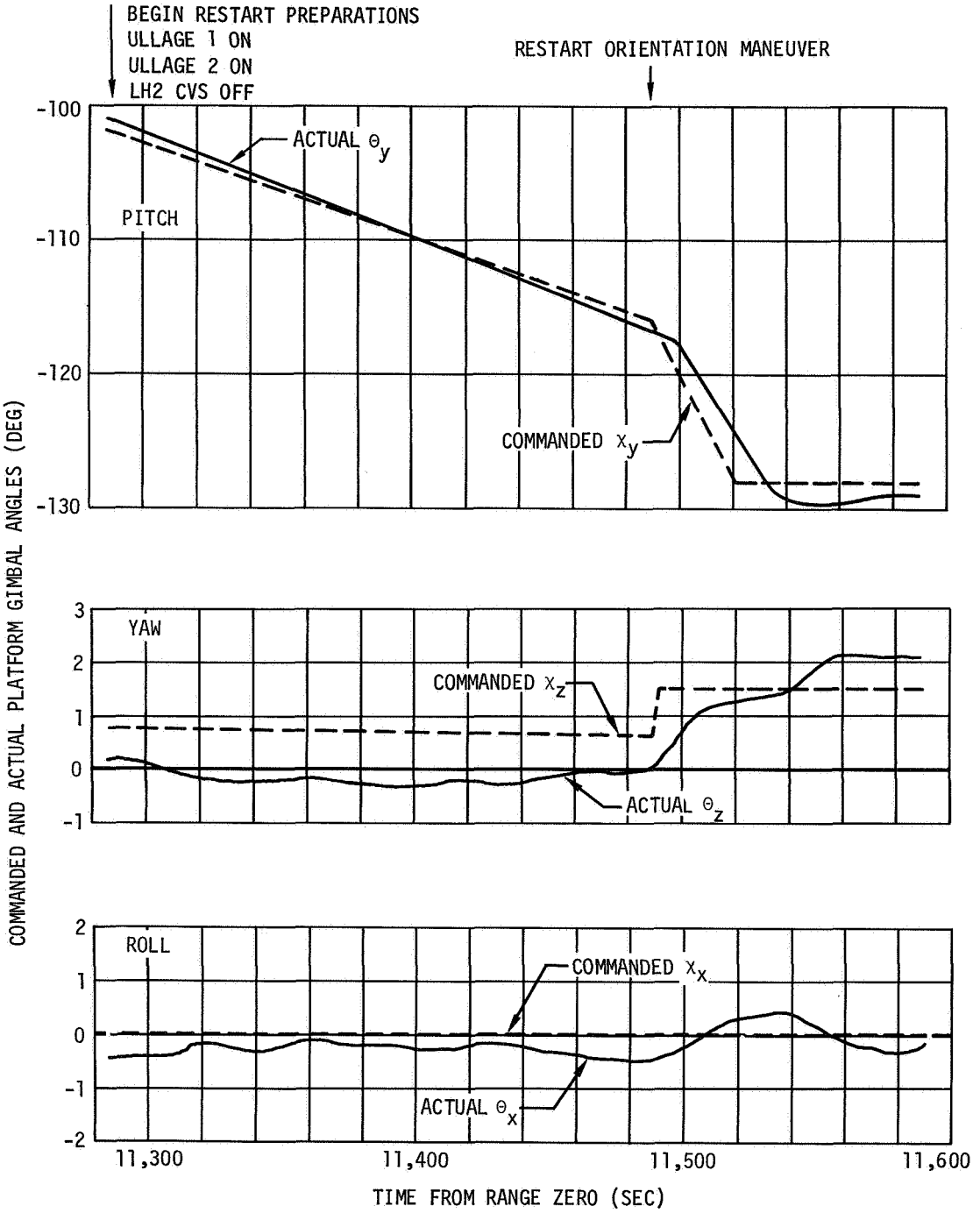

Figure 21-24. Commanded and Actual Vehicle Attitudes - Restart Orientation Maneuver

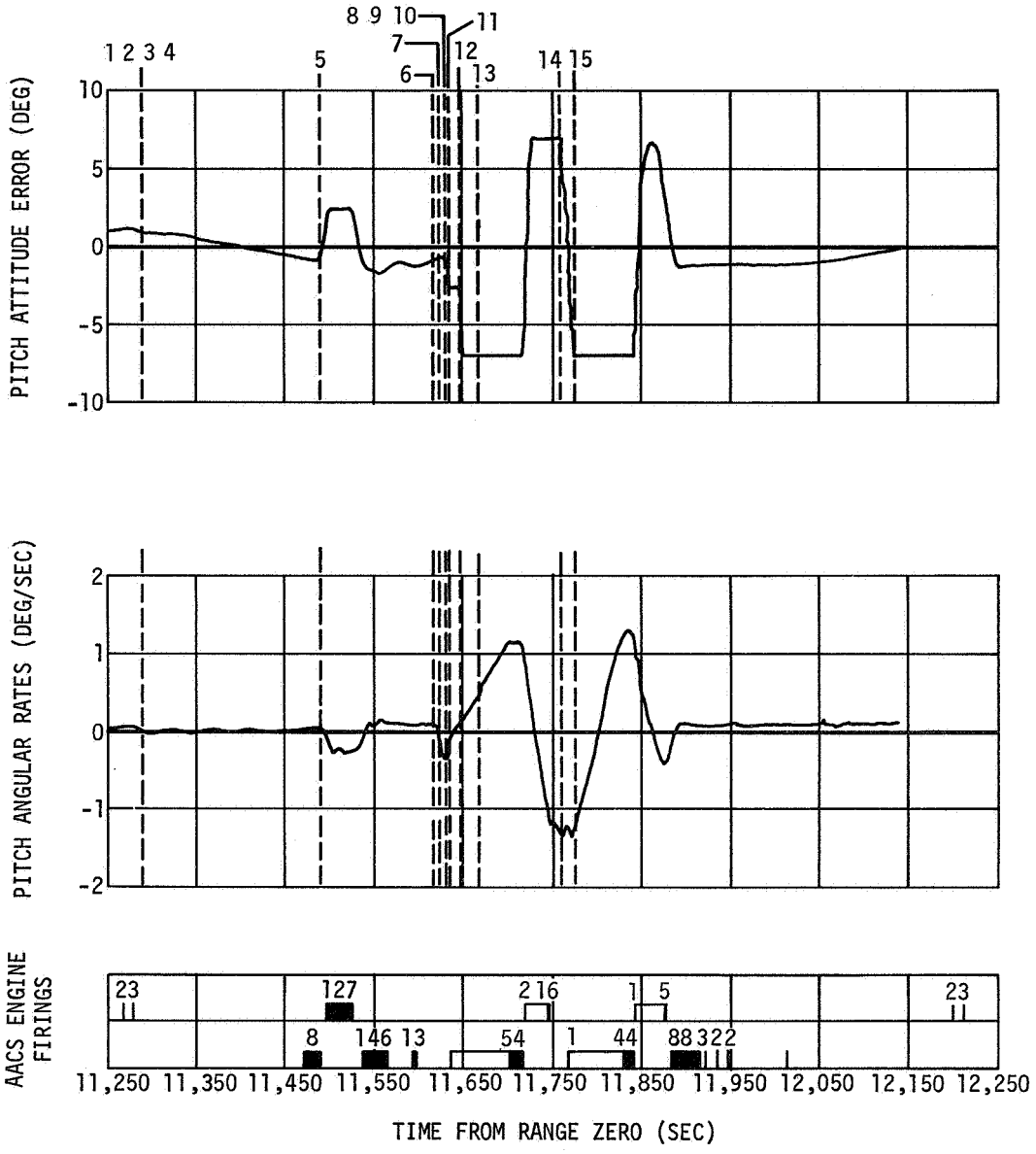

1. INITIATE RESTART PREPARATIONS
2. ULLAGE 1 ON
3. ULLAGE 2 ON
4. LH2 CVS OFF
5. RESTART ORIENTATION MANEUVER
6. S-IVB ENGINE START COMMAND
7. S-IVB BURN MODE ON
8. S-IVB ENGINE OUT INTERRUPT
9. LOX VENT OPEN
10. LH2 VENT OPEN
11. S-IV BURN MODE OFF
12. S/C SEPARATION MANEUVER
13. S/C SEPARATION INITIATION
14. χ_y FROZEN
15. χ_x FROZEN

Figure 21-25. Pitch Attitude Control - Restart Orientation Maneuver and Restart Attempt

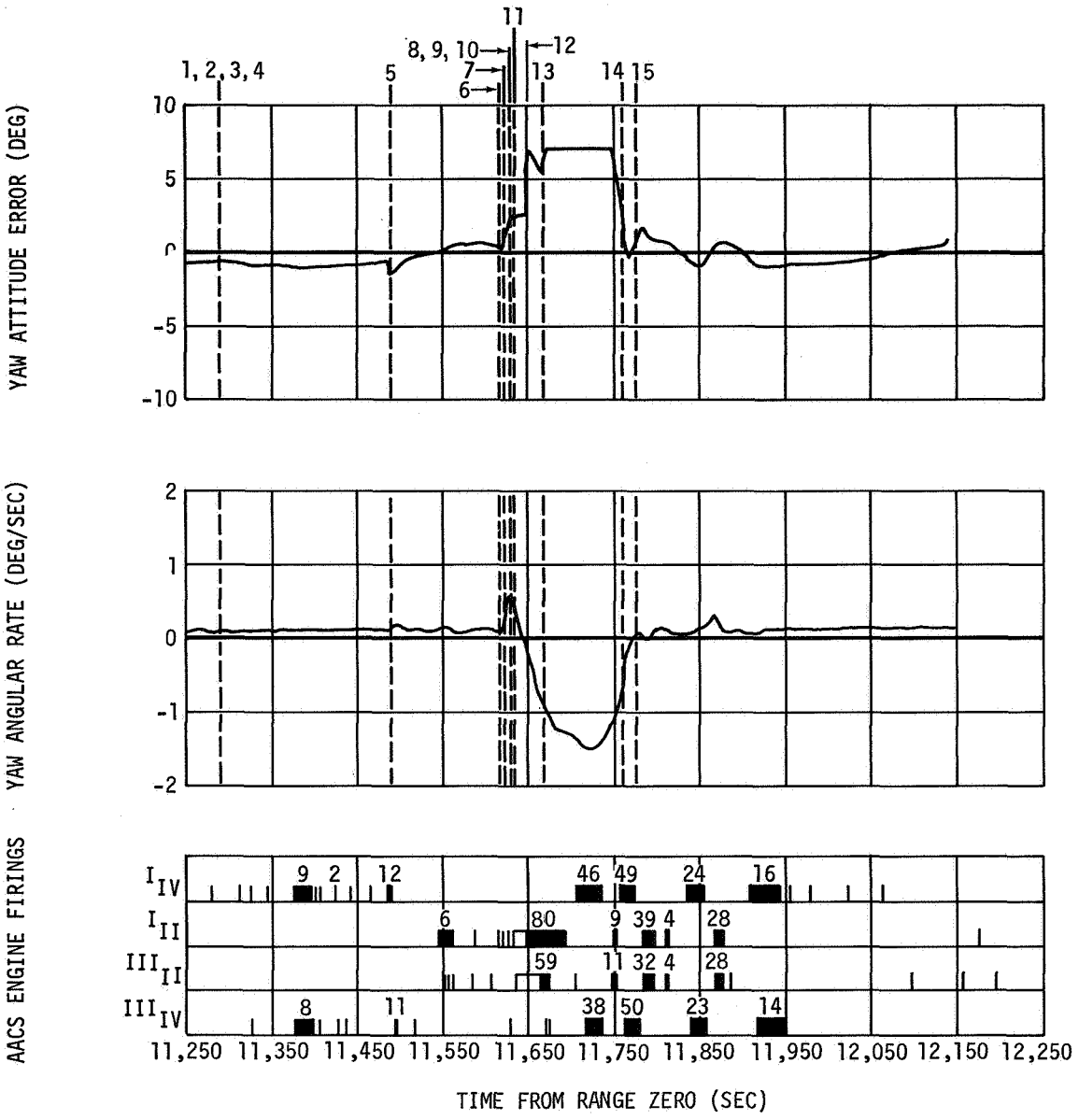

1. INITIATE RESTART PREPARATIONS
2. ULLAGE 1 ON
3. ULLAGE 2 ON
4. LH2 CVS OFF
5. RESTART ORIENTATION MANEUVER
6. S-IVB ENGINE START COMMAND
7. S-IVB BURN MODE ON
8. S-IVB ENGINE OUT INTERRUPT
9. LOX VENT OPEN
10. LH2 VENT OPEN
11. S-IV BURN MODE OFF
12. S/C SEPARATION MANEUVER
13. S/C SEPARATION INITIATION
14. χ_y FROZEN
15. χ_x FROZEN

Figure 21-26. Yaw Attitude Control - Restart Orientation Maneuver and Restart Attempt

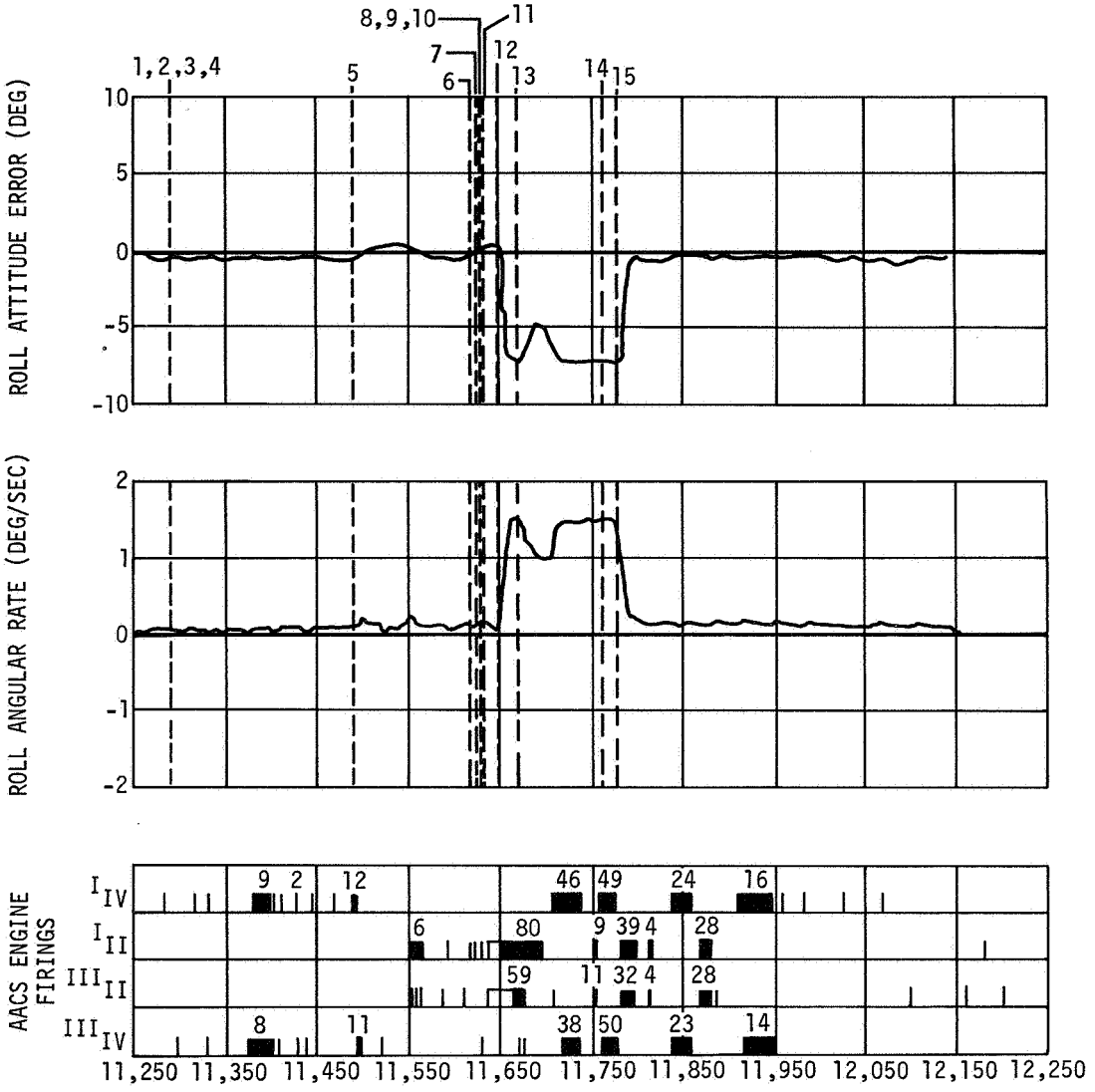

DENOTES FULL ON PULSE

DENOTES MULTIPLE PULSES WITH TOTAL NUMBER OF PULSES ABOVE

1. INITIATE RESTART PREPARATIONS
2. ULLAGE 1 ON
3. ULLAGE 2 ON
4. LH2 CVS OFF
5. RESTART ORIENTATION MANEUVER
6. S-IVB ENGINE START COMMAND
7. S-IVB BURN MODE ON
8. S-IVB ENGINE OUT INTERRUPT
9. LOX VENT OPEN
10. LH2 VENT OPEN
11. S-IVB BURN MODE OFF
12. S/C SEPARATION MANEUVER
13. S/C SEPARATION INITIATION
14. χ_y FROZEN
15. χ_x FROZEN

Figure 21-27. Roll Attitude Control - Restart Orientation Maneuver and Restart Attempt

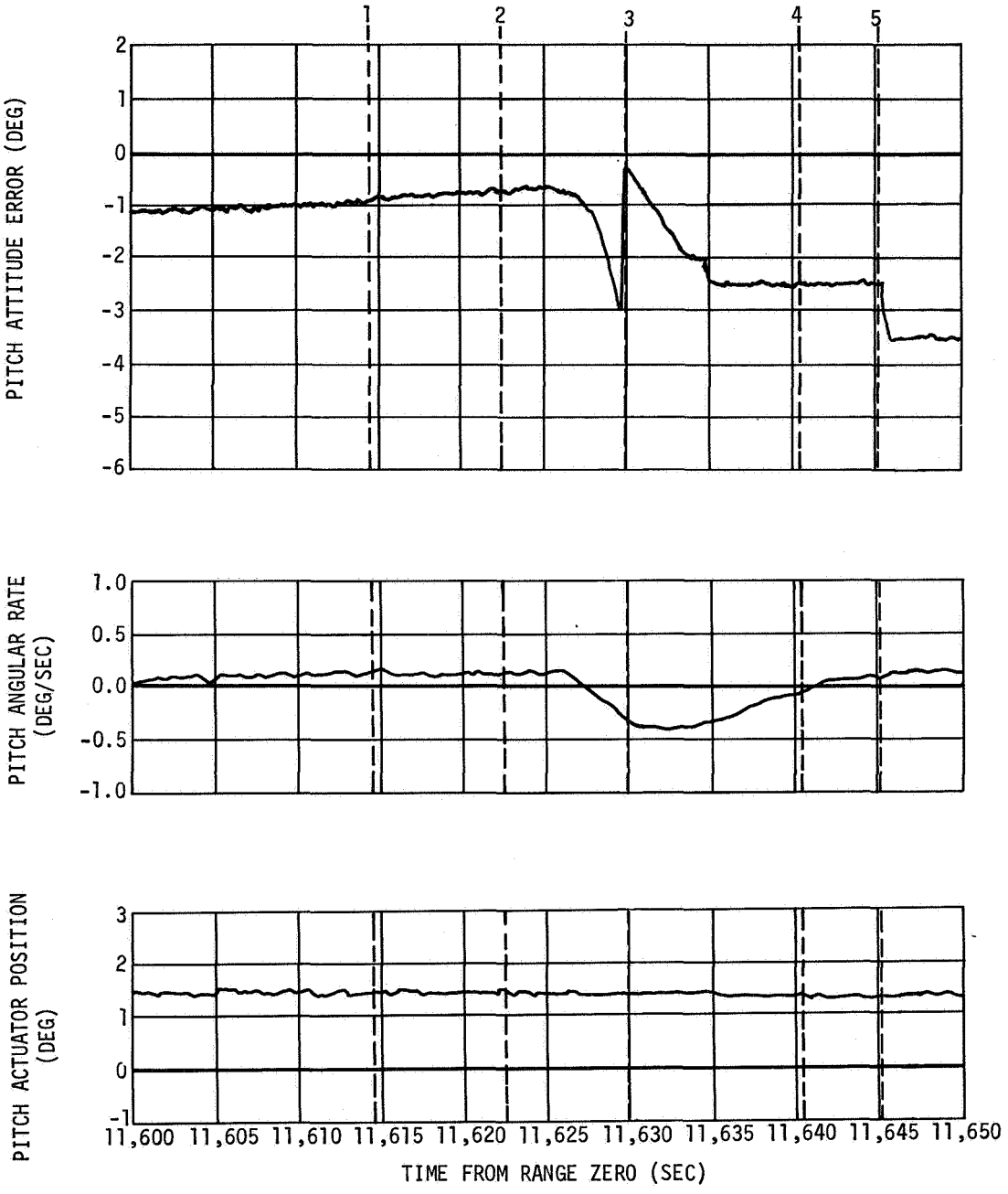

1. ENGINE START COMMAND
2. S-IVB BURN MODE ON
3. S-IVB CUTOFF, LOX VENT OPEN, LH2 VENT OPEN
4. LOX VENT CLOSE
5. ATTITUDE ERROR LIMIT CHANGE

Figure 21-28. Pitch Attitude Control - Restart Attempt

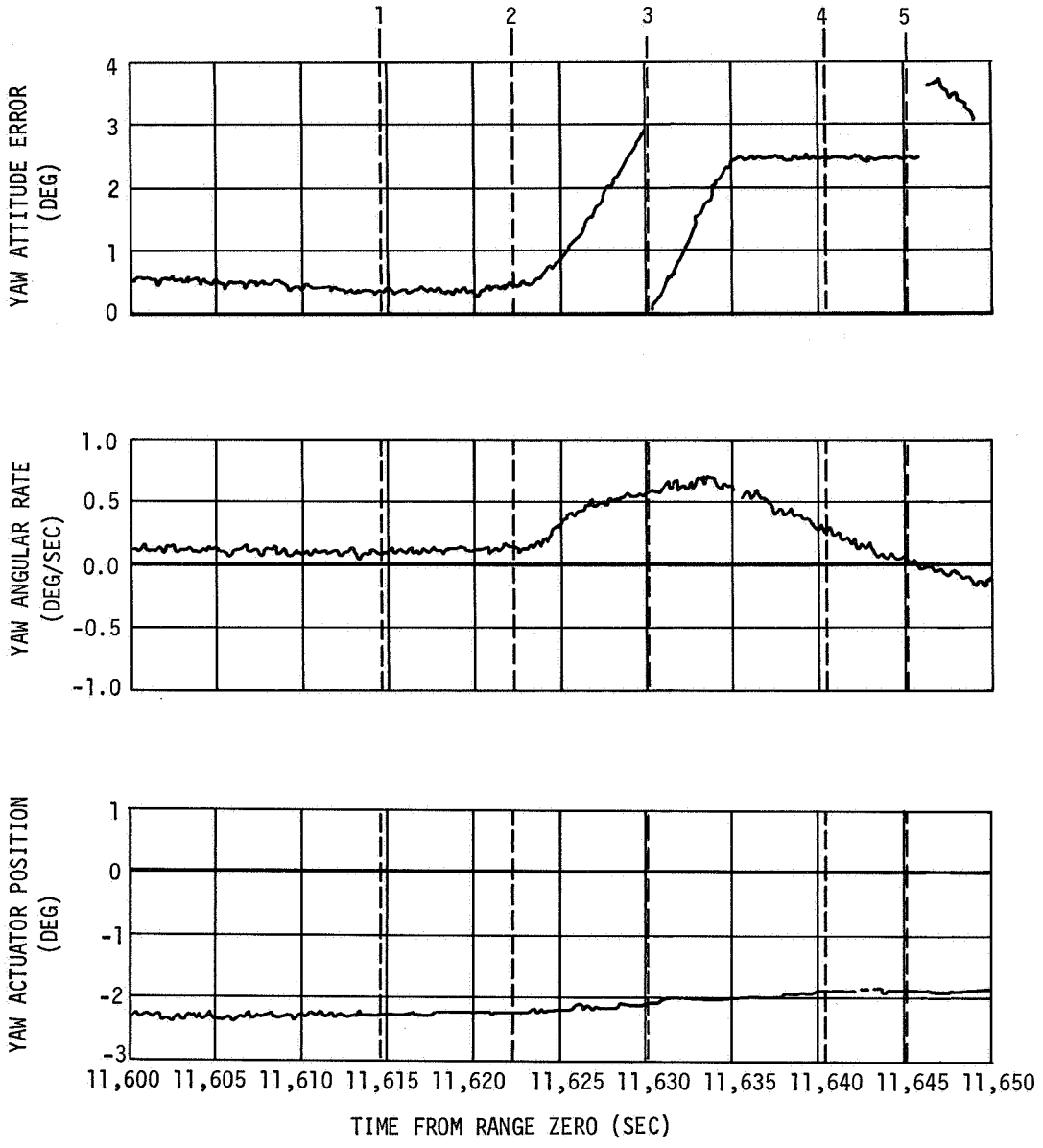

1. ENGINE START COMMAND
2. S-IVB BURN MODE ON
3. S-IVB CUTOFF, LOX VENT OPEN, LH2 VENT OPEN
4. LOX VENT CLOSE
5. ATTITUDE ERROR LIMIT CHANGE

Figure 21-29. Yaw Attitude Control - Restart Attempt

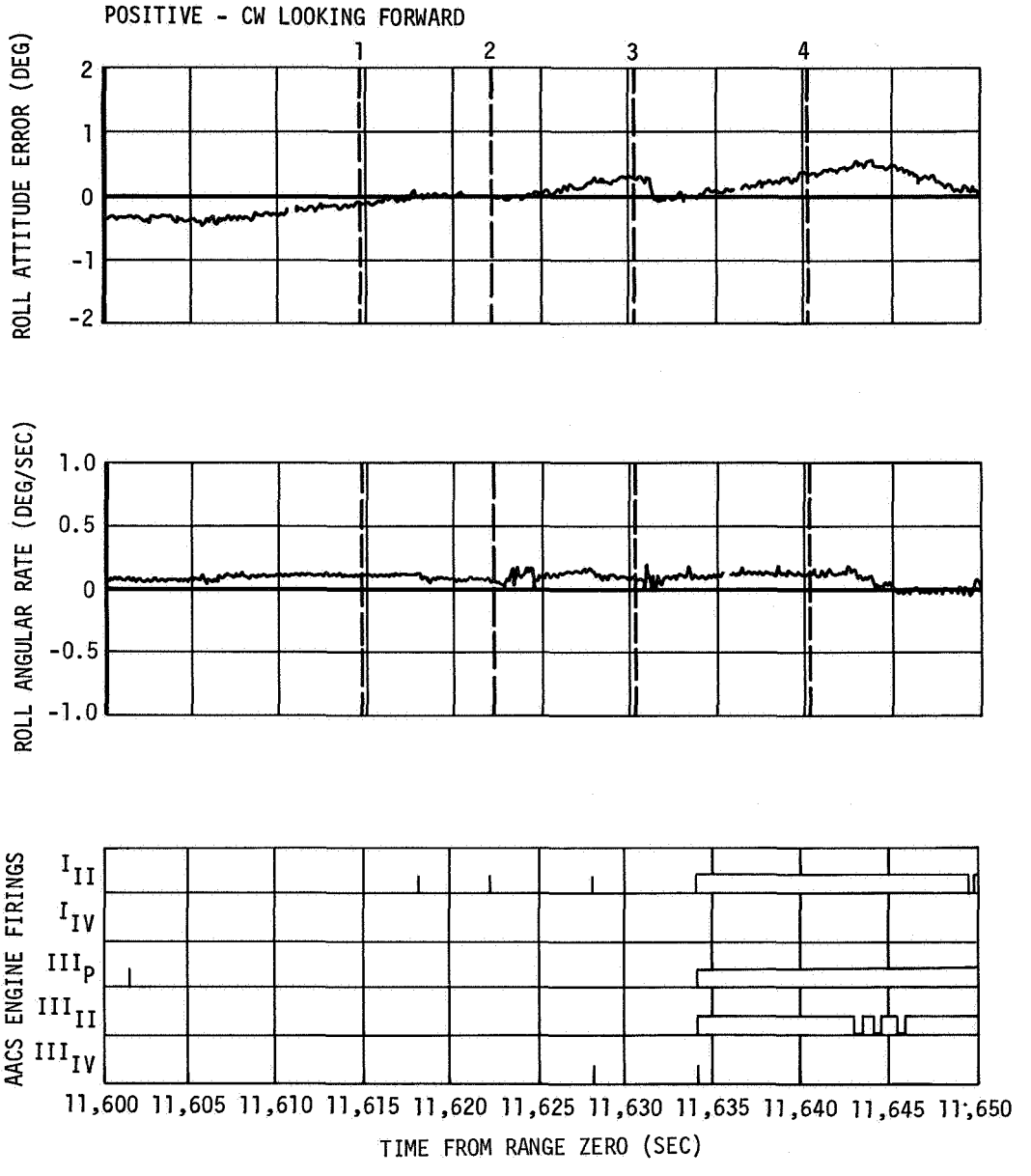

DENOTES FULL ON PULSE POSITIVE - CW LOOKING FORWARD

1. ENGINE START COMMAND
2. S-IVB BURN MODE ON
3. S-IVB CUTOFF, LOX VENT OPEN, LH2 VENT OPEN
4. LOX VENT CLOSE

Figure 21-30. Roll Attitude Control - Restart Attempt

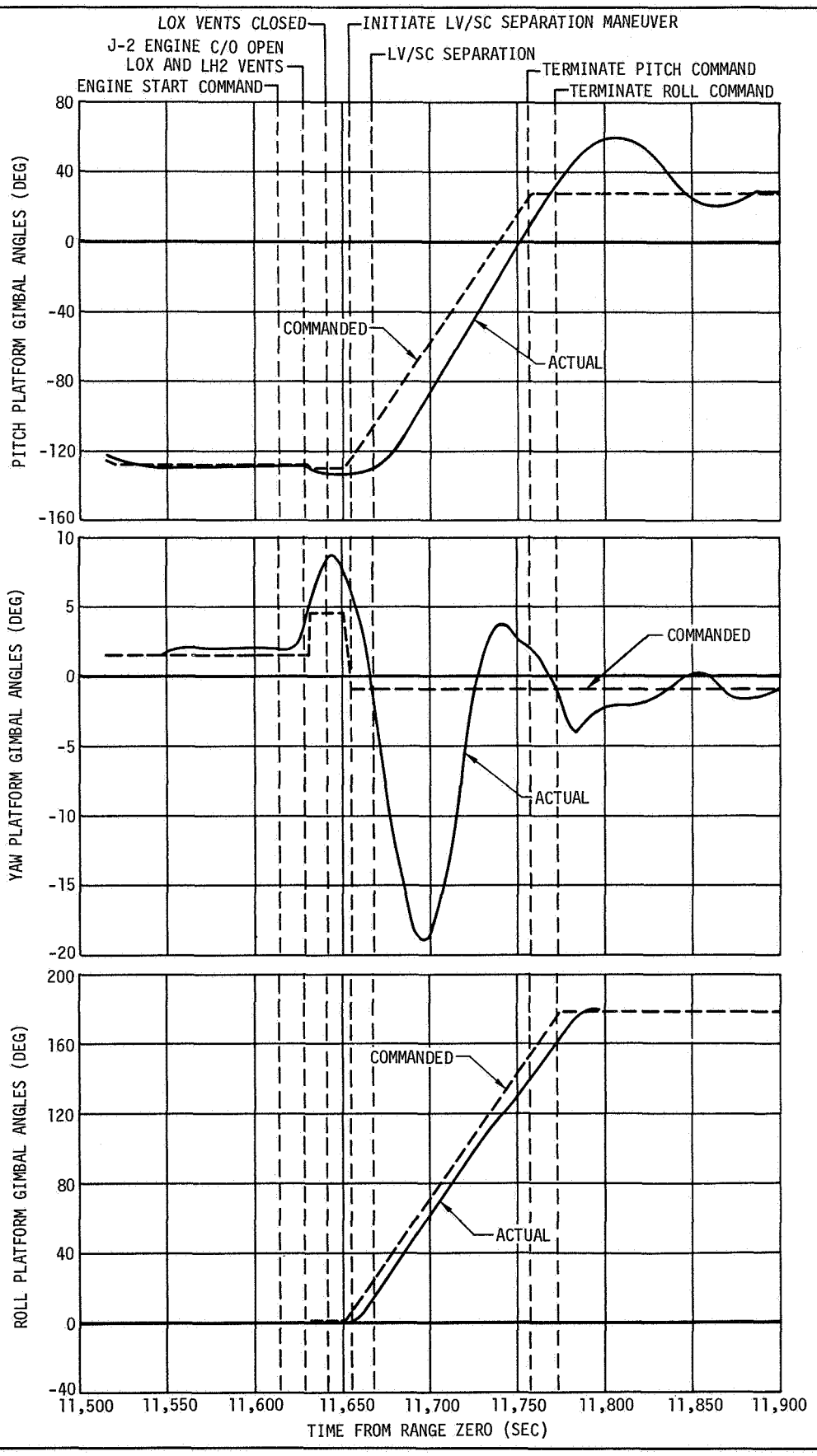

Figure 21-31. Pitch, Yaw, and Roll Commanded and Actual Vehicle Attitudes following Attempted Restart

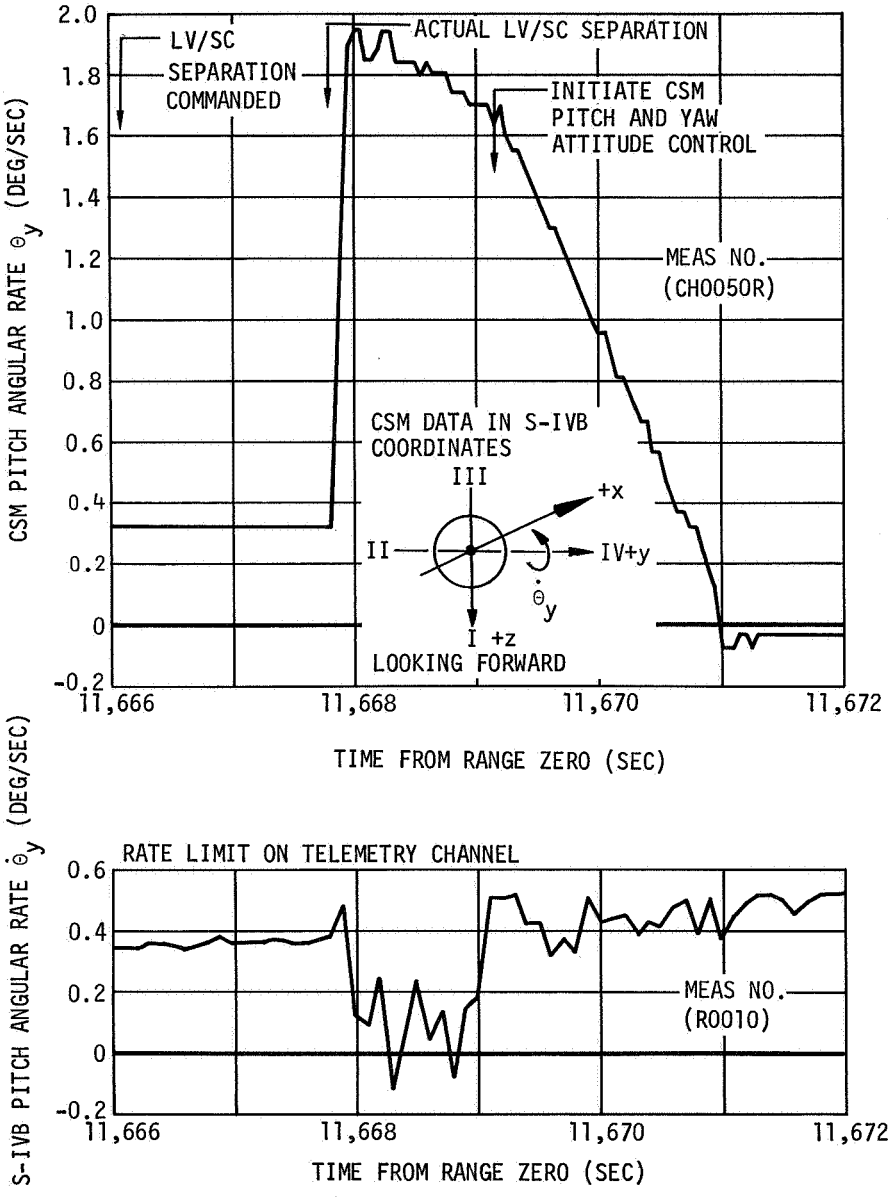

Figure 21-32. LV/SC Pitch Angular Rates at Separation

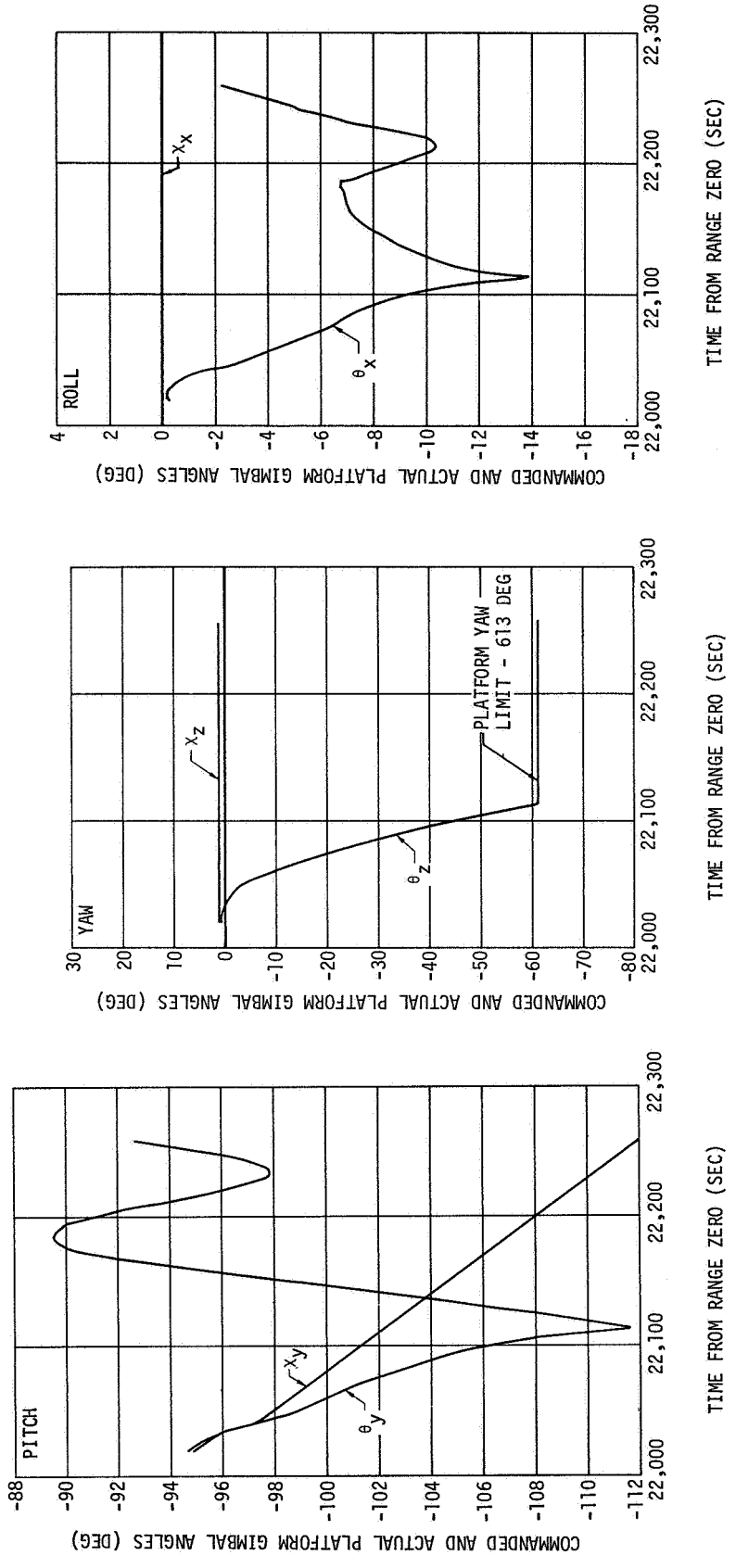

Figure 21-33. Commanded and Actual Vehicle Attitudes at Loss of Attitude Control (Hawaii - Revolution 4)

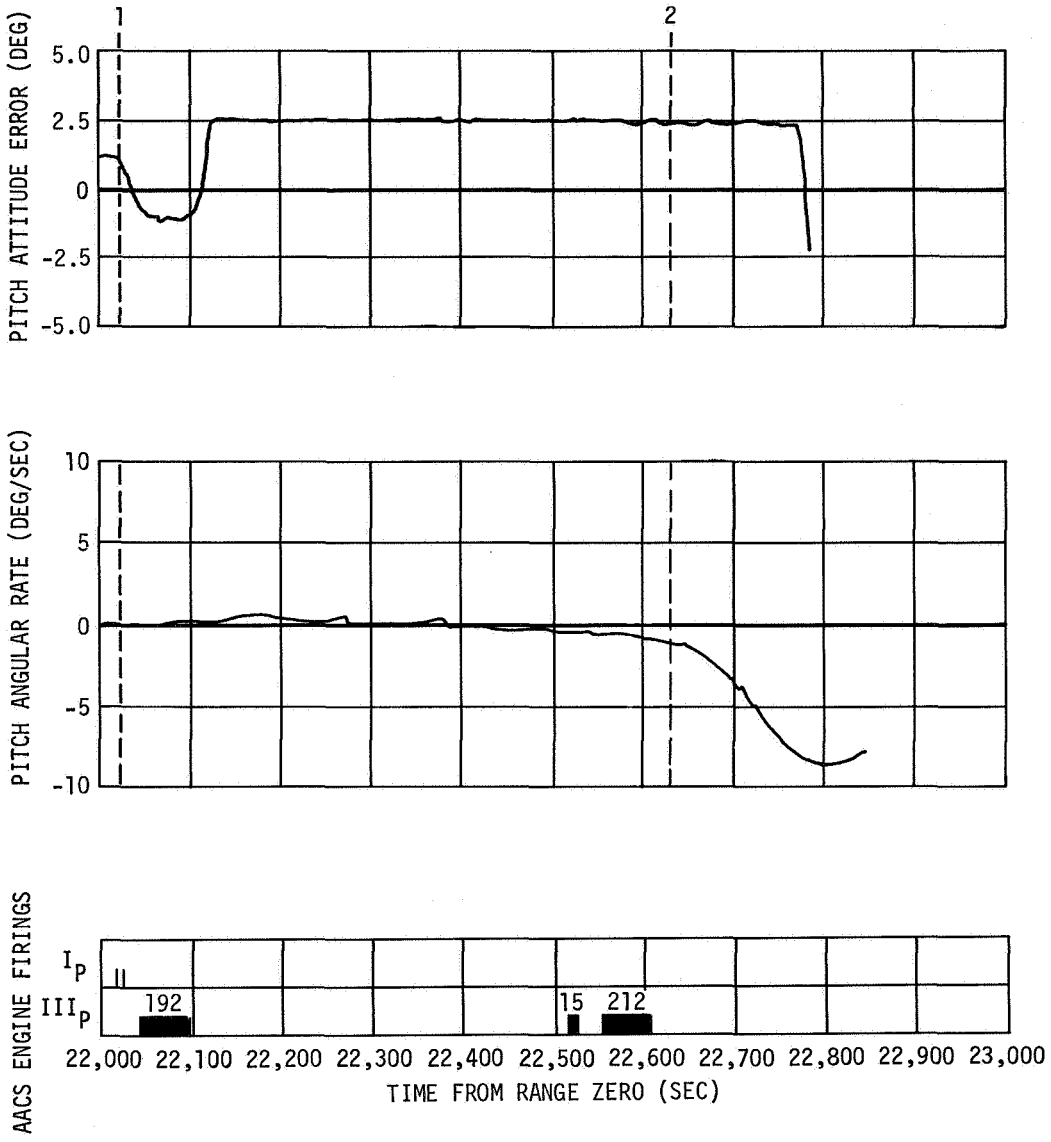

Figure 21-34. Pitch Axis Parameters at Loss of Attitude Control

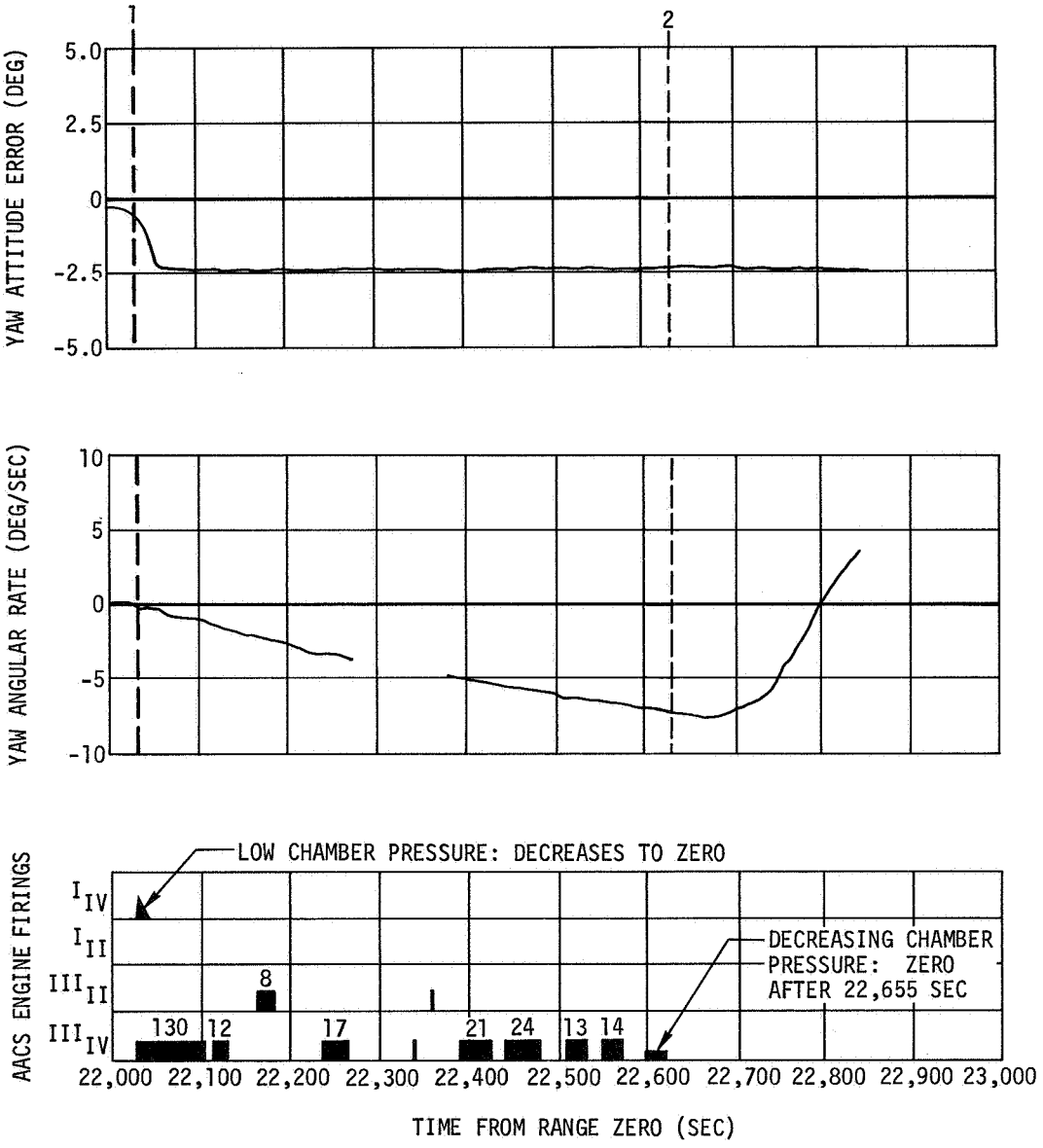

Figure 21-35. Yaw Axis Parameters at Loss of Attitude Control

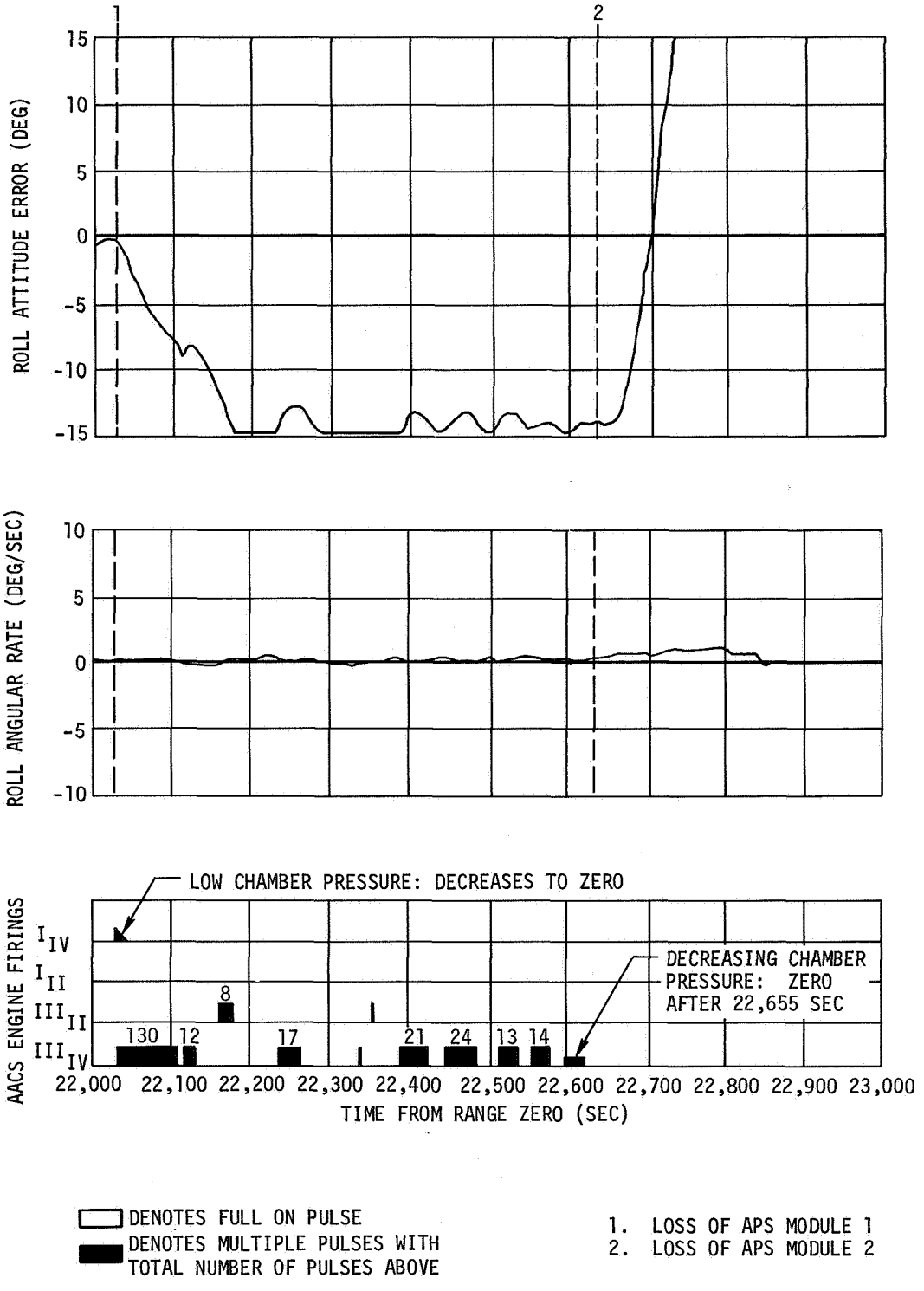

Figure 21-36. Roll Axis Parameters at Loss of Attitude Control

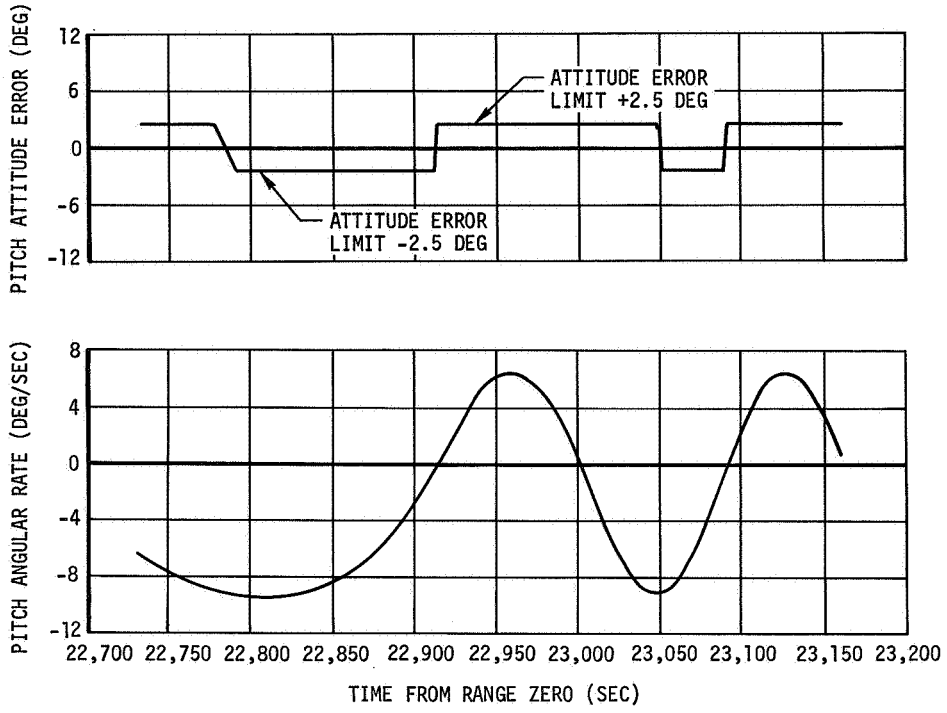

Figure 21-37. Pitch Axis Parameters After Loss of Attitude Control

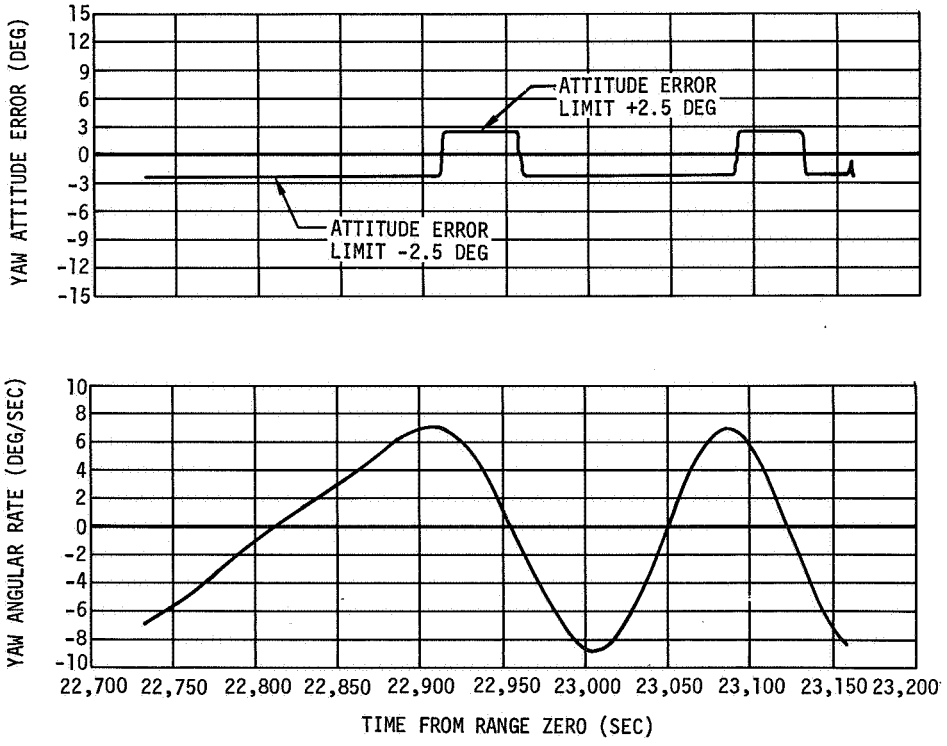

Figure 21-38. Yaw Axis Parameters After Loss of Attitude Control

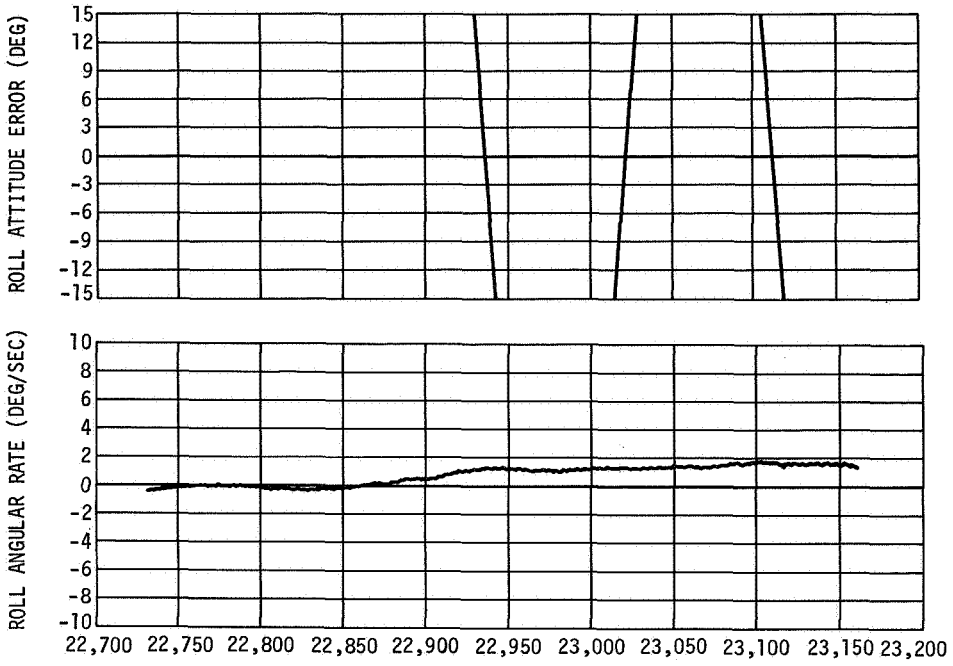

Figure 21-39. Roll Axis Parameters After Loss of Attitude Control

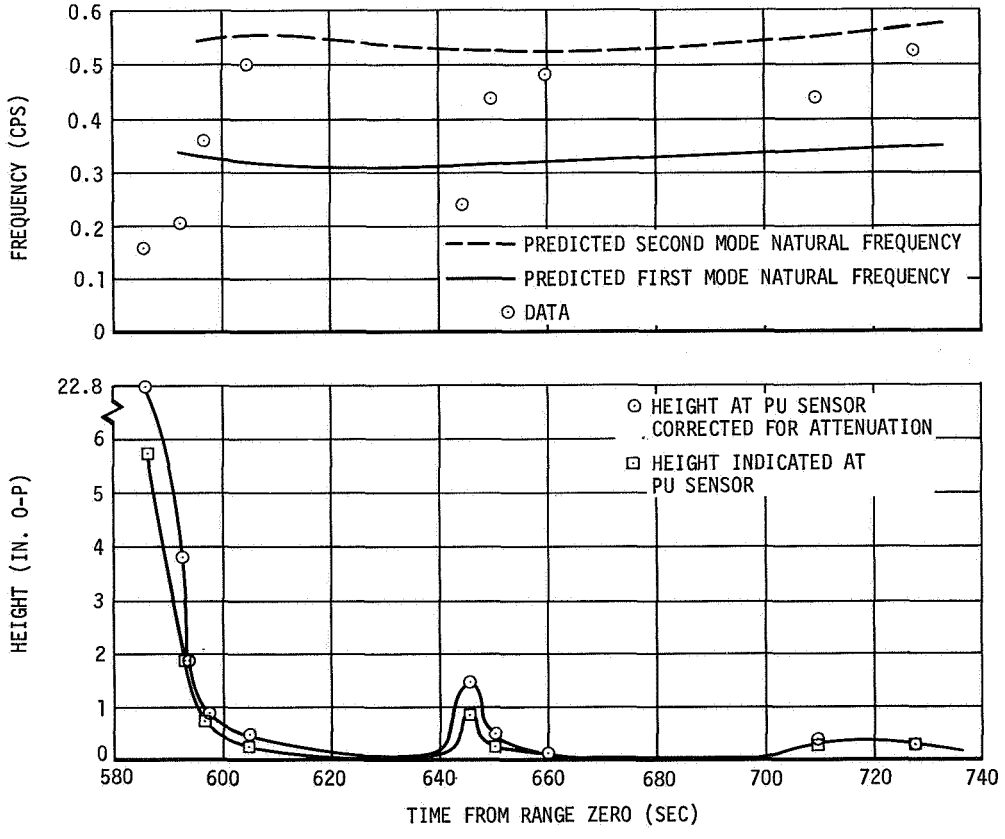

Figure 21-40. LH2 Slosh Frequencies and Amplitudes - First Burn

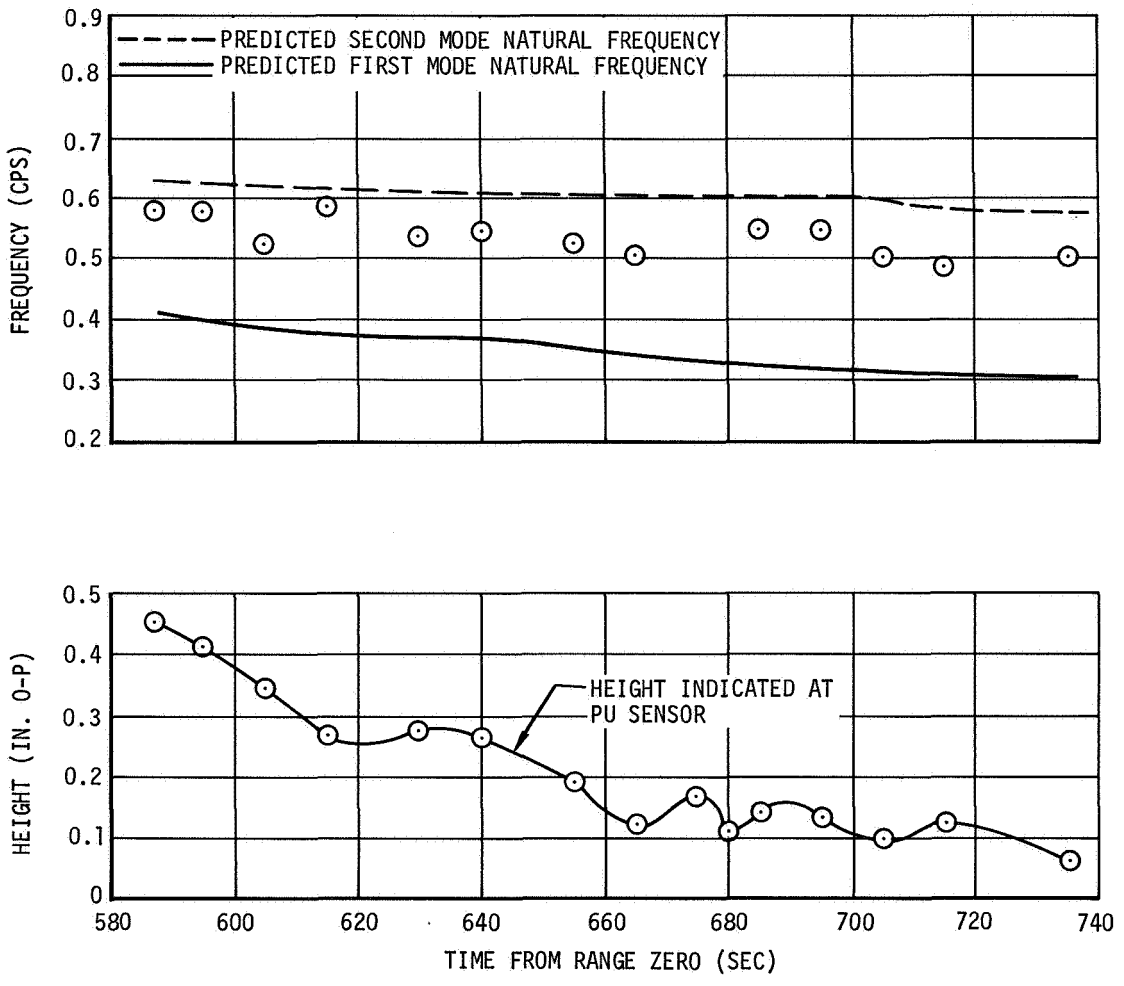

Figure 21-41. LOX Slosh Frequencies and Amplitudes - First Burn

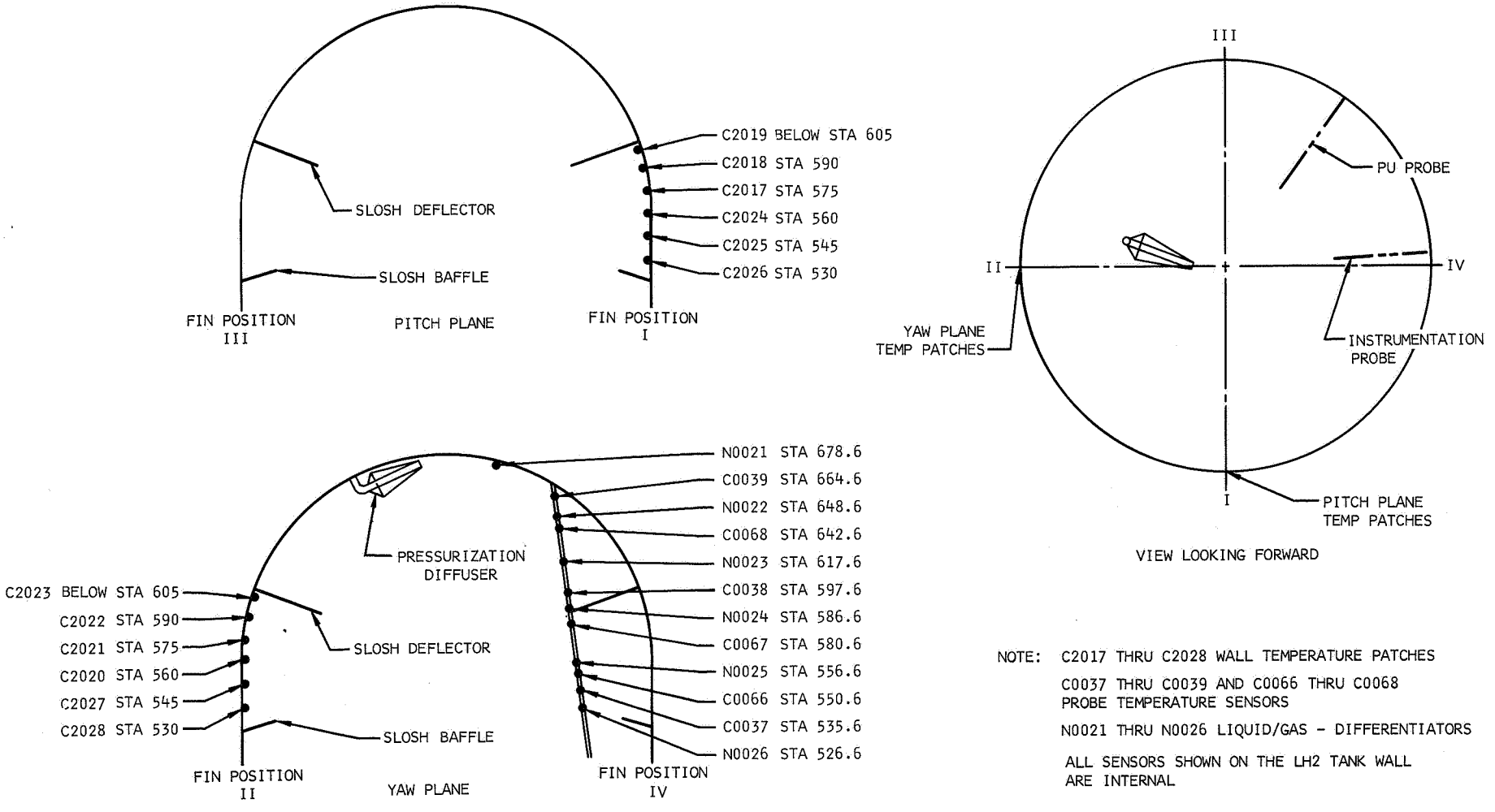

Figure 21-42. LH2 Instrumentation Location in Forward Dome Area

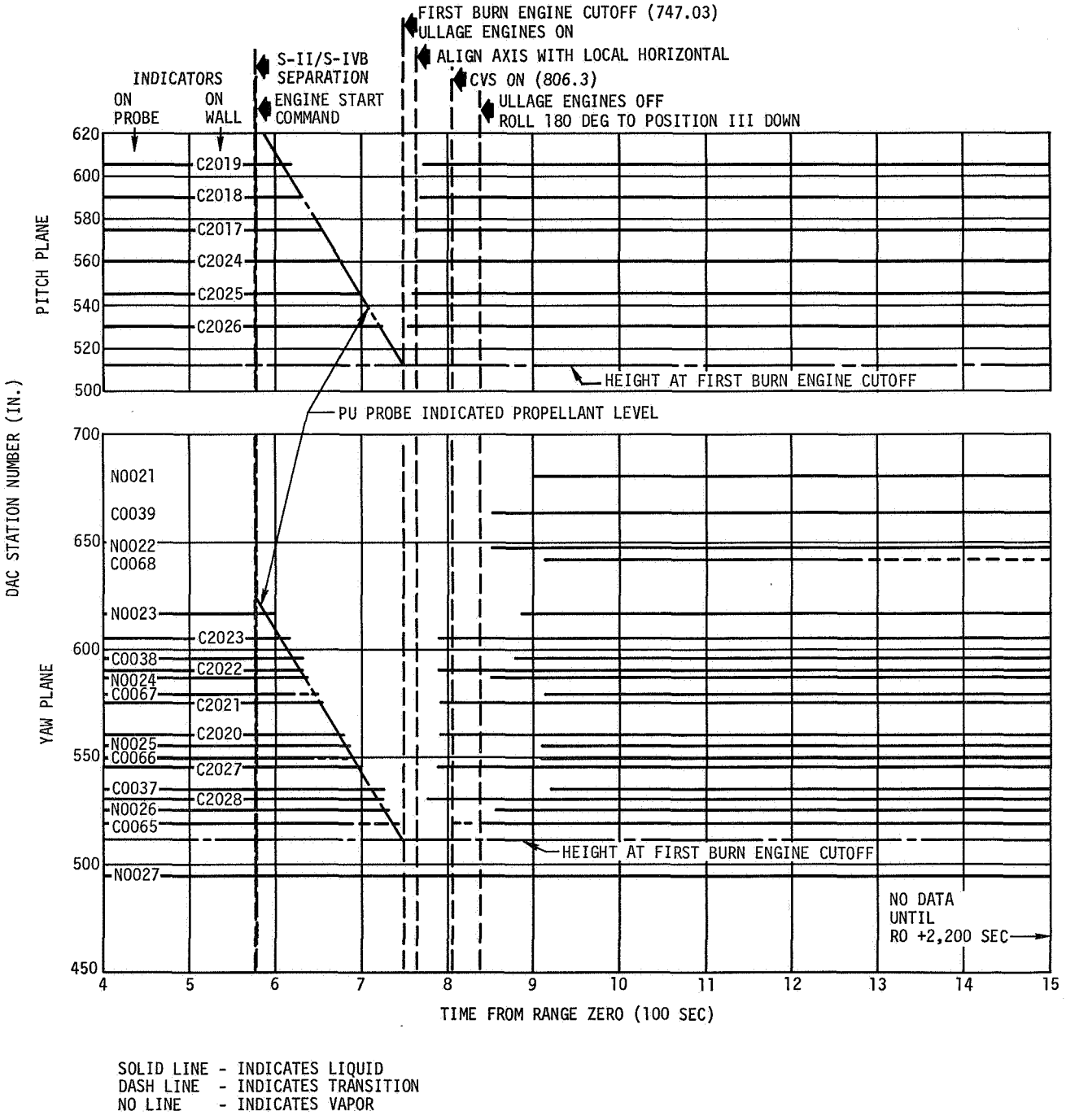

SOLID LINE - INDICATES LIQUID
DASH LINE - INDICATES TRANSITION
NO LINE - INDICATES VAPOR

Figure 21-43. LH2 Sensor Data - S-IVB First Burn and Engine Cutoff

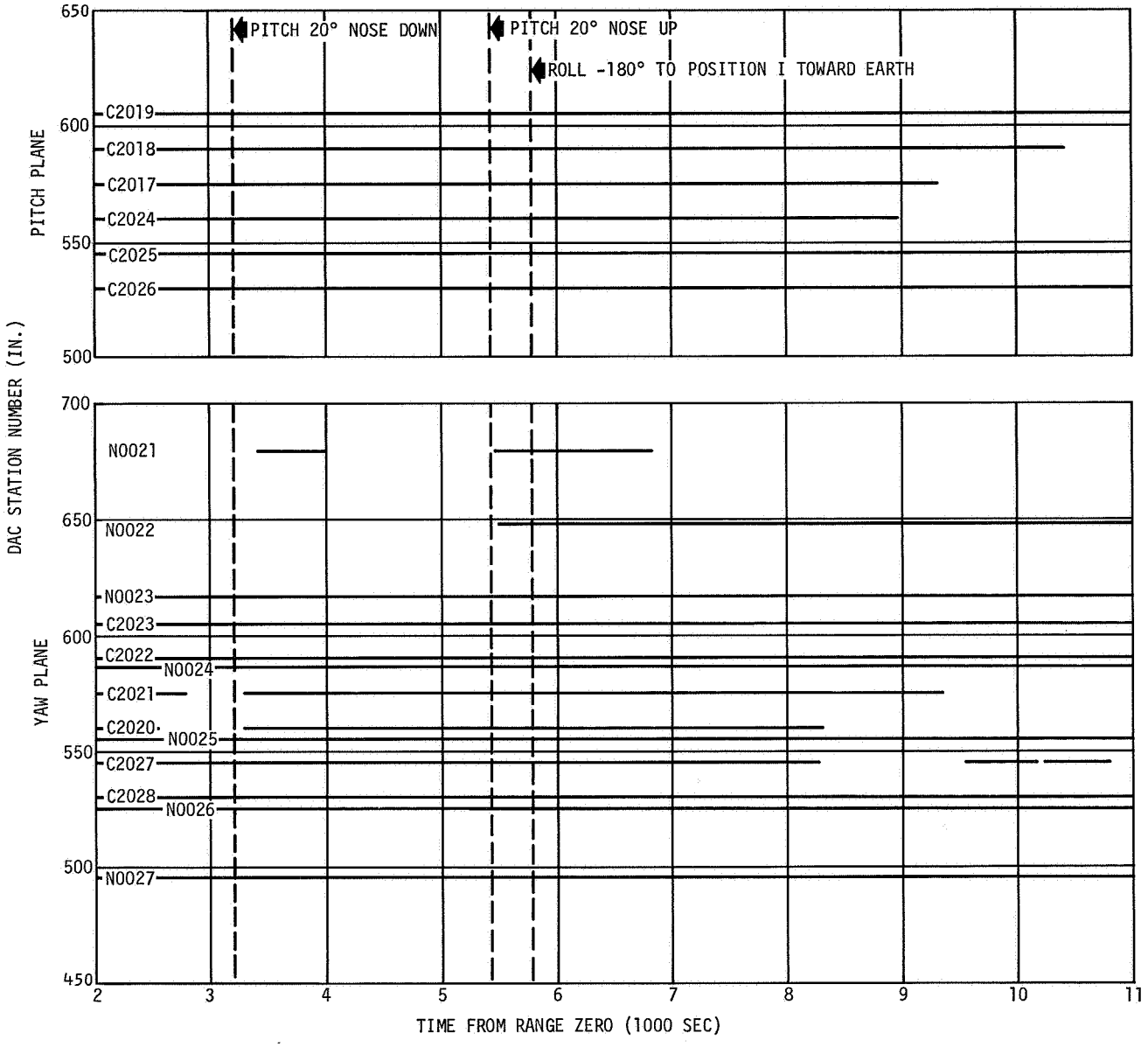

Figure 21-44. Sensor Data - Orbital Coast

1. TB6 BEGIN RESTART PREPARATIONS
2. ULLAGE ENGINES ON
3. LH2 CVS OFF
4. RESTART ORIENTATION MANEUVER
5. LH2 TANK REPRESSURIZATION
6. ENGINE START COMMAND
7. ENGINE CUTOFF COMMAND

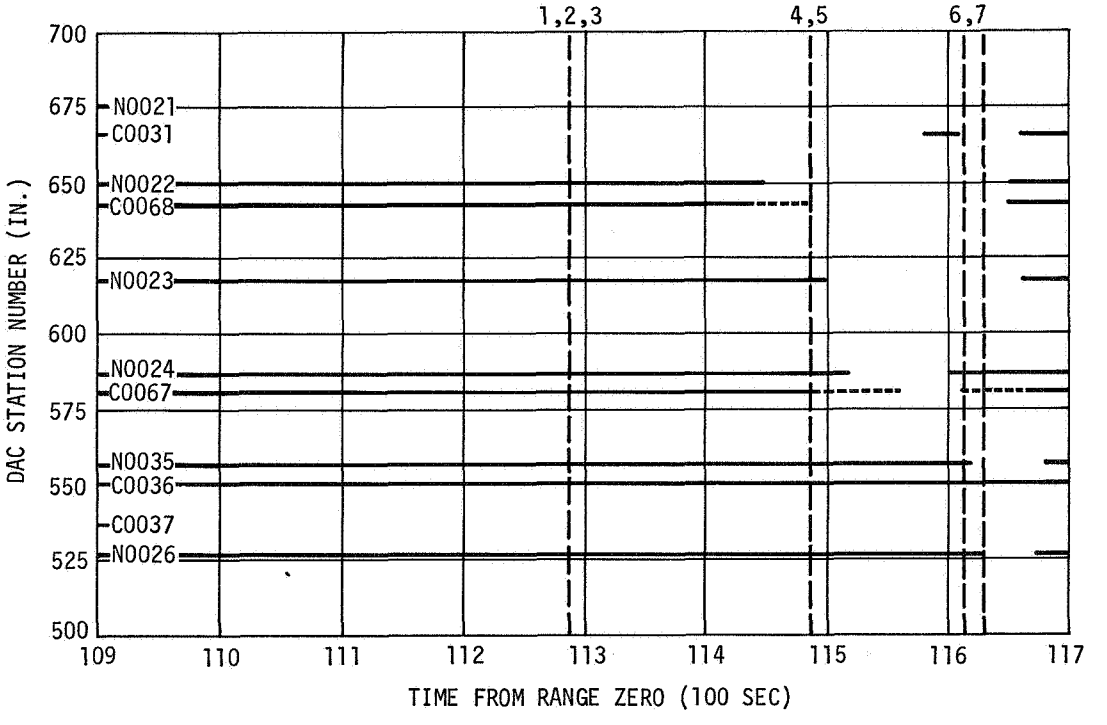

SOLID LINE - SENSOR INDICATES LIQUID
NO LINE - SENSOR INDICATES VAPOR
DOTTED LINE - SENSOR INDICATES TRANSITION

Figure 21-45. Instrumentation Probe Sensor Data - Prior to Restart

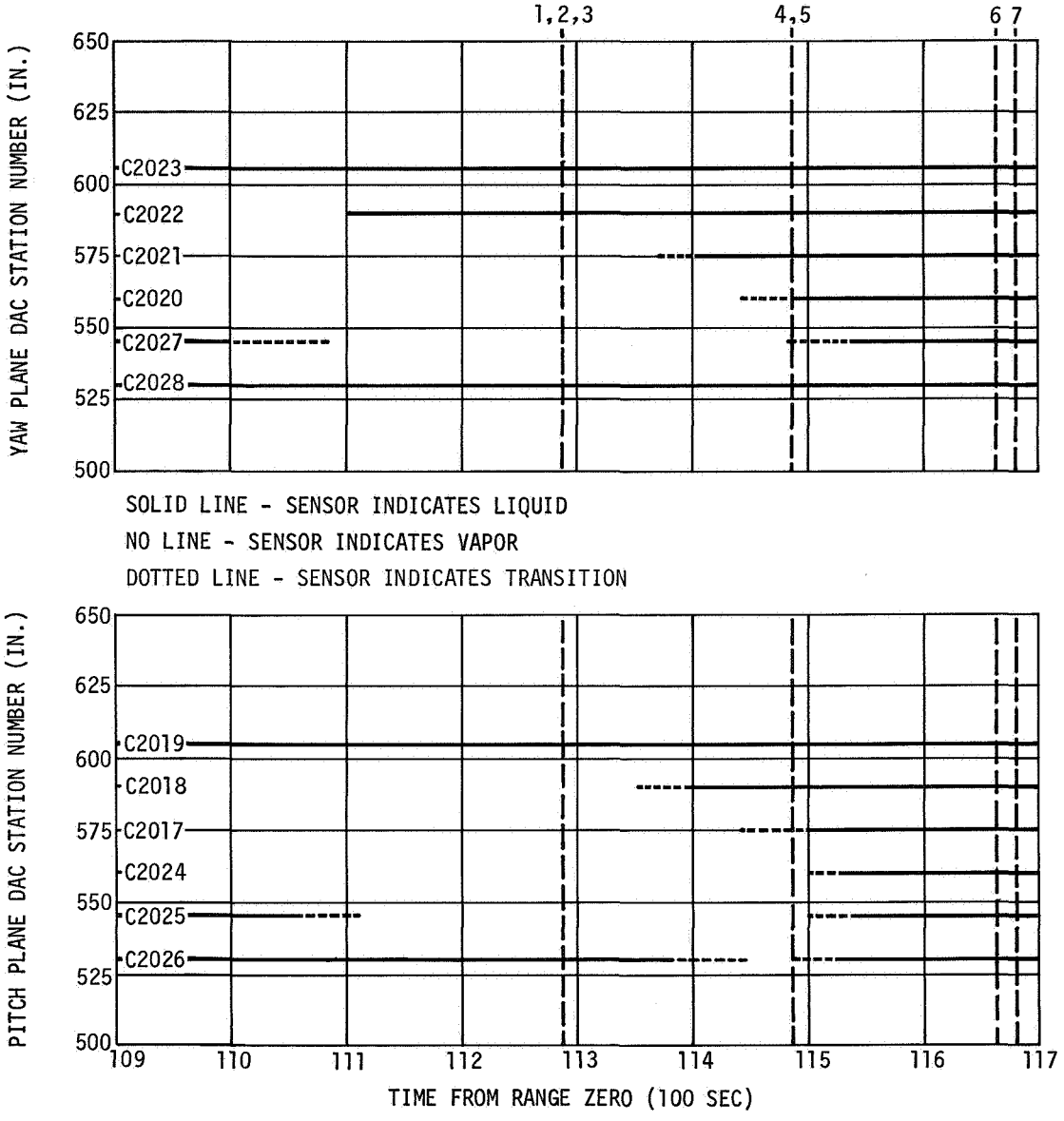

1. TB6 BEGIN RESTART PREPARATIONS
2. ULLAGE ENGINES ON
3. LH2 CVS OFF
4. RESTART ORIENTATION MANEUVER
5. LH2 TANK REPRESSURIZATION
6. ENGINE START COMMAND
7. ENGINE CUTOFF COMMAND

Figure 21-46. Tank Wall Temperature Sensor Data - Prior to Restart

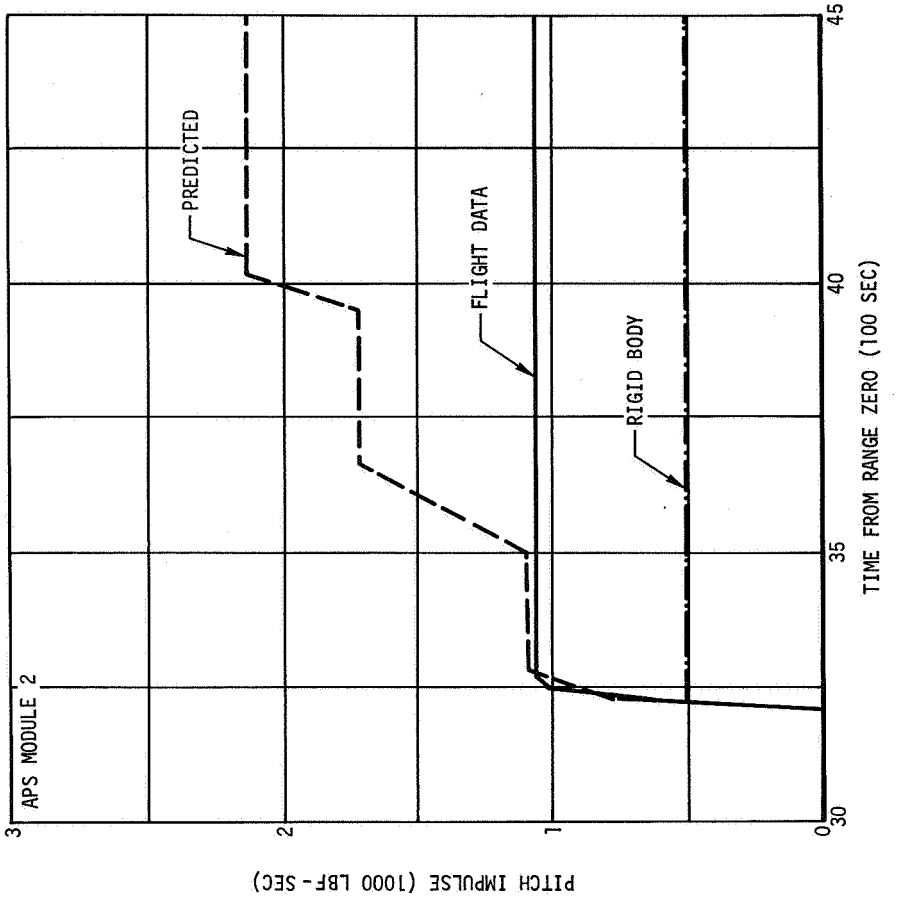

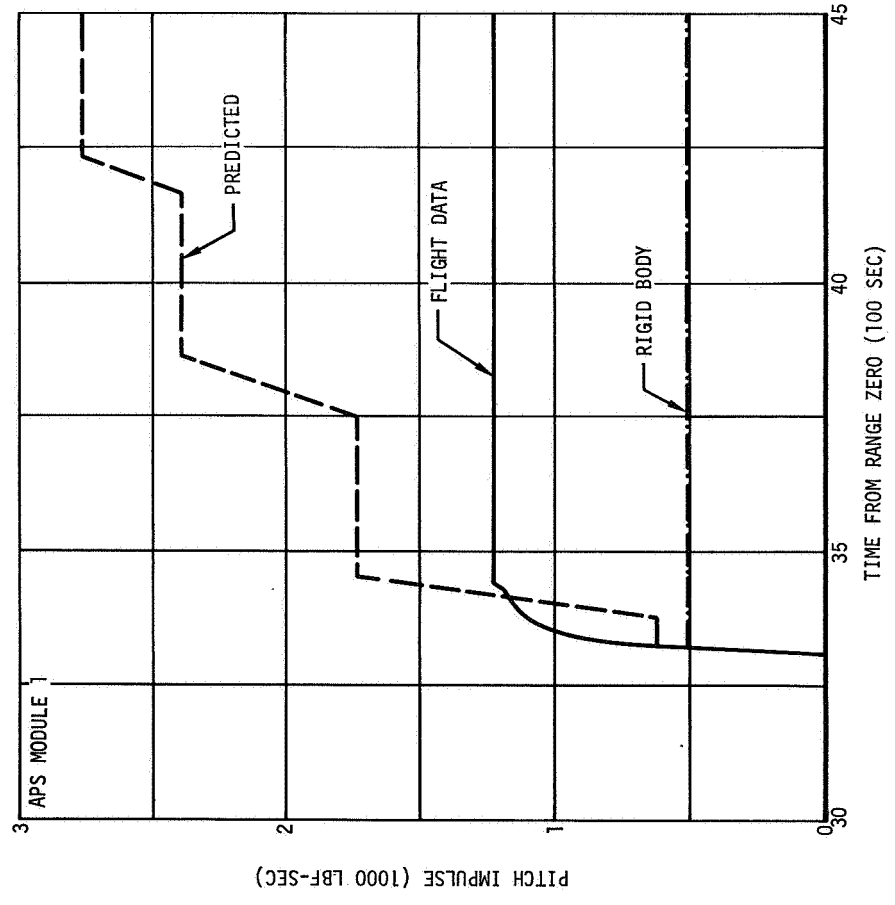

Figure 21-47. APS Impulse Requirements for 20 deg Pitch Down Maneuver

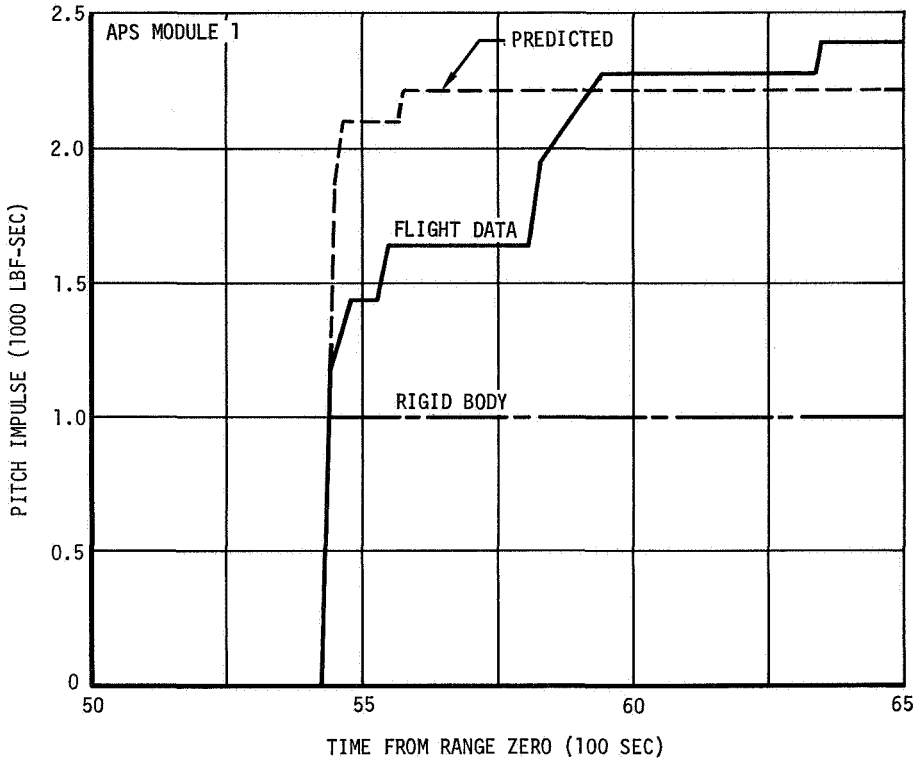

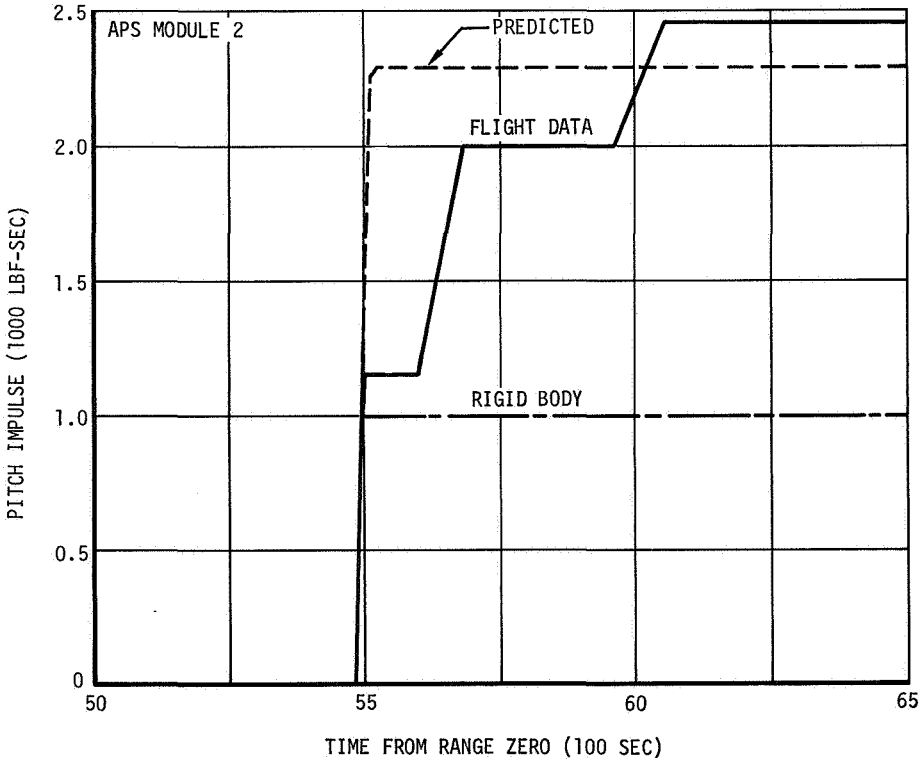

Figure 21-48. APS Impulse Requirements for 20 deg Pitch Up Maneuver

SECTION 22

HYDRAULIC SYSTEM

22. HYDRAULIC SYSTEM

The S-IVB hydraulic system performance was within predicted limits and the entire system operated satisfactorily during liftoff and first burn. There was no loss of system fluid due to overboard venting as a result of reservoir fluid thermal expansion. System internal leakage was 0.64 gpm which is within the 0.4 to 0.8 gpm allowable range. The hydraulic pump required 5.6 hp from the engine during first burn.

Both the auxiliary and main hydraulic pumps failed to develop pressure in the period preceding and during second burn. It is believed that the pumps were cavitating due to an obstruction of frozen hydraulic fluid in the pump suction line between the reservoir and main pump. Flight data indicated that the freezing was in a localized area and possibly caused by fluid impingement from a leaking cryogenic fuel line. Reservoir fluid level, temperature and pressure levels were normal during this time period.

A summary of system pressure measurements obtained during various phases of flight is presented in table 22-1. Figures 22-1 through 22-5 graphically depict various system parameters plotted against time from liftoff.

22.1 Prelaunch

During countdown the auxiliary hydraulic pump was switched to coast thermal mode ON at RO -6.5 hr, just prior to start of propellant loading. The accumulator was precharged to 2,200 psia at 40 deg F. Reservoir fluid level (auxiliary pump OFF) was 78.5 percent at 26 deg F. There were no thermal cycles prior to launch.

The auxiliary hydraulic pump was switched to flight mode ON, coast mode OFF at RO -8.5 min (11:51:20 GMT). After stabilization the following measurements were recorded:

System pressure (D0041):	3,600 psia
Reservoir pressure (D0042):	170 psia
Pump inlet fluid temperature (C0050):	52 deg F
Reservoir fluid temperature (C0051):	45 deg F
Reservoir fluid level (L0007):	17 percent

22.2 Boost and First Burn Phases

During boost the pump inlet and reservoir fluid temperatures rose steadily as auxiliary pump operation warmed the fluid. Accumulator gas and actuator cylinder temperatures remained low during boost but started to rise as soon as the engine driven pump started.

The pitch actuator differential pressure recorded a 5.5 cps pressure oscillation between RO +121.5 to RO +135.0 sec. The maximum amplitude recorded was 400 psi (peak to peak). The yaw actuator differential pressure did not show a change in pressure during this interval of time. These oscillations occurred when the maximum S-IC stage pogo effect was taking place.

System temperatures did not rise normally during first burn. The following characteristics have not been experienced on previous flights:

a. At Engine Start Command (ESC) +111 sec (RO +688 sec) the yaw actuator suddenly started to lose temperature at the rate of approximately 0.3 deg F/sec.

b. At ESC +124 sec (RO +701 sec) the pump inlet fluid temperature suddenly jumped 30 deg F in 14 sec and then decreased 12 deg F at cutoff.

c. The main pump discharge line temperature rose normally from the start of engine burn. At ESC +107 sec (RO +684 sec) it suddenly started to drop and then leveled off at engine cutoff.

Engine deflections in the pitch plane exceeded previously observed excursions on other Saturn flights by a considerable amount. The deflections in the yaw plane were much less than those encountered in the pitch plane throughout first burn. The large amount of pitch actuator activity was due to abnormal SII/S-IVB separation transients caused by engines No. 2 and 3 on the S-II cutting off earlier than scheduled during the S-II boost portion of the powered flight. These engines are symmetrical about the S-IVB pitch plane.

Prior to the event Flight Control Computer S-IVB Burn Mode ON, the pitch and yaw actuator positions (G0001 and G0002) were at null. During S-IVB first burn, their average offset values were +0.37 and -0.75 deg respectively. At engine cutoff after the event Flight Control Computer S-IVB Burn Mode OFF, the actuators returned to their original null positions. The actuators were offset from null during powered flight due to the displacement of the vehicle's center of gravity off the vehicle's longitudinal axis, and due to J-2 engine installation tolerances, thrust misalignment, and uncompensated gimbal clearances and thrust structure compression effects.

The pitch actuator's first movement at separation occurred at RO +577.5 sec, the yaw actuator at RO +577.9 sec. A maximum deflection of 6.69 deg occurred in the pitch plane due to separation transients at RO +580.9 sec; thus the displacement of the engine from its offset during this portion of powered flight was 6.32 deg. The maximum slew rate of the engine was 15.1 deg/sec. This rate falls within the hydraulic servo flow limit of 10.5 $\pm$1.5 gal/min. The actuator did not retract to its limit since full differential pressure was not developed. The engine responded to pitch guidance commands at RO +643.8 sec and moved to -0.437 deg, or 0.807 deg from the offset position. At RO +747.30 sec, the S-IVB engine cutoff signal was received. At this time, the pitch attitude rate signal was causing the pitch actuator to retract at a rate of 0.68 deg/sec. The vehicle could not respond to the guidance signals since engine thrust was cutoff. The actuator continued to move and reached +2.79 deg. At RO +750.76 sec the guidance signal was removed. This caused the engine to null at a rate of 16.3 deg/sec. The actuator was able to return to null since hydraulic pressure was still on the system. The yaw actuator experienced its maximum deflection of -1.35 deg at RO +586.0 sec which is 0.6 deg from its offset position. The maximum pitch and yaw actuator differential pressures during first burn were -800 psi at

RO +577.6 sec and -650 psi at RO +585.3 sec respectively. This is equivalent to 25.7 and 18.9 percent of the respective actuator's maximum torque capability at that particular time. A differential pressure bias of -200 psi existed in both planes at the beginning of powered flight. A differential pressure of +900 psi was developed in the pitch actuator at RO +750.76 sec when guidance was removed. This is equivalent to 26.2 percent of the actuator's maximum torque capability.

Actuator separation transient loads were not considered excessive. Proper operation of the actuator dynamic pressure feedback mechanism is indicated by noting the damping of the pitch and yaw actuator differential pressure traces. The hydraulic servoactuators responded properly to the guidance signals.

Figure 22-1 shows the activity of various system measurements during this phase of flight.

22.3 Parking Orbit

After engine cutoff the pump inlet fluid temperature continued to rise as heat was transferred from the LOX turbine dome to the pump manifold. It rose to a peak of 185 deg F at RO +8,300 sec and then started to decrease at a rate of 0.39 deg F/min. Reservoir fluid temperature dropped approximately 30 deg F during orbital coast prior to second burn. The pitch actuator temperature fell off very sharply. Just prior to restart it was -60 deg F. The yaw actuator was at -28 deg F prior to restart. The pump discharge line declined to a minimum of 2 deg F at restart.

The auxiliary hydraulic pump was commanded to coast mode ON (thermal switch control) after engine cutoff. There were no thermal cycles during the coast phase.

At RO +10,822 sec the pump was commanded to flight mode ON and coast mode OFF but the pump failed to produce any discernable hydraulic pressure. There was an increase in current draw to the pump motor of 12 amp which is an indication that the pump was cavitating. Normal motor current is 45 amp. A 10 psi reservoir pressure increase occurred approximately 250 sec later but this was of short duration.

Flight history during this phase is shown on figures 22-2 through 22-4.

22.4 Second Burn

After second burn Engine Start Command, the main engine driven hydraulic pump failed to produce any measurable hydraulic system pressure. Flight data was carefully analyzed at RO +11,622 sec which corresponds to start of LOX turbine spin after second burn Engine Start Command. At this time there was a small fluctuation in reservoir oil pressure, the actuators moved slightly and there was 27 deg F momentary drop in pump inlet fluid temperature. This indicated that the main pump was turning and moving fluid but unable to develop system pressure.

It has been concluded that both the auxiliary and main hydraulic pumps did not produce pressure preceding and during second burn due to cavitation. Since the reservoir fluid level

and pressure were normal it is believed that the condition was caused by localized freezing of the pump suction line hydraulic fluid by an unusual source such as fluid impingement from a leaking cryogenic fuel line. The pump suction line runs across the gimbal plane in line with position III between the accumulator reservoir on the thrust structure and the main hydraulic pump on the LOX turbine dome. If this line is subjected to cryogenic freezing, a blockage of fluid would result in the line (pour point of MIL-H-5606 is -90 deg F) which would prevent reservoir fluid from reaching the inlets of both pumps.

The pitch and yaw hydraulic actuators were offset from null +1.2 and -3.0 deg respectively at RO +10,822.83 sec when the hydraulic auxiliary pump was commanded ON for second burn. The actuators attempted to center the engine, however, since hydraulic system pressure was not sufficiently developed nor sustained they were only able to move to +0.9 and -2.1 deg positions. At RO +11,070 and RO +11,500 sec both actuators attempted to center and at RO +11,620 sec the yaw actuator again moved indicating some hydraulic pressure activity. Other hydraulic parameters also indicated activity at these times. The pitch and yaw actuators were unable to respond to the incoming IU signals. Their differential pressures were zero during this portion of the flight.

Two attempts were made to start the auxiliary hydraulic pump by ground command but with no success. The pump inlet and reservoir fluid temperatures continued to sink at approximately the same rates. The pump discharge line temperature measurement which was located near the system thermal switch, apparently varied with exposure to solar radiation or earth's shadow. Curve plots of flight measurements during attempted second burn are shown in figures 22-2 through 22-5.

TABLE 22-1
HYDRAULIC SYSTEM PERFORMANCE

PRESSURES	PREDICTED DURING PUMP OPERATION (psia)	LIFTOFF (psia)	FIRST BURN (psia)	PARKING ORBIT (psia)	SECOND BURN (psia)
System fluid (D0041)	3,500 to 3,650	3,600	3,600	-	-
Accumulator gas (D0043)	3,500 to 3,650	3,610	3,610	2,370*	2,380*
Reservoir fluid (D0042)	165 to 185	170	172	67	62
Aux pump air tank (D0223)	250 to 450	425	430	430	425
Aux pump motor air (D0209)	15 to 35 psig	20 psig	36 psig	35 psig	36 psig
RESERVOIR FLUID LEVEL	PREDICTED (percent)	LIFTOFF (percent)	FIRST BURN (percent)	PARKING ORBIT (percent)	SECOND BURN (percent)
Pump ON	20 to 25	18	21	-	-
Pump OFF	80 to 90	-	-	82	83

*Corrected to 68 deg F

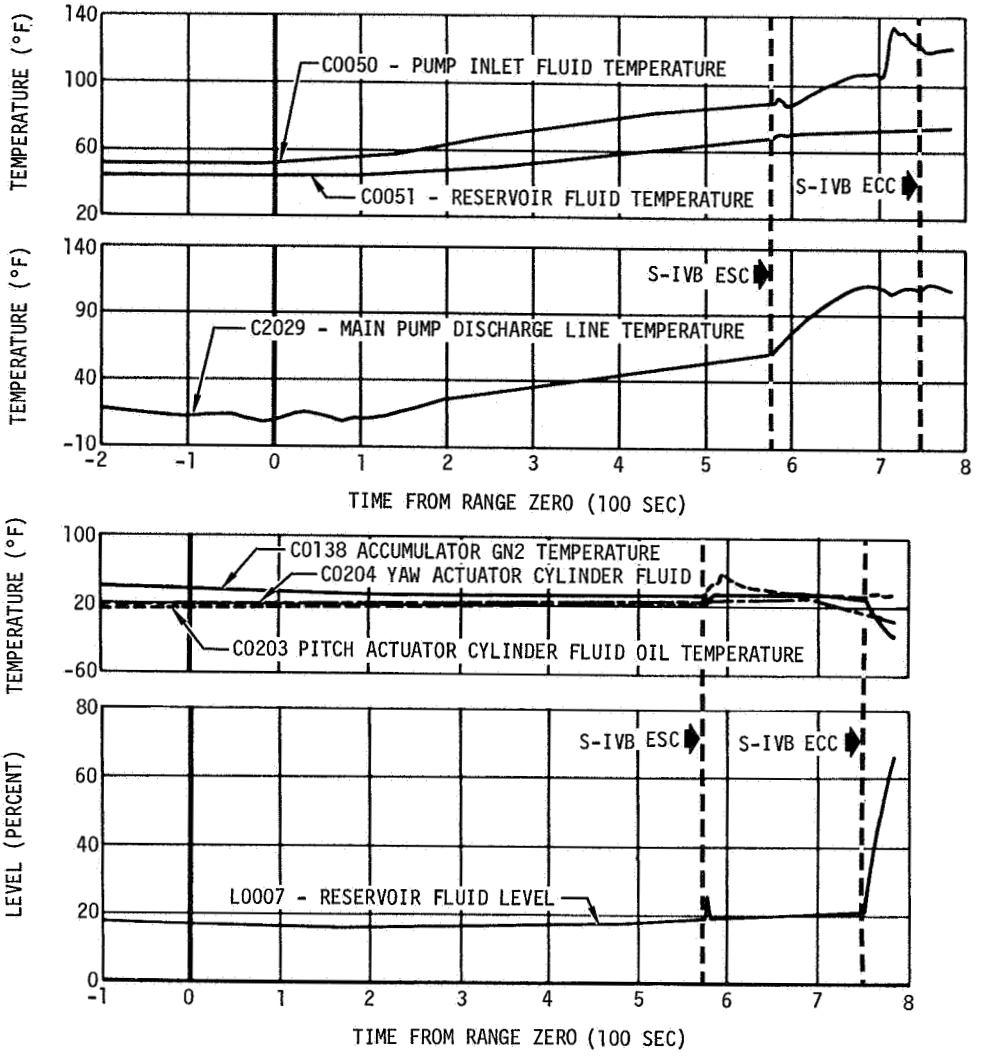

Figure 22-1. Hydraulic System Temperature and Reservoir Fluid Level - Boost and First Burn

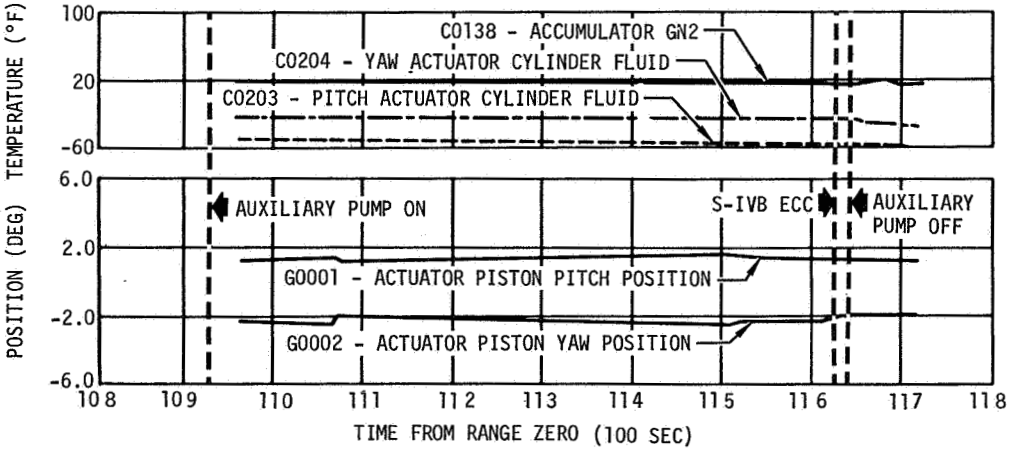

Figure 22-2. Hydraulic System Temperature and Actuator Piston Position - Restart

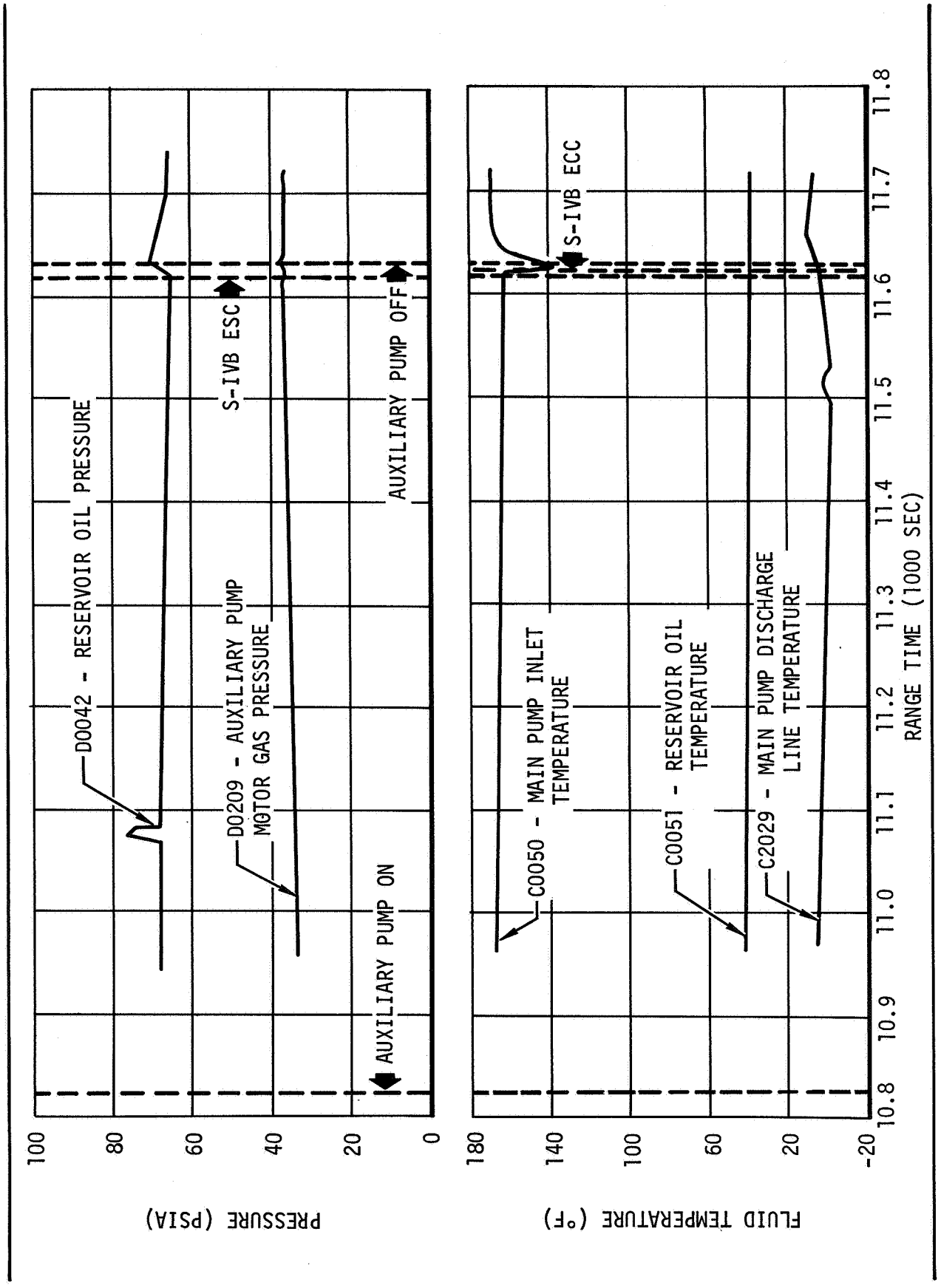

Figure 22-3. Hydraulic System Pressures and Fluid Temperatures - Restart

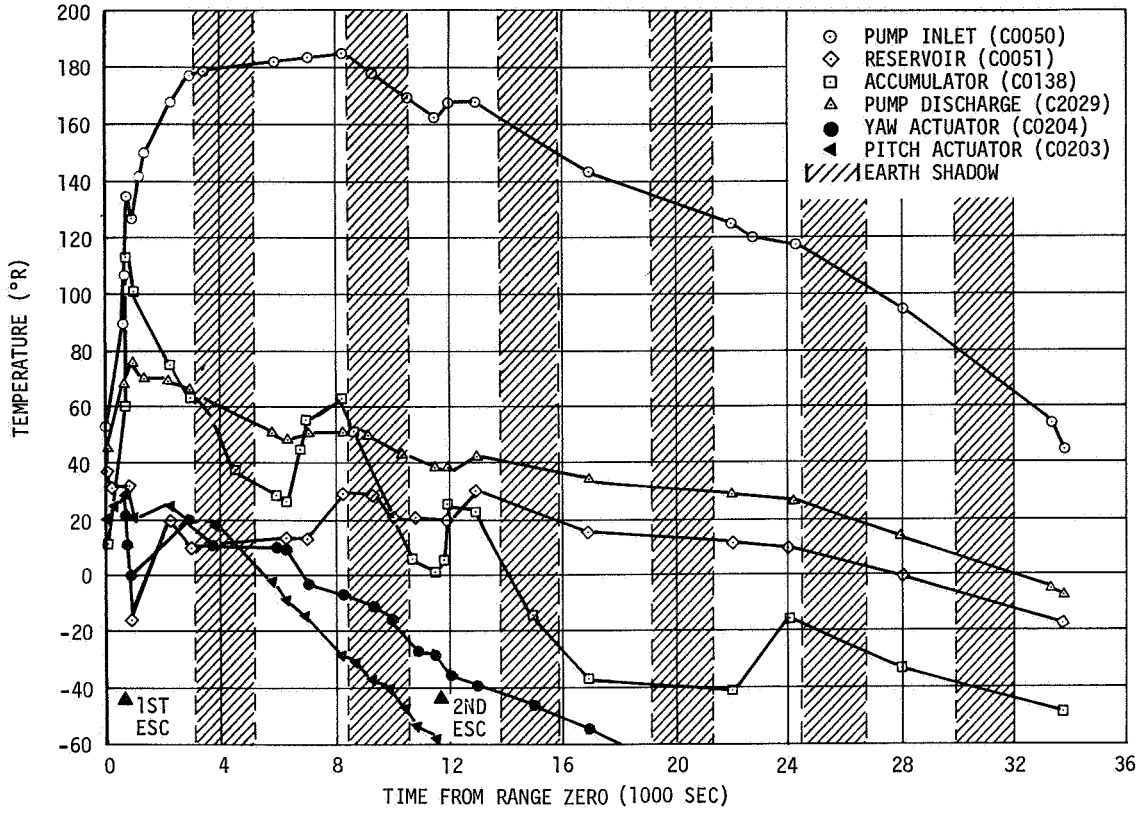

Figure 22-4. Hydraulic System Temperatures - First Burn to End of Data

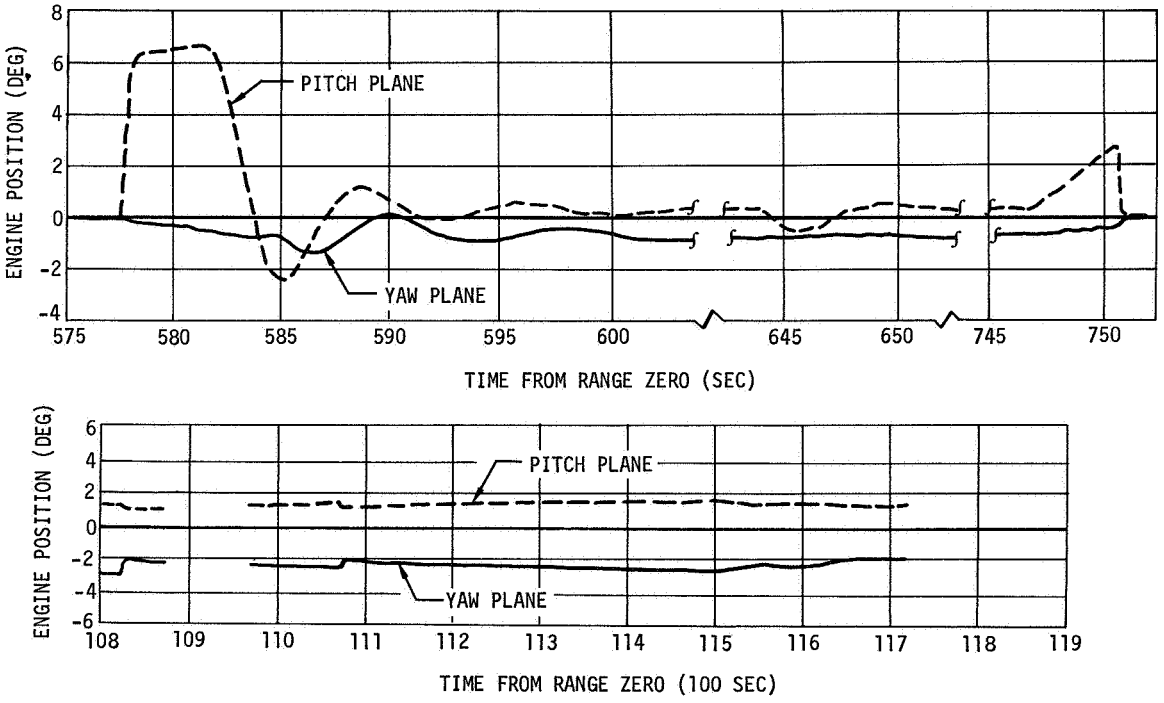

Figure 22-5. Engine Position

SECTION 23

STAGE STRUCTURE AND ENVIRONMENT

23. STAGE STRUCTURE AND ENVIRONMENT

23.1 Flight Load Conditions and Structural Integrity

An evaluation of strain, acceleration, pressure, and temperature data from the S-IVB for the AS-502 trajectory indicated adequate structural strength existed in the stage for the conditions encountered.

The flight environment of the S-IVB deviated from expected conditions in two structurally significant respects. First, during S-IC boost, the AS-502 vehicle and spacecraft experienced relatively severe 5 1/2 cps longitudinal vibrations as reported in section 25. Second, during S-IC boost at RO +133 sec, the S-IVB experienced an unusual load redistribution in the forward skirt as indicated by strain gage measurements at skirt stringers. This load redistribution was evident throughout the remainder of the high axial loads of first stage boost to center engine cutoff (CECO) at RO +144 sec. The combined loads from the load redistribution and the longitudinal vibrations were within the structural capability of the S-IVB forward skirt.

The load distribution to the aft skirt was normal, which indicates the propellant tank structure was effective in uniformly distributing the unusual axial load distributions of the forward skirt to the aft skirt.

The flight test data indicate that the sudden change in axial load distribution through the S-IVB forward skirt at RO +133 sec resulted from changes in structure located above the forward skirt. The character of these structural changes and their causes were investigated by an engineering task group at NASA Manned Spacecraft Center, Houston, Texas. The results of that investigation are to be published in a NASA/MSC report entitled, Anomaly Report No. 6 - Unexpected Structural Indications During Launch Phase, unpublished as of this writing.

Body bending moments and skin differential pressures were less than the maximum predicted values due to comparatively moderate wind shears and gusts. Vehicle axial accelerations were close to predicted values which verified the computed preflight axial loads for the S-IVB, except for the structurally noncritical anomaly of two S-II engines cutting out prematurely at about RO +414 sec. Axial loads computed from flight strain gage aft skirt data are in agreement with preflight computed axial loads from liftoff to approximately RO +60 sec. Beyond this flight time, the axial loads computed from stringer strain gage data appeared to be low apparently due to thermal effects on the structure from aerodynamic heating and to an approximate integration resulting from the limited number of instrumented stringers.

Recorded maximum temperatures of the S-IVB structure subjected to aerodynamic heating indicated the flight temperatures did not exceed maximum predicted temperatures.

The LH2 and LOX tank ullage pressures did not exceed corresponding design ullage pressures. The differential tankage pressures acting on the common bulkhead were as expected. The internal pressure of the common bulkhead remained substantially constant at less than 1 psia as predicted.

23.1.1 Body Strains and Stringer Loads

Thirty-two axial strain gages were installed on external hat stringers of the S-IVB. The gages were located at vehicle sta 3145 of the forward skirt and sta 2821 of the aft skirt. Eight measurement locations at each station were approximately equally spaced around the circumference. Two strain gages were installed at each measurement location, of which one gage was mounted to the side of the stringer near the neutral axis, and the other to the top of the stringer. The dual stringer strain gage installation permitted the evaluation of strains at the stringer neutral axis and hence more accurate calculations of stringer axial loads and body bending moments. The dual gage installations also provided data from which stringer internal bending moments could be evaluated. All strain gages were temperature compensated.

The recorded data from the strain gages were determined to be valid by the S-IVB-502 Data Qualification Review Board. These data were reviewed thoroughly and in detail and no electrical anomalies were detected. In particular, the unusual strain changes which occurred at RO +133 sec and which remained through CECO at approximately RO +144 sec were found to be valid by the Review Board. An analytical calculation at S-II engine ignition indicated that measured thrust computed from S-IVB strain measurements and predicted thrust were within 3 percent, and that the strain gages at that later time were performing normally.

The strain histories for the 16 gages on the aft skirt are presented in figure 23-1, and those for the 16 gages on the forward skirt are shown in figure 23-2. At RO -10 sec all measured strains have been adjusted to the computed correct strain corresponding to the 1 g axial load condition. This adjustment was necessary since the initial strain readings had drifted considerably due to the combined effects of added payload and propellant weights, propellant cryogenic temperatures, and ullage pressurizations. The adjustment to each measured strain at liftoff was applied uniformly to the corresponding measured strain trace throughout flight, so that measured strain increments during flight were not affected. The increments of strain on the S-IVB due to bending moments from ground winds were computed and found to be relatively small. Ground wind strains have been neglected in the adjustments to corrected strains at liftoff.

The maximum and minimum strain envelopes shown in figures 23-1 and 23-2 were calculated from design conditions and include the effects of maximum expected aerodynamic gusts and wind shears. The envelope also includes the tolerances of ± 7 percent for the telemetry system and ± 3 percent for predicted engine thrust. The predicted strains for the top mounted gages were computed using coefficients obtained from the AS-501 vehicle calibration conducted 19 April 1967.

The stringer side mounted gages on the aft skirt (figure 23-1) provided strain histories substantially as predicted except at times approaching CECO and outboard engines cutoff (OECO). At these flight times, airloads should be nearly non-existent and body bending negligible. Hence, the side gage strain traces ideally would converge approximately to

a common value at OECO. The non-convergence of the measured strains after RO +80 sec is apparently due in part to differential structural expansion or contraction from aerodynamic heating. However, the heating did not significantly affect the evaluation of flight body bending moments which peaked at approximately RO +68 sec. Also, the aerodynamic heating influence was minimized in the evaluation of maximum axial loads at CECO by using differential strains referenced to zero thrust strains at S-IC separation.

The stringer top mounted gages on the aft skirt (figure 23-1) provided strain data having less convergence at OECO than in the side gage data. The top gages were displaced from the stringer neutral axis and were sensitive to local stringer bending. These data were useful in analyzing the stringers for local bending. The strains from the top gages, like those from the side gages, were less than the maximum design strains shown in the figures. It is to be noted that the aft skirt strain traces indicate no unusual strain changes at RO +133 sec, such as subsequently will be discussed for the forward skirt. It appears that the propellant tankage structure distributed axial loads from the forward skirt uniformly to the aft skirt.

Figure 23-3 illustrates the effect of aerodynamic heating on stringer strains. The strain data from gages No. 70 and No. 74 have been plotted to show typical trends for side mounted gages, and the broken line curves show the traces adjusted to remove temperature effects. The adjustments result from the assumption that without aerodynamic heating, the measured strain traces would ideally decrease to zero strain (zero thrust) at S-IC separation (RO +148 sec). However, the actual measured strain traces, after correction to the 1 g condition, did not decrease to zero strains at RO +148 sec and the residual strains were assumed to be measurements of thermally induced strains. Residual compressive strains at RO +148 sec were subtracted from measured strains at CECO (RO +144 sec) to show flight strains independently of temperature effects. Similarly, residual tension strains were additive to show flight strains without internal temperature effects. These adjustments were assumed constant from CECO (RO +144 sec) back to RO +120 sec, and to decrease linearly to zero strain adjustment at RO +60 sec. This strain adjustment distribution corresponds with the aerodynamic heating which began at approximately RO +60 sec and stabilized at higher temperatures near RO +120 sec. These adjustments to remove temperature effects were applied to all side gage strain data to allow more accurate calculations of body bending moments and stage axial loads. However, thermally induced strains were reacted internally by the structure, and hence these increments of strain were included in detailed stringer stress analyses.

The strain histories (figure 23-2) for the 16 forward skirt strain gages indicate greater aerodynamic heating effects than occurred in the aft skirt. It is also seen that a number of strain measurements experienced load shifts at RO +133 sec, and that these shifts were retained throughout the remainder of S-IC powered flight. These strain shifts at RO +133 sec are summarized in the polar bar chart of figure 23-4. In the chart, negative values indicate increases in compression and positive values indicate decreases in

compression. Figure 23-4 includes identification of gage or measurement numbers, skirt stringer numbers, vehicle position numbers (I through IV), and values of strain changes in micro inches per inch. The strain shift at the side gage of stringer No. 81 was 0.00115 in./in. which corresponds to an increase of the stringer axial compression load of approximately 4,800 lbf. Stringers No. 95 and No. 27 experienced much smaller increases in compression. Stringers No. 14, 27, 54, 81, 95 and 108 experienced relatively small changes in strain at the top mounted gages. These gages reflected the combined effects of axial loads, local stringer bending, and shifts of the locations of the applied axial stringer loads. Changes in readings of the stringer top mounted gages and side mounted gages could result from changes in stiffnesses or load paths of structure above the S-IVB forward skirt.

The sudden change in stringer axial loads is further illustrated by figure 23-5 which shows polar plots at RO +132 sec compared to RO +134 sec for the S-IVB-502 forward skirt. The large change is evident at stringer No. 81. For purposes of comparison, a similar plot is shown for the S-IVB-501 forward skirt at RO +135.5 sec. Only the S-IVB-502 plots have been adjusted to represent the total axial load.

The strain changes at RO +133 sec in the S-IVB forward skirt stringers appear to be due to a change in load path through the skirt apparently caused by a load path shift in structure above the skirt. This conclusion resulted after it was determined that the gross loads on the vehicle were normal, that the temperatures of the forward skirt were normal, and that the forward skirt stringer strain gage data were valid throughout powered flight. The indicated load change in stringer No. 81 from strain measurements was 4,800 lbf at the g loading of RO +133 sec, or about 1,200 lbf when related to a 1 g weight condition. Assuming several stringers adjacent to stringer No. 81 were also affected, then the total load change may have been of the order of approximately 2,500 lb or more related to the 1 g condition. The largest single weight in the S-IVB forward skirt was 100 lb and the largest in the instrument unit (IU) was approximately 150 lb. In contrast, the LM weighed 26,000 lb and the weight above the service lunar adapter panels was 64,000 lb. Hence, the large load change in the load path at stringer No. 81 evidently resulted from load redistributions from the large weights above the forward skirt rather than from any failure of supports for the relatively small weights in the skirt. A detailed postflight stress analysis of the forward skirt using measured strains throughout flight indicated that there was no stringer buckling and that positive margins of safety existed for the skirt. The strain gage data showed increasing compressive stringer loads with increasing axial load factors after the anomaly at RO +133 sec thereby providing supporting evidence that skirt stringer buckling did not occur. Thus, it appears evident that the forward skirt structural integrity was maintained and that a change in load path originated in structure above the S-IVB stage forward skirt.

The strain changes at RO +133 sec involved eight strain gages. However, at RO +107 sec there was an indication of a similar sudden shift of increased compressive strain from the

single measurement of side gage No. 66 at stringer No. 95. This strain shift is shown in figure 23-2. This single strain shift may have been the result of a preliminary change in structure above the S-IVB forward skirt preceeding the more pronounced structural changes at RO +133 sec. Further details of the anomalies, including considerations of the structure above the forward skirt, are presented in the Anomaly Report No. 6 referenced in paragraph 23.1.

The local stringer bending moments and axial loads for the aft and forward skirts at respective strain measurement sta 2821 and 3145 are shown in table 23-1. The table compares the maximum flight loads derived from strain gage data to the corresponding stringer local design loads. For the aft skirt, the critical maximum αq condition design loads were not exceeded, and including temperature effects a positive margin of safety existed. The forward skirt flight moments and axial loads calculated from measured strains exceeded design values. The results of the corresponding postflight stress analysis are presented in table 23-2. Stringer No. 95 was critical and the corresponding minimum margin of safety was +97 percent.

23.1.2 Axial Loads

The strain data measured for sta 2821 and 3145 during flight were used for computing axial load histories as presented in figures 23-6 and 23-7. The measured strain data were converted to stringer neutral axis strains, and adjusted to remove the internal strains induced by differential expansions and contractions from aerodynamic heating. From these adjusted data, the axial flight loads at the respective stations were computed. These axial load histories are shown compared to preflight computed axial loads. The divergence of the flight measured plots above RO +60 to RO +80 sec is attributed to thermal effects on the structure from aerodynamic heating and to the limited number of instrumented stringers which prevents a full integration of stringer loads.

Axial load factors measured during powered flight are presented in table 23-3. The maximum acceleration of 4.78 g occurred at S-IC CECO. This was slightly higher than the 4.73 g predicted value, and greater than the design limit axial load factor of 4.68 g at CECO as expected. Detailed stress analysis, including the effects of S-IVB flight measured temperatures, indicated positive margins of safety for the 4.78 g axial load condition.

23.1.3 Body Bending Moments

The strain data measured during flight was also used in computing bending moment histories, as shown in figure 23-8 for the aft skirt and figure 23-9 for the forward skirt. In each case, the measured strain data at three stringer locations was converted to stringer neutral axis strains, and adjusted to remove internal strains induced by aerodynamic heating. From these adjusted data, the maximum bending moments at the respective stations from flight loads were computed. In the figures, the computed flight moment histories are shown compared to preflight computed design limit moments. The design curve is a partial

envelope covering the time of maximum αq and showing the total effect of discrete wind shears and gusts occurring at each time point. The curves show the S-IVB was subjected to relatively moderate aerodynamic loading as compared to maximum design values.

During S-II powered flight, two adjacent outboard engines cut out inadvertently at about RO +414 sec (reference figure 8-6). The bending moment at sta 2821 of the aft skirt was computed using flight measured strains. The resulting moment was 9,600,000 in.-lb which was only about one-sixth of the limit design maximum bending moment, indicating ample margin of safety for the S-IVB with this anomalous condition.

23.1.4 Pressures - Skirts and Interstage

For the forward skirt of the S-IVB, no pressure measurements were taken because of confidence in prediction methods gained from S-IVB/IB flight test experience.

For the aft skirt and interstage, the maximum calculated bursting pressure during flight, based on pressure sensor measurements was 2.9 psid at RO +75 sec. This was less than the maximum limit design bursting pressure of 3.9 psid at RO +73 sec. The peak flight measured differential crushing pressure was -0.80 psid at RO +60 sec, which compares favorably to the maximum limit design crushing pressure of -1.66 psid at RO +58 sec.

23.1.5 Temperatures

A summary of maximum measured temperatures for the major structural assemblies subject to aerodynamic heating is given in table 23-4. The temperatures are shown separately for stringers and skin. Predicted maximum temperatures based on the maximum heating trajectory are also shown. A comparison of values shows flight temperatures did not exceed maximum predicted temperatures. This supports other evidence that S-IVB structural integrity was maintained.

23.1.6 LH2 and LOX Tank Ullage Pressures

The maximum LH2 ullage pressure recorded during prelaunch and through powered flight to S-IVB first burn engine cutoff was 37.0 psia. Subsequent ullage pressures during orbital coast reached a maximum of 34.0 psia. These values compare favorably with the limit design ullage pressure of 37.0 psia for the LH2 tank.

The limit design ullage pressure for the LOX tank is 44 psia, and the maximum ullage pressure recorded during prelaunch and powered flight through first burn was 43.0 psia. The maximum LOX tank ullage pressure recorded during orbital coast was 42.0 psia.

23.1.7 Common Bulkhead Pressure Environment

The S-IVB-502 ullage differential pressures on the common bulkhead during prelaunch, powered flight, and typical orbital coast are shown in figure 23-10. A positive differential pressure indicates the LOX tank ullage pressure exceeds the LH2 tank ullage pressure. At the apex of the common bulkhead these differential ullage pressures are the pressures across

the bulkhead after allowances for the liquid hydrogen head. Also included in the figures are curves showing the limit structural capability of the common bulkhead, and these limit curves have been calculated to include the liquid hydrogen head effects.

The maximum negative operational pressure during flight occurred due to a temporary decrease in LOX ullage pressure from 41.0 psid to 34.5 psid after S-IVB first burn ignition. The resultant negative differential pressure was -1.0 psid at R0 +600 sec (figure 23-10). This applied pressure was well below the limit bulkhead capability of -24.2 psid corresponding to this period of flight.

The largest positive differential pressure occurred during initial pressurization of the LOX tank while the LH2 tank was vented and stabilized at a saturation pressure condition. The pressure obtained was +24.8 psid, and this was expected since the sequencing permits pressurization to the LOX tank vent and relief valve setting of 44 psia while the LH2 tank is unpressurized. The measured maximum positive differential pressure was below the corresponding bulkhead limit structural capability of 30.0 psid.

The ullage differential pressures at all other times were normal and also below the limit structural capability.

Common bulkhead internal vacuum pressure during prelaunch and through powered flight to first burn engine cutoff and through orbital coast did not exceed 0.3 psia. This favorably corresponds to expected values of less than 1.0 psia.

23.2 Explosive Ordnance Equipment

All exploding bridgewire initiated ordnance systems performed as required. The stage separation system, which utilizes a dual mild detonating fuse assembly, functioned on command and effected a complete disconnection of the S-IVB from the S-II. The two ullage rockets and four retrorockets fired, thus accomplishing a normal separation sequence.

Approximately 12 sec after separation, the two ullage rockets and their fairings were jettisoned. This has been verified by telemetry data. The jettison indication was a drop to zero of the chamber pressure transducer potentiometer excitation voltage.

The safety and arming device, an element of the range safety system, was cycled electrically from ARMED to SAFE position several times during terminal countdown and functioned as required.

TABLE 23-1
MAXIMUM LOCAL STRINGER BENDING MOMENTS AND AXIAL LOADS IN AFT AND FORWARD SKIRTS

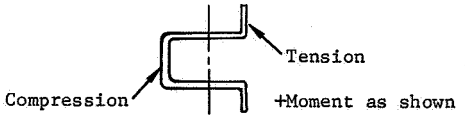

Axial Load
- Compression
+ Tension

SKIRT	STATION	CONDITION	MAX. FLIGHT LOAD (CALCULATED FROM TOP AND SIDE STRAIN GAGES)		LOAD USED IN DESIGN ANALYSIS (LIMIT)	
			MOMENT (in.-lb)	AXIAL LOAD (lb)	MOMENT (in.-lb)	AXIAL LOAD (lb)
Aft	2821	Max αq	-1,364	-7,319	-6,800	-14,168
		CECO	-2,611	-13,047	-5,700	-11,756
Fwd	3145	Max αq	+118	-3,065	+1,857	-8,287
		CECO	-1,217	-6,853	+1,080	-4,804

TABLE 23-2
FORWARD SKIRT LOCAL STRINGER LOADS AND MINIMUM MARGIN
OF SAFETY AT STA 3145 - CONDITION OF RO +144 SEC

STRINGER NO.	GAGE* NO.	STRAIN** (micro in./in.)	STRINGER*** MOMENT (in.-lb)	STRINGER AXIAL LOAD (lb)	MINIMUM MARGIN OF SAFETY (percent)
14	54	-1,040	-184	-4,437	--
	55	-890			
27	56	-560	719	-3,319	--
	57	-1,210			
41	58	-840	-50	-3,695	--
	59	-800			
54	60	-600	127	-2,794	--
	61	-700			
68	62	-1,250	-800	-4,813	--
	63	-580			
81	64	-1,810	-925	-6,785	--
	65	-1,010			
95	66	-1,890	-1,217	-6,853	+97.0
	67	-830			
108	68	-520	154	-2,471	--
	69	-640			

*Even numbered gages were stringer side mounted, and odd numbered were top mounted.

**Measured strain values were adjusted to 1 g calculated conditions at RO -10 sec.

***Positive moment corresponds to tension in skin.

TABLE 23-3
AXIAL LOAD FACTORS - POWERED FLIGHT

CONDITION	MAXIMUM MEASURED LOAD FACTOR (g)	FLIGHT TIME OF MEASUREMENT (sec)	PREDICTED LOAD FACTOR (g)	FLIGHT TIME OF PRED. L.F. (g)
S-IC Liftoff	1.27	2.0	1.27	2.0
*S-IC CECO	4.78	144.7	4.73	143.4
S-IC OECO	3.98	148.4	3.96	148.4
S-II ECO (Max g)	1.58	410	2.02	515
S-IVB (First Burn)	0.85	747	0.84	660

*Condition S-IC CECO design load factor = 4.68 g

TABLE 23-4
MAXIMUM TEMPERATURES OF MAJOR STRUCTURAL ASSEMBLIES
SUBJECT TO AERODYNAMIC HEATING

STRUCTURAL ASSEMBLY	MEASURED* MAX. TEMP. (deg F)	FLIGHT TIME OF MEASUREMENT (sec)	THERMAL DESIGN TRAJECTORY		EXTERNALLY** INSULATED STRUCTURE
			MAXIMUM TEMPERATURE (deg F)	FLIGHT TIME OF MAX. TEMP. (sec)	
Stringers					
Forward skirt	220	150	320	150	No
Aft skirt	140	140	243	150	Yes
Interstage	191	160	248	150	Yes
Skin					
Forward skirt	286	160	389	150	No
LH2 tank cyl. wall	90	130	159	150	No
Aft skirt	176	130	258	150	Yes
Interstage	185	160	265	180	Yes

*Measured temperatures are adjusted for measurement lag due to mass of temperature sensors.

**At location of temperature sensor.

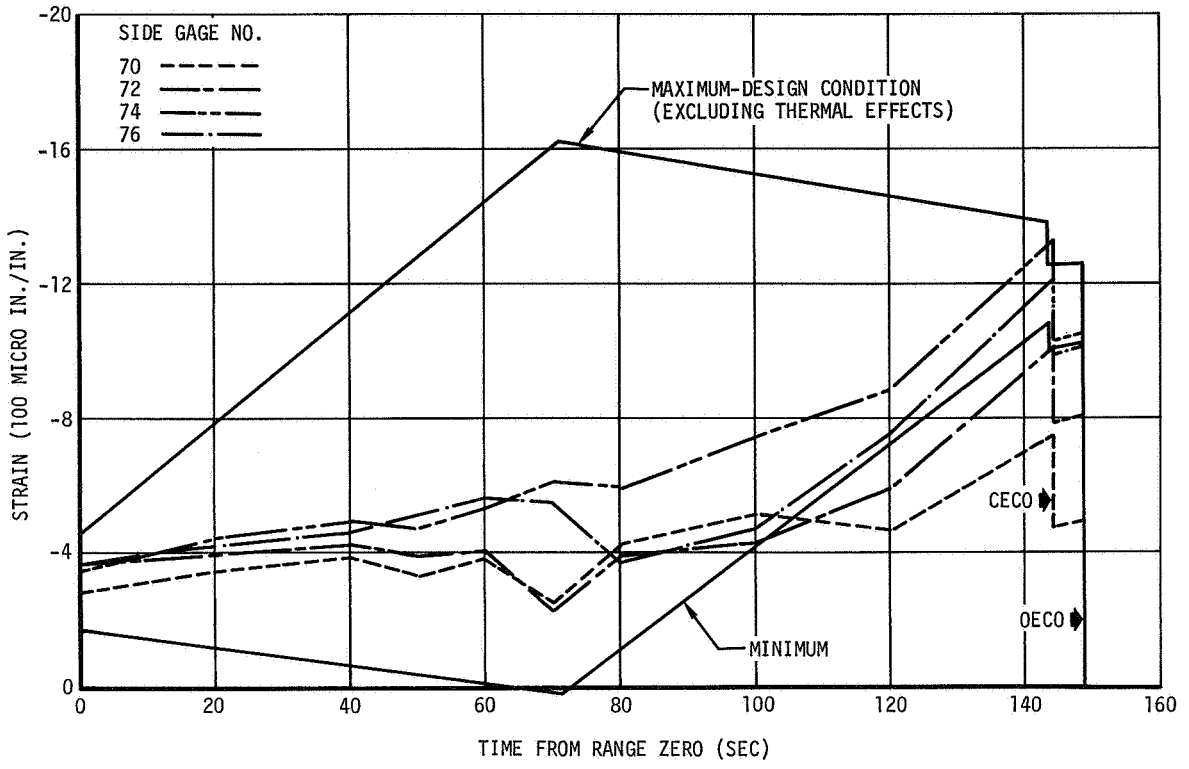

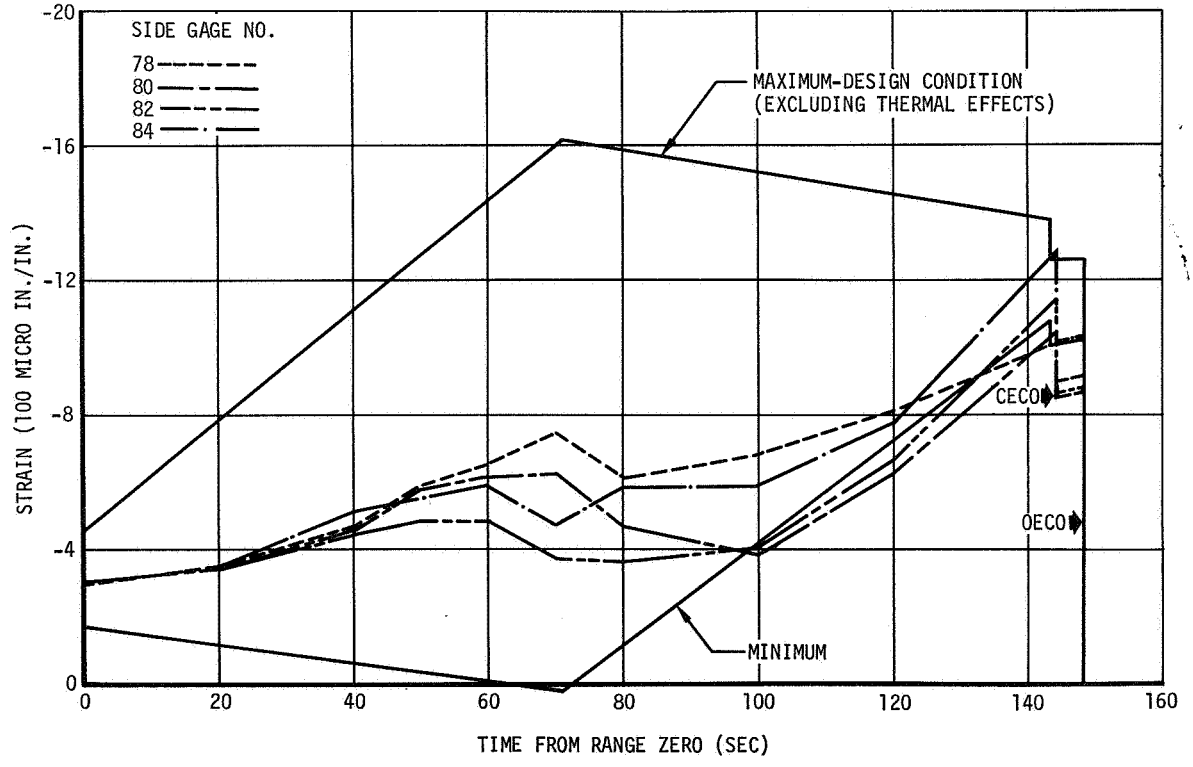

Figure 23-1. Flight Axial Strain vs Flight Time - Aft Skirt Sta 2821 (Sheet 1 of 2)

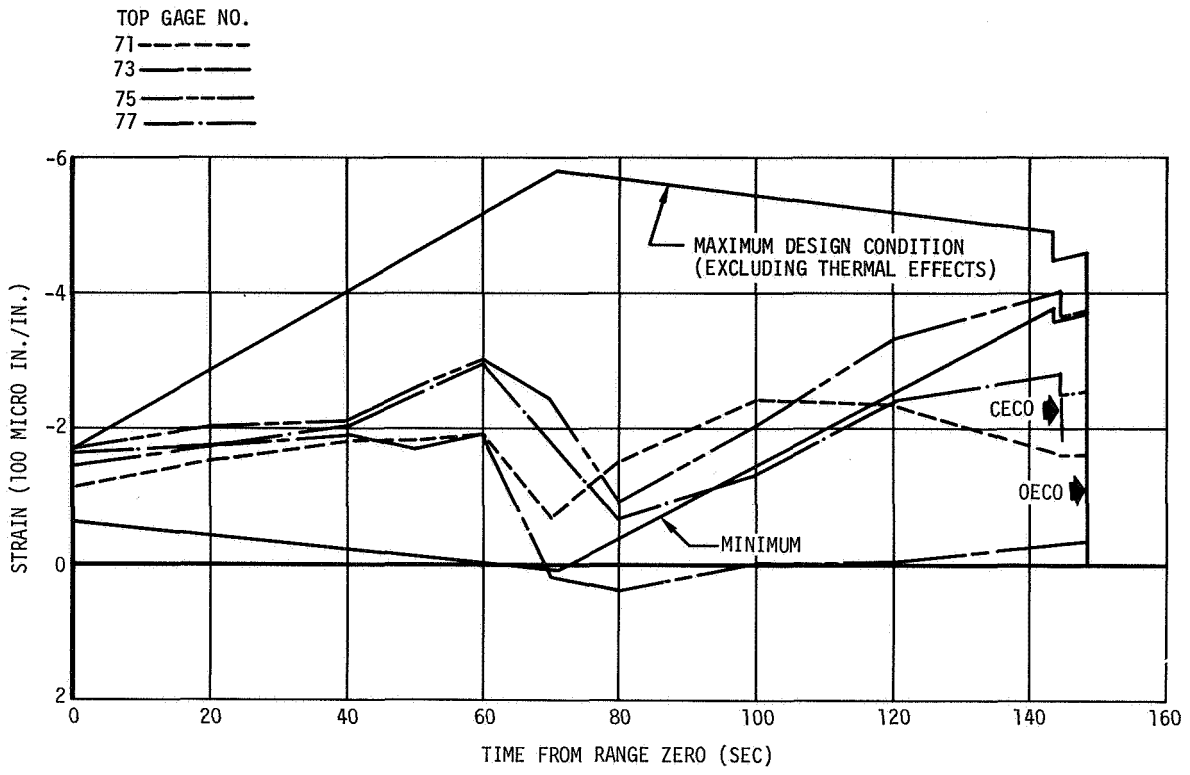

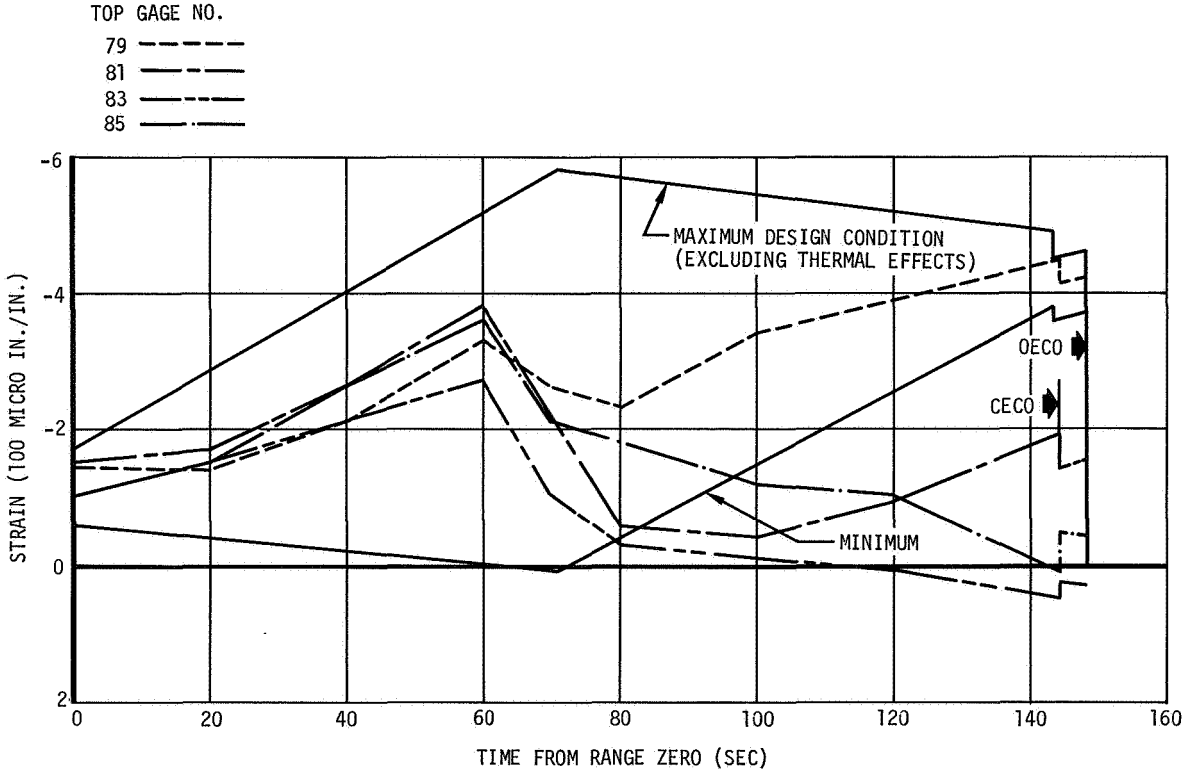

Figure 23-1. Flight Axial Strain vs Flight Time - Aft Skirt Sta 2821 (Sheet 2 of 2)

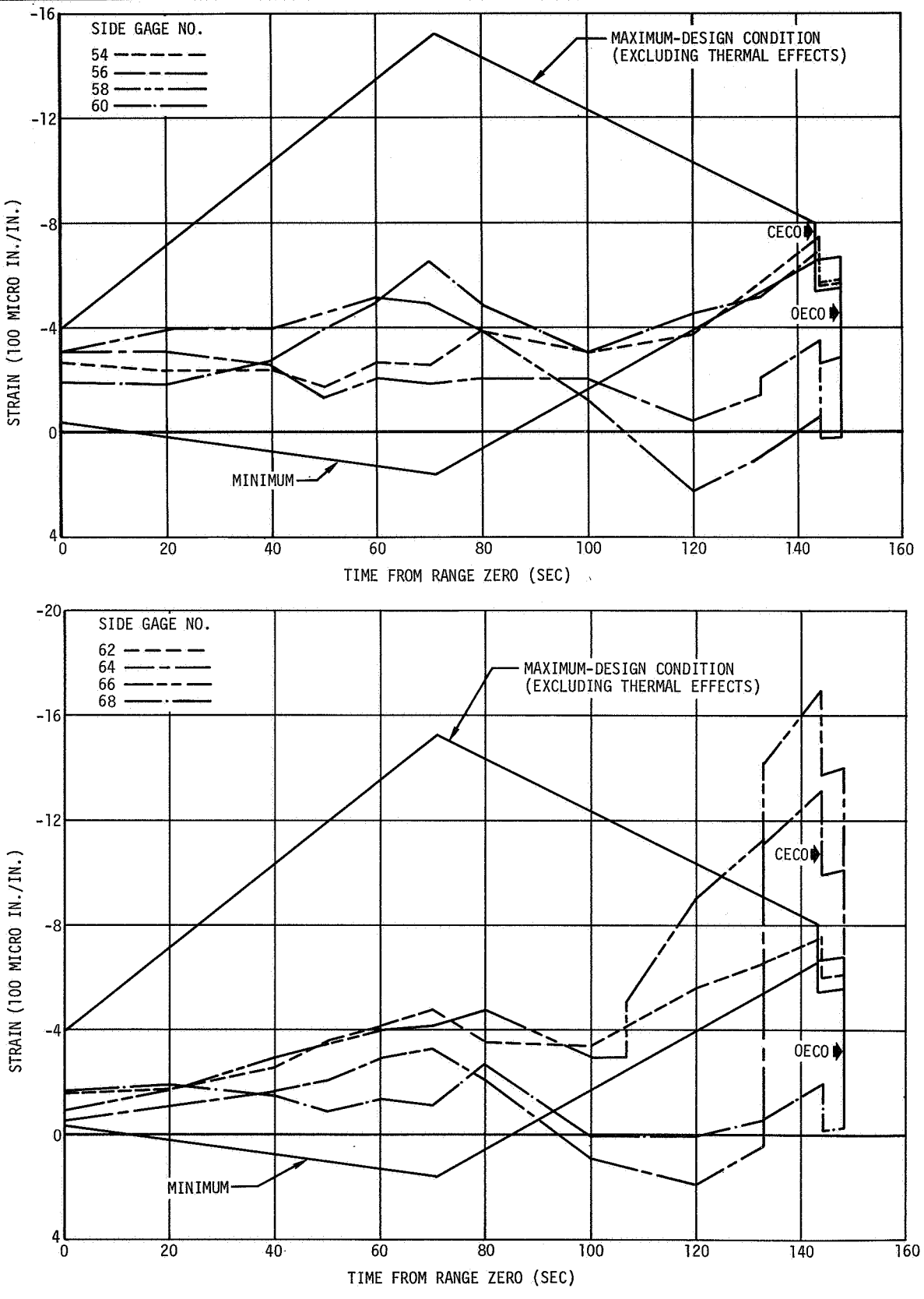

Figure 23-2. Flight Axial Strain vs Flight Time - Forward Skirt Sta 3145 (Sheet 1 of 2)

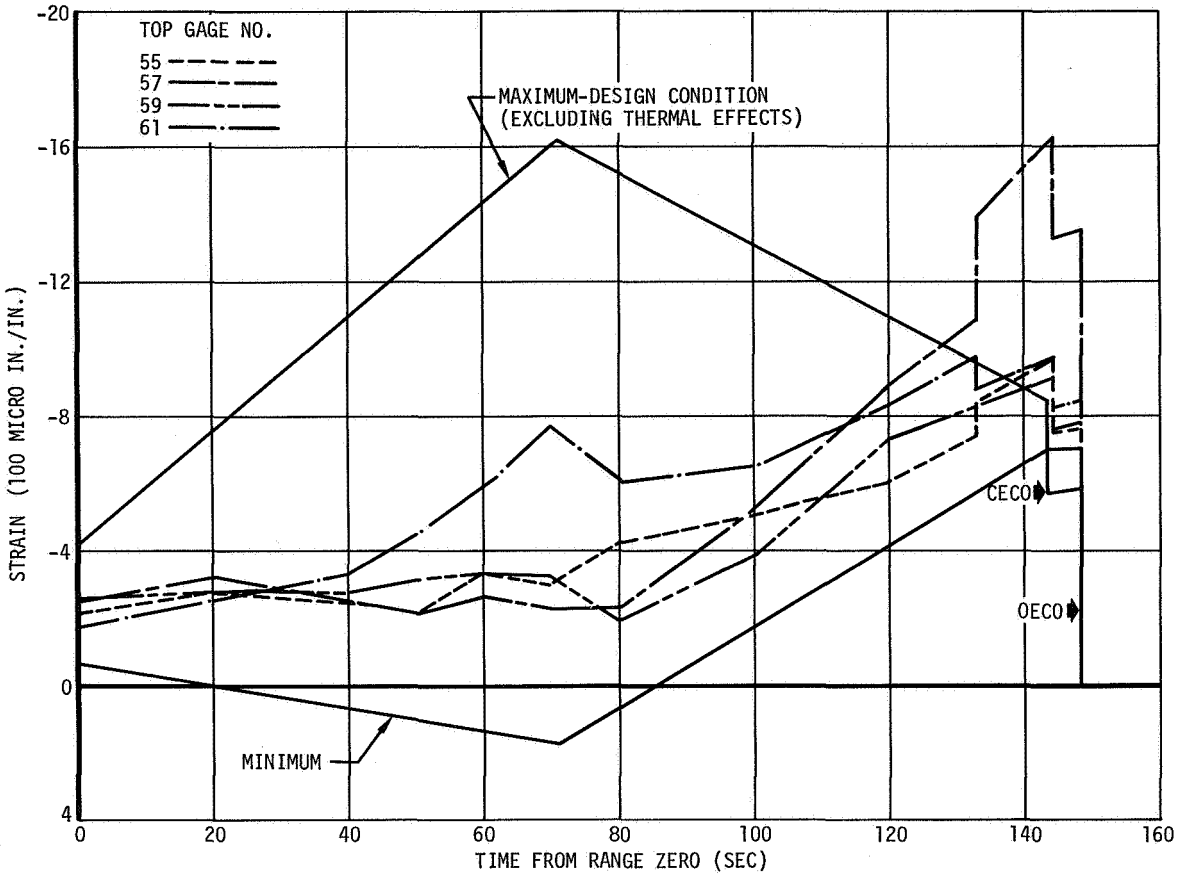

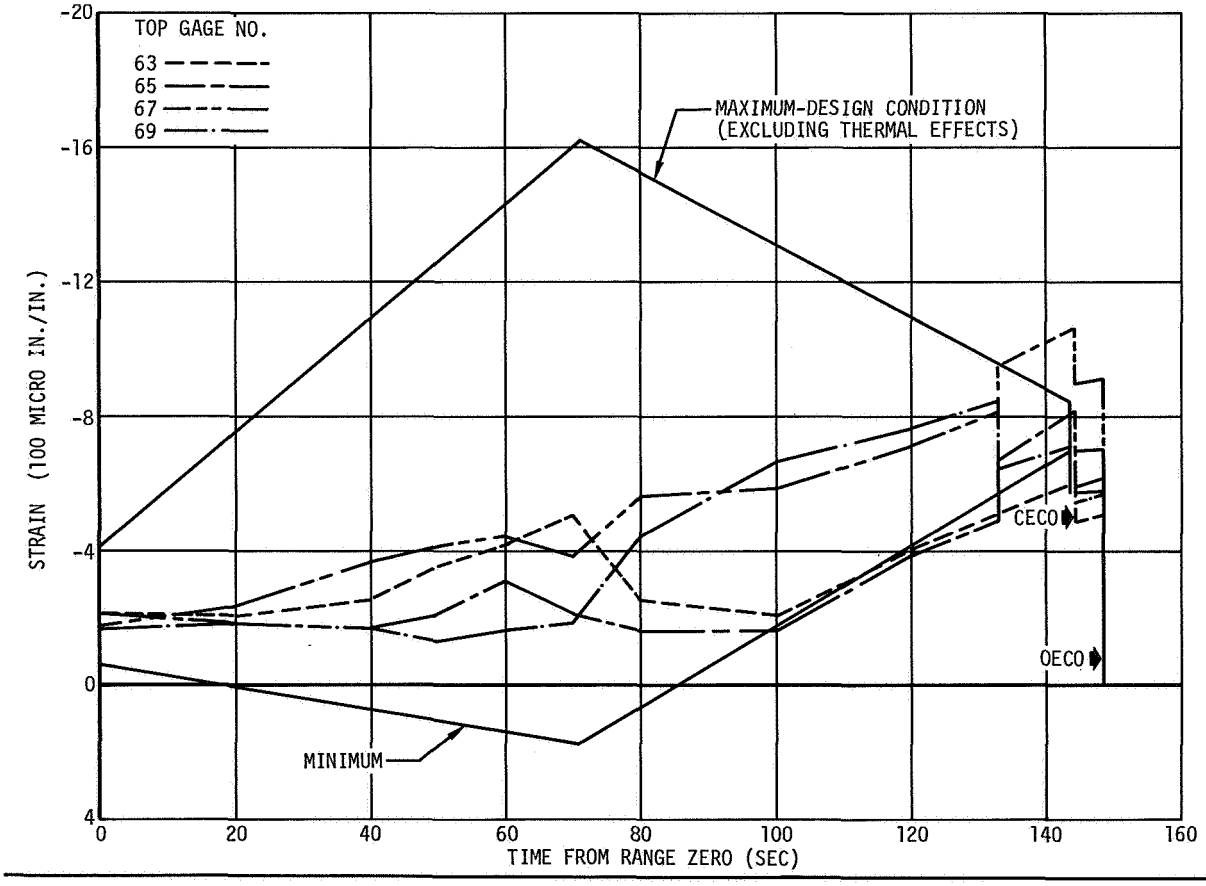

Figure 23-2. Flight Axial Strain vs Flight Time - Forward Skirt Sta 3145 (Sheet 2 of 2)

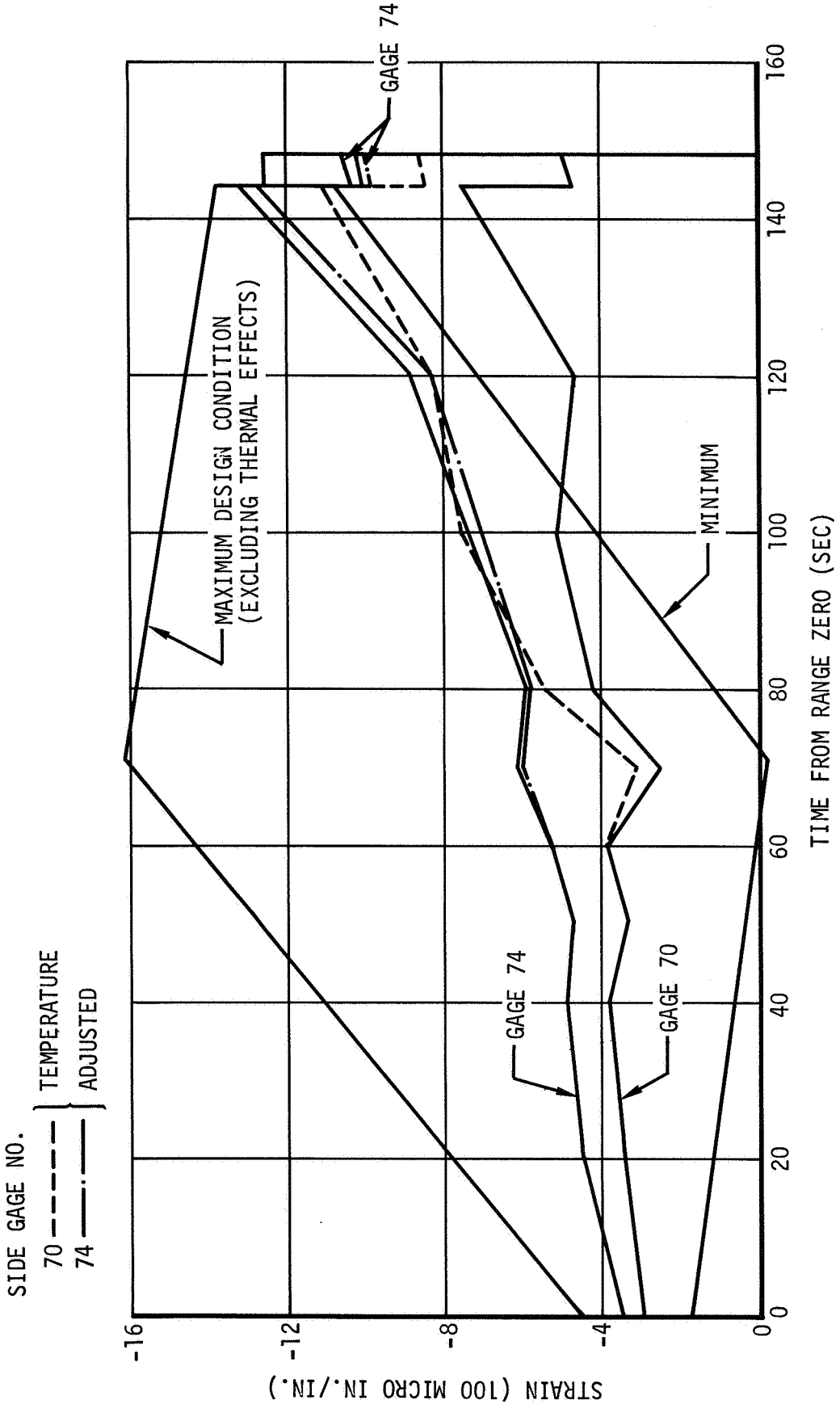

Figure 23-3. Flight Axial Strain vs Flight Time Including Temperature Adjustments - Aft Skirt Sta 2821

BAR CHART SHOWING STRAIN CHANGES AT RO +133 SEC

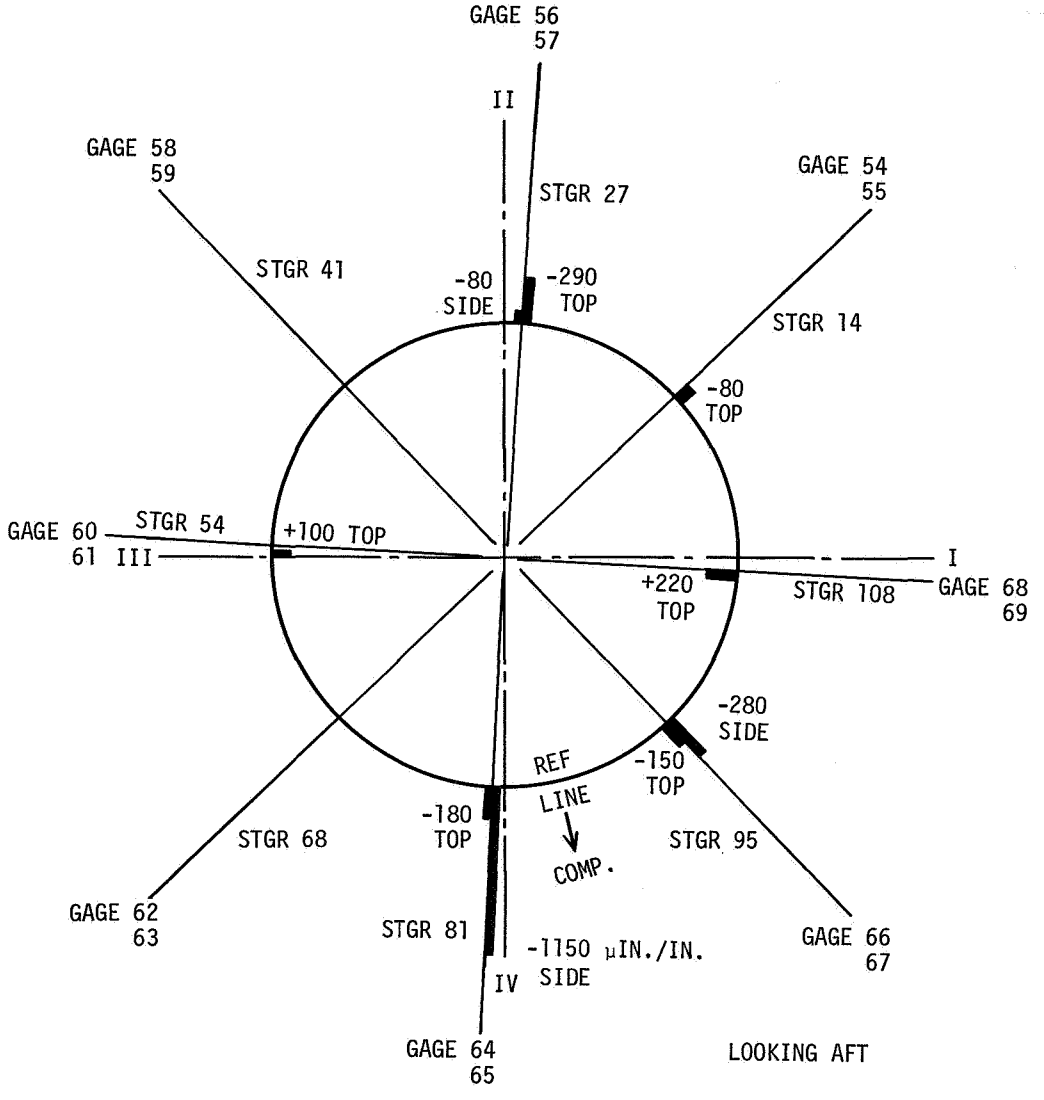

NOTE: THESE CHANGES HELD UNTIL CECO. BAR VALUES ARE STRAIN (MICRO INCHES PER IN.). NEGATIVE VALUES INDICATE INCREASES IN COMPRESSION. POSITIVE VALUES INDICATE DECREASES IN COMPRESSION

Figure 23-4. Forward Skirt Strains

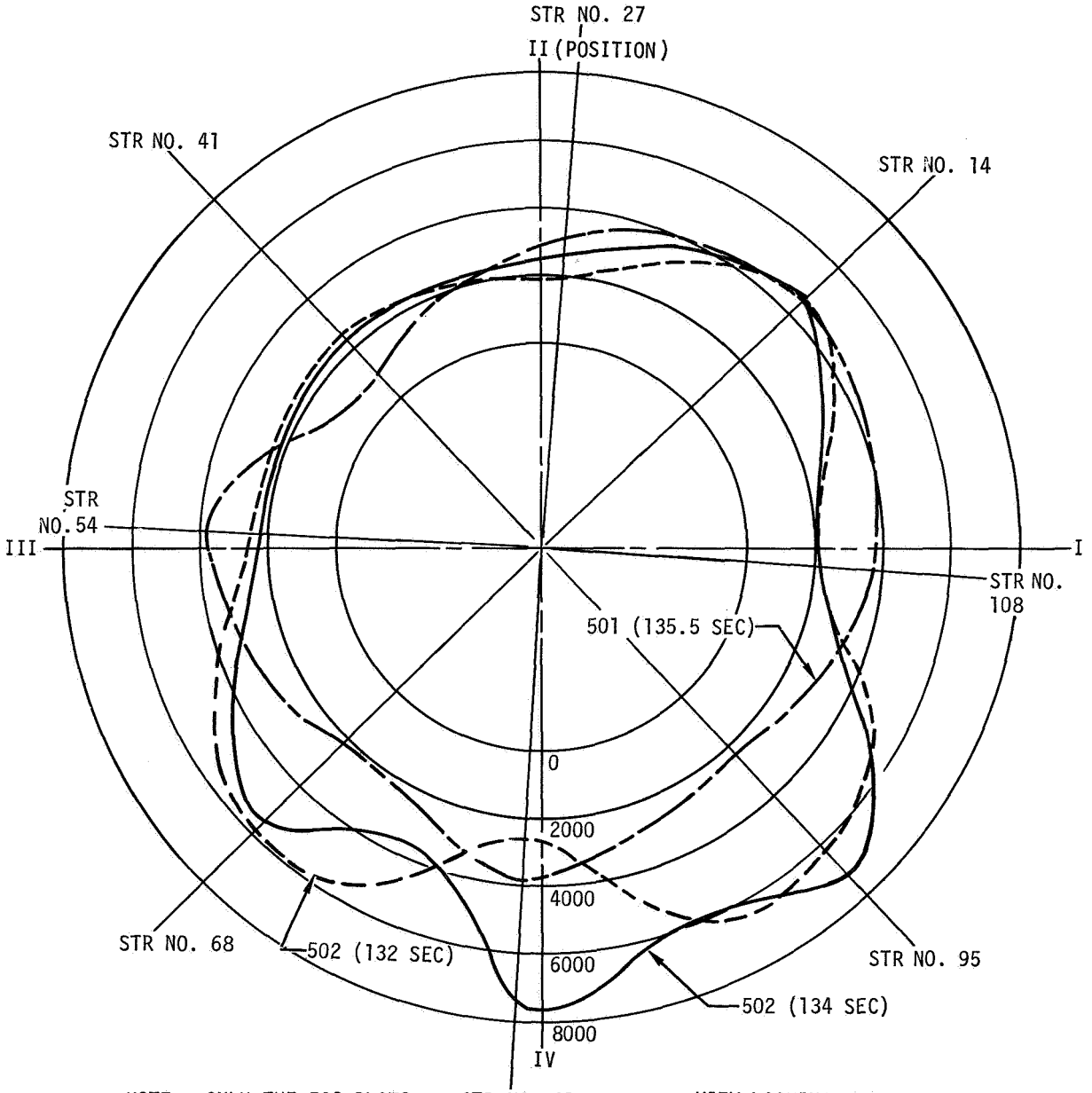

NOTE: ONLY THE 502 PLOTS HAVE BEEN ADJUSTED TO REPRESENT THE TOTAL AXIAL LOAD

LOADS ARE IN LBF

Figure 23-5. Forward Skirt Stringer Load

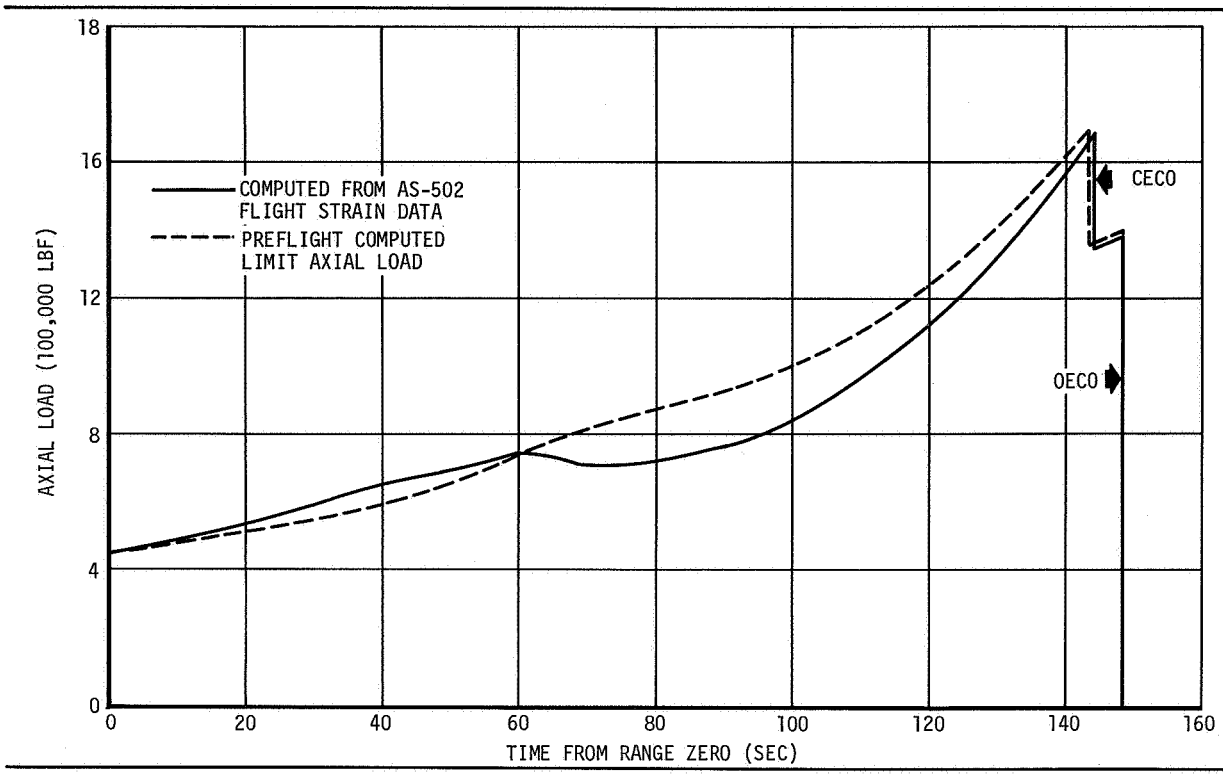

Figure 23-6. Flight Axial Load vs Time - Aft Skirt Sta 2821

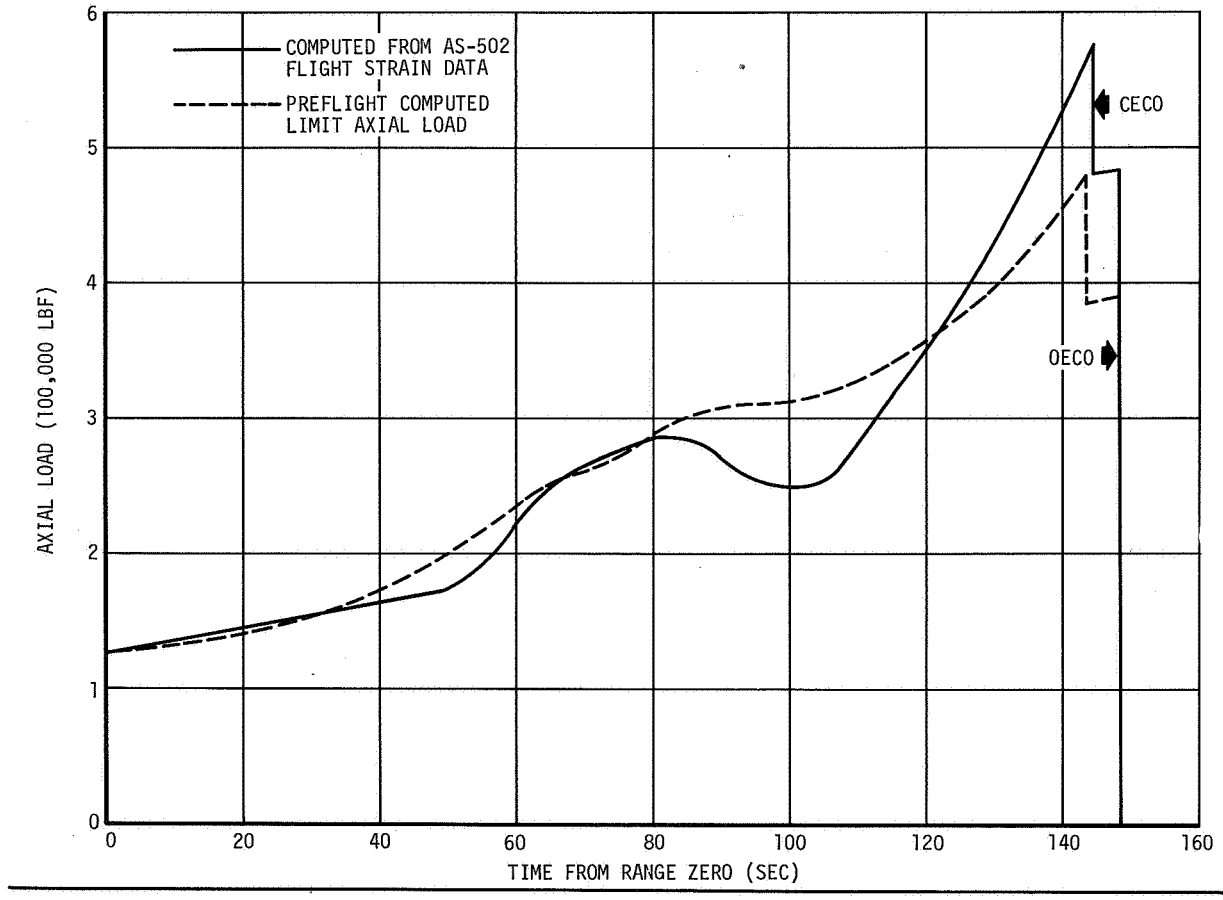

Figure 23-7. Flight Axial Load vs Time - Forward Skirt Sta 3145

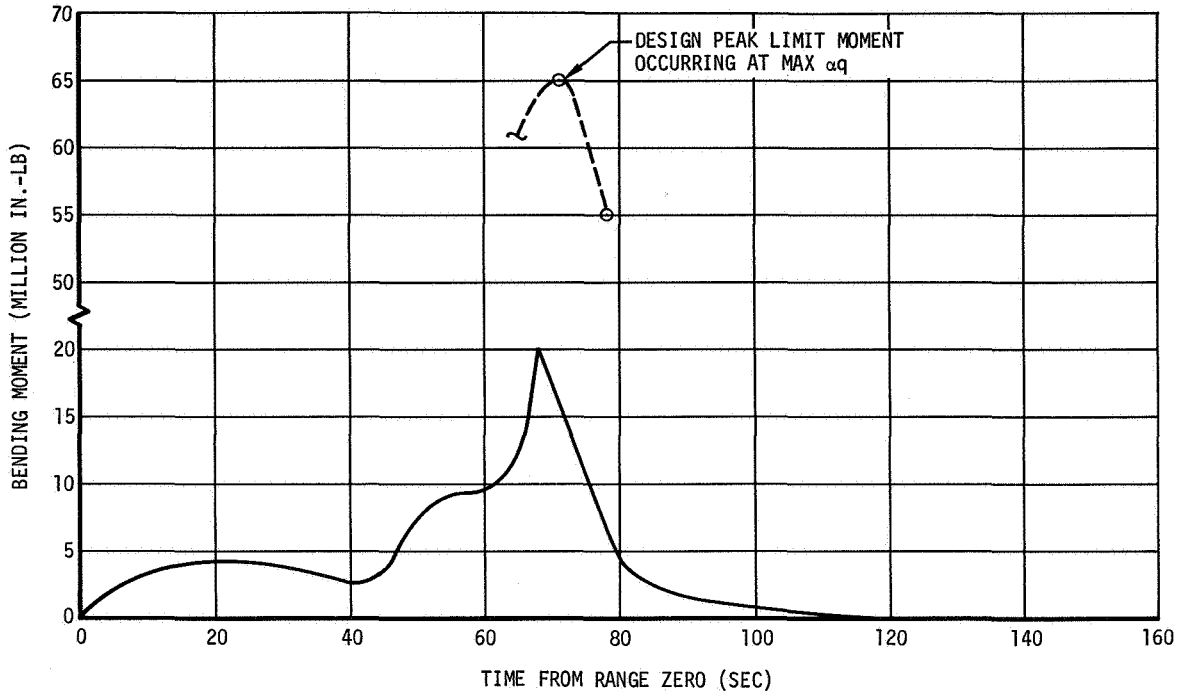

Figure 23-8. Flight Stage Bending Moment vs Time - Aft Skirt Sta 2821

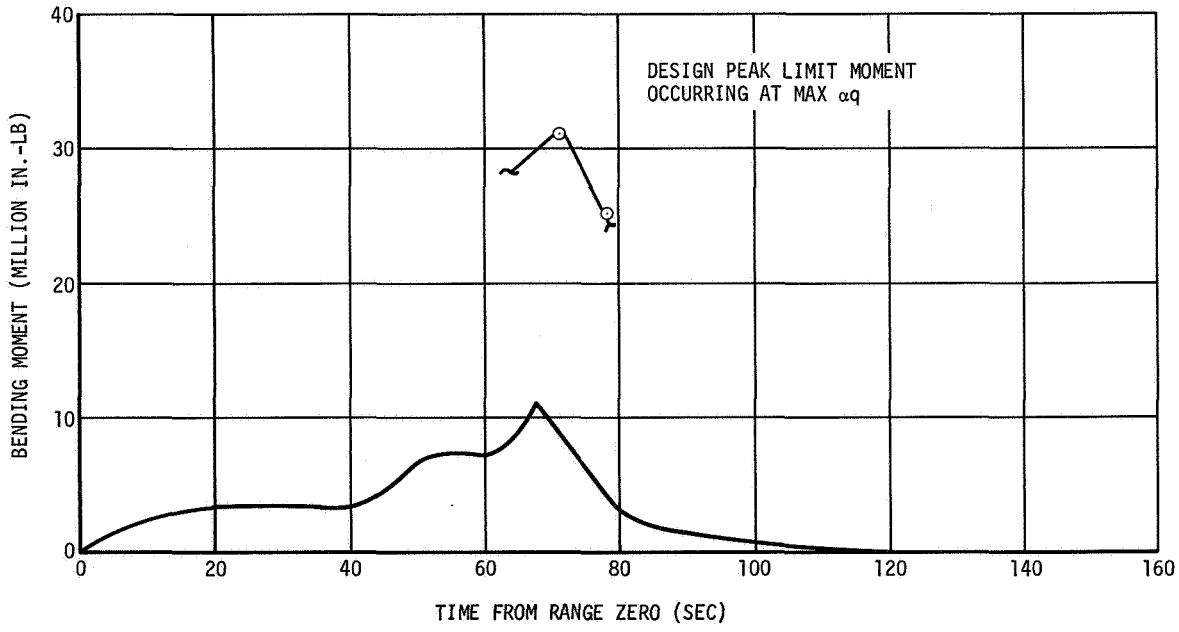

Figure 23-9. Flight Stage Bending Moment vs Time - Forward Skirt Sta 3145

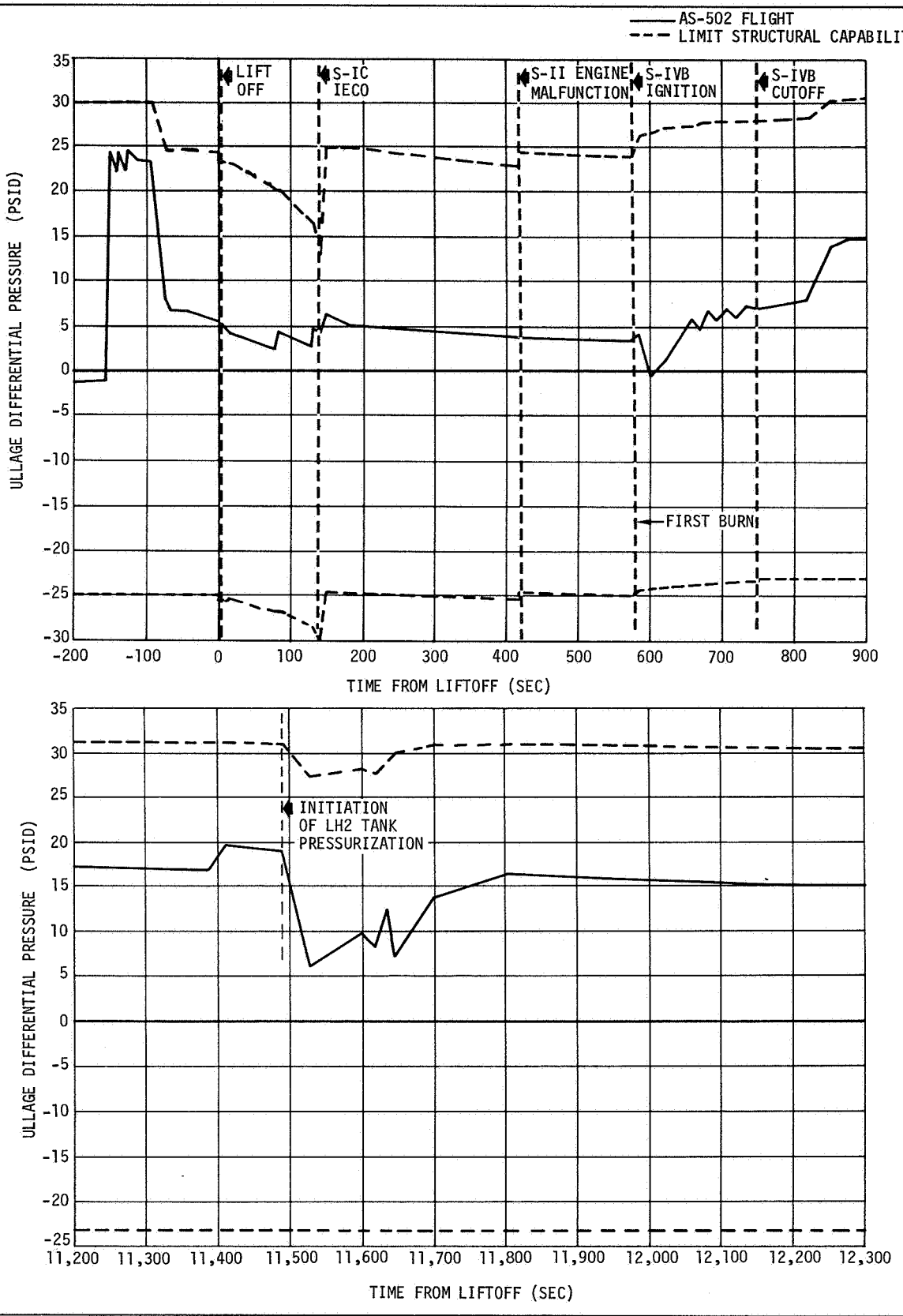

Figure 23-10. Ullage Differential Pressure vs Flight Time

SECTION 24

FORWARD SKIRT THERMOCONDITIONING SYSTEM

24. FORWARD SKIRT THERMOCONDITIONING SYSTEM

The thermoconditioning system operated normally during flight. All parameters (temperature, pressure, and flowrate) were within their design limits.

24.1 Temperature

The methanol/water control temperature (C0015-601), which is the inlet temperature for the S-IVB thermoconditioning panel system, was 59.2 deg F at liftoff and increased to 63.5 deg F in 32 sec, decreased to 62.2 deg F by RO +115 sec, increased to 66.4 deg F at RO +496 sec, and decreased to 63.5 deg F at the end of first burn (approximately RO +560 sec). During the remainder of the monitored flight periods, the control temperature varied between a minimum of 53 deg F and a maximum of 66 deg F. This temperature range is entirely within the acceptable inlet temperature range of 45 to 70 deg F.

The exit temperature from the S-IVB thermoconditioning system (C0026-601) was 62.2 deg F at liftoff and decreased to 60.8 deg F after 93 sec and increased to 66.9 deg F at RO +560 sec. The exit temperature varied between a minimum of 53 deg F and a maximum of 66 deg F for the remainder of the monitored flight periods.

24.2 Pressure

The coolant manifold inlet pressure (D0017-601) was approximately constant at 41.3 psia during the first 560 sec of flight. The inlet pressure varied between 41 and 44 psia from RO +560 sec until RO +33,780 sec. These pressure levels are all below the maximum allowable operating pressure of 53 psia.

The coolant manifold exit temperature (D0018-601) increased from 26.8 psia at liftoff to 30.0 psia during the first 148 sec of flight. At 148 sec, there was a pressure drop from 30.0 to 26.8 psia. The pressure then gradually increased from 26.8 psia to 27.5 psia at RO +400 sec. The pressure then decreased back to 26.8 psia at RO +420 sec and stabilized for the remainder of the first 560 sec of flight. From RO +560 sec until RO +33,750 sec, the exit pressure remained between 26.5 and 28.0 psia.

24.3 Flowrate

The S-IVB coolant inlet flowrate (F0010-601) was 7.9 gal/min at liftoff and decreased to 7.8 gal/min at RO +17 sec. It then increased to 8.0 gal/min at RO +560 sec. From RO +560 sec until RO +33,780, the flowrate varied between 7.9 and 8.3 gal/min.

SECTION 25

ACOUSTIC VIBRATION AND DYNAMIC STRAIN MEASUREMENTS

25. ACOUSTIC, VIBRATION, AND DYNAMIC STRAIN MEASUREMENTS

A total of 65 acoustic, vibration and dynamic strain measurements were monitored on the S-IVB-502 stage. Four measurements did not provide data. In general, the acoustic and vibration environments were similar to those measured on the AS-501 flight. The dynamic strain levels were higher than those measured on the AS-204 flight; however, there were no indications of panel flutter. The fatigue life of the forward skirt skin panels, as demonstrated in the wind tunnel qualification test, was not impaired during the flight.

There were two unexpected dynamic occurrences noted on the S-IVB. The first was a 5.5 cps oscillation (POGO) during the latter period of S-IC powered flight and secondly a shock transient at approximately RO +133.3 sec. There were no adverse effects on the S-IVB due to these events.

25.1 Data Acquisition and Reduction

A list of the 37 vibration and 12 acoustic measurements is presented in table 25-1. The transducer locations are shown in figure 25-1. The 16 dynamic strain measurements are listed in table 25-2 and gage locations are detailed in paragraph 25.4. Overall levels during specific flight periods are also presented in both tables.

Three separate telemetry systems were used to acquire the data: PAM/FM, FM/FM, and SSB/FM. The PAM/FM system, in conjunction with a filtering and averaging circuit, was used to provide acoustical levels for frequencies above 2,400 cps. The FM/FM system was used to provide low frequency (5 to 220 cps) vibration data. Both systems provided extended frequency information to supplement the data from the SSB/FM system which has a nominal frequency range of 50 to 3,000 cps. The preflight sweep calibration showed the low frequency rolloff for this SSB set was not as severe as expected, and therefore, 30 cps information was recoverable on this flight. The FM/FM system was also used to provide the dynamic strain data (0 to 800 cps).

A time sharing arrangement was utilized to obtain more measurements than the number of allocated telemetry channels. This method of acquisition provided data for 3 or 6 sec for every 12 sec commutation period. Time sharing, however, prevented the acquisition of maximum response amplitudes and specific events (liftoff, separation, etc.) for some of the measurements. The time shared channels are reflected in the time-history plots by interpolated lines between the time intervals of the actual measured data.

The data from the SSB/FM and FM/FM measurements were corrected for data acquisition system and data reduction filter rolloff characteristics. The corrections were applied to the spectrum plots and to the overall levels in tables 25-1 and 25-2. Because there was no convenient way to correct the time-history plots, the levels shown may differ from the values in the tables. The levels below 40 cps in the power spectral density (PSD) plots from the SSB measurements are to be disregarded because the system did not provide valid data below this frequency.

Both analog and digital techniques were utilized in reducing the data. The final analysis consisted of both instantaneous and root-mean square (rms) composite time history, and one-third octave band and PSD spectrum plots (figures 25-2 through 25-57).

25.2 Vibration Environment

The S-IVB vibration environment was induced by acoustical noise, aerodynamic pressure fluctuations, and mechanical excitation. The predominant sources were the F-1 engine exhaust noise during launch, unsteady aerodynamic flow conditions during the transonic period of flight, boundary layer turbulence during the period of high dynamic pressures, J-2 engine combustion chamber processes during S-IVB powered flight, and staging transients at separation and S-IVB engine ignition and cutoff. Thirty-seven vibration pickups were located on the S-IVB to determine the response amplitudes of the stage structure and components to these excitation sources.

For discussion purposes, the measurements were grouped into engine, thrust structure, aft skirt and LH2 tank, and forward skirt measurements. Data from corresponding measurements from the AS-501 flight are presented for comparison purposes.

25.2.1 Engine Measurements

Vibration measurements were made on the combustion chamber dome in the thrust direction and on the flange above the turbopump housing, in the radial direction, of each main propellant pump. The data from the LH2 turbopump measurement were invalid. A detailed discussion of the problems associated with this measurement system is presented in section 18. Although the data were invalid for determining the LH2 turbopump vibration, the data were considered usable for trend purposes. The rms composite time-history (figure 25-2) showed changes in amplitude which correlate in time with other measurement anomalies. A discussion of the anomalous behavior is presented in section 2.

The vibration amplitudes on the combustion chamber dome and LOX turbopump were similar to those measured on the AS-501 flight (figures 25-3 and 25-4). Between RO +685 and RO +694 sec the measurement on the combustion chamber dome failed and did not provide data for the remainder of the flight. The failure appears to be related to other measurement anomalies noted during this time period (section 2).

25.2.2 Thrust Structure Measurements

The thrust structure measurements were located on the gimbal block and at the attach points of an ambient helium bottle and the LH2 feedline. Three measurements on the gimbal block were oriented in the thrust, pitch, and yaw directions. The data (figures 25-5, 6, and 7) showed the amplitudes were nearly identical in the three axes. The highest vibration levels occurred during S-IVB powered flight.

Three helium bottle measurements were located on the thrust structure at one of the tie-down straps and oriented in the thrust, pitch, and yaw directions. The measurement at the LH2 feedline was located on the thrust structure near the support bracket. The data from these measurements are shown in figure 24-8 through 24-11. The measured amplitudes during the flight were approximately 75 percent lower than those measured during acceptance firing. In general, the vibration energy was concentrated below 300 cps at liftoff and above 300 cps during S-IVB powered flight and acceptance firing.

25.2.3 Aft Skirt and LH2 Tank Measurements

The aft skirt measurements were monitored on the separation ring frame, at two vibration-isolated ambient panels, and at APS module No. 1. The measurement on the separation ring frame was located at position II and oriented in the thrust direction. The PSD levels (figures 25-12) were in good agreement with those measured on the AS-501 flight. The increased amplitude in the composite time-history at RO +125 sec was due to a 5.5 cps longitudinal oscillation (POGO). The vibration level was approximately 70 percent higher than that measured on the AS-501 flight.

The ambient panel measurements provided the vibration input and response of the sequencer (panel No. 1) and switch selector (panel No. 2) panels. The data from these measurements are shown in figures 25-13 through 25-18. In addition, the PSD's from corresponding AS-501 flight measurements are shown. The comparisons show the peaks in the spectrum for the panel input data were at a lower frequency on this flight. However, the panel response data were in good agreement. Similar differences were noted in the acceptance firing data.

The measurements at the APS module monitored the vibration input to the module at the forward and aft attach points. The levels shown in figures 25-19, 20, and 21 show good agreement with those measured on the AS-501 flight.

There was one measurement located on the LH2 tank near the PU probe support structure. The maximum amplitude was measured during launch with most of the energy concentrated at approximately 100 cps (figure 25-22).

25.2.4 Forward Skirt Measurements

The vibration environment in the forward skirt was measured on the field splice, at two vibration-isolated cold plate panels, and at battery No. 1. Except for short duration transients at approximately RO +133.3 sec and stage separation, the vibration amplitudes diminished to negligible values (less than 1 grms) after RO +110 sec.

The measurements on the field splice were monitored near positions I and II. There were three measurements at each location monitored via SSB. The thrust measurement system at position I was also monitored on FM/FM to provide low frequency (figure 25-23) data. The 5.5 cps longitudinal oscillation noted on the aft skirt was also measured in the forward skirt. The maximum amplitude was ± 0.5 g, measured on both the aft and forward skirts.

The vibration amplitudes on the field splice were similar to those measured on the AS-501 flight (figures 25-24 through 25-28), except for measurement E0097-411 (figures 25-29). The AS-501 flight data were considerably higher due to a 700 cps peak which was absent in the AS-502 data. This difference in vibration response was also noticed during the acceptance firing.

The cold plate panel measurements provided the vibration input and response of the PU electronics (panel No. 9) and EBW range safety (panel No. 16) panels. The data from these measurements are shown in figures 25-30 through 25-34. In general, the amplitudes were in good agreement with those measured on the AS-501 flight.

The accelerometers at the battery were mounted on the structure adjacent to the battery support bracket. Rms time-history and PSD plots are presented in figures 25-35, 36, and 37. Measurement E0117-411 did not provide valid data throughout the flight due to an instrumentation malfunction (section 18). The vibration characteristics at the battery were similar to those measured at the cold plate panels.

A shock transient with four separate impulses within a time interval of 0.25 sec was noted at approximately RO +133.3 sec. Due to time-sharing, only three forward skirt measurements were monitored at this time. The maximum measured level was $\pm$17 g which was slightly higher than that measured during stage separation. The transient was hardly noticeable on the aft skirt, thrust structure, or engine measurements. The RO +133.3 sec incident is discussed in greater detail in section 2.

25.3 Acoustic Environment

The acoustic environment was produced by F-1 engine exhaust noise at launch, unsteady flow conditions during the transonic period of flight (near mach 1), and by boundary layer pressure fluctuations during the period of high dynamic pressures. There were four microphones on the S-IVB to measure this environment. Two (external and internal) were located on the aft skirt near position I, approximately 36 in. forward of the separation plane. The other two were located on the forward skirt near position I (external) and II (internal), approximately 6 in. aft of the field splice. Each transducer system had a multiple output capability with the data signal below 3,000 cps transmitted by SSB/FM and the data level for the 7th (2,400 to 4,800 cps) and 8th (4,800 to 9,600 cps) octave bands transmitted via PAM/FM.

Rms time-history and one-third octave band plots for these measurements are shown in figures 25-38 through 25-41. Data from similar AS-501 flight measurements are also presented. In general, the comparisons during selected flight periods were in reasonable agreement between flights.

One of the discrepancies noted in the AS-501 aft skirt acoustical data at liftoff was that the internal levels were higher than the external in the low frequencies. The internal levels on this flight were lower than the external throughout the spectrum.

No comparison was made of the forward skirt external data because the AS-501 flight measurement was located at a different location. The major difference noted on this flight was the increase in amplitude between RO +85 to RO +96 sec. This phenomenon correlates in time with the increased wind shear loading noted at this time and reported in appendices 3 and 5.

25.4 Dynamic Strain Measurements

Sixteen dynamic strain measurements were made to detect the possible existence and degree of skin panel flutter in the forward skirt during supersonic flight. The strain gages were installed on approximately every 7th panel at sta 3135, oriented in the thrust axis, located midway between stringers and 4 in. forward of the panel trailing edge. The installation was similar to AS-204. The gages were external to the skin and at the same location as the internal gages used in the panel flutter qualification test performed on a full scale segment of the S-IVB forward skirt in the Arnold Engineering Development Center transonic wind tunnel.

A location sketch and a comparison of rms composite time histories of the measurements are shown in figure 25-42. PSD plots, samples of the instantaneous wave forms and rms composite time histories are shown for selected flight periods in figures 25-43 through 25-57. The composite dynamic strain levels at liftoff, transonic, and supersonic periods of flight are presented in table 25-2.

One measurement, S0087, was found to be operating erratically prior to launch and was deleted. Two measurements, S0100 and S0101, were not found to be malfunctioning prior to launch; but the signals that they were sending back during launch and later in flight during periods of maxima cross winds aloft indicated high wide-band random noise levels on the channels, as well as a dc shift of approximately one volt which occurred on the channel of S0101 at 91.5 sec. The high wide-band random noise levels seemed to be a function of the high external excitation environments. The spectrum level over a broad frequency band was raised, which is not the expected response of a vibrating skin panel as shown in the other flight dynamic strain measurements. The noise levels dropped to satisfactory values during low external excitation. These two measurements were investigated for electrical malfunction and no single failure mode could be identified (see section 18, table 18-5) but because of their peculiar behavior, they have been classified as aberrant. The data from these measurements are included in this report, see figures 25-56 and 25-57.

The time history of the composite dynamic strain levels from most measurements followed a trend similar to the external acoustic levels measured on the forward skirt as shown in figure 25-40. The first maxima levels occurred at liftoff followed by lower levels during subsonic flight. The next maxima levels occurred during transonic flight followed by lower levels during low supersonic flight before maximum dynamic pressure. The flight vehicle then encountered transient air loads as it traversed the maxima cross winds aloft which ranged from approximately 50 to 80 ft/sec, between R0 +75 and R0 +85 sec, as shown in appendix 3 and appendix 5. During the period of cross winds the measured dynamic strain increased on individual panels then decreased as indicated in figure 25-42.

The dynamic strain transients during supersonic flight can be explained as follows: The wind tunnel tests showed that (with the Mach number, differential pressure, and dynamic pressure held constant) the dynamic strain levels due to the fluctuating pressures in the boundary layer increased as the compression loads applied to the skin panels were increased. The maximum dynamic strain levels occurred when the panel compression load was equal to or greater than the static buckling load. Similarly in flight the dynamic strain response increased as the static strain in the skin panel approached the critical buckling ratio. The critical buckling ratios during flight were estimated from the static strains measured on eight forward skirt stringers as a result of bending moments induced by the cross winds. The static strains, reported in section 23, were adjusted for this dynamic analysis to reflect the total load on each stringer, including the strain-effects due to loading the S-IVB with cryogenic fuels. The effects of differential pressure were included in the estimation of the static buckling load.

The dynamic strain data were analyzed by high speed oscillograph traces and power spectral density analysis as shown in figures 25-43 through 25-57. Panel flutter, which was searched for, was to be distinguished by the sustained characteristic of a single dominant mode with a wave shape that was primarily periodic and of constant amplitude, significantly higher than the expected random and narrow band random vibration. No such dominant mode was found in the dynamic strain data during supersonic flight. Therefore, it is concluded that panel flutter did not occur. The predominant dynamic response was narrow band random vibration of two or more modes of the panels occurring simultaneously as shown in the figures. This dynamic response is typical of skin panel vibration response to acoustic noise or random pressure fluctuations in the aerodynamic boundary layer.

The composite dynamic strain levels which are tabulated in table 25-2 show that the aberrant measurements S0100 and S0101 indicated the highest values; 498 μin./in. rms and 460 μin./in. rms, respectively. These values are approximately four times higher than the maxima values of rms strain measured on AS-204 but only approximately one-half of the maximum levels recorded in the wind tunnel panel flutter qualification testing. If the aberrant measurements are disregarded because of the peculiarities noted in this report, the highest dynamic strain during supersonic flight occurred on measurement S0092. The dynamic strain level would then be approximately 253 μin./in. rms, approximately twice as high as the maximum value measured on AS-204, and approximately one-third of the levels recorded in the wind tunnel panel flutter qualification testing.

The dynamic strains after 100 sec (figure 25-42) were all due to the predominantly low frequency (approximately 5.5 Hz) vibration which was attributed to POGO, (section 2). These dynamic strains were not due to random pressure fluctuations in the boundary layer.

In summary it is concluded that panel flutter did not occur and that the fatigue life of the forward skirt skin panels, as demonstrated in the wind tunnel qualification test, was not impaired by the dynamic strains measured during the AS-502 flight.

TABLE 25-1 (Sheet 1 of 2)
COMPOSITE VIBRATION AND ACOUSTIC LEVELS

MEASUREMENT NO.	MEASUREMENT	DIRECTION	FREQUENCY RANGE (cps)	S-IC POWERED FLIGHT LEVELS		S-II POWERED FLIGHT LEVELS	S-IVB POWERED FLIGHT LEVELS	MAX AS-501 FLIGHT LEVEL
				LIFTOFF	MAX INFLIGHT		FIRST BURN	
	Vibration			Acceleration (grms)				
E0041-403	Helium Bottle, Thrust Struct	Thrust	40 to 3,000	1.8	1.0	NF	1.8	NM
E0042-403	Helium Bottle, Thrust Struct	Pitch	40 to 3,000	2.2	1.4	NF	2.2	NM
E0043-403	Helium Bottle, Thrust Struct	Yaw	40 to 3,000	2.1	1.2	NF	2.1	NM
E0061-403	LH2 Feedline, Thrust Struct	Thrust	40 to 3,000	2.2	1.4	NF	1.7	NM
E0062-409	PU Probe, LH2 Tank Cylinder	Radial	40 to 3,000	6.8	4.6	NF	0.4	NM
E0090-403	Gimbal Point	Thrust	40 to 3,000	0.4	0.3	NF	4.5	3.0
E0091-411	Field Splice Position I	Thrust	10 to 220	0.7	0.4	NF	NF	1.1*
E0092-404	Station 2748 Position II	Thrust	10 to 220	0.8	0.5	NF	NF	0.9*
E0093-411	Field Splice Position I	Thrust	40 to 3,000	2.9	5.0	NF	0.2	4.8
E0094-411	Field Splice Position I	Pitch	40 to 3,000	6.5	7.6	NF	0.2	8.2
E0095-411	Field Splice Position I	Yaw	40 to 3,000	2.1	4.7	NF	0.2	2.7
E0096-411	Field Splice Position II	Thrust	40 to 3,000	1.3*	4.4	NF	0.2	5.0
E0097-411	Field Splice Position II	Pitch	40 to 3,000	1.1	3.0	NF	0.1	5.7
E0098-411	Field Splice Position II	Yaw	40 to 3,000	4.2	8.6	NF	0.2	7.2
E0103-404	Sequencer Panel	Thrust	40 to 3,000	4.2	5.9	NF	0.4	6.3
E0104-404	Sequencer Assembly	Radial	40 to 3,000	1.6	2.8	NF	0.3	3.5
E0105-404	Sequencer Panel	Radial	40 to 3,000	4.4	7.8	NF	0.4	7.5
E0106-404	Switch Selector Panel	Thrust	40 to 3,000	4.1	4.8	NF	0.4	10.9
E0107-404	Switch Selector Unit	Radial	40 to 3,000	3.5	3.1	NF	0.3	3.6
E0108-404	Switch Selector Panel	Radial	40 to 3,000	4*	6.6	NF	0.4	8.1
E0109-411	PU Electronic Panel	Thrust	40 to 3,000	3.2	4.3	NF	0.2	5.9
E0110-411	PU Electronic Assembly	Radial	40 to 3,000	5.5	4.9	NF	0.2	3.5
E0111-411	PU Electronic Panel	Radial	40 to 3,000	10.6	9.8	NF	0.3	9.0
E0112-411	EBW Range Safety Panel	Thrust	40 to 3,000	1.3*	3.2	NF	0.2	5.2
E0113-411	EBW Range Safety Unit	Radial	40 to 3,000	2.2	1.6	NF	0.2	2.3
E0114-411	EBW Range Safety Panel	Radial	40 to 3,000	I	I	I	I	8.1
E0115-411	Forward Skirt Battery 1	Thrust	40 to 3,000	1.0	2.1	NF	0.2	2.6
E0116-411	Forward Skirt Battery 1	Radial	40 to 3,000	3.2	4.2	NF	0.3	5.7
E0117-411	Forward Skirt Battery 1	Tangential	40 to 3,000	1.9	I	I	I	4.8

TABLE 25-1 (Sheet 2 of 2)
COMPOSITE VIBRATION AND ACOUSTIC LEVELS

MEASUREMENT NO.	MEASUREMENT	DIRECTION	FREQUENCY RANGE (cps)	S-IC POWERED FLIGHT LEVELS		S-II POWERED FLIGHT LEVELS	S-IVB POWERED FLIGHT LEVELS	MAX AS-501 FLIGHT LEVEL
				LIFTOFF	MAX INFLIGHT		FIRST BURN	
	Vibration				Acceleration (grms)			
E0118-427	APS Mod 1 Aft Attach Point	Thrust	40 to 3,000	0.8*	2.8	NF	0.6	2.6
E0119-427	APS Mod 1 Aft Attach Point	Radial	40 to 3,000	2.7	4.2	NF	0.4	4.5
E0120-427	APS Mod 1 Fwd Attach Point	Radial	40 to 3,000	4.7	5.7	NF	0.8	5.5
E0209-401	Combustion Chamber Dome	Thrust	40 to 3,000	NF	NF	NF	9.1	7.7
E0210-401	LH2 Turbopump	Radial	40 to 3,000	NF	NF	NF	I	I
E0211-401	LOX Turbopump	Radial	40 to 3,000	NF	NF	NF	21.0	28*
E0212-403	Gimbal Point	Yaw	40 to 3,000	I	0.3	NF	4.2	NM
E0213-403	Gimbal Point	Pitch	40 to 3,000	0.7*	0.4	NF	5.3	NM
	Acoustics				Sound Pressure Level (db)			
B0016-411	Forward Skirt	Internal	30 to 3,000	140.7	132.6	NF	NF	139.5
B0017-411	Forward Skirt	Internal	2,400 to 4,800	111C	121	NF	NF	126
B0018-411	Forward Skirt	Internal	4,800 to 9,600	105C	119.5	NF	NF	119
B0019-427	Aft Skirt	External	30 to 3,000	151.9	150.2	NF	NF	150
B0020-427	Aft Skirt	External	2,400 to 4,800	130C	138	NF	NF	129C
B0021-427	Aft Skirt	External	4,800 to 9,600	120C	133C	NF	NF	130C
B0022-404	Aft Skirt	Internal	30 to 3,000	144.1	129.4	NF	NF	145
B0023-404	Aft Skirt	Internal	2,400 to 4,800	N	N	N	N	110C
B0024-404	Aft Skirt	Internal	4,800 to 9,600	108C	108C	NF	NF	101C
B0025-426	Forward Skirt	External	30 to 3,000	152.0	151.8	NF	NF	NM
B0026-426	Forward Skirt	External	2,400 to 4,800	130C	138	NF	NF	NM
B0027-426	Forward Skirt	External	4,800 to 9,600	123C	134	NF	NF	NM

NF - System Noise Floor
NM - Not Monitored
* - Estimated Level
I - Data Invalid
N - No Data
C - Data Corrected for System Noise

TABLE 25-2
COMPOSITE DYNAMIC STRAIN LEVELS

MEASUREMENT NO.	MEASUREMENT	DIRECTION	FREQUENCY RANGE (cps)	S-IC POWERED FLIGHT LEVELS STRAIN (μin./in. rms)*		
				LIFTOFF	TRANSONIC	SUPERSONIC
S0086-426	Forward Skirt Panel 13	Thrust	2 to 800	39.8K	29.9	25.8
S0087-426	Forward Skirt Panel 17	Thrust	2 to 800	D	D	D
S0088-426	Forward Skirt Panel 26	Thrust	2 to 800	44**K	40**	28.6
S0089-426	Forward Skirt Panel 33	Thrust	2 to 800	30.1K	30.6	25.8
S0090-426	Forward Skirt Panel 40	Thrust	2 to 800	144.0	73.7	112.3
S0091-426	Forward Skirt Panel 46	Thrust	2 to 800	60**	93.2	66.7
S0092-426	Forward Skirt Panel 55	Thrust	2 to 800	80**	100**	252.6
S0093-426	Forward Skirt Panel 61	Thrust	2 to 800	67.1	36.2	106.8
S0094-426	Forward Skirt Panel 69	Thrust	2 to 800	115.3	77.6	182.5
S0095-426	Forward Skirt Panel 76	Thrust	2 to 800	40**K	25.7	31.8
S0096-426	Forward Skirt Panel 80	Thrust	2 to 800	115.3K	67.4	46.4
S0097-426	Forward Skirt Panel 87	Thrust	2 to 800	102.4	74**	105.0
S0098-426	Forward Skirt Panel 94	Thrust	2 to 800	56.9	65.5	36.6
S0099-426	Forward Skirt Panel 101	Thrust	2 to 800	90**	67.6	64.4
S0100-426	Forward Skirt Panel 108	Thrust	2 to 800	133.8A	51.8A	497.7A
S0101-426	Forward Skirt Panel 7	Thrust	2 to 800	95.0A	64.2A	459.8A

*The possible accumulated measurement error is ±25 percent.

**Estimated level.

K = Panel either partially or completely coated with 0.010 in. thickness of Korotherm for thermal protection near protuberances.

A = Aberrant measurement.

D = Deleted prior to launch.

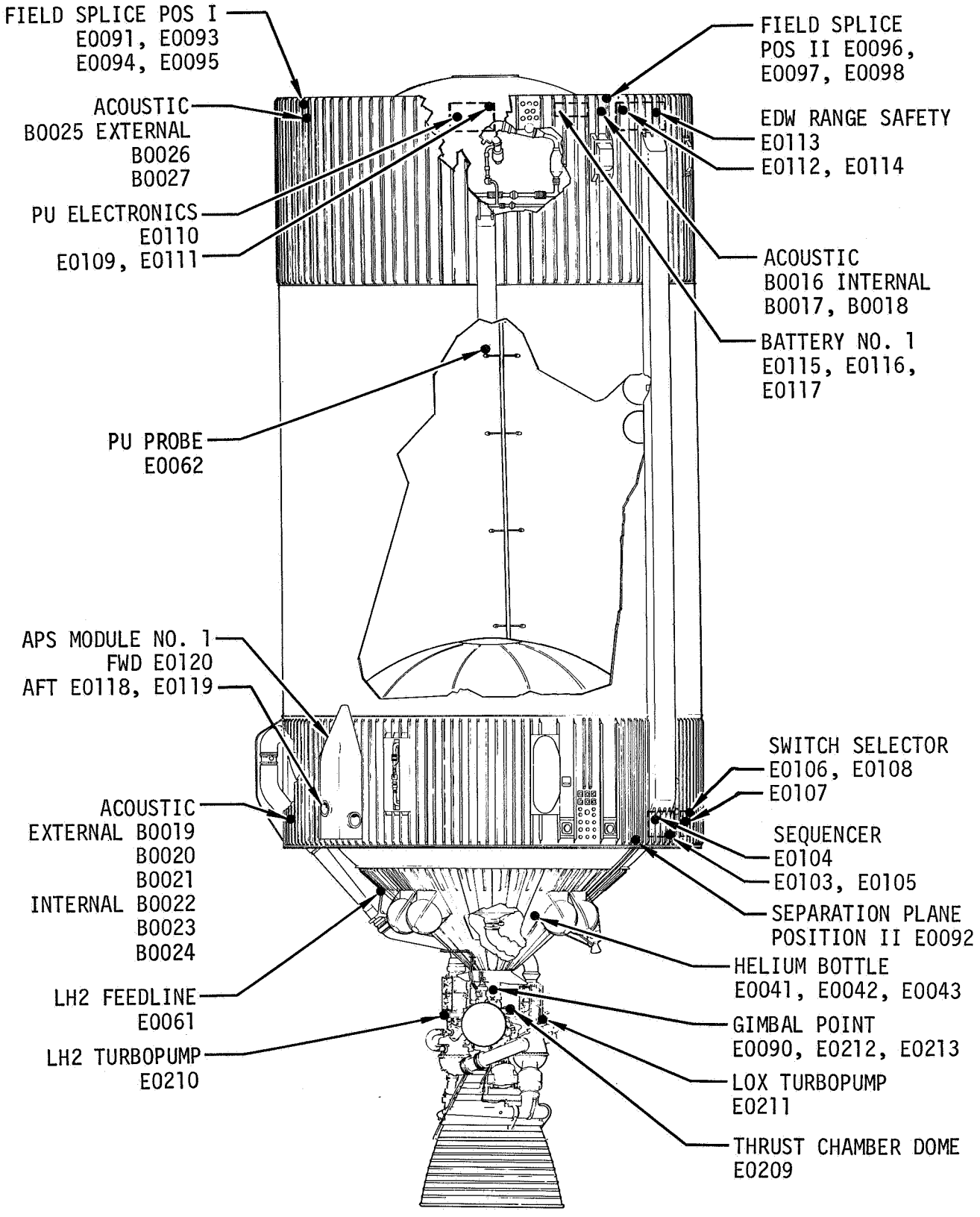

Figure 25-1. Acoustic and Vibration Measurement Locations

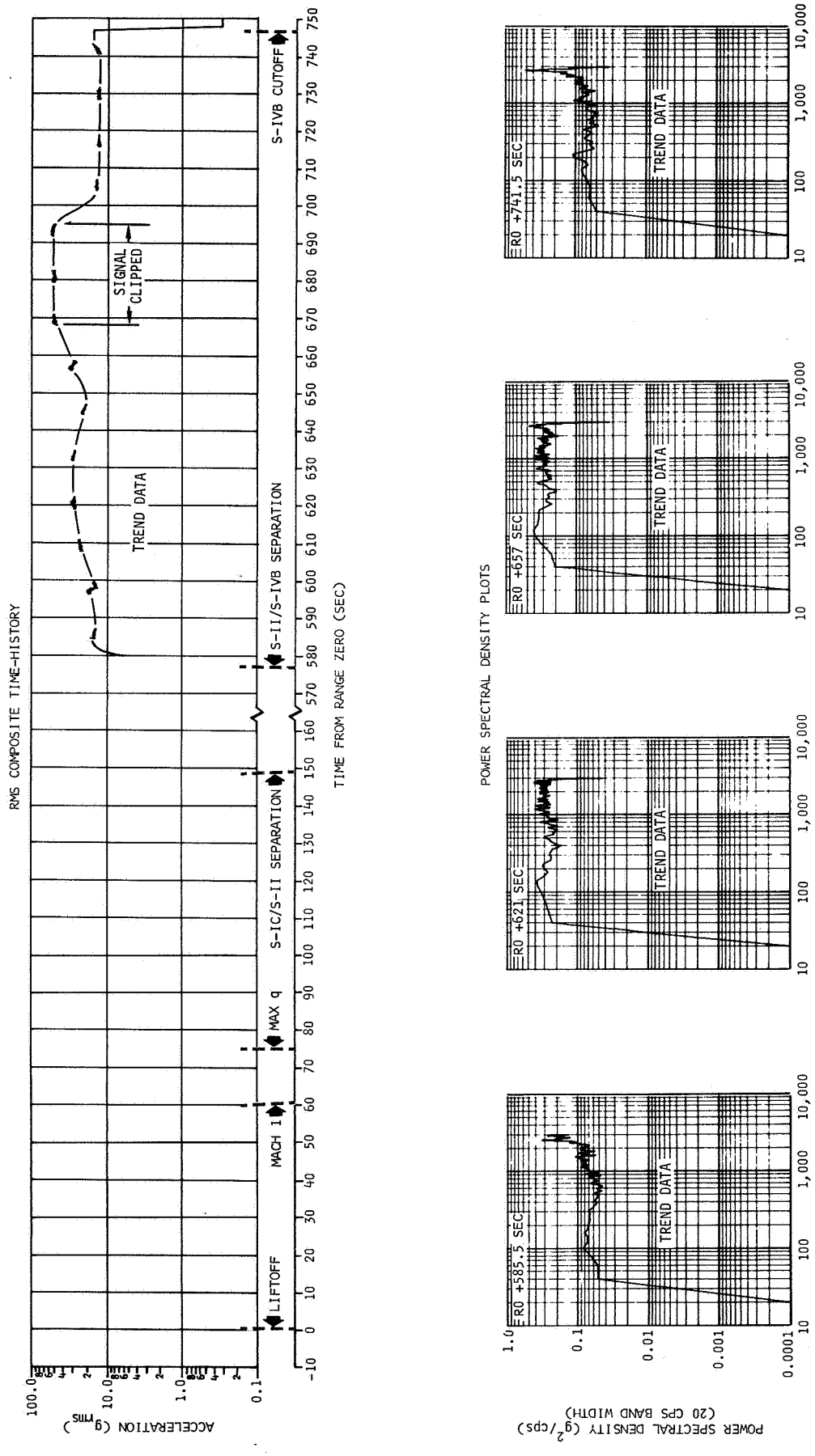

Figure 25-2. Vibration Measured at LH2 Turbopump, Radial Direction - E0210-401

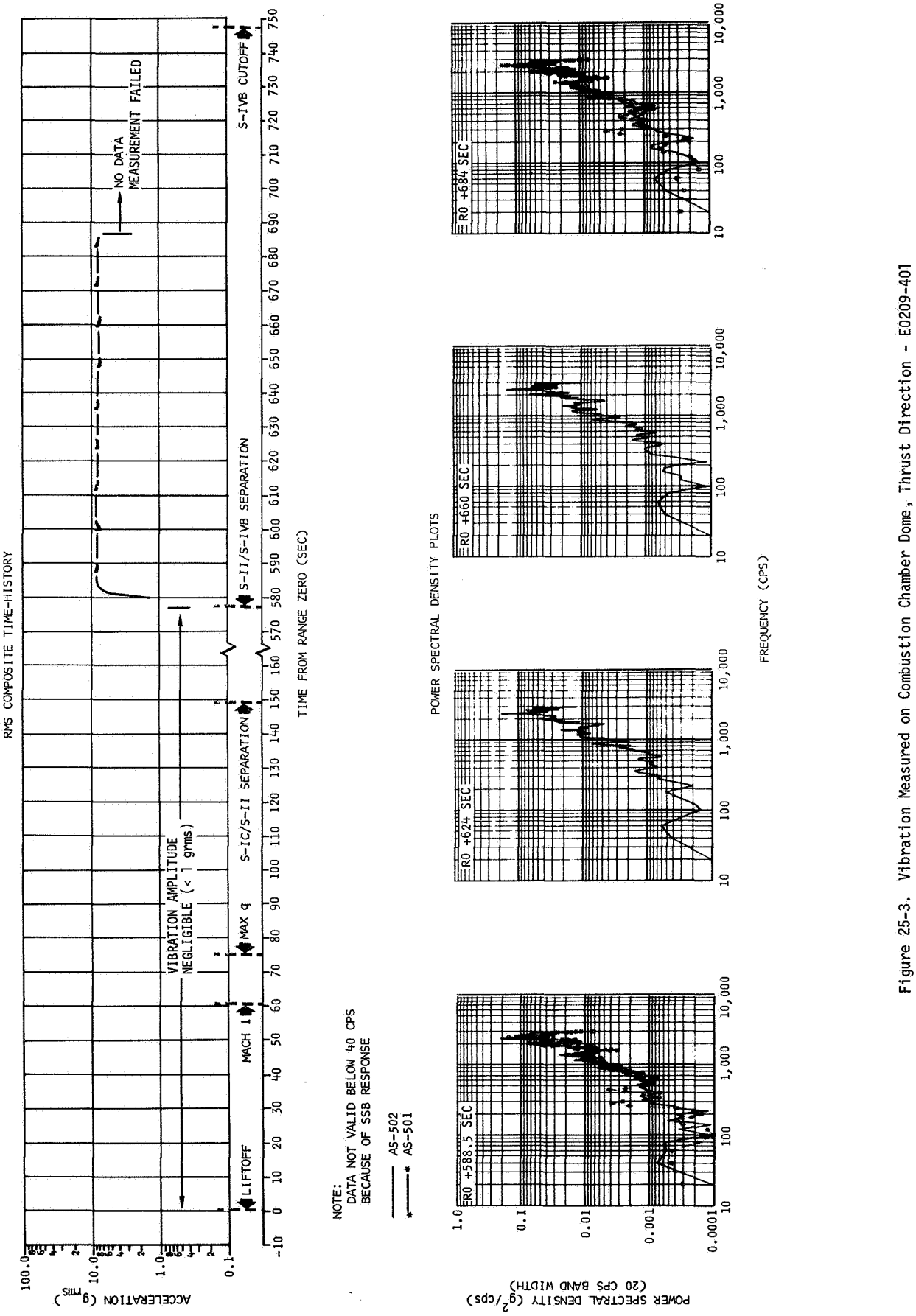

Figure 25-3. Vibration Measured on Combustion Chamber Dome, Thrust Direction - E0209-401

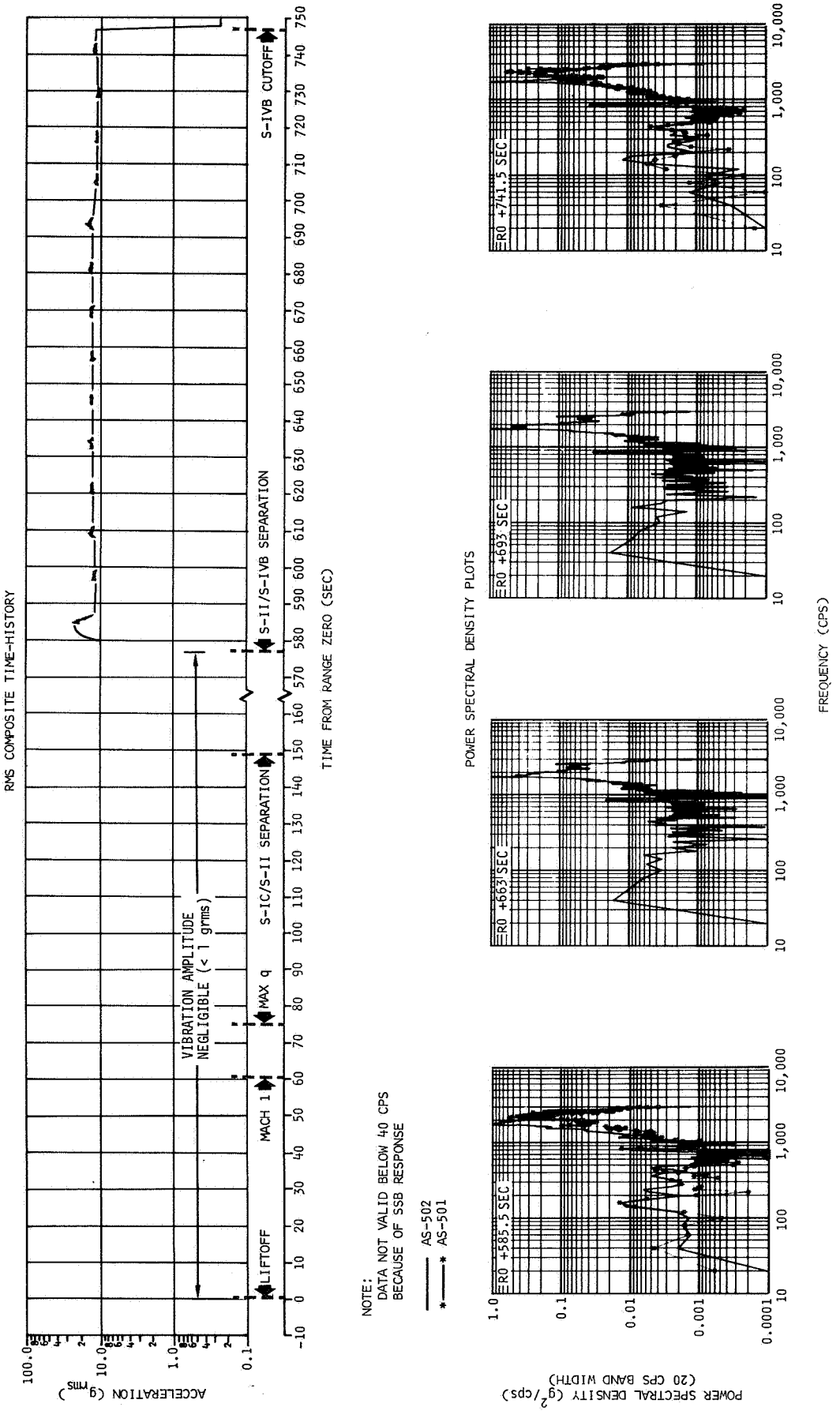

Figure 25-4. Vibration Measured at LOX Turbopump, Radial Direction - E0211-401

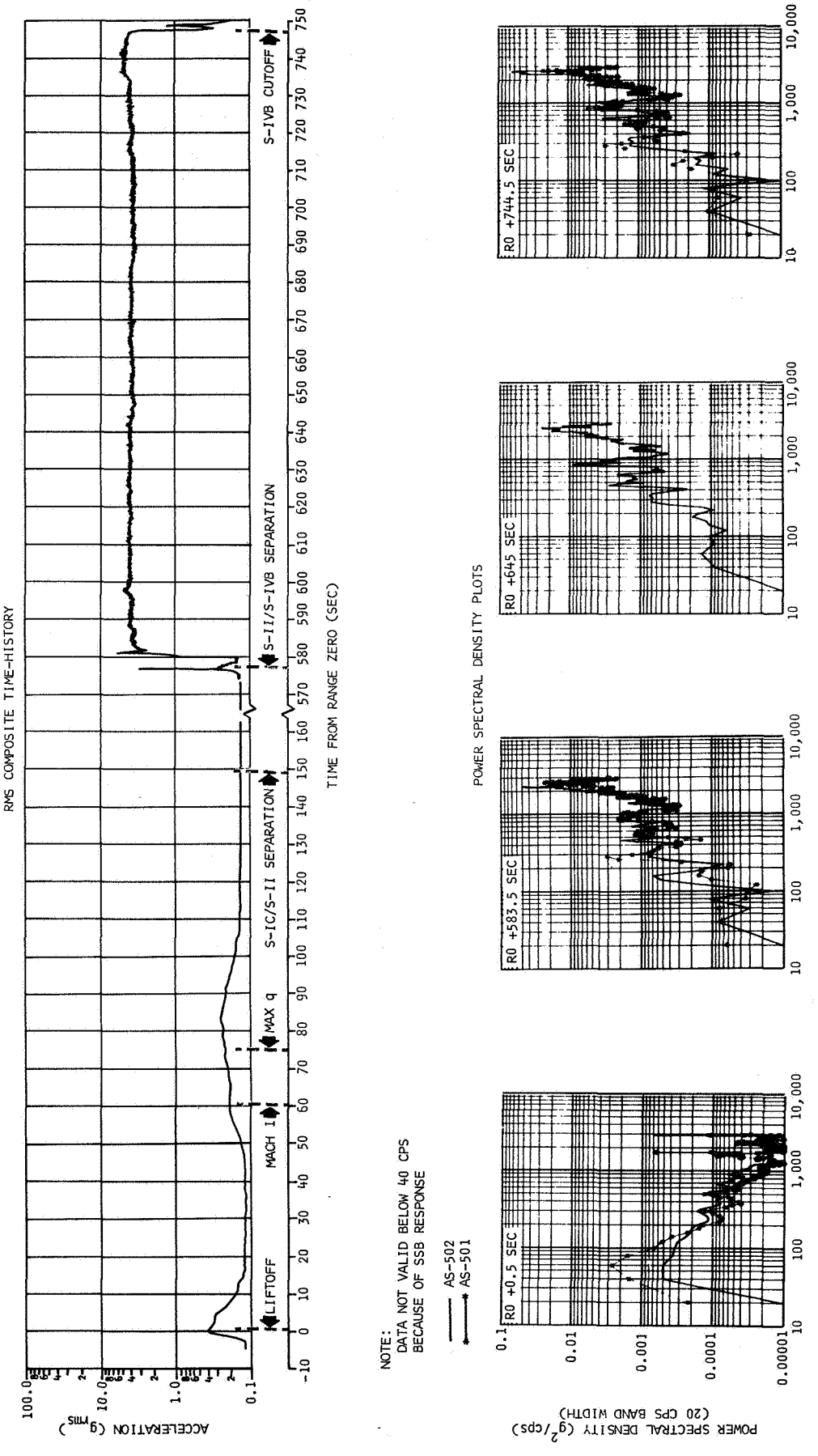

Figure 25-5. Vibration Measured on Gimbal Block, Thrust Direction - E0090-403

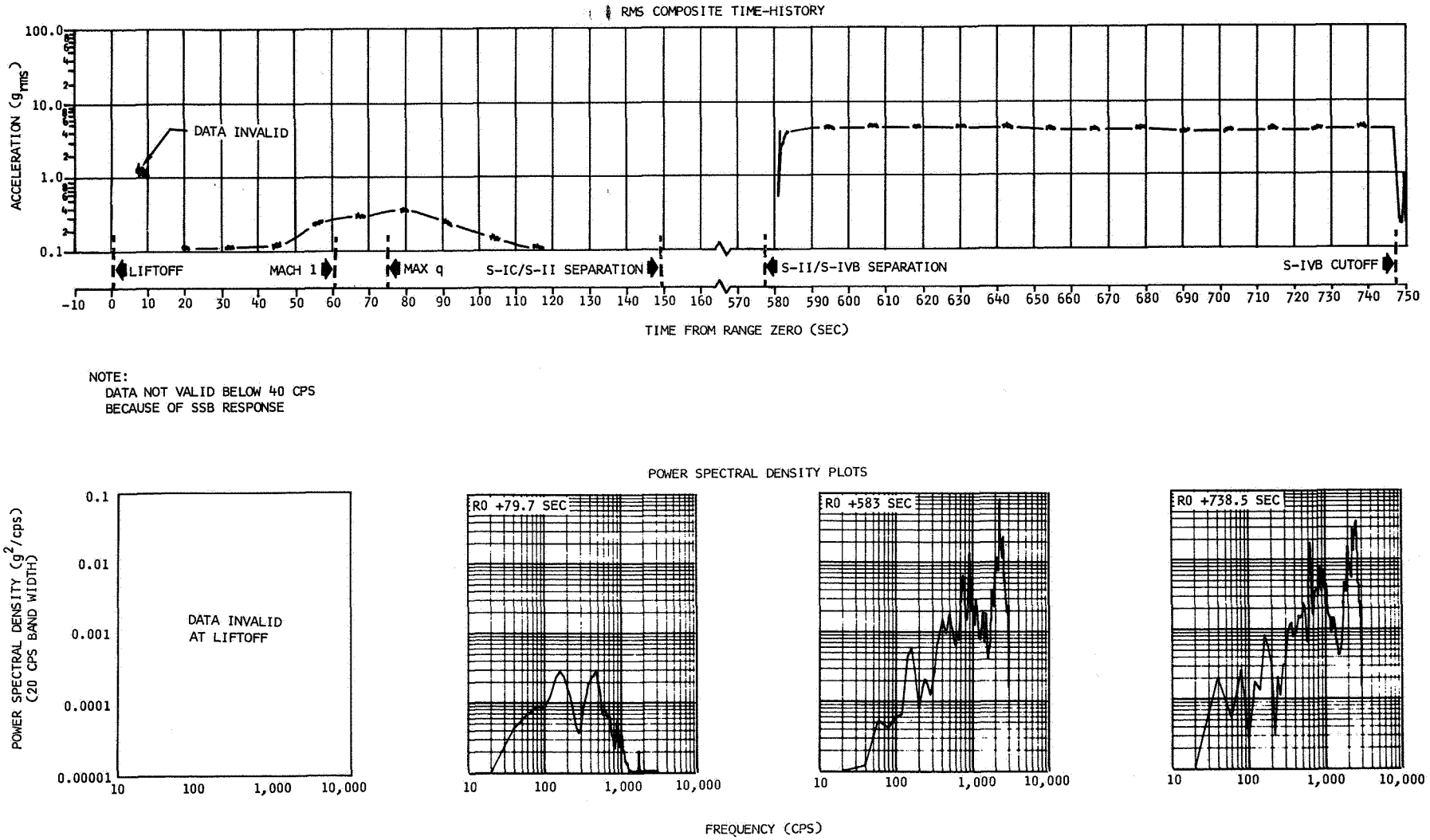

Figure 25-6. Vibration Measured on Gimbal Block, Yaw Direction - E0212-403

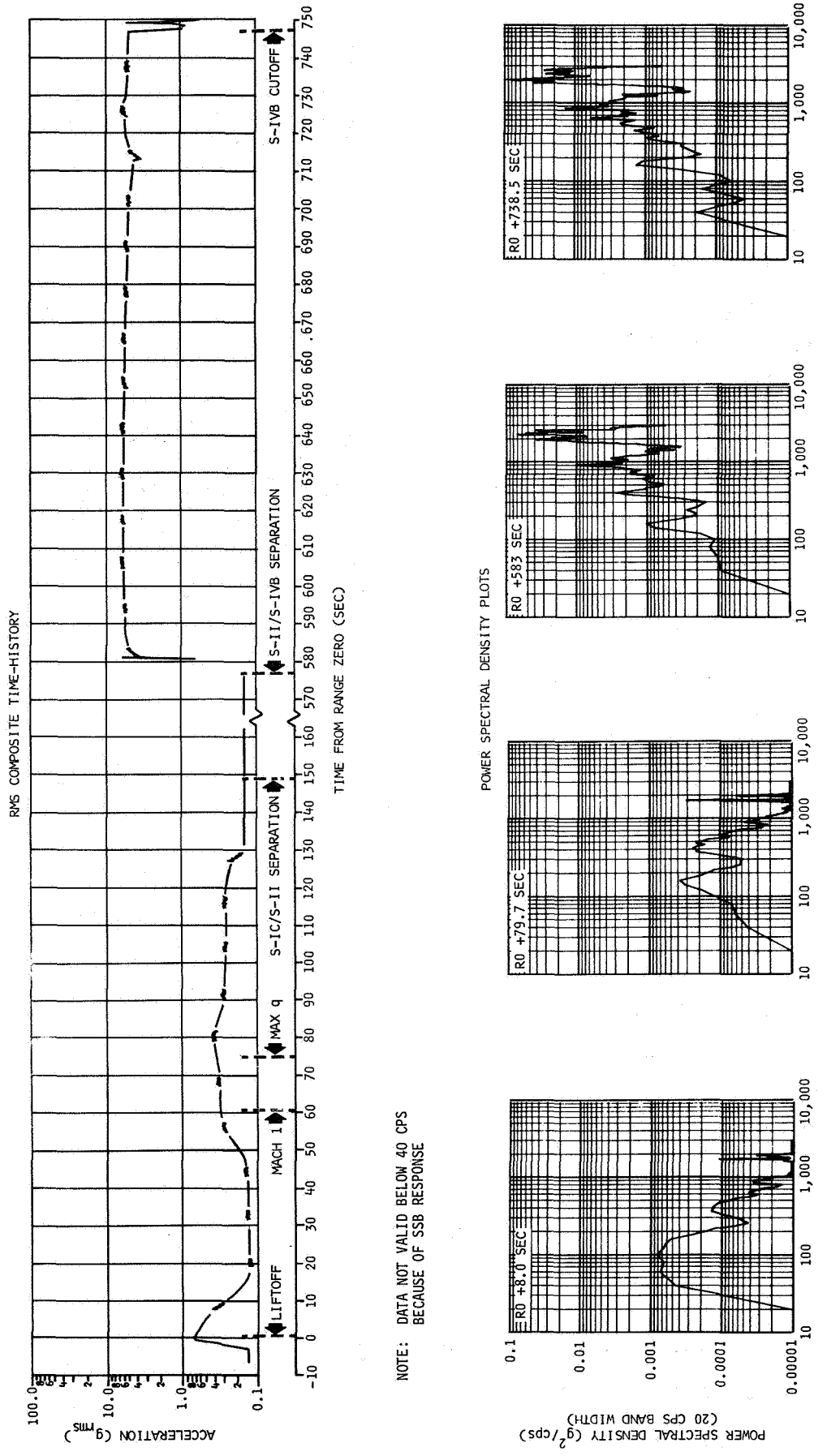

Figure 25-7. Vibration Measured on Gimbal Block, Pitch Direction - E0213-403

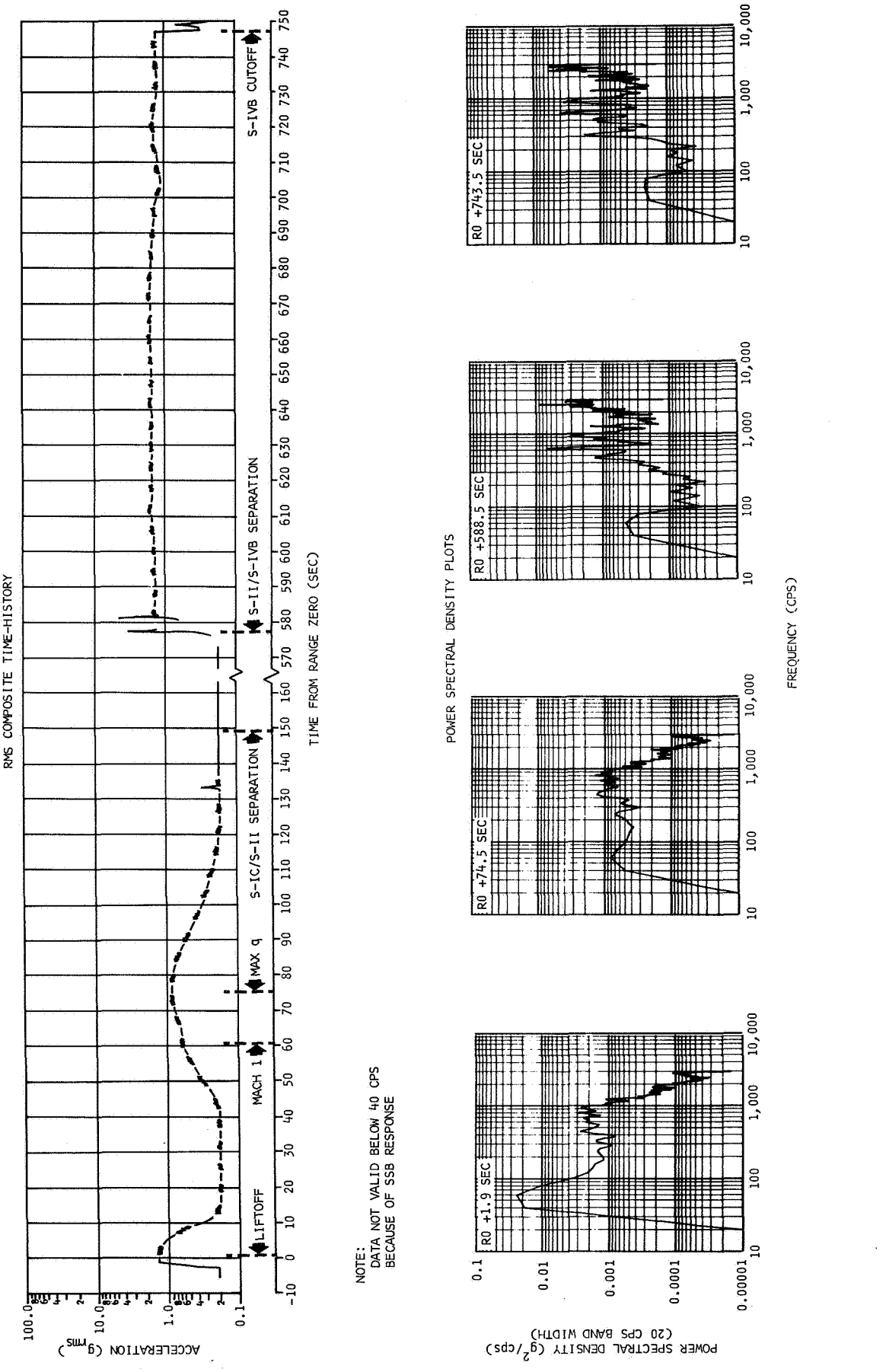

Figure 25-8. Vibration Measured at Input to Helium Bottle, Thrust Direction - E0041-403

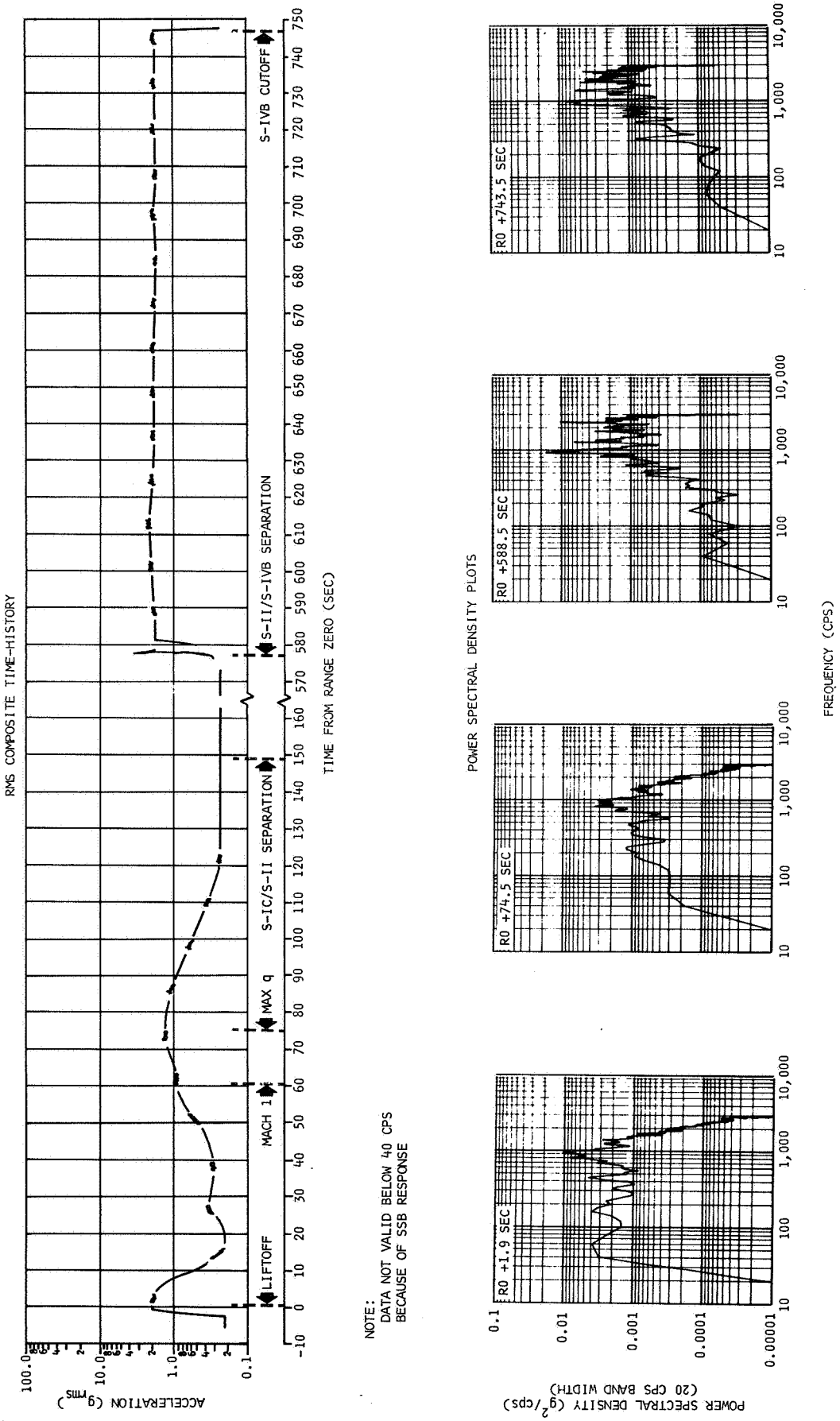

Figure 25-9. Vibration Measured at Input to Helium Bottle, Pitch Direction - E0042-403

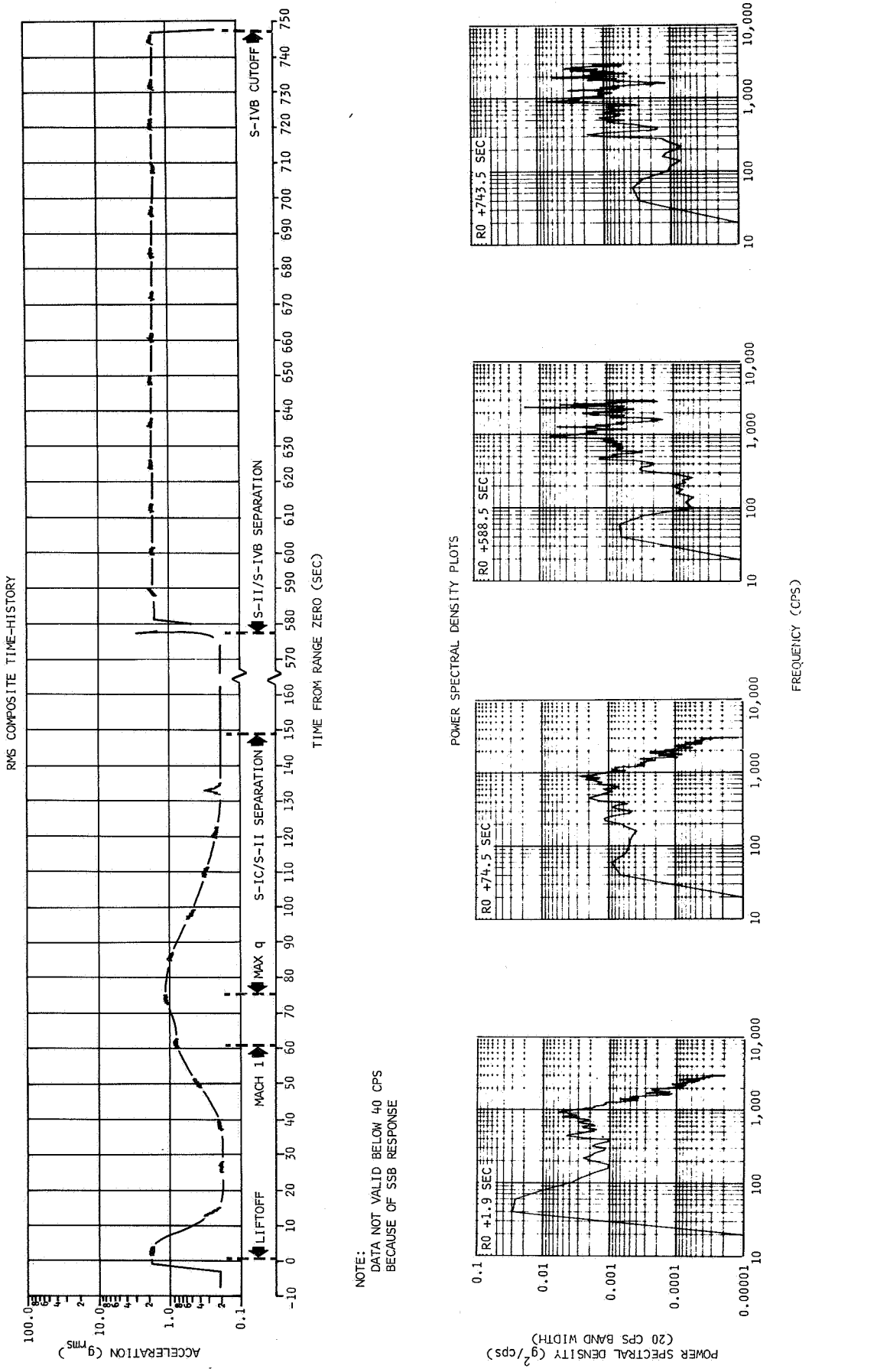

Figure 25-10. Vibration Measured at Input to Helium Bottle, Yaw Direction - E0043-403

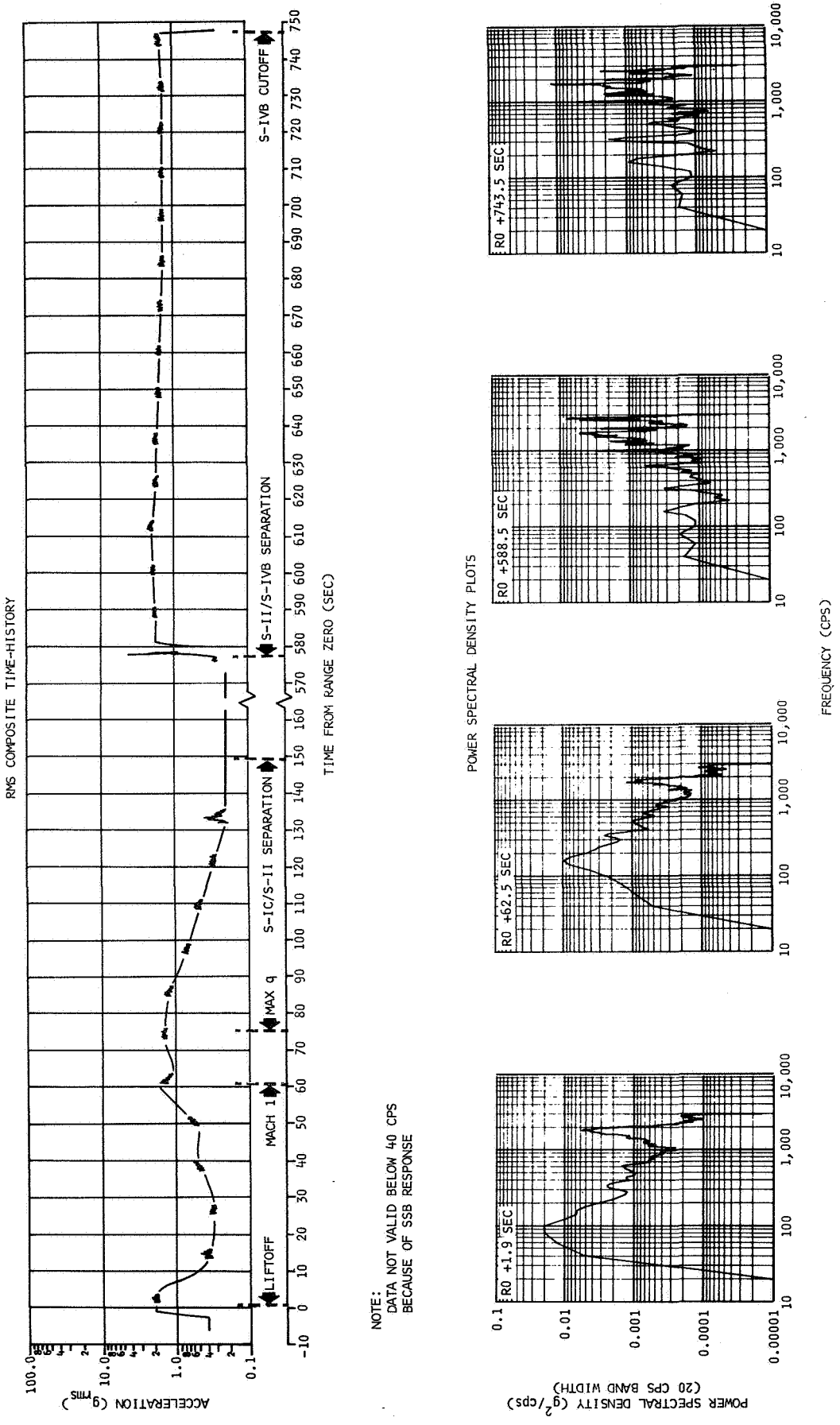

Figure 25-11. Vibration Measured at LH2 Feedline Attach Point on Thrust Structure, Thrust Direction - E0061-403

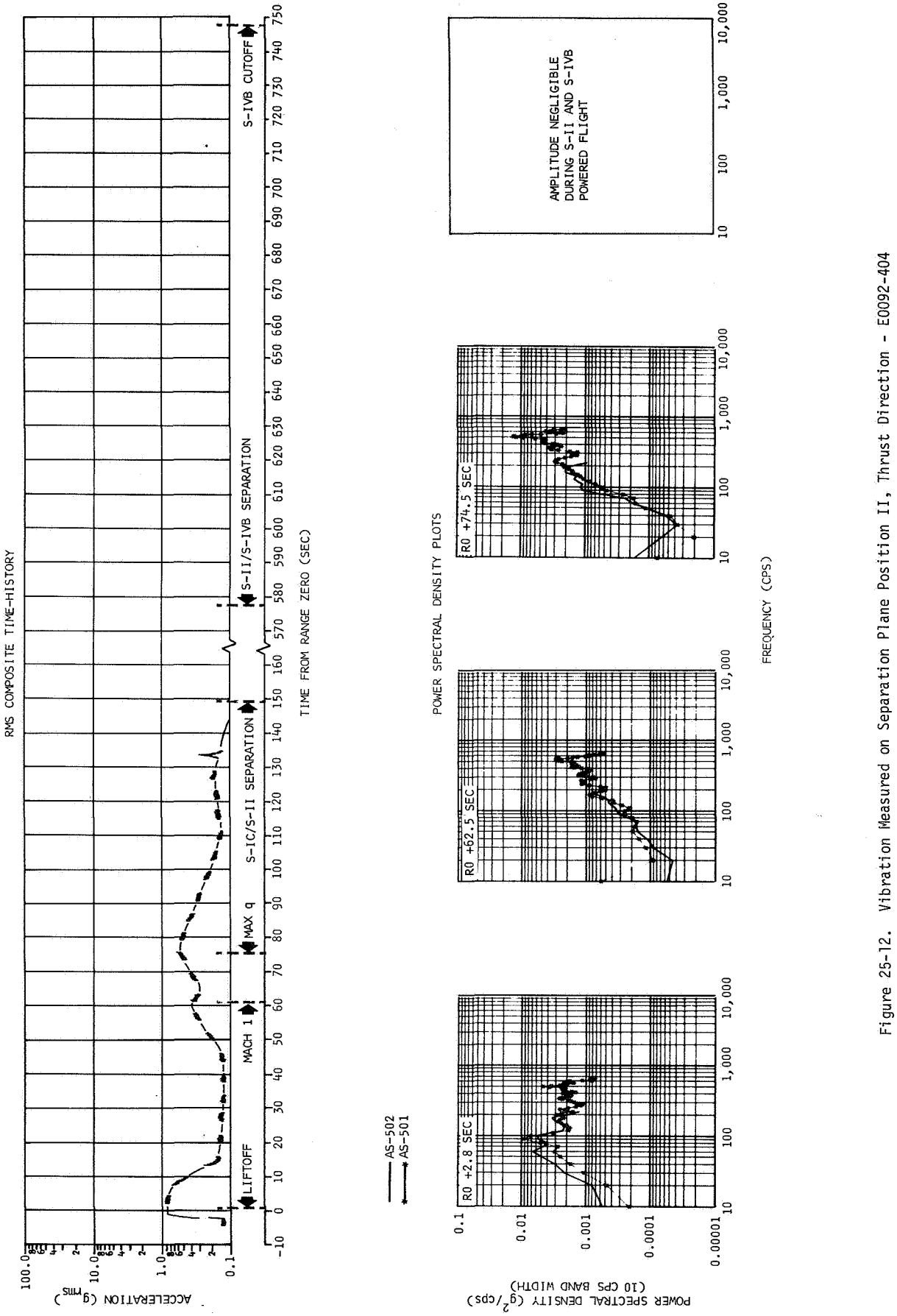

Figure 25-12. Vibration Measured on Separation Plane Position II, Thrust Direction - E0092-404

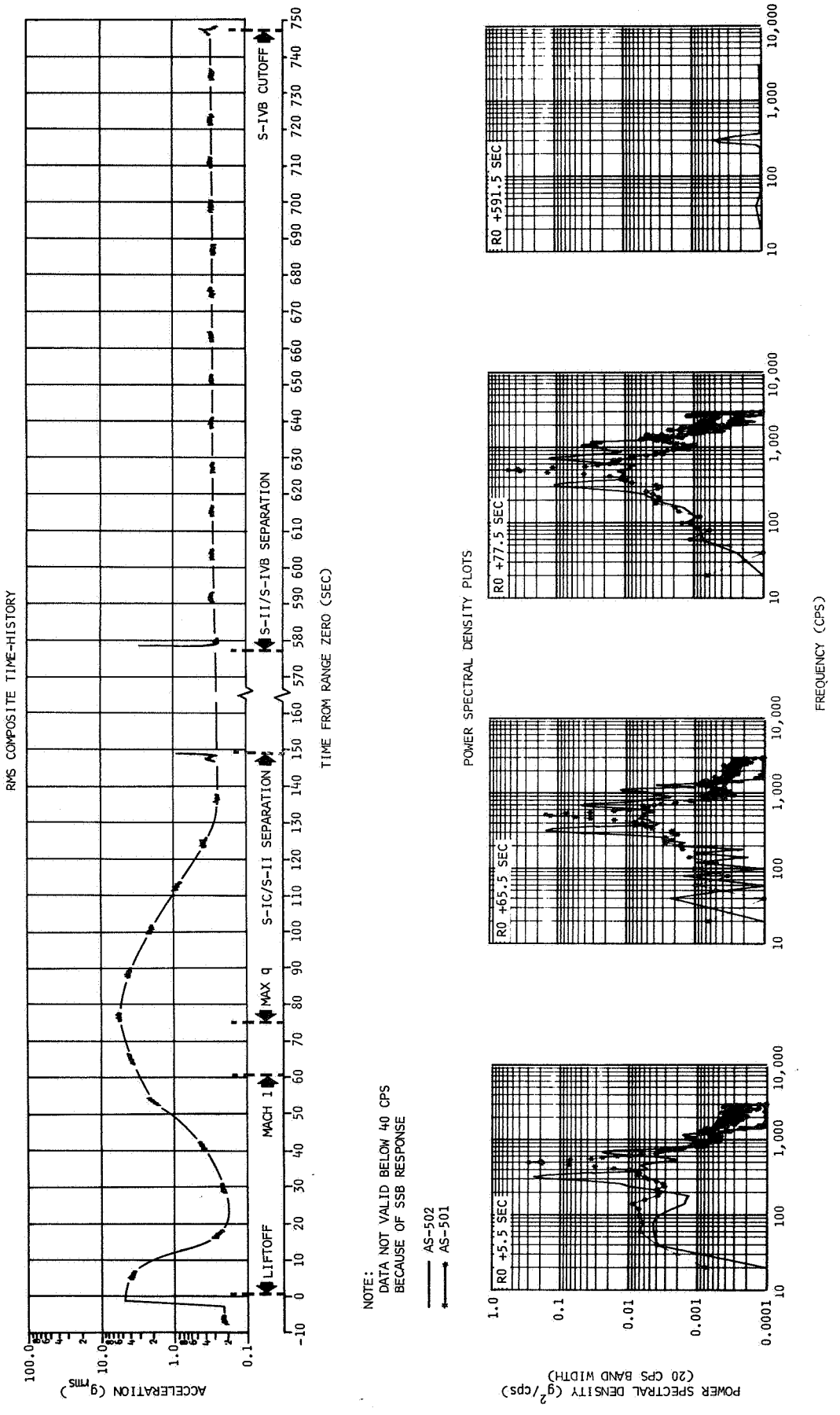

Figure 25-13. Vibration Measured at Input to Sequencer Panel, Thrust Direction - E0103-404

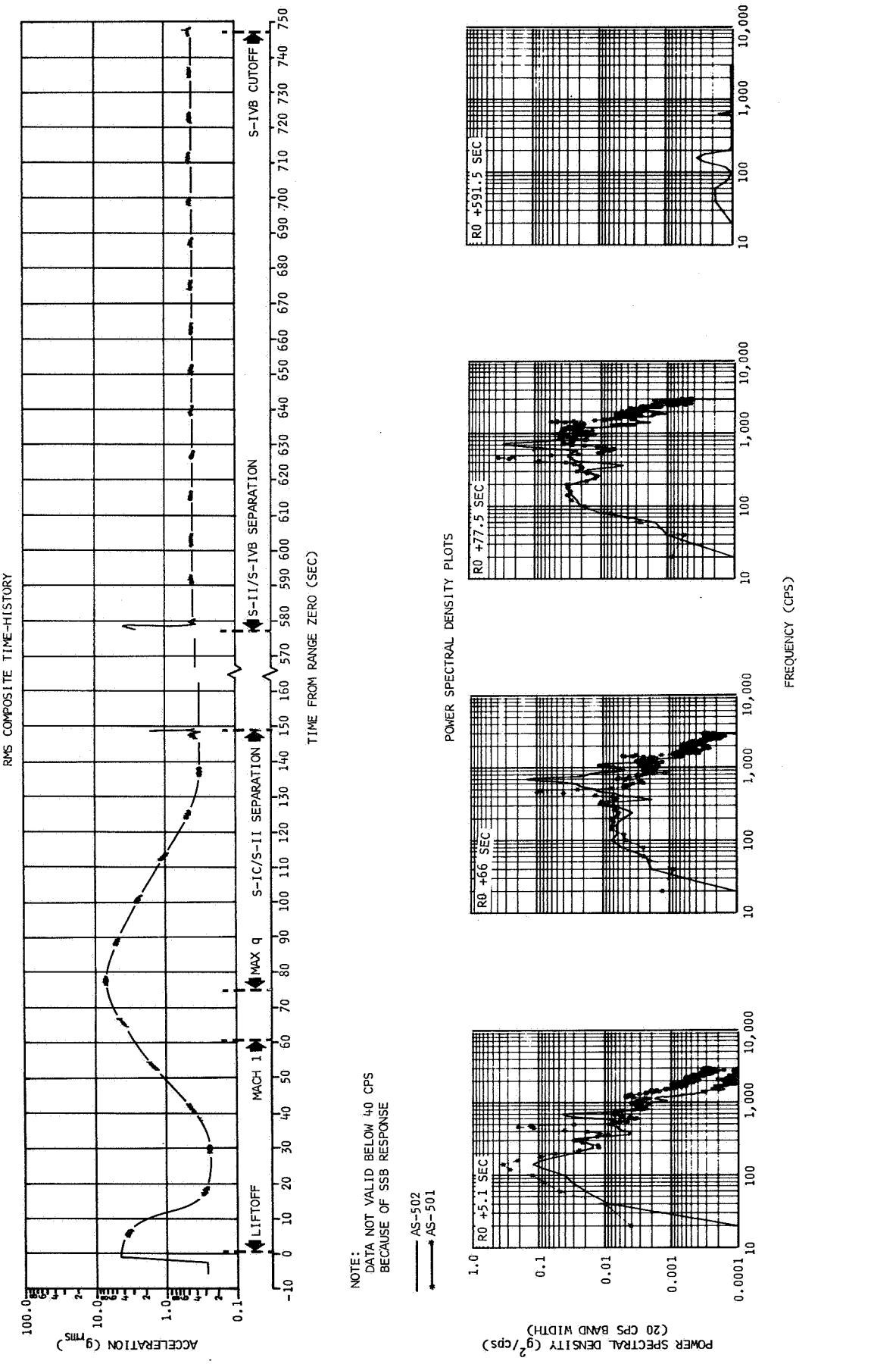

Figure 25-14. Vibration Measured at Input to Sequencer Panel, Radial Direction - E0105-404

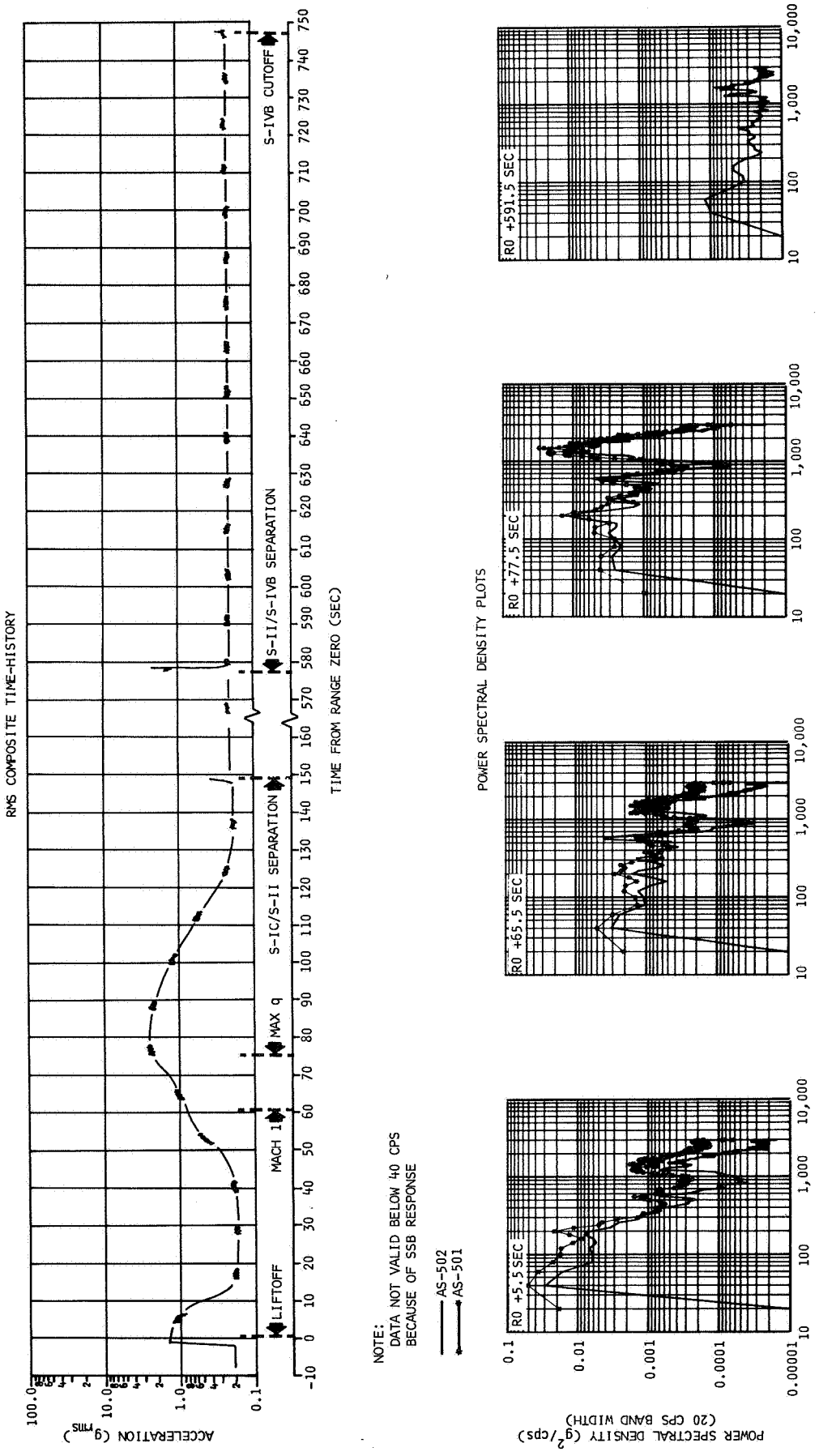

Figure 25-15. Vibration Measured at Input to Sequencer Assembly, Radial Direction - E0104-404

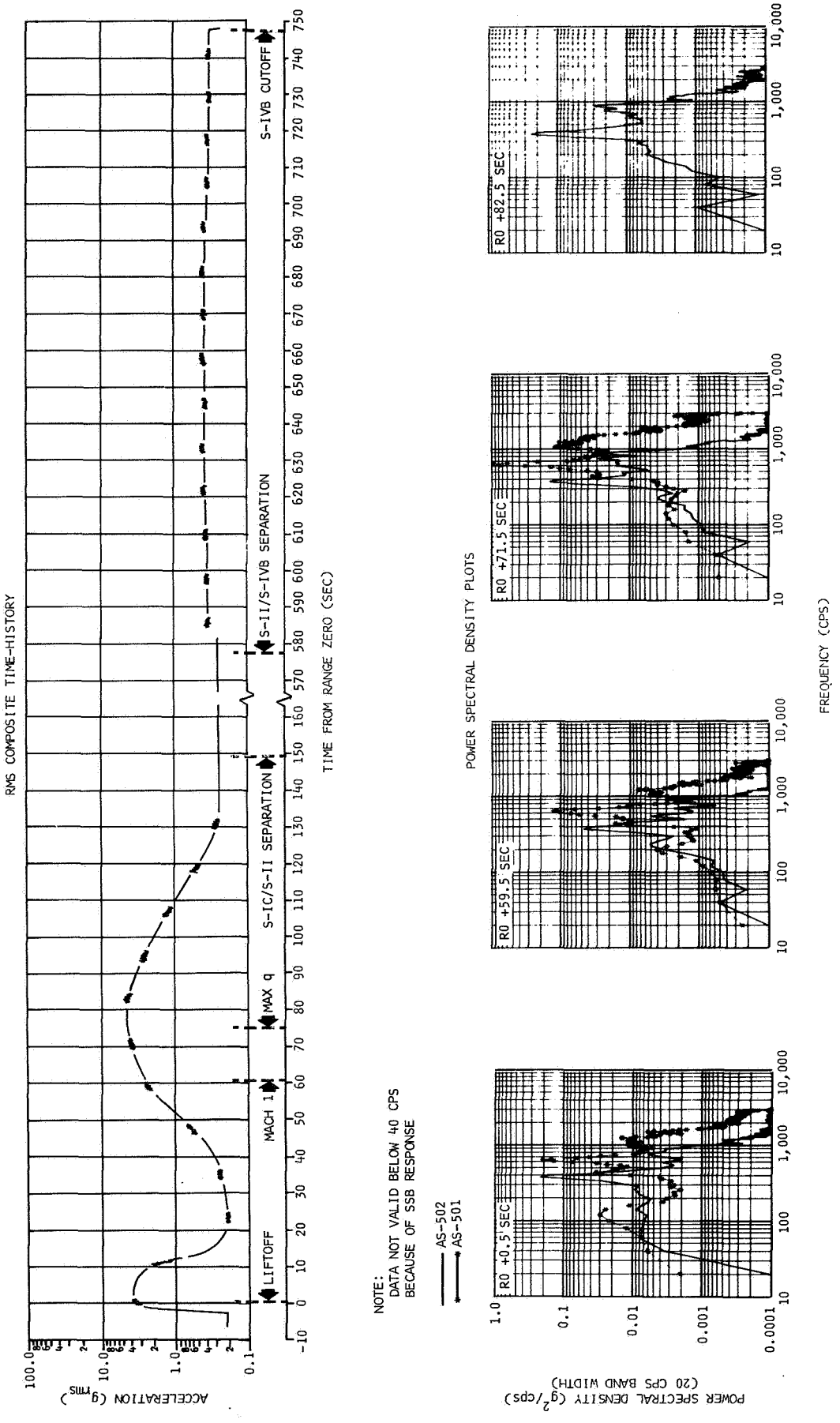

Figure 25-16. Vibration Measured at Input to Switch Selector Panel, Thrust Direction - E0106-404

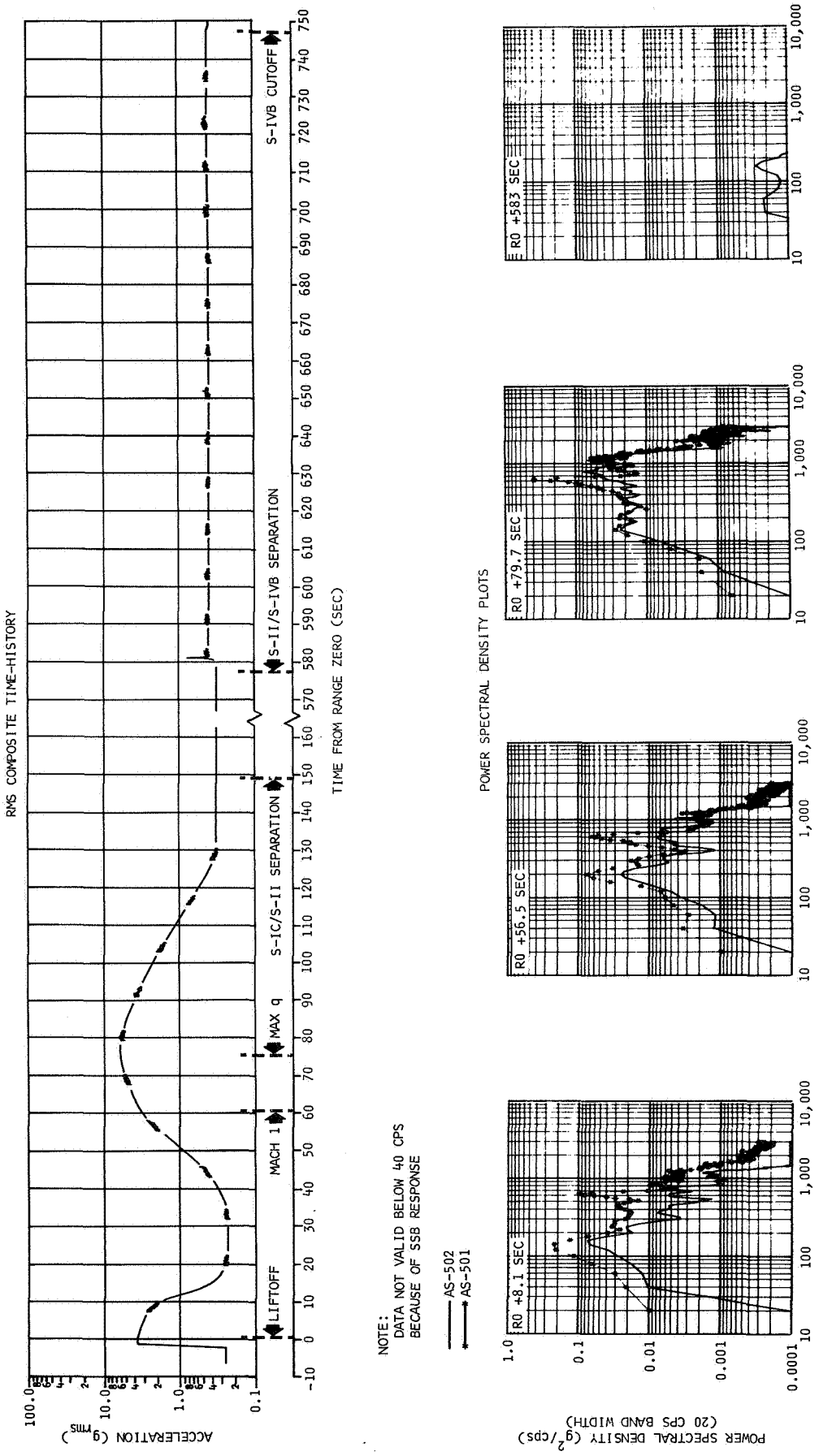

Figure 25-17. Vibration Measured at Input to Switch Selector Panel, Radial Direction - E0108-404

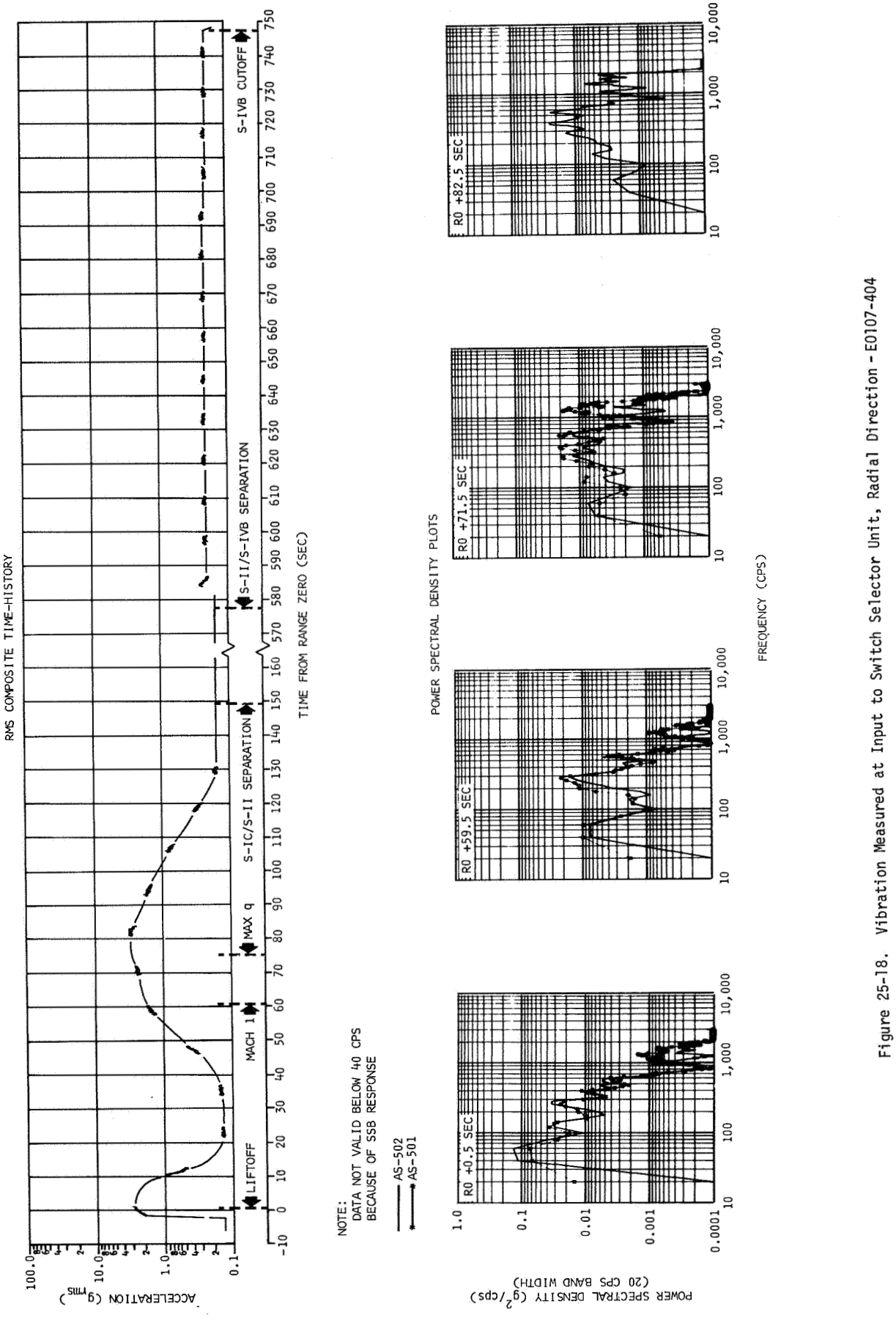

Figure 25-18. Vibration Measured at Input to Switch Selector Unit, Radial Direction - E0107-404

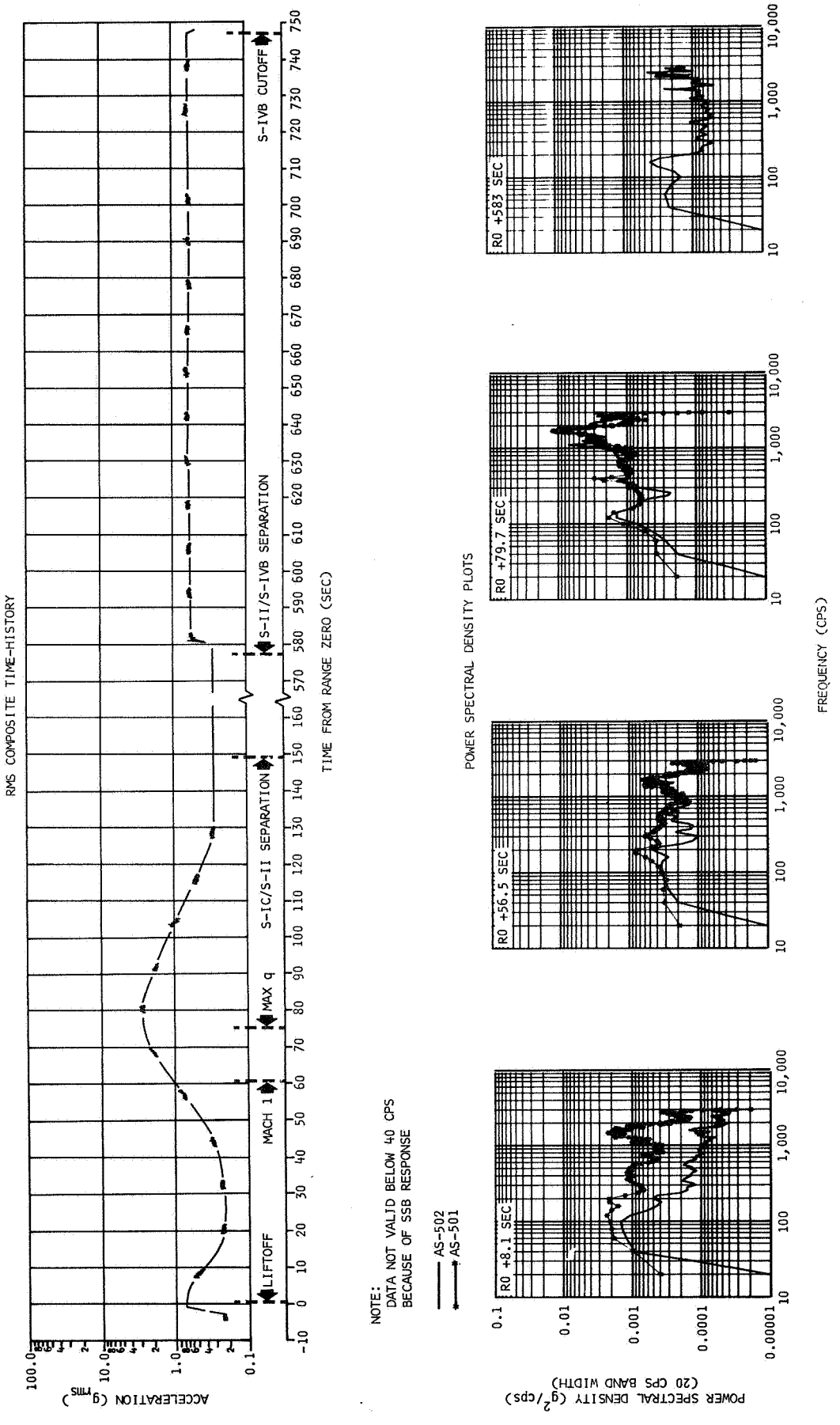

Figure 25-19. Vibration Measured at Aft Attach Point of APS Module 1, Thrust Direction - E0118-427

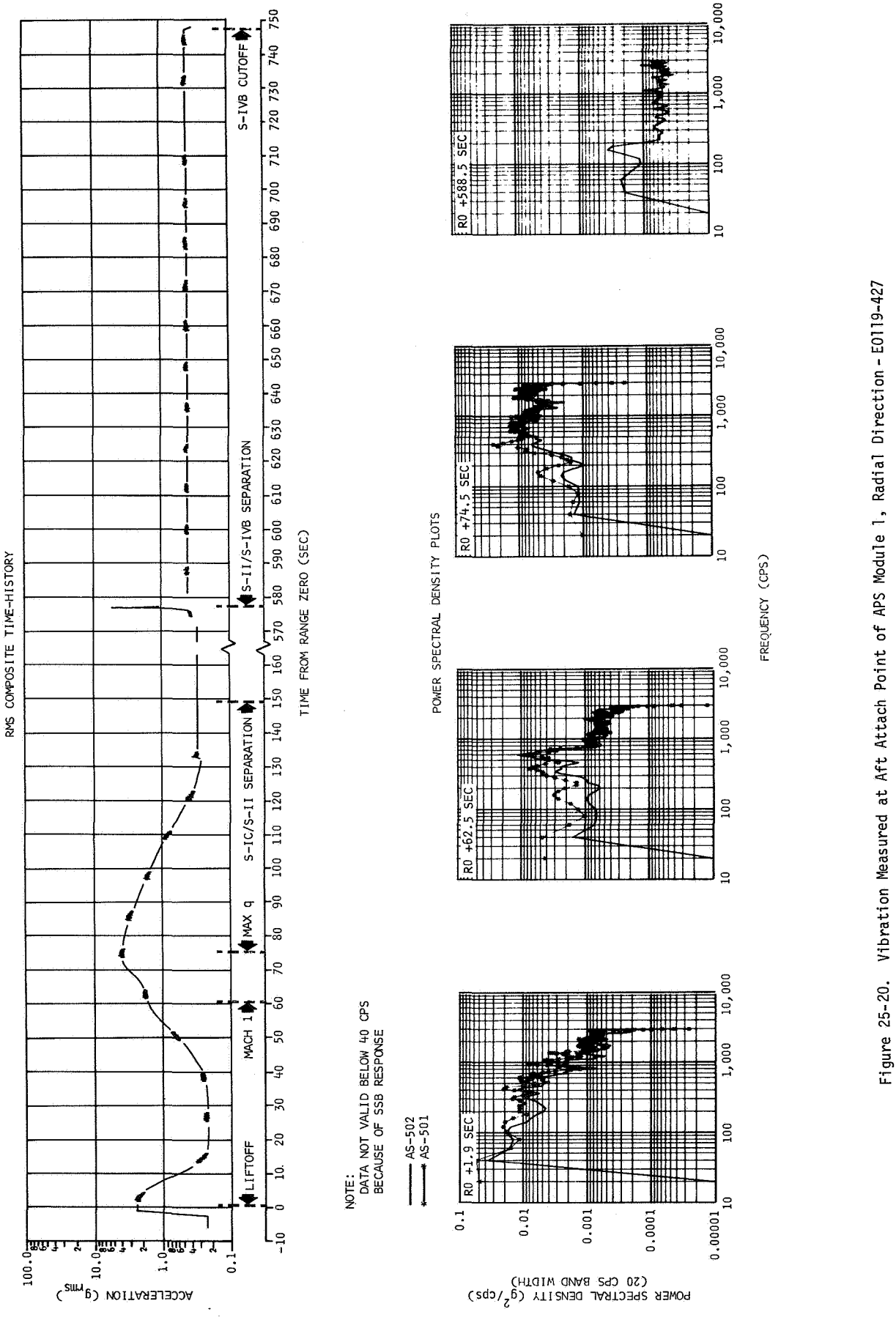

Figure 25-20. Vibration Measured at Aft Attach Point of APS Module 1, Radial Direction - E0119-427

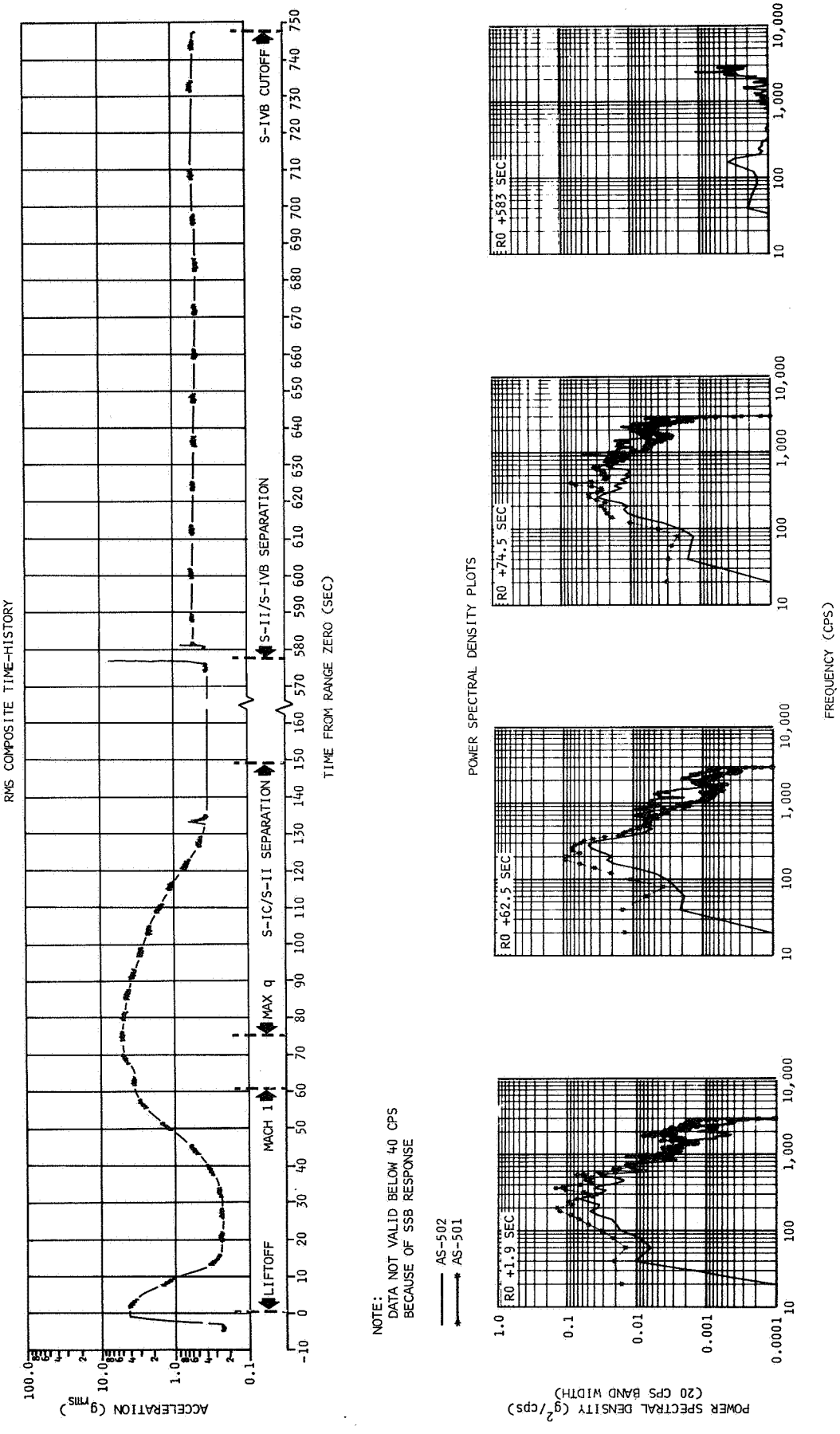

Figure 25-21. Vibration Measured at Forward Attach Point of APS Module 1, Radial Direction - E0120-427

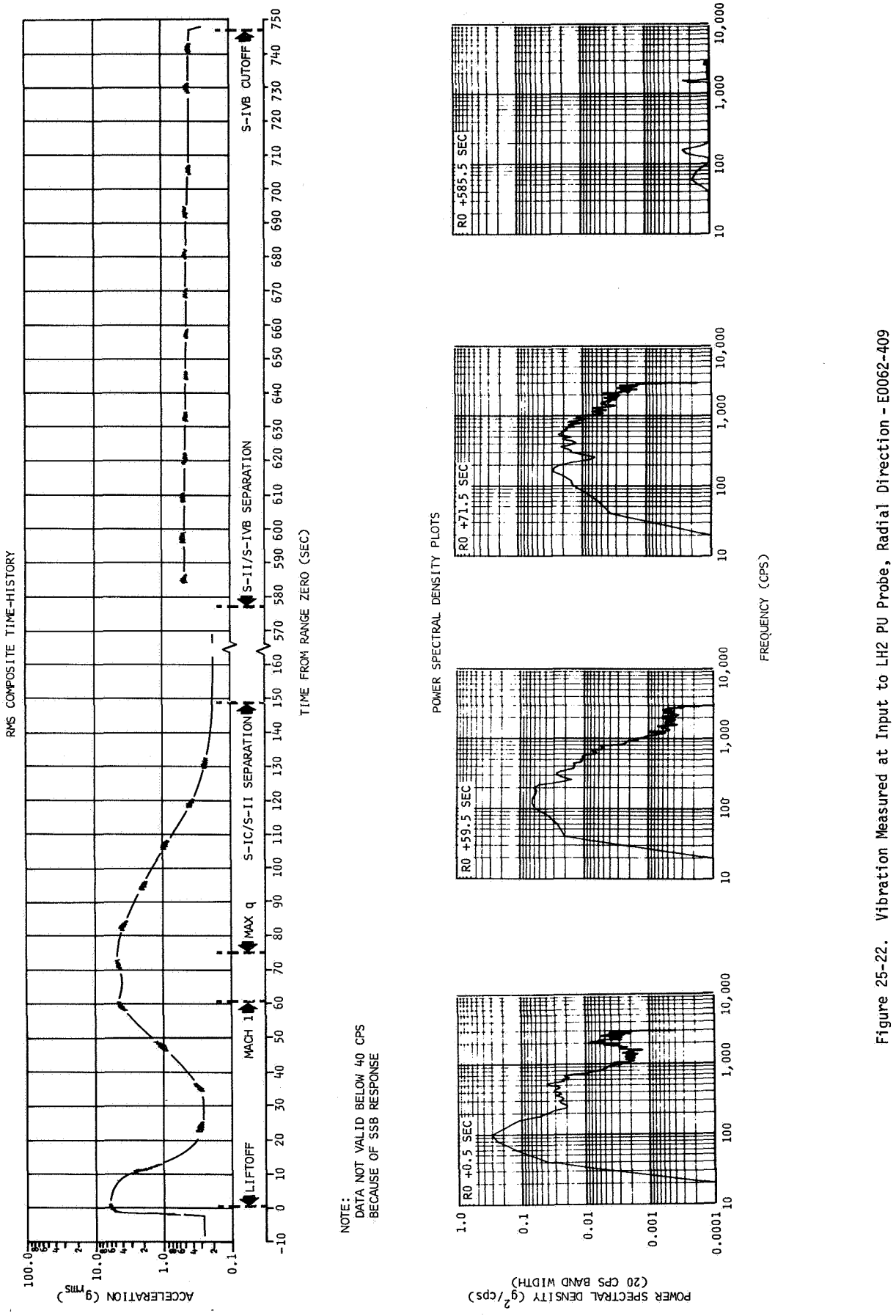

Figure 25-22. Vibration Measured at Input to LH2 PU Probe, Radial Direction - E0062-409

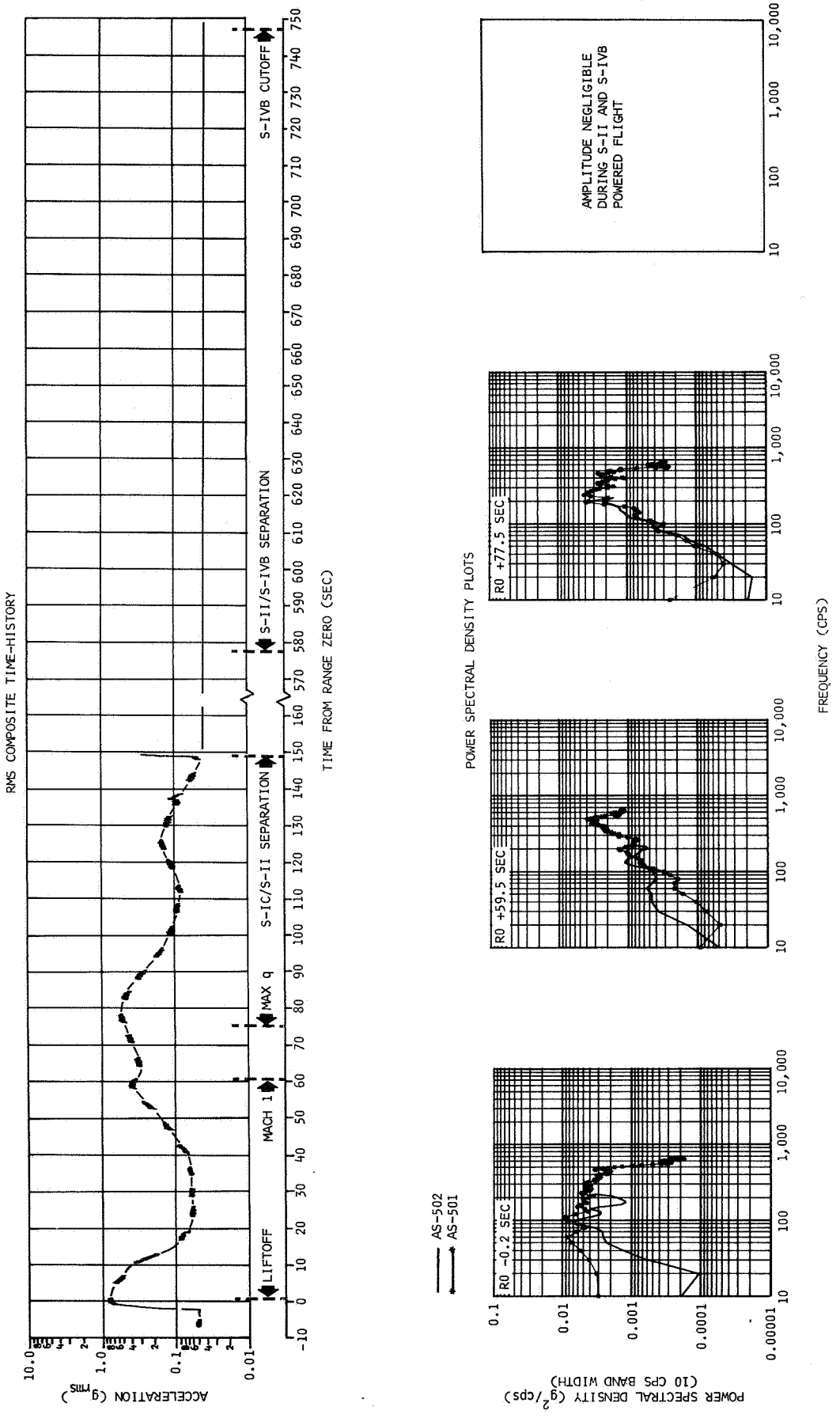

Figure 25-23. Low Frequency Vibration Measured on Field Splice Position I, Thrust Direction - E0091-411

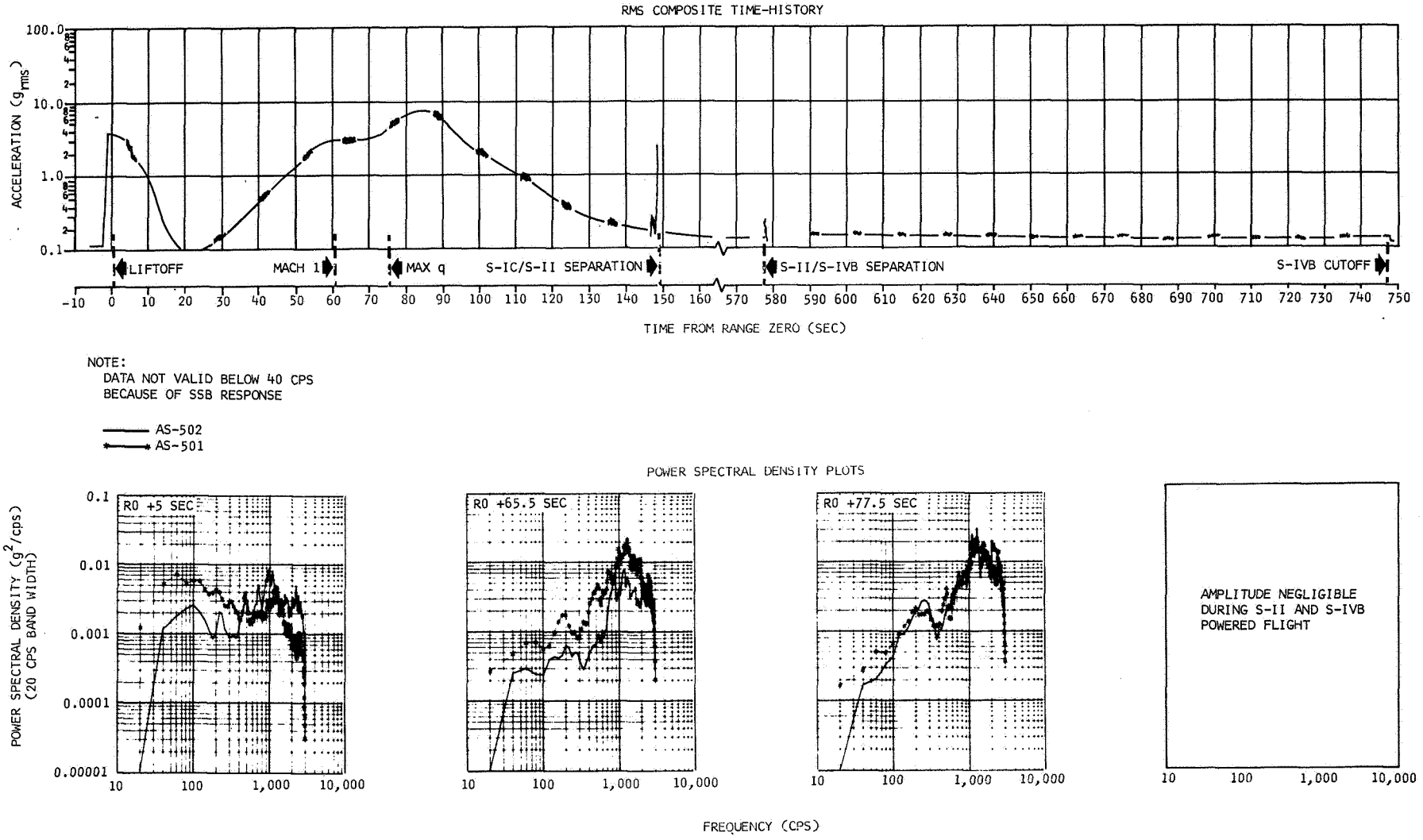

Figure 25-24. Vibration Measured on Field Splice Position I, Thrust Direction - E0093-411

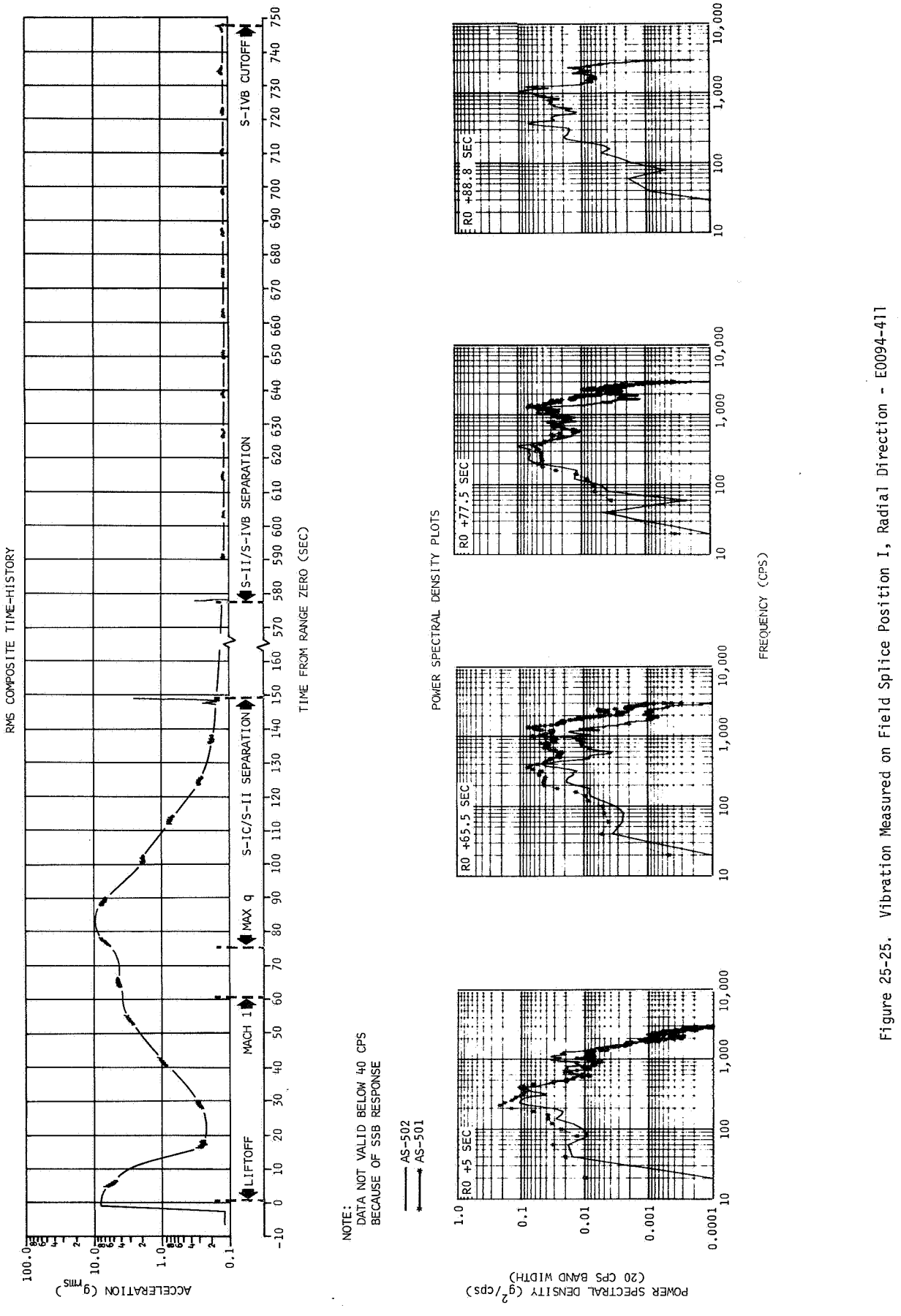

Figure 25-25. Vibration Measured on Field Splice Position I, Radial Direction - E0094-411

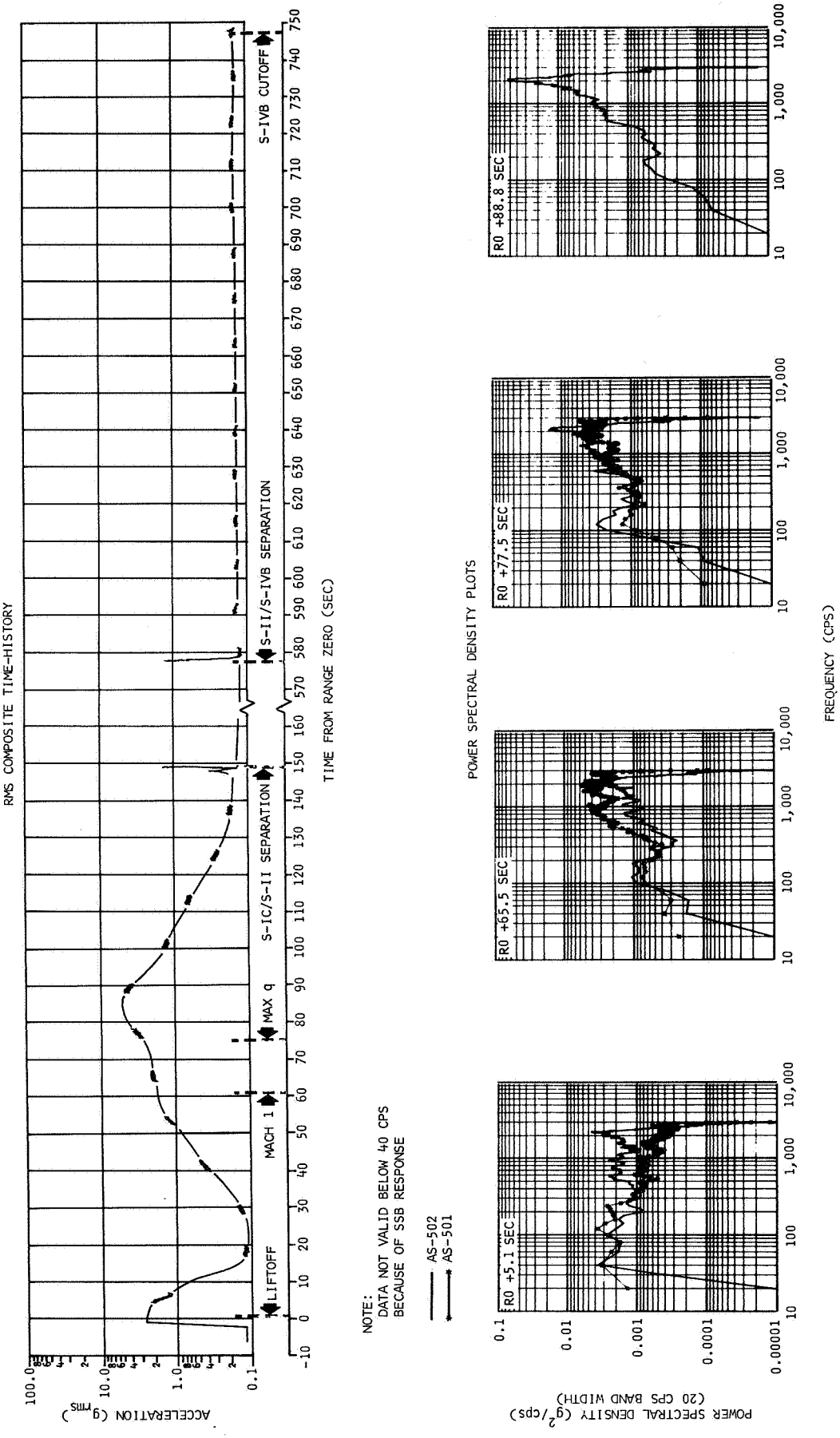

Figure 25-26. Vibration Measured on Field Splice Position I, Tangential Direction - E0095-411

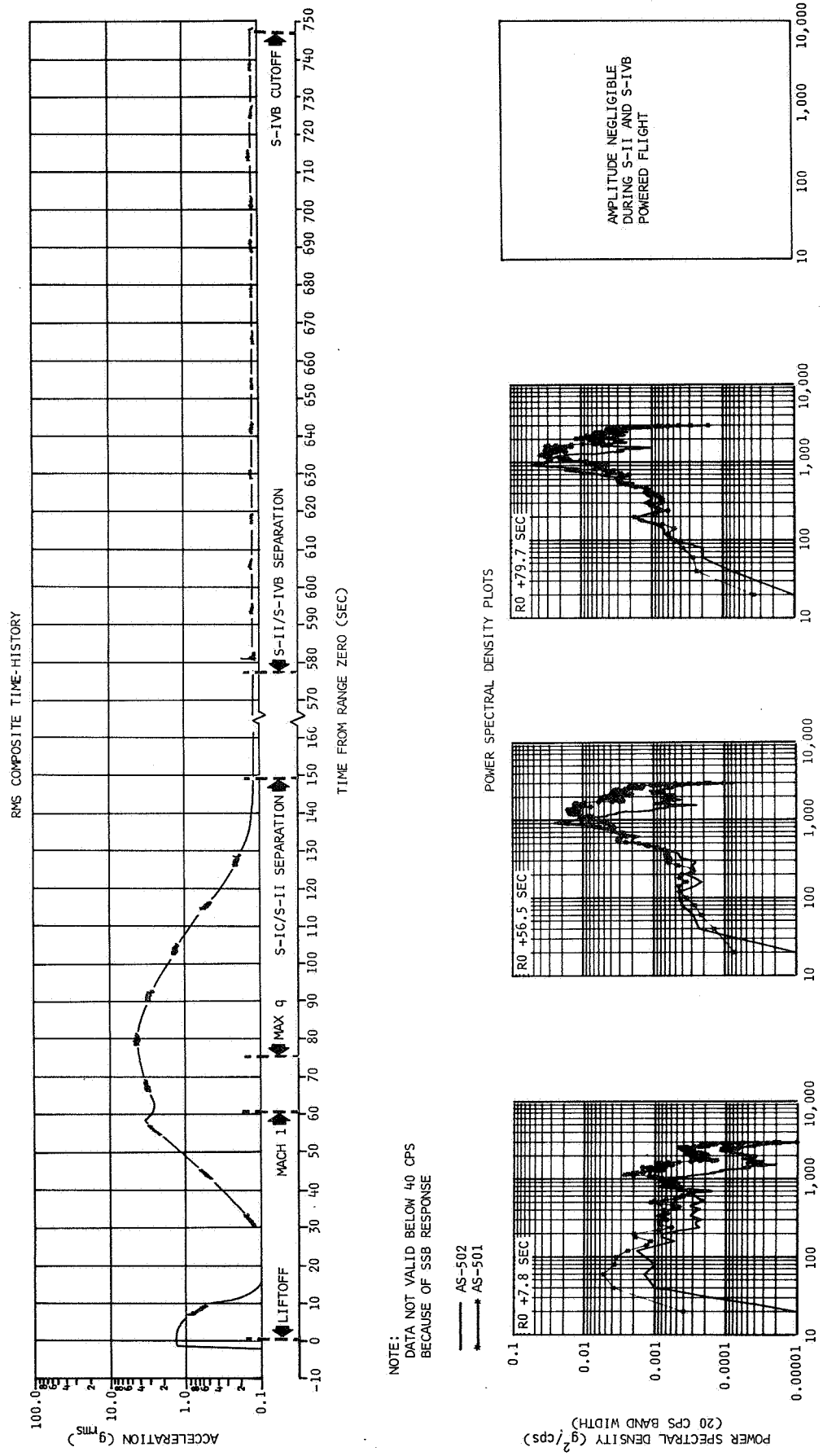

Figure 25-27. Vibration Measured on Field Splice Position II, Thrust Direction - E0096-411

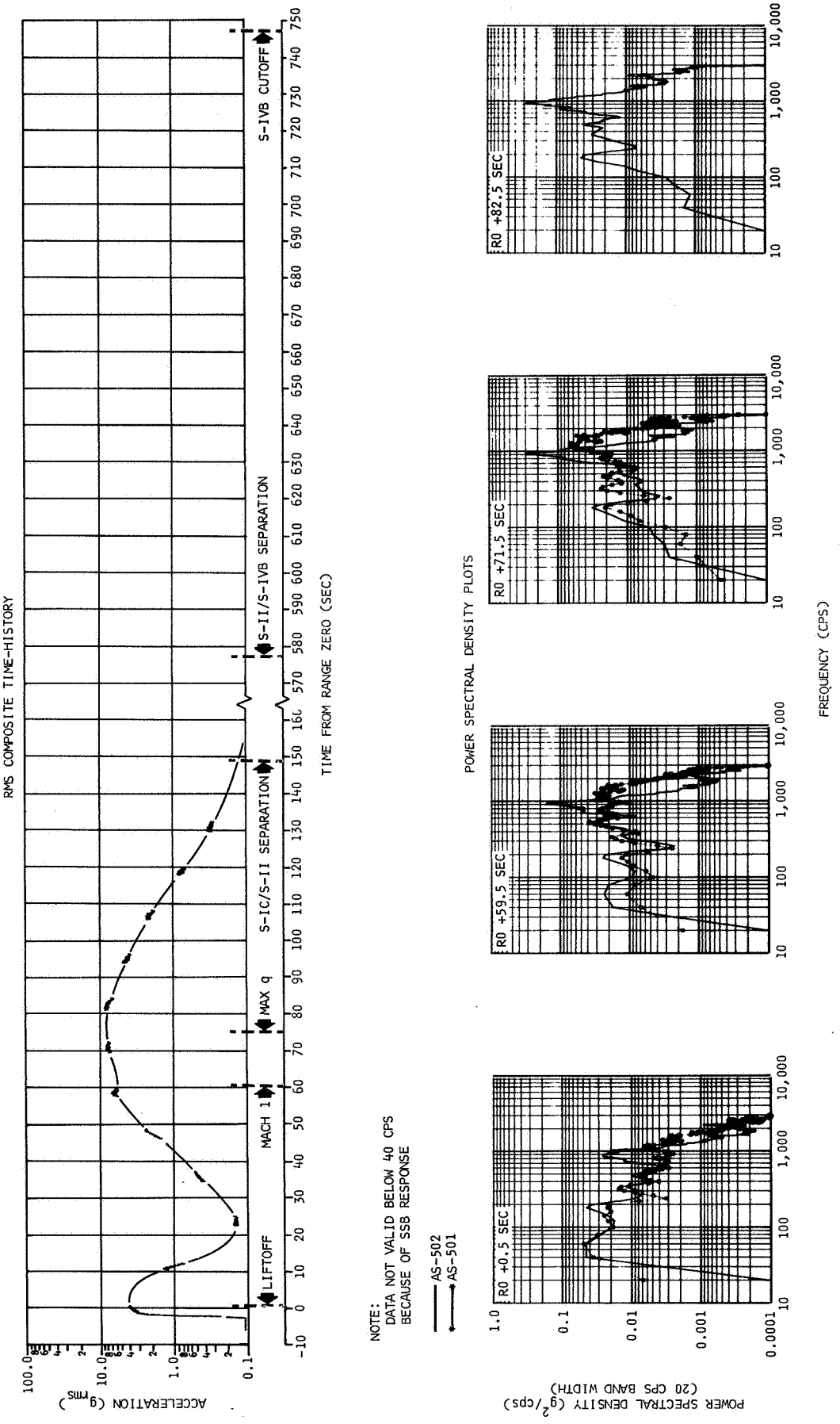

Figure 25-28. Vibration Measured on Field Splice Position II, Radial Direction - E0098-411

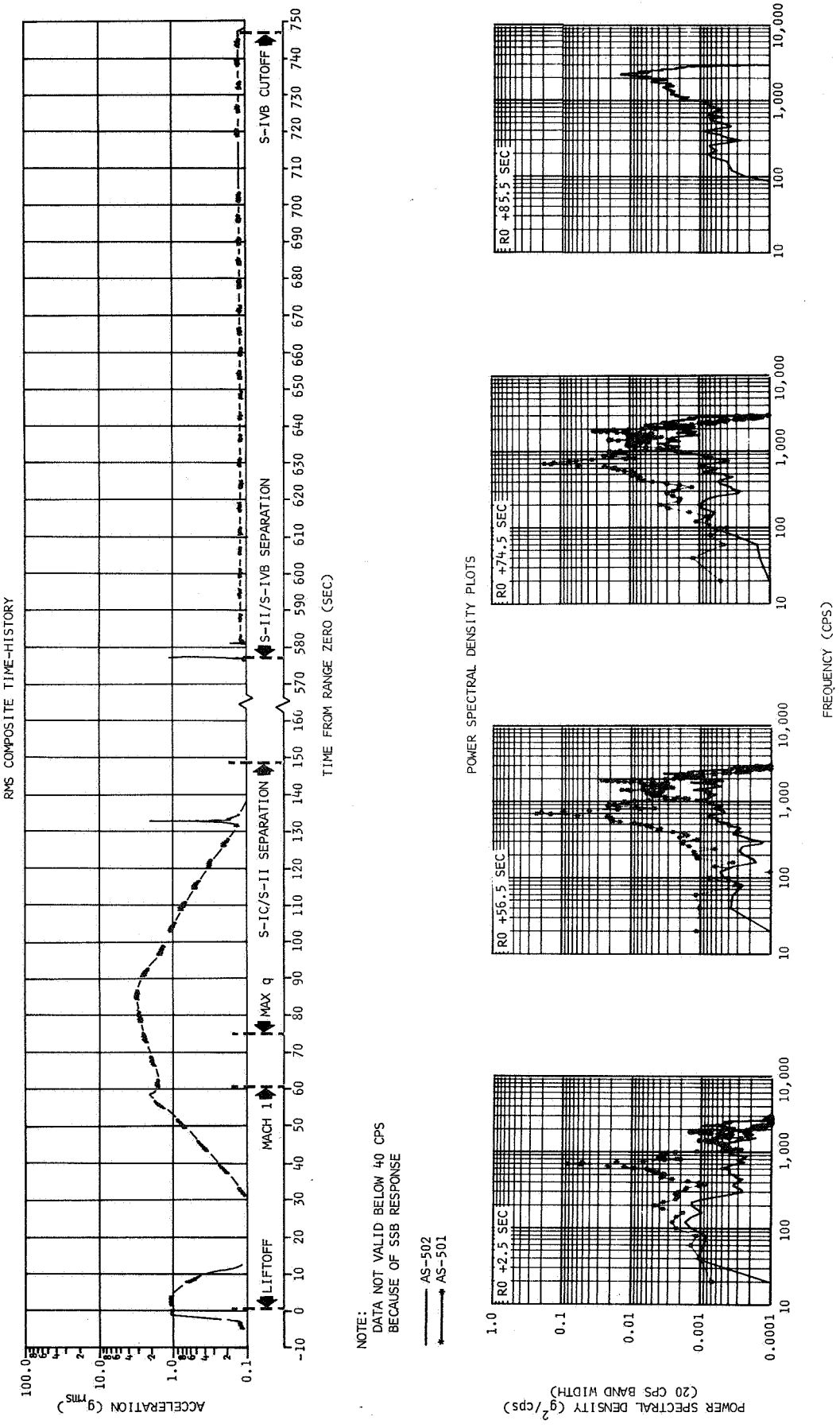

Figure 25-29. Vibration Measured on Field Splice Position II, Tangential Direction - E0097-411

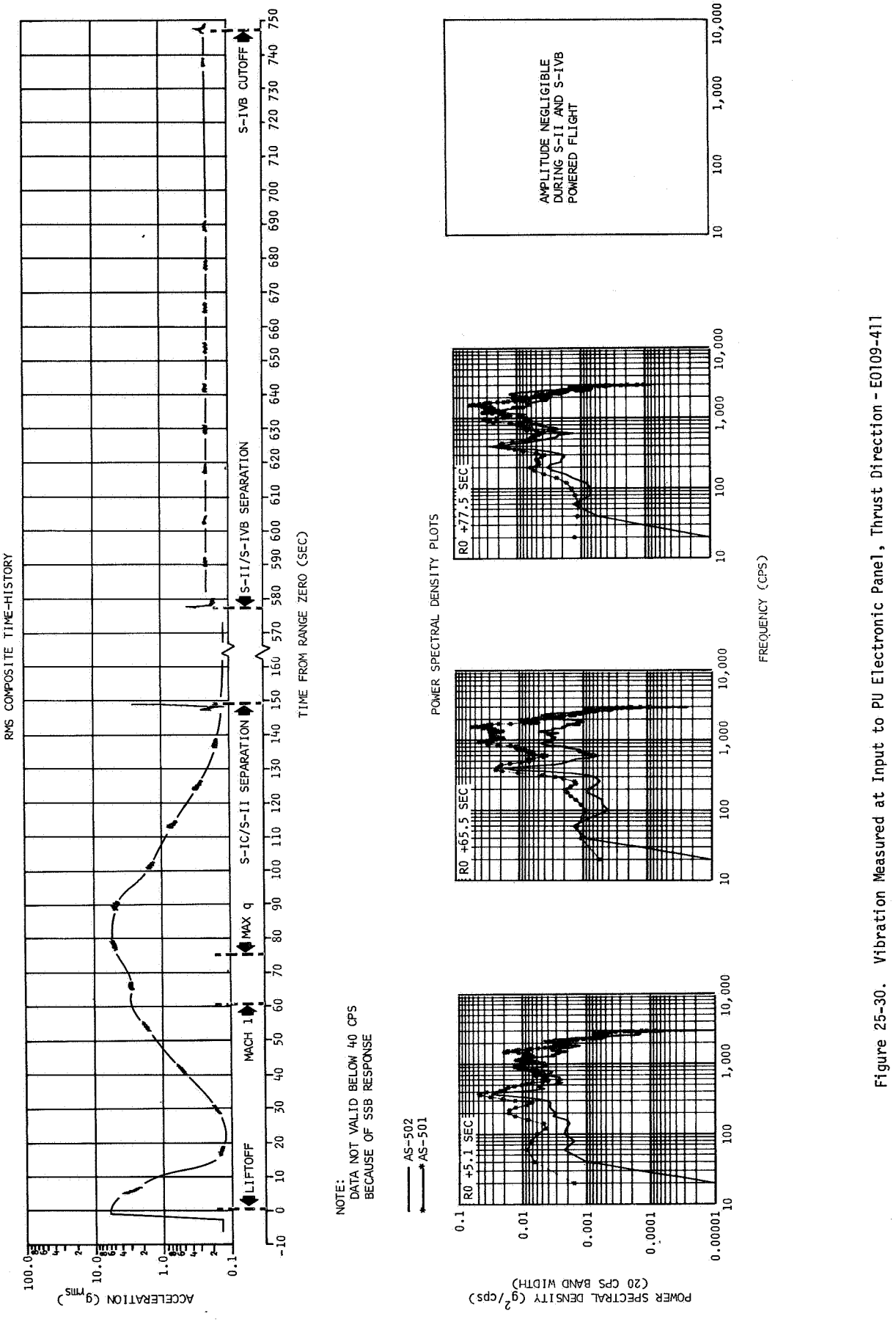

Figure 25-30. Vibration Measured at Input to PU Electronic Panel, Thrust Direction - E0109-411

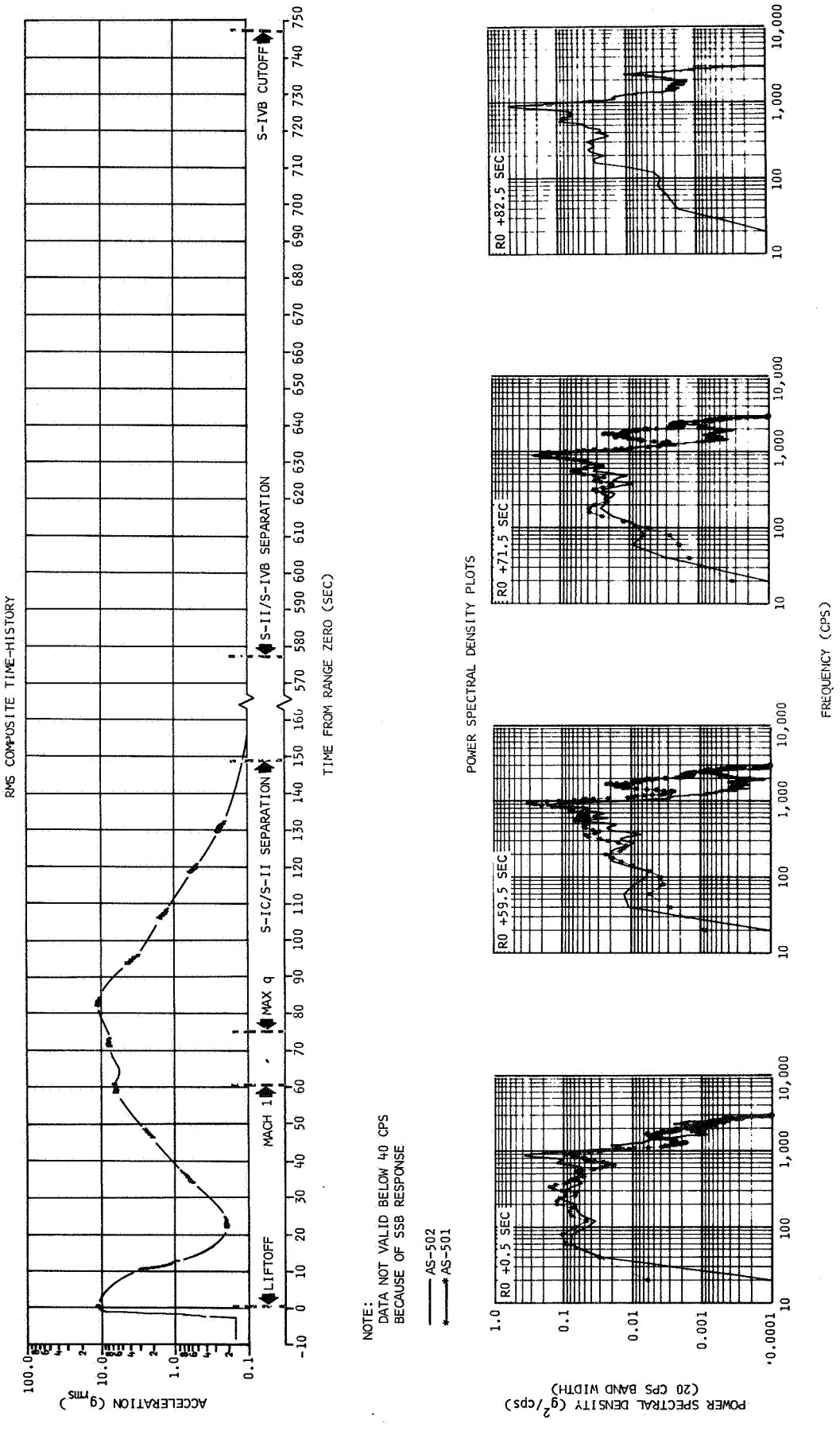

Figure 25-31. Vibration Measured at Input to PU Electronic Panel, Radial Direction - E0111-411

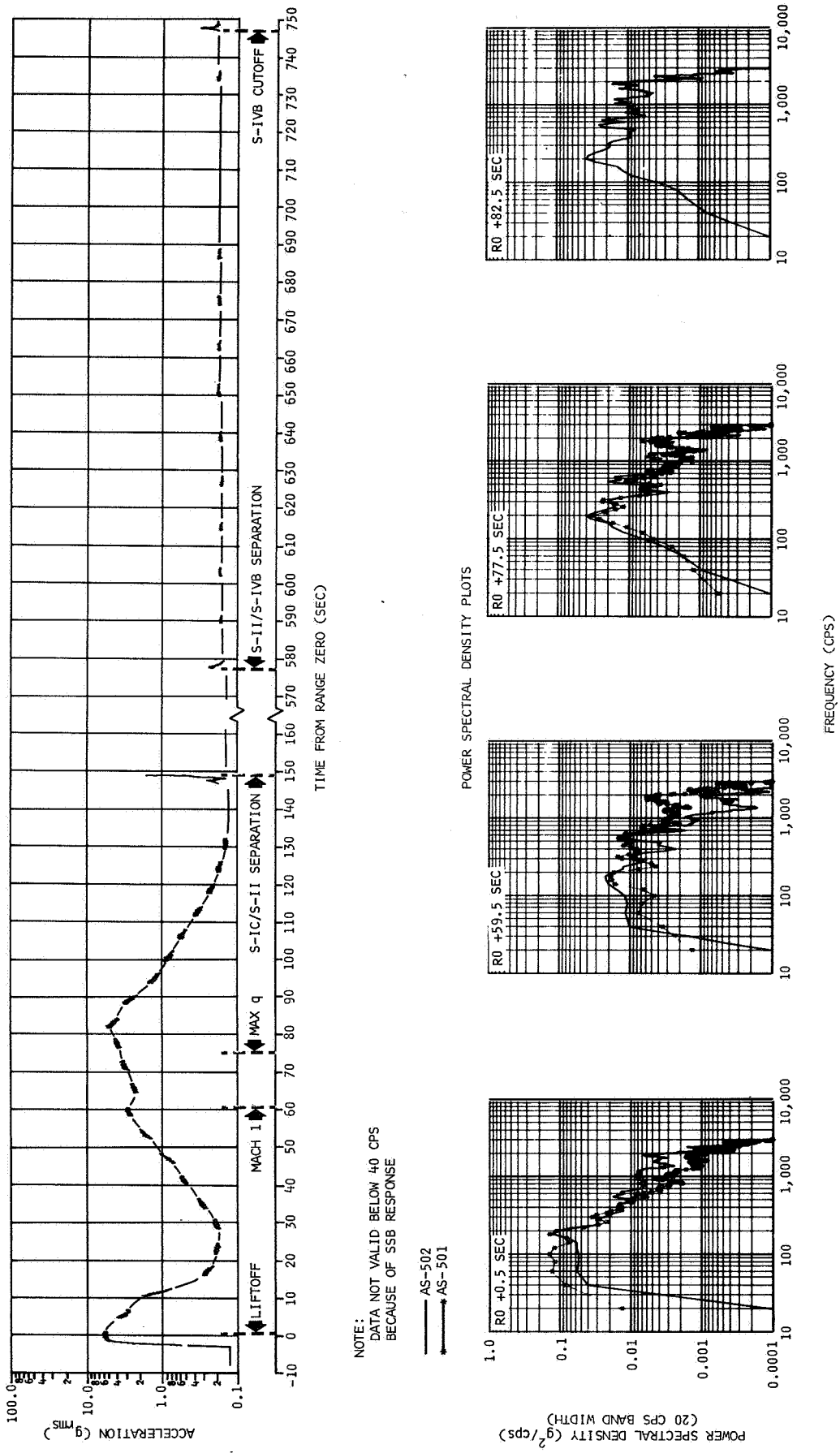

Figure 25-32. Vibration Measured at Input to PU Electronic Assembly, Radial Direction - E0110-411

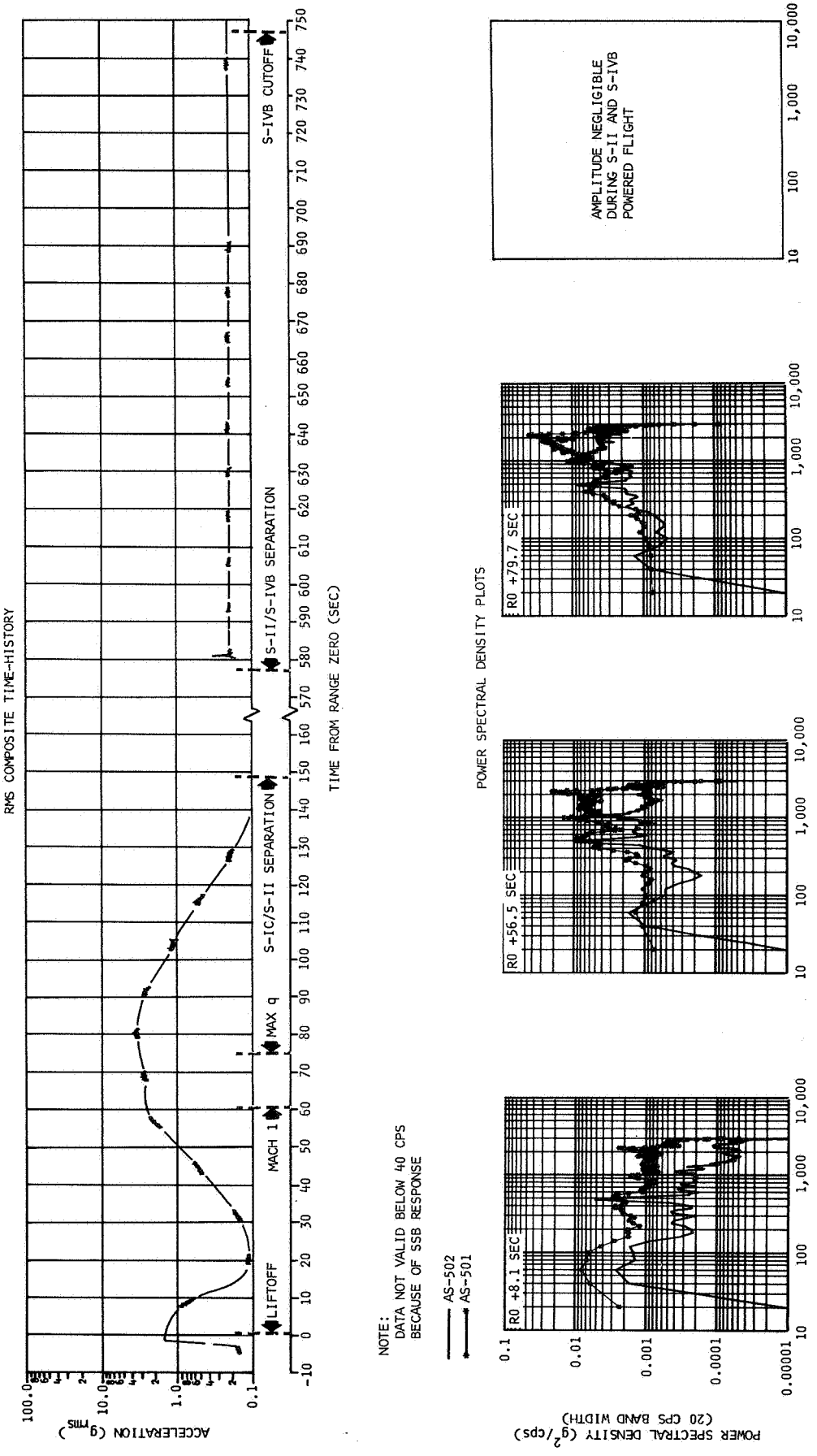

Figure 25-33. Vibration Measured at Input to EBW Range Safety Panel, Thrust Direction - E0112-411

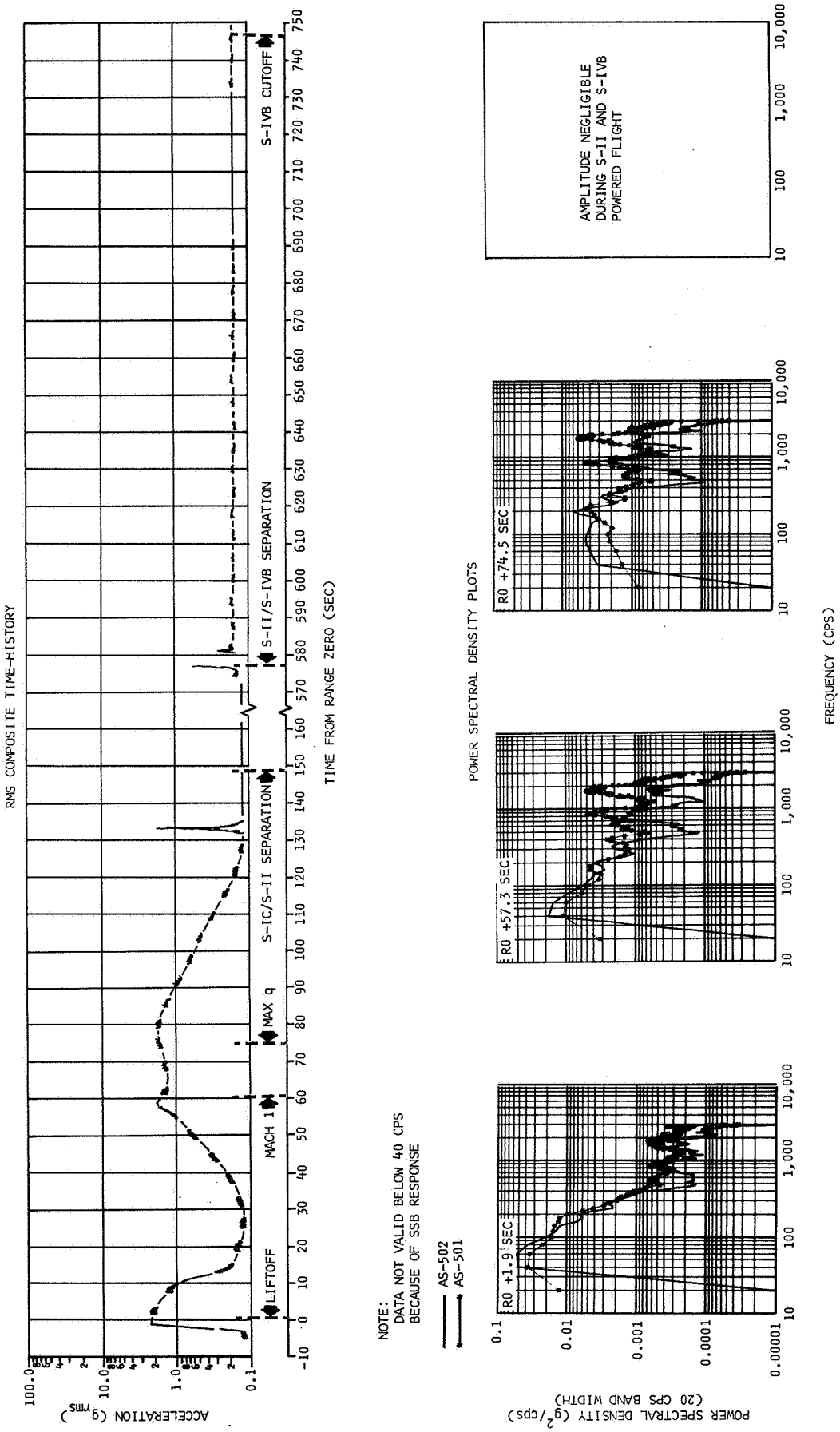

Figure 25-34. Vibration Measured at Input to EBW Range Safety Unit, Radial Direction - E0113-411

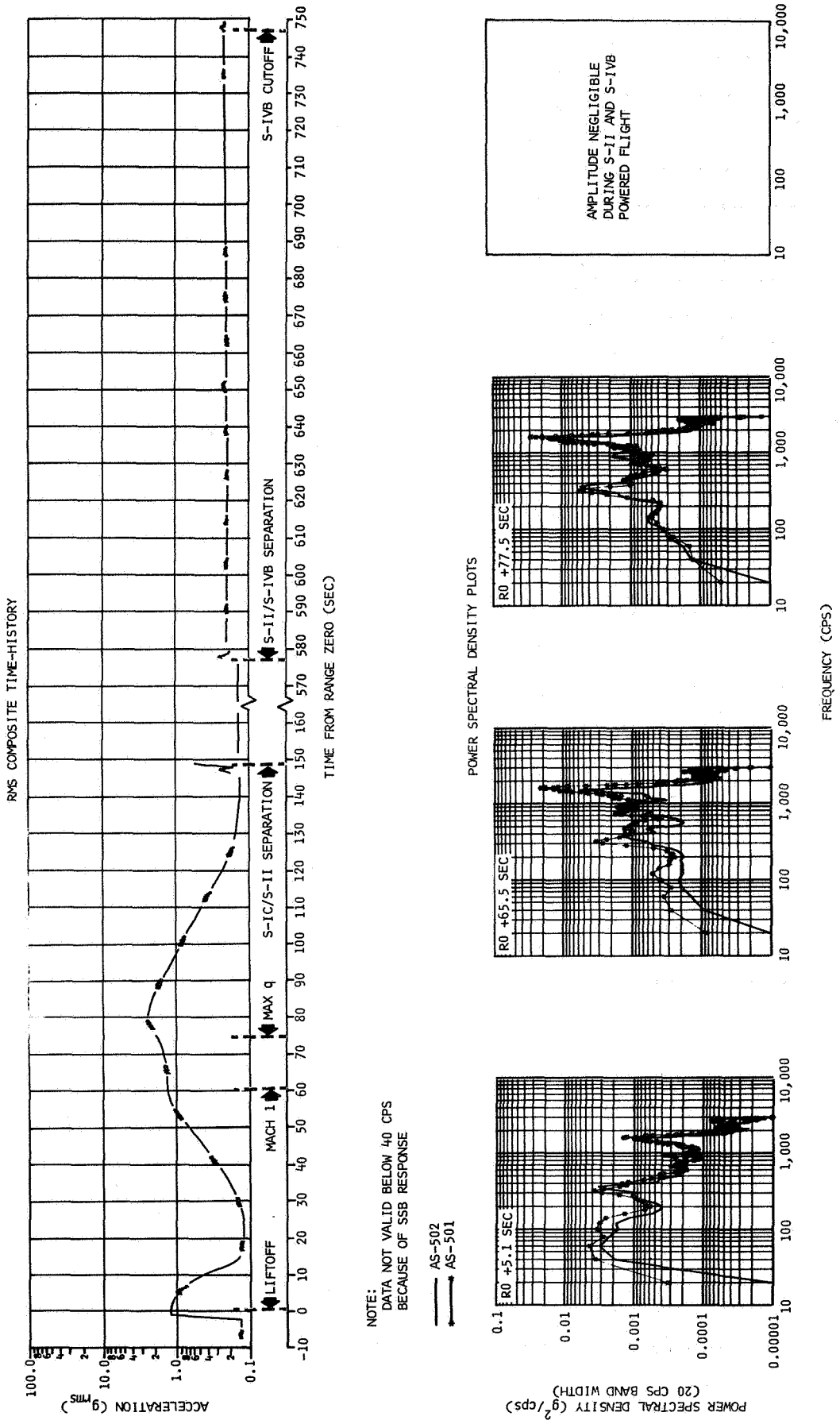

Figure 25-35. Vibration Measured at Input to Forward Skirt Battery No. 1, Thrust Direction - E0115-411

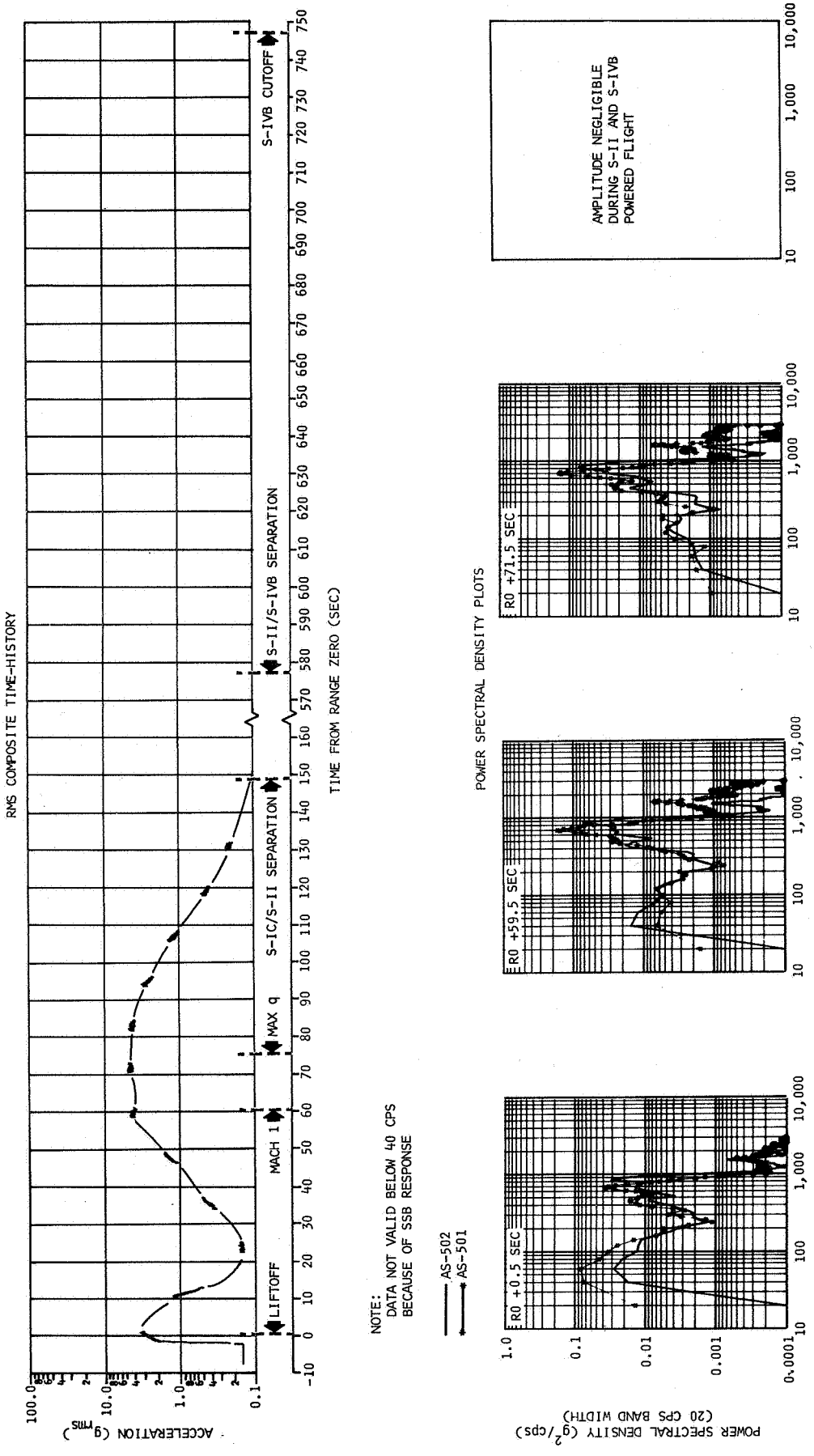

Figure 25-36. Vibration Measured at Input to Forward Skirt Battery No. 1, Radial Direction- E0116-411

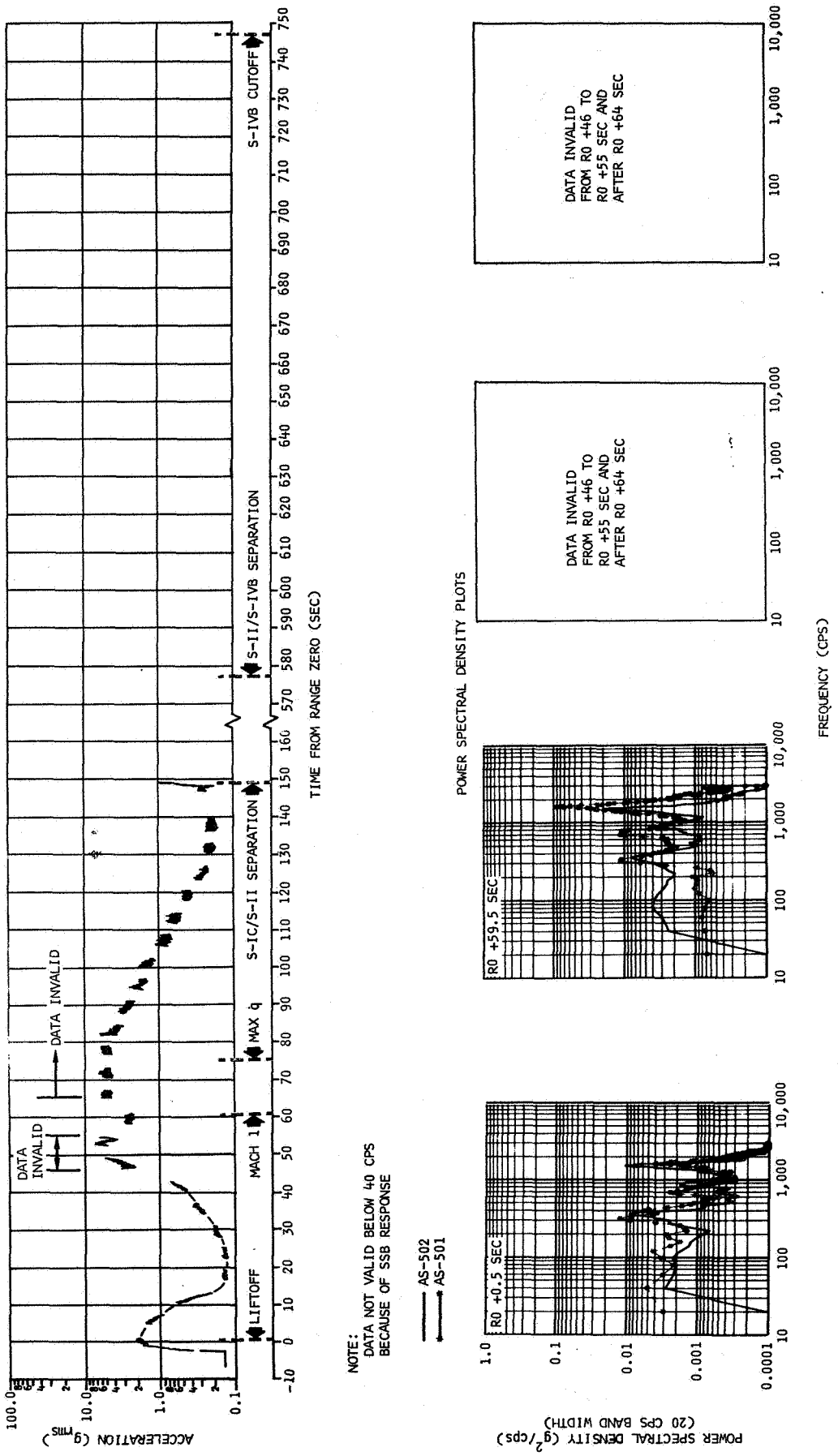

Figure 25-37. Vibration Measured at Input to Forward Skirt Battery No. 1, Tangential Direction - E0117-411

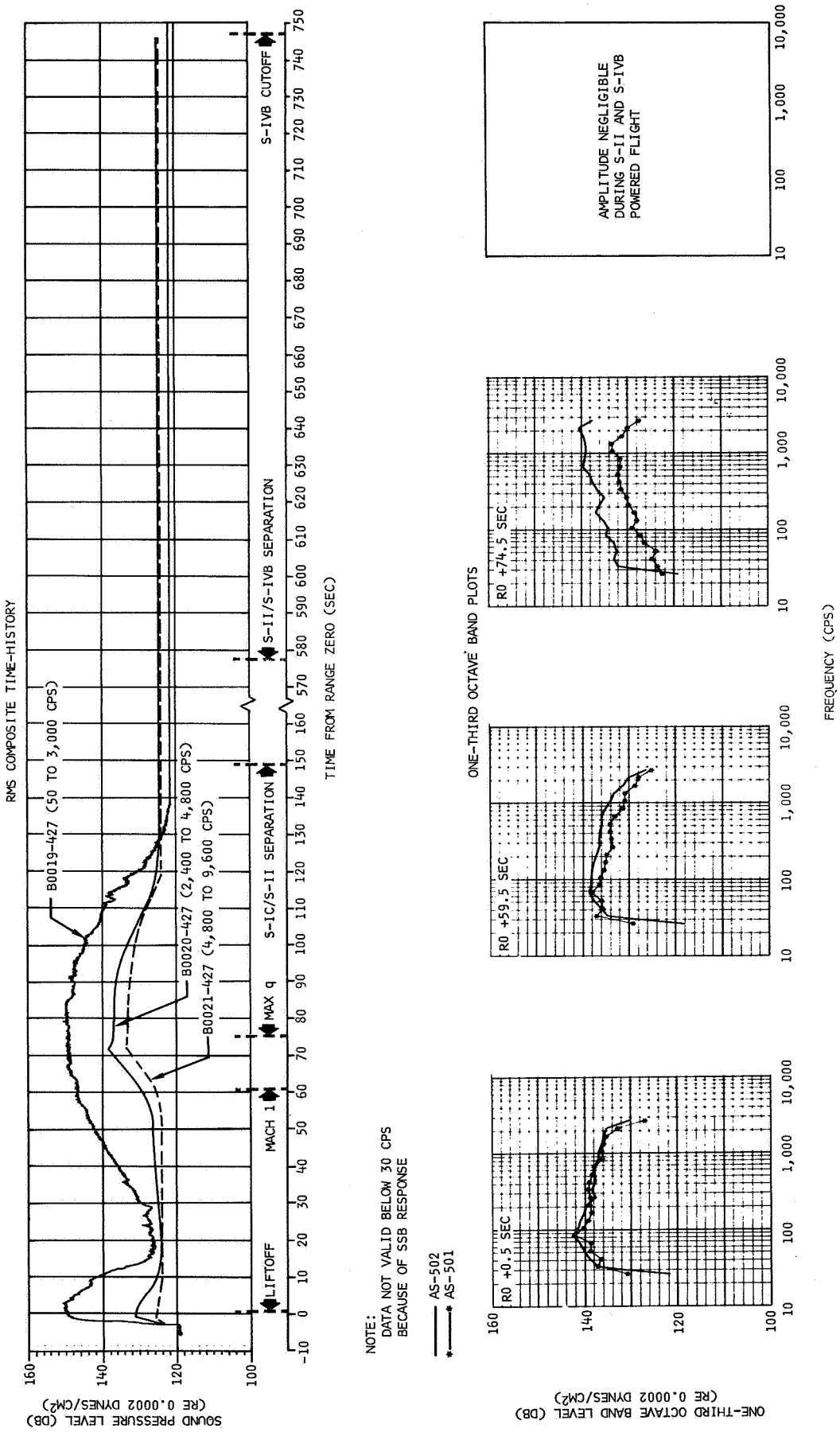

Figure 25-38. External Sound Pressure Levels Measured on Aft Skirt

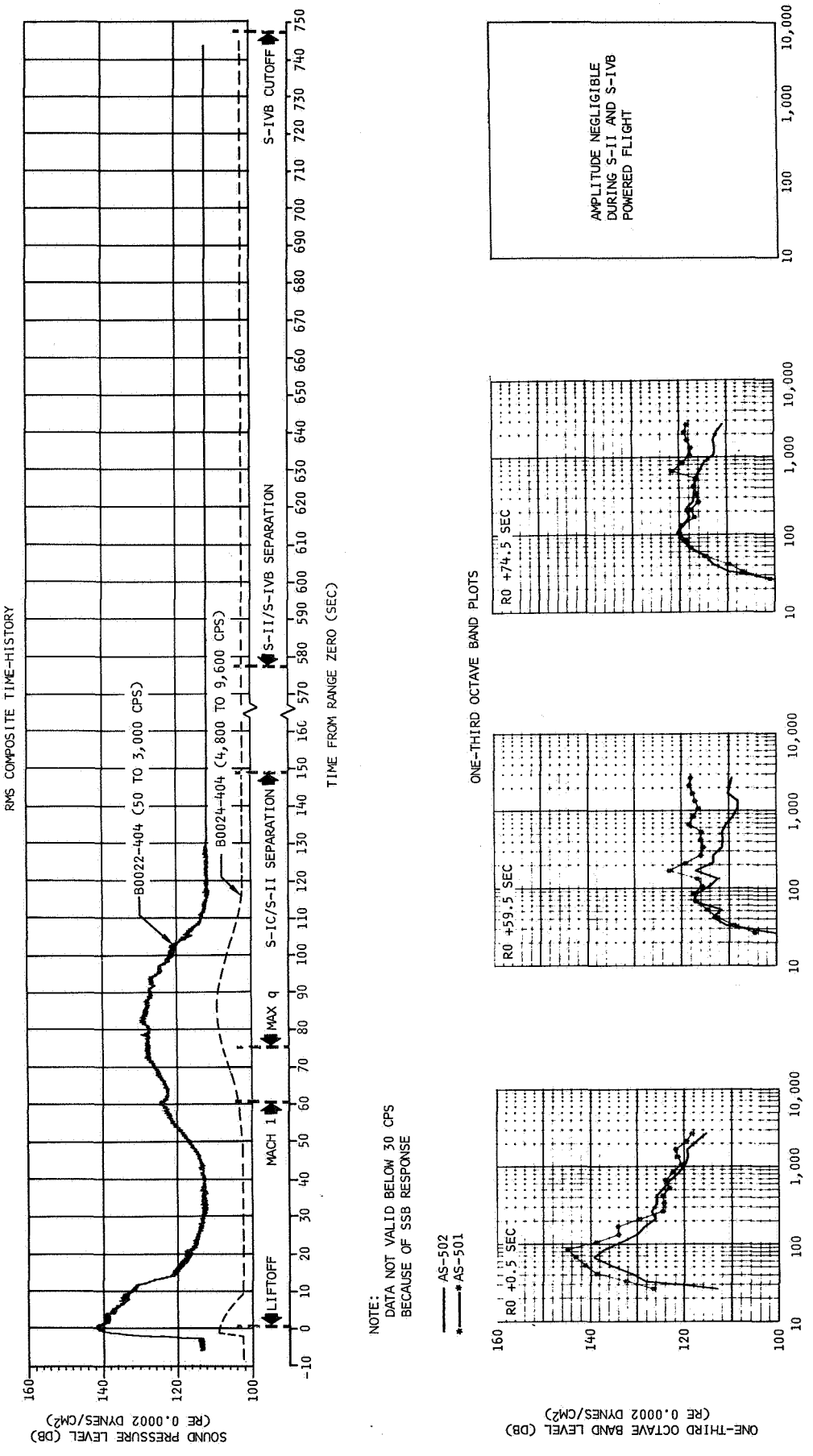

Figure 25-39. Internal Sound Pressure Levels Measured on Aft Skirt

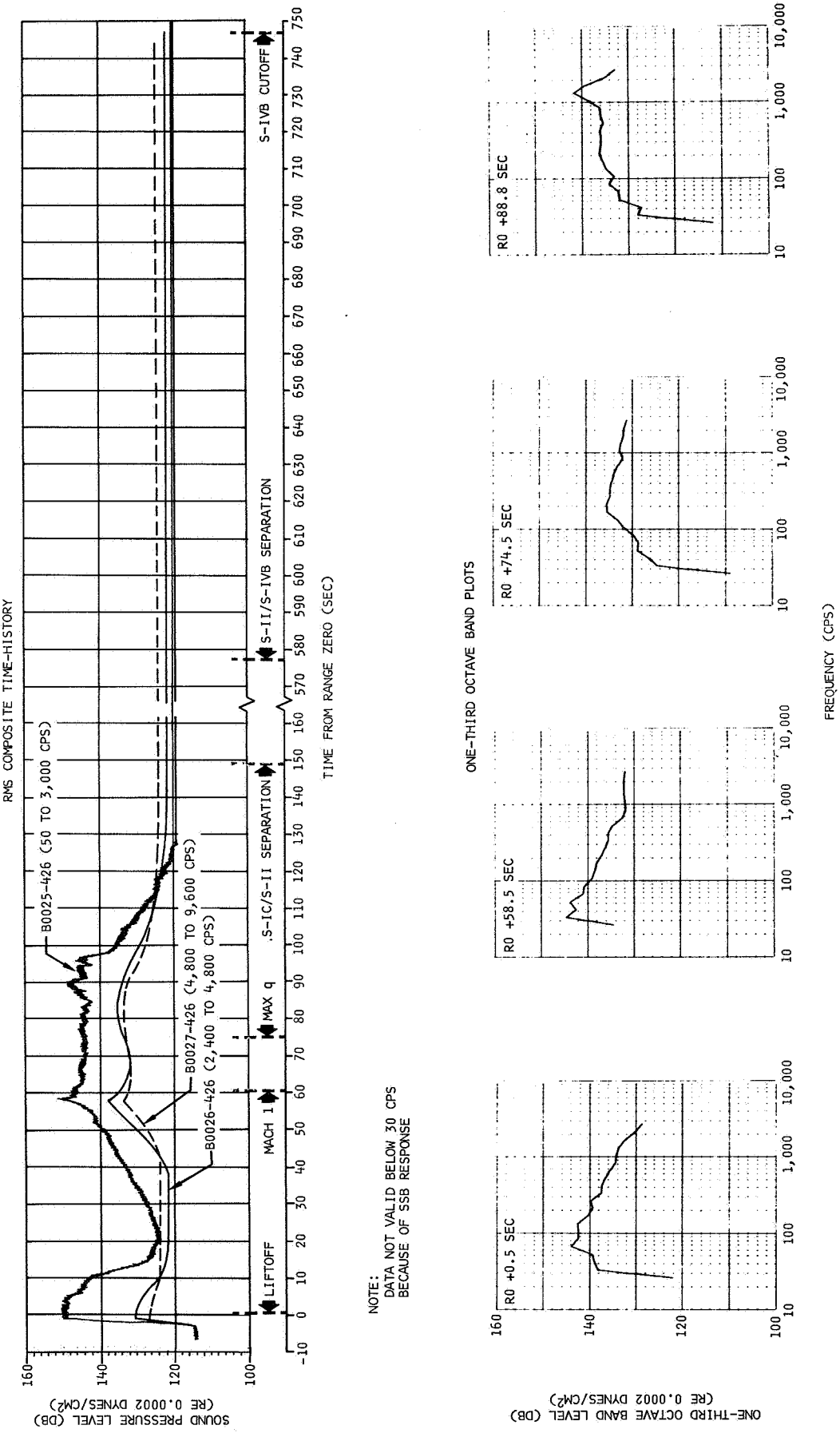

Figure 25-40. External Sound Pressure Levels Measured on Forward Skirt

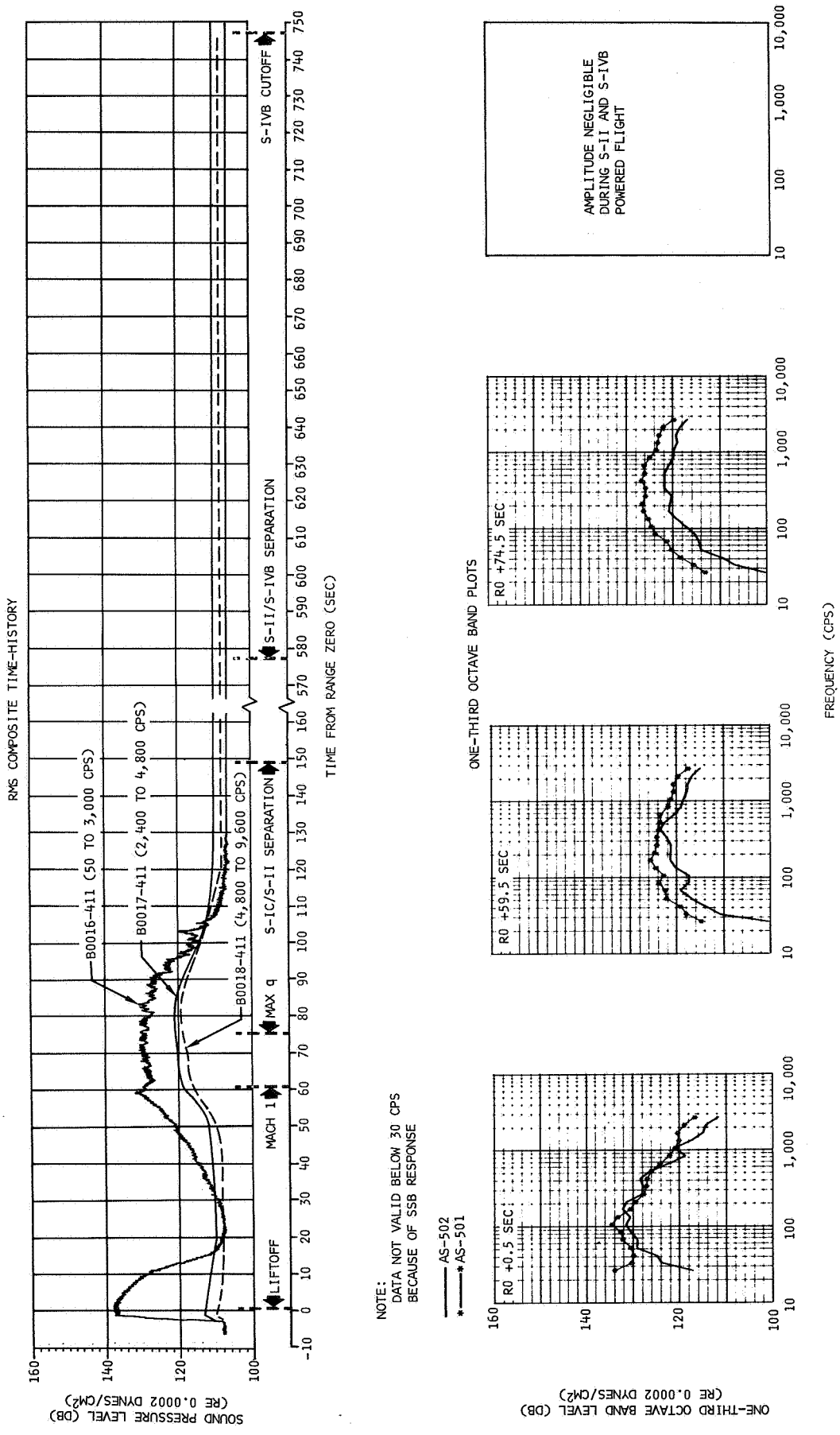

Figure 25-41. Internal Sound Pressure Levels Measured on Forward Skirt

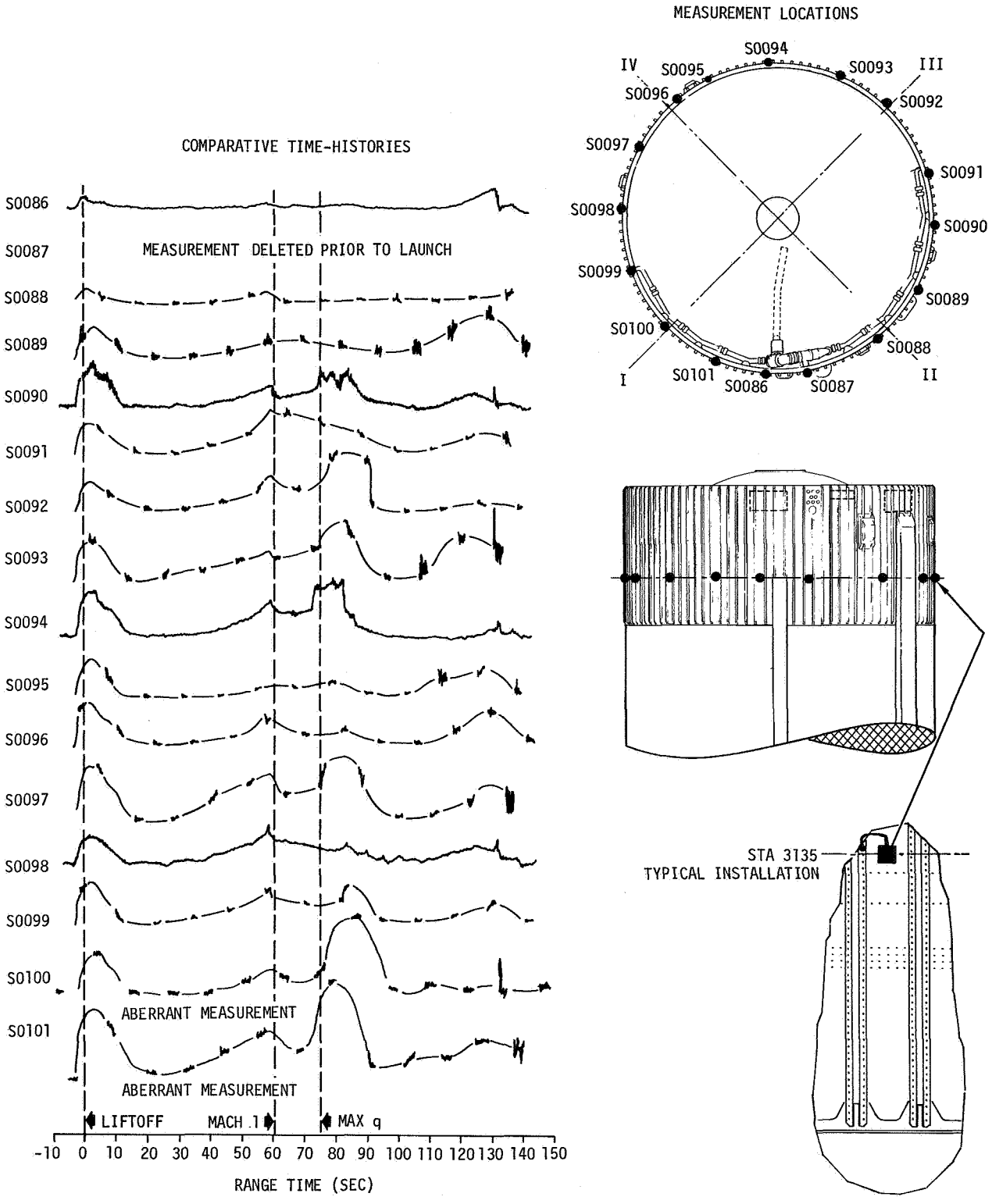

Figure 25-42. Forward Skirt Dynamic Strains

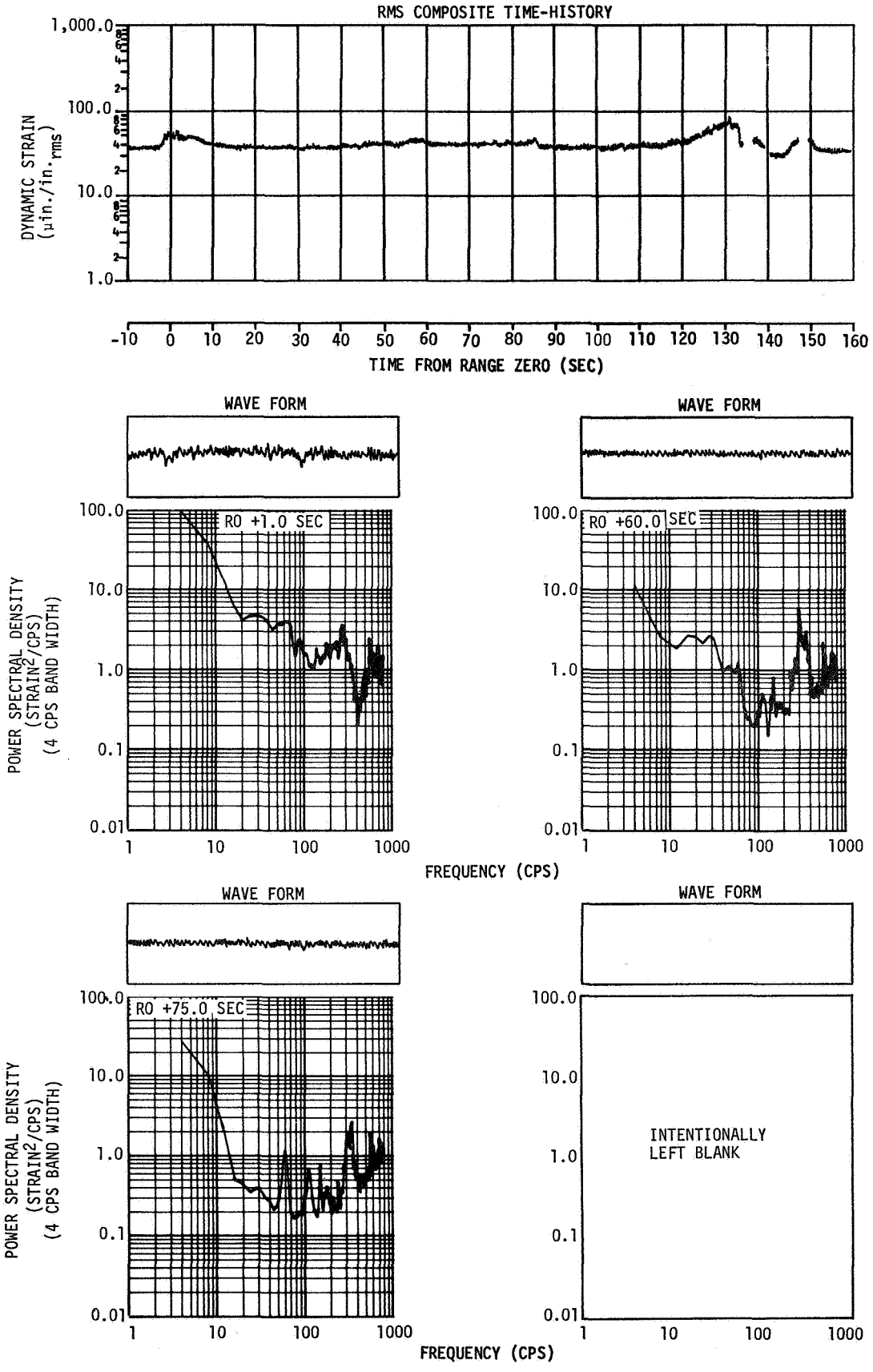

Figure 25-43. Dynamic Strain Measured on Forward Skirt Panel 13 - S0086-426

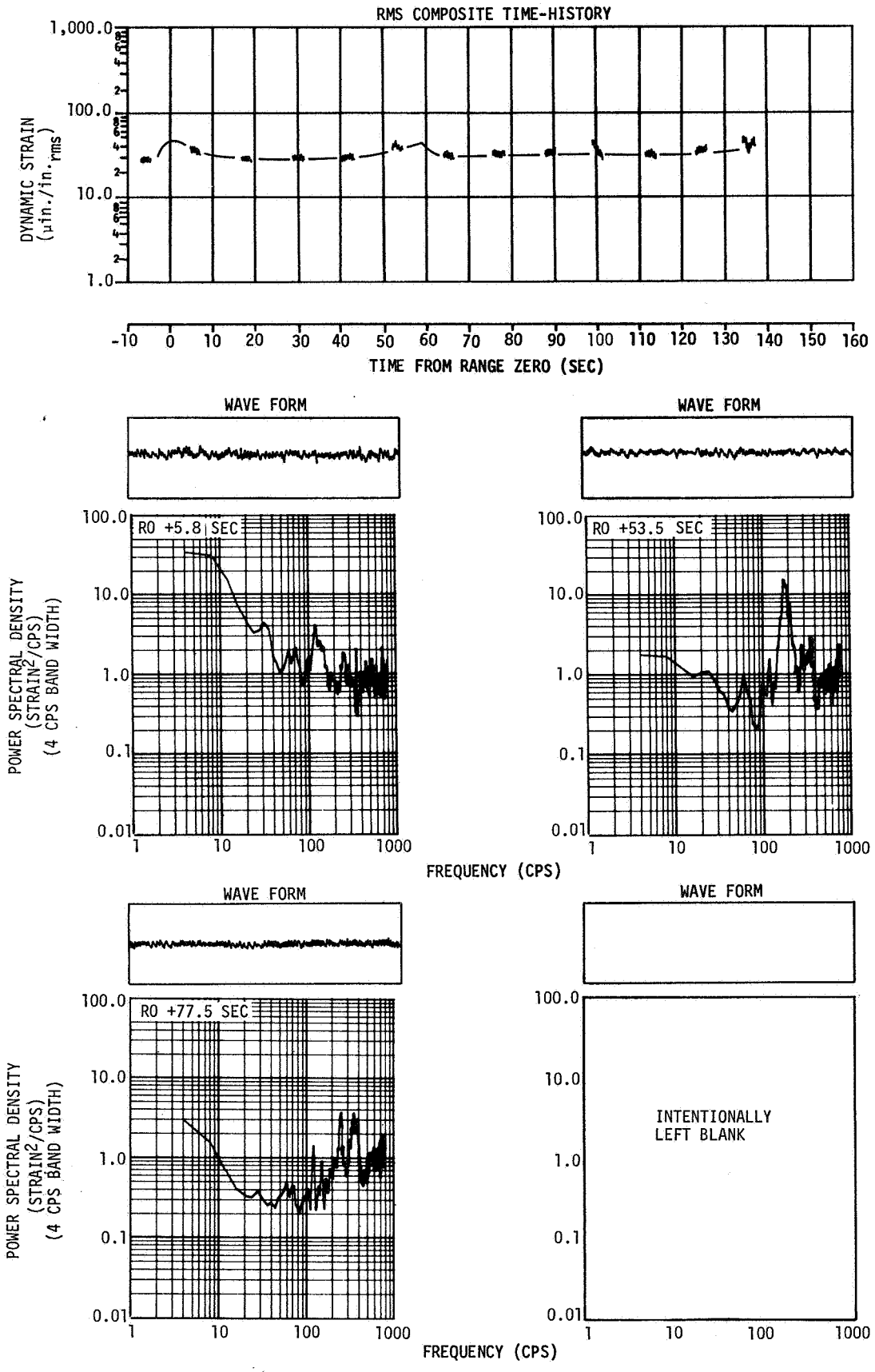

Figure 25-44. Dynamic Strain Measured on Forward Skirt Panel 26 - S0088-426

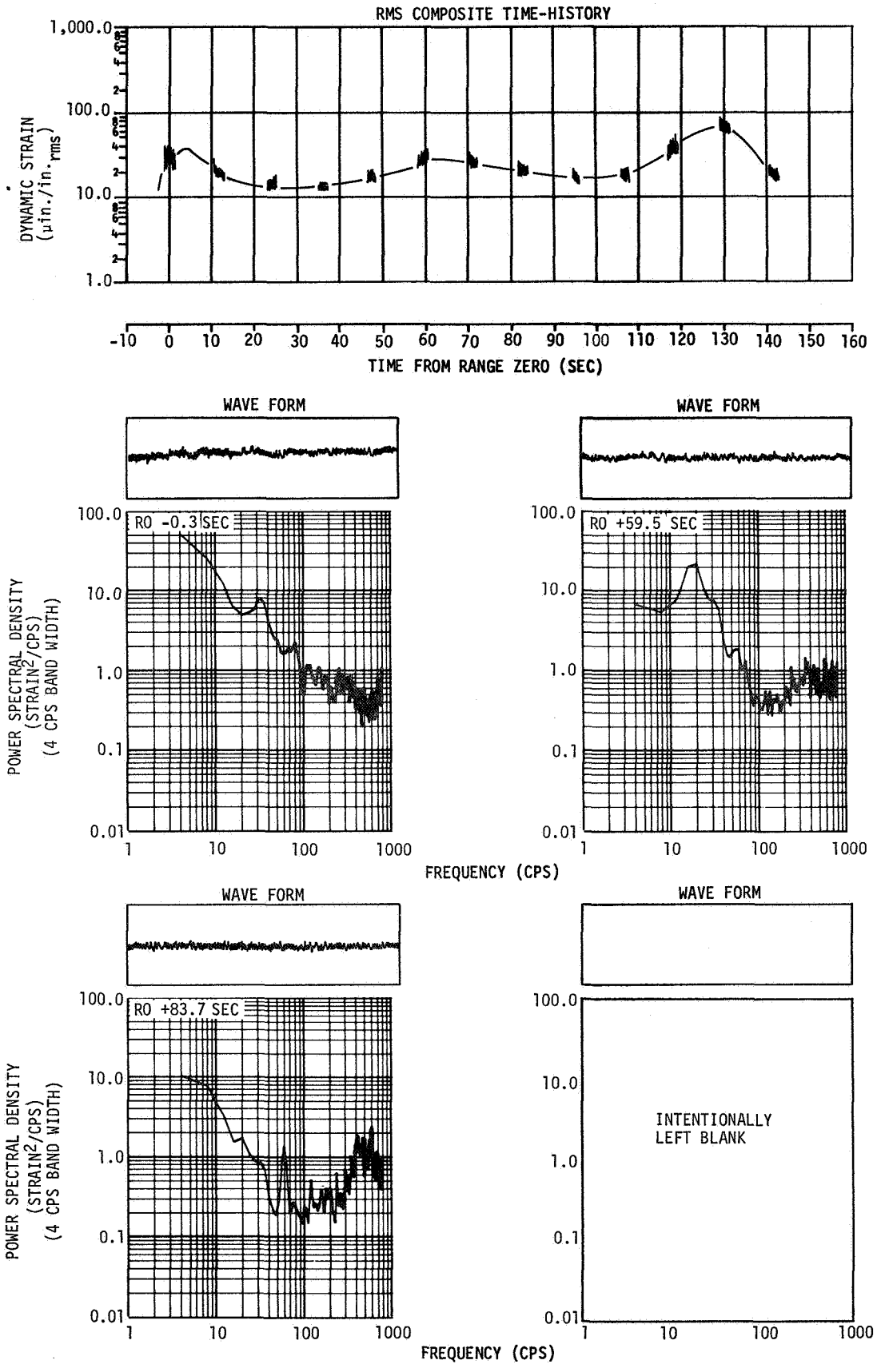

Figure 25-45. Dynamic Strain Measured on Forward Skirt Panel 33 - S0089-426

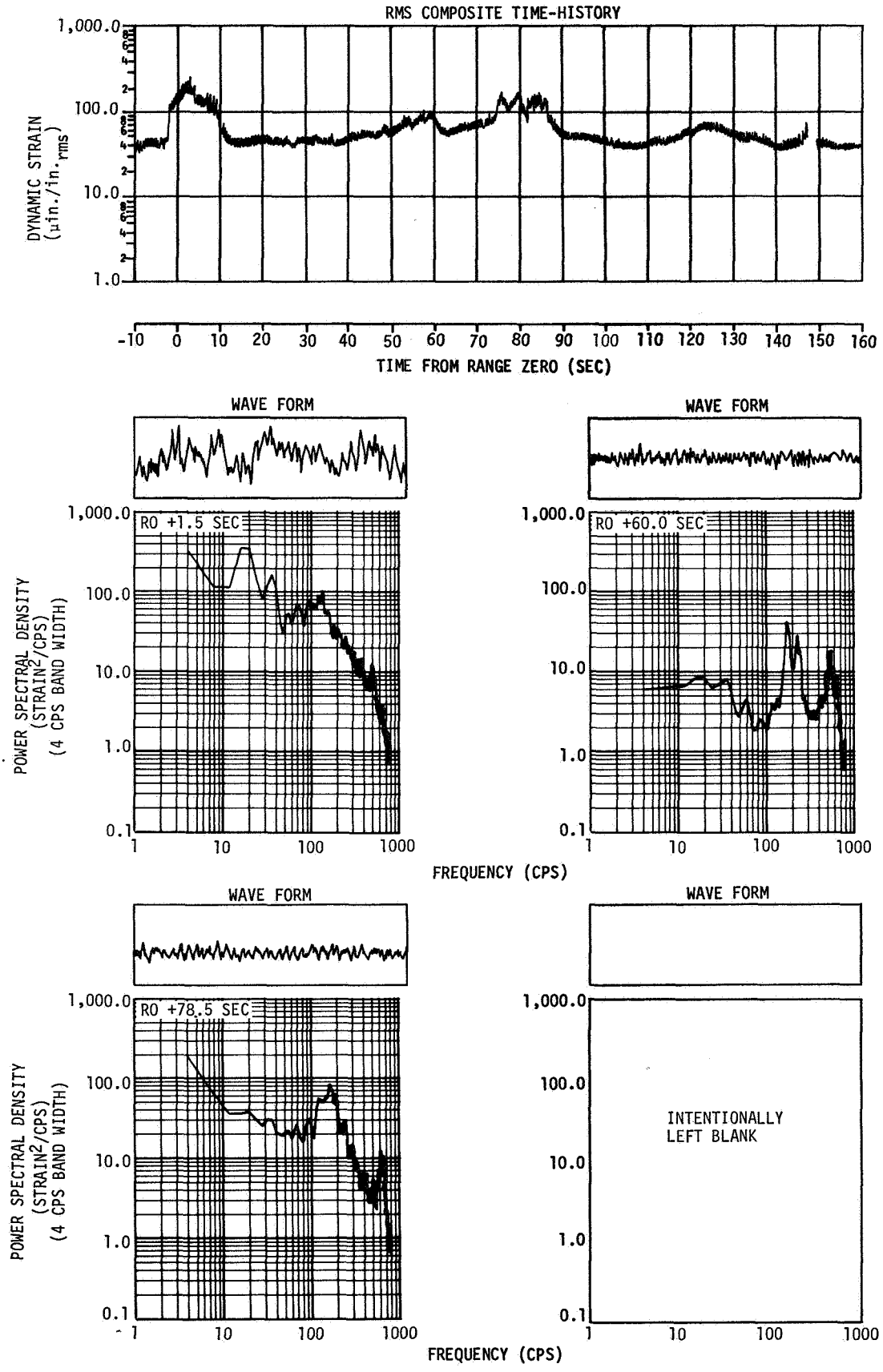

Figure 25-46. Dynamic Strain Measured on Forward Skirt Panel 40 - S0090-426

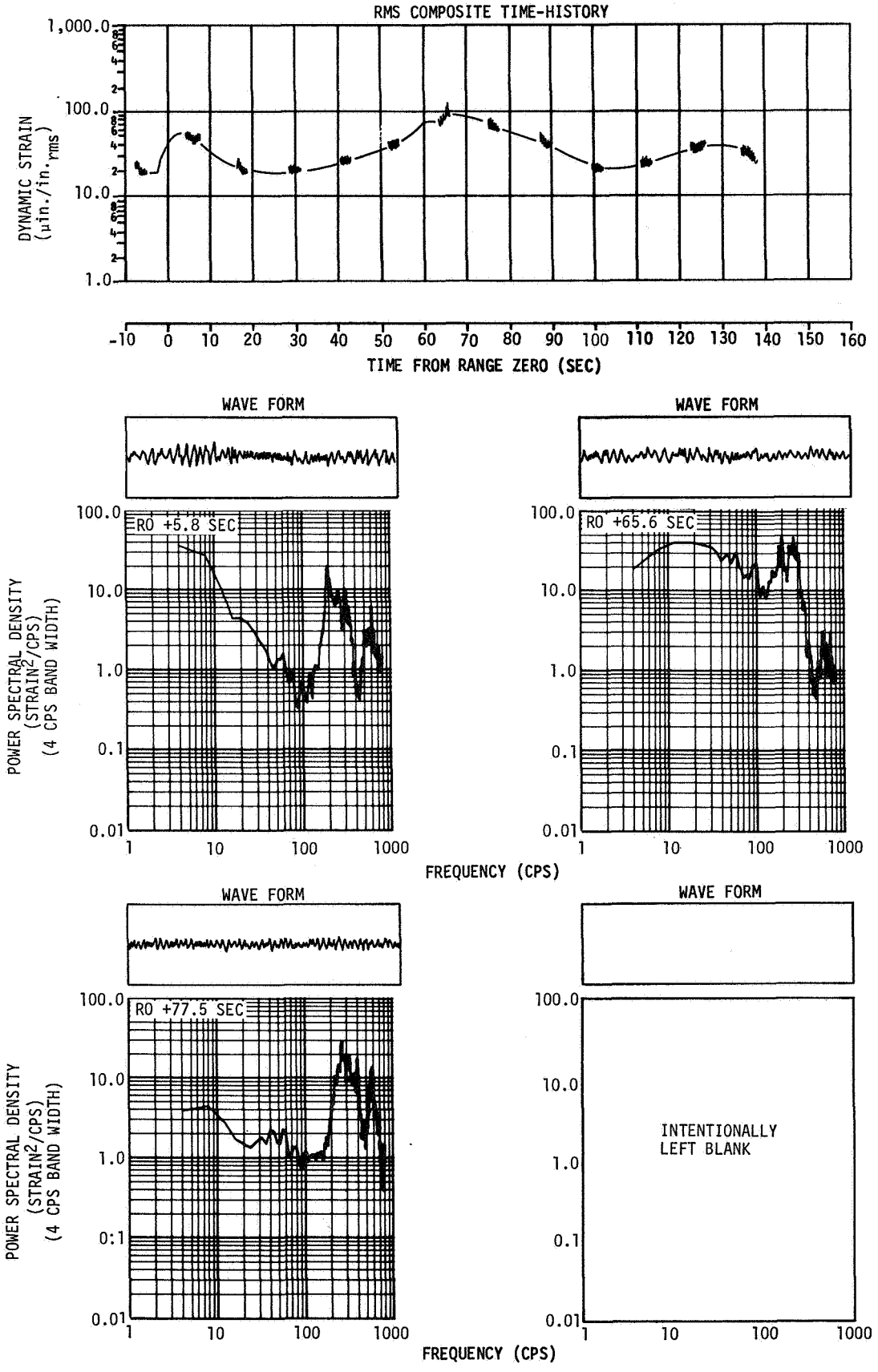

Figure 25-47. Dynamic Strain Measured on Forward Skirt Panel 46 - S0091-426

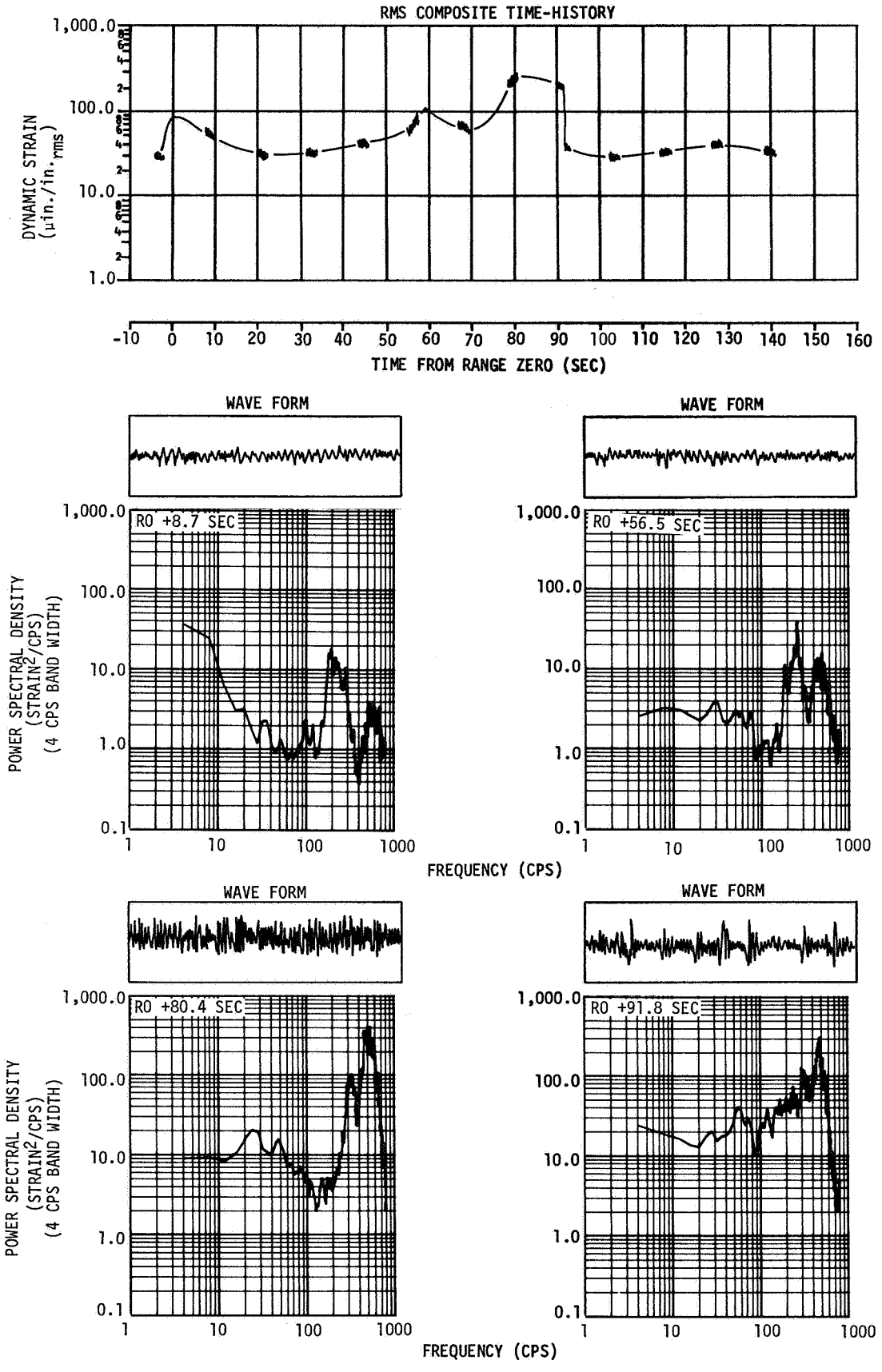

Figure 25-48. Dynamic Strain Measured on Forward Skirt Panel 55 - S0092-426

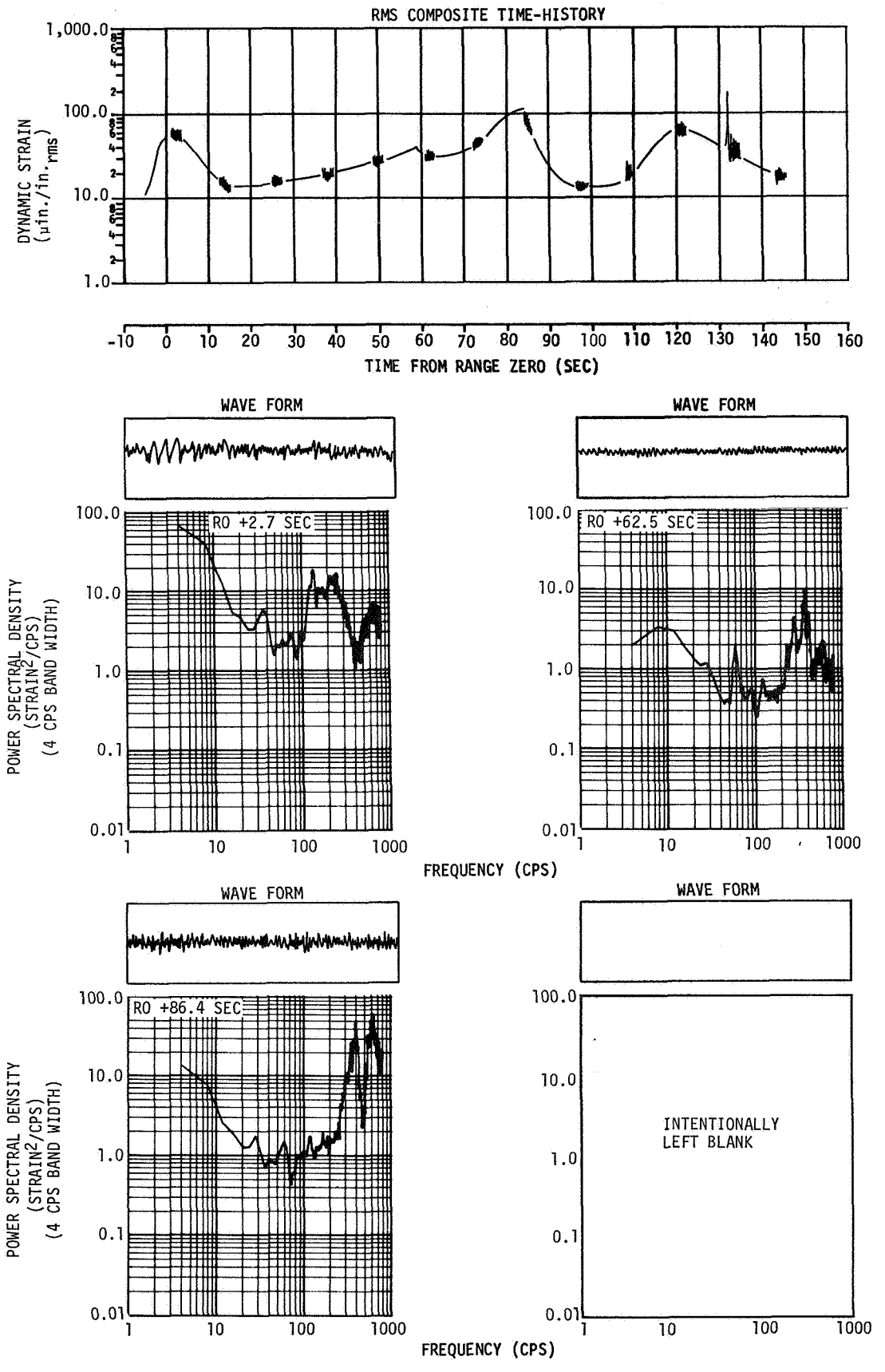

Figure 25-49. Dynamic Strain Measured on Forward Skirt Panel 61 - S0093-426

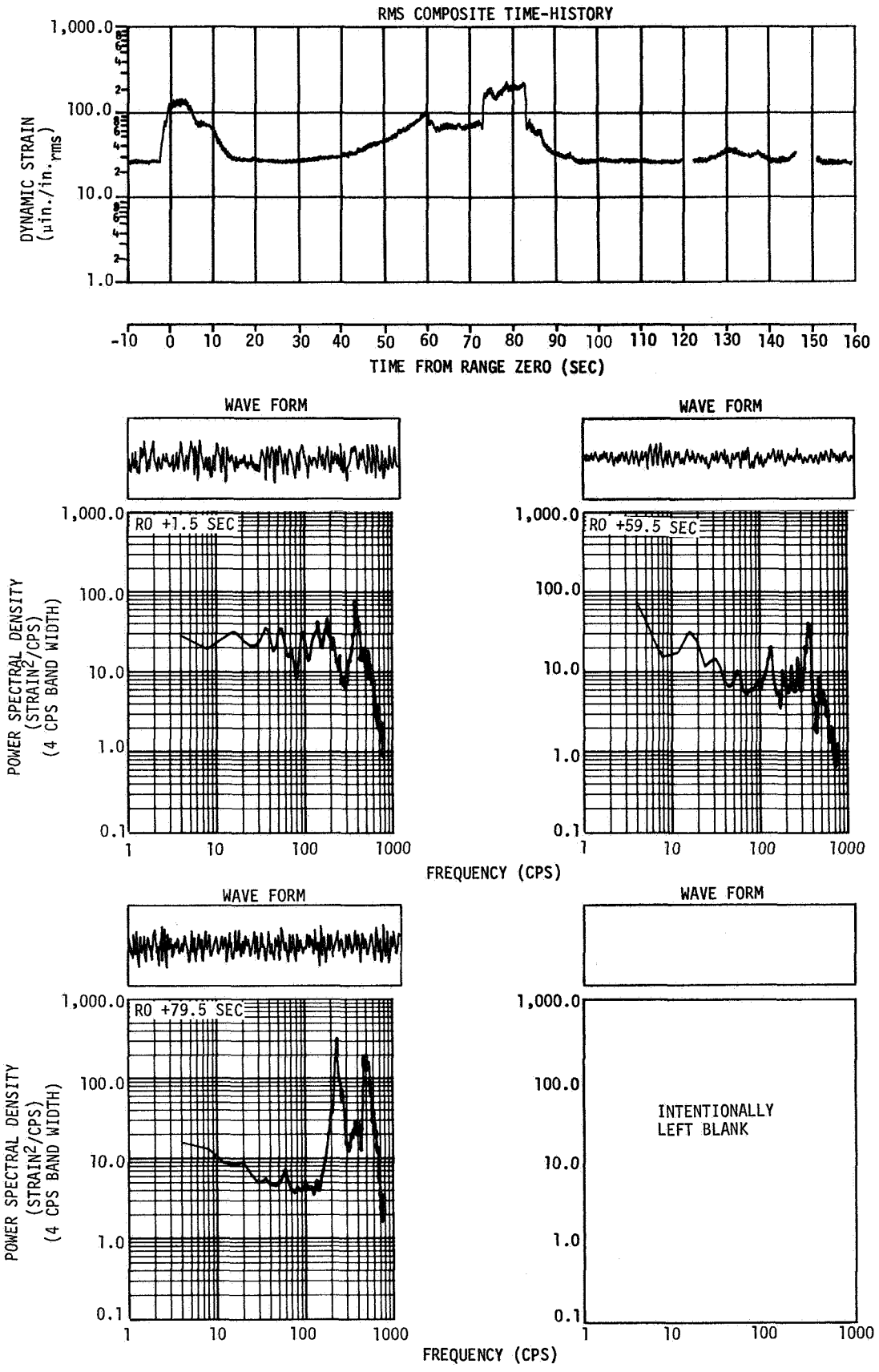

Figure 25-50. Dynamic Strain Measured on Forward Skirt Panel 69 - S0094-426

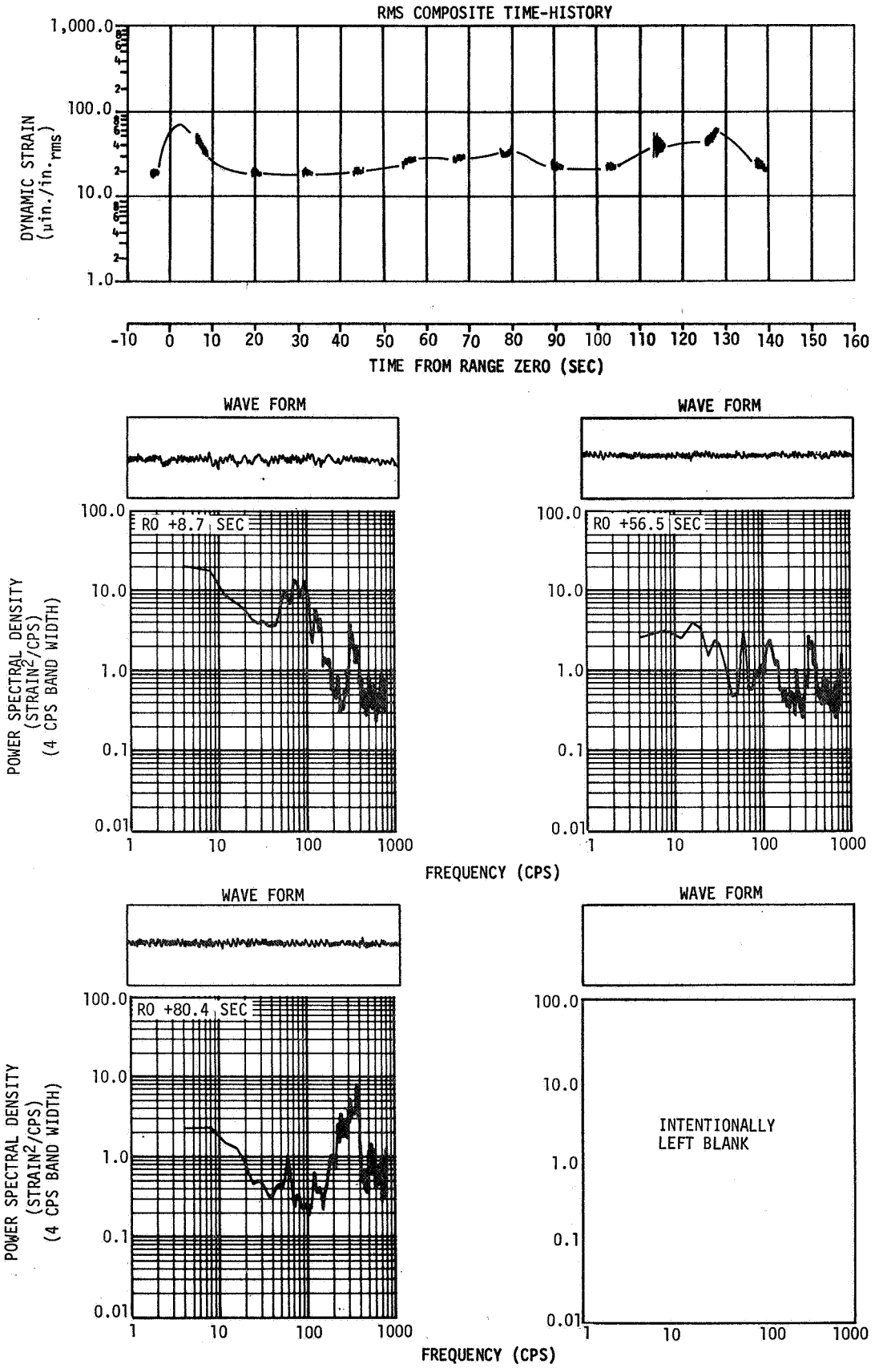

Figure 25-51. Dynamic Strain Measured on Forward Skirt Panel 76 - S0095-426

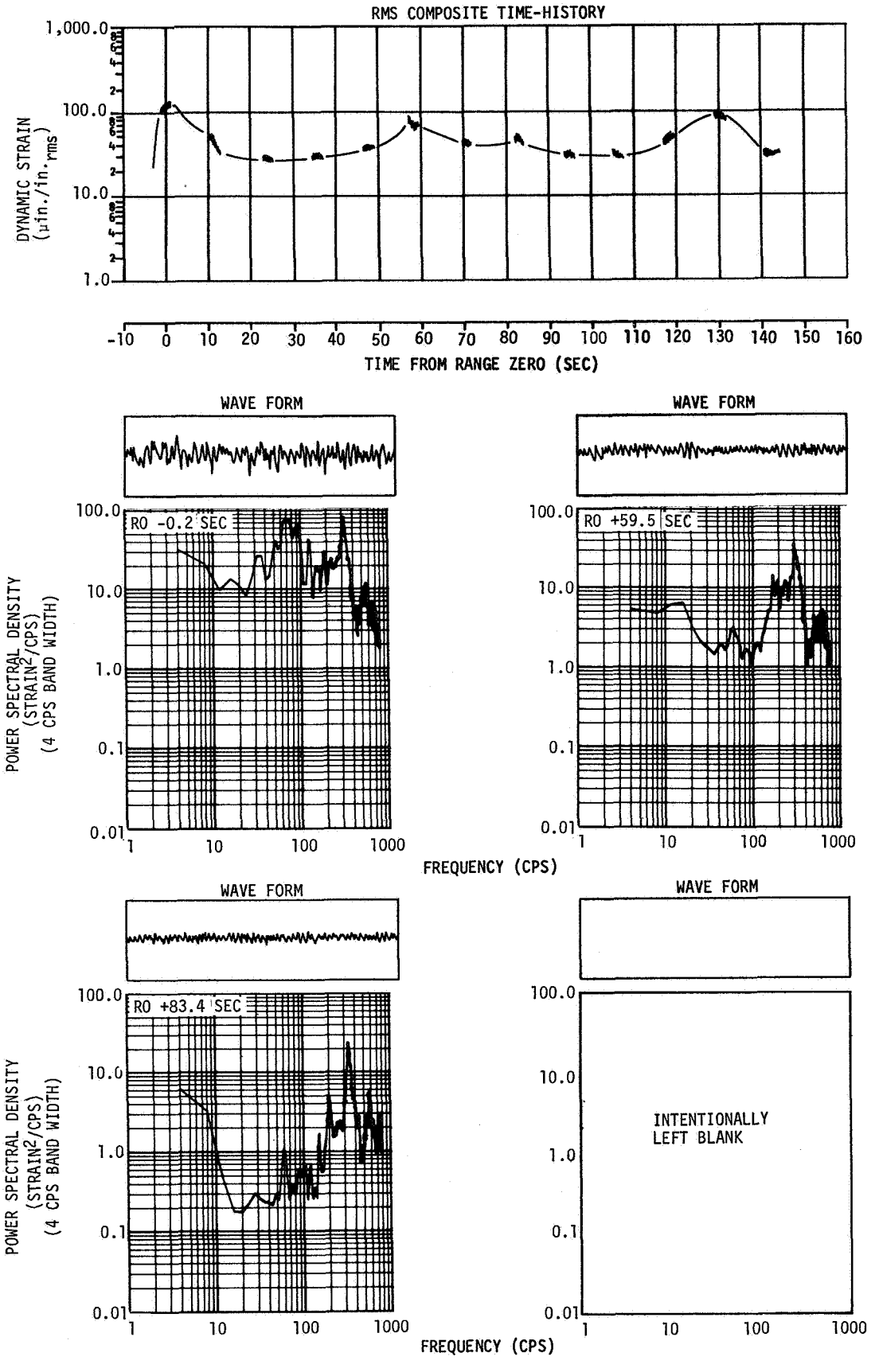

Figure 25-52. Dynamic Strain Measured on Forward Skirt Panel 80 - S0096-426

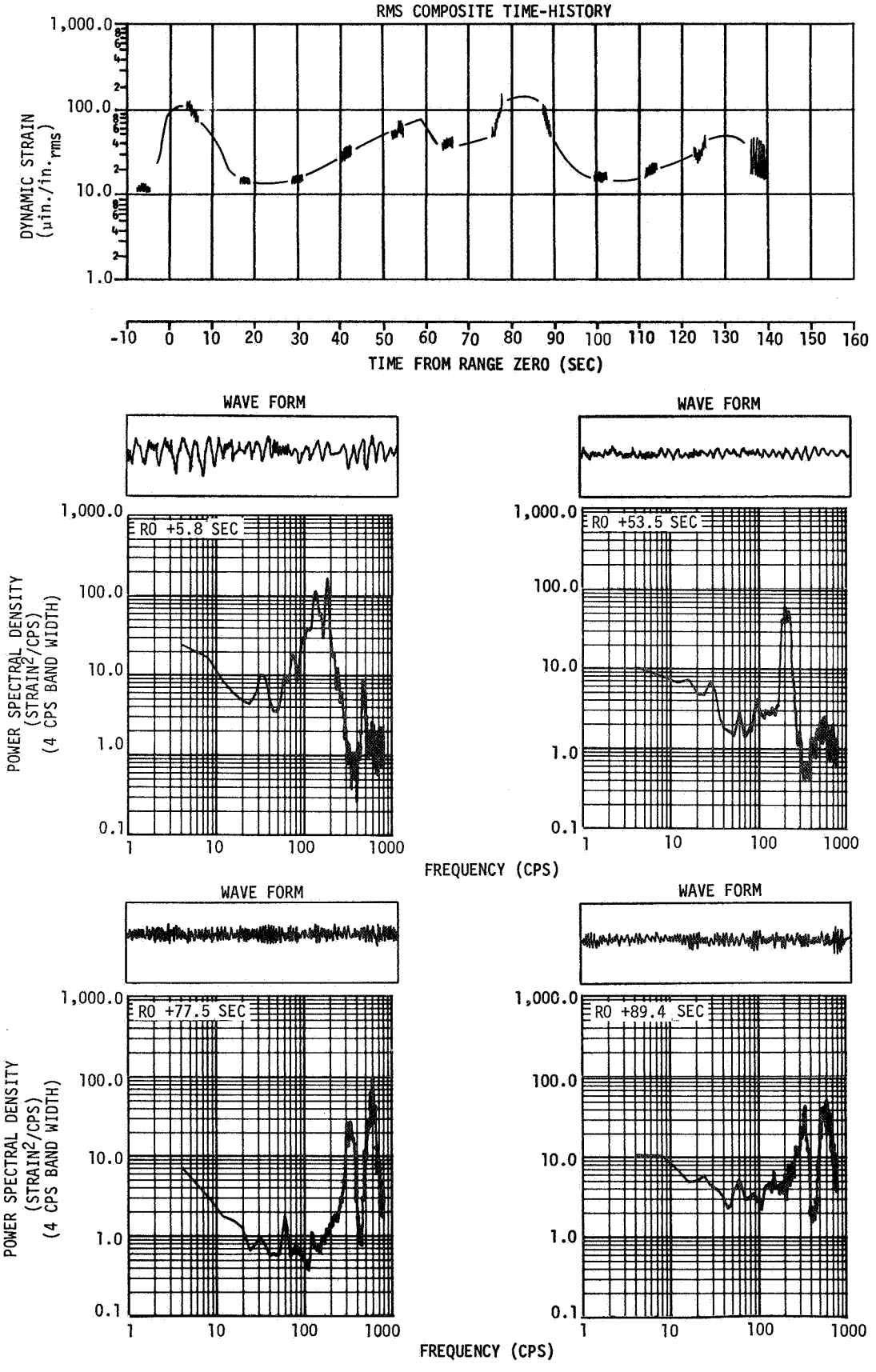

Figure 25-53. Dynamic Strain Measured on Forward Skirt Panel 87 - S0097-426

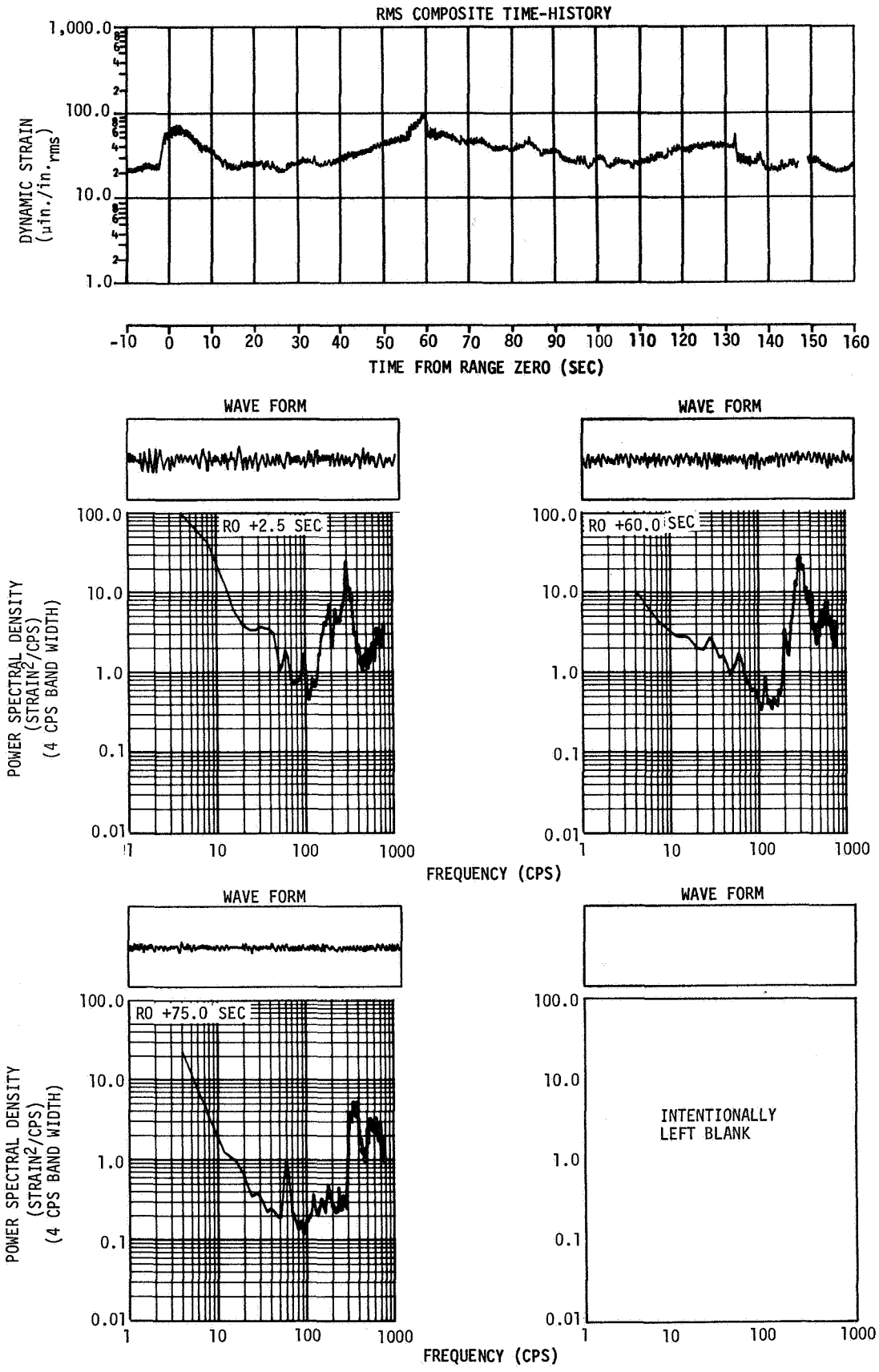

Figure 25-54. Dynamic Strain Measured on Forward Skirt Panel 94 - S0098-426

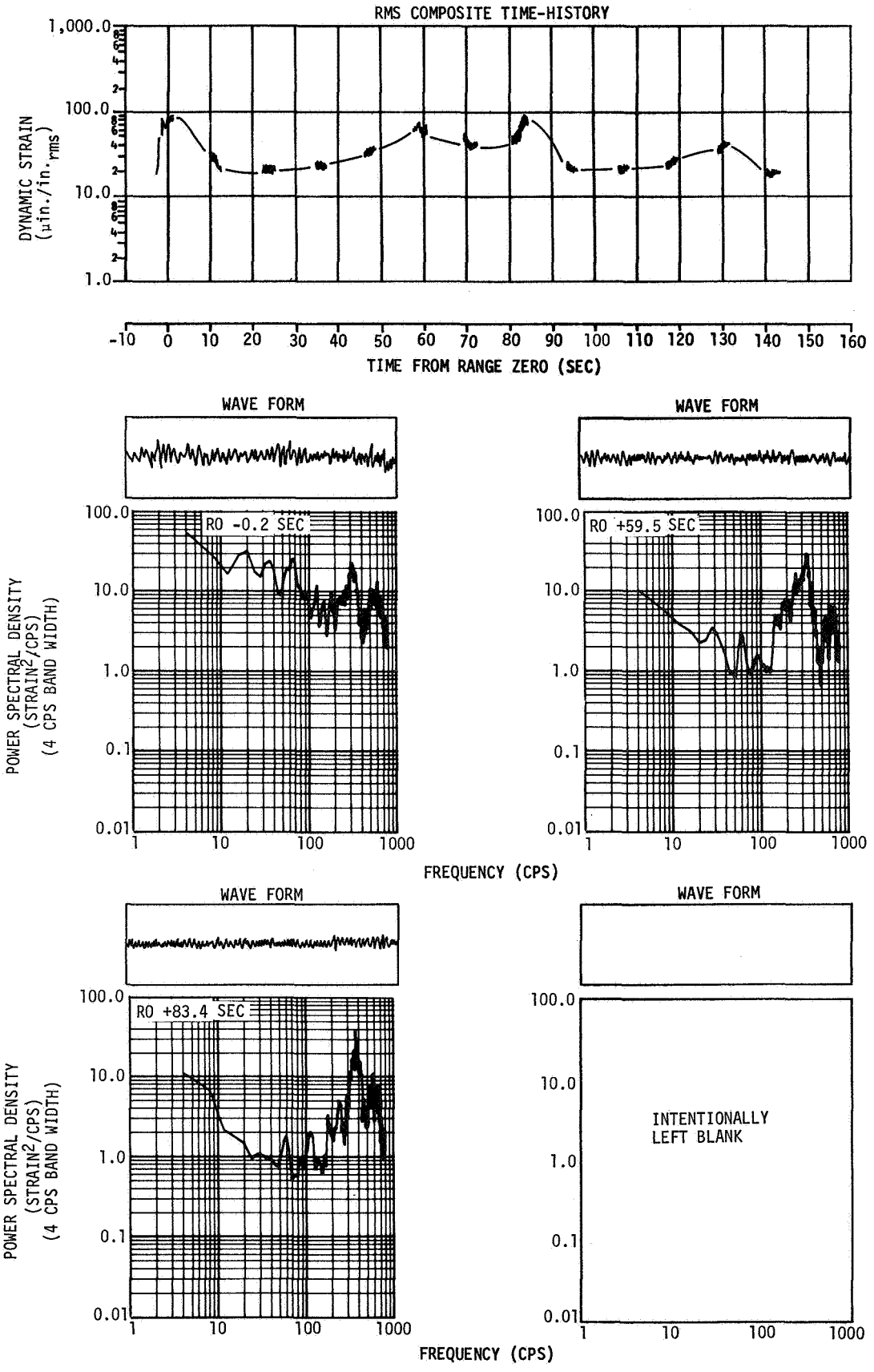

Figure 25-55. Dynamic Strain Measured on Forward Skirt Panel 101 - S0099-426

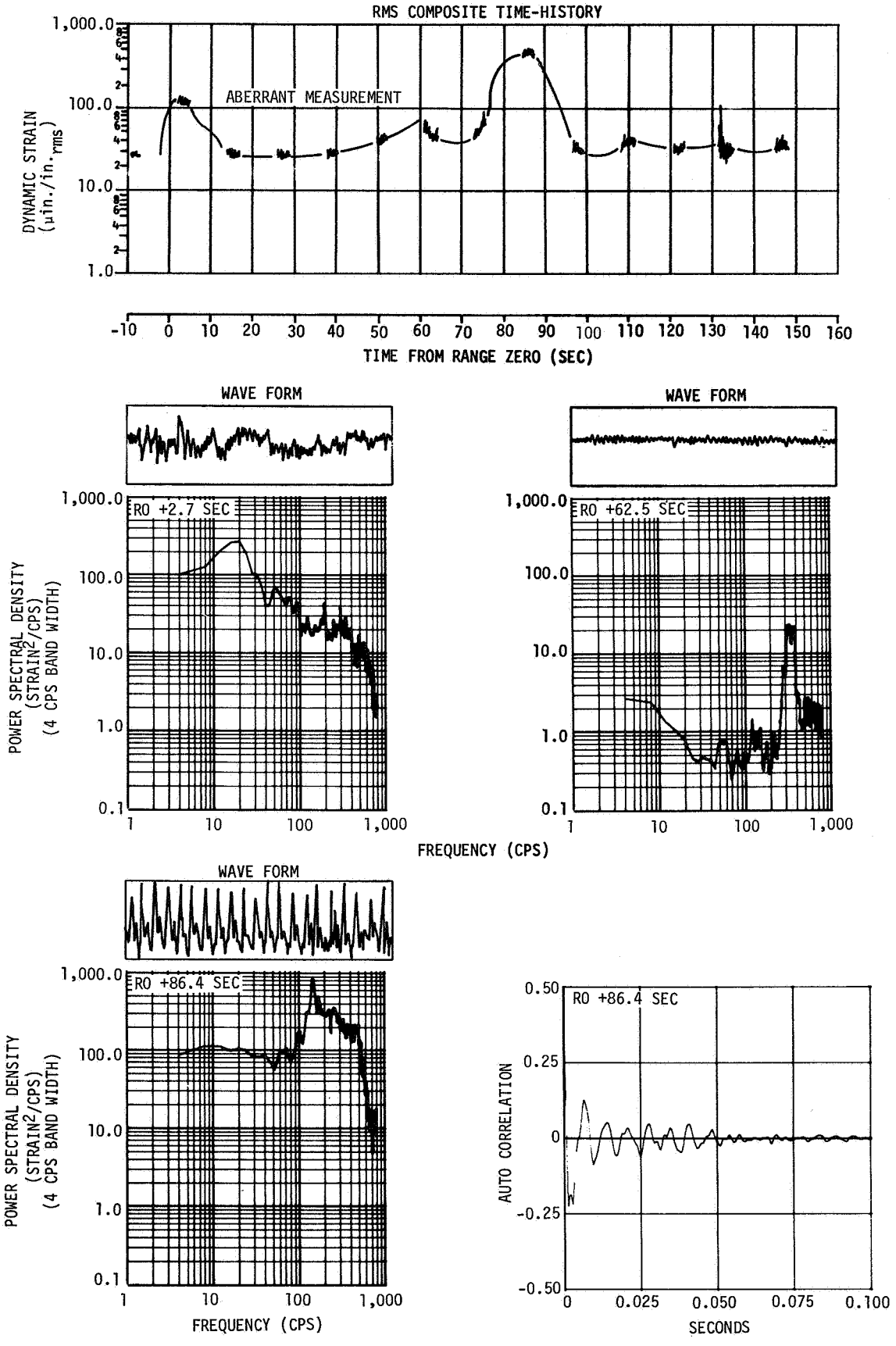

Figure 25-56. Dynamic Strain Measured on Forward Skirt Panel 108 - S0100-426

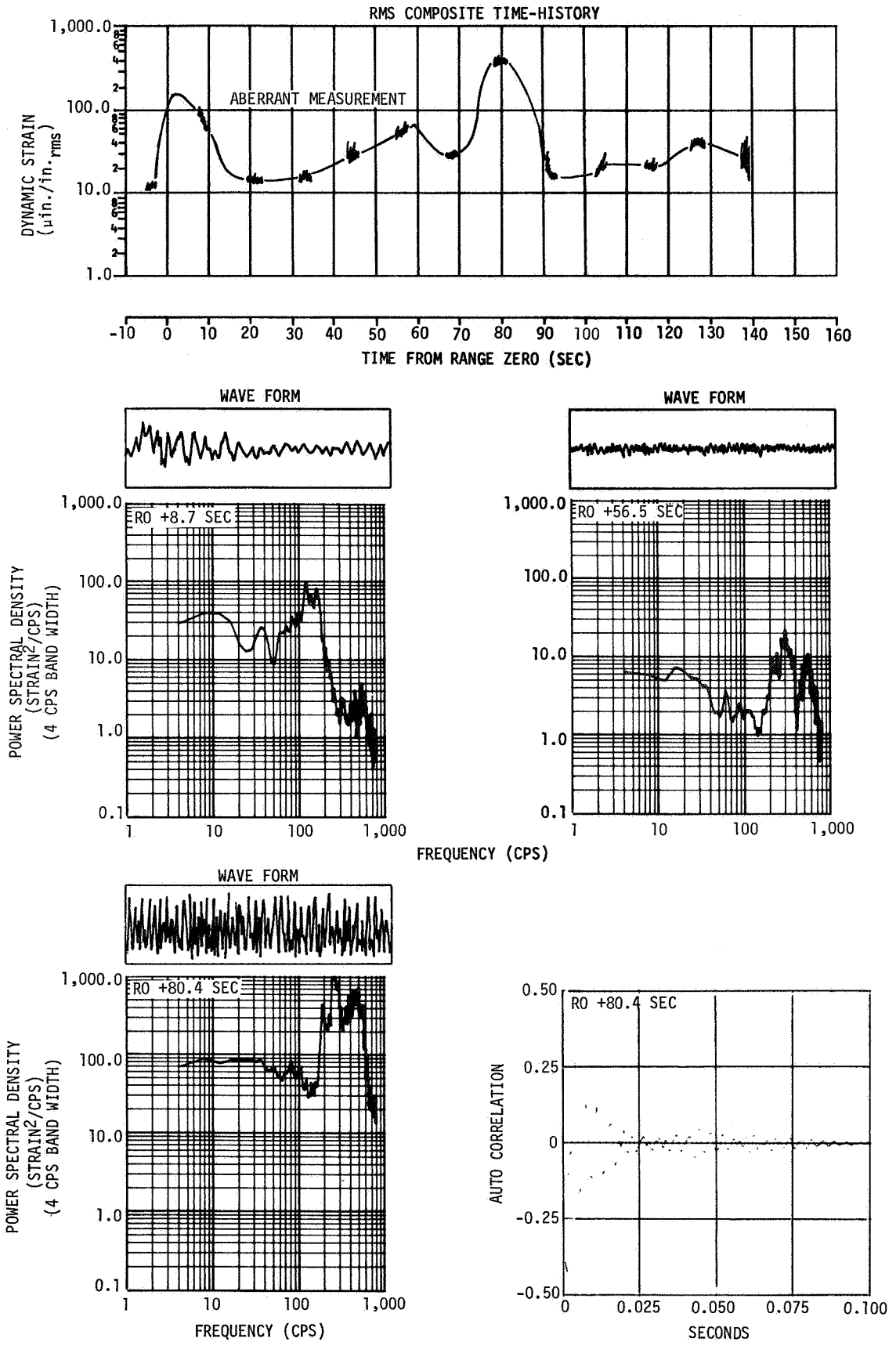

Figure 25-57. Dynamic Strain Measured on Forward Skirt Panel 7 - S0101-426

SECTION 26

AERO/THERMODYNAMIC ENVIRONMENT

26. AERO/THERMODYNAMIC ENVIRONMENT

26.1 Surface Pressure and Compartment Venting

Pressures on the S-IVB were measured by 1 internal transducer in the forward compartment and 21 external and 3 internal measurements for the aft compartment.

Figure 26-1 shows the predicted internal minus ambient pressure differentials for the forward compartment together with flight data for both AS-501 and AS-502. The vent area for AS-502 was 150 sq in. as compared to 200 sq in. for AS-501. With the trajectories flown, the smaller vent area on AS-502 should have resulted in higher internal pressures than AS-501 and correspondingly higher pressure differentials. The lower internal pressures shown in figure 26-1 for the first 60 sec of the AS-502 flight (0.05 psid) are attributed to instrumentation accuracy ($\pm$0.75 psi). Also, the fact that the AS-502 data exceed the predicted by a maximum of 0.08 psid is considered to be within the data accuracy.

Figure 26-2 shows pressure data for measurement D0051 at approximately R0 +133 sec. The pressure dropped approximately 0.2 psi. Tests conducted at Douglas to support the overall vehicle evaluation of unusual behavior at R0 +133 sec produced the following results:

a. The maximum response time required to release the transducer mechanical static friction pressure buildup was 70 ms. The maximum response time for a sudden pressure drop from 0.2 psia to 0 psia was 180 ms. The flight data were recorded every 250 ms. Therefore, it was possible that either a pressure drop or a static friction release occurred during the flight since both responses occurred in less than 250 ms during the tests.

b. Preflight and pretest calibrations on the flight and test transducers compared to test calibrations of the test transducers showed that ageing can increase the static friction buildup percentage. Based on test data and the latter fact, it was possible for the flight transducer to build up an indicated static friction pressure of 0.2 psi or greater.

It must, therefore, be concluded that the ground tests were inconclusive in showing whether a static friction release or an actual pressure drop of 0.2 psi occurred at R0 +133 sec.

Figures 26-3 and 26-4 show predicted and measured pressure differentials for the aft compartment as internal-minus-ambient and internal-minus-external, respectively. The flight data fall within the predicted band during the critical flight period and the maximum bursting and crushing pressures (2.9 psid and 0.8 psid, respectively) are well below the design values (4.69 psid and 2.24 psid).

26.2 Thermodynamic Environment

26.2.1 Structural Heating (Boost)

Figure 26-5 presents the vehicle geometry and indicates the locations of the temperature measurements used for the structural heating evaluation. All measured temperatures were below design temperatures as was expected from the relatively cool boost trajectory flown.

Table 26-1 tabulates the sensors liftoff temperatures, simulated maximum sensor and structural temperatures, AS-501 maximum measured sensor temperatures, AS-502 maximum measured sensor temperatures, and estimated maximum AS-502 structural temperatures. From table 26-1 it can be seen that the AS-502 flew a somewhat hotter trajectory than the AS-501 flight.

Comparisons between flight data and simulations are shown in figures 26-6 through 26-20. The simulations used the actual AS-502 flight trajectory and assumed boundary layer transition from turbulent to laminar flow at the time the wall-temperature-to-recovery-temperature ratio (T_w/T_r) equals 0.5. This method resulted in a closer simulation with measured data than the design method of analysis (using a transition Reynolds number of 500,000) and gave maximum simulated temperatures, with few exceptions, higher than the recorded flight data. The simulations matched the AS-502 flight data very well during the subsonic flight from RO to RO +60 sec.

26.2.1.1 Forward Skirt

The forward skirt temperature data are shown in figures 26-6 through 26-9, along with the sensor and structural temperature simulations. All of the sensors were located in regions unaffected by protuberance induced heating (i.e., $h/h_o = 1$). Good correlation between the sensor simulation and flight data is indicated. The maximum structural temperature simulations are found to be from 17 to 57 deg R higher than the maximum sensor simulated temperatures. The estimated maximum structural temperature was 746 deg R for the skin near sensor C0081, which is at the forward end of the skirt and positioned toward the sun.

26.2.1.2 LH2 Tank

The LH2 tank temperatures are shown in figure 26-10 along with the simulated sensor and skin temperatures. All of the sensors were located in regions unaffected by protuberance induced heating (i.e., $h/h_o = 1$). The simulations start at the liftoff sensor temperature, but do not consider the presence of frost and ice formation which was evident from the low liftoff temperatures (391 to 490 deg R). As a result, both sensor and skin temperature simulations gave much higher values than the recorded temperature. The estimated maximum structural temperature was 550 deg R based on sensor C0078. Only two sensors recorded temperatures higher than the freezing point of water and these were C0078 (541 deg R) and C0106 (497 deg R).

26.2.1.3 Aft Skirt

The aft skirt temperature data are shown in figures 26-11 through 26-16, along with the simulated sensor and structural temperatures. The estimated maximum structural temperature was 646 deg R based on sensor C0048 which was not insulated by Korotherm.

Figure 26-11 and 26-12 present the temperatures in the insulated (0.01 in. Korotherm) protuberance induced heating area adjacent to the APS. The simulations employ a disturbed aerodynamic heating rate 50 percent higher ($h/h_o = 1.5$) than experienced in undisturbed regions of the stage. This approach gives good simulation for the sensors in the higher heating areas (adjacent to the protuberance), and values as much as 100 deg R higher in the lower heating areas as seen for sensor C0291. The simulated skin temperatures were found

to be approximately the same as the simulated sensor temperatures. The maximum structural temperature in a protuberance induced heating area insulated with 0.01 in. of Korotherm was 636 deg R (sensor C0165).

Figures 26-13 and 26-14 present the temperatures in the insulated protuberance induced heating area adjacent to the LH2 feedline fairing (C0045, C0113, C0114, and C0115) and adjacent to the LOX vent (C0046). The simulations employed a disturbed heating rate factor, $h/h_o = 1.5$, which gave simulations up to 65 deg R higher than the data for the skin simulation and up to 30 deg R higher for the stringer simulation. The simulated structural temperatures were found to be nearly equal to the simulated sensor temperature. The low initial and maximum temperature recorded by C0046 were due to the influence of the LOX venting which was not considered in the simulation. The maximum temperature recorded for this sensor (C0046) was 562 deg R and was 92 deg R lower than the simulation.

Figure 26-15 presents the temperature data and simulations for the uninsulated aft skirt skin. Sensors C0047, C0048, C0116, and C0117 were located on the skin sufficiently removed from protuberances so as to require no insulation and the simulation employed a heating rate factor of $h/h_o = 1.0$. This approach gives excellent correlation and predicts temperatures from 0 to 15 deg R higher than the recorded temperatures. The estimated maximum structural temperature was 631 deg R based on sensor C0048.

26.2.1.4 Aft Interstage

Figure 26-16 presents the aft interstage temperature data and the sensor and structural temperature simulations. The temperature sensors on the aft interstage were covered with ablative insulation. The simulated temperatures were analyzed with $h/h_o = 1.0$ and boundary layer transition at the time $T_w/T_r = 0.5$. This method predicts temperatures slightly higher than the data with the simulation being 20 to 24 deg R higher for the stringers and 27 to 47 deg R higher for the skin. The estimated maximum structural temperature was 647 deg R based on skin sensor C0305.

26.2.1.5 LH2 Feedline Fairing

The temperature data and simulation of the LH2 feedline fairing forebody is presented in figure 26-17. For the simulation, local flow properties were assumed to be those for a 30 deg semi-apex angle cone. The simulated maximum skin temperature is seen to be 14 deg R higher than the maximum sensor temperature. The estimated maximum skin temperature is 754 deg R.

26.2.1.6 Main Tunnel

The main tunnel centerbody temperature data are shown in figure 26-18 with the simulated sensor and skin temperatures. The forebody sensor C0049 was listed as a failure during boost and therefore was not analyzed. The estimated maximum structural temperature was 685 deg R based on sensor C0227. Good correlation between data and simulated sensor temperatures is indicated.

26.2.1.7 APS Fairing

Figure 26-19 shows the temperature data of the APS centerbody with their corresponding simulated skin and sensor temperatures. Sensor C0288 is located on top of the fairing and sensors C0287 and C0289 are located approximately half way down either side of the fairing. As indicated in the data, there is little difference between the aerodynamic heating on the top or sides. The simulated sensor temperatures were found to match the recorded sensor temperature quite well. The simulated skin temperatures were found to be approximately 41 deg R higher than the simulated sensor temperatures. The maximum estimated structural temperature was 711 deg R based on sensor C0288.

26.2.2 Plume Impingement Heating

26.2.2.1 J-2 Engine Heat Flux - S-II/S-IVB Separation

The heat flux on the J-2 engine bell during retrorocket firing (RO +577.076 sec) was measured by calorimeters C2000 and C2004. The recorded heat flux histories are shown in figure 26-20 along with the simulated heat fluxes. Sensor C2000 indicated a maximum heat flux of 0.56 Btu/ft^2-sec and sensor C2004 indicated a maximum heat flux of 1.13 Btu/ft^2-sec. The simulation indicates no heating until the S-IVB was sufficiently separated from the S-II to orient the J-2 engine bell within the retrorocket flow field (approximately 1 sec after retrorocket start). The initial heating indicated by the data is due to retrorocket gases entering the aft compartment during initial separation whereas the predicted values are based only on flow impingement. The simulation also shows a maximum condition for sensor C2000 (with maximum heat flux equal to 2.29 Btu/ft^2-sec) whereas the data indicate a maximum condition for sensor C2004. It is suspected that this is attributable to the simplified analysis method which does not consider flowfield interrelation between retrorockets as well as between retrorockets and ullage rockets.

26.2.2.2 APS Ullage Rocket Plume Impingement on J-2 Engine

Calorimeters C2000 and C2004 were also used for measuring the heating rates on the J-2 engine during the auxiliary propulsion system (APS) ullage rocket firing (initiated at RO +11,288 sec). The maximum increase in heat flux for these measurements during this time was 0.014 Btu/ft^2-sec; however, the initial increase occurred approximately 40 sec prior to ullage ignition. Examination of the data from the previous orbit (RO +5,760 sec), when the ullage rockets were not firing, indicated similar trends with approximately the same (0.012 Btu/ft^2-sec) heat flux. This would indicate that solar influences are the primary source of heating measured during the ullage rocket firing and the heating due to the APS ullage rocket plume impingement is much less than the design heat flux (0.15 Btu/ft^2-sec).

26.2.3 Auxiliary Propulsion System

The orbital temperatures for the APS were determined by 10 sensors (C0294 through C0303) mounted internally to the APS fairing, on various components and propellant transfer lines,

and 4 sensors (C0286 through C0289) mounted on the fairing. One component measurement (C0303) and one fairing measurement (C0288) were selected for analytical correlation with the flight data. All measurements were evaluated with regard to their proper operation and whether the temperatures were within the allowable operational limits and the predicted range.

Sensor C0301 was found to be inoperable and was deleted prior to the flight. Sensor C0286 did not respond properly after liftoff and it is believed that this measurement partially debonded during the boost phase of the flight.

Table 26-2 lists the maximum and minimum temperatures during the flight for the APS measurements. The values for the AS-501 flight are also included for comparison. It can be seen that all components remained within their allowable limits with the exception of the propellant transfer lines. Four line measurements (C0294, C0295, C0297, and C0298) exceeded their maximum allowable temperature of 585 deg R because of extended APS engine firing resulting from failure of the engine to restart. Two measurements (C0295 and C0298) were within 5 deg R of the maximum allowable value, and two measurements (C0294 and C0297) were within 20 deg R of the maximum allowable value.

The excessive line temperatures were produced by radiation from the APS engines. The engines have a direct radiation path to the propellant transfer lines and components in the aft engine compartment. The effect of this radiation on the oxidizer control module can be seen in figure 26-21 where correlation of measurement C0303 is presented. The analytically predicted temperatures (which do not include the radiation effects of the abnormal engine temperatures) agree fairly well with the flight data until after restart attempt (approximately R0 +11,615 sec). After this time, the flight data, although still well within the operational limits, exceed the analytically predicted values by as much as 20 deg R. The engines, which have a relatively large heat capacitance, retain the high temperatures until telemetry data drop out.

Figure 26-22 presents a comparison of the APS fairing orbital flight data with respect to the predicted design temperature envelope. The figure shows that the fairing flight data fall within the design limits and indicates that the high internal line and component temperatures were internally produced (i.e., due to the warmer than expected APS engines). If the increase in component temperature was a result of the external environment (through a change in vehicle orientation or a degradation of external surface optical properties) the fairing flight data would have reflected this condition. Figure 26-22, however, indicates that while the line and component temperatures were increasing in temperature after restart attempt, the APS fairings were decreasing in temperature. The fairing temperatures would need to be considerably outside the range of the maximum design temperature envelope to produce the response indicated by the flight data on the lines and components.

Figure 26-23 shows the correlation of measurement C0288 located on the APS fairing. This figure indicates that no appreciable change in optical properties occurred such as was encountered during the AS-501 flight. Fairly good correlation was achieved for the first two orbits. After this time, it is believed that the flight simulation parameters (e.g., inertial hold) used to establish the vehicle orientation did not match the actual flight parameters.

26.2.4 Propellant Heating

This section presents the LH2 and LOX tank heating values during boost and the first two orbits of the AS-502 flight.

26.2.4.1 LH2 Heating - Boost

The net heat transferred to the LH2 during boost was analytically determined by two methods. A comparison between the results obtained from these two methods and the maximum and minimum design heating values is shown in figure 26-24. Curve A is a simulation using the recovery temperature and tank wall heat transfer coefficient histories based on the flight trajectory. Initial LH2 tank skin temperatures from flight data were used. Maximum values of insulation thermal conductivity as a function of temperature as determined from S-IVB loading and acceptance firing test data were used. The heat transferred through heat shorts (i.e., heating paths other than the cylindrical tank) was taken from a recent S-IVB propellant heating analysis. Curve B was calculated by integrating LH2 bulk temperature change resulting from propellant heating during ascent. The LH2 heating values fall within the design range.

26.2.4.2 LH2 Heating - Orbit

The predicted LH2 heating values during the first two orbits were determined using the actual AS-502 orbital path. A comparison between the analysis results, the calculated maximum and minimum design heating values, and LH2 heating values obtained from LH2 boiloff data is shown in figure 26-25.

The heating values were based on the maximum values of internal insulation thermal conductivity discussed in paragraph 26.2.4.1. For the cylindrical tank optical properties, an average solar absorptivity (α) of 0.42 and infrared emissivity (ε) of 0.87 were used. These average values were determined by measurements taken on the LH2 tank a few days before the flight. (Design values for maximum heating were $\alpha = 0.40$ and $\varepsilon = 0.87$.) The LH2 was assumed to be settled at the aft end of the tank with the effective liquid level at the deflector. This assumption was based at the liquid-vapor indications given by interior wall temperature sensors (C2017 to C2028).

The LH2 heating value derived from boiloff data is equivalent to 2,600 lbm of boiloff. This boiloff occurred during the period between first burn engine cutoff and second burn Engine Start Command and did not include the boiloff during blowdown. The LH2 evaporation which occurred during blowdown was the result of heat accumulated during boost and was subtracted from the total. As shown in figure 26-25, the calculated heating values agree well with each other and fall within the design range.

26.2.4.3 LOX Heating - Orbit

The predicted LOX heating values during the first two orbits were determined using the actual AS-502 orbital path. The LOX was assumed to be settled at the aft end of the tank with the effective liquid level at sta 256 (just above the common bulkhead joint). Heating of the LOX caused by the helium pressurant gas was considered negligible in the analysis. The results of this analysis are presented in figure 26-26. As shown, the total heat transferred to the LOX was approximately 2,800 Btu.

26.2.4.4 LH2 Tank External Temperatures - Orbit

Figure 26-27 compares the LH2 tank skin temperature histories for three tank regions during the second orbit. The figure shows the tank temperature at a point 30 deg from position I toward IV, position IV, and a point 30 deg from position III toward IV.

During most of the first orbit, the vehicle position III was facing the earth. At the end of the first orbit. the vehicle rolled 180 deg; thus, during the second orbit, vehicle position I was toward earth. For simplification, the initial temperature distributions for the simulated curves were estimated using flight temperature data. As shown in the figures, the simulated curves are slightly higher than the measured ones and account for the calculated heat input being slightly high.

26.3 Electronic Components Thermal Environment

The electronic component temperature data appear to be valid throughout the flight. The temperature extremes recorded during the first 33,800 sec of flight are presented in table 26-3.

The temperatures of the aft skirt components mounted on fiberglass panels ranged from 10 to 20 deg R cooler than those recorded on vehicle AS-501 at liftoff. The forward skirt components mounted on cold plates ranged up to 9 deg R warmer than those on vehicle AS-501. All temperatures at liftoff were well within the components' upper and lower temperature limits.

All components, except the chilldown inverters and the propellant utilization assembly, remained within their respective temperature limits throughout the flight. Ground hold and orbital data through the first 16,000 sec of flight are presented in figure 26-28 for the chilldown inverters. The results of the postflight analysis, simulating the environment experienced by the LOX inverter (C0139), are also presented. As indicated, there is satisfactory correlation between the flight data and the analytical results. The chilldown inverters (C0139 and C0140) exceeded their lower temperature limit at approximately RO +24,000 sec. The propellant utilization (PU) assembly exceeded its low temperature limit at 33,400 sec. Neither event is considered to be a problem because the normal operation period of both the chilldown inverters and the PU assembly extends only over the first 16,200 sec of a nominal Saturn V flight.

26.4 Propellant Behavior

Figure 26-29 shows the location of temperature sensors on the instrumentation probe, liquid-vapor sensors and temperature sensors attached to the insulation which were used to evaluate the propellant behavior immediately after orbital insertion. Only the sensors attached to the internal insulation were used to evaluate the propellant behavior during the orbital coast period. The temperature sensors on the instrumentation probe could not be used for liquid-vapor indication because the ullage temperature decreased to liquid hydrogen temperature after the initial phases of orbital coast. The liquid-vapor sensors could not be used because most of these sensors gave continuous liquid indications after the ullage

temperature decreased to liquid temperature level. This was probably caused by liquid droplet collection at the sensors. The wall temperature sensors gave very definite liquid-vapor indications. Since external tank heating creates a warm vapor layer at the tank wall, these sensors increased in temperature when the tank wall at the sensor location dried.

The wall temperature sensors became wet shortly after S-IVB engine cutoff and the sensors located on the instrumentation probe became wet approximately 100 sec later. At the time the wall temperature sensors became wet, the continuous venting system was still closed and the bulk of the liquid was in a subcooled state. Hence, boiling could not cause any significant disturbances and the wall sensor wetting was probably caused by propellant dynamic disturbances. Sensors on the instrumentation probe became wet after the pressure in the tank decreased below saturation pressure. Hence, boiling within the liquid bulk was a contributing factor to the propellant disturbances at this time. The sensor wetting could have been caused by either propellant disturbances or liquid level rise induced by propellant boiling.

All of the sensors remained wet during the first orbit. During the second orbit, some of the sensors became dry as shown in figure 26-30. The first sensors to dry were located between the nominal liquid level and the slosh deflector. As can be seen in figure 26-30, the sensors dried in the following sequence: C2024, C2017, C2018 and C2025 on position I, C2020, C2021, and C2022 on position II. Sensor C2027 fluctuated between liquid and vapor readings. A drying trend which goes up from the forward dome joint area towards the slosh deflector is indicated. Such behavior can be explained by assuming that the liquid height reached the deflector during the initial phases of the orbital coast period, then receded, leaving some of the liquid attached to the slosh deflector. The maximum volume of liquid that can be trapped under the slosh deflector cannot be calculated accurately. A stable configuration depends on the Bond number, based on a typical dimension of attached fluid. Hence, for any settling acceleration level, some fluid can be maintained under the slosh deflector.

The total liquid level rise depends on the volume of vapor generated during pressure decrease after orbital insertion and the vapor volume generated by boundary layer boiling caused by external tank heating. Since both the pressure decrease and the maximum propellant heating occur immediately after orbital insertion, the liquid level rise should reach a maximum early in the first orbit, then recede. Such behavior is indicated by the flight data.

Sensors C2017, C2018, C2021, and C2022 became wet again after the ullage rockets were fired as shown in figure 26-30. The sequence of wetting suggests that liquid was flowing from the top down the sidewall, first wetting the higher sensors. This lends support to the assumption that a liquid volume existed under the slosh deflector prior to the ullage rocket ignition.

At the time of ullage rocket ignition, the liquid level was close to sensors C2025 and C2027. This is indicated by continuous liquid readings recorded by sensors C2026 and C2028 and a fluctuation between liquid and vapor readings, recorded by sensor C2027. Such liquid height is equivalent to 1,300 ft^3 of entrained vapor.

During the tank pressurization, all of the sidewall temperature sensors measured the saturation temperature corresponding to the tank pressure. This period is indicated by the shaded areas in figure 26-30. Such behavior is possible when a sensor is covered by a thin liquid film or is in the vicinity of a two phase system, such as a boiling boundary layer.

The decrease in pressure after the restart attempt caused the wetting of all temperature sensors. The sensors remained wet up to 17,700 sec or longer. At approximately 20,000 sec, sensors between the slosh deflector and the nominal liquid level were already dry. This is shown in figure 26-31. Data between 17,700 and 20,000 sec are not available; hence, it is not possible to determine the sequence of drying. The pattern of dry and wet sensors is very similar to that during the second orbit. It can be concluded, therefore, that after both the orbital insertion and the restart attempt, propellant behavior was very similar. In both cases at least one temperature sensor located under the slosh deflector remained wet indicating trapped liquid.

The propellant behavior results obtained during the flight indicate that the effective tank sidewall wetted area was much larger than the minimum possible area and this factor must be considered in such areas as the propellant heating analysis and the design of the pressurization system. The minimum wetted area is defined as the area for a completely settled propellant with no vapor entrained within the liquid, dry tank sidewalls in the ullage space, and zero meniscus height at the tank sidewall. The wetted area is very close to minimum in a 1 g environment, but deviates from the minimum considerably in a low gravity field, as indicated by the flight data.

For additional information concerning propellant behavior refer to paragraph 21.3 and 21.4.

26.5 Unusual Changes in Thermal Environment

26.5.1 First Burn Thermal Environment

Thrust structure and engine temperatures experienced an unexpected and significant change during boost beginning at approximately R0 +675 sec. The temperatures in the affected regions decreased at an abnormal rate for approximately 20 sec, underwent a 3 to 10 sec increase and, again, cooled at a rate higher than normal. A comparison of the rate of change of the affected S-IVB-502 temperatures with the temperatures experienced on S-IVB-501 for the same relative flight time is shown in figure 26-32. Sensors C0010 and C0275 are ambient gas temperature probes while C0203 and C0204 are hydraulic oil temperature probes. The remaining temperature sensors shown in the figures are external temperature patches installed on plumbing and structure.

The gas temperature probes show a high cooling rate (relative to S-IVB-501) indicating that convective cooling of the probes occurred at this time. A comparison of the rate of cooling of sensor C0087 with the temperature rise rate that occurred during S-IVB/S-II staging (retrorocket plume impingement heating of 3 Btu/sec-ft^2) produces a thrust structure cooling rate of 0.25 Btu/sec-ft^2. This cooling rate is 20 times that possible due to radiation cooling. The response of sensor C0088 showed the same trends as C0087, but the temperature changes were less due to its location under the LH2 feedline.

The thrust structure temperature (C0087) increases at an average rate of 2.5 deg F/sec during this time. This rate is approximately one-half the rate that resulted from retrorocket plume impingement. The maximum heating rate available from the natural environment and J-2 engine is approximately 30 percent of the heating rate required to produce the 2.5 deg F/sec temperature rise. Thus, to produce the observed temperature rise requires a heating environment other than the natural environment. The two gas temperature probes indicate convective heating is occurring at this time which indicates either plume impingement from a hot gas source or external combustion. Sensors C0204, C2005, C2013, C2014, and C2016 showed the initial cooling response, but did not increase in temperature at RO +695 sec. Except for C2016, all of the sensors that did not respond to heating were located between position I-IV and III-IV. C2015 showed little initial cooling, but responded with a rapid temperature rise approximately 22 sec after the other sensor responses.

Figure 26-32 shows the temperature decrease rates during the second cooling phase (RO +705 to RO +715 sec) that were two to six times as great as during the initial cooling phase that started at RO +675 sec. Comparing C0087 for the two cooling phases shows that the convective cooling environment was more severe (1.8 deg F/sec versus 0.35 deg F/sec) during the latter phase which indicates the possibility that either the initial gas mass flowrate has increased or that the flow had shifted direction.

26.5.2 Thermal Environment During Attempted Restart

The attempted restart (RO +11,614 sec) provided the next opportunity for the thrust structure and J-2 engine instrumentation to be subjected to a cold, gaseous environment. Figure 26-32 shows a comparison during restart of the rate of temperature change of selected instrumentation for both S-IVB-501 and S-IVB-502. In general, those sensors that responded to the cooling environment during boost responded during the attempted restart. The magnitude of the cooling rates was less than during boost except for C2005 (main oxidizer valve pneumatic line temperature). This measurement was very near the ASI LH2 line (suspected failure point) and was probably in the denser portion of the flow for both boost and restart.

TABLE 26-1
STRUCTURAL TEMPERATURES (BOOST)

MEASUREMENT NUMBER AND LOCATION	LIFTOFF TEMPERATURE (deg R)	MAXIMUM INFLIGHT TEMPERATURE (deg R)					REMARKS
		SIMULATED		MEASURED		TRUE STRUCTURE* AS-502	
		SENSOR	SKIN	AS-501	AS-502		
Forward Skirt							
C0081	546	687	744	645	690	746	
C0082	528	687	744	680	680	735	
C0083	528	687	744	690	660	715	
C0084	528	687	744	660	677	733	
C0108	542	653	670	640	663	680	Stringer adjacent to C0081
C0109	525	692	745	599	663	713	
C0110	528	653	670	610	618	635	Stringer adjacent to C0109
C0111	510	692	745	610	Failed		off-scale-high
C0112	490	690	735	492	624	664	
C0239	530	658	673	610	650	665	
C0240	496	631	620	540	538	528	
LH2 Tank External							
C0075	436	560	565	550	468	475	
C0076	476	570	575	510	490	495	
C0077	451	565	572	475	475	482	
C0078	490	573	582	505	541	550	
C0079	422	560	565	490	465	470	
C0080	460	565	572	490	478	485	
C0106	480	570	575	480	497	502	
C0107	391	550	560	480	470	480	
Aft Skirt (Insulated with 0.01 in. Korotherm except as noted)							
C0024	533	670	669	595	588	588	
C0025	534	670	669	633	634	634	
C0026	530	686	685	625	628	628	
C0027	526	686	685	590	588	588	
C0028	530	686	685	590	593	593	
C0029	534	670	669	615	615	615	
C0045	527	660	659	595	595	595	
C0046	503	654	652	480	562	562	
C0047	518	600	630	593	590	625	No insulation
C0048	528	600	630	593	601	631	No insulation
C0113	528	626	626	585	600	600	Stringer adjacent to C0045
C0114	550	664	664	585	605	605	
C0115	547	630	630	580	598	598	Stringer adjacent to C0114
C0116	522	600	630	580	597	627	No insulation
C0117	511	600	630	485	585	615	No insulation
C0164	531	686	685	583	591	591	
C0165	534	686	685	620	636	636	
C0291	495	654	652	570	565	565	
C0292	470	-	-	465	480	480	Covered by APS fairing
C0293	515	634	644	608	613	622	
Aft Interstage (Insulated with 0.01 in. Korotherm)							
C0119	520	660	670	595	640	650	Stringer adjacent to C0306
C0120	520	660	670	592	636	646	Stringer adjacent to C0121
C0121	517	672	670	-	627	625	
C0123	520	660	670	623	641	651	Stringer adjacent to C0305
C0305	518	672	670	617	647	645	
C0306	520	672	670	575	628	626	
LH2 Feedline Fairing							
C0091	505	740	754	670	740	754	
Main Tunnel							
C0049	-	-	-	702	Failed		Off-scale-high
C0227	500	648	698	612	635	684	
C0242	510	650	700	590	626	675	
APS Fairing							
C0286	-	-	-	755	Failed		No response
C0287	547	665	706	657	665	706	
C0288	540	665	706	655	670	711	
C0289	544	665	706	641	653	694	

*True structural temperature was estimated from analysis by the temperature differences of the structure calculated with and without the sensor installation.

TABLE 26-2
APS ORBITAL TEMPERATURES

MEASUREMENT NO. AND DESCRIPTION OR LOCATION	LIFTOFF TEMPERATURE (deg R)			INFLIGHT MAXIMUM TEMPERATURE (deg R)				INFLIGHT MINIMUM TEMPERATURE (deg R)		
	EXPECTED	MEASURED		MAX LIMIT	MEASURED		EXCEED TIME* (sec)	MIN LIMIT	MEASURED	
		AS-501	AS-502		AS-501	AS-502			AS-501	AS-502
FAIRING										
C0286 Forebody		533	533		585	508**			485	498
C0287 Right side		542	546		650	600			496	490
C0288 Top		537	540		610	582			507	505
C0289 Left side		537	542		505	540			465	475
INTERNAL										
C0294 Fuel line	545 ±7	547	545	535	575	603	16,500	480	545	550
C0295 Fuel inlet (right side)	545 ±7	546	545	535	566	587	16,850	480	546	550
C0296 Fuel inlet (left side)	545 ±7	545	545	585	557	576		480	540	548
C0297 Ox line	545 ±7	545	545	585	550	601	16,500	480	545	550
C0298 Ox inlet (left side)	545 ±7	545	545	585	559	590	16,850	480	544	548
C0299 Ox inlet (right side)	545 ±7	546	545	585	566	570		480	543	550
C0300 Fuel tank support	545 ±7	545	548	585	563	560		480	550	550
C0301 Ox tank support	545 ±7	545	†	585	555	†		480	540	†
C0302 Fuel cont mod	545 ±7	545	546	585	570	563		480	550	548
C0303 Ox cont mod	545 ±7	545	546	585	550	554		480	528	548

*Time at which temperature limit was exceeded (available data)
**Apparent failure during boost
†No Data

TABLE 26-3
FORWARD AND AFT SKIRT COMPONENT TEMPERATURE*

MEASUREMENT NO. AND DESCRIPTION OR LOCATION	LIFTOFF TEMPERATURE (deg R)			MAX FLIGHT TEMP (deg R)			MIN FLIGHT TEMP (deg R)			REMARKS
	EXPECTED	MEASURED		LIMIT	MEASURED		LIMIT	MEASURED		
		AS-501	AS-502		AS-501	AS-502		AS-501	AS-502	
LOX CHILLDOWN INVERTER										
C0139	495 - 540	530	515	610	536	523	470	500	435	Exceeded minimum limit approximately 24,000 sec after liftoff
C2032	495 - 540	-	505	-	-	516	-	-	444	
LH2 CHILLDOWN INVERTER										
C0140	495 - 540	535	515	610	545	527	470	509	440	Exceeded minimum limit approximately 24,000 sec after liftoff
C2033	495 - 540	-	505	-	-	516	-	-	447	
BRIDGE MODULES										
Forward										
C0233	500 - 540	516	525	620	524	529	395	516	490	
C0234	500 - 540	516	524	620	524	526	395	516	490	
C0235	500 - 540	516	517	620	524	523	395	516	487	
Aft										
C0236	460 - 540	508	499	620	508	499	395	467	424	
C0237	460 - 540	505	489	620	505	489	395	474	411	
C0238	460 - 540	525	511	620	525	511	395	434	422	
PU ASSEMBLY										
C0017	500 - 560	528	527	570	537	530	500	521	493	Exceeded minimum limit 33,400 sec after liftoff
STATIC INVERTER/ CONVERTER										
C0061	500 - 560	533	541	570	537	546	500	515	505	

*During first 33,800 sec of flight.

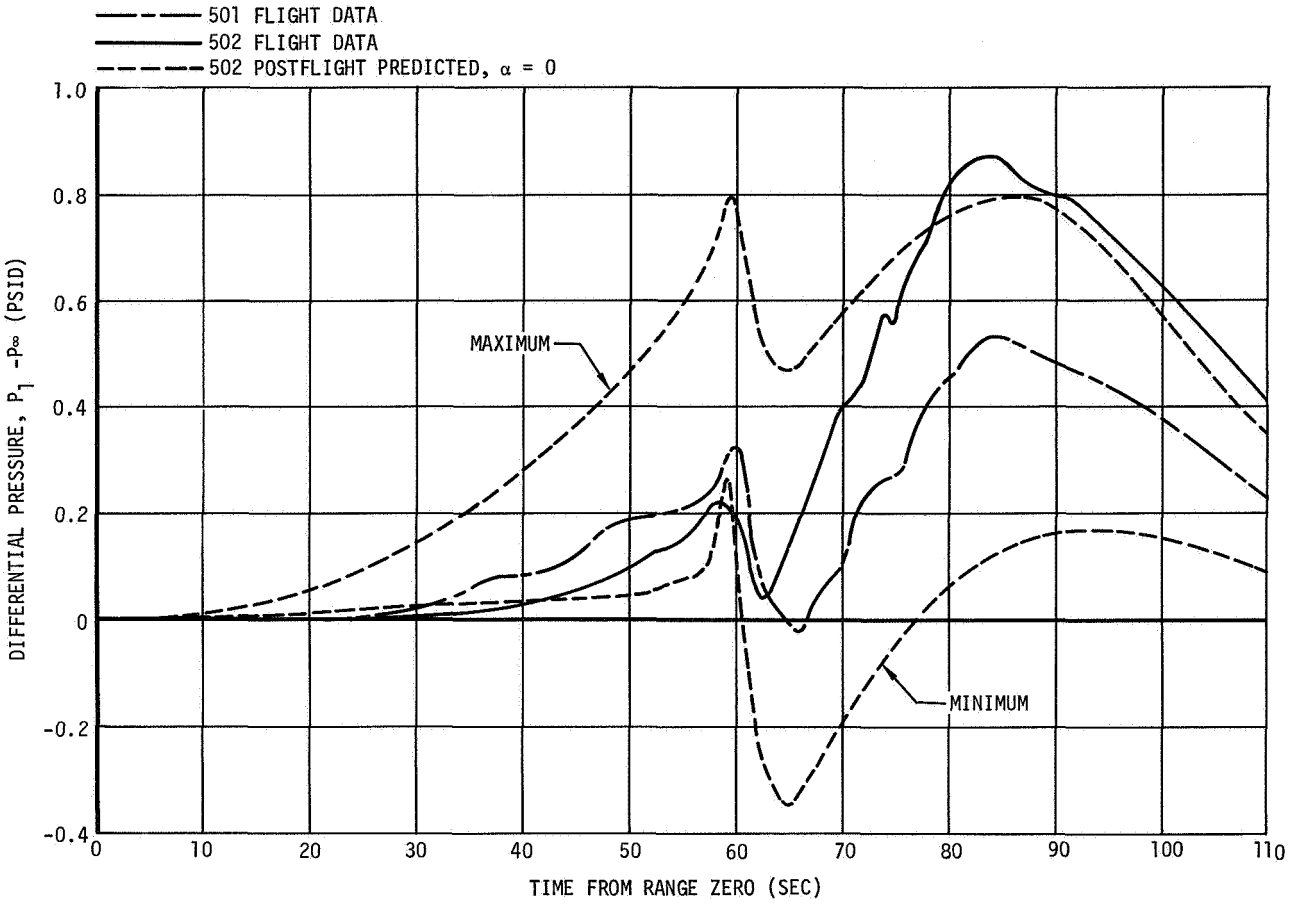

Figure 26-1. Forward Compartment Internal Pressure Minus Ambient Pressure

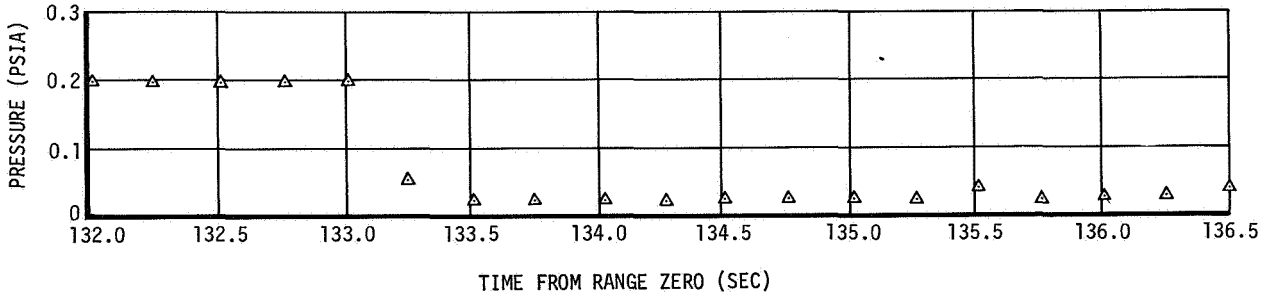

Figure 26-2. Raw Data Output From Measurement D0051

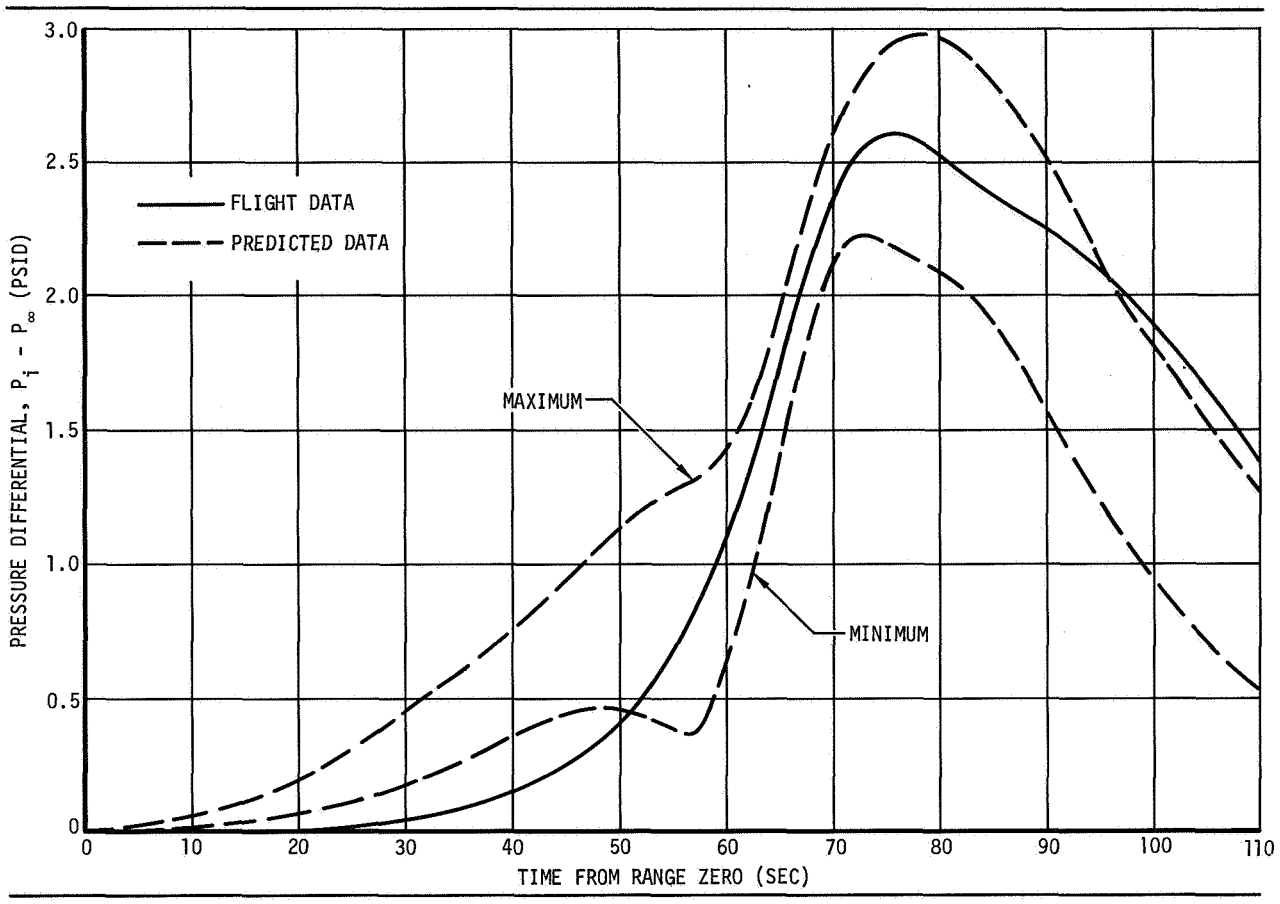

Figure 26-3. Aft Skirt and Interstage Internal Pressure Minus Ambient Pressure

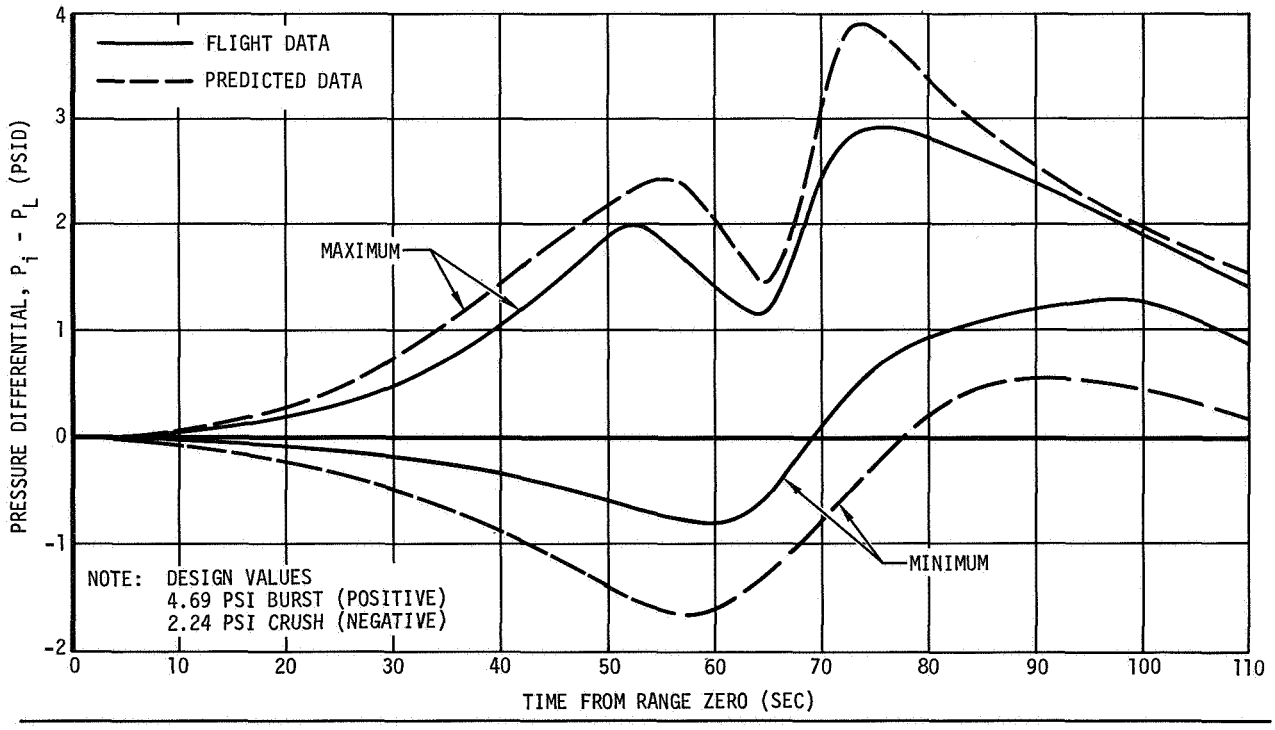

Figure 26-4. Aft Skirt and Interstage Internal Pressure Minus Local External Pressure

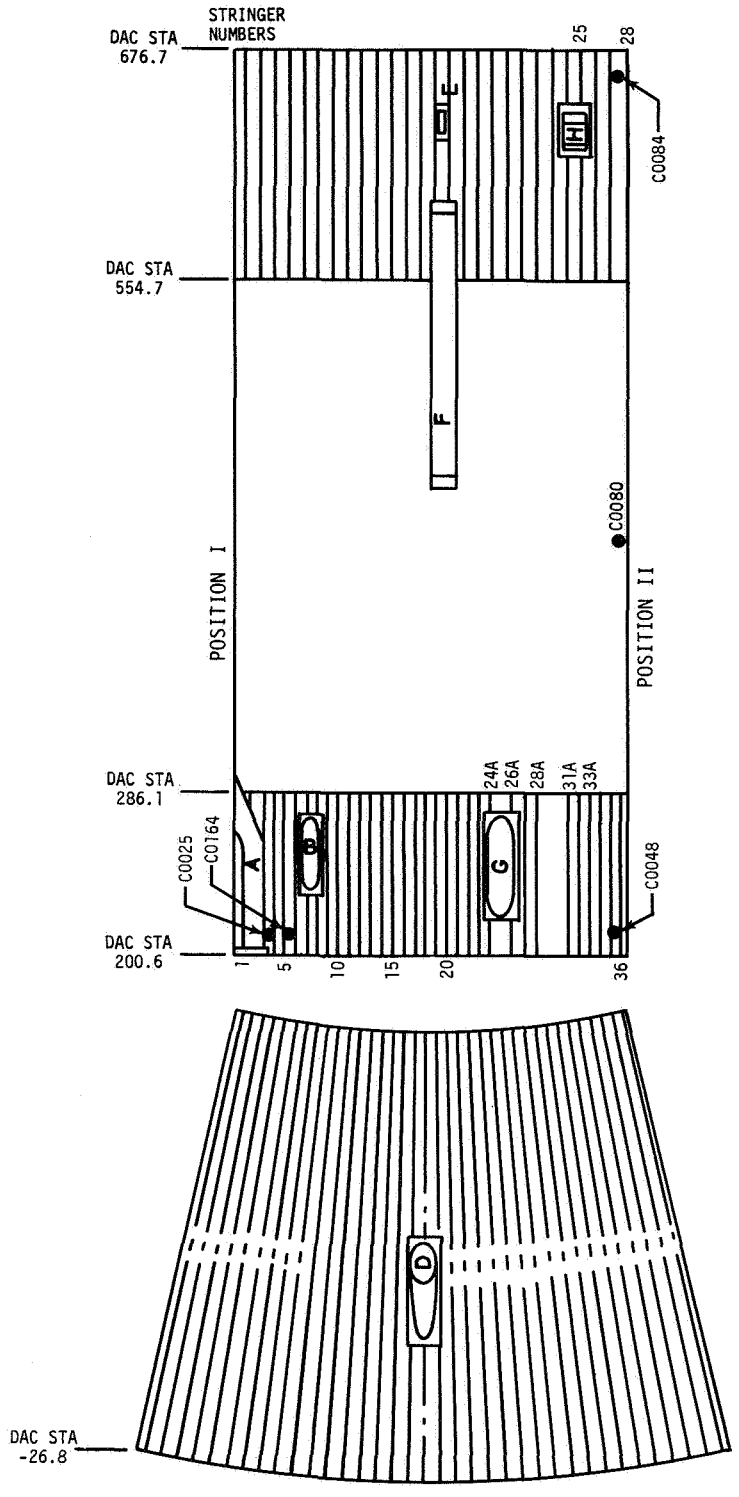

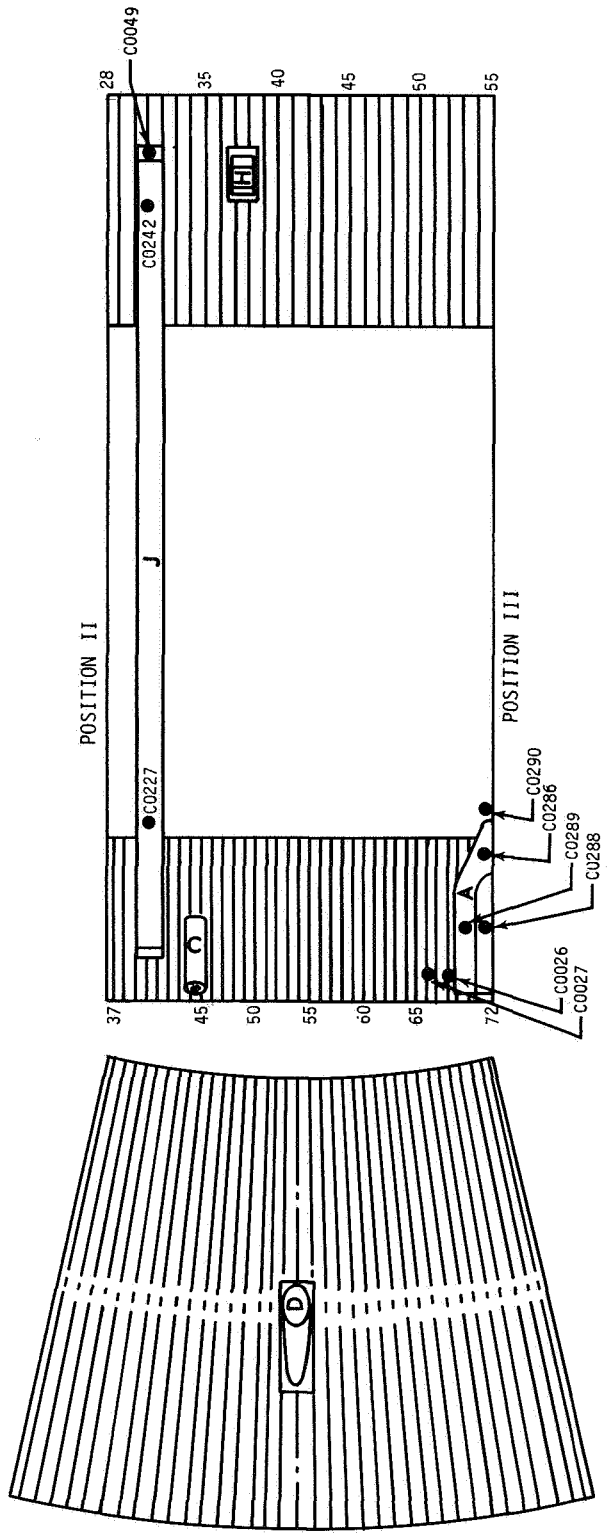

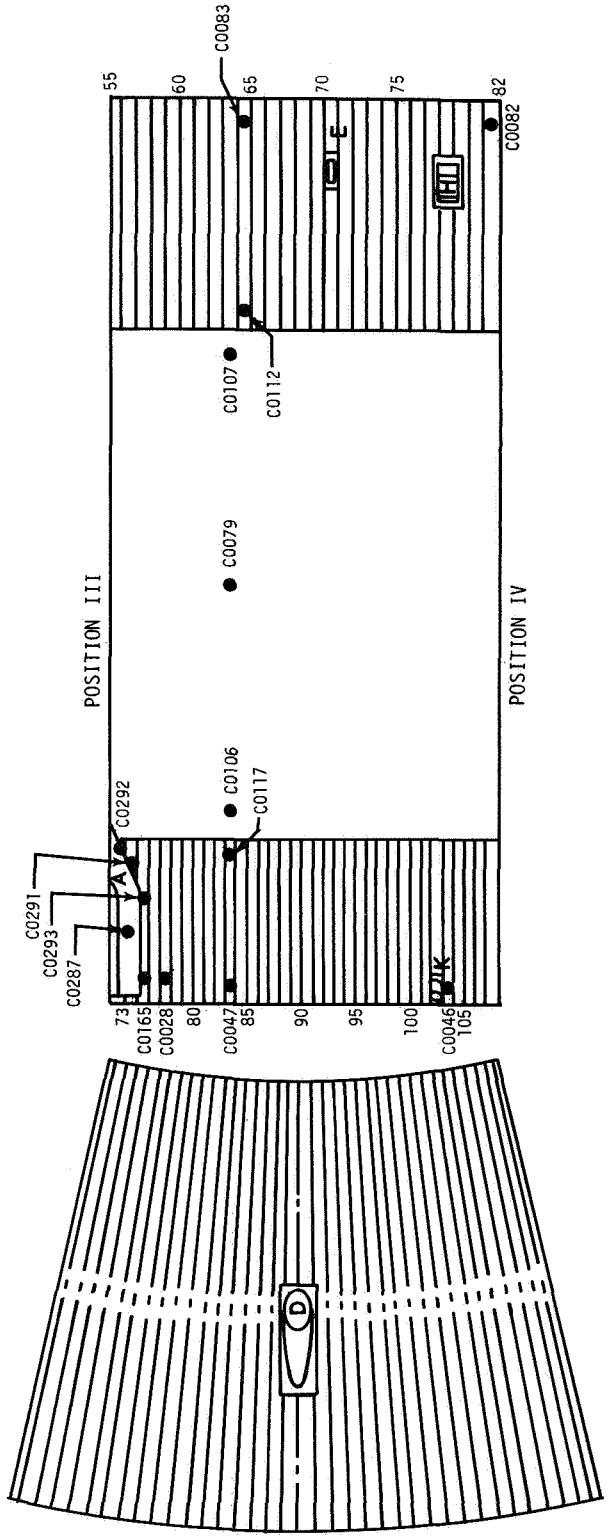

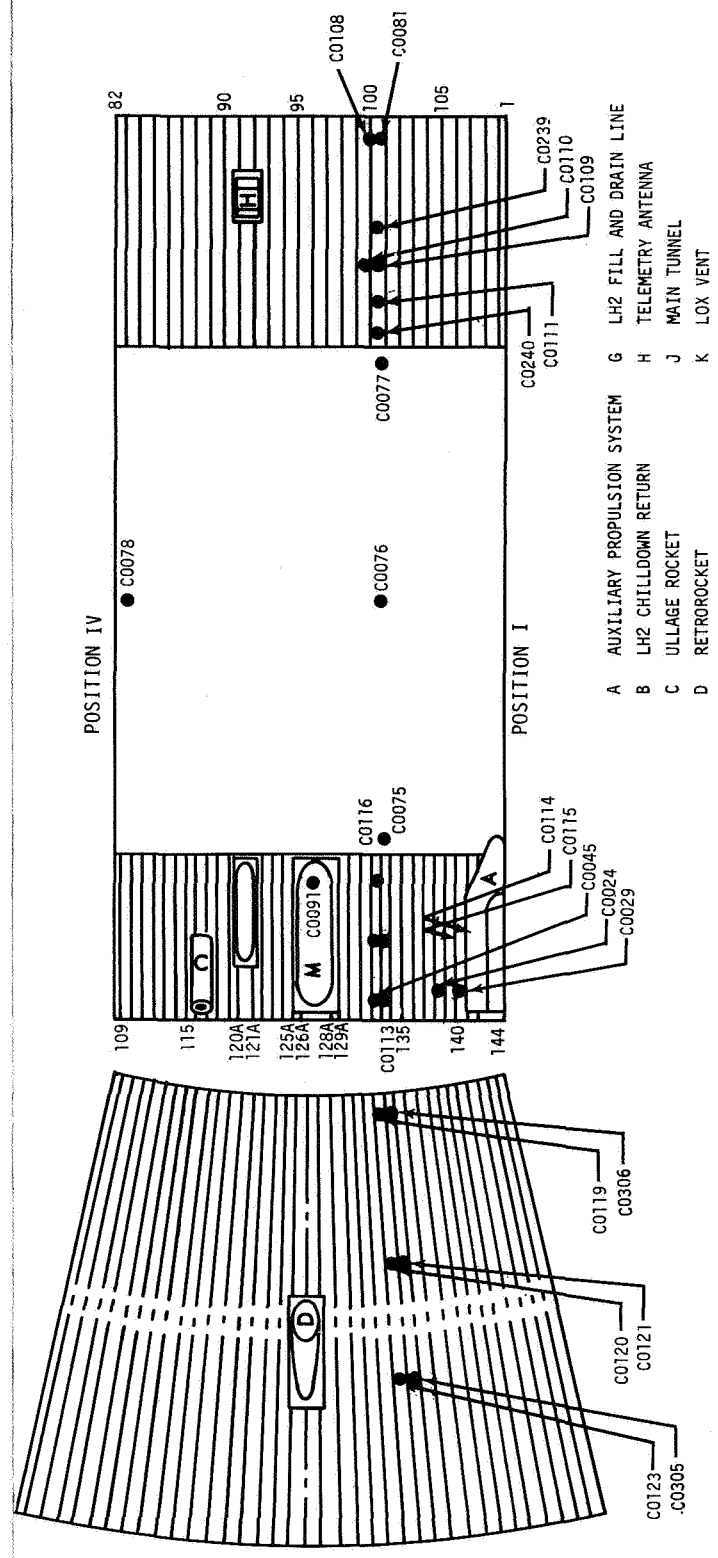

Figure 26-5. Temperature Sensor Locations

FOLDOUT FRAME 1

FOLDOUT FRAME

FOLDOUT FRAME 2

		SIMULATION	
SENSOR	DATA	SENSOR	SKIN
C0081	⊙	———	—·—
C0082	△	———	—·—
C0083	⊡	———	—·—
C0084	▽	———	—·—
C0108	◇	— —	- - -

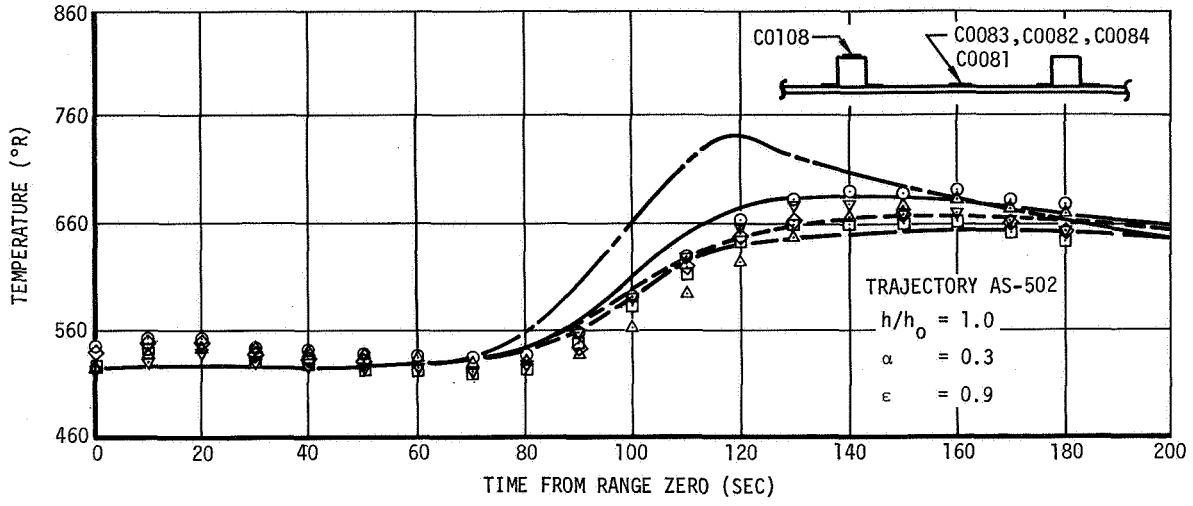

Figure 26-6. Forward Skirt Temperature Histories - Sta 670

		SIMULATION		
SENSOR	DATA	SENSOR	SKIN	DAC STA
C0109	⊙	———	—·—	600
C0110	⊡	- - -	— —	600
C0111	△	———	—·—	570

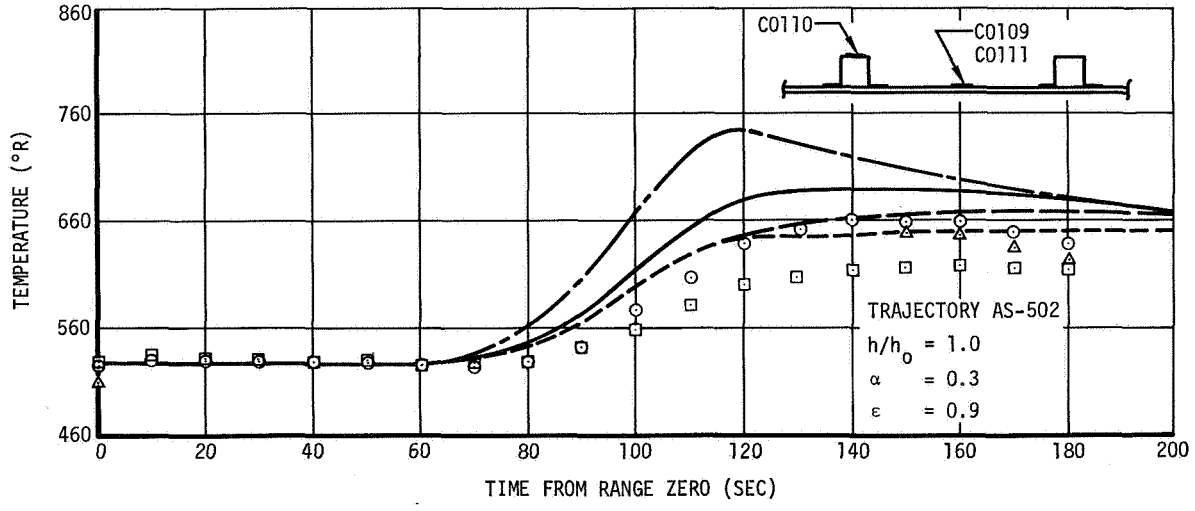

Figure 26-7. Forward Skirt Temperature Histories - Sta 600 and 570

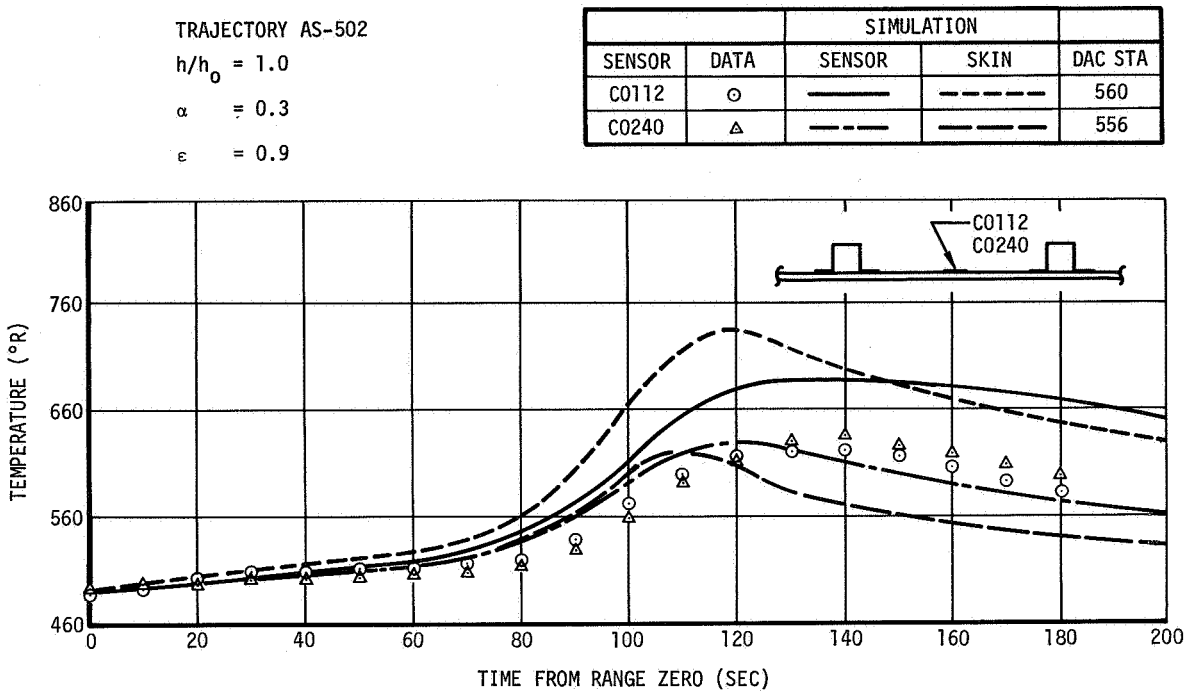

Figure 26-8. Forward Skirt Temperature Histories - Sta 556 & 560

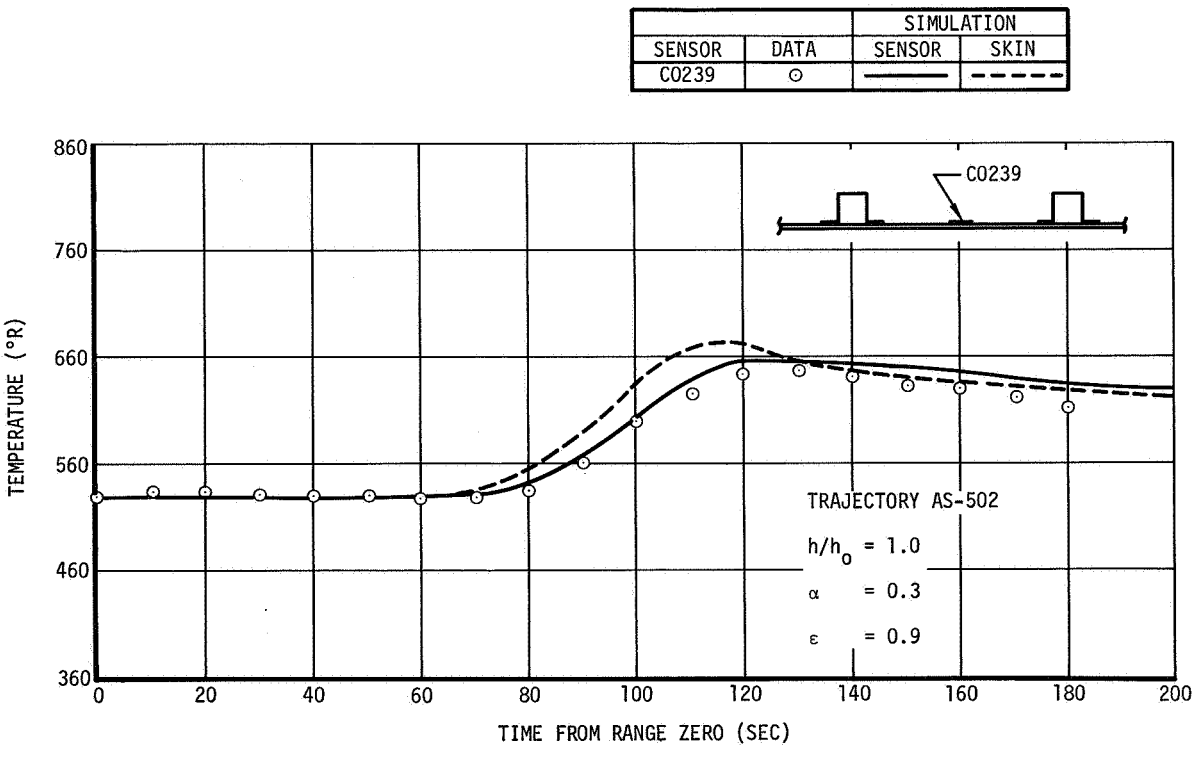

Figure 26-9. Forward Skirt Temperature History - Sta 615

TRAJECTORY AS-502

h/h_o = 1.0

α = 0.42

ε = 0.87

SENSOR	DATA	SIMULATION SENSOR	SIMULATION SKIN	DAC STA
C0075	⊙	———	— - —	296
C0079	△	———	— · —	421
C0076	⊡	- - - -	———	421
C0106	▽	- - - -	— —	296

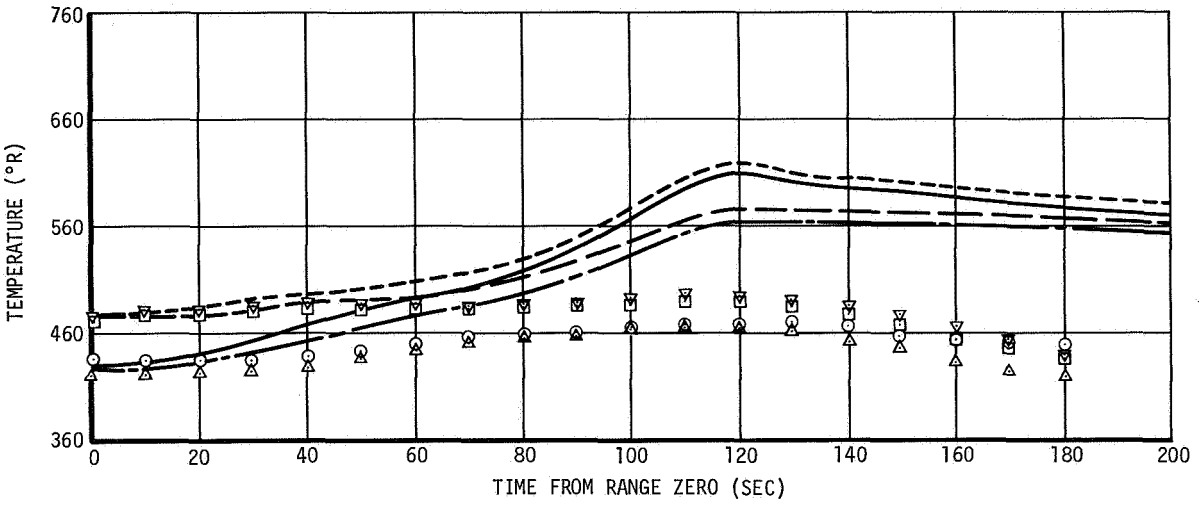

TRAJECTORY AS-502

h/h_o = 1.0

α = 0.42

ε = 0.87

SENSOR	DATA	SIMULATION SENSOR	SIMULATION SKIN	DAC STA
C0077	⊙	———	— - - —	544
C0080	△	———	— · - —	421
C0078	⊡	- - - -	———	421
C0107	▽	— · —	— · - —	544

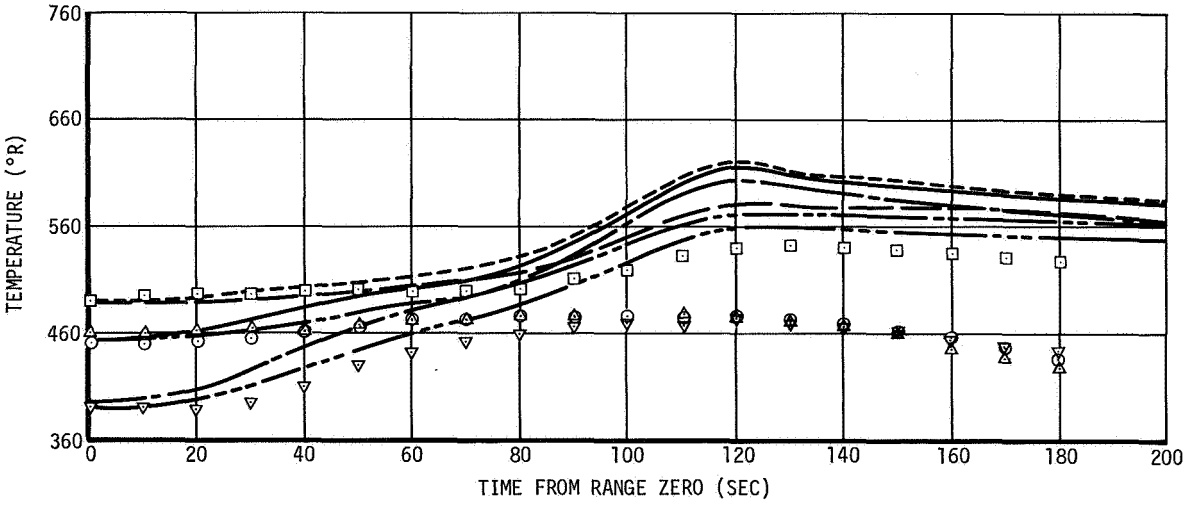

Figure 26-10. LH2 Tank Temperature Histories

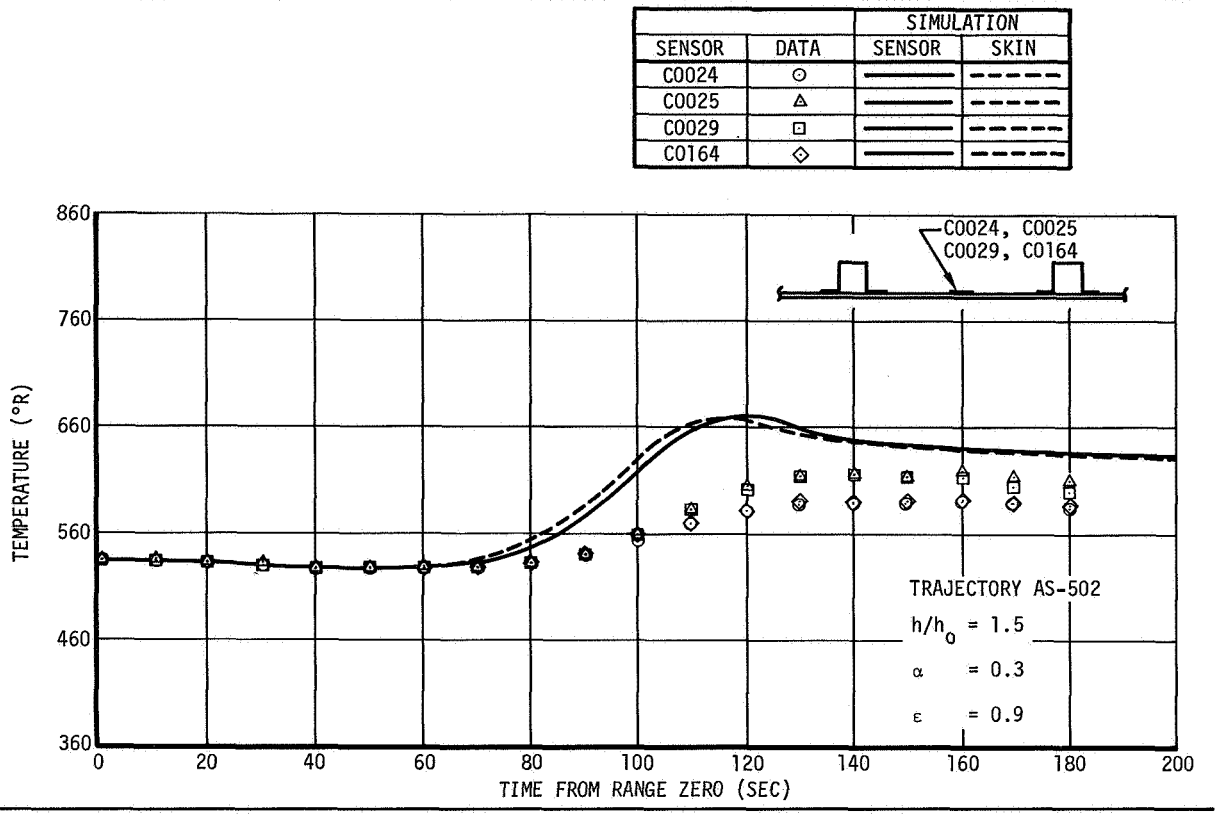

Figure 26-11. Aft Skirt Temperature Histories Near APS NO. 1 - Sta 215

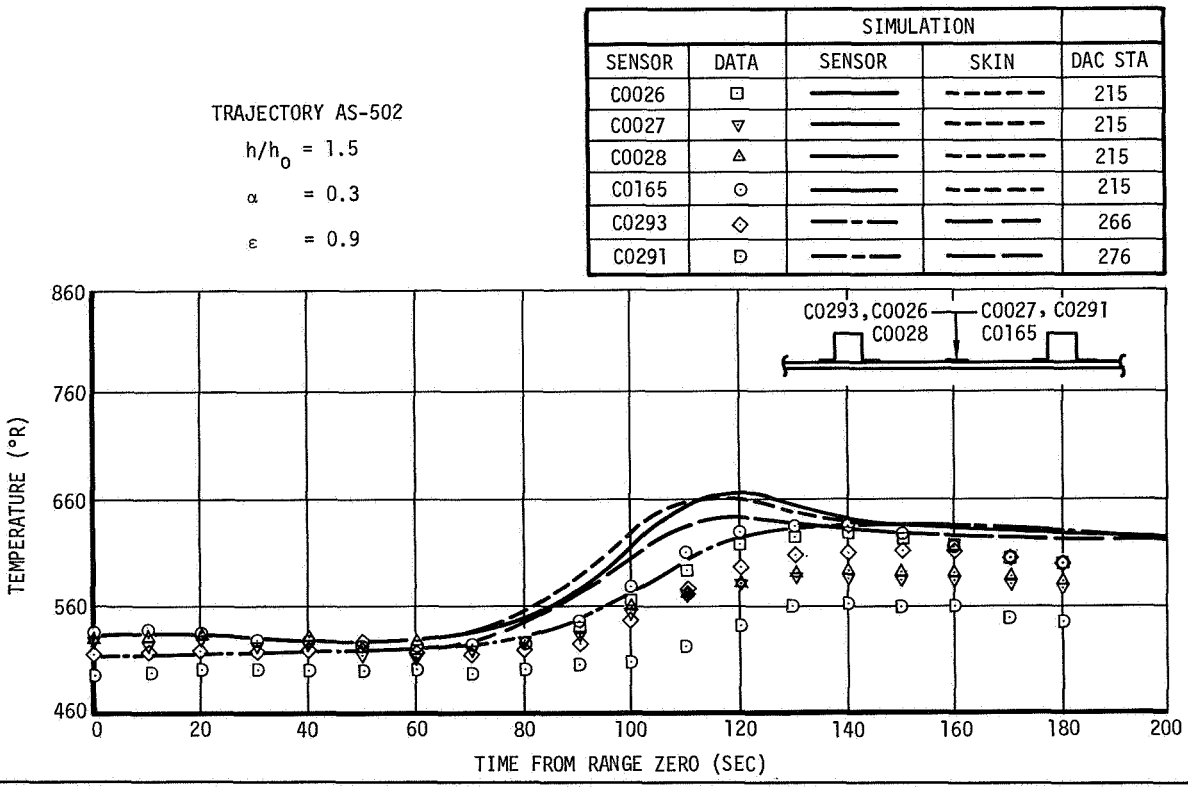

Figure 26-12. Aft Skirt Temperature Histories Near APS NO. 2

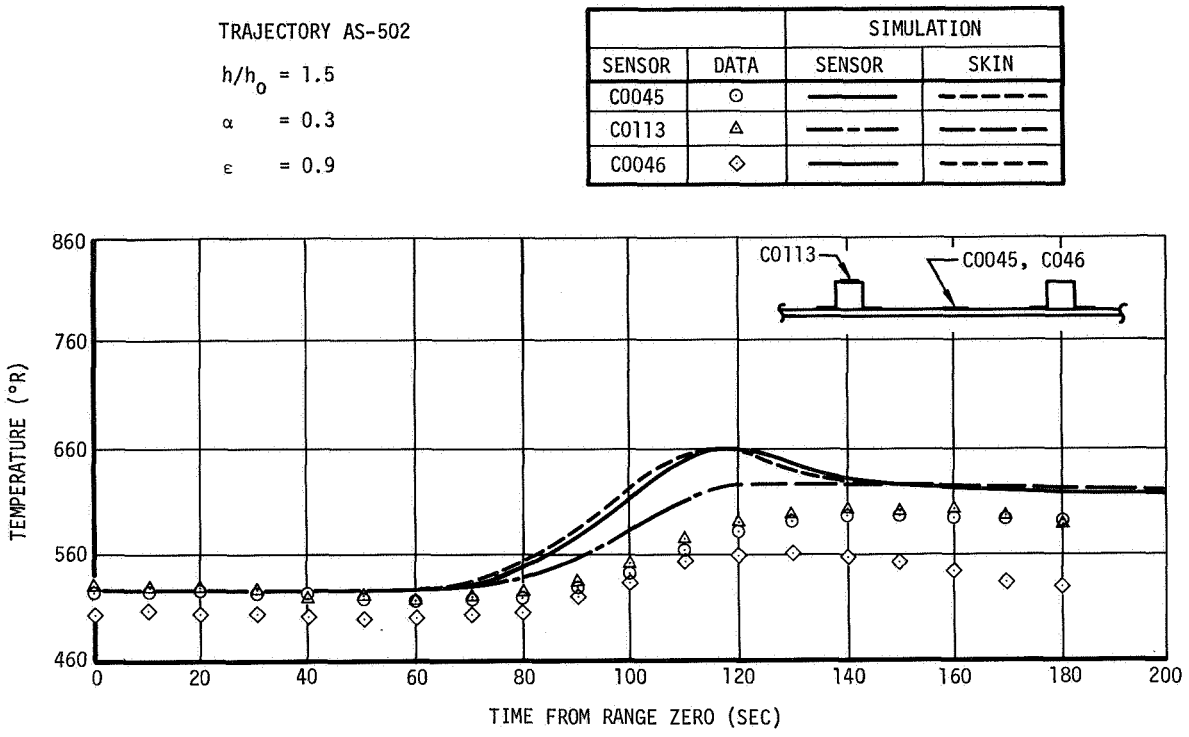

Figure 26-13. Aft Skirt Temperature Histories - Insulated (Sta 210.65)

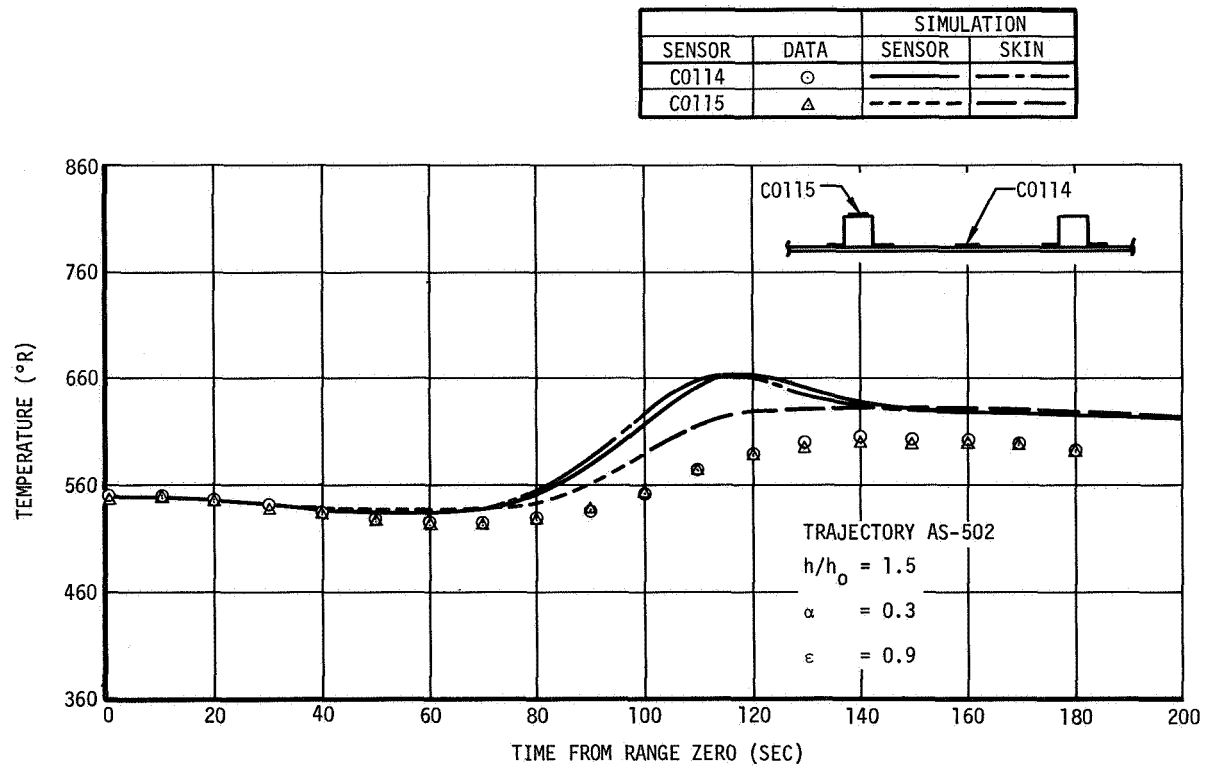

Figure 26-14. Aft Skirt Temperature Histories - Insulated (Sta 250)

TRAJECTORY AS-502

h/h_o = 1.0

α = 0.3

ϵ = 0.9

		SIMULATION		
SENSOR	DATA	SENSOR	SKIN	DAC STA
C0047	⊙	———	- - - - -	210
C0048	△	———	- - - - -	210
C0116	⊡	———	- - - - -	280
C0117	▽	———	- - - - -	280

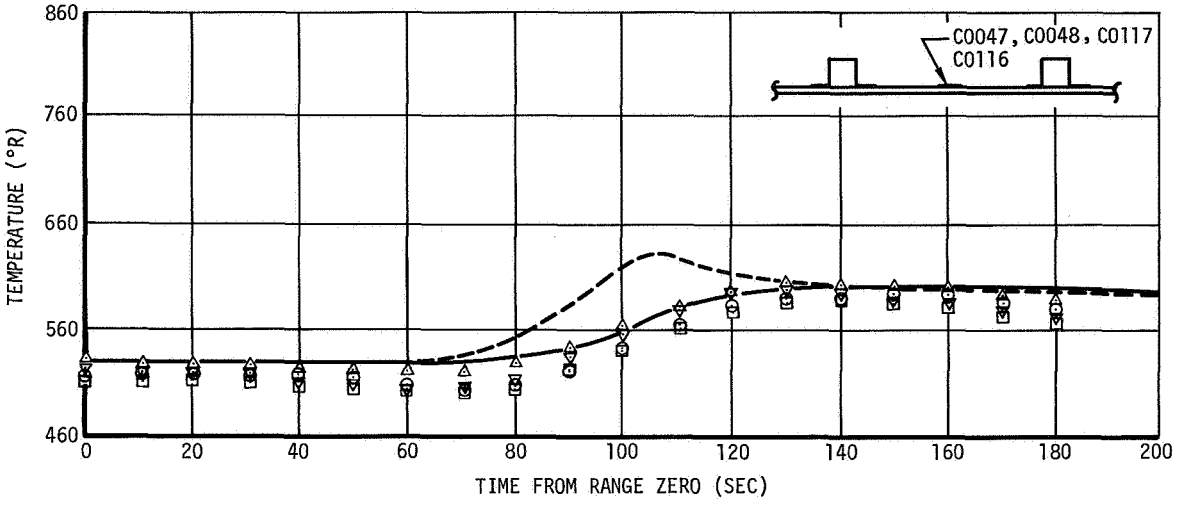

Figure 26-15. Aft Skirt Skin Temperature Histories - Uninsulated

TRAJECTORY AS-502

h/h_o = 1.0

α = 0.3

ϵ = 0.9

		SIMULATION		
SENSOR	DATA	SENSOR	SKIN	DAC STA
C0119	⊡	———	—·—·—	192
C0120	▽	———	—·—·—	156
C0121	◇	- - - - -	— — —	156
C0123	⊙	———	—·—·—	81
C0305	△	- - - - -	— — —	81
C0306	◁	- - - - -	— — —	192

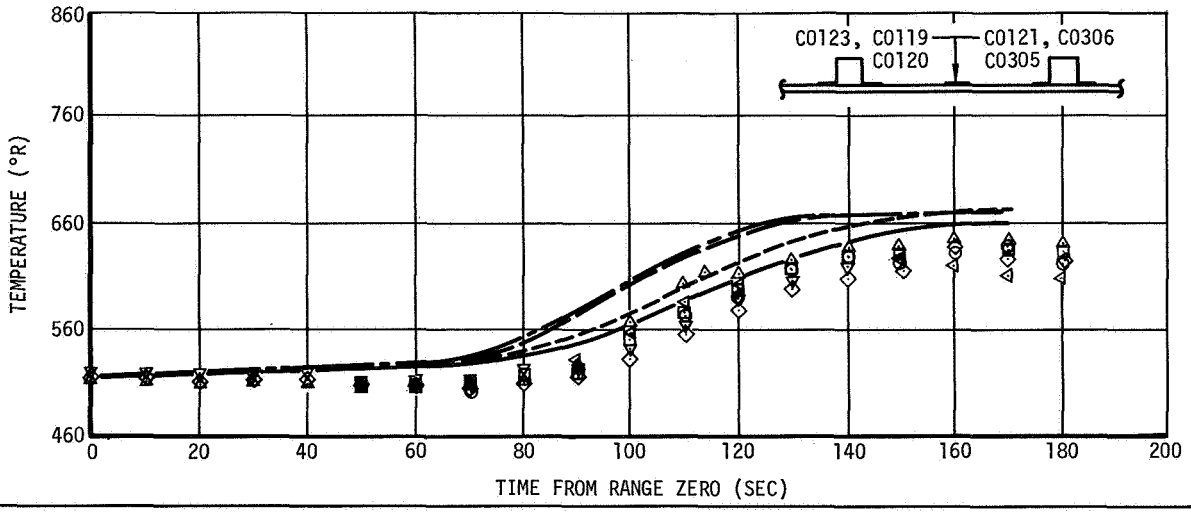

Figure 26-16. Aft Interstage Temperature Histories - Insulated

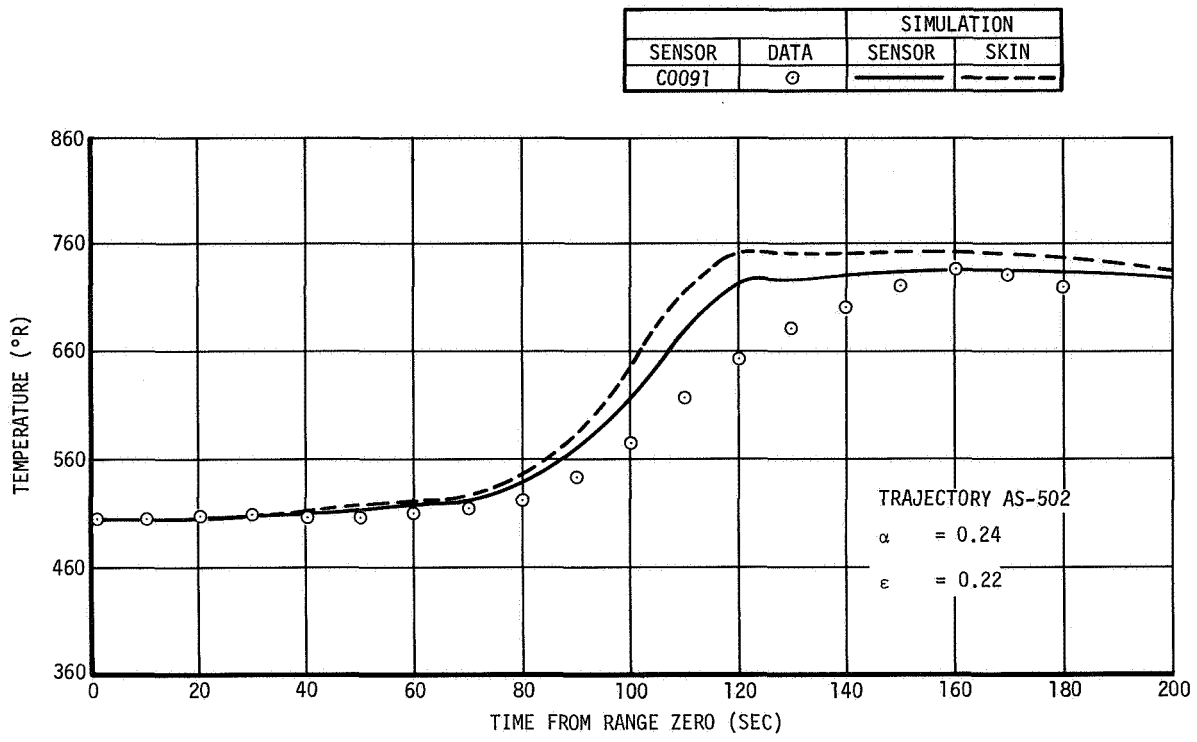

Figure 26-17. LH2 Feedline Fairing Temperature History

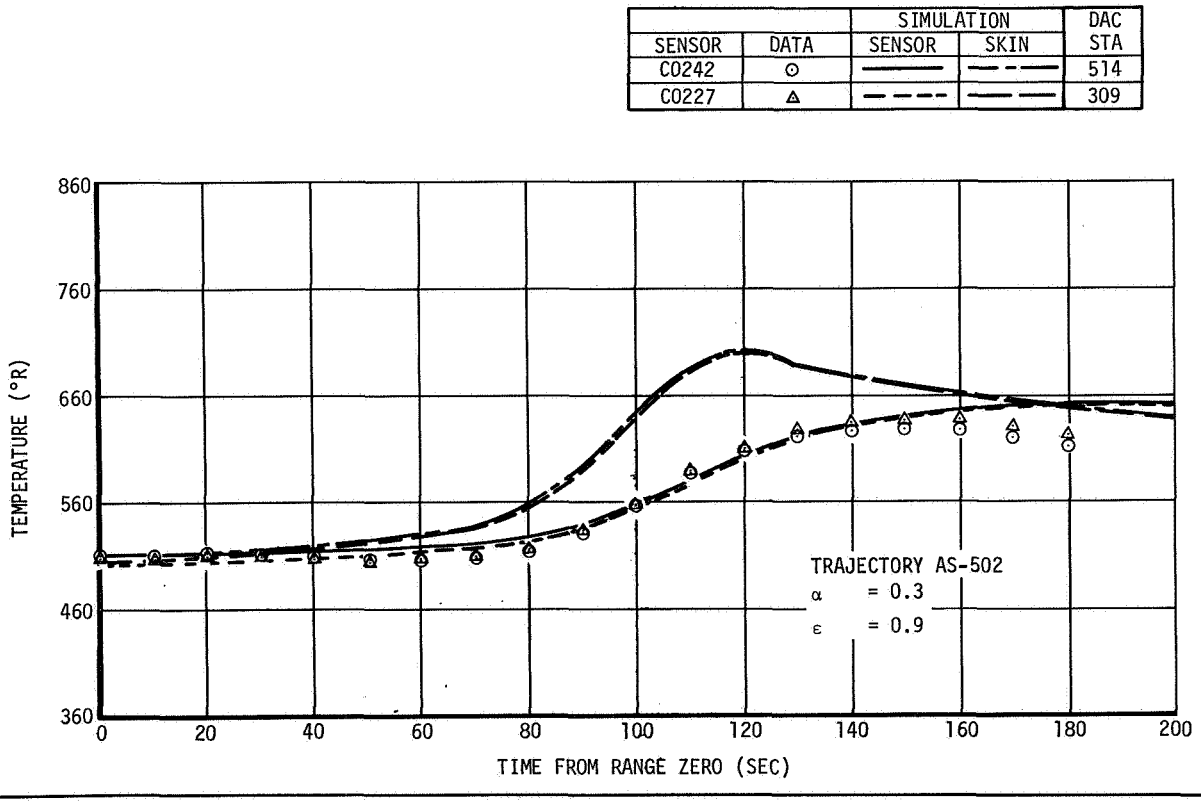

Figure 26-18. Main Tunnel Temperature Histories

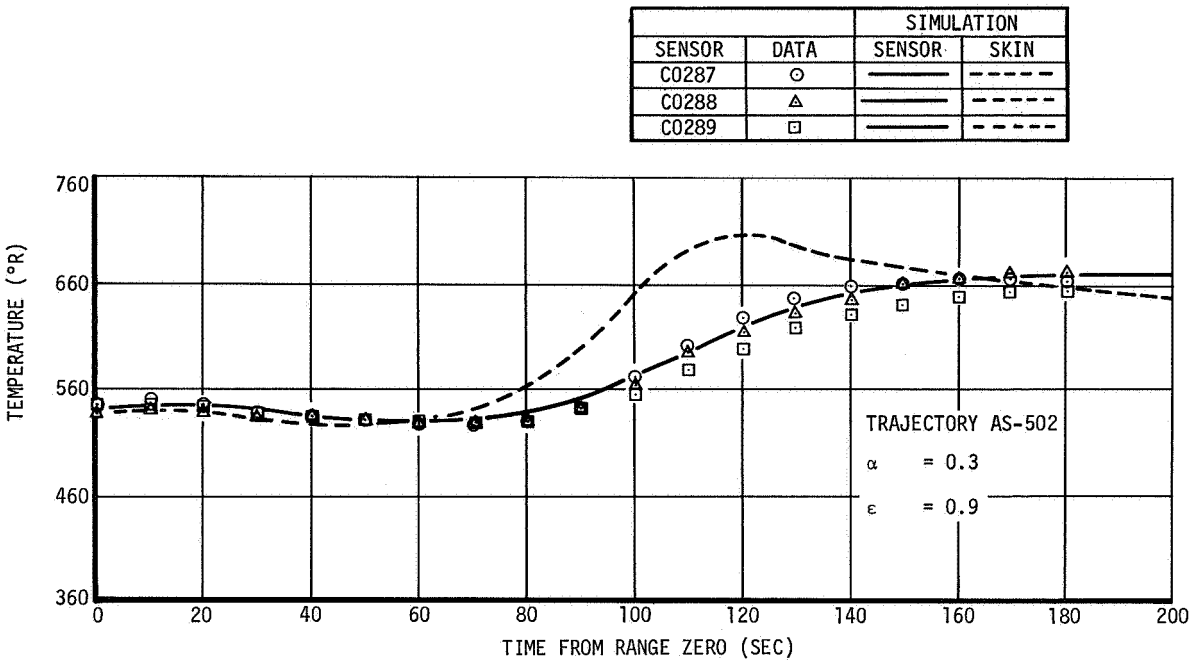

Figure 26-19. APS Centerbody Temperature Histories

HEAT FLUX-BTU/SEC-FT^2	SENSOR		501	502	
ENGINE NOZZLE	C2000	6.2* (10)**	0.4 (2.3)**	0.55	45° FROM POSITION III TOWARD
					POSITION IV
HEAT FLUX	C2004	3.6*	0.35(1.1)**	1.10	POSITION III

* AS-202 FLIGHT DATA

** NUMBERS IN PARENTHESIS REPRESENT ANALYTICALLY PREDICTED MAXIMUMS

SENSOR	DATA	SIMULATION
C2000	△	———
C2004	⊙	— — —

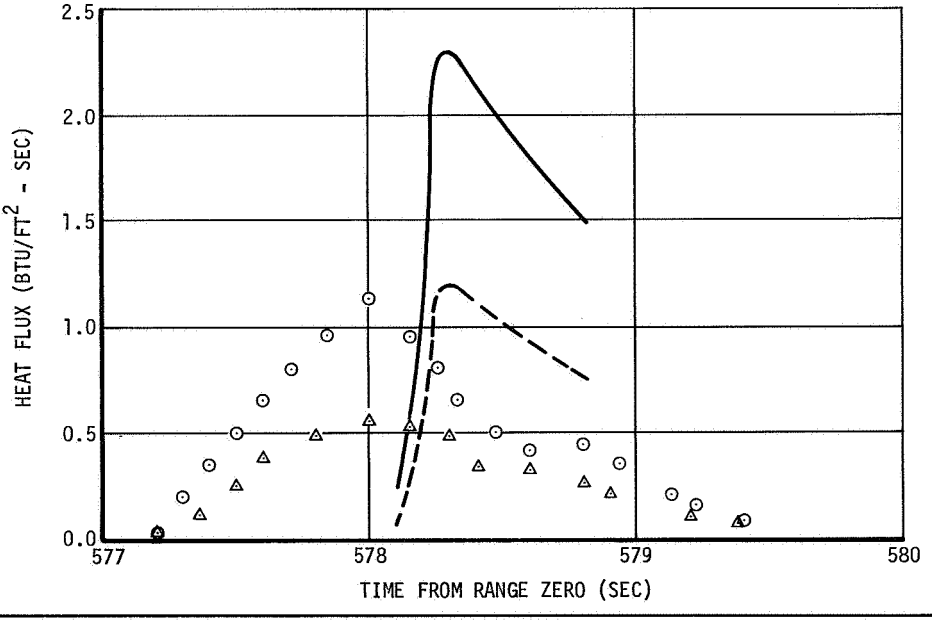

Figure 26-20. J-2 Engine Heat Flux Due to Retrorocket Impingement

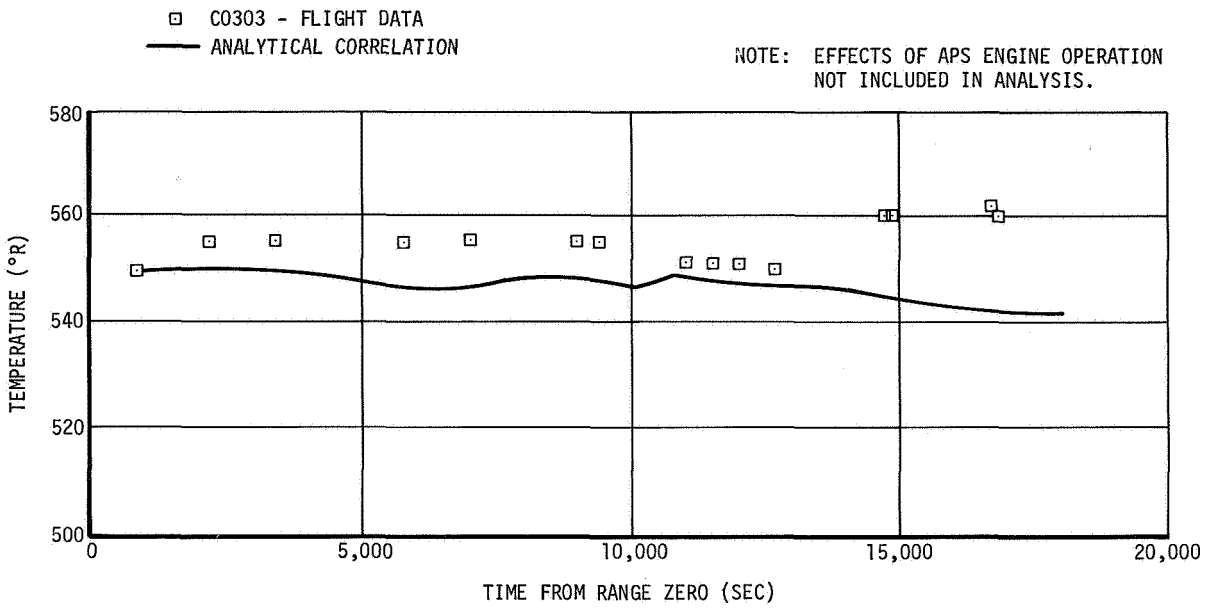

Figure 26-21. APS Oxidizer Control Module Temperature Correlation

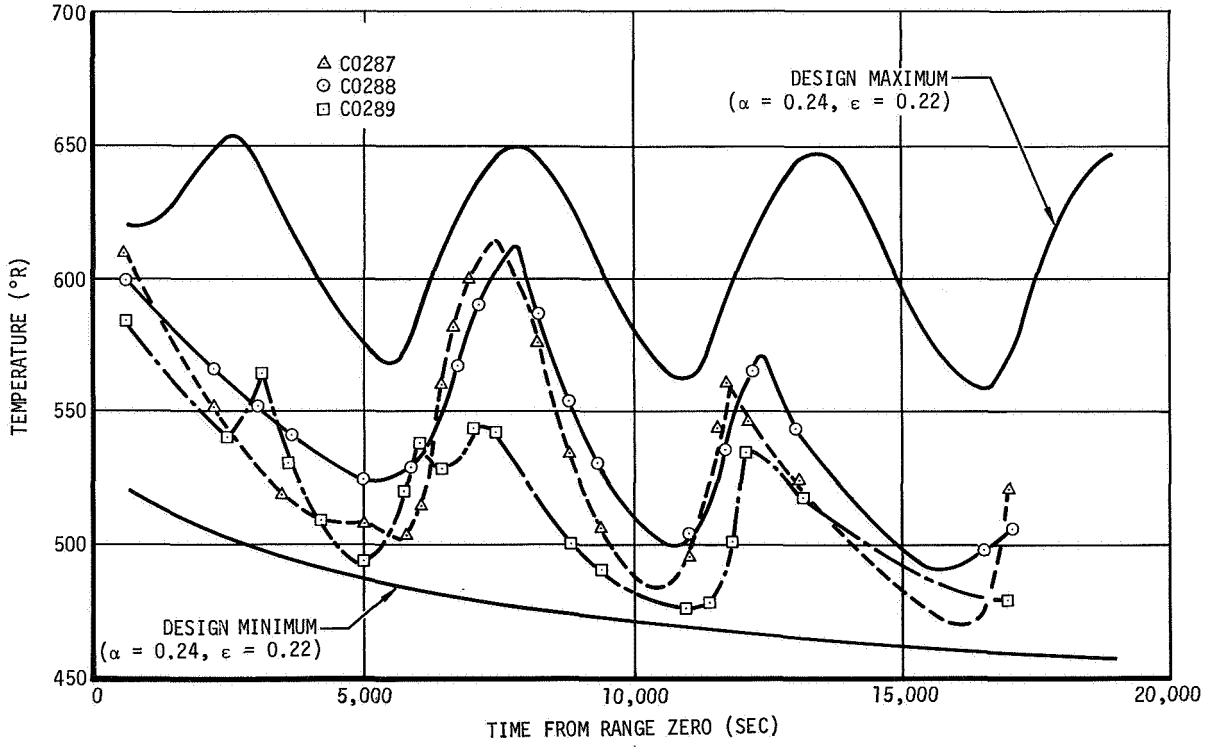

Figure 26-22. APS Fairing Temperature Comparison

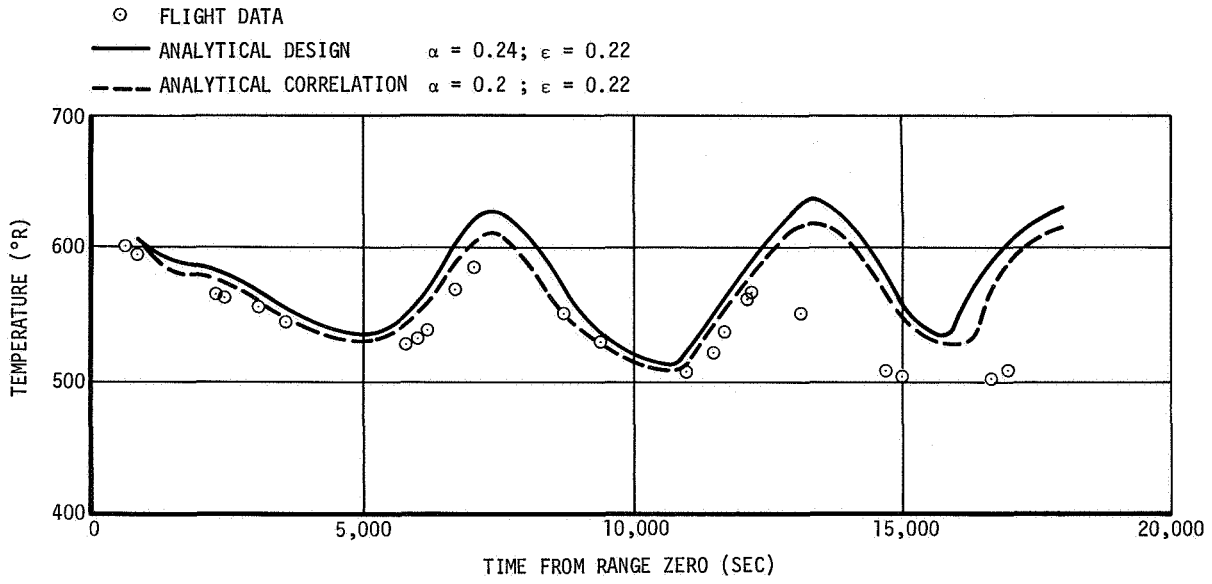

Figure 26-23. APS Fairing Temperature Correlation

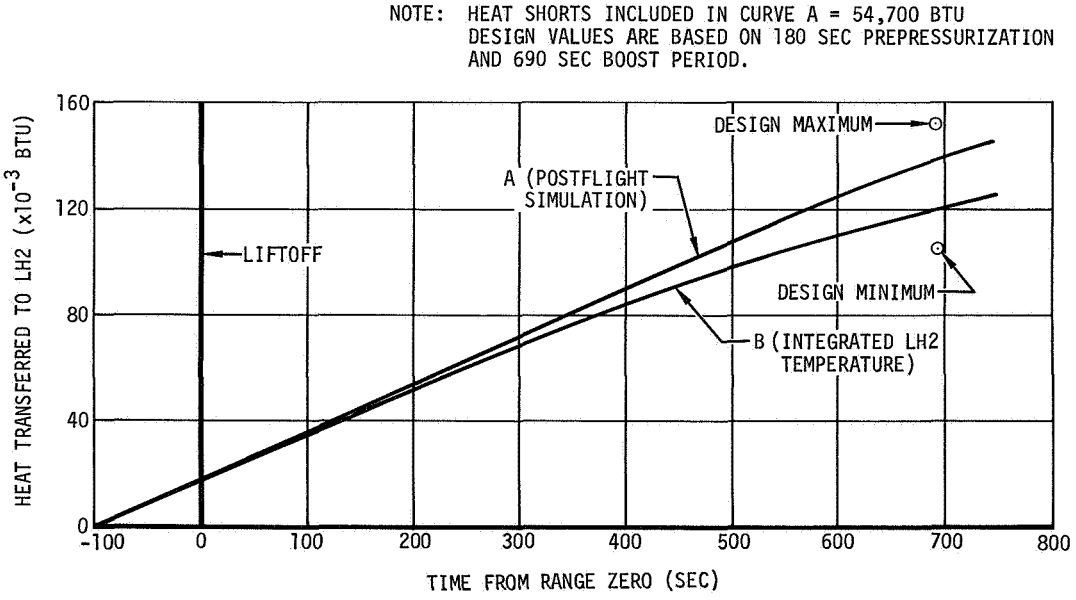

Figure 26-24. LH2 Heating - Boost

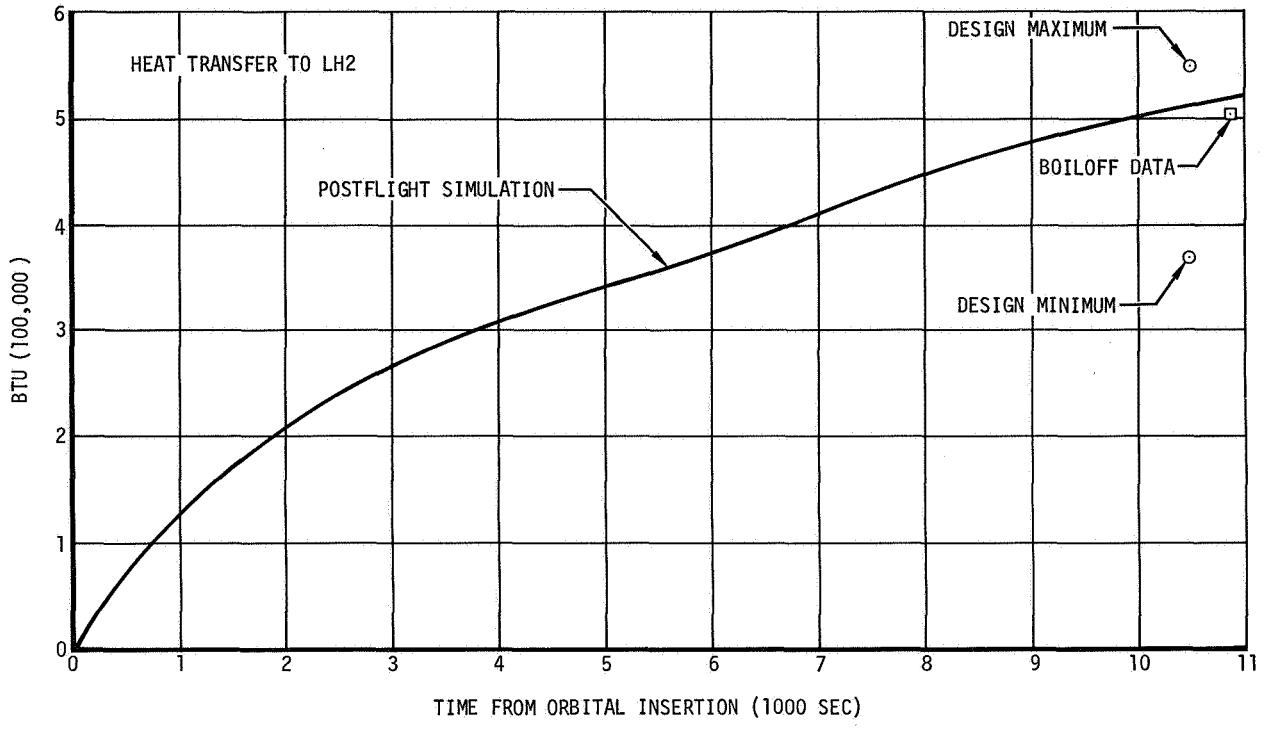

Figure 26-25. LH2 Heating - Orbit

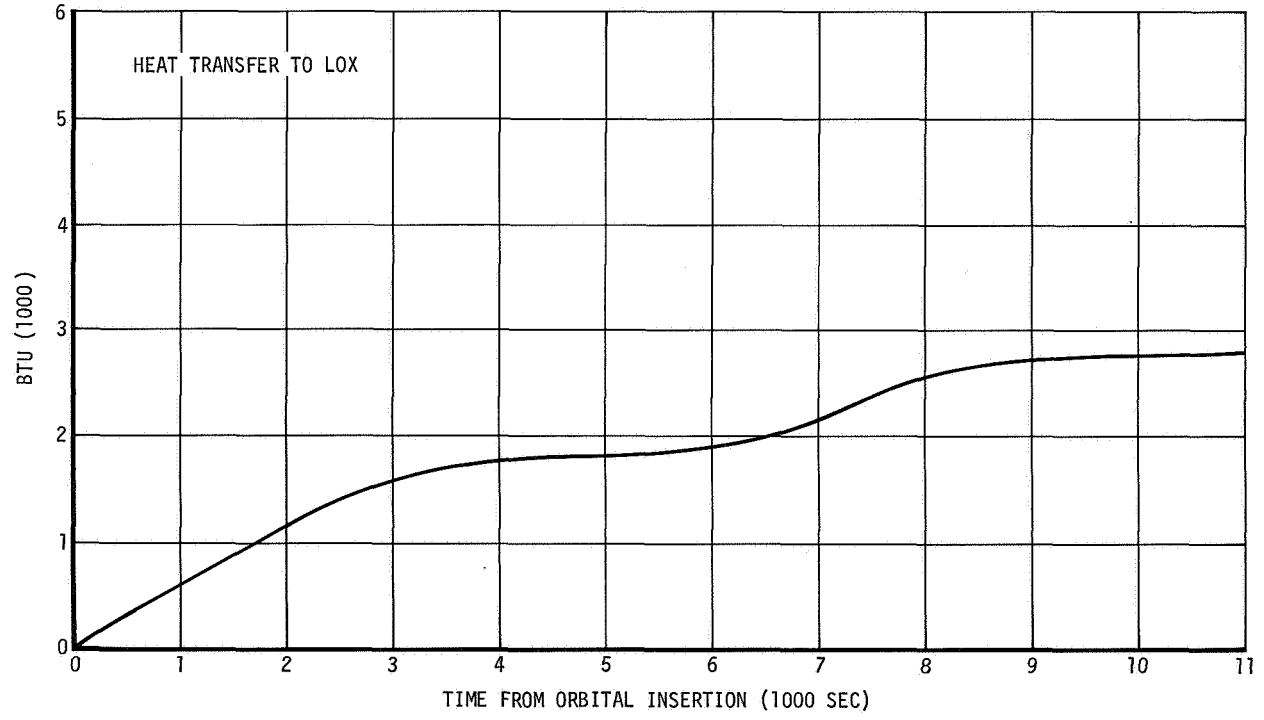

Figure 26-26. LOX Heating - Orbit

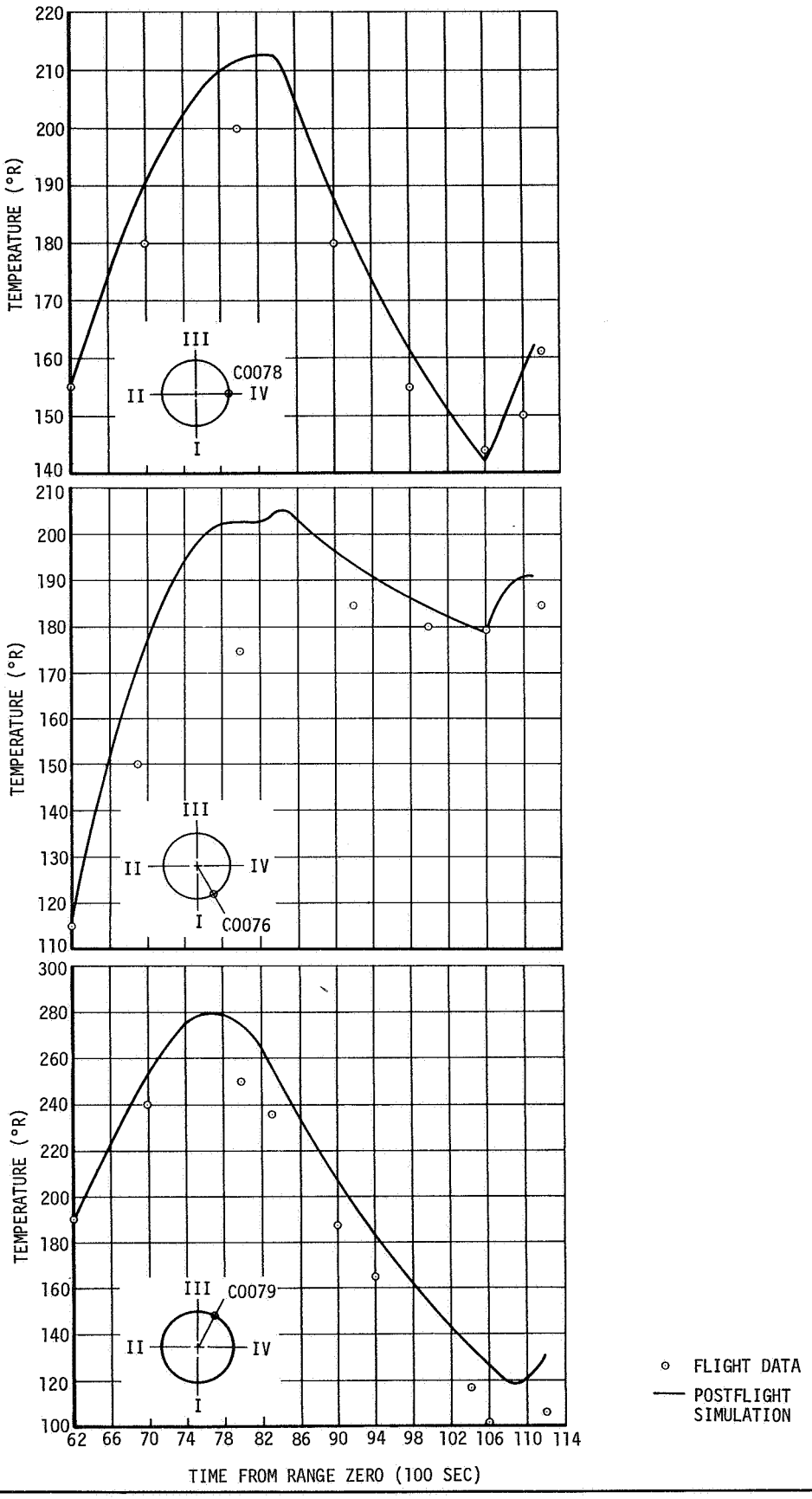

Figure 26-27. LOX and LH2 Chilldown Inverters Temperatures

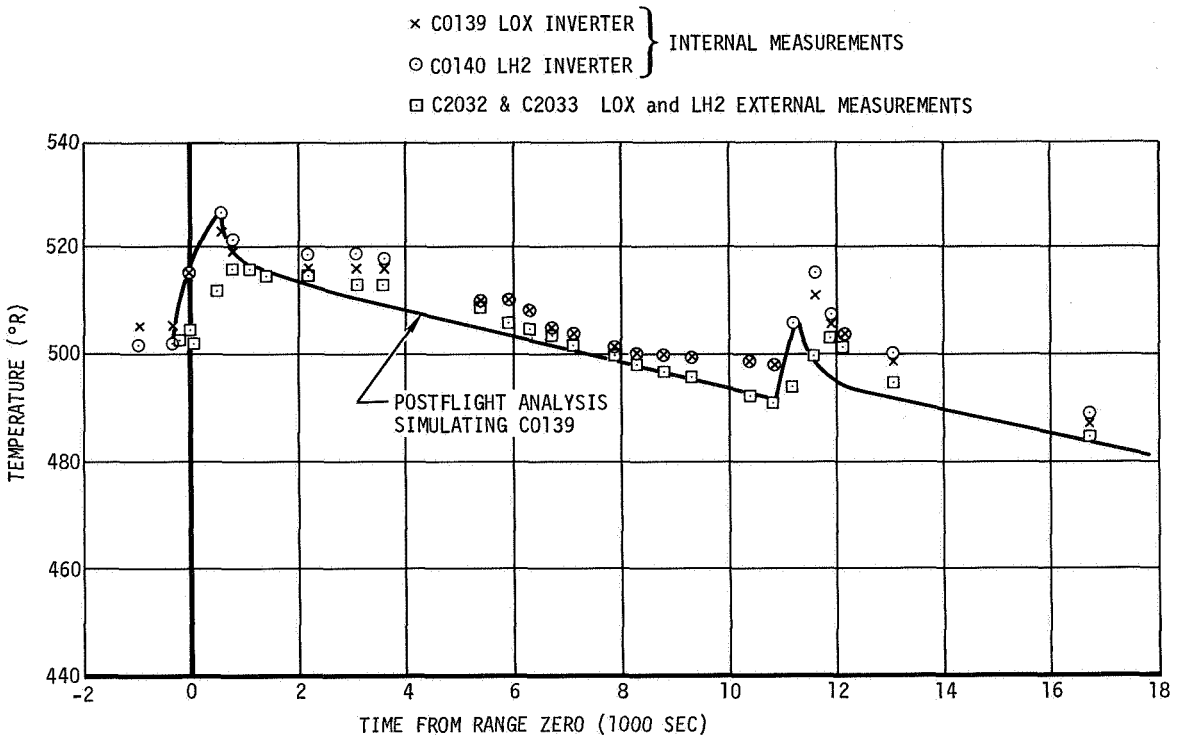

Figure 26-28. LOX and LH2 Chilldown Inverters Temperatures

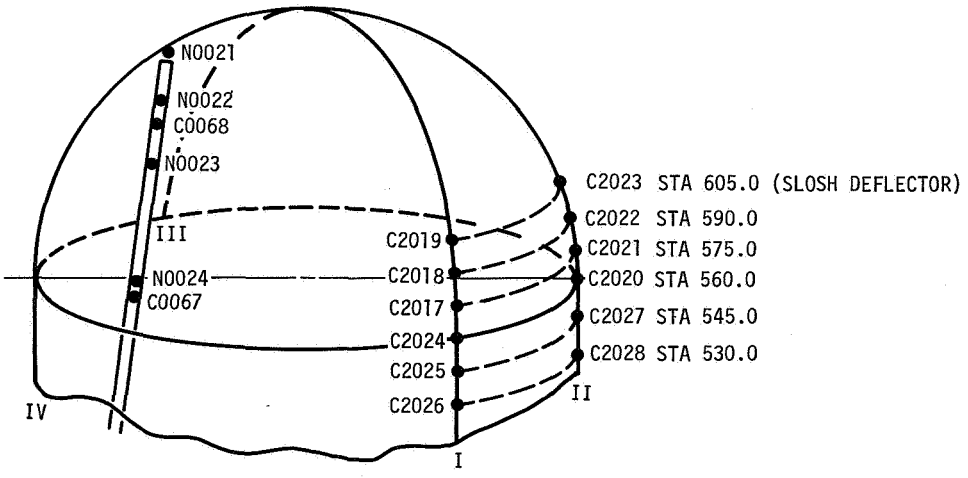

Figure 26-29. Ullage Space Instrumentation

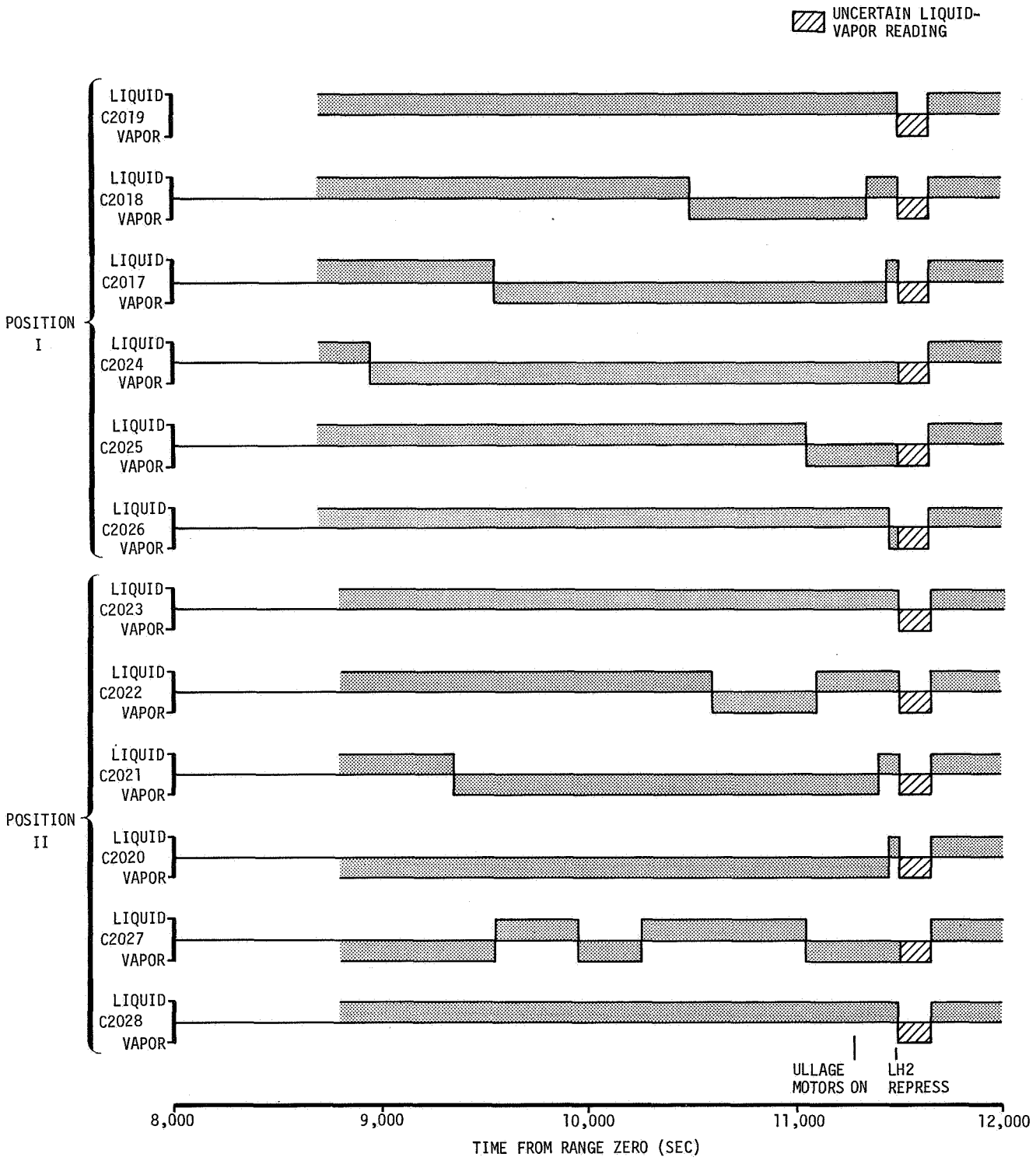

Figure 26-30. Wall Temperature Sensors Liquid-Vapor Indications - Second Orbit through Restart Attempt

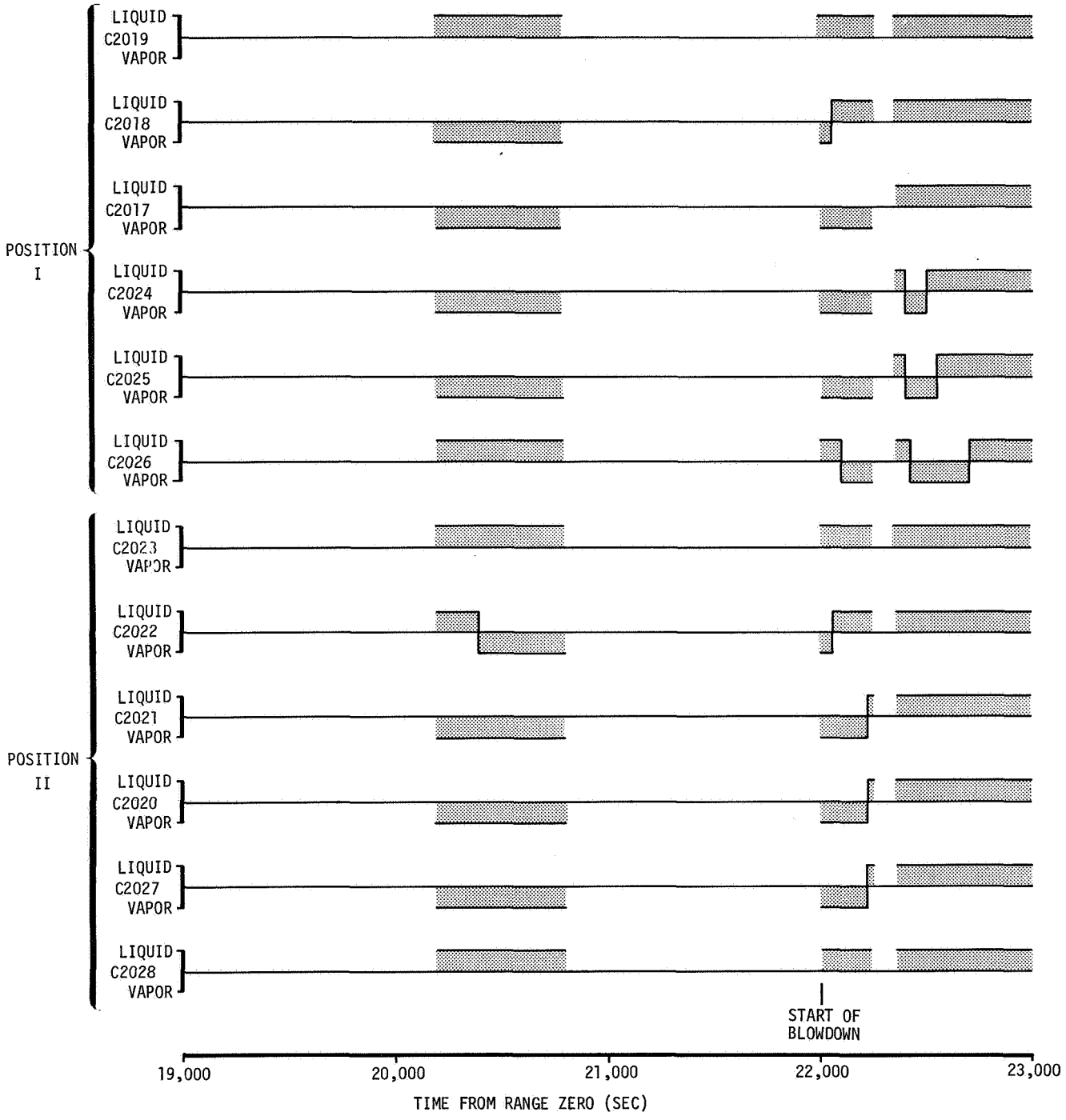

Figure 26-31. Wall Temperature Sensors Liquid-Vapor Indications - Fourth Orbit through Blowdown

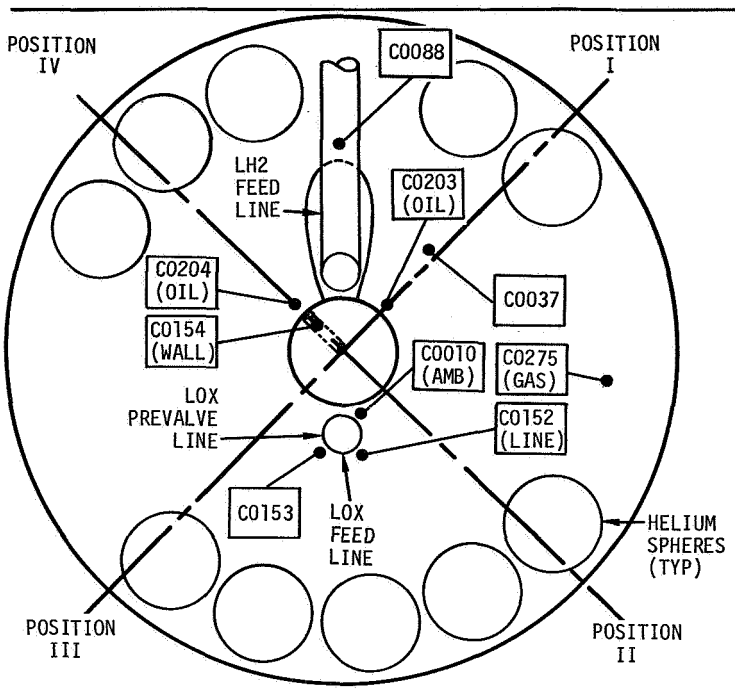

THRUST STRUCTURE
(VIEW LOOKING FWD

VIEW B-B

DETAILS OMITTED FOR CLARITY

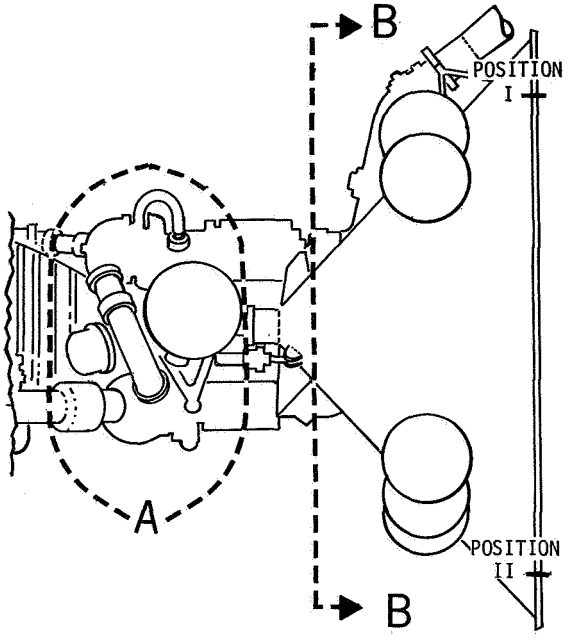

TEMPERATURE CHANGE RATES ($\Delta T/\Delta\theta$ DEG F/SEC)

MEASUREMENT	TIME FROM RANGE ZERO (SEC)							
	675 TO 695		695 TO 705		705 TO 715		11,614	
	502	501	502	501	502	501	502	501
C0204 (Oil)	-0.05	0	-0.10	0	-0.40	0	-0.14	0
C0154 (Wall)	0	+0.03	+0.22	+0.03	-0.10	+0.03	+0.017	0
C0153	0	+0.05	+0.78	+0.05	+0.41	+0.05	0	-0.05
C0088	-0.20	-0.10	+0.50	0	-0.25	0	0	0
C0087	-0.35	+0.05	+2.5	+0.05	-1.8	+0.05	-0.78	0
C0203 (Oil)	-0.05	0	-0.05	0	-0.10	0	0	+0.05
C0010 (Amb)	-0.80	0	+30.7	0	OSL	0	OSL	0
C0152 (Line)	-0.65	-0.075	OSH	-0.005	OSH	-0.005	OSH	0
C0275 (Gas)	-2.36	-0.08	+25.6	-0.08	-5.0	-0.08	+0.02	0
C2014	+5.5	0	+4.0	0	+3.0	0	0	0
C2013	+1.75	+2.5	+1.0	+3.5	+1.0	+2.0	+1.4	+0.1
C2037	-0.46	0	+16.7	0	-0.21	0	-1.0	--
C2005	-6.4	+0.2	-7.1	0	-5.0	0	-5.0	-0.1
C0050 (Oil)	+0.05	+0.13	0	-0.3	+2.9	+0.3	-15.0	+0.07
C2016	+1.0	-1.5	+1.0	-1.0	+1.0	-1.0	+0.15	+33.3
C2015	-0.40	-1.2	-0.20	-1.0	-0.50	-1.0	0	+4.76

NOTE: OSH - off-scale-high
OSL - off-scale-low

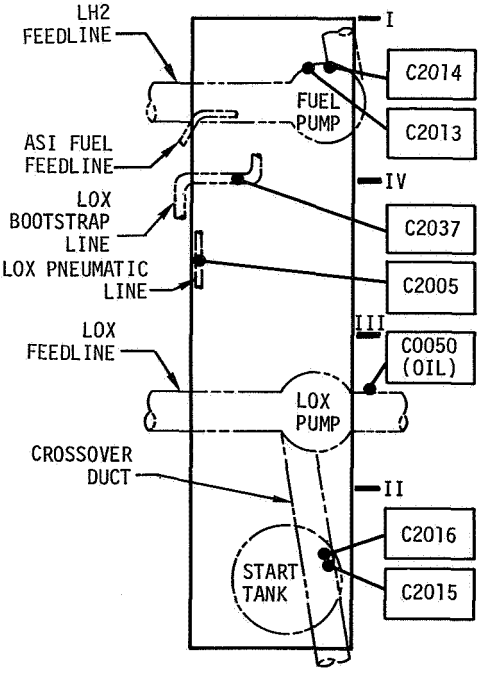

DETAIL A

ENGINE CYLINDRICAL SECTION FLAT PATTERN DIAGRAM

Figure 26-32. Thrust Structure and Engine Instrumentation Temperature Change Rates

APPENDIX 1

MASS CHARACTERISTICS DATA (WS11)

1. MASS CHARACTERISTICS DATA (WS11)

This appendix presents the mass breakdown summary and the mass characteristics summary as calculated by the WS11 computer program for the AS-502 third flight stage (S-IVB stage, IU, spacecraft, lunar module, and the launch escape system).

Table AP 1-1 defines the terms and abbreviations used in the printouts.

The mass breakdown (table AP 1-2) is an itemized listing of major components (including all propellants, gases, etc) giving mass, center of gravity and moments of inertia including a summation for the indicated time. In addition to the above, a jettisoned item summary is presented at the appropriate time. The mass characteristics summary (table AP 1-3) is a time listing of the S-IVB-502 third flight stage mass characteristics.

All mass characteristics parameters are time referenced to AS-502 vehicle range zero and progress chronologically from range zero to LV/SC separation.

Figure AP 1-1 is a diagram of the coordinate system used in the WS11 computing program and S-IVB Douglas station numbers.

TABLE AP 1-1 (Sheet 1 of 2)
DEFINITIONS FOR MASS CHARACTERISTICS
COMPUTER PROGRAM WS11

Term	Definitions	Units
Time	Time is referenced to range time. All computing was done in the pounds, inches, and pound inches squared system of units. (Items below the TOTAL REMAINING line were converted to other unit systems.) Pound mass is defined as 1/32.174 slugs.	Seconds
DAC Station	Distance along the H axis from an arbitrary S-IVB-502 stage reference zero. The ZERO station is located so that the S-IVB-502 stage engine gimbal point is station 100.0. Positive values increase in the forward direction and negative values are aft of station zero.	Inches
H Arm	Distance along the centerline of the S-IVB-502 stage from the center of gravity of the item under consideration to S-IVB-502 stage DAC station zero.	Inches
L Arm	Distance from the center of gravity of the item under consideration to the centerline of the S-IVB-502 stage along an axis perpendicular to the centerline and coinciding with position II and IV. Position II is negative and position IV is positive.	Inches
V Arm	Distance from the center of gravity of item under consideration to the centerline of the stage along an axis perpendicular to the H and L axes and coinciding with positions I and III. Position I is negative and position II is positive.	Inches
Pound Inches Square	Moment of inertia about the center of gravity of each item or total of items.	Lbm-In.^{2}

TABLE AP 1-1 (Sheet 2 of 2)
DEFINITIONS FOR MASS CHARACTERISTICS
COMPUTER PROGRAM WS11

Term	Definitions	Units
Roll MOI	Moment of inertia of any item of total, about an axis through its own center of gravity and parallel to the H axis.	Lbm-In.^{2}
Pitch MOI	Moment of inertia of any item of total about an axis through its own center of gravity and parallel to the V axis.	Lb-In.^{2}
Yaw MOI	Moment of inertia of any item or total, about an axis through its own center of gravity and parallel to the L axis.	Lb-In.^{2}
Items Remaining	A listing of all items being considered at the current computing time that will be considered at the next computing time.	None
Total Remaining	A summation of the above.	None
Items Jettisoned	A listing of all items being considered at the current computing time that will not be considered at the next computing time.	None
Total Jettisoned	A summation of the items being jettisoned at the current computing time.	None
KGM	Kilograms	
SLG	Slugs	
VS	Vehicle station (when center of gravity is expressed in coordinates other than S-IVB-502 stage).	Inches
GS	Center of gravity expressed in terms of distance from engine gimbal point of the stage being considered.	Inches
SS	Center of gravity expressed in terms of stage coordinates when individual items are in another coordinate system.	Inches
SLF	Slug feet squared.	
KM^2	Kilogram meters squared.	

TABLE AP 1-2 (Sheet 1 of 9)
MASS BREAKDOWN SUMMARY

S-IC LIFTOFF — TIME 0.690 SEC — ITEMS REMAINING

ITEM	MASS (LBM)	X ARM (STA-IN)	Y ARM (STA-IN)	Z ARM (STA-IN)	IXX (LB-IN2)	IYY (LB-IN2)	IZZ (LB-IN2)
LAUNCH ESCAPE	8886.00	1510.50	-.3	-1.3	.34206159+07	.13915493+09	.13904376+09
FROST	100.00	420.40	.0	.0	.16926009+07	.14472090+07	.14472090+07
SEPARATION PKG	51.00	200.69	.0	.0	.85792657+06	.60659825+06	.60659825+06
ULLAGE ROCKETS	253.20	223.50	.0	.0	.49627200+07	.51341386+06	.44526262+07
COMMAND MODULE	12543.00	1249.90	.3	6.7	.30485636+08	.27825516+08	.22443064+08
SERVICE MODULE	9836.00	1122.20	.1	.5	.29862195+08	.50565793+08	.49165147+08
SM PROPELLANT	32785.00	1111.50	11.3	-4.8	.74282940+08	.87970022+08	.11181521+09
ADAPTER RING	91.00	1047.70	.6	-1.8	.52285323+06	.26831259+06	.25949196+06
ADAPTER (SLA)	3795.00	850.60	1.2	-1.8	.44519034+08	.58881507+08	.58186549+08
LUNAR MODULE	26001.00	799.10	.1	.0	.80089580+08	.92050040+08	.96749721+08
VEH INSTR UNIT	4874.00	699.00	-.7	-10.8	.71596330+08	.39831107+08	.33173662+08
S4B502 DRY STG	26252.80	325.46	6.2	-2.8	.29793359+09	.11660329+10	.11662542+10
LOX IN TANK	193773.00	241.92	.0	.0	.00000000	.00000000	.00000000
LOX ULLAGE GAS	28.00	318.61	.0	.0	.00000000	.00000000	.00000000
LOX BELOW TANK	367.00	114.94	3.2	6.5	.19821582+06	.46607650+06	.46669026+06
LH2 IN TANK	42400.00	454.28	.0	.0	.00000000	.21238044+09	.21238044+09
LH2 ULLAGE GAS	78.00	644.37	.0	.0	.00000000	.00000000	.00000000
LH2 BELOW TANK	48.00	148.00	-39.2	-42.5	.58934476+05	.23972394+06	.23305451+06
COLD HELIUM	332.00	494.30	100.5	-27.8	.82139044+06	.10579520+07	.36220565+06
APS PROP FP 1	314.00	246.20	1.8	-140.3	.13847400+06	.11335400+06	.11335400+06
APS PROP FP 3	315.00	246.20	-1.8	140.3	.13891500+06	.11371500+06	.11371500+06
GH2 IN STRTANK	5.00	88.40	-22.0	14.6	.00000000	.00000000	.00000000
HELIUM-REPRESS	78.00	153.50	.0	.0	.19500000+06	.95550001+05	.95550001+05
SERVICE ITEMS	73.00	442.63	5.8	3.8	.70984703+06	.54597656+07	.54290643+07
TOTAL REMAINING	363279.00	493.70	1.6	-.6	.66495918+09	.51025550+11	.51036281+11
					(SLUG-FT2) .14352483+06	(SLUG-FT2) .11013358+08	(SLUG-FT2) .11015674+08

S-II/S-IVB SEPARATION — TIME 577.079 SEC — ITEMS JETTISONED

ITEM	MASS (LBM)	X ARM (STA-IN)	Y ARM (STA-IN)	Z ARM (STA-IN)	IXX (LB-IN2)	IYY (LB-IN2)	IZZ (LB-IN2)
FROST	.00	420.40	.0	.0	.00000000	.00000000	.00000000
SEPARATION PKG	51.00	200.69	.0	.0	.85792657+06	.60659825+06	.60659825+06
TOTAL JETTISONED	51.00	200.69	.0	.0	.85792657+06	.60659835+06	.60659835+06
					(SLUG-FT2) .18517493+03	(SLUG-FT2) .13092823+03	(SLUG-FT2) .13092823+03

S-II/S-IVB SEPARATION — TIME 577.079 SEC — ITEMS REMAINING

ITEM	MASS (LBM)	X ARM (STA-IN)	Y ARM (STA-IN)	Z ARM (STA-IN)	IXX (LB-IN2)	IYY (LB-IN2)	IZZ (LB-IN2)
ULLAGE ROCKETS	249.94	223.50	.0	.0	.48987310+07	.50679393+06	.43952142+07
COMMAND MODULE	12543.00	1249.90	.3	6.7	.30485636+08	.27825516+08	.22443064+08
SERVICE MODULE	9836.00	1122.20	.1	.5	.29862195+08	.50565793+08	.49165147+08
SM PROPELLANT	32785.00	1111.50	11.3	-4.8	.74282940+08	.87970022+08	.11181521+09
ADAPTER RING	91.00	1047.70	.6	-1.8	.52285323+06	.26831259+06	.25949196+06
ADAPTER (SLA)	3795.00	850.60	1.2	-1.8	.44519034+08	.58881507+08	.58186549+08
LUNAR MODULE	26001.00	799.10	.1	.0	.80089580+08	.92050040+08	.96749721+08
VEH INSTR UNIT	4874.00	699.00	-.7	-10.8	.71596330+08	.39831107+08	.33173662+08
S4B502 DRY STG	26252.80	325.46	6.2	-2.8	.29793359+09	.11660329+10	.11662542+10
LOX IN TANK	193768.03	241.92	.0	.0	.00000000	.00000000	.00000000
LOX ULLAGE GAS	33.00	318.60	.0	.0	.00000000	.00000000	.00000000
LOX BELOW TANK	367.00	114.94	3.2	6.5	.19821582+06	.46607650+06	.46669026+06
LH2 IN TANK	42400.00	455.84	.0	.0	.00000000	.21945602+09	.21945602+09
LH2 ULLAGE GAS	78.00	646.81	.0	.0	.00000000	.00000000	.00000000
LH2 BELOW TANK	48.00	148.00	-39.2	-42.5	.58934476+05	.23972394+06	.23305451+06
COLD HELIUM	332.00	494.30	100.5	-27.8	.82139044+06	.10579520+07	.36220565+06
APS PROP FP 1	314.00	246.20	1.8	-140.3	.13847400+06	.11335400+06	.11335400+06
APS PROP FP 3	315.00	246.20	-1.8	140.3	.13891500+06	.11371500+06	.11371500+06
GH2 IN STRTANK	5.00	88.40	-22.0	14.6	.00000000	.00000000	.00000000
HELIUM-REPRESS	78.00	153.50	.0	.0	.19500000+06	.95550001+05	.95550001+05
SERVICE ITEMS	73.00	442.63	5.8	3.8	.70984703+06	.54597656+07	.54290643+07
TOTAL REMAINING	354238.76	468.45	1.6	-.6	.65888723+09	.41468216+11	.41478981+11
					(SLUG-FT2) .14221427+06	(SLUG-FT2) .89505026+07	(SLUG-FT2) .89528261+07

TABLE AP 1-2 (Sheet 2 of 9)
MASS BREAKDOWN SUMMARY

S-IVB FIRST ENGINE START COMMAND — TIME 577.280 SEC — ITEMS REMAINING

ITEM	MASS (LBM)	X ARM (STA-IN)	Y ARM (STA-IN)	Z ARM (STA-IN)	IXX (LB-IN2)	IYY (LB-IN2)	IZZ (LB-IN2)
ULLAGE ROCKETS	243,86	223,50	,0	,0	,47796312+07	,49447258+06	,42883962+07
COMMAND MODULE	12543,00	1249,90	,3	6,7	,30485636+08	,27825516+08	,22443064+08
SERVICE MODULE	9836,00	1122,20	,1	,5	,29862195+08	,30565793+08	,49165147+08
SM PROPELLANT	32785,00	1111,50	11,3	-4,8	,74282940+08	,87970022+08	,11181521+09
ADAPTER RING	91,00	1047,70	,6	-1,8	,52285323+06	,26831259+06	,25949196+06
ADAPTER (SLA)	3795,00	850,60	1,2	-1,8	,44519034+08	,58881507+08	,58186549+08
LUNAR MODULE	26001,00	799,10	,1	,0	,80089580+08	,92050040+08	,96749721+08
VEH INSTR UNIT	4874,00	699,00	-,7	-10,8	,71596330+08	,39831107+08	,33173662+08
S4B302 DRY STG	26252,80	325,46	6,2	-2,8	,29793359+09	,11660329+10	,11662542+10
LOX IN TANK	193768,03	241,92	,0	,0	,00000000	,00000000	,00000000
LOX ULLAGE GAS	33,00	318,60	,0	,0	,00000000	,00000000	,00000000
LOX BELOW TANK	367,00	114,94	3,2	6,5	,19821582+06	,46407650+06	,46669026+06
LH2 IN TANK	42400,00	455,84	,0	,0	,00000000	,21945845+09	,21945845+09
LH2 ULLAGE GAS	78,00	646,81	,0	,0	,00000000	,00000000	,00000000
LH2 BELOW TANK	48,00	148,00	-39,2	-42,5	,58934476+05	,23972394+06	,23305451+06
COLD HELIUM	332,00	494,30	100,5	-27,8	,82139044+06	,10579520+07	,36220565+06
APS PROP FP 1	314,00	246,20	1,8	-140,3	,13847400+06	,11335400+06	,11335400+06
APS PROP FP 3	315,00	246,20	-1,8	140,3	,13891500+06	,11371500+06	,11371500+06
GH2 IN STRTANK	5,00	88,40	-22,0	14,6	,00000000	,00000000	,00000000
HELIUM-REPRESS	78,00	153,50	,0	,0	,19500000+06	,95550001+05	,95550001+05
SERVICE ITEMS	73,00	442,63	5,8	3,8	,70984703+06	,54597656+07	,54290643+07
TOTAL REMAINING	354232,69	468,45	1,6	-,6	,65876811+09	,41467842+11	,41478513+11
					(SLUG-FT2) ,14218856+06	(SLUG-FT2) ,89504219+07	(SLUG-FT2) ,89527251+07

END FUEL LEAD — TIME 580.280 SEC — ITEMS REMAINING

ITEM	MASS (LBM)	X ARM (STA-IN)	Y ARM (STA-IN)	Z ARM (STA-IN)	IXX (LB-IN2)	IYY (LB-IN2)	IZZ (LB-IN2)
ULLAGE ROCKETS	153,17	223,50	,0	,0	,30020592+07	,31057541+06	,26934922+07
COMMAND MODULE	12543,00	1249,90	,3	6,7	,30485636+08	,27825516+08	,22443064+08
SERVICE MODULE	9836,00	1122,20	,1	,5	,29862195+08	,30565793+08	,49165147+08
SM PROPELLANT	32785,00	1111,50	11,3	-4,8	,74282940+08	,87970022+08	,11181521+09
ADAPTER RING	91,00	1047,70	,6	-1,8	,52285323+06	,26831259+06	,25949196+06
ADAPTER (SLA)	3795,00	850,60	1,2	-1,8	,44519034+08	,58881507+08	,58186549+08
LUNAR MODULE	26001,00	799,10	,1	,0	,80089580+08	,92050040+08	,96749721+08
VEH INSTR UNIT	4874,00	699,00	-,7	-10,8	,71596330+08	,39831107+08	,33173662+08
S4B302 DRY STG	26252,80	325,46	6,2	-2,8	,29793359+09	,11660329+10	,11662542+10
LOX IN TANK	193768,00	241,92	,0	,0	,00000000	,00000000	,00000000
LOX ULLAGE GAS	34,09	318,60	,0	,0	,00000000	,00000000	,00000000
LOX BELOW TANK	367,00	114,94	3,2	6,5	,19821582+06	,46407650+06	,46669026+06
LH2 IN TANK	42392,00	455,82	,0	,0	,00000000	,21931984+09	,21931984+09
LH2 ULLAGE GAS	79,09	646,78	,0	,0	,00000000	,00000000	,00000000
LH2 BELOW TANK	53,45	148,00	-39,2	-42,5	,65621854+05	,26692575+06	,25949953+06
COLD HELIUM	330,98	494,30	100,5	-27,8	,81887195+06	,10547082+07	,36109509+06
APS PROP FP 1	313,95	246,20	1,8	-140,3	,13845069+06	,11333492+06	,11333492+06
APS PROP FP 3	314,95	246,20	-1,8	140,3	,13889169+06	,11369592+06	,11369592+06
GH2 IN STRTANK	2,82	88,40	-22,0	14,6	,00000000	,00000000	,00000000
HELIUM-REPRESS	78,00	153,50	,0	,0	,19500000+06	,95550001+05	,95550001+05
SERVICE ITEMS	73,00	442,63	5,8	3,8	,70984703+06	,54597656+07	,54290643+07
TOTAL REMAINING	354138,28	468,51	1,6	-,6	,65699850+09	,41462398+11	,41471649+11
					(SLUG-FT2) ,14180660+06	(SLUG-FT2) ,89492467+07	(SLUG-FT2) ,89512435+07

TABLE AP 1-2 (Sheet 3 of 9)
MASS BREAKDOWN SUMMARY

FIRST 90 PERCENT THRUST — TIME 582.788 SEC — ITEMS REMAINING

ITEM	MASS (LBM)	X ARM (STA-IN)	Y ARM (STA-IN)	Z ARM (STA-IN)	IXX (LB-IN2)	IYY (LB-IN2)	IZZ (LB-IN2)
ULLAGE ROCKETS	135.30	223.50	.0	.0	.26518800+07	.27434793+06	.23793062+07
COMMAND MODULE	12543.00	1249.90	.3	6.7	.30485636+08	.27825516+08	.22443064+08
SERVICE MODULE	9836.00	1122.20	.1	.5	.29862195+08	.50565793+08	.49165147+08
SM PROPELLANT	32785.00	1111.50	11.3	-4.8	.74282940+08	.87970022+08	.11181521+09
ADAPTER RING	91.00	1047.70	.6	-1.8	.52285323+06	.26831259+06	.25949196+06
ADAPTER (SLA)	3795.00	850.60	1.2	-1.8	.44519034+08	.58881507+08	.58186549+08
LUNAR MODULE	26001.00	799.10	.1	.0	.80089580+08	.92050040+08	.96749721+08
VEH INSTR UNIT	4874.00	699.00	-.7	-10.8	.71596330+08	.39831107+08	.33173662+08
S48502 DRY STG	26252.80	325.46	6.2	-2.8	.29793359+09	.11660329+10	.11662542+10
LOX IN TANK	193470.00	241.81	.0	.0	.00000000	.00000000	.00000000
LOX ULLAGE GAS	35.00	318.34	.0	.0	.00000000	.00000000	.00000000
LOX BELOW TANK	397.00	114.94	3.2	6.5	.21441875+06	.50201190+06	.50483932+06
LH2 IN TANK	42278.00	455.37	.0	.0	.00000000	.21667198+09	.21667198+09
LH2 ULLAGE GAS	80.00	646.07	.0	.0	.00000000	.00000000	.00000000
LH2 BELOW TANK	58.00	148.00	-39.2	-42.5	.71212492+05	.28966642+06	.28160753+06
COLD HELIUM	330.13	494.30	100.5	-27.8	.81676650+06	.10519964+07	.36016665+06
APS PROP FP 1	313.90	246.20	1.8	-140.3	.13843121+06	.11331897+06	.11331897+06
APS PROP FP 3	314.90	246.20	-1.8	140.3	.13887221+06	.11367997+06	.11367997+06
GH2 IN STRTANK	1.00	88.40	-22.0	14.6	.00000000	.00000000	.00000000
HELIUM-REPRESS	78.00	153.50	.0	.0	.19500000+06	.95550001+05	.95550001+05
SERVICE ITEMS	73.00	442.63	5.8	3.8	.70984703+06	.54597656+07	.54290643+07
TOTAL REMAINING	353742.03	468.57	1.6	-.6	.65667175+09	.41457207+11	.41466172+11
					(SLUG-FT2) .14173608+06	(SLUG-FT2) .89481264+07	(SLUG-FT2) .89500614+07

SUMMARY PRINTOUT — TIME 600.000 SEC — ITEMS REMAINING

ITEM	MASS (LBM)	X ARM (STA-IN)	Y ARM (STA-IN)	Z ARM (STA-IN)	IXX (LB-IN2)	IYY (LB-IN2)	IZZ (LB-IN2)
COMMAND MODULE	12543.00	1249.90	.3	6.7	.30485636+08	.27825516+08	.22443064+08
SERVICE MODULE	9836.00	1122.20	.1	.5	.29862195+08	.50565793+08	.49165147+08
SM PROPELLANT	32785.00	1111.50	11.3	-4.8	.74282940+08	.87970022+08	.11181521+09
ADAPTER RING	91.00	1047.70	.6	-1.8	.52285323+06	.26831259+06	.25949196+06
ADAPTER (SLA)	3795.00	850.60	1.2	-1.8	.44519034+08	.58881507+08	.58186549+08
LUNAR MODULE	26001.00	799.10	.1	.0	.80089580+08	.92050040+08	.96749721+08
VEH INSTR UNIT	4874.00	699.00	-.7	-10.8	.71596330+08	.39831107+08	.33173662+08
S48502 DRY STG	26252.80	325.46	6.2	-2.8	.29793359+09	.11660329+10	.11662542+10
LOX IN TANK	185641.68	239.08	.0	.0	.00000000	.00000000	.00000000
LOX ULLAGE GAS	50.93	312.00	.0	.0	.00000000	.00000000	.00000000
LOX BELOW TANK	397.00	114.94	3.2	6.5	.21441875+06	.50201190+06	.50483932+06
LH2 IN TANK	40827.42	449.63	.0	.0	.00000000	.18506171+09	.18506171+09
LH2 ULLAGE GAS	88.38	637.31	.0	.0	.00000000	.00000000	.00000000
LH2 BELOW TANK	58.00	148.00	-39.2	-42.5	.71212492+05	.28966642+06	.28160753+06
COLD HELIUM	324.29	494.30	100.5	-27.8	.80231707+06	.10333855+07	.35379494+06
APS PROP FP 1	313.60	246.20	1.8	-140.3	.13829748+06	.11320950+06	.11320950+06
APS PROP FP 3	314.60	246.20	-1.8	140.3	.13873848+06	.11357050+06	.11357050+06
GH2 IN STRTANK	3.07	88.40	-22.0	14.6	.00000000	.00000000	.00000000
HELIUM-REPRESS	78.00	153.50	.0	.0	.19500000+06	.95550001+05	.95550001+05
SERVICE ITEMS	73.00	442.63	5.8	3.8	.70984703+06	.54597656+07	.54290643+07
TOTAL REMAINING	344347.76	471.72	1.7	-.6	.65390463+09	.41250469+11	.41257280+11
					(SLUG-FT2) .14113882+06	(SLUG-FT2) .89035041+07	(SLUG-FT2) .89049741+07

TABLE AP 1-2 (Sheet 4 of 9)
MASS BREAKDOWN SUMMARY

SUMMARY PRINTOUT — TIME 650.000 SEC — ITEMS REMAINING

ITEM	MASS (LBM)	X ARM (STA-IN)	Y ARM (STA-IN)	Z ARM (STA-IN)	IXX (LB-IN2)	IYY (LB-IN2)	IZZ (LB-IN2)
COMMAND MODULE	12543.00	1249.90	.3	6.7	.30485636+08	.27825516+08	.22443064+08
SERVICE MODULE	9836.00	1122.20	.1	.5	.29862195+08	.50565793+08	.49165147+08
SM PROPELLANT	32785.00	1111.50	11.3	-4.8	.74282940+08	.87970022+08	.11181521+09
ADAPTER RING	91.00	1047.70	.6	-1.8	.52285323+06	.26831259+06	.25949196+06
ADAPTER (SLA)	3795.00	850.60	1.2	-1.8	.44519034+08	.58881507+08	.58186549+08
LUNAR MODULE	26001.00	799.10	.1	.0	.80089580+08	.92050040+08	.96749721+08
VEH INSTR UNIT	4874.00	699.00	-.7	-10.8	.71596330+08	.39831107+08	.33173662+08
S48502 DRY STG	26252.80	325.46	6.2	-2.8	.29793359+09	.11660329+10	.11662542+10
LOX IN TANK	162900.83	231.78	.0	.0	.00000000	.00000000	.00000000
LOX ULLAGE GAS	97.20	299.29	.0	.0	.00000000	.00000000	.00000000
LOX BELOW TANK	397.00	114.94	3.2	6.5	.21441875+06	.50201190+06	.50483932+06
LH2 IN TANK	36613.57	433.40	.0	.0	.00000000	.11223433+09	.11229433+09
LH2 ULLAGE GAS	112.74	615.22	.0	.0	.00000000	.00000000	.00000000
LH2 BELOW TANK	58.00	148.00	-39.2	-42.5	.71212492+05	.28966642+06	.28160753+06
COLD HELIUM	307.32	494.30	100.5	-27.8	.76036222+06	.97932184+06	.33528544+06
APS PROP FP 1	312.72	246.20	1.8	-140.3	.13790899+06	.11289148+06	.11289148+06
APS PROP FP 3	313.72	246.20	-1.8	140.3	.13836999+06	.11325248+06	.11325248+06
GH2 IN STRTANK	7.00	88.40	-22.0	14.6	.00000000	.00000000	.00000000
HELIUM-REPRESS	78.00	153.50	.0	.0	.19500000+06	.95550001+05	.95550001+05
SERVICE ITEMS	73.00	442.63	5.8	3.8	.70984703+06	.54597656+07	.54290643+07
TOTAL REMAINING	317448.89	483.03	1.8	-.7	.65356077+09	.40504506+11	.40511165+11
					(SLUG-FT2) .14106461+06	(SLUG-FT2) .87424953+07	(SLUG-FT2) .87439325+07

SUMMARY PRINTOUT — TIME 700.000 SEC — ITEMS REMAINING

ITEM	MASS (LBM)	X ARM (STA-IN)	Y ARM (STA-IN)	Z ARM (STA-IN)	IXX (LB-IN2)	IYY (LB-IN2)	IZZ (LB-IN2)
COMMAND MODULE	12543.00	1249.90	.3	6.7	.30485636+08	.27825516+08	.22443064+08
SERVICE MODULE	9836.00	1122.20	.1	.5	.29862195+08	.50565793+08	.49165147+08
SM PROPELLANT	32785.00	1111.50	11.3	-4.8	.74282940+08	.87970022+08	.11181521+09
ADAPTER RING	91.00	1047.70	.6	-1.8	.52285323+06	.26831259+06	.25949196+06
ADAPTER (SLA)	3795.00	850.60	1.2	-1.8	.44519034+08	.58881507+08	.58186549+08
LUNAR MODULE	26001.00	799.10	.1	.0	.80089580+08	.92050040+08	.96749721+08
VEH INSTR UNIT	4874.00	699.00	-.7	-10.8	.71596330+08	.39831107+08	.33173662+08
S48502 DRY STG	26252.80	325.46	6.2	-2.8	.29793359+09	.11660329+10	.11662542+10
LOX IN TANK	140159.96	224.99	.0	.0	.00000000	.00000000	.00000000
LOX ULLAGE GAS	143.47	289.75	.0	.0	.00000000	.00000000	.00000000
LOX BELOW TANK	397.00	114.94	3.2	6.5	.21441875+06	.50201190+06	.50483932+06
LH2 IN TANK	32399.72	417.12	.0	.0	.00000000	.13788752+09	.13788752+09
LH2 ULLAGE GAS	137.09	596.58	.0	.0	.00000000	.00000000	.00000000
LH2 BELOW TANK	58.00	148.00	-39.2	-42.5	.71212492+05	.28966642+06	.28160753+06
COLD HELIUM	290.36	494.30	100.5	-27.8	.71836738+06	.92525818+06	.31677594+06
APS PROP FP 1	311.84	246.20	1.8	-140.3	.13752050+06	.11257347+06	.11257347+06
APS PROP FP 3	312.84	246.20	-1.8	140.3	.13796150+06	.11293447+06	.11293447+06
GH2 IN STRTANK	7.00	88.40	-22.0	14.6	.00000000	.00000000	.00000000
HELIUM-REPRESS	78.00	153.50	.0	.0	.19500000+06	.95550001+05	.95550001+05
SERVICE ITEMS	73.00	442.63	5.8	3.8	.70984703+06	.54597656+07	.54290643+07
TOTAL REMAINING	290546.07	498.29	2.0	-.7	.65319806+09	.39563227+11	.39569722+11
					(SLUG-FT2) .14098632+06	(SLUG-FT2) .85393296+07	(SLUG-FT2) .85407315+07

TABLE AP 1-2 (Sheet 5 of 9)
MASS BREAKDOWN SUMMARY

S-IVB FIRST ENGINE CUTOFF COMMAND — TIME 747.032 SEC — ITEMS REMAINING

ITEM	MASS (LBM)	X ARM (STA-IN)	Y ARM (STA-IN)	Z ARM (STA-IN)	IXX (LB-IN2)	IYY (LB-IN2)	IZZ (LB-IN2)
COMMAND MODULE	12543.00	1249.90	.3	6.7	.30485636+08	.27825516+08	.22443064+08
SERVICE MODULE	9836.00	1122.20	.1	.5	.29862195+08	.30565793+08	.49165147+08
SM PROPELLANT	32785.00	1111.50	11.3	-4.8	.74282940+08	.87970022+08	.11181521+09
ADAPTER RING	91.00	1047.70	.6	-1.8	.52285323+06	.26831259+06	.25949196+06
ADAPTER (SLA)	3795.00	850.60	1.2	-1.8	.44519034+08	.58881507+08	.58186549+08
LUNAR MODULE	26001.00	799.10	.1	.0	.80089580+08	.92050040+08	.96749721+08
VEH INSTR UNIT	4874.00	699.00	-.7	-10.8	.71596330+08	.39831107+08	.33173662+08
S4B502 DRY STG	26252.80	325.46	6.2	-2.8	.29793359+09	.11660329+10	.11662542+10
LOX IN TANK	118769.00	218.67	.0	.0	.00000000	.00000000	.00000000
LOX ULLAGE GAS	187.00	282.07	.0	.0	.00000000	.00000000	.00000000
LOX BELOW TANK	397.00	114.94	3.2	6.5	.21441875+06	.50201190+06	.50483932+06
LH2 IN TANK	28436.00	401.94	.0	.0	.00000000	.11776071+09	.11776071+09
LH2 ULLAGE GAS	160.00	580.74	.0	.0	.00000000	.00000000	.00000000
LH2 BELOW TANK	58.00	148.00	-39.2	-42.5	.71212492+05	.28966642+06	.28160753+06
COLD HELIUM	274.40	494.30	100.5	-27.8	.67888416+06	.87440374+06	.29936516+06
APS PROP FP 1	311.01	246.20	1.8	-140.3	.13715507+06	.11227633+06	.11227633+06
APS PROP FP 3	312.01	246.20	-1.8	140.3	.13759607+06	.11263533+06	.11263533+06
GH2 IN STRTANK	7.00	88.40	-22.0	14.6	.00000000	.00000000	.00000000
HELIUM-REPRESS	78.00	153.50	.0	.0	.19500000+06	.95550001+05	.95550001+05
SERVICE ITEMS	73.00	442.63	5.8	3.8	.70984703+06	.54597656+07	.54290643+07
TOTAL REMAINING	265240.21	517.05	2.1	-.8	.65283817+09	.38320220+11	.38326547+11
					(SLUG-FT2) .14090864+06	(SLUG-FT2) .82710390+07	(SLUG-FT2) .82724045+07

S-IVB FIRST END OF THRUST DECAY — TIME 748.432 SEC — ITEMS REMAINING

ITEM	MASS (LBM)	X ARM (STA-IN)	Y ARM (STA-IN)	Z ARM (STA-IN)	IXX (LB-IN2)	IYY (LB-IN2)	IZZ (LB-IN2)
COMMAND MODULE	12543.00	1249.90	.3	6.7	.30485636+08	.27825516+08	.22443064+08
SERVICE MODULE	9836.00	1122.20	.1	.5	.29862195+08	.30565793+08	.49165147+08
SM PROPELLANT	32785.00	1111.50	11.3	-4.8	.74282940+08	.87970022+08	.11181521+09
ADAPTER RING	91.00	1047.70	.6	-1.8	.52285323+06	.26831259+06	.25949196+06
ADAPTER (SLA)	3795.00	850.60	1.2	-1.8	.44519034+08	.58881507+08	.58186549+08
LUNAR MODULE	26001.00	799.10	.1	.0	.80089580+08	.92050040+08	.96749721+08
VEH INSTR UNIT	4874.00	699.00	-.7	-10.8	.71596330+08	.39831107+08	.33173662+08
S4B502 DRY STG	26252.80	325.46	6.2	-2.8	.29793359+09	.11660329+10	.11662542+10
LOX IN TANK	118609.00	218.62	.0	.0	.00000000	.00000000	.00000000
LOX ULLAGE GAS	187.00	282.02	.0	.0	.00000000	.00000000	.00000000
LOX BELOW TANK	367.00	114.94	3.2	6.5	.19821582+06	.46407650+06	.46669026+06
LH2 IN TANK	28407.00	401.82	.0	.0	.00000000	.11764510+09	.11764510+09
LH2 ULLAGE GAS	160.00	580.63	.0	.0	.00000000	.00000000	.00000000
LH2 BELOW TANK	48.00	148.00	-39.2	-42.5	.58936476+05	.23972394+06	.23305451+06
COLD HELIUM	274.39	494.30	100.5	-27.8	.67884955+06	.87435918+06	.29934990+06
APS PROP FP 1	310.51	246.20	1.8	-140.3	.13693504+06	.11209422+06	.11209422+06
APS PROP FP 3	311.70	246.20	-1.8	140.3	.13745978+06	.11252377+06	.11252377+06
GH2 IN STRTANK	7.00	88.40	-22.0	14.6	.00000000	.00000000	.00000000
HELIUM-REPRESS	78.00	153.50	.0	.0	.19500000+06	.95550001+05	.95550001+05
SERVICE ITEMS	73.00	442.63	5.8	3.8	.70984703+06	.54597656+07	.54290643+07
TOTAL REMAINING	265010.39	517.27	2.1	-.8	.65275616+09	.38303221+11	.38309564+11
					(SLUG-FT2) .14089093+06	(SLUG-FT2) .82673700+07	(SLUG-FT2) .82687389+07

TABLE AP 1-2 (Sheet 6 of 9)
MASS BREAKDOWN SUMMARY

SUMMARY PRINTOUT TIME 3,600.000 SEC ITEMS REMAINING

ITEM	MASS (LBM)	X ARM (STA-IN)	Y ARM (STA-IN)	Z ARM (STA-IN)	IXX (LB-IN2)	IYY (LB-IN2)	IZZ (LB-IN2)
COMMAND MODULE	12543.00	1249.90	.3	6.7	.30485636+08	.27825516+08	.22443064+08
SERVICE MODULE	9836.00	1122.20	.1	.5	.29862195+08	.30565793+08	.49165147+08
SM PROPELLANT	32785.00	1111.50	11.3	-4.8	.74282940+08	.87970022+08	.11181521+09
ADAPTER RING	91.00	1047.70	.6	-1.8	.52285323+06	.26831259+06	.25949196+06
ADAPTER (SLA)	3795.00	850.60	1.2	-1.8	.44519034+08	.58881507+08	.58186549+08
LUNAR MODULE	26001.00	799.10	.1	.0	.80089580+08	.92050040+08	.96749721+08
VEH INSTR UNIT	4874.00	699.00	-.7	-10.8	.71596330+08	.39831107+08	.33173662+08
S4B502 DRY STG	26252.80	325.46	6.2	-2.8	.29793359+09	.11660329+10	.11662542+10
LOX IN TANK	118546.51	218.69	.0	.0	.00000000	.00000000	.00000000
LOX ULLAGE GAS	249.49	282.10	.0	.0	.00000000	.00000000	.00000000
LOX BELOW TANK	367.00	114.94	3.2	6.5	.19821582+06	.46407650+06	.46669026+06
LH2 IN TANK	27588.90	398.82	.0	.0	.00000000	.11450271+09	.11450271+09
LH2 ULLAGE GAS	226.28	577.63	.0	.0	.00000000	.00000000	.00000000
LH2 BELOW TANK	48.00	148.00	-39.2	-42.5	.58934476+05	.23972394+06	.23305451+06
COLD HELIUM	247.19	494.30	100.5	-27.8	.61156201+06	.78769273+06	.26967835+06
APS PROP FP 1	220.07	246.20	1.8	-140.3	.97049342+05	.79444019+05	.79444019+05
APS PROP FP 3	258.45	246.20	-1.8	140.3	.11397458+06	.93298919+05	.93298919+05
GH2 IN STRTANK	7.00	88.40	-22.0	14.6	.00000000	.00000000	.00000000
HELIUM-REPRESS	78.00	153.50	.0	.0	.19500000+06	.95550001+05	.95550001+05
SERVICE ITEMS	73.00	442.63	5.8	3.8	.70984703+06	.54597656+07	.54290643+07
TOTAL REMAINING	264087.68	517.52	2.1	-.8	.64951724+09	.38287751+11	.38296723+11
					(SLUG-FT2) .14019185+06	(SLUG-FT2) .82640307+07	(SLUG-FT2) .82659675+07

SUMMARY PRINTOUT TIME 7,200.000 SEC ITEMS REMAINING

ITEM	MASS (LBM)	X ARM (STA-IN)	Y ARM (STA-IN)	Z ARM (STA-IN)	IXX (LB-IN2)	IYY (LB-IN2)	IZZ (LB-IN2)
COMMAND MODULE	12543.00	1249.90	.3	6.7	.30485636+08	.27825516+08	.22443064+08
SERVICE MODULE	9836.00	1122.20	.1	.5	.29862195+08	.30565793+08	.49165147+08
SM PROPELLANT	32785.00	1111.50	11.3	-4.8	.74282940+08	.87970022+08	.11181521+09
ADAPTER RING	91.00	1047.70	.6	-1.8	.52285323+06	.26831259+06	.25949196+06
ADAPTER (SLA)	3795.00	850.60	1.2	-1.8	.44519034+08	.58881507+08	.58186549+08
LUNAR MODULE	26001.00	799.10	.1	.0	.80089580+08	.92050040+08	.96749721+08
VEH INSTR UNIT	4874.00	699.00	-.7	-10.8	.71596330+08	.39831107+08	.33173662+08
S4B502 DRY STG	26252.80	325.46	6.2	-2.8	.29793359+09	.11660329+10	.11662542+10
LOX IN TANK	118467.61	218.79	.0	.0	.00000000	.00000000	.00000000
LOX ULLAGE GAS	328.39	282.21	.0	.0	.00000000	.00000000	.00000000
LOX BELOW TANK	367.00	114.94	3.2	6.5	.19821582+06	.46407650+06	.46669026+06
LH2 IN TANK	26556.08	395.02	.0	.0	.00000000	.11084309+09	.11084309+09
LH2 ULLAGE GAS	309.96	573.85	.0	.0	.00000000	.00000000	.00000000
LH2 BELOW TANK	48.00	148.00	-39.2	-42.5	.58934476+05	.23972394+06	.23305451+06
COLD HELIUM	226.55	494.30	100.5	-27.8	.56050967+06	.72193725+06	.24716599+06
APS PROP FP 1	205.52	246.20	1.8	-140.3	.90633896+05	.74192373+05	.74192373+05
APS PROP FP 3	249.81	246.20	-1.8	140.3	.11016541+06	.90180753+05	.90180753+05
GH2 IN STRTANK	7.00	88.40	-22.0	14.6	.00000000	.00000000	.00000000
HELIUM-REPRESS	78.00	153.50	.0	.0	.19500000+06	.95550001+05	.95550001+05
SERVICE ITEMS	73.00	442.63	5.8	3.8	.70984703+06	.54597656+07	.54290643+07
TOTAL REMAINING	263094.71	517.71	2.1	-.8	.64878108+09	.38282438+11	.38291722+11
					(SLUG-FT2) .14003295+06	(SLUG-FT2) .82628839+07	(SLUG-FT2) .82648879+07

TABLE AP 1-2 (Sheet 7 of 9)
MASS BREAKDOWN SUMMARY

S-IVB SECOND ENGINE START COMMAND — TIME 10,800.000 SEC — ITEMS REMAINING

ITEM	MASS (LBM)	X ARM (STA-IN)	Y ARM (STA-IN)	Z ARM (STA-IN)	IXX (LB-IN2)	IYY (LB-IN2)	IZZ (LB-IN2)
COMMAND MODULE	12543.00	1249.90	.3	6.7	.30485636+08	.27825516+08	.22443064+08
SERVICE MODULE	9836.00	1122.20	.1	.5	.29862195+08	.50565793+08	.49165147+08
SM PROPELLANT	32785.00	1111.50	11.3	-4.8	.74282940+08	.87970022+08	.11181521+09
ADAPTER RING	91.00	1047.70	.6	-1.8	.52285323+06	.26831259+06	.25949196+06
ADAPTER (SLA)	3795.00	850.60	1.2	-1.8	.44519034+08	.58881507+08	.58186549+08
LUNAR MODULE	26001.00	799.10	.1	.0	.80089580+08	.92050040+08	.96749721+08
VEH INSTR UNIT	4874.00	699.00	-.7	-10.8	.71596330+08	.39831107+08	.33173662+08
S4B502 DRY STG	26252.80	325.46	6.2	-2.8	.29793359+09	.11660329+10	.11662542+10
LOX IN TANK	118388.71	218.88	.0	.0	.00000000	.00000000	.00000000
LOX ULLAGE GAS	407.29	282.31	.0	.0	.00000000	.00000000	.00000000
LOX BELOW TANK	367.00	114.94	3.2	6.5	.19821582+06	.46407650+06	.46669026+06
LH2 IN TANK	25523.25	391.19	.0	.0	.00000000	.10746063+09	.10746063+09
LH2 ULLAGE GAS	393.64	570.08	.0	.0	.00000000	.00000000	.00000000
LH2 BELOW TANK	48.00	148.00	-39.2	-42.5	.58934476+05	.23972394+06	.23305451+06
COLD HELIUM	205.72	494.30	100.5	-27.8	.50895436+06	.65553392+06	.22443182+06
APS PROP FP 1	190.97	246.20	1.8	-140.3	.84218450+05	.68940727+05	.68940727+05
APS PROP FP 3	241.17	246.20	-1.8	140.3	.10635624+06	.87062588+05	.87062588+05
GH2 IN STRTANK	7.00	88.40	-22.0	14.6	.00000000	.00000000	.00000000
HELIUM-REPRESS	78.00	153.50	.0	.0	.19500000+06	.95550001+05	.95550001+05
SERVICE ITEMS	73.00	442.63	5.8	3.8	.70984703+06	.54597656+07	.54290643+07
TOTAL REMAINING	262101.55	517.92	2.1	-.8	.64804231+09	.38276245+11	.38285839+11
					(SLUG-FT2) .13987350+06	(SLUG-FT2) .82615475+07	(SLUG-FT2) .82636181+07

SUMMARY PRINTOUT — TIME 11,614.667 SEC — ITEMS REMAINING

ITEM	MASS (LBM)	X ARM (STA-IN)	Y ARM (STA-IN)	Z ARM (STA-IN)	IXX (LB-IN2)	IYY (LB-IN2)	IZZ (LB-IN2)
COMMAND MODULE	12543.00	1249.90	.3	6.7	.30485636+08	.27825516+08	.22443064+08
SERVICE MODULE	9836.00	1122.20	.1	.5	.29862195+08	.50565793+08	.49165147+08
SM PROPELLANT	32785.00	1111.50	11.3	-4.8	.74282940+08	.87970022+08	.11181521+09
ADAPTER RING	91.00	1047.70	.6	-1.8	.52285323+06	.26831259+06	.25949196+06
ADAPTER (SLA)	3795.00	850.60	1.2	-1.8	.44519034+08	.58881507+08	.58186549+08
LUNAR MODULE	26001.00	799.10	.1	.0	.80089580+08	.92050040+08	.96749721+08
VEH INSTR UNIT	4874.00	699.00	-.7	-10.8	.71596330+08	.39831107+08	.33173662+08
S4B502 DRY STG	26252.80	325.46	6.2	-2.8	.29793359+09	.11660329+10	.11662542+10
LOX IN TANK	118378.00	218.91	.0	.0	.00000000	.00000000	.00000000
LOX ULLAGE GAS	423.00	282.34	.0	.0	.00000000	.00000000	.00000000
LOX BELOW TANK	367.00	114.94	3.2	6.5	.19821582+06	.46407650+06	.46669026+06
LH2 IN TANK	25383.00	390.69	.0	.0	.00000000	.10701311+09	.10701311+09
LH2 ULLAGE GAS	448.00	569.58	.0	.0	.00000000	.00000000	.00000000
LH2 BELOW TANK	48.00	148.00	-39.2	-42.5	.58934476+05	.23972394+06	.23305451+06
COLD HELIUM	201.00	494.30	100.5	-27.8	.49728759+06	.64050710+06	.21928716+06
APS PROP FP 1	102.17	246.20	1.8	-140.3	.45057476+05	.36883784+05	.36883784+05
APS PROP FP 3	138.56	246.20	-1.8	140.3	.61103367+05	.50018856+05	.50018856+05
GH2 IN STRTANK	7.00	88.40	-22.0	14.6	.00000000	.00000000	.00000000
HELIUM-REPRESS	30.00	153.50	.0	.0	.75000000+05	.36750000+05	.36750000+05
SERVICE ITEMS	73.00	442.63	5.8	3.8	.70984703+06	.54597656+07	.54290643+07
TOTAL REMAINING	261776.53	518.22	2.1	-.8	.64400397+09	.38250674+11	.38264004+11
					(SLUG-FT2) .13900186+06	(SLUG-FT2) .82560281+07	(SLUG-FT2) .82589053+07

TABLE AP 1-2 (Sheet 8 of 9)
MASS BREAKDOWN SUMMARY

END FUEL LEAN — TIME 11,623.239 SEC — ITEMS REMAINING

ITEM	MASS (LBM)	X ARM (STA-IN)	Y ARM (STA-IN)	Z ARM (STA-IN)	IXX (LB-IN2)	IYY (LB-IN2)	IZZ (LB-IN2)
COMMAND MODULE	12543.00	1249.90	.3	6.7	.30485636+08	.27825516+08	.22443064+08
SERVICE MODULE	9836.00	1122.20	.1	.5	.29862195+08	.50565793+08	.49165147+08
SM PROPELLANT	32785.00	1111.50	11.3	-4.8	.74282940+08	.87970022+08	.11181521+09
ADAPTER RING	91.00	1047.70	.6	-1.8	.52285323+06	.26831259+06	.25949196+06
ADAPTER (SLA)	3795.00	850.60	1.2	-1.8	.44519034+08	.58881507+08	.58186549+08
LUNAR MODULE	26001.00	799.10	.1	.0	.80089580+08	.92050040+08	.96749721+08
VEH INSTR UNIT	4874.00	699.00	-.7	-10.8	.71596330+08	.39831107+08	.33173662+08
S4B502 DRY STG	26252.80	325.46	6.2	-2.8	.29793359+09	.11660329+10	.11662542+10
LOX IN TANK	118378.00	218.91	.0	.0	.00000000	.00000000	.00000000
LOX ULLAGE GAS	423.00	282.34	.0	.0	.00000000	.00000000	.00000000
LOX BELOW TANK	367.00	114.94	3.2	6.5	.19821582+06	.46407650+06	.46669026+06
LH2 IN TANK	25098.24	389.57	.0	.0	.00000000	.10614574+09	.10614574+09
LH2 ULLAGE GAS	448.00	568.48	.0	.0	.00000000	.00000000	.00000000
LH2 BELOW TANK	55.74	148.00	-39.2	-42.5	.68440154+05	.27838957+06	.27064441+06
COLD HELIUM	199.63	494.30	100.5	-27.8	.49390046+06	.63614447+06	.21779355+06
APS PROP FP 1	99.89	246.20	1.8	-140.3	.44059032+05	.36061553+05	.36061553+05
APS PROP FP 3	135.90	246.20	-1.8	140.3	.59929859+05	.49058229+05	.49058229+05
GH2 IN STRTANK	2.35	88.40	-22.0	14.6	.00000000	.00000000	.00000000
HELIUM-REPRESS	30.00	153.50	.0	.0	.75000000+05	.36750000+05	.36750000+05
SERVICE ITEMS	73.00	442.63	5.8	3.8	.70984703+06	.54597656+07	.54290643+07
TOTAL REMAINING	261488.55	518.25	2.1	-.8	.64391777+09	.38252087+11	.38265500+11
					(SLUG-FT2) .13898326+06	(SLUG-FT2) .82563331+07	(SLUG-FT2) .82592282+07

S-IVB SECOND ENGINE CUTOFF COMMAND — TIME 11,630.320 SEC — ITEMS REMAINING

ITEM	MASS (LBM)	X ARM (STA-IN)	Y ARM (STA-IN)	Z ARM (STA-IN)	IXX (LB-IN2)	IYY (LB-IN2)	IZZ (LB-IN2)
COMMAND MODULE	12543.00	1249.90	.3	6.7	.30485636+08	.27825516+08	.22443064+08
SERVICE MODULE	9836.00	1122.20	.1	.5	.29862195+08	.50565793+08	.49165147+08
SM PROPELLANT	32785.00	1111.50	11.3	-4.8	.74282940+08	.87970022+08	.11181521+09
ADAPTER RING	91.00	1047.70	.6	-1.8	.52285323+06	.26831259+06	.25949196+06
ADAPTER (SLA)	3795.00	850.60	1.2	-1.8	.44519034+08	.58881507+08	.58186549+08
LUNAR MODULE	26001.00	799.10	.1	.0	.80089580+08	.92050040+08	.96749721+08
VEH INSTR UNIT	4874.00	699.00	-.7	-10.8	.71596330+08	.39831107+08	.33173662+08
S4B502 DRY STG	26252.80	325.46	6.2	-2.8	.29793359+09	.11660329+10	.11662542+10
LOX IN TANK	116685.00	218.39	.0	.0	.00000000	.00000000	.00000000
LOX ULLAGE GAS	423.00	281.76	.0	.0	.00000000	.00000000	.00000000
LOX BELOW TANK	397.00	114.94	3.2	6.5	.21441875+06	.50201190+06	.50483932+06
LH2 IN TANK	24863.00	388.65	.0	.0	.00000000	.10544098+09	.10544098+09
LH2 ULLAGE GAS	448.00	567.57	.0	.0	.00000000	.00000000	.00000000
LH2 BELOW TANK	58.00	148.00	-39.2	-42.5	.71212492+05	.28966642+06	.28160753+06
COLD HELIUM	198.50	494.30	100.5	-27.8	.49110241+06	.63254059+06	.21655971+06
APS PROP FP 1	98.01	246.20	1.8	-140.3	.43223284+05	.35382325+05	.35382325+05
APS PROP FP 3	133.70	246.20	-1.8	140.3	.58960450+05	.48264677+05	.48264677+05
GH2 IN STRTANK	1.00	88.40	-22.0	14.6	.00000000	.00000000	.00000000
HELIUM-REPRESS	30.00	153.50	.0	.0	.75000000+05	.36750000+05	.36750000+05
SERVICE ITEMS	73.00	442.63	5.8	3.8	.70984703+06	.54597656+07	.54290643+07
TOTAL REMAINING	259586.01	519.96	2.2	-.8	.64383817+09	.38141670+11	.38155145+11
					(SLUG-FT2) .13896608+06	(SLUG-FT2) .82325007+07	(SLUG-FT2) .82354093+07

TABLE AP 1-2 (Sheet 9 of 9)
MASS BREAKDOWN SUMMARY

COMMAND SERVICE MODULE SEPARATION — TIME 11,667.820 SEC — ITEMS JETTISONED

ITEM	MASS (LBM)	X ARM (STA-IN)	Y ARM (STA-IN)	Z ARM (STA-IN)	IXX (LB-IN2)	IYY (LB-IN2)	IZZ (LB-IN2)
COMMAND MODULE	12543.00	1249.90	.3	6.7	.30485636+08	.27825516+08	.22449064+08
SERVICE MODULE	9836.00	1122.20	.1	.5	.29862195+08	.50565793+08	.49165147+08
SM PROPELLANT	32785.00	1111.50	11.3	-4.8	.74282940+08	.87970022+08	.11181521+09
ADAPTER RING	91.00	1047.70	.6	-1.8	.52285323+06	.26891259+06	.25949196+06
TOTAL JETTISONED	55255.00	1144.72	6.8	-1.2	.13802856+09	.34865249+09	.36610768+09
					(SLUG-FT2) .29792094+05	(SLUG-FT2) .75253166+05	(SLUG-FT2) .79020707+05

COMMAND SERVICE MODULE SEPARATION — TIME 11,667.820 SEC — ITEMS REMAINING

ITEM	MASS (LBM)	X ARM (STA-IN)	Y ARM (STA-IN)	Z ARM (STA-IN)	IXX (LB-IN2)	IYY (LB-IN2)	IZZ (LB-IN2)
ADAPTER (SLA)	3795.00	836.80	4.6	-3.5	.10909879+09	.89479114+08	.85320414+08
LUNAR MODULE	26001.00	799.10	.1	.0	.80089580+08	.92050040+08	.96749721+08
VEH INSTR UNIT	4874.00	699.00	-.7	-10.8	.71596330+08	.39831107+08	.33173662+08
S4B502 DRY STG	26252.80	325.46	6.2	-2.8	.29793359+09	.11660329+10	.11662542+10
LOX IN TANK	116685.00	218.39	.0	.0	.00000000	.00000000	.00000000
LOX ULLAGE GAS	345.00	281.76	.0	.0	.00000000	.00000000	.00000000
LOX BELOW TANK	367.00	114.94	3.2	6.5	.19821582+06	.46407650+06	.46669026+06
LH2 IN TANK	24863.00	388.65	.0	.0	.00000000	.10544025+09	.10544025+09
LH2 ULLAGE GAS	448.00	567.57	.0	.0	.00000000	.00000000	.00000000
LH2 BELOW TANK	48.00	148.00	-39.2	-42.5	.58934476+05	.23972394+06	.23305451+06
COLD HELIUM	197.50	494.30	100.5	-27.8	.48864017+06	.62936921+06	.21547394+06
APS PROP FP 1	88.05	246.20	1.8	-140.3	.38829084+05	.31785260+05	.31785260+05
APS PROP FP 3	122.06	246.20	-1.8	140.3	.53826633+05	.44062165+05	.44062165+05
GH2 IN STRTANK	1.00	88.40	-22.0	14.6	.00000000	.00000000	.00000000
HELIUM-REPRESS	30.00	153.50	.0	.0	.75000000+05	.36750000+05	.36750000+05
SERVICE ITEMS	73.00	442.63	5.8	3.8	.70984703+06	.54597656+07	.54290643+07
TOTAL REMAINING	204190.40	350.84	1.0	-.7	.56843321+09	.10369130+11	.10360643+11
					(SLUG-FT2) .12269067+06	(SLUG-FT2) .22380737+07	(SLUG-FT2) .22362420+07

TABLE AP 1-3 (Sheet 1 of 2)
MASS CHARACTERISTICS SUMMARY

TIME (SEC)	MASS (LBM)	X ARM (STA-IN)	Y ARM (STA-IN)	Z ARM (STA-IN)	IXX (SLUG-FT2)	IYY (SLUG-FT2)	IZZ (SLUG-FT2)
0.690	363279.00	493.70	1.6	-.6	.14352483+06	.11013358+08	.11015674+08
184.766	363217.51	493.77	1.6	-.6	.14330012+06	.11013225+08	.11015541+08
184.766	354331.51	468.27	1.6	-.6	.14255396+06	.89508000+07	.89531346+07
300.000	354293.01	468.31	1.6	-.6	.14241329+06	.89508924+07	.89532269+07
576.971	354293.03	468.41	1.6	-.6	.14241329+06	.89514659+07	.89538004+07
577.079	354289.76	468.41	1.6	-.6	.14239947+06	.89514227+07	.89537463+07
577.079	354238.76	468.45	1.6	-.6	.14221427+06	.89505026+07	.89528261+07
577.280	354232.69	468.45	1.6	-.6	.14218856+06	.89504219+07	.89527251+07
580.280	354138.28	468.51	1.6	-.6	.14180660+06	.89492467+07	.89512435+07
580.871	354031.25	468.53	1.6	-.6	.14173220+06	.89488001+07	.89507365+07
582.788	353742.03	468.57	1.6	-.6	.14173608+06	.89481264+07	.89500614+07
589.066	350364.86	469.63	1.6	-.6	.14172707+06	.89332543+07	.89351855+07
589.066	350229.56	469.73	1.6	-.6	.14115460+06	.89314246+07	.89329012+07
590.000	349727.13	469.89	1.6	-.6	.14115326+06	.89291394+07	.89306155+07
600.000	344347.76	471.72	1.7	-.6	.14113882+06	.89035041+07	.89049741+07
610.000	338968.40	473.69	1.7	-.6	.14112429+06	.88757345+07	.88771980+07
620.000	333589.04	475.80	1.7	-.6	.14110963+06	.88458014+07	.88472584+07
630.000	328209.68	478.06	1.7	-.6	.14109486+06	.88136636+07	.88151143+07
632.788	326709.91	478.71	1.8	-.6	.14109073+06	.88043060+07	.88057551+07
640.000	322829.45	480.47	1.8	-.6	.14107984+06	.87792455+07	.87806898+07
650.000	317448.89	483.03	1.8	-.7	.14106461+06	.87424953+07	.87439325+07
660.000	312068.31	485.75	1.8	-.7	.14104925+06	.87033477+07	.87047781+07
670.000	306687.75	488.63	1.9	-.7	.14103375+06	.86617164+07	.86631397+07
680.000	301307.20	491.68	1.9	-.7	.14101810+06	.86175013+07	.86189178+07
690.000	295926.64	494.88	1.9	-.7	.14100229+06	.85878519+07	.85892609+07
700.000	290546.07	498.29	2.0	-.7	.14098632+06	.85393296+07	.85407315+07
710.000	285165.52	501.90	2.0	-.7	.14097016+06	.84880123+07	.84894067+07
720.000	279784.96	505.70	2.0	-.7	.14095382+06	.84337542+07	.84351408+07
730.000	274404.39	509.71	2.1	-.8	.14093728+06	.83763925+07	.83777715+07
740.000	269023.84	513.94	2.1	-.8	.14092054+06	.83157529+07	.83171236+07
747.032	265240.21	517.05	2.1	-.8	.14090864+06	.82710390+07	.82724045+07
747.556	265154.48	517.13	2.1	-.8	.14090324+06	.82696716+07	.82710373+07
748.432	265010.39	517.27	2.1	-.8	.14089093+06	.82673700+07	.82687389+07
835.210	264908.44	517.35	2.1	-.8	.14054955+06	.82657798+07	.82674786+07
1800.000	264623.31	517.41	2.1	-.8	.14043102+06	.82652125+07	.82669865+07
3074.000	264246.81	517.49	2.1	-.8	.14027452+06	.82644509+07	.82663240+07

TABLE AP 1-3 (Sheet 2 of 2)
MASS CHARACTERISTICS SUMMARY

TIME (SEC)	MASS (LBM)	X ARM (STA-IN)	Y ARM (STA-IN)	Z ARM (STA-IN)	IXX (SLUG-FT2)	IYY (SLUG-FT2)	IZZ (SLUG-FT2)
3202.000	264207.79	517.49	2.1	-.8	.14025354+06	.82643474+07	.82662357+07
3300.000	264174.51	517.51	2.1	-.8	.14022283+06	.82642019+07	.82661160+07
3369.000	264151.39	517.51	2.1	-.8	.14020202+06	.82640988+07	.82660311+07
3600.000	264087.68	517.52	2.1	-.8	.14019185+06	.82640307+07	.82659675+07
5400.000	263591.24	517.61	2.1	-.8	.14011254+06	.82634789+07	.82654494+07
6000.000	263425.77	517.64	2.1	-.8	.14008611+06	.82632861+07	.82652675+07
7200.000	263094.71	517.71	2.1	-.8	.14003295+06	.82628839+07	.82648879+07
9000.000	262598.13	517.81	2.1	-.8	.13995323+06	.82622426+07	.82642799+07
10800.000	262101.55	517.92	2.1	-.8	.13987350+06	.82615475+07	.82636181+07
11287.733	261966.99	517.95	2.1	-.8	.13985189+06	.82613499+07	.82634293+07
11287.888	261966.95	517.95	2.1	-.8	.13985188+06	.82613504+07	.82634298+07
11288.867	261966.12	517.95	2.1	-.8	.13984942+06	.82613384+07	.82634203+07
11387.670	261908.62	518.01	2.1	-.8	.13960025+06	.82601251+07	.82624480+07
11487.678	261831.46	518.10	2.1	-.8	.13933659+06	.82583092+07	.82608763+07
11613.668	261777.26	518.22	2.1	-.8	.13900448+06	.82560461+07	.82589207+07
11614.486	261776.63	518.22	2.1	-.8	.13900232+06	.82560308+07	.82589074+07
11614.667	261776.53	518.22	2.1	-.8	.13900186+06	.82560281+07	.82589053+07
11623.239	261488.55	518.25	2.1	-.8	.13898326+06	.82563331+07	.82592282+07
11625.739	260836.84	518.82	2.2	-.8	.13898101+06	.82486750+07	.82515746+07
11630.320	259586.01	519.96	2.2	-.8	.13896608+06	.82325007+07	.82354093+07
11630.490	259584.54	519.96	2.2	-.8	.13896517+06	.82324516+07	.82353606+07
11635.320	259504.50	520.06	2.2	-.8	.13893919+06	.82305829+07	.82335041+07
11640.276	259462.01	520.10	2.2	-.8	.13892636+06	.82300370+07	.82329704+07
11667.720	259445.47	520.11	2.2	-.8	.13885556+06	.82296961+07	.82326955+07
11667.820	259445.41	519.91	2.2	-.8	.15280335+06	.82289854+07	.82312363+07
11667.820	204190.40	350.84	1.0	-.7	.12269067+06	.22380737+07	.22362420+07
11668.000	204190.30	350.84	1.0	-.7	.12269020+06	.22380731+07	.22362418+07

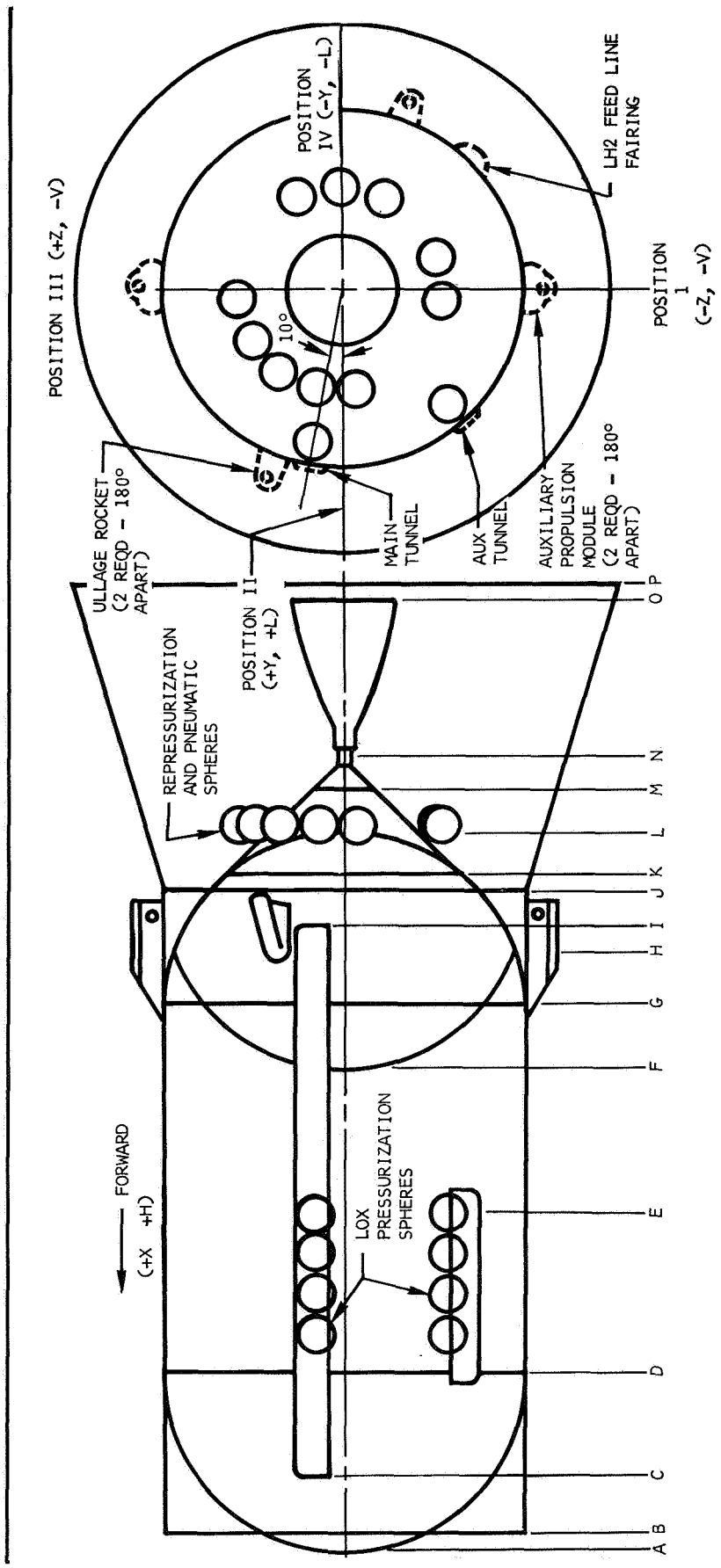

	INSTALLATION	STATION
A.	FWD BULKHEAD (FWD END)	684.6
B.	FWD SKIRT (FWD END)	676.7
C.	MAIN TUNNEL (FWD END)	647.7
D.	FWD SKIRT (AFT END)	554.7
	FWD BULKHEAD (AFT END)	553.0
E.	COLD HELIUM SPHERES (8 REQD - 269" ℄ TO ℄)	454.0
F.	COMMON BULKHEAD (FWD END)	335.2
	AUXILIARY PROPULSION MODULE (FWD END)	298.4
	AFT BULKHEAD (FWD END)	287.9
G.	AFT SKIRT (FWD END)	286.1
	LH2 FEED LINE FAIRING (FWD END)	286.1
	ULLAGE ROCKET (FWD END)	245.3
H.	COMMON BULKHEAD (AFT END)	244.4

	INSTALLATION	STATION
I.	MAIN TUNNEL (AFT END)	220.9
	ULLAGE ROCKET FAIRING (AFT END)	204.6
	AUXILIARY PROPULSION MODULE (AFT END)	203.6
	LH2 FEED LINE FAIRING (AFT END)	202.7
J.	AFT SKIRT (AFT END)	200.6
	INTERSTAGE (FWD END)	200.6
K.	THRUST STRUCTURE/AFT BULKHEAD TANGENT POINT	186.7
L.	AFT BULKHEAD (AFT END)	156.3
	AMBIENT HELIUM SPHERES	153.5
M.	THRUST STRUCTURE SKIN (AFT END)	121.4
N.	GIMBAL STATION	100.0
O.	ENGINE NOZZLE (AFT END)	-16.0
P.	INTERSTAGE (AFT END)	-26.9

Figure AP 1-1. Saturn S-IVB/V Installation - Station List

APPENDIX 2

ENGINE PERFORMANCE PROGRAM (PA49)

1. ENGINE PERFORMANCE PROGRAM (PA49)

This appendix contains the digital printout of computer program PA49 which is a compilation of computer programs G105 and AA89. These computer programs are employed in the propulsion system performance reconstruction of the S-IVB-502 stage flight. The performance analysis and associated plots are presented in section 10.

Table AP 2-1 defines the printout symbols; table AP 2-2 is the digital printout for S-IVB engine burn.

TABLE AP 2-1
PROGRAM PA49 PRINTOUT SYMBOLS

FSUB1	Stage thrust from G105 (lbf)	EMR 2	Engine mixture ratio from AA89
WDOTT1	Total flowrate from G105 (lbm/sec)	ISP 2	Specific impulse from AA89 (sec)
WDOTO1	LOX flowrate from G105 (lbm/sec)	MSUBO2	LOX mass on board from AA89
WDOTF1	LH2 flowrate from G105 (lbm/sec)	MSUBF2	LH2 mass on board from AA89 (lbm)
EMR 1	Engine mixture ratio from G105	THRUST	Composite stage thrust (lbf)
ISP 1	Specific impulse from G105 (sec)	T FLOW	Composite total flowrate (lbm/sec)
MSUBO1	LOX mass on board from G105 (lbm)	O FLOW	Composite LOX flowrate (lbm/sec)
MSUBF1	LH2 mass on board from G105 (lbm)	F FLOW	Composite LH2 flowrate (lbm/sec)
FSUB2	Stage thrust from AA89 (lbf)	*EMR*	Composite engine mixture ratio
WDOTT2	Total flowrate from AA89 (lbm/sec)	*ISP*	Composite specific impulse (sec)
WDOTO2	LOX flowrate from AA89 (lbm/sec)	O MASS	Composite LOX mass on board (lbm)
WDOTF2	LH2 flowrate from AA89 (lbm/sec)	F MASS	Composite LH2 mass on board (lbm)

TABLE AP 2-2 (Sheet 1 of 17)
FIRST BURN ENGINE PERFORMANCE PROGRAM (PA49)

TIME FSUB 1 I FLOW WDOTF2 ISP 1 O MASS	FSUB 2 WDOTO1 F FLOW ISP 2 MSUBF1	THRUST WDOTO2 EMR 1 *ISP* MSUBF2	WDOTI1 O FLOW EMR 2 MSUBO1 F MASS	WDOTI2 WDOTF1 *EMR* MSUBO2
.000				
.000	.000	.000	1.029	.000
1.029	.000	.000	.000	1.029
.000	1.029	.000	.000	.000
.000	.000	.000	193335.000	193273.000
193335.000	42470.001	42493.001	42470.001	
1.000				
.000	180.679	.000	.343	2.566
.343	.000	.000	.000	.343
2.566	.343	.000	.000	.000
.000	70.417	.000	193334.630	193272.610
193334.630	42468.971	42490.473	42468.971	
2.000				
.000	180.711	.000	.338	2.566
.338	.000	.000	.000	.338
2.566	.338	.000	.000	.000
.000	70.422	.000	193334.240	193272.220
193334.240	42467.941	42487.905	42467.941	
3.000				
.000	180.744	.000	4.475	2.612
4.475	.000	.046	.000	4.475
2.566	4.475	.000	.018	.000
.000	69.191	.000	193333.850	193271.790
193333.850	42465.980	42485.337	42465.980	
4.000				
5258.775	38871.720	5258.775	105.366	106.026
105.366	55.004	59.369	55.004	50.362
46.657	50.362	1.092	1.272	1.092
49.910	366.624	49.910	193315.660	193234.140
193315.660	42432.372	42456.556	42432.372	
5.000				
155344.420	132585.030	155344.420	355.443	283.324
355.443	286.800	223.692	286.800	68.643
59.633	68.643	4.178	3.751	4.178
437.044	467.962	437.044	193182.200	193114.910
193182.200	42374.393	42404.085	42374.393	
6.000				
188282.500	187957.900	188282.500	435.281	433.833
435.281	356.871	357.780	356.871	78.410
76.054	78.410	4.551	4.704	4.551
432.554	433.249	432.554	192842.820	192802.180
192842.820	42298.063	42334.162	42298.063	
7.000				
191079.680	200737.010	191079.680	442.983	460.553
442.983	363.769	381.270	363.769	79.214
79.283	79.214	4.592	4.809	4.592
431.348	435.841	431.348	192482.520	192432.580
192482.520	42218.486	42255.492	42218.486	
8.000				
193610.810	215768.340	193610.810	450.420	492.729
450.420	370.731	411.166	370.731	79.690
81.563	79.690	4.652	5.041	4.652
429.845	437.905	429.845	192115.370	192037.360
192115.370	42138.250	42174.363	42138.250	

TABLE AP 2-2 (Sheet 2 of 17)
FIRST BURN ENGINE PERFORMANCE PROGRAM (PA49)

9.000				
207081.360	229785,570	207081.360	483.593	527.740
483.593	402.361	445.144	402.361	81.232
82.596	81,232	4.953	5.389	4.953
428.214	435,414	428.214	191726.600	191610.430
191726.600	42057,193	42091.666	42057.193	
10.000				
219319.260	230108,870	219319.260	515.356	541.606
515.356	432,687	458.968	432.687	82.669
82.638	82,669	5.234	5.554	5.234
425.568	424,864	425.568	191309.600	191158.030
191309.600	41974,785	42008.400	41974.785	
11.000				
224239.840	230064,560	224239.840	524.820	541.517
524.820	441.071	458.832	441.071	83.749
82.685	83,749	5.267	5.549	5.267
427.270	424,852	427.270	190871.880	190698.730
190871.880	41891,237	41925.088	41891.237	
12.000				
224689.260	230010,520	224689.260	528.406	541.417
528.406	444,865	458.700	444.855	83.551
82.717	83,551	5.324	5.545	5.324
425.221	424,831	425.221	190428.470	190239.560
190428.470	41807,146	41841.735	41807.146	
13.000				
224727.270	229958,650	224727.270	531.064	541.308
531.064	447,825	458.571	447.825	83.239
82.738	83,239	5.380	5.542	5.380
423.164	424,820	423.164	189982.820	189780.530
189982.820	41723,103	41758.354	41723.103	
14.000				
225955.790	229907,190	225955.790	531.683	541.193
531.683	448,123	458.442	448.123	83.560
82.752	83,560	5.363	5.540	5.363
424.982	424,815	424.982	189534.670	189321.610
189534.670	41639,094	41674.958	41639.094	
15.000				
225195.370	230181,050	225195.370	532.408	541.449
532.408	449,456	458.666	449.456	82.952
82.782	82,952	5.418	5.541	5.418
422.975	425,121	422.975	189085.630	188862.670
189085.630	41554,923	41591.539	41554.923	
16.000				
227513.710	230455,010	227513.710	534.223	541.704
534.223	450,676	458.891	450.676	83.547
82.813	83,547	5.394	5.541	5.394
425.877	425,426	425.877	188634.560	188403.490
188634.560	41470,921	41508.090	41470.921	
17.000				
227524.850	230426,680	227524.850	535.569	541.607
535.569	452,182	458.787	452.182	83.386
82.820	83,386	5.423	5.540	5.423
424.829	425,450	424.829	188182.070	187944.250
188182.070	41386,727	41424.620	41386.727	
18.000				
229049.990	230398,220	229049.990	535.963	541.505
535.963	452,372	458.683	452.372	83.591
82.822	83,591	5.412	5.538	5.412
427.362	425,477	427.362	187728.930	187485.110
187728.930	41302,516	41341.149	41302.516	

TABLE AP 2-2 (Sheet 3 of 17)
FIRST BURN ENGINE PERFORMANCE PROGRAM (PA49)

19.000				
228566.670	230369.770	228566.670	536.811	541.403
536.811	453.090	458.579	453.090	83.721
82.824	83.721	5.412	5.537	5.412
425.786	425.505	425.786	187275.100	187026.080
187275.100	41218.073	41257.674	41218.073	
20.000				
229321.320	230341.310	229321.320	537.890	541.302
537.890	454.296	458.475	454.296	83.594
82.826	83.594	5.435	5.535	5.435
426.335	425.532	426.335	186820.870	186567.160
186820.870	41133.974	41174.197	41133.974	
21.000				
228167.210	230331.380	228167.210	537.685	541.258
537.685	454.046	458.428	454.046	83.641
82.830	83.641	5.429	5.535	5.429
424.350	425.548	424.350	186366.390	186108.310
186366.390	41049.719	41090.717	41049.719	
22.000				
229228.910	230321.440	229228.910	536.038	541.214
536.038	453.526	458.381	453.526	82.511
82.833	82.511	5.497	5.534	5.497
427.636	425.564	427.636	185911.530	185649.500
185911.530	40965.629	41007.235	40965.629	
23.000				
230278.910	230332.490	230278.910	539.740	541.224
539.740	456.409	458.385	456.409	83.331
82.839	83.331	5.477	5.533	5.477
426.648	425.577	426.648	185455.710	185190.710
185455.710	40881.625	40923.748	40881.625	
24.000				
227773.470	230343.620	227773.470	537.037	541.239
537.037	453.627	458.390	453.627	83.410
82.849	83.410	5.438	5.533	5.438
424.130	425.586	424.130	185000.480	184731.920
185000.480	40797.630	40840.253	40797.630	
25.000				
229840.910	230341.610	229840.910	537.738	541.241
537.738	454.446	458.380	454.446	83.292
82.861	83.292	5.456	5.532	5.456
427.421	425.581	427.421	184545.340	184273.140
184545.340	40713.532	40756.747	40713.532	
26.000				
230276.850	230339.590	230276.850	538.147	541.243
538.147	454.762	458.370	454.762	83.385
82.873	83.385	5.454	5.531	5.454
427.907	425.575	427.907	184090.260	183814.370
184090.260	40629.495	40673.228	40629.495	
27.000				
229696.970	230343.160	229696.970	537.990	541.259
537.990	454.952	458.373	454.952	83.038
82.886	83.038	5.479	5.530	5.479
426.954	425.569	426.954	183636.670	183355.590
183636.670	40545.718	40589.697	40545.718	
28.000				
228476.940	230346.720	228476.940	539.232	541.276
539.232	456.127	458.377	456.127	83.105
82.898	83.105	5.489	5.529	5.489
423.708	425.563	423.708	183181.300	182896.820
183181.300	40461.940	40506.154	40461.940	

TABLE AP 2-2 (Sheet 4 of 17)
FIRST BURN ENGINE PERFORMANCE PROGRAM (PA49)

29.000				
228190.080	230355,460	228190,080	539,756	541.305
539.756	456,528	458,393	456.528	83.229
82.912	83,229	5,485	5,529	5.485
422.765	425,556	422.765	182724.830	182438.040
182724.830	40378,110	40422.597	40378.110	
30.000				
228057.880	230364,210	228057,880	538,315	541.335
538.315	455,604	458.410	455.604	82.711
82.925	82,711	5,508	5.528	5.508
423.651	425,549	423.651	182269.280	181979.240
182269.280	40294,320	40339.027	40294.320	
31.000				
50421.930	230373,200	50421,930	541.025	541.365
541.025	457,903	458,426	457,903	83.122
82.939	83,122	5.509	5.527	5.509
93.197	425,542	93.197	181813.730	181520.420
181813.730	40210,596	40255.443	40210.596	
32.000				
228138.250	230382,170	228138,250	536.046	541.395
536.046	452,954	458,442	452.954	83.091
82.953	83,091	5,451	5.527	5.451
425.595	425,535	425.595	181358.330	181061.590
181358.330	40127,604	40171,846	40127.604	
33.000				
229481.950	230394,360	229481,950	540.318	541.439
540.318	457,160	458,472	457.160	83.159
82.967	83,159	5.497	5.526	5.497
424.716	425,522	424.716	180902.920	180602.730
180902.920	40043,685	40088.235	40043.685	
34.000				
229914.460	230406,770	229914,460	539.851	541.484
539.851	456,509	458,502	456.509	83.342
82.982	83,342	5,478	5.525	5.478
425.885	425,510	425,885	180445.700	180143.840
180445.700	39960,004	40004.610	39960.004	
35.000				
228067.200	230419,180	228067,200	540.507	541.529
540.507	457,351	458,533	457.351	83.156
82.996	83,156	5.500	5.525	5.500
421.950	425,498	421.950	179988.340	179684.930
179988.340	39876.261	39920.969	39876.261	
36.000				
229340.550	230431,590	229340,550	539,822	541.573
539,822	456,802	458.563	456,802	83.020
83.010	83,020	5.502	5.524	5.502
424.845	425,485	424,845	179530.610	179225.980
179530.610	39792,484	39837.314	39792.484	
37.000				
228864.180	230444,000	228864,180	539.616	541.618
539.616	456,592	458.593	456,592	83.023
83.025	83,023	5,500	5.524	5.500
424.124	425,473	424,124	179072,530	178767.000
179072.530	39708,856	39753.645	39708,856	
38.000				
227890.120	230456,400	227890.120	538,309	541.663
538.309	456,135	458.624	456.135	82.174
83.039	82,174	5.551	5.523	5.551
423.344	425,461	423.344	178615.270	178308.000
178615.270	39625,249	39669,961	39625.249	

TABLE AP 2-2 (Sheet 5 of 17)
FIRST BURN ENGINE PERFORMANCE PROGRAM (PA49)

39.000				
230466.440	230468.810	230466.440	536.295	541.708
536.295	453.601	458.654	453.601	82.694
83.054	82.694	5.485	5.522	5.485
429.738	425.448	429.738	178158.090	177848.960
178158.090	39541.675	39586.264	39541.675	
40.000				
229870.740	230481.210	229870.740	541.343	541.753
541.343	458.314	458.685	458.314	83.029
83.068	83.029	5.520	5.522	5.520
424.631	425.436	424.631	177701.530	177389.880
177701.530	39458.025	39502.551	39458.025	
41.000				
229084.370	230493.750	229084.370	540.194	541.798
540.194	457.287	458.715	457.287	82.907
83.083	82.907	5.516	5.521	5.516
424.078	425.424	424.078	177244.140	176930.790
177244.140	39374.449	39418.823	39374.449	
42.000				
228991.330	230506.280	228991.330	540.869	541.843
540.869	457.856	458.745	457.856	83.014
83.098	83.014	5.515	5.521	5.515
423.376	425.412	423.376	176786.610	176471.660
176786.610	39290.718	39335.082	39290.718	
43.000				
229931.230	230518.810	229931.230	541.392	541.887
541.392	458.346	458.775	458.346	83.046
83.111	83.046	5.519	5.520	5.519
424.703	425.400	424.703	176329.190	176012.490
176329.190	39207.160	39251.326	39207.160	
44.000				
228844.030	230531.330	228844.030	541.461	541.930
541.461	458.442	458.806	458.442	83.019
83.124	83.019	5.522	5.520	5.522
422.642	425.389	422.642	175871.460	175553.310
175871.460	39123.529	39167.557	39123.529	
45.000				
229947.960	230543.670	229947.960	540.652	541.976
540.652	457.584	458.838	457.584	83.068
83.138	83.068	5.509	5.519	5.509
425.316	425.376	425.316	175414.580	175094.080
175414.580	39039.791	39083.774	39039.791	
46.000				
230900.530	230556.180	230900.530	541.222	542.023
541.222	458.190	458.872	458.190	83.032
83.151	83.032	5.518	5.519	5.518
426.628	425.363	426.628	174956.340	174634.830
174956.340	38956.268	38999.978	38956.268	
47.000				
227915.910	230568.690	227915.910	539.149	542.069
539.149	456.195	458.905	456.195	82.954
83.164	82.954	5.499	5.518	5.499
422.733	425.349	422.733	174499.740	174175.550
174499.740	38872.627	38916.169	38872.627	
48.000				
228539.130	230581.200	228539.130	540.156	542.116
540.156	457.156	458.938	457.156	82.999
83.178	82.999	5.508	5.518	5.508
423.099	425.336	423.099	174043.450	173716.220
174043.450	38789.179	38832.346	38789.179	

TABLE AP 2-2 (Sheet 6 of 17)
FIRST BURN ENGINE PERFORMANCE PROGRAM (PA49)

49.000				
230015.860	230593.710	230015.860	542.340	542.162
542.340	459.118	458.971	459.118	83.222
83.191	83.222	5.517	5.517	5.517
424.118	425.322	424.118	173585.790	173256.870
173585.790	38705.295	38748.510	38705.295	
50.000				
227908.600	230606.220	227908.600	535.846	542.209
535.846	452.719	459.004	452.719	83.127
83.204	83.127	5.446	5.517	5.446
425.325	425.309	425.325	173128.120	172797.490
173128.120	38621.490	38664.661	38621.490	
51.000				
228459.430	230618.770	228459.430	540.427	542.255
540.427	457.369	459.038	457.369	83.058
83.218	83.058	5.507	5.516	5.507
422.739	425.296	422.739	172670.890	172338.060
172670.890	38537.745	38580.798	38537.745	
52.000				
228248.770	230631.310	228248.770	540.718	542.302
540.718	457.622	459.071	457.622	83.095
83.231	83.095	5.507	5.516	5.507
422.122	425.282	422.122	172213.710	171878.610
172213.710	38453.897	38496.923	38453.897	
53.000				
228226.890	230643.850	228226.890	541.421	542.348
541.421	458.314	459.104	458.314	83.107
83.244	83.107	5.515	5.515	5.515
421.533	425.269	421.533	171755.210	171419.120
171755.210	38370.100	38413.034	38370.100	
54.000				
229870.930	230656.390	229870.930	540.777	542.395
540.777	457.712	459.137	457.712	83.065
83.258	83.065	5.510	5.515	5.510
425.075	425.256	425.075	171297.130	170959.600
171297.130	38286.314	38329.131	38286.314	
55.000				
229013.580	230668.940	229013.580	540.124	542.439
540.124	456.954	459.170	456.954	83.169
83.269	83.169	5.494	5.514	5.494
424.002	425.244	424.002	170838.990	170500.050
170838.990	38202.627	38245.216	38202.627	
56.000				
230400.460	230681.480	230400.460	539.775	542.481
539.775	456.498	459.203	456.498	83.277
83.278	83.277	5.482	5.514	5.482
426.845	425.234	426.845	170382.460	170040.460
170382.460	38118.812	38161.291	38118.812	
57.000				
230662.550	230694.030	230662.550	540.034	542.524
540.034	456.903	459.236	456.903	83.132
83.288	83.132	5.496	5.514	5.496
427.126	425.224	427.126	169924.780	169580.840
169924.780	38035.081	38077.356	38035.081	
58.000				
230174.320	230706.560	230174.320	538.027	542.567
538.027	454.828	459.269	454.828	83.199
83.297	83.199	5.467	5.514	5.467
427.812	425.213	427.812	169466.610	169121.190
169466.610	37951.226	37993.412	37951.226	

TABLE AP 2-2 (Sheet 7 of 17)
FIRST BURN ENGINE PERFORMANCE PROGRAM (PA49)

59.000				
229755.160	230719.220	229755.160	541.742	542.610
541.742	458.583	459.303	458.583	83.159
83.307	83.159	5.514	5.513	5.514
424.104	425.203	424.104	169008.430	168661.500
169008.430	37867.402	37909.459	37867.402	
60.000				
229771.170	230731.900	229771.170	540.770	542.652
540.770	457.516	459.336	457.516	83.253
83.316	83.253	5.495	5.513	5.495
424.897	425.193	424.897	168550.690	168201.780
168550.690	37783.708	37825.496	37783.708	
61.000				
230136.950	230744.950	230136.950	541.191	542.696
541.191	458.327	459.370	458.327	82.864
83.326	82.864	5.531	5.513	5.531
425.241	425.183	425.241	168091.840	167742.030
168091.840	37699.816	37741.523	37699.816	
62.000				
230427.120	230758.000	230427.120	541.951	542.740
541.951	458.610	459.403	458.610	83.340
83.336	83.340	5.503	5.513	5.503
425.181	425.173	425.181	167633.060	167282.250
167633.060	37615.905	37657.541	37615.905	
63.000				
230343.460	230771.060	230343.460	541.233	542.783
541.233	458.029	459.437	458.029	83.204
83.346	83.204	5.505	5.512	5.505
425.591	425.163	425.591	167174.770	166822.430
167174.770	37532.149	37573.548	37532.149	
64.000				
230860.610	230784.110	230860.610	541.851	542.827
541.851	458.743	459.470	458.743	83.109
83.356	83.109	5.520	5.512	5.520
426.059	425.153	426.059	166716.230	166362.570
166716.230	37448.394	37489.546	37448.394	
65.000				
230120.410	230797.160	230120.410	541.722	542.870
541.722	458.466	459.504	458.466	83.256
83.366	83.256	5.507	5.512	5.507
424.794	425.143	424.794	166257.640	165902.690
166257.640	37364.480	37405.533	37364.480	
66.000				
230035.210	230810.210	230035.210	542.312	542.914
542.312	458.493	459.537	458.493	83.818
83.376	83.818	5.470	5.512	5.470
424.175	425.132	424.175	165798.760	165442.760
165798.760	37280.574	37321.511	37280.574	
67.000				
229420.840	230823.260	229420.840	540.638	542.957
540.638	457.519	459.571	457.519	83.119
83.386	83.119	5.504	5.511	5.504
424.352	425.122	424.352	165340.080	164982.810
165340.080	37196.650	37237.478	37196.650	
68.000				
230607.990	230836.300	230607.990	541.558	543.001
541.558	458.327	459.605	458.327	83.231
83.396	83.231	5.507	5.511	5.507
425.823	425.112	425.823	164881.930	164522.830
164881.930	37112.724	37153.435	37112.724	

TABLE AP 2-2 (Sheet 8 of 17)
FIRST BURN ENGINE PERFORMANCE PROGRAM (PA49)

69.000				
229788.820	230849.360	229788.820	541.787	543.044
541.787	458.654	459.638	458.654	83.133
83.406	83.133	5.517	5.511	5.517
424.131	425.102	424.131	164424.130	164062.810
164424.130	37028.827	37069.383	37028.827	
70.000				
228529.100	230862.400	228529.100	541.452	543.088
541.452	458.176	459.672	458.176	83.276
83.416	83.276	5.502	5.511	5.502
422.067	425.092	422.067	163966.110	163602.750
163966.110	36944.897	36985.320	36944.897	
71.000				
228745.200	230875.710	228745.200	541.946	543.132
541.946	458.541	459.705	458.541	83.405
83.426	83.405	5.498	5.510	5.498
422.081	425.082	422.081	163507.300	163142.660
163507.300	36860.890	36901.248	36860.890	
72.000				
230533.330	230889.010	230533.330	541.654	543.176
541.654	458.372	459.739	458.372	83.282
83.437	83.282	5.504	5.510	5.504
425.610	425.073	425.610	163048.320	162682.540
163048.320	36777.061	36817.165	36777.061	
73.000				
230169.270	230902.370	230169.270	541.743	543.220
541.743	458.272	459.773	458.272	83.471
83.447	83.471	5.490	5.510	5.490
424.868	425.063	424.868	162589.010	162222.390
162589.010	36693.118	36733.072	36693.118	
74.000				
230610.040	230915.790	230610.040	542.640	543.264
542.640	459.477	459.807	459.477	83.164
83.457	83.164	5.525	5.509	5.525
424.978	425.053	424.978	162129.700	161762.190
162129.700	36609.115	36648.969	36609.115	
75.000				
230218.430	230929.220	230218.430	535.552	543.308
535.552	452.239	459.841	452.239	83.312
83.467	83.312	5.428	5.509	5.428
429.872	425.043	429.872	161671.090	161301.970
161671.090	36525.264	36564.855	36525.264	
76.000				
230539.680	230942.640	230539.680	540.378	543.352
540.378	457.086	459.875	457.086	83.292
83.478	83.292	5.488	5.509	5.488
426.627	425.033	426.627	161213.490	160841.710
161213.490	36441.394	36480.730	36441.394	
77.000				
229890.860	230956.070	229890.860	543.562	543.397
543.562	460.521	459.909	460.521	83.040
83.488	83.040	5.546	5.509	5.546
422.934	425.023	422.934	160755.050	160381.420
160755.050	36357.468	36396.596	36357.468	
78.000				
230567.460	230969.500	230567.460	542.043	543.441
542.043	458.699	459.943	458.699	83.343
83.498	83.343	5.504	5.508	5.504
425.368	425.013	425.368	160296.160	159921.090
160296.160	36273.497	36312.451	36273.497	

TABLE AP 2-2 (Sheet 9 of 17)
FIRST BURN ENGINE PERFORMANCE PROGRAM (PA49)

79.000				
230302.340	230982.920	230302.340	537.825	543.485
537.825	454.362	459.977	454.362	83.462
83.509	83.462	5.444	5.508	5.444
428.211	425.003	428.211	159838.230	159460.740
159838.230	36189.286	36228.297	36189.285	
80.000				
229752.640	230996.350	229752.640	540.109	543.529
540.109	456.636	460.011	456.636	83.472
83.519	83.472	5.471	5.508	5.471
425.382	424.993	425.382	159381.170	159000.340
159381.170	36105.160	36144.131	36105.160	
81.000				
228272.080	231009.070	228272.080	540.228	543.572
540.228	456.898	460.044	456.898	83.329
83.528	83.329	5.483	5.508	5.483
422.548	424.984	422.548	158924.360	158539.910
158924.360	36021.145	36059.956	36021.145	
82.000				
229711.300	231021.780	229711.300	538.570	543.613
538.570	455.344	460.077	455.344	83.227
83.536	83.227	5.471	5.508	5.471
426.521	424.974	426.521	158467.800	158079.460
158467.800	35937.250	35975.774	35937.250	
83.000				
229566.360	231034.500	229566.360	541.132	543.655
541.132	457.801	460.111	457.801	83.331
83.544	83.331	5.494	5.507	5.494
424.233	424.965	424.233	158011.210	157618.960
158011.210	35853.203	35891.582	35853.203	
84.000				
228614.610	231047.220	228614.610	539.332	543.697
539.332	456.092	460.144	456.092	83.241
83.552	83.241	5.479	5.507	5.479
423.885	424.956	423.885	157555.520	157158.430
157555.520	35769.384	35807.382	35769.384	
85.000				
227995.020	230230.820	227995.020	540.756	542.737
540.756	457.456	459.223	457.456	83.300
83.514	83.300	5.492	5.499	5.492
421.623	424.203	421.623	157099.140	156698.350
157099.140	35685.400	35723.197	35685.400	
86.000				
228194.630	230202.660	228194.630	537.581	542.675
537.581	454.241	459.157	454.241	83.339
83.518	83.339	5.451	5.498	5.451
424.485	424.200	424.485	156642.260	156238.760
156642.260	35601.372	35639.030	35601.372	
87.000				
229910.870	230174.790	229910.870	541.629	542.612
541.629	458.168	459.091	458.168	83.461
83.521	83.461	5.490	5.497	5.490
424.480	424.197	424.480	156185.810	155779.240
156185.810	35517.320	35554.859	35517.320	
88.000				
229545.660	230146.930	229545.660	541.204	542.550
541.204	458.073	459.026	458.073	83.131
83.524	83.131	5.510	5.496	5.510
424.139	424.195	424.139	155728.380	155319.790
155728.380	35433.270	35470.685	35433.270	

TABLE AP 2-2 (Sheet 10 of 17)
FIRST BURN ENGINE PERFORMANCE PROGRAM (PA49)

89.000				
228345.500	230119.150	228345.500	540.851	542.488
540.851	457.045	458.961	457.045	83.806
83.528	83.806	5.454	5.495	5.454
422.197	424.192	422.197	155269.700	154860.390
155269.700	35349.072	35386.506	35349.072	
90.000				
230000.590	230091.390	230000.590	542.629	542.427
542.629	458.881	458.896	458.881	83.747
83.531	83.747	5.479	5.494	5.479
423.864	424.189	423.864	154811.990	154401.070
154811.990	35264.798	35302.327	35264.798	
91.000				
229765.130	230063.880	229765.130	541.149	542.365
541.149	457.445	458.831	457.445	83.704
83.535	83.704	5.465	5.493	5.465
424.587	424.186	424.587	154354.310	153941.810
154354.310	35180.520	35218.143	35180.520	
92.000				
230103.000	230036.380	230103.000	542.578	542.304
542.578	458.543	458.766	458.543	84.035
83.538	84.035	5.457	5.492	5.457
424.092	424.184	424.092	153896.760	153482.620
153896.760	35096.166	35133.954	35096.166	
93.000				
230564.280	230008.870	230564.280	542.876	542.242
542.876	459.240	458.700	459.240	83.636
83.542	83.636	5.491	5.491	5.491
424.709	424.181	424.709	153437.850	153023.480
153437.850	35011.724	35049.763	35011.724	
94.000				
230377.560	229981.360	230377.560	541.947	542.181
541.947	458.353	458.635	458.353	83.594
83.545	83.594	5.483	5.490	5.483
425.093	424.178	425.093	152979.430	152564.420
152979.430	34927.529	34965.568	34927.529	
95.000				
230100.440	229953.860	230100.440	539.769	542.120
539.769	456.172	458.570	456.172	83.596
83.549	83.596	5.457	5.489	5.457
426.294	424.176	426.294	152521.690	152105.420
152521.690	34843.241	34881.368	34843.241	
96.000				
229861.200	229926.360	229861.200	541.471	542.058
541.471	457.875	458.505	457.875	83.596
83.553	83.596	5.477	5.488	5.477
424.513	424.173	424.513	152064.570	151646.480
152064.570	34758.937	34797.166	34758.937	
97.000				
229878.870	230736.800	229878.870	540.979	543.020
540.979	456.296	459.417	456.296	84.683
83.603	84.683	5.388	5.495	5.388
424.931	424.914	424.931	151605.930	151187.120
151605.930	34674.578	34712.935	34674.578	
98.000				
229969.290	230759.020	229969.290	542.972	543.086
542.972	459.255	459.473	459.255	83.717
83.613	83.717	5.486	5.495	5.486
423.538	424.903	423.538	151148.190	150727.280
151148.190	34590.130	34628.676	34590.130	

TABLE AP 2-2 (Sheet 11 of 17)
FIRST BURN ENGINE PERFORMANCE PROGRAM (PA49)

99.000				
230445.820	230780,930	230445.820	542.498	543.151
542.498	458,443	459.528	458,443	84.054
83.623	84,054	5,454	5.495	5.454
424.787	424,893	424.787	150689.590	150267.380
150689.590	34505,757	34544,406	34505,757	
100.000				
230227.850	230802,850	230227.850	542.845	543.216
542,845	459,382	459.584	459,382	83.462
83.632	83,462	5.504	5.495	5.504
424.114	424,882	424,114	150230.680	149807.420
150230.680	34421,390	34460.127	34421,390	
101.000				
229560.390	230824,810	229560.390	539.840	543.281
539,840	455,633	459,639	455.633	84.207
83.642	84,207	5.411	5.495	5.411
425.238	424,872	425.238	149771.500	149347.410
149771.500	34337,010	34375,838	34337,010	
102.000				
229443.360	230846,770	229443,360	540.582	543.346
540.582	456,971	459,694	456,971	83.611
83.652	83,611	5,465	5.495	5.465
424.438	424,861	424.438	149315.010	148887.340
149315.010	34252,493	34291,540	34252,493	
103.000				
229721.750	230868,730	229721.750	540.245	543.411
540.245	456,722	459.750	456.722	83.524
83.661	83,524	5.468	5.495	5.468
425.217	424,851	425.217	148857.680	148427.230
148857.680	34168,216	34207,233	34168,216	
104.000				
229725.840	230890.680	229725,840	540.697	543.475
540.697	457,197	459,805	457,197	83.500
83.670	83,500	5.475	5.495	5.475
424.870	424,842	424,870	148400.560	147967.050
148400.560	34084,029	34122,916	34084,029	
105.000				
227658.710	230912,680	227658.710	538.913	543.538
538.913	455,269	459.861	455.269	83.644
83.678	83,644	5.443	5.496	5.443
422.441	424,832	422,441	147945.200	147506.810
147945.200	33999,909	34038.591	33999,909	
106.000				
227655.540	230934,720	227655.540	537.888	543.602
537.888	454,194	459.916	454,194	83.694
83.686	83,694	5,427	5.496	5.427
423.239	424,823	423,239	147490.410	147046.520
147490.410	33915,590	33954,258	33915,590	
107.000				
228999.270	230956,770	228999,270	536,888	543.665
536.888	453,310	459,972	453,310	83.577
83.693	83,577	5,424	5.496	5.424
426.531	424,814	426.531	147034.880	146586.180
147034.880	33831,276	33869,916	33831,276	
108.000				
229302.060	230978,820	229302,060	537,575	543.729
537.575	454,050	460,027	454,050	83.526
83.701	83,526	5,436	5.496	5.436
426.549	424,805	426.549	146578.570	146125.780
146578.570	33746,902	33785,567	33746,902	

TABLE AP 2-2 (Sheet 12 of 17)
FIRST BURN ENGINE PERFORMANCE PROGRAM (PA49)

109.000				
227642.890	231000.860	227642.890	537.260	543.792
537.260	453.460	460.083	453.460	83.800
83.709	83.800	5.411	5.496	5.411
423.711	424.796	423.711	146123.130	145665.330
146123.130	33662.480	33701.210	33662.480	
110.000				
227715.970	231022.910	227715.970	534.685	543.855
534.685	451.146	460.138	451.146	83.540
83.717	83.540	5.400	5.496	5.400
425.888	424.787	425.888	145668.650	145204.820
145668.650	33578.227	33616.846	33578.227	
111.000				
227953.990	230201.690	227953.990	536.868	542.882
536.868	453.341	459.205	453.341	83.527
83.677	83.527	5.427	5.488	5.427
424.600	424.037	424.600	145213.210	144744.750
145213.210	33493.925	33532.497	33493.925	
112.000				
228260.980	230168.700	228260.980	539.965	542.804
539.965	456.343	459.126	456.343	83.623
83.678	83.623	5.457	5.487	5.457
422.733	424.036	422.733	144758.090	144285.180
144758.090	33409.588	33448.167	33409.588	
113.000				
228271.160	230136.000	228271.160	541.710	542.728
541.710	457.677	459.048	457.677	84.033
83.680	84.033	5.446	5.486	5.446
421.390	424.036	421.390	144300.520	143825.690
144300.520	33325.204	33363.836	33325.204	
114.000				
229202.110	230103.310	229202.110	540.016	542.651
540.016	456.873	458.971	456.873	83.143
83.681	83.143	5.495	5.485	5.495
424.436	424.035	424.436	143843.360	143366.280
143843.360	33240.917	33279.505	33240.917	
115.000				
228601.440	230070.610	228601.440	540.502	542.575
540.502	457.247	458.893	457.247	83.254
83.682	83.254	5.492	5.484	5.492
422.943	424.035	422.943	143386.120	142906.950
143386.120	33156.676	33195.173	33156.676	
116.000				
228314.180	230037.910	228314.180	541.022	542.498
541.022	457.360	458.815	457.360	83.662
83.683	83.662	5.467	5.483	5.467
422.005	424.034	422.005	142927.940	142447.700
142927.940	33072.206	33110.838	33072.206	
117.000				
228351.320	230005.210	228351.320	542.410	542.422
542.410	458.659	458.737	458.659	83.751
83.685	83.751	5.476	5.482	5.476
420.994	424.034	420.994	142471.480	141988.520
142471.480	32987.695	33026.502	32987.695	
118.000				
227679.130	229972.510	227679.130	541.450	542.345
541.450	457.495	458.659	457.495	83.955
83.686	83.955	5.449	5.481	5.449
420.499	424.034	420.499	142013.270	141529.430
142013.270	32903.141	32942.167	32903.141	

TABLE AP 2-2 (Sheet 13 of 17)
FIRST BURN ENGINE PERFORMANCE PROGRAM (PA49)

119.000				
227373.030	229939.820	227373.030	540.422	542.269
540.422	456.423	458.582	456.423	83.999
83.687	83.999	5.434	5.480	5.434
420.732	424.033	420.732	141555.250	141070.410
141555.250	32818.514	32857.829	32818.514	
120.000				
225784.640	229907.130	225784.640	542.465	542.192
542.465	458.615	458.504	458.615	83.851
83.688	83.851	5.469	5.479	5.469
416.219	424.033	416.219	141097.330	140611.470
141097.330	32733.975	32773.489	32733.975	
121.000				
225617.820	230709.490	225617.820	540.939	543.132
540.939	457.087	459.395	457.087	83.852
83.736	83.852	5.451	5.486	5.451
417.086	424.776	417.086	140639.820	140152.120
140639.820	32649.276	32689.127	32649.276	
122.000				
226006.310	230723.610	226006.310	541.383	543.175
541.383	457.464	459.431	457.464	83.919
83.744	83.919	5.451	5.486	5.451
417.461	424.769	417.461	140182.990	139692.310
140182.990	32564.613	32604.736	32564.613	
123.000				
225790.230	230737.620	225790.230	542.787	543.218
542.787	458.757	459.467	458.757	84.030
83.751	84.030	5.459	5.486	5.459
415.983	424.761	415.983	139725.990	139232.460
139725.990	32479.843	32520.339	32479.843	
124.000				
224612.500	230751.640	224612.500	539.909	543.260
539.909	455.926	459.503	455.926	83.983
83.758	83.983	5.429	5.486	5.429
416.019	424.753	416.019	139268.820	138772.570
139268.820	32395.268	32435.935	32395.268	
125.000				
223565.290	230765.660	223565.290	542.144	543.303
542.144	458.266	459.539	458.266	83.877
83.765	83.877	5.464	5.486	5.464
412.373	424.746	412.373	138810.740	138312.650
138810.740	32310.588	32351.524	32310.588	
126.000				
223723.540	230779.690	223723.540	539.729	543.346
539.729	455.882	459.575	455.882	83.847
83.772	83.847	5.437	5.486	5.437
414.511	424.738	414.511	138353.600	137852.690
138353.600	32226.010	32267.106	32226.010	
127.000				
224609.940	230793.710	224609.940	541.732	543.389
541.732	457.882	459.610	457.882	83.850
83.779	83.850	5.461	5.486	5.461
414.614	424.730	414.614	137896.450	137392.700
137896.450	32141.488	32182.681	32141.488	
128.000				
224760.800	230807.740	224760.800	541.244	543.432
541.244	457.327	459.646	457.327	83.917
83.786	83.917	5.450	5.486	5.450
415.267	424.723	415.267	137440.380	136932.670
137440.380	32056.864	32098.249	32056.864	

TABLE AP 2-2 (Sheet 14 of 17)
FIRST BURN ENGINE PERFORMANCE PROGRAM (PA49)

129.000				
224289.340	230821,760	224289.340	536.645	543.475
536.645	452,867	459.682	452.867	83.778
83.793	83,778	5,406	5,486	5,406
417.947	424,715	417,947	136984,390	136472.610
136984.390	31972,425	32013,810	31972,425	
130.000				
224539.720	230835,790	224539.720	540.999	543.518
540.999	457,344	459.718	457.344	83.655
83.800	83,655	5,467	5,486	5.467
415.046	424,707	415.046	136529.350	136012.510
136529.350	31887,973	31929,363	31887.973	
131.000				
223197.250	230849,820	223197.250	536,284	543.560
536.284	452,432	459.754	452,432	83.852
83.807	83,852	5.396	5.486	5.396
416.192	424,699	416.192	136075.090	135552.370
136075.090	31803,422	31844,910	31803,422	
132.000				
223279.500	230863,850	223279,500	539.331	543.603
539.331	455,482	459,790	455,482	83.849
83.814	83,849	5,432	5.486	5,432
413.994	424,692	413,994	135617.730	135092.200
135617.730	31718,820	31760,450	31718,820	
133.000				
223396.570	230089,320	223396.570	540.519	542.749
540.519	456,716	458,970	456.716	83.803
83.779	83,803	5,450	5.478	5.450
413.300	423,933	413.300	135163.070	134632.420
135163.070	31634,142	31676,003	31634.142	
134.000				
224303.950	230103,060	224303,950	538,626	542.791
538,626	454,845	459,005	454.845	83.781
83.786	83,781	5,429	5,478	5.429
416,437	423,926	416,437	134706.910	134173.040
134706.910	31549,690	31591,570	31549,690	
135.000				
224298.150	230117,090	224298,150	538.361	542.833
538.361	454,788	459,041	454,788	83.572
83.792	83,572	5.442	5,478	5.442
416,632	423,919	416,632	134251.650	133713.610
134251.650	31465,112	31507,131	31465,112	
136.000				
224542.590	230131,130	224542,590	538.211	542.873
538.211	454,399	459,077	454,399	83.812
83.797	83,812	5,422	5,478	5,422
417.202	423,913	417,202	133796.790	133254.160
133796.790	31380,729	31422,686	31380,729	
137.000				
224261.540	230145,160	224261,540	536.020	542.914
536.020	452,128	459,112	452,128	83.892
83.802	83,892	5,389	5,479	5.389
418.383	423,907	418,383	133344.180	132794.660
133344.180	31296,153	31338,236	31296,153	
138.000				
224695.590	230159,200	224695,590	539.464	542.955
539.464	455,786	459,148	455,786	83.678
83.807	83,678	5,447	5,479	5,447
416,516	423,901	416,516	132889.830	132335.130
132889.830	31211,554	31253,782	31211,554	

TABLE AP 2-2 (Sheet 15 of 17)
FIRST BURN ENGINE PERFORMANCE PROGRAM (PA49)

139.000				
224456.300	230173,240	224456,300	539.185	542.996
539.185	455,389	459.184	455.389	83.796
83.812	83,796	5.435	5.479	5.435
416.288	423,895	416,288	132433,880	131875.570
132433,880	31126,968	31169,322	31126.968	
140.000				
224415.420	12420,031	224415.420	539.288	31.097
539.288	455,400	26.399	455.400	83.887
4.697	83,887	5.429	5.621	5.429
416.133	399,286	416.133	131978.050	131574.560
131978.050	31042,391	31113.838	31042.391	
141.000				
222946.320		222946.320	538.543	
538.543	454,765		454.765	83.778
	83,778	5,428		5.428
413.980		413.980	131522.280	
131522.280	30957,820		30957.820	
142.000				
224669.170		224669.170	539.428	
539.428	455,651		455.651	83.777
	83,777	5,439		5.439
416.495		416,495	131066.281	
131066.281	30873,138		30873.138	
143.000				
224444.580		224444.580	540.636	
540.636	456,724		456.724	83.913
	83,913	5,443		5.443
415.149		415,149	130609.304	
130609.304	30788,509		30788.509	
144.000				
225025.210		225025.210	541.629	
541.629	457,693		457.693	83.935
	83,935	5,453		5.453
415.460		415,460	130153.355	
130153.355	30703,886		30703.886	
145.000				
224353.250		224353,250	540.451	
540.451	456,630		456.630	83.821
	83,821	5,448		5.448
415.122		415,122	129694.726	
129694.726	30619,241		30619.241	
146.000				
224669,890		224669,890	540.899	
540.899	456,845		456.845	84.054
	84,054	5,435		5.435
415.364		415,364	129237.829	
129237.829	30534,592		30534.592	
147.000				
224896.860		224896.860	541.719	
541.719	457,740		457.740	83.979
	83,979	5,451		5.451
415.154		415,154	128779.852	
128779.852	30449,952		30449.952	
148.000				
225386.150		225386.150	540.615	
540.615	456,547		456.547	84.068
	84,068	5,431		5.431
416.907		416,907	128322.962	
128322.962	30365,326		30365.326	

TABLE AP 2-2 (Sheet 16 of 17)
FIRST BURN ENGINE PERFORMANCE PROGRAM (PA49)

149.000				
225016.690		225016.690	541.448	
541.448	457.310		457.310	84.137
	84.137	5.435		5.435
415.584		415.584	127866.484	
127866.484	30280.495		30280.495	
150.000				
225108.600		225108.600	540.710	
540.710	456.950		456.950	83.760
	83.760	5.455		5.455
416.321		416.321	127409.787	
127409.787	30195.924		30195.924	
151.000				
225496.760		225496.760	539.424	
539.424	455.472		455.472	83.953
	83.953	5.425		5.425
418.032		418.032	126952.808	
126952.808	30111.243		30111.243	
152.000				
225220.310		225220.310	539.454	
539.454	455.437		455.437	84.017
	84.017	5.421		5.421
417.497		417.497	126495.737	
126495.737	30026.636		30026.636	
153.000				
225218.470		225218.470	540.865	
540.865	456.890		456.890	83.975
	83.975	5.441		5.441
416.404		416.404	126038.913	
126038.913	29941.934		29941.934	
154.000				
225042.770		225042.770	542.467	
542.467	458.439		458.439	84.028
	84.028	5.456		5.456
414.851		414.851	125579.953	
125579.953	29857.334		29857.334	
155.000				
225802.750		225802.750	542.547	
542.547	458.708		458.708	83.840
	83.840	5.471		5.471
416.190		416.190	125121.784	
125121.784	29772.700		29772.700	
156.000				
223911.580		223911.580	533.813	
533.813	449.709		449.709	84.104
	84.104	5.347		5.347
419.457		419.457	124663.974	
124663.974	29687.960		29687.960	
157.000				
224793.790		224793.790	537.950	
537.950	453.992		453.992	83.958
	83.958	5.407		5.407
417.871		417.871	124209.274	
124209.274	29603.530		29603.530	
158.000				
224858.590		224858.590	536.670	
536.670	453.067		453.067	83.603
	83.603	5.419		5.419
418.989		418.989	123753.367	
123753.367	29519.179		29519.179	

TABLE AP 2-2 (Sheet 17 of 17)
FIRST BURN ENGINE PERFORMANCE PROGRAM (PA49)

159.000				
224660.860		224660.860	536.215	
536.215	452.186		452.186	84.029
	84.029	5.381		5.381
418.975		418.975	123300.418	
123300.418	29434.635		29434.635	
160.000				
224160.050		224160.050	538.173	
538.173	454.179		454.179	83.994
	83.994	5.407		5.407
416.521		416.521	122845.946	
122845.946	29349.955		29349.955	
161.000				
224610.880		224610.880	538.673	
538.673	454.576		454.576	84.097
	84.097	5.405		5.405
416.971		416.971	122390.111	
122390.111	29265.362		29265.362	
162.000				
224324.030		224324.030	538.079	
538.079	454.267		454.267	83.811
	83.811	5.420		5.420
416.898		416.898	121934.351	
121934.351	29180.820		29180.820	
163.000				
223175.990		223175.990	535.810	
535.810	451.994		451.994	83.816
	83.816	5.393		5.393
416.520		416.520	121479.160	
121479.160	29096.319		29096.319	
164.000				
224201.490		224201.490	538.887	
538.887	454.861		454.861	84.026
	84.026	5.413		5.413
416.046		416.046	121024.568	
121024.568	29011.693		29011.693	
165.000				
223765.750		223765.750	538.777	
538.777	455.046		455.046	83.731
	83.731	5.435		5.435
415.322		415.322	120568.615	
120568.615	28927.140		28927.140	
166.000				
223119.670		223119.670	534.258	
534.258	450.465		450.465	83.794
	83.794	5.376		5.376
417.625		417.625	120113.976	
120113.976	28842.513		28842.513	
167.000				
224565.040		224565.040	538.407	
538.407	454.641		454.641	83.767
	83.767	5.427		5.427
417.091		417.091	119658.943	
119658.943	28757.957		28757.957	
168.000				
223492.730		223492.730	538.863	
538.863	455.095		455.095	83.768
	83.768	5.433		5.433
414.748		414.748	119204.098	
119204.098	28673.478		28673.478	
169.000				
224158.990		224158.990	535.965	
535.965	452.077		452.077	83.888
	83.888	5.389		5.389
418.234		418.234	118750.471	
118750.471	28588.966		28588.966	
169.766				
222836.240		222836.240	519.595	
519.595	435.632		435.632	83.963
	83.963	5.189		5.189
428.908		428.908	118403.599	
118403.599	28524.238		28524.238	

APPENDIX 3

OBSERVED TRAJECTORY (AA83)

1. OBSERVED TRAJECTORY (AA83)

This appendix presents a detailed tabulation of the AS-502 vehicle observed trajectory from guidance reference release (R0 -16.845 sec) to launch vehicle/spacecraft (LV/SC) separation (R0 +11,667.8 sec). The trajectory data was obtained from various radar tracking histories, explained in table AP 3-1, while the aerodynamic data is based on the final meteorological summary of appendix 5.

Table AP 3-2 presents the definition of symbols for the trajectory parameters furnished in tables AP 3-3 and AP 3-4. All trajectory parameters are consistent with Project Apollo Coordinate System Standards. Table AP 3-3 presents the observed trajectory from guidance reference release to parking orbit insertion. Vehicle radar parameters were calculated for KSC launch complex 39A, Cape Tel 4, Grand Bahama, Bermuda, and the Insertion Ship, sites one through five, respectively. Table AP 3-4 presents the observed trajectory from parking orbit insertion to LV/SC separation. Vehicle radar parameters were calculated for Bermuda, Canary Island, Carnarvon, Hawaii, and Guaymas, sites one through five, respectively. Table AP 3-5 presents the vehicle acquisition and loss times for each of these radar stations.

TABLE AP 3-1
TRACKING HISTORY

-16.845 sec to 757.04 sec	Boost composite fit of final Glotrac (Sta 1) and Bermuda, 3.18, 1.16, 0.18, and 19.18 C-band radars (CMP)
757.04 sec to 11,667.8 sec	Orbit fit of Redstone tracking ship, Carnarvon, White Sands, Mila, and Hawaii C-band radars

TABLE AP 3-2 (Sheet 1 of 39)
SATURN OBSERVED TRAJECTORY - BOOST PHASE (AA83)

1	TIME (SEC)	ALTITUDE (FEET)	RANGE (FEET)	GAMMA SB 1 (DEG,)	GAMMA SB 2 (DEG,)
2	V SB E (FT/SEC)	V SB I (FT/SEC)	A SB I (FT/SSQ)	GAMMA(1I) PR (DEG,)	GAMMA(2I) PR (DEG,)
3	X SB E (FEET)	X SB S (FEET)	X SB SFE (FEET)	XI (METERS)	X SB GS (FEET)
4	Y SB E (FEET)	Y SB S (FEET)	Y SB SFE (FEET)	ETA (METERS)	Y SB GS (FEET)
5	Z SB E (FEET)	Z SB S (FEET)	Z SB SFE (FEET)	ZETA (METERS)	Z SB GS (FEET)
6	D-X SB E (FT/SEC)	D-X SB S (FT/SEC)	D-X SB SFE (FT/SEC)	D-XI (M/SEC)	D-X SB GS (FT/SEC)
7	D-Y SB E (FT/SEC)	D-Y SB S (FT/SEC)	D-Y SB SFE (FT/SEC)	D-ETA (M/SEC)	D-Y SB GS (FT/SEC)
8	D-Z SB E (FT/SEC)	D-Z SB S (FT/SEC)	D-Z SB SFE (FT/SEC)	D-ZETA (M/SEC)	D-Z SB GS (FT/SEC)
9	DD-X SB E (FT/SSQ)	V SB W (FT/SEC)	ALPHA SB WIND (DEG,)	MU (DEG,)	RHO (DEG,)
10	DD-Y SB E (FT/SSQ)	E SB W (DEG,)	BETA SB WIND (DEG,)	TEMPERATURE (DEG R)	DENSITY (SL/FT3)
11	DD-Z SB E (FT/SSQ)	V SB RM (FT/SEC)	MACH NUMBER	PRESSURE (LB/FT2)	DYN PRESS Q (LB/FT2)
12	RANGE ANGLE (DEG,)	REYN/L (1/FT)	VISCOSITY (LB-S/FT2)	REL HUMID (PERCENT)	SOUND VEL (FT/SEC)
13	D* SB 1 (FEET)	D* SB 2 (FEET)	D* SB 3 (FEET)	D* SB 4 (FEET)	D* SB 5 (FEET)
14	A* SB 1 (DEG,)	A* SB 2 (DEG,)	A* SB 3 (DEG,)	A* SB 4 (DEG,)	A* SB 5 (DEG,)
15	E* SB 1 (DEG,)	E* SB 2 (DEG,)	E* SB 3 (DEG,)	E* SB 4 (DEG,)	E* SB 5 (DEG,)

GUIDANCE REFERENCE RELEASE

1	-16.8450	193.3564	.5455	90.0000	.0000
2	.0000	1340.6744	32.140	.0000	90.0000
3	193.6	.0	-3137778.700	.000	.000
4	.0	.0	18115556.0	.000	.000
5	.0	.0	9960274.6	.000	.000
6	.000	.000	-1321.021	-.0000	.000
7	.000	414.291	-228.716	.0012	.000
8	.000	1275.057	.0000	.0036	.000
9	.000	27.596	-90.0000	-80.6042	28.6084
10	.000	147.200	-75.1764	526.9597	.0023224
11	.000	27.571	.0244	2115.2772	.8827
12	.0000	555417.8200	.0000	.8546	344.1884
13	193.4	54911.5	1036753.1	5186520.1	11129393.7
14	.0000	16.6024	314.4925	259.0173	273.9795
15	89.9901	.1262	-1.4115	-7.1129	-15.4072

S-IC ENGINE START COMMAND

1	-8.7700	193.3564	.5455	90.0000	.0000
2	.0000	1340.6744	32.140	.0000	90.0000
3	193.6	-2.8	-3148445.300	319.245	-1050.189
4	.0	3343.9	18113706.0	.027	-1.509
5	.0	10296.6	9960274.4	.081	.300
6	.000	-.693	-1320.886	79.0699	-260.109
7	.000	413.932	-229.494	.0076	-.381
8	.000	1275.174	.0000	.0230	.053
9	.000	27.596	-90.0000	-80.6042	28.6084
10	.000	147.200	-75.1602	526.9597	.0023224
11	.000	27.571	.0244	2115.2772	.8827
12	.0000	555417.8200	.0000	.8546	344.1884
13	193.4	54911.5	1036753.1	5186520.1	11129393.6
14	.0000	16.6024	314.4925	259.0173	273.9795
15	89.9901	.1262	-1.4115	-7.1129	-15.4072

TABLE AP 3-2 (Sheet 2 of 39)
SATURN OBSERVED TRAJECTORY - BOOST PHASE (AA83)

RANGE ZERO

1	.0000	193.3564	.5455	90.0000	.0000
2	.0000	1340.6744	32.140	.0000	90.0000
3	193.6	-12.2	-3160028.800	1389.251	-4570.086
4	.0	6972.4	18111689.0	.176	-6.829
5	.0	21480.4	9960274.1	.535	.490
6	.000	-1.446	-1320.739	164.9451	-542.604
7	.000	413.541	-230.339	.0288	-.841
8	.000	1275.300	.0000	.0881	-.035
9	.000	27.596	-90.0000	-80.6042	28.6084
10	.000	147.200	-75.1425	526.9597	.0023224
11	.000	27.571	.0244	2115.2772	.8827
12	.0000	555417.8300	.0000	.8546	344.1884
13	193.4	54911.5	1036753.1	5186520.1	11129393.7
14	.0000	16.6024	314.4925	259.0173	273.9795
15	89.9901	.1262	-1.4115	-7.1129	-15.4072

FIRST MOTION

1	.3800	193.3564	.5455	90.0000	.0000
2	.0000	1340.6744	35.420	.0000	90.0000
3	193.6	-12.7	-3160530.600	1452.637	-4778.601
4	.0	7129.6	18111601.0	.187	-7.153
5	.0	21965.0	9960274.1	.569	.476
6	.000	-1.478	-1320.733	168.6661	-554.845
7	.000	413.524	-230.376	.0301	-.862
8	.000	1275.306	.0000	.0920	-.042
9	3.281	27.596	-90.0000	-80.6042	28.6084
10	.000	147.200	-75.1417	526.9597	.0023224
11	.000	27.571	.0244	2115.2772	.8827
12	.0000	555417.8300	.0000	.8546	344.1884
13	193.4	54911.5	1036753.1	5186520.1	11129393.7
14	.0000	16.6024	314.4925	259.0173	273.9795
15	89.9901	.1262	-1.4115	-7.1129	-15.4072

LIFTOFF SIGNAL - TB 1

1	.6900	193.6412	.1954	87.2967	220.3412
2	1.3122	1340.6350	37.474	.0560	90.0019
3	193.8	-12.9	-3160940.300	1505.477	-4952.151
4	.6	7258.4	18111531.0	.391	-7.423
5	-.0	22360.3	9960273.7	.594	.462
6	1.311	-.194	-1320.890	172.1011	-564.830
7	.032	413.543	-229.243	.0412	-.879
8	-.053	1275.259	.5862	.0796	-.048
9	5.335	27.598	-82.3214	-80.6042	28.6084
10	-.012	147.183	103.5285	526.9600	.0023224
11	-.025	27.619	.0245	2115.2572	.8858
12	.0000	556374.2300	.0000	.8545	344.1885
13	193.6	54911.0	1036752.6	5186520.3	11129393.7
14	160.9496	16.6028	314.4925	259.0173	273.9795
15	89.8336	.1265	-1.4114	-7.1129	-15.4072

START YAW MANEUVER

1	1.9000	205.3166	1.8164	88.5130	236.7543
2	11.2023	1340.4789	40.923	.4787	90.0055
3	205.3	-3.3	-3162540.600	1723.906	-5659.176
4	2.4	7760.4	18111262.0	.959	-8.528
5	-.2	23903.3	9960277.6	.655	.389
6	11.198	9.590	-1322.172	186.9632	-603.806
7	.076	413.537	-220.720	.0601	-.947
8	-.280	1275.060	5.2222	.0269	-.073
9	8.783	27.676	-34.1508	-80.6042	28.6084
10	.002	146.483	115.9181	526.9701	.0023214
11	-.146	29.807	.0264	2114.4174	1.0312
12	.0000	600190.9700	.0000	.8524	344.1896
13	205.2	54909.5	1036751.5	5186521.9	11129396.9
14	167.3974	16.6036	314.4924	259.0173	273.9795
15	89.3457	.1385	-1.4108	-7.1127	-15.4072

1	5.0000	278.5015	10.1728	87.8164	207.8672
2	39.2345	1340.5555	41.432	1.6761	90.0518
3	278.7	64.6	-3166645.300	2362.321	-7685.752
4	10.2	9049.8	18110614.0	3.496	-11.739
5	-3.9	27853.3	9960305.1	-.043	.044
6	39.206	37.332	-1326.008	225.8549	-703.662
7	1.041	414.379	-196.172	.3708	-1.125
8	-1.073	1274.357	17.6125	-.1634	-.152
9	9.291	28.070	-13.6248	-80.6042	28.6084
10	.035	142.409	143.9750	527.0345	.0023154
11	-.372	48.541	.0430	2109.0626	2.7279
12	.0000	974824.8800	.0000	.8390	344.1968
13	278.7	54901.3	1036748.2	5186534.7	11129419.4
14	182.9297	16.6052	314.4921	259.0172	273.9795
15	87.7468	.2151	-1.4068	-7.1119	-15.4068

TABLE AP 3-2 (Sheet 3 of 39)
SATURN OBSERVED TRAJECTORY - BOOST PHASE (AA83)

	STOP YAW MANEUVER				
1	9.8000	579.7837	46.3304	87.7315	207.3903
2	85.8435	1341.8853	42.304	3.6653	90.1187
3	579.9	355.9	-3173034.600	3593.673	-11434.400
4	46.0	11069.1	18109783.0	14.718	-17.827
5	-13.7	33965.9	9960416.6	-2.013	-1.049
6	85.776	83.492	-1332.301	287.0503	-858.274
7	2.386	415.545	-155.420	.8145	-1.414
8	-2.419	1273.188	38.4227	-.4714	-.311
9	10.164	39.013	-12.1743	-80.6042	28.6083
10	.066	133.930	155.4622	527.2987	.0022911
11	-.374	94.623	.0838	2087.2172	10.2566
12	.0001	1879530.3000	.0000	.7839	344.2246
13	581.8	54869.0	1036729.1	5186582.6	11129506.7
14	178.6588	16.6179	314.4906	259.0168	273.9793
15	85.2678	.5300	-1.3901	-7.1087	-15.4053
1	10.0000	597.7240	48.2867	87.6995	206.1970
2	87.8661	1342.0236	42.350	3.7513	90.1248
3	597.8	373.3	-3173301.800	3651.504	-11606.699
4	47.9	11153.7	18109753.0	15.333	-18.111
5	-14.2	34220.6	9960423.5	-2.095	-1.112
6	87.795	85.494	-1332.624	289.6240	-864.716
7	2.529	415.681	-153.625	.8595	-1.426
8	-2.459	1273.157	39.2598	-.4786	-.319
9	10.210	39.128	-12.0179	-80.6042	28.6083
10	.067	133.712	155.7761	527.3145	.0022897
11	-.339	96.545	.0855	2085.9277	10.6709
12	.0001	1916469.9000	.0000	.7807	344.2262
13	599.7	54867.5	1036728.2	5186585.3	11129511.9
14	178.5024	16.6186	314.4906	259.0168	273.9793
15	85.2300	.5485	-1.3891	-7.1085	-15.4052
	START PITCH AND ROLL MANEUVERS				
1	11.0100	688.4146	61.2536	87.9138	207.3361
2	98.2897	1342.6667	42.581	4.1957	90.1241
3	688.3	461.4	-3174652.100	3949.566	-12496.491
4	61.0	11584.1	18109603.0	19.405	-19.582
5	-16.6	35506.6	9960455.4	-2.549	-1.454
6	98.225	95.836	-1334.115	302.6923	-897.248
7	2.515	415.632	-144.684	.8637	-1.489
8	-2.545	1273.114	44.2415	-.4795	-.358
9	10.442	39.476	-11.1010	-80.6042	28.6083
10	.069	133.000	158.0676	527.3940	.0022824
11	-.172	106.210	.0940	2079.4148	12.8734
12	.0002	2101395.4000	.0000	.7641	344.2339
13	691.1	54856.4	1036720.1	5186599.2	11129537.5
14	177.2592	16.6243	314.4901	259.0166	273.9792
15	84.7518	.6434	-1.3841	-7.1075	-15.4048
1	15.0000	1165.8328	33.5763	88.9147	191.9210
2	141.8243	1347.6661	43.568	6.0400	90.0953
3	1165.8	928.7	-3179969.200	5261.341	-16332.903
4	23.6	13194.8	18109080.0	8.478	-26.025
5	-27.6	40585.8	9960711.9	-4.514	-3.223
6	141.799	139.068	-1341.742	355.0406	-1025.764
7	2.328	415.311	-107.845	.8433	-1.743
8	-1.340	1274.512	65.5887	.0002	-.534
9	11.425	39.770	-6.5898	-80.6042	28.6084
10	-.270	137.787	163.8387	525.9172	.0022508
11	.679	147.639	.1309	2044.8427	24.5303
12	.0001	2886850.5000	.0000	.7906	343.7510
13	1166.3	54889.6	1036770.3	5186668.6	11129677.1
14	211.4033	16.5927	314.4906	259.0171	273.9794
15	88.2111	1.1413	-1.3577	-7.1022	-15.4024
1	20.0000	2015.2902	33.5427	88.2522	65.4979
2	201.3768	1361.3462	44.844	8.5024	89.8675
3	2015.6	1763.8	-3186704.500	7201.856	-21864.318
4	28.7	15264.4	18108656.0	10.837	-35.563
5	-25.9	46967.5	9961114.9	-1.526	-6.534
6	201.283	198.108	-1356.425	422.1200	-1186.800
7	-.695	412.130	-60.417	-.0253	-2.075
8	6.102	1282.251	98.6146	2.4395	-.799
9	12.640	39.203	-3.7112	-80.6042	28.6083
10	-.576	142.574	-10.3686	521.9185	.0022004
11	2.429	205.333	.1827	1984.1742	46.3865
12	.0001	3948445.4000	.0000	.9012	342.4658
13	2015.8	54912.2	1036787.4	5186772.4	11129901.1
14	203.9888	16.5973	314.4905	259.0170	273.9794
15	88.9010	2.0278	-1.3108	-7.0929	-15.3982

TABLE AP 3-2 (Sheet 4 of 39)
SATURN OBSERVED TRAJECTORY - BOOST PHASE (AA83)

1	25.0000	3187.3901	40.3526	84.9441	62.8328
2	269.1644	1388.1521	46.399	11.1352	89.5126
3	3187.6	2918.8	-3193538.300	9485.276	-28200.878
4	18.8	17318.3	18108483.0	8.905	-46.801
5	36.2	53411.3	9961701.0	20.809	-11.291
6	268.117	264.465	-1381.253	491.4248	-1347.821
7	-3.779	408.892	-9.744	-.9059	-2.423
8	23.418	1299.936	137.8883	7.9255	-1.112
9	14.038	37.850	-1.8328	-80.6040	28.6084
10	-.517	148.864	-7.7885	516.7385	.0021324
11	4.596	271.951	.2433	1902.7431	78.8535
12	.0001	5107285.2000	.0000	.9589	340.6704
13	3187.7	55012.6	1036798.5	5186856.4	11130153.7
14	99.3865	16.6447	314.4938	259.0171	273.9794
15	89.2659	3.2461	-1.2460	-7.0800	-15.3923
1	30.0000	4710.3303	217.8133	81.2853	65.1723
2	345.1702	1429.9006	47.896	13.8018	89.0542
3	4710.6	4422.2	-3200525.200	12120.279	-35342.494
4	-5.0	19357.4	18108570.0	3.019	-59.819
5	213.0	59971.7	9962498.0	79.239	-17.740
6	341.185	337.007	-1417.534	562.6082	-1508.821
7	-6.218	406.297	43.058	-1.5859	-2.787
8	51.931	1328.896	182.6462	16.8636	-1.476
9	15.316	25.982	-1.2561	-80.6035	28.6086
10	-.447	144.931	-4.1078	521.6689	.0020084
11	6.570	346.785	.3095	1801.5315	120.7636
12	.0006	6088788.5000	.0000	.2522	341.5679
13	4715.2	55243.7	1036778.5	5186870.3	11130390.5
14	70.6323	16.7819	314.5030	259.0173	273.9796
15	87.4094	4.8157	-1.1618	-7.0631	-15.3845
	STOP ROLL MANEUVER				
1	30.2000	4778.9596	227.9530	81.1398	65.2415
2	348.3831	1431.8664	47.962	13.9077	89.0336
3	4779.1	4489.9	-3200808.300	12233.084	-35644.902
4	-6.3	19438.6	18108579.0	2.694	-60.378
5	223.0	60237.1	9962534.5	82.494	-18.037
6	344.225	340.025	-1419.204	565.4910	-1515.260
7	-6.315	406.194	45.204	-1.6131	-2.802
8	53.290	1330.275	184.5522	17.2886	-1.492
9	15.372	24.640	-1.2014	-80.6035	28.6086
10	-.442	144.605	-3.8538	522.1051	.0020022
11	6.654	349.895	.3121	1797.1188	122.5591
12	.0006	6120411.8000	.0000	.2255	341.6785
13	4784.2	55256.2	1036776.8	5186869.0	11130399.1
14	70.4025	16.7898	314.5035	259.0173	273.9796
15	87.3272	4.8860	-1.1580	-7.0623	-15.3842
1	35.0000	6614.3062	564.9877	77.8481	67.2242
2	430.4680	1485.8959	49.474	16.4479	88.5418
3	6614.8	6304.1	-3207718.100	15116.000	-43289.044
4	-40.5	21384.1	18108927.0	-6.063	-74.695
5	556.4	66701.2	9963532.4	189.778	-26.135
6	420.820	416.056	-1464.292	635.7673	-1669.794
7	-7.546	404.807	98.862	-1.9245	-3.166
8	90.312	1367.814	232.2989	28.8521	-1.891
9	16.571	14.069	-1.3436	-80.6026	28.6090
10	-.173	114.648	-1.2638	517.0748	.0018879
11	8.779	432.681	.3873	1682.6462	176.7212
12	.0015	7190529.6000	.0000	.5993	340.4737
13	6638.1	55665.1	1036703.2	5186767.0	11130569.3
14	67.8341	17.0532	314.5206	259.0176	273.9799
15	85.1789	6.7486	-1.0564	-7.0417	-15.3746
1	40.0000	8934.6454	1133.4366	74.3954	68.7740
2	526.5972	1558.9647	51.174	18.9802	87.9508
3	8935.0	8598.9	-3215176.100	18482.858	-52040.383
4	-79.2	23406.8	18109570.0	-15.819	-91.506
5	1121.4	73655.3	9964828.6	369.450	-36.733
6	507.180	501.749	-1524.109	710.9410	-1830.735
7	-7.977	404.200	156.799	-1.9893	-3.561
8	141.455	1419.592	287.8842	44.7765	-2.358
9	17.778	10.607	.5060	-80.6009	28.6096
10	-.083	189.191	-1.0281	512.3436	.0017578
11	11.404	525.230	.4732	1546.8794	242.4642
12	.0031	8185550.6000	.0000	.1421	338.3121
13	9005.3	56344.7	1036542.5	5186496.6	11130646.3
14	67.9571	17.5063	314.5491	259.0179	273.9803
15	82.8283	9.0478	-.9278	-7.0155	-15.3623

TABLE AP 3-2 (Sheet 5 of 39)
SATURN OBSERVED TRAJECTORY - BOOST PHASE (AA83)

1	45.0000	11702.4139	1993.2403	70.9241	69.7341
2	634.2538	1650.2335	53.099	21.2915	87.2606
3	11702.7	11337.6	-3222968.700	22230.267	-61596.331
4	-120.3	25426.0	18110505.0	-25.980	-110.330
5	1978.4	80904.8	9966420.6	639.894	-49.801
6	599.405	593.202	-1598.245	787.8588	-1991.637
7	-8.209	403.765	215.264	-1.9969	-3.971
8	207.181	1486.054	350.0678	65.1930	-2.879
9	18.964	2.757	.1304	-80.5984	28.6104
10	.000	308.594	-1.6401	500.2997	.0016247
11	14.560	633.798	.5776	1397.1695	326.3275
12	.0055	9301096.5000	.0000	.3568	334.4356
13	11869.2	57376.8	1036266.3	5185994.2	11130562.4
14	68.5186	18.1930	314.5919	259.0182	273.9808
15	80.3871	11.6914	-.7742	-6.9840	-15.3474
1	50.0000	14946.4124	3219.3185	67.5514	70.4582
2	754.7344	1760.1701	55.126	23.3369	86.5107
3	14946.4	14548.1	-3231170.200	26366.653	-71956.673
4	-160.3	27445.4	18111735.0	-35.493	-131.243
5	3202.4	88525.2	9968339.0	1024.253	-65.618
6	697.498	690.397	-1687.525	866.5124	-2152.492
7	-7.782	403.952	274.198	-1.8102	-4.397
8	288.201	1567.921	418.6602	90.3221	-3.457
9	20.066	5.414	.0595	-80.5948	28.6116
10	.061	333.230	-1.5506	486.4273	.0014789
11	17.856	754.506	.6976	1235.8408	420.9454
12	.0088	10304155.5000	.0000	.3911	329.6817
13	15286.4	58867.3	1035841.1	5185189.7	11130253.8
14	69.1341	19.1624	314.6524	259.0184	273.9815
15	77.8921	14.6303	-.5938	-6.9467	-15.3296
1	55.0000	18696.0310	4893.0071	64.2185	70.7453
2	889.4163	1889.8537	57.257	25.0614	85.6508
3	18695.8	18259.5	-3239859.200	30900.826	-83121.159
4	-200.4	29463.2	18113256.0	-44.779	-154.322
5	4874.7	96598.5	9970621.2	1547.570	-84.474
6	800.793	792.641	-1793.347	946.6885	-2313.293
7	-8.524	402.917	331.524	-1.9912	-4.838
8	386.935	1667.611	495.5256	120.9023	-4.095
9	20.989	17.558	1.0126	-80.5899	28.6131
10	.125	242.788	-.8963	473.6992	.0013131
11	21.505	881.976	.8265	1068.0469	510.7034
12	.0134	10921820.4000	.0000	.3567	325.2606
13	19321.7	60938.9	1035236.3	5184007.1	11129650.0
14	69.6443	20.4536	314.7349	259.0184	273.9823
15	75.3742	17.7870	-.3848	-6.9033	-15.3088
1	60.0000	22972.4240	7106.0755	60.9198	70.9732
2	1038.5323	2039.7182	59.167	26.4068	84.7516
3	22971.5	22491.5	-3249121.500	35838.674	-95089.498
4	-244.0	31476.0	18115059.0	-54.939	-179.644
5	7087.3	105217.2	9973304.9	2238.133	-106.678
6	907.444	898.057	-1917.379	1027.8127	-2474.032
7	-9.144	401.936	385.633	-2.1512	-5.294
8	504.986	1786.727	579.1352	157.4227	-4.797
9	21.624	19.389	.9322	-80.5834	28.6151
10	.192	260.916	-1.1758	458.0027	.0011449
11	24.870	1029.383	.9813	899.9074	606.5891
12	.0195	11418278.7000	.0000	.1697	319.7367
13	24041.0	63724.5	1034419.7	5182359.4	11128669.5
14	70.0279	22.0958	314.8439	259.0184	273.9832
15	72.8439	21.0492	-.1457	-6.8533	-15.2845
	MACH 1				
1	60.5050	23434.6810	7363.8911	60.6146	71.0001
2	1054.4861	2055.7883	59.361	26.5327	84.6642
3	23433.6	22948.8	-3250093.200	36360.122	-96342.983
4	-248.1	31679.5	18115256.0	-55.859	-182.330
5	7345.2	106122.3	9973599.5	2318.517	-109.120
6	918.633	909.111	-1930.685	1036.1291	-2490.263
7	-9.133	401.907	391.244	-2.1458	-5.341
8	517.659	1799.515	587.9219	161.3433	-4.872
9	21.683	15.079	.7181	-80.5827	28.6153
10	.199	250.875	-.9769	456.1771	.0011280
11	25.204	1047.161	1.0003	883.0795	618.4738
12	.0202	11481140.6000	.0000	.1471	319.0924
13	24558.9	64050.8	1034323.4	5182163.1	11128545.6
14	70.0656	22.2826	314.8566	259.0184	273.9834
15	72.5872	21.3798	-.1199	-6.8478	-15.2819

TABLE AP 3-2 (Sheet 6 of 39)
SATURN OBSERVED TRAJECTORY - BOOST PHASE (AA83)

1	65.0000	27789.0820	9948.7718	57.8853	71.3179
2	1200.6319	2206.0397	61.503	27.4327	83.9221
3	27786.8	27256.4	-3259044.100	41183.882	-107861.359
4	-286.8	33487.6	18117126.0	-64.751	-207.285
5	9931.2	114472.7	9976417.5	3123.951	-132.559
6	1016.615	1005.800	-2056.891	1109.6247	-2634.701
7	-7.767	402.877	437.651	-1.7207	-5.765
8	638.710	1921.632	666.5374	198.7763	-5.567
9	22.451	20.600	.6795	-80.5750	28.6176
10	.259	288.193	-1.3443	437.7597	.0009803
11	28.504	1192.032	1.1624	736.3311	696.4651
12	.0273	11742336.2000	.0000	.0976	312.5639
13	29509.5	67347.4	1033355.1	5180159.6	11127228.7
14	70.3462	24.0992	314.9839	259.0183	273.9844
15	70.3251	24.2855	.1244	-6.7964	-15.2567
1	70.0000	33162.6500	13503.2101	55.0582	71.5725
2	1380.1774	2391.9372	64.207	28.2098	83.1046
3	33158.6	32570.1	-3269708.000	46941.166	-121436.375
4	-321.5	35504.9	18119448.0	-72.109	-237.320
5	13489.5	124448.9	9979983.7	4230.622	-162.470
6	1130.870	1118.403	-2214.399	1192.8938	-2795.291
7	-6.177	403.944	488.106	-1.2471	-6.251
8	791.191	2075.420	761.2841	245.9080	-6.410
9	23.526	30.936	1.0307	-80.5646	28.6207
10	.319	267.000	-.8875	413.9691	.0008192
11	32.186	1363.338	1.3672	581.8676	761.3281
12	.0370	11748450.4000	.0000	.1500	303.9439
13	35798.7	71919.3	1032010.3	5177329.4	11125253.0
14	70.6344	26.4448	315.1590	259.0179	273.9858
15	67.8568	27.3712	.4270	-6.7324	-15.2251
1	75.0000	39123.7740	17868.5680	52.3809	71.7822
2	1579.1306	2599.3143	67.530	28.7428	82.3125
3	39116.3	38460.9	-3281209.400	53119.026	-135814.130
4	-348.0	37527.5	18122017.0	-77.088	-269.824
5	17862.2	135246.3	9984044.5	5588.964	-196.789
6	1249.985	1235.601	-2392.282	1277.5372	-2955.794
7	-4.108	405.382	536.082	-.6560	-6.753
8	964.973	2250.643	863.7366	299.5966	-7.331
9	24.138	69.029	2.0340	-80.5516	28.6245
10	.425	254.999	-.4890	388.4236	.0006615
11	37.505	1537.994	1.5923	440.8581	782.4078
12	.0490	11285035.2000	.0000	.1870	294.4093
13	43003.1	77564.2	1030355.4	5173775.9	11122655.4
14	70.8838	29.0947	315.3744	259.0172	273.9875
15	65.4524	30.2001	.7643	-6.6606	-15.1895
	MAXIMUM DYNAMIC PRESSURE				
1	75.2430	39428.8810	18103.3950	52.2490	71.7888
2	1589.3845	2610.0664	67.733	28.7605	82.2730
3	39421.5	38762.6	-3281791.700	53430.198	-136533.330
4	-348.9	37626.1	18122149.0	-77.209	-271.468
5	18097.5	135794.0	9984255.2	5662.019	-198.576
6	1255.853	1241.368	-2401.589	1281.6717	-2963.592
7	-4.042	405.414	538.235	-.6387	-6.778
8	974.145	2259.888	868.9793	302.4289	-7.378
9	24.163	67.664	1.9777	-80.5510	28.6247
10	.431	251.000	-.3052	387.1465	.0006540
11	37.830	1548.836	1.6061	434.4215	784.4783
12	.0496	11266792.9000	.0000	.1762	293.9245
13	43378.3	77868.1	1030266.3	5173582.9	11122511.8
14	70.8954	29.2305	315.3861	259.0171	273.9876
15	65.3371	30.3293	.7816	-6.6569	-15.1877
1	80.0000	45689.7640	23172.0630	49.6128	71.9483
2	1801.9943	2834.4722	71.187	28.9387	81.5229
3	45677.4	44944.6	-3293669.100	59722.129	-150994.160
4	-363.8	39557.3	18124811.0	-79.084	-304.674
5	23177.8	146994.1	9988641.0	7238.474	-235.926
6	1371.258	1354.613	-2598.285	1362.7039	-3116.200
7	-1.744	406.957	576.289	-.0184	-7.270
8	1169.116	2456.348	975.2125	362.6025	-8.338
9	24.211	83.143	2.0593	-80.5360	28.6290
10	.552	259.000	-.5206	375.5370	.0004957
11	43.662	1749.653	1.8422	319.3946	758.7882
12	.0635	9897887.5000	.0000	.0000	289.4806
13	51222.6	84408.4	1028349.4	5169376.6	11119318.8
14	71.1008	32.0006	315.6369	259.0162	273.9894
15	63.0927	32.6747	1.1379	-6.5808	-15.1496

TABLE AP 3-2 (Sheet 7 of 39)
SATURN OBSERVED TRAJECTORY - BOOST PHASE (AA83)

1	85.0000	52860.3350	29568.3020	46.7673	72.0932
2	2048.3097	3096.6103	75.545	28.7859	80.7643
3	52839.7	52017.2	-3307229.700	66749.118	-166975.950
4	-367.1	41595.2	18127775.0	-77.825	-342.545
5	29592.7	159849.3	9993813.1	9227.085	-280.327
6	1490.374	1471.077	-2833.208	1447.0617	-3276.501
7	1.234	408.953	604.616	.7520	-7.801
8	1405.118	2694.010	1093.7866	435.3770	-9.438
9	23.509	63.018	1.0545	-80.5170	28.6345
10	.711	288.603	-1.1070	371.2888	.0003505
11	51.225	2014.345	2.1331	223.2801	711.1321
12	.0810	8135418.3000	.0000	.0000	287.8376
13	60563.0	92577.2	1025943.9	5163979.5	11115092.9
14	71.2894	35.0994	315.9547	259.0148	273.9916
15	60.7473	34.7149	1.5486	-6.4926	-15.1052
1	90.0000	60619.3150	37224.3290	43.8563	72.1840
2	2319.7543	3386.5947	79.508	28.3049	80.0284
3	60586.7	59660.2	-3322045.200	74194.172	-183758.970
4	-351.7	43646.3	18130845.0	-71.724	-382.911
5	37275.9	173981.4	9999593.7	11606.659	-330.478
6	1604.274	1581.878	-3098.524	1529.6585	-3436.687
7	3.807	410.312	617.156	1.3329	-8.348
8	1675.575	2966.198	1219.5480	518.7064	-10.640
9	22.300	7.263	.0305	-80.4943	28.6409
10	-.152	328.377	-.1288	368.0797	.0002387
11	58.063	2318.523	2.4658	150.7507	641.6328
12	.1020	6424564.5000	.0000	.0000	286.5904
13	71136.1	102187.1	1023086.5	5157418.3	11109813.6
14	71.4594	38.3118	316.3371	259.0129	273.9942
15	58.3969	36.2732	1.9967	-6.3958	-15.0560
1	95.0000	68943.2320	46308.2870	41.0051	72.1323
2	2619.4485	3705.2339	83.617	27.6062	79.2694
3	68892.2	67845.0	-3338259.600	82048.390	-201342.610
4	-335.8	45691.2	18133935.0	-66.678	-426.049
5	46398.0	189561.1	10006031.7	14429.383	-386.911
6	1714.318	1688.345	-3393.061	1610.8964	-3596.748
7	2.273	407.308	613.565	.5885	-8.910
8	1980.561	3272.973	1356.2595	612.6116	-11.953
9	21.618	6.807	.0869	-80.4674	28.6485
10	-.407	279.640	-.1434	381.6109	.0001521
11	64.146	2614.911	2.7313	99.6052	520.1317
12	.1269	4478616.0000	.0000	.0000	291.8135
13	83060.2	113357.2	1019754.2	5149524.1	11103313.3
14	71.5852	41.5312	316.7942	259.0107	273.9972
15	56.0395	37.3358	2.4818	-6.2904	-15.0020
1	100.0000	77816.9420	56982.5110	38.3475	72.1117
2	2946.6365	4050.6436	87.701	26.7974	78.5950
3	77739.5	76552.5	-3356017.700	90305.770	-219726.230
4	-326.9	47721.1	18136974.0	-65.311	-472.033
5	57124.3	206754.1	10013169.9	17745.934	-450.214
6	1821.890	1791.839	-3714.985	1691.1878	-3756.678
7	1.219	404.523	598.115	-.0848	-9.486
8	2315.898	3610.179	1499.6210	715.8298	-13.390
9	21.800	12.292	-.1476	-80.4357	28.6575
10	-.131	70.669	-.1646	393.5225	.0000967
11	69.250	2956.291	3.0407	65.2616	422.3897
12	.1561	3135067.0000	.0000	.0000	296.3350
13	96471.3	126203.7	1015928.2	5140135.4	11095431.6
14	71.6721	44.6600	317.3362	259.0082	274.0009
15	53.6905	37.9320	3.0044	-6.1762	-14.9430
1	105.0000	87248.1410	69380.7240	36.0306	72.1209
2	3301.8072	4421.6111	92.487	26.0225	78.0130
3	87133.0	85784.5	-3375446.200	98966.632	-238909.160
4	-321.4	49738.2	18139922.0	-66.955	-520.938
5	69591.9	225698.1	10021045.1	21598.502	-521.032
6	1933.330	1898.701	-4060.886	1772.4629	-3916.467
7	1.016	402.342	577.967	-.5692	-10.078
8	2676.596	3972.871	1651.0040	826.8575	-14.961
9	22.808	24.937	-.1565	-80.3989	28.6680
10	.005	124.574	-.3412	409.3605	.0000601
11	74.493	3314.143	3.3422	42.1834	329.8386
12	.1901	2113288.4000	.0000	.0000	302.2425
13	111513.6	140836.2	1011607.8	5129120.9	11086040.9
14	71.7353	47.6168	317.9722	259.0054	274.0051
15	51.3858	38.1282	3.5662	-6.0528	-14.8787

TABLE AP 3-2 (Sheet 8 of 39)
SATURN OBSERVED TRAJECTORY - BOOST PHASE (AA83)

1	110.0000	97262.8410	83629.3350	34.0016	72.1379
2	3686.7237	4820.2279	97.760	25.2878	77.5007
3	97095.5	95561.4	-3396668.400	108036.980	-258890.650
4	-316.4	51744.4	18142757.0	-71.028	-572.834
5	83931.5	246524.4	10029700.8	26027.262	-600.076
6	2049.457	2009.704	-4432.376	1854.9547	-4076.106
7	.991	400.070	552.917	-1.0771	-10.683
8	3064.581	4362.985	1811.8855	946.2887	-16.682
9	23.422	6.331	-.0350	-80.3567	28.6800
10	.062	123.153	-.1570	417.6503	.0000376
11	80.523	3690.024	3.6841	26.9544	256.0911
12	.2292	1449472.2000	.0000	.0000	305.2889
13	128343.7	157376.8	1006813.2	5116361.0	11075025.9
14	71.7839	50.3463	318.7114	259.0021	274.0101
15	49.1589	38.0026	4.1701	-5.9196	-14.8088

1	115.0000	107880.3270	99868.6500	32.1481	72.1668
2	4102.4476	5248.5687	103.432	24.5409	77.0512
3	107641.6	105894.6	-3419818.900	117520.085	-279669.960
4	-310.5	53739.5	18145444.0	-77.544	-627.796
5	100287.8	269378.3	10039182.3	31076.825	-688.124
6	2166.372	2120.882	-4832.553	1937.4514	-4235.586
7	1.474	397.990	518.439	-1.5220	-11.304
8	3483.807	4784.448	1981.1953	1075.3248	-18.566
9	23.245	9.770	.0278	-80.3085	28.6937
10	-.025	185.402	-.1256	426.1803	.0000230
11	87.416	4099.180	4.0514	16.7919	192.9371
12	.2737	966846.1300	.0000	.0000	308.3922
13	147120.5	175958.7	1001578.5	5101720.1	11062255.5
14	71.8226	52.8218	319.5645	258.9983	274.0157
15	47.0254	37.6238	4.8186	-5.7758	-14.7330

1	120.0000	119104.0680	118262.2450	30.4100	72.1765
2	4551.6505	5709.6002	109.452	23.7617	76.6341
3	118768.9	116778.7	-3445049.900	127414.000	-301246.230
4	-304.7	55720.7	18147925.0	-87.343	-685.893
5	118829.9	294429.5	10049535.0	36799.083	-786.031
6	2281.775	2229.870	-5264.048	2019.2294	-4394.899
7	.537	394.127	470.439	-2.5062	-11.938
8	3938.404	5241.363	2160.5629	1215.2210	-20.628
9	23.050	38.405	.2236	-80.2539	28.7092
10	-.234	228.350	-.1976	436.3288	.0000144
11	94.553	4521.379	4.4164	10.7998	147.4524
12	.3241	657173.8700	.0000	.0000	312.0442
13	168007.9	196727.8	995951.5	5085037.6	11047571.2
14	71.8530	55.0380	320.5444	258.9941	274.0221
15	44.9852	37.0453	5.5131	-5.6211	-14.6509

1	125.0000	130935.1030	138980.6200	28.7982	72.1897
2	5037.7882	6206.6806	115.970	22.9789	76.2609
3	130472.1	128204.8	-3472518.800	137715.780	-323618.640
4	-305.0	57680.3	18150136.0	-102.758	-747.197
5	139734.4	321854.8	10060809.4	43248.267	-894.727
6	2397.496	2338.428	-5729.718	2100.8226	-4554.034
7	-.659	389.610	410.157	-3.6856	-12.586
8	4430.725	5736.101	2350.5321	1366.7049	-22.885
9	23.223	29.425	.0510	-80.1924	28.7266
10	-.234	324.624	-.6828	452.0599	.0000086
11	101.909	5030.119	4.8271	6.6520	108.4957
12	.3808	422357.9200	.0000	.0000	317.6220
13	191177.1	219841.0	990008.7	5066146.0	11030808.4
14	71.8749	57.0020	321.6651	258.9893	274.0294
15	43.0366	36.3132	6.2551	-5.4548	-14.5624

1	130.0000	143387.7300	162220.0900	27.3141	72.2067
2	5563.7190	6742.6161	123.889	22.2103	75.9279
3	142756.2	140173.9	-3502410.700	148425.470	-346786.270
4	-312.0	59615.4	18152012.0	-124.626	-811.774
5	163204.6	351858.2	10073063.7	50486.863	-1015.232
6	2514.653	2447.611	-6231.753	2182.5488	-4712.983
7	-2.130	384.385	337.791	-5.0764	-13.247
8	4963.012	6270.912	2552.2619	1530.4679	-25.354
9	23.847	37.866	.1405	-80.1234	28.7461
10	-.286	291.263	-.6673	475.4911	.0000050
11	110.491	5537.812	5.1816	4.0678	76.4530
12	.4445	259617.9600	.0000	.0000	325.7532
13	216829.7	245486.3	983848.5	5044853.5	11011779.3
14	71.8904	58.7322	322.9431	258.9840	274.0376
15	41.1763	35.4668	7.0463	-5.2763	-14.4669

TABLE AP 3-2 (Sheet 9 of 39)
SATURN OBSERVED TRAJECTORY - BOOST PHASE (AA83)

1	135.0000	156486.4100	188176.1600	25.9615	72.2285
2	6134.9688	7322.8765	132.843	21.4757	75.6312
3	155635.8	152696.6	-3534912.200	159545.940	-370748.150
4	-326.7	61523.0	18153498.0	-153.865	-879.693
5	189444.3	384643.9	10086360.9	58577.470	-1148.656
6	2636.025	2560.106	-6774.694	2265.2248	-4871.735
7	-3.850	378.438	254.260	-6.6833	-13.922
8	5539.783	6850.341	2768.2858	1707.9016	-28.056
9	24.735	103.605	.4291	-80.0463	28.7679
10	-.505	252.947	-.4862	493.6024	.0000029
11	119.989	6042.016	5.5487	2.4745	53.3308
12	.5156	161149.4100	.0000	.0000	331.9015
13	245176.9	273862.5	977612.8	5020971.3	10990300.0
14	71.9011	60.2498	324.3957	258.9781	274.0468
15	39.4044	34.5410	7.8885	-5.0845	-14.3640

1	140.0000	170269.2100	217080.1700	24.7261	72.2471
2	6757.2790	7953.2786	143.430	20.7762	75.3602
3	169136.1	165792.9	-3570244.100	171083.080	-395503.270
4	-352.7	63396.7	18154536.0	-192.383	-951.019
5	218694.3	420453.8	10100781.0	67594.104	-1296.211
6	2762.683	2676.876	-7363.497	2349.1409	-5030.279
7	-6.734	370.794	158.259	-8.8036	-14.610
8	6166.714	7480.074	3001.4201	1900.7444	-31.010
9	25.823	.000	.0000	-79.9604	28.7922
10	-.658	.000	-.5443	481.5559	.0000017
11	131.088	6757.279	6.2827	1.4191	39.2093
12	.5948	108025.5330	.0000	.0000	327.8248
13	276467.5	305209.5	971488.5	4994276.6	10966155.2
14	71.9075	61.5780	326.0432	258.9716	274.0572
15	37.7180	33.5628	8.7835	-4.8783	-14.2532

STOP PITCH MANEUVER

1	140.9000	172825.7600	222614.3600	24.5134	72.2506
2	6875.4384	8072.8221	145.442	20.6526	75.3142
3	171633.9	168212.7	-3576922.100	173204.430	-400043.350
4	-358.7	63730.0	18154671.0	-200.412	-964.224
5	224298.2	427239.9	10103502.3	69321.349	-1324.371
6	2786.012	2698.305	-7475.074	2364.3639	-5058.795
7	-7.347	369.261	139.383	-9.2328	-14.735
8	6285.677	7599.557	3045.3758	1937.3336	-31.570
9	26.150	.000	.0000	-79.9440	28.7968
10	-.674	.000	-.5574	478.5488	.0000016
11	133.135	6875.438	6.4126	1.2821	36.9038
12	.6100	100423.9860	.0000	.0000	326.7993
13	282432.3	311186.6	970415.8	4989155.2	10961508.9
14	71.9083	61.7987	326.3621	258.9704	274.0593
15	37.4233	33.3830	8.9502	-4.8395	-14.2323

S-IC CENTER ENGINE CUTOFF SIGNAL - TB 2

1	144.7200	183944.8100	247301.1100	23.6529	72.2686
2	7395.2501	8598.2129	153.857	20.1445	75.1313
3	182473.2	178700.9	-3606414.900	182361.800	-419599.000
4	-392.0	65127.6	18155044.0	-239.340	-1021.534
5	249309.2	457274.3	10115504.6	77029.426	-1449.653
6	2886.750	2790.586	-7965.155	2429.3571	-5179.746
7	-10.008	362.484	54.765	-11.1350	-15.271
8	6808.546	8124.686	3237.6818	2098.1488	-34.050
9	27.115	.000	.0000	-79.8706	28.8175
10	-.674	.000	-.6101	464.7552	.0000010
11	141.839	7395.250	6.9991	.8252	28.2972
12	.6776	73278.9500	.0000	.0000	322.0529
13	308952.5	337766.4	966028.1	4966274.4	10940701.1
14	71.9098	62.6780	327.7974	258.9649	274.0682
15	36.2009	32.6097	9.6774	-4.6691	-14.1406

1	145.0000	184776.5100	249186.2100	23.5935	72.2699
2	7430.6367	8633.9922	138.940	20.1077	75.1198
3	183282.4	179483.0	-3608649.200	183042.630	-421050.580
4	-394.8	65229.0	18155058.0	-242.469	-1025.815
5	251219.9	459553.6	10116412.6	77618.244	-1459.213
6	2892.858	2796.085	-7998.605	2433.7336	-5188.606
7	-10.227	361.965	48.227	-11.2811	-15.310
8	5844.387	8160.682	3250.5133	2109.1779	-34.239
9	23.086	.000	.0000	-79.8650	28.8191
10	-.670	.000	-.6143	463.5667	.0000010
11	127.362	7430.637	7.0416	.7984	27.7121
12	.6828	71568.6040	.0000	.0000	321.6409
13	310972.6	339791.1	965719.9	4964525.0	10939107.4
14	71.9099	62.7389	327.9078	258.9644	274.0689
15	36.1133	32.5526	9.7318	-4.6562	-14.1937

TABLE AP 3-2 (Sheet 10 of 39)
SATURN OBSERVED TRAJECTORY - BOOST PHASE (AA83)

S-IC OUTBOARD ENGINE CUTOFF SIGNAL - TB 3

1	148.4000	195026.7700	272840.4900	22.9120	72.2915
2	7822.7281	9030.7097	128.078	19.6673	75.0048
3	193234.5	189093.6	-3636511.600	191404.710	-438874.660
4	-433.3	66449.8	18155085.0	-283.582	-1078.690
5	275206.1	488018.3	10127716.5	85009.643	-1579.605
6	2951.395	2847.425	-8370.658	2482.1580	-5296.138
7	-12.375	356.263	-33.443	-12.8720	-15.794
8	7244.597	8562.650	3388.9078	2232.4187	-36.604
9	16.485	.000	.0000	-79.7946	28.8389
10	.131	.000	-.6552	447.9166	.0000007
11	118.319	7822.728	7.5416	.5278	21.0136
12	.7476	52992.4180	.0000	.0000	316.1625
13	336270.9	365149.1	962179.1	4942551.6	10919053.6
14	71.9097	63.4398	329.3031	258.9592	274.0776
15	35.0743	31.8613	10.4033	-4.4962	-14.0476

S-IC/S-II SEPARATION COMMAND

1	149.0800	197117.0300	277721.2800	22.7375	72.2982
2	7862.6768	9071.9847	4.923	19.5302	74.9961
3	195259.7	191047.6	-3642229.700	193100.230	-442483.350
4	-442.2	66691.4	18155069.0	-292.539	-1089.463
5	280157.9	493866.7	10130037.1	86535.586	-1604.662
6	2942.580	2837.479	-8411.599	2485.6775	-5317.631
7	-12.500	355.538	-56.761	-13.0634	-15.891
8	7291.279	8609.485	3397.4563	2246.8433	-37.094
9	-32.518	.000	.0000	-79.7801	28.8429
10	.162	.000	-.6601	444.5499	.0000006
11	-5.321	7862.677	7.6088	.4843	19.6247
12	.7610	49539.8070	.0000	.0000	314.9714
13	341489.3	370379.3	961528.1	4938015.1	10914908.2
14	71.9095	63.5712	329.5932	258.9581	274.0794
15	34.8750	31.7260	10.5401	-4.4633	-14.0299

S-II ENGINE START COMMAND

1	149.7700	199245.7100	282678.9200	22.6245	72.3024
2	7858.9073	9069.1714	4.249	19.4309	74.9993
3	197321.5	193036.6	-3648038.500	194827.140	-446160.020
4	-451.0	66936.6	18155056.0	-301.571	-1100.462
5	285188.8	499807.5	10132396.1	88086.039	-1630.430
6	2925.063	2819.260	-8411.362	2486.7705	-5339.436
7	-12.878	354.780	-73.761	-13.2642	-15.990
8	7294.261	8612.536	3390.1930	2247.9267	-37.597
9	-32.518	.000	.0000	-79.7654	28.8471
10	.191	.000	-.6690	441.0795	.0000006
11	-4.559	7858.907	7.6350	.4433	18.0870
12	.7746	45971.3430	.0000	.0000	313.7391
13	346797.6	375698.6	960897.3	4933408.5	10910698.8
14	71.9093	63.7006	329.8885	258.9570	274.0813
15	34.6792	31.5929	10.6792	-4.4298	-14.0119

1	150.0000	199917.4900	284327.2700	22.5763	72.3059
2	7858.3658	9069.0350	3.263	19.3890	75.0018
3	197970.5	193661.4	-3649964.700	195392.130	-447388.950
4	-453.7	67018.4	18155020.0	-304.575	-1104.143
5	286861.2	501782.9	10133162.9	88601.401	-1639.097
6	2918.154	2812.104	-8412.298	2486.8046	-5346.704
7	-12.727	354.793	-80.622	-13.2501	-16.023
8	7296.446	8614.732	3387.3516	2248.6474	-37.766
9	-32.518	.000	.0000	-79.7605	28.8485
10	.199	.000	-.6680	439.9762	.0000006
11	-3.441	7858.366	7.6440	.4311	17.6305
12	.7791	44905.0210	.0000	.0000	313.3462
13	348542.4	377448.6	960685.8	4931871.5	10909289.4
14	71.9093	63.7427	329.9869	258.9566	274.0819
15	34.6105	31.5448	10.7233	-4.4191	-14.0061

1	155.0000	214661.4400	320267.8600	21.6921	72.3704
2	7851.4340	9069.4775	24.259	18.6202	75.0472
3	212189.3	207337.6	-3691978.700	207829.350	-474517.220
4	-513.0	68789.8	18154278.0	-371.038	-1186.063
5	323354.5	544868.2	10149919.8	99851.078	-1837.399
6	2790.137	2678.762	-8430.934	2494.2793	-5504.569
7	-11.173	353.428	-209.727	-13.4454	-16.747
8	7338.939	8657.642	3336.2851	2262.8968	-41.606
9	-21.346	.000	.0000	-79.6535	28.8784
10	.389	.000	-.6705	415.3297	.0000003
11	21.613	7851.434	7.8607	.2289	9.9015
12	.8776	26460.0290	.0000	.0000	304.4392
13	386759.2	415755.9	956908.7	4898382.9	10878576.6
14	71.9090	64.5658	332.1499	258.9485	274.0952
15	33.2733	30.5992	11.6855	-4.1825	-13.8790

TABLE AP 3-2 (Sheet 11 of 39)
SATURN OBSERVED TRAJECTORY - BOOST PHASE (AA83)

ACTIVATE PU SYSTEM

1	155.2600	215414.9600	322145.7800	21.6450	72.3739
2	7854.1657	9072.5863	24.476	18.5803	75.0488
3	212913.7	208033.0	-3694170.300	208477.850	-475949.450
4	-515.9	68881.7	18154223.0	-374.532	-1190.422
5	325262.5	547119.0	10150786.6	100439.377	-1848.243
6	2784.415	2672.732	-8434.673	2494.9414	-5512.771
7	-11.081	353.353	-216.552	-13.4569	-16.785
8	7344.033	8662.764	3334.8507	2264.5216	-41.814
9	-21.233	.000	.0000	-79.6479	28.8800
10	.398	.000	-.6704	414.0672	.0000003
11	21.800	7854.166	7.8755	.2214	9.6131
12	.8827	25745.0250	.0000	.0000	303.9759
13	388752.0	417753.3	956749.9	4896631.0	10876966.7
14	71.9091	64.6043	332.2638	258.9481	274.0959
15	33.2083	30.5521	11.7345	-4.1702	-13.8724
1	160.0000	228941.8500	356633.5100	20.7954	72.4409
2	7918.3198	9143.4148	25.855	17.8650	75.0767
3	225874.0	220450.3	-3734338.400	220335.190	-502434.250
4	-563.4	70554.2	18152899.0	-438.560	-1271.631
5	360319.8	588428.3	10166541.6	111251.564	-2055.686
6	2684.801	2567.313	-8514.905	2508.3584	-5662.209
7	-8.995	352.278	-340.745	-13.5717	-17.483
8	7449.265	8768.515	3313.9601	2297.9574	-45.761
9	-20.665	.000	.0000	-79.5452	28.9087
10	.514	.000	-.6632	391.7893	.0000002
11	23.040	7918.320	8.1625	.1197	5.5819
12	.9772	15525.1972	.0000	.0000	295.6815
13	425264.3	454349.2	954508.2	4864419.8	10847310.7
14	71.9103	65.2470	334.3706	258.9401	274.1087
15	32.0824	29.7218	12.6081	-3.9478	-13.7531
1	165.0000	242778.3100	393521.2100	19.9227	72.5133
2	7993.3818	9225.0962	26.270	17.1316	75.1070
3	239040.7	233013.8	-3777134.800	232913.760	-531138.950
4	-602.3	72313.0	18150867.0	-506.625	-1360.908
5	397853.7	632559.7	10183060.2	122832.754	-2295.543
6	2582.086	2458.325	-8604.009	2523.1209	-5819.631
7	-6.618	351.213	-471.198	-13.6685	-18.230
8	7564.849	8884.577	3294.1496	2334.6965	-50.234
9	-20.407	.000	.0000	-79.4353	28.9392
10	.541	.000	-.6537	370.1301	.0000001
11	23.363	7993.382	8.4777	.0615	3.0957
12	1.0783	8948.4771	.0000	.0000	287.3879
13	464142.6	493314.8	953518.7	4829886.1	10815402.1
14	71.9132	65.8219	336.6501	258.9313	274.1224
15	30.9985	28.8949	13.4871	-3.7147	-13.6281
1	170.0000	256182.5900	430946.6900	19.0731	72.5872
2	8072.7998	9310.7342	26.533	16.4177	75.1391
3	251697.0	245035.5	-3820381.900	245566.890	-560630.220
4	-628.9	74066.8	18148183.0	-575.086	-1453.949
5	435970.9	677276.6	10199482.3	134599.470	-2558.566
6	2480.440	2350.277	-8694.894	2538.1056	-5976.841
7	-4.065	350.224	-601.352	-13.7388	-18.989
8	7682.285	9002.407	3275.2067	2372.0724	-55.029
9	-20.279	.000	.0000	-79.3237	28.9700
10	.560	.000	-.6426	350.0627	.0000001
11	23.574	8072.800	8.8040	.0311	1.6889
12	1.1809	5070.2129	.0000	.0000	279.4843
13	503410.7	532669.1	953990.6	4794765.9	10782837.4
14	71.9173	66.3139	338.9837	258.9220	274.1363
15	29.9989	28.1094	14.3181	-3.4829	-13.5041
1	175.0000	269161.5700	468919.2300	18.2475	72.6612
2	8156.0165	9399.7751	26.880	15.7238	75.1718
3	263847.5	256518.8	-3864087.100	258295.390	-590907.000
4	-643.1	75815.0	18144849.0	-644.101	-1550.814
5	474679.6	722586.8	10215812.2	146554.540	-2846.372
6	2379.766	2243.079	-8787.045	2553.2863	-6133.844
7	-1.546	349.101	-731.227	-13.8462	-19.759
8	7801.110	9121.541	3257.1352	2409.9449	-60.148
9	-20.113	.000	.0000	-79.2104	29.0012
10	.576	.000	-.6327	330.4033	.0000000
11	23.860	8156.016	9.1557	.0155	.9100
12	1.2849	2843.2903	.0000	.0000	271.5183
13	543080.6	572423.9	955972.6	4759048.7	10749609.0
14	71.9223	66.7400	341.3653	258.9123	274.1504
15	29.0672	27.3587	15.0963	-3.2523	-13.3810

TABLE AP 3-2 (Sheet 12 of 39)
SATURN OBSERVED TRAJECTORY - BOOST PHASE (AA83)

S-II SECOND PLANE SEPARATION

1	179.0600	279393.2600	500159.2100	17.5931	72.7216
2	8226.0568	9474.2774	27.177	15.1735	75.1990
3	273344.0	265449.5	-3899915.600	268686.820	-616068.940
4	-645.0	77230.6	18141664.0	-700.461	-1632.320
5	506549.1	759817.6	10229005.7	156401.790	-3099.428
6	2298.405	2156.330	-8862.601	2565.6580	-6261.183
7	.505	348.123	-836.694	-13.9511	-20.393
8	7898.440	9219.057	3242.8693	2441.0081	-64.546
9	-19.935	.000	.0000	-79.1171	29.0268
10	.588	.000	-.6253	325.3700	.0000000
11	24.090	8226.057	9.3056	.0088	.5308
12	1.3705	1666.6738	.0000	.0000	269.4412
13	575594.8	605005.9	958723.0	4729602.8	10722135.8
14	71.9270	67.0463	343.3294	258.9041	274.1621
15	28.3522	26.7712	15.6865	-3.0658	-13.2817

1	180.0000	281723.3300	507444.7800	17.4440	72.7361
2	8242.7338	9491.9546	27.245	15.0481	75.2057
3	275495.8	267467.1	-3908254.900	271099.910	-621968.320
4	-644.3	77557.7	18140866.0	-713.571	-1651.559
5	513984.4	768494.3	10232052.5	158699.780	-3160.594
6	2279.704	2136.368	-8880.343	2568.5543	-6290.647
7	1.041	347.948	-861.058	-13.9593	-20.541
8	7921.213	9241.866	3239.6453	2448.2802	-65.595
9	-19.893	.000	.0000	-79.0953	29.0327
10	.592	.000	-.6228	325.3700	.0000000
11	24.141	8242.734	9.3244	.0077	.4677
12	1.3905	1465.6588	.0000	.0000	269.4412
13	583162.3	612589.1	959508.1	4722728.0	10715711.6
14	71.9281	67.1128	343.7876	258.9022	274.1648
15	28.1913	26.6377	15.8175	-3.0227	-13.2587

LAUNCH ESCAPE TOWER JETTISON

1	184.7700	293324.1600	544721.9200	16.7017	72.8084
2	8329.2633	9583.3515	27.823	14.4237	75.2393
3	286144.2	277416.5	-3950828.600	283387.060	-652331.100
4	-633.4	79214.7	18136461.0	-780.455	-1751.338
5	552044.1	812853.8	10247466.3	170466.110	-3486.496
6	2185.441	2035.640	-8970.947	2583.3920	-6440.055
7	3.602	346.846	-984.474	-14.0647	-21.297
8	8037.441	9358.232	3223.9040	2485.4270	-71.102
9	-19.691	.000	.0000	-78.9839	29.0631
10	.609	.000	-.6129	325.3700	.0000000
11	24.660	8329.263	9.4223	.0040	.2494
12	1.4926	773.3412	.0000	.0000	269.4412
13	621797.0	651301.9	964365.5	4687506.5	10682742.9
14	71.9342	67.4275	346.1292	258.8921	274.1787
15	27.3993	25.9738	16.4490	-2.8047	-13.1428

1	185.0000	293874.4600	546532.7100	16.6666	72.8119
2	8333.5284	9587.8429	27.854	14.3941	75.2409
3	286646.4	277884.2	-3952892.600	283981.350	-653813.150
4	-632.7	79294.3	18136235.0	-783.722	-1756.241
5	553893.6	815007.1	10248207.9	171038.020	-3502.881
6	2180.937	2030.822	-8975.356	2584.1179	-6447.255
7	3.729	346.794	-990.402	-14.0694	-21.334
8	8043.084	9363.880	3223.1726	2487.2316	-71.375
9	-19.683	.000	.0000	-78.9785	29.0645
10	.610	.000	-.6124	325.3700	.0000000
11	24.689	8333.528	9.4271	.0039	.2421
12	1.4976	750.3313	.0000	.0000	269.4412
13	623670.2	653178.8	964637.0	4685793.8	10681137.6
14	71.9345	67.4418	346.2427	258.8916	274.1794
15	27.3621	25.9424	16.4781	-2.7942	-13.1373

1	190.0000	305626.4600	586195.3000	15.9153	72.8889
2	8428.5274	9687.5868	28.234	13.7617	75.2775
3	297306.6	287776.6	-3998011.300	296941.380	-686440.560
4	-667.1	81025.4	18130957.0	-854.343	-1864.918
5	594418.2	862135.9	10264283.6	183573.110	-3874.903
6	2083.471	1926.439	-9072.303	2599.9781	-6603.674
7	6.532	345.652	-1119.330	-14.1722	-22.139
8	8166.957	9487.819	3207.7683	2526.8723	-77.490
9	-19.460	.000	.0000	-78.8599	29.0967
10	.621	.000	-.6013	342.0947	.0000000
11	24.983	8428.527	-.2942	.0020	.1237
12	1.6063	362.6910	.0000	.0000	276.4104
13	664623.6	694212.2	971393.9	4648234.0	10645877.1
14	71.9414	67.7346	348.7224	258.8805	274.1943
15	26.5725	25.2696	17.0749	-2.5664	-13.0165

TABLE AP 3-2 (Sheet 13 of 39)
SATURN OBSERVED TRAJECTORY - BOOST PHASE (AA83)

INITIATE ITERATIVE GUIDANCE MODE

1	190.9000	307700.1100	593396.3900	15.7820	72.9032
2	8445.7297	9705.6142	28.320	13.6494	75.2846
3	299173.7	289501.7	-4006184.400	299282.570	-692396.510
4	-600.9	81336.4	18129938.0	-867.089	-1884.908
5	601778.7	870685.2	10267169.0	185850.580	-3945.154
6	2065.864	1907.576	-9089.674	2602.8045	-6631.809
7	7.092	345.492	-1142.553	-14.1764	-22.285
8	8189.170	9510.035	3204.8965	2533.9900	-78.626
9	-19.408	.000	.0000	-78.8383	29.1025
10	.625	.000	-.5987	345.4408	.0000000
11	25.050	8445.730	9.2671	.0018	.1102
12	1.6260	319.6929	.0000	.0000	277.7854
13	672043.7	701646.5	972785.3	4641405.9	10639456.4
14	71.9427	67.7839	349.1706	258.8784	274.1970
15	26.4342	25.1507	17.1754	-2.5254	-12.9948

1	195.0000	316988.2400	626439.6500	15.1941	72.9682
2	8526.2802	9789.7407	28.416	13.1542	75.3168
3	307481.4	297148.6	-4043616.700	309981.040	-719849.590
4	-566.9	82751.1	18125036.0	-925.368	-1977.645
5	635564.3	909886.3	10280283.4	196307.220	-4278.347
6	1987.549	1823.479	-9169.967	2616.2163	-6759.908
7	9.598	344.681	-1247.106	-14.2196	-22.954
8	8291.382	9612.240	3193.0343	2566.7631	-83.944
9	-18.633	.000	.0000	-78.7394	29.1292
10	.709	.000	-.5876	360.4137	.0000000
11	24.801	8526.280	9.1552	.0011	.0667
12	1.7166	184.7042	.0000	.0000	283.8624
13	706036.1	735702.7	979807.3	4610041.4	10609924.6
14	71.9488	67.9970	351.2172	258.8689	274.2094
15	25.8173	24.6170	17.6058	-2.3392	-12.8963

1	200.0000	327979.2700	667265.6200	14.5506	73.0532
2	8625.3491	9892.6757	28.868	12.6126	75.3625
3	317186.9	306016.0	-4089711.000	323104.870	-754039.330
4	-509.6	84473.6	18118485.0	-996.120	-2094.480
5	677330.7	958256.9	10296212.3	209240.480	-4714.919
6	1899.915	1728.720	-9267.059	2634.8994	-6915.963
7	13.464	344.468	-1366.781	-14.0324	-23.782
8	8413.488	9734.368	3180.9717	2606.0595	-90.742
9	-16.227	.000	.0000	-78.6172	29.1620
10	.813	.000	-.5636	378.0990	.0000000
11	24.087	8625.349	9.0378	.0007	.0379
12	1.8284	99.5275	.0000	.0000	290.8896
13	747920.1	777662.3	989900.8	4571218.3	10573284.9
14	71.9568	68.2337	353.7174	258.8566	274.2247
15	25.0932	23.9836	18.0697	-2.1123	-12.7768

1	205.0000	338663.3600	708653.4700	13.9887	73.1405
2	8724.6942	9995.3645	29.225	12.1405	75.4116
3	326484.4	314439.5	-4136286.800	336331.070	-789008.930
4	-431.9	86196.1	18111366.0	-1065.588	-2215.480
5	719697.9	1007228.7	10312092.0	222367.600	-5186.345
6	1821.377	1642.986	-9362.770	2656.2800	-7071.843
7	17.626	344.524	-1477.586	-13.7597	-24.620
8	8532.442	9853.387	3172.1620	2644.5141	-97.886
9	-14.782	.000	.0000	-78.4931	29.1950
10	.843	.000	-.5361	405.7513	.0000000
11	23.637	8724.694	8.8089	.0004	.0220
12	1.9418	53.6884	.0000	.0000	301.8855
13	790289.4	820103.3	1001701.4	4531794.6	10535994.5
14	71.9655	68.4486	356.2115	258.8438	274.2402
15	24.4010	23.3720	18.4691	-1.8849	-12.6575

1	210.0000	349076.0800	750593.2400	13.4716	73.2282
2	8825.5972	10099.2905	29.375	11.7062	75.4620
3	335406.4	322451.4	-4183340.200	340669.260	-824757.480
4	-333.3	87918.8	18103708.0	-1133.726	-2340.699
5	762656.0	1056791.5	10327934.6	235686.060	-5694.368
6	1747.146	1561.458	-9458.637	2678.8902	-7227.552
7	21.814	344.543	-1584.611	-13.4948	-25.470
8	8650.906	9971.902	3165.2605	2682.9220	-105.381
9	-14.774	.000	.0000	-78.3673	29.2284
10	.862	.000	-.5093	432.6000	.0000000
11	23.784	8825.597	8.6145	.0003	.0135
12	2.0568	30.7264	.0000	.0000	312.2698
13	833151.6	863033.5	1015222.4	4491785.9	10498071.8
14	71.9749	68.6447	358.6891	258.8303	274.2560
15	23.7393	22.7823	18.8054	-1.6566	-12.5382

TABLE AP 3-2 (Sheet 14 of 39)
SATURN OBSERVED TRAJECTORY - BOOST PHASE (AA83)

INITIATE STEERING MISALIGNMENT CORRECTION

1	210.6000	350308.1400	755663.0700	13.4106	73.2388
2	8837.7830	10111.8274	29.419	11.6549	75.4682
3	336452.2	323385.5	-4189018.600	351277.450	-829099.600
4	-320.1	88125.4	18102754.0	-1141.822	-2356.012
5	767850.6	1062778.8	10329833.3	237297.130	-5757.873
6	1738.240	1551.668	-9470.143	2681.5980	-7246.226
7	22.325	344.549	-1597.458	-13.4619	-25.572
8	8665.127	9986.125	3164.4270	2687.5385	-106.304
9	-14.791	.000	.0000	-78.3521	29.2324
10	.866	.000	-.5061	435.7631	.0000000
11	23.844	8837.783	8.5932	.0002	.0127
12	2.0707	28.8341	.0000	.0000	313.4757
13	838328.4	868218.3	1016960.6	4486945.7	10493478.5
14	71.9760	68.6671	358.9848	258.8286	274.2579
15	23.6618	22.7129	18.8415	-1.6292	-12.5239

1	215.0000	359225.8500	793089.8300	12.9667	73.3161
2	8928.9039	10205.4648	29.700	11.2814	75.5130
3	343956.8	330054.8	-4230874.800	363120.110	-861284.160
4	-213.8	89641.3	18095515.0	-1200.607	-2470.195
5	806208.9	1106949.5	10343743.3	249197.560	-6240.750
6	1672.603	1479.488	-9555.646	2701.3145	-7383.092
7	26.011	344.474	-1692.473	-13.2536	-26.331
8	8770.807	10091.778	3158.5909	2721.8527	-113.230
9	-14.971	.000	.0000	-78.2397	29.2620
10	.907	.000	-.4838	458.5764	.0000000
11	24.254	8928.904	8.4501	.0002	.0086
12	2.1732	18.4925	.0000	.0000	322.0694
13	876515.3	906461.6	1030462.8	4451188.3	10459513.7
14	71.9847	68.8245	1.1410	258.8161	274.2719
15	23.1048	22.2123	19.0794	-1.4272	-12.4191

1	220.0000	369113.0800	836156.0400	12.4698	73.4076
2	9035.8116	10315.1265	30.078	10.8628	75.5674
3	352132.7	337246.2	-4278901.100	376682.300	-898588.140
4	-71.9	91364.6	18086778.0	-1265.906	-2604.024
5	850368.7	1157714.0	10359518.4	262906.170	-6827.271
6	1597.305	1396.613	-9655.110	2723.4124	-7538.468
7	30.729	344.813	-1801.779	-12.8844	-27.203
8	8893.456	10214.325	3151.8709	2761.7063	-121.437
9	-15.158	.000	.0000	-78.1103	29.2959
10	.945	.000	-.4531	505.1200	.0000000
11	24.770	9035.812	8.1278	.0001	.0055
12	2.2912	10.8110	.0000	.0000	338.8509
13	920393.6	950400.9	1047414.1	4409988.7	10420307.7
14	71.9951	68.9901	3.5592	258.8011	274.2881
15	22.4942	21.6598	19.2922	-1.1965	-12.2999

1	225.0000	378737.3300	879804.4000	11.9797	73.4995
2	9145.6135	10427.5592	30.406	10.4491	75.6224
3	359929.6	344020.4	-4327428.800	390354.000	-936668.570
4	93.8	93089.5	18077490.0	-1329.404	-2742.243
5	895147.0	1209096.2	10375260.1	276815.850	-7455.728
6	1520.856	1312.443	-9756.184	2745.0662	-7693.680
7	35.487	345.080	-1912.852	-12.5337	-28.086
8	9018.203	10338.879	3145.1359	2802.2822	-130.006
9	-15.347	.000	.0000	-77.9790	29.3301
10	.980	.000	-.4235	554.1485	.0000000
11	25.221	9145.614	7.8342	.0001	.0037
12	2.4108	6.6732	.0000	.0000	355.8215
13	964799.1	994864.5	1066063.4	4368173.9	10380440.7
14	72.0059	69.1433	5.9361	258.7854	274.3045
15	21.9046	21.1229	19.4454	-.9645	-12.1807

1	230.0000	388098.1500	924047.2500	11.4989	73.5926
2	9258.6457	10543.0961	30.700	10.0424	75.6789
3	367341.8	350371.0	-4376466.500	404133.000	-975524.670
4	283.3	94815.5	18067642.0	-1391.205	-2884.907
5	940555.0	1261106.9	10390968.6	290930.440	-8127.939
6	1443.663	1227.377	-9859.223	2766.3986	-7848.734
7	40.413	345.403	-2025.379	-12.1625	-28.981
8	9145.312	10465.712	3138.5437	2843.6640	-138.939
9	-15.471	.000	.0000	-77.8459	29.3646
10	1.011	.000	-.3934	601.3302	.0000000
11	25.590	9258.646	7.8946	.0001	.0026
12	2.5321	4.3641	.0000	.0000	371.8846
13	1009744.4	1039865.1	1086393.9	4325731.2	10339899.7
14	72.0172	69.2857	8.2651	258.7688	274.3212
15	21.3336	20.5998	19.5414	-.7309	-12.0615

TABLE AP 3-2 (Sheet 15 of 39)
SATURN OBSERVED TRAJECTORY - BOOST PHASE (AA83)

1	235.0000	397196.5200	968896.0700	11.0288	73.6876
2	9374.4175	10661.2496	30.981	9.6442	75.7375
3	374366.8	356294.6	-4426023.400	418018.030	-1015155.640
4	498.2	96543.6	18057229.0	-1450.997	-3032.073
5	986603.3	1313756.3	10406643.9	305253.600	-8845.741
6	1365.839	1141.536	-9963.826	2787.4467	-8003.631
7	45.625	345.900	-2139.054	-11.7347	-29.887
8	9274.271	10594.315	3131.9144	2885.6976	-148.243
9	-15.576	.000	.0000	-77.7108	29.3993
10	1.028	.000	-.3614	665.5474	.0000000
11	25.929	9374.418	7.2929	.0001	.0019
12	2.6550	2.8536	.0000	.0000	391.7951
13	1055242.5	1085415.7	1108385.3	4282648.9	10298673.2
14	72.0288	69.4184	10.5402	258.7514	274.3380
15	20.7792	20.0891	19.5830	-.4958	-11.9422
1	240.0000	406034.5200	1014361.4000	10.5712	73.7828
2	9493.2235	10782.3013	31.344	9.2559	75.7965
3	381001.4	361787.3	-4476107.500	432007.670	-1055560.700
4	739.3	98274.2	18046246.0	-1508.664	-3183.798
5	1033301.3	1367053.5	10422286.8	319788.670	-9610.991
6	1287.676	1055.204	-10070.165	2808.2984	-8158.374
7	50.821	346.270	-2253.832	-11.3425	-30.805
8	9405.350	10724.956	3125.7097	2928.4665	-157.919
9	-15.648	.000	.0000	-77.5737	29.4343
10	1.049	.000	-.3313	756.5958	.0000000
11	26.340	9493.224	6.9138	.0000	.0014
12	2.7796	1.8560	.0000	.0000	418.5159
13	1101305.6	1131529.0	1132014.2	4238916.7	10256750.9
14	72.0409	69.5427	12.7565	258.7331	274.3552
15	20.2400	19.5899	19.5733	-.2589	-11.8229
1	245.0000	414615.4600	1060454.8000	10.1275	73.8785
2	9614.9353	10906.1264	31.721	8.8786	75.8565
3	387244.9	366847.7	-4526727.300	446101.250	-1096739.200
4	1006.5	100006.3	18034685.0	-1564.420	-3340.137
5	1080659.7	1421008.7	10437899.8	334539.320	-10425.566
6	1209.371	968.579	-10178.177	2829.0150	-8312.966
7	56.077	346.588	-2369.470	-10.9625	-31.733
8	9538.410	10857.502	3119.9251	2971.9309	-167.973
9	-15.703	.000	.0000	-77.4346	29.4696
10	1.068	.000	-.3021	844.3369	.0000000
11	26.753	9614.935	6.6166	.0000	.0010
12	2.9059	1.2884	.0000	.0000	442.9185
13	1147948.1	1178219.3	1157257.9	4194523.5	10214122.4
14	72.0533	69.6592	14.9100	258.7138	274.3725
15	19.7147	19.1012	19.5160	-.0200	-11.7034
1	250.0000	422943.4700	1107186.6000	9.6966	73.9750
2	9739.2669	11032.4490	32.090	8.5117	75.9177
3	393096.0	371473.8	-4577890.900	460297.940	-1138690.100
4	1300.3	101740.0	18022545.0	-1618.286	-3501.148
5	1128687.9	1475630.9	10453484.5	349508.900	-11291.365
6	1130.732	881.470	-10287.626	2849.5384	-8467.410
7	61.432	346.892	-2486.044	-10.5833	-32.673
8	9673.210	10991.708	3114.3698	3016.0177	-178.409
9	-15.748	.000	.0000	-77.2935	29.5052
10	1.091	.000	-.2733	928.8692	.0000000
11	27.148	9739.267	6.3787	.0000	.0008
12	3.0339	.9400	.0000	.0000	465.3811
13	1195183.0	1225499.7	1184090.2	4149459.8	10170777.6
14	72.0659	69.7689	16.9975	258.6934	274.3902
15	19.2020	18.6224	19.4148	.2211	-11.5838
1	255.0000	431023.2400	1154567.5000	9.2805	74.0714
2	9866.5925	11161.6379	32.475	8.1568	75.9792
3	398554.1	375664.0	-4629606.200	474597.070	-1181413.000
4	1620.4	103474.6	18009819.0	-1670.455	-3666.888
5	1177395.6	1530929.4	10469043.4	364700.810	-12210.308
6	1052.121	794.231	-10398.830	2869.9779	-8621.708
7	66.722	347.016	-2603.425	-10.2556	-33.625
8	9810.109	11127.936	3109.4519	3060.8387	-189.232
9	-15.790	.000	.0000	-77.1503	29.5410
10	1.111	.000	-.2468	1010.2899	.0000000
11	27.557	9866.592	6.1856	.0000	.0007
12	3.1638	.7135	.0000	.0000	486.1820
13	1243023.8	1273383.9	1212484.8	4103715.6	10126707.1
14	72.0788	69.8724	19.0168	258.6721	274.4080
15	18.7012	18.1528	19.2734	.4645	-11.4640

TABLE AP 3-2 (Sheet 16 of 39)
SATURN OBSERVED TRAJECTORY - BOOST PHASE (AA83)

1	260.0000	438858.0400	1202608.8000	8.8769	74.1706
2	9996.7246	11293.5342	32.927	7.8118	76.0437
3	403618.0	379416.6	-4681882.200	488997.810	-1224907.000
4	1968.1	105210.6	17996504.0	-1720.715	-3837.412
5	1226792.9	1586914.1	10484577.3	380118.640	-13184.336
6	973.127	706.448	-10511.802	2890.2081	-8775.862
7	72.440	347.451	-2721.737	-9.8297	-34.587
8	9948.984	11266.062	3104.5290	3106.3572	-200.445
9	-15.849	.000	.0000	-77.0050	29.5772
10	1.131	.000	-.2171	1088.6943	.0000000
11	28.042	9996.725	6.0273	.0000	.0006
12	3.2954	.5592	.0000	.0000	505.5372
13	1291484.5	1321886.0	1242414.3	4057280.5	10081900.4
14	72.0918	69.9702	20.9663	258.6495	274.4262
15	18.2113	17.6918	19.0957	.7106	-11.3439
1	265.0000	446452.2900	1251322.9000	8.4853	74.2700
2	10130.2879	11428.7543	33.309	7.4766	76.1086
3	408286.6	382729.4	-4734728.900	503499.360	-1269171.400
4	2344.6	106948.7	17982595.0	-1768.869	-4012.779
5	1276891.4	1643595.9	10500088.3	395766.370	-14215.415
6	893.720	618.081	-10626.956	2910.2170	-8929.875
7	78.155	347.756	-2841.389	-9.4396	-35.561
8	10090.485	11406.730	3100.1233	3152.7710	-212.052
9	-15.930	.000	.0000	-76.8575	29.6136
10	1.151	.000	-.1891	1164.1745	.0000000
11	28.457	10130.288	5.8969	.0000	.0005
12	3.4289	.4501	.0000	.0000	523.6150
13	1340580.1	1371020.8	1273851.6	4010143.4	10036346.0
14	72.1051	70.0630	22.8456	258.6258	274.4447
15	17.7317	17.2389	18.8854	.9595	-11.2235
1	270.0000	453808.9600	1300720.1000	8.1060	74.3700
2	10266.0671	11566.0891	33.772	7.1512	76.1747
3	412556.6	385598.5	-4788153.200	518100.240	-1314205.500
4	2749.7	108688.0	17968084.0	-1815.140	-4193.044
5	1327700.2	1700983.7	10515577.2	411647.280	-15305.530
6	813.848	529.094	-10743.210	2929.9947	-9083.750
7	83.907	347.983	-2962.022	-9.0702	-36.547
8	10233.413	11548.741	3095.8516	3199.7158	-224.060
9	-16.030	.000	.0000	-76.7078	29.6503
10	1.169	.000	-.1624	1236.8020	.0000000
11	28.964	10266.067	5.7887	.0000	.0004
12	3.5643	.3704	.0000	.0000	540.5505
13	1390323.1	1420801.2	1306769.5	3962294.6	9990033.7
14	72.1186	70.1511	24.6544	258.6008	274.4634
15	17.2616	16.7936	18.6458	1.2115	-11.1029
1	275.0000	460931.0800	1350812.5000	7.7383	74.4703
2	10405.3465	11706.8276	34.169	6.8352	76.2414
3	416426.1	388021.1	-4842164.200	532799.450	-1360008.600
4	3183.3	110427.9	17952967.0	-1859.738	-4378.264
5	1379230.4	1759088.0	10531046.2	427765.180	-16456.693
6	733.476	439.429	-10861.731	2949.5239	-9237.487
7	89.668	348.089	-3084.106	-8.7342	-37.543
8	10379.075	11693.399	3092.0740	3247.5907	-236.472
9	-16.134	.000	.0000	-76.5559	29.6873
10	1.194	.000	-.1372	1306.6623	.0000000
11	29.396	10405.346	5.6995	.0000	.0004
12	3.7015	.3108	.0000	.0000	556.4565
13	1440727.9	1471241.6	1341142.3	3913723.5	9942953.0
14	72.1322	70.2350	26.3933	258.5745	274.4825
15	16.8004	16.3556	18.3805	1.4669	-10.9818
1	280.0000	467823.0200	1401614.7000	7.3829	74.5725
2	10547.8099	11850.6639	34.602	6.5291	76.3101
3	419892.8	389993.9	-4896773.600	547595.750	-1406580.100
4	3646.6	112168.9	17937236.0	-1902.469	-4568.498
5	1431495.4	1817922.1	10546497.0	444124.710	-17670.937
6	652.689	349.170	-10982.345	2968.8311	-9391.089
7	95.682	348.318	-3207.375	-8.3570	-38.552
8	10527.162	11840.398	3088.5445	3296.3038	-249.293
9	-16.242	.000	.0000	-76.4017	29.7245
10	1.215	.000	-.1110	1373.8335	.0000000
11	29.864	10547.810	5.6262	.0000	.0003
12	3.8407	.2651	.0000	.0000	571.4257
13	1491811.7	1522359.0	1376946.5	3864416.5	9895089.5
14	72.1459	70.3150	28.0634	258.5468	274.5019
15	16.3476	15.9244	18.0925	1.7260	-10.8604

TABLE AP 3-2 (Sheet 17 of 39)
SATURN OBSERVED TRAJECTORY - BOOST PHASE (AA83)

1	285.0000	474487.2200	1453137.9000	7.0377	74.6756
2	10692.8015	11996.9477	35.068	6.2313	76.3802
3	422953.0	391512.5	-4951989.400	562487.590	-1453919.300
4	4140.2	113911.0	17920886.0	-1943.328	-4763.801
5	1484505.2	1877495.1	10561929.6	460729.380	-18950.321
6	571.078	257.919	-11104.369	2987.7951	-9544.559
7	101.811	348.534	-3332.035	-7.9803	-39.571
8	10677.055	11989.111	3085.0151	3345.6659	-262.529
9	-16.358	.000	.0000	-76.2452	29.7621
10	1.237	.000	-.0852	1438.3845	.0000000
11	30.366	10692.802	5.5661	.0000	.0003
12	3.9819	.2294	.0000	.0000	585.5366
13	1543587.4	1574166.6	1414157.3	3814364.2	9846432.9
14	72.1597	70.3915	29.6661	258.5176	274.5216
15	15.9028	15.4997	17.7848	1.9890	-10.7385
1	290.0000	480926.9300	1505394.8000	6.7040	74.7793
2	10841.3900	12146.7449	35.494	5.9428	76.4512
3	425604.2	392573.4	-5007820.700	577473.720	-1502025.500
4	4664.5	115653.9	17903908.0	-1982.395	-4964.230
5	1538271.2	1937818.4	10577346.2	477583.170	-20296.928
6	488.924	165.935	-11228.781	3006.4956	-9697.896
7	107.975	348.648	-3458.228	-7.6311	-40.602
8	10829.822	12140.608	3081.9750	3396.0039	-276.183
9	-16.471	.000	.0000	-76.0863	29.7999
10	1.264	.000	-.0608	1500.3914	.0000000
11	30.820	10841.390	5.5179	.0000	.0003
12	4.1251	.2010	.0000	.0000	598.8569
13	1596069.9	1626679.4	1452752.7	3763555.1	9796971.2
14	72.1737	70.4646	31.2029	258.4867	274.5416
15	15.4655	15.0812	17.4601	2.2562	-10.6161
1	295.0000	487146.5900	1558400.1000	6.3819	74.8851
2	10992.8113	12299.3034	35.934	5.6639	76.5245
3	427843.3	393172.5	-5064279.600	592552.700	-1550898.000
4	5220.7	117398.0	17886297.0	-2019.497	-5169.844
5	1592807.3	1998905.0	10592747.8	494690.780	-21712.864
6	406.215	73.213	-11355.002	3024.9318	-9851.104
7	114.443	348.934	-3585.616	-7.2263	-41.645
8	10984.707	12294.136	3078.9903	3447.0906	-290.262
9	-16.587	.000	.0000	-75.9250	29.8381
10	1.296	.000	-.0348	1559.9284	.0000000
11	31.285	10992.811	5.4798	.0000	.0002
12	4.2704	.1782	.0000	.0000	611.4467
13	1649276.2	1679914.3	1492713.5	3711976.5	9746690.6
14	72.1877	70.5348	32.6759	258.4542	274.5620
15	15.0352	14.6686	17.1207	2.5282	-10.4931
1	300.0000	493149.4400	1612166.2000	6.0706	74.9915
2	11147.5965	12455.1523	36.354	5.3937	76.5987
3	429667.1	393306.0	-5121374.700	607723.120	-1600536.300
4	5809.1	119143.1	17868044.0	-2054.686	-5380.699
5	1648124.2	2060765.4	10608135.0	512056.040	-23200.266
6	322.781	-20.425	-11483.396	3043.0496	-10004.184
7	120.945	349.112	-3714.634	-6.8508	-42.699
8	11142.266	12450.243	3076.3559	3499.0941	-304.770
9	-16.700	.000	.0000	-75.7612	29.8765
10	1.320	.000	-.0103	1614.6772	.0000000
11	31.723	11147.597	5.4552	.0000	.0002
12	4.4177	.1599	.0000	.0000	622.8521
13	1703220.7	1733885.8	1534020.3	3659618.0	9695579.6
14	72.2019	70.6022	34.0871	258.4199	274.5827
15	14.6117	14.2617	16.7691	2.8051	-10.3696
1	305.0000	498939.6600	1666706.4000	5.7715	75.0990
2	11305.2817	12613.8306	36.848	5.1336	76.6744
3	431072.7	392969.6	-5179116.100	622983.540	-1650939.700
4	6430.2	120889.0	17849144.0	-2088.035	-5596.852
5	1704234.3	2123411.6	10623510.2	529683.200	-24761.294
6	238.906	-114.692	-11613.626	3060.9372	-10157.137
7	127.571	349.278	-3844.855	-6.4755	-43.764
8	11302.037	12608.473	3074.0071	3551.8772	-319.713
9	-16.819	.000	.0000	-75.5949	29.9152
10	1.345	.000	.0000	1656.1229	.0000000
11	32.238	11305.282	5.4580	.0000	.0002
12	4.5672	.1465	.0000	.0000	631.3347
13	1757919.0	1788609.4	1576656.2	3606468.5	9643625.5
14	72.2161	70.6670	35.4388	258.3836	274.6038
15	14.1947	13.8601	16.4072	3.0875	-10.2454

TABLE AP 3-2 (Sheet 18 of 39)
SATURN OBSERVED TRAJECTORY - BOOST PHASE (AA83)

1	310.0000	504521.9200	1722034.9000	5.4835	75.2085
2	11466.2816	12775.7628	37.393	4.8828	76.7524
3	432057.1	392159.6	-5237514.700	638332.580	-1702107.500
4	7085.4	122636.2	17829588.0	-2119.335	-5818.362
5	1761150.1	2186855.6	10638873.9	547576.700	-26398.133
6	154.394	-209.796	-11746.116	3078.5311	-10309.964
7	134.489	349.591	-3976.529	-6.0519	-44.841
8	11464.453	12769.257	3071.8266	3605.5727	-335.096
9	-16.944	.000	.0000	-75.4261	29.9542
10	1.373	.000	.0000	1695.9360	.0000000
11	32.805	11466.281	5.4659	.0000	.0002
12	4.7188	.1350	.0000	.0000	639.4059
13	1813387.2	1844101.5	1620606.2	3552516.7	9590815.8
14	72.2304	70.7294	36.7333	258.3453	274.6253
15	13.7838	13.4639	16.0368	3.3757	-10.1205

1	315.0000	509900.6700	1778165.9000	5.2076	75.3182
2	11630.8260	12941.1718	37.854	4.6421	76.8309
3	432617.9	390872.5	-5296581.400	653769.050	-1754039.100
4	7774.9	124384.4	17809370.0	-2148.689	-6045.285
5	1818885.1	2251110.3	10654228.0	565741.050	-28112.999
6	69.425	-305.562	-11880.981	3095.8854	-10462.667
7	141.354	349.704	-4109.716	-5.6858	-45.930
8	11629.760	12932.838	3070.2557	3660.2568	-350.925
9	-17.070	.000	.0000	-75.2546	29.9934
10	1.400	.000	.0000	1734.1684	.0000000
11	33.278	11630.826	5.4785	.0000	.0002
12	4.8726	.1252	.0000	.0000	647.0880
13	1869642.1	1900378.7	1665857.7	3497751.1	9537137.0
14	72.2448	70.7896	37.9730	258.3047	274.6472
15	13.3790	13.0728	15.6597	3.6704	-9.9949

1	320.0000	515081.2200	1835114.1000	4.9420	75.4284
2	11798.2247	13109.3751	38.289	4.4099	76.9104
3	432751.7	389103.9	-5356326.900	669291.370	-1806733.900
4	8498.7	126132.8	17788482.0	-2176.330	-6277.679
5	1877452.4	2316188.6	10669574.9	584180.880	-29908.135
6	-16.347	-402.327	-12017.569	3112.8975	-10615.246
7	148.215	349.666	-4244.479	-5.3618	-47.030
8	11797.282	13098.535	3068.9053	3715.7233	-367.204
9	-17.218	.000	.0000	-75.0805	30.0329
10	1.428	.000	.0000	1770.8681	.0000000
11	33.727	11798.225	5.4952	.0000	.0002
12	5.0287	.1167	.0000	.0000	654.4020
13	1926700.2	1957457.7	1712399.9	3442160.0	9482575.6
14	72.2593	70.8477	39.1601	258.2618	274.6696
15	12.9798	12.6865	15.2773	3.9720	-9.8685

1	325.0000	520067.1200	1892891.1000	4.6867	75.5406
2	11968.2851	13280.1907	38.780	4.1863	76.9922
3	432454.3	386848.7	-5416759.000	684897.810	-1860191.400
4	9257.4	127881.2	17766917.0	-2202.263	-6515.602
5	1936862.0	2382099.7	10684914.7	602899.750	-31785.809
6	-102.931	-500.101	-12155.813	3129.5650	-10767.702
7	155.341	349.750	-4380.660	-4.9974	-48.141
8	11966.834	13266.163	3067.4952	3771.9177	-383.941
9	-17.384	.000	.0000	-74.9037	30.0728
10	1.456	.000	.0000	1806.0730	.0000000
11	34.237	11968.285	5.5158	.0000	.0002
12	5.1870	.1093	.0000	.0000	661.3644
13	1984574.7	2015351.7	1760220.3	3385735.5	9427121.4
14	72.2738	70.9039	40.2970	258.2163	274.6923
15	12.5862	12.3051	14.8910	4.2811	-9.7412

1	330.0000	524863.6500	1951510.6000	4.4417	75.6542
2	12141.8202	13454.4316	39.332	3.9713	77.0757
3	431722.6	384102.8	-5477888.500	700586.940	-1914410.700
4	10052.3	129630.2	17744667.0	-2226.327	-6759.111
5	1997126.6	2448856.0	10700248.5	621902.050	-33748.323
6	-190.334	-598.909	-12296.415	3145.8799	-10920.037
7	162.632	349.844	-4518.581	-4.6265	-49.264
8	12139.239	13436.543	3066.3279	3829.0920	-401.141
9	-17.556	.000	.0000	-74.7242	30.1128
10	1.482	.000	.0000	1839.8353	.0000000
11	34.807	12141.820	5.5402	.0000	.0002
12	5.3476	.1029	.0000	.0000	667.9937
13	2043281.7	2074076.8	1809309.6	3328467.5	9370761.4
14	72.2883	70.9582	41.3859	258.1682	274.7155
15	12.1979	11.9283	14.5018	4.5983	-9.6129

TABLE AP 3-2 (Sheet 19 of 39)
SATURN OBSERVED TRAJECTORY - BOOST PHASE (AA83)

1	335.0000	529474.1000	2010988.5000	4.2068	75.7690
2	12318.8189	13632.0877	39.864	3.7648	77.1607
3	430551.7	380860.0	-5539726.800	716356.670	-1969391.600
4	10883.9	131379.6	17721722.0	-2248.538	-7008.265
5	2058260.4	2516471.0	10715576.9	641192.680	-35798.004
6	-278.584	-698.781	-12439.348	3161.8335	-11072.251
7	170.044	349.899	-4658.283	-4.2640	-50.399
8	12314.495	13609.670	3065.4290	3887.2466	-418.809
9	-17.736	.000	.0000	-74.5419	30.1532
10	1.509	.000	.0000	1860.7384	.0000000
11	35.353	12318.819	5.5855	.0000	.0002
12	5.5106	.0982	.0000	.0000	672.2388
13	2102838.3	2133650.2	1859661.8	3270343.8	9313480.7
14	72.3029	71.0108	42.4292	258.1170	274.7392
15	11.8147	11.5560	14.1108	4.9243	-9.4837

1	340.0000	533903.4900	2071341.1000	3.9820	75.8857
2	12499.7476	13813.6321	40.443	3.5668	77.2478
3	428936.8	377114.6	-5602286.000	732205.090	-2025133.100
4	11753.2	133129.3	17698075.0	-2268.908	-7263.120
5	2120278.3	2584959.2	10730901.1	660776.760	-37937.211
6	-367.730	-799.784	-12585.085	3177.4057	-11224.343
7	177.720	350.050	-4799.918	-3.8685	-51.545
8	12493.073	13786.017	3064.7817	3946.5272	-436.952
9	-17.887	.000	.0000	-74.3567	30.1938
10	1.536	.000	.0000	1880.5936	.0000000
11	35.935	12499.748	5.6338	.0000	.0002
12	5.6760	.0941	.0000	.0000	676.2624
13	2163262.5	2194089.8	1911272.1	3211353.0	9255264.3
14	72.3175	71.0619	43.4290	258.0628	274.7633
15	11.4365	11.1881	13.7188	5.2599	-9.3535

1	345.0000	538157.9900	2132585.1000	3.7682	76.0028
2	12683.8154	13998.2677	41.034	3.3782	77.3358
3	426875.0	372862.4	-5665579.200	748130.720	-2081634.800
4	12660.7	134879.4	17673715.0	-2287.420	-7523.736
5	2183195.5	2654335.4	10746223.3	680659.500	-40168.333
6	-457.525	-901.652	-12732.849	3192.6771	-11376.315
7	185.351	349.999	-4943.136	-3.5313	-52.703
8	12674.206	13964.815	3064.5537	4006.7013	-455.576
9	-18.059	.000	.0000	-74.1686	30.2347
10	1.564	.000	.0000	1899.6093	.0000000
11	36.531	12683.815	5.6845	.0000	.0002
12	5.8438	.0904	.0000	.0000	680.1046
13	2224573.0	2255414.4	1964138.6	3151483.8	9196096.9
14	72.3322	71.1115	44.3874	258.0051	274.7880
15	11.0631	10.8244	13.3266	5.6059	-9.2221

1	350.0000	542242.0400	2194736.5000	3.5632	76.1217
2	12871.6788	14186.6623	41.652	3.1970	77.4257
3	424361.2	368097.3	-5729618.000	764131.550	-2138896.000
4	13607.1	136629.5	17648634.0	-2304.163	-7790.170
5	2247026.6	2724613.5	10761544.6	700845.900	-42493.790
6	-548.497	-1004.935	-12883.230	3207.4809	-11528.167
7	193.196	349.988	-5088.512	-3.1782	-53.872
8	12858.536	14146.697	3064.4514	4067.9640	-474.687
9	-18.236	.000	.0000	-73.9776	30.2759
10	1.592	.000	.0000	1917.8136	.0000000
11	37.152	12871.679	5.7377	.0000	.0002
12	6.0141	.0871	.0000	.0000	683.7728
13	2286787.3	2317641.5	2018259.2	3090725.5	9135963.8
14	72.3469	71.1596	45.3064	257.9437	274.8132
15	10.6944	10.4649	12.9349	5.9633	-9.0895

1	355.0000	546161.8500	2257812.5000	3.3693	76.2415
2	13063.4218	14378.8964	42.375	3.0255	77.5170
3	421390.8	362813.4	-5794415.300	780205.590	-2196916.200
4	14592.8	138379.1	17622820.0	-2319.261	-8062.479
5	2311787.5	2795808.8	10776866.7	721341.360	-44916.034
6	-640.131	-1109.123	-13036.356	3221.9721	-11679.898
7	201.097	349.860	-5235.705	-2.8571	-55.053
8	13046.179	14331.788	3064.8840	4130.3551	-494.292
9	-18.410	.000	.0000	-73.7835	30.3173
10	1.620	.000	.0000	1935.2368	.0000000
11	37.874	13063.422	5.7935	.0000	.0002
12	6.1870	.0841	.0000	.0000	687.2745
13	2349924.3	2380790.3	2073634.7	3029067.4	9074848.7
14	72.3616	71.2064	46.1881	257.8782	274.8389
15	10.3302	10.1094	12.5443	6.3331	-8.9557

TABLE AP 3-2 (Sheet 20 of 39)
SATURN OBSERVED TRAJECTORY - BOOST PHASE (AA83)

1	360.0000	549923.6100	2321831.5000	3.1853	76.3619
2	13258.9996	14574.9259	42.980	2.8624	77.6092
3	417960.1	357005.9	-5859984.800	796351.160	-2255694.800
4	15617.8	140127.5	17596266.0	-2332.916	-8340.723
5	2377494.9	2867937.7	10792192.4	742151.630	-47437.846
6	-732.712	-1214.503	-13192.088	3236.0634	-11831.508
7	208.938	349.495	-5384.995	-2.6049	-56.246
8	13237.090	14520.032	3065.7998	4193.8598	-514.396
9	-18.613	.000	.0000	-73.5863	30.3590
10	1.647	.000	.0000	1951.9150	.0000000
11	38.478	13259.000	5.8518	.0000	.0002
12	6.3624	.0815	.0000	.0000	690.6187
13	2414004.1	2444880.7	2130267.8	2966498.5	9012735.7
14	72.3763	71.2520	47.0342	257.8085	274.8652
15	9.9704	9.7578	12.1552	6.7165	-8.8205

1	365.0000	553533.5000	2386810.5000	3.0111	76.4843
2	13458.1672	14774.5153	43.617	2.7079	77.7036
3	414064.0	350668.3	-5926339.300	812566.130	-2315231.100
4	16682.6	141874.2	17568961.0	-2345.244	-8624.959
5	2444164.5	2941015.1	10807522.8	769282.020	-50060.846
6	-826.251	-1321.085	-13350.327	3249.7511	-11982.998
7	217.032	349.206	-5536.193	-2.3258	-57.450
8	13431.026	14711.191	3066.8665	4258.4072	-535.008
9	-18.835	.000	.0000	-73.3860	30.4009
10	1.675	.000	.0000	1967.8788	.0000000
11	39.113	13458.167	5.9123	.0000	.0002
12	6.5405	.0791	.0000	.0000	693.8126
13	2479045.5	2509931.4	2188161.2	2903009.6	8949608.7
14	72.3910	71.2963	47.8466	257.7339	274.8921
15	9.6149	9.4101	11.7682	7.1147	-8.6838

1	370.0000	556996.5800	2452768.5000	2.8448	76.6083
2	13661.7890	14978.5319	44.369	2.5600	77.8000
3	409696.5	343793.5	-5993492.900	828848.130	-2375524.600
4	17788.7	143619.8	17540893.0	-2356.086	-8915.245
5	2511813.4	3015057.7	10822859.0	784738.420	-52788.482
6	-921.283	-1429.428	-13511.716	3262.8651	-12134.366
7	225.333	348.930	-5690.061	-2.0395	-58.666
8	13628.828	14906.088	3068.0938	4324.2506	-556.132
9	-19.058	.000	.0000	-73.1825	30.4431
10	1.702	.000	.0000	1983.1568	.0000000
11	39.862	13661.789	5.9755	.0000	.0002
12	6.7213	.0770	.0000	.0000	696.8627
13	2545068.6	2575962.7	2247319.3	2838590.6	8885450.5
14	72.4057	71.3395	48.6269	257.6542	274.9196
15	9.2636	9.0662	11.3835	7.5291	-8.5456

1	375.0000	560318.4700	2519725.2000	2.6885	76.7336
2	13869.3754	15186.4830	45.159	2.4209	77.8979
3	404851.4	336373.7	-6061460.400	845194.630	-2436574.500
4	18936.2	145363.4	17512050.0	-2365.669	-9211.640
5	2580460.0	3090083.1	10838202.4	806526.970	-55623.037
6	-1017.257	-1538.975	-13675.884	3275.5749	-12285.612
7	233.694	348.526	-5846.036	-1.7885	-59.894
8	13830.045	15104.284	3069.7463	4391.2581	-577.777
9	-19.327	.000	.0000	-72.9757	30.4855
10	1.729	.000	.0000	1993.8248	.0000000
11	40.653	13869.375	6.0469	.0000	.0002
12	6.9047	.0753	.0000	.0000	699.0990
13	2612094.3	2642995.6	2307748.9	2773231.2	8820242.2
14	72.4204	71.3817	49.3768	257.5687	274.9478
15	8.9163	8.7259	11.0015	7.9614	-8.4059

1	380.0000	563505.9700	2587700.8000	2.5403	76.8608
2	14081.5195	15398.9685	45.887	2.2888	77.9980
3	399523.2	328402.5	-6130257.000	861603.430	-2498380.500
4	20126.3	147105.4	17482422.0	-2373.882	-9514.200
5	2650122.8	3166109.2	10853554.5	828653.920	-58567.131
6	-1114.710	-1650.280	-13843.315	3287.7114	-12436.735
7	242.306	348.171	-6004.699	-1.5192	-61.133
8	14035.238	15306.326	3071.5600	4459.5985	-599.948
9	-19.600	.000	.0000	-72.7655	30.5282
10	1.760	.000	.0000	2002.9429	.0000000
11	41.375	14081.520	6.1223	.0000	.0002
12	7.0910	.0738	.0000	.0000	701.0510
13	2680144.4	2711051.9	2369457.9	2706922.8	8753965.6
14	72.4350	71.4228	50.0977	257.4770	274.9766
15	8.5729	8.3892	10.6223	8.4133	-8.2644

TABLE AP 3-2 (Sheet 21 of 39)
SATURN OBSERVED TRAJECTORY - BOOST PHASE (AA83)

1	385.0000	566563.8200	2656715.7000	2.4008	76.9900
2	14297.8948	15615.6631	46.650	2.1643	78.1003
3	393704.0	319870.2	-6199897.800	878071.440	-2560941.700
4	21359.9	148845.5	17451993.0	-2380.736	-9822.986
5	2720820.2	3243154.0	10868915.8	851125.550	-61623.417
6	-1213.499	-1763.198	-14013.742	3299.3182	-12587.733
7	251.160	347.857	-6165.828	-1.2336	-62.383
8	14244.091	15511.902	3073.5249	4529.1788	-622.654
9	-19.872	.000	.0000	-72.5520	30.5711
10	1.791	.000	.0000	2011.6688	.0000000
11	42.126	14297.895	6.1999	.0000	.0002
12	7.2801	.0725	.0000	.0000	702.9184
13	2749240.1	2780152.5	2432454.7	2639657.3	8686601.2
14	72.4497	71.4630	50.7912	257.3784	275.0062
15	8.2333	8.0560	10.2463	8.8869	-8.1210
1	390.0000	569499.4400	2726790.8000	2.2705	77.1208
2	14518.8561	15836.9212	47.477	2.0480	78.2046
3	387387.7	310769.4	-6270398.400	894596.210	-2624257.600
4	22638.0	150583.7	17420752.0	-2386.287	-10138.053
5	2792571.6	3321235.9	10884288.0	873948.340	-64794.583
6	-1313.526	-1877.645	-14187.489	3310.4211	-12738.606
7	260.195	347.516	-6329.493	-.9527	-63.646
8	14456.975	15721.380	3075.8395	4600.1137	-645.902
9	-20.151	.000	.0000	-72.3349	30.6143
10	1.822	.000	.0000	2020.0258	.0000000
11	42.939	14518.856	6.2797	.0000	.0002
12	7.4722	.0714	.0000	.0000	704.7066
13	2819403.6	2850320.2	2496749.6	2571428.0	8618130.4
14	72.4644	71.5022	51.4586	257.2721	275.0365
15	7.8975	7.7261	9.8735	9.3844	-7.9758
1	395.0000	572318.7500	2797948.7000	2.1483	77.2529
2	14744.3847	16062.7246	48.264	1.9387	78.3104
3	380567.0	301091.4	-6341776.000	911174.900	-2688327.600
4	23961.3	152319.7	17388684.0	-2390.560	-10459.462
5	2865397.9	3400375.5	10899672.5	897129.310	-68083.356
6	-1415.137	-1993.968	-14364.396	3320.9132	-12889.353
7	269.270	347.002	-6496.034	-.7212	-64.920
8	14673.846	15934.706	3078.4441	4672.3884	-669.698
9	-20.443	.000	.0000	-72.1143	30.6577
10	1.852	.000	.0000	2028.0356	.0000000
11	43.705	14744.385	6.3618	.0000	.0002
12	7.6672	.0703	.0000	.0000	706.4198
13	2890659.0	2921578.7	2562355.1	2502228.9	8548531.4
14	72.4790	71.5406	52.1012	257.1572	275.0676
15	7.5652	7.3996	9.5041	9.9085	-7.8286
1	400.0000	575030.2700	2870209.3000	2.0352	77.3876
2	14974.2730	16292.8726	49.188	1.8375	78.4190
3	373235.6	290828.5	-6414045.700	927804.890	-2753150.900
4	25331.1	154053.7	17355780.0	-2393.480	-10787.268
5	2939317.2	3480590.0	10915070.0	920674.640	-71492.501
6	-1518.029	-2111.868	-14544.482	3330.8855	-13039.970
7	278.724	346.655	-6665.005	-.4349	-66.205
8	14894.521	16151.705	3081.1499	4745.9526	-694.051
9	-20.729	.000	.0000	-71.8900	30.7013
10	1.876	.000	.0000	2035.7213	.0000000
11	44.605	14974.273	6.4460	.0000	.0002
12	7.8652	.0694	.0000	.0000	708.0637
13	2963027.4	2993949.2	2629282.0	2432059.0	8477786.6
14	72.4937	71.5782	52.7203	257.0328	275.0995
15	7.2364	7.0763	9.1383	10.4621	-7.6791
1	405.0000	577641.4600	2943596.7000	1.9311	77.5235
2	15209.1968	16528.0360	50.020	1.7443	78.5292
3	365385.9	279971.4	-6487225.400	944483.290	-2818727.000
4	26748.3	155785.7	17322022.0	-2395.077	-11121.531
5	3014352.0	3561901.2	10930482.6	946591.790	-75024.815
6	-1622.334	-2231.495	-14728.196	3340.2917	-13190.458
7	288.219	346.123	-6836.881	-.2018	-67.502
8	15119.677	16373.045	3084.3619	4821.0118	-718.968
9	-21.027	.000	.0000	-71.6621	30.7451
10	1.898	.000	.0000	2043.1061	.0000000
11	45.406	15209.197	6.5325	.0000	.0002
12	8.0663	.0686	.0000	.0000	709.6426
13	3036534.2	3067457.1	2697545.3	2360915.6	8405873.7
14	72.5083	71.6150	53.3169	256.8978	275.1322
15	6.9111	6.7561	8.7760	11.0486	-7.5275

TABLE AP 3-2 (Sheet 22 of 39)
SATURN OBSERVED TRAJECTORY - BOOST PHASE (AA83)

1	410.0000	580160.5800	3018133.6000	1.8350	77.6608
2	15448.9744	16768.0350	50.964	1.6583	78.6411
3	357011.6	268512.3	-6561332.600	961207.390	-2885055.300
4	28213.2	157514.5	17287398.0	-2395.622	-11462.309
5	3090523.5	3644329.8	10945912.3	968887.870	-78683.140
6	-1728.324	-2353.123	-14915.304	3349.0476	-13340.612
7	297.767	345.416	-7011.827	-.0186	-68.811
8	15349.105	16598.510	3087.8806	4897.5023	-744.457
9	-21.355	.000	.0000	-71.4303	30.7891
10	1.925	.000	.0000	2050.2176	.0000000
11	46.320	15448.974	6.6213	.0000	.0002
12	8.2706	.0678	.0000	.0000	711.1631
13	3111203.6	3142126.8	2767160.4	2288801.5	8332772.3
14	72.5230	71.6510	53.8922	256.7508	275.1659
15	6.5892	6.4391	8.4174	11.6720	-7.3733
	S-II NO. 2 ENGINE OUT				
1	412.9000	581574.2900	3061898.9000	1.7827	77.7394
2	15587.4585	16906.6320	39.849	1.6113	78.7054
3	351902.7	261578.2	-6604741.900	970924.600	-2923870.000
4	29084.7	158515.4	17266908.0	-2395.586	-11662.968
5	3135228.8	3692654.8	10954865.5	983155.000	-80863.840
6	-1790.341	-2424.278	-15022.703	3353.9210	-13427.956
7	302.827	344.465	-7113.759	-.0753	-69.575
8	15481.338	16728.374	3089.8347	4941.6716	-759.505
9	-21.511	.000	.0000	-71.2941	30.8148
10	1.934	.000	.0000	2054.2018	.0000000
11	35.048	15587.458	6.6727	.0000	.0002
12	8.3905	.0674	.0000	.0000	712.0149
13	3155050.0	3185972.9	2808158.5	2246532.0	8289820.0
14	72.5314	71.6716	54.2165	256.6594	275.1858
15	6.4039	6.2565	8.2110	12.0520	-7.2829
	S-II NO. 3 ENGINE OUT				
1	414.2000	582199.3600	3081636.0000	1.7562	77.7725
2	15636.9917	16956.2090	34.775	1.5874	78.7331
3	349555.9	258404.8	-6624294.900	975285.740	-2941351.600
4	29479.3	158962.5	17257630.0	-2395.836	-11753.639
5	3155385.4	3714431.8	10958879.9	989589.700	-81855.615
6	-1817.833	-2455.550	-15059.154	3356.2914	-13467.005
7	304.226	343.348	-7155.294	-.3111	-69.919
8	15527.989	16773.952	3088.1587	4957.6392	-766.315
9	-21.318	.000	.0000	-71.2326	30.8263
10	1.937	.000	.0000	2055.9625	.0000000
11	29.827	15636.992	6.6904	.0000	.0002
12	8.4446	.0672	.0000	.0000	712.3911
13	3174825.2	3205748.0	2826677.3	2227489.3	8270443.3
14	72.5352	71.6807	54.3596	256.6169	275.1949
15	6.3212	6.1751	8.1190	12.2271	-7.2420
1	415.0000	582580.4500	3093813.3000	1.7390	77.7926
2	15663.3072	16982.5500	32.762	1.5717	78.7501
3	348093.8	256431.5	-6636351.400	977971.050	-2952135.000
4	29723.1	159236.9	17251894.0	-2396.148	-11809.659
5	3167820.1	3727862.9	10961349.6	993559.980	-82470.355
6	-1834.635	-2474.572	-15077.744	3357.8167	-13491.031
7	304.900	342.534	-7179.418	-.4946	-70.131
8	15552.503	16797.804	3086.2010	4966.1928	-770.525
9	-20.521	.000	.0000	-71.1947	30.8334
10	1.938	.000	.0000	2057.0353	.0000000
11	27.575	15663.307	6.6995	.0000	.0002
12	8.4780	.0670	.0000	.0000	712.6204
13	3187026.2	3217948.8	2838111.7	2215746.6	8258486.4
14	72.5375	71.6862	54.4469	256.5903	275.2005
15	6.2705	6.1251	8.0625	12.3362	-7.2168
1	420.0000	584914.4200	3170303.9000	1.6853	77.9229
2	15799.5532	17118.9420	31.631	1.5236	78.8625
3	338684.7	243789.7	-6711977.700	994792.510	-3019965.400
4	31258.8	160938.6	17215659.0	-2400.942	-12163.638
5	3245903.5	3812163.1	10976743.4	1018506.020	-86389.376
6	-1922.592	-2575.785	-15173.095	3372.7121	-13641.114
7	309.719	338.543	-7306.399	-1.3051	-71.463
8	15679.082	16920.666	3074.4013	5011.7655	-797.180
9	-14.662	.000	.0000	-70.9564	30.8776
10	1.937	.000	.0000	2063.5993	.0000000
11	24.233	15799.553	6.7445	.0000	.0002
12	8.6876	.0660	.0000	.0000	714.0233
13	3263674.8	3294596.2	2910088.4	2142106.6	8183349.1
14	72.5517	71.7204	54.9795	256.4158	275.2360
15	5.9565	5.8156	7.7130	13.0434	-7.0584

TABLE AP 3-2 (Sheet 23 of 39)
SATURN OBSERVED TRAJECTORY - BOOST PHASE (AA83)

1	425.0000	587250.6700	3247426.4000	1.6913	78.0694
2	15928.8821	17248.4490	31.970	1.5304	78.9904
3	328890.6	230696.4	-6788077.200	1011705.030	-3088545.900
4	32826.9	162629.2	17178846.0	-2407.112	-12524.304
5	3324601.9	3897061.1	10992092.6	1043675.350	-90443.147
6	-1994.885	-2661.344	-15267.840	3392.3362	-13791.057
7	318.619	338.758	-7416.634	-.8301	-72.806
8	15800.259	17038.530	3065.2294	5055.9950	-824.426
9	-14.667	.000	.0000	-70.7159	30.9217
10	1.926	.000	.0000	2070.1560	.0000000
11	24.526	15928.882	6.7864	.0000	.0002
12	8.8989	.0649	.0000	.0000	715.4245
13	3340991.4	3371910.8	2982930.9	2068116.0	8107560.2
14	72.5656	71.7535	55.4900	256.2256	275.2723
15	5.6494	5.5126	7.3714	13.7993	-6.8978

1	430.0000	589607.0900	3325180.9000	1.6761	78.2318
2	16064.9492	17384.7720	32.371	1.5177	79.1329
3	318722.9	217162.7	-6864662.700	1028711.680	-3157875.700
4	34453.0	164333.8	17141473.0	-2406.917	-12891.714
5	3403916.4	3982558.5	11007381.7	1069069.400	-94634.631
6	-2075.312	-2755.332	-15367.629	3409.3479	-13940.856
7	331.822	343.034	-7534.157	.8858	-74.160
8	15926.882	17161.608	3050.0468	5101.9950	-852.266
9	-17.252	.000	.0000	-70.4731	30.9656
10	1.896	.000	.0000	2076.7580	.0000000
11	25.931	16064.949	6.8309	.0000	.0002
12	9.1120	.0639	.0000	.0000	716.8352
13	3418979.0	3449895.3	3056623.4	1993820.8	8031122.1
14	72.5798	71.7861	55.9801	256.0168	275.3093
15	5.3490	5.2161	7.0376	14.6100	-6.7347

1	435.0000	591941.1000	3403607.4000	1.6316	78.3835
2	16207.8458	17527.8860	32.794	1.4780	79.2656
3	308125.2	203130.5	-6941752.800	1045794.590	-3227954.100
4	36139.7	166053.7	17103480.0	-2400.005	-13265.924
5	3483878.8	4068684.9	11022590.1	1094697.900	-98966.812
6	-2166.410	-2860.216	-15468.912	3422.9934	-14090.510
7	341.924	343.941	-7663.932	1.5786	-75.526
8	16058.768	17289.526	3033.7712	5149.6525	-880.705
9	-19.023	.000	.0000	-70.2280	31.0093
10	1.854	.000	.0000	2083.2845	.0000000
11	26.855	16207.846	6.8782	.0000	.0002
12	9.3269	.0630	.0000	.0000	718.2297
13	3497664.6	3528576.8	3131180.0	1919212.9	7953983.7
14	72.5943	71.8183	56.4514	255.7866	275.3470
15	5.0540	4.9249	6.7104	15.4815	-6.5694

1	440.0000	594218.0400	3482735.4000	1.5642	78.5238
2	16356.1524	17676.3630	33.213	1.4169	79.3878
3	297050.7	188552.1	-7019350.100	1062939.000	-3298780.500
4	37866.1	167766.7	17064813.0	-2393.115	-13646.992
5	3564510.9	4155460.1	11037718.7	1120568.100	-103442.691
6	-2266.523	-2974.309	-15570.645	3433.7870	-14240.015
7	348.591	341.171	-7804.220	1.1543	-76.903
8	16194.600	17420.992	3017.1187	5198.5750	-909.747
9	-20.789	.000	.0000	-69.9805	31.0528
10	1.806	.000	.0000	2089.6395	.0000000
11	27.648	16356.152	6.9281	.0000	.0002
12	9.5438	.0621	.0000	.0000	719.5875
13	3577067.3	3607974.6	3206615.3	1844301.9	7876108.5
14	72.6086	71.8498	56.9045	255.5325	275.3855
15	4.7635	4.6379	6.3885	16.4207	-6.4020

1	445.0000	596402.8300	3562594.4000	1.4771	78.6715
2	16510.3450	17830.7550	33.623	1.3376	79.5169
3	285452.6	173379.5	-7097463.600	1080130.000	-3370354.100
4	39629.1	169468.5	17025421.0	-2387.528	-14034.975
5	3645834.1	4242903.7	11052753.6	1146686.700	-108065.297
6	-2375.070	-3097.091	-15675.329	3441.8856	-14389.367
7	357.149	340.045	-7952.600	1.2343	-78.292
8	16334.717	17556.431	2996.0116	5248.8940	-939.396
9	-22.165	.000	.0000	-69.7305	31.0962
10	1.760	.000	.0000	2095.7283	.0000000
11	28.248	16510.345	6.9808	.0000	.0002
12	9.7626	.0613	.0000	.0000	720.8882
13	3657206.5	3688108.3	3282939.5	1769107.4	7797458.8
14	72.6227	71.8804	57.3406	255.2507	275.4251
15	4.4766	4.3544	6.0711	17.4361	-6.2327

TABLE AP 3-2 (Sheet 24 of 39)
SATURN OBSERVED TRAJECTORY - BOOST PHASE (AA83)

1	450.0000	598475.8700	3643205.1000	1.3828	78.8256
2	16667.5400	17988.1650	33.997	1.2516	79.6522
3	273298.8	157579.6	-7176103.900	1097357.300	-3442674.000
4	41440.2	171169.5	16985276.0	-2380.038	-14429.930
5	3727862.2	4331028.3	11067673.3	1173058.500	-112837.677
6	-2488.268	-3224.716	-15781.298	3448.4617	-14538.567
7	367.284	340.318	-8105.111	1.7443	-79.692
8	16476.666	17693.488	2971.8566	5299.8927	-969.657
9	-23.060	.000	.0000	-69.4778	31.1394
10	1.727	.000	.0000	2101.4949	.0000000
11	28.676	16667.540	7.0352	.0000	.0002
12	9.9835	.0606	.0000	.0000	722.1202
13	3738096.6	3768992.3	3360155.4	1693673.4	7718008.3
14	72.6368	71.9105	57.7608	254.9361	275.4655
15	4.1927	4.0737	5.7576	18.5377	-6.0615

1	455.0000	600427.9200	3724582.7000	1.2852	78.9746
2	16827.8980	18148.6990	34.432	1.1623	79.7830
3	260568.5	141130.6	-7255275.000	1114614.000	-3515739.400
4	43298.6	172868.1	16944356.0	-2371.160	-14831.914
5	3810605.3	4419842.8	11082471.5	1199687.300	-117762.905
6	-2605.162	-3356.206	-15887.691	3453.8121	-14687.611
7	375.664	338.657	-8262.322	1.6683	-81.104
8	16620.775	17832.457	2947.9838	5351.6622	-1000.536
9	-23.683	.000	.0000	-69.2225	31.1825
10	1.700	.000	.0000	2106.9144	.0000000
11	29.103	16827.898	7.0915	.0000	.0002
12	10.2066	.0599	.0000	.0000	723.2778
13	3819749.1	3850638.0	3438267.5	1618067.2	7637739.7
14	72.6509	71.9401	58.1660	254.5829	275.5069
15	3.9115	3.7955	5.4476	19.7380	-5.8883

1	460.0000	602253.3500	3806742.8000	1.1890	79.1191
2	16991.2420	18312.1840	34.845	1.0742	79.9097
3	247246.0	124016.1	-7334978.500	1131894.900	-3589549.800
4	45193.5	174552.5	16902640.0	-2364.456	-15240.984
5	3894074.0	4509356.5	11097152.4	1226576.600	-122844.082
6	-2724.464	-3490.278	-15994.767	3458.3274	-14836.497
7	382.387	335.171	-8423.086	1.0394	-82.526
8	16767.033	17973.363	2924.9242	5404.2117	-1032.037
9	-24.046	.000	.0000	-68.9645	31.2254
10	1.679	.000	.0000	2111.9765	.0000000
11	29.465	16991.242	7.1497	.0000	.0002
12	10.4317	.0594	.0000	.0000	724.3590
13	3902176.8	3933058.6	3517284.5	1542373.8	7556637.9
14	72.6648	71.9689	58.5567	254.1843	275.5495
15	3.6328	3.5196	5.1408	21.0520	-5.7132

1	465.0000	603955.4600	3889699.6000	1.0971	79.2692
2	17157.3740	18478.4600	35.268	.9900	80.0419
3	233322.3	106225.9	-7415221.800	1149196.600	-3664104.200
4	47124.8	176221.9	16860114.0	-2360.130	-15657.196
5	3978278.9	4599579.5	11111714.8	1253730.600	-128084.329
6	-2845.313	-3626.098	-16103.721	3462.2615	-14985.224
7	390.429	332.842	-8585.477	.7666	-83.961
8	16915.296	18116.130	2900.5670	5457.5201	-1064.166
9	-24.278	.000	.0000	-68.7037	31.2682
10	1.662	.000	.0000	2116.6908	.0000000
11	29.816	17157.374	7.2096	.0000	.0002
12	10.6591	.0590	.0000	.0000	725.3660
13	3985393.7	4016267.8	3597213.8	1466705.7	7474689.7
14	72.6786	71.9971	58.9338	253.7311	275.5933
15	3.3563	3.2459	4.8371	22.4978	-5.5361

1	470.0000	605540.9100	3973464.4000	1.0122	79.4242
2	17325.5970	18646.8270	35.720	.9122	80.1789
3	218791.7	87753.7	-7496013.600	1166517.000	-3739401.800
4	49100.0	177882.9	16816775.0	-2356.167	-16080.608
5	4063228.7	4690519.4	11126152.3	1281152.600	-133486.800
6	-2966.819	-3762.760	-16214.132	3465.8896	-15133.789
7	399.582	331.478	-8748.624	.7915	-85.406
8	17065.012	18260.229	2875.3618	5511.4274	-1096.928
9	-24.344	.000	.0000	-68.4402	31.3107
10	1.643	.000	.0000	2121.0743	.0000000
11	30.178	17325.597	7.2709	.0000	.0002
12	10.8886	.0586	.0000	.0000	726.3023
13	4069411.2	4100277.0	3678059.2	1391210.3	7391885.1
14	72.6922	72.0248	59.2980	253.2112	275.6382
15	3.0820	2.9743	4.5364	24.0973	-5.3567

TABLE AP 3-2 (Sheet 25 of 39)
SATURN OBSERVED TRAJECTORY - BOOST PHASE (AA83)

1	475.0000	607018.7800	4058049.0000	.9355	79.5776
2	17496.0410	18817.3910	36.124	.8419	80.3146
3	203652.5	68596.5	-7577360.300	1183854.900	-3815441.800
4	51119.5	179535.2	16772615.9	-2352.649	-16511.274
5	4148931.9	4782184.4	11140465.4	1308846.000	-139054.670
6	-3088.646	-3899.919	-16325.513	3469.3158	-15282.189
7	407.903	329.135	-8913.069	.5213	-86.862
8	17216.426	18405.885	2851.1578	5566.0032	-1130.327
9	-24.355	.000	.0000	-68.1738	31.3531
10	1.623	.000	.0000	2125.1559	.0000000
11	30.484	17496.041	7.3336	.0000	.0002
12	11.1204	.0583	.0000	.0000	727.1740
13	4154241.5	4185098.6	3759827.8	1316073.4	7308215.9
14	72.7058	72.0519	59.6501	252.6091	275.6844
15	2.8099	2.7048	4.2387	25.8772	-5.1751
1	480.0000	608400.4000	4143461.4000	.8681	79.7291
2	17668.3630	18989.8100	36.622	.7801	80.4487
3	187904.3	48753.3	-7659265.100	1201209.600	-3892223.400
4	53177.1	181172.1	16727632.0	-2351.623	-16949.251
5	4235395.3	4874580.4	11154661.5	1336813.600	-144791.150
6	-3210.410	-4037.183	-16437.637	3472.6597	-15430.423
7	415.235	325.663	-9078.452	-.0897	-88.330
8	17369.282	18552.844	2828.2014	5621.1730	-1164.371
9	-24.308	.000	.0000	-67.9046	31.3953
10	1.605	.000	.0000	2128.9676	.0000000
11	30.878	17668.364	7.3975	.0000	.0002
12	11.3545	.0581	.0000	.0000	727.9882
13	4239894.8	4270742.7	3842525.9	1241533.5	7223677.1
14	72.7193	72.0785	59.9904	251.9044	275.7320
15	2.5401	2.4373	3.9441	27.8695	-4.9910
1	485.0000	609699.8800	4229713.3000	.8112	79.8859
2	17842.9190	19164.4640	36.742	.7281	80.5879
3	171548.4	28224.2	-7741736.200	1218581.200	-3969745.700
4	55274.4	182794.2	16681821.2	-2352.843	-17394.593
5	4322628.3	4967716.3	11168742.2	1365059.200	-150699.470
6	-3331.783	-4174.259	-16551.790	3476.0085	-15578.487
7	423.797	323.275	-9243.781	-.3668	-89.809
8	17523.965	18701.545	2804.9009	5677.0711	-1199.063
9	-24.223	.000	.0000	-67.6324	31.4372
10	1.588	.000	.0000	2132.5485	.0000000
11	30.888	17842.919	7.4628	.0000	.0002
12	11.5909	.0579	.0000	.0000	728.7531
13	4326384.0	4357222.2	3926161.6	1167892.4	7138261.5
14	72.7325	72.1045	60.3196	251.0692	275.7810
15	2.2725	2.1720	3.6525	30.1130	-4.8041
1	490.0000	610930.1000	4316807.3000	.7631	80.0442
2	18016.1040	19337.7410	36.227	.6841	80.7290
3	154587.1	7011.2	-7824775.700	1235969.800	-4048008.000
4	57415.4	184405.0	16635186.1	-2355.236	-17847.355
5	4410632.1	5061592.8	11182705.8	1393583.700	-156782.870
6	-3452.535	-4310.800	-16664.325	3479.4680	-15726.377
7	432.384	320.833	-9408.101	-.6574	-91.298
8	17676.908	18848.405	2781.4036	5732.6078	-1234.409
9	-24.116	.000	.0000	-67.3574	31.4790
10	1.578	.000	.0000	2135.9356	.0000000
11	30.257	18016.104	7.5277	.0000	.0002
12	11.8295	.0578	.0000	.0000	729.4766
13	4413713.6	4444541.6	4010734.0	1095544.8	7051969.5
14	72.7457	72.1301	60.6383	250.0641	275.8314
15	2.0072	1.9089	3.3640	32.6539	-4.6144
	S-II EMR SHIFT (GUIDANCE SENSED)				
1	493.7000	611801.9300	4381791.4000	.7313	80.1597
2	18141.7470	19463.4380	35.347	.6551	80.8321
3	141647.7	-9125.5	-7886581.600	1248848.600	-4106397.700
4	59025.5	185587.2	16600148.5	-2358.514	-18187.208
5	4476241.8	5131528.6	11192963.3	1414869.300	-161399.250
6	-3541.732	-4411.670	-16744.635	3482.0452	-15835.702
7	437.828	318.091	-9529.031	-1.1548	-92.407
8	17787.282	18954.194	2764.0929	5772.9537	-1260.990
9	-24.032	.000	.0000	-67.1520	31.5097
10	1.571	.000	.0000	2138.3344	.0000000
11	29.287	18141.747	7.5749	.0000	.0002
12	12.0076	.0577	.0000	.0000	729.9888
13	4478871.2	4509691.4	4073911.9	1043137.4	6987559.2
14	72.7554	72.1487	60.8675	249.1791	275.8697
15	1.8123	1.7156	3.1526	34.7570	-4.4721

TABLE AP 3-2 (Sheet 26 of 39)
SATURN OBSERVED TRAJECTORY - BOOST PHASE (AA83)

1	495.0000	612101.1000	4404729.6000	.7206	80.2001
2	18184.9860	19506.6940	35.019	.6454	80.8682
3	137023.1	-14883.6	-7908366.900	1253375.900	-4127009.200
4	59595.8	186000.0	16587732.1	-2360.157	-18307.593
5	4499390.1	5156192.8	11196552.1	1422383.300	-163044.660
6	-3573.011	-4447.036	-16771.918	3482.9663	-15874.091
7	439.605	316.995	-9571.206	-1.3696	-92.799
8	17825.096	18990.380	2757.8907	5786.8564	-1270.415
9	-23.991	.000	.0000	-67.0794	31.5204
10	1.568	.000	.0000	2139.1569	.0000000
11	28.926	18184.986	7.5911	.0000	.0002
12	12.0705	.0576	.0000	.0000	730.1645
13	4501870.4	4532687.7	4096227.6	1025004.7	6964819.0
14	72.7588	72.1551	60.9467	248.8335	275.8834
15	1.7442	1.6480	3.0787	35.5460	-4.4217
1	500.0000	613220.5900	4493453.0000	.6852	80.3573
2	18347.8690	19669.6420	34.088	.6131	81.0092
3	118859.2	-37456.9	-7992480.500	1270800.100	-4206748.600
4	61811.0	187574.6	16539469.5	-2369.042	-18775.360
5	4588872.5	5251485.9	11210278.9	1451449.400	-169488.140
6	-3692.313	-4582.030	-16873.802	3486.7887	-16021.625
7	446.676	313.024	-9731.314	-2.1196	-94.310
8	17966.958	19125.948	2733.3477	5839.3548	-1307.086
9	-23.740	.000	.0000	-66.7987	31.5616
10	1.559	.000	.0000	2142.2324	.0000000
11	27.858	18347.869	7.6523	.0000	.0002
12	12.3136	.0575	.0000	.0000	730.8215
13	4590827.5	4621634.0	4182613.0	956935.0	6876839.0
14	72.7716	72.1796	61.2453	247.2950	275.9371
15	1.4836	1.3894	2.7965	38.8498	-4.2258
1	505.0000	614299.6800	4582952.2000	.6594	80.5196
2	18505.7300	19828.5770	33.765	.5898	81.1552
3	100102.3	-60701.6	-8077094.200	1288244.400	-4287225.200
4	64064.5	189132.2	16490414.3	-2380.769	-19250.707
5	4679052.2	5347444.6	11223878.7	1480774.800	-176116.650
6	-3809.870	-4715.281	-16972.475	3491.0858	-16168.975
7	454.806	310.095	-9888.195	-2.5485	-95.831
8	18104.616	19257.271	2707.6157	5890.7630	-1344.426
9	-23.255	.000	.0000	-66.5153	31.6025
10	1.549	.000	.0000	2145.1946	.0000000
11	27.369	18506.730	7.7118	.0000	.0002
12	12.5589	.0574	.0000	.0000	731.4540
13	4680561.1	4711356.0	4269862.4	892176.3	6788057.8
14	72.7844	72.2037	61.5344	245.3212	275.9925
15	1.2255	1.1332	2.5176	42.6301	-4.0267
1	510.0000	615357.1600	4673215.9000	.6486	80.6832
2	18664.1410	19986.0540	33.725	.5805	81.3027
3	80764.3	-84606.0	-8162198.500	1305711.900	-4368438.000
4	66358.7	190675.0	16440581.5	-2394.665	-19733.691
5	4769916.3	5444056.2	11237352.3	1510356.700	-182933.530
6	-3924.389	-4845.577	-17070.395	3496.2266	-16316.137
7	462.875	307.052	-10042.176	-3.0090	-97.364
8	18241.027	19387.329	2683.0517	5941.9917	-1382.440
9	-22.590	.000	.0000	-66.2292	31.6430
10	1.539	.000	.0000	2148.0952	.0000000
11	27.134	18664.141	7.7708	.0000	.0002
12	12.8063	.0573	.0000	.0000	732.0738
13	4771061.4	4801844.4	4357962.3	831786.7	6698493.2
14	72.7970	72.2272	61.8144	242.7058	276.0496
15	.9699	.8795	2.2421	46.9477	-3.8241
1	515.0000	616417.8700	4764236.0000	.6557	80.8461
2	18820.0840	20142.0530	33.782	.5879	81.4499
3	60861.1	-109154.8	-8247790.600	1323207.300	-4450386.200
4	68691.7	192201.1	16389985.1	-2411.347	-20224.362
5	4861460.0	5541315.5	11250706.9	1540194.300	-189942.180
6	-4034.822	-4971.871	-17167.761	3502.5287	-16463.107
7	470.269	303.288	-10192.683	-3.6860	-98.906
8	18376.469	19516.426	2660.7450	5993.1339	-1421.133
9	-21.319	.000	.0000	-65.9404	31.6831
10	1.529	.000	.0000	2151.0024	.0000000
11	26.880	18820.084	7.8291	.0000	.0002
12	13.0557	.0571	.0000	.0000	732.6947
13	4862326.1	4893096.8	4446907.6	777085.6	6608158.3
14	72.8094	72.2504	62.0857	239.0964	276.1085
15	.7172	.6285	1.9701	51.8391	-3.6176

TABLE AP 3-2 (Sheet 27 of 39)
SATURN OBSERVED TRAJECTORY - BOOST PHASE (AA83)

1	520.0000	617521.6100	4856000.0000	.7011	81.0108
2	18971.2870	20293.3070	34.330	.6310	81.5990
3	40425.1	-134315.8	-8333867.200	1340739.900	-4533068.800
4	71061.8	193708.4	16338654.6	-2431.381	-20722.771
5	4953675.1	5639214.7	11263957.8	1570286.500	-197146.010
6	-4133.737	-5086.687	-17264.733	3512.2690	-16609.880
7	477.677	299.603	-10332.506	-4.3358	-100.459
8	18509.289	19643.172	2643.2298	6043.7676	-1460.508
9	-19.265	.000	.0000	-65.6490	31.7229
10	1.529	.000	.0000	2154.0253	.0000000
11	26.903	18971.287	7.8851	.0000	.0002
12	13.3072	.0570	.0000	.0000	733.3402
13	4954349.6	4985107.8	4536689.8	729688.4	6517077.7
14	72.8218	72.2731	62.3486	233.8519	276.1694
15	.4675	.3805	1.7020	57.2719	-3.4069

1	525.0000	618732.6500	4948491.6000	.7578	81.1774
2	19124.0470	20446.1200	34.488	.6848	81.7501
3	19512.6	-160033.1	-8420434.500	1358326.400	-4616484.600
4	73469.2	195197.5	16286639.1	-2454.591	-21228.968
5	5046557.3	5737751.1	11277130.2	1600633.500	-204548.420
6	-4230.945	-5199.974	-17363.525	3522.4137	-16756.450
7	485.327	296.047	-10471.476	-4.9435	-102.022
8	18643.839	19771.609	2626.7992	6095.1261	-1500.570
9	-19.207	.000	.0000	-65.3551	31.7623
10	1.536	.000	.0000	2157.3377	.0000000
11	26.945	19124.047	7.9409	.0000	.0002
12	13.5607	.0568	.0000	.0000	734.0477
13	5047129.7	5077874.9	4627303.8	691470.7	6425283.1
14	72.8340	72.2953	62.6034	225.7324	276.2324
15	.2215	.1361	1.4385	63.0524	-3.1911

1	530.0000	620058.3500	5041723.3000	.8234	81.3448
2	19278.4910	20600.6200	34.801	.7471	81.9021
3	-1881.4	-186312.8	-8507500.700	1375964.700	-4700632.900
4	75914.9	196668.5	16233930.7	-2480.912	-21743.007
5	5140117.3	5836934.5	11290223.9	1631239.300	-212152.860
6	-4327.243	-5312.525	-17463.830	3532.7187	-16902.810
7	492.851	292.240	-10610.416	-5.6243	-103.595
8	18780.104	19901.690	2611.3749	6147.1961	-1541.322
9	-19.164	.000	.0000	-65.0585	31.8012
10	1.543	.000	.0000	2160.9604	.0000000
11	27.150	19278.491	7.9966	.0000	.0002
12	13.8162	.0565	.0000	.0000	734.8216
13	5140678.0	5171409.8	4718757.9	664339.3	6332766.3
14	72.8461	72.3172	62.8506	212.3157	276.2975
15	-.0210	-.1049	1.1792	68.6232	-2.9701

1	535.0000	621509.9200	5135695.4000	.8960	81.5139
2	19432.6050	20754.7930	34.996	.8158	82.0559
3	-23756.1	-213154.9	-8595067.300	1393654.600	-4785512.400
4	78398.0	198120.1	16180528.4	-2510.773	-22264.934
5	5234357.6	5936767.1	11303241.0	1662105.600	-219962.810
6	-4422.812	-5424.457	-17563.809	3543.1471	-17048.956
7	500.452	288.425	-10748.683	-6.3047	-105.178
8	18915.983	20031.314	2596.1309	6199.3383	-1582.768
9	-19.112	.000	.0000	-64.7593	31.8397
10	1.547	.000	.0000	2164.9234	.0000000
11	27.231	19432.605	8.0513	.0000	.0002
12	14.0737	.0561	.0000	.0000	735.6683
13	5234998.3	5265716.5	4811052.6	650026.7	6239528.1
14	72.8580	72.3386	63.0905	190.0445	276.3648
15	-.2600	-.3425	.9241	72.6880	-2.7435

1	540.0000	623100.8800	5230411.3000	.9735	81.6855
2	19588.0450	20910.3000	35.354	.8893	82.2122
3	-46109.5	-240557.7	-8683135.900	1411396.000	-4871122.100
4	80920.4	199553.4	16126433.0	-2543.751	-22794.799
5	5329279.8	6037250.2	11316180.8	1693233.800	-227981.720
6	-4518.603	-5536.772	-17664.751	3553.3911	-17194.880
7	508.464	284.898	-10887.474	-6.8946	-106.770
8	19052.958	20161.936	2580.7340	6251.9974	-1624.912
9	-19.062	.000	.0000	-64.4575	31.8777
10	1.544	.000	.0000	2169.2609	.0000000
11	27.480	19588.045	8.1055	.0000	.0002
12	14.3333	.0557	.0000	.0000	736.5948
13	5330093.4	5360797.6	4904187.8	649729.2	6145572.1
14	72.8698	72.3597	63.3233	160.3966	276.4346
15	-.4957	-.5768	.6732	73.2700	-2.5109

TABLE AP 3-2 (Sheet 28 of 39)
SATURN OBSERVED TRAJECTORY - BOOST PHASE (AA83)

1	545.0000	624843.3300	5325876.0000	1.0579	81.8573
2	19744.7370	21067.0590	35.731	.9693	82.3688
3	-68941.2	-268521.9	-8771711.600	1429188.500	-4957460.800
4	83481.9	200968.1	16071642.6	-2580.007	-23332.649
5	5424890.4	6138389.6	11329045.9	1724626.900	-236213.100
6	-4614.006	-5648.857	-17766.537	3563.6356	-17340.575
7	516.094	280.867	-11026.605	-7.6350	-108.372
8	19191.124	20293.658	2566.1657	6305.2052	-1667.756
9	-19.011	.000	.0000	-64.1531	31.9153
10	1.519	.000	.0000	2172.5021	.0000000
11	27.747	19744.737	8.1618	.0000	.0002
12	14.5949	.0553	.0000	.0000	737.3613
13	5425970.6	5456660.3	4998167.9	663809.8	6050896.6
14	72.8816	72.3804	63.5495	135.3205	276.5069
15	-.7280	-.8079	.4263	69.9505	-2.2720

1	550.0000	626752.3500	5422093.6000	1.1494	82.0302
2	19902.7750	21225.1690	36.095	1.0560	82.5267
3	-92248.2	-297045.3	-8860799.000	1447032.500	-5044527.400
4	86081.4	202361.9	16016156.4	-2620.146	-23878.530
5	5521194.9	6240190.5	11341839.7	1756287.400	-244660.460
6	-4708.897	-5760.597	-17869.439	3573.9133	-17486.034
7	523.672	276.663	-11165.887	-8.4253	-109.983
8	19330.611	20426.621	2552.2438	6359.0056	-1711.305
9	-18.962	.000	.0000	-63.8460	31.9523
10	1.538	.000	.0000	2175.7636	.0000000
11	28.000	19902.775	8.2183	.0000	.0002
12	14.8586	.0548	.0000	.0000	738.1537
13	5522636.2	5553311.5	5092997.0	691729.3	5955503.1
14	72.8932	72.4007	63.7692	119.7242	276.5819
15	-.9571	-1.0357	.1834	64.5576	-2.0263

1	555.0000	628841.3000	5519068.2000	1.2471	82.2052
2	20061.9250	21384.3960	36.464	1.1487	82.6868
3	-116029.2	-326127.3	-8950402.900	1464927.700	-5132320.700
4	88719.1	203734.9	15959973.2	-2664.191	-24432.492
5	5618199.3	6342658.5	11354564.7	1788218.100	-253327.330
6	-4803.545	-5872.255	-17973.261	3584.1419	-17631.251
7	531.522	272.610	-11305.326	-9.1668	-111.603
8	19471.114	20560.515	2538.4878	6413.3058	-1755.561
9	-18.919	.000	.0000	-63.5362	31.9889
10	1.595	.000	.0000	2179.3260	.0000000
11	28.259	20061.925	8.2743	.0000	.0002
12	15.1243	.0542	.0000	.0000	739.0197
13	5620097.4	5650757.8	5188679.7	732229.8	5859391.5
14	72.9046	72.4207	63.9827	110.4053	276.6598
15	-1.1830	-1.2605	-.0557	58.6637	-1.7732

1	560.0000	631124.2800	5616806.0000	1.3516	82.3824
2	20222.5580	21545.1140	36.776	1.2478	82.8491
3	-140282.8	-355767.3	-9040529.200	1482874.000	-5220839.500
4	91397.1	205088.3	15903092.3	-2711.712	-24994.574
5	5715909.7	6445799.3	11367221.0	1820421.900	-262217.260
6	-4897.803	-5983.701	-18078.423	3594.3583	-17776.217
7	539.662	268.720	-11444.939	-9.8558	-113.232
8	19613.060	20695.774	2525.0668	6468.2388	-1800.527
9	-18.875	.000	.0000	-63.2237	32.0249
10	1.606	.000	.0000	2183.2111	.0000000
11	28.458	20222.558	8.3299	.0000	.0002
12	15.3922	.0535	.0000	.0000	739.9652
13	5718361.2	5749006.6	5285220.4	783671.6	5762562.3
14	72.9160	72.4404	64.1903	104.5031	276.7407
15	-1.4057	-1.4821	-.2910	53.0051	-1.5124

1	565.0000	633616.1100	5715309.8000	1.4620	82.5608
2	20384.0140	21706.6580	36.940	1.3525	83.0127
3	-165006.9	-385964.2	-9131183.000	1500871.300	-5310082.500
4	94115.6	206421.8	15845512.7	-2762.830	-25564.826
5	5814332.2	6549618.4	11379811.6	1852901.500	-271333.800
6	-4991.790	-6095.029	-18184.149	3604.5326	-17920.923
7	547.765	264.678	-11584.712	-10.5888	-114.870
8	19755.758	20831.697	2512.0111	6523.5915	-1846.208
9	-18.829	.000	.0000	-62.9086	32.0604
10	1.611	.000	.0000	2187.4416	.0000000
11	28.505	20384.014	8.3847	.0000	.0002
12	15.6622	.0527	.0000	.0000	740.9957
13	5817434.3	5848064.3	5382623.4	844349.8	5665017.5
14	72.9273	72.4598	64.3923	100.5092	276.8249
15	-1.6254	-1.7007	-.5226	47.8628	-1.2433

TABLE AP 3-2 (Sheet 29 of 39)
SATURN OBSERVED TRAJECTORY - BOOST PHASE (AA83)

1	570.0000	636329.8400	5814580.2000	1.5773	82.7404
2	20545.0280	21867.7680	36.924	1.4619	83.1777
3	-190199.7	-416716.9	-9222364.900	1518919.400	-5400048.300
4	96874.4	207734.6	15787234.9	-2817.767	-26143.288
5	5913467.8	6654116.5	11392337.5	1885658.300	-280680.540
6	-5085.541	-6206.225	-18289.243	3614.6656	-18065.364
7	555.778	260.456	-11724.246	-11.3737	-116.516
8	19897.904	20966.980	2498.9935	6578.9672	-1892.604
9	-18.797	.000	.0000	-62.5907	32.0953
10	1.617	.000	.0000	2192.0374	.0000000
11	28.371	20545.029	8.4382	.0000	.0002
12	15.9342	.0519	.0000	.0000	742.1165
13	5917318.7	5947933.0	5480888.6	912693.0	5566763.2
14	72.9385	72.4788	64.5889	97.6534	276.9125
15	-1.8420	-1.9163	-.7506	43.3093	-.9653
1	575.0000	639275.5500	5914610.7000	1.6964	82.9217
2	20705.6420	22028.4810	36.942	1.5751	83.3445
3	-215861.9	-448026.3	-9314069.500	1537017.800	-5490735.600
4	99673.4	209026.2	15728259.8	-2876.630	-26730.002
5	6013311.7	6759288.5	11404797.3	1918691.600	-290261.050
6	-5179.364	-6317.598	-18393.671	3624.6607	-18209.530
7	563.856	256.209	-11863.731	-12.1638	-118.171
8	20039.457	21101.573	2485.7257	6634.3523	-1939.720
9	-18.772	.000	.0000	-62.2701	32.1296
10	1.494	.000	.0000	2197.0113	.0000000
11	28.273	20705.642	8.4903	.0000	.0002
12	16.2083	.0509	.0001	.0000	743.3307
13	6018010.3	6048608.8	5580010.4	987358.0	5467810.7
14	72.9495	72.4976	64.7802	95.5203	277.0037
15	-2.0556	-2.1290	-.9750	39.3243	-.6778
	S-II ENGINE CUTOFF SIGNAL = TB 4				
1	576.2800	640066.8500	5940340.5000	1.7222	82.9684
2	20742.9620	22065.8320	36.939	1.5996	83.3876
3	-222507.9	-456132.0	-9337629.000	1541658.700	-5514067.400
4	100396.5	209353.5	15713049.5	-2892.315	-26881.533
5	6038984.6	6786319.8	11407975.6	1927192.500	-292751.680
6	-5204.335	-6346.928	-18416.405	3626.9560	-18246.391
7	565.839	255.096	-11898.852	-12.3735	-118.596
8	20071.502	21131.787	2480.8074	6647.2734	-1951.898
9	-18.758	.000	.0000	-62.1876	32.1383
10	1.478	.000	.0000	2198.3454	.0000000
11	28.238	20742.962	8.5018	.0000	.0002
12	16.2789	.0507	.0001	.0000	743.6568
13	6043916.1	6074510.6	5605522.0	1007349.6	5442367.8
14	72.9524	72.5024	64.8284	95.0590	277.0277
15	-2.1098	-2.1830	-1.0319	38.3890	-.6026
	S-II/S-IVB SEPARATION COMMAND				
1	577.0800	640569.5300	5956445.2000	1.7196	82.9986
2	20752.7320	22075.6370	8.890	1.5973	83.4157
3	-226677.0	-461216.4	-9352369.600	1544560.900	-5528673.800
4	100849.8	209557.4	15703520.5	-2902.234	-26976.516
5	6055052.4	6803235.3	11409959.5	1932514.300	-294316.250
6	-5223.150	-6367.935	-18416.654	3627.5726	-18269.420
7	567.019	254.614	-11918.423	-12.4395	-118.862
8	20076.680	21135.715	2472.2173	6650.7974	-1959.533
9	-25.793	.000	.0000	-62.1360	32.1437
10	1.469	.000	.0000	2199.1924	.0000000
11	.976	20752.732	8.5035	.0000	.0002
12	16.3230	.0505	.0001	.0000	743.8639
13	6060132.9	6090724.8	5621494.0	1020009.9	5426444.3
14	72.9541	72.5053	64.8583	94.7854	277.0428
15	-2.1436	-2.2166	-1.0673	37.8211	-.5553
	S-IVB ENGINE START SIGNAL				
1	577.2680	128392.3510	1195064.3000	.3429	16.6319
2	4157.8241	4422.8712	.331	.3185	16.7153
3	-45853.2	-92939.5	-1875289.200	309756.100	-1109199.700
4	20253.0	42006.0	3145173.2	-582.485	-5414.714
5	1214816.6	1364803.1	2286178.8	387738.050	-59130.894
6	-1048.659	-1278.207	-3688.765	726.7854	-3662.674
7	113.723	50.978	-2389.722	-2.4941	-23.842
8	4021.801	4233.838	494.0017	1332.5180	-393.394
9	-5.274	.000	.0000	-12.4434	6.4405
10	.293	.000	.0000	.0401	.0000000
11	-1.253	.000	.0000	.0000	.0000
12	3.2749	.0000	.0000	.0000	.0000
13	1215850.3	1221979.1	1127943.9	205703.0	1085500.9
14	14.6164	14.5267	12.9974	18.9621	55.5067
15	-.4330	-.4476	-.2175	7.5186	-.1062

TABLE AP 3-2 (Sheet 30 of 39)
SATURN OBSERVED TRAJECTORY - BOOST PHASE (AA83)

S-II/S-IVB SEPARATION COMPLETE

1	578.1060	641225.2400	5977133.3000	1.7005	83.0382
2	20753.7540	22076.7170	1.018	1.5794	83.4530
3	-232041.3	-467758.1	-9371299.600	1548285.000	-5547433.000
4	101433.2	209818.4	15691271.3	-2914.998	-27098.642
5	6075691.7	6824960.6	11412502.5	1939351.800	-296331.760
6	-5249.941	-6397.080	-18405.135	3627.6878	-18298.943
7	568.501	254.194	-11941.439	-12.4634	-119.203
8	20070.706	21128.044	2456.5316	6651.4524	-1969.352
9	-26.319	.000	.0000	-62.0697	32.1506
10	1.456	.000	.0000	.2000	.0000000
11	-6.920	.000	.0000	.0000	.0000
12	16.3797	.0000	.0000	.0000	.0000
13	6080967.0	6111555.5	5642015.6	1036431.7	5405991.8
14	72.9564	72.5091	64.8965	94.4496	277.0623
15	-2.1869	-2.2597	-1.1126	37.1106	-.4942

1	580.0000	642371.8900	6015240.6000	1.6618	83.1115
2	20753.4740	22076.5430	1.101	1.5433	83.5219
3	-242035.0	-479928.0	-9406122.900	1555155.100	-5582143.100
4	102512.7	210299.6	15668614.7	-2938.502	-27325.010
5	6113679.3	6864947.6	11417120.8	1951945.900	-300078.950
6	-5299.915	-6451.301	-18381.555	3627.7933	-18353.412
7	571.283	253.514	-11983.478	-12.4785	-119.834
8	20057.198	21111.377	2426.6154	6651.9213	-1987.558
9	-26.301	.000	.0000	-61.9474	32.1632
10	1.447	.000	.0000	.2000	.0000000
11	-6.880	.000	.0000	.0000	.0000
12	16.4841	.0000	.0000	.0000	.0000
13	6119326.9	6149909.3	5679806.3	1067067.7	5368304.3
14	72.9606	72.5161	64.9662	93.8737	277.0987
15	-2.2668	-2.3393	-1.1964	35.8524	-.3816

GUIDANCE INITIATION-START ARTIFICIAL TAU

1	582.5000	643860.7100	6065566.5000	1.6263	83.2070
2	20765.0860	22088.2790	13.435	1.5102	83.6116
3	-255363.6	-496142.6	-9452049.500	1564225.600	-5628116.400
4	103945.4	210931.9	15638582.4	-2969.835	-27625.638
5	6163814.1	6917712.8	11423142.4	1968580.800	-305078.040
6	-5363.529	-6520.983	-18362.314	3628.4193	-18425.246
7	574.821	252.232	-12041.454	-12.6149	-120.668
8	20052.206	21102.258	2391.8471	6656.5148	-2011.748
9	-24.847	.000	.0000	-61.7859	32.1797
10	1.440	.000	.0000	.2000	.0000000
11	5.318	.000	.0000	.0000	.0000
12	16.6220	.0000	.0000	.0000	.0000
13	6169977.1	6200551.4	5729716.6	1108289.6	5318529.4
14	72.9661	72.5253	65.0570	93.1877	277.1473
15	-2.3720	-2.4441	-1.3067	34.2890	-.2318

1	585.0000	645330.0300	6115948.9000	1.6117	83.2996
2	20801.0410	22124.3340	18.791	1.4969	83.6979
3	-268849.6	-512530.9	-9497959.000	1573297.800	-5674269.300
4	105386.3	211559.7	15608394.1	-3001.910	-27928.354
5	6213970.8	6970489.5	11429088.0	1985237.800	-310137.850
6	-5426.253	-6590.690	-18365.736	3629.0454	-18497.008
7	577.950	250.005	-12107.606	-13.0385	-121.505
8	20072.495	21118.393	2364.7056	6668.8609	-2036.118
9	-25.252	.000	.0000	-61.6242	32.1960
10	1.443	.000	.0000	.2000	.0000000
11	10.679	.000	.0000	.0000	.0000
12	16.7601	.0000	.0000	.0000	.0000
13	6220676.6	6251242.8	5779689.0	1150346.4	5268695.5
14	72.9715	72.5343	65.1464	92.5734	277.1969
15	-2.4770	-2.5486	-1.4166	32.8278	-.0806

S-IVB PU ACTIVATE ON

1	585.3000	645505.6400	6122000.5000	1.6095	83.3107
2	20805.9780	22129.2820	19.014	1.4948	83.7083
3	-270478.5	-514509.3	-9503468.600	1574386.500	-5679819.500
4	105559.8	211634.6	15604760.2	-3005.824	-27964.819
5	6219992.9	6976825.3	11429796.7	1987238.700	-310749.110
6	-5434.122	-6599.417	-18366.568	3629.0087	-18505.614
7	578.330	249.727	-12116.024	-13.0929	-121.605
8	20075.472	21120.855	2361.4279	6670.5065	-2039.055
9	-25.327	.000	.0000	-61.6048	32.1979
10	1.443	.000	.0000	.2000	.0000000
11	10.900	.000	.0000	.0000	.0000
12	16.7767	.0000	.0000	.0000	.0000
13	6226765.7	6257330.8	5785691.7	1155447.1	5262710.0
14	72.9722	72.5354	65.1571	92.5040	277.2029
15	-2.4896	-2.5612	-1.4297	32.6589	-.0623

TABLE AP 3-2 (Sheet 31 of 39)
SATURN OBSERVED TRAJECTORY - BOOST PHASE (AA83)

S-IVB PU VALVE REACHES HARDOVER POSITION

1	589.0000	647654.6200	6196759.9000	1.5847	83.4513
2	20872.4830	22195.9440	20.515	1.4721	83.8393
3	-290765.1	-539127.4	-9571449.100	1587812.700	-5748486.700
4	107709.7	212553.5	15559732.3	-3055.132	-28417.056
5	6294348.0	7055036.6	11438458.1	2011959.600	-318360.900
6	-5532.098	-6708.203	-18381.978	3628.1785	-18611.676
7	584.438	247.562	-12221.974	-13.3740	-122.847
8	20117.527	21156.529	2320.8243	6692.4842	-2075.486
9	-26.477	.000	.0000	-61.3647	32.2216
10	2.437	.000	.0000	.2000	.0000000
11	12.326	.000	.0000	.0000	.0000
12	16.9816	.0000	.0000	.0000	.0000
13	6301980.8	6332533.6	5859854.7	1219251.2	5188764.9
14	72.9803	72.5487	65.2868	91.7136	277.2783
15	-2.6445	-2.7154	-1.5917	30.6803	.1650

1	590.0000	648231.3600	6217005.1000	1.5788	83.4916
2	20891.5770	22215.0850	20.688	1.4668	83.8768
3	-296310.4	-545850.3	-9589833.000	1591440.700	-5767112.700
4	108295.1	212800.9	15547494.7	-3068.495	-28540.072
5	6314471.7	7076198.5	11440773.0	2018655.200	-320441.340
6	-5558.687	-6737.767	-18387.382	3627.8962	-18640.313
7	586.924	247.782	-12250.754	-13.2046	-123.184
8	20129.941	21167.219	2309.3852	6698.7642	-2085.401
9	-26.799	.000	.0000	-61.2996	32.2279
10	2.449	.000	.0000	.2000	.0000000
11	12.472	.000	.0000	.0000	.0000
12	17.0371	.0000	.0000	.0000	.0000
13	6322347.5	6352897.1	5879941.4	1236765.1	5168739.4
14	72.9825	72.5523	65.3214	91.5190	277.2990
15	-2.6863	-2.7570	-1.6354	30.1770	.2271

1	595.0000	651081.1700	6318514.0000	1.5359	83.6937
2	20990.2480	22313.9940	21.175	1.4273	84.0652
3	-324447.2	-579919.9	-9681836.500	1609573.100	-5860671.900
4	111261.9	214043.3	15485865.2	-3132.172	-29160.203
5	6415281.2	7182172.2	11452169.7	2052229.000	-330993.060
6	-5698.040	-6892.065	-18414.179	3624.4562	-18783.326
7	599.477	248.861	-12400.521	-12.3614	-124.870
8	20193.154	21221.496	2249.3277	6730.5499	-2135.406
9	-28.723	.000	.0000	-60.9733	32.2591
10	2.492	.000	.0000	.2000	.0000000
11	12.712	.000	.0000	.0000	.0000
12	17.3153	.0000	.0000	.0000	.0000
13	6424443.6	6454976.2	5980661.1	1325889.5	5068336.1
14	72.9935	72.5702	65.4918	90.6479	277.4052
15	-2.8948	-2.9647	-1.8531	27.8390	.5422

1	600.0000	653849.3000	6420496.9000	1.4753	83.8972
2	21091.5740	22415.5630	21.391	1.3713	84.2551
3	-353302.5	-614782.9	-9773968.800	1627681.600	-5954945.500
4	114291.1	215290.4	15423468.4	-3191.834	-29788.789
5	6516406.3	7288415.7	11463256.0	2085961.800	-341796.620
6	-5845.705	-7054.712	-18439.063	3618.3807	-18926.040
7	612.283	250.028	-12557.241	-11.4893	-126.565
8	20256.045	21275.010	2184.9922	6762.3238	-2186.138
9	-30.400	.000	.0000	-60.6453	32.2894
10	2.525	.000	.0000	.2000	.0000000
11	12.545	.000	.0000	.0000	.0000
12	17.5947	.0000	.0000	.0000	.0000
13	6526977.3	6557492.5	6081858.2	1417314.2	4967460.3
14	73.0047	72.5881	65.6579	89.9169	277.5156
15	-3.1029	-3.1721	-2.0702	25.7633	.8649

1	605.0000	656500.3000	6522967.4000	1.3945	84.1006
2	21195.0510	22519.2820	21.603	1.2962	84.4450
3	-382919.4	-650482.3	-9866218.300	1645752.200	-6049931.800
4	117383.7	216542.3	15360268.4	-3247.464	-30425.867
5	6617843.3	7394923.2	11474009.2	2119852.900	-352855.660
6	-6002.575	-7226.559	-18460.799	3609.4095	-19068.453
7	624.744	250.692	-12721.583	-10.7678	-128.268
8	20317.701	21326.793	2116.2020	6793.7919	-2237.597
9	-32.215	.000	.0000	-60.3155	32.3188
10	2.553	.000	.0000	.2000	.0000000
11	12.194	.000	.0000	.0000	.0000
12	17.8756	.0000	.0000	.0000	.0000
13	6629951.2	6660448.5	6183533.9	1510716.0	4866095.3
14	73.0161	72.6060	65.8198	89.2953	277.6306
15	-3.3110	-3.3795	-2.2869	23.9080	1.1953

TABLE AP 3-2 (Sheet 32 of 39)
SATURN OBSERVED TRAJECTORY - BOOST PHASE (AA83)

1	610.0000	658997.1800	6625933.1000	1.2955	84.3058
2	21299.8750	22624.3440	21.812	1.2039	84.6367
3	-413341.9	-687062.1	-9958567.800	1663771.300	-6145629.500
4	120539.3	217797.8	15296230.2	-3299.384	-31071.480
5	6719583.6	7501683.3	11484406.1	2153900.000	-364173.810
6	-6167.832	-7406.762	-18479.090	3597.7982	-19210.563
7	637.512	251.531	-12892.324	-9.9908	-129.978
8	20377.342	21376.099	2042.5928	6824.7272	-2289.785
9	-33.970	.000	.0000	-59.9838	32.3474
10	2.581	.000	.0000	.2000	.0000000
11	11.691	.000	.0000	.0000	.0000
12	18.1577	.0000	.0000	.0000	.0000
13	6733363.5	6763842.3	6285684.9	1605836.7	4764227.6
14	73.0276	72.6239	65.9778	88.7607	277.7506
15	-3.5194	-3.5871	-2.5038	22.2384	1.5336
1	615.0000	661303.7800	6729401.2000	1.1767	84.5123
2	21405.3420	22730.0420	21.996	1.0929	84.8299
3	-444612.5	-724564.8	-10050997.600	1681725.500	-6242036.900
4	123759.1	219057.6	15231322.5	-3347.369	-31725.666
5	6821614.7	7608681.2	11494422.6	2188099.700	-375754.740
6	-6341.873	-7595.677	-18492.875	3583.4384	-19352.365
7	650.430	252.401	-13069.500	-9.2015	-131.697
8	20433.949	21421.878	1963.8292	6854.8112	-2342.706
9	-35.747	.000	.0000	-59.6503	32.3751
10	2.615	.000	.0000	.2000	.0000000
11	10.978	.000	.0000	.0000	.0000
12	18.4413	.0000	.0000	.0000	.0000
13	6837208.6	6867668.6	6388304.8	1702468.7	4661847.7
14	73.0393	72.6417	66.1320	88.2966	277.8758
15	-3.7285	-3.7955	-2.7210	20.7257	1.8798
1	620.0000	663381.2400	6833374.9000	1.0391	84.7207
2	21510.6230	22835.5430	22.180	.9642	85.0251
3	-476774.8	-763033.1	-10143484.000	1699601.200	-6339152.600
4	127044.2	220322.2	15165513.8	-3391.268	-32388.467
5	6923920.1	7715898.2	11504031.7	2222447.300	-387602.100
6	-6524.195	-7792.762	-18501.489	3566.4938	-19493.857
7	663.654	253.486	-13252.299	-8.3445	-133.424
8	20486.614	21463.241	1879.7763	6883.7725	-2396.361
9	-37.390	.000	.0000	-59.3149	32.4019
10	2.653	.000	.0000	.2000	.0000000
11	10.152	.000	.0000	.0000	.0000
12	18.7263	.0000	.0000	.0000	.0000
13	6941478.3	6971919.0	6491384.1	1800442.9	4558948.0
14	73.0511	72.6596	66.2827	87.8902	278.0067
15	-3.9385	-4.0048	-2.9390	19.3463	2.2340
1	625.0000	665191.1900	6937852.6000	.8817	84.9306
2	21615.5350	22940.6570	22.341	.8167	85.2217
3	-509870.3	-802508.2	-10235999.400	1717385.400	-6436975.000
4	130395.8	221592.3	15098776.4	-3430.844	-33059.923
5	7026477.9	7823309.9	11513207.3	2256936.700	-399719.580
6	-6715.093	-7998.286	-18504.364	3546.8821	-19635.039
7	676.989	254.598	-13440.872	-7.4767	-135.160
8	20534.863	21499.684	1790.3254	6911.4596	-2450.755
9	-38.936	.000	.0000	-58.9777	32.4278
10	2.695	.000	.0000	.2000	.0000000
11	9.182	.000	.0000	.0000	.0000
12	19.0126	.0000	.0000	.0000	.0000
13	7046159.3	7076580.1	6594908.3	1899616.9	4455525.9
14	73.0631	72.6774	66.4298	87.5317	278.1438
15	-4.1496	-4.2153	-3.1581	18.0805	2.5964
1	630.0000	666695.6000	7042832.1000	.7063	85.1422
2	21719.1990	23044.5000	22.485	.6522	85.4203
3	-543939.3	-843029.4	-10328513.400	1735065.800	-6535502.400
4	133814.7	222868.6	15031084.6	-3465.910	-33740.077
5	7129263.8	7930889.4	11521922.1	2291560.500	-412110.890
6	-6913.700	-8211.345	-18500.949	3524.8785	-19775.908
7	690.580	255.912	-13634.114	-6.5448	-136.903
8	20577.839	21530.382	1695.5395	6937.6212	-2505.889
9	-40.503	.000	.0000	-58.6387	32.4528
10	2.738	.000	.0000	.2000	.0000000
11	7.985	.000	.0000	.0000	.0000
12	19.3003	.0000	.0000	.0000	.0000
13	7151236.0	7181636.4	6698861.2	1999871.7	4351581.1
14	73.0752	72.6953	66.5737	87.2135	278.2874
15	-4.3623	-4.4272	-3.3785	16.9122	2.9670

TABLE AP 3-2 (Sheet 33 of 39)
SATURN OBSERVED TRAJECTORY - BOOST PHASE (AA83)

1	635.0000	667856.0500	7148306.4000	.5124	85.3561
2	21821.0210	23146.4740	22.679	.4701	85.6212
3	-579021.0	-884635.1	-10420992.500	1752630.000	-6634733.500
4	137302.4	224152.1	14962415.5	-3496.101	-34428.971
5	7232249.4	8038605.8	11530148.8	2326310.800	-424779.710
6	-7119.996	-8431.882	-18490.549	3500.5002	-19916.463
7	704.568	257.588	-13831.652	-5.4999	-138.656
8	20614.709	21554.496	1595.0845	6962.0028	-2561.767
9	-42.007	.000	.0000	-58.2979	32.4768
10	2.775	.000	.0000	.2000	.0000000
11	6.685	.000	.0000	.0000	.0000
12	19.5893	.0000	.0000	.0000	.0000
13	7256689.7	7287069.3	6803223.3	2101104.7	4247116.2
14	73.0875	72.7133	66.7144	86.9296	278.4382
15	-4.5766	-4.6409	-3.6004	15.8275	3.3460
1	640.0000	668634.4100	7254266.8000	.3005	85.5713
2	21920.5040	23246.0690	22.828	.2711	85.8235
3	-615152.4	-927361.0	-10513401.500	1770066.700	-6734666.500
4	140860.1	225444.0	14892748.9	-3521.036	-35126.648
5	7335403.3	8146425.8	11537860.2	2361178.300	-437729.810
6	-7333.557	-8659.435	-18472.552	3473.8873	-20056.704
7	718.561	259.257	-14033.052	-4.4543	-140.416
8	20644.881	21571.434	1489.3283	6984.4250	-2618.392
9	-43.367	.000	.0000	-57.9553	32.4998
10	2.810	.000	.0000	.2000	.0000000
11	5.231	.000	.0000	.0000	.0000
12	19.8797	.0000	.0000	.0000	.0000
13	7362499.1	7392857.0	6907972.2	2203226.2	4142137.2
14	73.1000	72.7312	66.8520	86.6749	278.5966
15	-4.7928	-4.8564	-3.8241	14.8152	3.7334
1	645.0000	668994.3100	7360699.8000	.0722	85.7879
2	22016.9160	23342.5530	23.071	.0564	86.0273
3	-652367.7	-971240.1	-10605698.800	1787365.500	-6835300.000
4	144488.0	226744.6	14822068.5	-3540.652	-35833.151
5	7438688.0	8254309.4	11545029.4	2396152.200	-450964.900
6	-7553.568	-8893.154	-18446.492	3445.2996	-20196.631
7	732.611	260.999	-14237.335	-3.3839	-142.186
8	20667.645	21580.514	1378.4275	7004.6806	-2675.769
9	-44.601	.000	.0000	-57.6110	32.5218
10	2.840	.000	.0000	.2000	.0000000
11	3.834	.000	.0000	.0000	.0000
12	20.1714	.0000	.0000	.0000	.0000
13	7468636.8	7498972.6	7013080.3	2306153.0	4036656.4
14	73.1127	72.7492	66.9866	86.4454	278.7634
15	-5.0110	-5.0741	-4.0498	13.8657	4.1294
1	650.0000	668906.2500	7467595.6000	-.1618	86.0056
2	22113.5090	23439.1670	23.333	-.1637	86.2323
3	-690694.8	-1016299.1	-10697851.800	1804517.600	-6936632.300
4	148186.0	228053.8	14750361.0	-3554.940	-36548.525
5	7542074.2	8362224.8	11551635.3	2431223.700	-464488.750
6	-7777.155	-9130.334	-18416.794	3415.5512	-20336.244
7	746.714	262.748	-14443.555	-2.3087	-143.965
8	20687.329	21586.168	1264.9345	7024.1224	-2733.900
9	-44.504	.000	.0000	-57.2650	32.5429
10	2.863	.000	.0000	.2000	.0000000
11	4.220	.000	.0000	.0000	.0000
12	20.4644	.0000	.0000	.0000	.0000
13	7575084.0	7605397.0	7118528.4	2409821.2	3930681.8
14	73.1255	72.7673	67.1184	86.2378	278.9392
15	-5.2315	-5.2939	-4.2776	12.9709	4.5342
1	655.0000	668380.1300	7574969.9000	-.3798	86.2247
2	22214.4760	23540.1090	23.464	-.3689	86.4386
3	-730133.3	-1062537.8	-10789865.100	1821522.600	-7038662.000
4	151955.7	229372.4	14677625.6	-3563.620	-37272.815
5	7645567.2	8470176.8	11557678.3	2466395.600	-478305.160
6	-7998.041	-9364.982	-18390.878	3386.4988	-20475.543
7	761.168	264.721	-14648.617	-1.1623	-145.753
8	20710.744	21595.459	1153.4531	7044.9041	-2792.790
9	-43.935	.000	.0000	-56.9173	32.5629
10	2.860	.000	.0000	.2000	.0000000
11	4.979	.000	.0000	.0000	.0000
12	20.7586	.0000	.0000	.0000	.0000
13	7681854.0	7712143.6	7224328.7	2514207.9	3824210.0
14	73.1385	72.7854	67.2475	86.0494	279.1248
15	-5.4540	-5.5158	-4.5074	12.1248	4.9489

TABLE AP 3-2 (Sheet 34 of 39)
SATURN OBSERVED TRAJECTORY - BOOST PHASE (AA83)

1	660.0000	667442.3600	7682843.7000	-.5824	86.4440
2	22319.3570	23644.9230	23.632	-.5596	86.6452
3	-770670.2	-1109944.1	-10881756.700	1838383.800	-7141387.200
4	155797.3	230700.4	14603866.9	-3566.747	-38006.068
5	7749185.9	8578183.5	11563169.2	2501674.400	-492417.920
6	-8216.272	-9597.128	-18368.235	3358.1035	-20614.528
7	775.526	266.477	-14852.608	-.0793	-147.550
8	20737.530	21608.021	1044.2385	7066.9150	-2852.442
9	-43.359	.000	.0000	-56.5678	32.5818
10	2.840	.000	.0000	.2000	.0000000
11	5.738	.000	.0000	.0000	.0000
12	21.0542	.0000	.0000	.0000	.0000
13	7788971.9	7819237.4	7330505.5	2619308.4	3717235.8
14	73.1517	72.8036	67.3740	85.8776	279.3213
15	-5.6783	-5.7396	-4.7390	11.3223	5.3748

1	665.0000	666120.7700	7791236.0000	-.7685	86.6635
2	22428.3140	23753.7750	23.872	-.7349	86.8521
3	-812290.8	-1158504.1	-10973544.000	1855105.000	-7244806.700
4	159710.5	232036.6	14529091.4	-3564.585	-38748.331
5	7852947.5	8686261.8	11568120.3	2537066.600	-506830.860
6	-8431.693	-9826.636	-18349.220	3330.4165	-20753.200
7	789.768	267.989	-15055.536	.9321	-149.357
8	20768.055	21624.230	937.4804	7090.2710	-2912.861
9	-42.809	.000	.0000	-56.2165	32.5997
10	2.807	.000	.0000	.2000	.0000000
11	6.513	.000	.0000	.0000	.0000
12	21.3513	.0000	.0000	.0000	.0000
13	7896461.6	7926702.5	7437081.9	2725120.0	3609757.1
14	73.1650	72.8218	67.4980	85.7206	279.5299
15	-5.9043	-5.9650	-4.9720	10.5591	5.8134

1	670.0000	664443.9000	7900169.9000	-.9380	86.8828
2	22541.5880	23866.9120	24.105	-.8946	87.0587
3	-854982.1	-1208205.7	-11065246.000	1871689.300	-7348918.700
4	163694.4	233379.5	14453303.1	-3557.661	-39499.651
5	7956872.1	8794431.5	11572543.8	2572579.200	-521547.820
6	-8644.350	-10053.571	-18334.095	3303.4179	-20891.556
7	803.713	269.064	-15257.652	1.8134	-151.173
8	20802.702	21644.466	833.4118	7115.0894	-2974.050
9	-42.180	.000	.0000	-55.8633	32.6166
10	2.751	.000	.0000	.2000	.0000000
11	7.294	.000	.0000	.0000	.0000
12	21.6498	.0000	.0000	.0000	.0000
13	8004348.9	8034564.5	7544083.3	2831645.8	3501771.8
14	73.1785	72.8401	67.6196	85.5765	279.7517
15	-6.1317	-6.1918	-5.2064	9.8317	6.2666

1	675.0000	662441.5500	8009665.8000	-1.0892	87.1019
2	22658.5580	23983.7200	24.298	-1.0371	87.2652
3	-898728.0	-1259033.8	-11156881.600	1888140.900	-7453721.800
4	167747.0	234726.4	14376507.8	-3546.710	-40260.077
5	8060979.6	8902711.5	11576454.6	2608219.400	-536572.660
6	-8853.507	-10277.191	-18322.803	3277.3329	-21029.595
7	817.363	269.717	-15458.250	2.5590	-152.999
8	20841.248	21668.537	732.3230	7141.3128	-3036.013
9	-41.422	.000	.0000	-55.5081	32.6324
10	2.683	.000	.0000	.2000	.0000000
11	8.077	.000	.0000	.0000	.0000
12	21.9499	.0000	.0000	.0000	.0000
13	8112659.2	8142848.9	7651534.5	2938890.5	3393281.6
14	73.1921	72.8583	67.7389	85.4439	279.9883
15	-6.3603	-6.4198	-5.4418	9.1369	6.7362

1	680.0000	660147.6700	8119742.1000	-1.2210	87.3208
2	22779.0570	24104.0350	24.505	-1.1613	87.4716
3	-943510.4	-1310971.1	-11248470.700	1904464.400	-7559214.100
4	171867.2	236075.7	14298713.7	-3532.254	-41029.658
5	8165289.9	9011122.0	11579867.9	2643994.300	-551909.250
6	-9058.693	-10497.038	-18315.586	3252.3007	-21167.316
7	830.719	269.950	-15656.990	3.1998	-154.835
8	20883.855	21696.633	634.4827	7169.0001	-3098.755
9	-40.597	.000	.0000	-55.1509	32.6471
10	2.614	.000	.0000	.2000	.0000000
11	8.860	.000	.0000	.0000	.0000
12	22.2516	.0000	.0000	.0000	.0000
13	8221417.5	8251580.8	7759459.8	3046860.3	3284291.8
14	73.2057	72.8766	67.8560	85.3216	280.2415
15	-6.5899	-6.6489	-5.6781	8.4721	7.2246

TABLE AP 3-2 (Sheet 35 of 39)
SATURN OBSERVED TRAJECTORY - BOOST PHASE (AA83)

1	685.0000	657599.5500	8230417.1000	-1.3321	87.5397
2	22902.4390	24227.2200	24.636	-1.2661	87.6781
3	-989307.3	-1363996.7	-11340033.600	1920665.900	-7665394.400
4	176053.8	237425.4	14219932.3	-3514.862	-41808.445
5	8269822.7	9119682.4	11582800.1	2679911.100	-567561.510
6	-9259.254	-10712.453	-18312.359	3228.5214	-21304.715
7	843.835	269.831	-15853.204	3.7262	-156.681
8	20930.262	21728.525	540.0887	7198.0827	-3162.278
9	-39.544	.000	.0000	-54.7917	32.6607
10	2.552	.000	.0000	.2000	.0000000
11	9.642	.000	.0000	.0000	.0000
12	22.5549	.0000	.0000	.0000	.0000
13	8330647.5	8360783.8	7867882.6	3155562.4	3174814.1
14	73.2195	72.8948	67.9709	85.2084	280.5132
15	-6.8203	-6.8787	-5.9150	7.8349	7.7346

1	690.0000	654837.1600	8341704.8000	-1.4203	87.7581
2	23028.2950	24352.8700	24.816	-1.3493	87.8842
3	-1036093.3	-1418086.2	-11431590.800	1936752.300	-7772260.800
4	180304.6	238772.9	14140177.5	-3495.323	-42596.486
5	8374597.2	9228412.0	11585270.8	2715977.000	-583533.350
6	-9454.191	-10922.447	-18313.368	3206.2954	-21441.790
7	856.458	269.115	-16046.199	4.0737	-158.537
8	20980.637	21764.423	449.8758	7228.6260	-3226.588
9	-38.446	.000	.0000	-54.4303	32.6733
10	2.480	.000	.0000	.2000	.0000000
11	10.424	.000	.0000	.0000	.0000
12	22.8599	.0000	.0000	.0000	.0000
13	8440371.6	8470480.4	7976824.7	3265003.8	3064866.3
14	73.2333	72.9131	68.0837	85.1033	280.8056
15	-7.0511	-7.1090	-6.1522	7.2235	8.2694

1	695.0000	651905.5900	8453619.6000	-1.4856	87.9765
2	23156.7910	24481.1590	25.010	-1.4109	88.0903
3	-1083840.1	-1473212.4	-11523163.800	1952731.500	-7879811.700
4	184617.8	240115.8	14059465.5	-3474.344	-43393.833
5	8479633.9	9337331.5	11587300.4	2752199.300	-599828.710
6	-9643.572	-11127.109	-18318.980	3185.5944	-21578.535
7	868.813	268.018	-16236.068	4.3080	-160.403
8	21035.295	21804.652	363.7091	7260.7300	-3291.687
9	-37.214	.000	.0000	-54.0668	32.6847
10	2.405	.000	.0000	.2000	.0000000
11	11.206	.000	.0000	.0000	.0000
12	23.1666	.0000	.0000	.0000	.0000
13	8550612.9	8580693.6	8086308.5	3375192.7	2954471.7
14	73.2472	72.9313	68.1944	85.0056	281.1216
15	-7.2822	-7.3395	-6.3895	6.6361	8.8325

1	700.0000	648851.1500	8566172.3000	-1.5240	88.1943
2	23286.0290	24610.1950	25.097	-1.4470	88.2958
3	-1132515.1	-1529343.5	-11614774.900	1968612.400	-7988045.500
4	188991.1	241451.4	13977816.7	-3452.734	-44200.537
5	8584952.4	9446461.0	11588912.0	2788585.400	-616451.560
6	-9825.097	-11324.106	-18328.761	3167.1280	-21714.946
7	880.579	266.271	-16420.667	4.3475	-162.280
8	21093.392	21848.466	282.7275	7294.1684	-3357.579
9	-35.529	.000	.0000	-53.7011	32.6951
10	2.324	.000	.0000	.2000	.0000000
11	11.984	.000	.0000	.0000	.0000
12	23.4750	.0000	.0000	.0000	.0000
13	8661392.0	8691444.2	8196354.6	3486136.2	2843662.7
14	73.2610	72.9494	68.3032	84.9145	281.4642
15	-7.5132	-7.5701	-6.6265	6.0715	9.4285

1	705.0000	645730.8500	8679368.7000	-1.5327	88.4121
2	23415.7640	24739.7370	25.181	-1.4551	88.5014
3	-1182076.1	-1586438.7	-11706447.500	1984407.000	-8096960.600
4	193422.6	242777.5	13895259.2	-3431.174	-45016.646
5	8690571.5	9555820.2	11590132.3	2825142.700	-633405.840
6	-9997.591	-11512.291	-18343.467	3151.2441	-21851.020
7	892.020	264.142	-16599.062	4.2735	-164.166
8	21155.388	21896.393	207.4004	7329.1030	-3424.267
9	-33.554	.000	.0000	-53.3333	32.7043
10	2.235	.000	.0000	.2000	.0000000
11	12.715	.000	.0000	.0000	.0000
12	23.7852	.0000	.0000	.0000	.0000
13	8772727.3	8802750.9	8306980.4	3597839.3	2732485.2
14	73.2749	72.9674	68.4101	84.8295	281.8372
15	-7.7438	-7.8002	-6.8630	5.5286	10.0624

TABLE AP 3-2 (Sheet 36 of 39)
SATURN OBSERVED TRAJECTORY - BOOST PHASE (AA83)

1	710.0000	642607.9700	8793209.1000	-1.5099	88.6299
2	23545.0230	24868.8220	25.379	-1.4333	88.7071
3	-1232474.4	-1644450.2	-11798205.700	2000129.600	-8206555.200
4	197910.7	244092.3	13811828.0	-3410.164	-45842.212
5	8796509.5	9665428.6	11590990.6	2861878.000	-650695.550
6	-10159.868	-11690.472	-18363.051	3138.3044	-21986.747
7	903.120	261.641	-16770.141	4.0891	-166.062
8	21220.970	21948.184	138.2226	7365.4587	-3491.753
9	-31.441	.000	.0000	-52.9633	32.7123
10	2.130	.000	.0000	.2000	.0000000
11	13.421	.000	.0000	.0000	.0000
12	24.0972	.0000	.0000	.0000	.0000
13	8884634.9	8914629.0	8418201.2	3710304.8	2620998.3
14	73.2888	72.9854	68.5151	84.7498	282.2448
15	-7.9738	-8.0297	-7.0985	5.0064	10.7404
	INTRODUCTION OF CHI TILDE GUIDANCE MODE				
1	712.5330	641045.4500	8851127.3000	-1.4865	88.7401
2	23610.1740	24933.8910	25.525	-1.4111	88.8112
3	-1258308.9	-1674171.8	-11844730.500	2008071.800	-8262334.200
4	200205.2	244753.2	13769240.5	-3399.995	-46264.067
5	8850304.7	9721057.3	11591297.7	2880558.400	-659583.770
6	-10238.114	-11776.853	-18374.760	3132.8925	-22055.372
7	908.547	260.169	-16853.962	3.9344	-167.027
8	21255.490	21975.829	105.5904	7384.3985	-3526.247
9	-30.387	.000	.0000	-52.7750	32.7160
10	2.050	.000	.0000	.2000	.0000000
11	13.747	.000	.0000	.0000	.0000
12	24.2559	.0000	.0000	.0000	.0000
13	8941549.9	8971529.0	8474777.1	3767570.9	2564423.9
14	73.2958	72.9944	68.5675	84.7114	282.4662
15	-8.0899	-8.1456	-7.2173	4.7495	11.1031
1	715.0000	639547.0400	8907694.0000	-1.4561	88.8470
2	23673.2130	24996.8560	25.701	-1.3822	88.9122
3	-1283658.0	-1703326.9	-11890073.400	2015795.000	-8316827.500
4	202452.6	245392.8	13727560.2	-3390.623	-46677.285
5	8902784.1	9775305.4	11591519.6	2898798.700	-668324.720
6	-10311.717	-11858.421	-18387.119	3128.3759	-22122.122
7	913.554	258.456	-16933.724	3.6994	-167.968
8	21289.784	22003.498	75.4704	7403.1323	-3560.040
9	-29.214	.000	.0000	-52.5911	32.7193
10	1.940	.000	.0000	.2000	.0000000
11	14.078	.000	.0000	.0000	.0000
12	24.4109	.0000	.0000	.0000	.0000
13	8997128.8	9027093.2	8530031.0	3823533.7	2509274.6
14	73.3026	73.0032	68.6182	84.6751	282.6924
15	-8.2026	-8.2581	-7.3327	4.5041	11.4699
1	720.0000	636612.8600	9022814.6000	-1.3713	89.0625
2	23799.0760	25122.5850	26.012	-1.3016	89.1158
3	-1335573.5	-1763016.4	-11982071.100	2031418.600	-8427775.700
4	207044.6	246675.3	13642494.7	-3373.636	-47521.914
5	9009408.7	9885465.7	11591751.1	2935910.400	-686297.300
6	-10452.439	-12015.400	-18414.888	3121.6813	-22257.137
7	922.933	254.231	-17089.058	2.9958	-169.885
8	21360.962	22061.503	19.5690	7441.8707	-3629.130
9	-27.069	.000	.0000	-52.2168	32.7250
10	1.871	.000	.0000	.2000	.0000000
11	14.514	.000	.0000	.0000	.0000
12	24.7264	.0000	.0000	.0000	.0000
13	9110217.6	9140152.1	8642477.6	3937521.7	2397403.3
14	73.3164	73.0209	68.7195	84.6049	283.1862
15	-8.4300	-8.4851	-7.5652	4.0213	12.2593
1	725.0000	633871.5300	9138559.1000	-1.2562	89.2791
2	23922.0340	25245.4330	26.311	-1.1924	89.3204
3	-1388164.8	-1823463.4	-12074216.900	2047016.900	-8539398.200
4	211682.6	247935.9	13556674.1	-3360.426	-48376.147
5	9116394.7	9995922.0	11591718.8	2973218.300	-704617.360
6	-10581.948	-12161.319	-18446.358	3118.2453	-22391.783
7	932.282	250.009	-17235.515	2.2958	-171.810
8	21434.013	22121.750	-30.4303	7481.5373	-3699.023
9	-24.741	.000	.0000	-51.8404	32.7296
10	1.873	.000	.0000	.2000	.0000000
11	14.763	.000	.0000	.0000	.0000
12	25.0436	.0000	.0000	.0000	.0000
13	9223907.0	9253811.5	8755546.0	4052261.3	2285493.6
14	73.3301	73.0385	68.8189	84.5388	283.7339
15	-8.6557	-8.7104	-7.7958	3.5571	13.1189

TABLE AP 3-2 (Sheet 37 of 39)
SATURN OBSERVED TRAJECTORY - BOOST PHASE (AA83)

1	730.0000	631388.0900	9254910.9000	-1.1119	89.4970
2	24040.9720	25364.2860	26.570	-1.0553	89.5264
3	-1441374.6	-1884611.2	-12166527.700	2062606.400	-8651693.000
4	216367.7	249175.8	13470145.0	-3350.543	-49240.033
5	9223748.4	10106683.1	11591450.7	3010726.100	-723288.880
6	-10699.933	-12295.828	-18480.808	3118.1712	-22526.049
7	941.764	245.986	-17372.427	1.6595	-173.746
8	21507.972	22183.308	-74.7770	7521.8488	-3769.720
9	-22.350	.000	.0000	-51.4621	32.7331
10	1.879	.000	.0000	.2000	.0000000
11	14.773	.000	.0000	.0000	.0000
12	25.3625	.0000	.0000	.0000	.0000
13	9338195.8	9368070.2	8869234.5	4167738.7	2173678.1
14	73.3437	73.0559	68.9166	84.4764	284.3447
15	-8.8792	-8.9335	-8.0239	3.1112	14.0605
1	735.0000	629225.5300	9371846.5000	-.9399	89.7159
2	24154.1860	25477.4340	26.820	-.8919	89.7333
3	-1495144.7	-1946402.3	-12259015.100	2078204.300	-8764658.000
4	221100.0	250395.7	13382956.8	-3343.840	-50113.618
5	9331470.9	10217752.0	11590974.9	3048436.300	-742315.900
6	-10806.099	-12418.557	-18516.741	3121.5692	-22659.926
7	951.115	241.948	-17499.062	1.0211	-175.690
8	21581.203	22244.564	-113.5521	7562.3133	-3841.221
9	-19.961	.000	.0000	-51.0818	32.7353
10	1.887	.000	.0000	.2000	.0000000
11	14.571	.000	.0000	.0000	.0000
12	25.6829	.0000	.0000	.0000	.0000
13	9453078.1	9482921.9	8983535.8	4283935.4	2062117.3
14	73.3572	73.0732	69.0126	84.4176	285.0301
15	-9.1004	-9.1543	-8.2494	2.6830	15.0986
1	740.0000	627445.3600	9489332.2000	-.7416	89.9361
2	24260.6710	25583.8740	27.089	-.7035	89.9415
3	-1549415.4	-2008776.7	-12351685.000	2093828.100	-8878291.600
4	225879.0	251595.8	13295162.6	-3340.193	-50996.947
5	9439556.0	10329125.2	11590318.8	3086348.600	-761702.430
6	-10900.282	-12529.300	-18553.416	3128.4986	-22793.403
7	960.503	238.096	-17614.874	.4425	-177.643
8	21652.747	22304.588	-147.0779	7602.6469	-3913.525
9	-17.627	.000	.0000	-50.6997	32.7362
10	1.894	.000	.0000	.2000	.0000000
11	14.200	.000	.0000	.0000	.0000
12	26.0049	.0000	.0000	.0000	.0000
13	9568538.1	9598351.3	9098433.6	4400823.4	1951010.7
14	73.3707	73.0903	69.1068	84.3620	285.8044
15	-9.3188	-9.3724	-8.4719	2.2720	16.2501
1	745.0000	626103.7100	9607331.8000	-.5186	90.1576
2	24359.8580	25683.0330	27.252	-.4914	90.1509
3	-1604128.4	-2071676.0	-12444538.000	2109495.000	-8992591.400
4	230704.7	252776.6	13206815.4	-3339.415	-51890.067
5	9547992.9	10440793.5	11589507.6	3124461.700	-781452.500
6	-10982.668	-12628.209	-18590.216	3138.9091	-22926.468
7	969.899	234.422	-17719.799	-.0791	-179.606
8	21721.948	22362.728	-175.5979	7642.6508	-3986.631
9	-15.375	.000	.0000	-50.3159	32.7360
10	1.901	.000	.0000	.2000	.0000000
11	13.551	.000	.0000	.0000	.0000
12	26.3283	.0000	.0000	.0000	.0000
13	9684555.5	9714338.1	9213906.4	4518370.2	1840598.4
14	73.3841	73.1073	69.1994	84.3095	286.6855
15	-9.5343	-9.5875	-8.6912	1.8778	17.5354
	CHI FREEZE				
1	746.1000	625872.2100	9633356.6000	-.4667	90.2064
2	24380.5100	25703.6800	27.266	-.4421	90.1971
3	-1616219.1	-2085578.7	-12464989.700	2112949.000	-9017826.100
4	231772.7	253034.1	13187310.1	-3339.545	-52087.869
5	9571894.6	10465398.7	11589310.2	3132873.300	-785846.640
6	-10999.301	-12648.461	-18598.080	3141.6419	-22955.685
7	971.955	233.632	-17741.414	-.1881	-180.039
8	21736.604	22375.010	-181.3027	7651.3291	-4002.822
9	-14.881	.000	.0000	-50.2313	32.7358
10	1.903	.000	.0000	.2000	.0000000
11	13.358	.000	.0000	.0000	.0000
12	26.3996	.0000	.0000	.0000	.0000
13	9710151.5	9739927.4	9239385.0	4544315.3	1816428.8
14	73.3870	73.1110	69.2195	84.2783	286.8958
15	-9.5813	-9.6344	-8.7389	1.7932	17.8385

13

TABLE AP 3-2 (Sheet 38 of 39)
SATURN OBSERVED TRAJECTORY - BOOST PHASE (AA83)

S-IVB GUIDANCE CUTOFF SIGNAL

1	747.0400	625694.4300	9655614.6000	-.4227	90.2484
2	24398.1380	25721.3040	27.313	-.4003	90.2368
3	-1626565.2	-2097476.6	-12482474.400	2115903.300	-9039416.600
4	232687.3	253253.5	13170623.5	-3339.733	-52257.282
5	9592333.2	10486436.3	11589137.0	3140069.100	-789615.860
6	-11013.670	-12665.920	-18604.695	3143.9257	-22980.637
7	973.771	233.014	-17759.959	-.2635	-180.409
8	21749.021	22385.391	-186.3308	7658.7195	-4016.688
9	-14.461	.000	.0000	-50.1589	32.7355
10	1.881	.000	.0000	.2000	.0000000
11	13.226	.000	.0000	.0000	.0000
12	26.4606	.0000	.0000	.0000	.0000
13	9732045.5	9761815.6	9261179.1	4566510.7	1795814.8
14	73.3895	73.1141	69.2367	84.2889	287.0807
15	-9.6213	-9.6744	-8.7796	1.7216	18.1038

REDUNDANT S-IVB CUTOFF SIGNAL = TB 5

1	747.3800	625632.9800	9663669.5000	-.4137	90.2638
2	24401.9200	25725.0840	17.886	-.3916	90.2514
3	-1630311.5	-2101784.7	-12488799.200	2116972.200	-9047231.600
4	233018.5	253332.7	13164582.8	-3339.836	-52318.647
5	9599727.8	10494047.4	11589072.9	3142673.400	-790982.480
6	-11020.309	-12673.505	-18603.536	3144.3635	-22989.659
7	974.392	232.831	-17766.610	-.2784	-180.543
8	21749.875	22385.444	-189.7958	7660.2663	-4021.711
9	-15.664	.000	.0000	-50.1327	32.7354
10	1.836	.000	.0000	.2000	.0000000
11	2.893	.000	.0000	.0000	.0000
12	26.4827	.0000	.0000	.0000	.0000
13	9739968.6	9769736.2	9269066.0	4574543.6	1788368.2
14	73.3904	73.1153	69.2429	84.2855	287.1488
15	-9.6357	-9.6888	-8.7943	1.6958	18.2011

S-IVB PU ACTIVATE OFF

1	748.1500	625497.8300	9681908.5000	-.4089	90.2994
2	24402.3430	25725.5000	3.294	-.3871	90.2852
3	-1638803.6	-2111550.3	-12503116.600	2119393.500	-9064941.300
4	233769.3	253511.9	13150897.8	-3340.019	-52457.777
5	9616470.1	10511278.2	11588921.2	3148571.200	-794083.470
6	-11037.651	-12692.511	-18591.212	3144.7953	-23010.081
7	975.719	232.584	-17779.979	-.2614	-180.846
8	21741.495	22375.153	-201.4811	7660.6009	-4033.098
9	-21.679	.000	.0000	-50.0734	32.7352
10	1.735	.000	.0000	.2000	.0000000
11	-10.695	.000	.0000	.0000	.0000
12	26.5326	.0000	.0000	.0000	.0000
13	9757910.5	9787673.9	9286927.1	4592736.1	1771528.5
14	73.3925	73.1179	69.2568	84.2779	287.3054
15	-9.6684	-9.7214	-8.8275	1.6377	18.4243

1	750.0000	625181.7100	9725742.7000	-.4045	90.3848
2	24404.1900	25727.3260	.051	-.3826	90.3662
3	-1659262.5	-2135074.7	-12537485.500	2125212.100	-9107555.500
4	235577.2	253941.4	13117970.8	-3340.536	-52793.019
5	9656678.2	10552654.3	11588522.8	3162745.500	-801570.100
6	-11082.284	-12741.100	-18560.380	3144.9290	-23059.109
7	978.784	231.840	-17814.443	-.2653	-181.577
8	21720.715	22349.633	-231.0492	7661.1853	-4060.536
9	-24.408	.000	.0000	-49.9308	32.7344
10	1.642	.000	.0000	.2000	.0000000
11	-12.244	.000	.0000	.0000	.0000
12	26.6528	.0000	.0000	.0000	.0000
13	9801024.3	9830776.2	9329848.2	4636461.4	1731200.4
14	73.3974	73.1241	69.2903	84.2599	287.6958
15	-9.7468	-9.7997	-8.9072	1.4991	18.9761

1	755.0000	624320.4200	9844211.5000	-.4006	90.6158
2	24405.1400	25728.2220	.053	-.3782	90.5852
3	-1714980.5	-2199112.5	-12630056.400	2140936.300	-9223181.800
4	240491.5	255095.7	13028662.7	-3341.856	-53705.847
5	9765123.4	10664211.5	11587158.3	3201050.200	-822059.200
6	-11203.970	-12873.165	-18471.679	3144.9722	-23191.316
7	986.960	229.861	-17906.442	-.2652	-183.556
8	21658.897	22274.880	-312.9122	7661.1698	-4135.238
9	-24.339	.000	.0000	-49.5455	32.7316
10	1.634	.000	.0000	.2000	.0000000
11	-12.422	.000	.0000	.0000	.0000
12	26.9774	.0000	.0000	.0000	.0000
13	9917490.7	9947211.7	9445807.1	4754649.4	1623275.4
14	73.4107	73.1409	69.3793	84.2133	288.8615
15	-9.9579	-10.0105	-9.1217	1.1318	20.5835

TABLE AP 3-2 (Sheet 39 of 39)
SATURN OBSERVED TRAJECTORY - BOOST PHASE (AA83)

1	755.5000	624235.3100	9856059.1000	-.4002	90.6389
2	24405.2450	25728.3230	.060	-.3778	90.6071
3	-1720585.5	-2205552.5	-12639289.500	2142508.700	-9234780.600
4	240985.2	255210.6	13019706.6	-3341.989	-53797.674
5	9775951.1	10675347.0	11586999.7	3206880.700	-824128.700
6	-11216.133	-12886.361	-18462.776	3144.9725	-23204.513
7	987.776	229.663	-17915.621	-.2652	-183.754
8	21652.682	22267.366	-321.1035	7661.1698	-4142.751
9	-24.324	.000	.0000	-49.5070	32.7312
10	1.633	.000	.0000	.2000	.0000000
11	-12.436	.000	.0000	.0000	.0000
12	27.0099	.0000	.0000	.0000	.0000
13	9929134.0	9958851.9	9457400.7	4766470.0	1612577.1
14	73.4120	73.1425	69.3881	84.2089	288.9879
15	-9.9790	-10.0315	-9.1430	1.0956	20.7543

1	756.0000	624149.8000	9867906.3000	-.3998	90.6620
2	24405.3510	25728.4230	.060	-.3774	90.6290
3	-1726196.8	-2211999.1	-12648517.900	2144081.200	-9246386.200
4	241479.3	255325.4	13010745.9	-3342.122	-53889.600
5	9786775.9	10686478.8	11586836.6	3208711.200	-826201.950
6	-11228.294	-12899.554	-18453.865	3144.9724	-23217.705
7	988.592	229.465	-17924.795	-.2652	-183.953
8	21646.461	22259.844	-329.2953	7661.1698	-4150.273
9	-24.317	.000	.0000	-49.4685	32.7309
10	1.633	.000	.0000	.2000	.0000000
11	-12.450	.000	.0000	.0000	.0000
12	27.0423	.0000	.0000	.0000	.0000
13	9940776.9	9970491.6	9468994.2	4778291.4	1601897.0
14	73.4134	73.1442	69.3969	84.2044	289.1163
15	-10.0000	-10.0525	-9.1644	1.0596	20.9272

1	756.5000	624064.8100	9879754.3000	-.3995	90.6851
2	24405.4570	25728.5230	.060	-.3770	90.6510
3	-1731814.0	-2218452.1	-12657742.100	2145653.700	-9257998.400
4	241973.8	255440.1	13001780.7	-3342.255	-53981.627
5	9797597.5	10697606.7	11586669.7	3212541.800	-828278.970
6	-11240.451	-12912.742	-18444.948	3144.9724	-23230.893
7	989.408	229.266	-17933.962	-.2652	-184.151
8	21640.233	22252.315	-337.4870	7661.1698	-4157.803
9	-24.311	.000	.0000	-49.4300	32.7305
10	1.632	.000	.0000	.2000	.0000000
11	-12.464	.000	.0000	.0000	.0000
12	27.0748	.0000	.0000	.0000	.0000
13	9952419.0	9982130.6	9480587.0	4790113.0	1591235.8
14	73.4147	73.1459	69.4057	84.1999	289.2467
15	-10.0210	-10.0735	-9.1857	1.0236	21.1020

1	757.0000	623979.7100	9891602.5000	-.3991	90.7082
2	24405.5620	25728.6230	.060	-.3766	90.6729
3	-1737437.3	-2224911.9	-12666961.700	2147226.100	-9269617.100
4	242468.7	255554.6	12992810.9	-3342.387	-54073.752
5	9808416.0	10708731.0	11586498.6	3216372.400	-830359.760
6	-11252.604	-12925.925	-18436.024	3144.9723	-23244.077
7	990.223	229.067	-17943.123	-.2652	-184.350
8	21633.997	22244.778	-345.6786	7661.1698	-4165.341
9	-24.304	.000	.0000	-49.3914	32.7301
10	1.631	.000	.0000	.2000	.0000000
11	-12.478	.000	.0000	.0000	.0000
12	27.1073	.0000	.0000	.0000	.0000
13	9964060.3	9993769.0	9492179.4	4801934.7	1580593.9
14	73.4160	73.1475	69.4145	84.1955	289.3792
15	-10.0420	-10.0945	-9.2071	.9877	21.2789

PARKING ORBIT INSERTION

1	757.0400	623978.9700	9892549.1000	-.3991	90.7100
2	24405.5710	25728.6310	.059	-.3766	90.6746
3	-1737881.6	-2225423.2	-12667700.600	2147353.700	-9270547.000
4	242504.2	255559.8	12992095.6	-3343.630	-54081.126
5	9809283.6	10709623.2	11586491.6	3216679.600	-830526.380
6	-11253.576	-12926.980	-18435.310	3144.9723	-23245.131
7	990.289	229.052	-17943.855	-.2651	-184.366
8	21633.498	22244.174	-346.3343	7661.1698	-4165.944
9	-24.304	.000	.0000	-49.3884	32.7301
10	1.631	.000	.0000	.2000	.0000000
11	-12.480	.000	.0000	.0000	.0000
12	27.1099	.0000	.0000	.0000	.0000
13	9964992.8	9994701.0	9493108.2	4802881.1	1579747.9
14	73.4161	73.1476	69.4151	84.1951	289.3900
15	-10.0437	-10.0961	-9.2087	.9849	21.2933

TABLE AP 3-3 (Sheet 1 of 14)
SATURN OBSERVED TRAJECTORY - ORBITAL PHASE (AA83)

1	TIME (SEC)	ALTITUDE (FEET)	RANGE (FEET)	GAMMA SB 1 (DEG.)	GAMMA SB 2 (DEG.)
2	V SB E (FT/SEC)	V SB I (FT/SEC)	A SB I (FT/SSQ)	GAMMA(1I) PR (DEG.)	GAMMA(2I) PR (DEG.)
3	X SB E (FEET)	X SB S (FEET)	X SB SFE (FEET)	XI (METERS)	X SB GS (FEET)
4	Y SB E (FEET)	Y SB S (FEET)	Y SB SFE (FEET)	ETA (METERS)	Y SB GS (FEET)
5	Z SB E (FEET)	Z SB S (FEET)	Z SB SFE (FEET)	ZETA (METERS)	Z SB GS (FEET)
6	D-X SB E (FT/SEC)	D-X SB S (FT/SEC)	D-X SB SFE (FT/SEC)	D-XI (M/SEC)	D-X SB GS (FT/SEC)
7	D-Y SB E (FT/SEC)	D-Y SB S (FT/SEC)	D-Y SB SFE (FT/SEC)	D-ETA (M/SEC)	D-Y SB GS (FT/SEC)
8	D-Z SB E (FT/SEC)	D-Z SB S (FT/SEC)	D-Z SB SFE (FT/SEC)	D-ZETA (M/SEC)	D-Z SB GS (FT/SEC)
9	DD-X SB E (FT/SSQ)	V SB W (FT/SEC)	ALPHA SB WIND (DEG.)	MU (DEG.)	RHO (DEG.)
10	DD-Y SB E (FT/SSQ)	E SB W (DEG.)	BETA SB WIND (DEG.)	TEMPERATURE (DEG R)	DENSITY (SL/FT3)
11	DD-Z SB E (FT/SSQ)	V SB RM (FT/SEC)	MACH NUMBER	PRESSURE (LB/FT2)	DYN PRESS Q (LB/FT2)
12	RANGE ANGLE (DEG.)	REYN/L (1/FT)	VISCOSITY (LB-S/FT2)	REL HUMID (PERCENT)	SOUND VEL (FT/SEC)
13	D* SB 1 (FEET)	D* SB 2 (FEET)	D* SB 3 (FEET)	D* SB 4 (FEET)	D* SB 5 (FEET)
14	A* SB 1 (DEG.)	A* SB 2 (DEG.)	A* SB 3 (DEG.)	A* SB 4 (DEG.)	A* SB 5 (DEG.)
15	E* SB 1 (DEG.)	E* SB 2 (DEG.)	E* SB 3 (DEG.)	E* SB 4 (DEG.)	E* SB 5 (DEG.)

PARKING ORBIT INSERTION

1	757.0400	623978.6700	9892549.1000	-.3991	90.7100
2	24405.5710	25728.6310	.059	-.3766	90.6746
3	-1737881.6	-2225423.2	-12667700.600	2147353.700	-9270547.000
4	242504.2	255559.8	12992095.6	-3343.630	-54081.126
5	9809283.6	10709623.2	11586491.6	3216679.600	-830526.380
6	-11253.576	-12926.980	-18435.310	3144.9723	-23245.131
7	990.289	229.052	-17943.855	-.2651	-184.366
8	21633.498	22244.174	-346.3343	7661.1698	-4165.944
9	-24.304	.000	.0000	-49.3884	32.7301
10	1.631	.000	.0000	.2000	.0000000
11	-12.480	.000	.0000	.0000	.0000
12	27.1099	.0000	.0000	.0000	.0000
13	4802881.1	10836326.8	41991656.0	31041832.0	18781310.0
14	84.1951	288.0704	300.8273	52.3082	68.6873
15	.9849	-11.5570	-81.5904	-46.1384	-24.5026

1	760.0000	623461.0800	9962698.9000	-.3968	90.8467
2	24406.2230	25729.2490	.000	-.3741	90.8043
3	-1771316.7	-2263820.5	-12722184.500	.000	.000
4	245443.1	256236.2	12938883.3	.000	.000
5	9873264.0	10775398.9	11585384.3	.000	.000
6	-11325.459	-13004.941	-18382.365	.0000	.000
7	995.100	227.865	-17997.977	.0000	.000
8	21596.469	22199.414	-394.8159	.0000	.000
9	-24.262	.000	.0000	-49.1603	32.7275
10	1.627	.000	.0000	.2000	.0000000
11	-12.561	.000	.0000	.0000	.0000
12	27.3021	.0000	.0000	.0000	.0000
13	4872876.6	10767415.9	41981643.0	31084058.0	18843640.0
14	84.1696	288.0700	300.5626	52.2157	68.6398
15	.7744	-11.4418	-81.5009	-46.2255	-24.6051

TABLE AP 3-3 (Sheet 2 of 14)
SATURN OBSERVED TRAJECTORY - ORBITAL PHASE (AA83)

ALIGN AXIS WITH LOCAL HORIZONTAL

1	764.0000	622777.4300	10057495.5000	-.3939	91.0314
2	24407.0780	25730.0590	.000	-.3707	90.9795
3	-1816823.6	-2316061.6	-12795563.300	.000	.000
4	249436.7	257144.6	12866732.3	.000	.000
5	9959548.3	10864073.6	11583666.5	.000	.000
6	-11422.400	-13110.041	-18310.435	.0000	.000
7	1001.589	226.264	-18070.793	.0000	.000
8	21546.021	22138.466	-460.3375	.0000	.000
9	-24.206	.000	.0000	-48.8520	32.7232
10	1.621	.000	.0000	.2000	.0000000
11	-12.671	.000	.0000	.0000	.0000
12	27.5619	.0000	.0000	.0000	.0000
13	4967475.6	10674255.0	41967943.0	31141029.0	18927809.0
14	84.1365	288.0694	300.2129	52.0907	68.5761
15	.4951	-11.2857	-81.3796	-46.3432	-24.7436

1	770.0000	621786.0600	10199689.3000	-.3894	91.3085
2	24408.3030	25731.2190	.000	-.3657	91.2423
3	-1885782.1	-2395182.5	-12905096.600	.000	.000
4	255475.2	258494.9	12757985.1	.000	.000
5	10088595.9	10996628.9	11580612.5	.000	.000
6	-11567.387	-13267.147	-18201.719	.0000	.000
7	1011.295	223.866	-18179.138	.0000	.000
8	21469.469	22046.052	-558.6313	.0000	.000
9	-24.123	.000	.0000	-48.3898	32.7152
10	1.613	.000	.0000	.2000	.0000000
11	-12.839	.000	.0000	.0000	.0000
12	27.9516	.0000	.0000	.0000	.0000
13	5109395.0	10534433.3	41947032.0	31226289.0	19053931.0
14	84.0898	288.0681	299.7059	51.9032	68.4815
15	.0872	-11.0506	-81.1972	-46.5197	-24.9511

1	780.0000	620143.0800	10436717.1000	-.3819	91.7700
2	24410.3670	25733.1700	.000	-.3573	91.6800
3	-2002659.7	-2529157.3	-13086189.000	.000	.000
4	265668.5	260713.4	12575288.0	.000	.000
5	10302644.4	11216309.5	11574202.8	.000	.000
6	-11807.874	-13527.516	-18018.510	.0000	.000
7	1027.359	219.840	-18357.766	.0000	.000
8	21339.744	21889.588	-722.3873	.0000	.000
9	-23.976	.000	.0000	-47.6194	32.6977
10	1.600	.000	.0000	.2000	.0000000
11	-13.108	.000	.0000	.0000	.0000
12	28.6011	.0000	.0000	.0000	.0000
13	5345978.2	10301118.5	41911125.0	31367815.0	19263774.0
14	84.0192	288.0650	298.9031	51.5906	68.3264
15	-.5676	-10.6560	-80.8918	-46.8139	-25.2965

1	790.0000	618532.8100	10673783.0000	-.3742	92.2311
2	24412.4020	25735.0910	.000	-.3487	92.1174
3	-2121934.7	-2665726.6	-13265436.700	.000	.000
4	276021.9	262891.6	12390817.6	.000	.000
5	10515381.7	11434410.2	11566156.0	.000	.000
6	-12046.902	-13786.025	-17832.740	.0000	.000
7	1043.284	215.785	-18533.840	.0000	.000
8	21207.288	21730.023	-886.0703	.0000	.000
9	-23.830	.000	.0000	-46.8493	32.6750
10	1.585	.000	.0000	.2000	.0000000
11	-13.383	.000	.0000	.0000	.0000
12	29.2508	.0000	.0000	.0000	.0000
13	5582592.5	10067480.7	41873921.0	31508631.0	19473158.0
14	83.9566	288.0607	298.1491	51.2779	68.1743
15	-1.1942	-10.2581	-80.5850	-47.1080	-25.6414

1	800.0000	616954.9700	10910885.5000	-.3665	92.6918
2	24414.3980	25736.9680	.000	-.3401	92.5544
3	-2243592.8	-2804871.6	-13442813.800	.000	.000
4	286533.7	265029.0	12204599.2	.000	.000
5	10726780.9	11650899.6	11556472.8	.000	.000
6	-12284.456	-14042.649	-17644.412	.0000	.000
7	1059.063	211.699	-18707.339	.0000	.000
8	21072.099	21567.355	-1049.6655	.0000	.000
9	-23.680	.000	.0000	-46.0795	32.6470
10	1.570	.000	.0000	.2000	.0000000
11	-13.655	.000	.0000	.0000	.0000
12	29.9005	.0000	.0000	.0000	.0000
13	5819208.3	9833528.4	41835424.0	31648726.0	19682071.0
14	83.9009	288.0550	297.4396	50.9649	68.0253
15	-1.7959	-9.8564	-80.2768	-47.4021	-25.9859

TABLE AP 3-3 (Sheet 3 of 14)
SATURN OBSERVED TRAJECTORY - ORBITAL PHASE (AA83)

ROLL 180 DEG. TO POSITION III DOWN

1	837.0000	611404.1900	11788473.3000	-.3374	94.3898
2	24421.4250	25743.5460	.000	-.3078	94.1648
3	-2714196.4	-3341783.7	-14082423.900	.000	.000
4	326780.6	272578.5	11500826.2	.000	.000
5	11496872.2	12437391.7	11506435.7	.000	.000
6	-13150.043	-14975.130	-16925.796	.0000	.000
7	1116.080	196.314	-19326.474	.0000	.000
8	20548.400	20938.892	-1653.8069	.0000	.000
9	-23.101	.000	.0000	-43.2359	32.4980
10	1.511	.000	.0000	.2000	.0000000
11	-14.649	.000	.0000	.0000	.0000
12	32.3053	.0000	.0000	.0000	.0000
13	6694293.5	8965328.7	41681745.0	32160682.0	20450778.0
14	83.7430	288.0206	295.1401	49.8041	67.4981
15	-3.8501	-8.3328	-79.1263	-48.4895	-27.2566

1	900.0000	603021.8000	13283767.7000	-.2865	97.2449
2	24432.0780	25753.3760	.000	-.2516	96.8721
3	-3587796.1	-4333607.1	-15108233.100	.000	.000
4	400017.6	284098.5	10252107.8	.000	.000
5	12761259.1	13720495.8	11369979.2	.000	.000
6	-14571.861	-16496.883	-15626.438	.0000	.000
7	1207.676	169.217	-20295.136	.0000	.000
8	19573.677	19775.254	-2675.5133	.0000	.000
9	-22.016	.000	.0000	-38.4211	32.0811
10	1.394	.000	.0000	.2000	.0000000
11	-16.282	.000	.0000	.0000	.0000
12	36.4027	.0000	.0000	.0000	.0000
13	8180716.6	7478871.2	41379502.0	33008306.0	21742989.0
14	83.5932	287.8978	292.0992	47.8098	66.6780
15	-6.9219	-5.5570	-77.1404	-50.3379	-29.4080

1	1000.0000	592592.4400	15659448.2000	-.2018	101.6250
2	24445.4520	25765.3190	.000	-.1600	101.0223
3	-5151909.7	-6096615.5	-16560374.600	.000	.000
4	527403.5	298787.3	8154863.8	.000	.000
5	14633093.9	15596529.4	11022462.1	.000	.000
6	-16677.690	-18722.247	-13384.179	.0000	.000
7	1336.339	124.181	-21598.945	.0000	.000
8	17822.710	17700.672	-4266.2743	.0000	.000
9	-20.053	.000	.0000	-30.8960	31.0086
10	1.172	.000	.0000	.2000	.0000000
11	-18.700	.000	.0000	.0000	.0000
12	42.9118	.0000	.0000	.0000	.0000
13	10523423.4	5105030.4	40795567.0	34287329.0	23745739.0
14	83.5248	287.3862	288.6578	44.5611	65.5376
15	-11.1925	-.2421	-73.9445	-53.2594	-32.7969

1	1500.0000	598329.9500	27547593.0000	.2624	118.3482
2	24441.0770	25753.8740	.000	.3017	116.7832
3	**********	**********	-20016649.000	.000	.000
4	1281570.3	300810.6	-3421068.0	.000	.000
5	20799581.0	21253956.0	7112256.4	.000	.000
6	-23594.674	-25398.822	-35.753	.0000	.000
7	1543.178	-117.483	-23329.880	.0000	.000
8	6186.775	4260.067	-10907.6817	.0000	.000
9	-5.849	.000	.0000	2.9314	19.4207
10	-.460	.000	.0000	.2000	.0000000
11	-26.529	.000	.0000	.0000	.0000
12	75.4695	.0000	.0000	.0000	.0000
13	21624275.0	6982014.7	36036228.0	39254182.0	32601438.0
14	84.1322	112.0271	280.0498	23.5458	61.3559
15	-29.2268	-4.5877	-57.6531	-67.2156	-49.4494

1	2000.0000	701475.1700	39360115.0000	.6855	124.5522
2	24316.3410	25629.9520	.000	.6574	122.5532
3	**********	**********	-16609958.400	.000	.000
4	1915789.4	186796.0	-13830215.3	.000	.000
5	20518120.0	19629490.0	753034.2	.000	.000
6	-23197.716	-23364.499	13226.440	.0000	.000
7	837.459	-326.577	-17096.820	.0000	.000
8	-7242.175	-10530.340	-13771.5119	.0000	.000
9	8.310	.000	.0000	30.9258	2.0096
10	-2.318	.000	.0000	.2000	.0000000
11	-25.698	.000	.0000	.0000	.0000
12	107.8115	.0000	.0000	.0000	.0000
13	31022324.0	18414602.0	28552914.0	41446120.0	38952855.0
14	85.1525	111.5665	274.7240	335.5732	57.1190
15	-45.9000	-23.6830	-41.1007	-76.5947	-65.7961

TABLE AP 3-3 (Sheet 4 of 14)
SATURN OBSERVED TRAJECTORY - ORBITAL PHASE (AA83)

1	2499.9999	873092.4700	50987577.0000	.8895	120.7420
2	24106.8680	25434.1790	.000	.7966	118.9803
3	**********	**********	-7578343.800	.000	.000
4	1985794.3	-8598.5	-19572355.0	.000	.000
5	13980097.0	11366403.5	-5870080.7	.000	.000
6	-15822.910	-13543.314	21821.682	.0000	.000
7	-653.219	-433.948	-5257.032	.0000	.000
8	-18175.530	-21524.123	-11961.7766	.0000	.000
9	20.305	.000	.0000	57.8878	-15.7209
10	-3.457	.000	.0000	.2000	.0000000
11	-16.946	.000	.0000	.0000	.0000
12	139.6771	.0000	.0000	.0000	.0000
13	37977200.0	28367085.0	19020072.0	40620968.0	42283033.0
14	86.2966	111.4730	268.6314	273.9261	42.5285
15	-62.1690	-40.3367	-24.0434	-71.5983	-81.6605
1	2999.9999	1052374.6000	62318141.0000	.7674	107.0060
2	23888.2010	25234.4250	.000	.6836	106.0751
3	**********	**********	3975312.000	.000	.000
4	1220261.0	-224415.9	-18844523.0	.000	.000
5	3300511.2	-663980.5	-10554796.3	.000	.000
6	-3993.508	485.886	23085.871	.0000	.000
7	-2391.611	-406.402	8030.221	.0000	.000
8	-23430.285	-25226.475	-6271.7125	.0000	.000
9	25.784	.000	.0000	88.8766	-28.8793
10	-3.248	.000	.0000	.2000	.0000000
11	-3.667	.000	.0000	.0000	.0000
12	170.7619	.0000	.0000	.0000	.0000
13	42006233.0	36088300.0	8425264.5	36859424.0	42386843.0
14	87.5247	110.6922	254.3300	248.4591	263.3013
15	-78.1970	-56.4700	-4.1981	-58.4790	-81.1733
		INITIATE 20 DEG. PITCH DOWN MANEUVER			
1	3207.0000	1112786.0000	63975197.0000	.6274	98.7675
2	23814.8820	25167.0930	.000	.5701	98.2946
3	**********	**********	8596742.000	.000	.000
4	658892.0	-303731.5	-16665265.4	.000	.000
5	-1586272.5	-5817201.1	-11541636.6	.000	.000
6	1374.554	6431.479	21357.777	.0000	.000
7	-3014.281	-356.481	12916.669	.0000	.000
8	-23583.327	-24328.823	-3222.9958	.0000	.000
9	25.869	.000	.0000	-256.6135	-31.7759
10	-2.728	.000	.0000	.2000	.0000000
11	2.175	.000	.0000	.0000	.0000
12	175.3154	.0000	.0000	.0000	.0000
13	42756376.0	38501793.0	4400437.8	34514894.0	41492061.0
14	88.1095	109.8691	230.6567	242.2608	254.7966
15	-84.7828	-63.0621	8.8753	-52.4584	-74.7748
1	3499.9999	1173830.6000	57598702.0000	.3671	85.9746
2	23741.3840	25098.0060	.000	.3582	86.1935
3	**********	**********	14257391.200	.000	.000
4	-326790.7	-393959.2	-12019878.5	.000	.000
5	-8287743.9	**********	-11821538.5	.000	.000
6	8721.210	14088.375	16925.913	.0000	.000
7	-3658.923	-253.791	18484.387	.0000	.000
8	-21776.273	-20769.287	1323.2124	.0000	.000
9	23.883	.000	.0000	-235.2573	-32.5379
10	-1.603	.000	.0000	.2000	.0000000
11	10.032	.000	.0000	.0000	.0000
12	157.8446	.0000	.0000	.0000	.0000
13	42882030.0	41058585.0	4753517.1	30500933.0	39324675.0
14	268.4939	107.3683	130.7297	234.9920	250.5405
15	-85.9272	-72.3174	8.0531	-43.7011	-65.5249
1	3999.9999	1197492.2000	46448741.0000	-.1391	66.9826
2	23714.7960	25067.1600	.000	-.0800	68.2893
3	**********	**********	20006458.000	.000	.000
4	-2252885.7	-464718.2	-1364008.4	.000	.000
5	**********	**********	-9314803.3	.000	.000
6	18815.763	23088.376	5451.407	.0000	.000
7	-3822.157	-20.967	22971.133	.0000	.000
8	-13919.400	-9761.611	8424.4771	.0000	.000
9	15.575	.000	.0000	-201.1131	-25.0562
10	1.063	.000	.0000	.2000	.0000000
11	20.635	.000	.0000	.0000	.0000
12	127.2657	.0000	.0000	.0000	.0000
13	40592793.0	42969743.0	15037995.7	22120684.0	33360155.0
14	269.8809	60.2034	100.1713	222.9836	247.9901
15	-70.1049	-87.0348	-16.0936	-28.3485	-49.5839

TABLE AP 3-3 (Sheet 5 of 14)
SATURN OBSERVED TRAJECTORY - ORBITAL PHASE (AA83)

1	4499.9998	1122267.9000	35259209.0000	-.5590	56.8462
2	23808.1870	25148.2920	.000	-.4966	58.8186
3	**********	**********	19408590.000	.000	.000
4	-3908562.3	-412588.7	9723053.6	.000	.000
5	**********	**********	-3845627.5	.000	.000
6	23577.484	24761.441	-7796.286	.0000	.000
7	-2559.315	225.641	20157.293	.0000	.000
8	-2093.302	4388.253	12858.3865	.0000	.000
9	2.985	.000	.0000	-172.6923	-10.1102
10	3.940	.000	.0000	.2000	.0000000
11	25.560	.000	.0000	.0000	.0000
12	96.5834	.0000	.0000	.0000	.0000
13	35307229.0	41701251.0	24962380.0	12783642.6	24918193.0
14	271.1402	305.2155	92.6413	203.0824	247.0307
15	-54.2167	-75.6442	-33.3749	-12.5428	-33.3626
1	4999.9999	979440.1700	23947041.0000	-.7716	56.1765
2	23982.8460	25313.7210	.000	-.7561	58.1729
3	**********	-6129758.8	12599142.600	.000	.000
4	-4597091.3	-249046.9	17689133.0	.000	.000
5	**********	**********	2853188.1	.000	.000
6	21592.586	18454.626	-18716.876	.0000	.000
7	-24.559	412.780	10791.676	.0000	.000
8	10437.265	17321.689	13191.0118	.0000	.000
9	-10.826	.000	.0000	-146.8514	7.5313
10	5.964	.000	.0000	.2000	.0000000
11	23.317	.000	.0000	.0000	.0000
12	65.5952	.0000	.0000	.0000	.0000
13	27367474.0	37318431.0	33201142.0	7156115.4	14576975.1
14	272.3847	299.5338	87.2320	137.6444	246.2081
15	-38.1048	-59.8140	-49.7574	-1.8271	-16.2517
		INITIATE 20 DEG. PITCH UP MANEUVER			
1	5426.9999	839000.8900	14161433.1000	-.7665	63.2555
2	24154.6030	25482.9080	.000	-.7801	64.7525
3	-3955019.0	-352685.5	3412410.800	.000	.000
4	-4043269.9	-55189.6	19976784.0	.000	.000
5	**********	-7102234.4	7910880.9	.000	.000
6	14744.912	8010.317	-23437.319	.0000	.000
7	2638.341	477.906	-331.957	.0000	.000
8	18949.183	24186.464	9998.0262	.0000	.000
9	-20.723	.000	.0000	-122.8690	21.4485
10	6.236	.000	.0000	.2000	.0000000
11	15.762	.000	.0000	.0000	.0000
12	38.7982	.0000	.0000	.0000	.0000
13	18879424.0	31312163.0	38381516.0	12546722.7	4827975.7
14	273.4378	297.0014	81.8469	84.0503	242.2577
15	-23.9197	-46.0811	-63.5613	-13.3970	3.5442
1	5499.9998	815650.0700	12479482.7000	-.7494	65.2233
2	24183.2510	25511.3910	.000	-.7640	66.5945
3	-2935062.4	156358.2	1691105.100	.000	.000
4	-3834155.0	-20270.7	19879644.0	.000	.000
5	**********	-5312829.4	8610870.8	.000	.000
6	13183.024	5926.449	-23692.887	.0000	.000
7	3089.328	478.227	-2326.191	.0000	.000
8	20037.305	24808.861	9168.8079	.0000	.000
9	-22.046	.000	.0000	-118.3427	23.4795
10	6.111	.000	.0000	.2000	.0000000
11	14.031	.000	.0000	.0000	.0000
12	34.1916	.0000	.0000	.0000	.0000
13	17303640.0	30098578.0	39068463.0	13916164.8	3152601.8
14	273.6174	296.5619	80.6433	79.7493	238.7257
15	-21.4127	-43.7123	-65.9098	-15.8324	10.8568
		ROLL 180 DEG. TO POSITION I DOWN			
1	5786.9999	730672.7900	5885424.5000	-.6397	75.0757
2	24287.8940	25615.2470	.000	-.6457	75.8674
3	-119583.1	640213.8	-5075752.600	.000	.000
4	-2706771.0	113759.1	18106715.0	.000	.000
5	-5366912.6	1972419.7	10706888.9	.000	.000
6	6255.940	-2603.832	-23014.203	.0000	.000
7	4719.152	447.211	-9923.854	.0000	.000
8	22989.010	25478.639	5291.9315	.0000	.000
9	-25.824	.000	.0000	-99.0203	29.8165
10	5.112	.000	.0000	.2000	.0000000
11	6.332	.000	.0000	.0000	.0000
12	16.1274	.0000	.0000	.0000	.0000
13	10843418.2	24867170.0	41157872.0	19507249.0	3932113.9
14	274.3288	294.5472	73.5673	68.3809	76.9706
15	-10.9703	-34.3228	-75.0725	-25.3372	5.4589

TABLE AP 3-3 (Sheet 6 of 14)
SATURN OBSERVED TRAJECTORY - ORBITAL PHASE (AA83)

1	5999.9998	678085.6800	1589152.2000	-.5182	84.1796
2	24353.1380	25679.1790	.000	-.5076	84.4826
3	615767.4	-586157.9	-9766748.200	.000	.000
4	-1594290.4	203582.3	15445970.9	.000	.000
5	-373613.9	7280700.7	11484645.0	.000	.000
6	608.871	-8858.420	-20798.848	.0000	.000
7	5682.437	391.786	-14931.515	.0000	.000
8	23673.076	24099.693	1969.2867	.0000	.000
9	-26.945	.000	.0000	-83.2638	32.3159
10	3.866	.000	.0000	.2000	.0000000
11	.047	.000	.0000	.0000	.0000
12	4.3549	.0000	.0000	.0000	.0000
13	5854625.9	20575415.0	42050724.0	23598647.0	8899712.3
14	274.8924	292.4666	60.6104	62.9497	72.8522
15	-1.2647	-27.2454	-81.6245	-32.3126	-7.7649

1	6499.9998	607464.8700	11179370.3000	-.1229	106.2817
2	24441.8960	25761.3720	.000	-.0743	105.4266
3	-2390703.5	-8229034.7	-17901172.000	.000	.000
4	1570632.5	349035.4	5775657.6	.000	.000
5	10851753.8	17396253.0	10447674.2	.000	.000
6	-12339.009	-20831.180	-10765.554	.0000	.000
7	6626.548	172.225	-22620.127	.0000	.000
8	20031.077	15155.216	-6006.7462	.0000	.000
9	-23.411	.000	.0000	-45.5400	29.2098
10	-.317	.000	.0000	.2000	.0000000
11	-14.233	.000	.0000	.0000	.0000
12	30.6336	.0000	.0000	.0000	.0000
13	6197484.9	9682427.6	41850578.0	32174326.0	20108275.0
14	95.7423	280.3682	286.8537	53.6705	71.8847
15	-2.7820	-9.6454	-80.4253	-48.5267	-26.7096

1	6999.9998	631574.7900	22962655.0000	.3512	120.6737
2	24413.6130	25726.6380	.000	.3804	118.9537
3	**********	**********	-19903105.000	.000	.000
4	4645956.8	364866.8	-5871253.2	.000	.000
5	18618052.0	21555194.0	5821585.3	.000	.000
6	-21528.681	-25707.045	2983.241	.0000	.000
7	5283.512	-112.013	-22589.371	.0000	.000
8	10228.632	997.635	-11944.8979	.0000	.000
9	-12.343	.000	.0000	-13.3112	15.7700
10	-4.979	.000	.0000	.2000	.0000000
11	-23.842	.000	.0000	.0000	.0000
12	62.9047	.0000	.0000	.0000	.0000
13	17696852.0	4520067.3	38451173.0	38485030.0	29785693.0
14	96.8747	169.4617	269.8851	43.8950	72.5832
15	-22.7369	1.9076	-64.4788	-64.4785	-43.6100

1	7499.9998	751259.5200	34681354.0000	.7469	124.5536
2	24267.0620	25583.6220	.000	.7010	122.5467
3	**********	**********	-15110884.800	.000	.000
4	6505706.2	242200.0	-15521178.4	.000	.000
5	20591719.0	18361852.0	-801406.6	.000	.000
6	-24067.032	-21817.232	15586.722	.0000	.000
7	1879.059	-365.579	-14903.228	.0000	.000
8	-2477.381	-13356.515	-13764.7961	.0000	.000
9	2.377	.000	.0000	13.9314	-2.1314
10	-8.273	.000	.0000	.2000	.0000000
11	-25.565	.000	.0000	.0000	.0000
12	94.9959	.0000	.0000	.0000	.0000
13	27803787.0	14965511.4	32141519.0	41895223.0	37127007.0
14	97.7962	131.4430	263.7712	18.0405	73.9543
15	-39.5724	-17.9057	-48.0794	-79.2729	-60.0383

1	7999.9998	929304.4700	46212361.0000	.8890	118.5218
2	24048.8030	25381.2500	.000	.7906	116.9006
3	**********	**********	-5232556.000	.000	.000
4	6354126.6	18742.4	-19965557.0	.000	.000
5	16341238.5	8997782.8	-7163018.0	.000	.000
6	-19382.943	-10749.839	22763.651	.0000	.000
7	-2537.208	-503.904	-2417.677	.0000	.000
8	-14007.463	-22986.842	-10962.6138	.0000	.000
9	15.756	.000	.0000	41.3888	-19.2532
10	-8.891	.000	.0000	.2000	.0000000
11	-19.408	.000	.0000	.0000	.0000
12	126.6031	.0000	.0000	.0000	.0000
13	35717060.0	25226875.0	23478694.0	42123898.0	41582836.0
14	98.4193	123.6429	258.7472	275.1480	76.6919
15	-55.8461	-34.5067	-31.3482	-79.8191	-76.1965

TABLE AP 3-3 (Sheet 7 of 14)
SATURN OBSERVED TRAJECTORY - ORBITAL PHASE (AA83)

1	8499.9996	1100962.6000	57489303.0000	.7012	102.6971
2	23839.1080	25189.6990	.000	.6303	102.0076
3	**********	**********	6379410.800	.000	.000
4	4041833.4	-235034.1	-17855818.0	.000	.000
5	7348294.3	-3328662.8	-11173602.5	.000	.000
6	-9183.542	3559.828	22386.786	.0000	.000
7	-6518.061	-483.971	10567.947	.0000	.000
8	-21011.437	-24932.196	-4655.2434	.0000	.000
9	23.975	.000	.0000	73.6456	-30.6709
10	-6.576	.000	.0000	.2000	.0000000
11	-8.036	.000	.0000	.0000	.0000
12	157.5372	.0000	.0000	.0000	.0000
13	40880736.0	33595917.0	13225736.8	39198770.0	42883296.0
14	98.1281	117.6879	251.5164	248.3501	236.7117
15	-71.8396	-50.4081	-13.3238	-65.3332	-87.6920

1	8999.9996	1203972.8000	62201654.0000	.2639	81.1973
2	23714.5880	25072.4420	.000	.2732	81.6782
3	**********	**********	15953681.000	.000	.000
4	133387.4	-439893.4	-10004377.5	.000	.000
5	-3620720.1	**********	-11587117.9	.000	.000
6	3437.039	16480.882	14878.594	.0000	.000
7	-8731.814	-313.460	19952.111	.0000	.000
8	-21778.978	-18892.054	3027.8894	.0000	.000
9	25.322	.000	.0000	-250.1950	-31.7687
10	-1.990	.000	.0000	.2000	.0000000
11	4.935	.000	.0000	.0000	.0000
12	170.4552	.0000	.0000	.0000	.0000
13	42979468.0	39431660.0	3116065.8	33388128.0	41007818.0
14	80.5505	108.4467	205.8169	240.5772	254.1828
15	-87.5419	-65.7724	18.8286	-49.6476	-71.9331

1	9499.9996	1206025.2000	51304784.0000	-.2379	63.8992
2	23713.9330	25064.9090	.000	-.1722	65.4023
3	**********	**********	20473481.000	.000	.000
4	-4250597.7	-531602.7	1022794.3	.000	.000
5	**********	**********	-8316541.8	.000	.000
6	14995.033	24092.579	2712.074	.0000	.000
7	-8333.187	-42.534	22953.909	.0000	.000
8	-16372.464	-6913.432	9696.0000	.0000	.000
9	19.848	.000	.0000	-217.3322	-22.2111
10	3.635	.000	.0000	.2000	.0000000
11	16.150	.000	.0000	.0000	.0000
12	140.5623	.0000	.0000	.0000	.0000
13	41906337.0	42349751.0	9988521.0	25138607.0	36133546.0
14	286.4699	78.3863	90.2671	235.7672	256.9838
15	-76.4601	-79.4540	-6.5655	-33.5551	-56.0847

1	9999.9996	1113626.7000	40140937.0000	-.6218	55.8967
2	23827.6370	25166.2570	.000	-.5676	57.9361
3	**********	**********	18506502.000	.000	.000
4	-7736877.9	-478631.8	11722640.8	.000	.000
5	**********	**********	-2405335.6	.000	.000
6	22364.022	24072.813	-10388.269	.0000	.000
7	-5185.270	250.793	18664.359	.0000	.000
8	-6381.204	7333.300	13306.6183	.0000	.000
9	8.888	.000	.0000	-189.9295	-6.3069
10	8.725	.000	.0000	.2000	.0000000
11	22.879	.000	.0000	.0000	.0000
12	109.9522	.0000	.0000	.0000	.0000
13	37736699.0	42161775.0	20491476.0	15065039.1	28602988.0
14	285.0244	345.0143	81.0440	229.8705	259.4961
15	-60.6135	-78.5623	-25.7150	-16.5741	-40.0778

1	10499.9995	962428.6300	28811545.0000	-.7876	57.2866
2	24011.9870	25342.9320	.000	-.7824	59.2003
3	**********	-4314962.2	10612594.800	.000	.000
4	-9088589.6	-291898.6	18657161.0	.000	.000
5	**********	**********	4272876.4	.000	.000
6	23388.527	16258.108	-20339.658	.0000	.000
7	18.669	477.956	8266.488	.0000	.000
8	5436.177	19434.755	12658.1079	.0000	.000
9	-4.996	.000	.0000	-164.0026	11.3285
10	11.584	.000	.0000	.2000	.0000000
11	23.232	.000	.0000	.0000	.0000
12	78.9227	.0000	.0000	.0000	.0000
13	30729453.0	38874444.0	29692899.0	4397226.6	18924504.0
14	284.6552	317.6847	76.6804	201.8102	262.7640
15	-44.5699	-64.5553	-42.5971	6.7463	-23.5852

TABLE AP 3-3 (Sheet 8 of 14)
SATURN OBSERVED TRAJECTORY - ORBITAL PHASE (AA83)

1	10999.9996	799627.6300	17293760.0000	-.7234	68.5677
2	24211.5940	25540.5700	.000	-.7366	69.7353
3	-6201162.6	627966.2	-738249.410	.000	.000
4	-7620285.7	-24716.0	19488323.0	.000	.000
5	*********	-2724287.6	9542582.9	.000	.000
6	17502.636	2898.573	-23782.564	.0000	.000
7	5793.483	562.178	-5084.840	.0000	.000
8	15693.775	25369.333	7800.9534	.0000	.000
9	-18.053	.000	.0000	-134.2905	26.2194
10	10.845	.000	.0000	.2000	.0000000
11	16.714	.000	.0000	.0000	.0000
12	47.3847	.0000	.0000	.0000	.0000
13	21349999.0	32725943.0	36787409.0	8714237.5	7825836.4
14	283.8095	306.9398	73.0032	74.9184	270.7819
15	-28.1324	-49.1555	-59.0689	-6.6065	-4.7460

BEGIN RESTART PREPARATIONS - TB 6

1	11287.7297	718846.1700	10595768.7000	-.5917	79.5944
2	24312.4390	25640.2370	.000	-.5893	80.1405
3	-1995040.3	225833.8	-7409690.100	.000	.000
4	-5530984.6	133694.9	16949172.0	.000	.000
5	-8922270.6	4591683.7	11202351.5	.000	.000
6	11470.803	-5683.526	-22144.695	.0000	.000
7	8621.234	528.629	-12407.253	.0000	.000
8	19626.250	24996.797	3618.6116	.0000	.000
9	-23.529	.000	.0000	-114.0487	31.3646
10	8.597	.000	.0000	.2000	.0000000
11	10.368	.000	.0000	.0000	.0000
12	29.0360	.0000	.0000	.0000	.0000
13	15140237.2	28085721.0	39667685.0	15094996.7	1804852.6
14	282.3921	301.5600	70.4131	67.2139	320.3424
15	-18.2476	-40.1333	-68.5021	-18.2016	21.2161

1	11299.9997	715783.6500	10309579.7000	-.5846	80.1230
2	24316.3110	25644.0290	.007	-.5812	80.6408
3	-1856069.3	153883.9	-7680612.900	47578.274	-2212.818
4	-5424557.9	140164.1	16795149.0	-1386305.100	-17.111
5	-8680683.6	4897904.2	11245566.6	-2905078.600	-490.667
6	11180.967	-6044.070	-22015.986	-1732.3495	-360.509
7	8725.963	525.833	-12695.369	34.8548	-2.807
8	19751.620	24916.039	3426.4009	7230.4187	-80.854
9	-23.713	.000	.0000	-113.1383	31.5042
10	8.473	.000	.0000	.2000	.0000000
11	10.067	.000	.0000	.0000	.0000
12	28.2518	.0000	.0000	.0000	.0000
13	14865620.3	27872883.0	39768948.0	15364102.3	1685143.6
14	282.2969	301.3187	70.2789	67.0287	329.8412
15	-17.8117	-39.7472	-68.9040	-18.6531	23.0557

1	11324.9996	709658.5300	9726480.0000	-.5698	81.2110
2	24324.0710	25651.6160	.008	-.5644	81.6708
3	-1583993.9	-6366.7	-8227577.800	4269.253	-20373.468
4	-5203787.6	153235.4	16470472.7	-1385433.600	-162.081
5	-8183811.7	5518590.7	11326293.6	-2726317.400	-4729.084
6	10583.559	-6775.155	-21739.328	-1732.3723	-1091.519
7	8934.587	519.798	-13274.488	34.8618	-8.866
8	19995.546	24735.249	3032.3347	7230.4799	-261.845
9	-24.076	.000	.0000	-111.2742	31.7663
10	8.215	.000	.0000	.2000	.0000000
11	9.446	.000	.0000	.0000	.0000
12	26.6541	.0000	.0000	.0000	.0000
13	14304028.9	27435829.0	39969640.0	15910842.1	1586722.0
14	282.0896	300.8217	69.9957	66.6711	352.9187
15	-16.9181	-38.9604	-69.7226	-19.5672	24.6297

1	11349.9996	703690.0200	9143459.5000	-.5546	82.3127
2	24331.6520	25659.0120	.008	-.5471	82.7142
3	-1326965.0	-184830.0	-8767385.300	-39040.357	-56744.783
4	-4977883.3	166150.2	16131455.0	-1384562.000	-464.146
5	-7681036.5	6134485.9	11397131.4	-2543554.600	-13763.757
6	9977.319	-7500.968	-21443.512	-1732.3966	-1817.252
7	9136.643	513.312	-13842.544	34.8689	-15.374
8	20223.852	24532.773	2635.2857	7230.5443	-464.532
9	-24.420	.000	.0000	-109.3985	31.9980
10	7.948	.000	.0000	.2000	.0000000
11	8.817	.000	.0000	.0000	.0000
12	25.0566	.0000	.0000	.0000	.0000
13	13739792.9	26994324.0	40162737.0	16455335.9	1704795.3
14	281.8624	300.3168	69.6981	66.3378	15.5779
15	-16.0164	-38.1732	-70.5411	-20.4741	22.2599

TABLE AP 3-3 (Sheet 9 of 14)
SATURN OBSERVED TRAJECTORY - ORBITAL PHASE (AA83)

1	11374.9996	697884.3100	8560615.3000	-.5389	83.4266
2	24339.0510	25666.2110	.009	-.5292	83.7694
3	-1085197.6	-381365.7	-9299559.100	-82350.592	-111186.604
4	-4747012.0	178897.3	15778380.2	-1383690.200	-934.519
5	-7172750.9	6745049.7	11458009.2	-2362790.100	-28135.330
6	9362.720	-8220.850	-21128.771	-1732.4223	-2537.050
7	9331.919	506.380	-14399.011	34.8760	-22.329
8	20436.344	24308.756	2235.6054	7230.6120	-688.771
9	-24.745	.000	.0000	-107.5123	32.1988
10	7.673	.000	.0000	.2000	.0000000
11	8.181	.000	.0000	.0000	.0000
12	23.4595	.0000	.0000	.0000	.0000
13	13173064.7	26548509.0	40348193.0	16997408.0	2001492.5
14	281.6126	299.8030	69.3840	66.0263	32.5515
15	-15.1056	-37.3858	-71.3594	-21.3743	17.8499

1	11399.9996	692245.5900	7978074.6000	-.5227	84.5511
2	24346.2580	25673.2060	.009	-.5108	84.8350
3	-858894.6	-595817.6	-9823629.500	-125661.489	-183542.340
4	-4511345.6	191465.6	15411544.6	-1382818.100	-1584.301
5	-6659352.6	7349745.6	11508866.3	-2182023.900	-48380.551
6	8740.245	-8934.146	-20795.358	-1732.4495	-3250.256
7	9520.206	499.007	-14943.372	34.8830	-29.726
8	20632.839	24063.365	1833.6491	7230.6831	-934.395
9	-25.050	.000	.0000	-105.6170	32.3683
10	7.389	.000	.0000	.2000	.0000000
11	7.538	.000	.0000	.0000	.0000
12	21.8632	.0000	.0000	.0000	.0000
13	12604006.1	26098525.0	40525962.0	17536891.0	2411719.6
14	281.3371	299.2795	69.0511	65.7347	43.9001
15	-14.1845	-36.5981	-72.1775	-22.2687	13.5349

1	11424.9995	686780.1700	7395999.4000	-.5061	85.6845
2	24353.2680	25679.9910	.010	-.4920	85.9093
3	-648246.9	-828012.7	-10339132.800	-168973.090	-273639.050
4	-4271061.6	203844.0	15031256.8	-1381946.000	-2424.476
5	-6141243.6	7948041.4	11549649.7	-2001255.900	-75031.756
6	8110.383	-9640.204	-20443.542	-1732.4784	-3956.220
7	9701.302	491.196	-15475.118	34.8901	-37.560
8	20813.172	23796.788	1429.7753	7230.7577	-1201.217
9	-25.336	.000	.0000	-103.7139	32.5062
10	7.097	.000	.0000	.2000	.0000000
11	6.888	.000	.0000	.0000	.0000
12	20.2681	.0000	.0000	.0000	.0000
13	12032788.7	25644522.0	40696001.0	18073624.0	2887347.9
14	281.0320	298.7454	68.6965	65.4610	51.4942
15	-13.2517	-35.8102	-72.9953	-23.1578	9.9437

1	11449.9995	681492.0300	6814605.4000	-.4890	86.8251
2	24360.0760	25686.5580	.011	-.4726	86.9906
3	-453432.9	-1077762.1	-10845612.900	-212285.430	-381287.580
4	-4026342.1	216021.8	14637838.9	-1381073.700	-3465.894
5	-5618830.0	8539410.1	11580316.4	-1820486.000	-108616.349
6	7473.633	-10338.378	-20073.612	-1732.5088	-4654.294
7	9875.009	482.954	-15993.752	34.8972	-45.825
8	20977.185	23509.232	1024.3455	7230.8359	-1489.029
9	-25.601	.000	.0000	-101.8043	32.6120
10	6.798	.000	.0000	.2000	.0000000
11	6.232	.000	.0000	.0000	.0000
12	18.6749	.0000	.0000	.0000	.0000
13	11459596.5	25186656.0	40858269.0	18607450.0	3400845.5
14	280.6931	298.1996	68.3167	65.2036	56.7796
15	-12.3053	-35.0221	-73.8127	-24.0420	7.0265

1	11474.9996	676387.2100	6234184.6000	-.4714	87.9712
2	24366.6740	25692.9030	.011	-.4527	88.0773
3	-274618.5	-1344860.6	-11342620.400	-255598.550	-506282.660
4	-3777374.3	227988.2	14231624.9	-1380201.100	-4719.267
5	-5092521.5	9123330.1	11600831.9	-1639714.100	-149656.290
6	6830.501	-11028.027	-19685.875	-1732.5407	-5343.838
7	10041.137	474.287	-16498.788	34.9042	-54.515
8	21124.740	23200.926	617.7236	7230.9180	-1797.604
9	-25.846	.000	.0000	-99.8897	32.6856
10	6.491	.000	.0000	.2000	.0000000
11	5.571	.000	.0000	.0000	.0000
12	17.0844	.0000	.0000	.0000	.0000
13	10884629.5	24725087.0	41012726.0	19138224.0	3937175.8
14	280.3146	297.6411	67.9076	64.9612	60.6232
15	-11.3434	-34.2339	-74.6298	-24.9217	4.6148

TABLE AP 3-3 (Sheet 10 of 14)
SATURN OBSERVED TRAJECTORY - ORBITAL PHASE (AA83)

MANEUVER TO OBTAIN RESTART ATTITUDE

1	11487.3998	673924.6000	5946773.9000	-.4625	88.5411
2	24369.8670	25695.9650	.012	-.4427	88.6177
3	-191909.3	-1483712.1	-11585488.000	-277082.400	-576649.080
4	-3652367.7	233841.9	14025498.8	-1379768.300	-5422.851
5	-4830151.8	9410034.7	11607233.3	-1550049.300	-172937.890
6	6509.295	-11366.737	-19487.048	-1732.5573	-5682.494
7	10120.667	469.832	-16744.097	34.9077	-58.982
8	21191.782	23040.382	415.7075	7230.9601	-1958.286
9	-25.960	.000	.0000	-98.9386	32.7101
10	6.336	.000	.0000	.2000	.0000000
11	5.242	.000	.0000	.0000	.0000
12	16.2967	.0000	.0000	.0000	.0000
13	10598850.8	24494825.0	41086426.0	19400312.0	4208900.4
14	280.1102	297.3591	67.6923	64.8461	62.1600
15	-10.8597	-33.8429	-75.0349	-25.3566	3.5604

1	11499.9996	671470.2400	5655145.1000	-.4534	89.1209
2	24373.0570	25699.0190	.012	-.4324	89.1676
3	-111956.7	-1629087.1	-11829714.200	-298912.480	-648403.070
4	-3524350.0	239732.7	13812960.4	-1379328.400	-6195.152
5	-4562731.3	9699285.6	11611171.2	-1458940.100	-198667.560
6	6181.502	-11708.516	-19280.656	-1732.5744	-6024.216
7	10199.499	465.201	-16989.753	34.9113	-63.625
8	21255.708	22872.119	210.2760	7231.0039	-2126.693
9	-26.070	.000	.0000	-97.9716	32.7268
10	6.177	.000	.0000	.2000	.0000000
11	4.906	.000	.0000	.0000	.0000
12	15.4976	.0000	.0000	.0000	.0000
13	10308107.4	24259985.0	41159333.0	19665797.0	4487877.9
14	279.8899	297.0688	67.4642	64.7325	63.5305
15	-10.3632	-33.4456	-75.4465	-25.7975	2.5658

1	11524.9996	666746.7300	5078075.5000	-.4349	90.2725
2	24379.2180	25704.9000	.013	-.4117	90.2597
3	34412.1	-1930204.8	-12306461.800	-342227.290	-807411.850
4	-3267465.6	251244.8	13382203.0	-1378455.600	-7903.945
5	-4029875.2	10266767.4	11611317.8	-1278163.900	-256159.660
6	5527.156	-12379.217	-18858.297	-1732.6098	-6694.802
7	10349.918	455.702	-17466.182	34.9183	-73.147
8	21369.980	22523.083	-197.6293	7231.0939	-2476.025
9	-26.274	.000	.0000	-96.0514	32.7354
10	5.856	.000	.0000	.2000	.0000000
11	4.236	.000	.0000	.0000	.0000
12	13.9161	.0000	.0000	.0000	.0000
13	9730275.3	23791525.0	41298055.0	20190031.0	5047942.9
14	279.4107	296.4815	66.9802	64.5163	65.8036
15	-9.3616	-32.6572	-76.2626	-26.6695	.7777

1	11549.9996	662220.3800	4503857.3000	-.4159	91.4242
2	24385.1520	25710.5410	.013	-.3905	91.3519
3	164360.9	-2247961.2	-12772438.800	-385543.000	-983056.370
4	-3006921.8	262514.4	12939721.9	-1377582.600	-9855.869
5	-3494372.3	10825273.4	11601265.4	-1097385.400	-322635.140
6	4867.988	-13039.512	-18419.159	-1732.6470	-7354.974
7	10492.219	445.798	-17927.625	34.9254	-83.074
8	21467.455	22154.105	-605.6226	7231.1881	-2845.312
9	-26.456	.000	.0000	-94.1306	32.7113
10	5.528	.000	.0000	.2000	.0000000
11	3.562	.000	.0000	.0000	.0000
12	12.3425	.0000	.0000	.0000	.0000
13	9151411.9	23319890.0	41428857.0	20710789.0	5614241.7
14	278.8665	295.8778	66.4477	64.3116	67.6307
15	-8.3346	-31.8687	-77.0781	-27.5382	-.8197

1	11574.9995	657897.1300	3933878.2000	-.3966	92.5740
2	24390.8510	25715.9340	.014	-.3689	92.4424
3	277775.8	-2582088.6	-13227230.800	-428859.650	-1175068.700
4	-2742923.6	273531.4	12485897.4	-1376709.300	-12060.962
5	-2956643.2	11374309.1	11581016.0	-916604.390	-398589.040
6	4204.532	-13688.787	-17963.618	-1732.6859	-8004.122
7	10626.240	435.496	-18373.647	34.9325	-93.399
8	21548.052	21765.495	-1013.3335	7231.2868	-3234.245
9	-26.617	.000	.0000	-92.2109	32.6547
10	5.193	.000	.0000	.2000	.0000000
11	2.885	.000	.0000	.0000	.0000
12	10.7805	.0000	.0000	.0000	.0000
13	8571839.7	22845274.0	41551705.0	21227936.0	6184717.6
14	278.2440	295.2565	65.8569	64.1176	69.1339
15	-7.2772	-31.0803	-77.8927	-28.4038	-2.2747

TABLE AP 3-3 (Sheet 11 of 14)
SATURN OBSERVED TRAJECTORY - ORBITAL PHASE (AA83)

1	11599.9995	653781.1500	3370442.1000	-.3767	93.7202
2	24396.3110	25721.0770	.015	-.3469	93.5293
3	374556.2	-2932303.7	-13670432.300	-472177.310	-1383165.600
4	-2475680.1	284286.0	12021119.9	-1375835.900	-14529.071
5	-2417110.9	11913387.5	11550581.6	-735820.930	-484508.400
6	3537.326	-14326.441	-17492.068	-1732.7268	-8641.642
7	10751.820	424.804	-18803.826	34.9395	-104.114
8	21611.702	21357.585	-1420.3905	7231.3899	-3642.494
9	-26.756	.000	.0000	-90.2936	32.5655
10	4.852	.000	.0000	.2000	.0000000
11	2.206	.000	.0000	.0000	.0000
12	9.2364	.0000	.0000	.0000	.0000
13	7991942.0	22367879.0	41666571.0	21741343.0	6757955.7
14	277.5260	294.6160	65.1951	63.9333	70.3949
15	-6.1829	-30.2919	-78.7065	-29.2665	-3.6214

1	11604.9996	652983.4200	3258852.7000	-.3727	93.9488
2	24397.3730	25722.0750	.015	-.3425	93.7462
3	391908.3	-3004251.3	-13757646.700	-480840.970	-1426689.100
4	-2421860.7	286404.5	11926885.2	-1375661.200	-15055.107
5	-2309025.3	12019965.9	11543274.2	-699663.930	-502930.400
6	3403.482	-14452.525	-17395.873	-1732.7351	-8767.698
7	10775.909	422.620	-18887.924	34.9409	-106.303
8	21622.394	21273.717	-1501.6908	7231.4110	-3726.431
9	-26.781	.000	.0000	-89.9105	32.5437
10	4.783	.000	.0000	.2000	.0000000
11	2.070	.000	.0000	.0000	.0000
12	8.9306	.0000	.0000	.0000	.0000
13	7875962.6	22272085.0	41688583.0	21843563.0	6872840.1
14	277.3691	294.4854	65.0528	63.8976	70.6234
15	-5.9589	-30.1342	-78.8691	-29.4387	-3.8800

1	11609.9995	652194.2400	3147723.3000	-.3687	94.1772
2	24398.4260	25723.0620	.015	-.3380	93.9627
3	408590.8	-3076828.1	-13844378.700	-489504.670	-1470841.700
4	-2367921.6	288512.1	11832231.9	-1375486.500	-15592.126
5	-2200888.0	12126123.3	11535560.5	-663506.810	-521773.960
6	3269.515	-14578.115	-17299.058	-1732.7436	-8893.261
7	10799.654	420.420	-18971.369	34.9423	-108.507
8	21632.405	21189.094	-1582.9471	7231.4324	-3811.124
9	-26.806	.000	.0000	-89.5277	32.5207
10	4.714	.000	.0000	.2000	.0000000
11	1.934	.000	.0000	.0000	.0000
12	8.6261	.0000	.0000	.0000	.0000
13	7759992.7	22176190.0	41710274.0	21945629.0	6987786.9
14	277.2072	294.3541	64.9069	63.8622	70.8450
15	-5.7330	-29.9766	-79.0316	-29.6108	-4.1354

S-IVB ENGINE START COMMAND

1	11614.6897	651462.2900	3043955.0000	-.3649	94.3912
2	24399.4030	25723.9770	.015	-.3338	94.1657
3	423628.9	-3145469.9	-13925285.800	-497630.660	-1512823.300
4	-2317223.3	290478.9	11743075.1	-1375322.600	-16105.863
5	-2099418.6	12225305.1	11527956.3	-629593.790	-539834.450
6	3143.753	-14695.458	-17207.689	-1732.7516	-9010.578
7	10821.611	418.344	-19049.037	34.9437	-110.588
8	21641.175	21109.039	-1659.1173	7231.4525	-3891.245
9	-26.828	.000	.0000	-89.1687	32.4979
10	4.649	.000	.0000	.2000	.0000000
11	1.806	.000	.0000	.0000	.0000
12	8.3417	.0000	.0000	.0000	.0000
13	7651233.4	22086157.0	41730328.0	22041216.0	7095650.4
14	277.0508	294.2300	64.7666	63.8293	71.0467
15	-5.5194	-29.8287	-79.1840	-29.7722	-4.3722

1	11614.9996	651413.3900	3037105.4000	-.3646	94.4054
2	24399.4690	25724.0380	.015	-.3336	94.1791
3	424603.3	-3150031.6	-13930624.900	-498168.410	-1515620.900
4	-2313864.7	290608.7	11737162.8	-1375311.800	-16140.205
5	-2092702.5	12231855.7	11527440.5	-627349.600	-541042.890
6	3135.427	-14703.208	-17201.624	-1732.7522	-9018.326
7	10823.053	418.206	-19054.157	34.9437	-110.727
8	21641.735	21103.719	-1664.1563	7231.4540	-3896.570
9	-26.829	.000	.0000	-89.1450	32.4964
10	4.645	.000	.0000	.2000	.0000000
11	1.798	.000	.0000	.0000	.0000
12	8.3229	.0000	.0000	.0000	.0000
13	7644036.9	22080196.0	41731644.0	22047538.0	7102790.0
14	277.0403	294.2218	64.7571	63.8272	71.0598
15	-5.5052	-29.8189	-79.1941	-29.7828	-4.3878

TABLE AP 3-3 (Sheet 12 of 14)
SATURN OBSERVED TRAJECTORY - ORBITAL PHASE (AA83)

1	11619.9996	650641.2400	2927058.3000	-.3606	94.6333
2	24400.5020	25725.0040	.016	-.3291	94.3952
3	439944.9	-3223859.4	-14016382.400	-506832.180	-1561024.100
4	-2259691.7	292694.2	11641681.5	-1375137.000	-16699.417
5	-1984471.8	12337159.4	11518914.7	-591192.280	-560740.930
6	3001.225	-14827.798	-17103.577	-1732.7607	-9162.888
7	10846.105	415.976	-19136.285	34.9452	-112.961
8	21650.384	21017.594	-1745.3157	7231.4757	-3982.766
9	-26.852	.000	.0000	-88.7625	32.4707
10	4.576	.000	.0000	.2000	.0000000
11	1.662	.000	.0000	.0000	.0000
12	8.0214	.0000	.0000	.0000	.0000
13	7528099.4	21984105.0	41752695.0	22149289.0	7217842.9
14	276.8679	294.0887	64.6034	63.7925	71.2683
15	-5.2753	-29.6612	-79.3566	-29.9547	-4.6372
1	11624.9996	649877.8200	2817650.4000	-.3565	94.8609
2	24401.5240	25725.9610	.016	-.3246	94.6111
3	454615.3	-3298308.8	-14101648.200	-515496.010	-1607048.900
4	-2205404.2	294768.4	11545791.2	-1374962.300	-17269.839
5	-1876199.7	12442030.5	11509983.2	-555034.840	-580871.810
6	2866.912	-14951.881	-17004.920	-1732.7695	-9266.942
7	10868.808	413.731	-19217.751	34.9466	-115.210
8	21658.352	20930.722	-1826.4222	7231.4977	-4069.710
9	-26.873	.000	.0000	-88.3802	32.4438
10	4.506	.000	.0000	.2000	.0000000
11	1.525	.000	.0000	.0000	.0000
12	7.7215	.0000	.0000	.0000	.0000
13	7412185.4	21887919.0	41773422.0	22250880.0	7332940.3
14	276.6900	293.9547	64.4455	63.7582	71.4708
15	-5.0433	-29.5036	-79.5190	-30.1266	-4.8839
	GUIDANCE INITIATION-START ARTIFICIAL TAU				
1	11627.7297	649464.8100	2758209.0000	-.3542	94.9851
2	24402.0780	25726.4790	.016	-.3221	94.7288
3	462342.1	-3339221.2	-14147996.300	-520226.660	-1632440.800
4	-2175714.5	295896.3	11493261.6	-1374867.000	-17586.059
5	-1817064.6	12499108.2	11504935.2	-535292.090	-592047.710
6	2793.529	-15019.417	-16950.794	-1732.7742	-9334.462
7	10881.057	412.499	-19261.952	34.9473	-116.445
8	21662.415	20882.975	-1870.6846	7231.5098	-4117.497
9	-26.885	.000	.0000	-88.1716	32.4286
10	4.468	.000	.0000	.2000	.0000000
11	1.451	.000	.0000	.0000	.0000
12	7.5586	.0000	.0000	.0000	.0000
13	7348905.6	21835358.0	41784604.0	22306284.0	7395802.5
14	276.5903	293.8812	64.3575	63.7395	71.5789
15	-4.9156	-29.4175	-79.6076	-30.2203	-5.0175
1	11629.9996	649123.5000	2708960.4000	-.3524	95.0882
2	24402.5370	25726.9060	.016	-.3200	94.8266
3	468613.9	-3373377.4	-14186419.200	-524159.880	-1653692.600
4	-2151004.2	296831.5	11449495.3	-1374787.600	-17851.546
5	-1767889.5	12546465.4	11500646.3	-518877.300	-601439.270
6	2732.492	-15075.452	-16905.656	-1732.7783	-9390.484
7	10891.162	411.471	-19298.550	34.9480	-117.475
8	21665.638	20843.108	-1907.4728	7231.5198	-4157.397
9	-26.894	.000	.0000	-87.9982	32.4156
10	4.436	.000	.0000	.2000	.0000000
11	1.389	.000	.0000	.0000	.0000
12	7.4237	.0000	.0000	.0000	.0000
13	7296299.7	21791638.0	41793828.0	22352313.0	7448076.5
14	276.5061	293.8198	64.2833	63.7242	71.6676
15	-4.8090	-29.3460	-79.6813	-30.2983	-5.1280
	TIME BASE 7				
1	11630.3197	649075.3400	2702029.3000	-.3521	95.1028
2	24402.6010	25726.9660	.016	-.3198	94.8404
3	469487.1	-3378203.8	-14191828.500	-524714.480	-1656699.600
4	-2147517.9	296963.1	11443317.1	-1374776.400	-17889.169
5	-1760954.9	12553135.6	11500034.8	-516562.720	-602770.810
6	2723.884	-15083.345	-16899.281	-1732.7788	-9398.375
7	10892.581	411.326	-19303.700	34.9481	-117.620
8	21666.081	20837.474	-1912.6591	7231.5212	-4163.035
9	-26.896	.000	.0000	-87.9737	32.4138
10	4.431	.000	.0000	.2000	.0000000
11	1.380	.000	.0000	.0000	.0000
12	7.4047	.0000	.0000	.0000	.0000
13	7288882.5	21785471.0	41795123.0	22358800.0	7455448.1
14	276.4941	293.8111	64.2728	63.7220	71.6800
15	-4.7939	-29.3359	-79.6917	-30.3093	-5.1435

TABLE AP 3-3 (Sheet 13 of 14)
SATURN OBSERVED TRAJECTORY - ORBITAL PHASE (AA83)

1	11634.9995	648377.1600	2601079.6000	-.3483	95.3153
2	24403.5390	25727.8410	.016	-.3155	95.0419
3	481940.1	-3449062.5	-14270692.000	-532823.790	-1700952.900
4	-2096493.2	298883.1	11352797.0	-1374612.900	-18444.610
5	-1659544.5	12650460.2	11490904.4	-482719.640	-622447.020
6	2597.970	-15198.506	-16805.788	-1732.7870	-9513.509
7	10913.166	409.197	-19378.681	34.9494	-119.754
8	21672.242	20754.753	-1988.4645	7231.5422	-4245.825
9	-26.914	.000	.0000	-87.6163	32.3861
10	4.366	.000	.0000	.2000	.0000000
11	1.253	.000	.0000	.0000	.0000
12	7.1280	.0000	.0000	.0000	.0000
13	7180448.0	21695265.0	41813914.0	22453585.0	7563246.8
14	276.3160	293.6840	64.1165	63.6905	71.8588
15	-4.5724	-29.1883	-79.8436	-30.4699	-5.3695

1	11639.9996	647639.7300	2494114.4000	-.3441	95.5420
2	24404.5320	25728.7640	.016	-.3110	95.2569
3	494593.4	-3525361.6	-14354464.400	-541487.750	-1748826.900
4	-2041873.1	300923.4	11255700.0	-1374438.100	-19049.109
5	-1551168.2	12754011.6	11480757.6	-446561.870	-643898.760
6	2463.351	-15321.040	-16705.321	-1732.7960	-9636.013
7	10934.817	406.908	-19458.140	34.9508	-122.048
8	21678.165	20665.661	-2069.3944	7231.5647	-4334.991
9	-26.933	.000	.0000	-87.2347	32.3554
10	4.295	.000	.0000	.2000	.0000000
11	1.116	.000	.0000	.0000	.0000
12	6.8349	.0000	.0000	.0000	.0000
13	7064635.8	21598803.0	41833676.0	22554694.0	7678446.2
14	276.1195	293.5473	63.9449	63.6571	72.0448
15	-4.3333	-29.0307	-80.0058	-30.6414	-5.6087

1	11644.9995	646911.8700	2388189.3000	-.3400	95.7684
2	24405.4670	25729.6320	.000	-.3064	95.4715
3	506573.4	-3602272.0	-14437732.500	-550151.740	-1797312.100
4	-1987145.6	302952.2	11158207.2	-1374263.400	-19665.112
5	-1442764.0	12857115.6	11470206.4	-410404.010	-665798.160
6	2328.621	-15443.030	-16604.217	-1732.7996	-9757.992
7	10956.095	404.601	-19536.896	34.9514	-124.356
8	21683.365	20575.789	-2150.2610	7231.5738	-4424.892
9	-26.957	.000	.0000	-86.8534	32.3233
10	4.217	.000	.0000	.2000	.0000000
11	.966	.000	.0000	.0000	.0000
12	6.5446	.0000	.0000	.0000	.0000
13	6948869.1	21502253.0	41853116.0	22655642.0	7793669.7
14	275.9162	293.4096	63.7682	63.6241	72.2258
15	-4.0916	-28.8731	-80.1679	-30.8128	-5.8455

1	11649.9996	646191.8800	2283451.0000	-.3359	95.9944
2	24406.3610	25730.4560	.001	-.3019	95.6858
3	517879.5	-3679790.9	-14520493.900	-558815.750	-1846405.900
4	-1932312.8	304969.4	11060322.5	-1374088.600	-20292.696
5	-1334335.7	12959768.2	11459250.9	-374246.140	-688148.910
6	2193.791	-15564.477	-16502.495	-1732.7996	-9879.439
7	10977.005	402.278	-19614.955	34.9514	-126.680
8	21687.856	20485.157	-2231.0606	7231.5738	-4515.525
9	-26.975	.000	.0000	-86.4723	32.2900
10	4.146	.000	.0000	.2000	.0000000
11	.830	.000	.0000	.0000	.0000
12	6.2576	.0000	.0000	.0000	.0000
13	6833154.6	21405616.0	41872235.0	22756425.0	7908913.0
14	275.7057	293.2709	63.5863	63.5914	72.4021
15	-3.8473	-28.7155	-80.3299	-30.9842	-6.0801

MANEUVER TO ATTAIN SEPARATION ATTITUDE

1	11650.0998	646177.5500	2281367.4000	-.3358	95.9989
2	24406.3790	25730.4730	.001	-.3018	95.6901
3	518098.9	-3681349.0	-14522145.500	-558989.190	-1847394.900
4	-1931214.0	305009.7	11058359.0	-1374085.100	-20305.379
5	-1332164.8	12961818.6	11459027.5	-373522.270	-688600.990
6	2191.091	-15566.903	-16500.452	-1732.7996	-9881.865
7	10977.420	402.231	-19616.511	34.9514	-126.726
8	21687.939	20483.334	-2232.6774	7231.5737	-4517.347
9	-26.975	.000	.0000	-86.4646	32.2893
10	4.145	.000	.0000	.2000	.0000000
11	.827	.000	.0000	.0000	.0000
12	6.2519	.0000	.0000	.0000	.0000
13	6830838.5	21403680.0	41872614.0	22758441.0	7911220.3
14	275.7014	293.2682	63.5826	63.5907	72.4056
15	-3.8424	-28.7123	-80.3332	-30.9876	-6.0847

TABLE AP 3-3 (Sheet 14 of 14)
SATURN OBSERVED TRAJECTORY - ORBITAL PHASE (AA83)

1	11654.9996	645480.6900	2180071.8000	-.3317	96.2201
2	24407.2440	25731.2710	.001	-.2974	95.8998
3	528511.2	-3757915.8	-14602744.700	-567479.740	-1896105.600
4	-1877376.1	306974.9	10962049.2	-1373913.900	-20931.932
5	-1225886.6	13061965.9	11447891.7	-338088.270	-710954.640
6	2058.876	-15685.390	-16400.182	-1732.7996	-10000.352
7	10997.559	399.940	-19692.332	34.9513	-129.017
8	21691.664	20393.796	-2311.7896	7231.5738	-4606.887
9	-26.991	.000	.0000	-86.0914	32.2554
10	4.075	.000	.0000	.2000	.0000000
11	.693	.000	.0000	.0000	.0000
12	5.9743	.0000	.0000	.0000	.0000
13	6717498.8	21308896.0	41891029.0	22857042.0	8024171.5
14	275.4877	293.1313	63.3988	63.5590	72.5737
15	-3.6001	-28.5579	-80.4919	-31.1554	-6.3125
1	11659.9996	644778.6500	2078256.3000	-.3276	96.4454
2	24408.1160	25732.0730	.001	-.2928	96.1134
3	538468.1	-3836643.9	-14684482.700	-576143.740	-1946408.500
4	-1822337.7	308968.8	10863391.0	-1373739.100	-21582.893
5	-1117420.2	13163705.0	11436128.9	-301930.410	-734218.990
6	1923.881	-15805.763	-16297.284	-1732.7996	-10120.725
7	11017.758	397.588	-19769.025	34.9513	-131.370
8	21694.788	20301.709	-2392.4450	7231.5738	-4698.973
9	-27.007	.000	.0000	-85.7109	32.2195
10	4.004	.000	.0000	.2000	.0000000
11	.557	.000	.0000	.0000	.0000
12	5.6952	.0000	.0000	.0000	.0000
13	6601909.0	21212094.0	41909502.0	22957495.0	8139441.4
14	275.2618	292.9907	63.2054	63.5269	72.7410
15	-3.3500	-28.4003	-80.6538	-31.3266	-6.5430
1	11664.9996	644085.2800	1978247.5000	-.3234	96.6703
2	24408.9770	25732.8640	.001	-.2883	96.3266
3	547749.8	-3915972.6	-14765704.600	-584807.750	-1997311.900
4	-1767199.2	310950.8	10764350.9	-1373564.300	-22245.652
5	-1008939.9	13264981.8	11423963.3	-265772.530	-757945.580
6	1788.809	-15925.592	-16193.803	-1732.7996	-10240.555
7	11037.599	395.221	-19845.030	34.9513	-133.736
8	21697.229	20208.900	-2473.0238	7231.5738	-4791.782
9	-27.022	.000	.0000	-85.3307	32.1823
10	3.932	.000	.0000	.2000	.0000000
11	.420	.000	.0000	.0000	.0000
12	5.4212	.0000	.0000	.0000	.0000
13	6486392.4	21115211.0	41927651.0	23057780.0	8254718.7
14	275.0275	292.8491	63.0059	63.4951	72.9041
15	-3.0967	-28.2427	-80.8156	-31.4976	-6.7715
		INITIATE SPACECRAFT SEPARATION SEQUENCE			
1	11666.0997	643934.0000	1956513.9000	-.3225	96.7198
2	24409.1650	25733.0370	.001	-.2873	96.3734
3	549701.4	-3933506.7	-14783505.500	-586713.980	-2008592.000
4	-1755054.4	311385.3	10742509.1	-1373525.900	-22393.063
5	-985070.6	13287202.3	11421232.5	-257817.090	-763228.280
6	1759.081	-15951.884	-16170.957	-1732.7996	-10266.846
7	11041.916	394.698	-19861.661	34.9513	-134.259
8	21697.674	20188.384	-2490.7421	7231.5737	-4812.298
9	-27.025	.000	.0000	-85.2471	32.1740
10	3.917	.000	.0000	.2000	.0000000
11	.390	.000	.0000	.0000	.0000
12	5.3616	.0000	.0000	.0000	.0000
13	6460987.2	21093885.0	41931599.0	23079822.0	8280082.6
14	274.9748	292.8178	62.9612	63.4882	72.9394
15	-3.0406	-28.2080	-80.8512	-31.5352	-6.8215
		S-IVB/CSM SEPARATION			
1	11667.7998	643700.9100	1923137.6000	-.3211	96.7961
2	24409.4550	25733.3030	.001	-.2857	96.4458
3	552652.6	-3960657.9	-14810962.500	-589659.580	-2026079.100
4	-1736278.5	312055.5	10708722.9	-1373466.500	-22621.977
5	-948186.1	13321493.6	11416974.5	-245524.120	-771435.720
6	1713.138	-15992.458	-16135.600	-1732.7996	-10307.419
7	11048.553	393.889	-19887.292	34.9513	-135.068
8	21698.298	20156.613	-2518.1134	7231.5738	-4844.069
9	-27.029	.000	.0000	-85.1179	32.1609
10	3.892	.000	.0000	.2000	.0000000
11	.343	.000	.0000	.0000	.0000
12	5.2702	.0000	.0000	.0000	.0000
13	6421738.3	21060923.0	41937673.0	23113866.0	8319275.8
14	274.8925	292.7694	62.8914	63.4775	72.9936
15	-2.9535	-28.1544	-80.9062	-31.5934	-6.8986

TABLE AP 3-4 (Sheet 1 of 3)
LIST OF SYMBOLS (PROGRAM AA83)

PRINTOUT SYMBOL	COMMON SYMBOL	DEFINITION
ALTITUDE	h	Height of vehicle above the Fischer Ellipsoid of 1960 (ft)
ALPHA SB WIND	α_w	Wind angle-of-attack in pitch plane (deg)
BETA SB WIND	β_w	Wind angle-of-attack in yaw plane (deg)
A SB I	A_I	Total inertial acceleration (ft/sec^2)
A * SB i (i=1 thru 5)	A^*_i	Radar azimuth angle measured in the plane tangent to the earth's surface at radar station i, positive clockwise from north to the perpendicular projection of the slant range vector onto the tangent plane
DD-X SB E DD-Y SB E DD-Z SB E	$\ddot{X}_e$ $\ddot{Y}_e$ $\ddot{Z}_e$	Component of acceleration vector of vehicle in earth-fixed right-handed cartesian coordinate system (same orientation as X_E, Y_E, Z_E) (ft/sec^2) (PACSS No. 10)
DENSITY	ρ_a	Ambient air density ($slugs/ft^3$)
D * SB i (i=1 thru 5)	D^*_i	Slant range distance from radar station i to vehicle (ft)
D-X SB GS D-Y SB GS D-Z SB GS	$\dot{X}_{gs}$ $\dot{Y}_{gs}$ $\dot{Z}_{gs}$	Components of gravitational velocity vector, in space-fixed coordinate system (same orientation as X_S, Y_S, Z_S) (ft/sec) (PACSS No. 13)
D-X1 D-ETA D-ZETA	$\dot{\xi}$ $\dot{\eta}$ $\dot{\zeta}$	Components of inertial platform velocity vector, in space-fixed coordinate system (same orientation as XI, ETA, ZETA) (ft/sec) (PACSS No. 12)
D-X SB S D-Y SB S D-Z SB S	$\dot{X}_s$ $\dot{Y}_s$ $\dot{Z}_s$	Components of velocity vector of vehicle, in space-fixed coordinate system (same orientation as X_S, Y_S, Z_S) (ft/sec) (PACSS No. 13)
D-X SB SFE D-Y SB SFE D-Z SB SFE	$\dot{X}_{SFE}$ $\dot{Y}_{SFE}$ $\dot{Z}_{SFE}$	Components of velocity vector in space-fixed ephemeris coordinate system (same orientation as X_{SFE}, Y_{SFE}, Z_{SFE}) (ft/sec) (PACSS No. 4)
D-X SB E D-Y SB E D-Z SB E	$\dot{X}_e$ $\dot{Y}_e$ $\dot{Z}_e$	Components of velocity vector of vehicle, in earth-fixed right-handed cartesian coordinate system (same orientation as X_E, Y_E, Z_E) (ft/sec) (PACSS No. 10)
E * SB i (i=1 thru 5)	E^*_i	Radar elevation angle measured positive up from plane tangent to the earth's surface at radar station i to the radar slant range vector (ft)
GAMMA SB 1	γ_1	Elevation angle of earth-fixed velocity vector from local horizontal measured positive above the plane (deg)
GAMMA SB 2	γ_2	Azimuth angle of earth-fixed velocity vector positive East of local North (deg)

TABLE AP 3-4 (Sheet 2 of 3)
LIST OF SYMBOLS (PROGRAM AA83)

PRINTOUT SYMBOL	COMMON SYMBOL	DEFINITION
GAMMA (1I) PR.	γ_{1_I}'	Angle between space-fixed velocity vector and plane normal to vector from geocentric center of earth, positive above plane (deg)
GAMMA (2I) PR.	γ_{2_I}'	Angle measured positive clockwise from north to projection of space-fixed velocity vector in plane normal to radius vector (deg)
MACH NUMBER	MACH	Mach number (dimensionless)
MU	μ	Longitude of vehicle (deg)
PRESSURE	P_a	Ambient air pressure (lbf/ft^2)
DYN. PRESS. Q	Q	Dynamic pressure (lbf/ft^2)
RANGE	S	Surface range referenced to spherical earth of instantaneous average radius (ft)
RANGE ANGLE	η	Angle measured from center of earth between launch site and subvehicle point (deg)
RE YN/L	RE/L	Reynolds number per unit length (dimensionless)
RHO	ρ	Latitude of vehicle (deg)
REL HUMID		Relative Humidity (percent)
SOUND VEL	V_s	Local velocity of sound (ft/sec)
TEMPERATURE	TEMP	Ambient air temperature (deg R)
TIME	t	Time from Range Zero (sec)
VISCOSITY	γ	Viscosity ($lb\text{-}sec/ft^2$)
V SB E	V_e	Magnitude of earth-fixed velocity vector of vehicle (ft/sec)
V SB 1	V_I	Magnitude of space-fixed velocity vector of vehicle (ft/sec)
V SB RM	V_{rm}	Magnitude of relative velocity vector of vehicle (ft/sec)
E SB W	ϵ_W	Wind direction azimuth, positive clockwise from North; direction is 0 deg when wind is coming from North (deg)
V SB W	V_W	Magnitude of wind velocity vector (ft/sec)
X SB GS Y SB GS Z SB GS	X_{gs} Y_{gs} Z_{gs}	Components of gravitational position vector, in space-fixed coordinate system (same orientation as X_S, Y_S, Z_S) (ft) (PACSS No. 13)
X1 ETA ZETA	ξ η ζ	Components of inertial platform displacement vector, in space-fixed coordinate system (same orientation as X_E, Y_E, Z_E at instant of launch (ft) (PACSS No. 12)
X SB S Y SB S Z SB S	X_s Y_s Z_s	Component of position vector of vehicle, in space-fixed coordinate system (same orientation as X_E, Y_E, Z_E at instant of launcy (ft) (PACSS No. 13)

TABLE AP 3-4 (Sheet 3 of 3)
LIST OF SYMBOLS (PROGRAM AA83)

PRINTOUT SYMBOL	COMMON SYMBOL	DEFINITION
X SB SFE Y SB SFE Z SB SFE	X_{SFE} Y_{SFE} Z_{SFE}	Components of position vector in space-fixed ephemeris coordinate system. Z_{SFE} is north along earth's rotational axis, X_{SFE} is through vernal equinox, Y_{SFE} completes a right-handed system, X_{SFE}-Y_{SFE} plane is in equatorial plane (ft) (PACSS No. 4)
X SB E Y SB E Z SB E	X_e Y_e Z_e	Components of position vector of vehicle, in earth-fixed right-handed cartesian coordinate system. Z_E is directed along firing direction, X_E is normal to horizontal plane and origin is on ellipsoid at launch site. Y_E completes the right-handed cartesian coordinate system (ft) (PACSS No. 10)

TABLE AP 3-5
RADAR STATION VEHICLE ACQUISITION AND LOSS TIMES

Station	Acquisition Time		Loss Time		Tracking Time Above 5°	
	Predicted	Actual	Predicted	Actual	Predicted	Actual
			Boost Phase of Flight			
Pad 39A	0	0	432	435	432	435
Cape Tel 4	30	30	432	435	402	405
Grand Bahama	116	115	459	460	343	345
Bermuda	335	335	688	710	353	375
Insertion Ship	645	655	945	950	300	295
			Orbital Phase of Flight - First Orbit			
Canary Island	1,044	1,075	1,344	1,360	300	285
Carnarvon	3,205	3,270	3,396	3,535	191	265
Hawaii	No Acquisition on First Orbit					
Guaymas	5,352	5,450	5,648	5,790	306	340
Bèrmuda	5,967	6,070	6,277	6,390	310	320
			Orbital Phase of Flight - Second Orbit			
Canary Island	6,705	6,820	6,824	6,890	119	70
Carnarvon	8,792	8,860	9,040	9,290	248	430
Hawaii	10,323	10,470	10,538	10,800	215	330
Guaymas	10,953	11,060	11,249	11,470	296	410
Bermuda	11,552	No Acquisition	11,918	-	366	-

APPENDIX 4

FLIGHT SIMULATED DATA (AD77)

1. FLIGHT SIMULATED DATA (AD77)

Presented in this appendix is a detailed five-degrees-of-freedom trajectory simulation constrained to the observed trajectory and employing adjusted engine analysis propulsion histories. Adjustments were determined by a differential correction technique. This technique correlated perturbations in thrust, weight flow, and pitch and yaw thrust vector misalignment with the resulting differences in altitude, earth-fixed velocity, earth-fixed velocity azimuth angle, and longitudinal acceleration, between the observed and simulated trajectories. A complete discussion of the trajectory simulation is presented in section 8.

Figures AP 4-1 and AP 4-2 illustrate the major coordinate systems. Tables AP 4-1 and AP 4-2 present the trajectory parameter definitions while table AP 4-3 furnishes the detailed reconstructed trajectory from S-II/S-IVB physical separation to guidance commanded engine cutoff. The ignition and cutoff weights are based on the composite best estimate ignition and cutoff weights as discussed in section 9.

TABLE AP 4-1 (Sheet 1 of 7)
LIST OF SYMBOLS (PROGRAM AD77)

PRINTOUT SYMBOL	COMMON SYMBOL	DEFINITION
A*SB i	A^*_i	Azimuth angle measured in the plane tangent to the earth's surface at radar station i; positive clockwise from north to the perpendicular projection of the vector drawn between the vehicle and the radar in the tangent plane (deg)
A SB XM A SB YM A SB ZM	a_{xm}, a_{ym}, a_{zm}	Vehicle accelerations in the vehicle coordinate system (ft/sec^2)
CHORD FORCE	C	Aerodynamic chord force (lbf)
D*SB i	D^*_i	Slant range distance between the vehicle and radar station i (ft)
ECCENTRICITY	e	Eccentricity of a conic section (dimensionless)
E*SB i	E^*_i	Elevation angle measured positively up from a plane tangent to the earth's surface at the radar site. Angle between the plane and the vector drawn between the missile and radar station i (ft)

TABLE AP 4-1 (Sheet 2 of 7)
LIST OF SYMBOLS (PROGRAM AD77)

PRINTOUT SYMBOL	COMMON SYMBOL	DEFINITION
F SB AX F SB AY F SB AZ	F_{A_x}, F_{A_y}, F_{A_z}	Aerodynamic forces in the vehicle coordinate system (lbf)
AVG F SB L	$\overline{F}_L$	Average Longitudinal thrust (lbf)
F SB T	F_T	Total effective engine thrust (lbf)
F SB TX F SB TY F SB TZ	F_{T_x}, F_{T_y}, F_{T_z}	Porpulsive forces in the vehicle system (lbf)
F SB X F SB Y F SB Z	F_x, F_y, F_z	Total forces in the vehicle coordinate system (lbf)
G (RHO)	g_ρ	Component of gravity due to the attractive force of the earth measured along r_c positive down (ft/sec^2)
G (PSI)	g_ψ	Component of gravity due to attractive force of the earth measured along the perpendicular to r_c positive down (ft/sec^2)
ALTITUDE	h	Vehicle altitude. Distance between the spheriod's surface and vehicle measured along the normal to the earth's surface positive up (ft)
I SB SP	I_{sp}	Specific impulse (sec)
AVG I SB SP	$\overline{I}_{sp}$	Average specific impulse (sec)
I SB XX I SB YY I SB ZZ	I_{xx}, I_{yy}, I_{zz}	Principal vehicle moments of inertia ($slug\text{-}ft^2$)
MACH NO.	M	Vehicle mach number
M SB X M SB Y M SB Z	M_x, M_y, M_z	Total moments about the axis of the vehicle coordinate system (ft-lbf)

TABLE AP 4-1 (Sheet 3 of 7)
LIST OF SYMBOLS (PROGRAM AD77)

PRINTOUT SYMBOL	COMMON SYMBOL	DEFINITION
M SB AX M SB AY M SB AZ	M_{A_x}, M_{A_y}, M_{A_z}	Aerodynamic moments in the vehicle coordinate system (ft-lbf)
NORMAL FORCE	N	Aerodynamic normal force (lbf)
P SB M	P_M	Total vehicle roll rate; positive roll clockwise looking forward along the X_m axis (deg/sec)
PRESSURE	P_a	Atmospheric pressure at the vehicle (lbf/ft^2)
Q	q	Vehicle dynamic pressure (lbf/ft^2)
Q SB M	Q_M	Total vehicle pitch rate, positive nose up (deg/sec)
R (AP)	r_a	Radius of apogee (nautical miles)
R (PER)	r_{PER}	Radius of perigee (nautical miles)
R SB C	r_c	Instantaneous distance between the center of the earth and the vehicle (ft)
R SB F	r_f	Geocentric missile distance at terminal altitude (ft)
R SB L	r_L	Earth radius at the launcher (ft)
S (BAR*)	$\bar{S}$*	Product of the average earth radius and the central angle traversed during glide (nautical miles)
S SB F	S_F	Downrange distance at terminal altitude (nautical miles)
R SB M	R_M	Total vehicle yaw rate; positive yaw-nose left (deg/sec)
RANGE	s	Spherical earth ground range (ft). Based on the spherical earth range angle and the average earth radius
SAF (i)	SAF_i	Space attenuation factor measured from radar station i
TIME	t	Current simulation time, measured from vehicle liftoff (sec)
T (1)	T_1	First stage time to go (sec)
T (3)	T_3	Second stage time to go (sec)

TABLE AP 4-1 (Sheet 4 of 7)
LIST OF SYMBOLS (PROGRAM AD77)

PRINTOUT SYMBOL	COMMON SYMBOL	DEFINITION
DELTA-T (3)	ΔT_3	Correction to T_3 (sec)
D-T (CO)	Δt_{co}	Time-to-go until Engine Cutoff Command (sec)
TEMPERATURE	T_T	The temperature specified at a certain altitude (deg R)
V SB E	V_e	Magnitude of the vehicle's earth fixed velocity (ft/sec)
V (F)	V_f	Magnitude of inertial velocity at terminal altitude (ft/sec)
V SB I	V_I	Magnitude of the vehicle's inertial velocity (ft/sec)
V SB RM	V_{RM}	Magnitude of the vehicle's velocity relative to the earth's atmosphere (ft/sec)
V SB W	V_W	Wind velocity relative to the earth (ft/sec)
WEIGHT	W	Total vehicle weight (lbm)
WEIGHT FLOW	$\dot{W}$	Time rate of change of total vehicle weight (lbm/sec)
AVG D-W	$\bar{\dot{W}}$	Average time rate of change of total vehicle weight (lbm/sec)
X, Y, Z D-X, D-Y, D-Z DD-X, DD-Y, DD-Z	X, Y, Z	Components of vehicle position, velocity, and accelerations. A subscript on these quantities indicates the coordinate system in which these quantities are measured. (ft, ft/sec, ft/sec^2, respectively)
X SB CG Y SB CG Z SB CG	X_{CG}, Y_{CG}, Z_{CG}	Components of vehicle center of gravity, with X_{CG} measured positive forward from the vehicle reference plane, Y_{CG} measured positive right from the missile centerline, and Z_{CG} measured positive down from the vehicle centerline (in.)
X SB CP X SB CP X SB CP	X_{CP}, Y_{CP}, Z_{CP}	Components of vehicle of pressure with X_{CP} measured positive forward from the vehicle reference plane. Y_{CP} measured positive right from the missile centerline, and Z_{CP} measured positive down from the vehicle centerline (in.)
X (V) Y (V) Z (V)	X^V, Y^V, Z^V	Positive coordinates in the terminal radius coordinate system. Origin is at the earth's center, Y^V along the desired terminal radius, X^V in the orbit plane in the direction of orbital motion, Z^V forming a right handed coordinate system (m)

TABLE AP 4-1 (Sheet 5 of 7)
LIST OF SYMBOLS (PROGRAM AD77)

PRINTOUT SYMBOL	COMMON SYMBOL	DEFINITION
D-X (V) D-Y (V) D-Z (V)	X^V, Y^V, Z^V	Velocity coordinates in terminal radius coordinate system (ms)
ALPHA*	α'	Total angle of attack. Angle between the centerline of the vehicle and the vehicle air velocity vector (deg)
ALPHA	α	Pitch angle of attack. Angle between the projection of the vehicle's air velocity vector onto the pitch plane and the centerline of the vehicle (deg)
BETA	β	Yaw angle of attack. Angle between the projection of the vehicle's air velocity vector onto the yaw plane and the centerline of the vehicle (deg)
BETA	β_f	True anomaly at terminal altitude (deg)
GAMMA (1)	γ_1	Elevation flight path angle. Angle between the earth fixed vehicle velocity and the local tangent plane positive for an ascending vehicle (deg)
GAMMA (2)	γ_2	Azimuthal flight path angle. Angle between the local north clockwise to the projection of the earth fixed vehicle velocity on the local tangent plane (deg)
GAMMA (1I)	γ_{1_I}	Inertial elevation flight path angle. Same as γ_1 except measured to inertial vehicle velocity (deg)
GAMMA (2I)	γ_{2_I}	Inertial azimuthal flight path angle. Same as γ_2 except measured to inertial vehicle velocity (deg)
GAMMA (1I) PR	$\gamma_{1_{I'}}$	Inertial elevation flight path angle. Angle between the inertial velocity vector and the $X_{L_{I'}}, Z_{L_{I'}}$ plane. Angle is positive for an ascending vehicle (deg)
GAMMA (2I) PR	$\gamma_{2_{I'}}$	Inertial azimuthal flight path angle measured in the $X_{L_{I'}}$, $Z_{L_{I'}}$ plane. Angle between Z_{L_I}, clockwise to the projection of the inertial velocity vector (deg)
GAMMA SB 1F	γ_{1_f}	Inertial flight path elevation angle at the terminal altitude (deg)

TABLE AP 4-1 (Sheet 6 of 7)
LIST OF SYMBOLS (PROGRAM AD77)

PRINTOUT SYMBOL	COMMON SYMBOL	DEFINITION
GAMMA SB 2F	γ_{2_f}	Inertial flight path azimuth angle, at the terminal altitude (deg)
DELTA (A) DELTA (B)	δ_A, δ_B	Engine "A" actuator and "B" actuator gimbal angles, respectively (deg)
SMCP	δMCP	Pitch thrust misalignment correction (radians)
SMCY	δMCY	Yaw thrust misalignment correction (radians)
E SB W	ε_W	Tabular wind azimuth angle, positive clockwise from north, as a function of altitude (at ε_W = zero wind is coming from the north) (deg)
EPS (THETA)	ε_θ, ε_ψ, ε_ϕ	Autopilot error signal rates (deg/sec)
RANGE ANGLE	η'	Spherical earth range angle. The angle is measured between lines connecting the following three points: the vehicle, the center of the earth, and the launcher with the earth's center as the vertex (radians)
D-THETA (M) QRP D-PSI (M) QRP D-PHI (M) QPR	θ_M, ψ_M, ϕ_M	Vehicle attitude pitch, yaw and roll Euler angle rates (deg/sec)
THETA SB C	θ_C	Commanded vehicle pitch Euler angle (deg)
THETA (M) QRP	θ_M	Vehicle pitch attitude Euler angle (deg)
THETA (P) THETA (Y) THETA (R)	θ_P, θ_Y, θ_R	For the three-gimbal stable platform, pitch, yaw and roll angles, respectively (deg)
MU	μ	Instantaneous vehicle longitude where Greenwich, England, is longitude zero. West of Greewich is positive (deg)
MU SB F	μ_f	Longitude of r_f (deg)
XI ETA ZETA	ξ, η, ζ	Vehicle position obtained by integrating $\dot{\xi}$, $\dot{\eta}$, $\dot{\zeta}$. The $\xi\eta\zeta$ system coincides with the "P" system at t - 0, and is falling with an acceleration equal to gravity at the vehicle position. Position and velocity in this system correspond to the position and velocity the vehicle would have if gravity were zero. (m)

TABLE AP 4-1 (Sheet 7 of 7)
LIST OF SYMBOLS (PROGRAM AD77)

PRINTOUT SYMBOL	COMMON SYMBOL	DEFINITION
D-XI D-ETA D-ZETA	$\dot{\xi}, \dot{\eta}, \dot{\zeta}$	Vehicle velocity obtained by integrating $\ddot{\xi}, \ddot{\eta}, \ddot{\zeta}$ (ms)
RHO	ρ	Instantaneous geodetic latitude, positive in the northern hemisphere (deg)
RHO PRIME	ρ'	Instantaneous geocentric latitude, positive in the northern hemisphere (deg)
RHO SB F	ρ_f	Longitude of r_f (deg)
TAU-P (i)	τ_{pi}	Radar polarization look angle for the ith radar station: angle between the projection of the vehicle centerline on a plane perpendicular to the radar line of sight and the line of intersection of the plane containing the radar line of sight, perpendicular to the earth's surface, and the plane perpendicular to the radar line of sight, measured positive counterclockwise from this line of intersection as viewed looking along the radar line of sight toward the vehicle (deg)
TAU (1G)	τ_{1G}	Ratio of $W/\dot{W}$ during first stage operation (sec)
TAU (3G)	τ_{3G}	Ratio of $W/\dot{W}$ during third stage operation (sec)
TAU SB F	τ_f	Time since/to perigee at terminal altitude (sec)
PHI SB C	ϕ_C	Commanded vehicle roll Euler angle (deg)
PHI (M) QRP	ϕ_M	Vehicle attitude roll Euler angle (deg)
PHI (T)	ϕ_T	Estimate of terminal range angle measured in the orbit plane from the descending node to the terminal radius vector, positive in the flight direction (radians)
PSI SB C	ψ_C	Commanded vehicle yaw Euler angle (deg)
PSI (M) QRP	ψ_M	Vehicle attitude yaw Euler angle (deg)
CHI SB P	χ_P	Guidance-commanded body attitude angle in the vehicle pitch plane (deg)
CHI SB R	χ_R	Guidance-commanded body attitude angle in the vehicle roll plane (deg)
CHI SB Y	χ_Y	Guidance-commanded body attitude angle in the vehicle yaw plane (deg)

TABLE AP 4-2
COORDINATE SUBSCRIPT DEFINITIONS

ee	Coordinate system on the surface of the spheriod representing the earth with origin at launch point latitude and longitude. X_{ee} perpendicular to the surface of the spheroid, positive up; Z_{ee} positive in the flight azimuth direction; and Y_{ee} crossrange forming a right-handed system.
LL	Instantaneous coordinate system located on the earth's surface under the vehicle with the X_{LL}, Z_{LL} plane tangent to the earth's surface. Positve directional are X_{LL} west, Y_{LL} up, and Z_{LL} north. (English)
L_I	Instantaneous inertial coordinate system coincidental with the L system. Velocities in this system are inertial. (English)
L'_I	Instantaneous inertial coordinate system located on the earth's surface under the vehicle where Z_L' points north, X_L' points west and Y_L' is along a line connecting the earth center and the vehicle. Velocities in this system are inertial. (English)
m	Vehicle coordinate system with origin at the vehicle center of gravity. The "m" system is related to the "s" system by the vehicle Euler angles θ_m, ψ_m, ϕ_m. X_m parallel to a radius from the vehicle centerline to position I, positive toward position I. If all Euler angles are zero, then X_m is up, Y_m crossrange positive right, Z_m positive in the flight azimuth direction.
P'	Inertial coordinate system with its origin at the center of the earth and with its X_p, axis along the line parallel to the local gravity vector at launch through the earth's center, positive up. The X_p, axis is parallel to the plane defined by the X_s and Y_x axis at launch and Z_p' forms a right-handed coordinate system. (Metric)
s	Coordinates initially coincident with the e system, but remaining fixed in space. (English)
SFE	Space Fixed Ephermeris System. The origin of the system is at the center of the earth, Z_{SFE} is positive north, X_{SFE} passes through the vernal equinox and Y_{SFE} completes the right handed system with the X_{SFE} -Y_{SFE} plane coincident with the equatorial plane. The directions of the axes remain fixed in space and the origin moves with the center of the earth. The reference equinox and equator are the true vernal equinox and equator for the epoch of midnight of the day of the launch.

TABLE 4-3 (Sheet 1 of 19)
FLIGHT SIMULATED DATA (AD77)

1	TIME	WEIGHT	F SB T	ALTITUDE	RANGE
2	V SB I	V SB E	R SB C	R SUB PF	RANGE ANGLE
3	X SB E	X SB P (M)	X SB S	XI	
4	Y SB E	Y SB P (M)	Y SB S	ETA	
5	Z SB E	Z SB P (M)	Z SB S	ZETA	
6	D-X SB E	D-X SB P (M)	D-X SB S	D-XI	A SB XM
7	D-Y SB E	D-Y SB P (M)	D-Y SB S	D-ETA	A SB YM
8	D-Z SB E	D-Z SB P (M)	D-Z SB S	D-ZETA	A SB ZM
9	F SB X	F SB TX	F SB AX	M SB X	M SB AX
10	F SB Y	F SB TY	F SB AY	M SB Y	M SB AY
11	F SB Z	F SB TZ	F SB AZ	M SB Z	M SB AZ
12	THETA(M) QRP	DTHETA(M)QRP	F AUX SB X	I SB XX	EPS(THETA)
13	PSI(M) QRP	D-PSI(M)QRP	F AUX SB Y	I SB YY	EPS(PSI)
14	PHI(M) QRP	D-PHI(M)QRP	F AUX SB Z	I SB ZZ	EPS(PHI)
15	CHI SB P	D-CHI SB P	THETA SB C	P SB M	X SB CG
16	CHI SB Y	D-CHI SB Y	PSI SB C	Q SB M	Y SB CG
17	CHI SB R	D-CHI SB R	PHI SB C	R SB M	Z SB CG
18	GAMMA SB 1	GAMMA SB 1I	GAMMA(1I)PR.	DELTA(A)	D-DELTA(A)
19	GAMMA SB 2	GAMMA SB 2I	GAMMA(2I)PR.	DELTA(B)	D-DELTA(B)
20	I SB SP	AVG I SB SP	WEIGHT FLOW	AVG D-W	AVG F SB L
21	Q	MACH NO.	PRESSURE	TEMPERATURE	X SB CP
22	ALPHA*	ALPHA	BETA	CHORD FORCE	Y SB RM
23	MU	RHO	RHO PRIME	G(RHO)	G(PSI)
24	T(2)	TAU(2)	PHI(T)	D-W(LOXBO)	DELTA-D-X(V)
25	T(3)	TAU(3)	SMCP	D-W(LH2BO)	DELTA-D-Y(V)
26	DELTA-T(CO)	DELTA-T(3)	SMCY	D-W(LH2PR)	DELTA-D-Z(V)
27	V(T)	CHI(P)-TILDE	K(1)	W(LOX)RES	WDOTSUBO
28	Y(V,T)	CHI(Y)-TILDE	K(3)	W(LH2)RES	WDOTSUBF
29	R(PER)	V(PER)	ECCENTRICITY	BETA	
30	R(AP)	V(AP)	INCLINATION	PERIOD	E/M
31	P	THETA(T)	E SUB T	THETA SUB N	C3 SUB T
32			I SUB T	THETA SUB NG	C SUB 3G
33	AVG FL HMR	AVG ISP HMR	AVG WDT HMR	DELTA SB R4	

S-II/S-IVB PHYSICAL SEPARATION

1	577.0800	354175.0	.0	640568.4	5956443.0
2	22075.6370	20752.7320	21546569.0	.0	16.3230
3	-226677.3	.0	-461024.9	.0	
4	100849.6	.0	209558.1	.0	
5	6055052.2	.0	6803241.1	.0	
6	-5223.1499	.0000	-6367.9395	.0000	-.0000
7	567.0190	.0000	254.6095	.0000	.0000
8	20076.6800	.0000	21135.7120	.0000	.0000
9	-.2	.0	-.2	.000	-.000
10	.0	-.0	-.0	.005	.005
11	.0	.0	-.0	.017	.017
12	-81.7590	.0000	.0	140640.0	-7.9002
13	-.7790	.0000	.0	9331642.1	-.0369
14	-.2310	-.0000	.0	9332777.3	.0000
15	-89.6600	.0000	-89.6600	.5500	473.82
16	-.8000	.0000	-.8000	.0000	-1.15
17	.0000	.0000	.0000	.0000	.34
18	1.7196	1.6165	1.5973	.0000	.0000
19	82.9987	83.4205	83.4158	.0000	.0000
20	-.0000	.0000	-30.4638	.0000	.0
21	.0002	8.5037	.0000	2478.3809	.00
22	24.9212	24.9077	.9365	-.180	20752.732
23	62.1360	32.1437	31.9757	-30.3279	-.0417
24	.0000	.0000	.0000	.0	.00
25	.0000	.0000	.00000	.0	.00
26	.00000	.0000	.00000	.0	.00
27	.0000	.0000	.00000	.0	.0000
28	.0	.0000	.00000	.0	.0000
29					
30					
31	.0	.00000	.00000	.00000	.0
32			.00000	.00000	.0
33	.0000	.0000	.0000	.0000	

TABLE 4-3 (Sheet 2 of 19)
FLIGHT SIMULATED DATA (AD77)

1	580.0000	354085.1	.0	642354.7	615208.1
2	22074.8860	20751.8150	21548333.0	.0	16.4840
3	-242041.7	.0	-479741.7	.0	
4	102511.6	.0	210300.1	.0	
5	6113644.4	.0	6864918.3	.0	
6	-5300.3491	.0000	-6451.6730	.0000	.7814
7	571.3511	.0000	253.6125	.0000	-.0000
8	20055.3660	.0000	2109.5290	.0000	.0000
9	8599.8	.0	-.2	.000	-.000
10	-.0	-.0	-.0	.005	.005
11	.0	.0	-.0	.017	.017
12	-81.7590	.0000	8600.0	140640.0	-7.9003
13	-.7790	.0000	.0	9331642.1	-.0210
14	-.0002	.0011	.0	9332777.3	.0000
15	-89.6600	.0000	-89.6600	.0004	473.82
16	-.8000	.0000	-.8000	.0000	-1.15
17	.0000	.0000	.0000	.0000	.34
18	1.6593	1.5598	1.5409	-.6610	.0002
19	83.1118	83.5268	83.5223	-6.2622	-.0000
20	273.1998	.0000	-31.4788	.0000	.0
21	.0002	8.4949	.0000	2483.2812	.00
22	25.1525	25.1358	1.0488	-.178	20751.815
23	61.9475	32.1632	31.9952	-30.3229	-.0417
24	.0000	.0000	.0000	.0	.00
25	.0000	.0000	.00000	.0	.00
26	.00000	.0000	.00000	.0	.00
27	.0000	.0000	.00000	.0	-.0000
28	.0	.0000	.00000	-.9	-1.0163
29					
30					
31	.0	.00000	.00000	.00000	.0
32			.00000	.00000	.0
33	7497.4357	243.2506	-30.8101	.0000	

1	585.0000	352620.9	193975.2	645304.2	6115892.2
2	22121.7690	20798.4720	21551247.0	.0	16.7600
3	-268858.0	.0	-512345.4	.0	
4	105387.1	.0	211562.6	.0	
5	6213909.5	.0	6970433.8	.0	
6	-5426.4507	.0000	-6590.7960	.0000	17.6561
7	578.4181	.0000	250.5271	.0000	-.2083
8	20069.7670	.0000	21115.6670	.0000	1.2092
9	193507.1	193507.3	-.2	1206.656	-.000
10	-2283.0	-2285.0	-.0	407515.270	.005
11	13252.6	13269.1	-.0	52604.690	.017
12	-91.9764	-2.1767	.0	139962.3	2.1102
13	-2.1232	-.2720	.0	9328606.0	1.4532
14	.0002	.0329	.0	9329346.6	.0000
15	-89.8656	.0000	-89.8656	.0802	473.97
16	-.6700	.0000	-.6700	-2.1752	-1.15
17	.0000	.0000	.0000	-.2720	.34
18	1.6091	1.5128	1.4944	.6766	.1580
19	83.3011	83.7038	83.6994	3.9227	1.3231
20	432.4584	432.5298	-447.4587	-443.5166	191834.8
21	.0002	8.5002	.0000	2491.3721	.00
22	15.4381	15.2706	2.3795	-.174	20798.473
23	61.6243	32.1959	32.0279	-30.3146	-.0417
24	.0000	.0000	.0000	.0	.00
25	.0000	.0000	.00000	.0	.00
26	.00000	.0000	.00000	.0	.00
27	.0000	.0000	.00000	-1113.9	-368.3971
28	.0	.0000	.00000	-304.7	-79.5934
29					
30					
31	.0	.00000	.00000	.00000	.0
32			.00000	.00000	.0
33	81316.4360	319.5458	-200.2992	.0000	

TABLE 4-3 (Sheet 3 of 19)
FLIGHT SIMULATED DATA (AD77)

1	590.0000	350102.9	225753.9	648194.0	6216938.9
2	22212.8530	20889.3520	21554101.0	.0	17.0369
3	-296326.0	.0	-545671.4	.0	
4	108293.6	.0	212801.7	.0	
5	6314397.5	.0	7076129.4	.0	
6	-5558.1291	.0000	-6737.1215	.0000	20.7427
7	586.0523	.0000	246.9605	.0000	.3168
8	20127.8110	.0000	21165.0910	.0000	-.2411
9	225712.3	225712.4	-.2	-152.669	-.000
10	3447.1	3453.2	-.0	-88363.659	.005
11	-2623.0	-2605.9	-.0	-129420.523	.017
12	-92.2047	-1.9074	.0	139404.6	-2.4312
13	1.9037	.6792	.0	9316692.9	.5970
14	-.0001	.0188	.0	9316989.1	.0000
15	-94.6376	.0000	-94.6376	-.0632	474.77
16	2.5007	.0000	2.5007	-1.9064	-1.16
17	.0000	.0000	.0000	.6792	.34
18	1.5785	1.4844	1.4665	-.8765	-.3286
19	83.4893	83.8790	83.8747	-.6615	1.4106
20	426.7224	429.1794	-528.9444	-491.9752	211077.8
21	.0002	8.5238	.0000	2499.2995	.00
22	15.4403	15.3604	-1.6462	-.172	20889.353
23	61.2998	32.2279	32.0597	-30.3065	-.0417
24	.0000	.0000	.0000	.0	.00
25	.0000	.0000	.00000	.0	.00
26	.00000	.0000	.00000	.0	.00
27	.0000	.0000	.00000	-3224.1	-446.1972
28	.0	.0000	.00000	-715.5	-83.3757
29					
30					
31	.0	.00000	.00000	.00000	.0
32			.00000	.00000	.0
33	134097.1400	362.2911	-319.4296	.0000	

1	595.0000	347309.0	228457.9	651040.3	6318433.9
2	22311.6110	20987.8690	21556914.0	.0	17.3150
3	-324461.9	.0	-579739.6	.0	
4	111257.9	.0	214041.9	.0	
5	6415192.9	.0	7182089.1	.0	
6	-5697.8838	.0000	-6891.8124	.0000	21.1632
7	598.9100	.0000	248.3466	.0000	-.1272
8	20190.7420	.0000	21219.0780	.0000	-.1159
9	228450.2	228450.4	-.2	-160.435	-.000
10	-1373.4	-1371.8	-.0	-45739.026	.005
11	-1251.0	-1245.5	-.0	20810.869	.016
12	-98.0721	-.6040	.0	139398.7	-1.4165
13	1.4321	.1811	.0	9303320.0	1.2158
14	.0000	.0035	.0	9303613.1	.0000
15	-99.4895	.0000	-99.4895	-.0151	475.71
16	2.6479	.0000	2.6479	-.6039	-1.17
17	.0000	.0000	.0000	.1811	.35
18	1.5343	1.4432	1.4258	.3440	-.2606
19	83.6922	84.0681	84.0639	-.3124	-.4191
20	426.7652	427.6601	-535.3069	-510.2004	218120.7
21	.0002	8.5506	.0000	2507.1073	.00
22	9.8948	9.8287	-1.1653	-.169	20987.869
23	60.9736	32.2590	32.0908	-30.2985	-.0417
24	.0000	.0000	.0000	.0	.00
25	.0000	.0000	.00000	.0	.00
26	.00000	.0000	.00000	.0	.00
27	.0000	.0000	.00000	-5474.3	-452.4282
28	.0	.0000	.00000	-1132.4	-83.5150
29					
30					
31	.0	.00000	.00000	.00000	.0
32			.00000	.00000	.0
33	160255.2500	380.1944	-379.6016	.0000	

TABLE 4-3 (Sheet 4 of 19)
FLIGHT SIMULATED DATA (AD77)

1	600.0000	344623.3	229553.3	653806.6	6420404.4
2	22413.4160	21089.4320	21559647.0	.0	17.5945
3	-353314.6	.0	-614599.3	.0	
4	114284.4	.0	215286.6	.0	
5	6516304.9	.0	7288319.8	.0	
6	-5845.1074	.0000	-7054.0311	.0000	21.4307
7	611.7306	.0000	249.5266	.0000	-.1005
8	20254.0030	.0000	21272.9790	.0000	.0793
9	229549.0	229549.2	-.2	52.648	-.000
10	-1076.9	-1077.5	-.0	19997.887	.005
11	849.0	857.2	-.0	11344.104	.016
12	-103.2668	-.8964	.0	139392.7	-1.0997
13	1.5616	-.0635	.0	9289817.1	1.0628
14	.0000	-.0026	.0	9290107.0	.0000
15	-104.3672	.0000	-104.3672	-.0245	476.66
16	2.6245	.0000	2.6245	-.8961	-1.17
17	.0000	.0000	.0000	-.0635	.35
18	1.4751	1.3879	1.3711	.2689	.0642
19	83.8958	84.2578	84.2538	.2140	-.1209
20	427.2368	427.3160	-537.2879	-518.5116	221512.1
21	.0002	8.5790	.0000	2514.6960	.00
22	5.1500	4.9891	-1.2838	-.167	21089.432
23	60.6456	32.2893	32.1210	-30.2908	-.0417
24	.0000	.0000	.0000	.0	.00
25	.0000	.0000	.00000	.0	.00
26	.00000	.0000	.00000	.0	.00
27	.0000	.0000	.00000	-7745.7	-454.3684
28	.0	.0000	.00000	-1549.9	-83.5580
29					
30					
31	.0	.00000	.00000	.00000	.0
32			.00000	.00000	.0
33	175401.2100	390.3903	-414.2535	.0000	

1	605.0000	341937.7	229739.2	656457.9	6522862.0
2	22517.1740	21192.9490	21562265.0	.0	17.8753
3	-382926.9	.0	-650293.9	.0	
4	117374.6	.0	216536.3	.0	
5	6617729.9	.0	7394815.1	.0	
6	-6001.3489	.0000	-7225.2592	.0000	21.6168
7	624.4405	.0000	250.4434	.0000	-.0593
8	20315.8800	.0000	21325.0110	.0000	.0368
9	229737.8	229738.0	-.2	21.075	-.000
10	-630.4	-630.6	-.0	5605.938	.005
11	391.2	400.6	-.0	-2804.516	.016
12	-107.9998	-1.0232	.0	139386.8	-1.2380
13	1.6142	-.0264	.0	9275408.5	.9868
14	-.0000	-.0006	.0	9275695.1	.0000
15	-109.2386	.0000	-109.2386	-.0288	477.67
16	2.6010	.0000	2.6010	-1.0228	-1.18
17	.0000	.0000	.0000	-.0264	.35
18	1.3960	1.3139	1.2976	.1573	.0306
19	84.0998	84.4481	84.4443	.0999	.0584
20	427.7394	427.2438	-537.0979	-522.9034	223363.0
21	.0002	8.6087	.0000	2521.9691	.00
22	1.4674	.6322	-1.3244	-.165	21192.950
23	60.3158	32.3187	32.1504	-30.2834	-.0417
24	.0000	.0000	.0000	.0	.00
25	.0000	.0000	.00000	.0	.00
26	.00000	.0000	.00000	.0	.00
27	.0000	.0000	.00000	-10018.2	-454.7052
28	.0	.0000	.00000	-1966.2	-83.0310
29					
30					
31	.0	.00000	.00000	.00000	.0
32			.00000	.00000	.0
33	185130.5400	396.9932	-436.4098	.0000	

TABLE 4-3 (Sheet 5 of 19)
FLIGHT SIMULATED DATA (AD77)

1	610.0000	339242.3	229394.2	658956.9	6625815.2
2	22622.1210	21297.6570	21564732.0	.0	18.1574
3	-413343.0	.0	-686866.8	.0	
4	120528.8	.0	217790.8	.0	
5	6719458.8	.0	7501564.1	.0	
6	-6166.4300	.0000	-7405.2845	.0000	21.7558
7	637.2677	.0000	251.3449	.0000	-.0687
8	20375.4560	.0000	21374.2600	.0000	.0126
9	229392.8	229393.0	-.2	-7.208	-.000
10	-724.2	-724.1	-.0	-2555.678	.005
11	132.8	141.8	-.0	77.328	.016
12	-112.8302	-.9833	.0	139380.8	-1.2751
13	1.5805	.0161	.0	9260773.5	1.0333
14	-.0000	.0004	.0	9261056.9	.0000
15	-114.1062	.0000	-114.1062	-.0271	478.69
16	2.6139	.0000	2.6139	-.9829	-1.19
17	.0000	.0000	.0000	.0161	.35
18	1.2973	1.2213	1.2056	.1809	-.0094
19	84.3051	84.6397	84.6362	.0354	.0150
20	425.3067	426.9289	-539.3590	-525.9924	224521.5
21	.0002	8.6395	.0000	2528.8241	.00
22	4.0088	-3.8013	-1.2770	-.164	21297.657
23	59.9841	32.3473	32.1790	-30.2764	-.0417
24	.0000	.0000	.0000	.0	.00
25	.0000	.0000	.00000	.0	.00
26	.00000	.0000	.00000	.0	.00
27	.0000	.0000	.00000	-12300.3	-456.5840
28	.0	.0000	.00000	-2381.9	-83.1392
29					
30					
31	.0	.00000	.00000	.00000	.0
32			.00000	.00000	.0
33	191898.4700	401.3624	-452.0958	.0000	

1	615.0000	336545.2	230056.6	661266.7	6729271.0
2	22727.7000	21403.0030	21567012.0	.0	18.4410
3	-444605.6	.0	-724361.0	.0	
4	123747.7	.0	219050.0	.0	
5	6821478.8	.0	7608551.2	.0	
6	-6340.1151	.0000	-7593.8433	.0000	21.9935
7	650.3131	.0000	252.3486	.0000	-.0710
8	20432.0490	.0000	21420.0440	.0000	.0189
9	230055.1	230055.3	-.2	-1.301	-.000
10	-742.5	-742.5	-.0	-552.534	.005
11	197.9	206.9	-.0	483.651	.016
12	-117.7163	-.9668	.0	139374.8	-1.2552
13	1.6248	.0084	.0	9245221.5	1.0341
14	-.0000	.0001	.0	9245501.6	.0000
15	-118.9724	.0000	-118.9724	-.0274	479.77
16	2.6589	.0000	2.6589	-.9664	-1.20
17	.0000	.0000	.0000	.0084	.36
18	1.1793	1.1106	1.0954	.1849	.0003
19	84.5120	84.8329	84.8297	.0515	-.0072
20	426.2314	426.7094	-539.7427	-528.1444	225328.2
21	.0002	8.6714	.0000	2535.1606	.00
22	8.3693	-8.2697	-1.3054	-.162	21403.004
23	59.6507	32.3750	32.2066	-30.2699	-.0417
24	.0000	.0000	.0000	.0	.00
25	.0000	.0000	.00000	.0	.00
26	.00000	.0000	.00000	.0	.00
27	.0000	.0000	.00000	-14585.5	-457.4189
28	.0	.0000	.00000	-2797.0	-82.9652
29					
30					
31	.0	.00000	.00000	.00000	.0
32			.00000	.00000	.0
33	196888.7500	404.5690	-463.6681	.0000	

TABLE 4-3 (Sheet 6 of 19)
FLIGHT SIMULATED DATA (AD77)

1	620.0000	333849.4	229734.0	663349.2	6833231.7
2	22833.4960	21508.5800	21569064.0	.0	18.7259
3	-476758.3	.0	-762819.2	.0	
4	127032.2	.0	220314.4	.0	
5	6923772.9	.0	7715757.3	.0	
6	-6522.3512	.0000	-7790.8549	.0000	22.1400
7	663.5566	.0000	253.4476	.0000	-.0724
8	20485.0590	.0000	21461.7560	.0000	.0219
9	229732.5	229732.7	-.2	1.440	-.000
10	-751.1	-751.0	-.0	369.071	.005
11	227.7	236.7	-.0	682.519	.016
12	-122.5847	-.9718	.0	139368.8	-1.2509
13	1.6723	.0102	.0	9229440.4	1.0429
14	-.0000	.0000	.0	9229717.0	.0000
15	-123.8365	.0000	-123.8365	-.0284	480.87
16	2.7153	.0000	2.7153	-.9714	-1.21
17	.0000	.0000	.0000	.0102	.36
18	1.0421	.9816	.9670	.1873	.0062
19	84.7205	85.0277	85.0248	.0590	-.0017
20	426.9690	426.7011	-538.0547	-529.6642	225977.1
21	.0001	8.7044	.0000	2540.8731	.00
22	12.7653	-12.6998	-1.3347	-.161	21508.580
23	59.3154	32.4018	32.2333	-30.2641	-.0417
24	.0000	.0000	.0000	.0	.00
25	.0000	.0000	.00000	.0	.00
26	.00000	.0000	.00000	.0	.00
27	.0000	.0000	.00000	-16870.1	-455.6697
28	.0	.0000	.00000	-3211.4	-83.0245
29					
30					
31	.0	.00000	.00000	.00000	.0
32			.00000	.00000	.0
33	200766.3200	407.1526	-472.5003	.0000	

1	625.0000	331154.1	228488.9	665165.9	6937697.1
2	22938.5900	21613.4710	21570852.0	.0	19.0122
3	-509842.7	.0	-802282.8	.0	
4	130383.5	.0	221584.6	.0	
5	7026320.8	.0	7823159.5	.0	
6	-6712.7835	.0000	-7995.9194	.0000	22.1992
7	677.0091	.0000	254.6803	.0000	-.0701
8	20533.4450	.0000	21498.3580	.0000	.0211
9	228487.5	228487.6	-.2	1.259	-.000
10	-722.0	-721.9	-.0	41.200	.005
11	217.2	226.2	-.0	-222.783	.016
12	-127.4470	-.9738	.0	139362.7	-1.2553
13	1.7570	.0152	.0	9212726.0	1.0403
14	-.0000	.0001	.0	9212999.5	.0000
15	-128.7034	.0000	-128.7034	-.0299	482.03
16	2.7974	.0000	2.7974	-.9734	-1.22
17	.0000	.0000	.0000	.0152	.36
18	.8859	.8347	.8207	.1810	.0018
19	84.9306	85.2242	85.2218	.0567	-.0007
20	427.1790	426.6889	-534.8756	-530.8056	226461.2
21	.0001	8.7382	.0000	2545.8568	.00
22	17.1544	-17.1038	-1.3981	-.160	21613.472
23	58.9782	32.4277	32.2592	-30.2590	-.0417
24	.0000	.0000	.0000	.0	.00
25	.0000	.0000	.00000	.0	.00
26	.00000	.0000	.00000	.0	.00
27	.0000	.0000	.00000	-19154.0	-453.2255
28	.0	.0000	.00000	-3626.0	-82.2858
29	2396.5336	33976.6700	.19419	176.59071	
30	3551.6269	22926.4600	32.57331	67.80278	263042100.
31	.0	.00000	.00000	.00000	.0
32			.00000	.00000	.0
33	203825.2000	409.1899	-479.4737	.0000	

TABLE 4-3 (Sheet 7 of 19)
FLIGHT SIMULATED DATA (AD77)

1	630.0000	328456.8	229912.7	666678.0	7042664.1
2	23042.2350	21716.9340	21572337.0	.0	19.2998
3	-543899.2	.0	-842791.0	.0	
4	133802.5	.0	222861.4	.0	
5	7129097.5	.0	7930730.2	.0	
6	-6911.0244	.0000	-8208.6101	.0000	22.5210
7	690.6837	.0000	256.0847	.0000	-.0710
8	20576.3440	.0000	21528.9980	.0000	.0219
9	229911.3	229911.4	-.2	1.813	-.000
10	-724.6	-724.5	-.0	156.341	.005
11	223.1	232.2	-.0	-393.394	.016
12	-132.3248	-.9757	.0	139356.7	-1.2552
13	1.8341	.0139	.0	9195778.4	1.0369
14	-.0000	.0001	.0	9196048.8	.0000
15	-133.5811	.0000	-133.5811	-.0312	483.20
16	2.8710	.0000	2.8710	-.9752	-1.23
17	.0000	.0000	.0000	.0139	.36
18	.7113	.6704	.6569	.1805	-.0010
19	85.1424	85.4225	85.4205	.0579	.0001
20	425.5544	426.5601	-540.2634	-531.7434	226794.7
21	.0001	8.7729	.0000	2550.0048	.00
22	21.5437	-21.5034	-1.4502	-.160	21716.935
23	58.6392	32.4527	32.2841	-30.2548	-.0417
24	.0000	.0000	.0000	.0	.00
25	.0000	.0000	.00000	.0	.00
26	.00000	.0000	.00000	.0	.00
27	.0000	.0000	.00000	-21439.1	-457.8701
28	.0	.0000	.00000	-4041.5	-83.0354
29	2434.0937	33607.0810	.18667	177.13544	
30	3551.3752	23034.1150	32.57246	68.44170	265425320.
31	.0	.00000	.00000	.00000	.0
32			.00000	.00000	.0
33	206263.8300	410.7364	-485.1629	.0000	

1	635.0000	325757.7	230616.1	667848.2	7148125.1
2	23144.2240	21818.7730	21573481.0	.0	19.5888
3	-578965.9	.0	-884381.5	.0	
4	137290.6	.0	224145.7	.0	
5	7232073.9	.0	8038438.3	.0	
6	-7116.9960	.0000	-8428.8260	.0000	22.7771
7	704.5542	.0000	257.6457	.0000	-.0737
8	20613.3650	.0000	21553.2730	.0000	.0234
9	230614.6	230614.7	-.2	2.544	-.000
10	-746.4	-746.3	-.0	533.118	.005
11	236.5	245.6	-.0	123.924	.016
12	-137.2009	-.9733	.0	139350.7	-1.2479
13	1.8940	.0136	.0	9178110.2	1.0410
14	-.0000	.0001	.0	9178377.5	.0000
15	-138.4499	.0000	-138.4499	-.0322	484.42
16	2.9350	.0000	2.9350	-.9728	-1.24
17	.0000	.0000	.0000	.0136	.37
18	.5182	.4885	.4756	.1854	-.0012
19	85.3560	85.6225	85.6211	.0610	.0023
20	426.9959	426.4995	-540.0865	-532.5319	227100.8
21	.0001	8.8085	.0000	2553.2149	.00
22	25.9132	-25.8813	-1.4809	-.160	21818.773
23	58.2984	32.4767	32.3080	-30.2515	-.0418
24	.0000	.0000	.0000	.0	.00
25	.0000	.0000	.00000	.0	.00
26	.00000	.0000	.00000	.0	.00
27	.0000	.0000	.00000	-23726.0	-457.4901
28	.0	.0000	.00000	-4456.9	-83.2383
29	2471.5497	33247.0690	.17925	177.82123	
30	3551.1059	23139.7730	32.57156	69.08051	267780950.
31	.0	.00000	.00000	.00000	.0
32			.00000	.00000	.0
33	208313.4500	412.0531	-489.8965	.0000	

TABLE 4-3 (Sheet 8 of 19)
FLIGHT SIMULATED DATA (AD77)

1	640.0000	323055.9	230967.6	668638.4	7254073.1
2	23243.9530	21918.3870	21574246.0	.0	19.8792
3	-615081.1	.0	-927090.9	.0	
4	140848.4	.0	225438.1	.0	
5	7335219.6	.0	8146250.6	.0	
6	-7330.2633	.0000	-8656.0959	.0000	23.0026
7	718.5901	.0000	259.3561	.0000	-.0728
8	20643.8020	.0000	21570.4920	.0000	.0220
9	230966.2	230966.4	-.2	1.371	-.000
10	-730.9	-730.8	-.0	-24.681	.005
11	220.5	229.6	-.0	-518.990	.017
12	-142.0530	-.9719	.0	139344.5	-1.2504
13	1.9564	.0102	.0	9159786.3	1.0303
14	-.0000	.0001	.0	9160050.1	.0000
15	-143.3046	.0000	-143.3046	-.0332	485.68
16	2.9867	.0000	2.9867	-.9714	-1.25
17	.0000	.0000	.0000	.0102	.37
18	.3072	.2897	.2774	.1813	-.0054
19	85.5712	85.8243	85.8234	.0570	.0014
20	427.5099	426.4778	-540.2597	-533.2292	227388.6
21	.0001	8.8450	.0000	2555.3825	.00
22	30.2412	-30.2157	-1.5092	-.160	21918.388
23	57.9559	32.4997	32.3310	-30.2493	-.0418
24	.0000	.0000	.0000	.0	.00
25	.0000	.0000	.00000	.0	.00
26	.00000	.0000	.00000	.0	.00
27	.0000	.0000	.00000	-26015.3	-458.4185
28	.0	.0000	.00000	-4872.7	-82.4833
29	2508.5861	32899.2760	.17201	178.66424	
30	3550.8717	23242.3690	32.57062	69.71467	27094450.
31	.0	.00000	.00000	.00000	.0
32			.00000	.00000	.0
33	210068.7200	413.1851	-493.9196	.0000	

1	645.0000	320352.4	230328.1	669011.3	7360495.6
2	23340.7020	22015.0640	21574594.0	.0	20.1708
3	-652279.9	.0	-970953.2	.0	
4	144476.6	.0	226739.4	.0	
5	7438499.3	.0	8254129.8	.0	
6	-7550.2957	.0000	-8889.8491	.0000	23.1320
7	732.7197	.0000	261.1716	.0000	-.0763
8	20666.8620	.0000	21579.8700	.0000	.1400
9	230322.4	230322.6	-.2	123.365	-.000
10	-759.6	-759.6	-.0	37798.817	.005
11	1393.7	1402.2	-.0	361.839	.017
12	-146.9006	-.8958	.0	139338.3	-.2249
13	1.9746	.0056	.0	9140583.2	1.0347
14	-.0000	-.0026	.0	9140843.6	.0000
15	-147.1257	.0000	-147.1257	-.0309	486.99
16	3.0093	.0000	3.0093	-.8952	-1.26
17	.0000	.0000	.0000	.0056	.37
18	.0790	.0745	.0628	.1890	-.0016
19	85.7880	86.0276	86.0274	.3488	.5799
20	426.5204	426.4606	-540.0036	-533.8398	227641.4
21	.0001	8.8822	.0000	2556.4056	.00
22	34.5454	-34.5263	-1.4873	-.161	22015.064
23	57.6116	32.5218	32.3530	-30.2483	-.0418
24	.0000	.0000	.0000	.0	.00
25	.0000	.0000	.00000	.0	.00
26	.00000	.0000	.00000	.0	.00
27	.0000	.0000	.00000	-28306.1	-457.3911
28	.0	.0000	.00000	-5288.6	-83.2543
29	2544.8146	32566.7920	.16503	179.68402	
30	3550.7392	23340.6180	32.56966	70.33853	27348310.
31	.0	.00000	.00000	.00000	.0
32			.00000	.00000	.0
33	211575.8100	414.1509	-497.3732	.0000	

TABLE 4-3 (Sheet 9 of 19)
FLIGHT SIMULATED DATA (AD77)

1	650.0000	317648.4	230512.4	668933.3	7467379.5
2	23436.2380	22110.5760	21574493.0	.0	20.4638
3	-690592.1	.0	-1015997.0	.0	
4	148175.6	.0	228049.9	.0	
5	7541877.3	.0	8362037.8	.0	
6	-7774.1000	.0000	-9127.1979	.0000	23.3480
7	746.9239	.0000	263.0484	.0000	-.0772
8	20685.3350	.0000	21584.3080	.0000	-.0590
9	230510.3	230510.4	-.2	-85.870	-.000
10	-762.6	-762.6	-.0	-26065.341	.005
11	-582.7	-587.1	-.0	329.481	.017
12	-145.7964	.4680	.0	139332.1	.3313
13	1.9979	.0010	.0	9121197.8	1.0340
14	.0000	.0030	.0	9121454.9	.0000
15	-145.4648	.0000	-145.4648	.0163	488.32
16	3.0319	.0000	3.0319	.4677	-1.27
17	.0000	.0000	.0000	.0010	.38
18	-.1568	-.1479	-.1590	.1896	.0042
19	86.0060	86.2323	86.2327	-.1459	.0521
20	425.3234	426.3976	-541.9650	-534.3661	227833.3
21	.0002	8.9211	.0000	2556.1916	.00
22	32.8976	-32.8762	-1.5017	-.163	22110.577
23	57.2657	32.5428	32.3739	-30.2485	-.0418
24	.0000	.0000	.0000	.0	.00
25	.0000	.0000	.00000	.0	.00
26	.00000	.0000	.00000	.0	.00
27	.0000	.0000	.00000	-30597.2	-459.4042
28	.0	.0000	.00000	-5704.8	-83.2049
29	2580.7679	32244.2810	.15820	-179.15475	
30	3550.7846	23435.6680	32.56871	70.96255	27583070.
31	.0	.00000	.00000	.00000	.0
32			.00000	.00000	.0
33	212854.9300	414.9398	-500.3592	.0000	

1	655.0000	314944.7	230584.2	668414.6	7574737.7
2	23536.7130	22211.0750	21573952.0	.0	20.7580
3	-730016.8	.0	-1062221.4	.0	
4	151946.1	.0	229370.0	.0	
5	7645358.9	.0	8469979.0	.0	
6	-7995.4735	.0000	-9362.3039	.0000	23.5558
7	761.3360	.0000	264.9904	.0000	-.0717
8	20708.0810	.0000	21592.9140	.0000	.0151
9	230583.0	230583.1	-.2	-6.914	-.000
10	-701.4	-701.7	-.0	-2466.599	.005
11	148.0	142.9	-.0	-1774.791	.018
12	-143.5850	.5329	.0	139325.9	.4765
13	1.9857	-.0275	.0	9100800.8	.9918
14	-.0000	.0002	.0	9101054.5	.0000
15	-143.1080	.0000	-143.1080	.0185	489.71
16	2.9774	.0000	2.9774	.5326	-1.28
17	.0000	.0000	.0000	-.0275	.38
18	-.3768	-.3555	-.3660	.1744	.0121
19	86.2250	86.4379	86.4390	.0355	-.0820
20	425.8439	426.3984	-541.4733	-534.8134	228025.7
21	.0002	8.9642	.0000	2554.7686	.00
22	30.1575	-30.1327	-1.4862	-.165	22211.075
23	56.9181	32.5628	32.3939	-30.2500	-.0418
24	.0000	.0000	.0000	.0	.00
25	.0000	.0000	.00000	.0	.00
26	.00000	.0000	.00000	.0	.00
27	.0000	.0000	.00000	-32887.9	-458.5636
28	.0	.0000	.00000	-6121.0	-83.5532
29	2618.7894	31911.0370	.15110	-177.94244	
30	3551.0304	23533.5310	32.56782	71.62790	276943180.
31	.0	.00000	.00000	.00000	.0
32			.00000	.00000	.0
33	213994.6300	415.6776	-502.9565	.0000	

TABLE 4-3 (Sheet 10 of 19)
FLIGHT SIMULATED DATA (AD77)

1	660.0000	312247.6	230247.3	667481.8	7682594.8
2	23641.4040	22915.8340	21572999.0	.0	21.0536
3	-770541.6	.0	-1109615.2	.0	
4	155788.8	.0	230699.4	.0	
5	7748963.6	.0	8577972.4	.0	
6	-8214.0937	.0000	-9594.8262	.0000	23.7246
7	775.7016	.0000	266.7573	.0000	-.0761
8	20734.5940	.0000	21605.1880	.0000	.0345
9	230245.7	230245.8	-.2	11.938	-.000
10	-739.0	-739.1	-.0	3584.048	.005
11	334.6	330.1	-.0	-631.723	.018
12	-141.2840	.4677	.0	139319.7	.4926
13	1.8762	-.0159	.0	9080151.0	1.0038
14	-.0000	-.0003	.0	9080401.1	.0000
15	-140.7909	.0000	-140.7909	.0153	491.12
16	2.8800	.0000	2.8800	.4675	-1.29
17	.0000	.0000	.0000	-.0159	.38
18	-.5806	-.5480	-.5579	.1839	-.0043
19	86.4444	86.6440	86.6456	.0821	-.0101
20	427.1514	426.4124	-539.0263	-535.1156	228163.2
21	.0002	9.0110	.0000	2552.2098	.00
22	27.3385	-27.3134	-1.3736	-.168	22315.834
23	56.5686	32.5817	32.4128	-30.2527	-.0418
24	.0000	.0000	.0000	.0	.00
25	.0000	.0000	.00000	.0	.00
26	.00000	.0000	.00000	.0	.00
27	.0000	.0000	.00000	-35171.3	-456.5822
28	.0	.0000	.00000	-6537.9	-83.0847
29	2658.7164	31569.3770	.14376	-176.67340	
30	3551.4703	23633.5970	32.56705	72.33201	279413040.
31	.0	.00000	.00000	.00000	.0
32			.00000	.00000	.0
33	214969.2800	416.3384	-505.1601	.0000	

1	665.0000	309552.4	230222.3	666162.5	7790968.9
2	23749.8020	22424.3370	21571659.0	.0	21.3506
3	-812152.5	.0	-1158164.7	.0	
4	159703.1	.0	232037.3	.0	
5	7852709.2	.0	8686035.1	.0	
6	-8429.7728	.0000	-9824.5668	.0000	23.9285
7	790.0027	.0000	268.3406	.0000	-.0763
8	20764.5300	.0000	21620.8010	.0000	.0337
9	230220.7	230220.9	-.2	11.020	-.000
10	-734.4	-734.9	-.0	3220.776	.005
11	324.0	319.5	-.0	-891.623	.019
12	-138.8979	.4784	.0	139313.5	.5296
13	1.7319	-.0495	.0	9058453.1	.9724
14	-.0000	-.0000	.0	9058699.8	.0000
15	-138.3680	.0000	-138.3680	.0145	492.60
16	2.7044	.0000	2.7044	.4782	-1.30
17	.0000	.0000	.0000	-.0495	.38
18	-.7681	-.7252	-.7345	.1829	.0106
19	86.6641	86.8505	86.8526	.0795	.0332
20	427.2389	426.3598	-538.8574	-535.3575	228239.0
21	.0002	9.0612	.0000	2548.5908	.00
22	24.4479	-24.4239	-1.2261	-.171	22424.337
23	56.2174	32.5996	32.4306	-30.2564	-.0419
24	.0000	.0000	.0000	.0	.00
25	.0000	.0000	.00000	.0	.00
26	.00000	.0000	.00000	.0	.00
27	.0000	.0000	.00000	-37453.2	-456.0272
28	.0	.0000	.00000	-6954.3	-83.4706
29	2700.4580	31220.8900	.13621	-175.33444	
30	3552.1006	23735.4490	32.56638	73.07354	281981880.
31	.0	.00000	.00000	.00000	.0
32			.00000	.00000	.0
33	215791.4200	416.8639	-507.0913	.0000	

TABLE 4-3 (Sheet 11 of 19)
FLIGHT SIMULATED DATA (AD77)

1	670.0000	306849.3	230921.0	664485.3	7899881.9
2	23862.4360	22537.1080	21569964.0	.0	21.6490
3	-854834.6	.0	-1207856.5	.0	
4	163688.3	.0	233382.1	.0	
5	7956614.6	.0	8794185.7	.0	
6	-8642.6155	.0000	-10051.6593	.0000	24.2126
7	804.0271	.0000	269.5089	.0000	-.0790
8	20798.5570	.0000	21640.4120	.0000	.0200
9	230919.5	230919.7	-.2	-4.078	-.000
10	-753.7	-754.1	-.0	-1196.560	.006
11	190.8	186.0	-.0	-449.995	.019
12	-136.3261	.5045	.0	139307.2	.5285
13	1.5147	-.0407	.0	9036493.4	.9800
14	-.0000	.0003	.0	9036736.6	.0000
15	-135.7973	.0000	-135.7973	.0133	494.09
16	2.4947	.0000	2.4947	.5043	-1.31
17	.0000	.0000	.0000	-.0407	.39
18	-.9387	-.8866	-.8953	.1871	-.0014
19	86.8836	87.0568	87.0595	.0461	.0140
20	426.0424	426.3086	-542.0109	-535.6626	228342.3
21	.0002	9.1150	.0000	2543.9899	.00
22	21.3835	-21.3639	-1.0065	-.175	22537.108
23	55.8642	32.6165	32.4474	-30.2611	-.0419
24	.0000	.0000	.0000	.0	.00
25	.0000	.0000	.00000	.0	.00
26	.00000	.0000	.00000	.0	.00
27	.0000	.0000	.00000	-39741.4	-459.0556
28	.0	.0000	.00000	-7372.4	-83.5994
29	2744.3365	30863.7470	.12840	-173.90544	
30	3552.9222	23839.6730	32.56586	73.85856	284663520.
31	.0	.00000	.00000	.00000	.0
32			.00000	.00000	.0
33	216558.6400	417.3283	-508.8990	.0000	

1	675.0000	304146.3	231060.2	662480.2	8009355.5
2	23979.1510	22653.9860	21567941.0	.0	21.9491
3	-898573.3	.0	-1258676.2	.0	
4	167742.8	.0	234731.7	.0	
5	8060700.6	.0	8902444.8	.0	
6	-8852.1804	.0000	-10275.6743	.0000	24.4425
7	817.7769	.0000	270.2649	.0000	-.0815
8	20836.8230	.0000	21664.1920	.0000	.0180
9	231058.7	231058.8	-.2	-6.972	-.000
10	-770.8	-771.2	-.0	-1917.511	.006
11	170.3	165.1	-.0	-16.631	.020
12	-133.6590	.5402	.0	139300.9	.5447
13	1.3067	-.0400	.0	9013444.3	.9842
14	-.0000	.0003	.0	9013683.9	.0000
15	-133.1140	.0000	-133.1140	.0123	495.65
16	2.2909	.0000	2.2909	.5401	-1.32
17	.0000	.0000	.0000	-.0400	.39
18	-1.0913	-1.0310	-1.0391	.1912	-.0011
19	87.1029	87.2631	87.2662	.0409	-.0032
20	426.9799	426.3268	-541.1469	-535.9343	228468.8
21	.0002	9.1722	.0000	2538.4896	.00
22	18.2407	-18.2256	-.7962	-.180	22653.986
23	55.5091	32.6323	32.4631	-30.2667	-.0419
24	.0000	.0000	.0000	.0	.00
25	.0000	.0000	.00000	.0	.00
26	.00000	.0000	.00000	.0	.00
27	.0000	.0000	.00000	-42029.5	-458.2013
28	.0	.0000	.00000	-7790.7	-83.5887
29	2790.4196	30498.3530	.12035	-172.37225	
30	3553.9307	23946.2190	32.56548	74.68859	287455660.
31	.0	.00000	.00000	.00000	.0
32			.00000	.00000	.0
33	217279.5500	417.8048	-510.5219	.0000	

TABLE 4-3 (Sheet 12 of 19)
FLIGHT SIMULATED DATA (AD77)

1	680.0000	301441.9	230149.7	660181.6	8119409.2
2	24099.2870	22774.3050	21565626.0	.0	22.2507
3	-943349.9	.0	-1310606.9	.0	
4	171865.5	.0	236084.0	.0	
5	8164988.1	.0	9010833.0	.0	
6	-9057.7884	.0000	-10495.9255	.0000	24.5646
7	831.2246	.0000	270.5953	.0000	-.0807
8	20879.0450	.0000	21691.8870	.0000	.0304
9	230148.1	230148.3	-.2	6.160	-.000
10	-756.3	-756.8	-.0	1866.392	.006
11	284.9	279.7	-.0	-506.902	.021
12	-130.9859	.5444	.0	139294.6	.6236
13	1.0953	-.0477	.0	8990122.6	.9744
14	-.0000	.0001	.0	8990358.9	.0000
15	-130.3621	.0000	-130.3621	.0104	497.23
16	2.0698	.0000	2.0698	.5443	-1.33
17	.0000	.0000	.0000	-.0477	.39
18	-1.2246	-1.1573	-1.1647	.1884	.0014
19	87.3220	87.4694	87.4728	.0696	.0245
20	426.3399	426.3202	-539.8235	-536.1910	228575.4
21	.0002	9.2324	.0000	2532.1838	.00
22	15.1099	-15.0997	-.5824	-.185	22774.306
23	55.1520	32.6470	32.4778	-30.2732	-.0419
24	.0000	.0000	.0000	.0	.00
25	.0000	.0000	.00000	.0	.00
26	.00000	.0000	.00000	.0	.00
27	.0000	.0000	.00000	-44318.5	-456.9242
28	.0	.0000	.00000	-8209.2	-83.5409
29	2838.5673	30126.7410	.11207	-170.71464	
30	3555.1225	24054.5250	32.56521	75.56155	290343840.
31	.0	.00000	.00000	.00000	.0
32			.00000	.00000	.0
33	217923.9200	418.2133	-5111.9991	.0000	

1	685.0000	298749.2	228120.3	657625.1	8230060.1
2	24221.8380	22897.0560	21563055.0	.0	22.5539
3	-989143.1	.0	-1363627.5	.0	
4	176054.3	.0	237436.8	.0	
5	8269495.1	.0	9119368.0	.0	
6	-9258.5198	.0000	-10711.4749	.0000	24.5675
7	844.2682	.0000	270.4227	.0000	-.0826
8	20924.6790	.0000	21722.9980	.0000	.0119
9	228118.9	228119.0	-.2	-13.726	-.000
10	-766.6	-767.0	-.0	-3887.210	.006
11	110.6	104.6	-.0	-56.354	.021
12	-127.8853	.6212	.0	139288.3	.6347
13	.8561	-.0464	.0	8972470.1	.9786
14	-.0000	.0005	.0	8972702.8	.0000
15	-127.2505	.0000	-127.2505	.0093	498.87
16	1.8347	.0000	1.8347	.6211	-1.34
17	.0000	.0000	.0000	-.0464	.40
18	-1.3371	-1.2639	-1.2708	.1926	-.0009
19	87.5408	87.6754	87.6792	.0263	.0049
20	423.0755	426.2616	-539.1923	-536.3075	228594.2
21	.0002	9.2950	.0000	2525.1708	.00
22	11.5706	-11.5658	-.3414	-.191	22897.056
23	54.7928	32.6606	32.4913	-30.2804	-.0420
24	.0000	.0000	.0000	.0	.00
25	.0000	.0000	.00000	.0	.00
26	.00000	.0000	.00000	.0	.00
27	.0000	.0000	.00000	-46596.7	-455.9923
28	.0	.0000	.00000	-8627.0	-83.8408
29	2888.4863	29751.9250	.10365	-168.91541	
30	3556.4847	24163.7570	32.56506	76.47244	293304960.
31	.0	.00000	.00000	.00000	.0
32			.00000	.00000	.0
33	218435.9200	418.5346	-513.2314	.0000	

TABLE 4-3 (Sheet 13 of 19)
FLIGHT SIMULATED DATA (AD77)

1	690.0000	296060.2	228570.8	654852.5	8341319.9
2	24346.9580	23022.3830	21560268.0	.0	22.8588
3	-1035926.2	.0	-1417712.9	.0	
4	180307.4	.0	238787.4	.0	
5	8374240.5	.0	9228068.5	.0	
6	-9453.8908	.0000	-10921.8656	.0000	24.8395
7	856.9070	.0000	269.7388	.0000	-.0843
8	20974.2650	.0000	21758.0910	.0000	.0369
9	228569.0	228569.2	-.2	11.669	-.000
10	-775.7	-776.2	-.0	3687.736	.007
11	339.5	333.3	-.0	84.285	.022
12	-124.7945	.6387	.0	139282.0	.7744
13	.6157	-.0484	.0	8956234.8	.9789
14	-.0000	.0002	.0	8956464.0	.0000
15	-124.0199	.0000	-124.0199	.0069	500.52
16	1.5946	.0000	1.5946	.6386	-1.35
17	.0000	.0000	.0000	-.0484	.40
18	-1.4272	-1.3495	-1.3558	.1946	.0003
19	87.7593	87.8813	87.8853	.0835	.0551
20	423.0588	426.1876	-540.2776	-536.3780	228584.9
21	.0002	9.3600	.0000	2517.5652	.00
22	8.0632	-8.0626	-.0987	-.198	23022.383
23	54.4315	32.6731	32.5038	-30.2882	-.0420
24	.0000	.0000	.0000	.0	.00
25	.0000	.0000	.00000	.0	.00
26	.00000	.0000	.00000	.0	.00
27	.0000	.0000	.00000	-48870.8	-457.0403
28	.0	.0000	.00000	-9045.1	-83.8794
29	2940.3664	29373.1590	.09505	-166.94075	
30	3558.0094	24274.2050	32.56502	77.42492	296343610.
31	.0	.00000	.00000	.00000	.0
32			.00000	.00000	.0
33	218877.7400	418.8075	-514.3212	.0000	

1	695.0000	293358.8	228105.0	651905.5	8453205.2
2	24474.7310	23150.3660	21557308.0	.0	23.1654
3	-1083672.6	.0	-1472837.2	.0	
4	184622.7	.0	240133.3	.0	
5	8479244.0	.0	9336955.1	.0	
6	-9643.4933	.0000	-11126.7138	.0000	25.0172
7	869.1326	.0000	268.5289	.0000	-.0852
8	21028.2440	.0000	21797.6290	.0000	.0104
9	228103.5	228103.7	-.2	-16.227	-.000
10	-776.9	-777.4	-.0	-4508.680	.007
11	95.1	87.8	-.0	63.121	.023
12	-121.0634	.7429	.0	139275.6	.7807
13	.3748	-.0485	.0	8932468.7	.9799
14	-.0000	.0004	.0	8932694.3	.0000
15	-120.2826	.0000	-120.2826	.0049	502.26
16	1.3546	.0000	1.3546	.7428	-1.37
17	.0000	.0000	.0000	-.0485	.40
18	-1.4938	-1.4130	-1.4186	.1953	.0007
19	87.9773	88.0869	88.0911	.0221	.0110
20	423.5906	426.0628	-538.5003	-536.5536	228592.8
21	.0002	9.4272	.0000	2509.4808	.00
22	3.9440	-3.9413	.1447	-.205	23150.366
23	54.0681	32.6846	32.5152	-30.2965	-.0420
24	.0000	.0000	.0000	.0	.00
25	.0000	.0000	.00000	.0	.00
26	.00000	.0000	.00000	.0	.00
27	.0000	.0000	.00000	-51156.8	-455.7776
28	.0	.0000	.00000	-9463.8	-83.3626
29	2994.3750	28989.9840	.08625	-164.73880	
30	3559.6939	24386.0540	32.56506	78.42238	299462810.
31	.0	.00000	.00000	.00000	.0
32			.00000	.00000	.0
33	219076.5100	418.9128	-514.8240	.0000	

TABLE 4-3 (Sheet 14 of 19)
FLIGHT SIMULATED DATA (AD77)

1	700.0000	290657.4	225699.8	648834.0	8565726.5
2	24603.4700	23279.3100	21554225.0	.0	23.4738
3	-1132348.6	.0	-1528967.8	.0	
4	188997.9	.0	241471.8	.0	
5	8584526.9	.0	9446049.0	.0	
6	-9825.6466	.0000	-11324.3063	.0000	24.9834
7	880.8893	.0000	266.7823	.0000	-.0850
8	21085.7060	.0000	21840.7810	.0000	.0589
9	225697.7	225697.9	-.2	33.905	-.000
10	-768.2	-768.6	-.0	10241.244	.007
11	532.3	522.8	-.0	-67.639	.024
12	-117.1087	.9672	.0	139269.3	1.0889
13	.1349	-.0481	.0	8906820.0	.9802
14	-.0000	.0003	.0	8907042.1	.0000
15	-116.0198	.0000	-116.0198	.0023	504.02
16	1.1150	.0000	1.1150	.9672	-1.38
17	.0000	.0000	.0000	-.0481	.41
18	-1.5344	-1.4518	-1.4568	.1951	.0001
19	88.1951	88.2923	88.2966	.1327	-.0775
20	418.7010	425.8093	-539.0431	-536.7142	228524.8
21	.0002	9.4957	.0000	2501.0552	.00
22	.5427	.3792	.3883	-.212	23279.311
23	53.7025	32.6949	32.5255	-30.3051	-.0421
24	.0000	.0000	.0000	.0	.00
25	.0000	.0000	.00000	.0	.00
26	.00000	.0000	.00000	.0	.00
27	.0000	.0000	.00000	-53441.7	-455.4691
28	.0	.0000	.00000	-9883.4	-84.2146
29	3049.9119	28607.2380	.07738	-162.27561	
30	3561.4987	24497.9890	32.56517	79.45381	302622100.
31	.0	.00000	.00000	.00000	.0
32			.00000	.00000	.0
33	219076.5100	418.9128	-514.8240	.0000	

1	705.0000	287956.2	225062.3	645692.3	8678889.3
2	24732.9390	23408.9730	21551073.0	.0	23.7839
3	-1181913.7	.0	-1586065.1	.0	
4	193430.7	.0	242800.2	.0	
5	8690107.2	.0	9555369.4	.0	
6	-9998.7635	.0000	-11513.0900	.0000	25.1465
7	892.1663	.0000	264.4935	.0000	-.0862
8	21147.3120	.0000	21888.2870	.0000	.0576
9	225060.2	225060.4	-.2	32.120	-.000
10	-771.6	-772.2	-.0	9695.006	.008
11	515.1	505.8	-.0	9.766	.026
12	-112.4316	.9423	.0	139262.9	1.1237
13	-.1171	-.0533	.0	8879990.0	.9765
14	-.0000	.0005	.0	8880208.7	.0000
15	-111.3078	.0000	-111.3078	-.0019	505.87
16	.8594	.0000	.8594	.9423	-1.39
17	.0000	.0000	.0000	-.0533	.41
18	-1.5450	-1.4623	-1.4667	.1966	.0019
19	88.4124	88.4975	88.5018	.1288	.0308
20	418.0851	425.5148	-538.3123	-536.8597	228428.2
21	.0002	9.5650	.0000	2492.4368	.00
22	5.4325	5.3944	.6462	-.220	23408.973
23	53.3348	32.7041	32.5346	-30.3140	-.0421
24	.0000	.0000	.0000	.0	.00
25	.0000	.0000	.00000	.0	.00
26	.00000	.0000	.00000	.0	.00
27	.0000	.0000	.00000	-55726.7	-454.9918
28	.0	.0000	.00000	-10302.9	-83.9602
29	3107.0288	28224.8650	.06841	-159.49522	
30	3563.3598	24610.3320	32.56533	80.51934	305815990.
31	.0	.00000	.00000	.00000	.0
32			.00000	.00000	.0
33	219076.5100	418.9128	-514.8240	.0000	

TABLE 4-3 (Sheet 15 of 19)
FLIGHT SIMULATED DATA (AD77)

1	710.0000	285264.7	225371.5	642542.7	8792698.2
2	24862.2090	23538.4210	21547914.0	.0	24.0958
3	-1232319.9	.0	-1644082.6	.0	
4	197918.6	.0	244115.7	.0	
5	8796004.9	.0	9664937.3	.0	
6	-10161.9565	.0000	-11692.1644	.0000	25.4187
7	902.8906	.0000	261.6128	.0000	-.0879
8	21212.6550	.0000	21939.7890	.0000	.0260
9	225369.8	225370.0	-.2	-1.137	-.000
10	-779.3	-779.8	-.0	33.041	.008
11	230.8	221.3	-.0	122.100	.027
12	-107.5118	.9539	.0	139256.5	1.0748
13	-.3773	-.0515	.0	8852864.7	.9805
14	-.0000	.0004	.0	8853080.1	.0000
15	-106.4370	.0000	-106.4370	-.0063	507.73
16	.6031	.0000	.6031	.9538	-1.40
17	.0000	.0000	.0000	-.0515	.42
18	-1.5246	-1.4434	-1.4473	.1983	.0016
19	88.6292	88.7023	88.7066	.0563	.0294
20	418.1021	425.2689	-539.0311	-536.9171	228320.7
21	.0002	9.6346	.0000	2483.7967	.00
22	10.6611	10.6235	.9155	-.228	23538.422
23	52.9649	32.7122	32.5427	-30.3229	-.0421
24	.0000	.0000	.0000	.0	.00
25	.0000	.0000	.00000	.0	.00
26	.00000	.0000	.00000	.0	.00
27	.0000	.0000	.00000	-58002.3	-455.3979
28	.0	.0000	.00000	-10722.0	-84.2737
29	3165.4061	27845.2930	.05941	-156.28639	
30	3565.2490	24722.4420	32.56554	81.61303	309021670.
31	.0	.00000	.00000	.00000	.0
32			.00000	.00000	.0
33	219076.5100	418.9128	-514.8240	.0000	

1	715.0000	282576.2	226035.8	639450.9	8907150.7
2	24990.6350	23667.0060	21544815.0	.0	24.4095
3	-1283515.8	.0	-1702969.7	.0	
4	202458.7	.0	245415.3	.0	
5	8902238.1	.0	9774772.2	.0	
6	-10314.6744	.0000	-11860.9720	.0000	25.7362
7	913.0540	.0000	258.1473	.0000	-.0732
8	21281.4710	.0000	21995.0590	.0000	.0217
9	226034.6	226034.9	-.2	-1.059	-.000
10	-642.8	-643.4	-.0	-1360.486	.008
11	190.8	181.1	-.0	-4704.293	.028
12	-102.6328	.9730	.0	139234.3	1.0700
13	-.6307	-.0633	.0	8833488.7	.8800
14	-.0000	.0004	.0	8833707.3	.0000
15	-101.5628	.0000	-101.5628	-.0107	509.02
16	.2493	.0000	.2493	.9729	-1.41
17	.0000	.0000	.0000	-.0633	.42
18	-1.4728	-1.3948	-1.3980	.1631	-.0546
19	88.8456	88.9068	88.9109	.0459	.0008
20	420.4019	425.0794	-537.6638	-536.9468	228231.9
21	.0002	9.7039	.0000	2475.3153	.00
22	15.8229	15.7830	1.1813	-.237	23667.006
23	52.5928	32.7191	32.5496	-30.3316	-.0421
24	.0000	.0000	.0000	.0	.00
25	.0000	.0000	.00000	.0	.00
26	.00000	.0000	.00000	.0	.00
27	.0000	.0000	.00000	-60274.9	-454.3655
28	.0	.0000	.00000	-11141.1	-83.9373
29	3224.7982	27470.2790	.05041	-152.45055	
30	3567.1703	24833.7190	32.56577	82.73076	312222970.
31	.0	.00000	.00000	.00000	.0
32			.00000	.00000	.0
33	219076.5100	418.9128	-514.8240	.0000	

TABLE 4-3 (Sheet 16 of 19)
FLIGHT SIMULATED DATA (AD77)

1	720.0000	279881.2	226155.4	636480.8	9022242.6
2	25116.9190	23793.4270	21541839.0	.0	24.7249
3	-1335448.3	.0	-1762674.2	.0	
4	207047.5	.0	246695.6	.0	
5	9008822.0	.0	9884890.8	.0	
6	-10456.4624	.0000	-12019.0112	.0000	25.9977
7	922.2463	.0000	253.7221	.0000	-.0985
8	21352.7280	.0000	22053.0880	.0000	.0272
9	226153.5	226153.7	-.2	-3.060	-.000
10	-856.9	-856.3	-.0	201.915	.009
11	236.7	227.0	-.0	2577.931	.029
12	-97.7838	.9747	.0	139219.2	1.0835
13	-.9950	.0602	.0	8833422.7	1.0679
14	-.0000	-.0004	.0	8833655.9	.0000
15	-96.7002	.0000	-96.7002	-.0169	509.02
16	.0729	.0000	.0729	.9746	-1.41
17	.0000	.0000	.0000	.0602	.42
18	-1.3903	-1.3170	-1.3196	.2169	-.0971
19	89.0606	89.1102	89.1141	.0575	.0005
20	418.0278	424.8627	-541.0016	-537.0223	228147.6
21	.0002	9.7718	.0000	2467.1677	.00
22	20.9342	20.8856	1.5606	-.245	23793.427
23	52.2186	32.7249	32.5553	-30.3399	-.0422
24	.0000	.0000	.0000	.0	.00
25	.0000	.0000	.00000	.0	.00
26	.00000	.0000	.00000	.0	.00
27	.0000	.0000	.00000	-62553.7	-457.3263
28	.0	.0000	.00000	-11560.5	-84.3182
29	3284.5379	27104.0690	.04153	-147.64405	
30	3569.1899	24942.4520	32.56602	83.86173	315386940.
31	.0	.00000	.00000	.00000	.0
32			.00000	.00000	.0
33	219076.5100	418.9128	-514.8240	.0000	

1	725.0000	277179.2	227186.5	633699.1	9137961.3
2	25240.2470	23916.8670	21539052.0	.0	25.0420
3	-1388061.5	.0	-1823141.2	.0	
4	211681.6	.0	247953.0	.0	
5	9115767.3	.0	9995305.5	.0	
6	-10587.0019	.0000	-12165.9502	.0000	26.3708
7	931.3126	.0000	249.2050	.0000	-.1013
8	21425.7930	.0000	22113.2920	.0000	.0266
9	227184.5	227184.7	-.3	-4.562	-.000
10	-872.5	-872.3	-.0	-106.194	.009
11	228.8	219.0	-.0	2990.177	.030
12	-92.8984	.9767	.0	139204.2	1.0830
13	-.9474	.0198	.0	8833356.6	1.0750
14	.0000	-.0001	.0	8833604.4	.0000
15	-91.8154	.0000	-91.8154	-.0161	509.02
16	.1276	.0000	.1276	.9766	-1.41
17	.0000	.0000	.0000	.0198	.42
18	-1.2774	-1.2104	-1.2125	.2200	-.0126
19	89.2764	89.3144	89.3180	.0552	.0004
20	419.9900	424.6528	-540.9289	-537.1422	228085.6
21	.0002	9.8377	.0000	2459.5369	.00
22	26.0271	25.9931	1.5337	-.254	23916.867
23	51.8424	32.7295	32.5599	-30.3478	-.0422
24	.0000	.0000	.0000	.0	.00
25	.0000	.0000	.00000	.0	.00
26	.00000	.0000	.00000	.0	.00
27	.0000	.0000	.00000	-64839.4	-457.3771
28	.0	.0000	.00000	-11980.1	-84.1946
29	3344.0144	26750.3600	.03290	-141.18031	
30	3571.5128	25046.4150	32.56623	84.99854	318492200.
31	.0	.00000	.00000	.00000	.0
32			.00000	.00000	.0
33	219076.5100	418.9128	-514.8240	.0000	

TABLE 4-3 (Sheet 17 of 19)
FLIGHT SIMULATED DATA (AD77)

1	730.0000	274480.3	227595.2	631169.7	9254289.9
2	25359.5140	24036.2230	21536519.0	.0	25.3608
3	-1441298.8	.0	-1884314.3	.0	
4	216360.7	.0	249187.8	.0	
5	9223080.1	.0	10106024.4	.0	
6	-10705.9588	.0000	-12301.4177	.0000	26.6781
7	940.3760	.0000	244.7518	.0000	-.0950
8	21499.7250	.0000	22174.7660	.0000	.0286
9	227593.4	227593.7	-.3	-.580	-.000
10	-810.8	-810.8	-.0	406.748	.009
11	244.2	234.6	-.0	839.030	.031
12	-88.0507	.9649	.0	139189.2	1.0736
13	-.8695	.0075	.0	8833290.5	1.0587
14	.0000	-.0000	.0	8833553.0	.0000
15	-86.9771	.0000	-86.9771	-.0146	509.03
16	.1892	.0000	.1892	.9648	-1.41
17	.0000	.0000	.0000	.0075	.42
18	-1.1352	-1.0760	-1.0774	.2041	.0059
19	89.4933	89.5198	89.5230	.0591	.0029
20	422.5327	424.4939	-538.6415	-537.2324	228038.6
21	.0002	9.9008	.0000	2452.5984	.00
22	31.0579	31.0345	1.4832	-.261	24036.224
23	51.4641	32.7329	32.5633	-30.3549	-.0422
24	.0000	.0000	.0000	.0	.00
25	.0000	.0000	.00000	.0	.00
26	.00000	.0000	.00000	.0	.00
27	.0000	.0000	.00000	-67121.6	-455.3852
28	.0	.0000	.00000	-12400.0	-83.8964
29	3402.0954	26416.0570	.02474	-131.60183	
30	3574.6730	25140.7470	32.56638	86.13011	321509700.
31	.0	.00000	.00000	.00000	.0
32			.00000	.00000	.0
33	219076.5100	418.9128	-514.8240	.0000	

1	735.0000	271781.0	226731.4	628957.1	9371204.4
2	25473.4910	24150.2680	21534304.0	.0	25.6812
3	-1495101.6	.0	-1946135.8	.0	
4	221085.2	.0	250400.6	.0	
5	9330762.6	.0	10217052.0	.0	
6	-10813.2307	.0000	-12425.2580	.0000	26.8408
7	949.4336	.0000	240.3965	.0000	-.0937
8	21573.3190	.0000	22236.3210	.0000	.0266
9	226729.6	226729.9	-.3	-2.205	-.000
10	-791.8	-791.5	-.0	-224.634	.009
11	224.8	215.1	-.0	290.341	.032
12	-83.1979	.9709	.0	139174.1	1.0860
13	-.7895	.0214	.0	8833224.3	1.0674
14	.0000	-.0002	.0	8833501.6	.0000
15	-82.1119	.0000	-82.1119	-.0134	509.03
16	.2779	.0000	.2779	.9708	-1.41
17	.0000	.0000	.0000	.0214	.42
18	-.9652	-.9151	-.9159	.2000	-.0015
19	89.7114	89.7264	89.7291	.0544	.0003
20	420.3371	424.3398	-539.4002	-537.3192	227992.5
21	.0002	9.9601	.0000	2446.5286	.00
22	36.0708	36.0546	1.4390	-.269	24150.269
23	51.0838	32.7352	32.5655	-30.3612	-.0422
24	.0000	.0000	.0000	.0	.00
25	.0000	.0000	.00000	.0	.00
26	.00000	.0000	.00000	.0	.00
27	.0000	.0000	.00000	-69404.6	-456.1636
28	.0	.0000	.00000	-12819.5	-83.8776
29	3456.5199	26115.5750	.01758	-115.49830	
30	3580.2125	25213.3100	32.56649	87.24290	324406620.
31	.0	.00000	.00000	.00000	.0
32			.00000	.00000	.0
33	219076.5100	418.9128	-514.8240	.0000	

TABLE 4-3 (Sheet 18 of 19)
FLIGHT SIMULATED DATA (AD77)

1	740.0000	269091.5	226073.8	627121.5	9488674.8
2	25580.8170	24257.6410	21532467.0	.0	26.0031
3	-1549411.3	.0	-2008547.0	.0	
4	225855.0	.0	251592.1	.0	
5	9438809.6	.0	10328384.8	.0	
6	-10908.4027	.0000	-12537.0014	.0000	27.0304
7	958.5541	.0000	236.2516	.0000	-.0935
8	21645.3480	.0000	22296.7710	.0000	.0060
9	226072.1	226072.4	-.3	-22.566	-.000
10	-782.3	-782.1	-.0	-6144.004	.010
11	50.5	39.4	-.0	44.866	.032
12	-77.8519	1.1119	.0	139159.1	1.1918
13	-.6850	.0197	.0	8833158.4	1.0654
14	.0000	-.0004	.0	8833450.2	.0000
15	-76.6601	.0000	-76.6601	-.0133	509.03
16	.3805	.0000	.3805	1.1119	-1.41
17	.0000	.0000	.0000	.0197	.42
18	-.7685	-.7287	-.7289	.1982	.0010
19	89.9309	89.9345	89.9367	.0100	-.0245
20	420.2387	424.2214	-537.9619	-537.3382	227937.3
21	.0003	10.0147	.0000	2441.4933	.00
22	41.5527	41.5421	1.3865	-.275	24257.642
23	50.7018	32.7362	32.5665	-30.3663	-.0423
24	.0000	.0000	.0000	.0	.00
25	.0000	.0000	.00000	.0	.00
26	.00000	.0000	.00000	.0	.00
27	.0000	.0000	.00000	-71678.0	-454.8598
28	.0	.0000	.00000	-13238.8	-83.7413
29	3502.0179	25883.8890	.01276	-86.30887	
30	3592.5506	25231.6110	32.56653	88.32070	327146330.
31	.0	.00000	.00000	.00000	.0
32			.00000	.00000	.0
33	219076.5100	418.9128	-514.8240	.0000	

1	745.0000	266403.3	225076.5	625724.5	9606660.8
2	25679.7290	24356.5840	21531070.0	.0	26.3264
3	-1604163.2	.0	-2071483.2	.0	
4	230670.6	.0	252763.4	.0	
5	9547209.5	.0	10440013.9	.0	
6	-10990.5514	.0000	-12635.6575	.0000	27.1824
7	967.6865	.0000	232.3234	.0000	-.0972
8	21714.3860	.0000	22354.7480	.0000	.1320
9	225072.2	225072.5	-.3	100.108	-.000
10	-805.0	-804.5	-.0	29438.026	.010
11	1093.3	1087.8	-.0	937.093	.033
12	-73.4761	.5558	.0	139144.1	1.0977
13	-.5318	.0560	.0	8833092.2	1.1020
14	.0000	.0003	.0	8833398.7	.0000
15	-72.3785	.0000	-72.3785	-.0052	509.04
16	.5702	.0000	.5702	.5558	-1.41
17	.0000	.0000	.0000	.0560	.42
18	-.5450	-.5169	-.5165	.2048	-.0143
19	90.1518	90.1440	90.1455	.2769	.5059
20	419.1978	424.0785	-536.9123	-537.3475	227864.7
21	.0003	10.0634	.0000	2437.6610	.00
22	46.0401	46.0334	1.2891	-.281	24356.584
23	50.3181	32.7359	32.5662	-30.3703	-.0423
24	.0000	.0000	.0000	.0	.00
25	.0000	.0000	.00000	.0	.00
26	.00000	.0000	.00000	.0	.00
27	.0000	.0000	.00000	-73949.9	-453.7758
28	.0	.0000	.00000	-13658.3	-83.7747
29	3529.8525	25778.4430	.01251	-46.62267	
30	3619.2901	25141.4220	32.56652	89.34175	329681480.
31	.0	.00000	.00000	.00000	.0
32			.00000	.00000	.0
33	219076.5100	418.9128	-514.8240	.0000	

TABLE 4-3 (Sheet 19 of 19)
FLIGHT SIMULATED DATA (AD77)

S-IVB ENGINE CUTOFF SIGNAL

1	747.0400	265308.2	224601.7	625292.5	9654937.1
2	25718.6240	24395.4870	21530639.0	.0	26.4587
3	-1626616.0	.0	-2097298.9	.0	
4	232648.6	.0	253235.9	.0	
5	9591534.7	.0	10485640.9	.0	
6	-11021.7562	.0000	-12673.5950	.0000	27.2373
7	971.5366	.0000	230.8748	.0000	-.0833
8	21742.0510	.0000	22377.9890	.0000	.0561
9	224599.9	224600.2	-.3	29.288	-.000
10	-687.0	-686.7	-.0	7951.317	.010
11	462.5	451.6	-.0	-3028.662	.033
12	-71.6988	1.1373	.0	139137.9	.6488
13	-.4269	.0383	.0	8833065.3	1.0469
14	.0000	-.0000	.0	8833377.7	.0000
15	-71.0500	.0000	-71.0500	-.0085	509.04
16	.6200	.0000	.6200	1.1372	-1.41
17	.0000	.0000	.0000	.0383	.42
18	-.4489	-.4258	-.4252	.1752	-.0351
19	90.2425	90.2300	90.2313	.1152	-2.0652
20	433.1752	424.0341	-518.4972	-537.3410	227838.2
21	.0003	10.0820	.0000	2436.4758	.00
22	47.8580	47.8528	1.2116	-.283	24395.487
23	50.1611	32.7355	32.5658	-30.3715	-.0423
24	.0000	.0000	.0000	.0	.00
25	.0000	.0000	.00000	.0	.00
26	.00000	.0000	.00000	.0	.00
27	.0000	.0000	.00000	-74875.4	-435.1269
28	.0	.0000	.00000	-13829.2	-83.9858
29	3535.7771	25774.0500	.01386	-32.78249	
30	3635.1953	25069.1600	32.56650	89.75127	330681050.
31	.0	.00000	.00000	.00000	.0
32			.00000	.00000	.0
33	219076.5100	418.9128	-514.8240	.0000	

APPENDIX 5

METEOROLOGICAL DATA (AA99)

1. METEOROLOGICAL DATA (AA99)

A summary of the meteorological data during the AS-502 vehicle launch and flight is presented in this appendix. Surface measurements at the Kennedy Space Center at the time of launch are recorded as follows:

TIME (GMT)	AMOUNT (%)	CLOUDS (Coverage)	BASE (ft)	VISIB (nmi)	PRESS AT MSL* (m bars)	DRY BULB TEMP (deg F)	RELATIVE HUMIDITY (%)	WIND** DIRECTION (deg)	WIND SPEED (knots)**
1200	20	High Scattered	3500	10	1021	70	89	160	20

*MSL - Mean sea level.

**Measured at launch pad light pole.

Table AP 5-1 presents definitions, units, and sign conventions for the meteorological data presented in table AP 5-2. Table AP 5-2 records the meteorological data to an altitude of 300,000 ft.

TABLE AP 5-1
PROGRAM AA99 METEOROLOGICAL DATA

Table of Definitions

Program Symbol	Definition
Alt	Altitude: Geocentric altitude (ft)
Density	Density: row 2, column B (slugs/feet^3) row 3, column E (lb/ft^3)
Elec/Ref	Electromagnetic Index of Refraction: (unitless)
Opt./Ref	Optical Index of Refraction: (unitless)
Pit. Shear	Shear of Wind Velocity Pitch Component: (1/sec)
Press	Ambient Pressure: row 1, column C (millibars) row 2, column C (lb/ft^2)
Rel Humd	Relative Humidity: (decimal)
Temp	Ambient Temperature: row 1, column B (deg Kelvin) row 4, column A (deg Centrigrade)
Vap. Press	Water Vapor Pressure: (lb/ft^2)
Vel/Sound	Velocity of Sound: (ft/sec)
Visc.	Coefficient of Viscosity: (slugs/ft-sec)
Wd. Merid.	Meridional Component of Wind Velocity: Component of wind velocity vector measured along lines of longitude, positive north (ft/sec)
Wd. Zonal	Zonal Component of Wind Velocity: Component of wind velocity vector measured along lines of latitude, positive east (ft/sec)
Wind Dir	Wind Direction: Direction from which wind is blowing, measured clockwise from north (deg)
Wind Pitch	Wind Velocity Pitch Component: Component of wind velocity vector along vehicle flight path, positive downrange (ft/sec)
Wind Vel	Magnitude of Wind Velocity: (ft/sec)
Wind Yaw	Wind Velocity Yaw Component: Component of wind velocity vector perpendicular to pitch component, lying in the local tangent plane, and positive right looking downrange (ft/sec)
Yaw Shear	Shear of Wind Velocity Yaw Component: (1/sec)

TABLE AP 5-2 (Sheet 1 of 14)
METEOROLOGICAL DATA (AA99)

	A	B	C	D	E	F
1	ALT	TEMP,	PRESS	WIND VEL	WIND DIR	REL HUMD
2	VAP, PRESS	DENSITY	PRESS	VEL/SOUND	OPT,/REF	ELEC/REF
3	WIND PITCH	WIND YAW	WD, ZONAL	WD, MERID,	DENSITY	VISC,
4	TEMP,	PIT, SHEAR	YAW SHEAR			

	A	B	C	D	E	F
1	-,0	292,55	1019,600	26,2467	160,000	,8900
2	41,8874	,0023	2129,475	1129,163	268,6568	357,9204
3	-1,4488	-,0001	-,1296	24,6638	,7384	,000000
4	19,400**********					

	A	B	C	D	E	F
1	1000,0	292,49	984,827	37,7814	138,192	,7663
2	35,9299	,0023	2056,850	1128,572	260,1264	336,3413
3	-,0859	-,0350	-,0083	28,1611	,7139	,000000
4	19,340**********					

	A	B	C	D	E	F
1	2000,0	289,89	950,558	39,0845	142,384	,8995
2	35,8054	,0022	1985,278	1123,658	253,1865	330,6045
3	-,0657	-,0306	-,0187	30,9600	,6951	,000000
4	16,736**********					

	A	B	C	D	E	F
1	3000,0	287,40	917,190	38,4748	146,424	,9566
2	32,4706	,0021	1915,589	1118,600	246,6854	317,9023
3	-,0875	-,0301	-,0389	32,0591	,6768	,000000
4	14,251**********					

	A	B	C	D	E	F
1	4000,0	287,45	884,811	32,7719	144,464	,5479
2	18,6581	,0021	1847,964	1117,238	239,5899	279,2183
3	-,1018	-,0415	-,0563	26,6692	,6545	,000000
4	14,301	,002822	,00099273			

	A	B	C	D	E	F
1	5000,0	290,32	853,697	22,6486	142,750	,1825
2	7,4648	,0020	1782,981	1121,529	230,2405	244,0180
3	-,1768	-,0380	-,0980	18,0282	,6267	,000000
4	17,166	,0[illegible]5	,00472447			

	A	B	C	D	E	F
1	6000,0	288,48	823,695	13,5118	119,304	,4009
2	14,5888	,0019	1720,321	1118,896	222,5962	252,8979
3	-,1240	-,0997	-,0420	6,6185	,6075	,000000
4	15,333	,000505	,00940384			

	A	B	C	D	E	F
1	7000,0	286,45	794,556	10,4968	121,312	,4490
2	14,3283	,0019	1659,462	1114,976	216,2132	246,4557
3	-,0618	-,1615	-,1298	5,4487	,5901	,000000
4	13,298	-1365,440100	,00857511			

	A	B	C	D	E	F
1	8000,0	285,30	766,305	7,3588	149,608	,1945
2	5,7553	,0018	1600,458	1111,670	210,4295	221,0687
3	-,1536	-,0919	-,3567	6,3532	,5725	,000000
4	12,148	,001832	,00532091			

TABLE AP 5-2 (Sheet 2 of 14)
METEOROLOGICAL DATA (AA99)

FLOATING POINT OVERFLOW AT LOCATION 020607

	A	B	C	D	E	F
1	9000.0	284.47	738.901	11.3226	189.000	.1405
2	3.9370	.0018	1543.225	1109.834	203.7070	210.2587
3	5.1403	-.0948	1.7712	11.1832	.5539	.000000
4	11.319	.004512	.00062113			

	A	B	C	D	E	F
1	10000.0	282.44	712.380	7.3675	237.520	.2038
2	4.9866	.0017	1487.835	1106.042	197.6456	206.8950
3	7.1301	-.7189	6.2116	3.9561	.5377	.000000
4	9.293	.004726	.00181869			

	A	B	C	D	E	F
1	11000.0	280.04	686.671	2.6940	293.336	.2652
2	5.5093	.0017	1434.139	1101.429	192.0534	202.8340
3	2.0224	1.7792	2.4732	-1.1466	.5226	.000000
4	6.890	.001104	.00260155			

	A	B	C	D	E	F
1	12000.0	277.00	661.568	3.8087	301.568	.3930
2	6.6075	1.16	1381.710	1095.631	186.887	200.7244
3	2.4627	2.8951	3.2368	-.3953	.5089	.000000
4	3.850	-103.467642	.00346560			

	A	B	C	D	E	F
1	13000.0	274.96	637.240	7.1869	327.488	.3620
2	5.2656	.0016	1330.901	1091.419	181.5002	192.2904
3	1.8061	6.9537	3.8665	-.0633	.4939	.000000
4	1.811	-52.078715	.00354180			

	A	B	C	D	E	F
1	14000.0	272.51	613.574	3.4861	352.312	.3428
2	4.1728	.0015	1281.474	1086.391	176.4581	184.7669
3	-1.5811	3.4299	.4678	-.2709	.4800	.000000
4	-.178	-99.921349	.00107056			

	A	B	C	D	E	F
1	15000.0	270.00	590.512	5.1365	333.880	.3944
2	3.9903	.0015	1233.309	1081.387	171.4034	179.4981
3	.7263	5.0848	2.2620	-.2438	.4662	.000000
4	-.027	-497.070680	.00085190			

	A	B	C	D	E	F
1	16000.0	267.74	568.199	1.9942	85.440	.4046
2	3.4505	.0014	1186.707	1076.773	166.3768	173.2876
3	-.6178	-3.0912	-.6504	-5.9331	.4525	.000000
4	-.020	-80.850806	-47.74938200			

	A	B	C	D	E	F
1	17000.0	265.76	546.560	14.2307	193.528	.4308
2	3.1560	.0014	1141.513	1072.761	161.2530	167.5772
3	7.4440	-.0312	3.3323	13.8333	.4385	.000000
4	-.005	.002489	-26.97998300			

	A	B	C	D	E	F
1	18000.0	263.93	525.617	17.0462	216.456	.4595
2	2.9175	.0013	1097.772	1069.042	156.1643	162.0243
3	13.8656	-.1003	10.1232	13.7139	.4246	.000000
4	-.013	.003492	-22.00061500			

TABLE AP 5-2 (Sheet 3 of 14)
METEOROLOGICAL DATA (AA99)

	A	B	C	D	E	F
1	19000.0	262.60	505.295	19.6648	250.648	.3201
2	1.8296	.0013	1055.328	1066.161	151.0244	154.0577
3	19.6588	-1.6955	18.5546	6.5121	.4104	.000000
4	-.011	.0[illegible]9	-100.16845300			

	A	B	C	D	E	F
1	20000.0	260.58	485.672	11.6772	260.360	.2623
2	1.2744	.0013	1014.345	1061.954	146.3544	147.9847
3	11.5507	1.6860	11.5064	1.9659	.3976	.000000
4	-.007	.000714	.00350763			

	A	B	C	D	E	F
1	21000.0	258.32	466.650	16.0283	272.096	.2500
2	1.0093	.0012	974.618	1057.300	141.8818	142.8836
3	15.0515	5.5078	16.0169	-2.0373	.3854	.000000
4	-.002	-476.618770	.00478764			

	A	B	C	D	E	F
1	22000.0	256.42	448.228	20.0759	271.896	.2171
2	.7474	.0012	936.143	1053.341	137.3264	137.6802
3	18.8678	6.8339	20.0561	-1.6930	.3730	.000000
4	-.007	.000419	.00286140			

	A	B	C	D	E	F
1	23000.0	254.28	430.400	19.1278	260.584	.1683
2	.4831	.0011	898.908	1048.881	133.0087	132.6853
3	18.9124	2.8582	18.8700	3.1259	.3612	.000000
4	-.006	.000877	.00075284			

	A	B	C	D	E	F
1	24000.0	252.00	413.157	16.7265	256.000	.1196
2	.2817	.0011	862.894	1044.141	128.8577	128.0175
3	16.6858	1.1668	16.2297	4.0465	.3499	.000000
4	-.005	.000834	-33.36934300			

	A	B	C	D	E	F
1	25000.0	249.54	396.463	22.0604	277.400	.0804
2	.1522	.0011	828.029	1038.995	124.8895	123.7267
3	19.9220	9.4637	21.8714	-.2183	.3391	.000000
4	-.004	.000741	.00177095			

	A	B	C	D	E	F
1	26000.0	247.15	380.223	19.7874	299.000	.0630
2	.0960	.0010	794.111	1034.003	120.9370	119.6624
3	13.4950	14.4716	17.3065	-.1103	.3284	.000000
4	-.003	-60.1[illegible]7	.00309922			

	A	B	C	D	E	F
1	27000.0	244.99	364.528	15.1394	302.448	.0784
2	.0977	.0010	761.332	1029.470	116.9669	115.7551
3	9.6378	11.6713	12.7727	-.1563	.3176	.000000
4	-.002	-18.202416	.00293762			

	A	B	C	D	E	F
1	28000.0	242.59	349.396	20.9231	284.000	.1014
2	.1007	.0010	729.728	1024.417	113.2187	112.0717
3	17.7438	11.0876	20.3016	-.1875	.3074	.000000
4	-.001	-113.632776	.00213921			

TABLE AP 5-2 (Sheet 4 of 14)
METEOROLOGICAL DATA (AA99)

	A	B	C	D	E	F
1	29000.0	240.17	334.642	20.9735	279.000	.1136
2	.0892	.0009	698.914	1019.285	109.5325	108.4029
3	18.6875	9.5218	20.7153	-.2348	.2974	.000000
4	-.004	.001694	-155.88920000			

	A	B	C	D	E	F
1	30000.0	237.60	320.485	17.8058	262.240	.1315
2	.0800	.0009	669.345	1013.821	106.0320	104.9242
3	17.5216	3.1656	17.6423	2.4038	.2879	.000000
4	-.003	.002319	-34.02806800			

FLOATING POINT OVERFLOW AT LOCATION 020715

	A	B	C	D	E	F
1	31000.0	235.24	306.761	19.9643	260.856	.1400
2	.0670	.0009	640.683	1008.773	102.5101	101.4098
3	19.7247	3.0758	19.7098	3.1701	.2783	.000000
4	-.003	.001102	-37.48742100			

	A	B	C	D	E	F
1	32000.0	232.82	293.446	29.6079	272.144	.1401
2	.0521	.0009	612.874	1003.565	99.0814	97.9795
3	27.7958	10.1973	29.5865	-1.0632	.2690	.000000
4	-.003	.002544	.00034367			

	A	B	C	D	E	F
1	33000.0	230.23	280.660	30.1606	268.328	.1500
2	.0423	[illegible]8	586.170	997.968	95.830	94.7403
3	28.9393	8.4815	30.1438	.8763	.2602	.000000
4	-.003	.002914	.00096454			

	A	B	C	D	E	F
1	34000.0	227.63	268.226	35.6354	259.944	.1545
2	.0327	.0008	560.201	992.310	92.6322	91.5532
3	35.2883	4.9226	35.0824	6.2231	.2515	.000000
4	-.002	.005104	.00144797			

	A	B	C	D	E	F
1	35000.0	225.01	256.242	44.4632	265.280	.1667
2	.0262	.0008	535.171	986.581	89.5240	88.4646
3	43.2734	10.2114	44.3109	3.6606	.2431	.000000
4	-.002	.005295	.00082205			

	A	B	C	D	E	F
1	36000.0	222.67	244.616	52.1026	265.000	.1700
2	.0204	.0007	510.891	981.436	86.3604	85.3226
3	50.7672	11.7205	51.9044	4.5410	.2345	.000000
4	-.002	.006736	.00071864			

	A	B	C	D	E	F
1	37000.0	220.31	233.501	54.4312	258.000	.1800
2	.0163	.0007	487.675	976.219	83.3192	82.3073
3	54.1331	5.6896	53.2418	11.3169	.2262	.000000
4	-.001	.006423	**********			

	A	B	C	D	E	F
1	38000.0	217.95	222.729	63.9898	253.704	.1800
2	.0122	.0007	465.178	970.991	80.3332	79.3459
3	63.9594	1.9030	61.4171	17.9547	.2181	.000000
4	-.001	.007000	-50.20767700			

TABLE AP 5-2 (Sheet 5 of 14)
METEOROLOGICAL DATA (AA99)

	A	B	C	D	E	F
1	39000.0	216.00	212.349	66.4942	254.488	.1855
2	.0099	.0007	443.500	966.621	77.2831	76.3272
3	66.4286	2.8954	64.0721	17.7739	.2098	.000000
4	-.001	.005216	-34.28013500			

FLOATING POINT OVERFLOW AT LOCATION 020715

	A	B	C	D	E	F
1	40000.0	214.21	202.351	72.2887	251.680	.0441
2	.0019	[illegible]6	422.618	962.599	74.261	73.3129
3	72.2852	-.2492	68.6236	22.7181	.2016	.000000
4	-.001	.005719	-45.77342000			

FLOATING POINT OVERFLOW AT LOCATION 020607

	A	B	C	D	E	F
1	41000.0	212.67	192.798	80.0981	251.872**********	
2**********		.0006	402.666	959.135	71.2666	70.3501
3	80.0966	-5999616.2000	76.1218	24.9192	.1935	.000000
4	-.000	.006839	-35.26215200			

	A	B	C	D	E	F
1	42000.0	210.56	183.569	82.6118	254.936**********	
2**********		.0006	383.392	954.368	68.5342	67.6535
3	82.5027	4.2298	79.7718	21.4720	.1861	.000000
4	-.000	.005904	-17.61506900			

FLOATING POINT OVERFLOW AT LOCATION 021123

	A	B	C	D	E	F
1	43000.0	209.09	174.743	82.8221	257.512**********	
2**********		.0006	364.958	951.041	65.6956	64.8520
3	82.4299	7.9513	80.8526	17.9100	.1784	.000000
4	-.002	.003728	.00260325			

	A	B	C	D	E	F
1	44000.0	209.21	166.284	78.1562	262.552**********	
2**********		.0005	347.291	951.319	62.4781	61.6766
3	76.8322	14.3086	77.4934	10.1342	.1696	.000000
4	-.000	-1103.657300	.00499651			

	A	B	C	D	E	F
1	45000.0	208.56	158.269	76.3622	255.360**********	
2**********		.0005	330.551	949.827	59.6528	58.8883
3	76.2286	4.4697	73.8789	19.3049	.1620	.000000
4	-.002	-72.872408**********				

	A	B	C	D	E	F
1	46000.0	208.56	150.592	76.3223	260.168**********	
2**********		.0005	314.517	949.826	56.7587	56.0319
3	75.5467	10.8416	75.1994	13.0342	.1541	.000000
4	-.002	-14.506442	.00190617			

	A	B	C	D	E	F
1	47000.0	208.74	143.321	67.1827	267.048**********	
2**********		.0005	299.332	950.241	53.9705	53.2801
3	64.8784	17.4409	67.0925	3.4613	.1466	.000000
4	-.002	-23.354703	-63.98852500			

	A	B	C	D	E	F
1	48000.0	208.27	136.351	54.9060	275.000**********	
2**********		.0004	284.774	949.173	51.4607	50.8028
3	50.5413	21.4535	54.6971	-.2220	.1397	.000000
4	-.002	-6.552878	.00378649			

TABLE AP 5-2 (Sheet 6 of 14)
METEOROLOGICAL DATA (AA99)

	A	B	C	D	E	F
1	49000.0	206.91	129.754	47.5961	280.574	**********
2	**********	.0004	270.995	946.063	49.2930	48.6632
3	41.7991	22.7634	46.7876	-.1372	.1339	.000000
4	-.002	-7.298424	.00389302			

	A	B	C	D	E	F
1	50000.0	205.59	123.404	45.9255	277.200	**********
2	**********	.0004	257.735	943.051	47.1804	46.5780
3	41.5543	19.5538	45.5629	-.1007	.1281	.000000
4	-.002	-13.639722	.00152254			

	A	B	C	D	E	F
1	51000.0	205.28	117.325	64.0004	281.610	**********
2	**********	.0004	245.039	942.321	44.9256	44.3523
3	55.6405	31.6233	62.6894	-.0076	.1220	.000000
4	-.002	.000863	.00313567			

	A	B	C	D	E	F
1	52000.0	206.01	111.585	70.8688	288.387	**********
2	**********	.0004	233.050	944.004	42.5750	42.0322
3	57.0512	42.0423	67.2507	-.0304	.1156	.000000
4	-.002	.003835	.00595773			

	A	B	C	D	E	F
1	53000.0	206.13	106.161	60.7904	288.433	**********
2	**********	.0003	221.722	944.272	40.4821	39.9663
3	48.9088	36.1027	57.6714	-.0549	.1099	.000000
4	-.002	.002435	.00467317			

	A	B	C	D	E	F
1	54000.0	205.55	100.974	53.0278	287.171	**********
2	**********	.0003	210.888	942.946	38.6121	38.1204
3	43.3465	30.5454	50.6640	-.0827	.1049	.000000
4	-.002	-33.074928	.00088044			

	A	B	C	D	E	F
1	55000.0	204.80	95.978	42.2607	291.568	**********
2	**********	.0003	200.453	941.228	36.8353	36.3665
3	32.5752	26.9211	39.2999	-.0837	.1000	.000000
4	-.002	-7.118618	-25.42141200			

	A	B	C	D	E	F
1	56000.0	203.95	91.238	36.0502	281.350	**********
2	**********	.0003	190.555	939.273	35.1621	34.7149
3	31.4226	17.6694	35.3448	-.1884	.0955	.000000
4	-.002	-11.872788	-10.55246200			

	A	B	C	D	E	F
1	57000.0	203.65	86.702	37.7056	278.032	**********
2	**********	.0003	181.080	938.590	33.4621	33.0367
3	33.8802	16.5481	37.3356	-.1616	.0909	.000000
4	-.002	-26.196335	-26.76338700			

	A	B	C	D	E	F
1	58000.0	203.42	82.387	39.3652	280.427	**********
2	**********	.0003	172.070	938.055	31.8332	31.4287
3	34.6186	18.7395	38.7151	-.1875	.0864	.000000
4	-.002	-392.913060	-33.64209200			

TABLE AP 5-2 (Sheet 7 of 14)
METEOROLOGICAL DATA (AA99)

	A	B	C	D	E	F
1	59000.0	204.01	78.318	30.1764	286.480	**********
2	**********	.0003	163.570	939.411	30.1732	29.7900
3	24.8761	17.0808	28.9369	-.1427	.0819	.000000
4	-.002	-33.619567	-176.45176000			

	A	B	C	D	E	F
1	60000.0	204.60	74.520	14.7496	303.196	**********
2	**********	.0002	155.639	940.779	28.6266	28.2633
3	9.2479	11.4885	12.3454	-.1580	.0777	.000000
4	-.002	-4.522089	-89.72830500			

	A	B	C	D	E	F
1	61000.0	204.61	70.810	5.3160	331.810	**********
2	**********	.0002	147.889	940.792	27.2003	26.8552
3	.9393	5.2322	2.5101	-.2345	.0739	.000000
4	-.002	-10.838432	-22.21466500			

	A	B	C	D	E	F
1	62000.0	205.17	67.333	2.9734	290.574	**********
2	**********	.0002	140.628	942.074	25.7942	25.4671
3	2.3238	1.8531	2.7827	-1.1921	.0700	.000000
4	-.002	-15.732132	-24.13893000			

	A	B	C	D	E	F
1	63000.0	205.57	64.006	8.4364	310.093	**********
2	**********	.0002	133.678	943.005	24.4710	24.1608
3	4.4573	7.1624	6.4525	-.1409	.0665	.000000
4	-.002	-39.498547	-12.88236620			

	A	B	C	D	E	F
1	64000.0	207.60	60.927	13.1913	255.926	**********
2	**********	.0002	127.248	947.632	23.0668	22.7746
3	-.3216	12.5604	-.1426	-.0292	.0626	.000000
4	-.002	-64.274601	.00187361			

	A	B	C	D	E	F
1	65000.0	209.05	57.921	18.7904	41.797	**********
2	**********	.0002	120.971	950.946	21.7762	21.5004
3	-.0782	9.4538	-.0188	-.0956	.0591	.000000
4	-.002	-19.315471	.00210283			

	A	B	C	D	E	F
1	66000.0	208.33	55.161	14.8273	55.713	**********
2	**********	.0002	115.207	949.305	20.8103	20.5469
3	-.0939	4.1592	-.0273	-.1491	.0565	.000000
4	-.002	-18.747076	-81.00910200			

	A	B	C	D	E	F
1	67000.0	208.81	52.480	9.6020	97.681	**********
2	**********	.0002	109.607	950.401	19.7531	19.5031
3	-.1399	-.3008	-.1130	1.2801	.0536	.000000
4	-.002	-51.485042	-25.26226500			

	A	B	C	D	E	F
1	68000.0	211.06	49.985	6.0827	196.189	**********
2	**********	.0002	104.397	955.508	18.6134	18.3780
3	3.4189	-.1920	1.6986	5.8360	.0506	.000000
4	-.000	.005703	-24.23542500			

TABLE AP 5-2 (Sheet 8 of 14)
METEOROLOGICAL DATA (AA99)

	A	B	C	D	E	F
1	69000.0	211.95	47.559	7.1260	283.882**********	
2	**********	.0002	99.328	957.517	17.6354	17.4124
3	6.0403	3.7682	6.9091	-.3095	.0479	.000000
4	-.000	.006443	-328.40972000			

	A	B	C	D	E	F
1	70000.0	213.34	45.308	12.7508	322.890**********	
2	**********	.0001	94.628	960.648	16.6915	16.4805
3	4.1737	12.0440	7.6912	-.0925	.0453	.000000
4	-.001	.004552	.00392507			

	A	B	C	D	E	F
1	71000.0	215.44	43.234	14.8810	350.022**********	
2	**********	.0001	90.297	965.366	15.7722	15.5729
3	7.6013	14.7343	2.5766	-.0906	.0428	.000000
4	-.001	-170.239980	.00627319			

	A	B	C	D	E	F
1	72000.0	216.28	41.164	16.0768	17.013**********	
2	**********	.0001	85.973	967.260	14.9581	14.7691
3	-.1219	13.1645	-.2322	-.0850	.0406	.000000
4	-.001	-26.828267	.00369437			

	A	B	C	D	E	F
1	73000.0	217.45	39.298	19.6890	55.029**********	
2	**********	.0001	82.075	969.863	14.2033	14.0238
3	-.0579	5.7468	-.0790	-.0575	.0386	.000000
4	-.001	-1.118342	-27.96067400			

	A	B	C	D	E	F
1	74000.0	217.82	37.464	20.7923	70.860**********	
2	**********	.0001	78.244	970.678	13.5176	13.3469
3	-.0426	.4134	-.0516	-.1971	.0367	.000000
4	-.001	-14.127966	-30.68734000			

	A	B	C	D	E	F
1	75000.0	218.09	35.677	13.1156	71.760**********	
2	**********	.0001	74.513	971.297	12.8567	12.6943
3	-.0002	-5504008.3000	-.0208	-.3071	.0349	.000000
4	-.001	-45.559435	-28.18582600			

	A	B	C	D	E	F
1	76000.0	218.08	34.038	10.9602	74.593**********	
2	**********	.0001	71.089	971.275	12.2663	12.1115
3	-.0679	-2.5965	-.0799	-.1844	.0333	.000000
4	-.001	.001563	-43.01641400			

	A	B	C	D	E	F
1	77000.0	218.23	32.455	6.9569	79.146**********	
2	**********	.0001	67.784	971.590	11.6885	11.5410
3	-.1944	-1.5512	-.1966	-.6596	.0317	.000000
4	-.001	.004742	-205.69990000			

	A	B	C	D	E	F
1	78000.0	218.55	30.981	13.4262	68.932**********	
2	**********	.0001	64.705	972.312	11.1409	11.0003
3	-.0979	.7188	-.0186	-.2169	.0303	.000000
4	-.001**********		.00010674			

TABLE AP 5-2 (Sheet 9 of 14)
METEOROLOGICAL DATA (AA99)

	A	B	C	D	E	F
1	79000.0	218.87	29.547	17.4430	61.357	**********
2	**********	.0001	61.710	973.016	10.6099	10.4760
3	-.0711	3.2214	-.0855	-.1488	.0288	.000000
4	-.001	-53.503897	.00112699			

	A	B	C	D	E	F
1	80000.0	220.14	28.205	23.2021	62.000	**********
2	**********	.0001	58.908	975.841	10.0694	9.9424
3	-.0265	4.0290	-.0450	-.0697	.0273	.000000
4	-.001	-27.030388	.00145008			

	A	B	C	D	E	F
1	81000.0	221.25	26.941	28.7124	65.105	**********
2	**********	.0001	56.268	978.309	9.5698	9.4491
3	-.0469	3.4466	-.0016	-.0324	.0260	.000000
4	-.001	-21.529219	.00101325			

	A	B	C	D	E	F
1	82000.0	222.03	25.725	29.5209	73.796	**********
2	**********	.0001	53.728	980.033	9.1057	8.9908
3	-.0449	-1.3201	-.0472	-.1527	.0247	.000000
4	-.002	-30.342570	-96.72653200			

	A	B	C	D	E	F
1	83000.0	223.56	24.523	34.1811	74.702	**********
2	**********	.0001	51.218	983.393	8.6210	8.5123
3	-.0358	-.1199	-.0381	-.1283	.0234	.000000
4	-.002	-30.276329	-46.23274800			

	A	B	C	D	E	F
1	84000.0	225.10	23.424	24.8355	76.047	**********
2	**********	.0001	48.923	986.769	8.1784	8.0753
3	-.0115	-.7644	-.0168	-.0716	.0222	.000000
4	-.002	.000770	-28.18509000			

	A	B	C	D	E	F
1	85000.0	225.83	22.391	24.4271	98.951	**********
2	**********	.0001	46.765	988.371	7.7923	7.6941
3	-.0350	-.0641	-.0166	3.8038	.0212	.000000
4	-.002	.002344	-12.57471650			

	A	B	C	D	E	F
1	86000.0	226.05	21.332	28.9667	118.390	**********
2	**********	.0001	44.552	988.855	7.4163	7.3229
3	-.0490	-.0412	-.0060	13.7738	.0201	.000000
4	-.002	.004600	-16.02757800			

	A	B	C	D	E	F
1	87000.0	227.10	20.443	25.9934	127.379	**********
2	**********	.0001	42.695	991.147	7.0744	6.9853
3	-.0897	-.0379	-.0437	15.7806	.0192	.000000
4	-.002	.003421	-12.28386370			

	A	B	C	D	E	F
1	88000.0	227.89	19.495	22.6804	112.243	**********
2	**********	.0001	40.715	992.881	6.7228	6.6381
3	-.0698	-.0906	-.0411	8.5851	.0183	.000000
4	-.002	.001509	-51.77767900			

TABLE AP 5-2 (Sheet 10 of 14)
METEOROLOGICAL DATA (AA99)

	A	B	C	D	E	F
1	89000.0	228.56	18.641	21.2314	93.767	**********
2	**********	.0001	38.932	994.319	6.4097	6.3289
3	-.0510	-.1641	-.0395	1.3952	.0174	.000000
4	-.002	.000233	.00331291			

	A	B	C	D	E	F
1	90000.0	229.14	17.788	22.0637	85.971	**********
2	**********	.0001	37.150	995.593	6.1008	6.0239
3	-.0378	-.1544	-.0331	-.4217	.0166	.000000
4	-.002	-42.182452	.00502403			

	A	B	C	D	E	F
1	91000.0	229.34	17.031	19.8568	87.818	**********
2	**********	.0001	35.570	996.035	5.8361	5.7626
3	-.0558	-.1437	-.0500	-.5104	.0159	.000000
4	-.002	-80.280591	.00347006			

	A	B	C	D	E	F
1	92000.0	230.65	16.299	19.6814	88.499	**********
2	**********	.0000	34.040	998.864	5.5535	5.4835
3	-.0576	-.1215	-.0513	-2.4375	.0151	.000000
4	-.003	.000448	.00114622			

	A	B	C	D	E	F
1	93000.0	232.00	15.566	17.0636	94.831	**********
2	**********	.0000	32.510	1001.778	5.2730	5.2066
3	-.0822	-.2033	-.0722	1.4353	.0143	.000000
4	-.003	.001362	-326.62670000			

	A	B	C	D	E	F
1	94000.0	232.55	14.896	13.1000	99.766	**********
2	**********	.0000	31.110	1002.971	5.0339	4.9705
3	-.0479	-.0574	-.0067	2.2220	.0137	.000000
4	-.003	.002651	-55.21714800			

	A	B	C	D	E	F
1	95000.0	232.47	14.287	10.3930	89.205	**********
2	**********	.0000	29.838	1002.793	4.8299	4.7691
3	-.0999	-.1028	-.0854	-4.8252	.0131	.000000
4	-.003	.002742	.00071650			

	A	B	C	D	E	F
1	96000.0	231.74	13.678	12.8167	81.532	**********
2	**********	.0000	28.567	1001.216	4.6387	4.5803
3	-.0151	-.5811	-.0140	-.6950	.0126	.000000
4	-.003	.001722	.00131483			

	A	B	C	D	E	F
1	97000.0	231.66	13.067	6.3799	112.998	**********
2	**********	.0000	27.291	1001.050	4.4329	4.3771
3	-.2185	-.2973	-.0863	2.4912	.0120	.000000
4	-.003	.001986	.00073192			

	A	B	C	D	E	F
1	98000.0	232.49	12.457	6.5131	142.741	**********
2	**********	.0000	26.016	1002.843	4.2108	4.1578
3	-.5663	-.0517	-.3273	5.1836	.0114	.000000
4	-.003	.002620	-184.98340000			

TABLE AP 5-2 (Sheet 11 of 14)
METEOROLOGICAL DATA (AA99)

	A	B	C	D	E	F
1	99000.0	233.03	11.918	4.2464	144.604	**********
2	**********	.0000	24.892	1004.006	4.0194	3.9688
3	-.7419	-.3137	-.4107	3.4615	.0109	.000000
4	-.003	.003249	-214.26389000			

	A	B	C	D	E	F
1	100000.0	233.52	11.432	3.2748	151.966	**********
2	**********	.0000	23.875	1005.056	3.8472	3.7988
3	-1.9977	-.0281	-.2028	2.8904	.0104	.000000
4	-.003	.001685	.00006935			

	A	B	C	D	E	F
1	105000.0	235.36	9.193	16.4042	181.016	**********
2	**********	.0000	19.201	1009.015	3.0698	3.0311
3	5.3450	-.0839	.2909	16.4016	.0083	.000000
4	-.003	.001212	-3.37203220			

	A	B	C	D	E	F
1	115000.0	241.11	6.146	22.9659	230.000	**********
2	**********	.0000	12.836	1021.268	2.0032	1.9780
3	21.2936	-.1413	17.5929	14.7622	.0054	.000000
4	-.004	.002948	-105.83675100			

	A	B	C	D	E	F
1	120000.0	243.02	4.981	33.4197	248.764	**********
2	**********	.0000	10.402	1025.306	1.6106	1.5904
3	33.3652	-.7421	31.1489	12.1056	.0044	.000000
4	-.001	.003410	.00667384			

	A	B	C	D	E	F
1	125000.0	249.29	4.055	41.3327	331.238	**********
2	**********	.0000	8.469	1038.443	1.2784	1.2623
3	7.7180	40.6057	19.8881	-.0318	.0035	.000000
4	-.004	-27.436673	.00169646			

	A	B	C	D	E	F
1	130000.0	250.38	3.308	29.5276	331.000	**********
2	**********	.0000	6.909	1040.716	1.0383	1.0252
3	5.6341	28.9851	14.3152	-.0033	.0028	.000000
4	-.005	-34.252934	-54.81344200			

	A	B	C	D	E	F
1	135000.0	253.36	2.705	35.3543	275.184	.0000
2	.0000	.0000	5.649	1046.881	.8390	.8284
3	32.4621	13.9928	35.1973	-.4301	.0023	.000000
4	-.006	.005915	-28.55761400			

	A	B	C	D	E	F
1	140000.0	260.70	2.220	52.4934	295.312	.0000
2	.0000	.0000	4.637	1061.947	.6693	.6609
3	38.1945	36.0078	47.4522	-.0297	.0018	.000000
4	-.007	-87.971567	.00201963			

	A	B	C	D	E	F
1	145000.0	264.31	1.831	40.5249	246.616	.0000
2	.0000	.0000	3.824	1069.273	.5444	.5376
3	39.6691	1.7121	36.3227	16.5820	.0015	.000000
4	-.014	-13.506067	-7.00462940			

TABLE AP 5-2 (Sheet 12 of 14)
METEOROLOGICAL DATA (AA99)

	A	B	C	D	E	F
1	150000.0	266.31	1.512	52.0997	233.480	.0000
2	.0000	.0000	3.158	1073.298	.4462	.4406
3	49.3818	-.0644	41.8451	31.0167	.0012	.000000
4	-.009	-30.889440	-102.09422300			

	A	B	C	D	E	F
1	155000.0	271.70	1.252	91.7848	243.904	.0000
2	.0000	.0000	2.615	1084.110	.3621	.3576
3	90.8657	-.0118	82.4259	40.3668	.0010	.000000
4	-.072	.008161	.00356888			

	A	B	C	D	E	F
1	160000.0	274.75	1.041	114.5932	273.072	.0000
2	.0000	.0000	2.174	1090.184	.2978	.2940
3	106.9306	41.1969	114.4276	-.0760	.0008	.000000
4	1.601	-3.971955	.01122213			

	A	B	C	D	E	F
1	165000.0	270.86	.838	.0000	.000	.0000
2	.0000	.0000	1.749	1082.445	.2430	.2400
3	.0000**********	**********	.0000	.0000	.0007	.000000
4	-.054	-.834013	-9.09914370			

	A	B	C	D	E	F
1	170000.0	267.60	.687	.0000	.000	.0000
2	.0000	.0000	1.434	1075.896	.2017	.1992
3	.0000**********	**********	.0000	.0000	.0005	.000000
4	-.019	.000000**********				

	A	B	C	D	E	F
1	175000.0	264.33	.563	.0000	.000	.0000
2	.0000	.0000	1.176	1069.308	.1674	.1653
3	.0000**********	**********	.0000	.0000	.0005	.000000
4	-.014	.000000**********				

	A	B	C	D	E	F
1	180000.0	261.06	.462	.0000	.000	.0000
2	.0000	.0000	.964	1062.678	.1390	.1372
3	.0000**********	**********	.0000	.0000	.0004	.000000
4	-.008	.000000**********				

	A	B	C	D	E	F
1	185000.0	257.25	.379	.0000	.000	.0000
2	.0000	.0000	.791	1054.887	.1158	.1143
3	.0000**********	**********	.0000	.0000	.0003	.000000
4	-.005	.000000**********				

	A	B	C	D	E	F
1	190000.0	253.11	.310	.0000	.000	.0000
2	.0000	.0000	.648	1046.371	.0963	.0951
3	.0000**********	**********	.0000	.0000	.0003	.000000
4	-.006	.000000**********				

	A	B	C	D	E	F
1	195000.0	248.76	.253	.0000	.000	.0000
2	.0000	.0000	.528	1037.330	.0799	.0789
3	.0000**********	**********	.0000	.0000	.0002	.000000
4	-.004	.000000**********				

TABLE AP 5-2 (Sheet 13 of 14)
METEOROLOGICAL DATA (AA99)

	A	B	C	D	E	F
1	200000.0	244.25	.206	.0000	.000	.0000
2	.0000	.0000	.430	1027.883	.0662	.0653
3	.0000**********		.0000	.0000	.0002	.000000
4	-.002	.000000**********				

	A	B	C	D	E	F
1	205000.0	239.64	.167	.0000	.000	.0000
2	.0000	.0000	.348	1018.137	.0546	.0539
3	.0000**********		.0000	.0000	.0001	.000000
4	-.004	.000000**********				

	A	B	C	D	E	F
1	210000.0	234.98	.134	.0000	.000	.0000
2	.0000	.0000	.281	1008.192	.0449	.0444
3	.0000**********		.0000	.0000	.0001	.000000
4	-.003	.000000**********				

	A	B	C	D	E	F
1	215000.0	230.31	.108	.0000	.000	.0000
2	.0000	.0000	.226	998.136	.0368	.0364
3	.0000**********		.0000	.0000	.0001	.000000
4	-.003	.000000**********				

	A	B	C	D	E	F
1	220000.0	225.68	.086	.0000	.000	.0000
2	.0000	.0000	.180	988.043	.0301	.0297
3	.0000**********		.0000	.0000	.0001	.000000
4	-.002	.000000**********				

	A	B	C	D	E	F
1	225000.0	221.10	.069	.0000	.000	.0000
2	.0000	.0000	.144	977.976	.0245	.0241
3	.0000**********		.0000	.0000	.0001	.000000
4	-.001	.000000**********				

	A	B	C	D	E	F
1	230000.0	216.61	.055	.0000	.000	.0000
2	.0000	.0000	.114	967.978	.0198	.0195
3	.0000**********		.0000	.0000	.0001	.000000
4	-.001	.000000**********				

	A	B	C	D	E	F
1	235000.0	212.20	.043	.0000	.000	.0000
2	.0000	.0000	.090	958.077	.0159	.0157
3	.0000**********		.0000	.0000	.0000	.000000
4	-.000	.000000**********				

	A	B	C	D	E	F
1	240000.0	207.88	.034	.0000	.000	.0000
2	.0000	.0000	.071	948.280	.0128	.0126
3	.0000**********		.0000	.0000	.0000	.000000
4	-.002	.000000**********				

	A	B	C	D	E	F
1	245000.0	203.65	.026	.0000	.000	.0000
2	.0000	.0000	.055	938.573	.0102	.0101
3	.0000**********		.0000	.0000	.0000	.000000
4	-.002	.000000**********				

TABLE AP 5-2 (Sheet 14 of 14)
METEOROLOGICAL DATA (AA99)

	A	B	C	D	E	F
1	250000.0	199.48	.021	.0000	.000	.0000
2	.0000	.0000	.043	928.917	.0081	.0080
3	.0000**********		.0000	.0000	.0000	.000000
4	-.002	.000000**********				

	A	B	C	D	E	F
1	255000.0	195.35	.016	.0000	.000	.0000
2	.0000	.0000	.033	919.246	.0064	.0063
3	.0000**********		.0000	.0000	.0000	.000000
4	-.002	.000000**********				

	A	B	C	D	E	F
1	260000.0	191.21	.012	.0000	.000	.0000
2	.0000	.0000	.025	909.465	.0050	.0049
3	.0000**********		.0000	.0000	.0000	.000000
4	-.001	.000000**********				

	A	B	C	D	E	F
1	265000.0	187.02	.009	.0000	.000	.0000
2	.0000	.0000	.019	899.447	.0039	.0039
3	.0000**********		.0000	.0000	.0000	.000000
4	-.001	.000000**********				

	A	B	C	D	E	F
1	270000.0	182.71	.007	.0000	.000	.0000
2	.0000	.0000	.015	889.029	.0030	.0030
3	.0000**********		.0000	.0000	.0000	.000000
4	-.001	.000000**********				

	A	B	C	D	E	F
1	275000.0	180.65	.005	.0000	.000	.0000
2	.0000	.0000	.011	883.994	.0023	.0023
3	.0000**********		.0000	.0000	.0000	.000000
4	-.001	.000000**********				

	A	B	C	D	E	F
1	280000.0	180.65	.004	.0000	.000	.0000
2	.0000	.0000	.008	883.994	.0018	.0017
3	.0000**********		.0000	.0000	.0000	.000000
4	-.001	.000000**********				

	A	B	C	D	E	F
1	285000.0	180.65	.003	.0000	.000	.0000
2	.0000	.0000	.006	883.994	.0013	.0013
3	.0000**********		.0000	.0000	.0000	.000000
4	-.001	.000000**********				

	A	B	C	D	E	F
1	290000.0	180.65	.002	.0000	.000	.0000
2	.0000	.0000	.005	883.994	.0010	.0010
3	.0000**********		.0000	.0000	.0000	.000000
4	-.001	.000000**********				

	A	B	C	D	E	F
1	295000.0	180.65	.002	.0000	.000	.0000
2	.0000	.0000	.004	883.994	.0008	.0008
3	.0000**********		.0000	.0000	.0000	.000000
4	-.001	.000000**********				

	A	B	C	D	E	F
1	300000.0	184.89	.001	.0000	.000	.0000
2	.0000	.0000	.003	894.501	.0006	.0006
3	.0000**********		.0000	.0000	.0000	.000000
4	-.001	.000000**********				

APPENDIX 6

GLOSSARY AND ABBREVIATIONS

1. GLOSSARY AND ABBREVIATIONS

This appendix (table AP 6-1) lists the commonly used S-IVB-502 stage flight evaluation terms and abbreviations together with their definitions.

TABLE AP 6-1 (Sheet 1 of 10)
GLOSSARY AND ABBREVIATIONS

ABBREVIATION	TERMS	DEFINITION
AACS	--	Auxiliary attitude control system (see APS)
ac	--	Alternating current
AEDC	--	Arnold Engineering Development Center
--	Aerodynamically induced vibration	The oscillation of a mechanical system when set into motion by the turbulent boundary layer during flight. It is dependent on the shape and velocity of the body
amp	--	Ampere
ANT	--	AFETR Station on Antigua Island
APS	--	Auxiliary propulsion system (see AACS)
AS	--	Apollo Saturn
ASC	--	AFETR Station on Ascension Island
ASI	--	Augmented spark igniter
AST	--	All systems test
A_t	--	Throat area
aux	--	Auxiliary
--	Average mixture ratio	The time average of the propellant mixture ratio over 1-sec time intervals between 90 percent thrust buildup and Engine Cutoff Command
--	Average thrust or specific impulse	Determined between the time of 90 percent thrust and Engine Cutoff Command
A_W	--	Wind azimuth (deg)
A_{XM}	--	Axial acceleration (ft/sec^2)
BDA	--	Bermuda
BGR	--	Bridge gain ratio
Btu	--	British thermal unit
CCS	--	Command communication system
CCW	--	Counterclockwise
CDDT	--	Countdown demonstration test
CECO	--	S-IC stage Center Engine Cutoff Command
CEI	--	Contract end item
CDF	--	Confined detonating fuse
C_F	--	Thrust coefficient
C_f	Collapse factor	A measure of the effectiveness of pressurization defined as: $C_f = \frac{M_{actual}}{M_{theoretical}}$, where M actual: is the mass necessary to pressure the propellant tank (lbm)

TABLE AP 6-1 (Sheet 2 of 10)
GLOSSARY AND ABBREVIATIONS

ABBREVIATION	TERMS	DEFINITION
C_f	(Continued)	$M_{theoretical}$: is the mass necessary to pressurize the propellant tank if heat and mass transfer across the ullage boundaries are neglected (lbm)
--	Composite data (acoustic and vibration)	The total energy of the oscillatory phenomen, consisting of all frequencies and amplitudes sensed by the transducers, and represents the phenomenon at the point of measurement within the limitations of the data acquisition and reduction systems
CPIF	--	Cost plus incentive fee
cpm	--	Cycles per minute
cps	--	Cycles per second
CRO	--	Carnarvon
CSM	--	Command service module
cu in.	--	Cubic inches
CVS	--	Continuous vent system
CW	--	Clockwise
CYI	--	Grand Canary Island
DAC	--	Douglas Aircraft Company, Inc.
DAC/FTC	--	Douglas Aircraft Company, Inc./Florida Test Center
DAC/HB	--	Douglas Aircraft Company, Inc./Huntington Beach
db	--	Decibel
dbm	--	10 log P (milliwatts) where p = power
dbw	--	10 log P (watts)
dc	--	Direct current
deg	--	Degree
--	Depletion Engine Cutoff Command	The time that engine cutoff was, or would be, initiated by the depletion level sensors
D/O	--	Dropout
e	--	Eccentricity
EA	--	Electronics assembly
EBW	--	Exploding bridgewire
ECA	--	Electrical control assembly
ECC	--	Engine Cutoff Command
ECF	--	End conditions of flight
ECP	--	Engineering change proposal
ECS	--	Environmental control system
EDS	--	Emergency detection system
--	Effective burntime	The engine burntime from 90 percent thrust buildup to Engine Cutoff Command

TABLE AP 6-1 (Sheet 3 of 10)
GLOSSARY AND ABBREVIATIONS

ABBREVIATION	TERMS	DEFINITION
EMC	--	Electromagnetic compatibility
EMI	--	Electromagnetic interference
EMR	Engine propellant mixture ratio	The ratio of engine LOX mass flowrate to LH2 mass flowrate includes gas generator operations
eng	--	Engine
--	Engine cutoff transient	Engine operation during the period from the Engine Cutoff Command until the end of thrust decay
ESC	--	Engine Start Command
EST	--	Eastern standard time
--	Engine start transient	Engine operation during the period from the Engine Start Command until the time of 90 percent thrust (approximately a 3-sec period)
--	Engine steady-state operation	Engine operation during the period from the time of 90 percent thrust until Engine Cutoff Command
ETD	--	End of thrust decay
ETR	--	Eastern Test Range
°F	--	Degree Fahrenheit
F	Stage longitudinal thrust	Thrust (lbf) developed by the J-2 engine. Ullage rocket thrust is not included
F_a	--	Ullage rocket thrust (lbf)
--	Flow integral propellant mass history	That propellant mass history determined by combining independent engine analyses by a statistical method
F/B	--	Feedback
FCC	--	Flight control computer
FM	--	Frequency modulation
fps	--	Feet per second
ft	--	Foot
FTC	--	Florida Test Center
fwd	--	Forward
g	Gravitational acceleration	The acceleration produced by the force of gravity, which varies with the altitude and elevation of the point of observation. The value 32.1739 ft/sec^2 has been chosen as the standard by international agreement for sea level at 45° north latitude
GBI	--	AFETR Station on Grand Bahama Island
GCC	--	Guidance Cutoff Command
GG	--	Gas generator
GH2	--	Gaseous hydrogen
GMT	--	Greenwich mean time
GN2	--	Gaseous nitrogen
GOX	--	Gaseous oxygen

TABLE AP 6-1 (Sheet 4 of 10)
GLOSSARY AND ABBREVIATIONS

ABBREVIATION	TERMS	DEFINITION
gpm	--	Gallons per minute
grms	--	Gravity root mean square
GSE	--	Ground support equipment
GYM	--	Guaymas
h	--	Altitude
h (AP)	--	Apogee altitude
HAW	--	Hawaii
He	--	Helium
HF	--	High frequency
hr	--	Hour
H/W	--	Hardwire
Hz	Hertz	Cycles per second
i	--	Inclination
IAS	--	Initiation of automatic sequence
IECO	--	S-IC stage Inboard Engine Cutoff Command
IGM	--	Iterative guidance mode
in.	--	Inches
in./in.	--	Inches per inch (strain)
IP&CL	--	Instrumentation Program and Components List
ips	--	Inches per second
IRIG	--	Inter range instrumentation group
Isp	--	Specific Impulse
IU	--	Instrument unit
k	--	Insulation thermal conductivity
kc	--	Kilocycles
KSC	--	Kennedy Space Center
ksi	--	1,000 $lb/in.^2$
L	--	Trajectory fit parameter
lbf	--	Pounds force
lbm	Pounds mass	1/32.1739 slug
lbm/hr	--	Pounds mass, hour
lbm/sec	--	Pounds mass, second
lb/pf	--	Pounds per picofarad
LC	--	Launch Complex
L/C	--	Loading Computer

TABLE AP 6-1 (Sheet 5 of 10)
GLOSSARY AND ABBREVIATIONS

ABBREVIATION	TERMS	DEFINITION
LCC	--	Launch control center
LES	--	Launch escape system
LET	--	Launch escape tower
--	Level sensor residuals	Those propellant residuals above the main propellant valves determined by combining data from one or more level sensors by a statistical method and extrapolating to Engine Cutoff Command
LH2	--	Liquid hydrogen
LM	--	Lunar module
LO	--	Vehicle liftoff time
--	Look angle	Angle between the vehicle centerline and the line of sight, measured from the rear of the vehicle (deg)
LOS	--	Loss of signal
LOX	--	Liquid oxygen
L/S	--	Level sensor
LTA	--	Lunar test article (Structural representation of LM)
LV	--	Launch vehicle
LVDC	--	Launch vehicle digital computer
M	--	Mach number
$\dot{M}$	Stage propellant mass flowrate (lbm/sec)	Engine propellant mass flowrate (includes propellant flowrate for gas generator operation)
$\dot{M}_f$	Stage LH2 mass flowrate (lbm/sec)	Engine LH2 mass flowrate (includes LH2 flowrate for gas generator operation)
$\dot{M}_o$	Stage LOX mass flowrate (lbm/sec)	Engine LOX mass flowrate (includes LOX flowrate for gas generator operation)
ma	--	Milliampere
M&A	--	Manufacturing and assembly building (STC)
max q	--	Maximum dynamic pressure
μin./in.	Micro inch per inch	Millionth of an inch per inch
MDF	--	Mild detonating fuse
MFV	--	Main fuel valve
MHz	--	Millihertz
MILA	--	Merritt Island Florida
MOI	--	Moment of inertia
MOV	--	Main oxidizer valve
ms	Millisecond	Thousandth of a sec
MSC	--	Manned Spacecraft Center, Houston, Texas
MSFC	--	Marshall Space Flight Center
MSL	--	Mean sea level

TABLE AP 6-1 (Sheet 6 of 10)
GLOSSARY AND ABBREVIATIONS

ABBREVIATION	TERMS	DEFINITION
MSSD	--	Missile and Space Systems Division, Huntington Beach, California
mv	--	Millivolt
mxr	--	Multiplexer
N/A	--	Not applicable
NASA	--	National Aeronautics and Space Administration
NC	--	Normally closed
--	Ninety percent thrust buildup	Time from Engine Start Command until the last engine chamber pressure (injector end) reaches 618 psia
nmi	--	Nautical miles
NO	--	Normally open
No.	--	Number
N_2O_4	NTO	Nitrogen Tetroxide
NPSP	--	Net positive suction pressure
NPV	--	Nonpropulsive vent
OAT	--	Overall test
OECO	--	S-IC stage Outboard Engine Cutoff Command
O-P	--	Zero to peak
P	--	Geodetic latitude
P	--	Pitch
P_a	--	Ambient pressure
P_c	--	Combustion chamber pressure measured at the injector
PA	--	Pressure actuated
PAM	--	Pulse amplitude modulation
PCF	--	Preconditions of flight
PCM	--	Pulse code modulation
--	Phase I	Time from liftoff to ECC1 +10 sec
--	Phase II	Time from liftoff to planned LV/SC separation
PMR	Programmed mixture ratio	A method of controlling the PU valve mixture ratio to obtain maximum efficiency of the stage. The propellant loading is provided to cause the PU system to command the PU valve against the LOX rich stop for the initial portion of flight and then decrease to a lower mixture ratio during the final portion of flight
P/N	--	Part number
P-P	--	Peak to peak
ppm	--	Parts per million
--	Propellant residuals	The sum of LOX and LH2 remaining onboard at Engine Cutoff Command. The residuals include both usable and trapped propellants

TABLE AP 6-1 (Sheet 7 of 10)
GLOSSARY AND ABBREVIATIONS

ABBREVIATION	TERMS	DEFINITION
PS	--	Pressurization system
P/S	--	Pulse sensor
PSD	--	Power spectral density
psia	--	Pounds per square inch absolute
psid	--	Pounds per square inch differential
psig	--	Pounds per square inch gauge
PTCS	--	Propellant tanking computer system
P/U	--	Pickup
PU	--	Propellant utilization
--	PU system propellant mass history	That propellant mass history determined for flight by the PU system
--	PU system residuals	Those propellant residuals above the main propellant valves determined by the PU system
q	--	Dynamic pressure
R	--	Rankine
RACS	--	Remote analog calibration system
reg	--	Regulator
RF	--	Radio frequency
RFI	--	Radio frequency interference
RMR	--	Reference mixture ratio
rms	--	Root mean square
R/NAA	--	Rocketdyne, North American Aviation
RO	--	An event time used as reference for S-IVB stage flight evaluation sequence of events. Defined as the first Greenwich mean time second prior to vehicle liftoff
rpm	--	Revolutions per minute
R/S	--	Range safety
RSCR	--	Range safety command receiver
rss	--	Root sum square
S	--	Surface range (ft)
SC	--	Spacecraft
scfm	--	Standard cubic ft/min
scim	--	Standard cubic in./min
sco	--	Subcarrier oscillator
sec	--	Seconds
S-IB	--	First stage of the Saturn IB (200) series of vehicles
S-IC	--	First stage of the Saturn V (500) series of vehicles

TABLE AP 6-1 (Sheet 8 of 10)
GLOSSARY AND ABBREVIATIONS

ABBREVIATION	TERMS	DEFINITION
S-II	--	Second Stage of the Saturn V (500) series of vehicles
S-IVB	--	Second stage of the Saturn IB (200) series of vehicles and third stage of Saturn V (500) series of vehicles
SLA	--	Spacecraft LM adapter
--	Slug	English system unit of mass
SLV	--	Saturn launch vehicle
SM	--	Santa Monica
SM	--	Service module
S/N	--	Serial number
SPS	--	Service propulsion system
SOV	--	Shutoff valve
SSB	--	Single sideband
SSS	--	Stage switch selector
sta	--	Station
--	Statistical weighted average loaded propellants	The most accurate determination of actual propellant load at liftoff as derived from the statistically weighted average mass
--	Statistical weighted average mass determination	A statistical combination of the PU system, engine system, flight simulation, and propellant level sensors at Engine Start Command and Engine Cutoff Command
--	Statistical weighted average residual propellants	The most accurate determination of actual propellant residual at Engine Cutoff Command as derived from the statistically weighted average mass determination method
STC	--	Sacramento Test Center
STD	--	Start tank discharge
STDV	--	Start tank discharge valve
S/V	--	Space vehicle
sw	--	Switch
Sw sel	--	Switch selector
T	--	Countdown time from prospective liftoff or as specifically defined in the text
Tel 2	--	Telemetry station at KSC
Tel 3	--	Cape Kennedy Telemetry Station IV
Tel 4	--	Merritt Island Telemetry Station IV
TEX	--	Cropus Christi, Texas
tk	--	Tank
T/M	--	Telemetry
--	Total depletion burntime	The engine burntime from Engine Start Command to the time that the Depletion Engine Cutoff Command would have been initiated

TABLE AP 6-1 (Sheet 9 of 10)
GLOSSARY AND ABBREVIATIONS

ABBREVIATION	TERMS	DEFINITION
--	Total propellants consumed	That amount of liquid propellants consumed from Engine Start Command to Engine Cutoff Command includes engine consumption, boiloff, and LH2 tank pressurant
TPEP	--	Telemetry performance evaluation period
--	Total stage burntime	The engine burntime from Engine Start Command to Engine Cutoff Command
--	Total stage mass history	A compilation of all final hardware, propellant, and gas masses. The measured and computed mass of each constituent is adjusted within its accuracy band so that the total stage mass at Engine Start Command and Engine Cutoff Command agrees with the total stage mass as determined by the Statistical Weighted Average mass determination method
TP&E	--	Test Planning and Evaluation
TVCS	--	Thrust vector control system
--	Unusable propellants	Those propellants remaining after a propellant depletion cutoff. This includes the propellant in the tank below the depletion sensor, propellant in the feed duct, and trapped propellants. It does not include sensor lag time or the propellant consumed during engine cutoff but does include sensor time delay
U/R	--	Ullage rocket
--	Usable residual	Propellants in excess of trapped propellants left onboard a stage after powered flight has been terminated by some specified cutoff criteria
USB	--	Unified S-band
v	--	Volt
V_E	--	Relative velocity
V_I	--	Inertial velocity
V_{RM}	--	Freestream velocity
V_W	--	Wind velocity (speed)
VAB	--	Vehicle Assembly Building, KSC, Florida
vac	--	Voltage, alternating current
VCO	--	Voltage controlled oscillator
vdc	--	Voltage, direct current
VHF	--	Very high frequency
VSE	--	Vehicle support equipment
VSWR	--	Voltage standing wave ratio
w	--	Watt
WRO	--	DAC work release order
wt	--	Weight
$\dot{W}_T$	--	Time rate of change of total vehicle weight
X_E	--	Downrange distance
$\dot{X}_E$	--	Downrange velocity

TABLE AP 6-1 (Sheet 10 of 10)
GLOSSARY AND ABBREVIATIONS

ABBREVIATION	TERMS	DEFINITION
Y	--	Yaw
Y_E	--	Vertical distance
$\dot{Y}_E$	--	Vertical velocity
Z_E	--	Crossrange distance
$\dot{Z}_E$	--	Crossrange velocity
α_P	--	Pitch angle of attack
αq	--	Product of angle of attack and dynamic pressure
α_Y	--	Yaw angle of attack
γ_1	--	Earth fixed flight path elevation angle
Δw	--	Delta weight
γ_{1_I}'	--	Inertial flight path elevation angle
γ_{2_I}'	--	Inertial flight path azimuth angle
μ	--	Longitude
μv	--	Microvolt

DISTRIBUTION LIST

HUNTINGTON BEACH (A3)

K010 Senior Director - Saturn/Apollo Programs
KY00 Director - Saturn Program Production
KOD0 Director - Huntington Beach Development Engineering
K0E0 Director Saturn/Apollo Program Ext
KWA0 Supervisor - System Engineering
KYC0 Manager - S-IVB Series Stages
N580 Branch Manger - Saturn Contracts
HAAA Manager - Vehicle Flight Readiness
KWA0 Supervisor - System Engineering
(Rocketdyne) via J. Boyde (KCDE)
KN00 Deputy Chief Design Engineer - Saturn Development Engineering
KA00 Chief Engineer - Mechanics & Reliability
KAB0 Branch Chief - Structural Mechanics (3)
KB00 Chief Engineer - Structural/Mechanical
KAC0 Branch Chief - Flight Mechanics (2)
KC00 Chief Engineer - Propulsion
KCB0 Branch Chief - Analysis
KCBC System Performance
KC00 Deputy Branch Chief - Propulsion Design
KCD0 Branch Chief - Test
KD00 Chief Engineer - Saturn Electronics
KDDH Section Chief - Electronics TP&E
KDLD Branch Chief - Electronic-Stage Design
L110 Chief - Data Reduction Engineering
LCC0 Branch Chief - Saturn Support Branch
KAD0 Branch Chief - Reliability Engineering (2)
KF00 Chief Engineer - Saturn Vehicle Checkout Laborities Qualification Test Programs
KKB0 Project Engineer - Test
KKBK Assistant Project Engineer - Test Special
KKBL Assistant Project Engineer - Operations Support
KKB0 Assistant Project Engineer - Test
KKBJ Assistant Project Engineer - System Test
5284 Library
KEBG Records

S-IVB TP&E Committee Members (A3)

AF02 Materials & Methods - Research & Engineering
KBDB Project Support
KCBC System Performance
KDDH Electronics
LCC0 Saturn Support Branch
KKBH TP&E - Flight Test

Propellant Utilization Panel (A3)

KKBH PU Panel Chairman - TP&E
KDLD PU Panel - Electronics

FLORIDA TEST CENTER (A41)

HE00 S. D. Truhan
HEBB H. N. Dell
KKG0 F. D. Comer
KA0C J. F. Ryan
KBDE G. C. Norvell

KCDD P. A. Kremer
KDDD L. H. Dybevick
KDDD D. W. Tutwiler
KKG0 J. R. Shaffer

SACRAMENTO TEST CENTER (A45)

KKH0 E. R. Jacobs (3)
KCDC A. C. Polansky

MANNED SPACE CENTER (A57)

K010 K. J. Patelski (3)
KLC0 L. A. Garrett (4)

NASA/MARSHALL SPACE FLIGHT CENTER

H. S. Garret (42)
TP&E - Files (10)